ANISOTROPY OF RESEDIMENTED BOSTON BLUE CLAY

by

Tian Ho Seah

BSc. (Hons) Civil Engineering
King's College
University of London
London, England
(1985)

Submitted to the Department of
Civil Engineering in partial fulfillment
of requirements for the degree of

Doctor of Science in Civil Engineering

at the

MASSACHUSETTS INSTITUTE OF TECHNOLOGY

April 1990

Signature of Author:.....
Dept. of Civil Engineering, April 10, 1990

Certified by:.....
Professor Charles C. Ladd, Thesis Co–Supervisor

Certified by:.....
Dr. John T. Germaine, Thesis Co–Supervisor

Accepted by:.....
Professor Ole S. Madsen
Chairman, Departmental Committee on Graduate Students

ANISOTROPY OF RESEDIMENTED BOSTON BLUE CLAY

by

Tian Ho Seah

Submitted to the Department of Civil Engineering on
April 12, 1990 in partial fulfillment of the requirements
for the Degree of Doctor of Science in Civil Engineering.

ABSTRACT

Rational analyses of complex clay–structure interaction problems should be able to predict the undrained and drained response of clay deposits under field conditions involving rotation of the principal stress directions. The set of constitutive relationship used to model soil behavior therefore must incorporate the stress–strain–strength anisotropy that is exhibited by natural clays. Laboratory experiments involving the effects of rotation of stress states on clay behavior are needed to validate and further develop realistic constitutive relationships.

The Directional Shear Cell (DSC) has the unique ability to fully control the major principal stress direction (δ) by varying the normal and shear stresses acting on four faces of a cubical sample constrained between two rigid end platens. The DSC has been used extensively at the Massachusetts Institute of Technology (MIT) to study the anisotropic drained behavior of sand and later to measure in detail the anisotropic response of overconsolidated resedimented Boston Blue Clay (BBC) under undrained shearing conditions.

This thesis includes: (1) preparation of resedimented BBC; (2) enhancement of the DSC equipment and testing procedure; (3) generation and analysis of results from undrained DSC tests on normally consolidated BBC; and (4) detailed comparisons of DSC experimental data with predictions by the MIT–E3 (Whittle, 1987) constitutive model.

The BBC is a lean illitic glacio–marine clay of low to medium sensitivity. The resedimentation process was introduced to control sample variability and the preparation of fully saturated resedimented BBC was developed by Germaine (1982). The equipment and the procedures have been modified and improved in this research. A significant amount of reference data including classification and index properties, consolidation and some undrained strength tests were performed to check sample uniformity on eight batches of BBC. The results obtained from this research are also compared with the data obtained from previous series of resedimented BBC.

Modifications of the DSC device include changes in the pressure bags, the shear sheets, the two platens, the sample corner design and the pore water pressure probe. Better uniformity of the sample is achieved by newly designed pressure bags and sample corner reinforcement. The stress state of the sample is now completely defined via the measurement of the intermediate principal stress (σ_2). Additional "proof" tests on rubber and BBC were performed to verify the DSC's ability to apply uniform states of stress.

A new technique has been developed to enable DSC testing of normally consolidated clay. Five DSC tests were conducted on normally consolidated BBC at δ_{inc} angles (incremental major principal stress direction relative to the depositional direction) of 0°, 45°, 60°, 75° and 90°. Results from the DSC test

program on normally consolidated BBC show very pronounced changes in the behavior of clay as a function of the δ angle. The experimental findings can be summarized as follows with increasing δ angle:

- The normalized undrained shear strength decreases from 0.33 at δ=0° to 0.16 at δ=90°.
- The stress–strain behavior changes from brittle to ductile;
- The shear induced pore pressure increases from 0.10 to 0.36 at failure.
- The shear modulus increases for given strain levels.

The maximum deviation between the ξ angle (major principal strain direction) and the δ angle is 15° when δ=25° at failure.

Predictions from the MIT–E3 model compare exceptionally well with the new DSC experimental data, which confirms the ability of this model in predicting the anisotropic behavior of clay at different overconsolidation ratio.

Thesis Co–Supervisor: **Dr. Charles C. Ladd**
Title: Professor of Civil Engineering

Thesis Co–Supervisor: **Dr. John T. Germaine**
Title: Principal Research Associate

ACKNOWLEDGEMENTS

The author would like to thank the following organization and people for making this research possible:

The National Science Foundation, whose financial support has made this research possible through a three–year research grant. This organization has been the sole sponsor for research on anisotropy at MIT since 1978.

Professor Charles C. Ladd, my thesis and academic advisor, for his contribution to the technical and literary content of this document. Professor Ladd had spent hundreds of hours reviewing and giving constructive and invaluable comments on the initial draft of this document. I am extremely grateful to have had the opportunity to work under him. "Sir, I thank you."

Dr. John T. Germaine, my thesis advisor, who taught me so much about laboratory testing, ranging from "measuring the water content" to "performing the DSC test." Dr. Germaine is always there when I needed a helping hand. I greatly admire his talent in tackling any kind of experimental problem.

Charles Aubeny, my colleague, for his preparation of several batches of resedimented Boston Blue Clay so that I would have enough soil samples to complete this research. Mr. Aubeny had spent two years working with me and had provided all his two year research in this document.

Professor Veneziano for helping to develop the strain analysis. Professor Whittle for providing the DSC predictions from the MIT–E3 soil model and reviewing my thesis.

To all my "soils and rocks" friends on the third floor, whom had made my stay at MIT a more memorable one. To Imitiaz Ahmed, Phillippe Bellward, "Magic" Elghaib, Youssef Hashash, Geraldo Iglesia, Paul Joseph, Aziz Malek, Atsuo Onoue, Anil Pahwa, Juan Pestana–Nascimen, "Libby" Reyes, Tom Sheahan and Naihsin Ting, many thanks!

Dr. Don. J. DeGroot, my MIT friend, his encouragement and support that were available in the difficult periods are sincerely appreciated.

My sister Khin, who did all the "cut and paste" for all the figures and tables presented in this thesis.

Annette Huber, for editing and typing this document before she left for the Peace Corps. She also helped me through the most difficult time at MIT, which was performing the DSC tests.

Finally, my parents who gave me the opportunity to pursue my studies abroad since I was seven. Their love and support was a continuous source of encouragement.

Dedicated to my
late Uncle Lee.

TABLE OF CONTENTS

LIST OF TABLES

LIST OF FIGURES

LIST OF SYMBOLS

Note:

1. Prefix Δ indicates a change.
2. Suffix $_f$ indicates a final or failure condition.
3. Suffix $_{max}$ indicates a maximum value.
4. A superscript prime on a stress indicates an effective stress.
5. A superscript prime on a property indicates value in terms of effective stress.

SYMBOL	DEFINITION
ASTM	American Society for Testing Materials
BBC	Boston Blue Clay
BRS	British Building Research Station
BS	British Standard
CD	Consolidated Drained Triaxial Test
CID	Hydrostatically Consolidated Drained Triaxial Test
CIU	Hydrostatically Consolidated Undrained Triaxial Test
CK_oD	K_o Consolidated Drained Triaxial Test
CK_oUDSS	K_o Consolidated Undrained Direct Simple Shear Test
CK_oU	K_o Consolidated Undrained Triaxial Test
CK_oUC	K_o Consolidated Undrained Compression Test
CK_oUE	K_o Consolidated Undrained Extension Test
CR	Compression Ratio
DSC	Plane Strain Directional Shear Cell
DSS	Direct Simple Shear
ESP	Effective Stress Path
LL	Liquid Limit
LL(BS)	Liquid Limit obtained from British Standard apparatus

LL(USA)	Liquid Limit obtained from ASTM apparatus
MCC	Modified Cam–Clay
MIT	Massachusetts Institute of Technology
NSF	National Science Foundation
OCR	Overconsolidation Ratio
PI	Plasticity Index
PL	Plastic Limit
PS	Plane Strain
PSC	Plane Strain Compression Test
PSE	Plane Strain Extension Test
RR	Recompression Ratio
SD	Standard Deviation
SHANSEP	Stress History and Normalized Soil Engineering Properties
SR	Swelling Ratio
TC	Triaxial Compression Test
TE	Triaxial Extension Test
TTA	True Triaxial Apparatus
TX	Triaxial Test
UCL	University College London
UU	Unconsolidated Undrained Triaxial Test
VCL	Virgin Compression Line
A_s	Cross sectional area of sample
A_a	Area of Pressure Bag A in contact with platen
A_b	Area of Pressure Bag B in contact with platen
A, (A_f)	Skempton's pore pressure parameter (at failure)
B	Skempton's pore pressure parameter
b	Relative Intermediate Principal Stress

C_c	Compression index
C_c'	Compression index in the remolded state
C_k	Permeability change index
C_r	Recompression Index
C_s	Swelling Index
$C_{\alpha\epsilon}$	Rate of secondary compression
c_v	Coefficient of consolidation
c	Cohesion intercept of effective envelope
d	Sample diameter
E	Young's modulus
E_r	Young's modulus of natural rubber
e	Void ratio
e_i, e_o	Initial void ratio
F_p	Total axial force acting on DSC platen
F_{piston}	Shear piston force
f	Ratio of number of non–zero weight data point to total number of data point
E_v, E_h	Young's modulus for vertical and horizontal loading
G_{50}	Shear Modulus at 50 % of maximum applied shear stress
G_s	Specific gravity of soil
G_{vh}	Shear modulus in vertical plane
G_y	Shear modulus after yielding in DSC test
H	Drainage path length
$\bar{H}$	Tansformation matrix
H_s	Height of sample
h	Radius of influence
I_1	First invariance of stress
I_2	Second invariance of stress

I_3	Third invariane of stress
K_o	Coefficient of earth pressure at rest
K_s	Anisotropy Strangth Ratio, $\left[\frac{S_u(\delta)}{S_u(0^\circ)}\right]$
k	Coefficient of permeability
k_v	Coefficient of vertical permeability
$\underline{m}'$	Estimate mean value matrix
m_v	Coefficient of volume change
p	Total mean stress, $\left[\frac{\sigma_1 + \sigma_3}{2}\right]$
q	Shear stress, $\left[\frac{\sigma_1 - \sigma_3}{2}\right]$
q_f	Shear stress at failure
q_y	Shear stress at yield point
r^2	Goodness of fit
R	Stress ratio, $\left[\frac{\sigma_1}{\sigma_3}\right]$
S	Degree of saturation
S_u	Undrained shear strength
$S_u(0^\circ)$	Undrained shear strength for vertical loading
$S_u(90^\circ)$	Undrained shear strength for horizontal loading
t_{100}, t_p	Time for primary consolidation
t_s	Time for which resedimented sample was stored before testing
u	Displacement of reference point in x direction
u_i	Excess pore pressure in sample exposed to atmospheric conditions
u_s	Shear induced pore pressure
v	Displacement of reference point in y direction
$\underline{W}$	Weight matrix
w_c	Water content
w_i	Initial water content
x_i, y_i	Coordinates of ith point in digitizer measuring system

Z	Deposition direction of the sample
α	Distortion angle on face A of DSC sample
β	Distortion angle on face B of DSC sample
γ	Shear strain
$\dot{\gamma}$	Shear strain rate
γ_1	Maximum shear strain obtained from Area No.1 of DSC sample
γ_2	Maximum shear strain obtained from Area No.2 of DSC sample
γ_{max}	Maximum shear strain
γ_{oct}	Octahedral shear strain $\{=\frac{1}{3}\sqrt{[(\epsilon_1-\epsilon_2)^2+(\epsilon_2-\epsilon_3)^2+(\epsilon_3-\epsilon_1)^2]}\}$
Δ	Deviation of axes of principal strain and principal stress
Δ_1	Deviation of axes of principal strain and principal stress for Area No.1
Δ_2	Deviation of axes of principal strain and principal stress for Area No.1
Δ_{inc}	Deviation of axes of principal strain and incremental principal stress
δ	Major principal stress direction measured from deposition axis
δ_{ave}	Average displacement of the soil sample due to platen separation
δ_{inc}	Incremental principal stress direction measured from the deposition axis
δ_{center}	Displacement at the center of the soil sample due to platen separation
δ_g	Change in grease thickness
δ_p	Deflections on DSC platens
δ_{obs}	Major Principal stress direction measured from orientations of failure planes
δ_r	Axial deformation of rubber membrane
ϵ	Strain, error in estimate
$\dot{\epsilon}$	Strain rate
ϵ_1	Major principal strain

ϵ_2	Intermediate principal strain
ϵ_{2g}	Average axial strain due to change in grease thickness
ϵ_{2p}	Average axial strain due to platen separation
ϵ_{2r}	Average axial strain due to deformation of rubber membrane
ϵ_3	Minor principal strain
ϵ_a	Axial strain
ϵ_c	Normal strain due to Poisson effect of rubber
ϵ_r	Radial strain of rubber membrane
ϵ_x	Normal strain in x direction
ϵ_y	Normal strain in y direction
ϵ_{xy}	Half of shear strain
ϵ_v	Volumetric strain
θ	Principal stress direction measured from the y axis
ν	Poisson's ratio
μ	Micrometer, mean
ξ	Total distortion angle of the DSC sample
ξ	Major principal strain direction
ξ_1	Major principal strain direction for Area No.1
ξ_2	Major principal strain direction for Area No.2
Σ	Sum
Σ	Variance
$\underline{\Sigma}$	Variance matrix
σ	Normal stress
σ_1	Major principal stress
σ_2	Intermediate principal stress
σ_{2c}	Consolidation stress in the plane strain direction
σ_3	Minor principal stress

σ_a	Applied normal stress of pressure bag A of DSC sample
σ_b	Applied normal stress of pressure bag B of DSC sample
σ_c	Cell pressure
σ_{hc}	Horizontal consolidation stress
σ_{ho}	Initial horizontal stress
σ_{piston}	Applied piston pressure
σ_{vc}	Vertical consolidation stress
σ_{vo}	Initial vertical stress
σ_x	Normal stress in x direction
σ_y	Normal stress in y direction
σ'_p	Preconsolidaton stress
σ'_{vm}	Maximum past vertical consolidation stress
τ	Shear stress
τ_a	Applied shear stress on face A of DSC sample
τ_b	Applied shear stress on face B of DSC sample
τ_h	Shear stress on horizontal plane
ϕ	Friction angle
ϕ_{obs}	Friction angle based on orientations of failure planes
ϕ_{tc}	Friction angle from triaxial compression
ϕ_{te}	Friction angle from triaxial extension
ψ	Major principal stress direction in the isotropic plane
ψ	Arctan (τ_h/σ'_v) for direct simple shear tests
ω	Rigid body rotation

CHAPTER 1

INTRODUCTION

1.1 BACKGROUND

Geotechnical engineering has historically been one of the more empirical disciplines within civil engineering because of the complex nature of soil, a multiphase particulate material. Foundations and other earth related structures involving soil were designed by rules of thumb before the eighteenth century. Coulomb, Rankine, Collin and Darcy were the pioneers in engineering aspects of soils involving problems of earth pressures against retaining walls, slope stability and seepage. Their work marked the beginning of a theoretical approach to geotechnical engineering, but without reliable experimental data, the analyses could not be applied with much certainty.

In 1925, the term "Soil Mechanics" was first used by the late Karl Terzaghi (1925). For the first time, soil was treated as an engineering material. Its nonlinear, inelastic, anisotropic and time dependent characteristics were more carefully studied in the laboratory and specific soil parameters were determined.

As noted by Ladd and Germaine (1985), "the design of structures founded in or on cohesive soils requires two key predictions by the geotechnical engineer: (1) the margin of safety against gross instability (failure); and (2) the expected magnitude of deformations during and after construction. Historically, limiting equilibrium analyses have been used to assess stability, with separate analyses employing simplified stress–strain relationships being used to predict deformations. Likewise, evaluation of soil properties required for design generally evaluated strength and stress–strain characteristics separately (e.g., field vane tests to measure undrained strength and laboratory oedometer tests to measure

compressibility)."

Advancements in both numerical methods and computer capabilities have now made it feasible to employ more sophisticated constitutive relationships to model soil behavior; through these models the full range of states of stress and strain can be encompassed. Constitutive soil models combined with the finite element method enable engineers to predict ground movements with more realistic boundary conditions. But the reliability of these constitutive relationships depends on extensive and accurate experimental data. The development of test devices and experimental procedures capable of obtaining reliable data under different drainage conditions and states of stress is an essential step in this process. The experimental data obtained for representative soil types can be used to identify and quantify important behavioral features, which can then be used to create or evaluate new constitutive relationships.

Due to a lack of reliable experimental data dealing with soil anisotropy, most soil models employed in design practice ignore anisotropy. A prime example is the widely used "Modified Cam–Clay" model (MCC) (Roscoe and Burland, 1968). This model provides an elegant framework for describing basic behavior observed in hydrostatically consolidated triaxial compression tests. But because most natural soils are anisotropic, the model cannot reliably predict the in–situ deformation–strength characteristics of natural cohesive soils. Recent developments in more sophisticated soil models, like the MIT–E3 generalized soil model (Whittle, 1987), have incorporated anisotropy, strain softening and bounding plasticity, etc. But sophisticated models face the same limitation: their predictions must be verified by experimental data regarding anisotropy.

Examples of field situations where anisotropy of soils can be important are shown in Figure 1.1. All of the examples shown involve the rotation of stress–states — one aspect of the study of anisotropy. Therefore, realistic

analyses will require better understanding of the effects of rotation of stress–states in an anisotropic material. Model development cannot proceed without first obtaining reliable experimental data on the effects of rotating stress–states on the behavior of anisotropic soils.

1.2 RESEARCH OBJECTIVES

The main objective of this research is to study the effects of the rotation of stress–states in anisotropic cohesive soils in order to achieve a better understanding of soil behavior. Because the research program also includes numerous conventional laboratory tests to check the variability of the soil, the results also provide reliable experimental data to form a data bank of the test material which will be available to engineers and researchers. This research concentrates on the undrained shear behavior of K_0 normally consolidated resedimented Boston Blue Clay (BBC) during the rotation of principal stress using the Directional Shear Cell (DSC), first developed by Dr. Arthur at University College London (UCL). This device is one of two laboratory shear apparatuses which has the capability to control the stress state rotation during a test. The chosen test material, resedimented Boston Blue Clay, has been extensively used at MIT for the past three decades to develop an understanding of soil behavior.

Germaine (1982) developed the basic technology needed to perform consolidated–undrained shear tests in the DSC on overconsolidated clay. O'Neill (1985) extended his data to obtain a comprehensive set of results for OCR=4 BBC at varying δ angles that was used by Whittle (1987) to evaluate the MIT–E3 model. The author improved the prior procedures used for conducting DSC tests and interpreting the data. New techniques were developed to enable K_0–consolidated–undrained DSC tests to be run on normally consolidated clay. These new results are compared to MIT–E3 predictions by Whittle.

Chapter 2 begins with a definition of soil anisotropy. A description of the laboratory devices used for investigation of soil anisotropy, and the merits and limitations of these devices follows. This chapter also includes an overview of research on anisotropy in soils in the context of principal stress rotation. Further details on this subject are given in Appendix C.

The modifications of the MIT Directional Shear Cell for the testing of K_o normally consolidated and K_o overconsolidated resedimented Boston Blue Clay are described in Chapter 3. Beginning with an overview of the modifications made to the DSC by different MIT researchers over the years, the chapter follows with an introduction to the measurement of the intermediate principal stress, and the changes made to the individual components of the DSC device.

The properties of resedimented Boston Blue Clay are given in Chapter 4. Index properties and consolidation behavior are determined for various batches of resedimented clay to check the consistency and the variability of the material and for comparison with prior data. Special testing was also needed to develop the final techniques used to conduct DSC tests on K_o normally consolidated clay.

Chapter 5 presents the principles underlying the Directional Shear Cell. The stress–strain measurements and analyses are discussed in detail in this chapter, as well as the testing procedures for clay in the DSC.

Chapter 6 evaluates the performance of the DSC device via the following experimental programs: 1) DSC tests run on an elastic material, namely rubber foam; and 2) DSC tests run on OCR=4 BBC in the isotropic plane, which simulates cavity expansion. In all cases, analysis of the uniformity of the strain distributions was a vital part of the performance evaluation process.

The undrained stress–strain–strength anisotropy of resedimented BBC is presented in Chapter 7. The testing programs and the results of overconsolidated and normally consolidated undrained tests are covered. Comparisons between the

DSC results and other experimental results are made to study the effects of the intermediate principal stress and other issues involving boundary conditions and interpretation of the state of stress in the DSC.

One of the objectives of this research is to evaluate the adequacy of the MIT–E3 generalized soil model (Whittle, 1987) regarding stress–strain anisotropy. Comparisons between the DSC experimental data and the model prediction are given in Chapter 8.

Chapter 9 summarizes principal conclusions and recommendations from the research.

There are a number of Appendices regarding descriptions of sample preparation, experimental results of the reference tests, results of the previous DSC tests on BBC at an OCR of 4, the construction and calibration of the DSC device, listings of various computer programs used for the stress–strain analysis, and the DSC experimental results. These are listed in the Table of Contents.

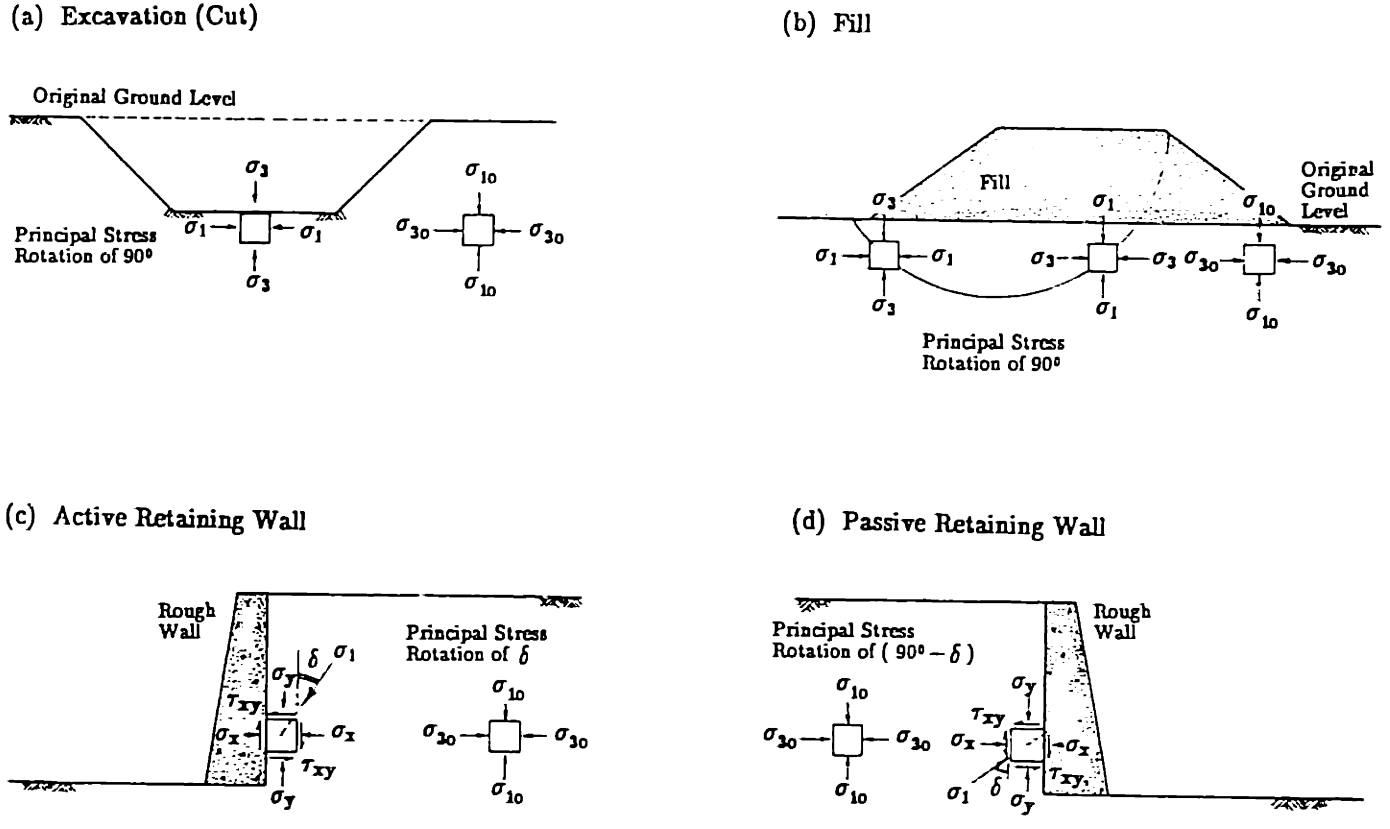

Assumptions:
Initial State of Stress, $\sigma_{vo}=\sigma_{1o}$ & $\sigma_{ho}=\sigma_{3o}$.
All the Elements are in the Failure Zones

Figure 1.1: Different Field Situations Involving Principal Stress Rotations.

CHAPTER 2

BACKGROUND

2.1 ANISOTROPY OF SOILS

Anisotropy is a complex and poorly understood subject within geotechnical engineering, even though most natural soils have moderate to high degrees of anisotropy in their stress–strain–strength properties. The change in soil behavior with direction of loading (i.e., anisotropy) can arise from several factors, such as the depositional environment and the consolidation stress–strain history of the soil and also due to subsequent changes in the loading conditions.

The nature of anisotropy in soils was first defined by Casagrande and Carrillo (1944) as one of two types, either induced or inherent anisotropy:

"If the anisotropic distribution of strength, exhibited by a material at failure, is due exclusively to the strain associated with the applied stresses, the material will be said to possess induced anisotropy. If, on the other hand, the non–isotropic behavior observed in a test is a physical characteristic inherent in the material, and entirely independent of the applied strains, the material will be said to possess inherent anisotropy."

A more recent description of anisotropy in natural clays was given by Ladd (1988):

"Initial anisotropy denotes changes in the stress–strain strength response of a soil with variations in the applied σ_1 direction (δ angle) during monotonic shearing. For natural clays having a one–dimensional strain history (K_o–consolidation and rebound), the resulting cross–anisotropic behavior has two components. An inherent anisotropy arises from the soil structure developed at the micro–level (preferred particle orientations and interparticle forces) and also at

the macro–level for certain soils like stiff fissured clays and varved glacial–lake deposits. Clays also exhibit directionally dependent undrained strengths whenever shearing starts from a $K_o \neq 1$ condition, as first predicted by Brinch–Hansen and Gibson (1949) and called initial shear stress anisotropy by Jamaiolkowski, et al. (1985)." These two components are inseparable in most natural clays so that the initial undrained strength anisotropy is the combined effect of both components. From a practical standpoint, it is also important to consider the influence of evolving anisotropy, which describes how the initial cross anisotropic properties of a K_o–consolidated clay change due to subsequent stressing and straining.

One approach to developing an understanding of the effects of anisotropy is to simulate the ground conditions in the laboratory by testing representative soil samples using special laboratory devices. The requirements of the devices are that:

- they should be able to simulate one–dimensional consolidation in order to either preserve or recreate the initial anisotropy;
- they should be able to load the soil sample in different directions relative to the depositional direction of the soil; and
- the drainage condition should be similar to the field situation, i.e., drained or undrained.

2.2 LABORATORY EQUIPMENT USED FOR MEASURING THE ANISOTROPIC BEHAVIOR OF SOILS

Many laboratory shear devices have been designed over the years to study the physical behavior of soils. This section provides an overview of six laboratory devices currently used to study the anisotropy of soils, along with their advantages and limitations.

Generally two parameters can be used to describe the shear mode of a soil sample (Germaine, 1982):

- the δ angle, defined as the direction of the major principal stress relative to the deposition direction (taken as vertical), as shown in Figure 2.1b; and
- the b value, defined as the relative magnitude of the intermediate principal stress, $b=(\sigma_2-\sigma_3)/(\sigma_1-\sigma_3)$.

The capabilities of different devices with respect to the δ–b space are shown in Figure 2.2. Table 2.1 summarizes the limitations and boundary conditions (flexible, rigid or mixed) of the devices.

2.2.1 Conventional Axisymmetric Triaxial Cell

Axisymmetric triaxial cells are the most widely used devices in soil mechanics to measure the stress–strain behavior of soil because of: its relative simplicity for testing and in the interpretation of results, and since the drainage condition can be well controlled. The axial stress ($\sigma_a=\sigma_v$) and radial stress ($\sigma_r=\sigma_h$) are applied to a cylindrical sample to produce an axisymmetric stress state, as shown in Figure 2.3a. The axial load is applied through rigid platens and the axial stress is assumed to be uniform over the cross–sectional area of the soil sample. The radial stress is imposed by fluid pressure in the chamber through a rubber membrane that encloses the sample. It is possible to produce K_o–consolidation by controlling the applied stresses such that the volumetric strain is the same as axial strain in an incremental manner. The specimens can then be sheared in either a triaxial compression (TC) mode (b=0) or a triaxial extension (TE) mode (b=1) as shown in Figure 2.2. Both drained and undrained shearing conditions can be achieved through stress–controlled and strain–controlled schemes.

The main disadvantage of the axisymmetric triaxial device is that the

major principal stress can act only in two directions, vertically (axial with δ=0°) or horizontally (radial with δ=90°). The principal stress cannot be rotated continuously during the tests. Another limitation of the axisymmetric triaxial device is the inability to separate the effects of b and δ since both change at the same time. But despite its limitations, the axisymmetric triaxial is still the simplest test to obtain the basic properties of a soil and the results are generally consistent and repeatable if good procedures are followed (Germaine and Ladd, 1988).

2.2.2 True Triaxial Apparatus

The concept behind true triaxial testing is very similar to that of axisymmetric triaxial cells, except that all three principal stresses are applied independently to a rectangular sample (Figure 2.3b). This apparatus is usually restricted in the study of the effects of the intermediate principal stress.

Various types of true triaxial apparatuses (TTA) have been designed over the years. The main difference among the devices is the applied loading boundaries, which can be characterized in three groups:

- flexible boundaries (Ko and Scott, 1967; Arthur and Menzies, 1972, Sture and Desai, 1979): where uniform stress can be applied;
- rigid platens (Hambly, 1969; Pearce, 1971): where the strain is uniform, and the deformation can be controlled in the test; and
- mixed boundaries (Shibata and Karube, 1965; Green, 1971; Lade and Duncan, 1973): this category is made up of a combination of flexible and rigid boundaries.

Each of these designs has its pros and cons. For example, flexible loading

boundaries have the advantage of applying nominally uniform stresses to the soil sample, but the strain in the soil sample is not always uniform due to imperfections in the devices. The strain distribution therefore should be measured and the technique involved can be very tedious and difficult. In contrast, a rigid loading device results in uniform strains, but the stresses are usually non–uniform and therefore should be measured using special load cells, such as the Cambridge load cell (Stroud, 1961).

True triaxial testing provides little improvement in studying the effects of the rotation of principal stresses over the conventional axisymmetric triaxial tests since the principal stresses must either act in or normal to the direction of deposition. However, it can perform tests at δ=0° and 90° with the same value of b in contrast to the axisymmetric triaxial cell. But this device is not suited for detailed study on the effects of principal stress rotation.

2.2.3 Plane Strain Device

Many practical problems in soil mechanics can be approximated by plane strain conditions. This led to the development of plane strain testing devices in which a rectangular specimen is used. The sample is restrained in the intermediate principal stress direction and normal stresses are applied in the other two directions, as shown in Figure 2.3c (e.g., Vaid and Campenella, 1974).

Plane strain devices face the same limitation as conventional and true triaxial devices, in that, the major principal stress can act in only two fixed directions (either in or normal to the direction of deposition).

2.2.4 Simple Shear and Direct Simple Shear Devices

There are two major types of "simple" shear devices. The first device (Roscoe, 1953) was the rigid boundary simple shear apparatus (SSA), where the

specimen deforms from a rectangular shape into a parallelepiped by loading the top platen of a ball–hinged box (dimensions of 6cm x 6cm x 2cm) in the horizontal direction. The major problems with this device are that: (1) the stresses are non–uniform, and; (2) the rotation of the principal stress is uncontrolled since the specimen is allowed to deform freely in a simple shear mode from the applied horizontal force.

The second device is known as the Direct Simple Shear (DSS) device. This device was developed by the Norwegian Geotechnical Institute (NGI) (Bjerrum and Landva, 1966) and based on an earlier design by the Swedish Geotechnical Institute. A version of this device as commonly used at MIT is shown in Figure 2.3d. The soil specimen is confined laterally with a wire–reinforced rubber membrane that allows only axial (vertical) deformation during consolidation. This restriction of lateral displacement allows K_o–consolidation as in an oedometer test. During shear, the sample deforms horizontally (in a simple shear mode) with little or no interference from the rubber membrane by displacing the top loading platen in the horizontal direction. Most of the tests performed on clays are sheared "undrained," which is achieved by keeping the height of the sample constant during shear. Since the cross–sectional area of the soil remains unchanged, the volume is kept constant by fixing the sample height. The main problem associated with this device is that the state of stress is not known because the stresses (τ and σ) are only measured on one plane. Therefore, the DSS device is not suited for this study.

2.2.5 Torsional Shear Hollow Cylinder

The torsional shear hollow cylinder (TSHC) apparatus rotates the principal stresses in a controlled fashion during monotonic shear. The principle behind this device is based on thin shell theory. A hollow cylindrical sample is subjected to a

combination of axial load (σ_a), torque (τ), internal (P_i) and external (P_o) cell pressures, giving control over the direction and magnitude of the major principal stress, as well as the magnitude of the intermediate stress (Figure 2.3e). Therefore, in theory, it can cover most of the b–δ range as shown Figure 2.2. In practice, however, it is difficult to prepare a thin–wall cylindrical specimen without causing substantial disturbance to the soil, and the required thickness of the wall is relatively large compared to the diameter of the cylinder. This large thickness causes non–uniform stresses across the sample when the internal cell pressure is not equal to the external cell pressure. Hight et al. (1983) evaluated the optimum sample dimensions to give reasonable uniformity by: "1) using samples in which the ratio of inner to outer radius is 0.8, and 2) monitoring displacements and pore pressures over a central gage length of the sample." They adopted an internal diameter of 203 mm, an external diameter of 254 mm, and an overall height of 254 mm. This device has been used to study anisotropy of sand.

2.2.6 Directional Shear Cell

The Directional Shear Cell (DSC) is the first laboratory device which is capable of rotating and controlling the principal stress direction under plane strain condition in order to study the anisotropy of soils in detail (Arthur et al., 1977). A cubical specimen is subjected to normal and shear stresses while constrained between two parallel rigid end platens to create a plane strain condition, as shown in Figure 2.3f. Further description of the components is given in Chapter 3 (Figures 3.1 to 3.4). The direction and magnitude of the principal stress can be controlled and applied in the plane of shearing by varying the normal and shear stresses which act parallel to the end platens (Figure 5.1). The principle underlying the stress application is given in Section 5.2. This capability enables rotation of the major principal stress by up to 90 degrees during a test. The

original DSC device designed by Arthur and his colleagues uses a 4 inch cube sample, it can apply a maximum normal stress of 2 ksc and a maximum shear stress of 0.5 ksc.

The normal stresses are applied via flexible pressure bags, which can produce reasonably uniform normal stresses to the sample. The shear stresses are applied using a set of rubber shear sheets, subdivided into hundreds of loading strips, so that shear stresses can be uniformly imposed through applying equal forces to each of these individual strips. Chapter 3 describes these components in detail. The use of flexible boundary conditions in the plane of shear minimizes stress concentrations and allows rupture surfaces to form with minimal restraints. The strain distributions of the sample during shearing are measured by either radiographic or photographic techniques. These methods of determining strain provide detailed information on the strain distribution across the sample, but the process of obtaining strain data is very time–consuming and labor intensive.

Another unique feature of the DSC is that its performance can be checked by conducting tests in the isotropic plane of the specimen (Figure 2.1a). The behavior of the material under this condition, referred to as ψ tests (or proof tests), should be independent of the principal stress direction. For example, the resedimented BBC used in this research is cross–anisotropic, that is the plane perpendicular to the depositional axis exhibits isotropic behavior. Therefore, by shearing the specimen in this isotropic plane (i.e., the plane normal to the depositional axis), the researcher can detect any device–induced errors. Tests with different orientations of the major principal stress (i.e., varying the components of normal and shear stresses) should give identical behavior.

The DSC was developed at University College London (Arthur et al., 1977) to study the effects of principal stress rotation in sand. The DSC was first used to investigate strain induced anisotropy in sand (Arthur et al, 1977, 1980). The same

device was later used at MIT to also study the inherent anisotropy of loose sand. Many tests were also performed at MIT for comparison with the induced anisotropy data obtained at UCL (Arthur et al., 1981).

Germaine (1982) extended the capability of the DSC to study of the effects of principal stress rotation in saturated clay under an undrained shearing condition. This was achieved by measuring and controlling the pore water pressure developed in the sample. O'Neill (1985) continued his study into the undrained anisotropy of overconsolidated BBC.

Today, there are a number of DSC devices used in different research institutes (MIT, UCL, University of Colorado, and Waterway Experiment Station). The DSC devices differ in sample sizes, strain measurement techniques, capacities and drainage conditions. The different methods of strain measurement used in the DSC are discussed in Section 5.3.1.

Sture et al. (1985) at the University of Colorado led a study using a different version of the Directional Shear Cell in the following aspects:

- Larger sample size (17.8 cm cube) and higher stress levels (σ=450 kPa, τ=110 kPa).
- Deformations are measured using 8 proxity transducers with two on each of the four vertical faces, and 12 LVDTs are used to correct for system flexibility.
- Stress–strain data can be obtained during the tests with data acquisition.

2.2.7 Discussion

The TSHC has the theoretical potential to fully investigate anisotropy under various (but constant) σ_2 conditions, that is to cover nearly the full range of b and δ in Figure 2.2. However, the only TSHC device that has apparently

succeeded in doing this (Hight et al., 1983) is essentially restricted to testing granular soils. Therefore, detailed studies of clay anisotropy can be best accomplished via the DSC.

The basic DSC device by Arthur et al. (1981) is considered the best plane strain device available for basic research into initial and evolving anisotropy. It also has the advantage of providing detailed information regarding strain distributions (magnitudes and directions). Other advantages includes: 1) K_o–consolidation can now be achieved in the DSC, which was one of the main tasks in this research – Section 5.5 describes the technique of K_o–consolidation of a DSC sample; 2) a smaller sample is used in the DSC testing than its counterpart, the TSHC, described by Hight et al. (1983). Large specimen dimensions make clay testing impractical.

The main limitation of the MIT DSC device for studying the effects of δ is that only low stress tests can be performed. In addition, it is not possible to "back pressure" the soil sample. Therefore, the undrained behavior of the soil can be evaluated only with a fully saturated sample capable of sustaining significant capillary stresses, i.e., undrained shear tests on sand are impossible. The DSC also is a stress–controlled device, and therefore cannot easily measure strain softening behavior due to the slow recovery of strain data.

2.3 OVERVIEW OF THE ANISOTROPY OF SOILS

Because of practical differences in field behavior, this overview of the soil anisotropy is presented separately for sand and clay. In sands, the typical field loading condition is drained because the large pore size and hence the high coefficient of permeability leads to quick dissipation of excess pore water pressure. Therefore most studies of anisotropy in sand were done under drained conditions with a few exceptions (e.g., Symes et al., 1984). The most critical loading

conditions for soft clays are usually undrained, therefore, most of the research on clays has concentrated on undrained behavior. The following sections present some experimental studies of the inherent and induced anisotropy in soils with varying major principal stress direction and the testing programs are summarized in Table 2.2.

2.3.1 Anisotropy of Sand

Early studies of the inherent anisotropy in sands involved drained triaxial testing (CID) on inclined specimens having σ_1 oriented at different δ angles to the vertical depositional direction. The samples were prepared by depositing dry sand into a tilting mold (Arthur & Phillips, 1975). Drained plane strain tests were also conducted on inclined specimens which were trimmed from a dense sand that had been solidified using a soap solution (Arthur & Assadi, 1977). These results showed a significant change in friction angles (ϕ'), as presented in Figure 2.4.

One of the most distinguished studies of anisotropy in sand was done at UCL and later at MIT using the UCL DSC device. The investigations focused on the drained shear behavior of Leighton Buzzard sand and included the following topics:

- Proof testing on dense and loose sand to verify the performance of the DSC device.
- Strain–induced anisotropy of dense and loose sand (Arthur et al., 1977, 1981).
- Inherent anisotropy of loose sand (Arthur et al., 1981).
- Inherent anisotropy of dense sand (Wong et al., 1985).

The results of the proof tests presented by Arthur et al. (1981) are discussed in Section 6.2.1. Other proof tests were conducted on dense Leighton

Buzzard by Wong et al. (1985) at different ψ angles to check the consistency of sample preparation and device. The results of these tests fall on a single stress–strain curve which have proven the performance of the DSC. The results of a monotonic test performed by Sture et al. (1985) at ψ=0° are compared with Arthur et al. (1981) and Wong et al. (1985) in Figure 2.11. The behavior is quite similar, except that the results from Sture et al. show a higher modulus at high strain levels and lower modulus at small strain levels (ϵ_1<1%) than the results from Arthur et al. (1981).

The DSC device was originally used for the investigation of strain–induced anisotropy in sands (Arthur et al., 1977). A similar study was conducted at MIT by Bekenstein (1980) to provide additional results on dense and loose sand. In the strain–induced anisotropy tests, the samples were first subjected to a very small hydrostatic stress (σ=14 kPa) before they were sheared to a fixed stress level in the isotropic plane with $\psi=\psi_A$. They were then unloaded to the initial hydrostatic stress state, and sheared to failure at different ψ angles (ψ_B). The experimental results showed that induced anisotropy produces a much stiffer response at small rotation angles ($\theta=\psi_B-\psi_A$) and a much softer response at larger rotation angles, as shown in Figures 2.5 and 2.6. The strains rise to a maximum at θ=70±10° and then decrease at θ=90° (see Figures 2.7 and 2.8).

The first study of inherent anisotropy in sands using the DSC was conducted at MIT (Arthur et al. 1981). Loose sand specimens were deposited one–dimensionally and then consolidated hydrostatically to a low level of stress (14 kPa) before they were sheared to failure at different δ angles. The study revealed important changes in stress–strain behavior; inherent anisotropy causes a decrease in stiffness as the δ angle rotates from 0° to 90° in the sand (Figure 2.9). The study was continued by Wong et al. (1985) at University College London, and the experimental program was extended to include the inherent anisotropy of

dense sand, the measurement of the intermediate stress and cyclic loading test. Wong et al. (1985) conducted three tests to study the effects of the inherent anisotropy of dense sand at δ=0°, 70° and 90°. The results indicate that the stiffness and the volumetric expansion decrease with increase in δ angle as shown in Figure 2.10. The friction angle (ϕ) is 50° at δ=0° and 46° at δ=90°, and the ϕ has a value of 45.5° at δ=70°.

A very interesting study of inherent anisotropy was done by Imperial College in the early 1980s using the Torsional Shear Hollow Cylinder (Hight et al., 1983) on Ham River sand. These tests included both undrained and drained shear, as described by Symes et al. (1984, 1988). Three sand samples with initial void ratios of 0.786 (medium to loose state) were deposited one–dimensionally and hydrostatically consolidated to 200 kPa, then subjected to undrained shear at different δ angles (δ=0°, 24.5° and 45°). The results from these tests show that the slope of the effective stress failure envelope and undrained shear strength decrease significantly with increasing δ angle (Figures 2.12 and 2.13). The q_f/σ'_c ratio decreases from 0.44 to 0.23 due to a combination of higher pore pressure and lower obliquities with increases in δ angle. The shear induced pore pressure ($u_s=\Delta u-\Delta\sigma_{oct}$) shown in Figure 2.14 indicates very small variations at the peak strength for these tests, but the u_s increases with increasing δ angles beyond peak . Figure 2.15 shows the large initial deviation between the principal stress direction and the incremental principal strain direction for the δ=24.5° and 45° tests.

Symes et al. (1988) performed drained shear tests at δ angles ranging from 0° to 45° on sand samples which were deposited one dimensionally and then were hydrostatically consolidated to 200 kPa. To define the drained initial strength and stiffness anisotropy of Ham River sand, tests were conducted in which the shear stress (q) was increased to failure with the direction of the major principal stress held constant at three different values of δ, δ=0°, 24.5° and 45°. The effective

octahedral normal stress was kept constant at 200 kPa, and the relative magnitude of the intermediate principal stress (b) was 0.5 throughout the tests. The results showed that the highest stiffness was associated with the δ=0° test and the softest response occurred with δ=45° (Figure 2.16). The highest drained strength occurred at δ=0° and the lowest at δ=45°, i.e., the friction angle (ϕ') decreases from 49° at δ=0° to 35° at δ=45°. Inherent anisotropy also affected the volumetric strain (contraction) rate, with the lowest rate occurring at δ=0° and the highest rate at δ=45° (Figures 2.17 and 2.18). But increases in the δ angle gave rise to less contraction near the end of shearing. The results of the drained tests are consistent with the undrained shear data since less contraction in the drained tests is equivalent to a lower shear induced pore pressure in the undrained tests. Figure 2.19 shows the deviation between the major principal stress and the incremental principal strain direction.

2.3.2 Anisotropy of Clay

Saada (1970) described the problems associated with performing UU tests in clay specimens cut at different orientations (δ angle) to the depositional axis. A number of unconfined compression tests were conducted on samples using frictional and lubricated end caps. When the end caps are frictional, bending moments and shear stresses are induced in the inclined samples. When the end caps are lubricated, the rigid platens still induce bending moments, but the sample is free to move laterally causing the sample to deform into an "S" shape. Jamiolkowski et al. (1985) state that results from UU tests on inclined samples are unreliable due to: "1) variable degrees of sample disturbance, which usually tends to mask anisotropic behavior; 2) neglect of the initial shear stress component of anisotropy; and 3) stress and strain non–uniformities generated within an inclined specimen having rigid end platens."

One of first studies of anisotropy of clays using CAU tests was done using the axisymmetric triaxial cell (e.g., Ladd and Varallyay, 1965). As mentioned earlier, such tests can only be performed at δ=0° and 90°. Therefore, for intermediate δ angles, either the TSHC or DSC should be used.

Saada and Bianchini (1975) ran CIU TSHC tests with P_o=P_i (to reduce non–uniformity) on one undisturbed and three remolded clay samples. The clays had been K_o–consolidated, rebounded to $\sigma'_c = K_o\ \sigma'_{vc}$ and sheared with different ratios of axial and torsional stress in order to vary σ_{1f} from δ=0° to δ=90°. Figure 2.20 shows the variation in the friction angle and undrained strength ratio for one of the "normally consolidated" clays. The data are scattered. The values of C_u/σ'_c generally increase between δ=0° and δ=30°, then decrease at greater inclinations of σ_1. The friction angle (ϕ') increases and then remains essentially constant at δ>45°. The authors considered ϕ' to "vary in a completely random fashion between 26.7°and 54.9°" and attributed the large variation to the invalidity of the Mohr–Coulomb failure criterion for anisotropic materials (Jamiolkowski et al., 1985). But due to the change in the intermediate principal stress (i.e., b=$\sin^2\delta$ in these tests) during the tests, it is very difficult to separate the relative effects rotation of principal stress versus b.

For example, Lade and Muscante (1978) conducted CIU TTA tests on remolded Grunite, indicating that the behavior is significantly influenced by the b value (Figure 2.21, prepared by C.C.Ladd). Therefore, conducting TSHC tests with P_i=P_o for basic research into anisotropy is severely hampered because of the unknown influence of the changes in the intermediate stress condition.

The first reliable and conclusive study on stress–strain–strength anisotropy of clay was done by Germaine (1982) using the DSC. Fully saturated resedimented Boston Blue Clay was used, with properties very similar to the natural material. The resedimented BBC was K_o–consolidated to a vertical stress

of 1 ksc, then rebounded to a hydrostatic stress with an overconsolidation ratio of 4. The samples were then extruded and trimmed into cubes before being tested in the DSC. The samples were reconsolidated to an OCR of 4, then sheared at different δ angles with no drainage in order to investigate the inherent anisotropy of clay under undrained shear. This undrained shear condition was accomplished by varying the mean stress in order to maintain a slightly negative pore water pressure in the clay samples during shear. Eleven undrained shear tests were performed by Germaine (1982) and O'Neill (1985); eight of these tests were judged successful. Five proof tests were performed on OCR=4 BBC and the results are discussed in Section 6.2.2.

The main setback to the above research was that the tested material was found to be thixotropic (O'Neill, 1985). Rational corrections were made, and the corrected stress–strain and effective stress path are shown in Figures 2.22 and 2.23. Figure 2.24 plots q_f, $(\sigma_1/\sigma_3)_f$, A_f and Δ versus the δ angle. The parameter Δ is defined as the difference between the major principal strain direction and the major principal stress direction. The results show that inherent anisotropy has a very significant effect on the nature of the shear stress–strain response and effective stress paths, e.g., a normalized undrained shear strength of 0.25 at δ=0° and a shear strength of 0.14 at δ=90°. Brittle behavior is observed in low δ angle tests, with the formation of distinct rupture surfaces at low strains (γ<2–4%). In contrast, more ductile behavior occurred at high δ angles with higher strains at failure (γ>5–10%). But inherent anisotropy had little effect on the shear induced pore pressure prior to yielding as shown in Figure 2.22. Thereafter, increasing δ angles caused much larger pore pressures. The results also show a very consistent decrease in p'_f and increase in A_f with increasing δ.

The above study clearly demonstrated the potential of the DSC for detailed investigations of anisotropy in clays. Further discussion of these data is given in

Section 7.3.7, combined with the tests performed in this research at an overconsolidation ratio of 1.

Hicher and Lade (1987) studied the effects of the principal stress rotation of normally consolidated Kaolin by comparing the results from CK_oU torsional shear hollow cylinder and true triaxial apparatus. Monotonic undrained shear tests on K_o–normally consolidated clay were performed at δ=0° in the true triaxial apparatus and at an incremental δ_{inc}=45° in the TSHC to investigate the combined anisotropy. The incremental magnitude of the intermediate principal stress ($\Delta b=\frac{\Delta\sigma_2-\Delta\sigma_3}{\Delta\sigma_1-\Delta\sigma_3}$) was maintained at 0.5 for both tests to provide a basis for the comparison of soil response with and without rotation of principal stresses. In the torsional shear test (shown in Figure 2.25), a sample was subjected to a plane stress state, wherein the inside and outside pressures are kept equal to reduce stress non–uniformity. This sample was sheared at a constant octahedral normal stress using $\Delta\sigma_1=-\Delta\sigma_3$. The resultant b value is a function of the principal stress direction angle δ ($b=\sin^2\delta$) and the initial value of K_o. In the cubical triaxial test (shown in Figure 2.26), the sample was subjected to an undrained shear condition with $\Delta b=(\Delta\sigma_2-\Delta\sigma_3)/(\Delta\sigma_1-\Delta\sigma_3)$ kept at 0.5. In this case, there was no stress rotation during shear, and σ_3 was kept constant with $\Delta\sigma_2=0.5\ \Delta\sigma_1$.

The results from Hicher and Lade (1987) are summarized in Table 2.3 and plotted in Figures 2.27 to 2.31. Some of the results presented in the figures were replotted from data provided in the paper. As the shearing begins, the b value increases from an initial zero value to a maximum at the peak shear strength (Figure 2.30). In the TSHC test, the major principal stress (δ) rotates continuously, reaching a maximum inclination at δ=20° (Figure 2.29), corresponding to b=0.12 at maximum shear stress. The inclination angle subsequently decreases to δ=19° and the parameter b to 0.11 at maximum obliquity. Since the TTA test is sheared at δ_{inc}=0°, there is no rotation of major

principal stress. The b value at peak strength of 0.15 is slightly higher than in the TSHC test. The b then continues to decrease to a value of 0.12 at maximum obliquity.

Figure 2.27a plots the stress–strain curves of these two tests. The shear stress (q) presented in the paper is proportional to octahedral shear stress, σ_{oct} (i.e., the σ_2 component is taken into account). An alternative plot of stress–strain is shown in Figure 2.27b which uses the conventional shear stress, q (i.e., q is equal to $(\sigma_1-\sigma_3)/2$). Both of these plots show lower strain at failure and higher shear strength from the TTA than the TSHC. The normalized undrained shear strengths (i.e., from conventional q) for TTA and TSHC tests are 0.327 and 0.301, respectively, which show that the rotation of principal stress causes a reduction in the undrained shear strength. The strain at failure in the TTA test is about 1.5% versus the strain at failure of 4.2% in the TSHC test. The rotation of principal stress direction does not significantly change the clay behavior at large strains since the stress–strain curves from the two tests converge. The effective stress paths for these tests are presented in Figures 2.28a and 2.28b, showing that the friction angle at peak strength was not altered by the rotation of principal stress.

Figure 2.27a shows the total pore water pressure versus octahedral shear strain. But since the total stress paths are different for these tests, it is more appropriate to compare the shear induced pore water pressure (u_s). A plot of u_s versus shear strain is shown in Figure 2.31. This graph indicates initial higher pore water pressure development in the TTA test than in the TSHC test, but the normalized u_s at peak strength for the TSHC test is higher than the TTA test because of the larger shear strain at failure for the TSHC test. Although both have the same ϕ' at failure, the TSHC had lower q_f due to higher u_s (lower p'_f). The pore pressure parameter at failure A_f for $\delta_{inc}=0^\circ$ TTA test gives a higher value than the $\delta_{inc}=45^\circ$ TSHC test.

It is unfortunate that the paper does not present any comparison of the results obtained from two devices (TSHC and TTA) under the same shearing condition or even the consolidation data which might help the reader to assess the quality of these tests.

DSC undrained shear tests conducted for this research on OCR=1 BBC at δ_{inc}=0°, 45°, 60°, 75° and 90° using the DSC device show a decrease in the undrained shear strength and an increase in the strain at failure with increasing δ angle. The friction angle does not vary very much with δ angle. In fact, the results from Hicher and Lade are very consistent with the experimental findings from this research. However, the data on BBC show that the changes in behavior for δ_{inc} angle from 0° to 45° is very small compared to δ_{inc} angle between 45° and 90°.

2.4 SUMMARY

The anisotropy of soils at intermediate δ angles can be realistically studied only by using the Torsional Shear Hollow Cylinder (TSHC) or the Directional Shear Cell (DSC).

Research on the anisotropy of sand has been focused on strain–induced and inherent anisotropy. Study of the drained strain–induced anisotropy was conducted in the DSC by Arthur et al. (1977). The sand samples were first sheared to a fixed stress level in the isotropic plane, then unloaded to the initial stress state, and finally sheared to failure at different major principal stress directions. The change in rotation angle is defined as θ. The results show that the stiffest response occurs in tests with small rotation angles and the softest response occurs with large rotation angles. The strains in these tests rise to a maximum at θ=70±10° and then decrease at θ=90° (Figures 2.7 and 2.8).

Several studies of the inherent anisotropy of sands were also presented.

Drained plane strain tests (Arthur and Assadi, 1977) performed on inclined specimens of dense Leighton Buzzard sand, showed a significant decrease in the friction angle from ϕ' of 51° at δ=0° to a ϕ' of 45° at δ=90° (Figure 2.4). The results from the study of inherent anisotropy of loose Leighton Buzzard sand in the DSC by Arthur et al. (1981) show that inherent anisotropy also causes a large decrease in stiffness with increasing δ angle (Figure 2.9). This anisotropy also produces consistent decrease in dilatancy with increases in δ angle. The same basic trends were also observed in the DSC tests by Wong and Arthur (1985) on dense Leighton Buzzard sand. Studies by Symes et al. (1988) in the TSHC on the inherent drained anisotropy on medium–loose Ham River sand show that as δ increases from 0° to 45°, the stiffness and the peak strength are significantly decreasing (Figure 2.16). The ϕ' angles at peak stress and at large strain also decrease substantially as δ increases from 0° to 45°.

The only reliable data on the inherent anisotropy of any clay with varying δ angles were presented by Germaine (1982) and O'Neill (1985). This study conducted CU tests in the DSC on OCR=4 resedimented BBC. The results, summarized in Figures 2.12 to 2.13, show very pronounced changes in the stress–strain behavior with increasing δ as follow: large decrease in peak undrained strength at much large strains due to a combination of large shear induced pore pressure and a decrease in effect stress failure envelope. Increase δ angle also caused significant reduction in the yield stress.

Hicher and Lade (1987) conducted CK_oU shear tests on normally consolidated kaolin to investigate the combined anisotropy of clay through compared results for two shear devices, both using Δb=0.5, TTA with δ_{inc}=0° and TSHC with δ_{inc}=45°. Although changes in behavior were relatively small compared to above results on BBC, trends in increasing δ are consistent with those observed by MIT.

In conclusion, the initial anisotropy of both sand and clay – soils, causes significant changes in the stress–strain–strength behavior of the material. The experimental findings can be summarized as follows with increase in δ angle:

- The friction angle (ϕ') decreases under drained shearing conditions; and in the case of undrained shear tests, the undrained shear strength (q_f) decreases even more significantly due to a combination of lower failure envelope and smaller effective stress at failure;
- A decrease in dilation occurred in the drained shear test; or an increase in shear induced pore pressure occurred in the undrained shear tests;
- The modulus and the strain at failure increases.

Since there is only one study on the undrained shear behavior of OCR=1 kaolin with relatively low degree of anisotropy and the tests were only performed at δ_{inc}=0° and 45°, there is a need for investigate the anisotropy of normally consolidated clay with rotation of stress states, e.g., varying δ_{inc} angles ranging from 0° to 90°.

Table 2.1: Capabilities and Limitations of Laboratory Devices for Measuring Anisotropy.

Devices	Boundary Conditions	State of Stress	State of Strain	Type of Control	Rotation of σ_1 Direction	Remarks
Triaxial Cell	Mixed* Surfaces	Known (average)	Known (average)	Stress or Strain	δ = 0° & 90°	$\sigma_2=\sigma_1$ or $\sigma_2=\sigma_3$.
True Triaxial(A)	Rigid	Known (average)	Known (Average)	Stress or Strain	δ = 0° & 90°	Stresses are non-uniform.
True Triaxial(B)	Flexible	Known (uniform)	Known (discrete)	Stress only	δ = 0° & 90°	Strains may be non-uniform.
Plane Strain	Mixed Surfaces	Known (average)	Known (average)	Stress or Strain	δ = 0° & 90°	Strains and stresses are non-uniform.
Direct Simple Shear	Mixed Surfaces	Unknown	Known (average)	Stress or Strain	Rotates continuously	State of stress is unknown.
Hollow Cylinder	Mixed‡ Surfaces	Known (average)	Known (average)	Stress only	δ = 0° to 90°	Uniform only when $P_i=P_o$, but b then changes with δ.
Directional Shear Cell	Mixed Surfaces	Known (uniform)	Known (discrete)	Stress only	δ = 0° to 90°	Low stress testing only, & no back pressure.

Notes: * σ_r is always flexible and σ_a is always rigid.

‡ Mainly flexible, i.e., only ϵ_2 is rigid.

Table 2.2: Summary of Research on Principal Stress Rotation in Soils.

Reference 1st Auth.	Research Group[1]	Year	Device[2]	Soil Type	Type of Consolid.[3]	Overcons. Ratio	Drainage[4] Condition	Test[5] Type	b Value	Remarks
Arthur	UCL	1977	DSC	Sand	I	-	D	Mψ	b(PS)[6]	
Arthur	UCL	1980	DSC	Sand	I	-	D	Cψ	b(PS)[6]	
Arthur	MIT	1981	DSC	Sand	I	-	D	Mψ,Mδ	b(PS)[6]	
Germaine	MIT	1982	DSC	Clay	K_o=1	4	U	Mψ,Mδ	b(PS)[6]	
O'Neill	MIT	1985	DSC	Clay	K_o=1	4	U	Mψ,Mδ	b(PS)[6]	
Hicher	UCLA	1987	TSHC	Clay	K_o	1	U	Mδ	b=sin$^2\delta$	b varies δ
Hicher	UCLA	1987	TTA	Clay	K_o	1	U	δ=0°	varies	b varies
Hight	IC	1983	TSHC	Sand	I	-	D	Rδ	0.5	No Proof Test
Sture	UC	1985	DSC	Sand	I	-	D	Mδ,Cδ	b(PS)	No Proof Test
Sture	UC	1985	DSC	Clay	I	-	D?	Rδ	b(PS)	No PWP Meas.
Sture	UC	1987	DSC	Sand	I	-	D	Rδ	b(PS)	No Proof Test
Symes	IC	1984	TSHC	Sand	I	-	U	Mδ,Rδ	0.5	
Symes	IC	1988	TSHC	Sand	I	-	D	Mδ,Rδ	0.5	
Wong	UCL	1985	DSC	Sand	I	-	D	Mψ,Cψ,Mδ,Cδ	Applied	

[1] MIT: Massachusetts Institute of Technology
UCLA: University of California, Los Angeles
IC: Imperial College London
UC: University of Colorado, Boulder
UCL: University College London

[2] DSC: Directional Shear Cell
TSHC: Torsional Shear Hollow Cylinder
TTA: True Triaxial Apparatus

[3] I: Hydrostatic Consolidation
K_o: K_o Consolidation

[4] U: Undrained Shear
D: Drained Shear

[5] M: Monotonic Loading
C: Cyclic Loading
R: Multi-Rotation of Principal Stress
ψ: Shear in Isotropic Plane
δ: Shear in Anisotropic Plane

[6] b(PS): b at plane strain condition

Table 2.3: Summary of Experimental Data for Undrained Shear Tests on OCR=1 Clay from Hicher and Lade (1987).

Parameter	At $(\sigma_1-\sigma_3)_{max}$		At Maximum Obliquity	
	TTA	TSHC	TTA	TSHC
δ_{inc} (°)	0	45	0	45
b	0.154	0.122	0.125	0.110
δ (°)	0.0	20.5	0.0	19.0
σ'_{vc} (kPa)	267	273	267	273
q/σ'_{vc} *	0.327	0.301	0.305	0.290
γ_{oct} (%)	1.5	4.2	6.2	9.2
ϕ (°)	35.0	34.5	38.0	36.9
A ‡	1.53	1.15	2.26	1.11
u_s/σ'_{vc} †	0.200	0.240	0.273	0.287

Notes:

* $q=0.5(\sigma_1-\sigma_3)$.

‡ $A=(\Delta u-\Delta\sigma_3)/(\Delta\sigma_1-\Delta\sigma_3)$.

† $u_s=\Delta u-\Delta\sigma_{oct}$.

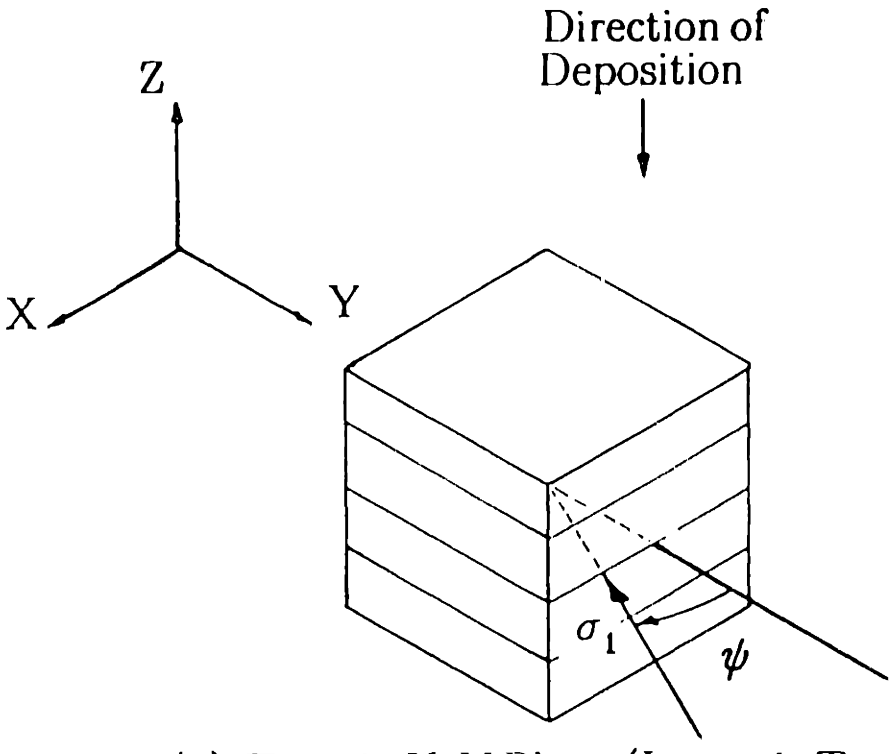

(a) Tests in X–Y Plane (Isotropic Test)

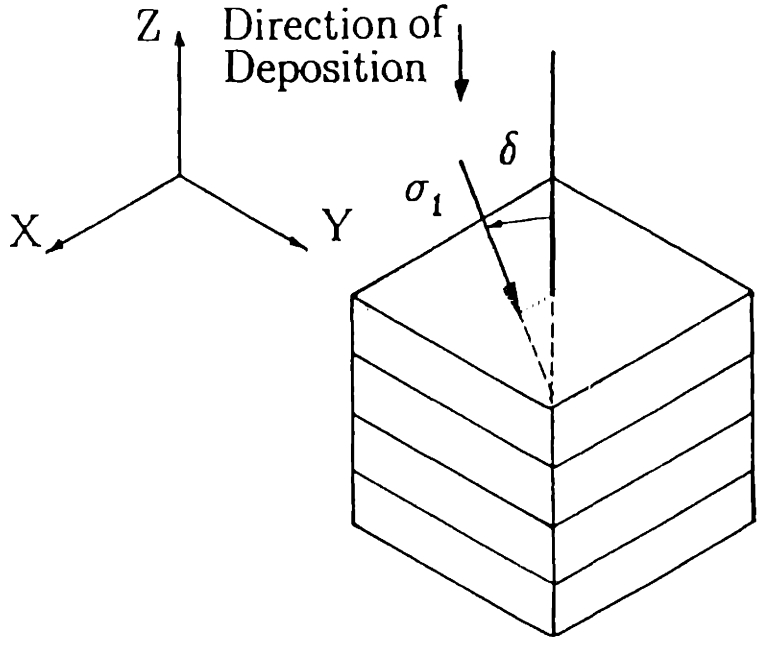

(b) Tests in X–Z Plane (with Inherent Anisotropy)

Figure 2.1: Definitions of ψ and δ Angles for DSC Testing.

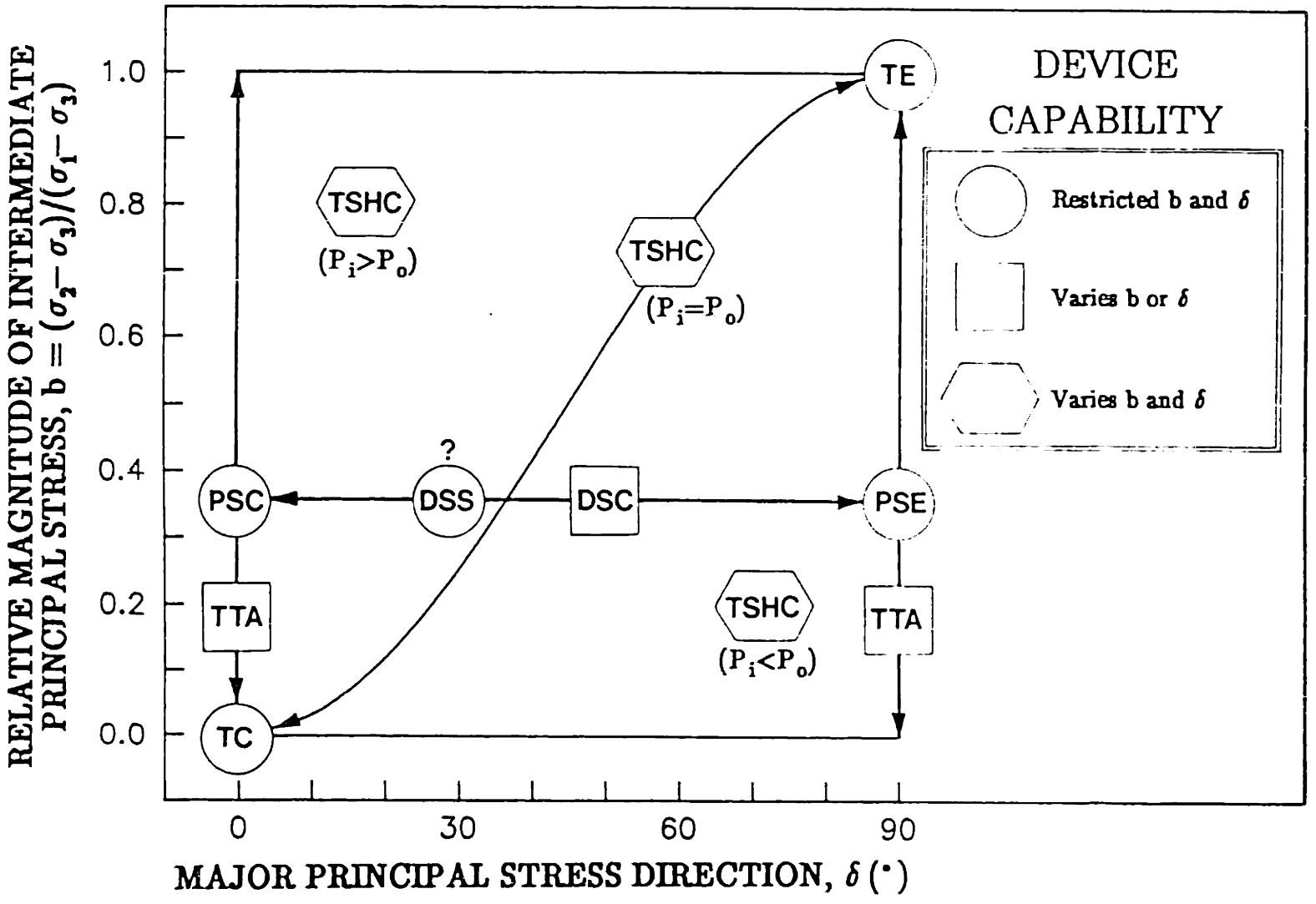

Figure 2.2: Stress Systems Achievable by Shear Devices from CK_oU Testing (after Germaine, 1982; and Ladd, 1988).

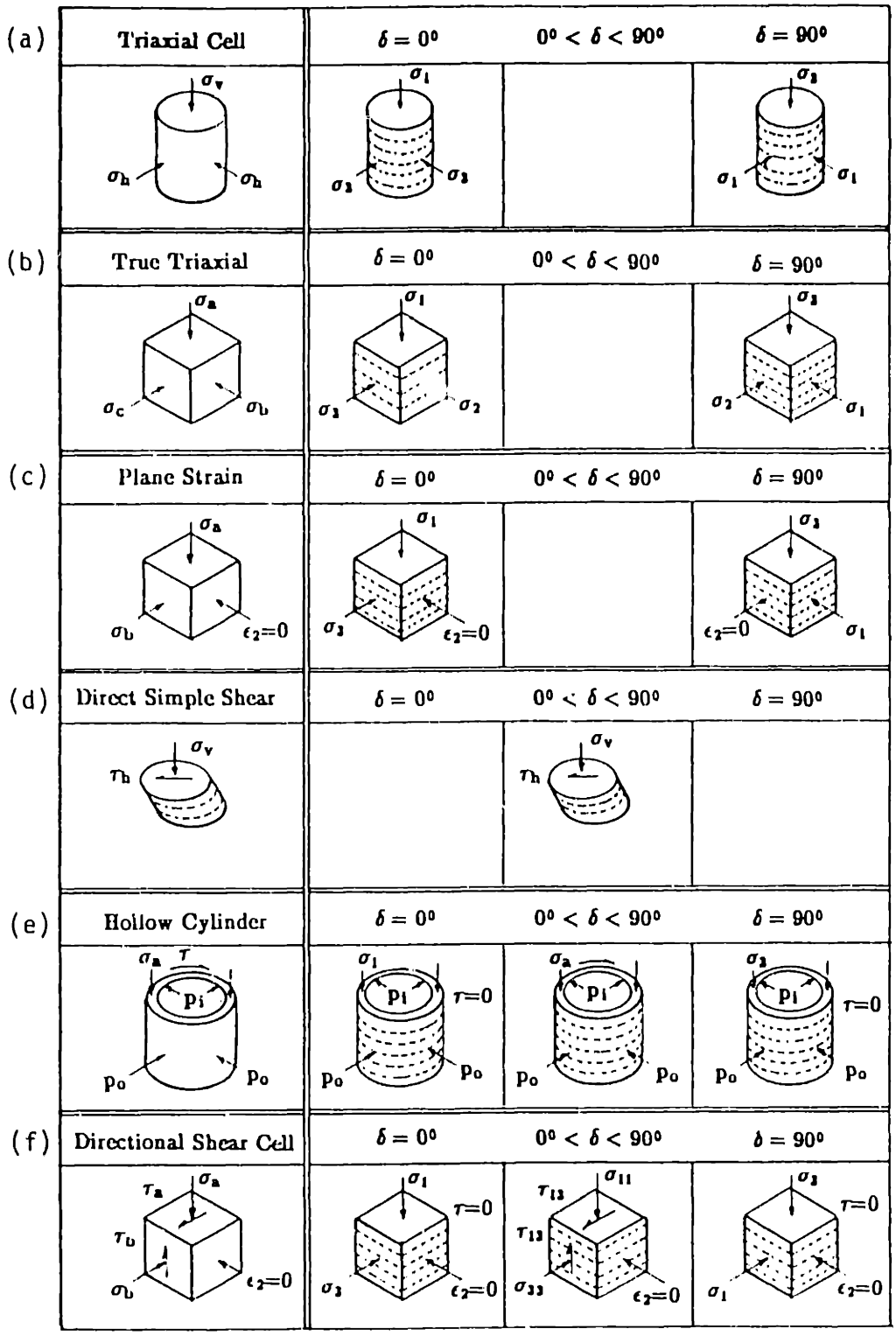

Figure 2.3: Capabilities of Different Laboratory Devices.

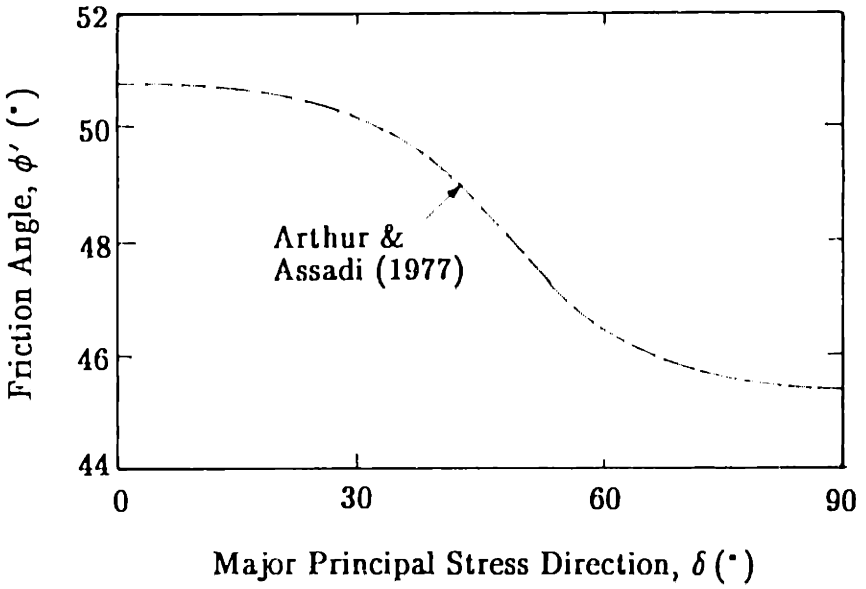

Figure 2.4: Relationship of ϕ' and δ Angles from CID Plane Strain Tests on Inclined Leighton Buzzard Sand Samples (from Wong and Arthur, 1985).

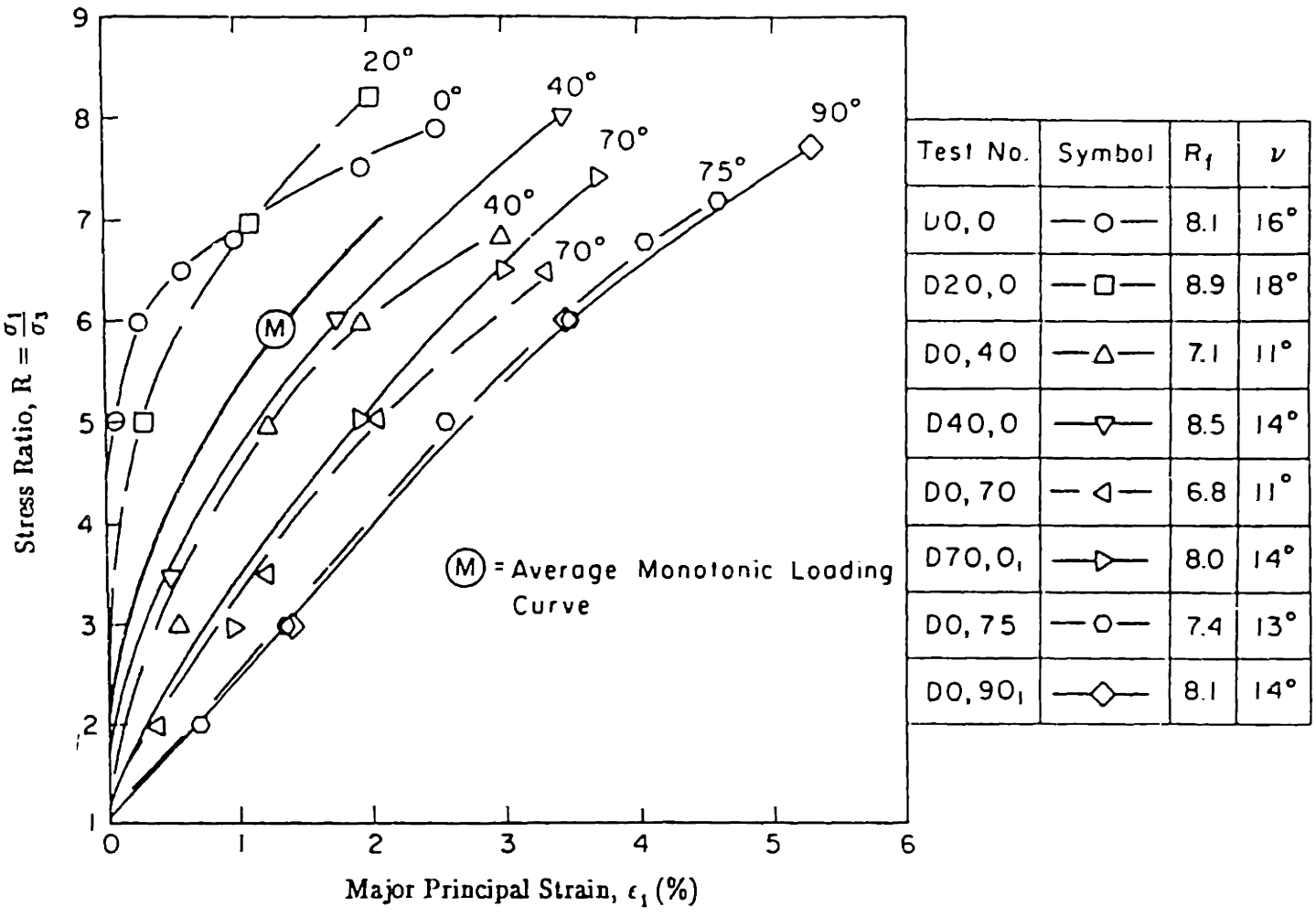

Figure 2.5: Stress–Strain Curves from Loading Tests on Dense Leighton Buzzard Sand with Induced Anisotropy (from Arthur et al., 1981).

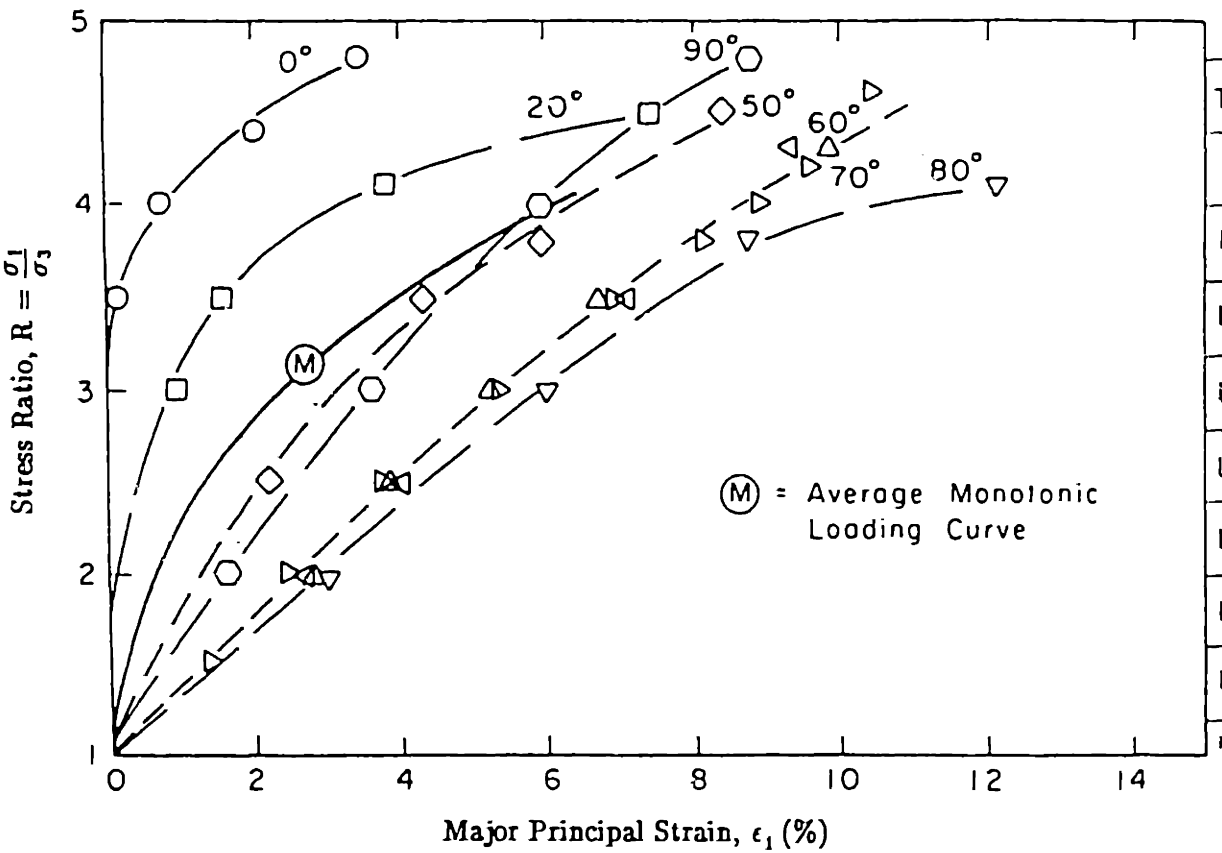

Test No.	Symbol	R_f	ν
L0,0	—○—	5.0	0°
L0,20	—□—	4.5	1°
L0,50	--◇--	4.9	-1°
L0,60	--△--	—	3°
$L0,70_1$	--◁--	—	0°
$L0,70_2$	--▷--	4.8	-1°
L0,80	—▽—	—	2°
L0,90*	—○—	5.5	3°

* No shear sheets

Figure 2.6: Stress–Strain Curves from Loading Tests on Loose Leighton Buzzard Sand with Induced Anisotropy; ϵ_1 Data from 16 Points (from Arthur et al., 1981).

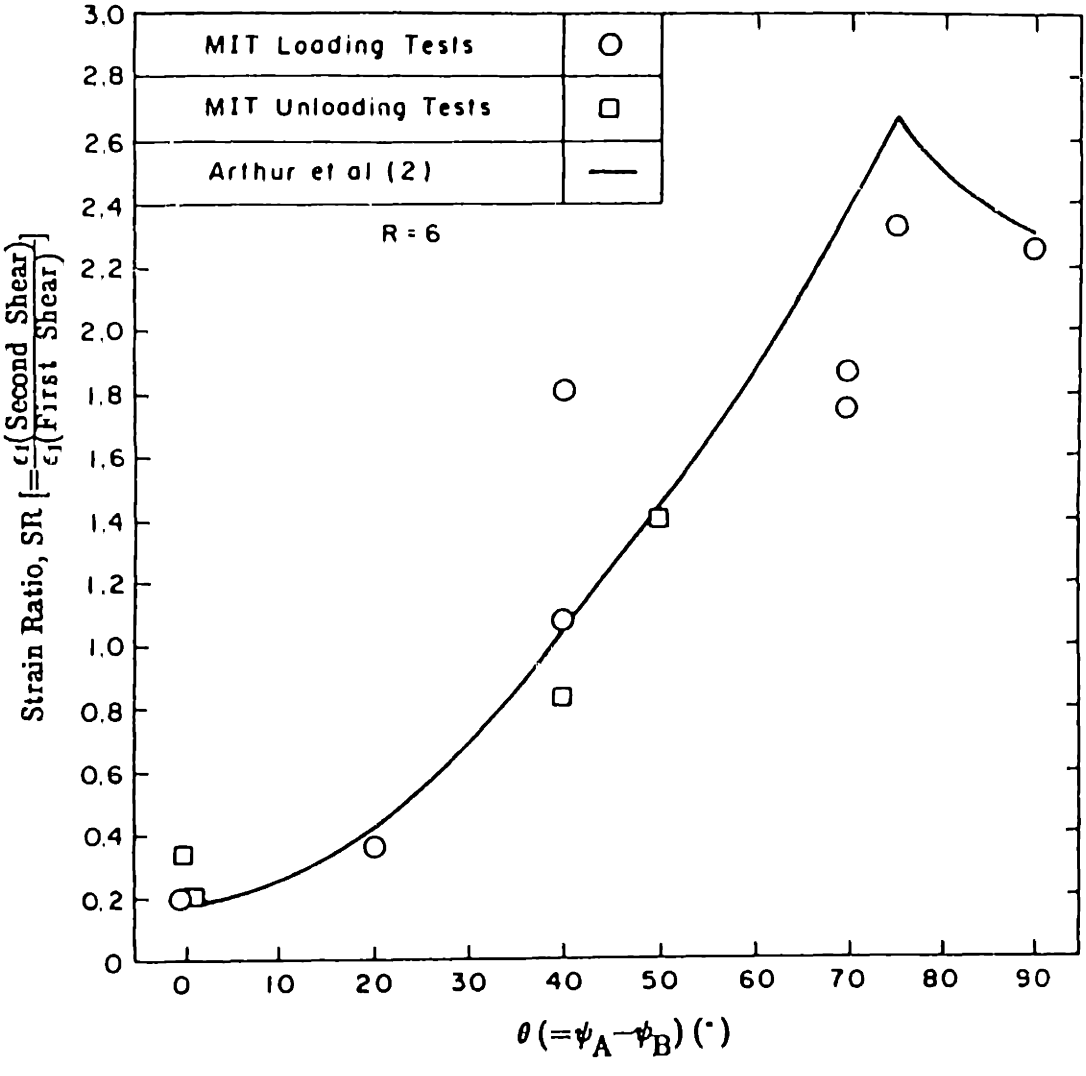

Figure 2.7: Strain Ratio versus Rotation Angle for Dense Leighton Buzzard Sand with Induced Anisotropy (from Arthur et al., 1981).

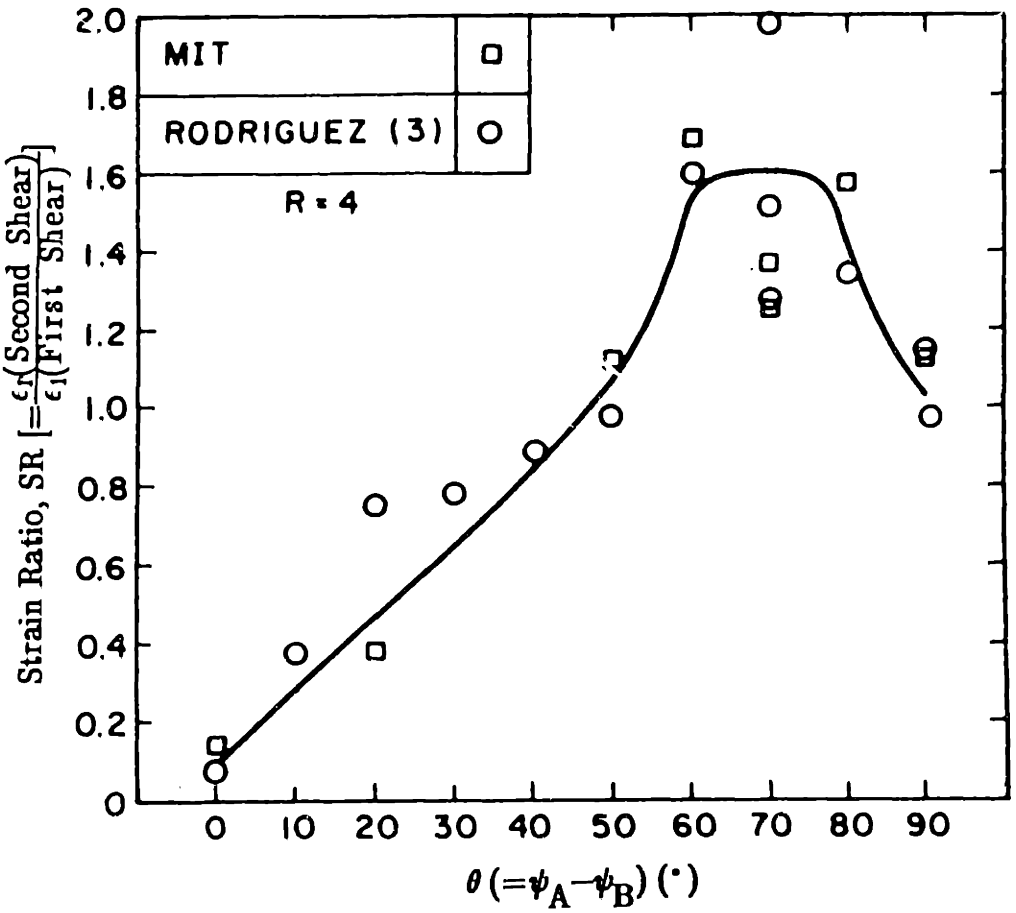

Figure 2.8: Strain Ratio versus Rotation Angle for Loose Leighton Buzzard Sand with Induced Anisotropy (from Arthur et al., 1981).

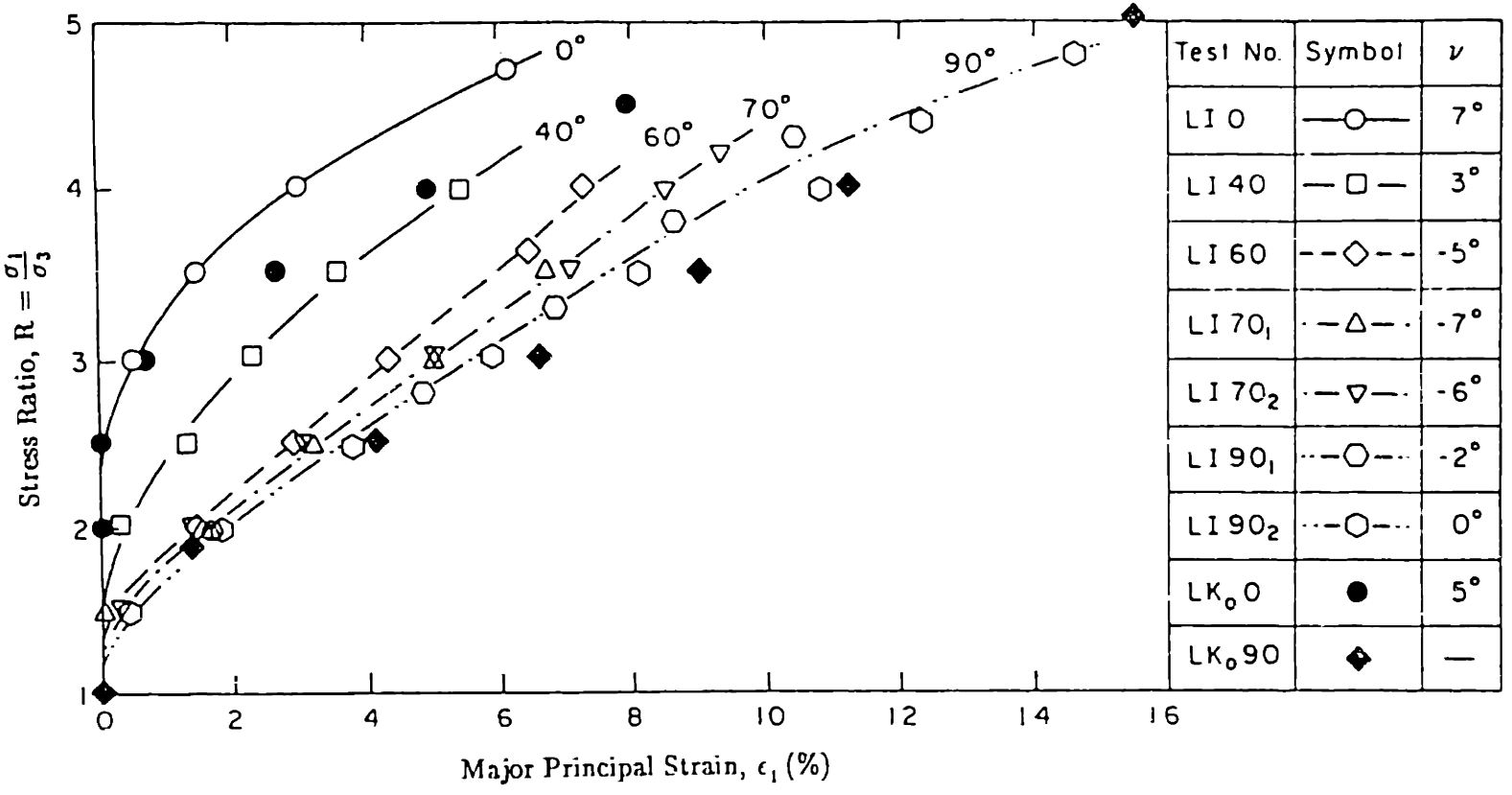

Figure 2.9: Stress–Strain Curves from Loading Tests on Loose Leighton Buzzard Sand with Inherent Anisotropy; ϵ_1 Data from 16 Points (from Arthur et al., 1981).

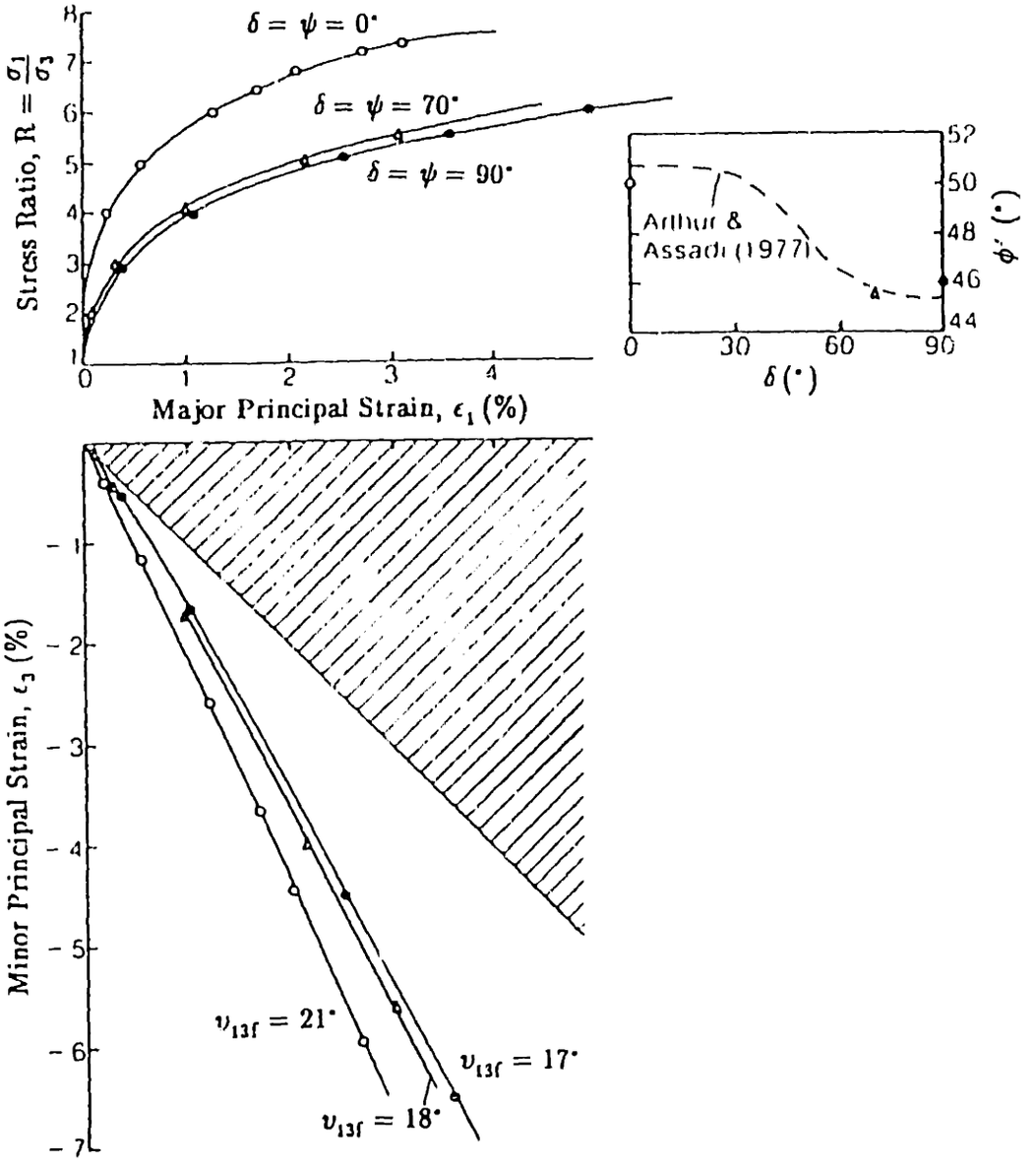

Figure 2.10: Stress–Strain Behavior for Monotonic δ Tests on Dense Leighton Buzzard Sand with Inherent Anisotropy (from Wong and Arthur, 1985).

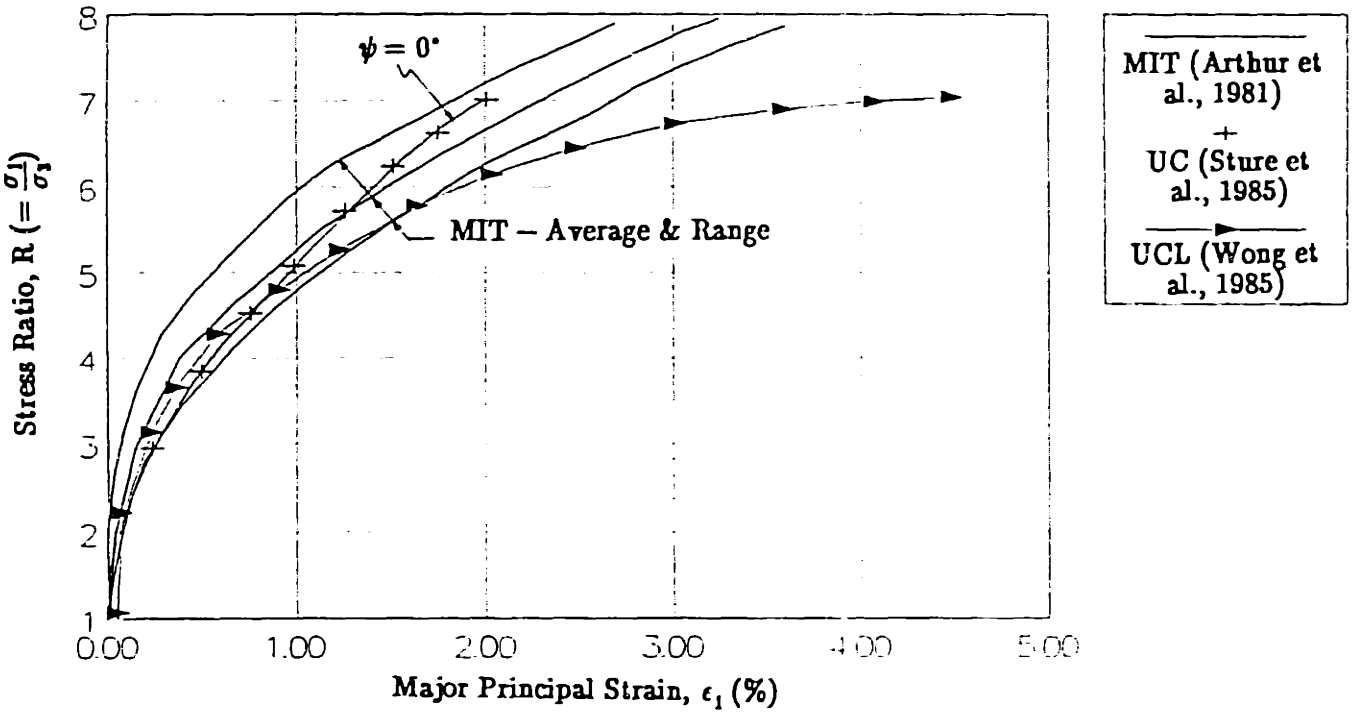

Figure 2.11: Comparison of Stress–Strain Relationships obtained by Different Research Groups on Dense Leighton Buzzard Sand in Directional Shear Cell.

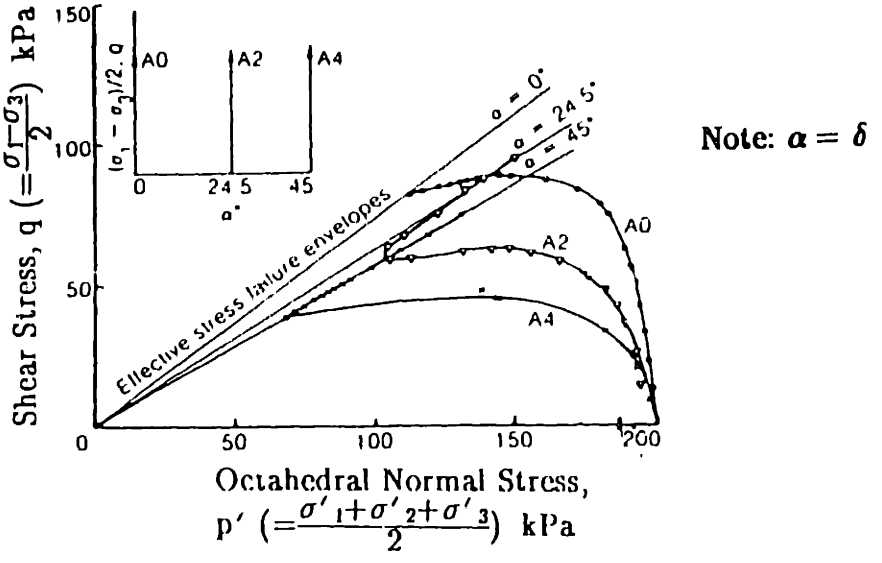

Figure 2.12: Effective Stress Paths from CIU Tests A0, A2 and A4 on Ham River Sand (from Symes et al., 1984).

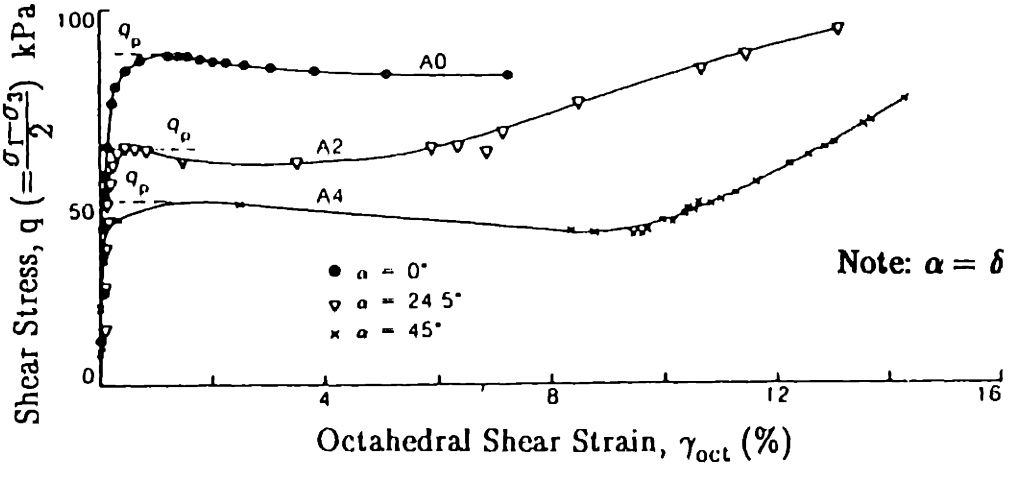

Figure 2.13: Stress–Strain ($q-\gamma_{oct}$) Behavior in CIU Tests A0, A2 and A4 on Ham River Sand (from Symes et al., 1984).

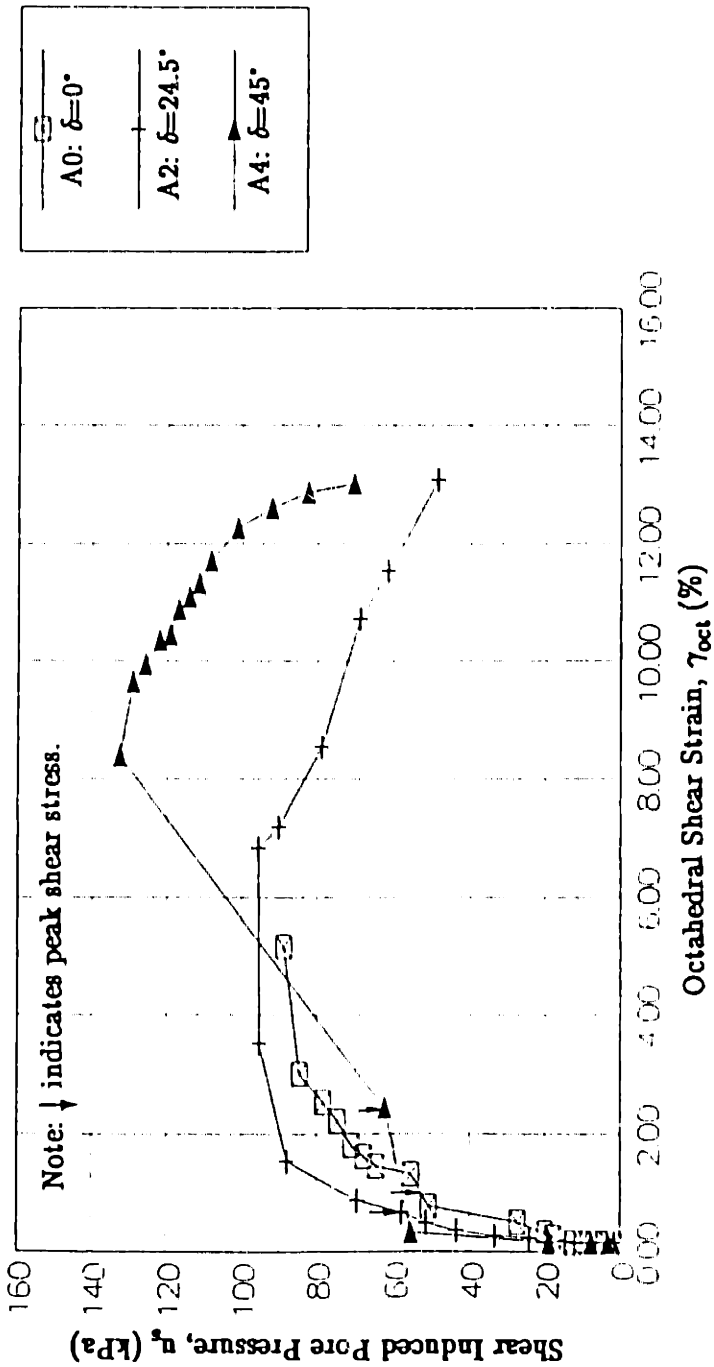

Figure 2.14: Shear Induced Pore Water Pressure versus Octahedral Shear Strain for CIU Tests A0, A2 and A4 on Ham Sand (Data replotted from Symes et al., 1984).

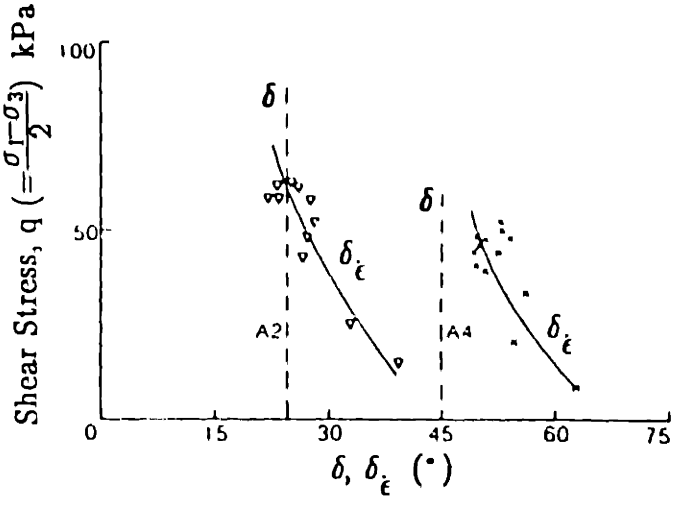

Figure 2.15: Principal Strain Incremental Directions in CIU Tests A2 and A4 on Ham River Sand (from Symes et al., 1984).

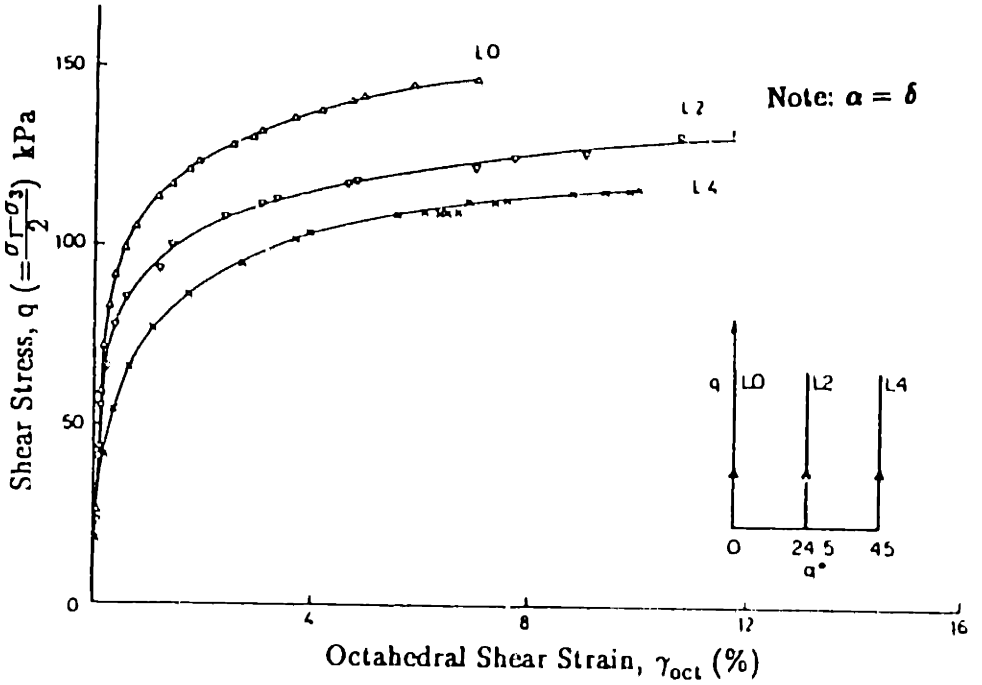

Figure 2.16: Development of Octahedral Shear Strain in CID Tests L0, L2 and L4 on Ham River Sand (from Symes et al., 1988).

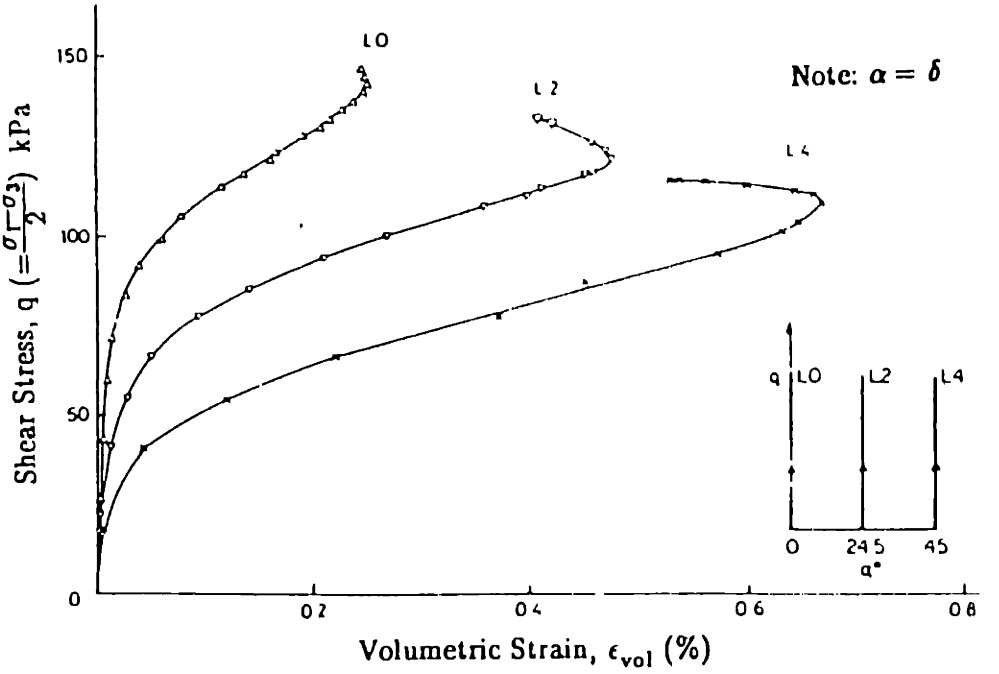

Figure 2.17: Development of Volumetric Strain in CID Tests L0, L2 and L4 on Ham River Sand (from Symes et al., 1988).

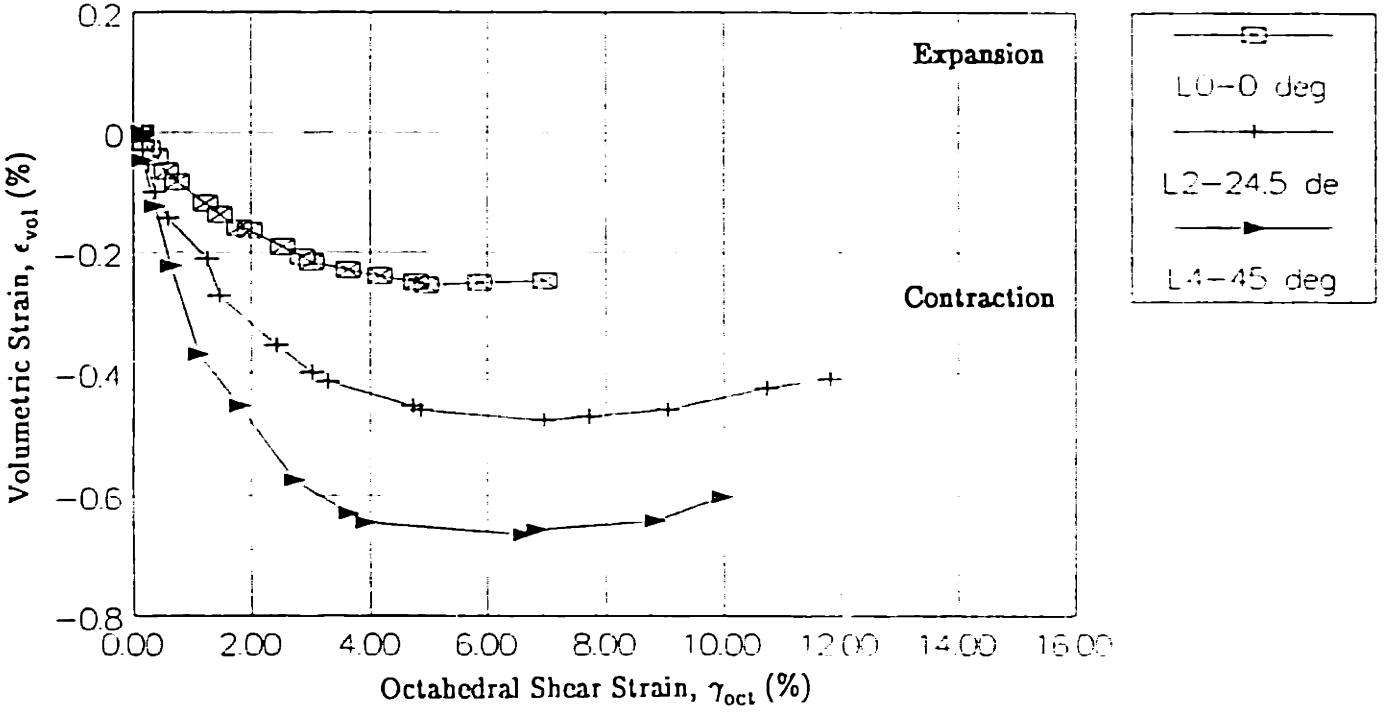

Figure 2.18 Volumetric Strain versus Octahedral Shear Strain in CID Tests L0, L2 and L4 on Ham River Sand (Data plotted from Symes et al., 1988).

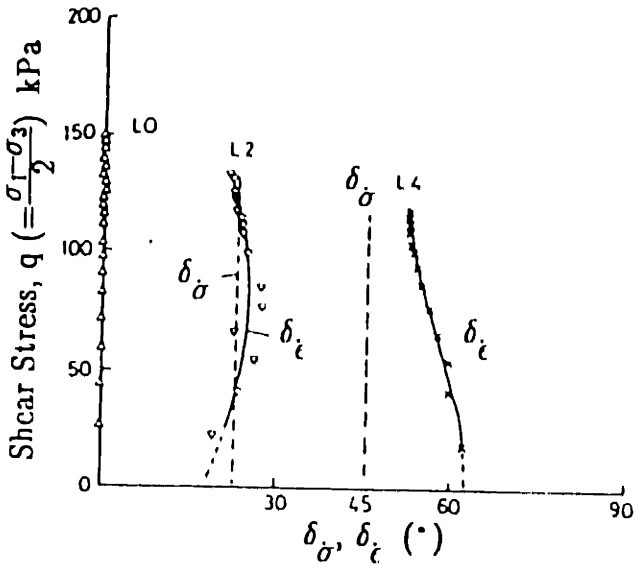

Figure 2.19: Stress and Strain Incremental Directions in CID Tests L0, L2 and L4 on Ham River Sand (from Symes et al., 1988).

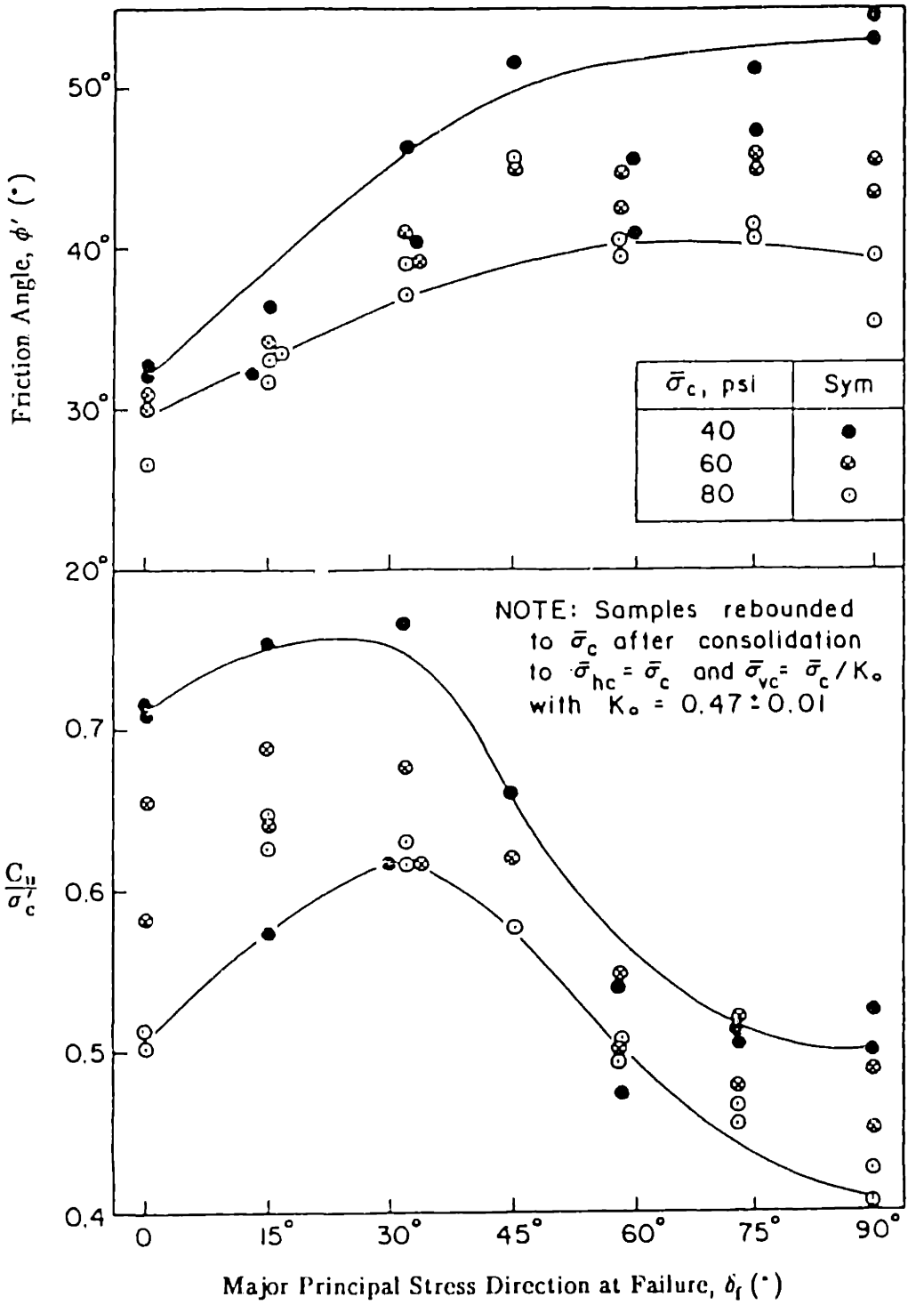

Figure 2.20: Results of CIU Hollow Cylinder Tests on Vertical Samples of Edgars Plastic Kaolin (EPK); Data plotted fromSaada and Bianchinin, 1985 (from Jamiolkwski, 1985).

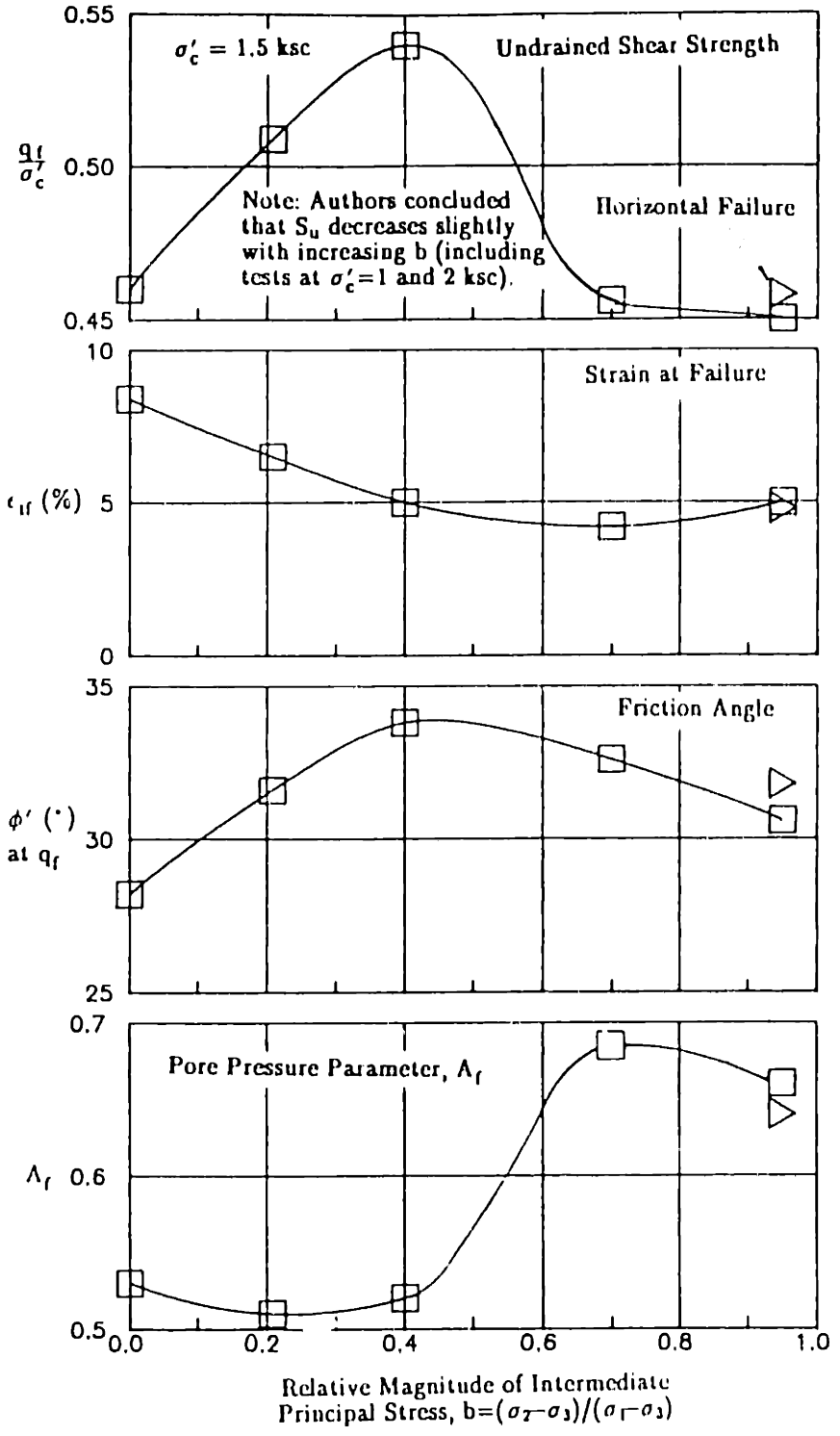

Figure 2.21: CIU True Triaxial Tests on Remolded Grundite; Prepared by Ladd (Data plotted from Lade and Musante, 1978).

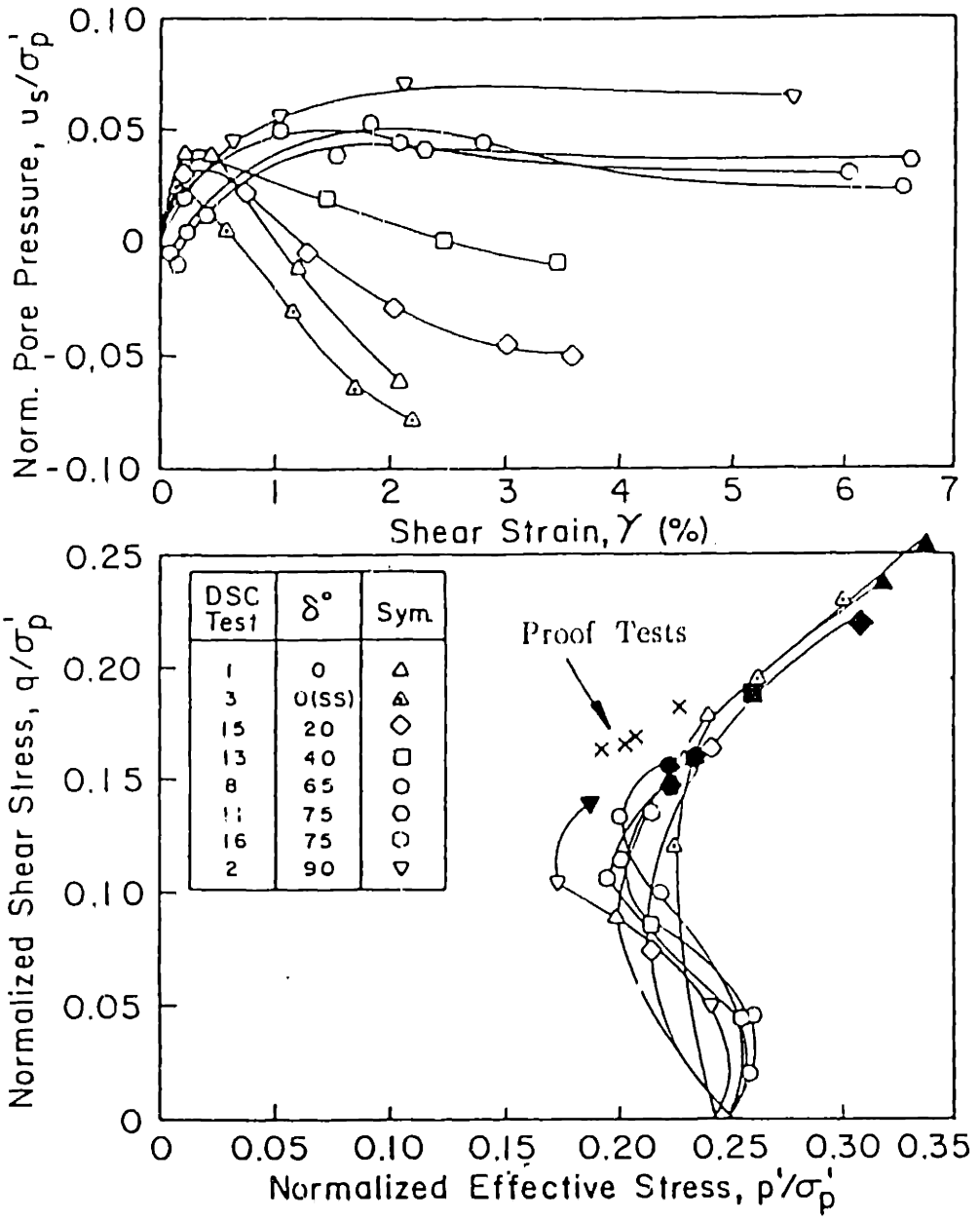

Figure 2.22: Normalized Pore Pressure and Effective Stress Paths for CU DSC Anisotropic Tests on BBC at OCR=4; Corrected Data from O'Neill, 1985 (from Ladd and Germaine; NSF Proposal, 1985).

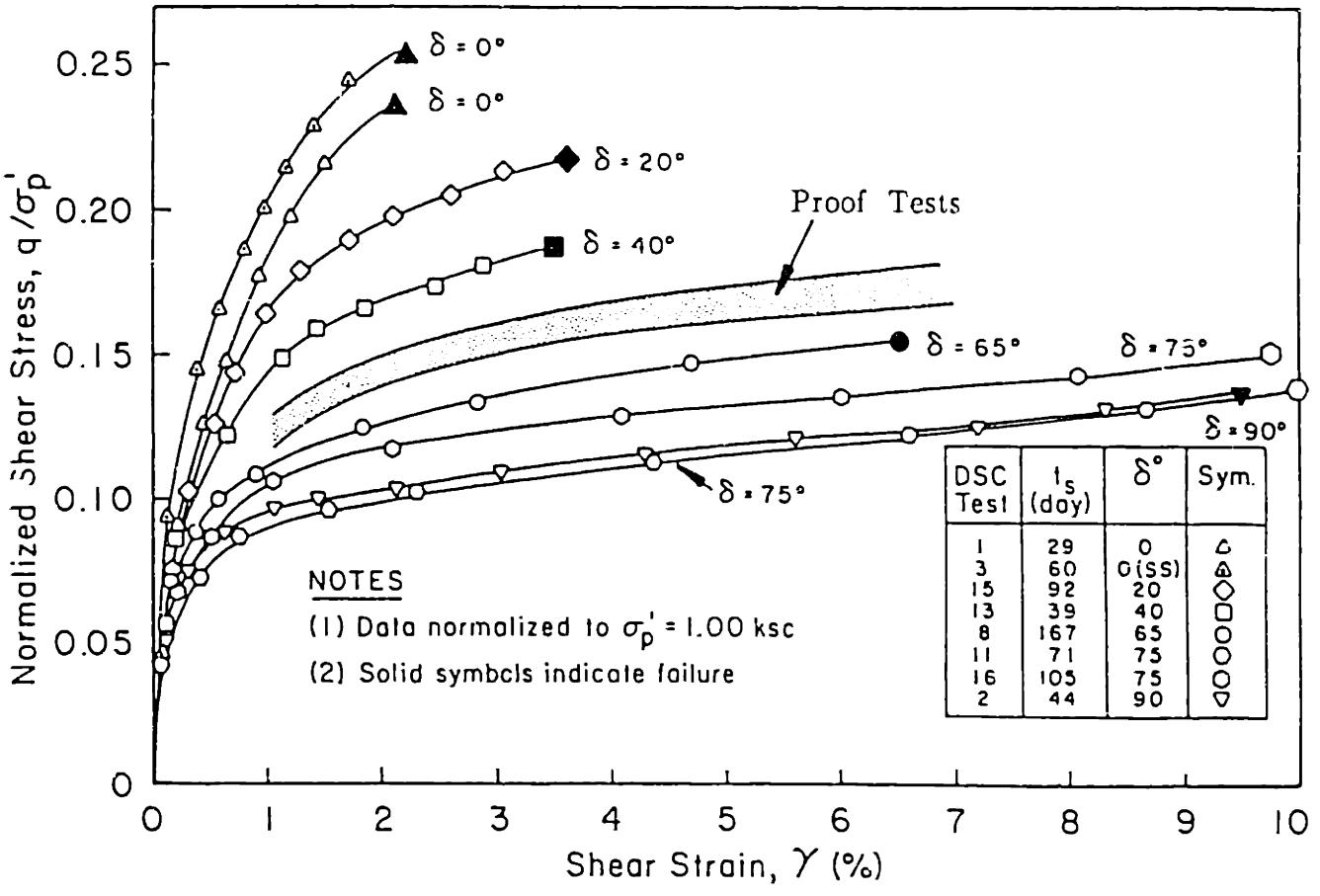

Figure 2.23: Normalized Shear Stress versus Strain from CU Anisotropic Tests on BBC at OCR=4; Corrected Data from O'Neill, 1985 (from Ladd and Germaine; NSF Proposal, 1985).

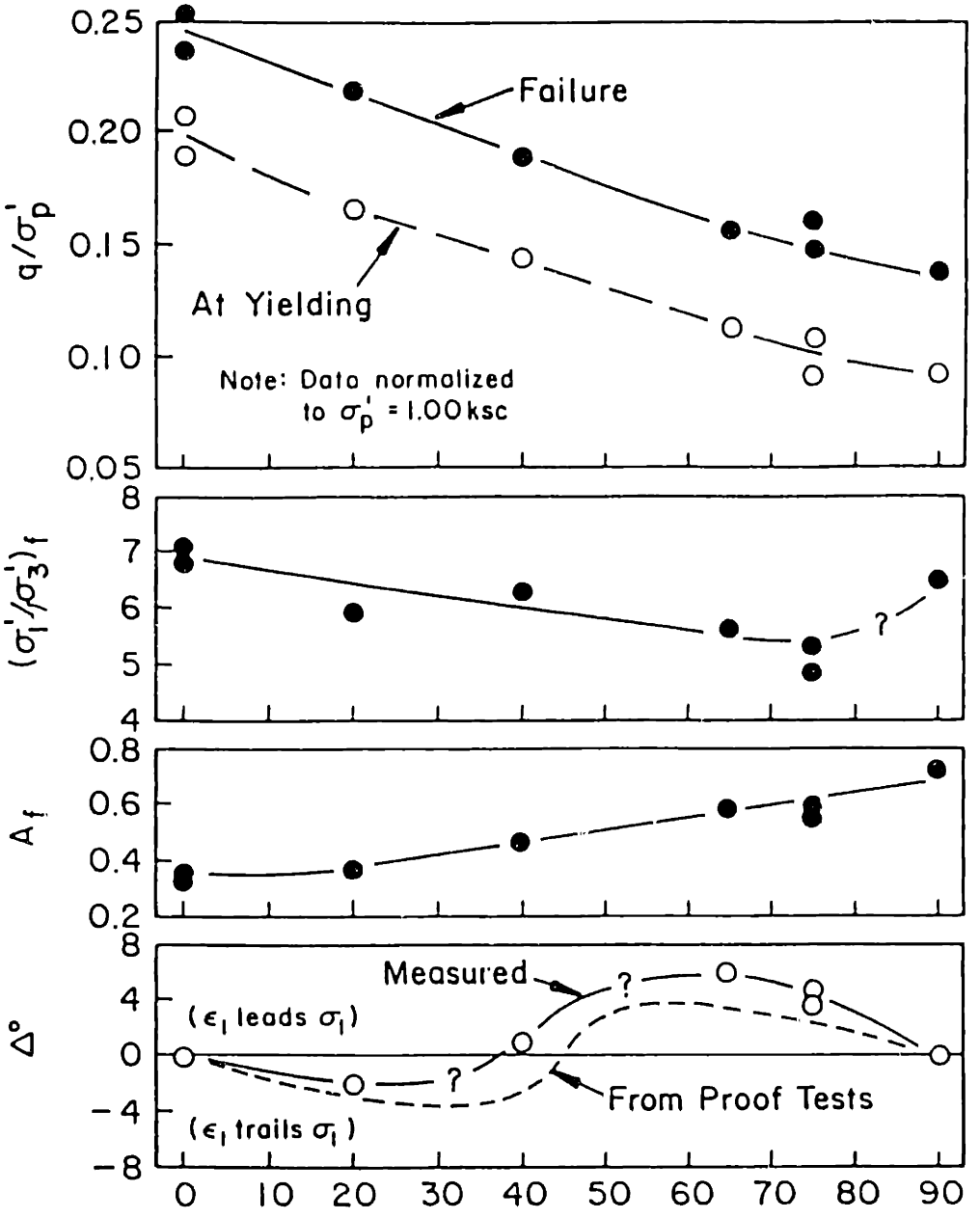

Figure 2.24: Effects of Inherent Anisotropy on Undrained Behavior of BBC at OCR=4; Corrected Data from O'Neill, 1985 (from Ladd and Germaine; NSF Proposal, 1985).

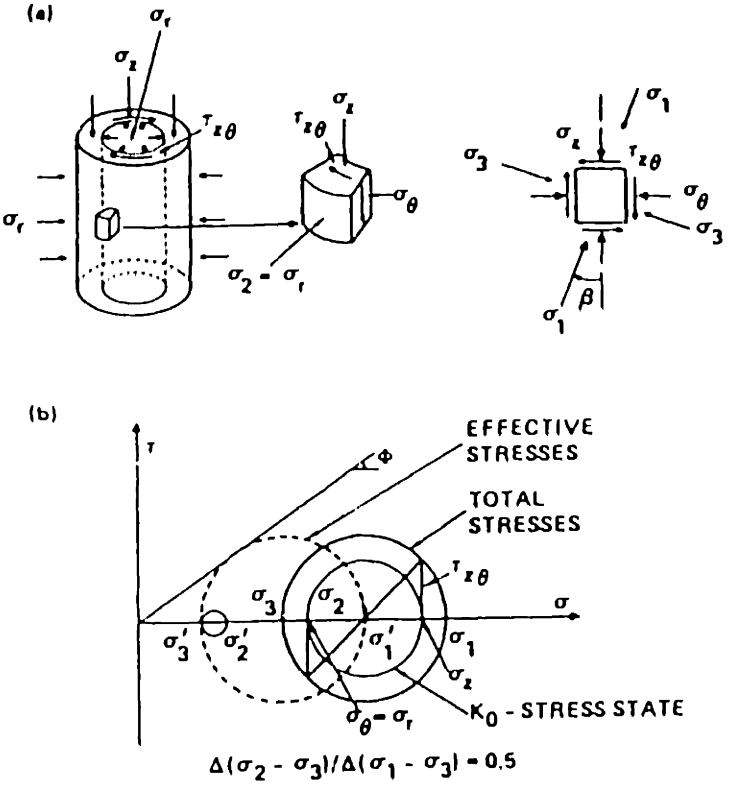

Figure 2.25: (a) Representative of Stress State; (b) Stress Path in Mohr Diagram for Torsion Shear Test (from Hicher and Lade, 1987).

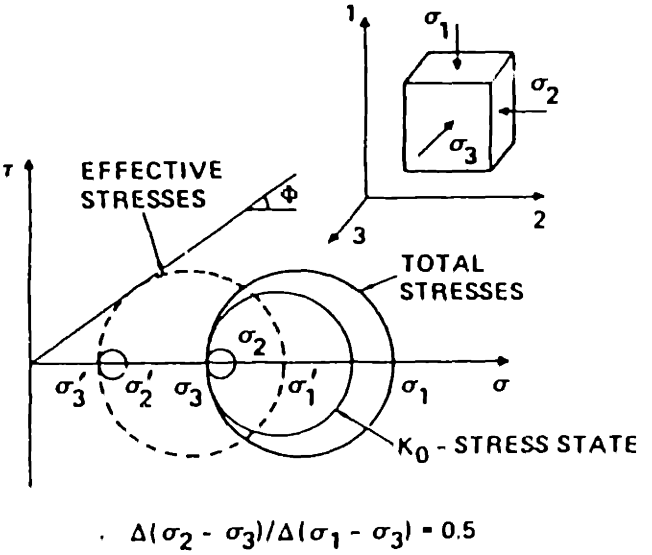

Figure 2.26: Stress Path in Mohr Diagram for Cubical Triaxial Tests (from Hicher and Lade, 1987).

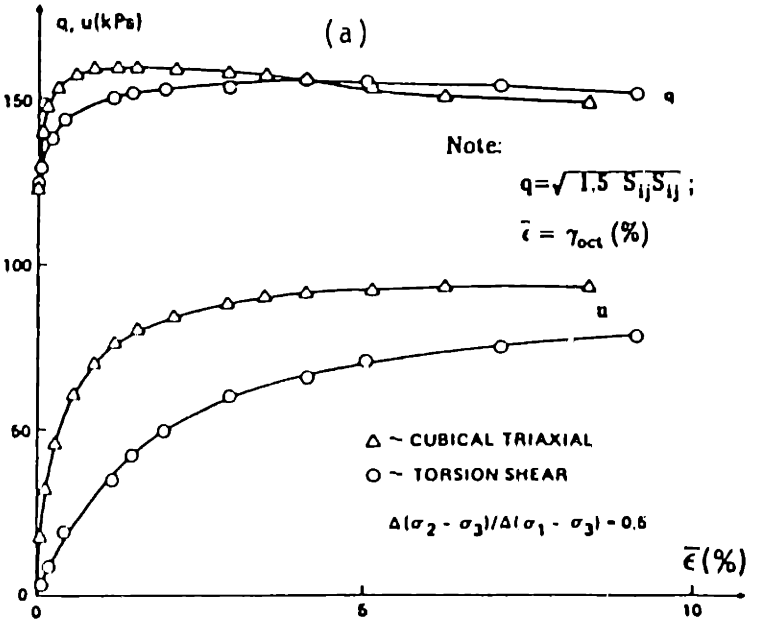

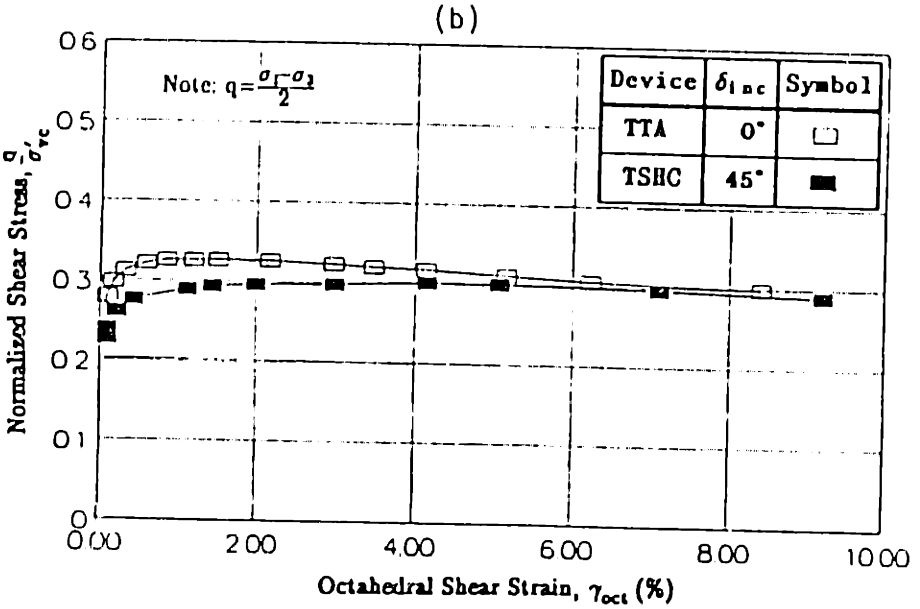

Figure 2.27: (a) Stress–Strain and Pore Pressure Relations from Monotonic Torsion Shear and Cubical Triaxial Tests on K_0–Consolidated EPK Clay (from Hicher and Lade, 1987); (b) Normalized Shear Stress (q) versus Octahedral Shear Strain for Two Tests (Data plotted from Hicher and Lade, 1987).

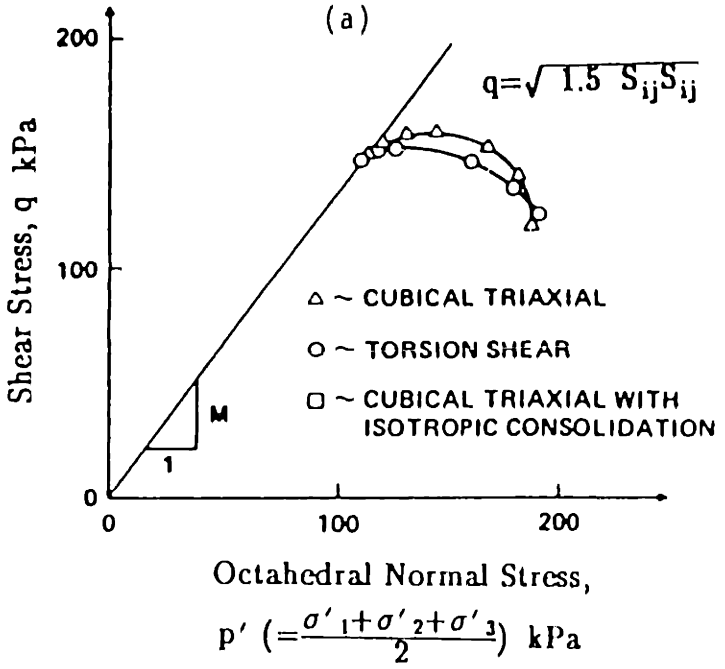

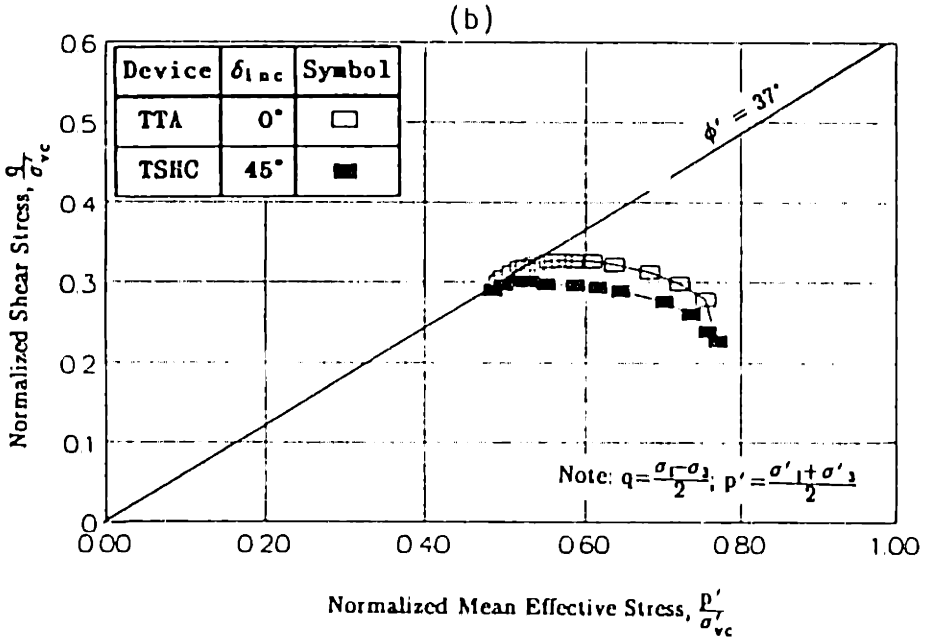

Figure 2.28: (a) Effective Stress Paths from Monotonic Torsion Shear and Cubical Triaxial Tests on K_0–Consolidated EPK Clay (from Hicher and Lade, 1987); (b) Normalized Effective Stress Paths for Two Tests (Data plotted from Hicher and Lade, 1987).

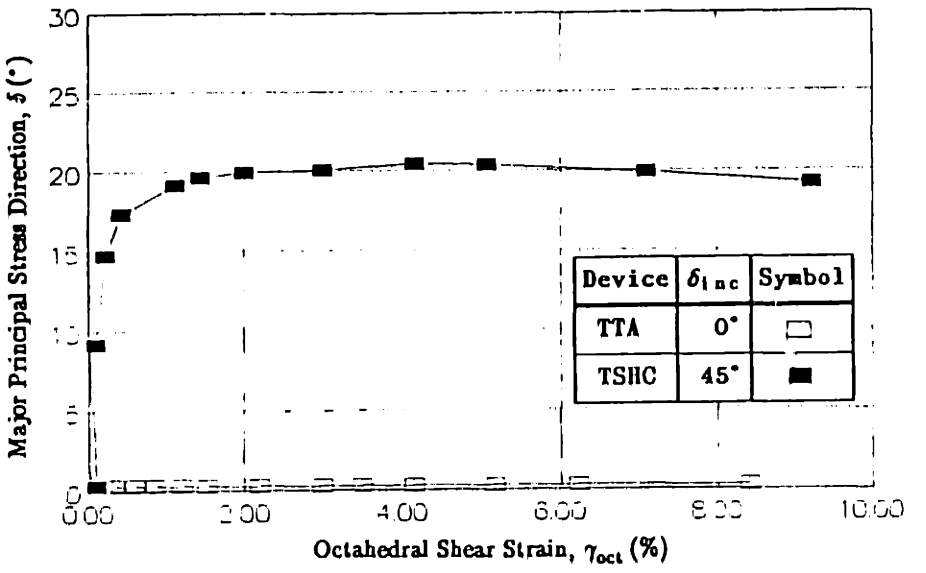

Figure 2.29: Principal Stress direction (δ) versus Octahedral Shear Strain for Monotonic Torsion Shear and Cubical Triaxial Tests on K_0–Consolidated EPK Clay (data plotted from Hicher and Lade, 1987).

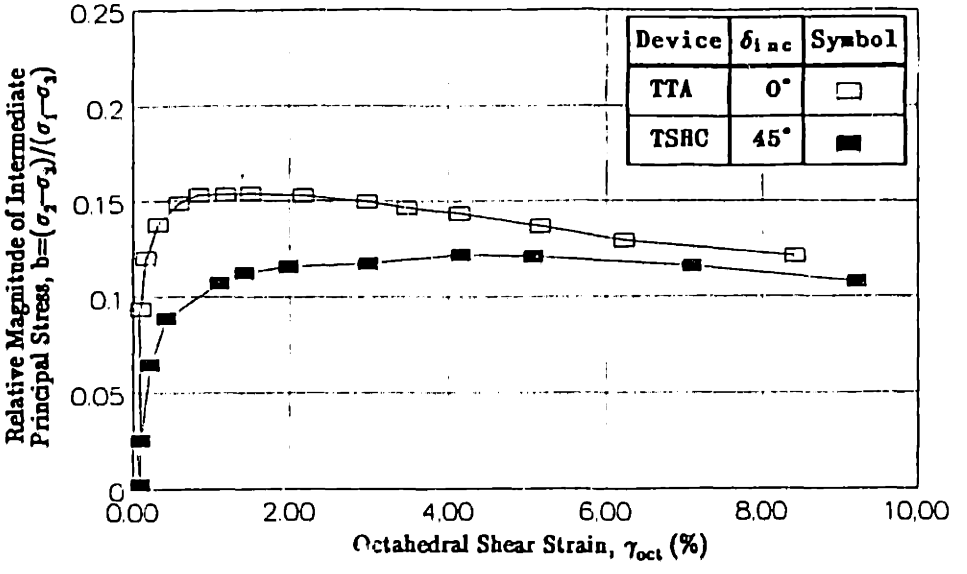

Figure 2.30: Relative Magnitude of Intermediate Principal Stress (b) versus Octahedral Shear Strain for Monotonic Torsion Shear and Cubical Triaxial Tests on K_0–Consolidated EPK Clay (Data plotted from Hicher and Lade, 1987).

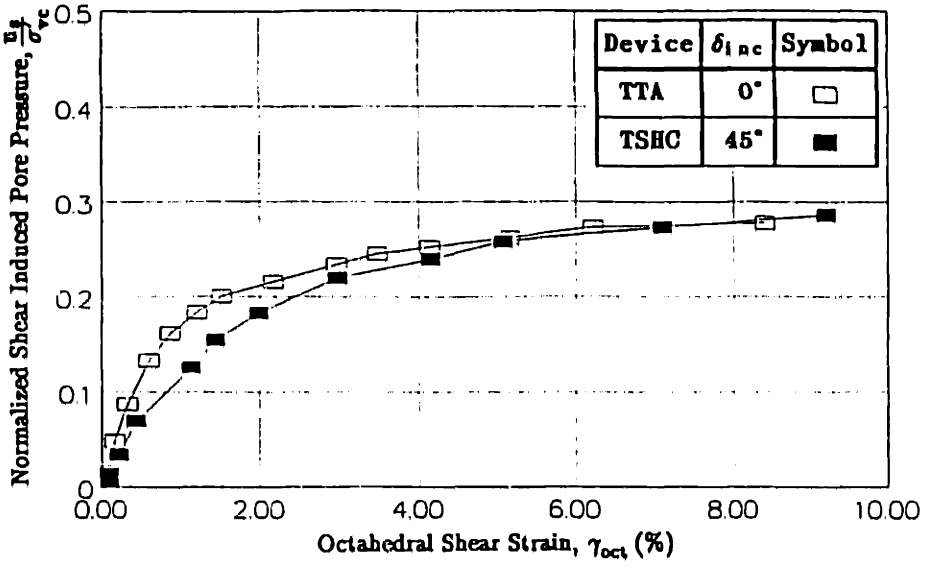

Figure 2.31: Normalized Shear Induced Pore Pressure versus Octahedral Shear Strain for Torsion Shear and Cubical Triaxial Tests on K_0–Consolidated EPK Clay (Data plotted from Hicher and Lade, 1987).

CHAPTER 3

DESCRIPTION OF THE MODIFIED DIRECTIONAL SHEAR CELL

3.1 INTRODUCTION

The Directional Shear Cell (DSC) was first developed by Dr. J. R. F. Arthur at University College London (UCL) in the mid–1970's. Arthur et al. (1977) and Rodriguez (1977) used the device to study the induced anisotropy of Leighton Buzzard sand. The MIT geotechnical group had foreseen the potential of the device, and acquired a DSC from UCL in 1978; Dr. Arthur spent a sabbatical leave at MIT to help with its instaliation and operation. Bekenstein (1980) at MIT conducted a number of DSC tests with the primary goal of reproducing the data obtained by UCL on induced anisotropy; the study was extended to include the effects of inherent anisotropy for Leighton Buzzard sand (Arthur et al., 1981). The results on induced anisotropy agreed with the trends reported by Arthur et al. (1977) for dense sand and Rodriguez (1977) for loose sand, except that the MIT tests generally produced somewhat smaller strains. The difference in strain levels was believed to be caused by differences in the amount of grease applied to the top and bottom platens. The device was later used by Germaine (1982) with substantial modifications in the testing procedure to study the undrained inherent anisotropy of resedimented Boston Blue Clay (BBC) at an overconsolidation ratio of 4. These tests required the measurement of pore water pressure in the clay, which led to the ingenious development of the Pore Water Pressure Probe. The design of this probe is described in Section 3.3.6. Germaine also developed a new technique for preparing saturated blocks of BBC, and a new trimming device. The

experimental program was continued by O'Neill (1985) to extend and refine the results obtained by Germaine (1982).

The Directional Shear Cell is far more complex than most soil testing devices. The cell has undergone several phases of modifications to improve the reliability and quality of experimental results, with new ideas and concepts introduced by each DSC researcher over the years. The changes made by each individual are briefly discussed in the following section and summarized in Table 3.1.

3.2 OVERVIEW OF PREVIOUS MODIFICATIONS TO THE DIRECTIONAL SHEAR CELL

The DSC device has been modified several times since its first use at MIT. The original device was used by Bekenstein (1980) to investigate the drained anisotropy of Leighton Buzzard sand in both loose and dense states.

The first modification to the DSC involved the pressure bags. Originally, the pressure bags used to apply the normal stresses to the soil specimen were made of accordion–like rubber bags with aluminum backing plates. The construction of the rubber bags is described in Rodriguez (1977) and a schematic diagram of the pressure bag (referred to as the Type A) is shown in Figure 3.1. The Type A pressure bag was used by all prior MIT researchers.

To provide the pressure bags with lateral stability, retaining (or restraining) vanes were attached to the sides of the backing plate. These vanes (shown in Figure 3.2, Type A) can be adjusted, along with the rigid backing plates, to maintain parallel alignment as the specimen deforms during the test. Further alterations to the pressure bags were necessary for testing conditions that used the shear sheets; the pressure bag vane immediately adjacent to the pulling strips of the shear sheets had to be removed. If the vanes were left in place, the

shear sheet strips would be displaced by 0.125 in. (the thickness of the vanes), causing a disruption to both the shear stress application at the corner of the specimen, as well as the sighting line used to locate the adjustable shear sheet pistons such that the pulling force is parallel to the distorting specimen face. The stressed reinforced pulling strips were considered sufficient to at least partially restrain the pressure bag during shear. This led to a new design of the retaining vane by O'Neill as shown in Figure 3.2, referred to as the Type B design. The new vanes have thicknesses of 0.067 in. They are placed on both vertical sides of each pressure bag, thus minimizing the interference with the alignment of the shear sheets.

Surface tractions are applied to the sample via shear sheets in the DSC. The original shear sheets (Figure 3.3, Type A) had three basic components: the inner rubber sleeves, the rubber elastic stretching strips and the outer reinforced pulling sheets. The shear sleeve transmits shear to the specimen by adhesion between the rubber surfaces of the sleeve and the sample membrane. The stretching strips serve the key function of distributing the applied tangential force to the shear sleeve. The two ends of these unreinforced rubber strips (6 by 25 mm long) are glued at 5 mm intervals to the outside of the shear sleeve and the inside of the reinforced pulling sheets. Silicone grease (described in Appendix E.1.3) allows these strips to reach 300–400% of their original length even though appreciable normal stress is transmitted across the strips from the pressure bags. An hydraulic piston load frame assembly applies the tangential shear force to the inextensible reinforced pulling sheets. Aluminum guide rails enable piston rotation during shear, thereby ensuring the applied shear forces are always parallel to the sample face. The original Type A shear sheets were used by Bekenstein, who observed premature failure and non–uniform strains in dense sand samples due to

the reduction in the thickness of the shear sheets in the area where they fold around the diagonal corners. As a result, tails were added to the shear sheets to fill in the gap created by stretching the strips in response to the applied tension. Figure 3.3 shows the locations of the tails (Type B).

The original design of the bottom platen consisted of a thick glass plate (thickness of 0.35 in.) inserted into an aluminum plate as shown in Figure 3.4 (Type A). The design of the top platen was identical to the bottom platen, except that four vertical poles (6 in. in length) were attached to the four corners of the bottom platen to support the top platen. There are eight slots in both platens where rods are inserted to support the pressure bags. The transparent nature of the glass on the top platen enables photographs of reference points on the top face of the membrane to be taken during the test; these reference points are used to determine the strains of the sample. It also enables the operator to see the sample during the test. No modification to the platens had been made by any of the prior MIT researchers.

In order to strengthen the two corners of the specimen where the interweaving shear sheets cross, two triangular acrylic prisms (Figure 3.5, Type A) were glued to diagonally opposite corners of the rubber membrane. Though the prisms were successful in preventing the excessive corner deformation for which they were originally designed, it became apparent after several DSC tests on BBC by O'Neill that there was considerable relative displacement between the prisms and the adjacent soil. The irregularities in the stress application at these corners resulted in forces which tended to push the prisms away from the soil; the only resistance was provided by the sample membrane. The triangular prisms were later replaced by chevron–shaped prisms as shown in Figure 3.5, referred to as the Type B design, which served to strengthen the two corners considerably, and

allowed much less corner twist. These prisms were adopted by O'Neill in her last DSC test.

One of the most remarkable achievements in DSC testing was the introduction of the pore water pressure probe by Germaine. This probe is inserted into the middle of the specimen to measure the pore water pressure of the soil. This probe not only measures the dissipation of excess pore water pressures during consolidation, but in addition makes undrained shear tests possible in the DSC (Germaine). The probe is made up of a fine porous ceramic stone (see Figure 3.9) connected to one end of a stainless steel tube, with a pressure transducer attached to the other end of the tube (see Figure 3.10). A stainless steel wire is inserted into the tube to reduce the volume of water required in the closed measuring system. The probe was designed with the same concept as adopted by Richardson (1963) for measuring pore water pressures in the middle third of a specimen during a triaxial test. Since then, this method of measuring the pore water pressure of a soil sample with a fine porous stone has been used in several other MIT testing devices; Wissa and Hedberg (1969) used this technique in the design of the constant rate of strain consolidometer, Malek (1987) and Walbaum (1988) used the same system in direct simple shear tests to measure the pore pressure at the base of the soil sample. The porous stones used in these devices are so fine that a special technique was developed to saturate the stone by Dr. R. T. Martin at MIT. The procedure is described by both Jordan (1979) and Walbaum (1988).

3.3 LATEST MODIFICATIONS OF MAJOR COMPONENTS OF THE DIRECTIONAL SHEAR CELL

This research has further modified the device, including changes in the pressure bags, the shear sheets, the two platens, the sample corner design and the pore water pressure probe. The changes to each component are described in the

following section (see summary of changes in Table 3.1).

3.3.1 Normal Pressure Bags

The normal stresses, σ_a and σ_b, in the DSC are applied to four faces of the soil sample using two sets of pressurized flexible rubber bags. In the original design, each bag was composed of three 1 cm thick rubber units mounted to an aluminum backing plate, which can move parallel or perpendicular to the initial sample face. Although this accordion design provided flexibility, there was poor control over the position of the bag relative to the sample face. The normal stresses applied to the sample faces are dependent on the relative positions of these pressure bags, therefore only an experienced researcher can determine where the bags should be. In order to reduce the dependency on the operator for the results, the pressure bags were redesigned. A schematic of the new pressure bag is shown in Figure 3.1 which referred to as the Type B bag. The new pressure bag still provides flexibility, but it consists of a single rubber unit with an electronic position sensor attached to the rubber bag. Appendix D.3 presents a detailed description of the design. The electronic sensor ensures that the displacement of the front face of each pressure bag is matched by an equal displacement of the pressure bag backing plate. This matching displacement system has several advantages: the most important is that regardless of the magnitude of the sample strain, the optimum position of the pressure bag to apply the correct boundary stress is maintained. Calibration results indicate that a 1 mm change in the position of the bag relative to the sample face gives rise to a 0.007 ksc change across the sample face. With the help of the position sensor, the error in applied normal stresses is no more than 0.007 ksc. The other advantage of this pressure bag is that there is no diminution of normal stress as a result of the internal

pressure stretching the bag itself, and the front face of the bag remains plane.

3.3.2 Shear Sheets

In the original shear sheet design, two corners (where the tails are located) of the shear sheets were joined together by the inner rubber sleeve. This attachment of the adjacent rubber sleeve defeats the objective of applying the shear stresses independently. If the interface between the rubber membrane and shear sheets failed, the shear forces in the shear sheets would be redistributed. There would be a resultant force acting at these corners of the soil sample, giving rise to an incorrect application of the shear stress across the sample. Furthermore, this design of the shear sheet makes it very difficult to identify any boundary interface failure. The new shear sheets (Figure 3.3, Type C) are separated from one another, so that independent shear stresses can be applied without causing any interference with the adjacent shear sheets. The resultant force at the corners where the tails are located must always be equal to zero. If there is any interface failure, the shear sheet will be displaced horizontally, and this type of failure will be more apparent. The test can then be evaluated more accurately. The new design also makes the cleaning of the shear sheets easier, because each shear sheet can be rested on a flat surface. The cleaning process is describe in Section 5.4.2.

3.3.3 Top and Bottom Platens

With the new pressure bags, the slots on the glass–aluminum platens had to be lengthened to provide as much travel as in the old design. Due to the size of the platens, the slots had to be extended to the edges of the platens. Eight plate extension adapters (Figure 3.6) were mounted to sides of the two platens as shown in Figure 3.4 (Type B); they also serve to stiffen the platens. An additional

supporting base frame was made for the intermediate principal stress measuring device (Figure 3.7). The frame has the same dimensions as the original base plate, but the glass plate is replaced by the intermediate principal stress measuring device, shown in Figure 3.4 as Type C.

It is difficult to design a completely rigid platen in the plane strain direction, since there will always be some axial strain due to the changes in stresses in that direction. The magnitude of the strain in the plane strain direction depends mainly on the relative stiffness of the soil and the platens, as well as the stiffness of the top and bottom platens, and the connecting rods. Measurement of the axial strain due to the separation of the platens is discussed in Appendix E.3.2. Furthermore, the thicknesses of the silicone grease layers on the top and bottom platens and of the rubber membrane prevent true plane strain conditions. Appendix E.3 describes the significance of each component of the strain; this strain is only calculated when σ_2 is measured.

Marachi et al. (1981) reported that a small amount of strain in the intermediate principal stress direction is tolerable because the measured peak drained strength of sand is unaffected by the small change in intermediate principal strain ($\epsilon_2/\epsilon_1<0.3$). Since there is no documented data on the influence of intermediate principal strain on the behavior of clay, the same assumption has been made.

3.3.4 Intermediate Principal Stress Measuring Device

In order to determine the complete state of stress of the soil sample, the stress in the plane strain direction (σ_2) has to be measured in the test (see Figure 3.8). Some DSC tests with σ_2 measurements were performed on Leighton Buzzard sand by Wong (1985) at UCL. A measuring device with a similar design is

adopted in this research. The design and calibration of the intermediate principal stress measuring device are described in Appendix D.4. The device consists of a flush–mounted rubber bag filled with de–aired water. The amount of water used is 7 cc. It is important that the volume of water be small, because the response time of the measurement is directly proportional to the volume of the water, since water is compressible. A pressure transducer is connected to the reservoir of water. This device is placed on the supporting base frame which replaced the glass–aluminum base platen. The lower face of the cubical sample covers the entire rubber bag during the test. As the applied stresses on the lateral faces vary, the change in stress in the plane strain direction can be measured. This is a flexible boundary stress measuring device. The rubber covers 62 % of the sample area, therefore the stress measured can be regarded as the average stress acting in the plane strain direction.

3.3.5 Sample Corner Design

The two corners of the soil sample with interweaving reinforced pulling strips were strengthened in the original design by two rigid prisms to prevent progressive boundary failure. Though the triangular prisms were replaced by chevron–shaped prisms (O'Neill), these corners were still more rigid than clay, leading to an incorrect strain distribution of soil close to these two corners. The area of influence from the prism on the strains is not known; O'Neill excluded the five closest reference points to each of the prism corners. This creates a bias in the calculation of average strains, because the average strain of the sample depends on the location of the reference points under consideration. A flexible corner design is used in this research to overcome this fundamental problem. It consists of a piece

of cheese cloth glued to the two corners of the rubber membrane with contact rubber cement, and is shown in Figure 3.5 as the Type C design. This fabric strengthens the rubber membrane at these corners. Two 3.5"x0.7" brass strips with 0.010" thickness are glued to the fabric 3 mm away from the corners using 5–minute epoxy. The technique for attaching the fabric and brass strips is discussed in Appendix D.1.3. These brass strips increase the rigidity of the corners. The combination of the fabric and brass strips acts as a hinge joint, allowing the corners of the sample to rotate freely, while preventing progressive boundary failure from occurring during the shear tests.

3.3.6 Pore Water Pressure Probe

The pore water pressure probe is essential for the undrained testing of clay. The probe was introduced by Germaine in 1982 to study the undrained anisotropy of resedimented Boston Blue Clay at an overconsolidation ratio of 4. A lighter and more versatile probe was designed for this research. The weight of the probe has been reduced from 25 to 15 g. The new probe has a longer porous stone tip and a smaller and lighter pressure transducer adapter as shown in Figures 3.9 and 3.10. Its lighter weight helps to reduce sample disturbance during the sample preparation. In three DSC tests (Test No. DSC32, DSC33 and DSC34), two probes, one located in the middle and the other midway between the middle of a corner of the sample, were used to determine the distribution of pore water pressure during consolidation, and to check the uniformity of stress in the soil sample during shear. The results are discussed in Chapter 7.

Table 3.1: The MIT Modifications of the Directional Shear Cell Device.

Research (Year)	Pressure Bag	Retaining Vane	Shear Sheet	Top & Bottom Platens	Corner Design	PWP Probe	Strain Measurement Techniques
Figures*	3.1	3.2	3.3	3.4	3.5	3.10	
Bekenstein (1980)	A‡	A	A	A	A	-	P1• & X‡
Germaine (1982)	A	A	B	A	A	A	P1
O'Neill (1985)	A	A to B	B	A	A to B	A	P1 to P2†
Author	B	B	C	A to B to C	C	B	P2

Notes:

- • P1 : Black & White Photography (Ilford FP 4).
- ‡ X : Radiography.
- † P2 : High Contrast Photography (Kodalith Ortho Film 3).
- * Refer to the figures for various types of designs.

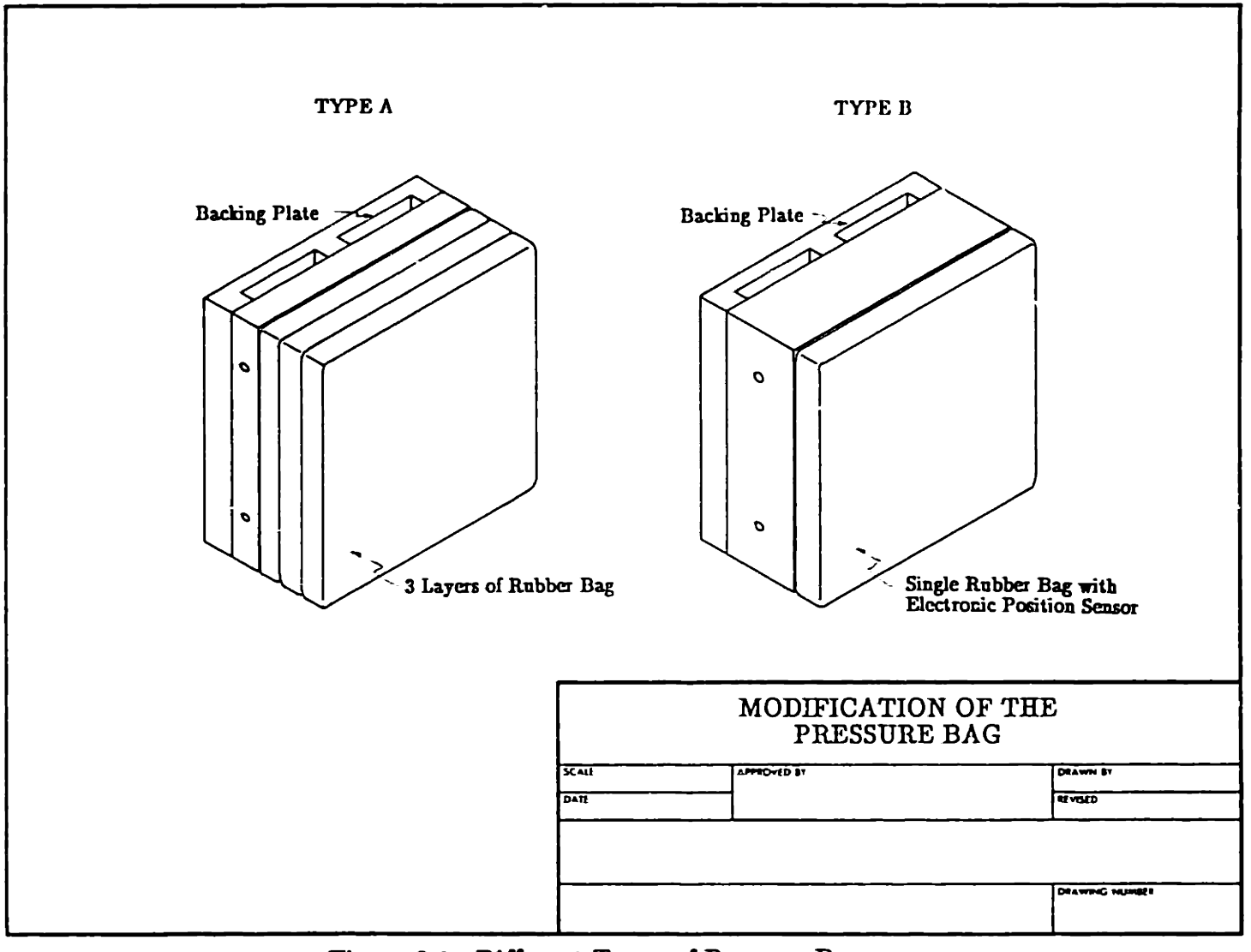

Figure 3.1: Different Types of Pressure Bags.

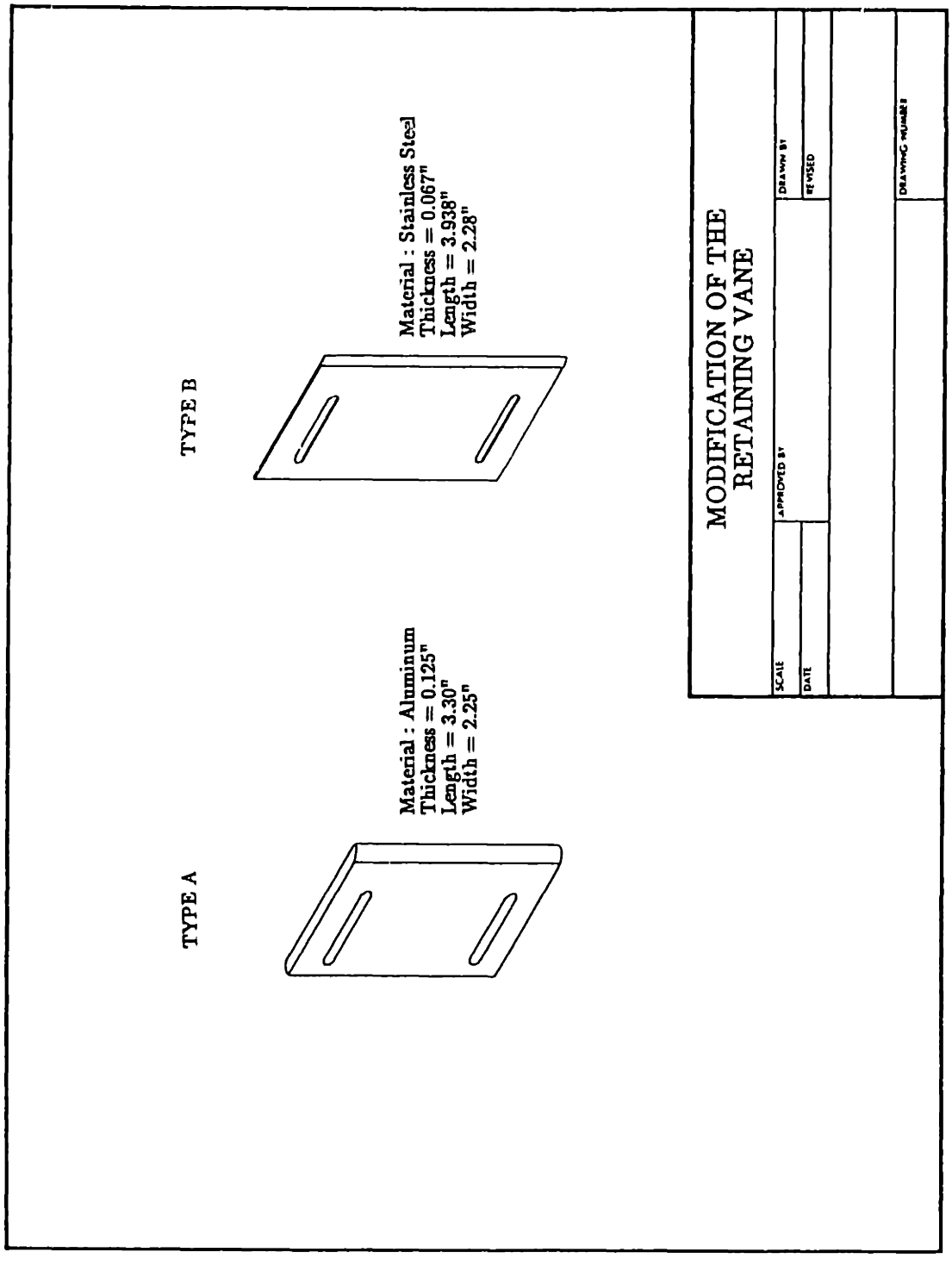

Figure 3.2: Different Types of Retaining Vanes.

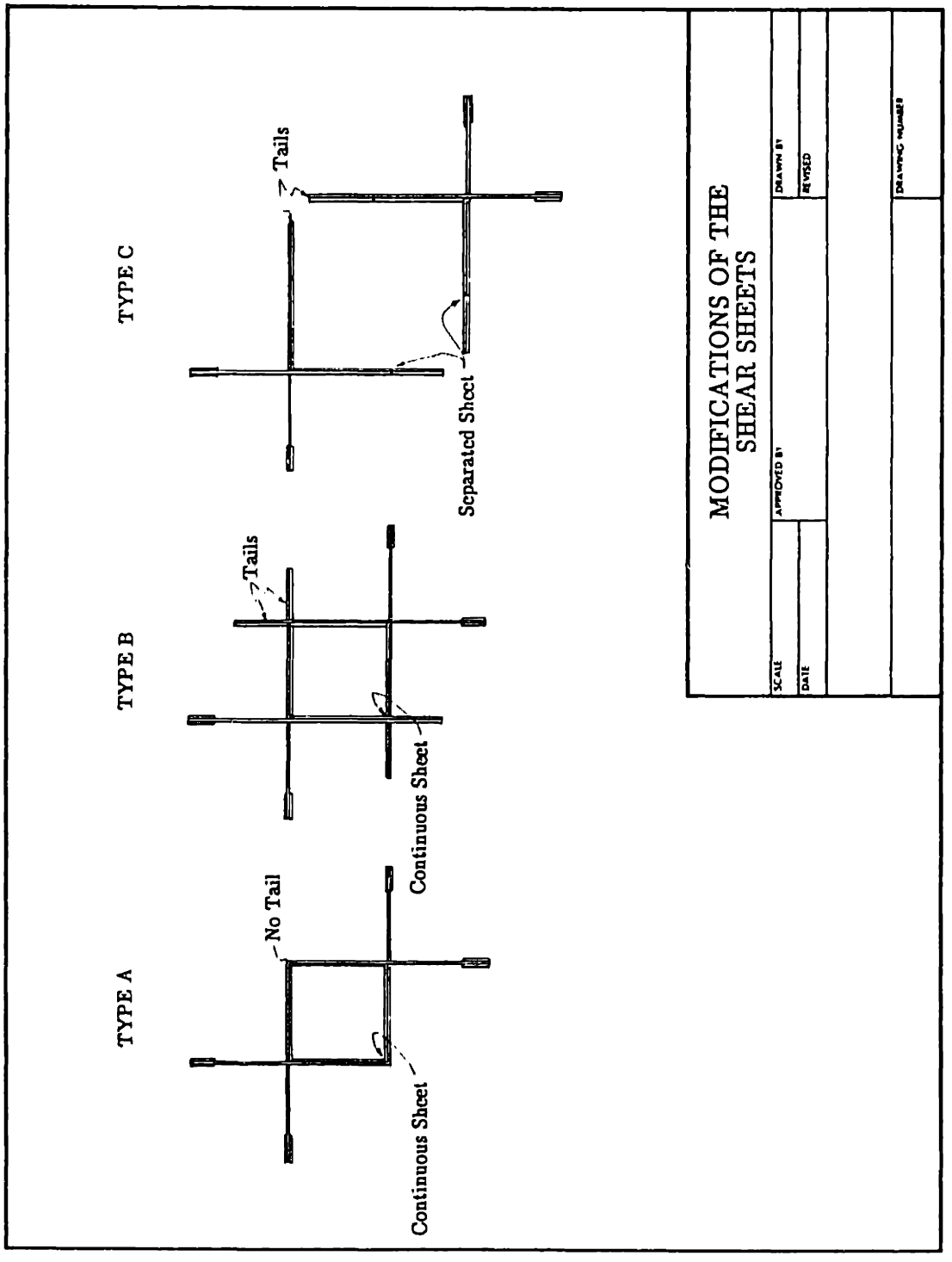

Figure 3.3: Different Types of Shear Sheets.

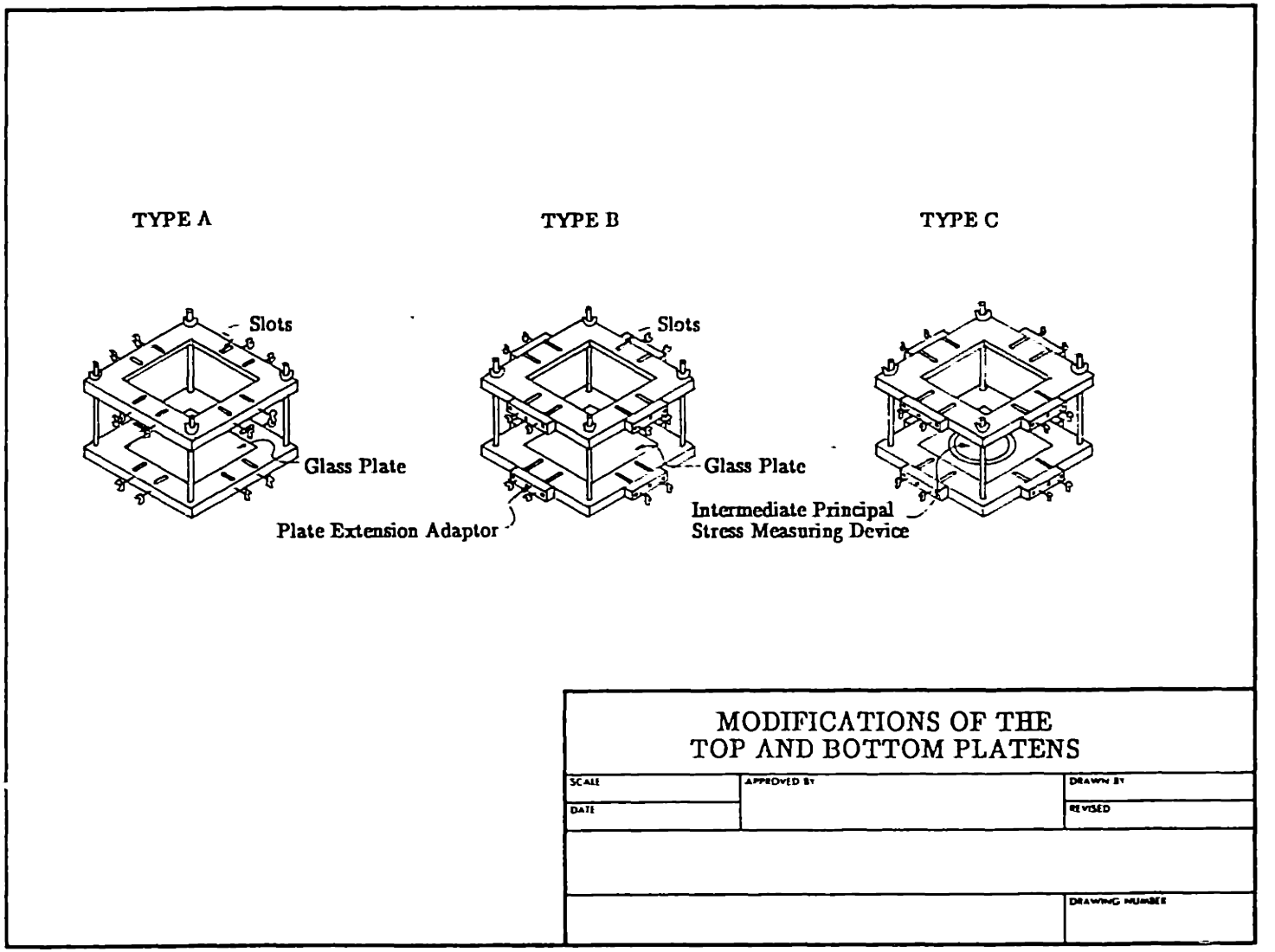

Figure 3.4: Different Types of Top and Bottom Platens.

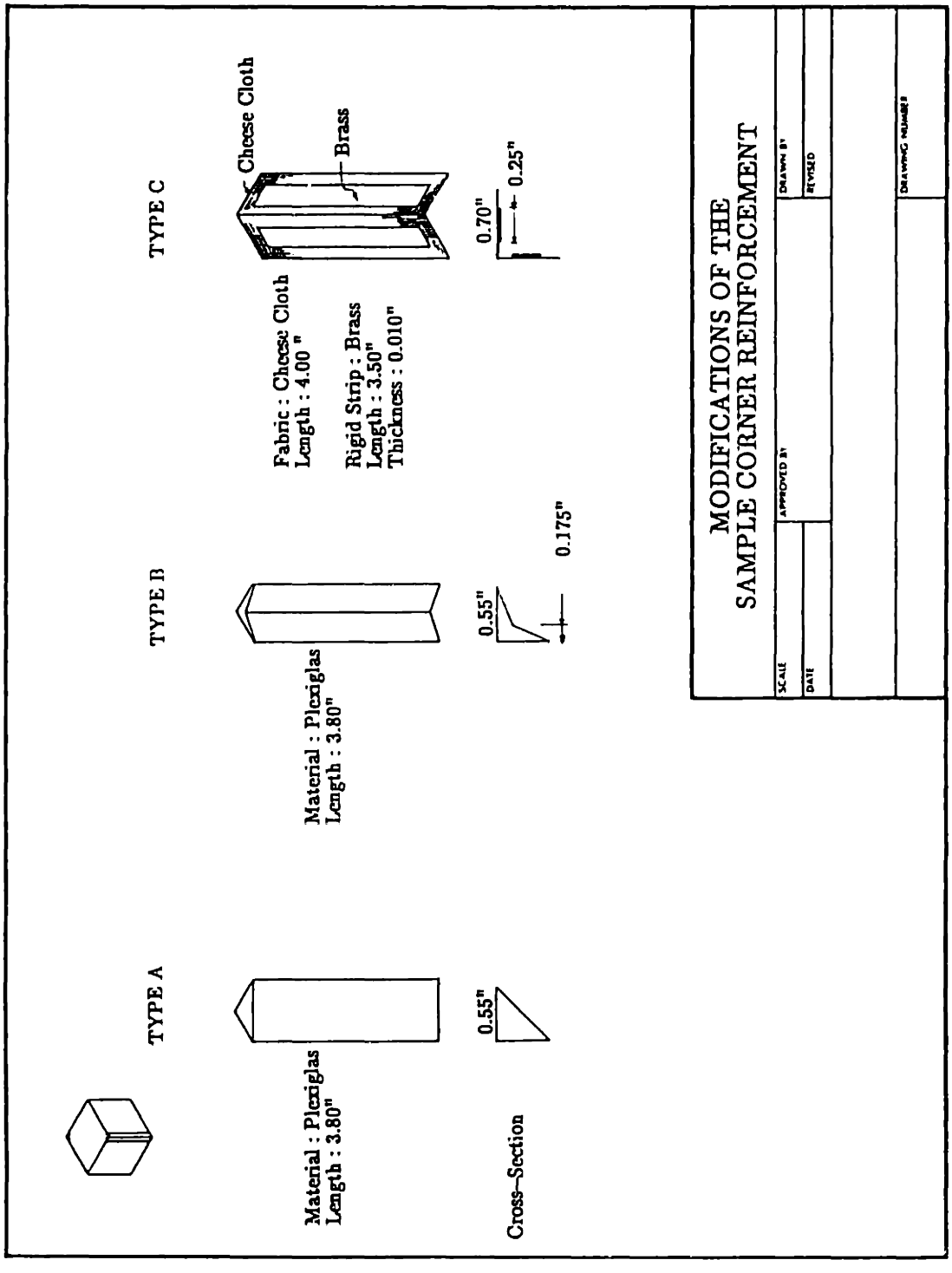

Figure 3.5: Different Types of Sample Corner Reinforcements.

PLATE EXTENSION ADAPTOR

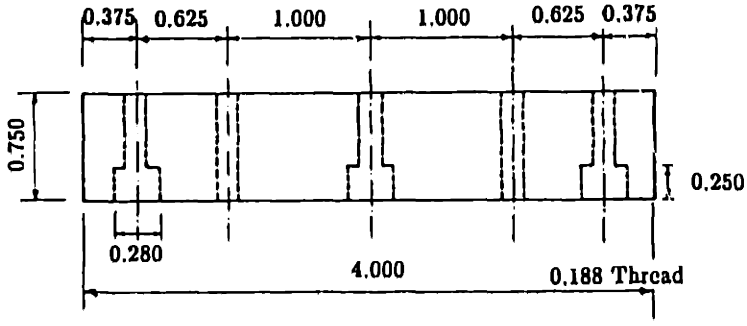

All Dimensions in Inches (")

Figure 3.6: Schematic of the Plate Extension Adapter.

SUPPORTING BASE FRAME

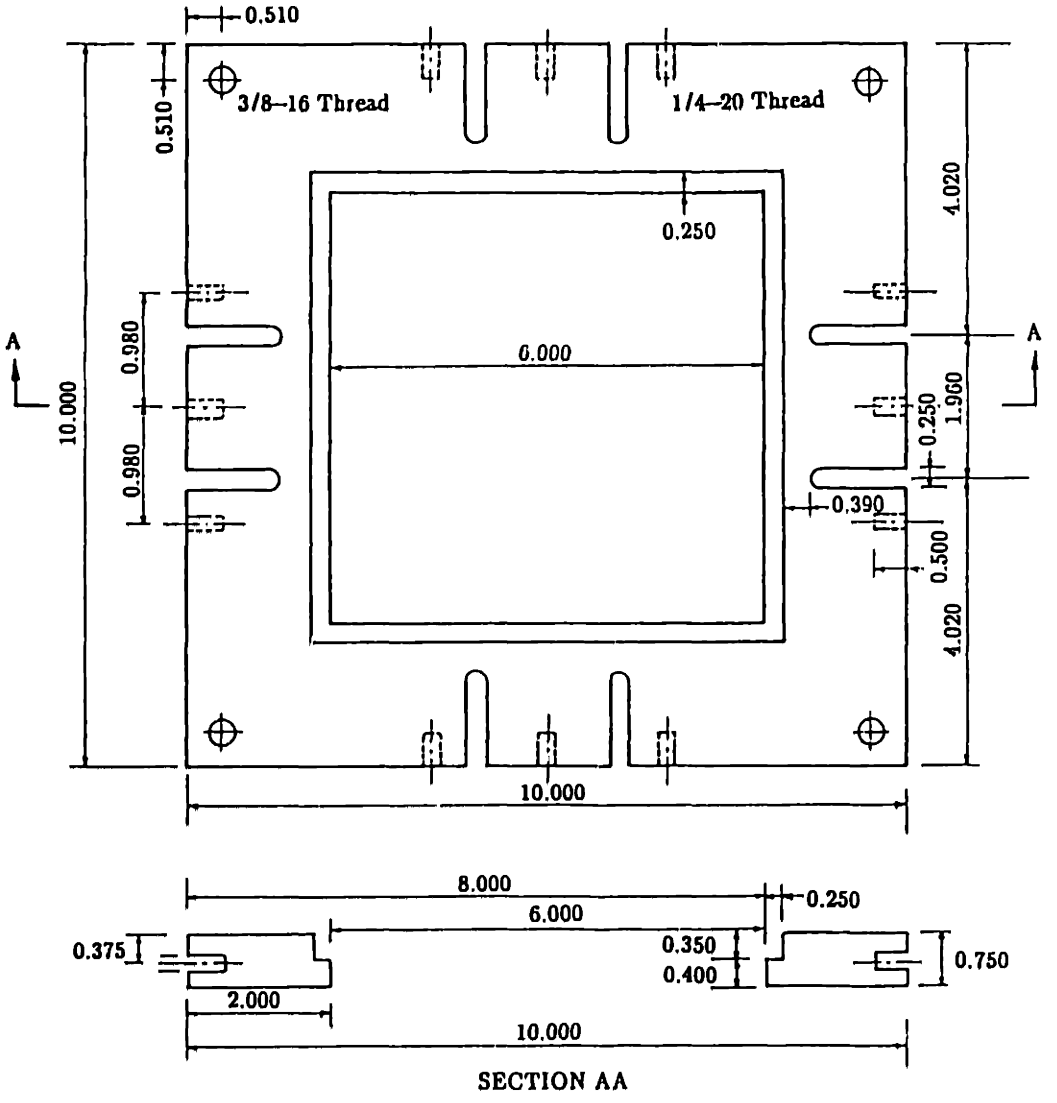

Figure 3.7: Schematic of the Supporting Base Frame.

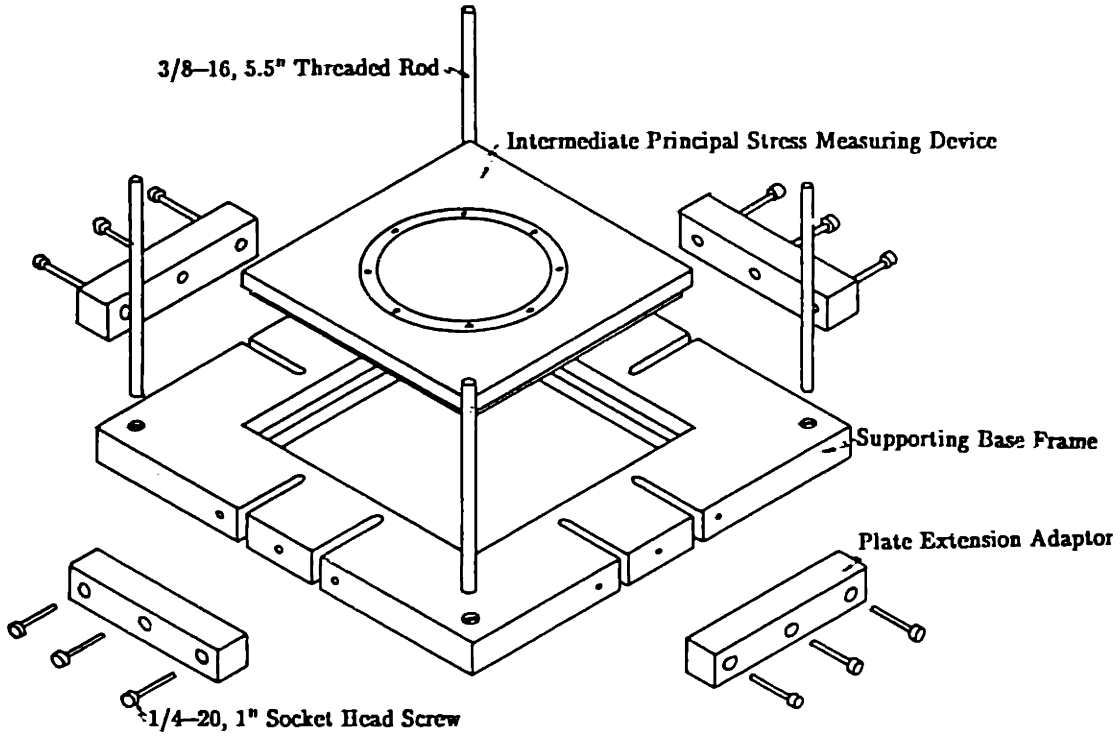

Figure 3.8: Assembly of the Bottom Platen with Intermediate Principal Stress Measuring Device.

Type B Pore Water Pressure Probe

PRESSURE TRANSDUCER CONNECTOR

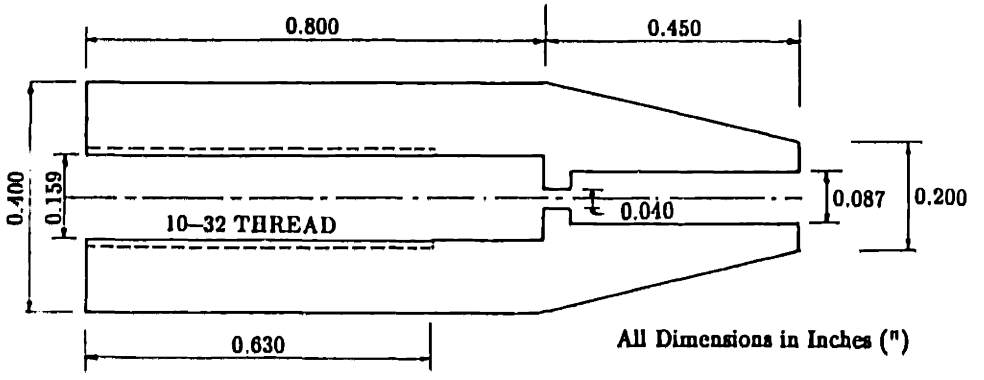

FINE POROUS STONE TIP

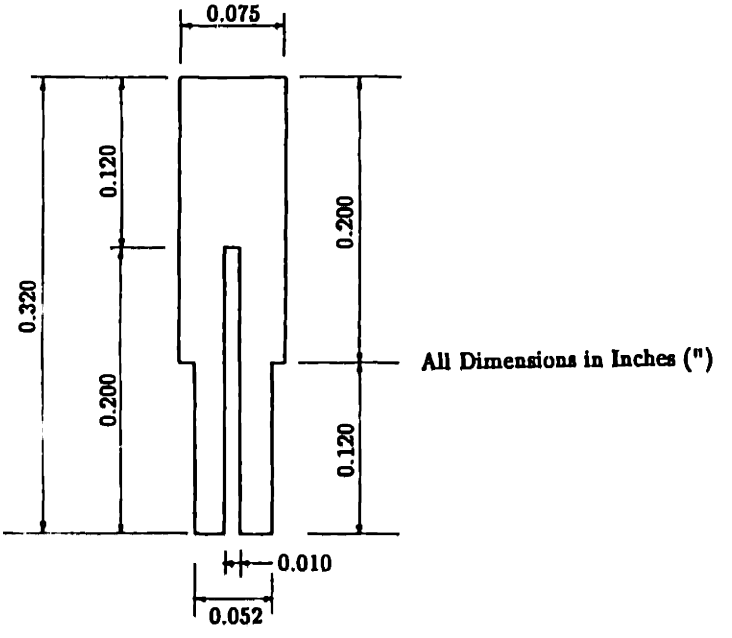

Figure 3.9: Schematic of the Pressure Transducer Connector and the Fine Porous Stone of the Pore Water Pressure Probe.

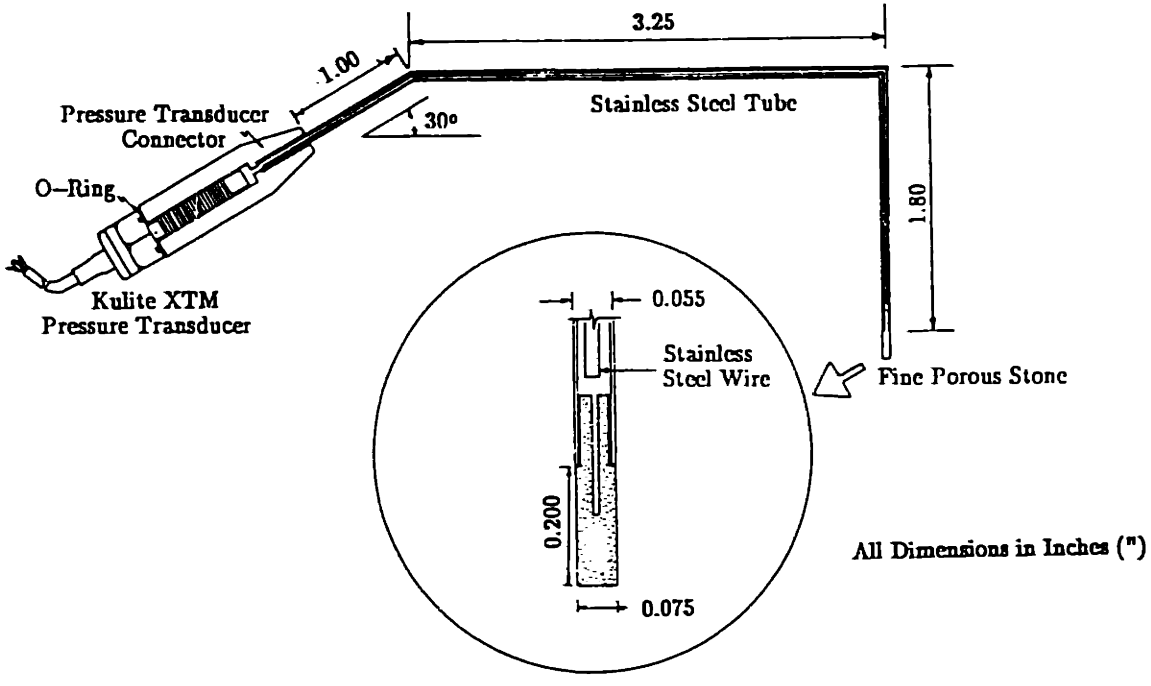

Figure 3.10: Schematic of the Pore Water Pressure Probe.

CHAPTER 4

TEST MATERIAL: RESEDIMENTED BOSTON BLUE CLAY

4.1 INTRODUCTION

The soil selected by the MIT research group to develop an understanding of fundamental soil behavior is Boston Blue Clay (BBC), a lean illitic glacio–marine clay of low to medium sensitivity. Boston Blue Clay was chosen for two principal reasons: its availability and relevance to local engineering practice; and, its behavior is significantly influenced by factors of interest such as sample disturbance and mode of shearing (anisotropy).

A substantial number of laboratory tests had been run on natural Boston Blue Clay before the 1960s because of construction in the Boston region, as well as interest in a basic understanding of soil behavior (e.g., studies of clay strength by A. Casagrande at Harvard and D.W. Taylor at MIT). Most of the test results on the natural Boston Blue Clay obtained for construction projects were never compiled, partly because the spatial variability in the properties of the natural material makes it difficult to generalize its behavior. In order to control sample variability, a resedimentation process was introduced. The basic idea of the resedimentation process is to mix dry clay with a known volume of water in the laboratory, then consolidate the slurry to a known vertical stress. During the course of the early studies, it was found that the resedimented material exhibits behavior fairly similar to natural Boston Blue Clay, making this process of soil preparation attractive from both practical and experimental points of view.

The material selection process can be the most important factor in experimental soil research. Natural BBC from different locations in the Boston

vicinity can exhibit different behavior. The properties of the clay depend on several factors, for example, the particle size distribution, the chemistry of the material and the mineralogy. Even material obtained from the same area at different depths can result in different properties. Therefore, the clay selected for resedimentation should at least be representative of typical natural BBC. The approach to material selection is described in Section 4.2.

The preparation of the resedimented clay used in this research was developed by Germaine (1982) for the study of anisotropy in overconsolidated clay using the DSC. The layout of the equipment and the procedure have been modified and improved in this research, as described in Appendix A. Section 4.3 describes the specifications of the resedimented material and the tests for verifying the final material properties. A large number of DSC samples were needed in this study, requiring many batches of resedimented BBC to be prepared since it is possible to obtain only two DSC samples per batch of resedimented clay. The properties of these batches of clay have to be checked for sample variability. Therefore,4 a group of reference tests were performed on each batch of clay. These tests include measurements of Atterberg limits, salt concentration, particle size analysis, degree of saturation, consolidation and some undrained strength tests. A summary of these "reference" tests is provided in Section 4.4.

Another group of tests were performed in preparation for the DSC tests on normally consolidated BBC. In a DSC test, the strain data cannot be obtained during actual testing, making it difficult to perform K_o–consolidation (i.e., allowing no lateral strain) without predetermining the consolidation stress path. This requires the horizontal stress at each consolidation increment to be known. Therefore, special oedometer tests measuring lateral stress were performed and compared with other results, as discussed in Section 4.5.1. Another important consideration before running the DSC tests was the validity of the concept of

normalized soil properties (NSP). The restriction of low stress levels in the DSC device brings several assumptions into question; therefore, special strength tests (Direct Simple Shear tests) were carried out at low consolidation stresses. The results are discussed in Section 4.5.2. This section also describes the behavior of normally consolidated BBC at different consolidation stresses, using results of DSS tests performed in other studies by MIT researchers.

The results of the reference tests are compared with other published results on Boston Blue Clay in Section 4.7.

4.2 MATERIAL SELECTION PROCESS

In the previous DSC research conducted by Germaine (1982) and O'Neill (1985), the resedimented BBC tested was found to be thixotropic, i.e. its properties changed with time. This effect caused significant increases in the preconsolidation pressure and undrained strength of the material with length of storage time, and served to substantially complicate the analysis of test results. Though a quantitative correction has been made with regard to this effect, the corrected results are somewhat less reliable. Another problem encountered by researchers (Ladd and Varallyay, 1965) was low plasticity BBC; this characteristic of soil results in lower compressibility.

The Boston Blue Clay used in this research is referred to as BBC III and was collected from a construction site at Kendall Square, Cambridge, Massachusetts (Figure 4.1). The natural material was collected by augering at a depth of approximately 75 ft. The natural Boston Blue Clay collected was inspected visually to assess the amount of organic matter and coarse particles. Atterberg limits were performed to check whether the material properties were representative of most BBC. Thixotropic effects could not be checked until after the resedimented clay was prepared. Several oedometer tests were performed on

samples with varying storage times to determine whether the material was thixotropic; the results described in Section 4.4 show that BBC III is not thixotropic.

4.3 PREPARATION OF RESEDIMENTED BOSTON BLUE CLAY

This section summarizes the specifications and the preparation of the resedimented clay for this research. Specifications of the resedimented Boston Blue Clay are:

- A final water content of 40±2%. The final water content is governed by the maximum vertical stress imposed on the sample during consolidation. It is important to keep the maximum vertical stress as low as possible because the DSC has a limitation on the maximum stress on the shear sheets of 0.5 ksc and a maximum normal stress on pressure bags of about 2 ksc. On the other hand, the maximum vertical stress should be high enough so that the sample block has sufficient strength to be trimmed and handled. Therefore, a maximum vertical stress of 1 ksc is applied to the sample in the consolidometer to produce a final water content of about 40% with a liquidity index of 0.8.
- K_o–consolidation to 1 ksc and rebound to 0.25 ksc for an overconsolidation ratio of 4 before extrusion and trimming. It has been shown that at an overconsolidation ratio of 4, the stress state of the soil is close to hydrostatic ($\sigma'_v \simeq \sigma'_h$). This state of stress helps to minimize sample disturbance caused by removal of an "in–situ" shear stress whenever K_o is not equal to unity. Verification of this assumption is discussed in Section 4.5.1.
- A salt concentration of 16 gram/liter to prevent segregation of the soil particles. This value of salt concentration has been used by MIT

researchers for the last 25 years. The primary reason for selecting this concentration is because studies have shown that the resedimented clay at this salt concentration will produce a flocculated clay structure which can prevent segregation of the soil particles during sedimentation. An increase in the salt concentration above 16 g/l can cause severe corrosion in the testing equipment and errors in the measurement of water content. Therefore this optimum value of salt concentration was chosen.

- 100% saturation, which is essential for undrained (constant volume) tests in the DSC. It is not possible to back–pressure the DSC clay sample; hence the only possible way to perform an undrained test in this device is to ensure that the clay is fully saturated. (Some undrained DSC tests on artificial clays were performed by Sture et al. (1985) with a maximum degree of saturation of 40%; back–pressure was not applied and hence the results do not represent constant volume clay behavior, unless the volume of the sample is controlled in a test.)

In order to achieve these requirements, a special technique of preparation was developed by Germaine (1982). The preparation process is illustrated in Figure 4.2. Once the material has passed preliminary inspection, it is wet–sieved through a #40 sieve to remove any coarse sand, large shells or organic materials in the clay. The wet soil is then placed in an oven at 105° C to remove the water in the soil before crushing it. The soil is crushed by a ball–grinding process and the particle size of the crushed soil is checked by sieving a small portion of it through a #100 sieve with at least 95% of the clay passing through this sieve. If the retained material is more than 5% of the total weight, then the clay is reprocessed to ensure consistency in the material size, as well as to make the mixture easier to pour into

the mixing chamber. The salt concentration of the crushed material is then measured to determine the amount of salt necessary to achieve a salt concentration of 16 gram/liter. Hydrometer analyses are conducted on the pre–processed and the post–processed clays to determine whether the grinding process alters the particle size distribution. The results shown in Figures 4.3 and 4.4 indicate no change in the particle distribution before and after processing.

Finally, Atterberg limits are performed on the processed material (after grinding) to check whether the material is representative of the natural BBC in terms of index properties. Once the powdered clay has satisfied these conditions, the material is ready for use in the resedimentation process, which is referred to as "batching."

The step–by–step procedure of preparing the resedimented BBC is described in Appendix A. In summary, the dry clay powder is mixed with distilled–deaired water and some salt under a vacuum in a mixing chamber, then rained through a 1/2" nylon tube into a 12" diameter consolidometer where the mixture will eventually be consolidated. In order to produce a final soil cake at least 4.5" in height and with a final water content of about 40% in the consolidometer, the initial water content has to be equal to or less than 100% due to the size restriction of the mixing chamber and the consolidometer. But at a water content much less than 100%, the mixture of clay and water is too plastic to form a uniform slurry, making it virtually impossible to transfer the mixture from the mixing chamber to the sedimentation chamber. Therefore, an initial water content of 100% is chosen. The sample is consolidated in the consolidometer from a vertical stress as low as 0.063 ksc to a maximum vertical consolidation stress of 1 ksc with a load increment ratio ($\Delta\sigma/\sigma$) of 1, before it is unloaded back to 0.25 ksc. The vertical stress is maintained at 0.25 ksc for 4 days before it is extruded to ensure that the pore water pressure in the soil is fully dissipated; otherwise, the

clay sample will be non–uniform. Once the sample is extruded, it is trimmed into different sizes according to the type of tests that will be performed.

In this research, a number of modifications have been made to the Germaine (1982) batching technique:

- additional lubrication is placed on the sidewall of the consolidometer to improve sample uniformity and to eliminate the excavation process;
- better general layout of the equipment to improve productivity, so that more batches of BBC can be made in a shorter time frame;
- an electric vibrator is introduced to ease the flow of dry clay into the mixing chamber; and
- remote data acquisition; the load and displacement can be monitored constantly with central computer data acquisition.

Each batch of soil yields a maximum of two DSC samples and a number of triaxial, direct simple shear and oedometer samples. Due to the large number of DSC samples needed for the research, an extensive testing program was carried out to check the uniformity of the batches and to verify the specifications of the final soil product, as summarized in the next section.

4.4 SUMMARY OF REFERENCE TESTS

Reference tests are referred to in this research as tests used primarily to quantify the batch–to–batch uniformity of the resedimented clay and to verify that the soil has satisfied the specifications discussed previously. Another purpose is to obtain basic engineering properties needed to characterize any cohesive soil that is used for research. Eight batches of resedimented Boston Blue Clay were prepared for this research. Reference tests, which include salt concentration, hydrometer analyses (to check signs of segregation), index properties, and

oedometer tests, were performed on the eight batches of clay. Other tests like unconsolidated–undrained triaxial compression (to check the degree of saturation) and lateral stress oedometer tests were conducted to supplement the reference tests.

4.4.1 Salt Concentration

The salt concentration is determined using a "conductivity" method recommended through research by Martin (1970). The conductivities of a known salt concentration (potassium chloride) solution are measured using platinum electrodes to form a basis for creating a calibration curve. A representative soil sample is mixed with a known quantity of distilled water in a test tube, then settled out by a centrifuge technique. The clear solution at the top of the test tube is poured into a small beaker and the conductivity of the solution is measured. The salt concentration of the solution is then determined from the calibration curve, by assuming the salt present in the solution is the same as the reference solution. The pore fluid salt concentration is then calculated from known differences in the water content.

Salt concentration tests were performed on each batch of resedimented clay; the results are summarized in Table 4.1. The measured salt concentrations of the soils compare well with the prescribed value of 16 gram/liter.

4.4.2 Hydrometer Analysis

Hydrometer analyses were performed on one batch of the clay (Batch 201) to investigate the possibility of particle segregation during the sedimentation process. Four samples were collected from different depths of a 4 inch thick soil sample, and the particle size distributions of each of the four samples were determined as shown in Figure 4.5. The results indicate no sign of particle

segregation in the resedimented clay. Therefore, a salt concentration of 16 g/l is judged to be sufficient to prevent segregation and to obtain sample uniformity.

4.4.3 Index Properties

Batch water content and Atterberg limits are the simplest tests to perform in quantifying the index properties and to check the uniformity of the batches. These tests were performed on all eight batches of resedimented clay. The liquid limits were determined using the Casagrande cup, and the plastic limits were determined from the "rolling" method which is described in ASTM D4318–84 (1988). The results are shown in Figure 4.6, indicating very little variation between batches of clay in terms of remolded properties. The value of the liquid limit is 45.20±0.44% and the value of the plastic limit is 21.74±0.44%. The final water content is 40.59±0.57% which gives a liquidity index of 0.82. The results are summarized in Table 4.1.

4.4.4 Unconsolidated–Undrained Triaxial Tests

The main objective of performing unconsolidated–undrained triaxial compression tests (UU) is to check the degree of saturation of the different batches of resedimented clay by means of Skempton's B parameter. A triaxial sample is trimmed and placed on a very fine saturated porous stone connected to a mounted pressure transducer. The sample is then subjected to a cell pressure of 0.25 ksc to ensure that a positive pressure is developed in the sample, and this pore pressure is measured with the pressure transducer. Since there is no drainage in the system and if the sample is fully saturated (i.e., B=1), the pore pressure measured is the capillary pressure or initial effective stress of the soil. If there were no sample disturbance or swelling during extrusion or trimming, and if K_o=1.0, the effective stress of the triaxial sample should equal the effective stress of the soil in the

consolidometer after the last unloading increment to 0.25 ksc. The results of the measured initial effective stress (σ'_s) of the trimmed samples, tabulated in Table 4.2, show some values of effective stresses much less than 0.25 ksc, which implies significant sample disturbance and/or swelling. This disturbance/swelling is very difficult to quantify because a number of factors can contribute, including: drawing out of water from the porous stones upon removal of the 0.25 ksc consolidation stress, the extrusion technique, duration of the extrusion process, storage time, storage conditions, trimming methods, and handling.

The triaxial samples were further subjected to an increase in cell pressure of 0.3 ksc to measure the Skempton's B parameter of the sample. Skempton's B coefficient, defined as the ratio of the change in pore water pressure to the change in the cell pressure, was calculated. A typical response curve of B versus time is shown in Figure 4.7. The results, summarized in Table 4.2, indicate that all batches have a B value of 1, implying that the clay specimens are fully saturated. Once the B value is measured, the soil sample is sheared by increasing the axial stress on the sample at a strain rate of 0.5%/hour. The three tests with the highest undrained strength also had the highest initial effective stress, σ'_s (see Figure 4.8), as would be expected from Ladd and Lambe (1963).

4.4.5 Consolidation Behavior

After the clay mixture slurry is rained into the consolidometer during the sedimentation process, the slurry is subjected to incremental loads. The displacements associated with each increment are recorded, so that the void ratio versus vertical effective stress relationship can be determined. The results for the eight batches of clay, shown in Figure 4.9, indicate very small variation between batches. In general, the compression index, C_c, decreases with increasing vertical effective stress (σ'_v) from a C_c value of about 0.55 at σ'_v=0.2 ksc to a C_c value of

0.45 at σ'_v=0.8 ksc (see Table 4.3). The swelling index (C_s) was also measured in most of the tests, indicating very small changes in C_s from σ'_v of 1 ksc to 0.25 ksc. The variation in water content for eight batches of resedimented BBC is also very small, with an average value of 40.59±0.57%.

Figure 4.10 presents the average coefficient of consolidation, c_v (average values obtained from log–time and root–time methods), versus vertical effective stress. The results show that the c_v value increases significantly with increasing σ'_v. One important observation from these tests is that the coefficients of consolidation computed from the Casagrande (log time) method and the Taylor ($\sqrt{t}$) method yield very similar results (as shown in Figure 4.11). This was not observed in one–day incremental oedometer tests with 2 cm height samples. One distinct advantage of performing consolidation tests on large samples is that the pore water pressure dissipation time is relatively long for each increment. The settlement curves are very well defined, and the secondary compression periods are relatively short. Flow parameters like coefficient of permeability (k) and permeability change index (C_k) are provided in Appendix B.

Oedometer tests are performed to check the preconsolidation pressure of the batches of BBC and general consolidation characteristics, which in turn can be used as a means of checking sample variability. Twelve oedometer tests were carried out on the eight batches of resedimented clay, specifically to accomplish the following goals:

- Figure 4.12 shows the relationship of the void ratio to the vertical effective stress for all the oedometer and two DSS consolidation tests. The variation between the different tests is partly due to the inaccuracy in water content measurements, which causes errors in the void ratios. Graphs of vertical strain versus vertical stress (Figure

4.13) show much smaller variation, implying that the sample variability between batches is small. The compressibilities from all oedometer tests are also compared as tabulated in Table 4.4; the results are summarized in Figure 4.14.

- The preconsolidation pressure was checked for each batch of clay. These preconsolidation pressures are determined from a plot of the vertical strain versus logarithm of vertical stress, using the Casagrande construction method.
- The possibility of any thixotropic effects was examined. Thixotropic behavior can be detected based on increases in preconsolidation pressure with storage time according to O'Neill (1985). Samples with storage times ranging from 1 to 248 days were tested and a graph of the preconsolidation pressure from the Casagrande construction method versus storage time is plotted in Figure 4.15. The results show no change in preconsolidation pressure with time. Therefore the material is non–thixotropic.
- The effects of lubrication on the inner walls of the consolidometer during batching were evaluated. As the soil sample consolidates in the large consolidometer, the vertical stress at the bottom of the sample might be less than the vertical stress at the top due to the side friction of the wall, which can affect the uniformity of the soil sample. Two oedometer tests (Figure 4.16) were conducted on soil samples from the top and the bottom of the large consolidometer sample taken from Batch number 204 that was prepared with an initial thickness of the lubricant (i.e., silicone grease) of about 0.1 mm. The results suggest that side friction has some effect on the preconsolidation pressures of the oedometer samples. The difference in preconsolidation pressure at

the top and bottom of the large consolidometer sample is about 0.03 ksc. Based on grease tests described in Appendix E, an initial grease thickness of less than 0.1 mm produces a shear force along the sidewalls of about 16 kg, assuming the shear resistance distribution due to the grease is linear with a zero value at the bottom of the wall to a maximum resistance of 0.03 ksc at the top of the wall. This implies that the preconsolidation pressure at the bottom of the soil cake in the consolidometer is about 0.02 ksc (16/732) less than a sample at the top. Therefore, the measured results are consistent with the theoretical value.

As a result of the above tests, more lubricant was added to the side wall of the consolidometer to reduce the friction in Batches 206 and 207, with the initial thickness of the grease increased to 1 mm. The oedometer results of two samples from the top and bottom of the consolidometer sample (Batch 206) show no difference in the preconsolidation pressures (Figure 4.17). Thus, the uniformity of the sample improved because of the additional lubrication. For a 1 mm grease thickness, the shear resistance (caused by the grease based on the grease test) is 0.007 ksc; the shear force along the wall of a 4.5 inch height sample will then be 3.77 kg, assuming the shear resistance distribution due to the grease is linear. The difference in preconsolidation pressures at the two drainage boundaries is only 0.005 ksc (3.77/732). Therefore, more grease was added for all subsequent batches.

- The effects of secondary compression on the coefficient of consolidation were investigated. Two samples from batch 206 were consolidated with 4 hour load increments, undergoing a few hours (at least 3) of

secondary compression. An additional sample from the same batch of clay was loaded only to the end–of–primary consolidation (EOP) for each increment, so that there would be a minimum amount of secondary compression in this test. The EOPs of this test were obtained from the 4–hour incremental oedometer tests. The consolidation should occur along the Virgin Compression Line with "constant" compressibility. It is known that secondary compression can lead to a higher c_v value due to an initially lower m_v and the root–time compression curves might reflect this behavior (1.322 Soil Behavior class at MIT). A comparison of the three tests shows a discrepancy in the coefficient of consolidation calculated from the Casagrande (log t) and the Taylor ($\sqrt{t}$) methods, possibly due to the secondary compression. However, the results, shown in Figures 4.18a and 4.18b, indicate that the EOP oedometer test gives the same results as the other two tests with secondary compression. In the writer's opinion, the difference in the coefficient of consolidation is due not to the amount of secondary compression, but probably to an error in the strain measurement during the first minute of the loading increment, in which both methods rely heavily to calculate the corresponding c_v values. One additional problem regarding the c_v values is concerns the time to the EOP obtained from the Casagrande method, which is discussed in the next section.

According Mesri and Choi (1985), for most clays the ratio of the rate of secondary compression ($C_{\alpha\epsilon}$) to the compression ratio (CR) is 0.04±0.01. The rate of secondary compression in the oedometer test is given from the change in strain after the end–of–primary consolidation over the change in the logarithm of time.

For most increments, the slope of the curve in the secondary compression range was not a straight line (see an example in Figure 4.19). In our tests, the minimum slopes of the strain versus the logarithm of time plots were taken as the rate of secondary compression. The mean ratio of about 0.02 is lower than the values reported by Mesri and Choi partly because of the non–linearity between the strain and the logarithm of time in the secondary compression range. Figure 4.19 shows the variation in the results depending on where the tangent to the point on the secondary compression time curve is being taken. As a result, the computed $(\frac{C\alpha\epsilon}{CR})$ values tabulated in Table 4.5 range from 0.017 to 0.045. The poorly defined "breaking point" also affects the computation of c_v from the log–time method since the time t_{50} is also depending on the magnitude of strain at the end–of–primary.

Figure 4.20 presents the relationship from oedometer tests between the average coefficient of consolidation and the vertical effective stress, showing a continuation of the trend from the batch consolidometer tests; that is, the c_v value increases with increasing vertical stress in the normally consolidated range.

The results of each oedometer test are provided in Appendix B, including a discussion on the empirical correlations with compression indices from the literature and the coefficients of permeability.

4.4.6 Consolidated–Undrained Triaxial Tests

Four recompression consolidated–undrained triaxial tests (two compression and two extension tests) were performed on resedimented material at an overconsolidation ratio of 4. The results are tabulated in Tables 4.9 and 4.10, and plotted in Figures 4.21 and 4.22. The initial state of stress is hydrostatic under these conditions since K_o is unity. The aim of these tests is to obtain undrained strength behavior from triaxial tests to compare with recompression DSC tests at

the same OCR on the same material. These results also provide a measure of the difference in undrained behavior of this material compared with other resedimented BBC or natural BBC.

The two recompression compression tests yield a normalized undrained shear strength ($\frac{q_f}{\sigma'_p}$) of 0.223±0.006 compared with an average value of 0.145±0.045 from the UU triaxial tests discussed earlier (Figure 4.8). A SHANSEP type triaxial compression test was performed by Sheahan (1990) at MIT on the same BBC at the OCR of 4.4, giving a $\frac{q_f}{\sigma'_p}$ value of 0.206 (see Table 4.9). The results of this test are consistent with the recompression test results, but give lower strength than from the the recompression tests conducted by O'Neill (1985).

The two recompression extension test results are somewhat disappointing. One test (CIUE–2) was stopped at a strain of 2.8 % due to some experimental problems, therefore the $\frac{q_f}{\sigma'_p}$ for this test is assumed to be the normalized shear stress at ϵ_a=2.8%. The other test (CIUE–1) has a $\frac{q_f}{\sigma'_p}$ value of 0.095, which is quite low. One problem in conducting triaxial tests at low stress is that the piston friction correction and membrane correction can amount to 10 to 20 % of the peak shear stress. Therefore, less emphasis is placed on these tests.

4.5 SPECIAL TESTS IN PREPARATION FOR DSC TESTS ON NORMALLY CONSOLIDATED CLAY

A number of tests were performed in preparation for DSC tests on normally consolidated clay. Since the DSC is a stress–controlled device, it is difficult to perform K_o–consolidation without predetermining the consolidation stress path because it requires at least 24 hours to obtain the strain data. The consolidation path can be estimated by performing a lateral stress oedometer test. Another difficulty associated with the DSC device is the limitation of applied surface tractions and normal stresses, which amounts to 0.5 ksc and 2 ksc respectively. There are two ways to reduce the applied stresses: one is to use a batch with a

lower preconsolidation pressure, and the other is to perform the test with consolidation stresses only slightly greater than the preconsolidation pressure of the batch. The minimum preconsolidation pressure has to be about 1 ksc in order to handle the sample. Hence, the second option was explored by performing undrained DSS shear tests at vertical consolidation stresses only 10 to 30% greater than preconsolidation pressure of the batch to check if these stresses yielded normally consolidated clay behavior. This testing program and the results are discussed in Section 4.5.2.

4.5.1 Lateral Stress Oedometer Test

The lateral stress oedometer measures the horizontal stress while restraining the sample from expanding radially, thus maintaining one–dimensional consolidation. The device is described by Dyvik et al. (1985). The results of a lateral stress oedometer test performed on the same series of BBC with the same stress history are tabulated in Table 4.6. When the void ratio versus vertical stress relationship from the test is compared with a regular oedometer test, the results should be identical, as shown in Figure 4.23. Figure 4.24 presents the stress path for the lateral stress oedometer test. The results from this test are also compared with a computer controlled CK_oUC test performed by Sheahan (1988). As shown in Figure 4.25, the results agree overall since they both yield very similar consolidation stress paths and vertical strains. Therefore, an average consolidation stress path obtained by these two methods is used in the DSC K_o normally consolidation process.

The results from the lateral stress oedometer test also show that the K_o value at an overconsolidation ratio of 4 is about 0.9 (Figure 4.26). Therefore, the assumed value of K_o (unity) during the batch rebound to an OCR of 4 is quite reasonable.

4.5.2 Direct Simple Shear Tests

Most soil models are based on the assumption that the stress–strain–strength behavior can be normalized with respect to a specified effective stress, such as a preconsolidation pressure or vertical consolidation stress (Henkel, 1960). Even the design method developed by Ladd and Foott (1974), which is referred to as SHANSEP (Stress History And Normalized Soil Engineering Properties), assumes that the Normalized Soil Properties (NSP) concept can be applied to soils. According to Ladd and Foott, the minimum vertical stress to obtain normally consolidated behavior should be at least 1.5 to 2 times the preconsolidation pressure of the natural soil to reduce the effects of sample disturbance. One of the problems associated with the DSC device is that it can perform tests only at relatively low stress levels. Even though the device is designed for a normal stress of 2 ksc and a surface traction of 0.5 ksc, creep of the rubber pressure bags and leaks between the rubber bags and the backing plates are inevitable, as shown in Figure 4.27, leading to a desired maximum normal stress of about 1.5 ksc. The problem is further complicated by the long duration of the consolidation process of clay in the DSC. Therefore, one wants to determine the minimum consolidation stress for which the sample still exhibits normally consolidation behavior. Special strength tests were carried out at maximum consolidation stresses (σ'_{vc}) just beyond the preconsolidation pressure of the soil ($\sigma'_p < \sigma'_{vc} < 1.3\ \sigma'_p$) so that the behavior at these stresses could be compared with results at higher consolidation stresses. The type of strength test selected is the Direct Simple Shear test (DSS), because of its relative simplicity and repeatability.

Two CK_oUDSS tests were performed in a Geonor device at a vertical consolidation stress slightly beyond the preconsolidation pressure of the clay (σ'_p=1 ksc). One sample was consolidated to a vertical stress of 1.12 ksc and the

other was consolidated to 1.3 ksc. The results are summarized in Table 4.7. Both of these samples were subjected to undrained shear by keeping the volume of the sample constant. The main objective of these tests is to investigate the behavior of a "normally consolidated" clay at a vertical consolidation close to the preconsolidation pressure. Figure 4.28 (as synthesized from data in DeGroot, 1989) shows typical stress paths and stress–strain curves for DSS tests on normally consolidated BBC. The results of the two tests are compared with published results (Walbaum, 1988 and DeGroot, 1989) on the same clay (having a batch preconsolidation pressure of about 1 ksc), but with higher consolidation stresses. Figure 4.29a shows no significant change in the normalized maximum shear stress of BBC with change in consolidation stress; the peak value remains at about 0.20 regardless of the vertical consolidation stress. But for a consolidation stress close to the preconsolidation pressure, the normalized vertical stress, σ'_v/σ'_{vc}, at failure has a higher value than at higher consolidation stresses, as shown in Figure 4.29b. The normalized shear modulus, defined as the shear modulus at 50% of the maximum shear stress divided by the undrained strength, decreases substantially at very high consolidation stresses (Figure 4.29c), but remains constant between a consolidation stress of 1.1 and 3 ksc. There is an increase in the shear strain at failure with increase in consolidation stress as shown in Figure 4.29d.

The results from these DSS tests show that at vertical stress consolidation stresses 12 to 30% greater than the preconsolidation pressure of the soil will give slightly different stress–strain relationships and stress paths, but the normalized undrained shear strength should not be affected by the low consolidation stress.

4.6 CONCLUSIONS ON RESULTS OF REFERENCE TESTS

The index properties indicate consistency between different batches of resedimented BBC; in other words, the variability between batches is relatively

small. The oedometer tests on various batches of the clay also yield very consistent results in terms of compressibilities (CR, RR and SR) as shown in Tables 4.3 and 4.4, with preconsolidation pressures close to the applied values from the large consolidometer tests. There is no sign of hardening due to thixotropic effects. Also, the unconsolidated–undrained triaxial tests on batches of clay indicate that the clay is fully saturated. Therefore, based on these reference tests, the prepared samples have satisfied our initial set of requirements, and have proven that the technique of resedimentation can produce very high quality samples with very little sample variability.

Regarding the K_o–consolidation stress path, an average consolidation stress path based on lateral stress oedometer and K_o triaxial tests is used. This stress path, shown in Figure 4.30, is used for the DSC tests on K_o normally consolidated BBC. Figure 4.31 shows the corresponding logarithmic relationship between K_o and the overconsolidation ratio. Finally, the maximum consolidation stress chosen for the DSC tests is between 1.12 to 1.3 ksc, which is about 12 to 30% above the preconsolidation pressure of the batches. There is some variation in the normalized behavior of this clay with consolidation stress, but as long as the maximum consolidation stress is within this range, the results of the tests should be fairly representative of normally consolidated BBC.

4.7 COMPARISON WITH THE PUBLISHED PROPERTIES OF RESEDIMENTED BOSTON BLUE CLAY

The resedimentation process has been used at MIT with BBC since 1960. During this time, the methodology has been refined and improved, resulting in better quality clay samples. A substantial number of laboratory tests have been conducted on resedimented clay in developing an understanding of clay behavior under different testing conditions.

4.7.1 History of Testing with Resedimented Boston Blue clay

Wissa (1961) developed the extrusion technique allowing the smaller clay samples to be trimmed from a large sample to the desired size with minimum amount of disturbance, which makes the process of preparing undisturbed clay in the laboratory feasible.

The effects of salt content on the shear strength of resedimented BBC was studied by Bailey (1961). Hydrostatically–consolidated undrained triaxial compression (CIUC) tests were performed on resedimented BBC samples with two different salt concentrations. The test results show that undrained shear strength does not vary with consolidation stress, provided the samples are at the same overconsolidation ratio. But the salt concentration does affect the consolidation behavior and shear strength.

Ladd and Varallyay (1965) used resedimented BBC to study undrained shear behavior under different failure conditions. The BBC used had a relatively low plasticity index due to a smaller fraction of clay size particles. As a result, the consolidation characteristics are significantly different from other resedimented BBC, but the undrained shear characteristics do not seem to be affected by the low plasticity index (see Table 4.11).

The first comprehensive summary of natural BBC was performed by Ladd and Luscher (1965) for undisturbed BBC collected from the MIT campus. Laboratory tests conducted on samples included consolidation, unconfined compression, unconsolidated–undrained triaxial compression, and non–hydrostatic consolidated–undrained triaxial compression and extension tests. Some of these results are compared with results from resedimented BBC in Table 4.12.

Preston (1965) and Braathen (1966) examined the effects of sample disturbance on resedimented BBC using undrained triaxial tests.

During the late 60's and early 70's, the study of soil behavior under plane strain conditions was fashionable. Dickey (1967) of MIT designed a prototype plane strain device to investigate the influence of the intermediate principal stress on shear behavior. But the early experimental results indicated that there were problems in measuring or applying the correct stress to the sample. Therefore, the results were considered unreliable. The plane strain device was further modified by Bovee (Bovee and Ladd, 1970). K_o–consolidated undrained plane strain tests were performed on the resedimented BBC at different overconsolidation ratios. One group of tests, referred to as active tests, yielded reliable plane strain data, but due to friction problems with the loading shaft, the results from the passive tests were somewhat less reliable.

Kinner and Ladd (1970) performed model footing tests on resedimented BBC. Theoretical predictions were then made using a finite element program with input parameters obtained from the laboratory tests. Laboratory tests included axisymmetric triaxial, plane strain and Direct Simple Shear tests.

In the late 70's, MIT soil researchers began to study the effects of principal stress rotation in soils using the Directional Shear Cell (DSC). The method of preparing the resedimented BBC was tremendously improved by Germaine (1982); the test results were more consistent and reproducible. This research was continued by O'Neill (1985), who later discovered that the resedimented BBC used (designated as BBC II) exhibited thixotropic behavior. The preconsolidation pressures of the material increased with storage time. Most of the tests conducted were recompression tests, making it very difficult to compare results from test specimens having different OCR values. Although corrections were made to "adjust" the data to a common OCR of 4, questions remain on the accuracy of the results.

A number of triaxial tests were conducted on the same resedimented BBC

to establish its yielding properties by Bensari (1984). The tests on overconsolidated clay were performed by recompression. Therefore, the results are faced with the same difficulty in defining the overconsolidation ratio due to thixotropic effects.

Fayad (1986) conducted an experimental program very similar to Bensari's, but extended the testing capability to include cyclic triaxial tests. Aware of the thixotropic effects of the resedimented clay, the SHANSEP method of determining the undrained behavior was used to produce the required overconsolidation ratio instead of the recompression technique. The compression test results were generally acceptable, but the extension tests gave extremely high friction angles and very questionable undrained strengths.

Cyclic Direct Simple Shear tests were carried out by Malek (1987) on the same clay at OCR=1, 2 and 4 to study the cyclic behavior of clay in more depth.

The resedimented BBC II was abandoned in 1986 beginning with this research, due to the obvious problems associated with thixotropic effects. Experimental data, as discussed in Section 4.4.4, have shown that the new material is non–thixotropic. During the course of this research, Walbaum (1988), Sheahan (1988) and DeGroot (1989) conducted laboratory tests on this new material for various studies, including investigation of sample disturbance using the DSS apparatus, the study of undrained K_o triaxial tests with a computer–controlled triaxial device and the investigation of evolving anisotropy using a new device called the Multi--Directional Direct Simple Shear apparatus (MDSS).

4.7.2 Comparisons with Other Series of Boston Blue Clay

There are at least four different series of resedimented BBC used at MIT during the last 25 years in various testing programs. Most of the experimental

programs included some index properties to be used as a basis for comparison.

Table 4.8 shows a comparison of properties from the different series of BBC. The specific gravity, G_s, does not vary very much, ranging from 2.75 to 2.78. The Atterberg limits change quite significantly among the different series. The plastic limit variation between 18 and 23% is relatively small compared with the 33 to 46% range for the liquid limits. This variation is primarily due to the amount of clay size fraction in the soils. Skempton (1953) introduced a quantity called the "activity of the soil," which is defined as plasticity index divided by clay size fraction ($<2\mu$). This quantity varies with the mineralogy and composition of the material. The results of the plasticity index versus clay fraction from Table 4.8 are plotted in Figure 4.32, showing an activity of 0.42. It is reasonable to assume from this plot that the activity of typical BBC is about 0.4.

The Atterberg limits have proven to be very useful not only in the identification and classification of soil type, but also in estimating consolidation characteristics and strength parameters. Empirical correlations have been established between the compressibility and the Atterberg limits for non–varved, low to medium sensitivity soils like Boston Blue Clay, as described in Appendix B.4.3. Ladd (1988) has developed an empirical correlation between the undrained strength ratio from laboratory CK_oU, field case histories and the plasticity index, as shown in Figure 4.33. Therefore, the importance of conducting limit tests to estimate basic soil properties from the empirical correlations should not be underestimated.

Table 4.11 summarized the triaxial data on three different series of resedimented BBC performed at MIT during the last three decades.

The results of normally consolidated compression tests indicate that there is no obvious differences between the three series of BBC, with normalized undrained strength ranging from 0.309 to 0.334. The strain at failure is between 0.13% and

0.3% in all the tests. The friction angles range from 32° to 35° at maximum obliquity.

The SHANSEP type triaxial compression results for overconsolidated clay show that the BBC III is weaker than BBC II. The results of the recompression triaxial tests performed at OCR=4 on BBC II and BBC III also indicate the same trend (see Table 4.9).

Four triaxial extension tests on normally consolidated BBC were presented here. The results in Table 4.11 indicate that BBC III exhibits lower normalized undrained strength than the other two series of BBC. The A_f does not change very much in these tests, ranging from 1.14 to 1.18. The strain at peak shear stress is between 10% and 14%.

The results of Geonor CK_oUDSS tests on normally consolidated BBC from the three series are summarized in Table 4.7. The results indicate that there is no significant difference in the three series of BBC at OCR=1.

Therefore, we conclude that there is no noticeable difference in behavior on the three series of BBC at an OCR of 1 in triaxial compression and DSS tests. But BBC III shows lower normalized undrained strength in compression at higher OCR than BBC II. In extension triaxial tests at OCR=1, the results indicate that BBC III is weaker than BBC II.

Table 4.12 summarizes the general properties between resedimented BBC II, BBC III and natural BBC (Ladd and Luscher, 1965) in terms of index properties, consolidation characteristics, and some undrained strength parameters. The two series of resedimented BBC show very small differences in all parameters, except coefficients of consolidation. The differences that do appear are due to the fact that the composition of the two series of clay are not identical. As for comparison with natural BBC from the MIT Campus, the difference again is small (except c_v), showing the value of using resedimented clay for studying realistic soil

behavioral trends. It is strongly advised to recycle BBC III, since this batch of clay has properties representative of the natural material. Furthermore, this clay is non–thixotropic and has a small rate of secondary compression which is ideal for research purposes.

Table 4.1: Index Properties of Resedimented Boston Blue Clay III.

Batch (Source)	σ'_{vm} • (ksc)	σ'_p ‡ (ksc)	w (%)	LL (%)	PL (%)	PI † (%)	LI †	Clay Fr. <2μ,(%)	Salt Conc. g/l	Remarks
(Ground)	-	-	-	44.90 ±0.14	22.45 ±0.07	22.45	-	52.1 ±4.1	1.98(g/kg) ±0.10	G_s = 2.785 (97% passed S. No.100)
200	1.00	1.04(3) ±0.04	41.10 ±0.80	45.90	21.95 ±0.35	23.95	0.80		22.13 ±2.02	
201	1.00	0.98(1)	39.42 ±1.90	44.82	21.19 ±0.35	23.63	0.77	57.6 ±1.1	14.53 ±1.43	
202	1.03	0.99(2) ±0.02	40.67 ±0.40	45.46	22.27 ±0.62	23.19	0.79		15.05 ±0.95	
203	1.00	1.00(1)	40.70 ±0.50	44.50	21.18 ±0.58	23.32	0.84		15.90 ±3.20	
204	1.01	0.97(2) ±0.02	40.19 ±0.40	45.60	21.47 ±0.58	24.13	0.78		13.63 ±3.02	
205	1.00	1.00(2) ±0.00	40.66 ±0.27	45.01	21.62 ±0.63	23.39	0.81		15.69 ±3.65	
206	0.98	0.98(2) ±0.00	41.24 ±0.30	45.17	22.10 ±0.64	23.07	0.83		17.38 ±2.52	
207	1.00	1.00(1)	40.75 ±0.10	45.12	22.15 ±0.57	22.97	0.81		16.25 ±1.73	
Mean, S.D.	-	-	40.59 ±0.57	45.20 ±0.44	21.74 ±0.44	23.46 ±0.42	0.82 ±0.02		16.34 ±2.60	

Notes:
- • Maximum applied vertical stress in the consolidometer.
- ‡ Preconsolidation pressure obtained from Casagrande Construction method.
- † Calculated from the mean.

No Standard Deviation means one measurement only.

Table 4.2: Unconsolidated Undrained Tests on Resedimented Boston Blue Clay III.

Test Number	Batch Number	Initial W_c (%)	σ'_s* (ksc)	B value	S_u (ksc)	ϵ_a (%) at Failure	Type of Failure	Remarks
1	203	41.0	0.125	1.00	0.175	2.1	Bulge	
2	204	40.5	0.068	1.00	0.083	1.2	Wedge‡	low u_c
3	204	41.0	0.110	1.00	0.171	2.4	Bulge	
4	205	41.0	0.037	1.00	0.121	1.2	Wedge‡	low u_c
7	206	41.0	0.113	1.00	0.202	4.0	Bulge	
8	207	40.8	0.060	1.00	0.112	1.5	Wedge‡	low u_c
9	205	40.5	0.138	1.00	-	-	-	Half Height Sample
10	207	40.5	0.121	1.00	-	-	-	Half Height Sample

Notes:
* Initial effective stress.
‡ Distinct rupture surface.

Table 4.3: Results of Consolidometer Tests for Resedimented Boston Blue Clay III.

Batch No.	H_c* (cm)	w_c† (%)	e_c†	σ'_{vm}* (ksc)	C_c (stress range, ksc)			C_s (stress range, ksc)		C_k from e-lgk	Remarks
					0.125-0.25	0.25-0.50	0.50-1.00	1.00-0.50	0.50-0.25		
200	10.272	41.10	1.145	1.00	0.482	0.509	0.409	-	0.010	0.686	
201	13.490	39.42	1.100	1.00	0.641	0.419	0.522	0.010	0.020	0.748	low w_c
202	13.822	40.67	1.132	1.03	0.568	0.453	0.453	0.011	0.006	0.813	
203	13.757	40.70	1.133	1.00	0.568	0.608	0.518	-	-	0.928	
204	13.238	40.19	1.119	1.01	0.512	0.487	0.463	-	-	0.676	
205	13.682	40.66	1.132	1.00	0.661	0.508	0.402	-	-	0.772	
206	11.646	41.24	1.148	0.98	0.548	0.439	0.416	0.023	0.025	0.728	
207	14.624	40.75	1.135	1.00	0.477	0.412	0.409	0.023	0.023	0.659	
Mean S.D.	-	40.59 ±0.57	-	-	0.557 ±0.068	0.479 ±0.064	0.449 ±0.049	0.017 ±0.007	0.017 ±0.008	0.751 ±0.088	

Notes:

* Final sample height.
† Final water content from Table 4.1.
† Final void ratio.
* Maximum applied vertical stress.

Table 4.4: Results of Oedometer Tests on Samples from Batches of Resedimented Boston Blue Clay III.

Test No.	Batch Label	Age t_s (days)	e_i	w_i (%)	σ'_p (ksc)	CR (stress range, ksc)			RR	SR	$\frac{RR}{SR}$	$\frac{CR}{RR}$ OCR=4	C_k from e-lgk
						1-2	2-4	4-8	2-8-2	16-2			
1	200-1[1]	23	1.127	40.47	1.05	0.187	0.162	0.141	0.012	0.015	0.76	11.8	0.44
2	200-2	24	1.179	42.33	1.08	0.152	0.173	0.139	0.010	0.018	0.54	13.9	0.49
3	200-3	79	1.160	41.66	1.00	0.187•	0.154	0.138	0.015	0.015	1.06	9.2	0.43
4	201	1	1.168	41.94	0.98	0.147•	0.165	0.138	0.012	0.016	0.77	11.5	0.57
5	202	9	1.164	41.80	0.98	0.159•	0.165	0.154	0.012	0.018	0.67	12.8	0.50
6	202-D[2]		1.133	40.70	1.00		0.189†						0.30
7	203-D		1.139	40.90	1.00		0.183†						0.33
8	204-T[3]	61	1.135	40.76	0.98	0.176•	0.156	0.152	0.025	0.010	2.45	6.1	0.45
9	204-B[4]	61	1.127	40.47	0.95	0.182•	0.155	0.165	0.008	0.015	0.55	20.6	0.55
10	205-T	248	1.115	40.03	1.00	0.156•	0.159	0.142	0.012	0.013	0.93	11.8	0.49
11	205LSD	257	1.115	40.04	1.00	0.172•	0.164	0.135	0.011	0.020	0.55	12.5	0.49

Table 4.4: (Cont.)

Test No.	Batch Label	Age t_s (days)	e_i	w_i (%)	σ'_p (ksc)	CR (stress range,ksc)			RR	SR	$\frac{RR}{SR}$	$\frac{CR^{\ddagger}}{RR}$ OCR=4	C_k from e-lgk
						1-2	2-4	4-8	2-8-2	16-2			
12	206-T	1	1.147	41.18	0.98	0.134	0.150	0.145	0.013	0.015	0.88	11.2	0.47
13	206-B	1	1.145	41.11	0.98	0.139	0.156	0.155	0.014	0.016	0.88	11.1	0.57
14	207-T	40	1.114	40.00	1.00	0.132•	0.159	0.152	0.016	0.017	0.96	9.5	0.50
Mean S.D	-	-	-	-	-	0.160 ±0.020	0.164 ±0.011	0.146 ±0.009	0.013 ±0.004	0.016 ±0.002	0.92 ±0.51	11.8 ±3.4	0.47 ±0.08

Note:
[1] Test Number on the Batch.
[2] Results obtained from DSS consolidation.
[3] Specimen taken at the top of the Consolidometer.
[4] Specimen taken at the bottom of the Consolidometer.
‡ CR taken from 4-8 ksc load increment.
• CR taken from 1.2-2 ksc load increment.
† CR taken from 1.5-3 ksc load increment.

Table 4.5: Interpretation of ϵ_{100} from a Typical Oedometer Load Increment (Refer to Figure 4.19, Batch No.207, σ'_{vc}= 4 to 8 ksc).

Tangent to point at time t (minutes)	Time at EOP, t_{100} (minutes)	Strain at EOP, ϵ_{100} (%)	Rate of 2nd. Compression $C\alpha\epsilon$	Compression Ratio, CR	Ratio of $C\alpha\epsilon$/CR
30	6.1	15.06	0.606	13.32	0.045
100	7.2	15.17	0.483	13.69	0.035
1000	12.0	15.62	0.260	15.18	0.017

Notes:

1. EOP: End of Primary
2. CR is assumed to be, $CR = \frac{\epsilon_{100} - 11.05\%}{\log (8/4)} / 100$

Table 4.6: Summary of Lateral Stress Oedometer Test Results.

Increment Numbernt	Load or Unload	σ'_v (ksc)	σ'_h (ksc)	K_o	OCR	ϵ_{100} (%)
1	Loading	0.25	0.26	1.044	4.00	0.38
2		0.50	0.32	0.640	2.00	0.80
3		0.80	0.43	0.533	1.25	1.47
4		1.20	0.65	0.538	1.00	3.10
5		2.00	1.05	0.525	1.00	7.25
6		4.00	2.06	0.515	1.00	12.40
7		8.00	4.18	0.522	1.00	16.40
8	Unloading	4.00	2.88	0.720	2.00	16.24
9		2.00	1.92	0.959	4.00	15.74
10	Loading	4.00	2.41	0.602	2.00	16.00
11		8.00	4.16	0.520	1.00	17.03
12		12.00	6.31	0.526	1.00	19.00
13		16.00	8.36	0.522	1.00	20.62
14	Unloading	14.00	7.53	0.538	1.14	20.62
15		12.00	7.02	0.585	1.33	20.61
16		10.00	6.20	0.620	1.60	20.54
17		6.00	4.73	0.788	2.67	20.30
18		4.00	3.62	0.904	4.00	20.03
19		2.00	2.22	1.111	8.00	19.70
20		1.00	1.36	1.360	16.00	18.70

Table 4.7: Results of Geonor CK_0UDSS Tests on Different Series of BBC at OCR=1.

Reference (Series)	Test No.	Batch No.	w_c (%)	σ'_{vc} (ksc)	ϵ_v (%)	At Peak τ_h					At τ_h/σ'_v Maximum					$\frac{G_{50}}{\sigma'_{vc}}$	Remarks
						γ (%)	$\frac{\tau_h}{\sigma'_{vc}}$	$\frac{\sigma'_v}{\sigma'_{vc}}$	$\frac{\tau_h}{\sigma'_v}$	ϕ (°)	γ (%)	$\frac{\tau_h}{\sigma'_{vc}}$	$\frac{\sigma'_v}{\sigma'_{vc}}$	$\frac{\tau_h}{\sigma'_v}$	ϕ (°)		
Ladd & Edgers, 1972 (BBC Ib)	202	200	37.4	4.0	15.5	6.0	0.211	0.566	0.372	20.4	32.5	0.128	0.199	0.643	32.8	33	
	301	300	37.2	3.0	13.7	4.5	0.199	0.575	0.346	19.1	33.1	0.098	0.141	0.695	34.8	50	
	303	300	35.6	8.0	17.0	6.2	0.194	0.565	0.342	18.9	29.8	0.111	0.210	0.525	27.7	26	
	1301	1300	35.2	4.0	9.9	5.4	0.187	0.567	0.330	18.3	Not Reached					43	
	1303	1300	35.6	8.0	15.0	9.0	0.196	0.531	0.369	20.3	Not Reached					30	
	Mean ±S.D	-	36.2 1.0	-	-	6.2 1.7	0.197 0.009	0.561 0.017	0.352 0.018	19.4 0.9	31.8 1.8	0.112 0.015	0.184 0.037	0.621 0.087	31.8 3.7	36 10	
Malek, 1987 (BBC II)	S1	111	39.8	3.1	10.1	2.4	0.201	0.592	0.340	18.8	Data Not Available					57	Low γ @ τ_{hmax}
	S2	111	39.7	3.1	10.1	10.7	0.192	0.447	0.430	23.2	Data Not Available					34	Good test
	S3	111	39.2	4.0	10.8	6.8	0.214	0.515	0.416	22.6	Data Not Available					50	Good test
	S4	111	39.5	4.0	10.0	6.8	0.195	0.505	0.386	21.1	Data Not Available					36	Good test
	S5	112	39.2	6.0	16.4	3.5	0.222	0.678	0.327	18.1	Data Not Available					50	High τ_{hmax}
	Mean ±S.D	-	39.6 0.3	-	-	6.7 3.4	0.201 0.010	0.515 0.060	0.393 0.040	21.4 2.0	Data Not Available					44 11	Excluding Test No.S5

Table 4.7: (Cont.)

Reference (Series)	Test No.	Batch No.	w_c (%)	σ'_{vc} (ksc)	ϵ_v (%)	At Peak τ_h					At τ_h/σ'_v Maximum					$\frac{G_{s0}}{\sigma'_{vc}}$	Remarks
						γ (%)	$\frac{\tau_h}{\sigma'_{vc}}$	$\frac{\sigma'_v}{\sigma'_{vc}}$	$\frac{\tau_h}{\sigma'_v}$	ϕ' (°)	γ (%)	$\frac{\tau_h}{\sigma'_{vc}}$	$\frac{\sigma'_v}{\sigma'_{vc}}$	$\frac{\tau_h}{\sigma'_v}$	ϕ' (°)		
Walbaum, 1983 (BBC III)	1	200	39.9	12.2	-	8.1	0.202	0.538	0.376	20.6	30.1	0.109	0.215	0.507	26.9	40	Incr. Consol.
	2	201	40.6	11.4	-	8.2	0.184	0.462	0.398	21.7	24.0	0.127	0.243	0.523	27.6	32	CRSC (low τ_f)
	3	201	41.5	11.6	-	6.0	0.195	0.543	0.359	19.8	27.4	0.114	0.219	0.521	27.2	27	CRSC
	4	201	40.9	11.4	-	6.8	0.194	0.545	0.356	19.6	27.5	0.104	0.202	0.515	27.2	24	Incr. Consol.
	5	202	41.1	3.0	-	4.9	0.195	0.600	0.325	18.0	31.0	0.105	0.176	0.597	30.8	54	
	Mean	-	40.9	-	-	7.3	0.194	0.522	0.372	20.4	27.3	0.114	0.220	0.517	27.3	31	Excluding
	±S.D		0.6			1.1	0.007	0.040	0.019	1.0	2.5	0.010	0.017	0.007	0.3	7	Test No.5
DeGroot, 1989 (BBC III)	G1	200	41.1	3.0	14.6	4.7	0.191	0.561	0.340	18.8	24.9	0.133	0.252	0.516	27.8	59	Poor ϵ_v data.
	G2	200	40.8	3.0	15.3	5.4	0.213	0.528	0.403	22.0	25.0	0.132	0.214	0.627	31.7	69	Poor ϵ_v data.
	G3	200	41.0	3.0	15.2	5.5	0.205	0.542	0.379	20.7	24.4	0.134	0.237	0.593	29.5	73	Poor ϵ_v data.
	Mean	-	41.0	3.0	-	5.2	0.203	0.544	0.374	20.5	24.8	0.133	0.234	0.579	29.7	67	
	±S.D		0.2			0.4	0.011	0.017	0.032	1.6	0.3	0.001	0.019	0.057	2.0	7	
This Research, (BBC III)	DSS6	203	40.5	1.12	5.1	2.5	0.201	0.667	0.301	16.8	24.2	0.095	0.153	0.621	31.8	62	
	DSS7	204	40.1	1.30	5.2	3.1	0.202	0.606	0.333	18.4	26.2	0.111	0.158	0.702	35.1	59	
	Mean	-	40.3	-	-	2.8	0.202	0.637	0.317	17.6	25.2	0.103	0.156	0.662	33.5	61	
	±S.D		0.3			0.4	0.001	0.043	0.023	1.1	1.4	0.011	0.004	0.057	2.3	2	

Table 4.8: Index Properties of the Different Batches of Resedimented BBC (after Fayad, 1986).

Year	Researchers	Series	Source Batch	G_s	LL (%)	PL (%)	PI (%)	Clay Fr. <2μ (%)	Salt (g/l)	Remarks Remarks
1961	Bailey	Ia	MIT 1139	2.77	30.0 34.7	17.5 17.7	12.5 17.0	40	2-3 35	Low PI
1963	Jackson				36.2	19.5	16.7		16.7	Low PI
1964	Varallyay		S4 S5 S6		32.6 33.3 32.8	19.5 20.4 20.3	13.1 12.9 12.5	35	 16.8 16.0	Low PI
1965	Ladd R.S.	Ib		2.77	45	22	23		16	
1965	Preston		S1	2.77	45.6	23.4	22.2	35	24	
1966	Braathen		S2	2.77	45.4	23.1	22.3		22	
1967	Dickey				34.5	23.9	19.6			
1970	Kinner		100 150 200 300 400 800 900 1000 1100	2.78	43.5 43.5 38.1 39.7 39.4 41.5 41.2 41.1 42.0	19.6 19.6 17.8 21.6 21.3 19.5 18.7 19.5 20.6	23.9 23.9 20.3 18.1 18.1 22.0 22.5 22.6 21.4	50 52 52 48 54 58	 8 10 10 16 16 16 16	

Table 4.8: (Cont.)

Year	Researchers	Series	Source Batch	G_s	LL (%)	PL (%)	PI (%)	Clay Fr. <2μ (%)	Salt (g/l)	Remarks
1970	Kinner	I	1200		40.2	18.6	21.6	48	16	
			M101		40.7	19.6	21.1	52		
			M104		40.3	19.6	20.7			
			M107		41.3	19.6	21.7			
			M200		42.3	18.5	23.8	52		
			M400		39.8	18.9	20.9	47		
1971	Ladd et al.		160	2.78	38.1	17.8	20.3		8	
			1300		42.1	22.1	20.0		16	
			1500		43.8	20.6	23.2		16	
1984	Bensari	II	105	2.75	47.6	23.3	24.3		16	
			111	2.75	47.1	24.9	22.2		16	
1985	O'Neill		105-112	2.78	41.3	22.1	19.2	52	16	
1989	Author	III	200-207	2.78	45.2	21.7	23.5	58	16	See Table 4.1

Table 4.9: Comparison of Triaxial Compression Data Between BBC III and BBC II.

BBC Series (Ref.)	Test Number	Method of Consolidation * (OCR)	σ'_p(R) or σ'_{vm}(S) (ksc)	σ'_{vc} (ksc)	At Failure					$\frac{G_{50}}{\sigma'_p}$	Remarks
					$\frac{q_f}{\sigma'_p}$	$\frac{p'_f}{\sigma'_p}$	ϵ_{af} (%)	$\frac{\sigma'_{1f}}{\sigma'_{3f}}$	A_f		
II O'Neill (1985)	TC-1	R (4.0)	1.0	0.25	0.275‡	0.444	5.9	4.25	0.15	28	
	TC-2	R (4.0)	1.0	0.25	0.273	-	5.2	-	-	20	
	TC-3	R (4.0)	1.0	0.25	0.290	0.438	4.3	4.92	0.18	24	
	TC-4	R (4.0)	1.0	0.25	0.259	0.428	6.0	4.07	0.15	26	
	TC-6	R (4.0)	1.0	0.25	0.291	0.432	4.3	5.13	0.19	20	
	TC-7	R (4.0)	1.0	0.25	0.286	0.436	4.3	4.81	0.18	23	
	TCSHAN	S (4.0)	2.46	0.62	0.252	0.449	2.5	3.56	0.06	67	
II Fayad (1986)		S (4.1)	4.1	1.01	0.258	0.463	1.1	3.52	0.02	64	
III Sheahan (1990)		S (4.4)	6.2	1.42	0.206	0.395	3.6	3.18	0.13		
III This Research	CIUC-1	R (4.0)	1.0	0.25	0.219	0.395	3.0	3.49	0.17	20	
	CIUC-2	R (4.1)	1.0	0.25	0.227	0.335	1.2	5.22	0.30	29	

Notes:
- * S=SHANSEP, R=Recompression.
- ‡ All recompression values corrected for thixotropic effect.

Table 4.10: Comparison of Triaxial Extension Data Between BBC III and BBC II.

BBC Series (Ref.)	Test Number	Method of Consolidation • (OCR)	σ'_p(R) or σ'_{vm}(S) (ksc)	σ'_{vc} (ksc)	At Failure					$\frac{G_{50}}{\sigma'_p}$	Remarks
					$\frac{q_f}{\sigma'_p}$	$\frac{p'_f}{\sigma'_p}$	ε_{af} (%)	$\frac{\sigma'_{1f}}{\sigma'_{3f}}$	A_f		
II O'Neill (1985)	TE-1	R (4.0)	1.0	0.25	0.147‡	0.137	-10.0	28	0.90	6.9	
	TE-2	R (3.9)	1.0	0.26	0.159	-	-10.0	-	-	3.3	
	TE-5	R (4.0)	1.0	0.25	0.132	0.140	-10.3	34	0.93	3.5	
	TE-7	R (4.0)	1.0	0.25	0.147	0.169	-11.8	14	0.78	3.6	
	TE-10	R (4.0)	1.0	0.25	0.132	0.154	-12.4	13	0.83	1.8	
II Fayad (1986)		S (4.0)	4.0	1.00	0.157	0.260	-9.0	4.05	-0.08	12	
II Sheahan (1988)	SPC7349	S (3.3)	8.7	2.68	0.124	0.224	-13.2	3.48	0.81	8.4	
III This Research	CIUE-1	R (4.2)	1.0	0.24	0.095	0.162	-6.4	3.84	0.93	30	
	CIUE-2	R (4.3)	1.0	0.23	0.088	0.165	<-2.8	3.29	0.84	37	q_f not reached

Notes:
- • S=SHANSEP, R=Recompression.
- ‡ All recompression values corrected for thixotropic effect.

Table 4.11: CK_oU Triaxial Data on Resedimented Boston Blue Clay (Prepared by C.C. Ladd).

Reference (Year)	Batch	Shear		Consolidation			At Peak					At Maximum Obliquity				Remarks
		C/E	$\dot{\epsilon}$ %/hr	σ'_p (ksc)	K_c	OCR	ϵ_f (%)	$\frac{q_f}{\sigma'_{vc}}$	$\frac{p'_f}{\sigma'_{vc}}$	A_f	ϕ'_p (°)	ϵ_f (%)	$\frac{q_f}{\sigma'_{vc}}$	$\frac{p'_f}{\sigma'_{vc}}$	ϕ' (°)	
Ladd & Varallyay (1965)	Ia	C	1	4 & 6	0.53	1.00	0.3	0.328	0.751 ±0.010	0.58 ±0.04	26.0 ±0.4	7.8 ±1.4	0.230 ±0.007	0.415	33.7 ±1.4	LL=33% PI=13%
		E	1	4 & 6	0.54	1.00	10	0.154	0.251	1.18	37.7	Same				Necking
Lutz (1985)	II	C	0.5	6 @ 3 1 @ 1	0.47	1.00	0.16 ±0.07	0.319 ±0.003	0.726 ±0.015	0.63 ±0.13	26.1 ±0.4	NA				7 Tests
Fayad (1986)	II	C	0.5	4	0.47	1.00	0.07	0.334	0.740	0.32	25.9	NA				
				4	0.63	2.05	0.27	0.623 0.304‡	1.148 0.560‡	0.24	-	0.17	0.599 0.292‡	1.084 0.529‡		
				4	0.82	4.06	1.06	1.049 0.258‡	1.878 0.463‡	0.02	-	0.42	0.936 0.231‡	1.589 0.391‡		
				4	1.10	8.04	2.97	1.749 0.218‡	2.939 0.366‡	-0.05	-	0.60	1.312 0.163‡	2.008 0.250‡		
Sheahan (1988)	II	C	0.5	3	0.485	1.00	0.18 ±0.02	0.317 ±0.004	0.739 ±0.013	0.53 ±0.04	25.4 ±0.1	8.4	0.244	0.432	34.4	2 Tests except MO
		E	0.5	4	0.484	1.00	13.5	0.156	0.210	1.14	48.0	12.1	0.153	-	48.6	ϕ' too large
	III	C	0.5	2	0.529	1.00	0.13	0.309	0.776	0.44	23.5	23.5	0.210	0.396	32.0	

Table 4.11: (Cont.)

Reference (Year)	Batch	Shear		Consolidation			At Peak					At Maximum Obliquity				Remarks
		C/E	$\dot{\epsilon}$ %/hr	σ'_p (ksc)	K_c	OCR	ϵ_a (%)	$\frac{q}{\sigma'_{vc}}$	$\frac{p'}{\sigma'_{vc}}$	A	ϕ' (°)	ϵ_a (%)	$\frac{q}{\sigma'_{vc}}$	$\frac{p'}{\sigma'_{vc}}$	ϕ' (°)	
Sheahan (1990)	III	E(F)	0.5	2.8	0.464	1.0	14.3	0.135	0.219	1.16	38.1	12.0	0.134	0.207	40.3	
		C(F)	0.5	2.9	0.466	1.0	0.13	0.322	0.749	0.52	25.4	11.0	0.249	0.445	34.0	
				6.2	1.098	4.36	3.6	0.900 0.206‡	1.723 0.395‡	0.13	-	6.0	0.874 0.200‡	1.657 0.380‡	31.8	
		C(L)	0.5	2.8	0.473	1.0	0.18	0.322	0.752	0.35	25.4	13.9	0.245	0.430	34.7	
				4.0	0.760	1.99	0.99	0.536 0.269‡	1.125 0.565‡	0.20	-	9.9	0.461 0.209‡	0.846 0.425‡	33.0	
				6.0	1.054	3.99	2.95	0.866 0.217‡	1.694 0.425‡	0.12	-	13.3	0.783 0.196‡	1.472 0.369‡	32.2	

Note: ‡ Normalized to σ'_p instead of σ'_{vc}.
(F)=Fixed ends used in test.
(L)=Lubricated ends in test.

Table 4.12: Comparison of Experimental Data Between the Resedimented Boston Blue Clay and Natural Boston Blue Clay.

Experimental Parameters		Resedimented BBC III	Resedimented BBC II•	Natural BBC (MIT Campus)‡
Index Properties	G_s	2.78	2.78	≃ 2.75
	LL(%)	45.2±0.4 (8)	41.3± ? (5)	44.4±5.4 (18)
	PL(%)	21.7±0.4 (8)	22.1± ? (5)	22.6±2.8 (18)
Consolid. Properties	C_c	0.34±0.02(12)[1]	0.33±0.02 (7)	0.37±0.08(30)
	C_r	0.03±0.01(12)[2]	0.03±0.001(2)	0.06±0.02(13)
	C_s	0.03±0.01(12)[3]	-	0.06±0.01(30)
	C_v(4-8) (cm^2/s)	0.0024 ±0.0005(12)	0.004 ± ? (7)	0.0095 ±0.0030 (4)
Triaxial (CK_oUC) OCR = 1	S_u/σ'_{vc}	0.318±0.008(3)	0.317±0.004(2)	0.32±0.01 (2)
	ϵ_a(%)	0.147±0.029	0.183±0.023	0.28±0.11
	A_f	0.44±0.09	0.53±0.04	0.55±0.04
Triaxial (CK_oUE) OCR = 1	S_u/σ'_{vc}	0.135 (1)	0.156 (1)	0.143 (1)
	ϵ_a(%)	14.3	13.5	11.6
	A_f	1.16	1.14	1.16

Notes:

• Data from O'Neill (1985)
‡ Data from Ladd & Luscher (1965)
1 Values taken from a stress of 4-8 ksc
2 Values taken from a stress of 2-8 ksc
3 Values Taken from a stress of 16-2 ksc

Parathesis = number of tests.

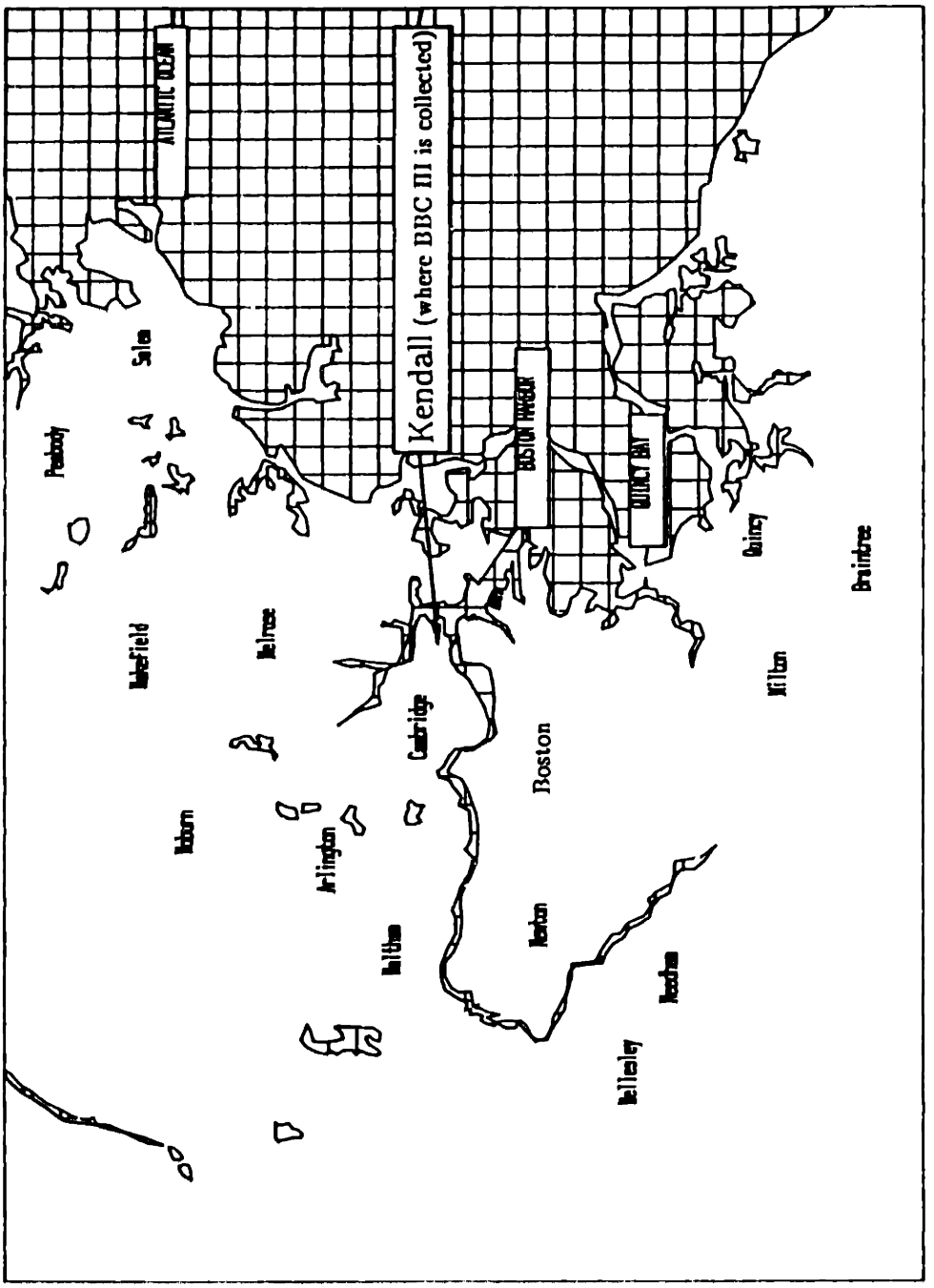

Figure 4.1: Location of the Site where Boston Blue Clay (III) was collected.

RECYCLING OF RESEDIMENTED BOSTON BLUE CLAY

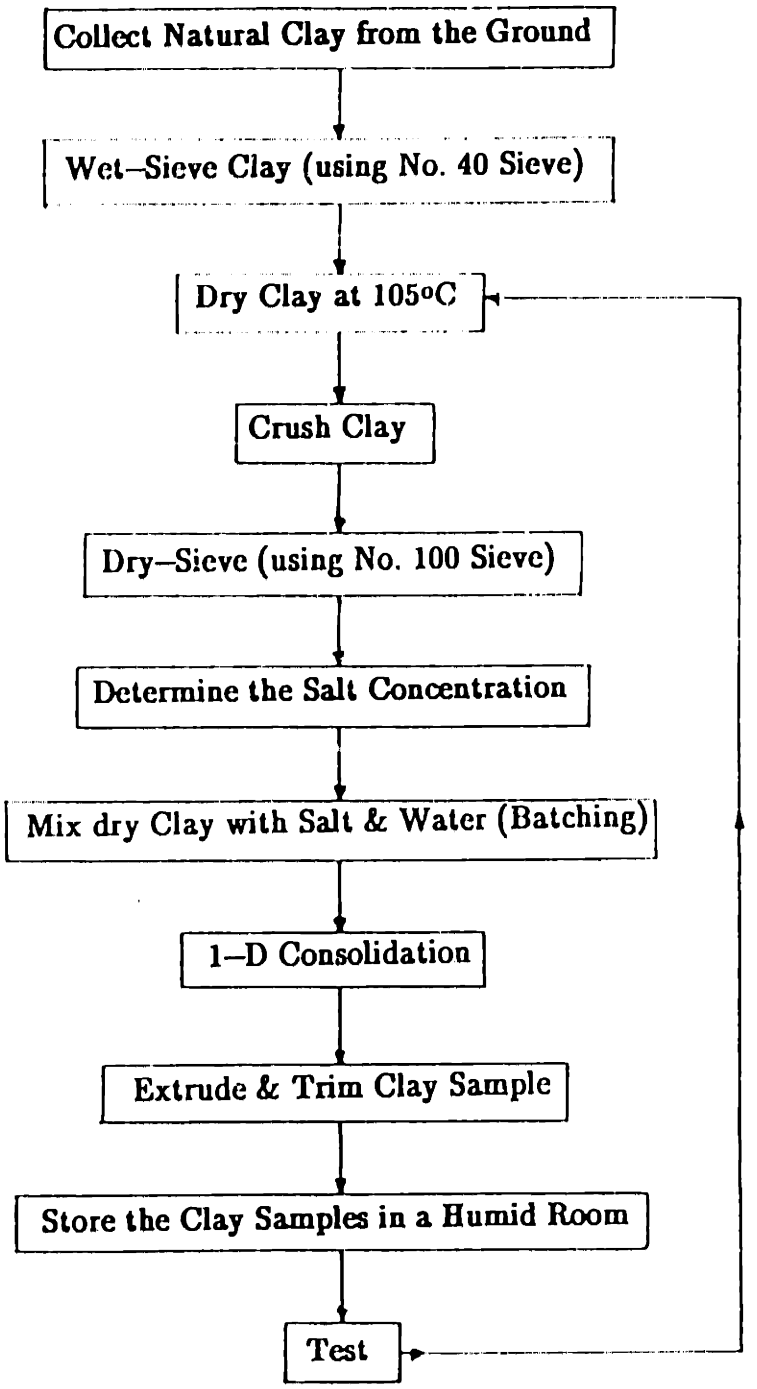

Figure 4.2: Recycling of Resedimented Boston Blue Clay for Testing.

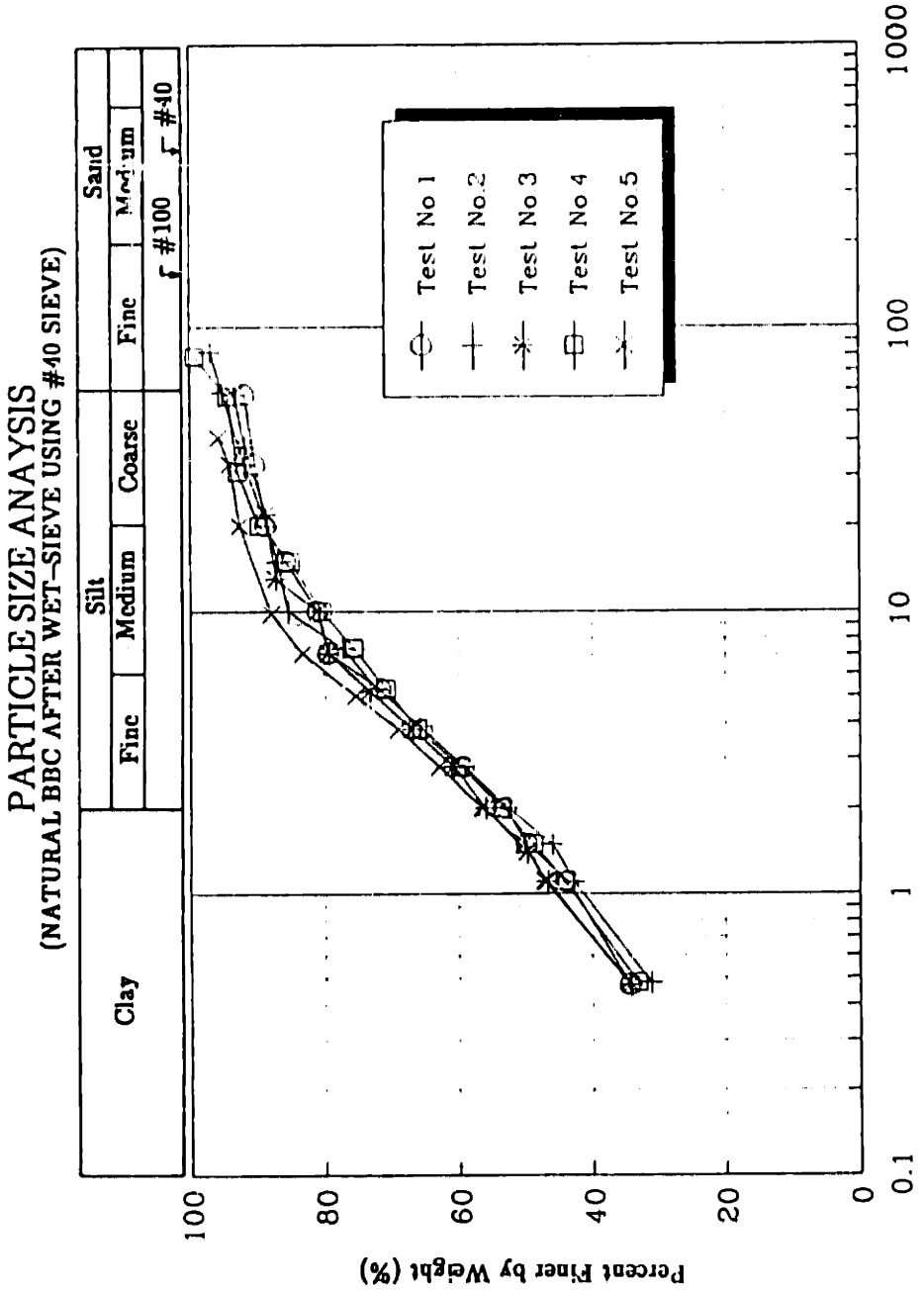

Figure 4.3: Particle Size Distribution of BBC III after Wet–Sieve.

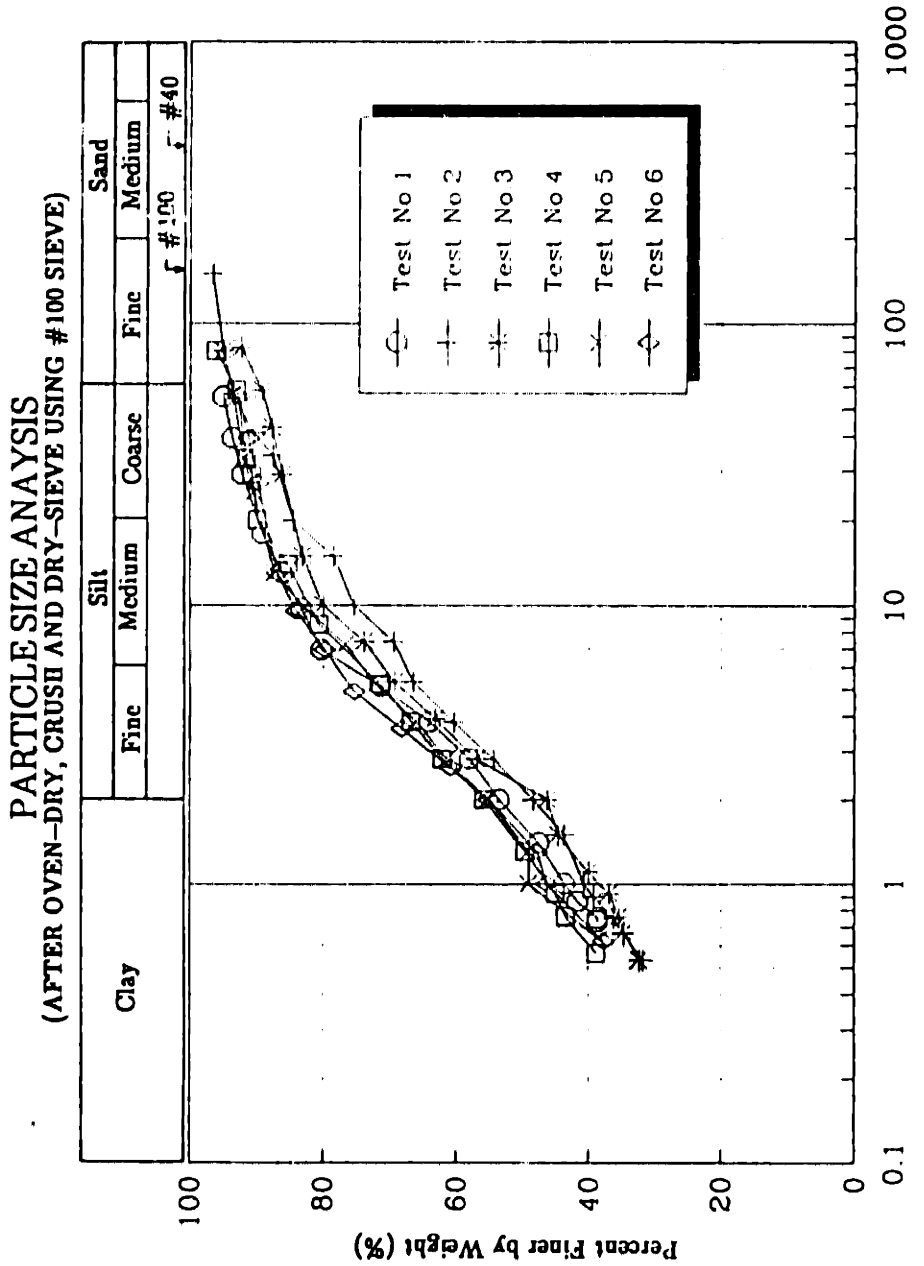

Figure 4.4: Particle Size Distribution of Post–Processed BBC III.

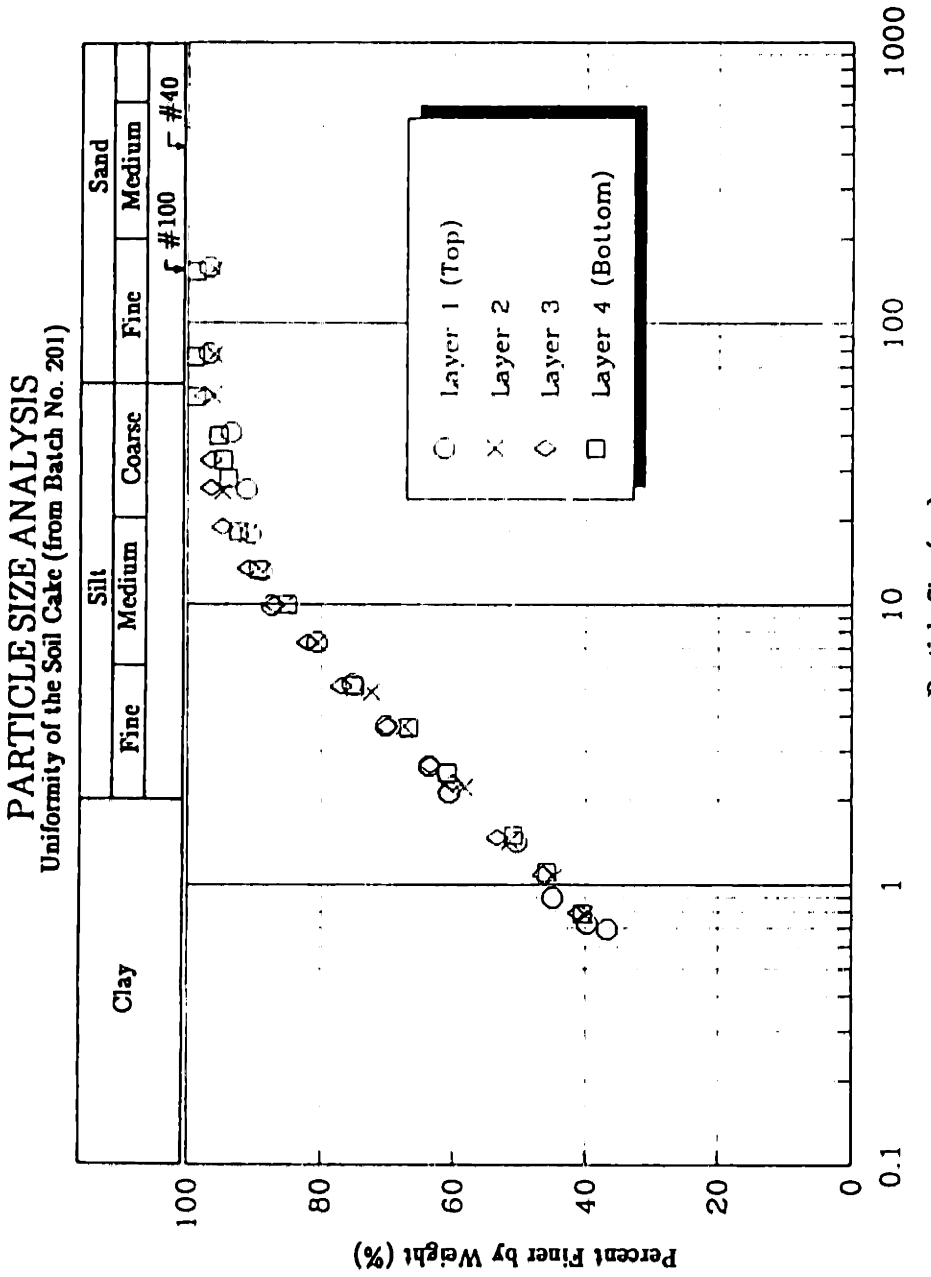

Figure 4.5: Particle Size Distributions of Four Layers from Batch 201 BBC III.

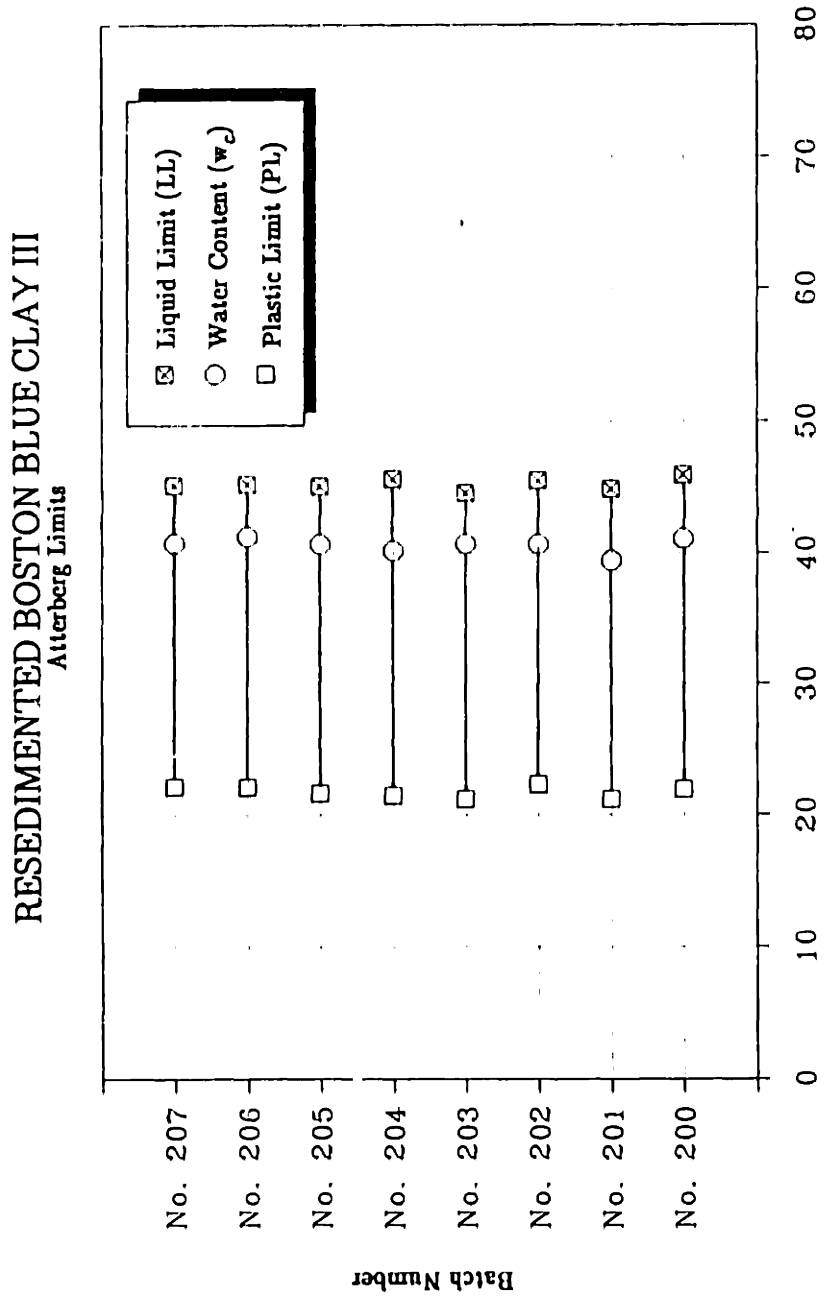

Figure 4.6: Atterberg Limits of Eight Batches of BBC III.

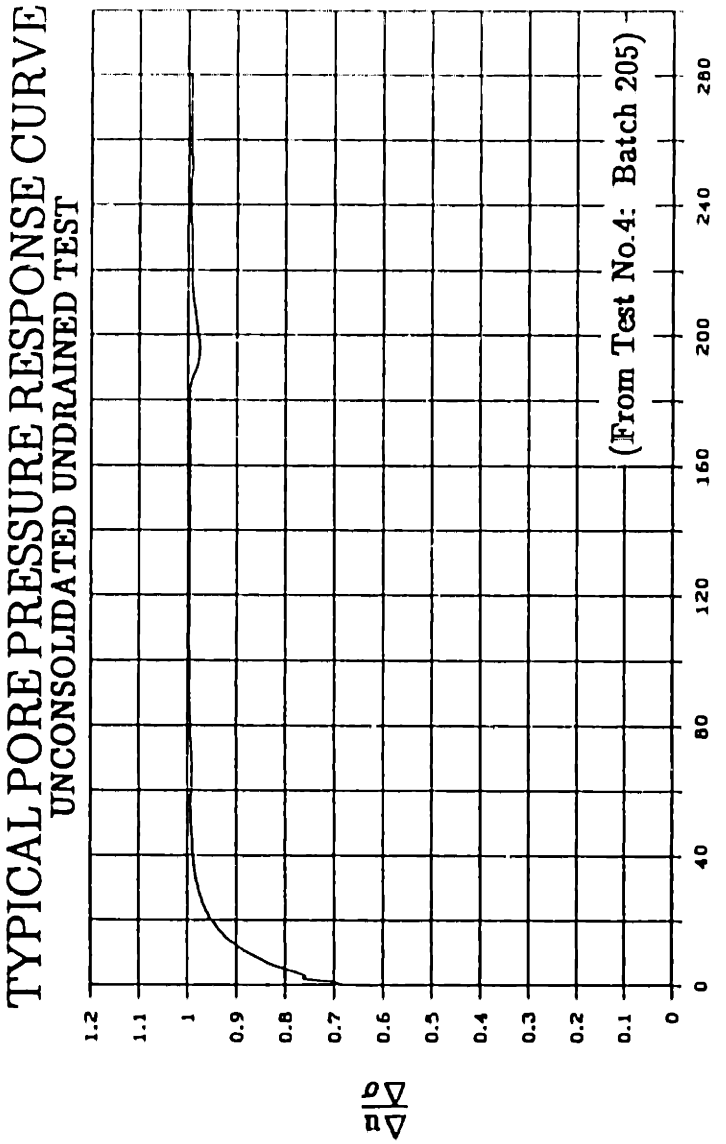

Figure 4.7: Typical Pore Water Pressure Response Curve of an Unconsolidated Undrained Triaxial BBC Sample.

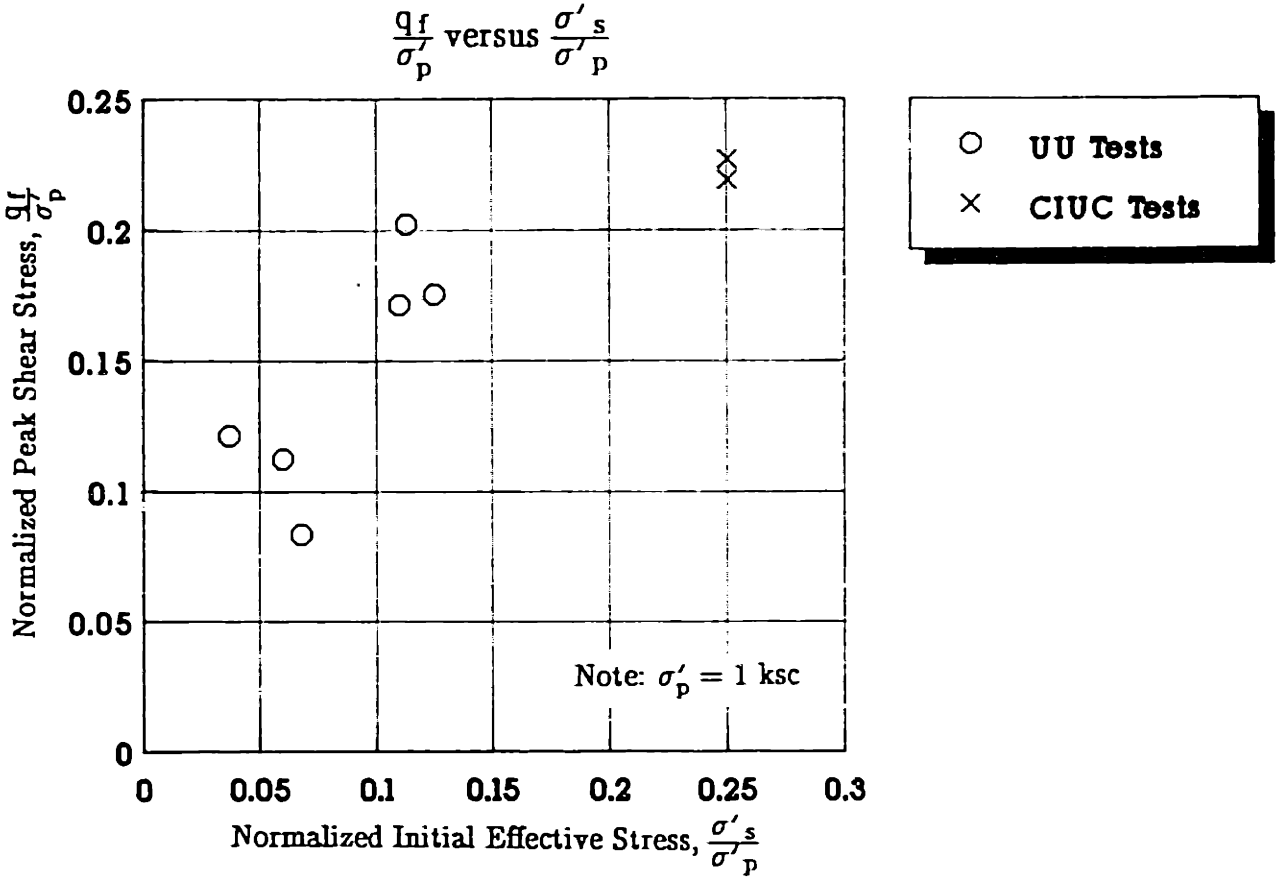

Figure 4.8: Normalized Peak Shear Stress versus Normalized Initial Effective Stress for UU and CIUC Triaxial Tests.

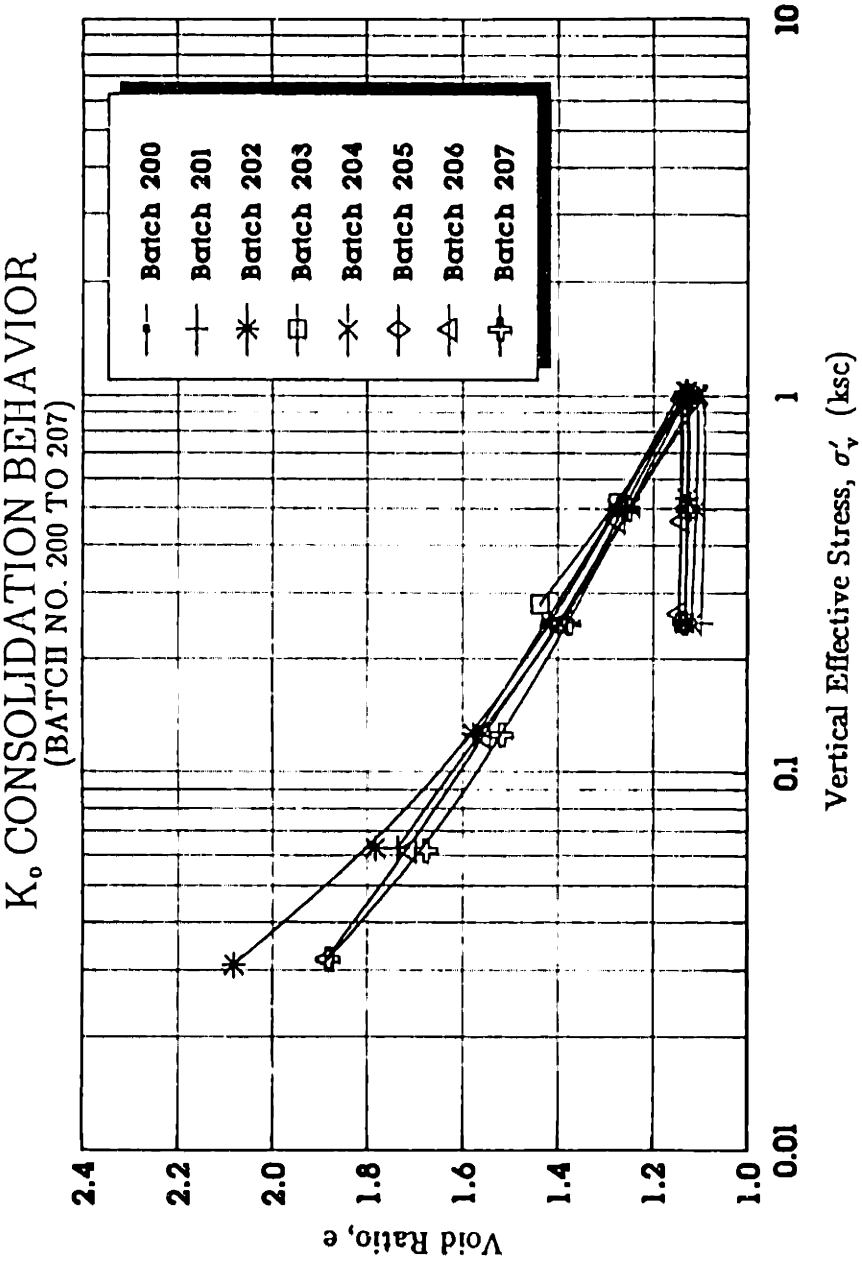

Figure 4.9: Compression Curves of Eight Batches of BBC from the Large Consolidometer Tests.

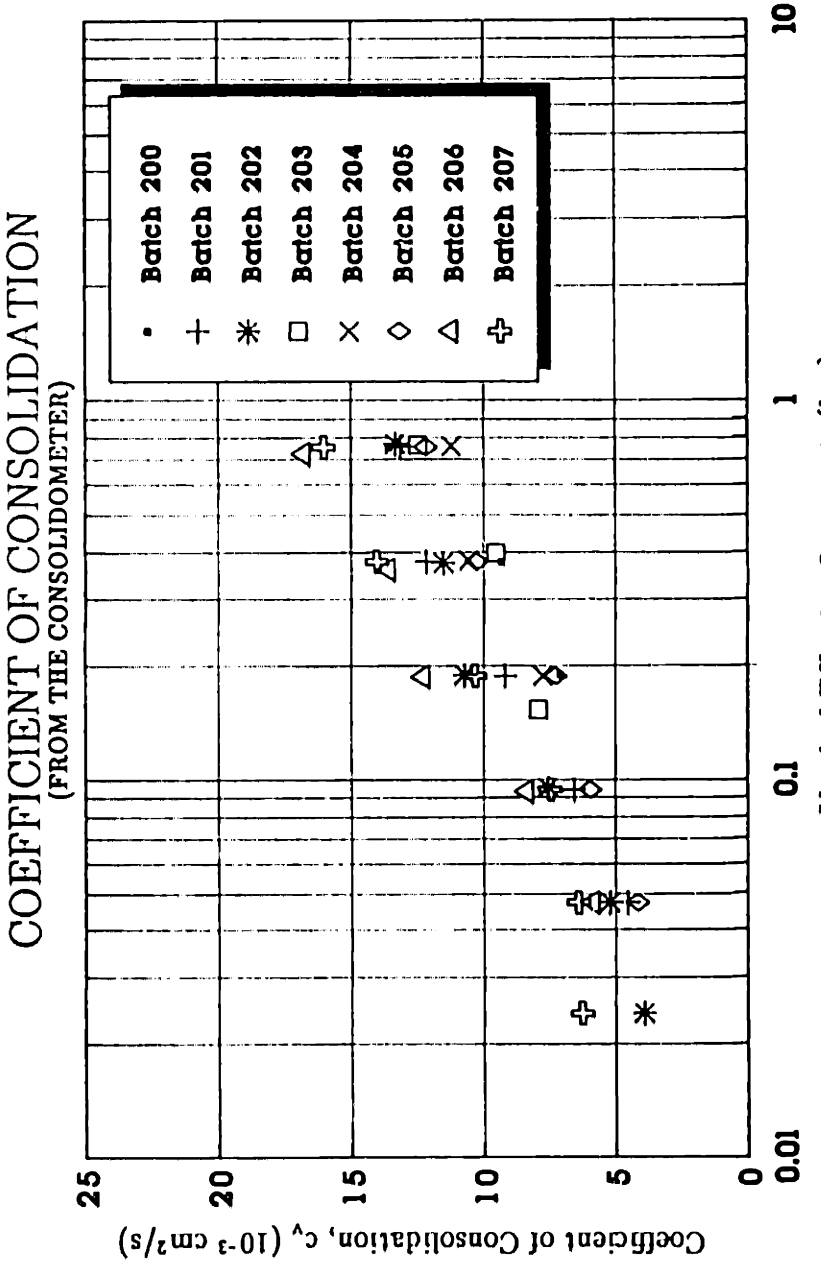

Figure 4.10: Relationship between Coefficient of Consolidation and Vertical Effective Stress for Eight Batches of BBC III.

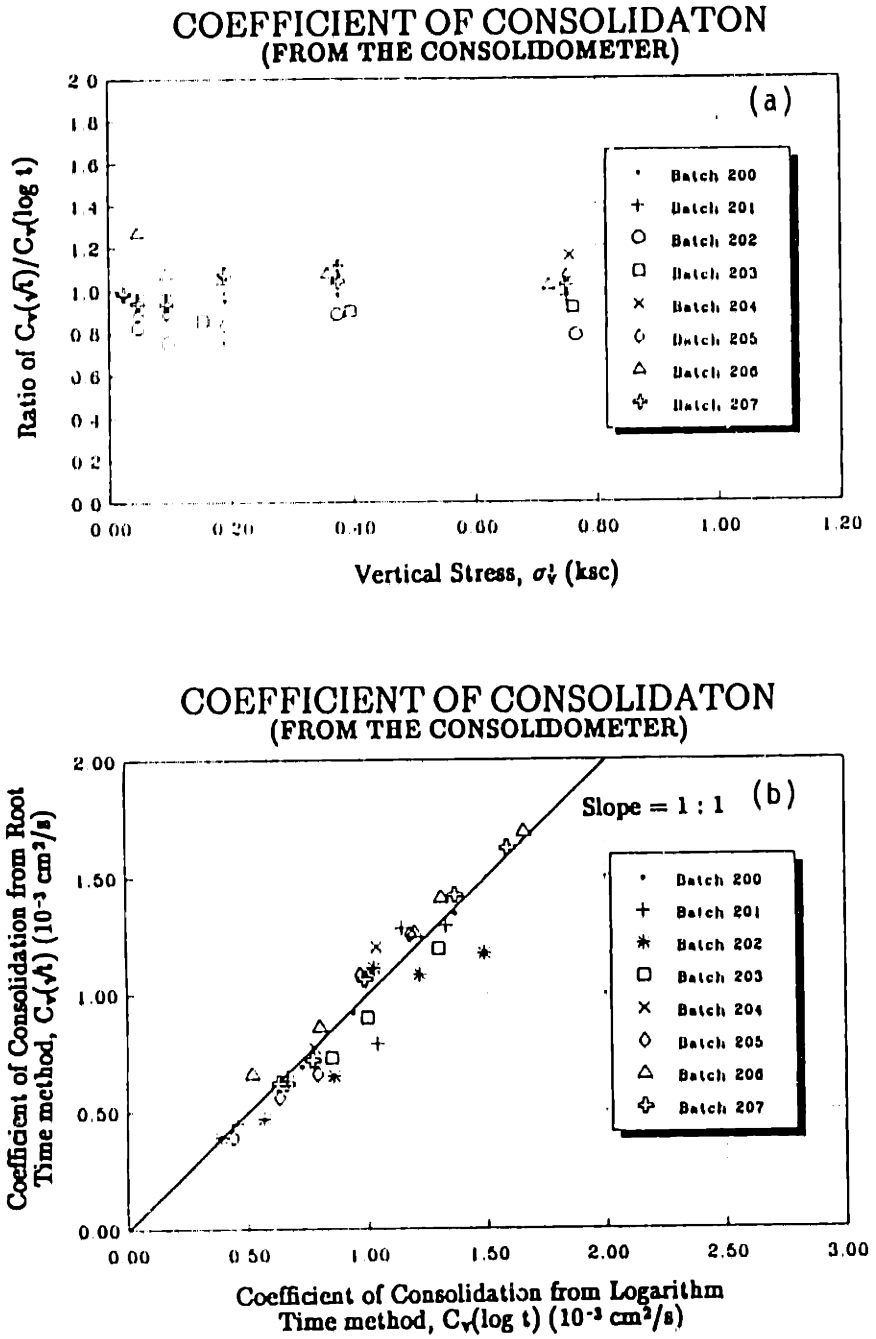

Figure 4.11: Coefficients of Consolidation of Eight Batches of BBC: (a) Ratio of $C_v(\sqrt{t})/C_v(\log t)$ versus Vertical Stress; (b) $C_v(\sqrt{t})$ versus $C_v(\log t)$.

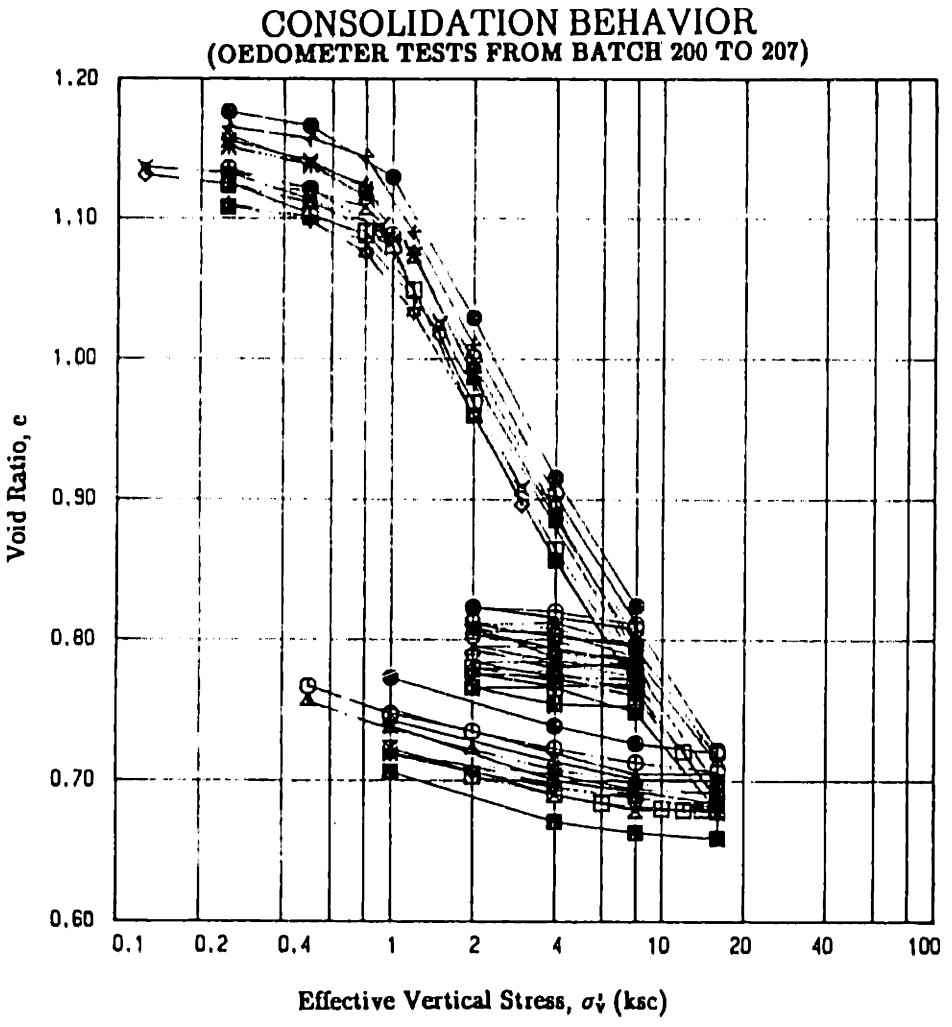

SYMBOL	BATCH NO.	POSITION
■	200	1ST TEST
●	200	2ND TEST
▲	200	3RD TEST
+	201	
×	202	Top
◇	202	DSS
⋈	203	DSS

SYMBOL	BATCH NO.	POSITION
✳	204	Top
⧖	204	Bottom
✿	205	Top
⊡	205	LSO
⊖	206	Top
⧋	206	Bottom
+	207	Top

Figure 4.12: Void Ratio versus Vertical Effective Stress for Twelve Oedometer Tests and Two DSS Tests from DeGroot (1989).

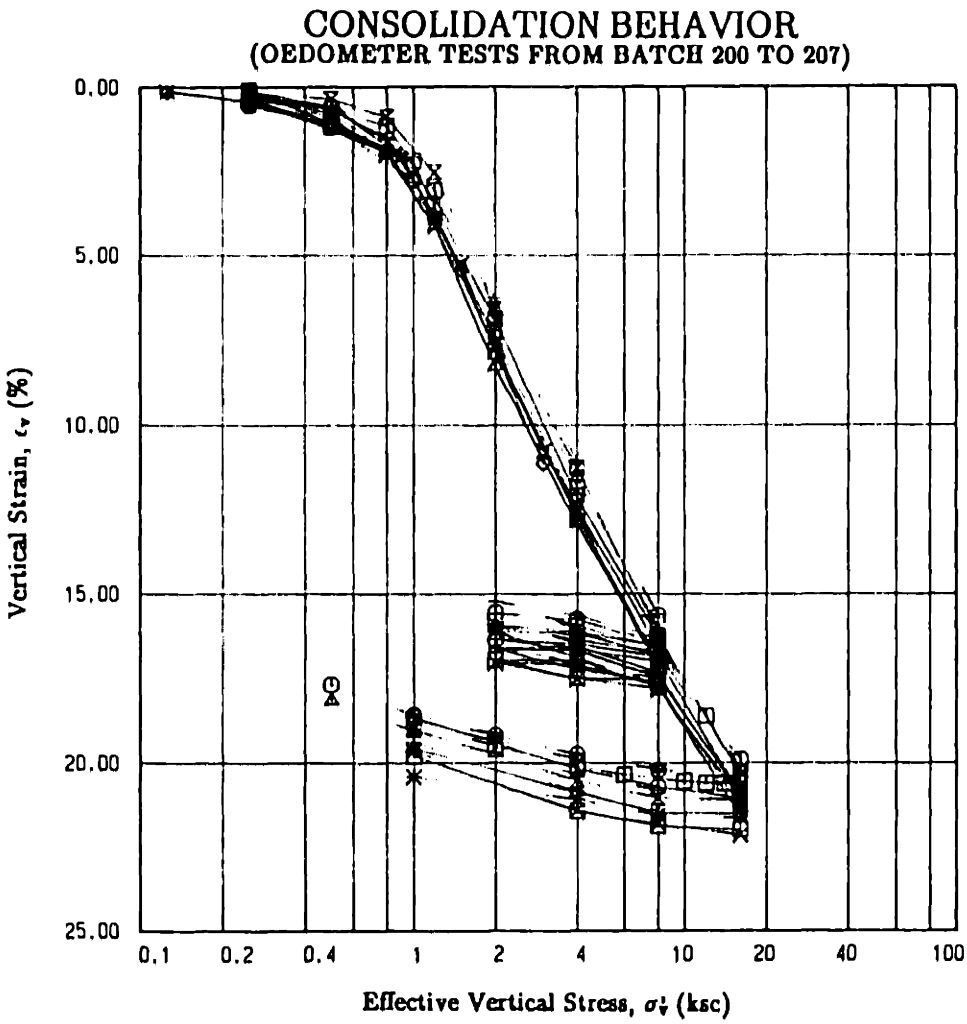

Figure 4.13: Vertical Strain versus Vertical Effective Stress for Twelve Oedometer Tests and Two DSS Tests from DeGroot (1989).

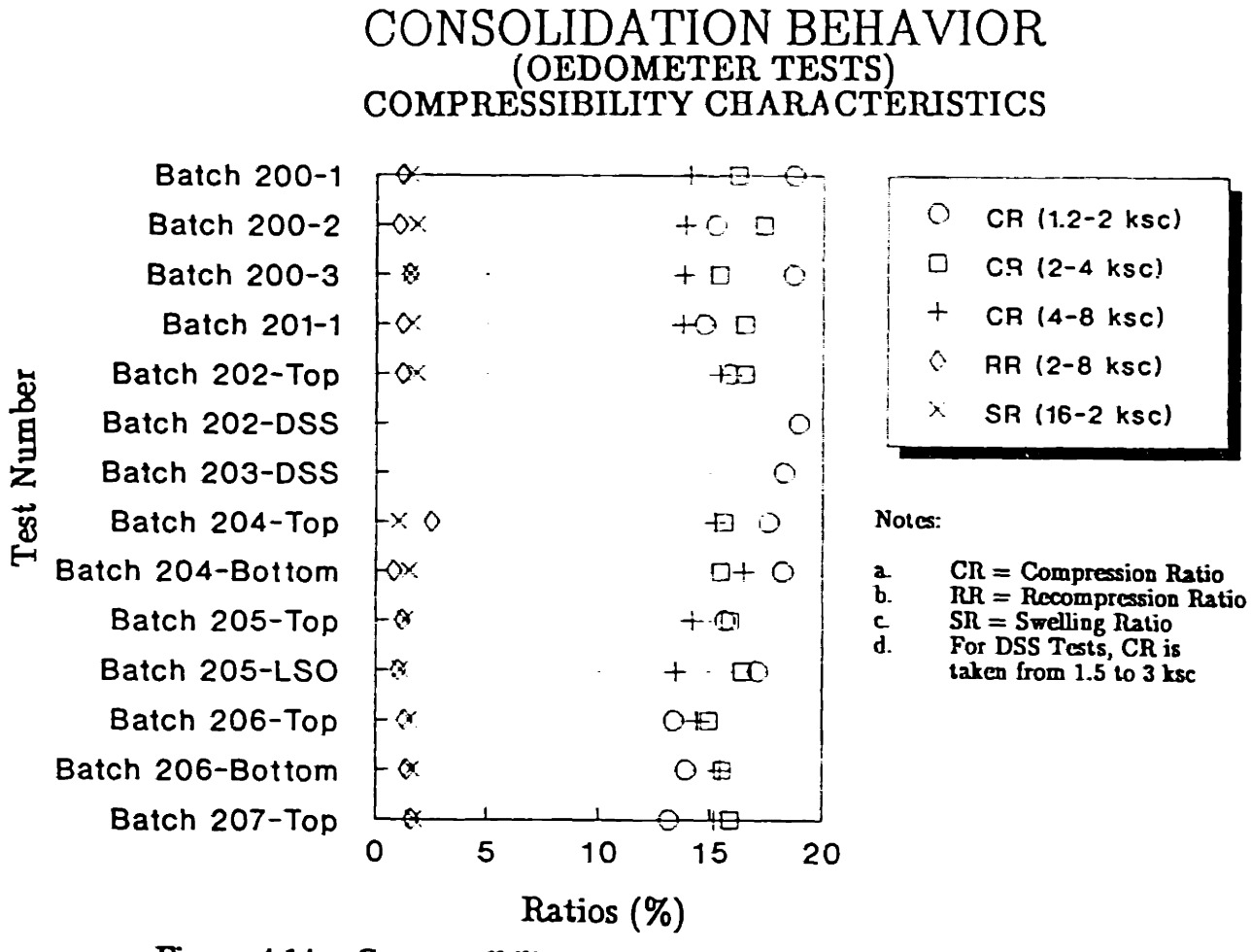

Figure 4.14: Compressibilities of Twelve Oedometer and Two DSS Tests.

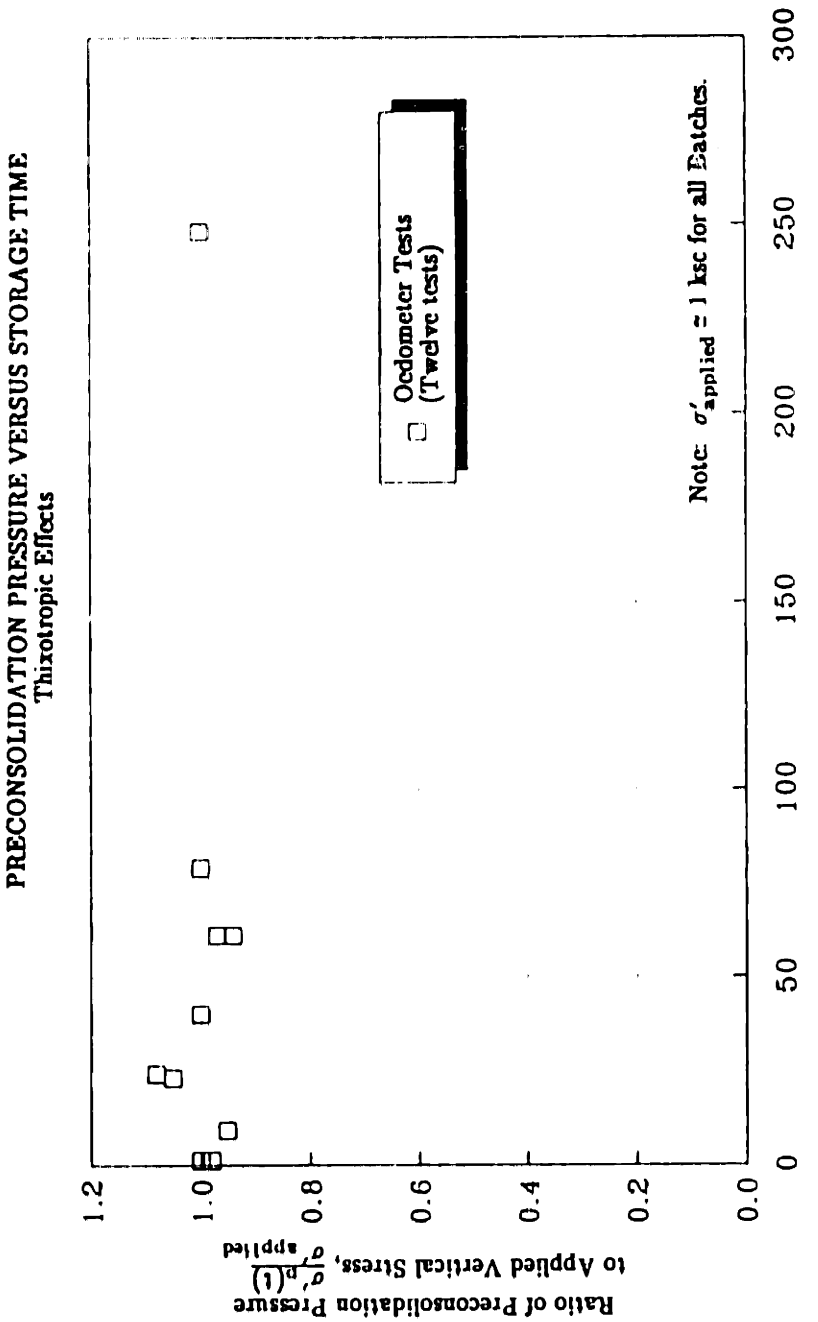

Figure 4.15: Ratio of Preconsolidation Pressure to Applied Vertical Stress versus Storage Time.

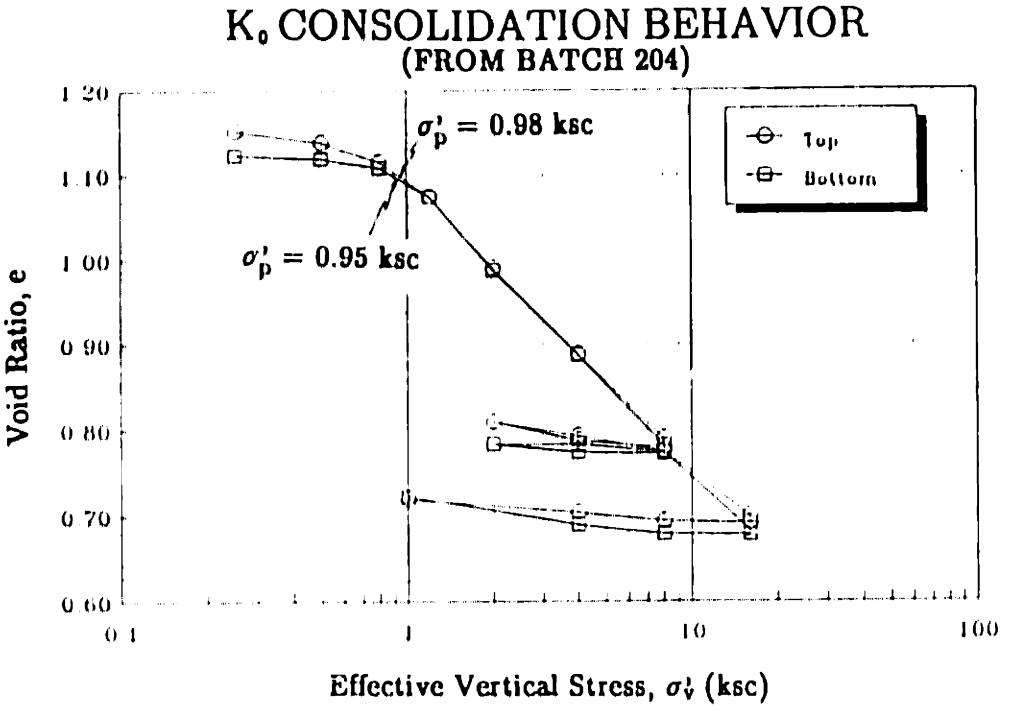

Figure 4.16: Void Ratio versus Vertical Effective Stress for Two Oedometer Tests from Batch 204.

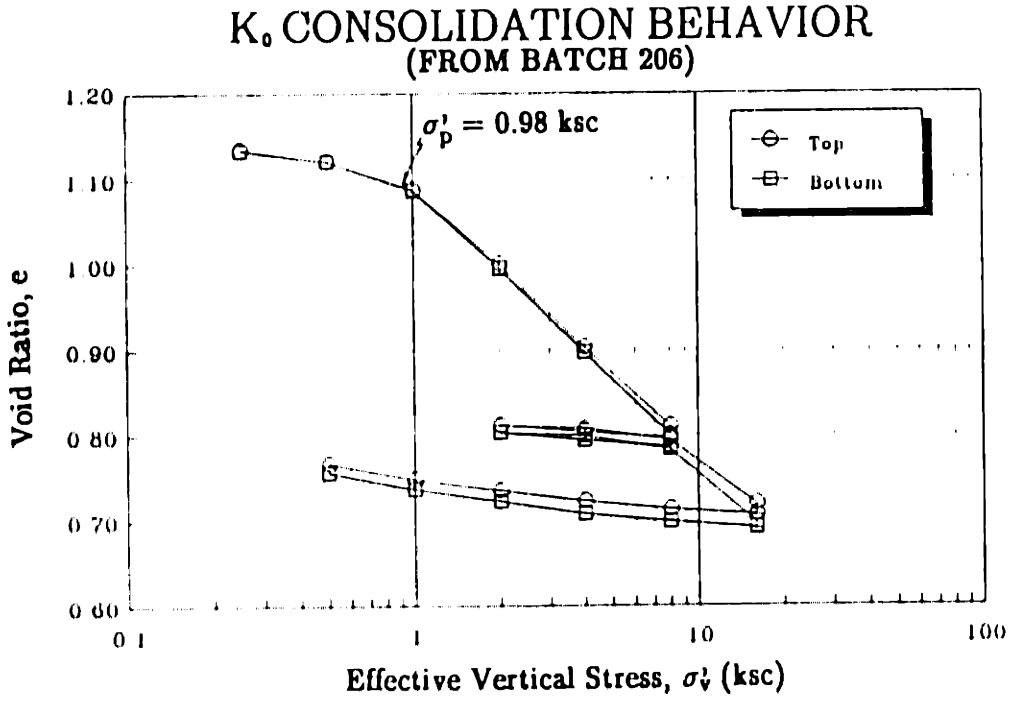

Figure 4.17: Void Ratio versus Vertical Effective Stress for Two Oedometer Tests from Batch 206.

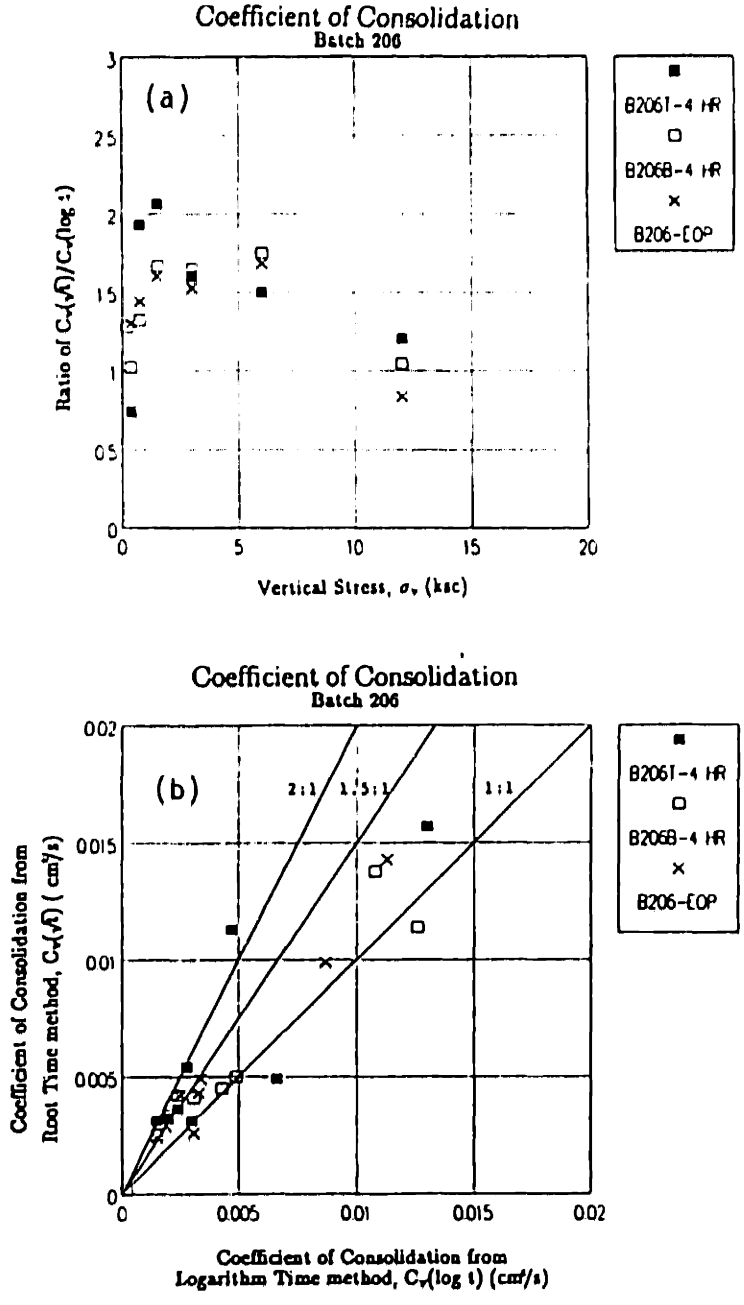

Figure 4.18: Coefficients of Consolidation of Three Oedometer Tests from Batch 206: (a) Ratio of $C_v(\sqrt{t})/C_v(\log t)$ versus Vertical Stress; (b) $C_v(\sqrt{t})$ versus $C_v(\log t)$.

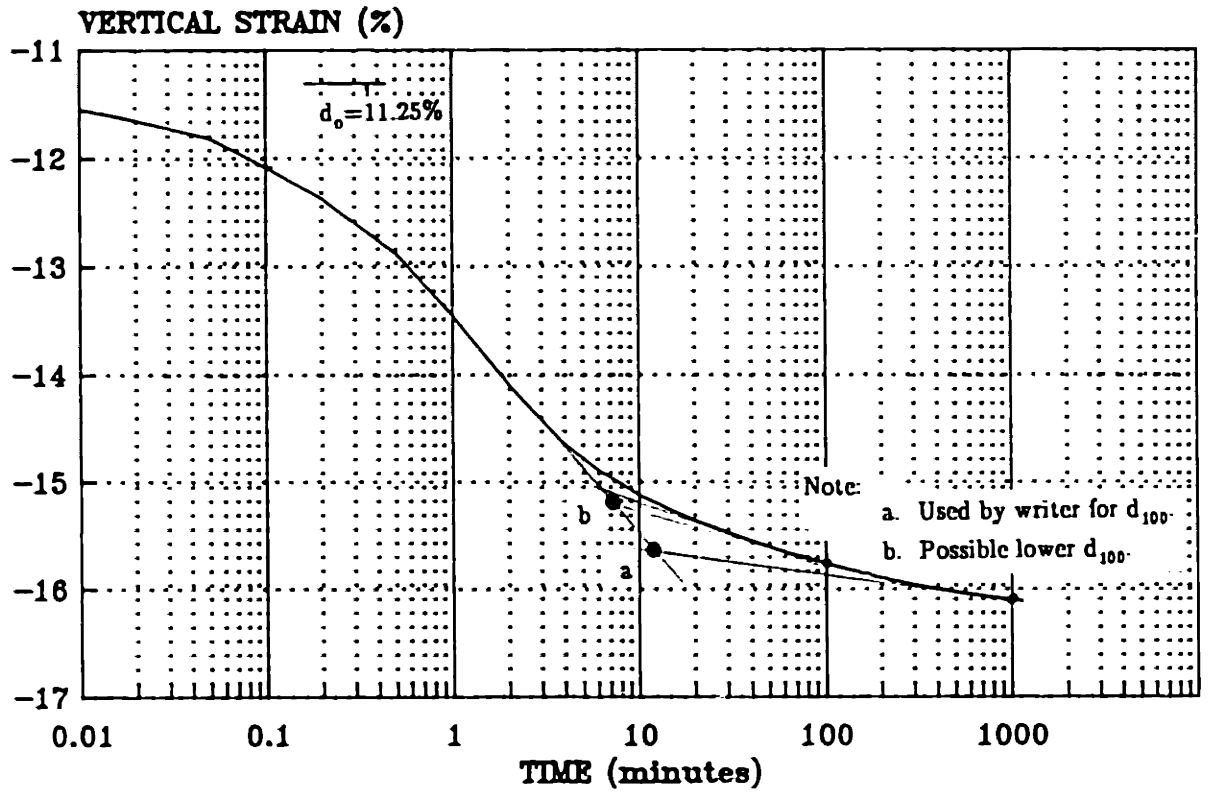

Figure 4.19: Typical Settlement–Time Curve of a Consolidation Increment in the Oedometer Test.

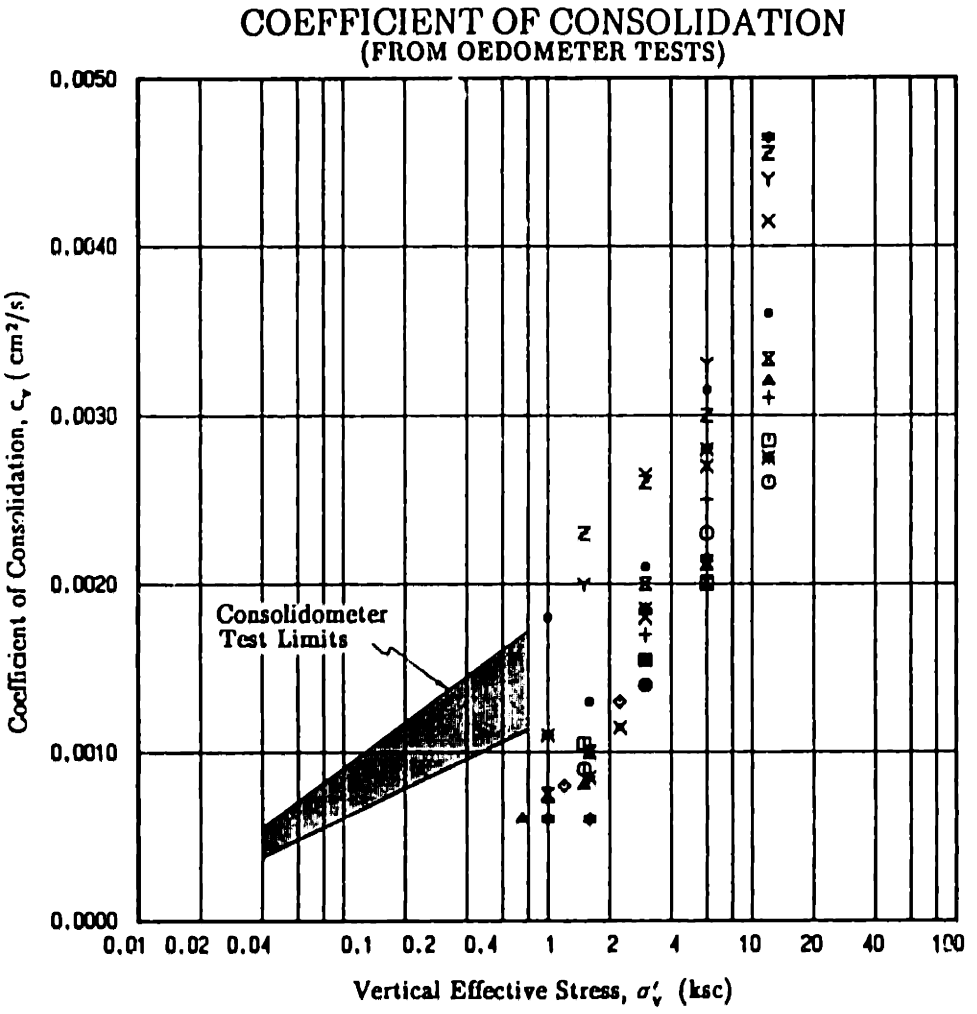

SYMBOL	BATCH NO.	POSITION	SYMBOL	BATCH NO.	POSITION
⊡	200	1ST TEST	✱	204	Top
⊙	200	2ND TEST	⧖	204	Bottom
▲	200	3RD TEST	❁	205	Top
+	201	1ST TEST	Z	206	Top
×	202	Top	Y	206	Bottom
◇	202	DSS	•	207	Top
✖	203	DSS			

Figure 4.20: Relationship between Coefficient of Consolidation and Vertical Effective Stress from Oedometer Tests.

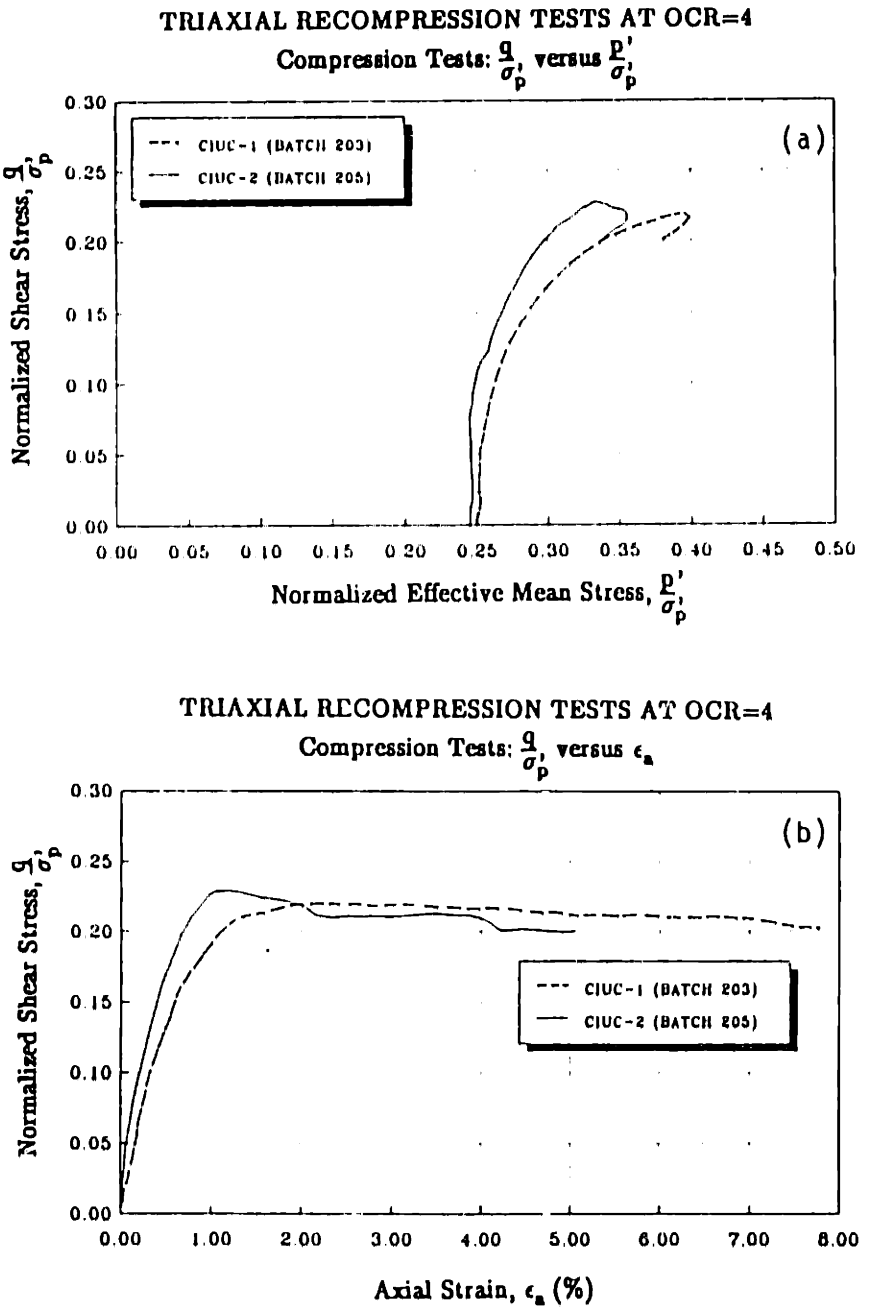

Figure 4.21: Results of CIUC Recompression Tests: (a) Effective Stress Paths; (b) Stress–Strain Relationships.

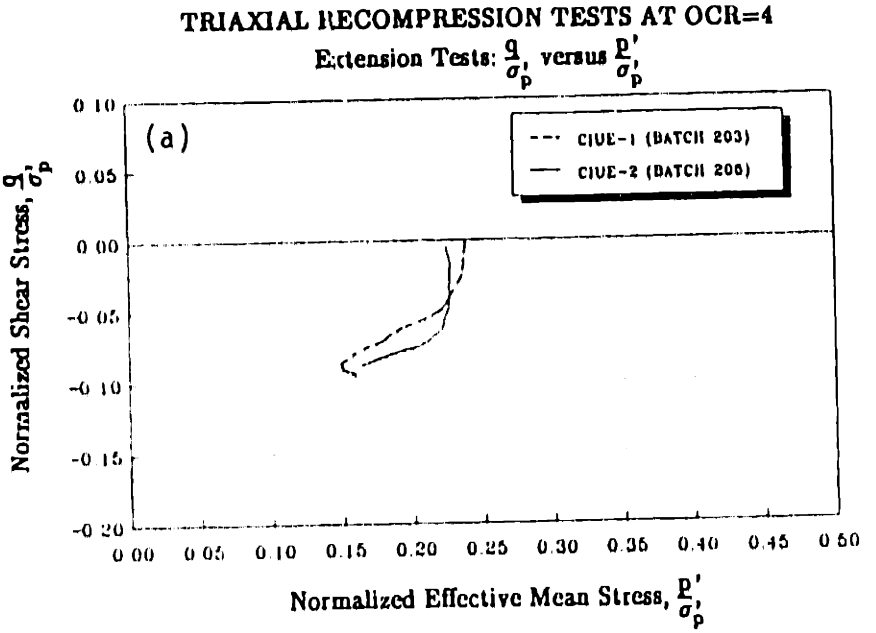

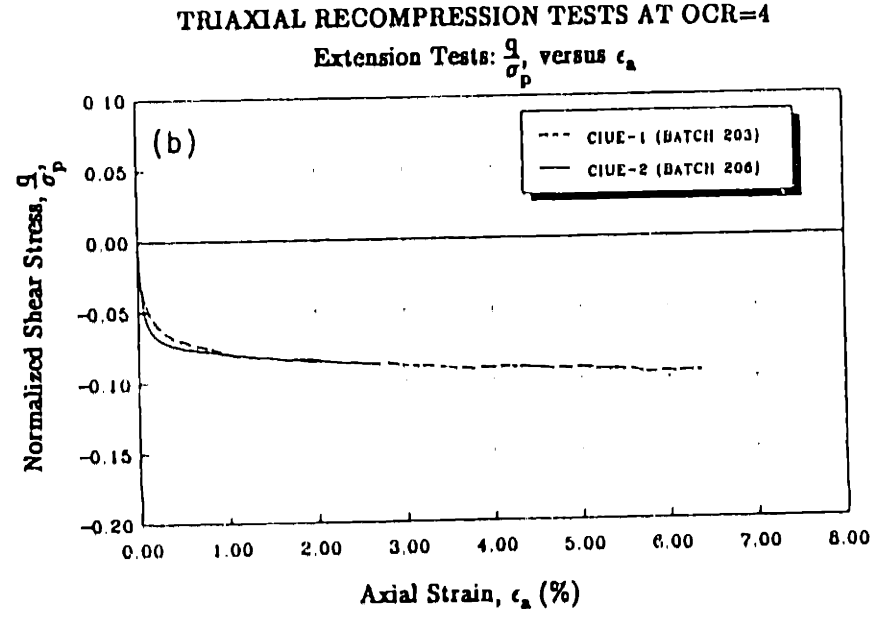

Figure 4.22: Results of CIUE Recompression Tests: (a) Effective Stress Paths; (b) Stress–Strain Relationships.

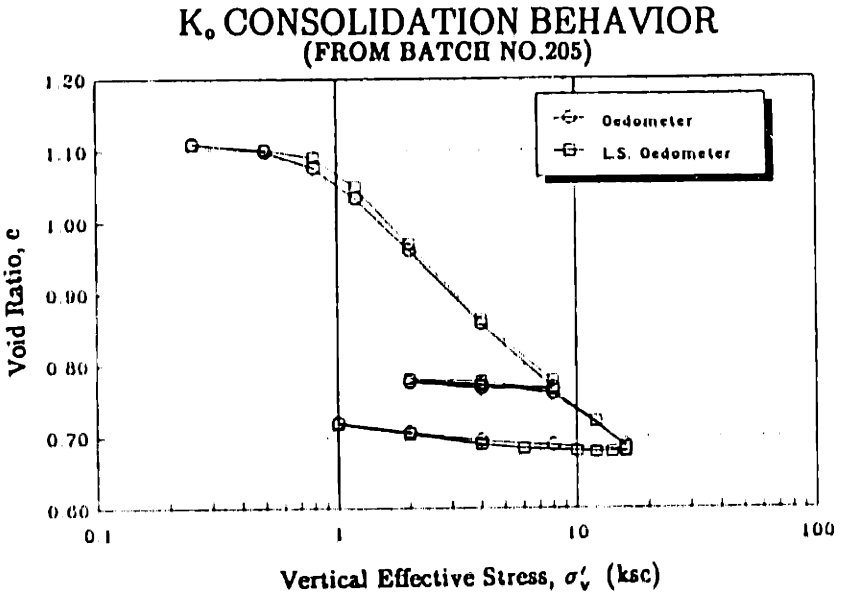

Figure 4.23: Void Ratio versus Vertical Effective Stress for Two Oedometer Tests (Standard and Lateral Stress).

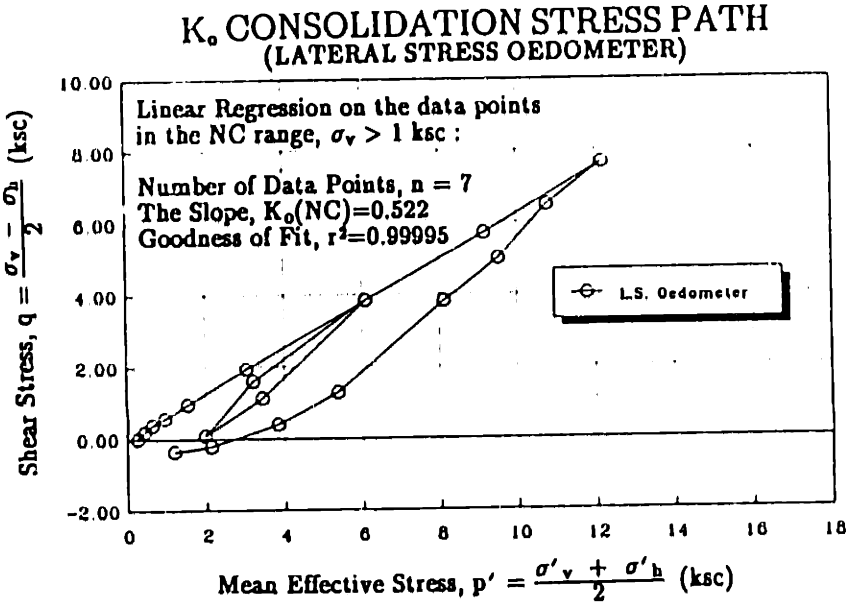

Figure 4.24: Consolidation Stress Path of the Lateral Stress Oedometer Test.

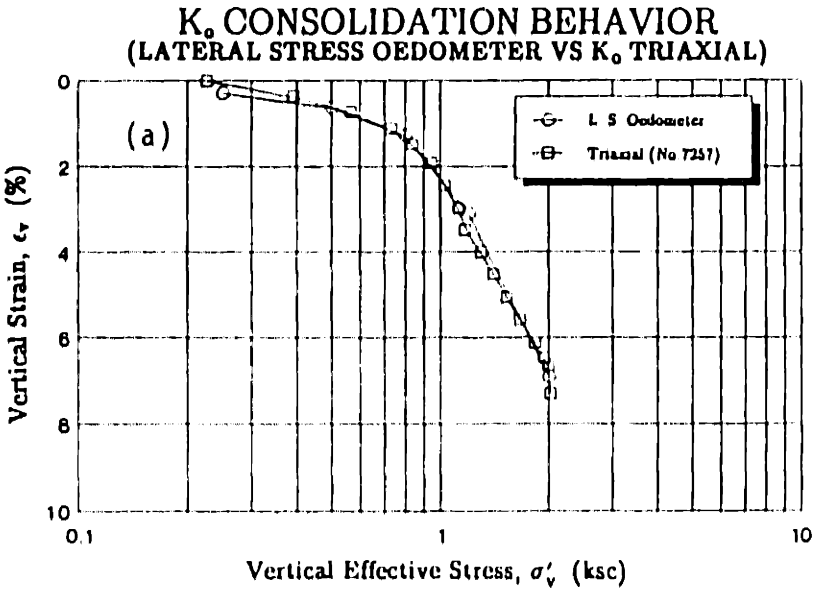

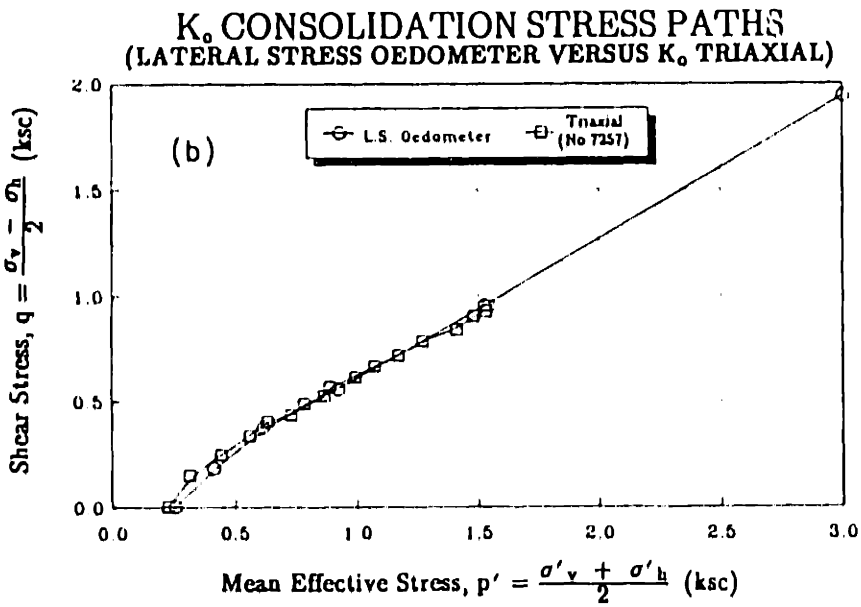

Figure 4.25: Comparison between LSO and K_o–Consolidation Triaxial Test: (a) Vertical Strain versus Vertical Effective Stress; (b) Effective Stress Paths.

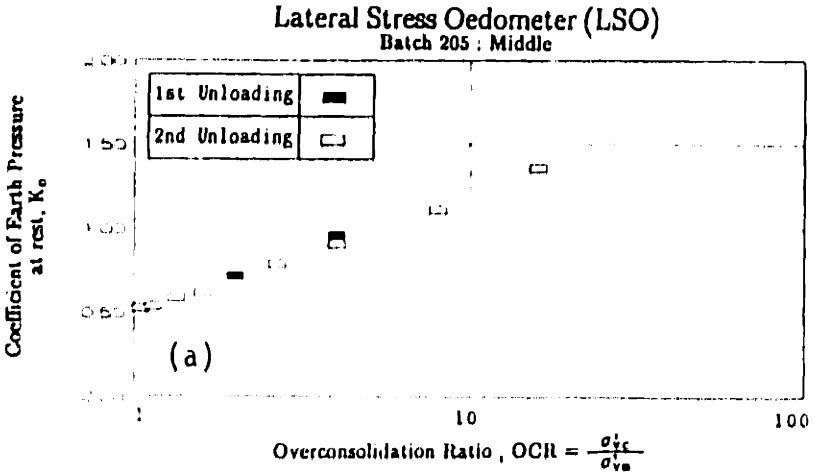

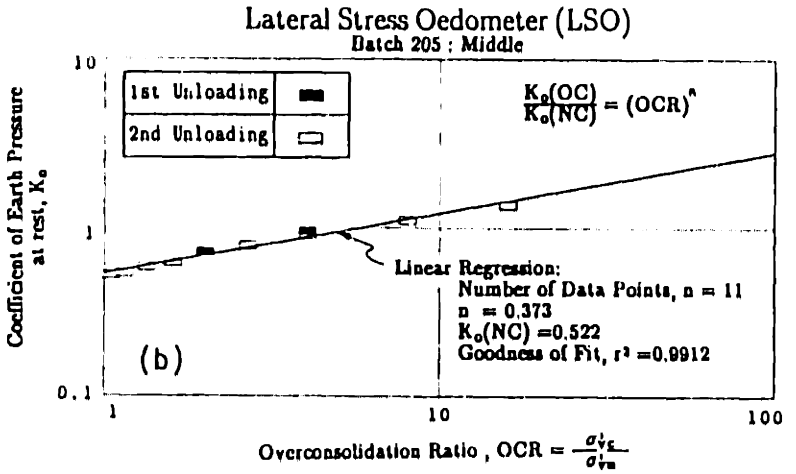

Figure 4.26: Coefficient of Earth Pressure at Rest (K_o) versus Overconsolidation Ratio (OCR) for the Lateral Stress Oedometer Test: (a) K_o versus Logarithm of OCR; (b) Logarithm of K_o versus Logarithm of OCR.

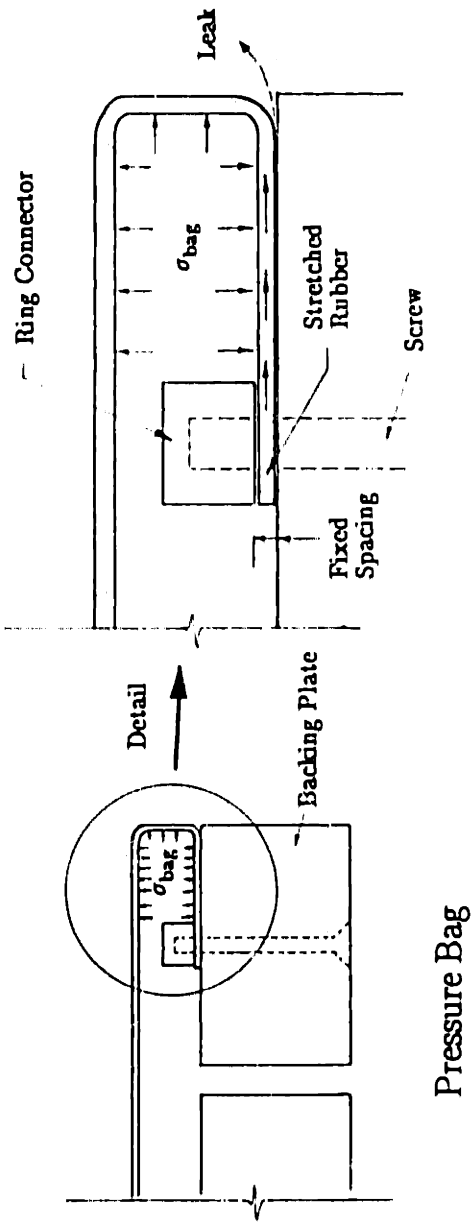

Figure 4.27: Location of the Leak in Pressure Bag.

TYPICAL STRESS PATH OF DIRECT SIMPLE SHEAR TEST
on Normally Consolidated Resedimented BBC

(From DeGroot, 1989)

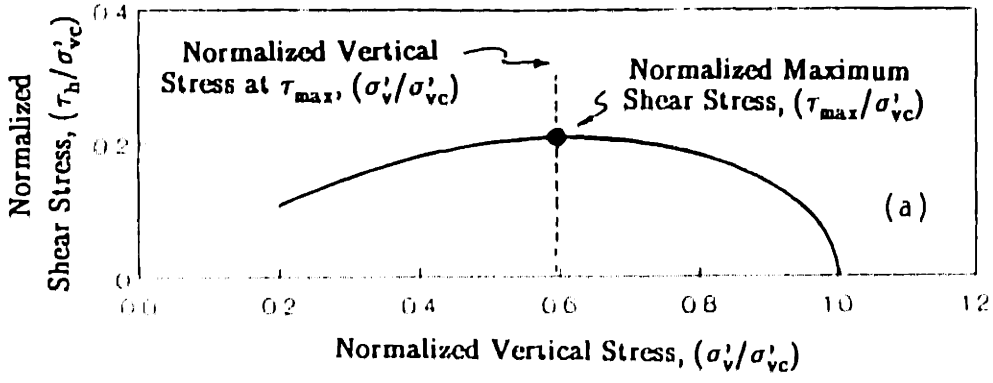

TYPICAL STRESS–STRAIN CURVE OF DIRECT SIMPLE SHEAR TEST
on Normally Consolidated Resedimented BBC

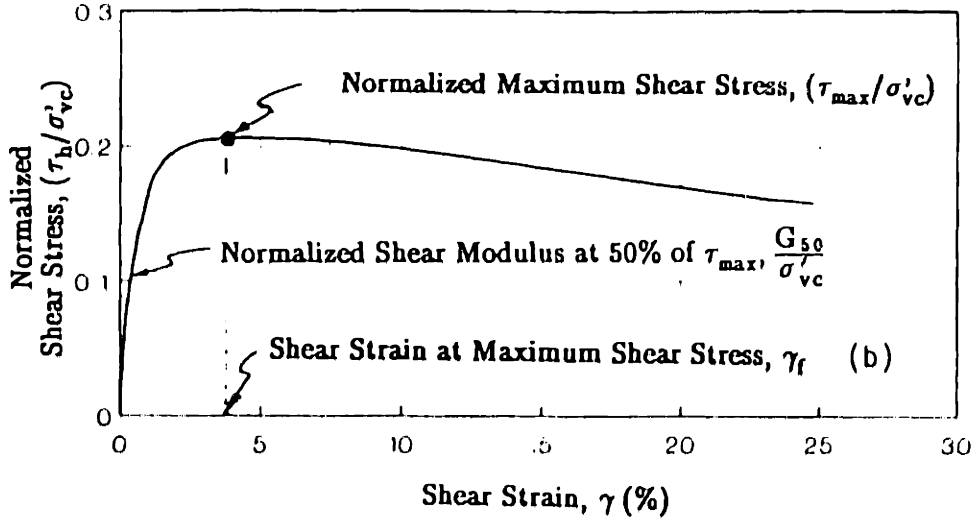

Figure 4.28: Typical Undrained Behavior of Normally–Consolidated BBC in DSS Test: (a) Stress Path; (b) Stress–Strain Relationship.

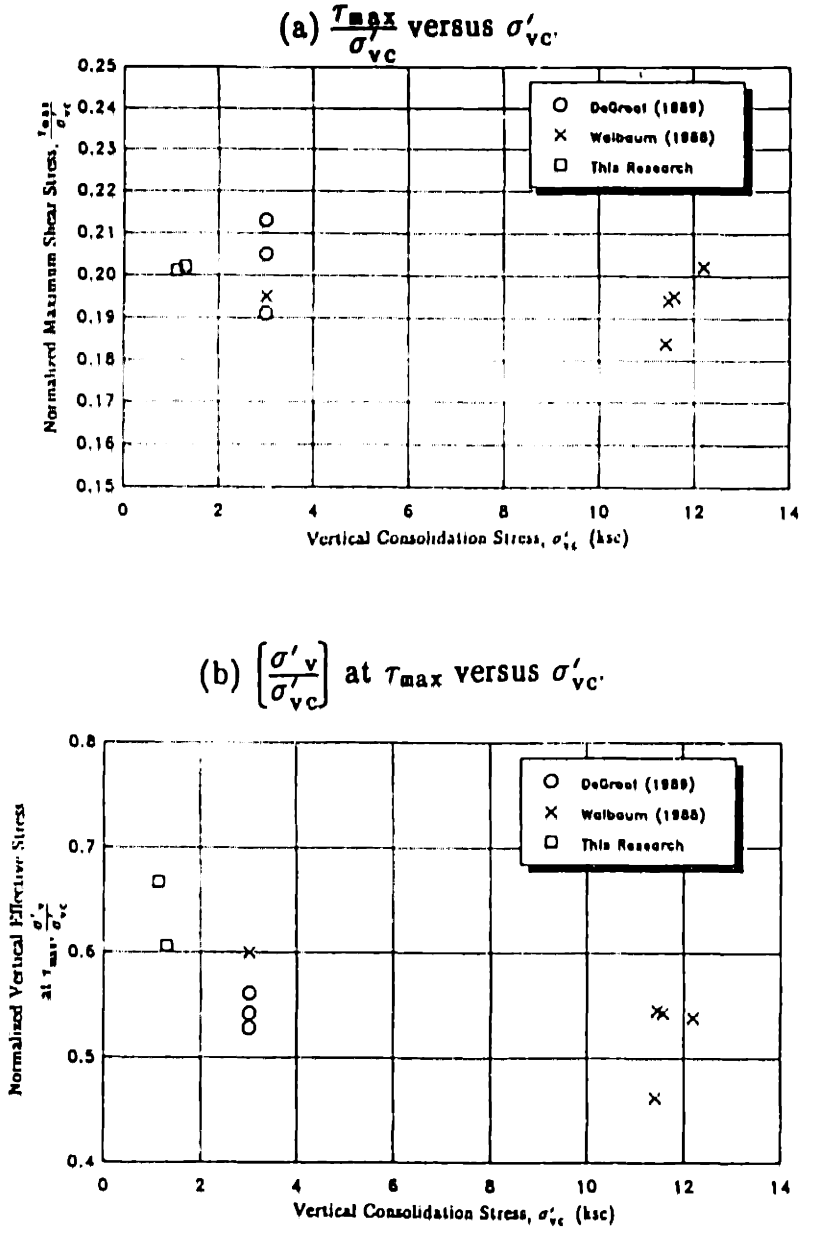

Figure 4.29: Undrained Strength Parameters versus Consolidation Stress on BBC at OCR=1.

(c) $\left[\frac{G_{50}}{\sigma'_{vc}}\right]$ versus σ'_{vc}.

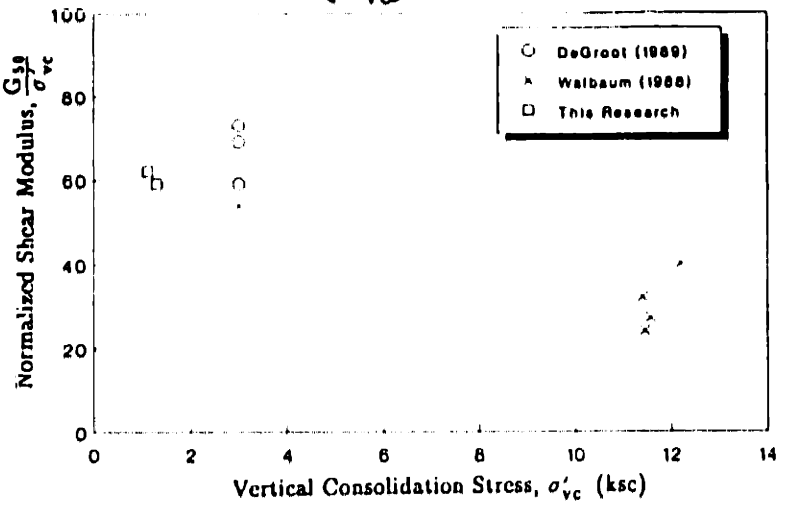

(d) γ_f versus σ'_{vc}.

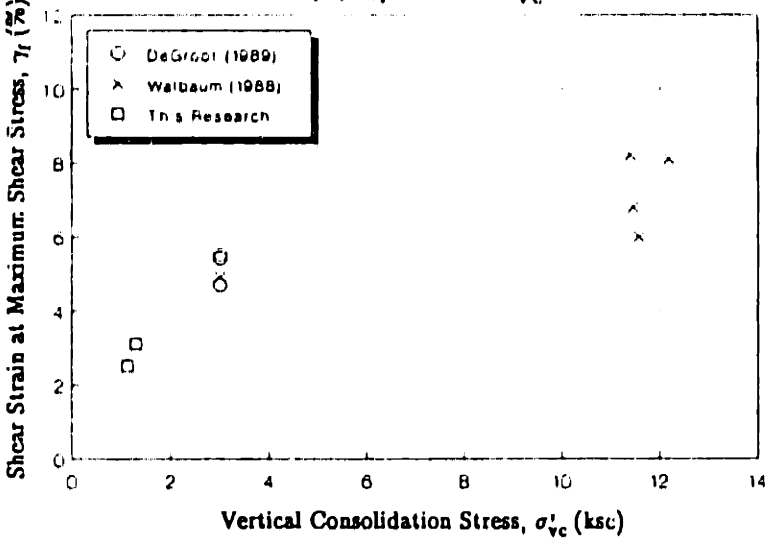

Figure 4.29: (Cont.)

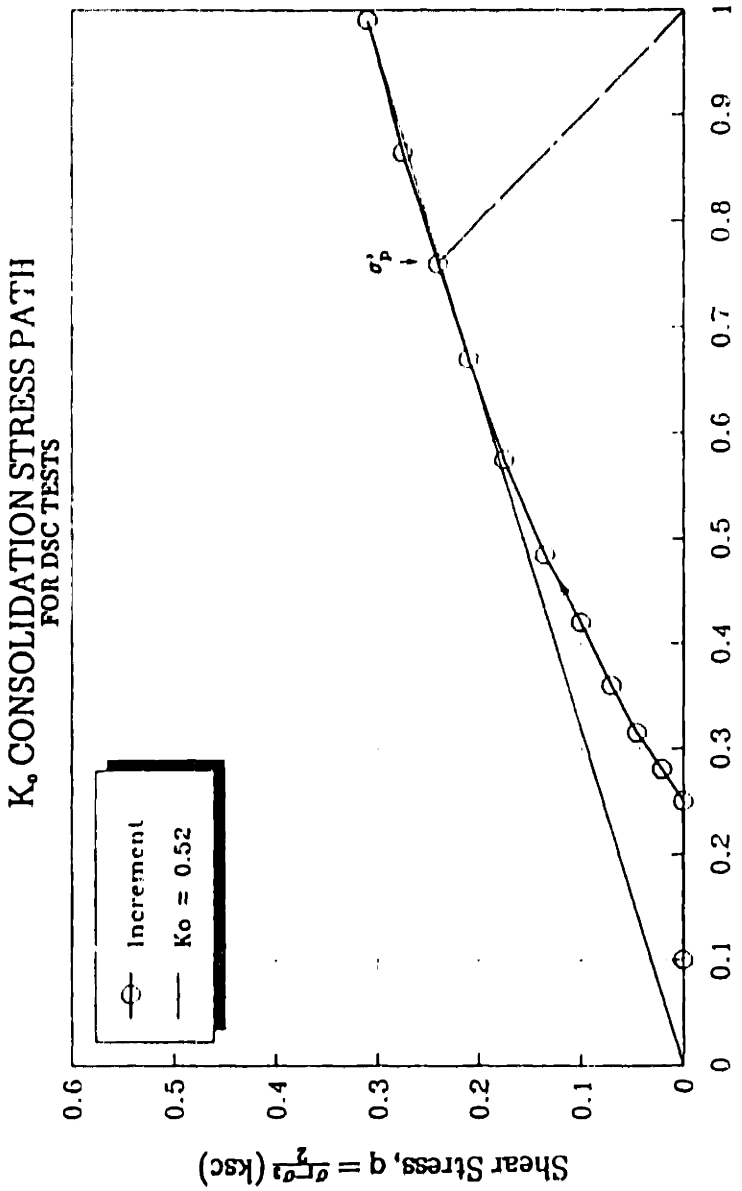

Figure 4.30: K_o–Consolidation Stress Path used in DSC Test.

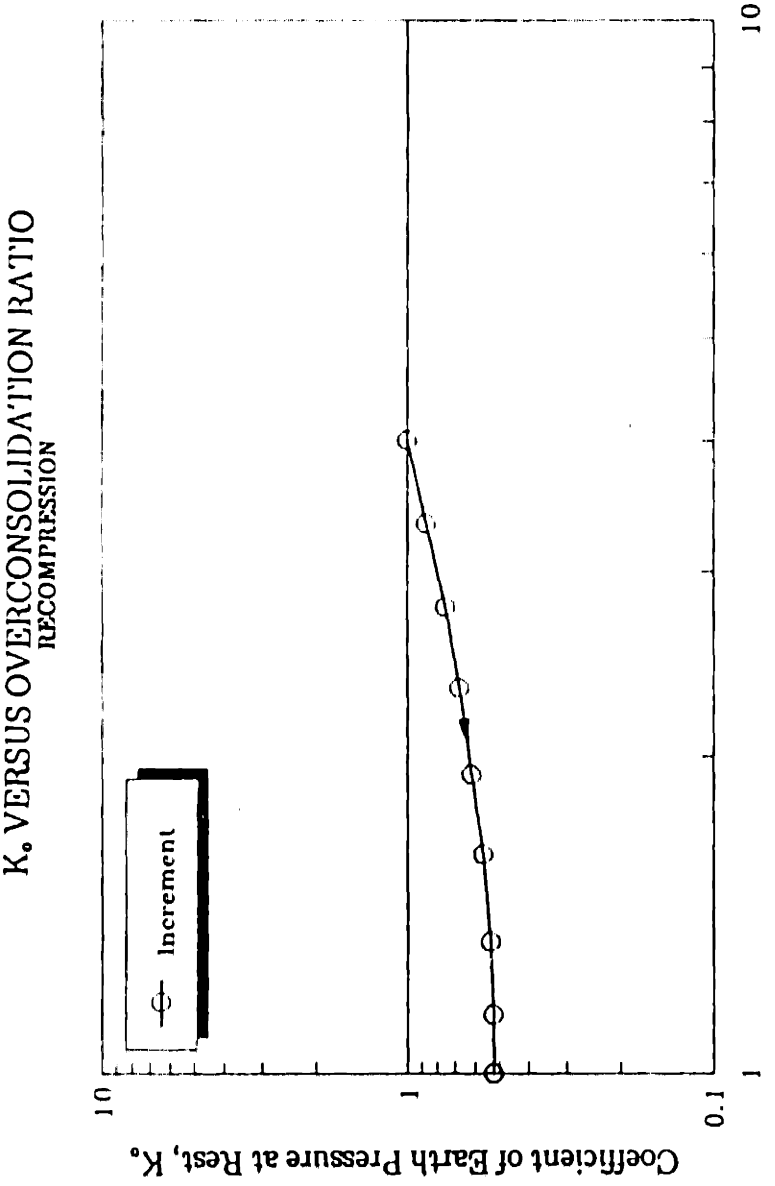

Figure 4.31: K_o–OCR Relationship for Reloading Range

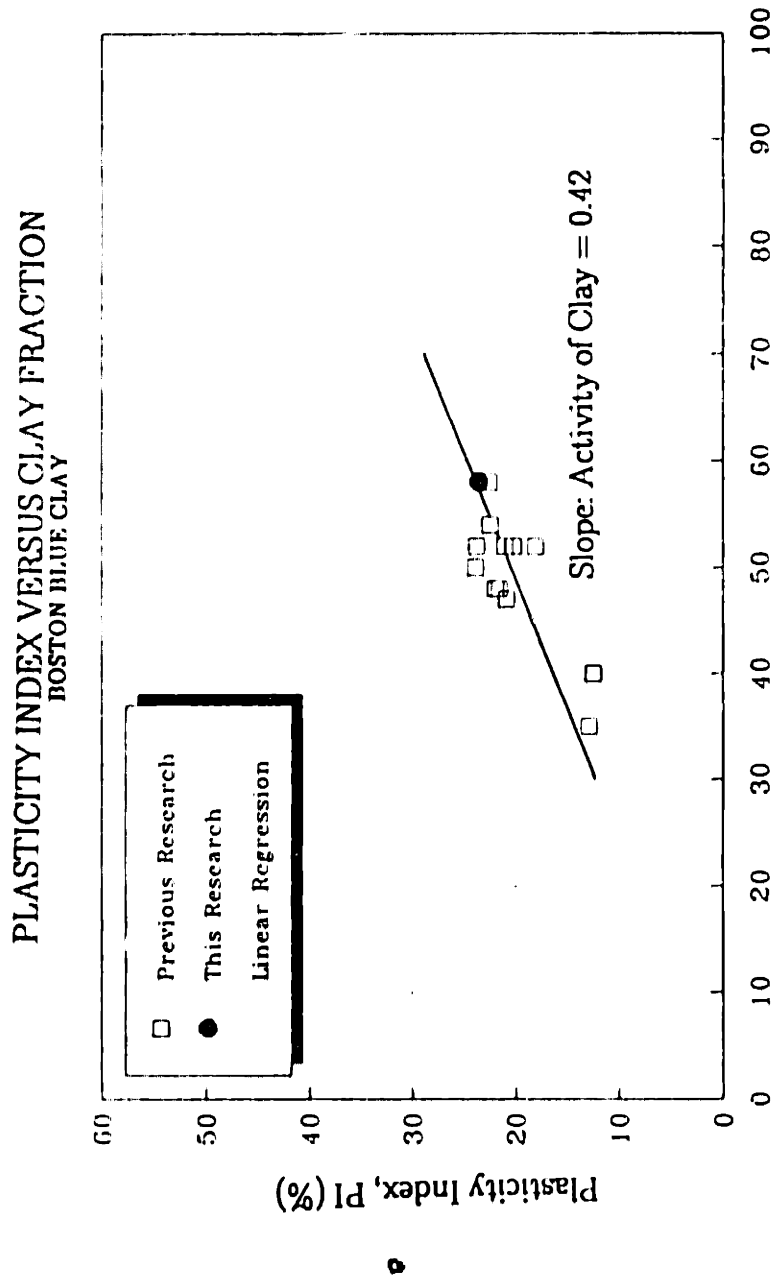

Figure 4.32: Activity of Boston Blue Clay.

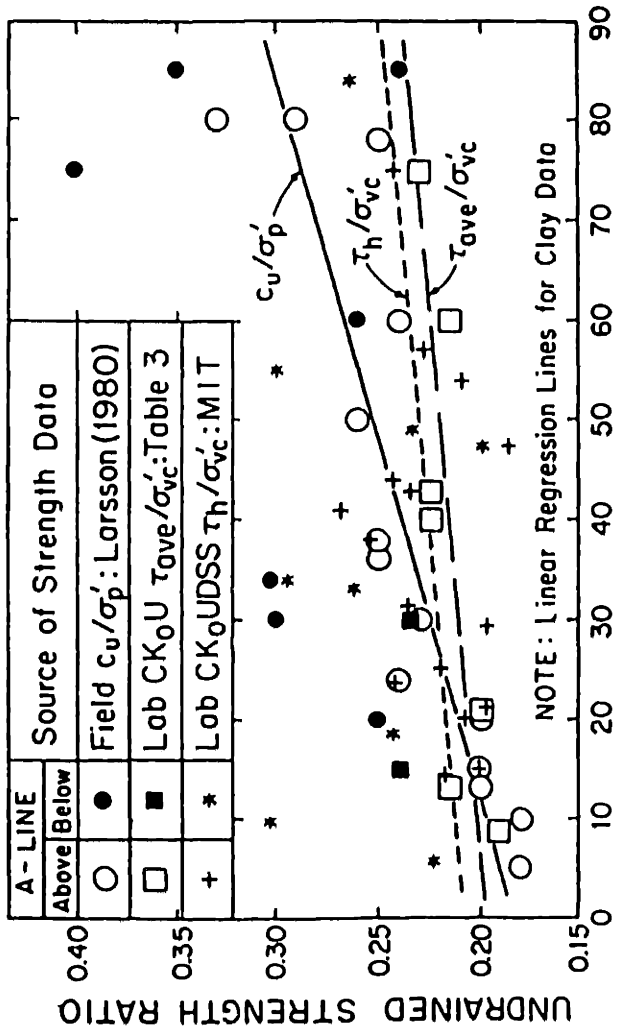

Figure 4.33: Comparison of Field and Laboratory Undrained Strength Ratios for Non–Varved Sedimentary Clays (OCR=1 for Laboratory CK_oU Testing; from Ladd, 1988).

CHAPTER 5

PRINCIPLES UNDERLYING THE DIRECTIONAL SHEAR CELL EXPERIMENTAL PROCEDURE

5.1 INTRODUCTION

The uniqueness of the Directional Shear Cell lies in its ability to completely control the principal stress direction during a test. For example, in a monotonic shear test starting from hydrostatic stresses, the major principal stress can be fixed at any desired direction and/or continuously rotated relative to the vertical depositional direction during shearing. The normal and shear stresses are applied to a sample by means of flexible pressure bags and shear sheets, respectively, according to the Mohr circle of stress for a given major principal stress direction, as discussed in Section 5.2. Due to potentially uneven stress application by the flexible pressure bags and shear sheets at the corners of the sample, the strains can be non–uniform. Determination of the strain distribution is therefore extremely vital to evaluate the quality of the tests, as well as to provide the stress–strain behavior of the material being tested. Different methods of determining strain and the method selected in this research are discussed in Section 5.3. A method called Normalized Area Ratio (NAR), is described in Section 5.3.4 to quantify the sample uniformity in a test.

A procedure for testing overconsolidated clay in the DSC was developed by Germaine (1982) and subsequently used by O'Neill (1985). The author made several improvements to that procedure (also see Chapter 3 for changes in the testing equipment) and, more importantly, developed a new technique to enable DSC testing of normally consolidated clay. Section 5.4 describes the sample preparation for clay testing in the DSC. The experimental procedures for the

consolidation and undrained shearing processes are given in Sections 5.5 and 5.6, respectively.

5.2 PRINCIPLES UNDERLYING APPLIED STRESSES

Components of both shear and normal stresses are applied in the Directional Shear Cell to give a specified major principal stress direction in an incremental manner. The corresponding strains are determined from the displacements of the reference markers on the soil sample. New approaches have been developed in this research to improve the accuracy and ease of taking stress and strain measurements. These measurements of stress and strain can then be combined to show the stress–strain behavior of the sample. The following sections describe the theory behind the application of stress and the measurements of stress.

5.2.1 Stress Representation in the Directional Shear Cell

The direction of the major principal stress is controlled by a combination of shear and normal stresses at the boundaries of the soil sample. By assuming the soil sample is a cubical element, the state of the stress in the element can be represented by shear and normal stresses on the four faces of the element as shown in Figure 5.1. If the major principal stress is to be applied in a direction, δ, relative to the y–axis, the stresses along the four faces are given as follows (see Figure 5.1):

$$\sigma_{yy}=\sigma_a=\frac{\sigma_1+\sigma_3}{2}+\frac{\sigma_1-\sigma_3}{2}\times\cos 2\,\delta \quad \text{(in the y–direction)} \qquad \text{Eq.5.1}$$

$$\sigma_{xx}=\sigma_b=\frac{\sigma_1+\sigma_3}{2}-\frac{\sigma_1-\sigma_3}{2}\times\cos 2\,\delta \quad \text{(in the x–direction)} \qquad \text{Eq.5.2}$$

$$\tau_{yx}\,(\tau_a) = -\tau_{xy}\,(-\tau_b) = \frac{\sigma_1 - \sigma_3}{2} \text{ x } \sin 2\,\delta \qquad \text{Eq.5.3}$$

As the stress level increases, the soil element undergoes deformation. In tests with non–zero boundary shear stresses (τ_{xy} and τ_{yx}), the adjacent faces of the sample lose their orthogonality because the shear components (τ_{xy} and τ_{yx}) cause the element to deform into a parallelepiped. In order to maintain equilibrium in the element, the applied stresses have to account for this distortion. These stresses after deformation (Figure 5.2) are given by equations 5.4 through 5.7:

$$\sigma_a = \frac{\sigma_1 + \sigma_3}{2} + \frac{\sigma_1 - \sigma_3}{2} \text{ x } \cos 2\,(\,\delta - \alpha\,) \qquad \text{Eq.5.4}$$

$$\sigma_b = \frac{\sigma_1 + \sigma_3}{2} - \frac{\sigma_1 - \sigma_3}{2} \text{ x } \cos 2\,(\,\delta + \beta\,) \qquad \text{Eq.5.5}$$

$$\tau_a = \frac{\sigma_1 - \sigma_3}{2} \text{ x } \sin 2\,(\,\delta - \alpha\,) \qquad \text{Eq.5.6}$$

$$\tau_b = \frac{\sigma_1 - \sigma_3}{2} \text{ x } \sin 2\,(\,\delta + \beta\,) \qquad \text{Eq.5.7}$$

where,

σ_a is the normal stress acting on face A;

σ_b is the normal stress acting on face B;

τ_a is the shear stress acting on face A;

τ_b is the shear stress acting on face B;

δ is the major principal stress direction;

α is the negative distortion angle of face A relative to the x–axis (where the positive direction is clockwise); and

β is the positive distortion angle of face B relative to y–axis (where the

positive direction is counterclockwise).

In DSC tests starting from a hydrostatic state of stress, the direction of the major principal stress is kept constant during shear. In an undrained shear test, since the DSC is a stress–controlled device, an assumed effective stress path has been used to determine the appropriate incremental stresses to be applied, and the pore water pressure is measured using a probe at the center of the soil sample. In order to achieve an undrained condition in the DSC, the effective stress path has to be the same as the total stress path to prevent any drainage during shear by keeping the pore water pressure at the center of the sample equal to zero. Alternatively, the pore pressure could always be kept constant at a slightly negative value as was done by Germaine (1982) and O'Neill (1985).

The determination of applied stresses requires a distortion angle to be known initially. This angle is measured using a protractor, assuming the preshear sample geometry to be cubical. It is extremely difficult to measure the angles α and β independently due to uncontrollable rigid body rotation of the sample during testing. Therefore, the distortion angle, α, is assumed to be equal in magnitude but opposite in sign to the distortion angle, β, so that the principal stress direction relative to the initial geometry can be calculated. From the estimated total distortion angle (summation of the absolute values of α and β), together with estimated incremental principal stresses ($\Delta\sigma_1$ and $\Delta\sigma_3$) from the stress path, the increment of applied stress can be computed using Equations 5.4 to 5.7. But the applied stresses of the DSC are not always identical to the measured values because of the coarse adjustment of the pressure regulators. Therefore, the principal stresses (σ_1, σ_3) and the angles (δ and α) have to be back–calculated from the following equations (assuming $\alpha = \beta$):

$$p \text{ (the mean stress)} = \frac{\sigma_1 + \sigma_3}{2} = \frac{(\sigma_a^2 - \sigma_b^2 + \tau_a^2 - \tau_b^2)}{2 (\sigma_a - \sigma_b)} \qquad \text{Eq.5.8}$$

$$q \text{ (the shear stress)} = \frac{\sigma_1 - \sigma_3}{2} = \sqrt{[(\sigma_a - p)^2 + \tau_a^2]} \qquad \text{Eq.5.9}$$

$$\delta \text{ (the major principal stress direction)} = \frac{1}{2} \tan^{-1} \left[\frac{\tau_a + \tau_b}{\sigma_a - \sigma_b} \right] \qquad \text{Eq.5.10}$$

$$\alpha \text{ (the distortion angle)} = \beta = \frac{1}{2} \tan^{-1} \left[\frac{\tau_a - \tau_b}{\sigma_a - \sigma_b} \right] \qquad \text{Eq.5.11}$$

The author wrote a computer program named "STRESS" to calculate the applied stresses based on the estimated effective stress path. It also computes the measured stresses using Equations 5.8 through 5.11.

5.2.2 Stress Measurements and Applications

The normal and shear stresses are applied during a test using a combination of pressure regulators, valves and pressure transducers. There are two separate control panels, one for controlling the normal stresses (σ_a, σ_b), and the other for the application of the shear stresses (τ_a, τ_b). The control of both normal and shear stresses assumes that opposite sample faces remain parallel during the test. Therefore, the applied stresses on opposite faces are equal.

The normal stresses are applied using flexible pressure bags. Each bag is supplied with air pressure which transfers the normal stress to the soil sample. The panel for controlling the normal stresses is shown in Figure 5.3. The compressed air is supplied by the general laboratory compressor which has a constant supply pressure. The air supply is regulated by two pressure regulators which in turn control the two applied normal stresses independently. The

pressures on each side of the panel are measured by pressure transducers. An alternative setup, shown as Option 2 in Figure 5.3, is used in most of the tests, with a differential pressure regulator and a pressure regulator, because it simplifies the controlling process during an undrained shear test. The pore water pressure at the middle of the soil can be kept at a constant value by adjusting the mean (hydrostatic) stress of the sample using a pressure regulator (A) instead of adjusting both regulators (A and B) in the other setup. The differential pressure regulator is used to adjust the pressure in pressure bags A (σ_a). The control process is described in Section 5.4.

The shear stresses (τ_a, τ_b) are applied using shear pistons and shear sheets. The shear sheets are connected to four shear pistons which are controlled pneumatically. A schematic of the shear stress control panel is shown in Figure 5.4. The layout of the system is very similar to the normal stress control panel, except that water is used to actually drive the shear pistons instead of compressed air. The panel is divided into two symmetrical independent halves with one side controlling the shear stress, τ_a, and the other side controlling the shear stress τ_b. The shear stresses are controlled by two pressure regulators. The pressures measured on the panel are proportional to the shear stresses; calibration curves are given in Appendix E.1. The procedure for applying the shear stresses is described in Section 5.6.

The schematic of the electrical setup of the DSC is shown in Figure 5.5. All of the pressure transducers are connected to the stress measurement unit which consists of a transducer connector box, six voltmeters, two DC power supply units and a remote central data acquisition system. The power is supplied to the transducers in order to activate them, and the voltmeters are used to give visual readings of the output voltages of the transducers during the test. The primary function of the central data acquisition system is to record the readings of the

transducers during consolidation and to act as a backup system during shear. The pressure bag position sensor unit consists of a DC power supply and a position sensor panel, which has four sets of red and green LED (light–emitting diode) lights. Each set of lights is responsible for controlling the position of one pressure bag in the DSC, so that the correct pressure can be applied to the sample during the test.

5.3 PRINCIPLES UNDERLYING STRAIN DETERMINATION

Since the DSC is a stress–control device, a known incremental stress is applied to the soil sample and the resulting displacement is measured. Different methods of strain or displacement measurement are discussed in Section 5.3.1. A new approach for strain analysis is developed which presents the results in two different ways: local and global analyses. The local analysis gives a strain distribution of the sample and the global analysis provides average strains for the study of the stress–strain behavior of the sample. Section 5.3.3 describes the analyses in detail.

5.3.1 Comparison of Alternative Methods of Strain Measurement

There are a number of existing techniques to determine the displacement or strain field of a soil sample in the laboratory, e.g., using displacement transducers, video technology, radiography and photography. The advantages and disadvantages are summarized in Table 5.1.

The most widely used technique to measure displacements during soil tests is through displacement transducers or dial gages. But due to the setup and design of the MIT DSC device, it is impossible to place the transducers along the boundaries of the sample. The DSC device developed at the University of Colorado in Boulder (Sture et. al., 1985) uses this technique to measure average

strains of the sample.

The video image method of strain measurement has been used for the US Army Corps of Engineers Waterways Experiment Station DSC research. The advantages of the video image method are that it can provide the strain field of the sample during the test and it can expand the testing capability of the DSC device to include a strain softening test with this instantaneous strain measurement technique. Unfortunately, the resolution of the strain measurement is on the order of 0.2% (which is the resolution of the pixels); therefore accurate strain measurement cannot be achieved. Due to the recent developments in video technology, a 0.03% strain measurement can be accomplished using a high resolution monitor and an electronic scanner with a resolution of 300 pixels per inch on a 13"x13" map. The cost of this equipment is beyond most soil research budgets, but this equipment will definitely be adopted in years to come.

Radiography was first used to measure the displacement field in soil modeling (Roscoe, et. al., 1963) at Cambridge University by Roscoe's soil mechanics research team in the 1960's. This method of strain measurement was adopted by Arthur (1977) as the primary technique to measure the strain field of Leighton Buzzard sand specimen in the DSC. Tungsten–carbide balls or lead shots, as reference points, were embedded in the sand sample midway between the top and bottom platens. Radiographs were then taken at successive stress increments and superimposed to determine the displacement field of the sample from digitizing the reference points of each radiograph. The displacement field was then converted into a strain field using a computer program. The resolution of these radiographs is reasonably good.

The photography method was first introduced by Rodriguez (1977) at UCL in the testing of loose sand, because of problems in embedding the tungsten balls at mid–height. Grids were drawn on the rubber sample membrane on the top face

of the sample as reference points. Photographs of these reference points were taken and the strain field of the sample was determined using the same procedure as the radiography method. The main assumption in the photography method is that the strains are uniform in the plane strain direction. In other words, for any planes orthogonal to the plane strain direction, the strain distribution on that plane is the same regardless of the location of the plane. This assumption was checked by Rodriguez in a series of DSC tests on dense sand using both radiography and photography methods. The conclusion was that both methods yield very similar results. The photography method was then adopted by the MIT soil research group in DSC testing of resedimented clay because it is impossible to embed the shots at mid–height without causing substantial disturbance to the soil sample.

The initial photography films (Ilford FP4, ASA 125, DIN 22) used by Bekenstein (1980) and Germaine (1982) had very large grain pigments, i.e., the resolution of the film was poor. O'Neill's (1985) research introduced a high contrast graphic film which improved the resolution of the film tremendously, producing sharper images and reducing the uncertainty in strain measurement. Therefore, this film was selected for use in this research.

During the course of this research, a different problem was encountered: the change in the magnitude of the intermediate principal stress distorts the strain measurement due to the Poisson effect on the rubber membrane where the reference points were placed. As the intermediate principal stress changes, the rubber membrane stretches or shrinks in the radial direction. The reference points on the membrane are therefore displaced radially, distorting the radial strain measurement of the sample, but not the maximum shear strain (γ_{max}). Therefore, the Mohr circle of strain is shifted along the x–axis, but the size of the Mohr circle remains unchanged. Special tests were performed (described in Appendix E.3) to

determine the magnitude of this apparent strain so that a correction could be made and the error could be quantified.

Given the pros and cons, the photography method is still the best method for determining the strain field of the clay sample in the DSC test.

5.3.2 Description of the Selected Method of Strain Measurement

There are a number of steps required to determine the strains of a sample in the DSC. They are:

- creating a photographic image of the deformed sample;
- digitizing the image using an optical comparator and storing the information in the computer;
- superimposing the images to yield the displacement field; and
- data analysis.

Strains are determined based on the boundary displacements along one plane strain surface of the soil sample. One hundred reference points are defined on this surface using pen dots in order to create a photographic image. The shape of the pen dots is very crucial. They should be circular with a diameter of 1±0.5 mm, and the dots should be placed on the rubber membrane before the membrane is removed from the form, as described in Appendix D.1. Photographs are then taken at representative stress levels using a camera mounted 36 cm above the center top platen of the device. The camera is made by Toyo–View and fitted with a Fujinon lens. The camera is adjusted such that the film plate is parallel to the top platen, and it is properly focused to ensure a sharp photographic image. All of these steps must be carefully done before the test. The soil sample image on the camera should have dimensions of 6 cm x 6 cm, due to the limitations of the digitizing board. The films used are made by Eastman Kodak with the trade name

Kodalith Ortho Type 3 graphic (4" x 5") film. They are inserted in a double dark slide holder with the lighter side of the film facing away from the holder. Special attention is required in mounting the film to ensure that the film is properly secured and flat during the mounting process. During the test, the aperture of the camera is set at f9.5 and the speed of exposure is fixed at 0.5 second with two 500 watt light bulbs placed two feet away on opposite sides of the DSC device. After the photograph is taken, the exposed film is temporarily stored in an opaque box so that a new film can be loaded in the holder. Immediately following the tests, the films are developed in a darkroom with a safelight. The developer used in this process is called Kodalith Developer (Cat. No. 1465152). At most, four films are placed on a tray of 800 ml of developer for 3 to 6 minutes; some judgment is required in determining when the developing is complete. If the film is underdeveloped, the reference dots will not show up very well on the film, increasing the uncertainty in strain measurement. Therefore, an operator should have a few trials before the actual tests. The same problem will happen if the film is overdeveloped. The developed films are then placed in a stop bath to prevent further development using Kodak Indicator Stop Bath (Cat. No. 1464247) for 30 to 60 seconds. Finally, the films are moved to a tray of 800 ml of Kodalith Fixer (Cat. No. 1971746) for 5 to 8 minutes. Once the process is complete, the films are cleaned in water for 5 to 20 minutes before they are dried. The drying duration is very important because the films have a thickness of 0.1 mm with Estar base which will shrink when dried. The shrinkage of the film depends on the temperature and duration of drying. In general, if the film is dried for at least 24 hours at 20°C before digitizing, the films are quite stable, and the shrinkage of different films is very uniform. To minimize the distortion due to film shrinkage, the standard procedure is to dry the film under the same conditions and digitize the films on the same day.

The digitizer unit consists of a 90 mm x 160 mm optical comparator (Germaine, 1982), a Magnescale display and an IBM personal computer. The dried film is placed on the optical comparator in a fixed orientation, with the reference points magnified 50 times and positioned by two adjustable knobs on the digitizing panel. The coordinates of the reference points are recorded and stored in the computer using a computer program called "DIGIT," which is developed in this research. This system can measure the displacement with a resolution of 0.002 mm. The accuracy of the strain measurements depends on the stability of the film, the quality of the film, the quality of the reference pen dots, and most of all, a patient and careful operator. If all of these conditions are satisfied, the repeatability of digitizing each reference point is within 0.006 mm. Once all of the films have been digitized, the strains of the sample are determined from the displacements of the reference points using a strain reduction program. The analysis used in this strain reduction process is described in the following section.

5.3.3 Development of New Strain Analysis

The strains of the DSC sample are determined based on the displacements of the reference points (or grids) on the rubber membrane on the top of the sample during the test.

The conventional method of determining the strain distribution from the displacements of a defined reference grid was developed by the Cambridge soils research group, as described by Roscoe et al.(1963) and Arthur et al. (1977).

The Cambridge method calculates the average strains of a rectangular element from the displacements of the four corners. The strains are assumed to be proportional to the first order differential of the displacements. A rectangular element is subdivided into four triangles and the total strain is based on the average strains of the four sub–elements.

In the DSC, the global grid is usually made up of many small squares with the same area. The global average strains of the system are computed from the average values of the individual rectangular elements. The variation of the strains is represented by the standard deviations of this one–dimensional array. This method of analysis was adopted by all previous DSC researchers.

The new strain analysis uses a multiple linear regression method to estimate the strains from the displacement field. It can be divided into two parts: global analysis and local analysis. This method of analysis is widely used as a tool by scientists and engineers (Draper and Smith, 1981). The local analysis uses a method called Locally Weighted Regression (Cleveland, 1979) for smoothing the data points. It provides visual information on strain distributions by means of a strain contour map. The general formulations of the two analyses are essentially the same; they differ in the weighting function, W, which will be discussed later in the chapter.

Consider an infinitesimal displacement field with the displacements at coordinates (x_i,y_i) in the Cartesian frame of (u_i,v_i), which can be written as follows:

$$u_i = b_{11} + b_{12}\,x_i + b_{13}\,y_i + \epsilon_{1i} \quad \text{in the x–direction.} \qquad \text{Eq.5.12}$$

$$v_i = b_{21} + b_{22}\,x_i + b_{23}\,y_i + \epsilon_{2i} \quad \text{in the y–direction.} \qquad \text{Eq.5.13}$$

where the coefficients b are constants which are related to the components of strains and rotations. ϵ_{1i} and ϵ_{2i} are error terms that are normally distributed random variables with means of zero and standard deviations equal to $\sigma_{1\epsilon}$ and $\sigma_{2\epsilon}$, respectively.

Let the displacement matrix be, $\underline{U} \equiv \begin{bmatrix} u_1 & v_1 \\ u_2 & v_2 \\ : & : \\ u_i & v_i \\ : & : \\ u_n & v_n \end{bmatrix}$,

where n is the number of data points.

The displacements in the matrix form can then be expressed as,

$$\underline{U} = \underline{H}\,\underline{b} + \underline{\epsilon} \qquad \text{Eq.5.14}$$

where $\underline{H} = \begin{bmatrix} 1 & x_1 & y_1 \\ 1 & x_2 & y_2 \\ : & : & : \\ 1 & x_i & y_i \\ : & : & : \\ 1 & x_n & y_n \end{bmatrix}$, $\underline{b} = \begin{bmatrix} b_{11} & b_{21} \\ b_{12} & b_{22} \\ b_{13} & b_{23} \end{bmatrix}$ and $\underline{\epsilon} = \begin{bmatrix} \epsilon_{11} & \epsilon_{21} \\ \epsilon_{12} & \epsilon_{22} \\ : & : \\ \epsilon_{1i} & \epsilon_{2i} \\ : & : \\ \epsilon_{1n} & \epsilon_{2n} \end{bmatrix}$.

The weight matrix is given by,

$$\underline{W} = \text{diag}\,(w_i) = \begin{bmatrix} w_1 & & & \\ & w_2 & & \underline{0} \\ & & \ddots & \\ & & & w_i \\ & \underline{0} & & \ddots \\ & & & & w_n \end{bmatrix} \qquad \text{Eq.5.15}$$

This weight matrix is introduced so that the different types of analyses (global and local) can be expressed using the same set of equations but with different weights.

The quantity, $\hat{b}$, is defined as the least square estimate of $\underline{b}$ for which $(\underline{U} - \underline{H}\,\hat{\underline{b}})^T\,\underline{W}\,(\underline{U} - \underline{H}\,\hat{\underline{b}})$ is minimum, and it is given by,

$$\hat{\underline{b}} = (\underline{H}^T \underline{W} \underline{H})^{-1} \underline{H}^T \underline{W} \underline{U} \qquad \text{Eq.5.16}$$

The $\hat{\underline{b}}$ matrix is determined from the Equation 5.16, and, as shown below, the strains are the products of this $\hat{\underline{b}}$ matrix.

The estimated or computed displacements are given by,

$$\hat{u}_i = \hat{b}_{11} + \hat{b}_{12}\, x_i + \hat{b}_{13}\, y_i$$
$$\hat{v}_i = \hat{b}_{21} + \hat{b}_{22}\, x_i + \hat{b}_{23}\, y_i$$

The infinitesimal strains are determined from the derivatives of displacements from equations 5.12 and 5.13,

The axial strain in the x–direction,

$$\epsilon_{xx} = \frac{\partial u}{\partial x} \qquad \text{Eq.5.17}$$
$$\epsilon_{xx} = \hat{b}_{12}$$

The axial strain in the y–direction,

$$\epsilon_{yy} = \frac{\partial v}{\partial y} \qquad \text{Eq.5.18}$$
$$\epsilon_{yy} = \hat{b}_{23}$$

The shear strain is,

$$\epsilon_{xy} = \epsilon_{yx} = \frac{\partial u}{\partial y} + \frac{\partial v}{\partial x} \qquad \text{Eq.5.19}$$
$$\epsilon_{xy} = \frac{1}{2} (\hat{b}_{13} + \hat{b}_{22})$$

The maximum shear strain, γ_{max}, is,

$$\gamma_{max} = \sqrt{[(\epsilon_{xx} - \epsilon_{yy})^2 + 4\, \epsilon_{xy}^2]} \qquad \text{Eq.5.20}$$

$$\gamma_{max} = \sqrt{[\,(\hat{b}_{12} - \hat{b}_{23})^2 + (\hat{b}_{13} + \hat{b}_{22})^2\,]}$$

The volumetric strain is as follows:

$$\epsilon_v = \epsilon_{xx} + \epsilon_{yy} \qquad \text{Eq.5.21}$$
$$\epsilon_v = \hat{b}_{12} + \hat{b}_{23}$$

The major and minor principal strains, ϵ_1 and ϵ_3, are,

$$\epsilon_1 = \frac{1}{2}(\epsilon_v + \gamma_{max})$$
$$\epsilon_1 = \frac{1}{2}\{\epsilon_{xx} + \epsilon_{yy} + \sqrt{[(\epsilon_{xx} - \epsilon_{yy})^2 + 4\,\epsilon_{xy}^2]}\} \qquad \text{Eq.5.22}$$
$$\epsilon_1 = \frac{1}{2}\{(\hat{b}_{12} + \hat{b}_{23}) + \sqrt{[(\hat{b}_{12} - \hat{b}_{23})^2 + (\hat{b}_{13} + \hat{b}_{22})^2]}\}$$

$$\epsilon_3 = \frac{1}{2}(\epsilon_v - \gamma_{max})$$
$$\epsilon_3 = \frac{1}{2}\{\epsilon_{xx} + \epsilon_{yy} - \sqrt{[(\epsilon_{xx} - \epsilon_{yy})^2 + 4\,\epsilon_{xy}^2]}\} \qquad \text{Eq.5.23}$$
$$\epsilon_3 = \frac{1}{2}\{(\hat{b}_{12} + \hat{b}_{23}) - \sqrt{[(\hat{b}_{12} - \hat{b}_{23})^2 + (\hat{b}_{13} + \hat{b}_{22})^2]}\}$$

Rigid Body Rotation, ω, is,

$$\omega = \frac{\partial v}{\partial x} - \frac{\partial u}{\partial y} \qquad \text{Eq.5.24}$$
$$\omega = \frac{1}{2}(\hat{b}_{22} - \hat{b}_{13})$$

The Major Principal Strain direction relative to the y–axis (vertical axis), ξ, is given by:

$$\xi = \frac{1}{2}\tan^{-1}\left[\frac{2\,\epsilon_{xy}}{\epsilon_{xx} - \epsilon_{yy}}\right] \qquad \text{Eq.5.25}$$

$$\xi = \frac{1}{2}\tan^{-1}\left[\frac{\hat{b}_{13} + \hat{b}_{22}}{\hat{b}_{12} - \hat{b}_{23}}\right]$$

(I) Global Strain Analysis

In the global strain analysis, the average strains are calculated using multiple linear regression, with the weight, w_i, at the ith data point equal to 1. Therefore, the weight matrix, $\underline{W}$, is defined as:

$$\underline{W} = \text{diag}\,(w_i) = \begin{bmatrix} 1 & & & \\ & 1 & & \underline{0} \\ & & \ddots & \\ & & & 1 \end{bmatrix} \qquad \text{Eq.5.26}$$

The average strains are computed from Equations 5.14 to 5.25 using this $\underline{W}$ matrix. The associated variances of the average strains have to be known in order to evaluate the uniformity of the sample. These variances are as follows.

Under the assumption that the model in Equation 5.16 is correct, the variance matrix of $\hat{\underline{b}}$ is,

$$\underline{\Sigma}_{\hat{b}} = \sigma_\epsilon^2 \left(\underline{H}^T \underline{W} \underline{H} \right)^{-1}$$

where σ_ϵ^2 is a measure of the scatter of the population about the regression line,

and an unbiased estimator of σ_ϵ^2 is given by,

$$s^2 = \frac{\left(\underline{U} - \underline{H}\,\hat{\underline{b}} \right)^T \underline{W} \left(\underline{U} - \underline{H}\,\hat{\underline{b}} \right)}{\text{tr}\ \underline{W} - \text{tr}\ \left[\left(\underline{H}^T \underline{W} \underline{H} \right)^{-1} \underline{H}^T \underline{W}^2 \underline{H} \right]}$$

$$s^2 = \begin{bmatrix} \sigma_{1\epsilon}^2 & 0 \\ 0 & \sigma_{2\epsilon}^2 \end{bmatrix} \qquad \text{Eq.5.27}$$

The variance matrix in the x direction is,

$$\underline{\Sigma}_1 = \sigma^2_{1\epsilon} \left(\underline{H}^T \underline{W} \underline{H} \right)^{-1}$$

$$\underline{\Sigma}_1 = \begin{bmatrix} \Sigma_{111} & \Sigma_{112} & \Sigma_{113} \\ \Sigma_{121} & \Sigma_{122} & \Sigma_{123} \\ \Sigma_{131} & \Sigma_{132} & \Sigma_{133} \end{bmatrix} \qquad \text{Eq.5.28}$$

and the variance matrix in the y direction is,

$$\underline{\Sigma}_2 = \sigma^2_{2\epsilon} \left(\underline{H}^T \underline{W} \underline{H} \right)^{-1}$$

$$\underline{\Sigma}_2 = \begin{bmatrix} \Sigma_{211} & \Sigma_{212} & \Sigma_{213} \\ \Sigma_{221} & \Sigma_{222} & \Sigma_{223} \\ \Sigma_{231} & \Sigma_{232} & \Sigma_{233} \end{bmatrix} \qquad \text{Eq.5.29}$$

The derivative of $\underline{U}$ from Equation 5.14 can be expressed as:

$$\underline{U}' = \underline{H}' \underline{b}$$

Combining equations 5.17 to 5.19 yields the components of strains, which is,

$$\underline{S} = \begin{bmatrix} \epsilon_{xx} \\ \epsilon_{yy} \\ \epsilon_{xy} \end{bmatrix} = \begin{bmatrix} 1 & 0 & 0 & 0 \\ 0 & 0 & 0 & 1 \\ 0 & 0.5 & 0.5 & 0 \end{bmatrix} \begin{bmatrix} \hat{b}_{11} \\ \hat{b}_{13} \\ \hat{b}_{22} \\ \hat{b}_{23} \end{bmatrix} \qquad \text{Eq.5.30}$$

Rewriting the above equation gives,

$$\underline{S} = \underline{G}\,\underline{B}$$

where $\underline{G}$ is referred to as the transformation matrix.

The variance matrix of strain:

$$\underline{\Sigma}_{\underline{S}} = \underline{G}\,\underline{\Sigma}\,\underline{G}^{T}$$

$$\underline{\Sigma}_{\underline{S}} = \begin{bmatrix} 1 & 0 & 0 & 0 \\ 0 & 0 & 0 & 1 \\ 0 & 0.5 & 0.5 & 0 \end{bmatrix} \begin{bmatrix} \underline{\Sigma}\begin{bmatrix} b_{12} \\ b_{13} \end{bmatrix} & \underline{0} \\ \underline{0} & \underline{\Sigma}\begin{bmatrix} b_{22} \\ b_{23} \end{bmatrix} \end{bmatrix} \begin{bmatrix} 1 & 0 & 0 \\ 0 & 0 & 0.5 \\ 0 & 0 & 0.5 \\ 0 & 1 & 0 \end{bmatrix}$$

The variance matrix. $\underline{\Sigma}$, is determined from Equations 5.28 and 5.29 yields the expression:

$$\underline{\Sigma}_{\underline{S}} = \begin{bmatrix} \Sigma_{122} & 0 & \frac{1}{2}\Sigma_{123} \\ 0 & \Sigma_{233} & \frac{1}{2}\Sigma_{223} \\ \frac{1}{2}\Sigma_{132} & \Sigma_{232} & \frac{1}{4}(\Sigma_{133}+\Sigma_{222}) \end{bmatrix} \qquad \text{Eq.5.31}$$

Variances:

The variances of ϵ_{xx}, ϵ_{yy} and ϵ_{xy} are the product of the variance matrix given in Equation 5.31 and they are given as follows:

$$\mathrm{Var}(\epsilon_{xx}) = \Sigma_{122} \qquad \text{Eq.5.32}$$

$$\mathrm{Var}(\epsilon_{yy}) = \Sigma_{233} \qquad \text{Eq.5.33}$$

$$\mathrm{Var}(\epsilon_{xy}) = \frac{1}{4}\left(\Sigma_{133} + \Sigma_{222}\right) \qquad \text{Eq.5.34}$$

The variances associated with the principal strains and the maximum shear strains can be determined using Taylor Series expansion. The first–order approximation to the variance of ϵ is:

$$\mathrm{Var}(\epsilon) \simeq \sum_{i,j} (\underline{\Sigma_s})_{ij} D(\epsilon)_i D(\epsilon)_j \qquad \text{Eq.5.35}$$

where i, j = 1, 2, 3.

$$D_1 = \left.\frac{\partial \epsilon}{\partial \epsilon_{xx}}\right|_m;$$

$$D_2 = \left.\frac{\partial \epsilon}{\partial \epsilon_{yy}}\right|_m; \text{ and}$$

$$D_3 = \left.\frac{\partial \epsilon}{\partial \epsilon_{xy}}\right|_m$$

The terms D_1, D_2 and D_3 are evaluated at ϵ_{xx}, ϵ_{yy} and ϵ_{xy}. The strain, ϵ, is replaced by the principal strains (ϵ_1 and ϵ_3), and maximum shear strain, γ_{max}.

The variances of the angles, which include the effects of rigid body rotation and the major principal strain direction, are determined using Equations 5.31 and 5.35, respectively. The major principal strain direction is calculated with ϵ being replaced by the angle (ξ) in radians. The resulting variance is:

$$\mathrm{Var}(\xi) = \sum_{i,j} (\underline{\Sigma_s})_{ij} D(\xi)_i D(\xi)_j \text{ and} \qquad \text{Eq.5.36}$$

the rigid body rotation is given by,

$$\mathrm{Var}(\omega) = \frac{1}{4}\left(\Sigma_{133} + \Sigma_{222}\right) \qquad \text{Eq.5.37}$$

The variances of each parameter shown above are the population variances of the estimates.

The number of data points depends on the size of the total sample area being considered. Figure 5.6 shows different sizes of areas taken into consideration. The average strains of the different areas are calculated to evaluate the uniformity of the sample from the boundaries to the center of the sample. This technique of evaluating strain uniformity has been used by Germaine (1982) and O'Neill (1985) in clay tests. Area Number 2 had been selected as a representative area of strain of the sample by these previous researchers, primary because boundary failure led to substantial deformation along the boundaries in Area Number 1. This introduces a bias in the strain analysis though, and a more correct approach is to abandon tests with boundary failures since the actual state of stress is not known. The conclusion is that Area Number 1 should be chosen as the reference area since it represents the strain of the maximum possible area of the soil sample (about 86% of the total area) instead of an arbitrarily selected one. An example of the output is shown in Table 5.2, presenting the means and their standard deviations of the <u>total</u> strains at failure for Test DSC31 with δ_{inc}=90° (see Figure 5.9). The total strains are computed based on the change in displacements relative to the initial coordinates.

(II) Local Strain Analysis

In order to enhance the visual information of the strain distribution of the sample, a technique called Locally Weighted Regression is used to smooth the scattered data points (Cleveland, 1979). The procedure is similar to the global strain analysis, except a non–linear weighting function is used at the point of

calculated strains.

The weighting function has the following properties:

- $W(z) > 0$ for $|z| < 1$;
- $W(-z) = W(z)$;
- $W(z)$ is a non–increasing function for $z \geq 0$;
- $W(z) = 0$ for $|z| \geq 1$.

The weighting function selected is called a "tricube" function (shown in Figure 5.7) which is expressed by,

$$W(z) = (1-|z|^3)^3 \qquad \text{Eq.5.38}$$

The procedure centers W to z_i with a value of 1 at that position and scales it so that the point at which W first becomes zero is at the rth nearest neighbor of z_i. The distance between this point and z_i is h times the average distance between two adjacent points. The larger the r values, the smoother the fit will be. It is rather difficult to select an appropriate r value. One method of choosing appropriate values of r is described by Cleveland. A quantity, f, is defined as the ratio of r to the number of data points, n. Let $\hat{u}_i(f)$ be the locally weighted regression fitted value of x_i for a given value of f with u_i not included in the computation. The f value is selected by minimizing,

$$R = \sum_{k=1}^{n} [u_k - \hat{u}(f)]^2$$

The value of f is large when the data points are randomly distributed. If

the deformation of the sample is non–uniform, but shows a trend, then the f value will be very low. Therefore, the f value has to be determined for each increment of a test. Figure 5.8 shows a typical relationship between R and f. In this case, the optimum f is 0.08 which is considered to be small. Figure 5.9 shows the distribution of strains (ϵ_1, ϵ_3 and γ_{max}) and the distribution of major principal strain direction for Test DSC31 at failure.

5.3.4 Strain Distribution Standard

A strain distribution standard was originally developed by Germaine (1982) to evaluate the uniformity of a DSC sample from the average strains of different rings and areas (Figure 5.10). The 81 elements within a 9x9 grid (or 10x10 grid lines) on the top of the square surface of the sample are divided into five rings: the outermost ring (Ring No.0) consists of 24 elements; the innermost ring (Ring No.4), which is located at the middle of the sample face, contains only one element. The strains of the three outermost rings (γ_r) are compared with the strains of the entire sample (γ_1) in a normalized form, $(\frac{\gamma_r - \gamma_1}{\gamma_1})$, which is called the Normalized Ring Strain (NRS). The parameter has proven to be very useful in evaluating sample uniformity. After performing a significant number of DSC tests, Germaine concluded that a |NRS| greater than approximately 40% (i.e., NRS>40% or NRS<40%) for one or more of the three outer rings is considered indicative of a testing problem; this was also verified by O'Neill (1985).

Instead of using the NRS parameter, an equivalent parameter called the Normalized Area Ratio (NAR) is introduced which is equal to the ratio of the strain for a given Area Number to the strain of the entire sample (i.e. the strain of Area No.1). For example, the NAR for Area No.2 (referred to in Figure 5.10) is the ratio of strain from Area No.2 (γ_2) to the strain from Area No.1 (γ_1). This NAR for Area No.2 is directly related to the NRS for Ring No.0 as (see Figure

5.11):

$$\text{NAR(Area No.2)} = \frac{\gamma_2}{\gamma_1} = 1 - 0.65\ \text{NRS(Ring No.0)}$$

Therefore, for a NRS limit of ±40%, the NAR limit is given by

$$\text{NAR(Area No.2)} = 1 \pm 0.26$$

In most cases, the |NRS| values are highest for Ring No.0. Therefore, it is reasonable and easier to use NAR (Area No.2) to evaluate the sample uniformity than using NRS values.

Some observations have been made by Germaine and O'Neill from DSC testing of BBC regarding strain distribution under different directions of loading. In tests with large applied surface tractions via shear sheets, the strains usually tend to be higher near the boundaries. This is probably caused by the improper transfer of surface tractions, causing the region close to the boundaries to experience larger surface tractions and hence larger strains. The NAR value in this case is less than unity (i.e., NAR<1).

In contrast, for tests with applied normal stresses only, the strains tend to be higher in the middle of the sample. This is probably caused by bowing of the sample; in this case, the NAR value will be greater than unity (i.e., NAR>1). Figure 5.9 is a good example of the test (Test DSC31 at δ_{inc}=90°) with applied normal stresses only, indicating higher strains in the middle of the sample.

5.4 SAMPLE PREPARATION FOR CLAY TESTING

The experimental procedure for clay testing has been described by Germaine (1982), but due to modifications of the device and the different

consolidation stress levels used for the current research, the procedure has been modified. This section describes the construction of the rubber membrane, the device preparation and the clay sample preparation for the DSC test.

5.4.1 Construction of Sample Membrane

In most soil strength tests, rubber membranes are used to separate the soil sample from the applied stress boundaries. The Directional Shear Cell test is no exception; the soil sample is placed in a cubical rubber membrane to help provide continuity in the stress transferred between the soil and the applied stresses. It also prevents drying of the clay sample. Another important feature of the membrane is that it provides a background on which markers are placed.

The criteria of the rubber membrane are:

- it should have a uniform thickness (0.15 to 0.2 mm);
- it should be white in color to enhance the photographic image of the markers on the rubber membrane;
- it should provide full stress transfer between the shear sheets and the soil sample.

The first two criteria can be achieved by using latex with white dye, as described in Appendix D.1.

In order to prevent slippage along the boundaries, the inner faces of the membrane are coated with a layer of sieve No. 40–50 clean Leighton Buzzard sand. The coating process must be done properly, otherwise slippage will occur during the test along the boundaries, and the test results will be very difficult to interpret. In the earlier part of this research, boundary failures occurred in a number of tests, leading to the development of a special coating technique. The method is discussed in more detail in Appendix D.1.

The strains of the soil sample are determined from the displacements of reference markers on the top face of the rubber membrane in the plane strain direction, under the assumption that the soil deforms uniformly in this direction. The markers are placed on the membrane before the membrane is removed from the form. Ten rows of 10 dots are marked on the top face of the membrane as shown in Figure 5.12. Note that the dots (Set No. 1) are at least 4 mm away from the edges of the membrane to ensure that the dots appear clearly on the film. The maximum area for the strain reduction is restricted to this boundary, which is about 86 % of the total cross–sectional area of the sample. A backup set of dots (Set No. 2) is marked on the membrane in case the quality of the first set is too poor to be digitized. The dots should be circular with a diameter between 0.5 and 1.5 mm. The top face of the membrane is coated with a film of silicone coating to prevent any smearing of the dots during the test.

The membrane dimensions of 107 mm x 107 mm shown in Figure 5.12 are those existing when the membrane is still on the mold used to form the membrane. The membrane contracts to dimensions of 100 mm x 100 mm when placed on the clay sample.

5.4.2 Device Preparation

Prior to trimming the clay sample for testing, there are several tasks to perform.

The pressure bags have to be checked for leakage, as described in Appendix E.2.2. Each pressure bag is placed on top of the intermediate principal stress measuring device and held together by restraining bars and tie rods. A pressure of about 1.3 times the maximum normal stress is applied to the pressure bag. The position of the bag is adjusted to the neutral position with the help of the position sensor in the bag. The bag is left at this pressure for at least 24 hours to check for

any leakage. If there is any evidence (the sound of a leak can be heard) that the bag is leaking during this time, the bag should be dismantled and checked for leakage in the bag and joints, then it is reassembled. The bag should be tested again until no leakage occurs. This procedure not only checks the pressure bags, but also verifies the performance of the intermediate principal stress measuring device.

The next crucial step is to clean the inner shear sleeves of the shear sheets to ensure proper bonding to the rubber membrane. Since adjacent shear sheets are no longer attached, the cleaning process is now much easier. The two sets of shear sheets are placed on a wooden platform with the reinforced pulling sheets passing through the slots as shown in Figure 5.13. The stretching strips and the tails of each of the shear sheets are arranged so that they are parallel to one another. The platform is placed under a ventilating hood for cleaning. A few drops of acetone are spread on each inner sleeve; the surface is then rubbed and cleaned using cotton balls. The cleanliness is checked by observing adhesion to a clean piece of rubber.

The top and bottom platens are lubricated with a layer of silicone grease. The initial grease thickness should be set to approximately 0.5±0.1mm. The technique for spreading the grease in this research is quite different from that used by Germaine (1982), which used plastic wrap to cover the grease. It was found that by covering the grease with plastic wrap the grease thickness is reduced when the wrap is removed because some of the grease adheres to the wrap making the final surface very uneven. The new method is much simpler: first, remove any old grease from the platens; then spread about 10 cc around the center portion of the platen with a spatula. Move the spatula in one direction until the grease is evenly spread. The thickness of the grease is measured at four different locations using a caliper. If the grease is too thick, remove some of the grease and smooth the face

again with the spatula. The process is repeated until the required thickness of the grease is achieved.

All of the stress measurements (σ_a, σ_b, τ_a, τ_b, u and σ_2) are taken using pressure transducers. Some of the transducers do not equilibrate immediately; therefore they should be connected to the power supply for 24 hours before the zero readings are taken. The procedure for measuring the zero readings of the normal stresses is as follows (see Figure 5.3):

- Close all the valves on the normal stress control panel.
- Close all the pressure regulators by turning the knobs of the regulators counter–clockwise all the way up.
- Open Valve Nos. 4, 6, 8, 12, 13, 15, 16 and 18.
- Record the readings of the two pressure transducers; these readings will be the zero readings of the normal stress pressure transducers.

The procedure for measuring the zero readings for shear stress pressure transducer is the following (see Figure 5.4):

- Close all the valves on the shear stress control panel.
- Open Valve Nos. 4, 5, 6, 7, 9, 10, 12, 13, 14 and 15.
- Record the readings of the two pressure transducers; these readings will be the zero readings of the shear stress pressure transducers.

Pore water pressure measurement is vital in undrained shear tests. The quality of the test depends on the performance of the probe. Therefore, its pore pressure response should be checked before the test. The setup is shown in Figure 5.14. The porous tip of the probe is placed in a Plexiglas container filled with distilled–deaired water. A pressure line is connected to one end of the container, so that water pressure can be applied via a mercury pot. The pressure in the system is increased by about 0.1 ksc, the reference (or applied) pressure is measured using a pressure transducer mounted next to a Bourdon gage, which provides a rough measurement of the applied pressure. Subsequently, the change

in pressure of the probe is also measured. A typical response curve is shown in Figure 5.15; the response time is about 20 seconds in this case. The porous stone tip of the probe should be submerged in deaired water at all times.

5.4.3 Sample Preparation

Once the device is ready for testing, the clay sample preparation can begin. The sample preparation usually takes a number of hours to complete. The following section describes the step–by–step procedure (see Figure 5.16):

a. *Trimming the clay sample* (Figure 5.16a)*:*
(detailed description is given by Germaine (1982).)

Note: DSC sample was enclosed in aluminum foil, plastic wrap and coated with wax for storage after removal from batch consolidometer.

- Place the wax coated sample on a 4.5"x4.5" glass plate in a humid room.
- Cut along the edges of the waxed sample with a razor blade until the clay is exposed.
- Slowly remove the aluminum foil and the plastic wrap on the sample.
- Place the clay sample with the glass plate on the sample trimmer.
- Cut the clay sample with wire saw on one face first and use this exposed face as a reference.

Note: All cuts should be less than 6 mm thick, otherwise the cuts will cause too much sample disturbance. Once the face of the sample is exposed, it should be covered by a piece of wax paper.

- Push the exposed face against the vertical side of the sample trimmer by rotating the sample 90° clockwise, slide the sample towards the two vertical poles so that the next face of the sample can be trimmed accordingly.
- Cut the next face, continue the cutting process in a systematic way until the final dimensions of the sample are a 100 mm cube.
- Position the clay sample so that the top and bottom faces of the sample will be perpendicular to the plane strain direction.

For a ψ test, the deposition direction of the clay sample will be the same as the plane strain direction.

For a δ test, the deposition direction of the clay sample will be orthogonal to the plane strain direction.

Note: The orientation of the sample should be noted at all times because it is not possible to determine the orientation of the sample visually.

- Measure the water contents at different locations from the trimmings.

b. *Attaching the filter strips:*
- Cut 12 strips of filter papers with dimensions of 0.25"x3.5".
- Fold the strips in halves along the longer sides.
- Soak them in water for a few minutes.
- Attach them to all 12 edges of the clay sample as shown in Figure 5.16b.

c. *Placing the sample in the rubber membrane* (Figure 5.16c)*:*
- Connect the membrane stretcher with the rubber membrane to the vacuum pump.
- Flip the stretcher upside down.
- Lower the stretcher over the clay sample until the rim of the stretcher touches the glass plate.
- Disconnect the vacuum pump.

d. *Removing the membrane stretcher* (Figure 5.16d)*:*
- Remove the tapes along the edges of the rubber membrane.
- Hold down the rubber membrane while pulling the stretcher up, as shown in Figure 5.16d.
- Flip the enclosed sample upside down using the two glass plates.
- Place the sample on a glass plate with the exposed face of the sample facing upwards.
- Bring the sample to the DSC testing laboratory.

e. *Installing the pore water pressure probe* (Figure 5.16e)*:*
- Lightly mark the diagonals of the bottom face of the sample with a needle.
- Dig a trench with a dental tool along the diagonal from the center of the sample to the corner of the unreinforced rubber membrane.

Note: The size of the trench should be about the size of the pore water pressure probe tube since the tube will eventually be buried in this trench.

- Place a drop of water at the end of the trench to prevent an air gap from forming behind the stone.
- Hold the pore water pressure probe in an upright position with the porous tip touching the center of the sample as shown in Figure 5.16e.
- Align the horizontal portion of the tube with the trench.
- Slowly push the probe into the soil vertically until the horizontal tube (50 mm in length) is flush with the sample surface.

- Fill the remaining gap with remolded clay from the trimming until the surface is smooth.
- Glue a plastic tube at the other unreinforced corner membrane with contact cement as a drainage line.

f. *Enclosing the sample* (Figure 5.16f):
- Clean the top face of the flap of the membrane with acetone.
- Apply some contact cement along the flap of the membrane as close to the sample as possible.
- Place a clean 5"x5" latex dental dam over the sample.
- Secure the latex sheet in place.
- Cut the excess flap about 5 mm away from the soil sample.

g. *Placing the enclosed sample on the bottom platen* (Figure 5.16g):
- Place a glass plate on one of the vertical sample faces.
- Rest the sample on this glass plate.
- Tilt the bottom platen at about 60° inclination.
- Slowly bring the bottom of the sample in contact with the bottom platen as shown in Figure 5.16g.
- Place the bottom platen in the testing frame.

h. *Centering the sample* (Figure 5.16h):
- Attach two strings on the opposite sides of the four poles as shown in Figure 5.16h.
- Center the sample by sliding the sample with a glass plate on the vertical faces with the help of the strings.
- Clean the four vertical faces of the sample thoroughly with acetone and cotton balls.

Note: The shear sheets will be bonded to the vertical sides of the sample membrane. The adhesion depends on the cleanliness of the membrane and the shear sheets. The cleanliness of the membrane is checked in the same manner as the shear sheets.

i. *Placing the fabric and the shear sheets* (Figure 5.16i):

The satin fabric strips are only necessary when testing normally consolidated clay in the DSC. This allows the sample to strain freely at the minor principal stress ($\sigma'_{hc} = K_o\sigma'_{vc}$) boundaries between the shear sheets and the soil sample during K_o consolidation. The strain in the plane strain direction is zero since the sample is restrained by the platens. To achieve an overconsolidation ratio of 1, the strain in the depositional direction is on the order of 3 to 5 percent at $\sigma'_{vc} \simeq 1.3\ \sigma'_p$. Using the previous setup of Germaine (1982), adhesive between the shear sheets and the sample membrane would restrict displacement of the sample at the boundaries

parallel to the deposition direction. Hence, a new method was developed to separate the shear sheets from the sample membrane during consolidation, but to subsequently "glue" them together before shearing. The new technique separates the two by strips of thin, smooth and flexible satin ribbons (as shown in Figure 5.17) during consolidation. The satin prevents the membrane from sticking to the shear sheets, and the sample can deform freely at this stage. It is then removed by hand after consolidation. The procedure is:

- Prepare eight 2–feet long double–face 1" satin ribbons.
- Fold the satin ribbons as shown in Figure 5.17.
- Place four ribbons on the two opposite minor principal stress faces of the specimen.
- Place one set of the shear sheets over two adjacent vertical faces, with one shear sheet covering the fabric and the other covering the major principal stress sample face.
- Repeat the above process on both faces.

j. *Positioning the pressure bags* (Figure 5.16j):

- Move the wing nuts on the bottom platens away from the soil sample.
- Place the four pressure bags behind the shear sheets.
- Move the four wing nuts on the vertical poles up to 4.5" away from the bottom platen.
- Connect the position sensors to the control panel.

k. *Placing the top platen and the guiding rods* (Figure 5.16k):

- Place the top platen on top of the device.
- Lower the four wing nuts on the poles until the top platen just touches the soil sample.
- Place the eight guiding rods through the slots on the top platen.
- Place another four wing nuts on the vertical poles to secure the top platen.
- Adjust the distance between the two platens until they are parallel to one another with an intermediate principal stress of 0.02 to 0.04 ksc.
- Measure the distance between the platens.
- Connect the pressure line to the pressure bags.

Note: Check the intensity of the light by taking a trial picture before starting the test.

The sample is ready for the consolidation stage.

5.5 CONSOLIDATION PROCEDURE

During K_o consolidation for the tests on normally consolidated clay, the sample should not experience any lateral strain. Because the time required to compute the strains in a DSC test is at least a day, it is difficult to have a feedback loop that can provide the strain data necessary to adjust the horizontal stress in order to maintain K_o conditions. Hence, the approach adopted uses a consolidation stress path obtained from the results of a lateral stress oedometer and K_o–consolidation triaxial test. The K_o triaxial test results were obtained from Sheahan (1988) on the same series of BBC. This consolidation stress path was compared with the results obtained from a lateral stress oedometer test performed in this research as described in Chapter 4. It was found that they yielded the same results. Therefore, this loading path was used for the DSC tests run on normally consolidated BBC. For these tests, the samples are consolidated to a vertical stress between 1.15 to 1.3 times the preconsolidation pressure of the batch in 11 to 13 loading increments.

For the overconsolidation ratio of 4 tests on resedimented Boston Blue Clay, the DSC samples are consolidated in two loading increments: first the samples are hydrostatically stressed to 0.1 ksc to measure the initial effective stress, σ'_s, of the soil. In the unconsolidated–undrained triaxial tests described in Chapter 4, the measured initial effective stress is about 0.11 to 0.14 ksc. Therefore, in order to reduce the suction pressure experienced by the pressure probe (to prevent the probe from desaturation), a stress of 0.1 ksc is applied. The initial effective stress of the sample is given by the sum of the magnitude of the (negative) pore pressure and the applied stress of 0.1 ksc. The samples are then consolidated to a hydrostatic stress of 0.25 ksc (for σ'_p equals 1 ksc, and an OCR of 4).

The duration for each consolidation increment for the above tests depends

on the stress level of the soil. For a high OCR, the dissipation of the pore water pressure is faster than for normally consolidated clay. Regardless of the test, the loading is increased when the pore water pressure dissipation has reached 95% in order to minimize the duration of the test. The time to reach this degree of consolidation ranges from 3 to 10 hours per increment. Although the pressure bags are designed for long duration tests, the natural rubber of the bags tends to undergo substantial creep under constant loading. Leaks can occur between the pressure bags and the backing plates (see Figure 4.27) if they are stressed for a long period of time (about a week).

The procedure for consolidation is as follows:

a. *Setup procedure for the normal stress control panel* (Figure 5.3):
   - Close Valve No. 15.
   - Open Valve Nos. 1, 20, 21, 22, 23 and 24.
   - Calculate the output voltages for 0.02 ksc hydrostatic stress.
   - Vary the hydrostatic stress using pressure regulator A.
   - Open Valve Nos. 5, 7, 14 and 17.
   - Adjust each pressure bag with a level at the back of the backing plate till the neutral position is reached (i.e. red light is lit up).
   - Set the position of the camera.
     (Fix the f–stop at 9.5 and the shutter speed at 0.5 seconds.)
   - Position two 500 watt spotlights about 1.5 feet away from the top platen at an angle of 45° on the opposite sides of the device.

b. *Determining the stress increments:*
   - Calculate the stresses for each stress increment.
   - Label the stress increment on the top platen so that it is printed on the film.

c. *Starting the central data acquisition with time delay:*
   - Record the readings of the two normal stresses and the pore water pressure using the central data acquisition. Set the time delay so that there will be enough time to place the stress increment.

Note: The readings are stored in the central data acquisition computer temporarily, then transferred to another computer for further analysis.

d. *Increasing the stresses, σ_a and σ_b:*
   - Increase the hydrostatic stress by turning the knob of pressure regulator A, and increase σ_1 (σ_a) by using the differential pressure regulator.

Note: In some tests, the hydrostatic stress is increased an hour before increasing the vertical stress, σ_1.

e. *Repositioning the pressure bags:*
- Move the pressure bags so that they are in the neutral position again with the help of both the position sensors and a level at the back of each backing plate which keeps the bag vertical.

Note: The bags should be constantly adjusted during each loading increment to keep the uniformity of the strains at the boundaries within an acceptable value.

f. *Taking Photographs:*
- Place the loaded film cartridge in the camera.
- Remove the cover of the cartridge.
- Turn on the two spotlights.
- Wind the shutter and press the button.
- Switch off the spotlights immediately.

Note: The heat from the spot lights can alter the readings of the pore pressure probe, therefore the lights are turned off immediately after the photographs are taken.

g. *Repeating step* (b) *through* (f)*:*
- Repeat the above steps until the last increment.
- Remove the satin ribbons before the last loading increment by pulling the ribbons one by one.

The films are developed to check the quality of the negatives before the undrained shearing stage of the test. The data for the consolidation process are collected and reduced. Consequently, the preshear consolidation stress was applied for a period of 3 to 6 days.

5.6 UNDRAINED SHEAR PROCEDURE

This part of the test requires the operator to be in an alert state, absolute concentration is necessary to achieve a successful test. The undrained shear procedure for resedimented Boston Blue Clay is as follows:

a. Connecting the shear sheets to the shear pistons (if shear sheets are in use) (refer to Figure 5.4)*:*
- Connect the shear pistons to the four shear sheets.
- Align each piston with corresponding shear sheet.
- Open Valve Nos. 1, 2, 3, 6, 7, 12, 13, 16 and 17 on the shear stress control panel.

b. Starting the stress reduction computer program:

- Run the stress reduction program on the personal computer.

This computer program calculates the applied stress for a given stress path.

c. Estimating the incremental stress:

- Extrapolate the effective stress path of the sample based on the initial effective stress path.
- Measure the distortion angle, α, of the soil sample using a protractor.
- Input the distortion angle and the estimated values of p' and q in the computer program.

Note: The number of stress increments (each applied for 8 to 10 minutes) was selected to give a shear strain rate of 0.1 to 0.8% per hour.

d. Increasing the applied stresses:

- Use the stress values computed.
- Adjust the hydrostatic stress using the pressure regulator (A) on the normal stress control panel (Figure 5.3).
- Vary the normal stress, σ_a, using differentiate pressure regulator.
- Increase the shear stresses, τ_a and τ_b, simultaneously, by adjusting the pressure in the two pressure regulators on the shear stress control panel (Figure 5.4).
- Adjust the positions of the four shear pistons by sliding the pistons along the piston supporting frame.

Note: As the sample deforms, the pistons have to be moved so that the shear stresses acting on the shear sheets and the pistons are concentric.

- Adjust the positions of the pressure bags if necessary, so that they are in the neutral positions using the position sensors and levels at the back of the backing plates.

e. Monitoring the pore water pressure of the soil:

- Measure the pore water pressure of the soil sample.
- Adjust the hydrostatic stress using pressure regulator (A) on the normal stress control panel in order to keep the pore water pressure at zero.
- Allow the sample to strain at this stress level for 8 to 10 minutes.

Note: Make sure that the pore water pressure is kept at zero and the pressure bags are at neutral positions during this time.

f. Taking photographs:

- Place the loaded film cartridge in the camera.
- Remove the cover of the cartridge.
- Turn on the two spotlights.
- Wind the shutter and press the button.
- Switch off the spotlights immediately.

g. *Increasing the stress level:*
- Measure the applied stress and input the information on the computer.
- Repeat the above steps (*c*) to (*f*) until failure occurs.

A typical number of increments for OCR=4 BBC is about 20, and the number of increments for OCR=1 varies from 20 at δ=0° to 40 at δ=90°.

Once the soil sample has reached failure (or yielded continuously), the shear stresses on the pistons are released and the normal stresses are brought back to an hydrostatic stress of 0.05 ksc before dismantling the device. No picture is taken at this stage. The air pressure supply to the two control panels is shut off, and the device is disassembled. The sample is cut into several horizontal layers to observe any failure planes in the soil sample. The water content of the soil sample is recorded at different locations to check the uniformity of the sample.

5.7 ANALYSIS OF EXPERIMENTAL DATA

The stress and strain reduction of the Directional Shear Cell is a very complicated process. A number of computer programs have been written to perform various tasks in the reduction process. A flowchart of the reduction process is shown in Figure 5.18.

The applied stresses are stored in the computer during the shear test. The data file can be retrieved and printed using a printing program called "STRESS–P." The data file contains all of the stresses (σ_a, σ_b, τ_a, τ_b, σ_2 and u) and the angles (δ or ψ and α), and can be read by any commercial software for IBM PC computers. Photographs of the sample are taken at representative stress increments. After the test, the films are developed and dried before they are digitized. The raw data on the reference points are stored in the computer using a program called "DIGIT." The strains are computed from the displacements of the reference points using a program called "STRAIN," described in Section 5.3.3.

The information on the applied stresses is combined with the results from the strain reduction to produce a more comprehensive data format, which can easily be read by any commercial software. The output from the sorting program separates the results into two parts: global results which include the general stress and strain results, and the local results, which include the strain distributions of the sample. The global results are then plotted using commercial plotting software, like Harvard Graphics or Lotus 123. A contouring program was written to plot the contours of the strain for each stress level; this program will only work on Roland DXY plotters (e.g., Roland DXY880). The plots are generated in color to make the contours easier to identify. It takes about 15 hours to reduce a DSC test with 20 strain increments.

Table 5.1: Different Techniques of Strain Measurements in the Directional Shear Cell.

Techniques	Resolutions	Data Processing	Material tested	Remarks
Displacement Transducer	Excellent	Very Fast	Clay & Sand	It cannot be used in MIT DSC device.
Video Image	Poor	Fast	Clay & Sand	It is too costly.
Radiography	Good	Slow	Dense sand only	It causes too much sample disturbance in clay.
Photography	Average	Slow	Clay & Sand	Overall performance is satisfactory.

Table 5.2: A Typical Output from Global Strain Analysis.

(From Test DSC31 at Failure, i.e., @ q/σ'_{vc} = 0.164)

Area Number (Fig. 5.6)	ϵ_y (%)		ϵ_x (%)		ϵ_{xy} (%)		ϵ_1 (%)		ϵ_3 (%)		γ_{max}* (%)		ϵ_v† (%)		ζ‡ (°)	
	Mean	S.D.	Mean	S.D.	Mean	S.D.	Mean	S.D.	Mean	S.D.	Mean	S.D.	Mean	S.D.	Mean	S.D.
1	-5.051	0.130	4.564	0.134	0.245	0.094	-5.057	0.130	4.570	0.134	9.627	0.187	-0.487	0.187	91.46	0.56
2	-5.895	0.127	5.333	0.138	0.302	0.094	-5.904	0.127	5.341	0.138	11.245	0.187	-0.562	0.187	91.54	0.48
3	-6.588	0.136	6.093	0.154	0.300	0.103	-6.595	0.136	6.100	0.154	12.696	0.205	-0.495	0.205	91.35	0.46
4	-7.274	0.198	6.568	0.220	0.298	0.148	-7.280	0.198	6.575	0.296	13.855	0.296	-0.706	0.296	91.23	0.61
5	-6.924	0.469	6.754	0.598	0.369	0.378	-6.934	0.469	6.764	0.776	13.698	0.760	-0.170	0.760	91.55	1.58

Notes:

* γ_{max} is the maximum shear strain.

† ϵ_v is the volumetric strain (negative values represent expansion).

‡ ζ is the major principal strain direction.

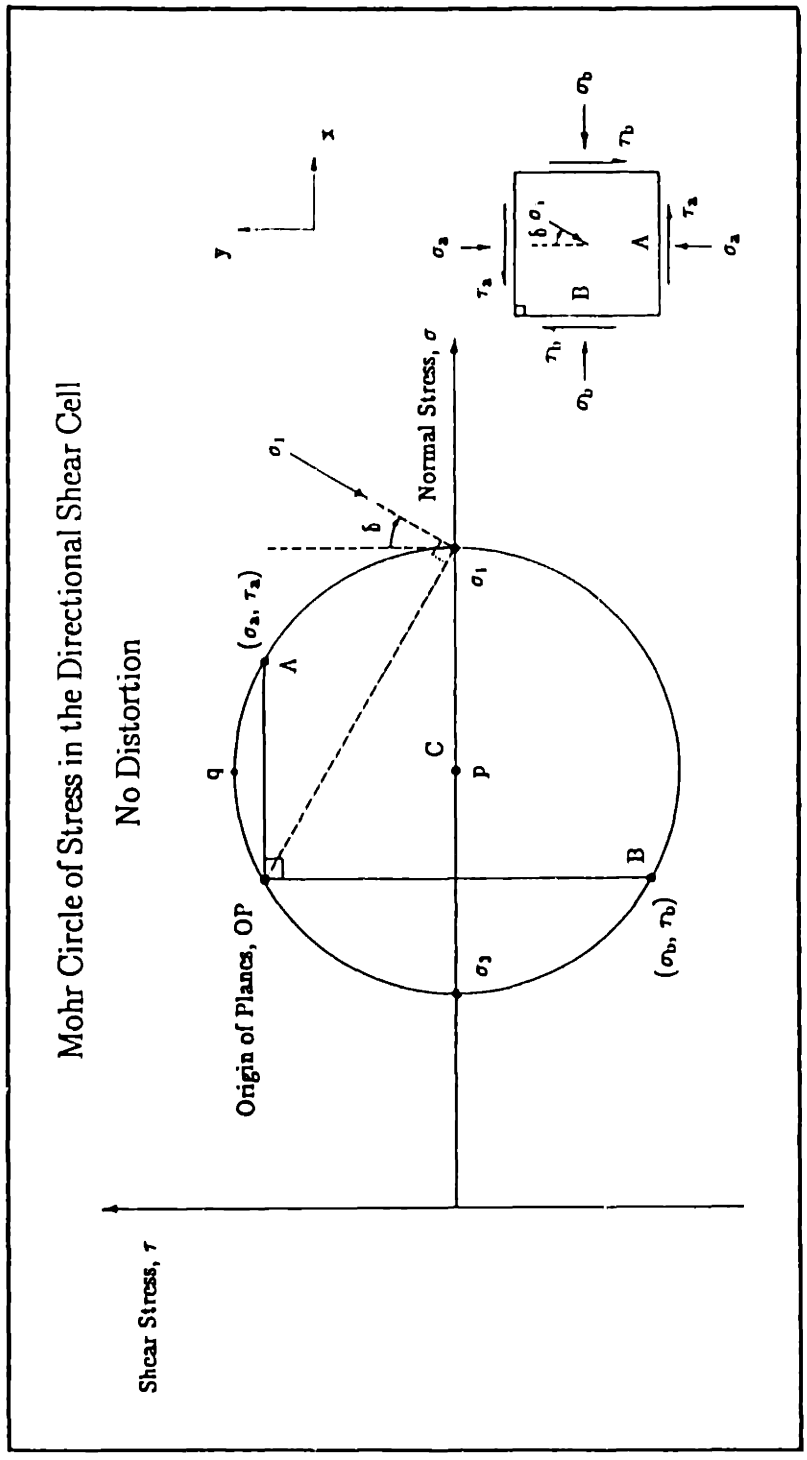

Figure 5.1: Mohr Circle of Stress in Directional Shear Cell with No Distortion Correction.

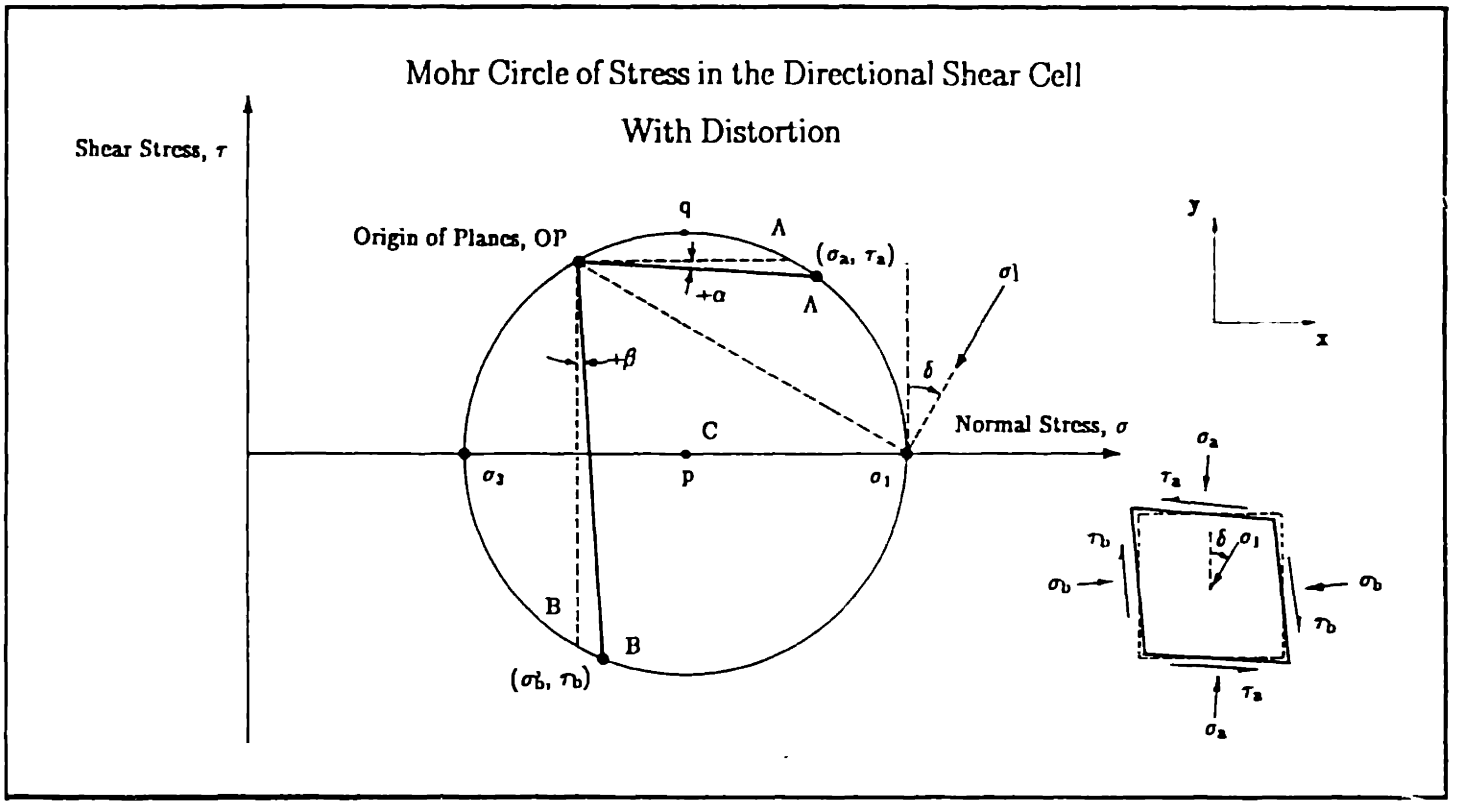

Figure 5.2: Mohr Circle of Stress in Directional Shear Cell with Distortion Correction.

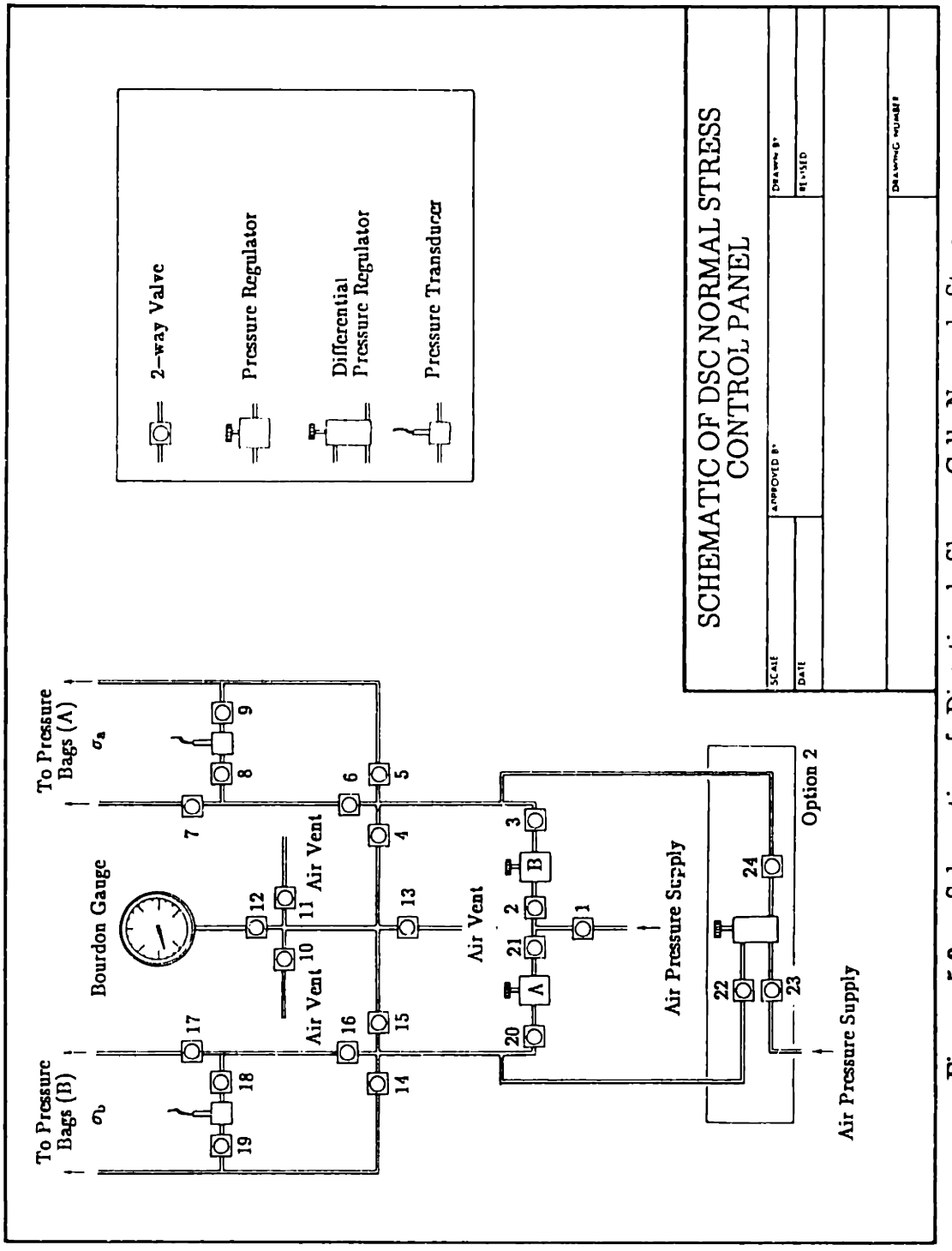

Figure 5.3: Schematic of Directional Shear Cell Normal Stress Control Panel.

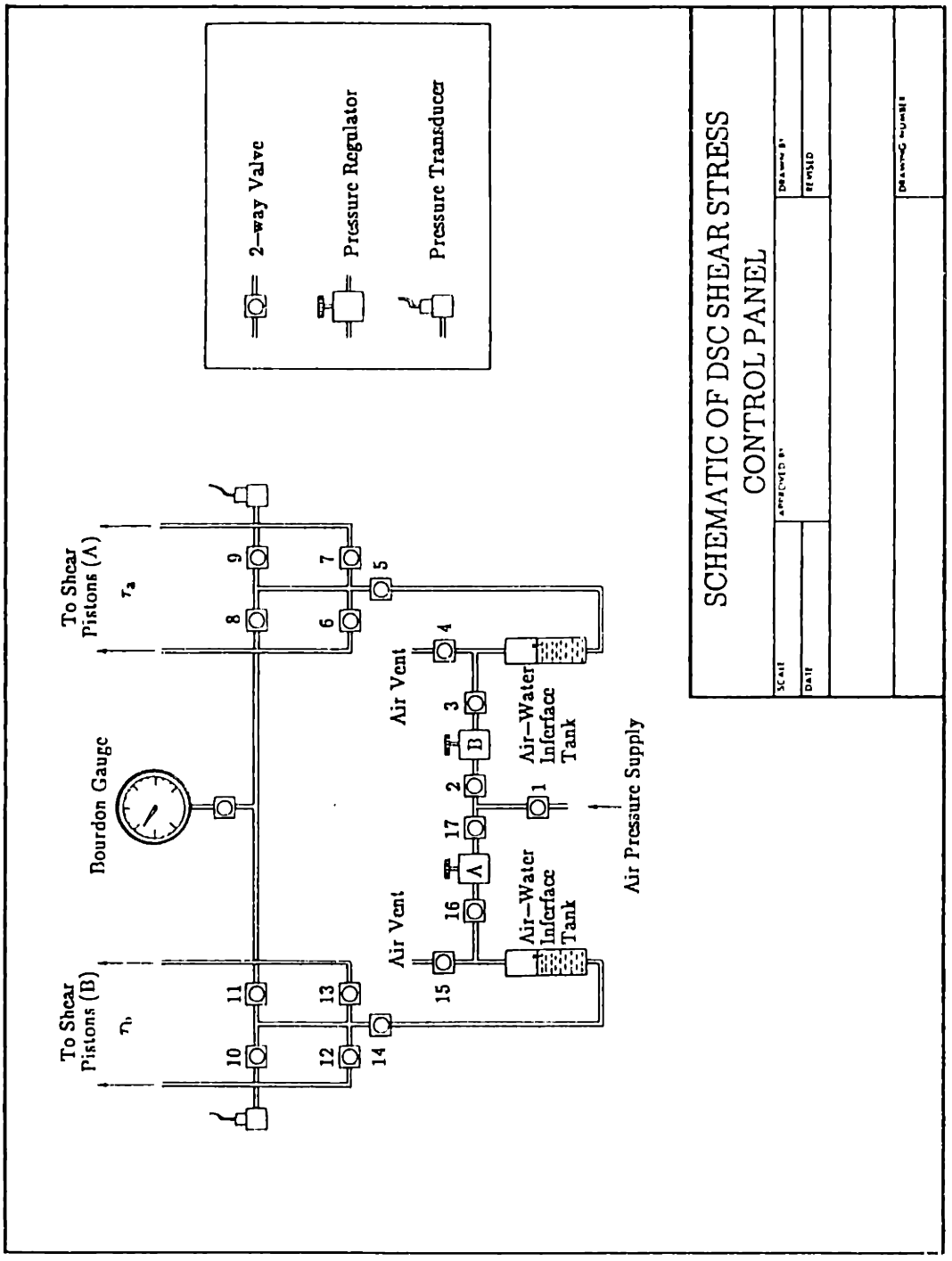

Figure 5.4: Schematic of Directional Shear Cell Shear Stress Control Panel.

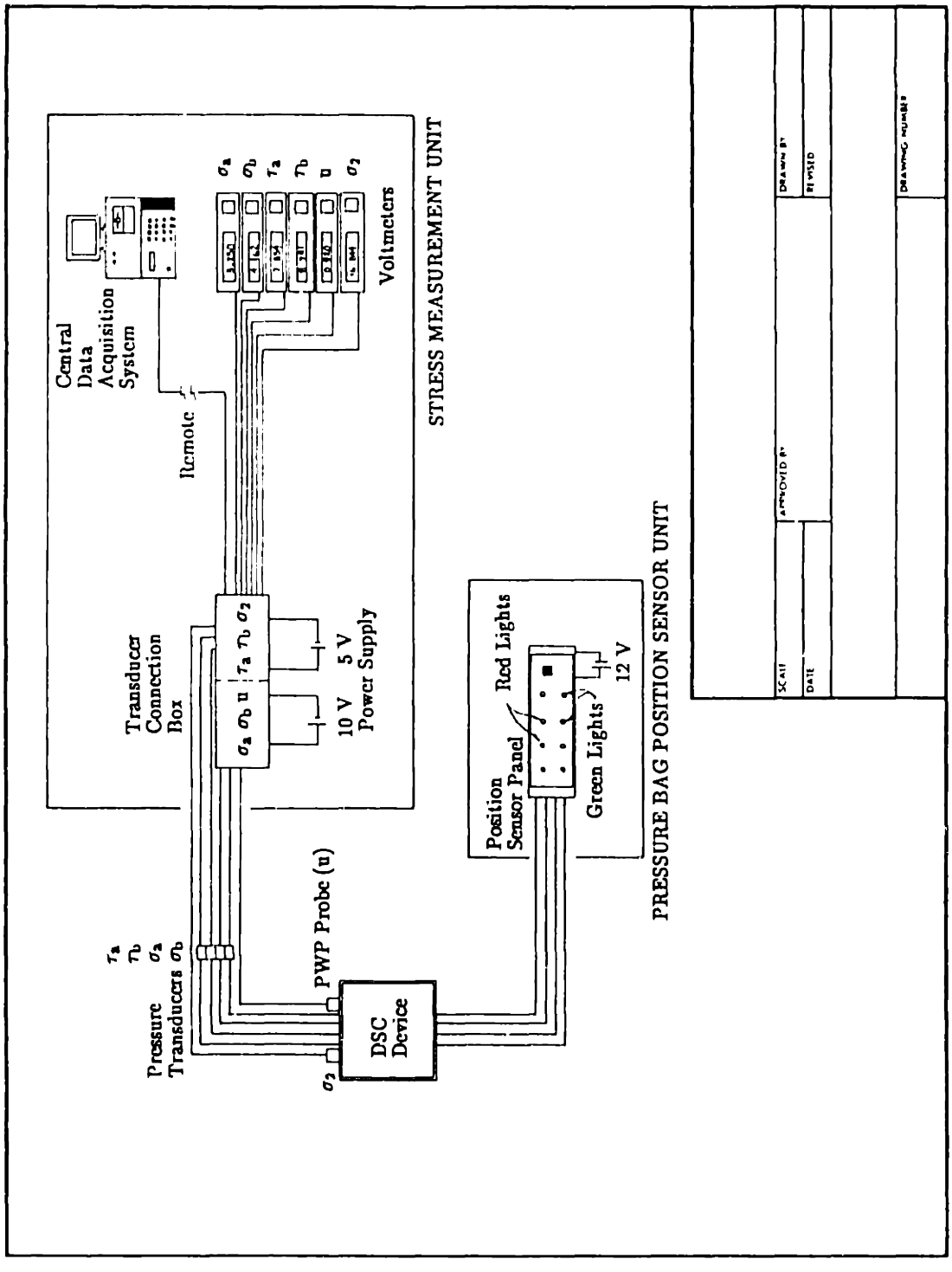

Figure 5.5: Schematic of Electrical Connections of the Directional Shear Cell.

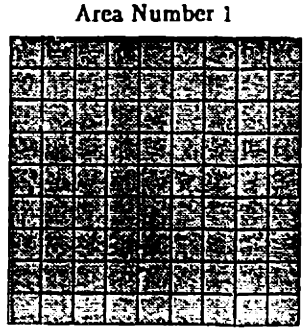

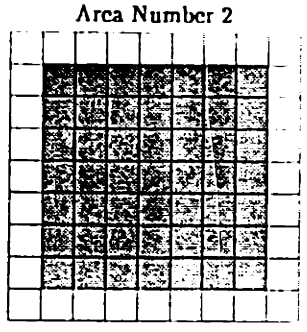

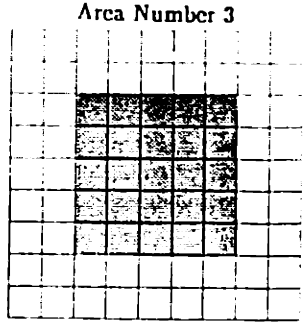

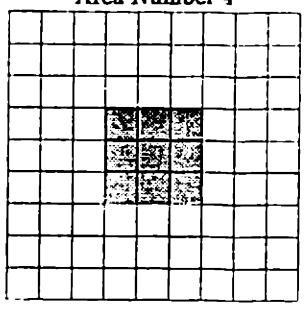

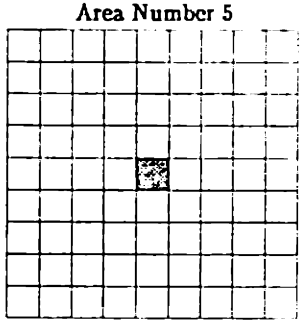

Area Number	Number of Data Points	% of Total Cross Sectional Area
1	100	85.6 %
2	64	51.8 %
3	36	26.4 %
4	16	9.5 %
5	4	1.1 %

Figure 5.6: Definition of Sample Zones over which the Average Strain Values are Calculated.

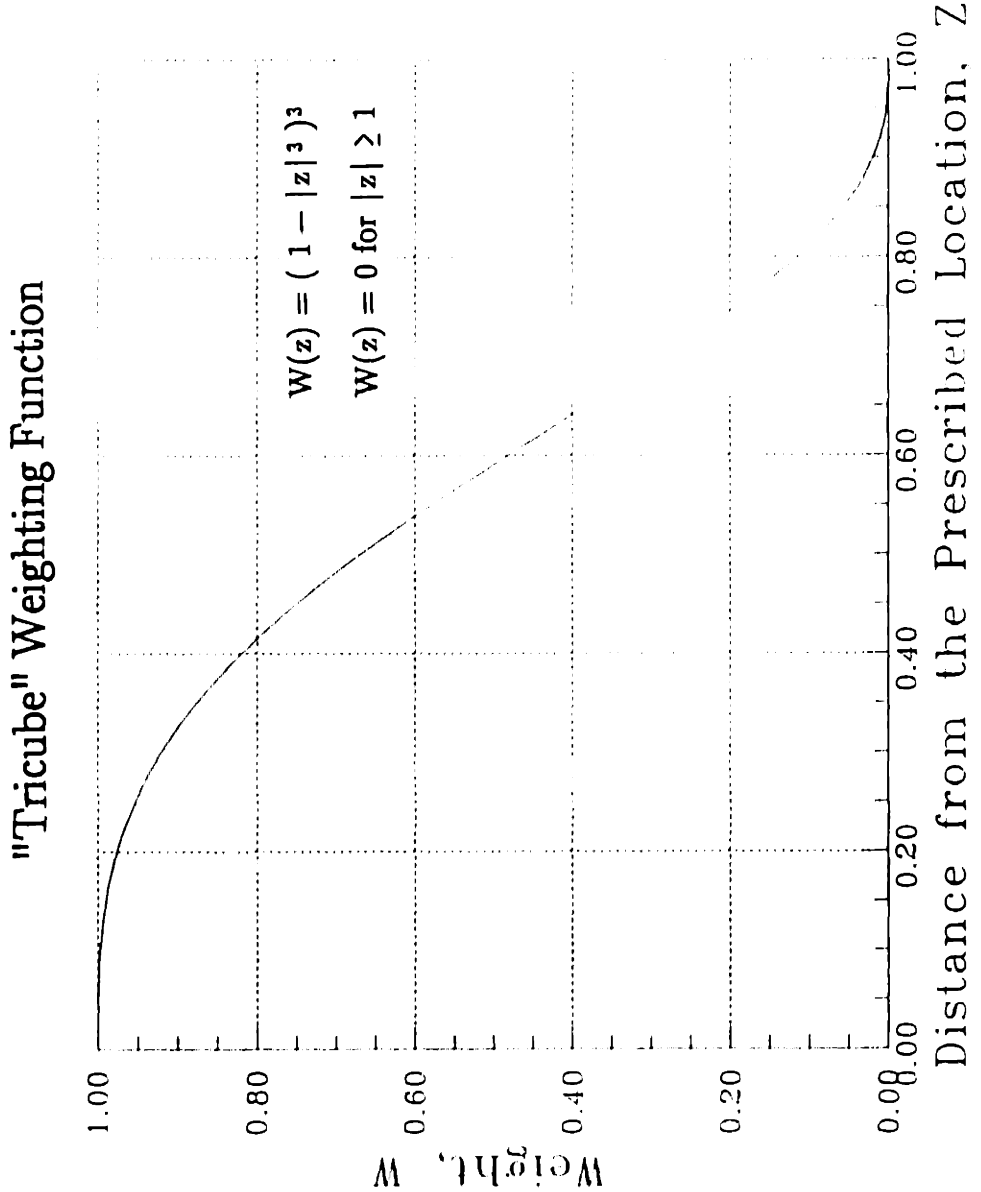

Figure 5.7: Weighting Function used in Local Strain Analysis.

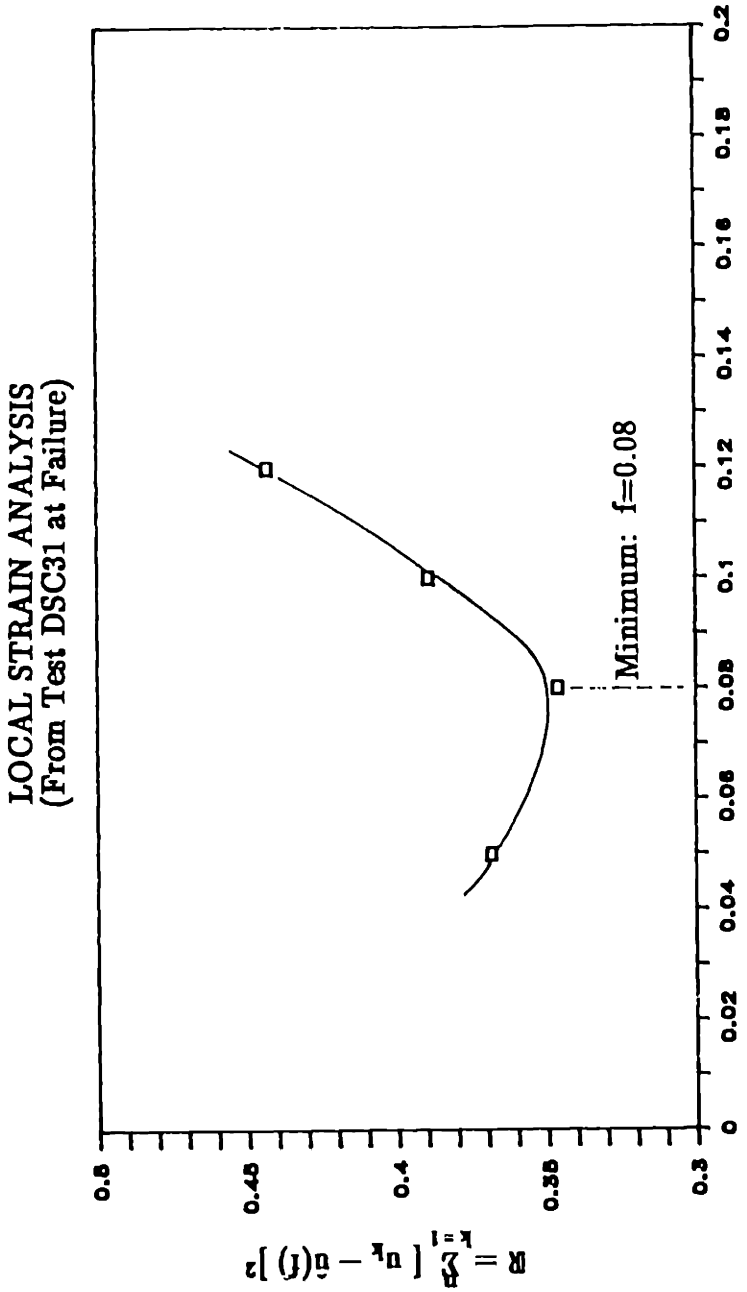

Figure 5.8: Determination of Optimum f Value.

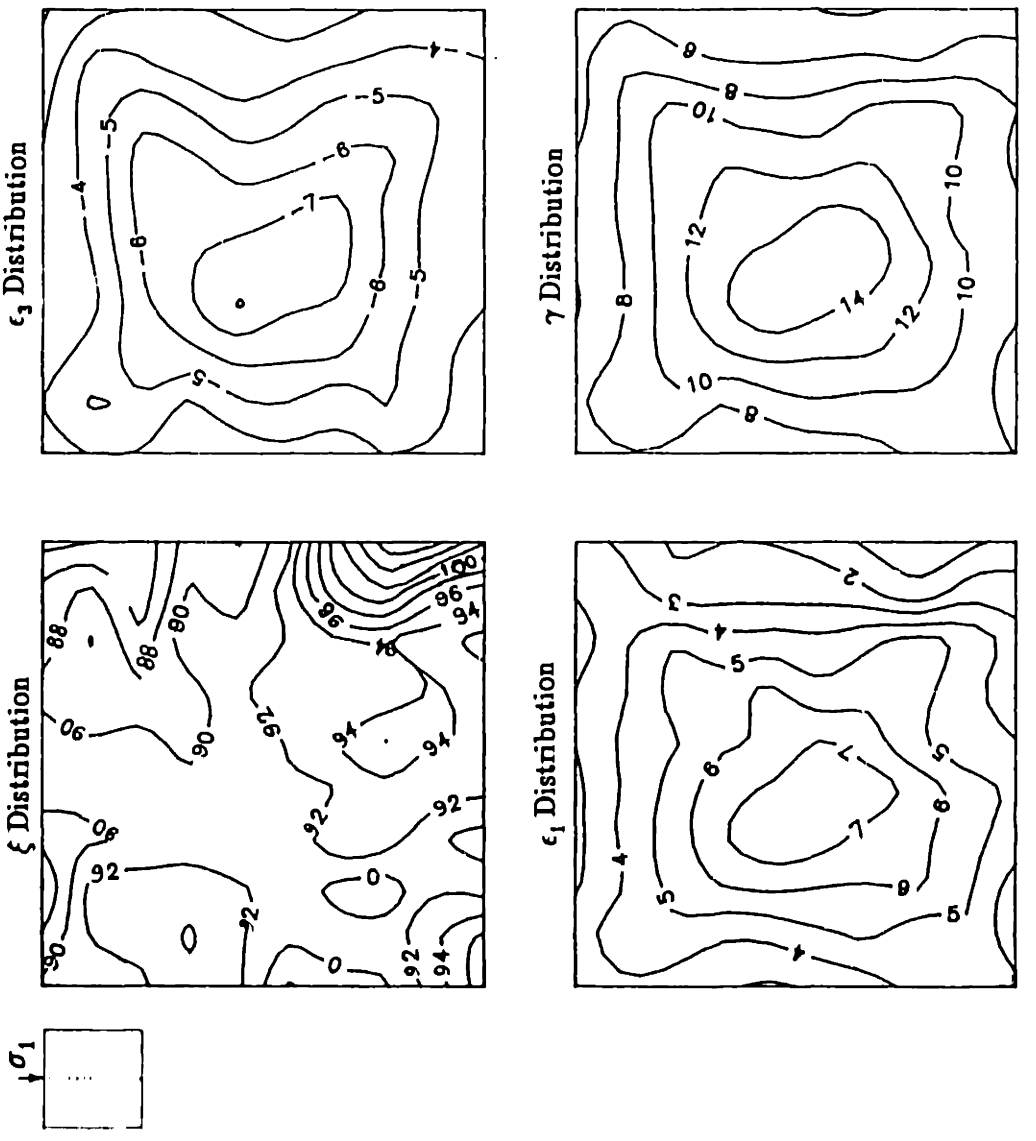

Figure 5.9: Example of Strain and ξ Distributions in Test DSC31.

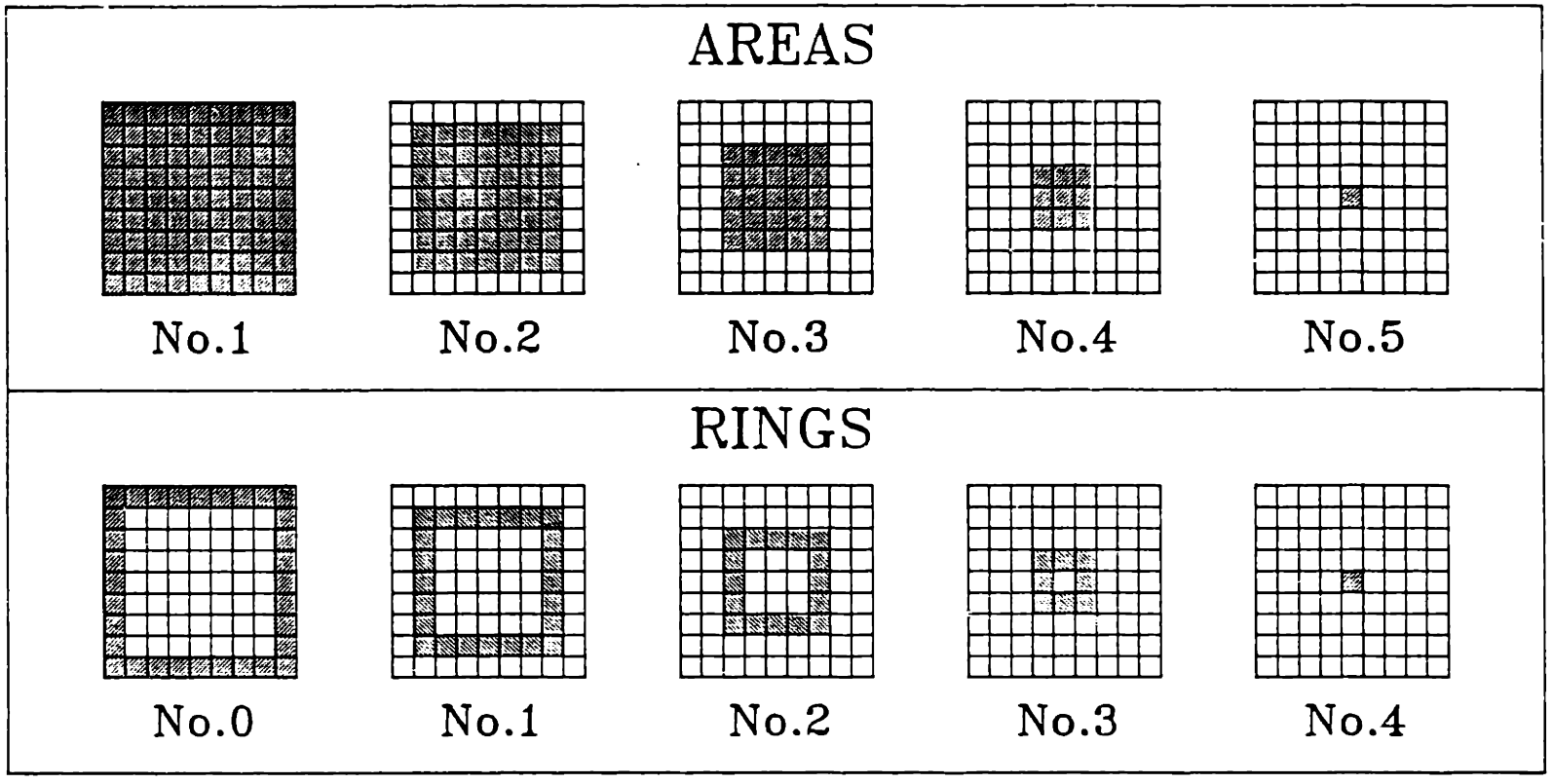

Figure 5.10: Definition of Sample Zones over which Average Strain Values are Computed (after Germaine, 1982).

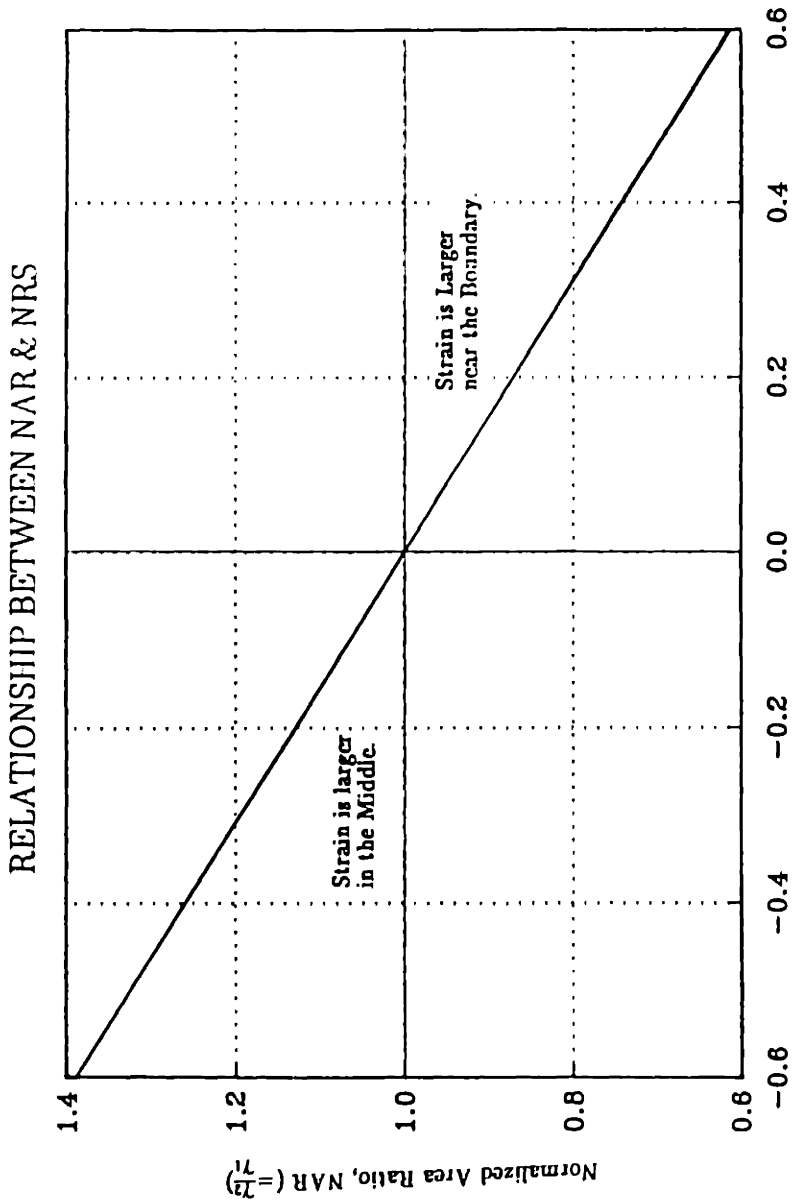

Figure 5.11: Relationship between Normalized Area Ratio (NAR) and Normalized Ring Standard (NRS).

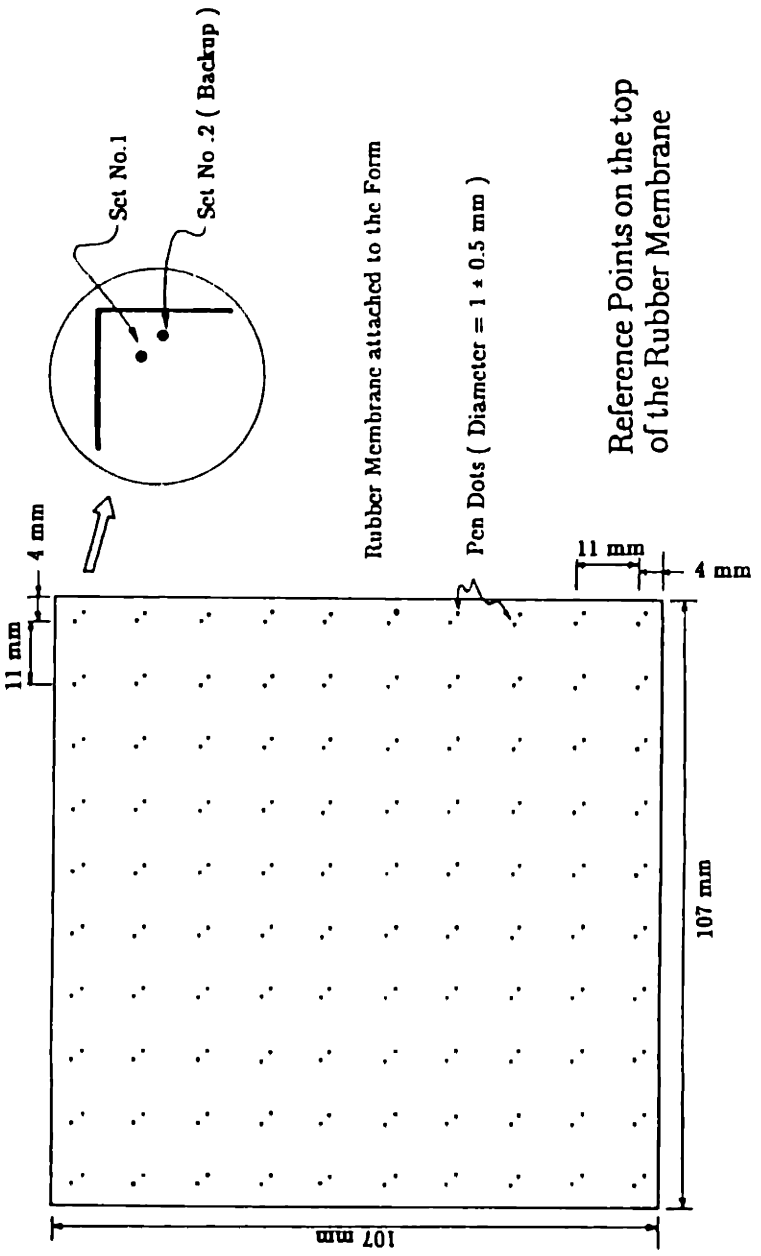

Figure 5.12: Locations of Pen Dots on the Rubber Membrane for Strain Determination.

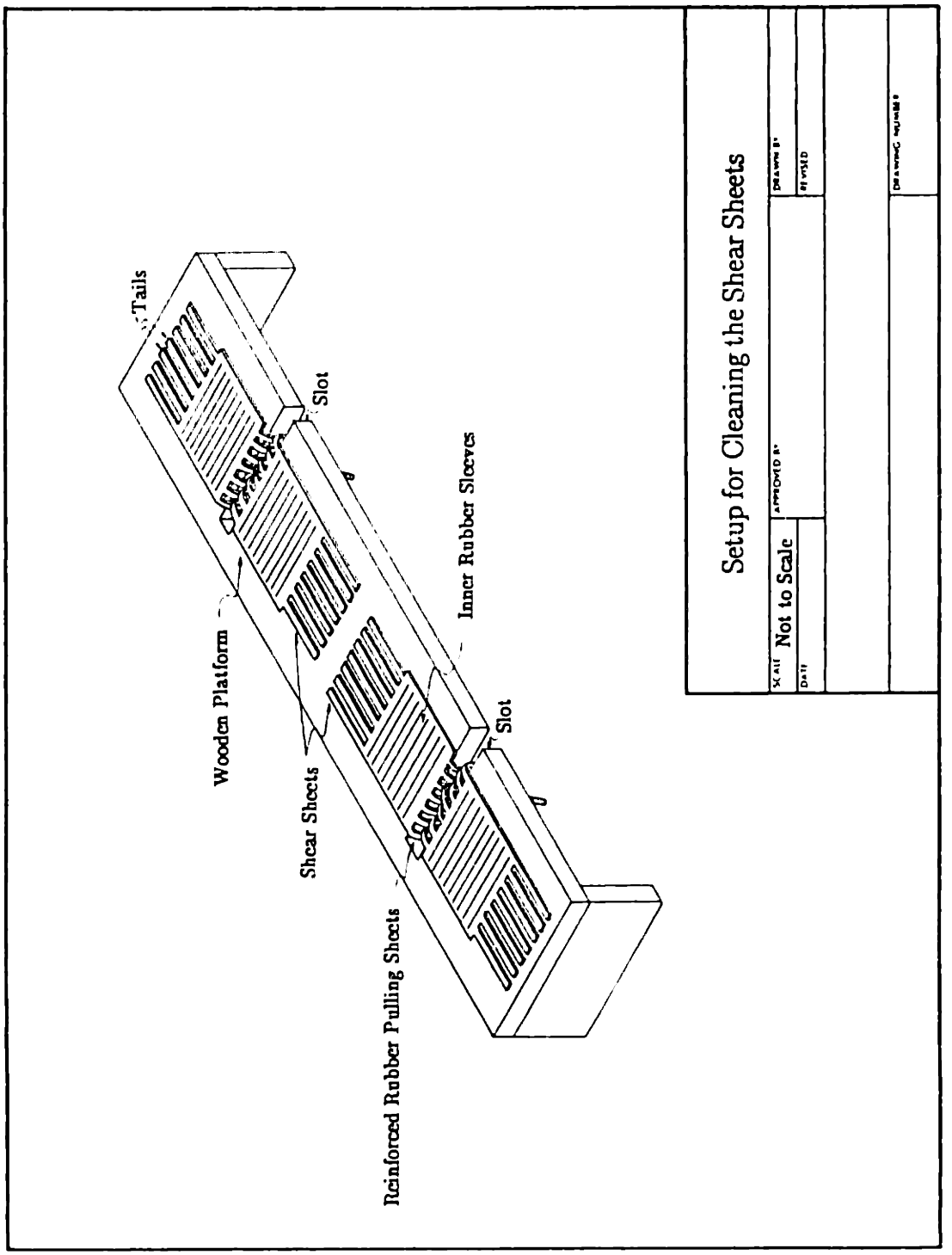

Figure 5.13: Setup for Cleaning the Shear Sheets.

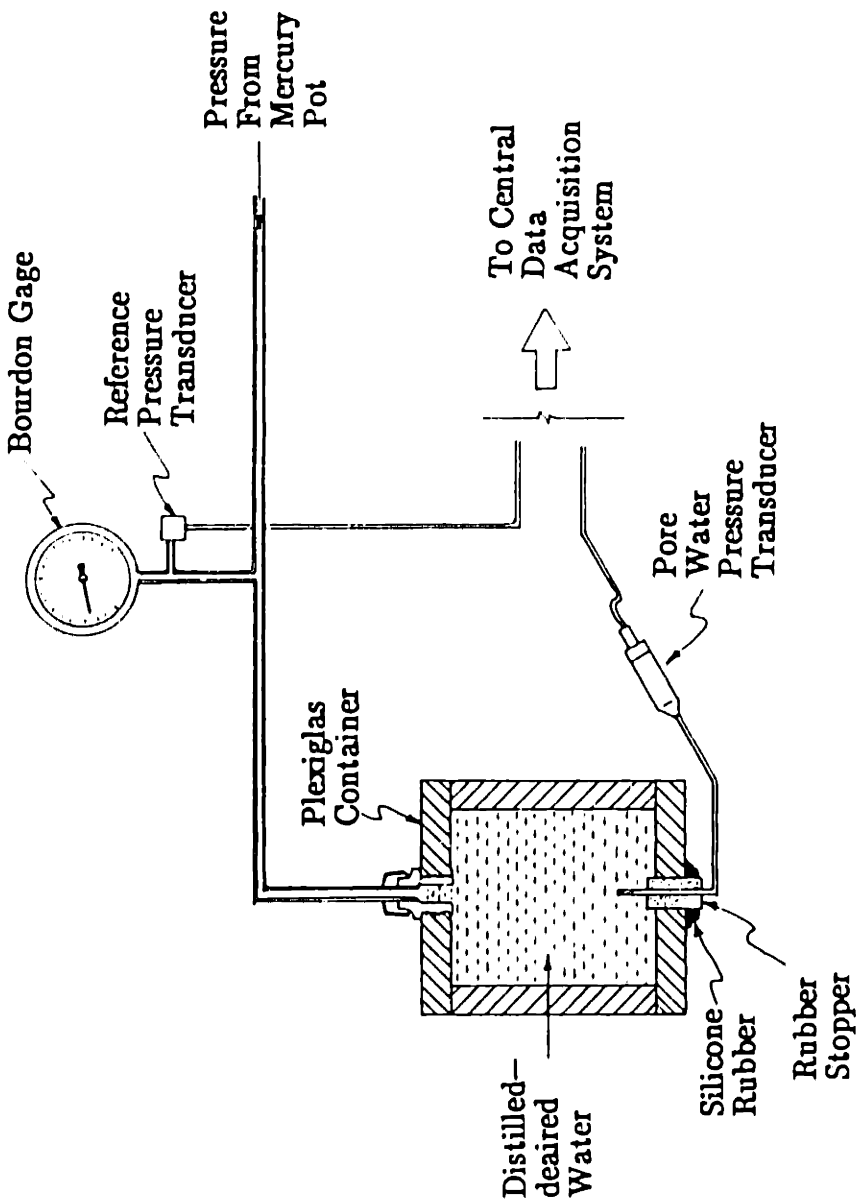

Figure 5.14: Setup for Pore Pressure Response Test.

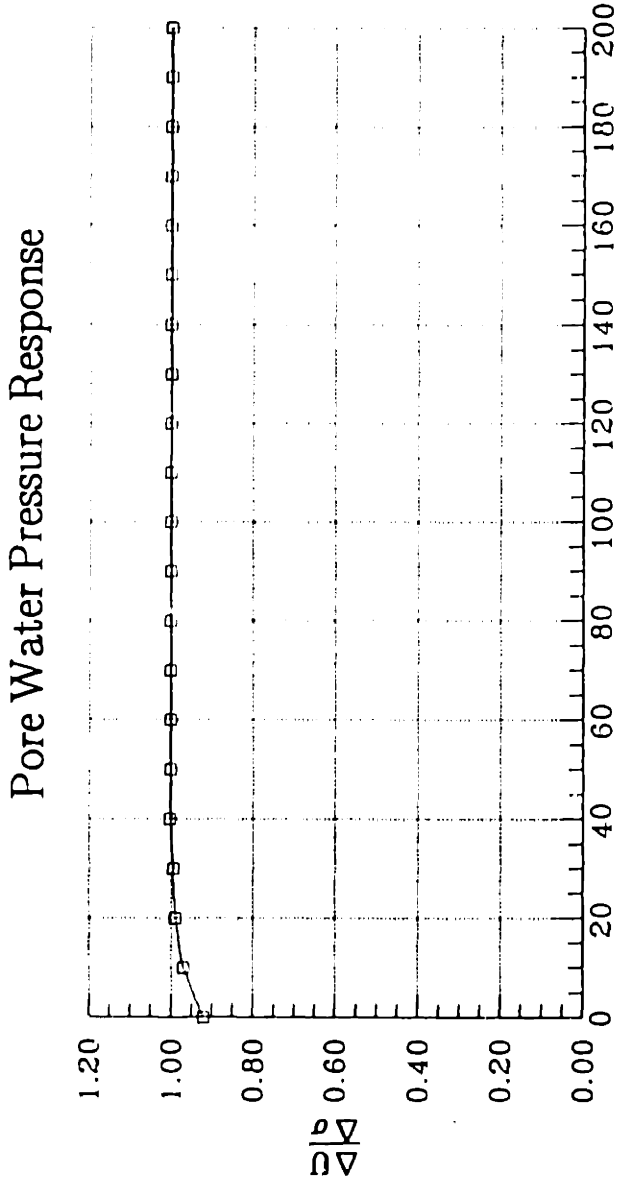

Figure 5.15: Typical Pore Water Pressure Response Curve of the Pore Water Pressure Probe.

PREPARATION OF DIRECTIONAL SHEAR CELL CLAY SAMPLE

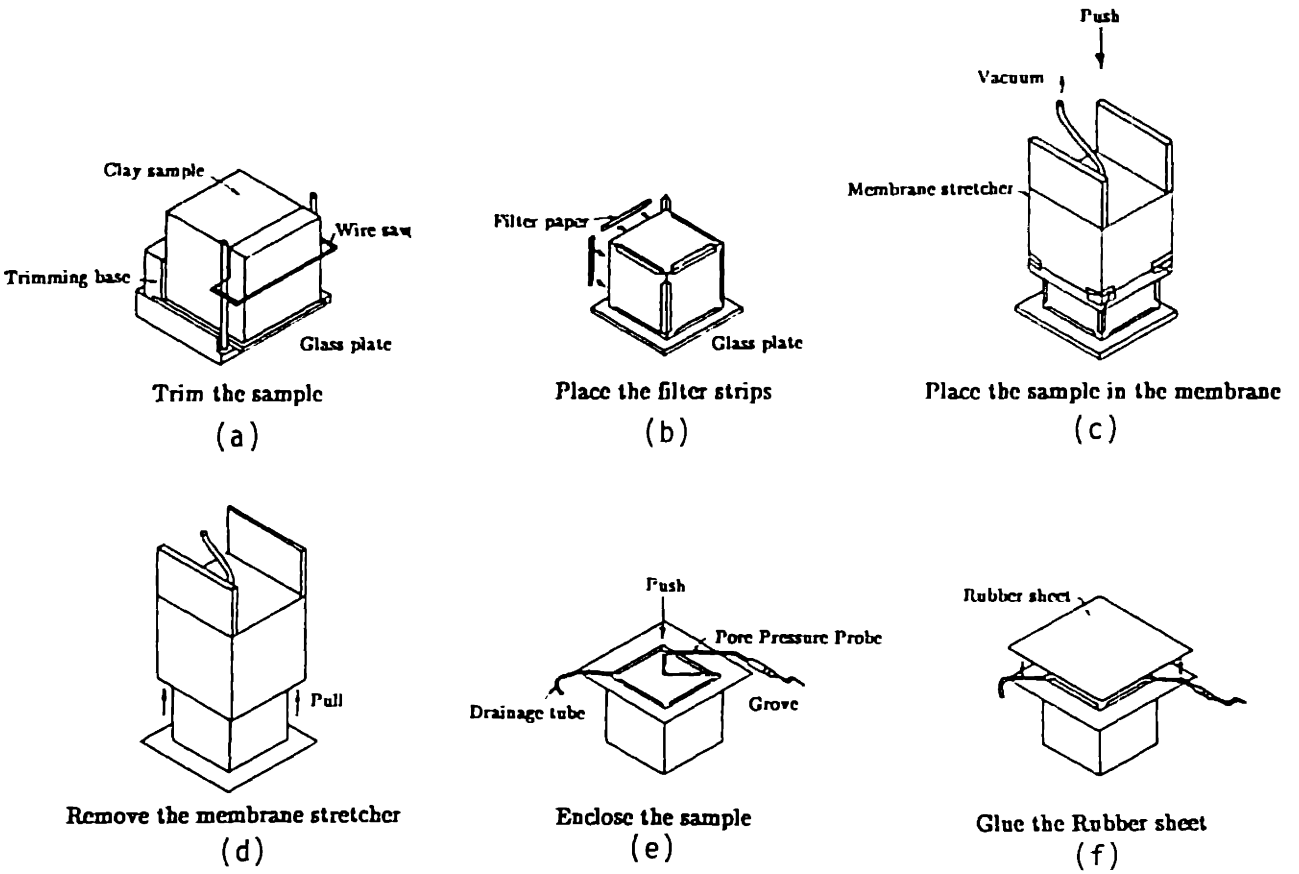

Figure 5.16: Preparation of Directional Shear Cell Clay Sample.

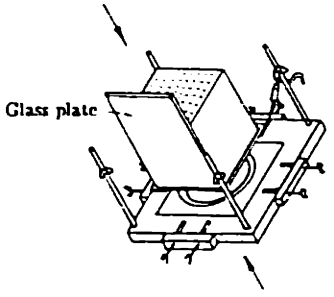

Place the sample on the Bottom Platen

(g)

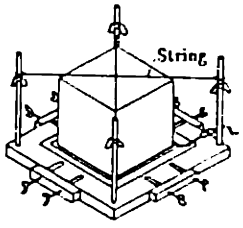

Center the sample

(h)

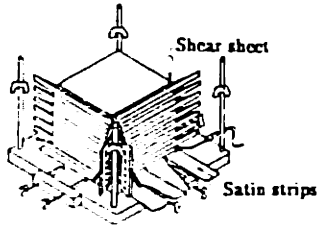

Place the fabric and the shear sheets

(i)

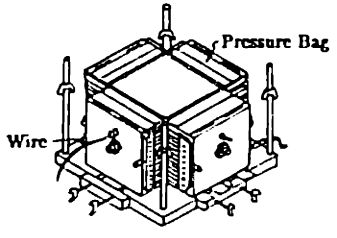

Place the Pressure Bags

(j)

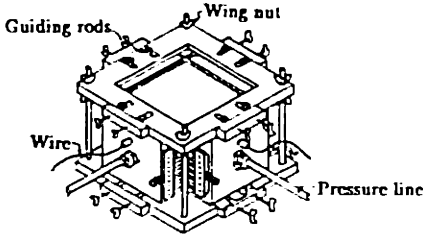

Place the top platen and the 8 Guiding rods

(k)

Figure 5.16: (Cont.)

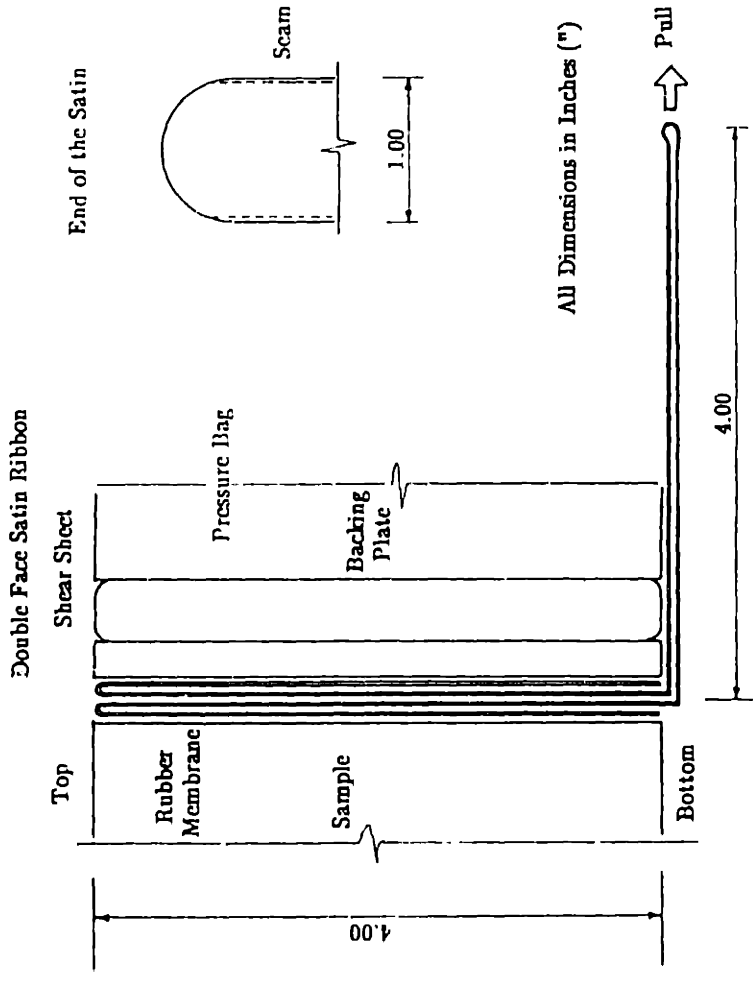

Figure 5.17: Arrangement of the Satin Fabric Ribbon on Face B of Directional Shear Cell Sample.

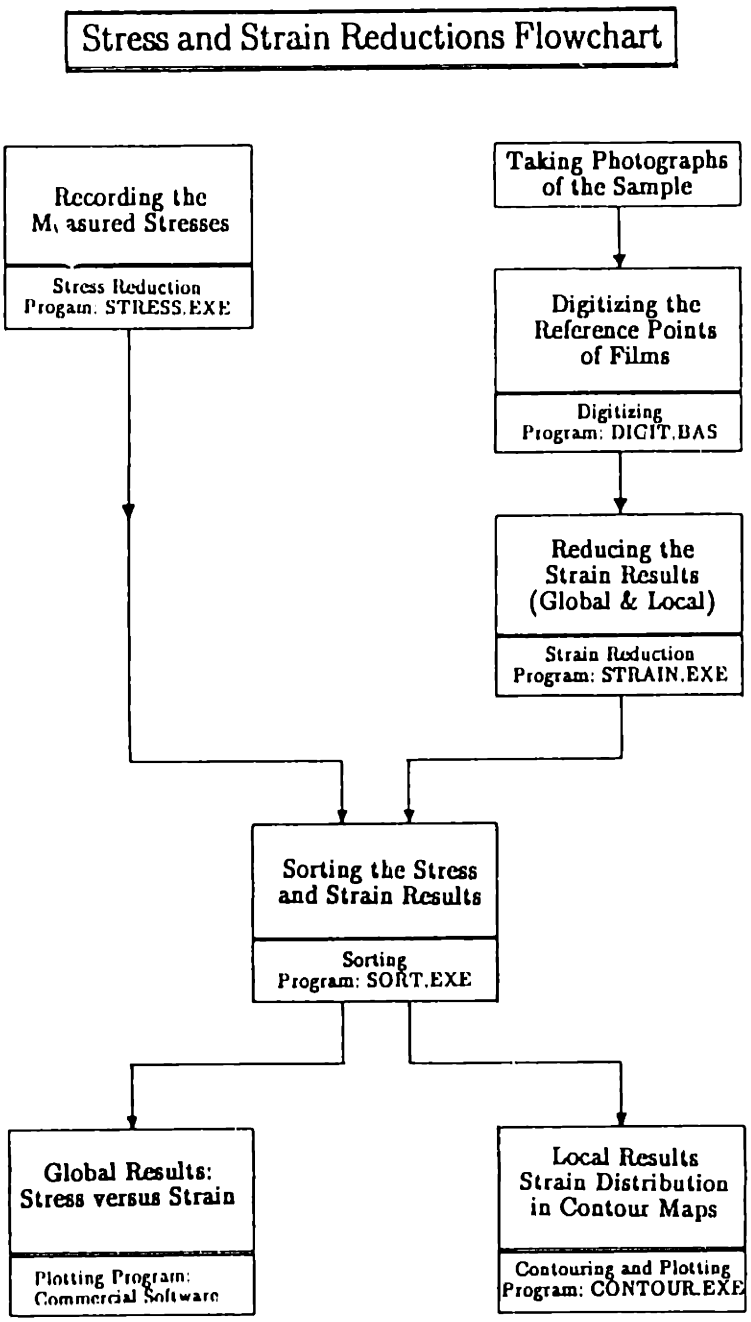

Figure 5.18: Analysis of Experimental Data.

CHAPTER 6

EXPERIMENTAL EVALUATION OF THE DIRECTIONAL SHEAR CELL

6.1 INTRODUCTION

A unique feature of the Directional Shear Cell (DSC) is that its performance can be verified by conducting tests on an isotropic material, which has a stress–strain relationship independent of the direction of the principal stress. This verification is referred to as "proof" testing. In other words, DSC tests that are run with changes in the relative magnitude of the normal and shear stress components (that is the ψ tests as indicated in Figure 2.1) should show identical behavior if the device and testing procedures operate as intended.

Proof testing has also been the primary method used to evaluate an operator's ability to perform DSC tests. The DSC device is highly operator–dependent. The stresses are applied manually using pressure regulators, and the alignment of the pressure bags and shear sheets is made according to the operator's judgment. Therefore, success is directly proportional to the operator ability to perform the tests.

The strain measuring technique described in Chapter 5 is one of the many special features of the MIT DSC device. The strains of the DSC specimen are computed from the displacements of reference points on one plane strain face of the sample. A new strain analysis has been developed in this research to further improve the interpretation and presentation of the data, which consists of both global strain analysis (to give an average value of strain) and local strain analysis (to show the distribution of strain). This method of analysis is described in Section 5.3. In order to quantify the uniformity of the sample, a parameter called

the Normalized Ring Strain (NRS) was used by Germaine (1982), and is described in Section 5.3.4. A different parameter, called the Normalized Area Ratio (NAR), was used in this research, and it serves the same purpose.

Since it is difficult to obtain a testing material with isotropic properties, proof tests were conducted in the isotropic plane of cross–anisotropic materials, such as sand and K_0–consolidated clay. Section 6.2 describes an overview of proof tests performed on Leighton Buzzard sand by Bekenstein (1980) and on resedimented Boston Blue Clay by Germaine (1982) and O'Neill (1985) at MIT.

Further evaluation of the DSC was done in this research by performing proof tests on the following materials:

1) Resedimented BBC at OCR=4 with shearing in the isotropic plane, as previously done (Section 6.3.2);
2) Cross–anisotropic rubber foam with shearing in the isotropic plane (Section 6.3.1);

Section 6.3.2 discusses the results from the DSC proof tests on BBC, including the stress–strain behavior, effective stress paths and failure planes of the tested samples.

The DSC tests performed in this research are compared with the previous DSC tests conducted by Germaine and O'Neill in Section 6.4.

6.2 OVERVIEW OF PREVIOUS PROOF TESTS OF THE DIRECTIONAL SHEAR CELL

A number of proof testing programs have been conducted over the years by both MIT and UCL research groups. Rodriguez (1977) and Wong (1985) conducted proof tests on Leighton Buzzard sand at UCL to verify the performance of the DSC device as well as to improve the testing technique. However, this

section discusses only the DSC proof tests performed by MIT researchers on sand and clay. Bekenstein (1980) performed a number of drained proof tests on Leighton Buzzard sand in both dense and loose states, as discussed in the section below. As Section 6.2.2 describes, this device was later used by Germaine (1982) to perform undrained proof tests on BBC.

6.2.1 Proof Tests with Leighton Buzzard Sand

DSC proof tests were conducted by Bekenstein (1980) on Leighton Buzzard sand at different ψ angles under drained conditions in the isotropic plane of the sand sample, i.e., the X–Y plane in Figure 2.1. The samples were hydrostatically consolidated to 14 kPa, then sheared with the minor principal stress kept at 14 kPa while the major principal stress was increased until failure occurred.

Figure 6.1 shows results of fifteen ψ tests on dense sand with initial void ratios of 0.53±0.01. The strains of the sample were calculated from the displacements of tungsten Carbide shot embedded in the middle of the sample using a radiographic technique. These strains represent 50% of the total sample area of a 7x7 sample grid, as shown in Figure 6.2. This area was used partly due to relatively non–uniform strains encountered close to the boundaries. The results in Figure 6.1 show good agreement for the Stress Ratio ($R=\frac{\sigma_1}{\sigma_3}$) versus the major principal strain (ϵ_1) for the ψ=0°, 40° and 50° tests, with a well–defined best estimate with relatively little scatter. But the tests performed at ψ=20° and ψ=70° generally showed excessive strain and/or premature failure. It was "thought to be caused by the reduced thickness of the shear sheets where they fold around diagonal corners, which produces a shear stress component from the pressure bags and local overstressing" (Arthur et al., 1981). It can be avoided by introducing uniformly thick shear sheets as used by Germaine (1982). Furthermore, tests conducted at ψ=0° and 90° with unstressed shear sheets gave

higher R values at failure (R_f=8.4±0.4), whereas the R_f measured at intermediate σ_i directions or on samples without shear sheets was 6.9±0.4. It is believed that the unstressed shear sheets apparently inhibit the formation of rupture layers. The difference (Δ) in the axes of major principal strain and major principal stress was within ±5°, this variation was thought to be within measurement capabilities.

Figure 6.3 displays the results of eleven ψ tests on loose sand with initial void ratios of 0.74±0.02. The conditions of the tests were identical to the dense sand, with the same drained conditions and loading stress path for all tests. The strains were determined by taking average values obtained from photographs of a 5x5 grid of lines inked on the top rubber membrane, representing about 50% of the total area. The stress–strain curves tended to be more randomly scattered than those observed with dense sand. The results indicate that the strains are consistently less uniform than the dense sand for the same amount of shear applied to the shear sheets. It was observed that larger interior strains occurred with unstressed shear sheets and more uniform strains with highly stressed shear sheets. The conclusion was that an arching effect was created in the tests with insufficient compression/extension of unstressed shear sheets. The problem can be corrected by using thinner shear sheets for these soils. Nevertheless, the results indicate that the DSC yields almost identical stress–strain curves at varying ψ angles. The difference in the axes of major principal strain and major principal stress is within ±5°, which is the same order of magnitude as the dense sand.

It should be noted that the area of the sample considered is 50% of the total area of the sample; by eliminating the region close the boundaries, the possibility of identifying or detecting boundary problems, such as premature boundary failure, is effectively removed. This problem will be discussed further in this chapter.

6.2.2 Proof Tests with Resedimented Boston Blue Clay

In order to check the performance of the DSC with a different material, undrained proof tests on clay were conducted. Germaine (1982) carried out two DSC proof tests on resedimented Boston Blue Clay that had been reconsolidated to an overconsolidation ratio of 4 in the isotropic plane (i.e., X–Y plane, as shown in Figure 2.1), one at ψ=0° (DSC6) and the other at ψ=45° (DSC7),. The test at ψ=45° was discarded by O'Neill (1985) due to its anomalous shear–induced pore pressure. O'Neill continued research on the same material in an attempt to verify the performance of the DSC device as well as to provide more data on the inherent anisotropy of this clay. Three additional proof tests were performed at ψ=0° (DSC12), 25° (DSC9) and 40° (DSC14), as shown in Figures 6.4 and 6.5. Test DSC9 at ψ=25° suffered from boundary slippage on the face of the sample where a lower normal stress was applied. This slippage occurred at γ=1.4% which led to a NRS (Ring No.0) value of about 0.55. Although this slippage did not increase with shear stress level, in this writer's opinion, the surface traction could not be transferred properly after the slippage unless the normal stress on that face was increased substantially, such that the ratio of (τ/σ) would be very small, say 0.3.

The above experimental results were further complicated by the fact the resedimented BBC tested was thixotropic. The procedure of separating the component of the behavior attributable to thixotropic effects based on the results from triaxial tests is described in Table 6.1. There are two main concerns regarding this correction:

1) The correction is based on results from low stress triaxial tests; the consolidation stress was only 0.25 ksc. The friction of the piston shaft and uplifts of the piston can amount to 10 to 20 percent of the peak shear strength. Unless extremely careful measurements had been taken, large

errors in the measurement are inevitable.

2) The correction procedure was based largely on one SHANSEP triaxial test, in which the sample was consolidated beyond its preconsolidation pressure before it was unloaded to an OCR of 4. It is possible that by consolidating the sample to a different preconsolidation pressure, the normalized behavior may be different even if the material is non–thixotropic. Furthermore, the SHANSEP technique is based on unloading consolidation, whereas the reconsolidation triaxial test is a recompression test. The behavior of the material may not be the same even if both were tested at the same OCR. Therefore, the correction procedure described is subject to debate.

The results of the uncorrected and corrected data from O'Neill (1985) are presented in Appendix C.

6.3 NEW PROOF TESTS OF THE DIRECTIONAL SHEAR CELL

One of the objectives of this research is to conduct more proof tests to verify the performance of the device. The simplest way to evaluate the DSC device is to conduct DSC tests on a material with the following properties:

- homogeneity;
- isotropic or at least cross–anisotropic, so that DSC shear tests can be carried out in the isotropic plane of the material;
- elastic, linear if possible; this is to ensure that only one sample is needed for the whole study since the strain is recoverable; and
- a modulus close to that of the soil tested, so that direct comparisons of stress and strain measurements can be made.

The material that best meets these criteria is rubber foam, which is described in the following section.

Proof tests were performed with varying ψ angles to help evaluate the stress application from the pressure bags and the shear sheets without complications due to sample–to–sample variability, since only one sample is used in the process. Furthermore, any corrections made based on the results from one direction can be verified from the results of a test done in another direction because the behavior of the material is independent of the direction of shear.

Proof tests were also performed on resedimented Boston Blue Clay to ensure that the device can be used on a elasto–plastic material under undrained shearing conditions. The test program and the results are described in Section 6.3.2.

6.3.1 Proof Tests on Rubber Foam

The elastic material chosen for the first series of proof tests is rubber foam. Specimens were cut into 2"x2"x2" cubes from a 10"x10"x2" rubber foam sheet, and tested uniaxially using a triaxial loading frame. The foam was compressed in three orthogonal directions, with the results shown in Figure 6.6. The modulus in the direction normal to Face 1 (see Figure 6.8) is approximately the same as the modulus in the direction normal to Face 2, but the modulus in the third direction has a lower modulus. Although the properties were far from ideal behavior, the foam was visco–elastic. Two 4"x4"x2" specimens were cut and glued together to form a 4"x4"x4" cubical sample with axes rotated 90° in order to produce a more cross–anisotropic material as shown in Figure 6.8. The direction normal to Face 3 was treated as the plane strain direction. This cubical sample was tested in three directions using an Intron compression machine; the results for two directions are shown in Figure 6.7. The stress–strain curves of the two directions normal to Face

1′ and Face 2′ were very similar, hence the DSC proof tests were performed in the plane where the properties are "isotropic."

One important factor to note is that the uniaxial testing machine has rigid loading platens. Therefore, the stress is computed based on an average stress over the cross–sectional area of the sample. This gives rise to identical stress–strain curves in the two directions normal to Face 1′ and Face 2′. On the other hand, if the uniaxial tests are performed using a flexible boundary loading mechanism, the axial strain across the sample is non–uniform because of the non–homogeneous nature of the glued specimen. Special precaution has to be taken when performing the DSC proof tests on this material since the DSC device is a flexible boundary apparatus. If this material is sheared with constant octahedral normal stress, the relationship between the octahedral shear stress and the octahedral shear strain will still be unique, i.e., the relationship is independent of the direction of loading. But the DSC is a plane strain device and the intermediate principal stress was not measured in this series of tests. Therefore, the equivalent unique relationship is the deviatoric stress versus maximum shear strain.

The 4 inch cubical rubber foam was dipped in liquid latex to produce a smooth surface to attach to the shear sheets, through which surface traction is transmitted to the sample. One advantage of this method of preparation is that boundary failure is unlikely to happen since the bonding between the rubber latex and the rubber foam is extremely strong. After the liquid latex sets for at least 24 hours, one hundred reference dots are placed on the top surface (Face 3) of the rubber foam. The sample is then sheared in the plane parallel to Face 3. The displacements of the sample can then be measured from the movements of the reference dots by superposition of films taken at different stress intervals.

A total of eight DSC proof tests were conducted on the rubber foam, all with 3 minute load increments and ten increments per test. The results of the

tests are described later in this section. The tests focused on the following items:

- Repeatability. This is evaluated by conducting shear tests with the same ψ angle twice; the difference in the results is a measure of the repeatability.
- Effects of rotation of the backing plates and the shear sheet pistons. In the tests with shear sheets, the axes of the loading planes have to be reoriented once the sample has deformed. This requires the backing plates of the pressure bags and the shear pistons to be rotated to accommodate the new geometry. Since the rotation is done manually, there exists a potential for over–rotating or under–rotating these loading components. Therefore, shear tests at ψ=45° were carried out to determine the effects of the rotation of the loading components.
- Effects of loading direction on sample uniformity. In previous DSC proof tests on resedimented BBC conducted by Germaine (1982), the results indicated that the strain distribution of the sample depends on the mechanism of loading (i.e., with or without the use of shear sheets). This is probably caused by: (1) non-uniform surfaces of the pressure bags along the boundaries, (2) poor transfer of surface traction through the sample, and (3) deflection of the top and bottom platens, also referred to as the end platens.

  The pressure bags that apply the larger stress, or the major principal stress, have a tendency to bulge. The pressure in the middle portion of the bags therefore transmits a larger stress than the corners of the bags, giving a higher axial strain in that location. Conversely, the pressure bags that apply the minor principal stress tend to under–inflate, may cause lower stress exerted from the

middle portion of the bags and reduced axial strains in the middle of the sample. The combined effects of the over–inflated and under–inflated pressure bags is a larger shear strain in the middle of the sample. The new pressure bags used in this research incorporate position sensors to reduce the non–uniformity caused by improperly inflated bags. Non–uniformity can still occur due to the deflections of the end platens; this could be addressed by stiffening the platens, but it is not done in this research.

In the tests conducted without any applied stress from the shear sheets (i.e., at ψ=0° and 90°), "larger interior strains occurred with unstressed shear sheets and more uniform strains with highly stressed shear sheets" (Arthur et al., 1981). But the DSC results on BBC by Germaine (1982) showed that larger strains occurred at the boundaries, probably due to the improper transfer of surface traction from the shear sheets, causing the sample to strain more near the boundaries than in the middle of the sample.

- Grease Corrections. Silicone grease is used to reduce friction in the region between the shear sheets and the pressure bags. It was determined experimentally that this grease has a cohesion of 0.007 ksc (refer to Appendix E.1.3). This cohesion force reduces the applied stress from shear sheets, therefore a grease correction of 0.007 ksc is made. Note that the magnitude of this correction depends on the applied normal stress. For a normal stress below 0.3 ksc, the grease correction is 0.007 ksc. But at a normal stress of 1.3 ksc, the grease correction is as high as 0.03 ksc.

6.3.1.1 Total Stress Paths

Although the rubber foam is not a true cross–anisotropic material, the validity of the proof tests rely more on the elastic properties of the material. The tests are conducted by keeping the mean stress or octahedral normal stress constant, while varying the deviatoric stress. Theoretically, the relationship between deviatoric stress ($\sigma_1-\sigma_3$) and maximum shear strain ($\epsilon_1-\epsilon_3$) of an isotropic elastic material is independent of the direction of loading. Using this relationship, one can check the performance of the DSC by applying known major and minor principal stresses in any direction.

The total stress paths were prescribed in the tests; the sample was hydrostatically compressed to a stress of 0.2 ksc, then sheared at a constant mean stress, p ($=\frac{\sigma_1+\sigma_3}{2}$), to a deviatoric stress of about 0.2 ksc with principal stress directions varying from 0° to 90°. The major and minor principal stresses were positive (i.e., compression) in all tests. The total stress paths of the tests are shown in Figure 6.9. The intermediate principal stress was not measured in these tests.

6.3.1.2 Stress and Strain Response

As discussed earlier, if the normal octahedral stress is kept at a constant value, the stress–strain relationship should be independent of the major principal stress direction. To review this relationship, graphs of shear stress, q ($=\frac{\sigma_1-\sigma_3}{2}$), versus maximum shear strain (γ_{max}) for the tests were generated as shown in Figures 6.10 and 6.11 for two different areas (Area No.1 and Area No.2). Area No.1 represents 95 % of the cross–sectional area of the specimen and Area No.2 represents 57% of the total area, which are different from the standard area sizes given in Figure 5.7. The maximum shear strain is selected because this parameter is not influenced by film shrinkage.

The results indicate that there are only small variations in the stress–strain relationship. The tests conducted at ψ=0° produce a slightly stiffer response than the tests performed at ψ=90°. This variation can be due to a number of reasons, including:

- The assumption of a unique stress versus strain relationship is not valid, and the measured stress–strain relationship is the true behavior. In this case, the chosen material failed to verify the performance of the DSC device.
- The variation is due to errors in the applied stress in the system. The locations of the pressure bags can be an important factor in the magnitude of the applied normal stress. It was found from calibrating the pressure bags that the position sensors of the pressure bags can only control the normal stress to within 0.007 ksc. Furthermore, a correction factor for grease friction added uncertainty to the shear stress measurement, also on the order of 0.007 ksc. This explanation can be evaluated by comparing the shear stresses, q, for a given strain as tabulated in Table 6.2. Figures 6.12 and 6.13 show the variation in shear stresses for given maximum shear strains. The results for γ=0.5% show larger scatter than the results for γ=1%. The tests performed at ψ=90° consistently yield softer behavior than the tests at other angles, implying that the material is probably slightly anisotropic. However, the variation of shear stresses for γ=1% is not very large, ranging from 0.075 ksc to 0.085 ksc, and therefore falling within an "error band" of 0.007 ksc.

Although either of these explanations is plausible, the variation is probably

caused by a combination of these two factors. Regardless, the range is at a tolerable level, and falls within measurement capabilities.

Two sets of tests were repeated to check the repeatability of the tests. The results are shown in Figures 6.14 and 6.15 with ψ=0° and 90°, respectively, and indicate remarkable similarity (Table 6.2). The stress–strain relationships are virtually the same for each ψ angle. These results have shown that tests under the same conditions can produce relatively good repeatability.

Another set of tests were performed to investigate the effects of rotating the backing plates of the normal stress system at small strain levels (γ_{max}<2%) with ψ equal to 45°, as shown in Figure 6.16. The test with rotated backing plates and shear pistons (designated as Rubber7) gives a higher stiffness than the test with no rotation of the backing plates (Rubber5). There are two possible explanations:

1) Excessive rotation of the backing plates can increase the friction between the shear sheets and the pressure bags, resulting in a higher modulus.
2) The alignment of the shear sheet pistons can also play an important role. If the pistons are not properly aligned, the applied surface traction by the shear sheets is reduced, which affects the stiffness of the material.

Therefore, additional precaution should be taken in the tests with stressed shear sheets, bearing in mind that "over–rotation" of the shear sheet pistons or the backing plates can result in misleading material behavior.

6.3.1.3 Volumetric Strain Behavior

For an elastic material, it is reasonable to assume that the volumetric

strain is proportional to the change in octahedral normal stress. Since the mean stress is kept constant in these proof tests, there should be no volumetric strain. This was evaluated, as shown in Figures 6.17 and 6.18 for Area No.1 and Area No.2, respectively. The volumetric strain behavior of the tests are scattered around zero volumetric strain, with the largest measured volumetric strain at 0.4%. Considering the effects of film shrinkage, and the Poisson effects of the reference rubber membrane due to changes in the intermediate principal stress (see Section 7.4), the magnitude of the volumetric strain is not very significant. Figure 6.19 shows variation in the volumetric strains with ψ angles; no clear trend is evident in the results except that tests at ψ=90° have larger volumetric strains.

6.3.1.4 Directions of Principal Strain and Stress

One means of evaluating the performance of the DSC is to check the direction of major principal stress and the direction of major principal strain. The directions of these two components should coincide for an elastic material.

Figures 6.20 and 6.21 show the difference (Δ) between the major principal strain and major principal stress with shear strain. At low strain levels, there is significant variation, but as the strain increases this variation diminishes. This initial variation is due to errors in both the stress and the strain measurements. The results are presented in a different form, in Figure 6.22, to illustrate the difference (Δ) in strain–stress direction for a given strain level. The Δ values fall close to zero, with a maximum of 2° at ψ=15° for γ_{max}=1%.

The major principal strain direction distributions at a shear stress of 0.1 ksc for the different tests are shown in Figures 6.25 to 6.32 using the local strain analysis described in Chapter 5. The directions of the major principal strain (ξ) are, in general, very close to the directions of loading. For example, in Test Rubber2 at ψ=0°, the ξ value varies from –4° to about 4° with a mean value of

0°, as shown in Figure 6.25. Considering the boundary and the end effects, this variation is considered small. The worst case is at ψ=45° (Rubber5), where the ξ value varies from 40° to 50°, with a mean of 45° (Figure 6.28). This test also reveals that the ξ value is larger on one of the corners where the shear sheets interweaved, probably because of slightly non–uniform shear sheet–applied stresses and normal stresses at this location.

6.3.1.5 Uniformity of Samples

Sample uniformity was examined using two methods. The first compares the strains for different areas (i.e., the ratio of γ_2 to γ_1 or NAR), as described in Section 5.3.4. Figures 6.23 and 6.24 show the NAR values for tests without any shear sheet applied stress (i.e., at ψ=0° and ψ=90°) and tests with shear sheets (i.e., at ψ=15°, 30° and 45°), respectively. All tests had NAR values greater than unity, which implies that the strains are higher in the middle of the samples. But the results from the clay tests by Germaine (1982) show higher strains near the boundaries for tests with surface tractions. In fact, it is not surprising that the NAR values for the rubber tests are greater than unity because the transfer of the surface tractions to the sample occurs easily since the shear sheets are essentially "glued" to the sample. The results of the individual tests for different areas are presented in Appendix F.

The second method of evaluating sample uniformity uses local strain analysis to determine the strain distribution of the whole sample. Figures 6.25 to 6.32 also show the strain distributions of different tests at a shear stress of about 0.1 ksc; the f value (defined in Section 5.3.3) is about 0.18 to 0.40, which implies that the variation of strain in the samples is relatively small. These tests also show that the strains are higher in the middle of the sample than at the boundaries, similar to the results from the NAR analysis.

The ψ=45° tests (Rubber5 and Rubber7) can be used to evaluate the performance of the shear sheets. Figures 6.28 and 6.30 show that the variation in strain is very similar to samples subjected only to normal stress. Therefore, the performance of the shear sheets is considered to be reasonable.

The ψ tests at 0° and 90° allow an evaluation of the performance of the pressure bags, since the shear sheets are not in use. The strains produced from the tests are quite uniform, although they are larger in the middle than at the boundaries. As explained earlier, the non–uniformity is probably caused either by the applied normal stress, in spite of the help from the position sensors, or by the deflections of the end platens caused by a change in the intermediate principal stress. It is not possible to prove which is dominant. However, the pressure bags still apply a reasonably uniform stress.

6.3.1.6 Summary

The stress–strain relationships for the tests on rubber foam are satisfactory, showing some variation in the behavior at different directions of loading probably due to slightly anisotropic material properties. But the variation is within measurement capabilities. Since the variation is not substantial, the grease correction of 0.007 ksc is considered to be acceptable at normal stresses less than 0.3 ksc. The same magnitude of grease correction was made by O'Neill (1985) in DSC tests on BBC at similar normal stress range.

The distributions of the strain and the major principal strain direction in all tests are extremely uniform, indicating that the applied stresses are also uniform. The NAR value for all the tests is about 1.1, giving an NRS (Ring No.0) value of –0.15, lower than any values measured in the previous tests on clay (O'Neill, 1985).

The results also show that the directions of the major principal strain

almost coincide with the major principal stress, with the a largest difference (Δ) of only 2° for Test Rubber8 at ψ=15°.

Despite the problems (i.e., slightly different stress–strain behavior) encountered, the results obtained from this study on rubber foam achieved better uniformity than the results obtained from the previous proof tests on clay.

The rubber tests have demonstrated the ability of the DSC to rotate the direction of σ_1. The results of these tests have also shown the capabilities of the new strain analysis in presenting valuable strain and ξ–distribution plots. This strain analysis is more efficient and yields more information than the previous analysis (Germaine, 1982).

6.3.2 Proof Tests with Resedimented Boston Blue Clay

Proof tests were conducted on resedimented Boston Blue Clay to check the performance of the DSC on an elasto–plastic material under undrained shearing conditions. There are several differences in the proof tests on clay, including:

- Interface or boundary performance: The success of the tests with shear sheets is determined by how well the shear stresses are transmitted through the sample. In the first DSC test with shear sheets (DSC25) on resedimented BBC, boundary failure was encountered on one of the boundaries. This led to an extensive study into the interface between the clay and the rubber membrane, as well as the rubber membrane and the shear sheets. As a result, better boundary conditions have been achieved. Note that the rubber foam tests did not have this problem because the rubber membrane is essentially glued to the foam, producing superb bonding.
- Effective stress paths are not prescribed by the operator: Undrained

DSC shear tests are performed by maintaining the total stress path equal to the effective stress path based on pore water pressure probe data in the middle of the sample; the average total normal stress is varied so that the pore water pressure is kept equal to zero.

A total of five proof tests were performed in this research, but two of the five tests were considered poor quality tests, DSC24 and DSC25. Both of these tests had boundary problems of different kinds. Test DSC24 with ψ=0° suffered from excessive straining on one face of the sample, causing substantial non–uniformity. This was probably due to a poor positioning of the pressure bag on that face. Test DSC25 with ψ=40° had a slippage problem on the boundary where the lower normal stress is applied. The results of these two tests are not compared with the other three proof tests, designated as DSC23 (ψ=0°), DSC29 (ψ=40°) and DSC30 (ψ=20°). A summary of all tests is given in Tables 6.3 and 6.4.

Each resedimented Boston Blue Clay DSC sample was prepared by the sedimentation process given in Appendix A. The general properties of each batch of clay are described in Chapter 4. The sample was trimmed into a 4"x4"x4" cube and placed in the DSC device such that the depositional direction was normal to the plane of shearing of the material. The testing procedure is described in Chapter 5. The intermediate principal stress was not measured in any of the tests. The samples were consolidated hydrostatically to 0.1 ksc using the normal pressure bags. This is to ensure that the pore water pressure measured in the middle of the sample is not subjected to a level of suction which would cause desaturation of the pore pressure probe as a result of the capillary suction of the clay. Since the clay sample is fully saturated, the negative pressure measured using the probe, added to the applied consolidation stress, will equal the initial effective stress of the sample.

This initial effective stress can be used as a tool to quantify sample disturbance, as discussed in Section 4.4. Once this stress is measured, the sample is consolidated to a hydrostatic stress of 0.25 ksc, giving an overconsolidation ratio of 4. The sample is maintained at this stress for at least 24 hours before it is subjected to undrained shear.

The undrained shear tests were conducted with ψ varying from 0 to 40 degrees; the results are summarized in Table 6.4. The tests were carried out at a loading rate of 10 minutes per increment, which is the standard rate set by Germaine (1982). The resulting strain rates for the three good tests are shown in Figure 6.33, ranging from about 0.04 %/hour at a low stress level ($\frac{\Delta q}{q_f}$=0.2) to approximately 0.5%/hour at a $\frac{\Delta q}{q_f}$ greater than 0.95. The shearing procedure is described in Section 5.6. Typically, twenty increments are used per test.

In the course of conducting these proof tests, a number of modifications have been made to the setup and to several components, including the clay–rubber membrane interface and the corner reinforcement of the sample as listed in Table 6.3.

Since the DSC is a stress controlled device, it is not possible to measure strain softening behavior. Therefore, once the material reaches its peak strength, the sample has the tendency to strain continuously, producing a flat curve beyond the failure stress in the stress versus strain relationship. In addition, it is very difficult to pinpoint when failure actually occurred in a DSC test. It has been observed that in a number of tests, the pore water pressure readings became very unstable at a certain stage during a test and the position sensors of the pressure bags showed significant deformation of the sample. It is believed that when failure planes start to develop in the soil sample close to the tip of the pore water pressure (PWP) probe, the sliding action between the failure planes can induce some pore pressure. In fact, a number of failure planes have been found on the sample cut

perpendicular to the plane strain direction, and there were a number of failure surfaces crossing the location of the probe (Figures 6.51 to 6.55), which explained why the pore pressure readings were unstable at failure Some knowledge of the estimated strength of the material is needed for guidance as to when failure would occur and to help estimating the number of loading increments.

6.3.2.1 Pore Pressure Response

The initial effective stresses (u_c) were measured for all tests, and are tabulated in Table 6.4. The values range from 0.12 to 0.15 ksc, with a mean of 0.134 ksc. If there is no sample disturbance, evaporation or swelling, the value would have been the same as the hydrostatic stress of the last consolidation increment in the consolidometer, which is 0.25 ksc.

The pore pressure parameter B is also measured for each test. B is calculated from the ratio of the change of the pore water pressure to the corresponding applied mean normal stress ($\frac{\sigma_1+\sigma_3}{2}$) from 0.1 to 0.25 ksc. Only two out of the five tests had a B value of 1; the B values for the other tests were about 0.85. But all the samples were fully saturated based on the results from unconsolidated–undrained triaxial tests as discussed in Chapter 4. A similar range of measurement was observed by Germaine; he concluded that it was unlikely that the variable B values were caused by variations in plate separations. Although the tests were performed under the same conditions, i.e., almost the same grease thickness and plate separations, a small variation in grease thickness can make a difference in the normal stress, σ_2. During consolidation from 0.1 to 0.25 ksc, the grease tends to be squeezed out due to the change in the σ_2 stress. The movement of soil in the plane strain direction can reduce the change in the σ_2 value. In other words, the change in the σ_2 value is less than the average of the other two applied normal stresses during consolidation from 0.1 to 0.25 ksc. Therefore, the

calculated B value is less than unity because it did not account for the actual $\Delta\sigma_2$. This explanation is supported by some DSC tests with σ_2 measured during the investigation of undrained anisotropy of normally consolidated clay presented in Chapter 7. To illustrate the problem, an example from Test DSC34 is given, where a change in the applied normal stress of $\Delta\sigma_1=\Delta\sigma_3=0.146$ ksc (from Increment No. 1 to 2) results in a change in the pore pressure of 0.117 ksc and a change in σ_2 of 0.062 ksc initially. If the B value is calculated by assuming a change in σ_2 of 0.146 ksc, then the B value would be 0.80 ($=\frac{0.117}{0.146}$), but the B value calculated using $\Delta\sigma_{oct}$ and the measured σ_2 is 0.99 ($=\frac{0.117}{0.118}$) as shown in Figure 6.34. This example clearly indicates that the low B value is due to an incorrect estimate of $\Delta\sigma_2$.

6.3.2.2 Effective Stress Paths

The effective stress paths of the three good proof tests are in excellent agreement as shown Figure 6.35. At low shear stress, the stress path has a tendency to move to the left, i.e., the effective mean stress is reduced. The mean effective stress reaches a minimum of 0.2 ksc before it changes direction and moves to the right. Thus, the mean effective stress increases until the sample fails. Table 6.4 summarizes the test results.

6.3.2.3 Stress and Strain Response

The most crucial information for judging the performance of the DSC, as well as the quality of the test, is the stress–strain response. The quality of the DSC test can be evaluated from the uniformity of the sample. Usually, a comparison of the average strains for Area No. 1 and No. 2 is sufficient to describe the quality of the tests. The parameter NAR is again used to describe sample uniformity. Most of the problems in uniformity appear in the region near the

boundaries. Local strain analysis is used solely to identify a problem such as boundary slippage or excessive corner straining. The sample uniformity is described further in Section 6.3.2.7. The errors in the measurement of average strains associated with Area Nos. 3, 4 and 5 are generally quite large due to the inaccuracies in digitizing the reference points for these small areas; the resolution is lost in the process. If the average strains of the different regions agree, the sample is uniform and the test is considered good in this aspect. Of course, a test has to satisfy other criteria to be accepted, but from past experience, the quality of the test is frequently governed by the uniformity of the sample. The stress–strain relationships of the tests are shown in Figures 6.36 and 6.37.

Test DSC23, performed with $\psi=0°$, has strains slightly higher in the middle ($\gamma\simeq1.5\%$) than at the region close to the boundary ($\gamma\lesssim1\%$) with a NAR value of 1.13 at failure as shown in Figure 6.40. The sample reached failure at $\gamma_{max}\simeq1.5\%$ with shear stress of 0.165 ksc.

In test DSC29 with $\psi=40°$, the material shows stiffer behavior than DSC23. Figure 6.38 shows the relationship between the normalized shear modulus ($\frac{G}{\sigma'_p}$) and the applied shear ratio ($\frac{\Delta q}{q_f}$). Another graph of normalized shear modulus versus shear strain (Figure 6.39) indicates very good agreement in the moduli of the three tests. The strain at failure for this test is very similar to the first test, with $\gamma_{max}\simeq1.5\%$ and an undrained shear strength of 0.163 ksc. But the average strain of Area No. 1 is slightly larger than Area No. 2 (see Figure 6.40) with a NAR value of 0.93. Germaine (1982) had made the same observation, that is, tests with the use of shear sheets yield higher strains near the boundaries. One possible explanation is that the surface tractions exerted by the shear sheets are not properly transferred through the sample, hence the strains are larger near the boundaries.

The last proof test (DSC30) was performed with $\psi=20°$. The stress–strain

curve is very similar to DSC29. The strain of the sample is slightly lower in the middle than the region close to the boundaries at failure with a NAR value of 0.93, and an undrained shear strength of 0.164 ksc. The secant shear modulus of this test falls in between the other two tests.

Figures 6.41 to 6.43 compare the shear stress for a given level of strain. The results fall within a band of ±0.007 ksc.

Test DSC25 at ψ=40° with a boundary failure has an NAR value of 0.4 at γ_{max} of 1.6 %, beyond the acceptable range of 1±0.26. Therefore, the NAR analysis has proven to be rather useful.

6.3.2.4 Volumetric Strain Behavior

Another criterion of a good test is governed by the volumetric strain behavior. In an undrained shear test, the volumetric strain should be zero. Figures 6.44 and 6.45 show the volumetric strain characteristics of two cross–sectional areas. The measured volumetric strain response of the tests were not zero because of several reasons:

1) Since the strain is measured only on one face of the sample, the effect of end friction between the glass end plate and the rubber membrane is not taken into account.
2) The effects of film shrinkage over time give incorrect measurements of strain; this is minimized by processing and digitizing the films at the same time.
3) The Poisson effects of the rubber membrane are not accounted for in these tests and can distort the volumetric strain behavior. Corrections can only be made if the intermediate principal stress is known, as described in Appendix E.3.

The effects of sample non–uniformity additionally result in a non–zero

volumetric strain; once the sample has reached failure, the front faces of the pressure bags cannot be kept flat even with the help of the position sensors.

Figure 6.46 displays the volumetric strain for given strain levels, indicating very small change in volumetric strains for all the tests. The magnitude of the volumetric strain is less than 0.1% at a shear strain of 1%.

6.3.2.5 Shear Induced Pore Pressure

The shear induced pore water pressure is computed based on an assumed σ'_2 of $0.35(\sigma'_1+\sigma'_3)$ since σ_2 is not measured in the test. The shear induced pore pressure, u_s, is given by,

$$u_s = \Delta u - \Delta\sigma_{oct}$$
$$u_s = -0.45\,(\Delta\sigma'_1+\Delta\sigma'_3)$$

Figure 6.47 presents the shear induced pore pressure response for the three good proof tests. Test DSC29 at ψ=40° shows a sharper increase in u_s than the other two tests, but all the tests reached a maximum u_s value of 0.04 ksc for γ_{max} ranging from 0.3 to 0.5%. This variation could be due to errors in the strain measurement at low strain levels and poor estimates of the magnitude of intermediate principal stress.

6.3.2.6 Directions of Principal Strain and Stress

The direction of the major principal stress can be controlled in a test, but the direction of the major principal strain (ξ) has to be measured. Since the material properties are isotropic in the ψ plane, the direction of the major principal strain should coincide with the direction of the major principal stress. Figures 6.48 and 6.49 show the difference between the major principal strain direction and the

major principal stress direction versus the maximum shear strain for two different cross–sectional areas, Area No.1 and Area No.2 (representing 86 and 52 percent of the total cross–sectional area, respectively). The difference in direction is relatively close to zero (±2°) for shear strains less than 1.5% for Area No.1. At higher strain levels, the difference is larger in the tests using shear sheets due to the over–rotation of the backing plates by the operator, which occurs because of the difficulty in estimating how much rotation is required at these strain levels. The deviation in strain–stress direction is even smaller when Area No.2 is considered. Figure 6.50 shows the variation in Δ with ψ angle, with a maximum deviation of 3° at ψ=20°.

Figures 6.51b to 6.55b present the distributions of major principal strain direction for all the tests using the local strain analysis. The distributions are not as good as the results from the rubber tests, except for Tests DSC23 and DSC24 at ψ=0°. The distributions of major principal strain direction for Tests DSC29 and DSC30 are erratic partly due to a low f value (f=0.08) or very non–uniform strain. Test DSC25 at ψ=40° has the worst distribution due to the boundary failure.

If the failure planes can be identified in the tested clay sample, they can be used to roughly check the direction of the major principal stress. Assuming the major principal stress acts in a direction between the two sets of failure planes, the direction of the major principal stress was determined. The "thin section" optical technique (Morgenstern and Tchanlenko, 1967) was used to identify the failure surfaces of the sample. Unfortunately, due to a lack of experience and appropriate equipment, the investigation was incomplete.

Usually, the failure planes can be seen on a cut surface by placing a light source next to the cut sample surface, and the light source is adjusted until the shadows of the failure planes become visible. Sketches of failure planes for these DSC samples are shown in Figures 6.51c through 6.55c, and the results are

tabulated in Table 6.6. The failure planes in Tests DSC23 and DSC24 at ψ=0° are oriented in a very similar manner, the friction angle for DSC23 is higher than DSC24 by about 3°. The observed angles, ψ_{obs}, are zero which coincide with the applied ψ angles. Note that the ψ_{obs} equals the bisector of the acute angle θ between the inclination of the two sets of failure planes and ϕ' is equal to $(90°-\theta)$. The observed ψ_{obs} angles for Tests DSC29 and DSC30 at ψ=40° and 20° also agree rather well with the applied ψ angles, with a maximum difference of about 3°. The friction angle for the three good tests is between 35° and 37°, which is a few degrees higher than the values obtained from normally consolidated triaxial compression tests (ϕ'=34°) at maximum obliquity on the same material. This is consistent with the predicted values of friction angles from Matsuoka and Lade isotropic failure criteria described in Appendix G.2. In fact, most isotropic failure criteria predict higher friction angles in the plane strain mode than in the triaxial compression mode Test DSC25 at ψ=40° has some failure planes on the cut sample surface, with an observed angle, ψ_{obs}, of 43°, even though boundary failures had occurred. The direction of the failure planes was not significantly affected.

The measured friction angles range from 32° to 38° based on the orientations of the failure planes, and the ψ_{obs} values seemed to agree with the applied values of ψ relatively well, which implies that the applied stress directions are correct. It should be emphasized that the measured ψ and ϕ angles do not include any geometric corrections.

6.3.2.7 Uniformity of Samples

There are three different ways of determining the uniformity of the sample. The first method, as described earlier, compares the NAR values of each test. The second method is based on a strain distribution map using a local strain analysis.

This technique helps to visualize the strain distribution in a more local sense, and can therefore be used to detect boundary problems not easily identified from the first method. The results are shown in Figures 6.51a to 6.55a. Figure 6.51a presents the strain distribution for test DSC23 at ψ=0°, and indicates that the strain is higher in the interior of the sample. The strain distribution for test DSC24 is shown in Figure 6.52a and excessive straining is evident on one side of the specimen. This is probably caused by poor control of the normal stress pressure bag on that face of the sample. This problem gives rise to a softer response than the other tests. One of the advantages of using the local strain analysis is that experimental problems can be identified easily; a problem like this would go undetected in the global strain analysis. Boundary slippage was found in test DSC25 (ψ=40°) which is clearly shown in Figure 6.53a. The slippage was caused by the detachment of the sand particles from the rubber membrane, therefore the strain on the slippage face was enormous. Once the slippage happened, the data obtained beyond this point are unreliable, and hence this test is abandoned. For test DSC29 at ψ=40°, the strain is high near the boundaries except one corner has a lower strain value as shown in Figure 6.54a. The last test, DSC30 at ψ=20°, has higher strains at two adjacent corners and lower strains at the remaining corners (see Figure 6.55a).

The last method uses observations of the final water content distribution. Basically, the sample is cut into several pieces, and the water content of each piece is taken. Figures 6.56 to 6.60 show the water content distribution of the different tests from the upper face (closest to the reference dots) of the sample with thickness of 1 inch. The water contents for all the tests are randomly distributed; there is no indication of a consistent trend in the distribution. This method provides very little information on sample uniformity.

6.3.2.8 Summary

The DSC proof tests on resedimented BBC have provided valuable information. The effective stress paths in Figure 6.35 are very consistent in the three tests used. The stress–strain relationships are somewhat less satisfactory, with a slightly stiffer response in the ψ=20° and ψ=40° tests than in the ψ=0° test. The measured volumetric strains at failure are very close to zero (i.e., about ±0.3%). In terms of matching the directions of the major principal strain and stress, the deviation between the stress and strain directions is quite small. Moreover, the measured directions of the major principal stress from the failure surfaces agree very well with what has been applied.

6.4 DISCUSSION

The results of the proof tests on rubber foam show better uniformity than the DSC results on BBC. This is not surprising since there are more variables involved in the tests on BBC than on the rubber foam tests, including sample variability, a non–prescribed stress path and a more complex boundary condition in the sand–rubber–clay interface.

Section 4.7.2 compared the recompression triaxial tests at OCR=4 and indicated that BBC III has a lower undrained strength and lower strain at failure in both compression and extension modes than BBC II. But the modulus of BBC III in the extension mode is significantly higher than the modulus of BBC II. The results of the new proof tests on BBC III are compared with the results of the proof tests performed by Germaine (1982) and O'Neill (1985) on the BBC II, in Figures 6.61 to 6.63. The results of these two series of DSC proof tests are summarized in Table 6.5.

Figures 6.62 and 6.63 show the effective stress paths and the stress–strain responses for the two series of DSC tests on the two materials. The BBC II data

shown in these figures have been corrected for thixotropic effects. The effective stress paths for these two series are very similar; the effective mean stress for BBC II tends to decrease more than BBC III at shear stresses below 0.1 ksc, but they converge at higher shear stress.

The stress–strain responses of the two series of DSC proof tests are shown in Figure 6.63. BBC III has a slightly lower normalized undrained strength (0.164±0.001) than BBC II, which has a mean of 0.170±0.009 (see Figure 6.61a). The strain at failure for BBC III is only 1.4%, compared to BBC II which ranges from 3 to 7% as shown in Figure 6.61e. The normalized shear modulus $(\frac{G_{50}}{\sigma'_p})$ of the DSC proof tests on BBC II ranges from 35 to 60, and the normalized shear modulus of the tests on BBC III is about 82±17 (Figure 6.61h), these results are tabulated in Table 6.5.

The pore pressure parameters at failure A_f for the two materials are very similar with an average value of 0.62 as shown in Figure 6.61c. The normalized shear induced pore pressure at failure $(\frac{u_{sf}}{\sigma'_p})$ for BBC III of 0.03 is lower than the average value from BBC II of 0.04 (Figure 6.61d).

Figure 6.61f presents the difference in major principal strain and major principal stress directions (Δ), which shows very similar trends. The variation is largest at ψ=20–25° with a Δ value of –1° to 2° for BBC III. The results from the new proof tests show smaller deviation than the previous results, probably because of the new strain reduction program which automatically corrects for rigid body rotation using the 100 reference points. In the old analysis, the rigid body rotation is corrected from the four outermost corner points. Therefore, any corner problems will distort the global rotation. Figure 6.61g shows that the NAR values for BBC III is closer to unity than BBC II, implying better strain uniformity in the new proof tests. Comparisons of the anisotropic behavior of the two materials are discussed in the next chapter.

The conclusion is that the new proof tests on both rubber foam and resedimented BBC have demonstrated the ability of the DSC device, as well as showing the repeatability of the tests under different shearing conditions. The proof tests also gave the operator some experience and confidence in conducting DSC tests.

The new strain analysis has proven valuable, providing information on the strain distribution which can help to identify boundary problems in the tests. The results from the clay tests have shown that the technique of conducting undrained tests works quite well, hence the device can be used to study the anisotropic behavior of resedimented Boston Blue Clay.

Table 6.1: Correction Method for Effect of Thixotropy on Undrained Shear Strength Tests (after O'Neill, 1985).

Correction for Thixotropic Effect		Triaxial Compression $\sigma_1 > \sigma_2 = \sigma_3$	Triaxial Extension $\sigma_1 = \sigma_2 > \sigma_3$	DSC (Plane Strain) $\sigma_1 > \sigma_2 > \sigma_3$, $\sigma'_2 = 0.35\ (\sigma'_1 + \sigma'_3)$
Correction of Shear Stress, $q = \frac{(\sigma_1 - \sigma_3)}{2}$	General	• Determine elapse storage time, t_s. [t_s(days)=date test recompressed-date batch unloaded to 0.25 ksc - 5]. • Find Δq_y using t_s.		
	$q \leq q_y$	$q_t = q - \Delta q_y\ (q/q_y)$		
	$q > q_y$	$q_t = q - \Delta q_y$		
Correction of Average Effective Stress, $p' = \frac{(\sigma'_1 + \sigma'_3)}{2}$	General	• Using t_s, find $\Delta(\Delta u_s)$.		
	Convert $\Delta(\Delta u_s) = \Delta(\Delta p')$	$\Delta(\Delta p') = \Delta q_y/3 - \Delta(\Delta u_s)$	$\Delta(\Delta p') = -[\Delta q_y/3 + \Delta(\Delta u_s)]$	$\Delta(p') = -1.1\ \Delta(\Delta u_s)$
	$q \leq q_e$	$p'_t = p'$		
	$q > q_p$	$p'_t = p' - \Delta(\Delta p')$		
	$q_e < q < q_p$ and $p_e < p' < p_p$	$p'_t = p' - \Delta(\Delta p') \left[\frac{p' - p'_e}{p'_p - p'_e} \right]$		

Table 6.2: Summary of DSC Rubber Foam Tests.

Test Number	ψ Angle (°)	γ_{max} = 0.5 % •			γ_{max} = 1 % •			Remarks
		q (ksc)	ϵ_v (%)•	Δ (°)‡	q (ksc)	ϵ_v (%)•	Δ (°)‡	
RUBBER2	0	0.060	0.05	-1	0.085	0.00	1	
RUBBER4	0	0.055	0.15	0	0.082	0.05	0	
RUBBER8	15	0.050	-0.10	6	0.086	-0.10	2	
RUBBER9	30	0.044	0.00	3	0.085	0.00	0	
RUBBER5	45	0.040	0.00	3	0.079	0.10	0	No rotation of B.P.
RUBBER7	45	0.056	0.10	2	0.085	0.10	1	With rotation of B.P.
RUBBER3	90	0.040	0.25	1	0.075	0.20	0	low q value
RUBBER6	90	0.042	0.30	0	0.078	0.30	0	low q value
Mean S.D.		0.049 ±0.008			0.082 ±0.004			

Notes:

• Strains taken from Area No.1.

‡ Difference between Major Principal Strain Direction (ξ) and Major Principal Stress Direction (δ).

Table 6.3: Summary of Setup of DSC Proof Tests on Resedimented Boston Blue Clay III at OCR=4.

Test Number	Batch Number	ψ Angle (°)	Setup (Refer to Table 3.1)			
			Pressure Bag	Corner Design	Shear Sheet	Rubber Membrane
DSC23	201	0	Type B	-	-	No Coating
DSC24	201	0	Type B	-	Type B	No Coating
DSC25	202	40	Type B	Type C	Type B	Old Sand-Coating
DSC29	204	40	Type B	Type B	Type C	New Sand-Coating
DSC30	204	20	Type B	Type C	Type C	New Sand-Coating

Table 6.4: Summary of DSC Proof Tests on OCR=4 Resedimented Boston Blue Clay III at Failure.

Test No.	Batch No.	ϕ Angle (°)	Shear Sheet	B * value	u_c* (ksc)	w_i/w_f (%)	At Failure							G_s : σ'_p	Remarks
							$\frac{q_f}{\sigma'_p}$	$\frac{p'_f}{\sigma'_p}$	A_f	$\frac{\sigma'_{3f}}{\sigma'_{3i}}$	γ_1 † (%)	γ_2 † (%)	$\frac{\gamma_2}{\gamma_1}$		
DSC23	201	0	No	0.99	0.12	40.87/ 40.90	0.165	0.212	0.61	8.02	1.34	1.52	1.13	65	
DSC29	204	40	Yes	0.87	0.14	40.70/ 40.43	0.163	0.222	0.59	6.53	1.42	1.32	0.93	100	
DSC30	204	20	Yes	1.00	0.15	40.68/ 40.83	0.164	0.205	0.63	9.00	~1.40	~1.30	0.93	80	
DSC24	201	0	Yes	0.84	0.13	41.20/ 41.40	0.165	0.225	0.56	6.50	~3.00	~3.40	1.13	47	Excessive ϵ on one face
DSC25	202	40	Yes	0.85	0.13	40.58/ 40.37	0.153	0.219	0.61	5.64	1.67	0.68	0.41	100	Bound.Failure @ q/σ'_p=0.143

Notes:

* The pore pressure parameter B is computed from the change in Δu over the change in $\Delta\sigma$ from a mean consolidation stress of 0.1 to 0.25 ksc.

• Initial effective Stress.

‡ Maximum Shear Strains taken from Area No.1 (86%).

† Maximum Shear Strains taken from Area No.2 (52%).

The preconsolidation pressure, σ'_p=1 ksc.

Table 6.5: Summary of All DSC Proof Tests on OCR=4 Resedimented Boston Blue Clay at Failure.

Test Number	Reference Year (Series)	ψ Angle (°)	At Failure								$\frac{G_{sec}}{\sigma'_p}$	Remarks
			q_f/σ'_p	p'_f/σ'_p	A_f	γ_1 (%)‡	γ_2 (%)†	γ_2/γ_1	Δ_{1f}, %	Δ_{2f}, %		
DSC06	Germaine 1982 (UBC II)	0	0.183	0.228	0.56	5.6	6.2	1.1	-0.3	-0.2	65	
DSC07		45	-	-	-	-	-	-	-	-	-	Boundary Failure
DSC09	O'Neill 1985 (UBC II)	25	0.163	0.200•	0.65•	5.4	4.0•	0.7	-2.4	-3.5	>35	Boundary Slippage
DSC12		0	0.169	0.210	0.62	6.2	7.0	1.1	0.9	-0.2	45	
DSC14		40	0.166	0.203	0.64	3.7	3.2•	0.9	-1.6	-2.9	60	
DSC23	This Research 1990 (UBC III)	0	0.165	0.212	0.61	1.3	1.5	1.2	-0.5	-0.5	65	
DSC24		0	0.165	0.225	0.56	~3.0	~3.4	1.1	0.2	0.2	47	Boundary Problem
DSC25		40	0.153	0.219	0.61	1.7	0.7	0.4	1.9	0.3	100	B.F. @ q/σ'_p=0.143
DSC29		40	0.163	0.222	0.59	1.4	1.3	0.9	0.5	0.9	100	
DSC30		20	0.164	0.205	0.63	~1.4	~1.3	0.9	2.3	-1.3	80	

Notes:

- • Values different from values reported in O'Neill's Thesis (1985).
- ‡ Maximum Shear Strain from Area No.1.
- † Maximum Shear Strain from Area No.2.

Table 6.6: Summary of Angular Parameters for DSC Proof Tests on OCR=4 Resedimented Boston Blue Clay III at Failure.

Test Number	ψ_f from Applied Stress (°)	From Strain Analysis		Δ_{1f} (Area 1) (°)	Δ_{2f} (Area 2) (°)	From Failure Planes*		Remarks
		ξ_f (Area 1) (°)	ξ_f (Area 2) (°)			τ_{obs} (°)	σ_{obs} (°)	
DSC23	0.0	-0.5	-0.5	-0.5	-0.5	0	35	
DSC29	39.7	40.2	40.6	0.5	0.9	37	35	
DSC30	19.1	21.4	17.8	2.3	-1.3	19	37	
DSC24	0.0	0.2	0.2	0.2	0.2	0	32	Excessive Strain on one face
DSC25	39.7	41.6	40.0	1.9	0.3	43	38	Boundary Slippage on one face

Notes:

* Angles calculated from the orientations of failure planes.

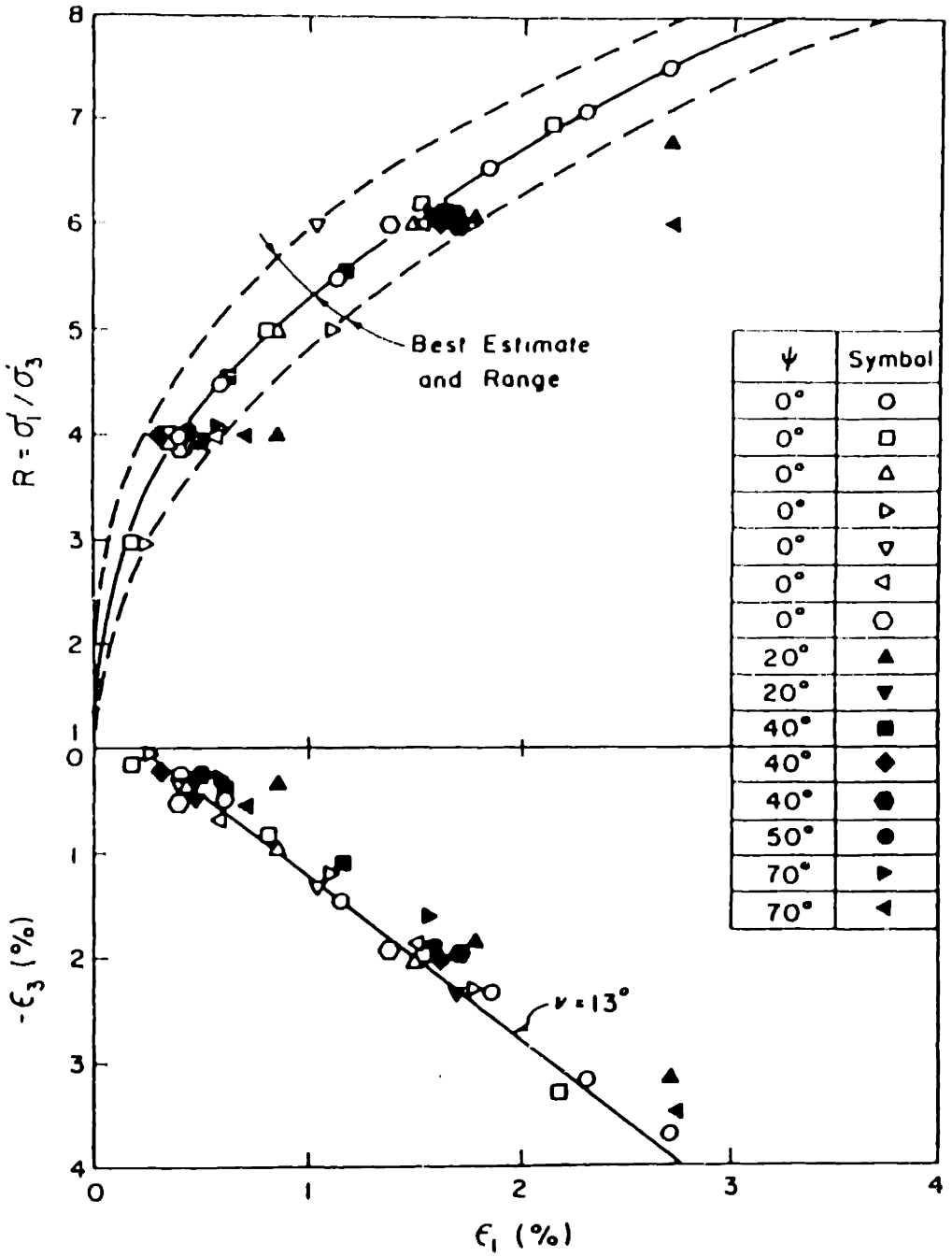

Figure 6.1: Stress–Strain Data from Monotonic Loading Tests on Dense Sand (from Arthur et al., 1981).

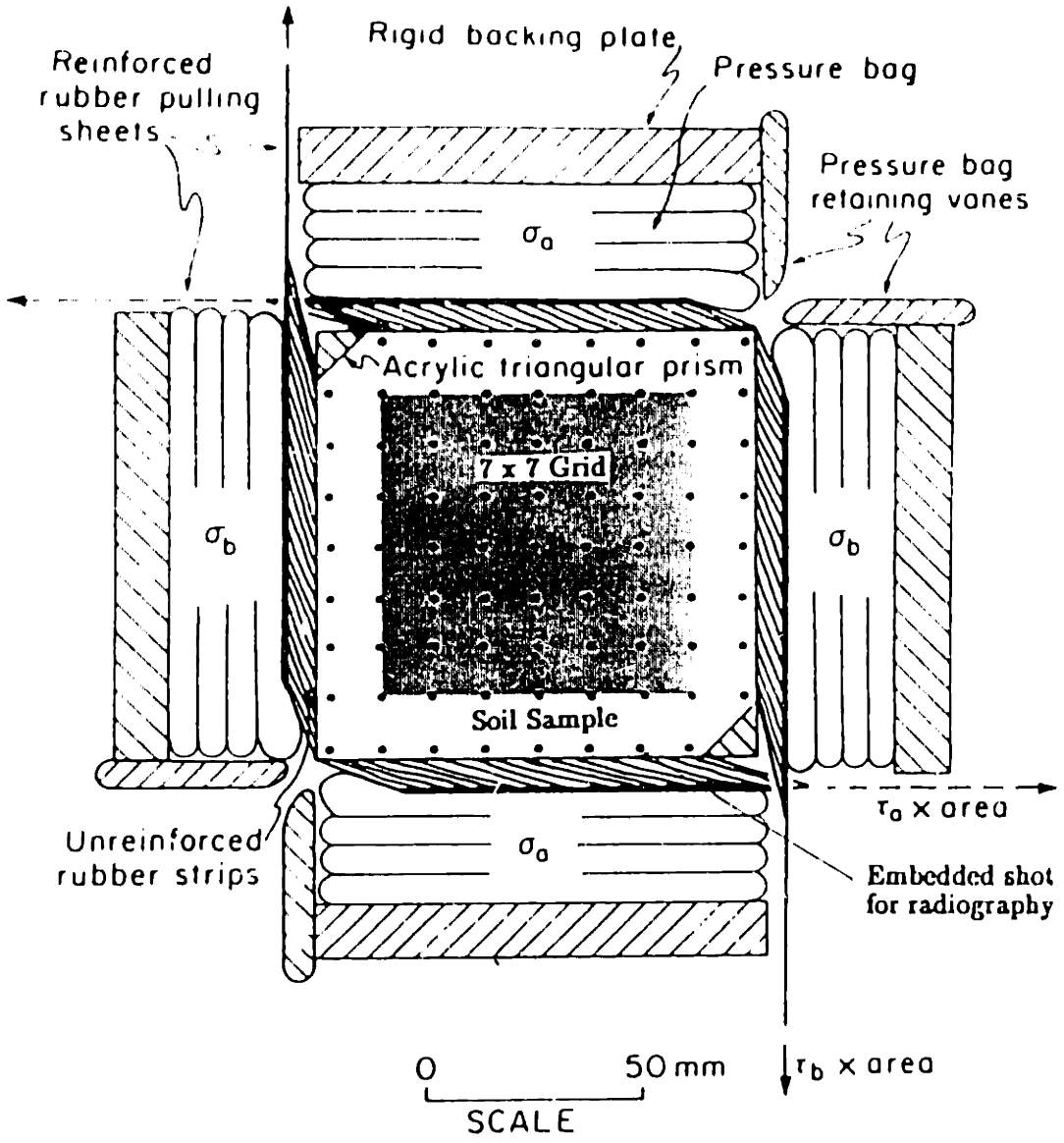

Figure 6.2: Diagram of Method used to apply Normal and Shear Stresses in DSC (from Arthur et al., 1981).

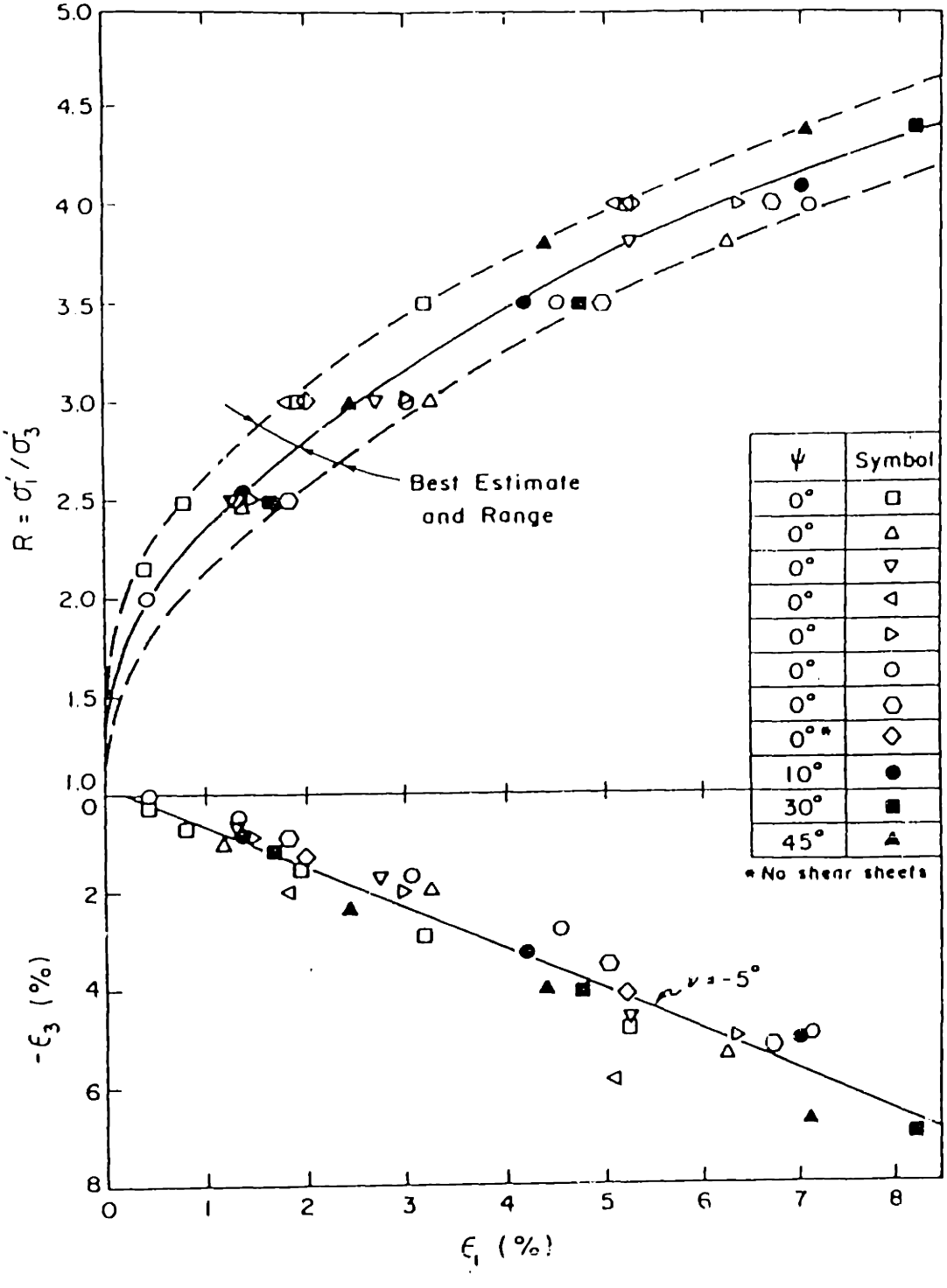

Figure 6.3: Stress–Strain Data from Monotonic Loading Tests on Loose Sand; ϵ_1 Data from 16 Points (from Arthur et al., 1981).

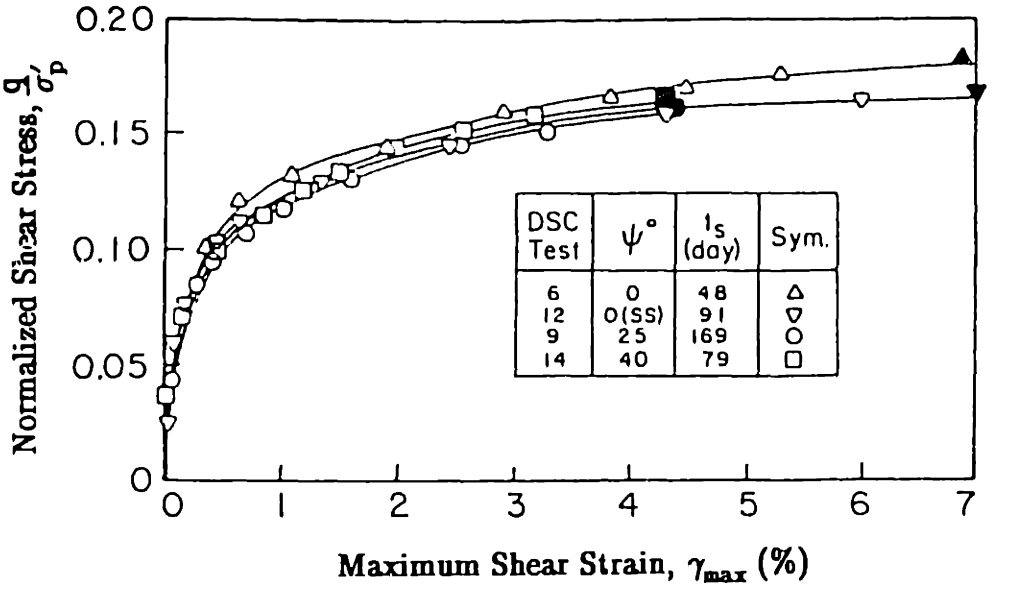

Figure 6.4: Normalized Stress–Strain Relationships from CU DSC Proof Tests on BBC at OCR=4 (Corrected Data from O'Neill, 1985).

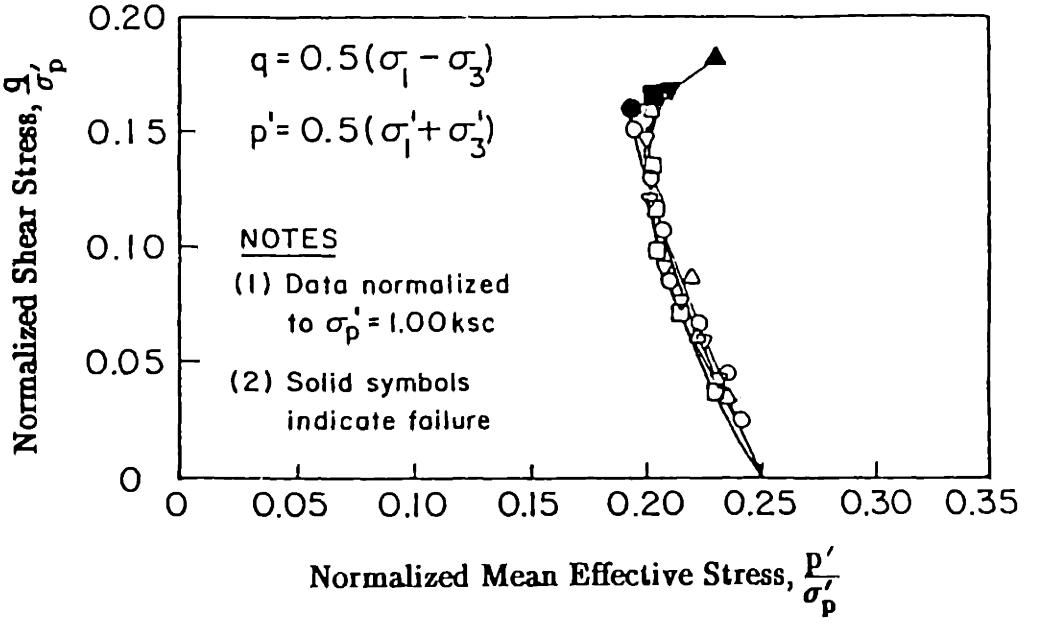

Figure 6.5: Effective Stress Paths from CU DSC Proof Tests on BBC at OCR=4 (Corrected Data from O'Neill,1985).

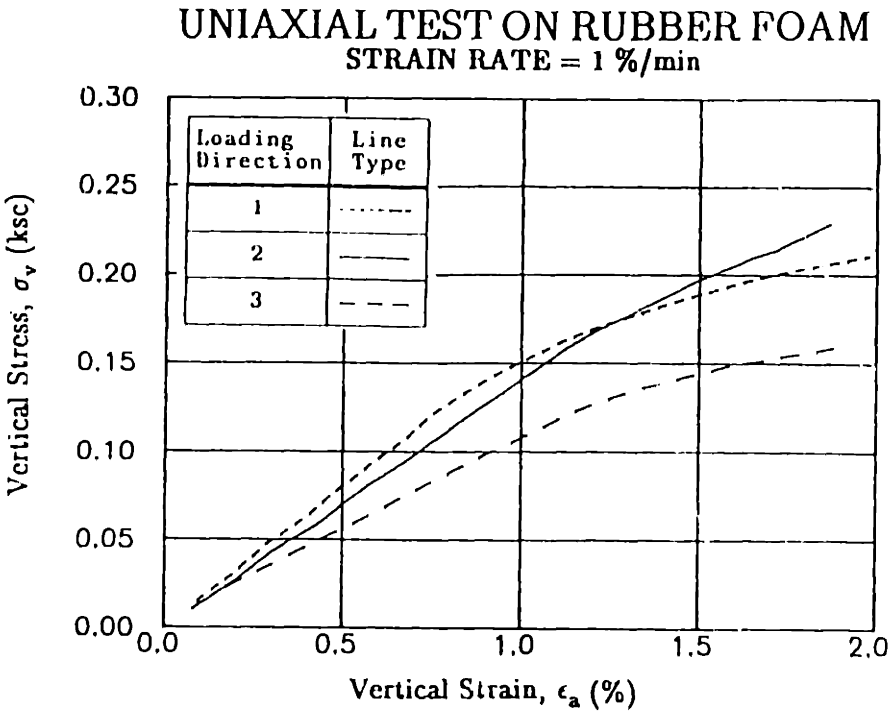

Figure 6.6: Uniaxial Compression Tests on a 2–Inch Cube of Rubber Foam.

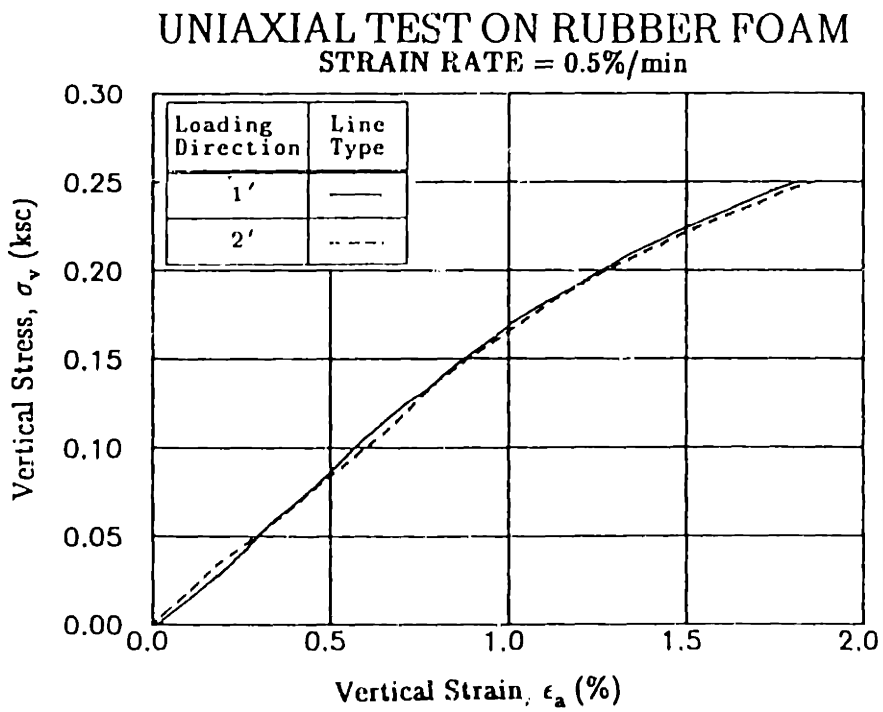

Figure 6.7: Uniaxial Compression Tests on a 4–Inch Cube of Rubber Foam.

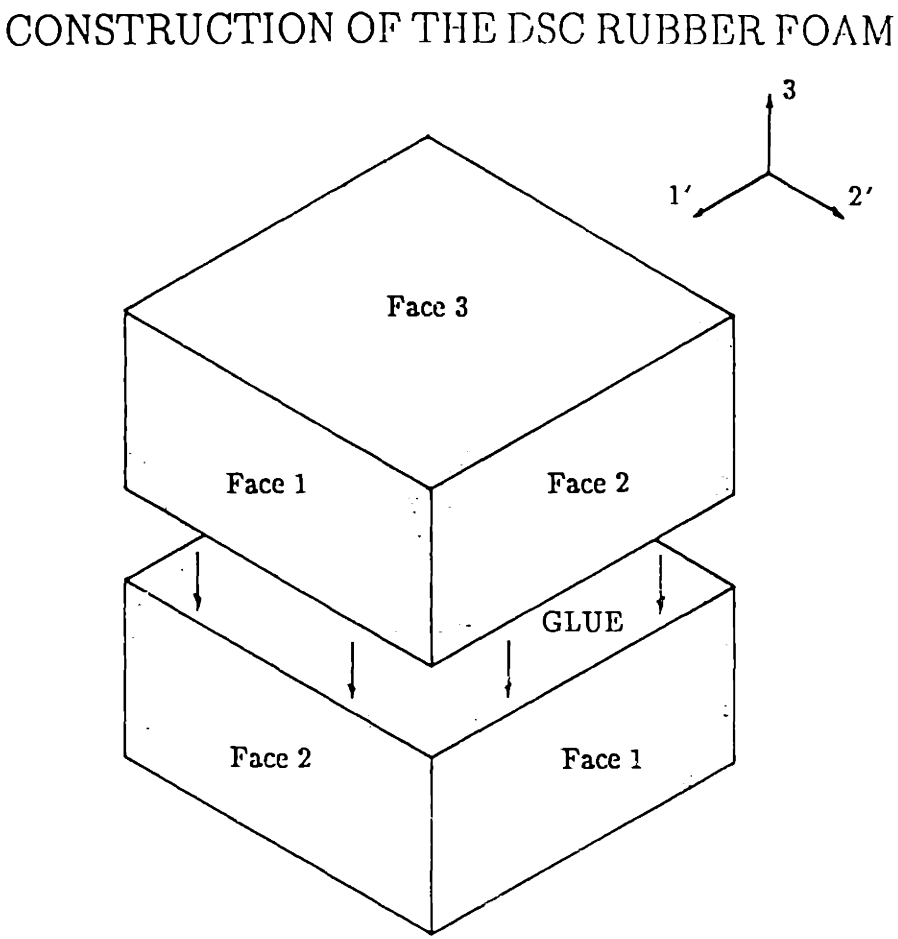

Figure 6.8: Orientation of DSC Rubber Foam Sample.

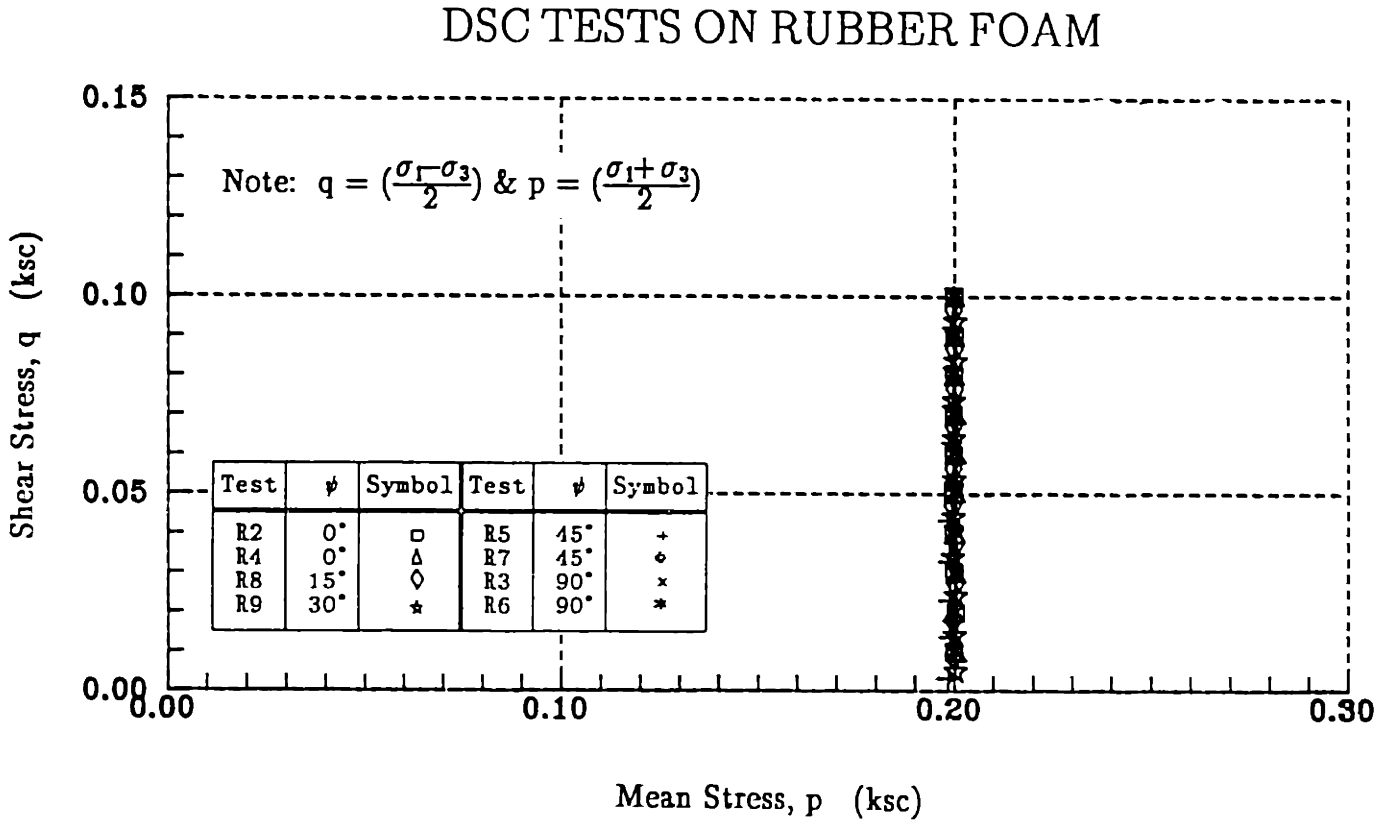

Figure 6.9: Total Stress Paths used in DSC Tests on Rubber Foam.

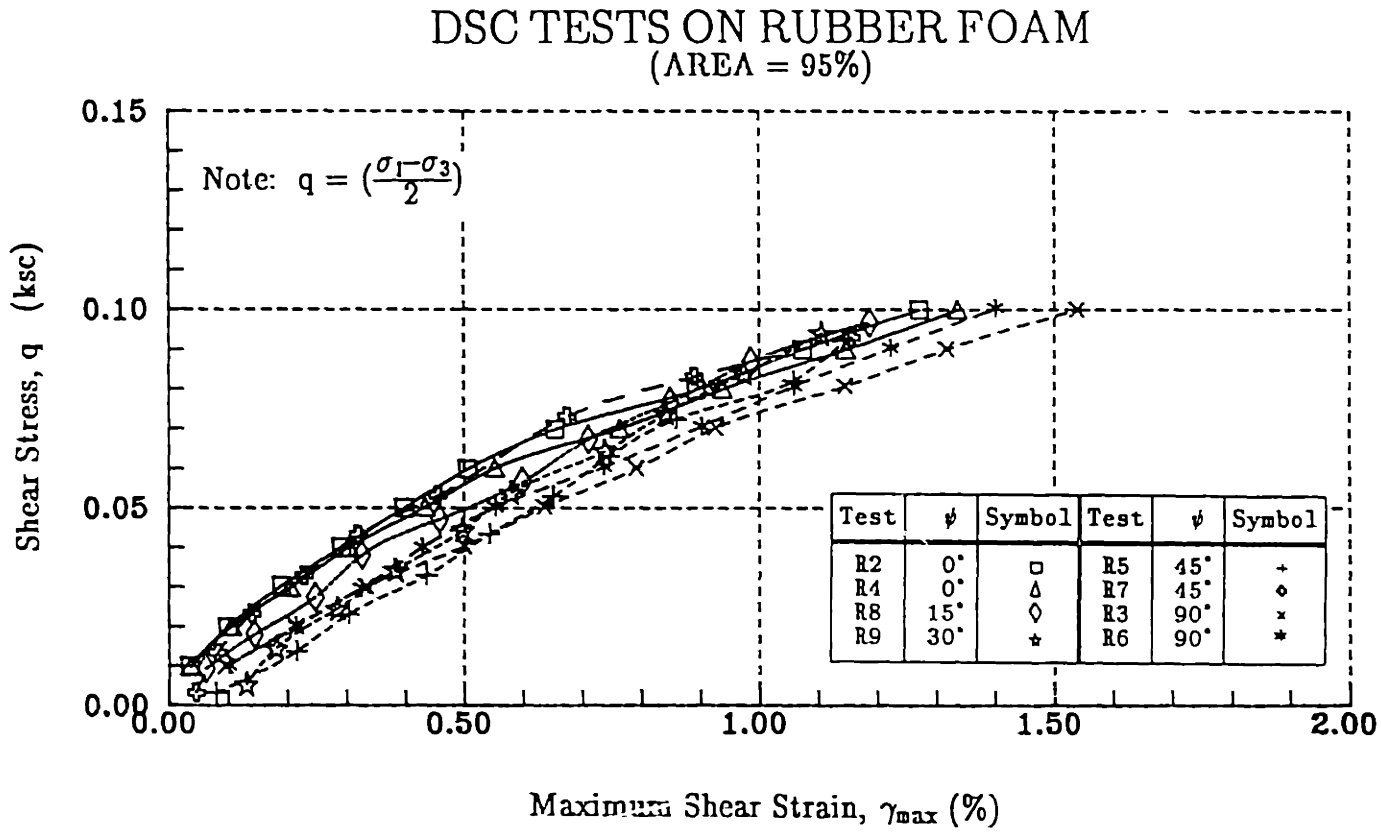

Figure 6.10: Stress–Strain Relationships from DSC Tests Rubber Foam (Area No. 1).

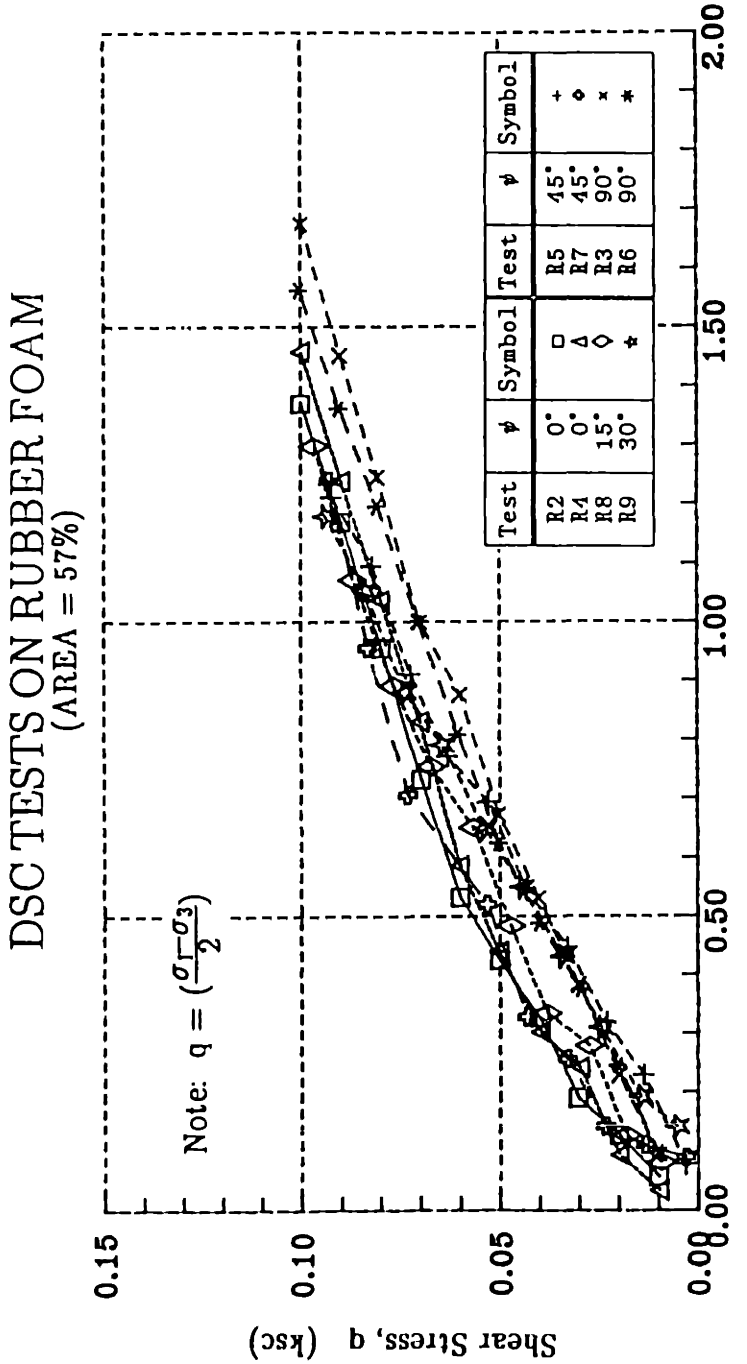

Figure 6.11: Stress–Strain Relationships from DSC Tests on Rubber Foam (Area No. 2).

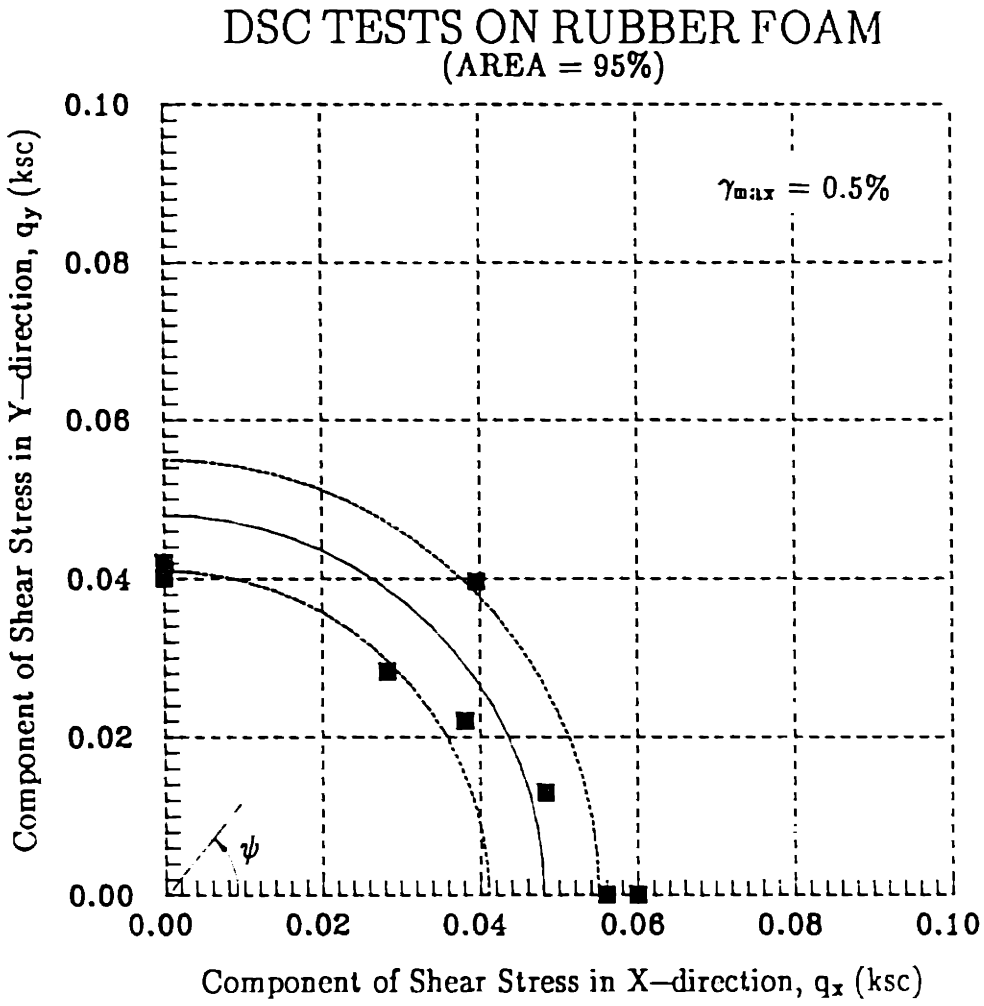

Figure 6.12: Variation of Shear Stress with ψ Angle at γ_{max}=0.5%.

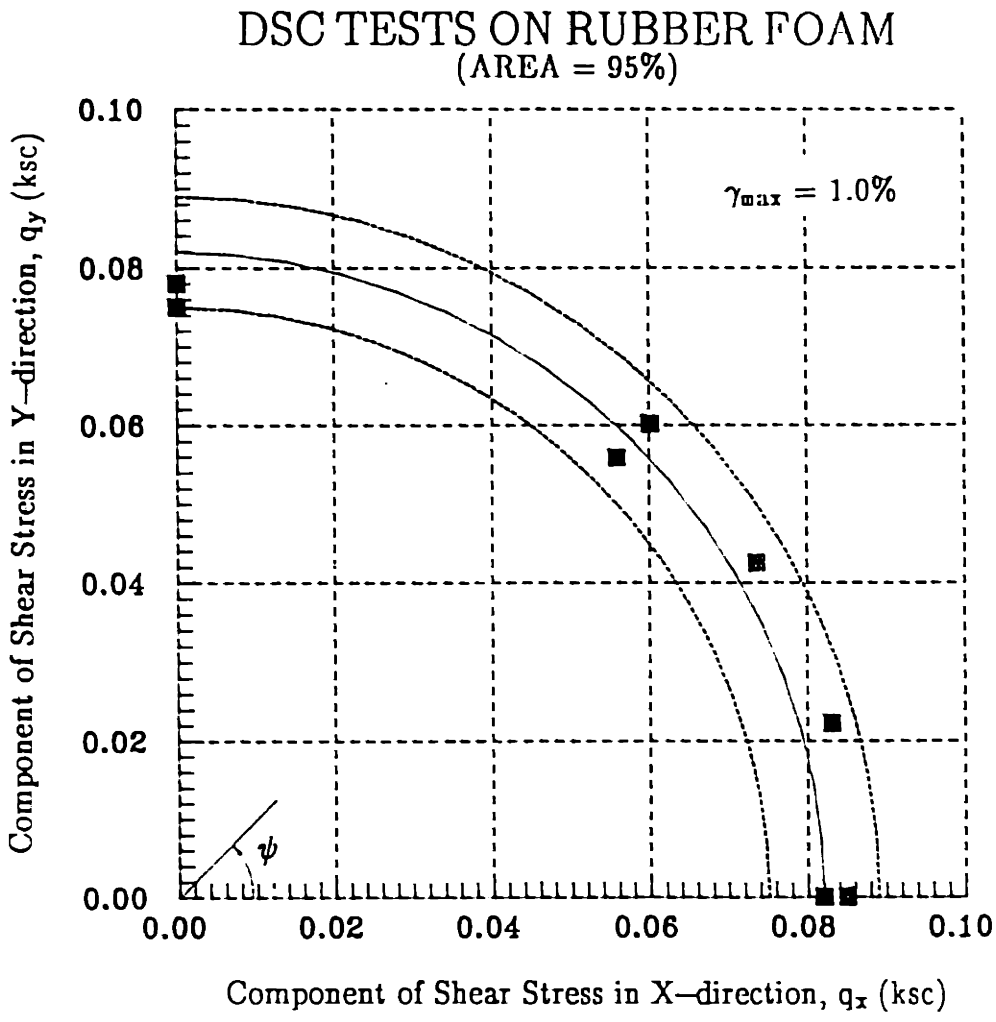

Figure 6.13: Variation of Shear Stress with ψ Angle at γ_{max}=1.0%.

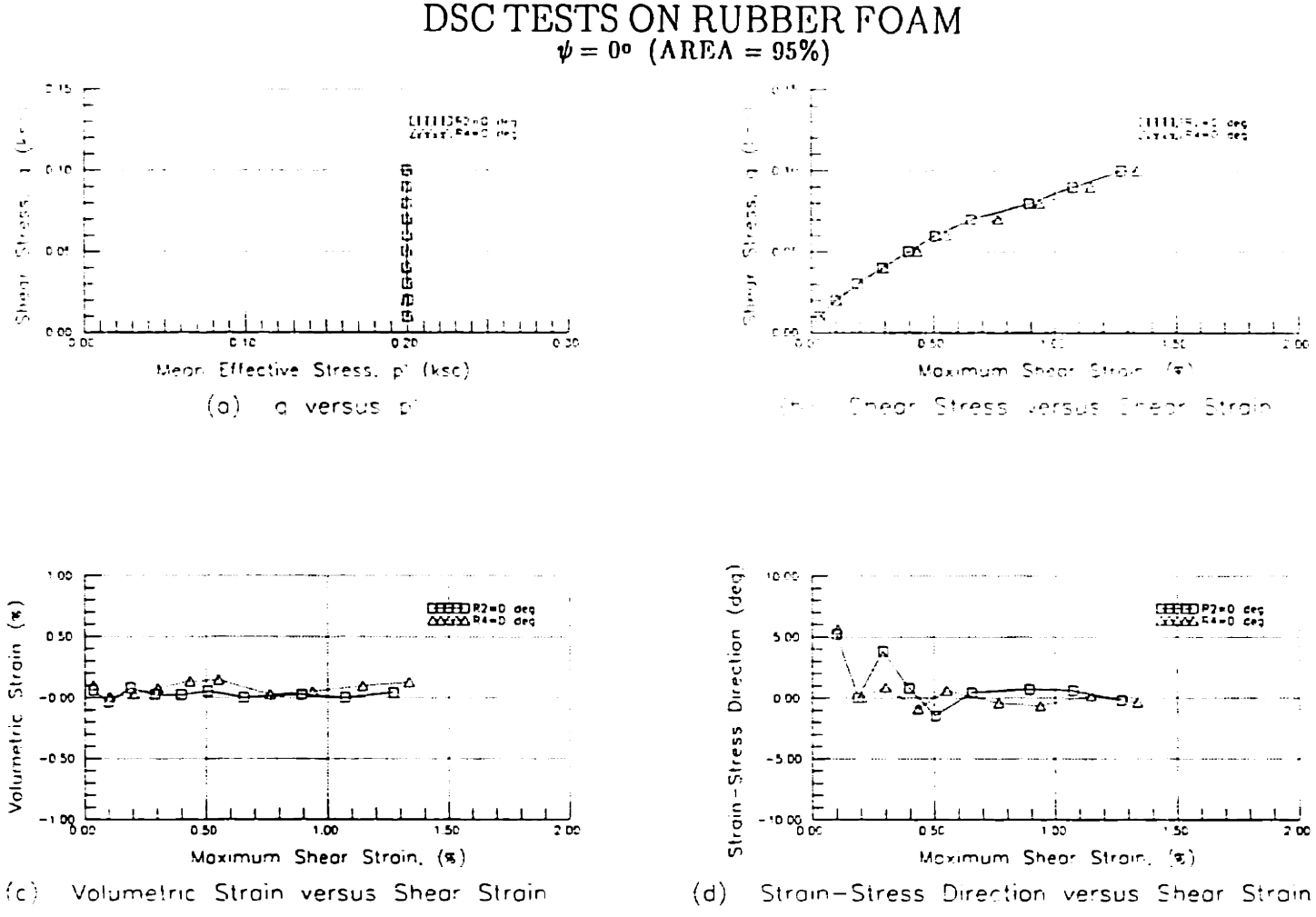

Figure 6.14: Results of Two Rubber Foam Tests at ψ=0°.

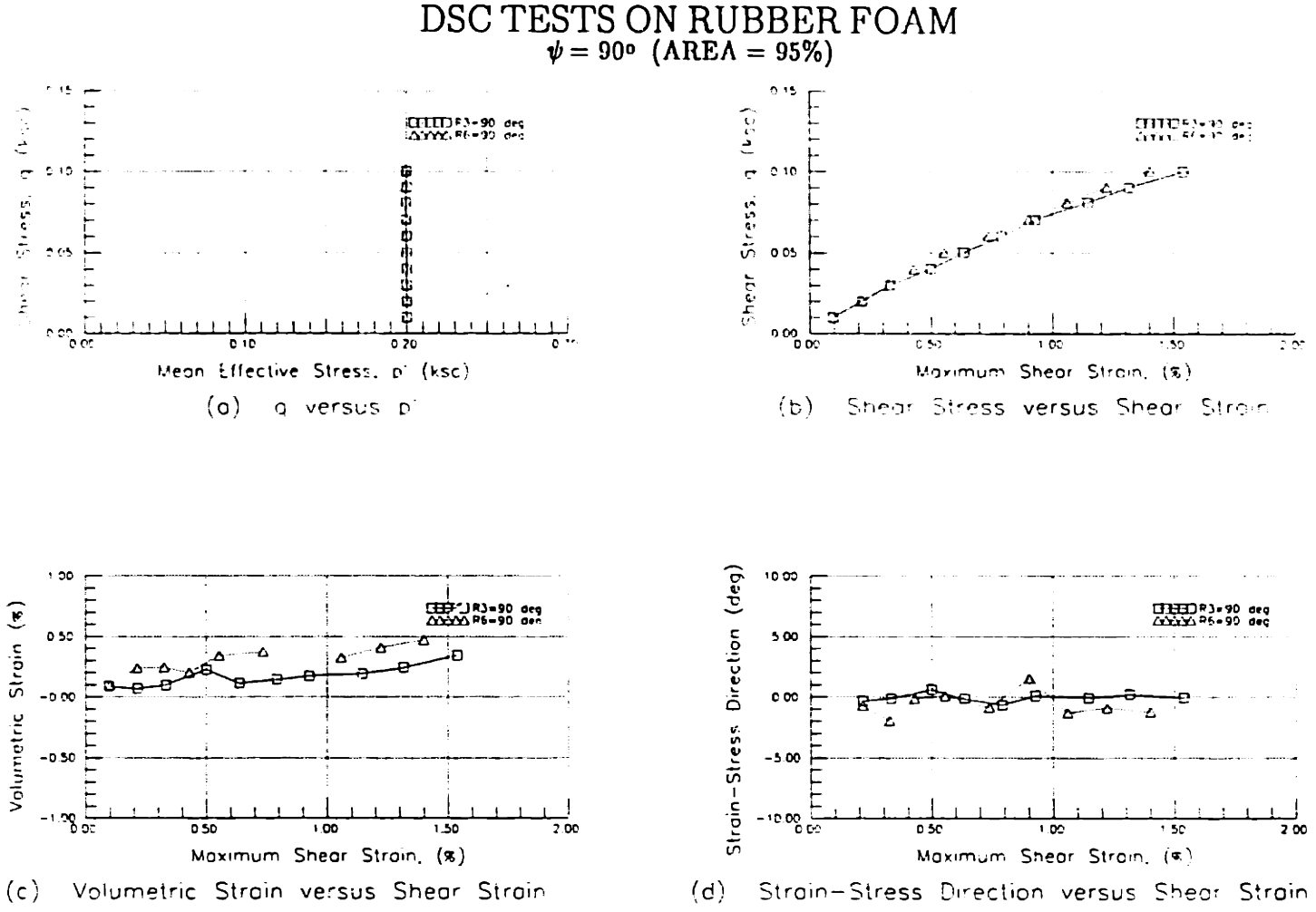

Figure 6.15: Results of Two Rubber Foam Tests at ψ=90°.

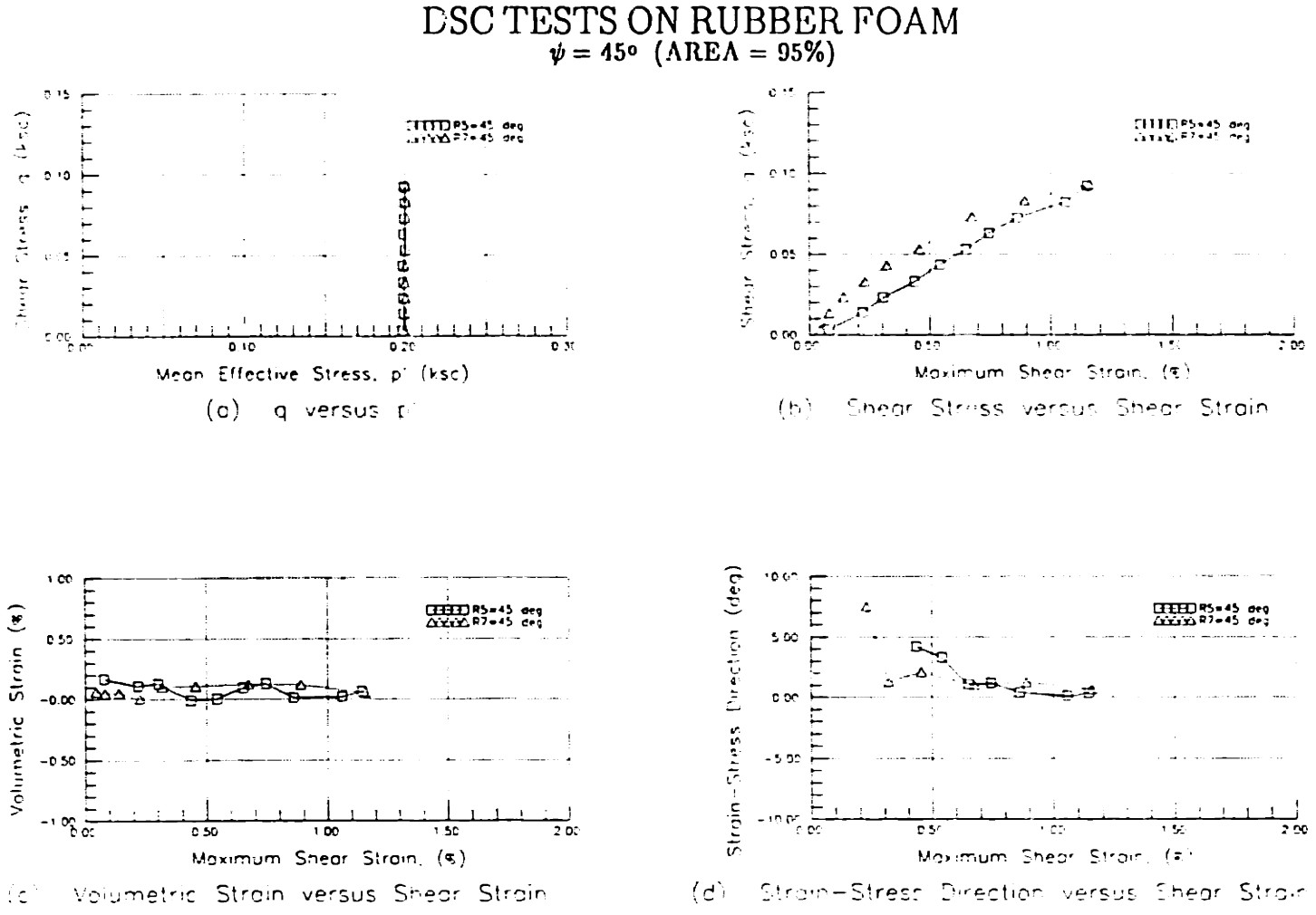

Figure 6.16: Results of Two Rubber Foam Tests at ψ=45°.

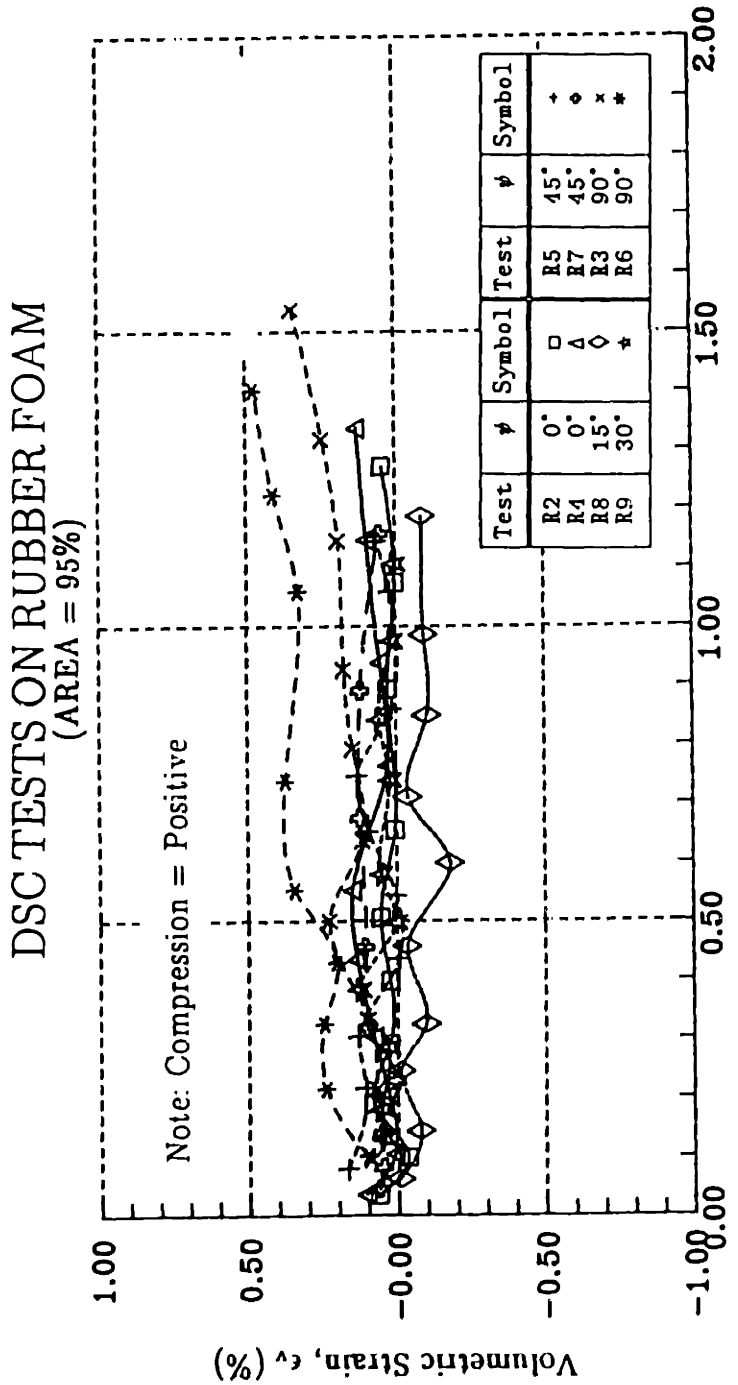

Figure 6.17: Volumetric Behavior of Rubber Foam (Area No. 1).

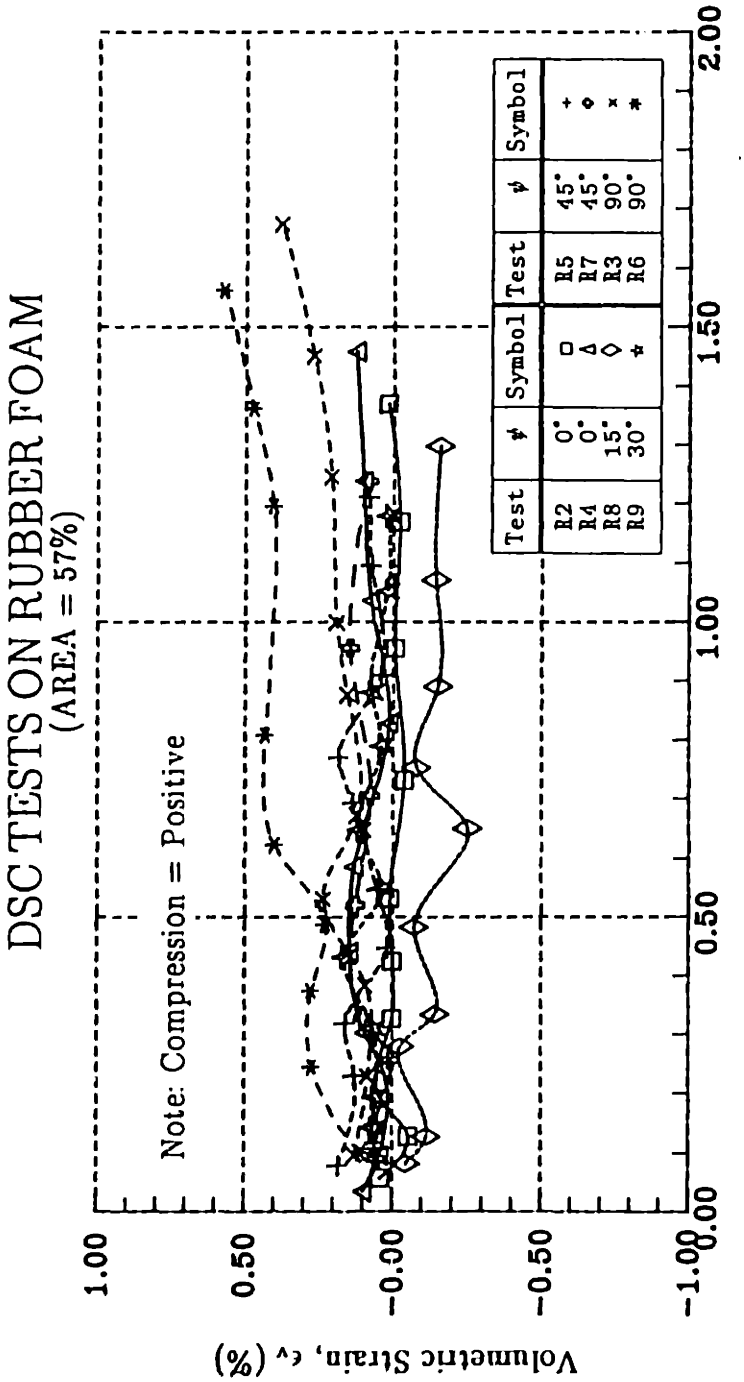

Figure 6.18: Volumetric Behavior of Rubber Foam (Area No. 2).

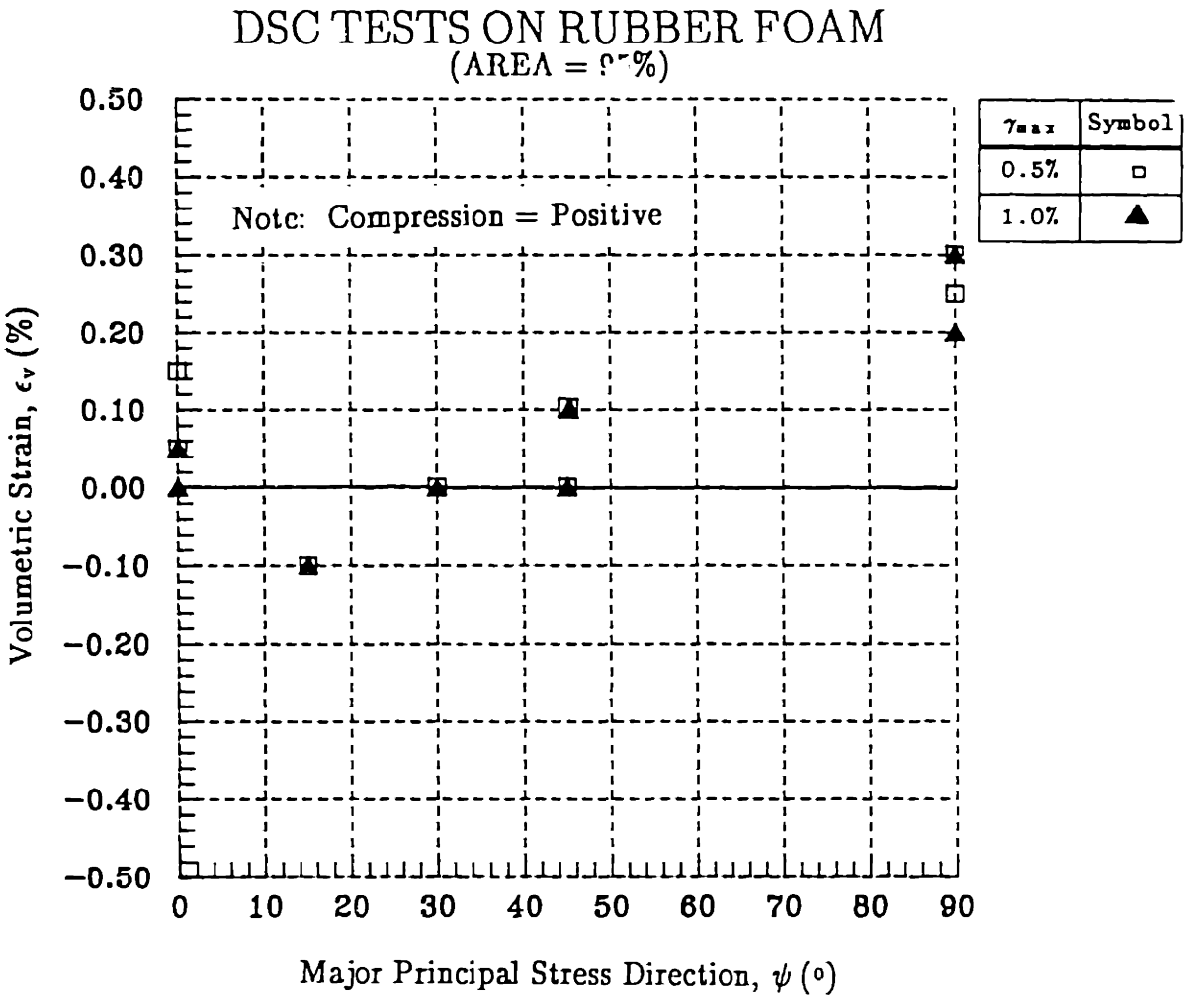

Figure 6.19: Volumetric Strain for Given Levels of Shear Strain.

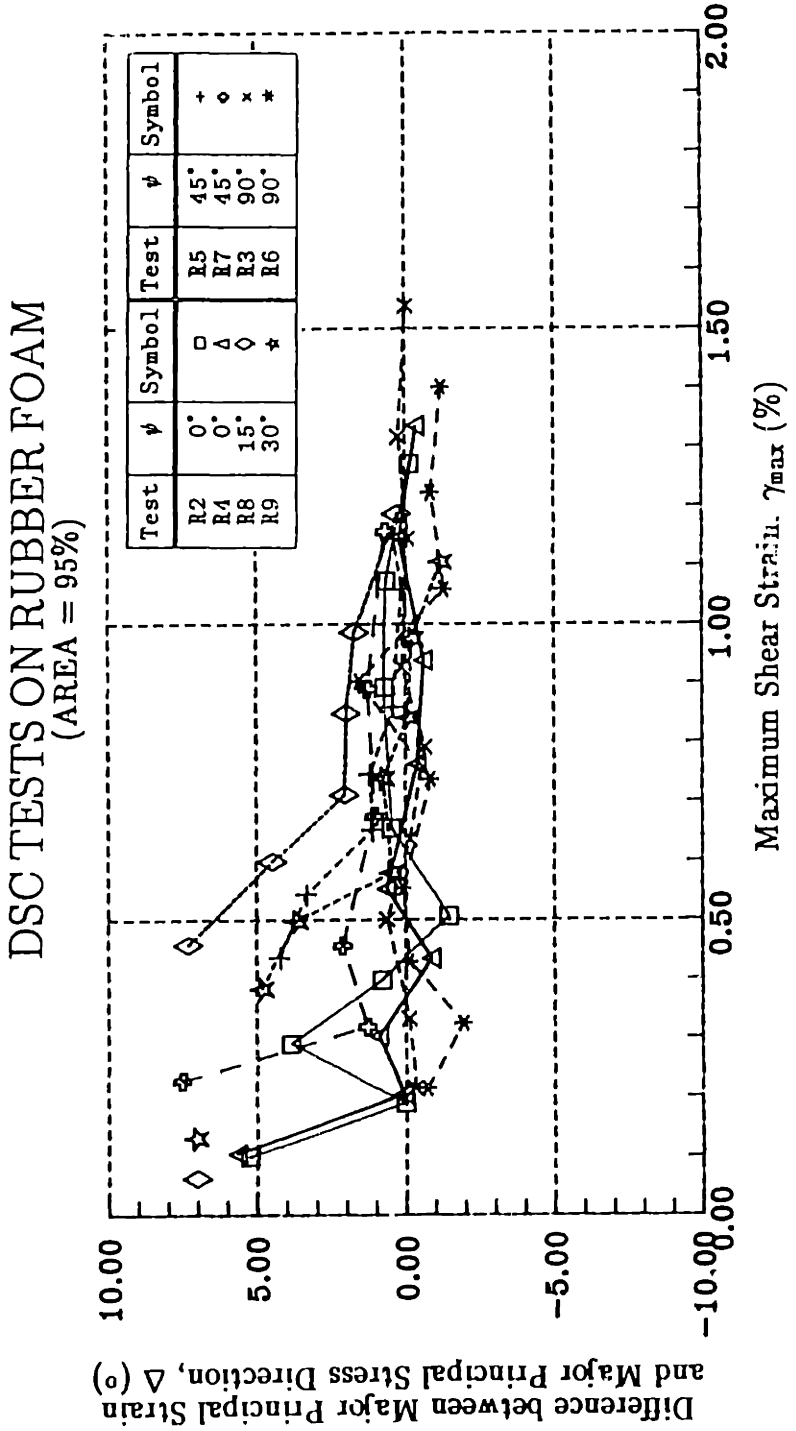

Figure 6.20: Characteristics of Strain–Stress Direction (Area No.1).

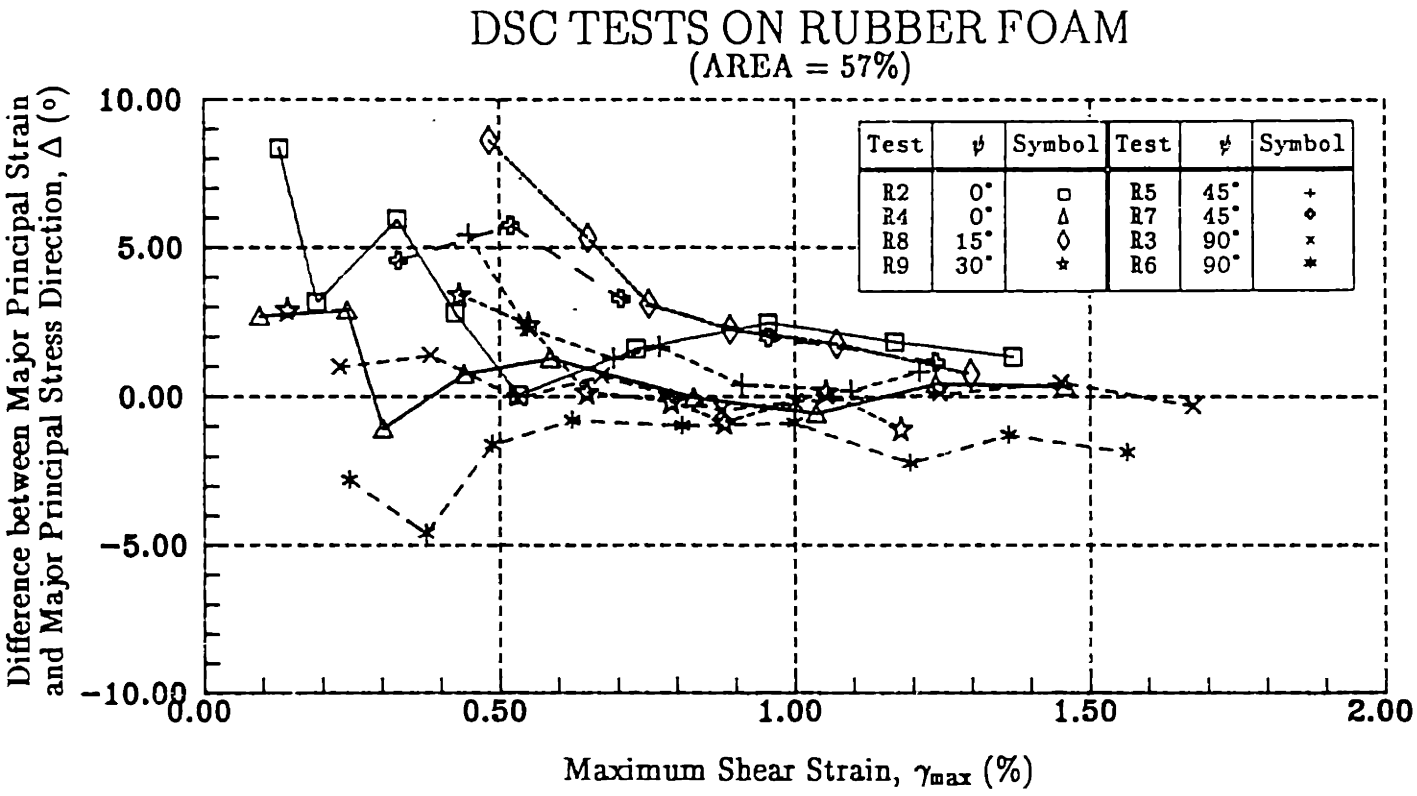

Figure 6.21: Characteristics of Strain–Stress Direction (Area No.2).

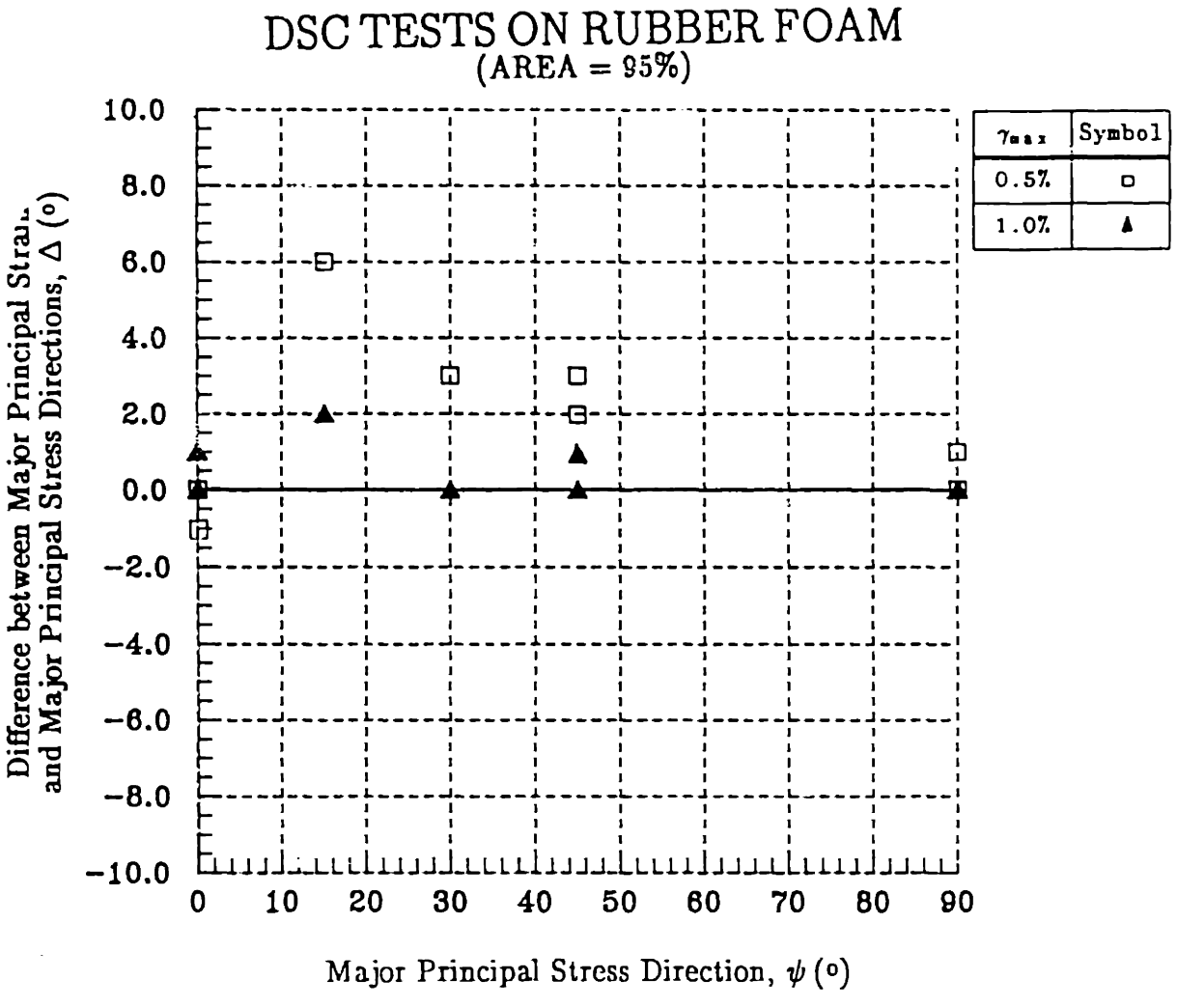

Figure 6.22: Strain–Stress Directions for Given Levels of Shear Strain.

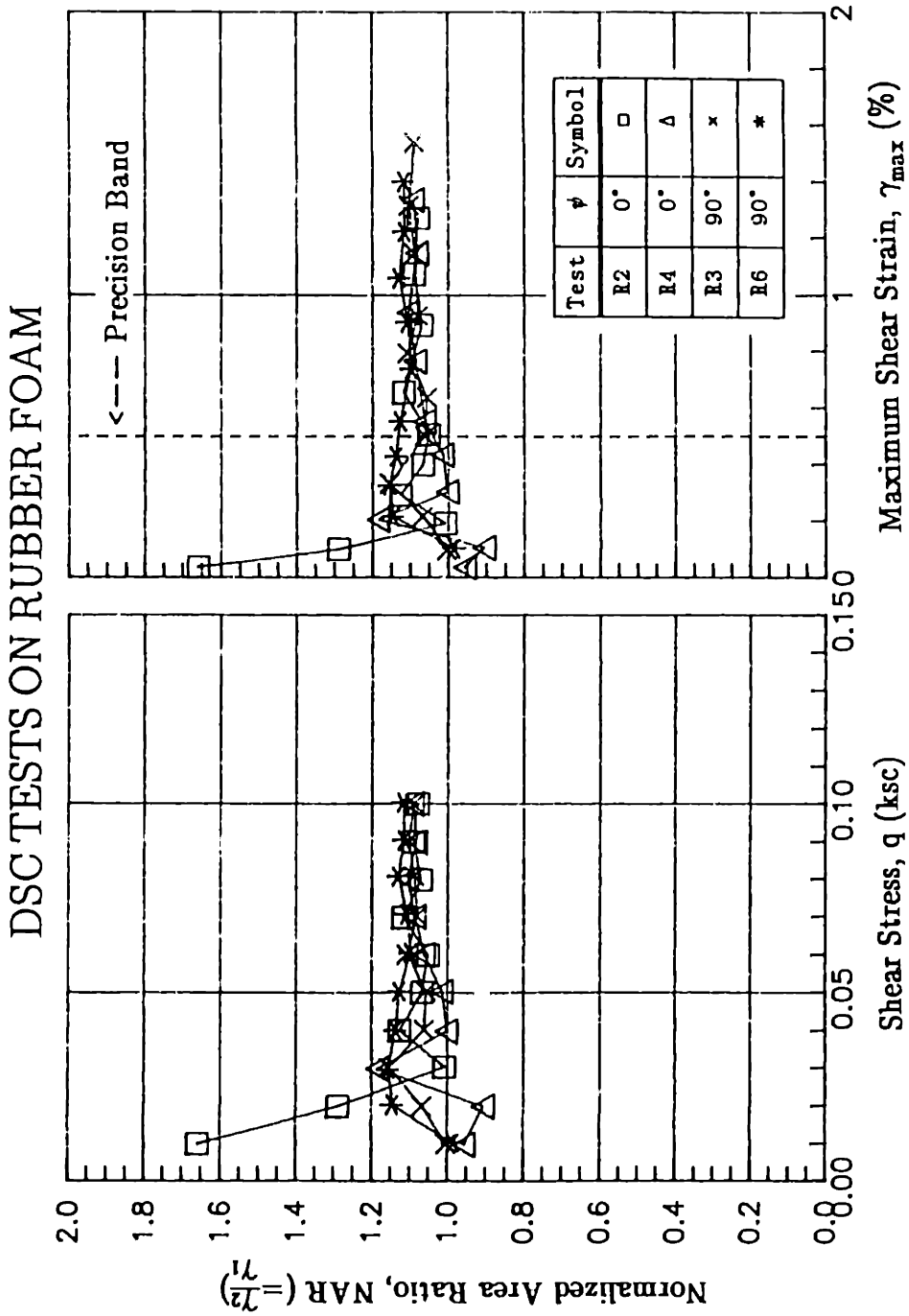

Figure 6.23: Variation of NAR with (a) Shear Stress and with (b) Maximum Shear Strain from DSC Tests on Rubber Foam (without Stressing Shear Sheets).

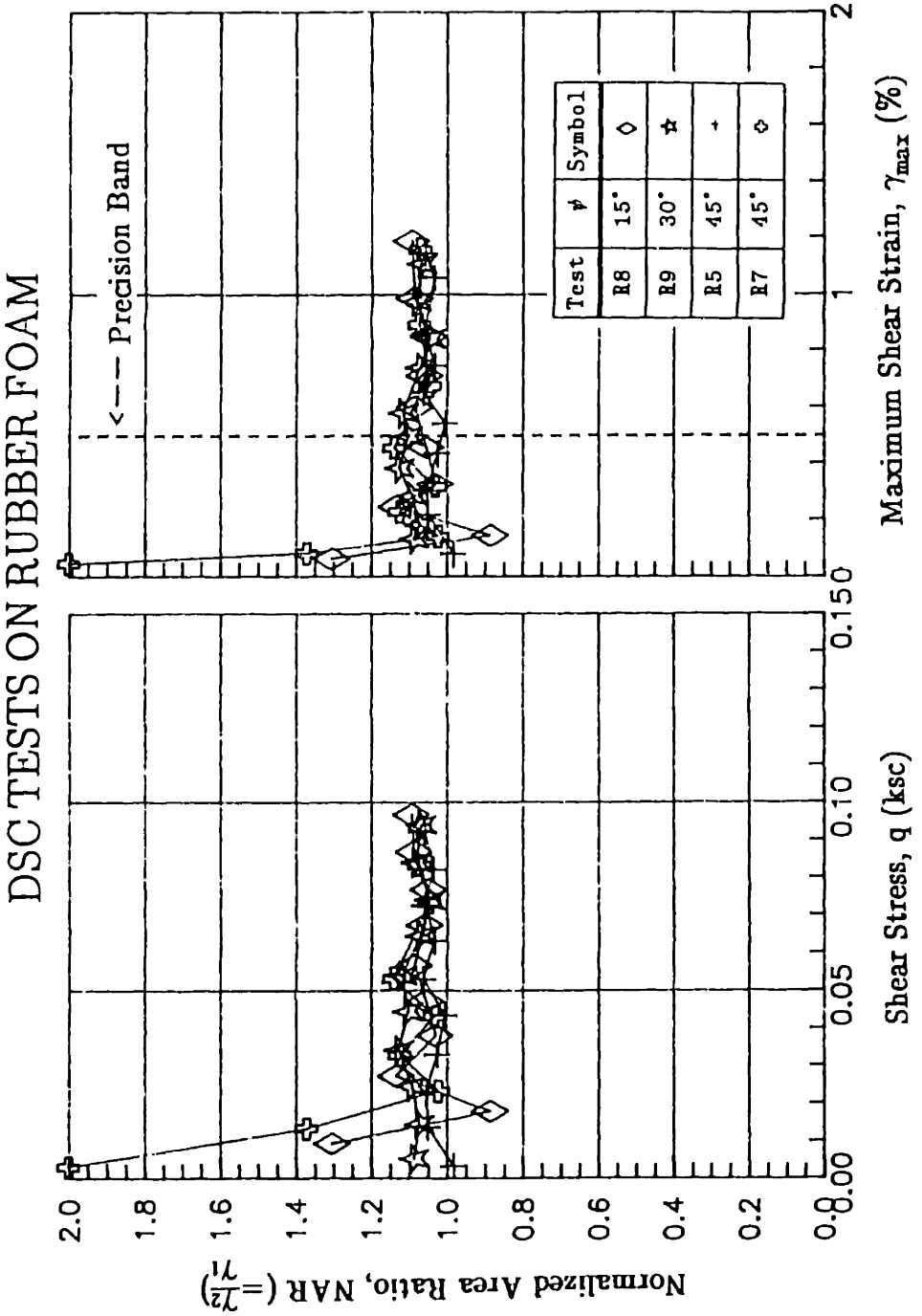

Figure 6.24: Variation of NAR with (a) Shear Stress and with (b) Maximum Shear Strain from DSC Tests on Rubber Foam (with Stressing Shear Sheets).

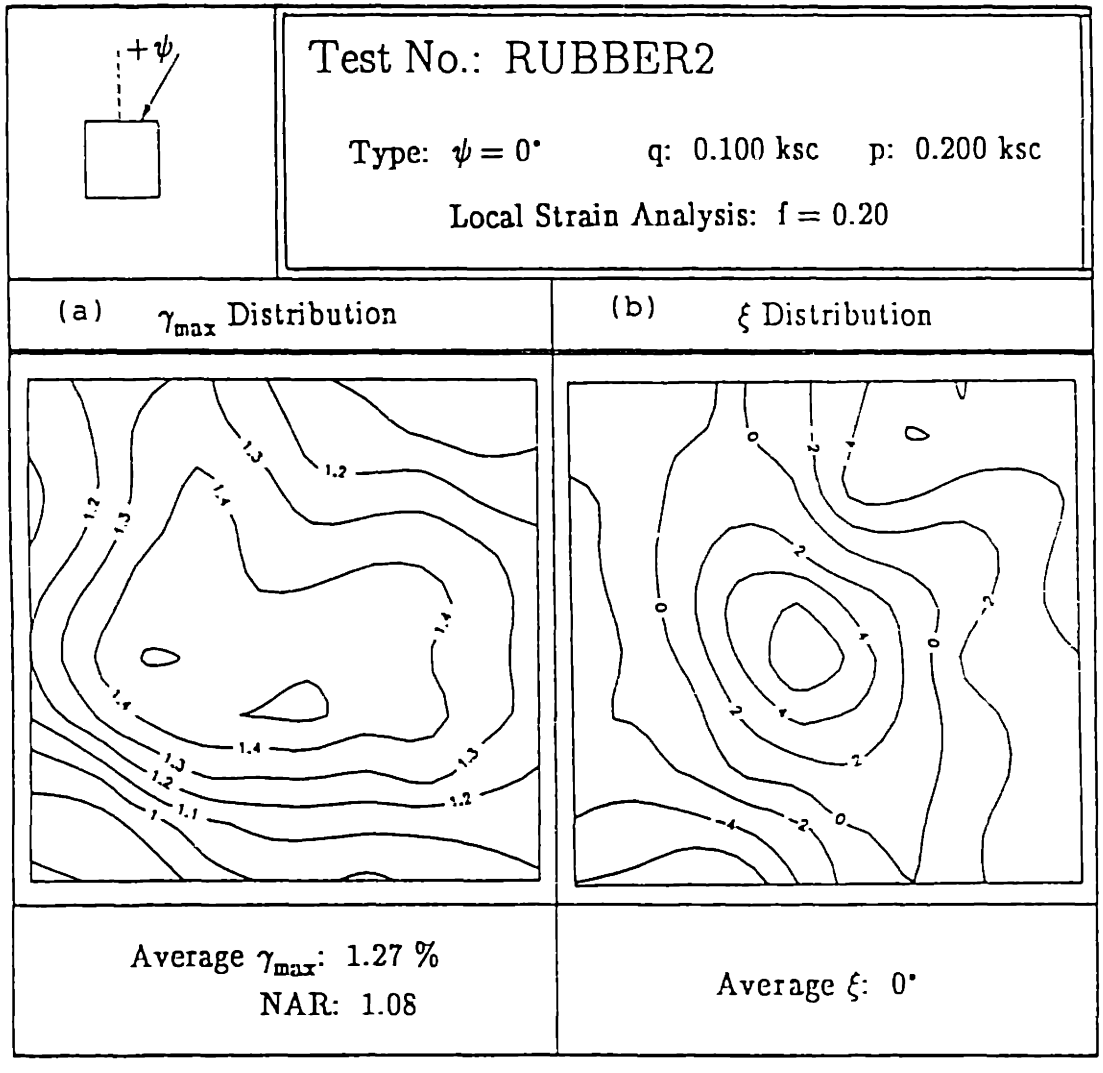

Figure 6.25: γ_{max} and ξ Distributions for Test Rubber2.

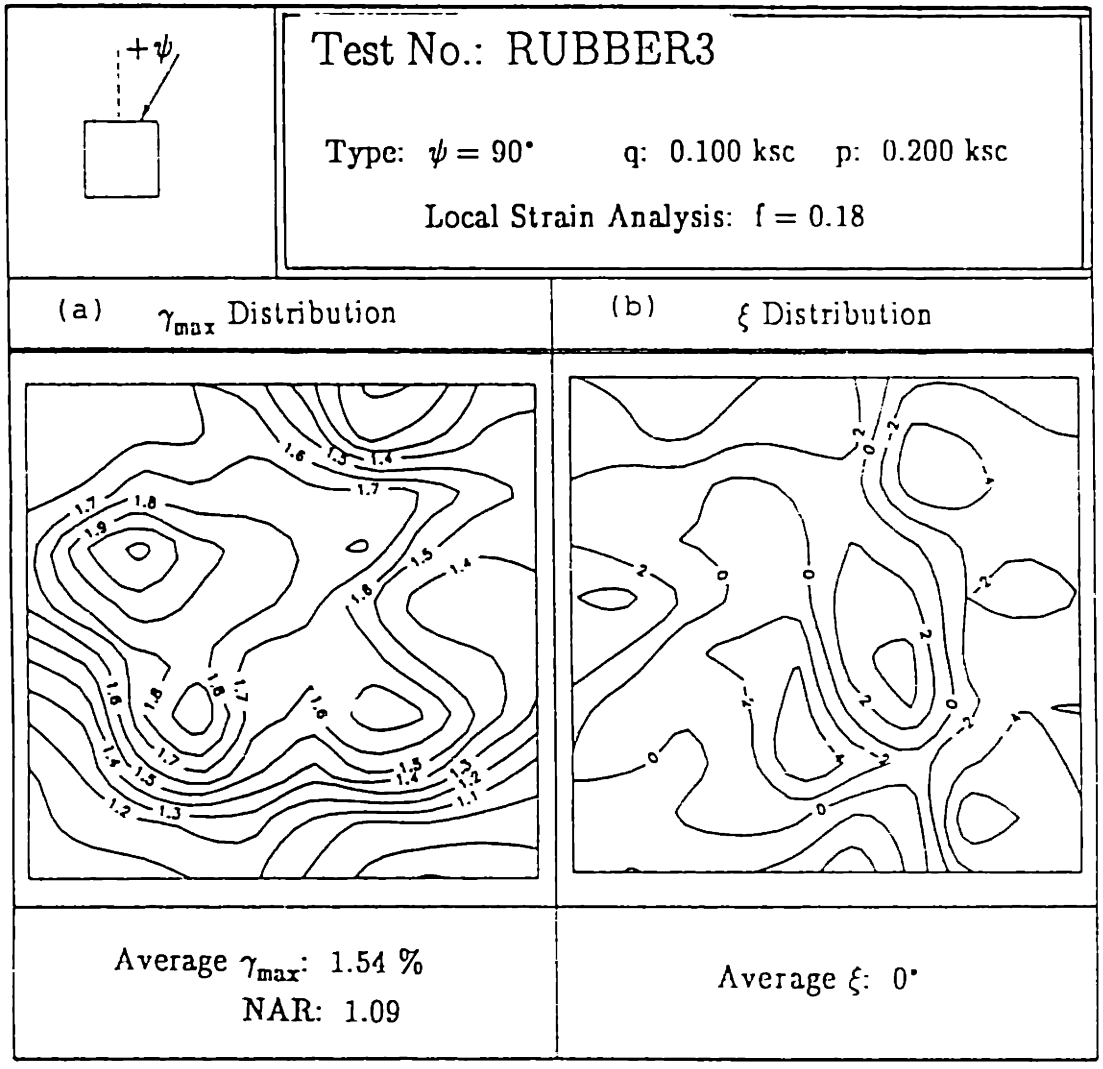

Figure 6.26: γ_{max} and ξ Distributions for Test Rubber3.

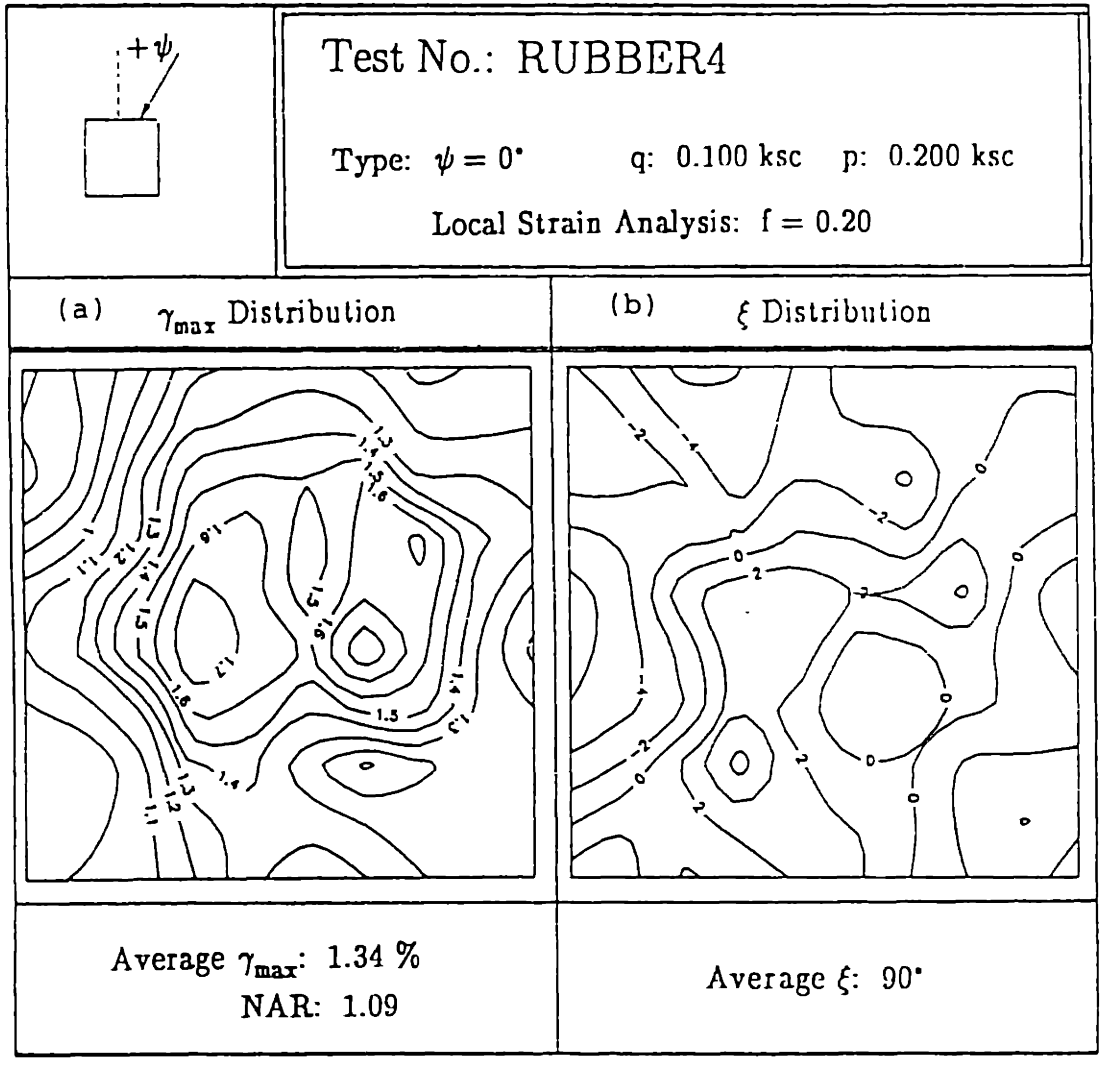

Figure 6.27: γ_{max} and ξ Distributions for Test Rubber4.

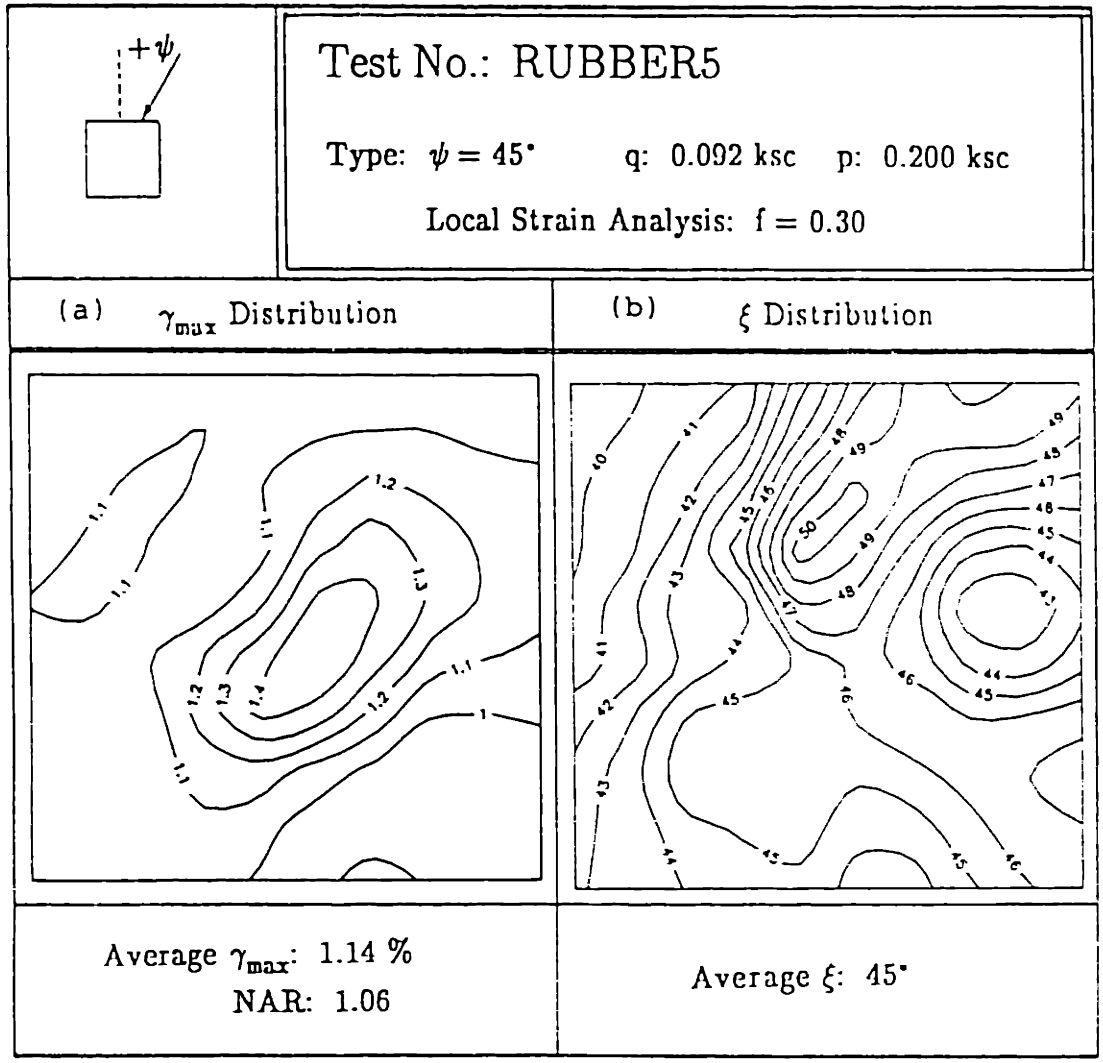

Figure 6.28: γ_{max} and ξ Distributions for Test Rubber5.

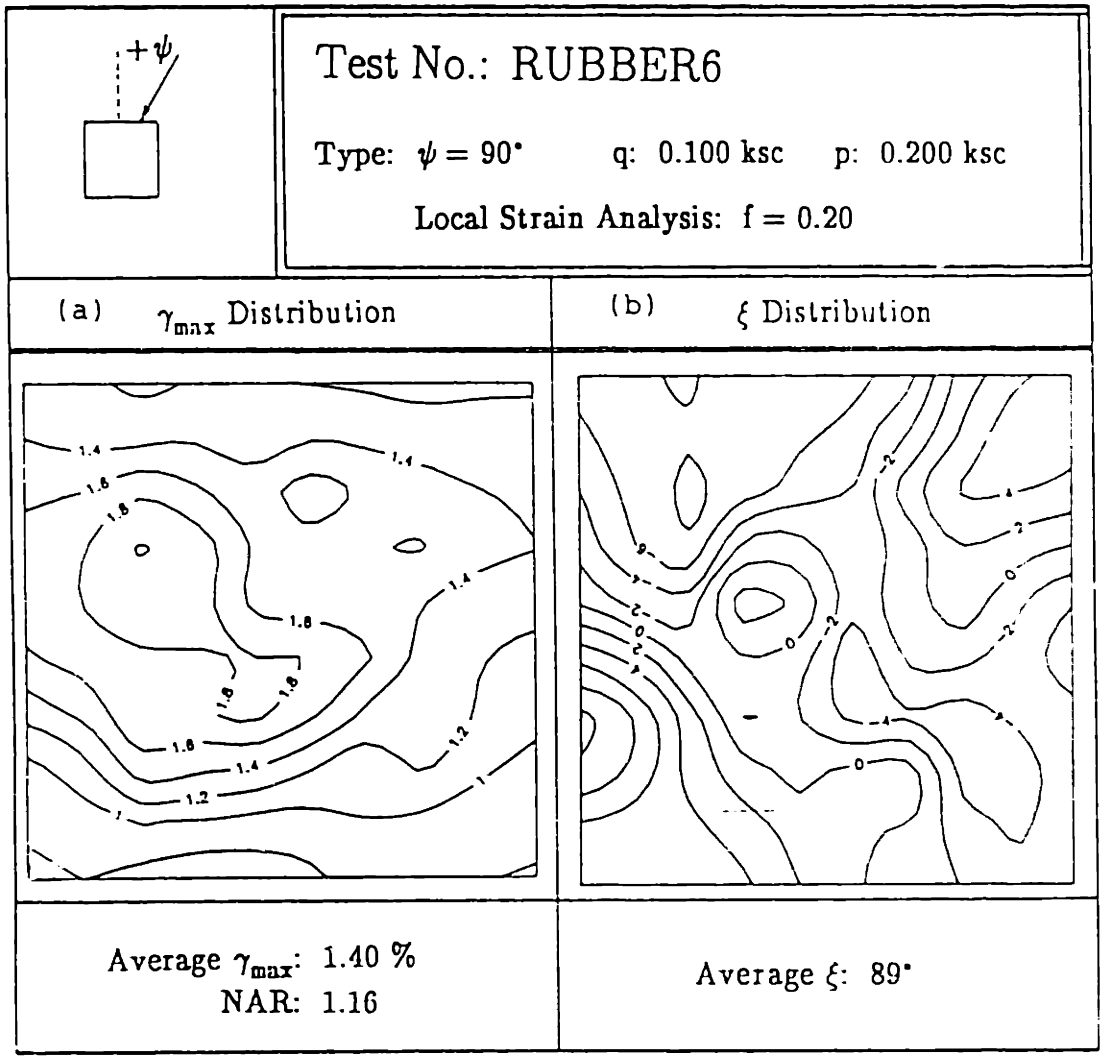

Figure 6.29: γ_{max} and ξ Distributions for Test Rubber6.

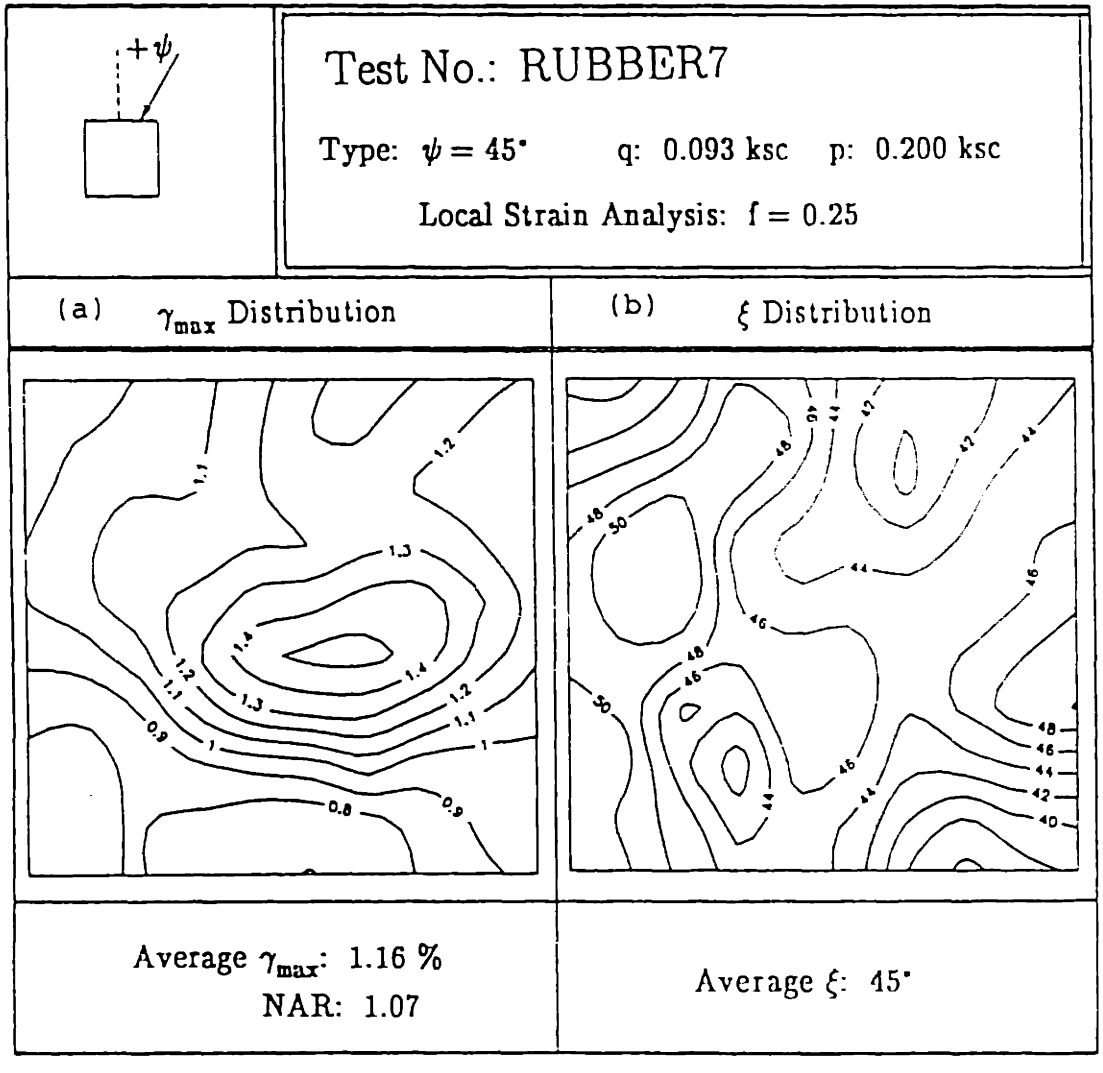

Figure 6.30: γ_{max} and ξ Distributions for Test Rubber7.

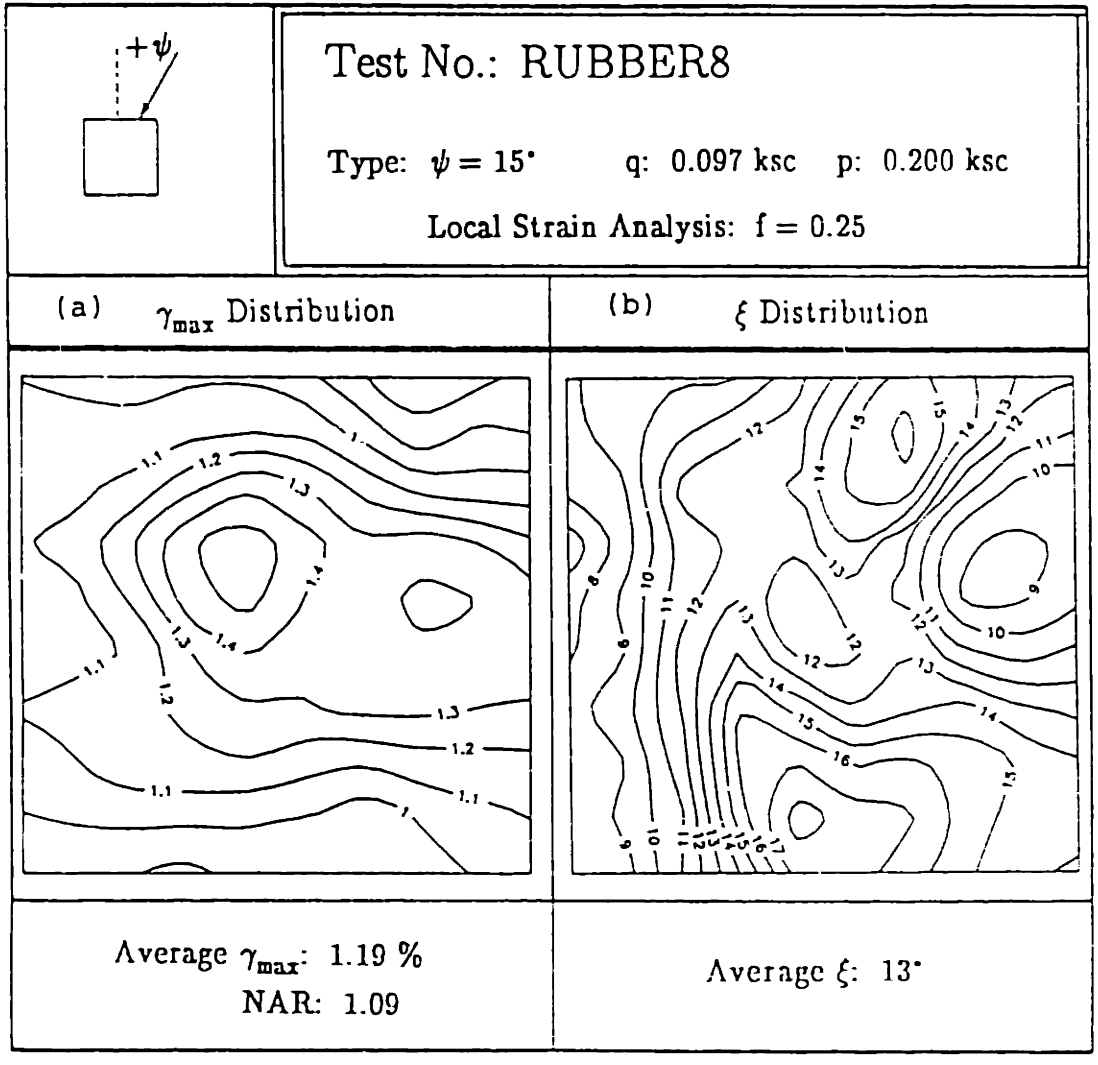

Figure 6.31: γ_{max} and ξ Distributions for Test Rubber8.

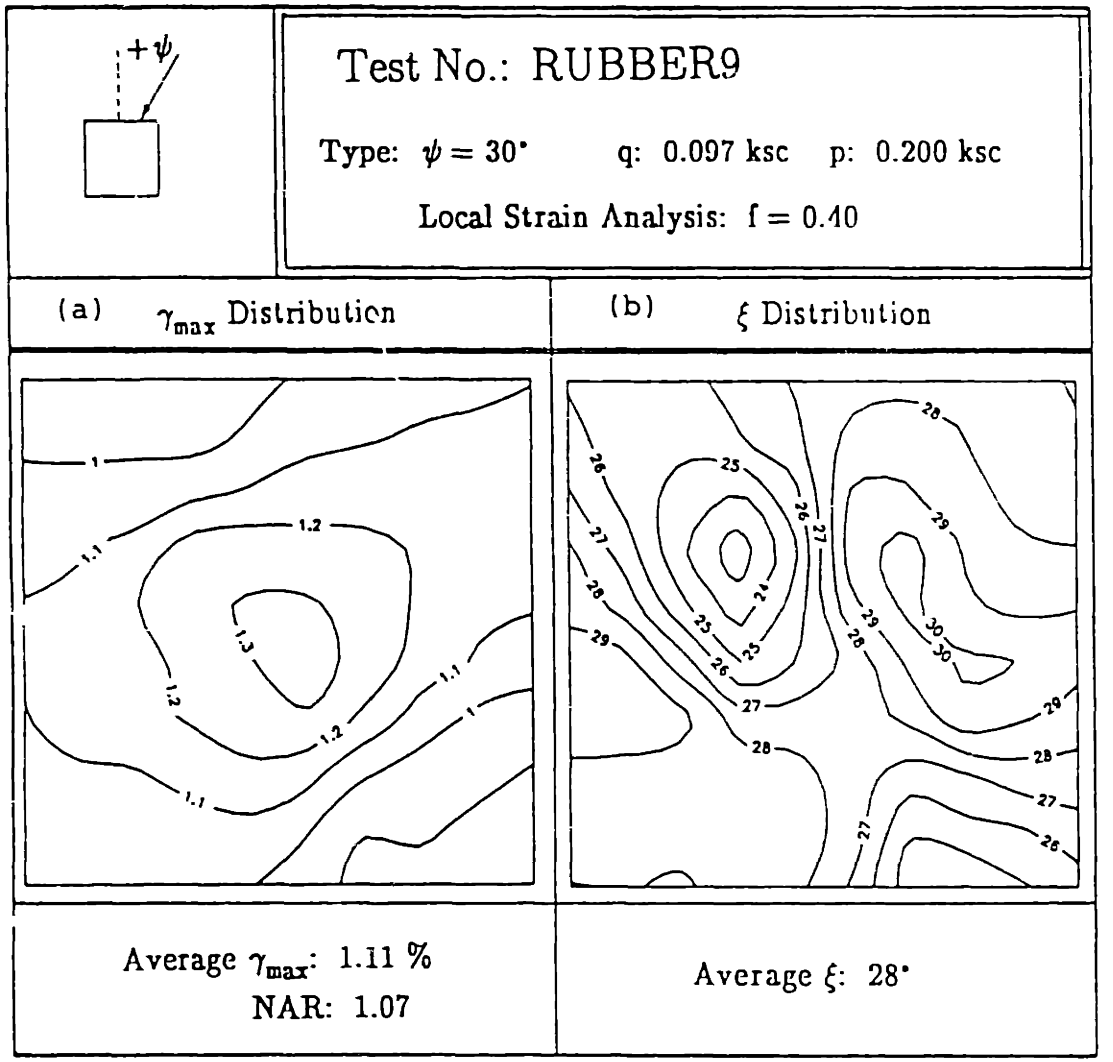

Figure 6.32: γ_{max} and ξ Distributions for Test Rubber9.

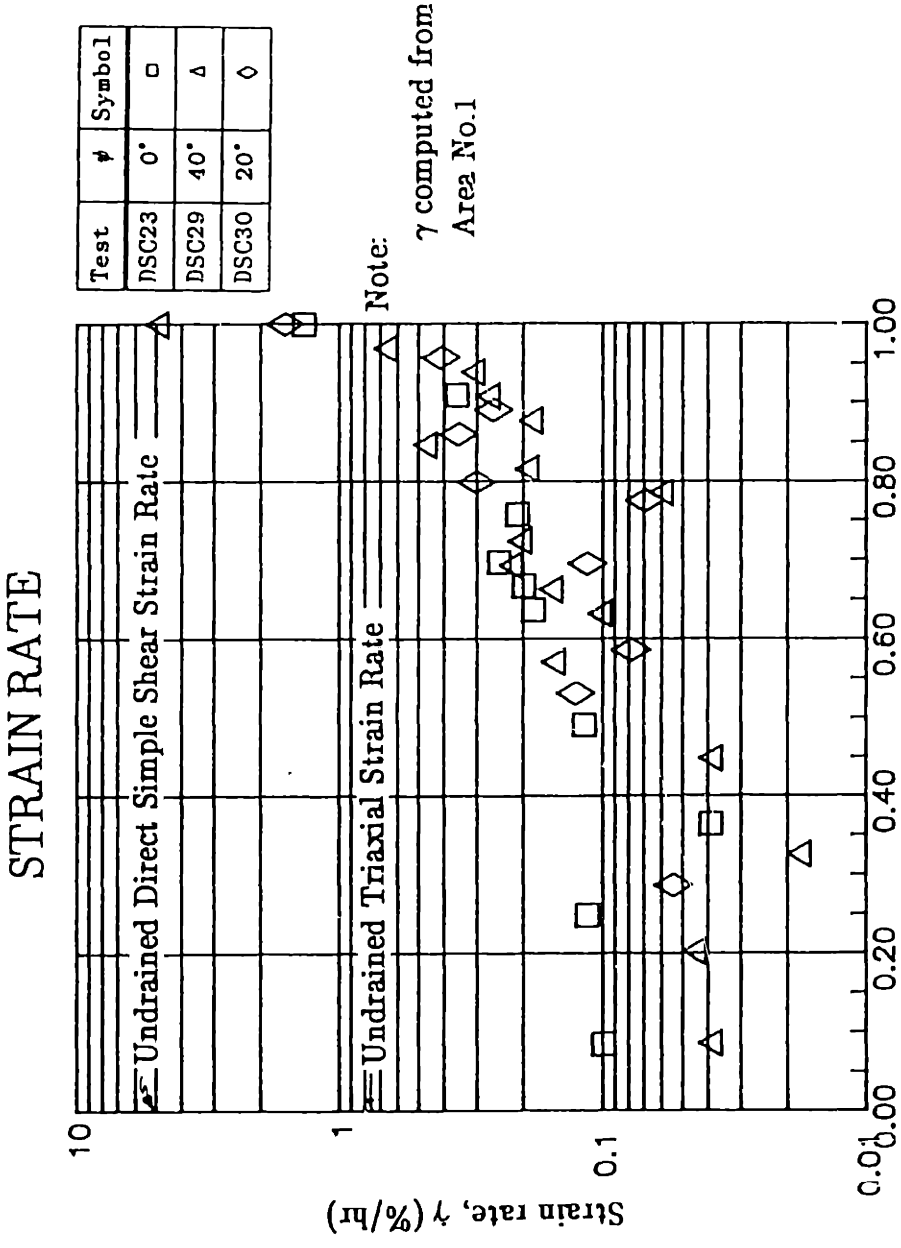

Figure 6.33: Shear Strain Rates from DSC Proof Tests on OCR=4 BBC.

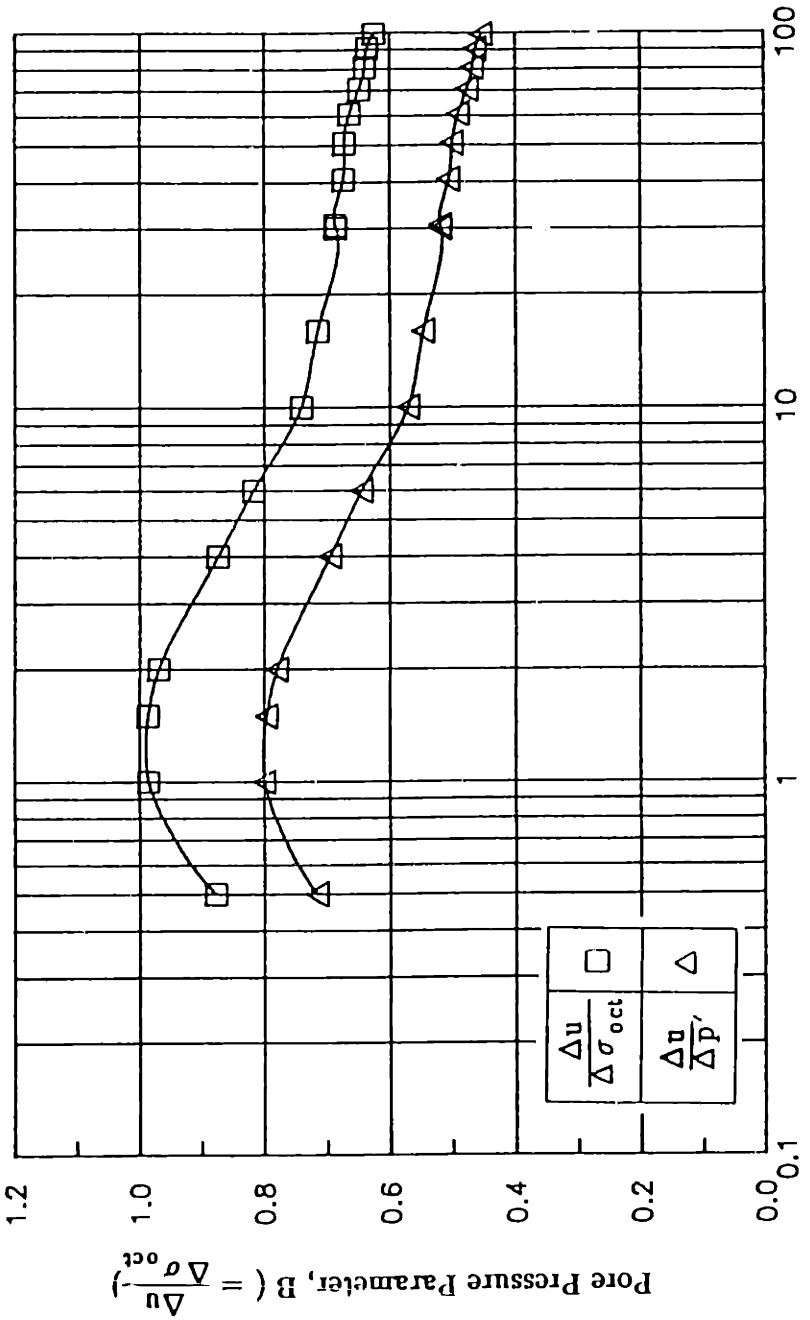

Figure 6.34: Pore Pressure Parameter B computed from $\Delta\sigma_{oct}$ and $\Delta p'$ for Test DSC34.

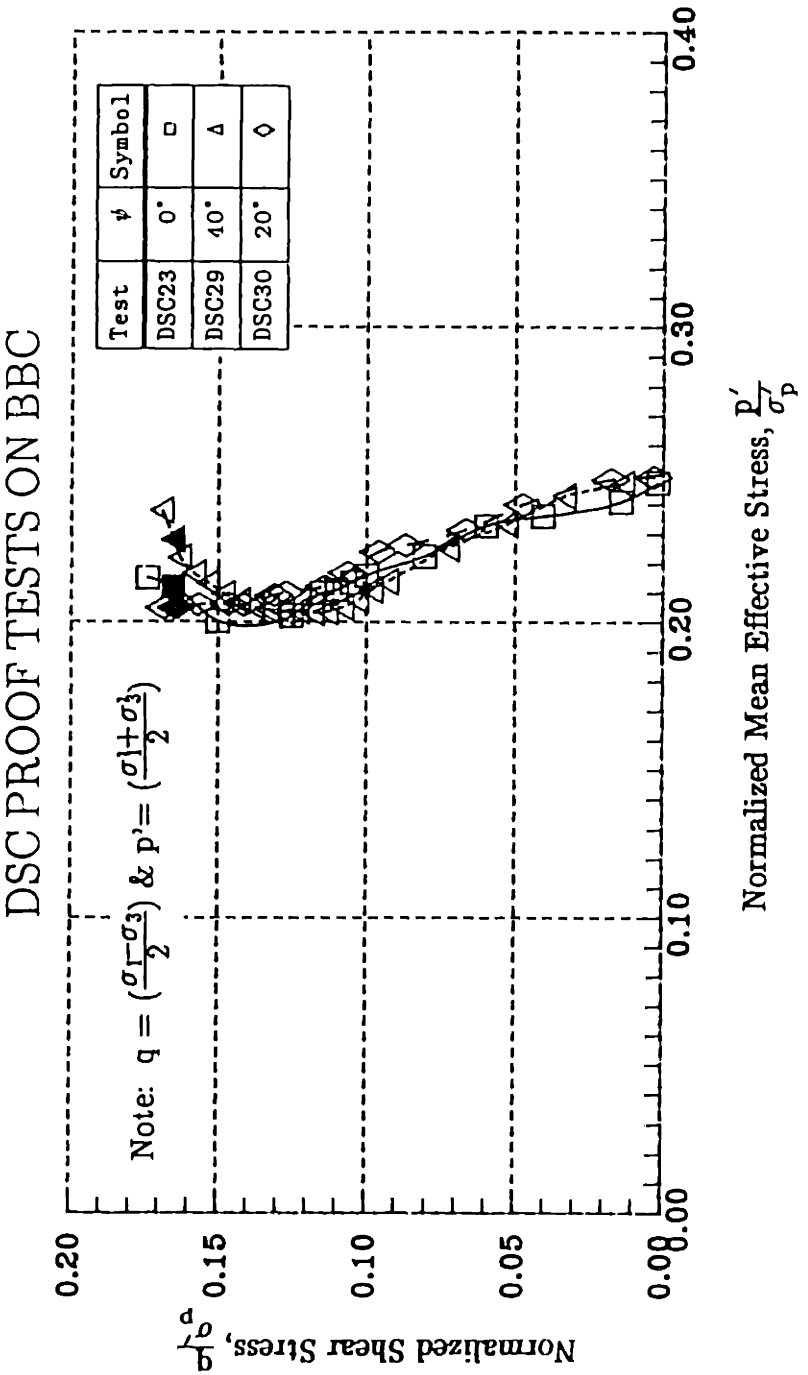

Figure 6.35: Effective Stress Paths for DSC Proof Tests on OCR=4 BBC.

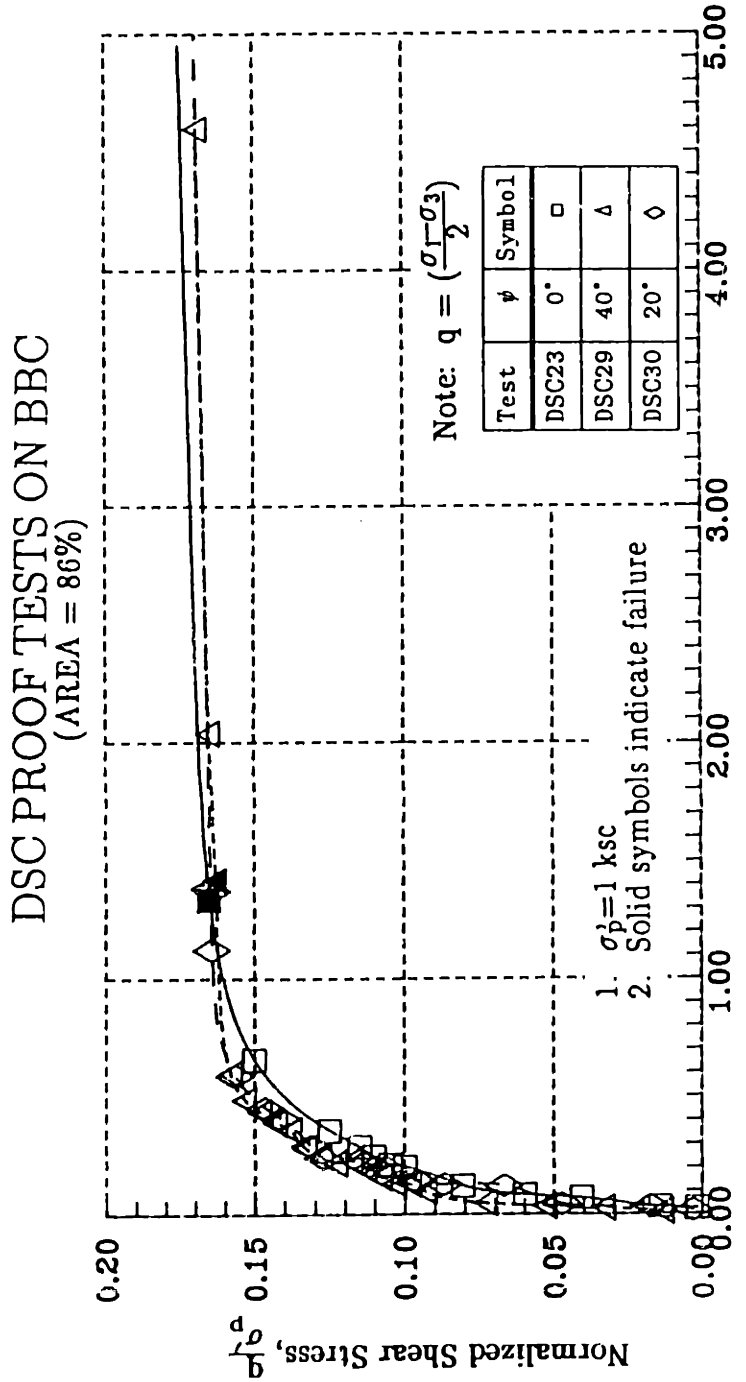

Figure 6.36a: Stress–Strain Relationships from DSC Proof Tests on OCR=4 BBC (Area No. 1).

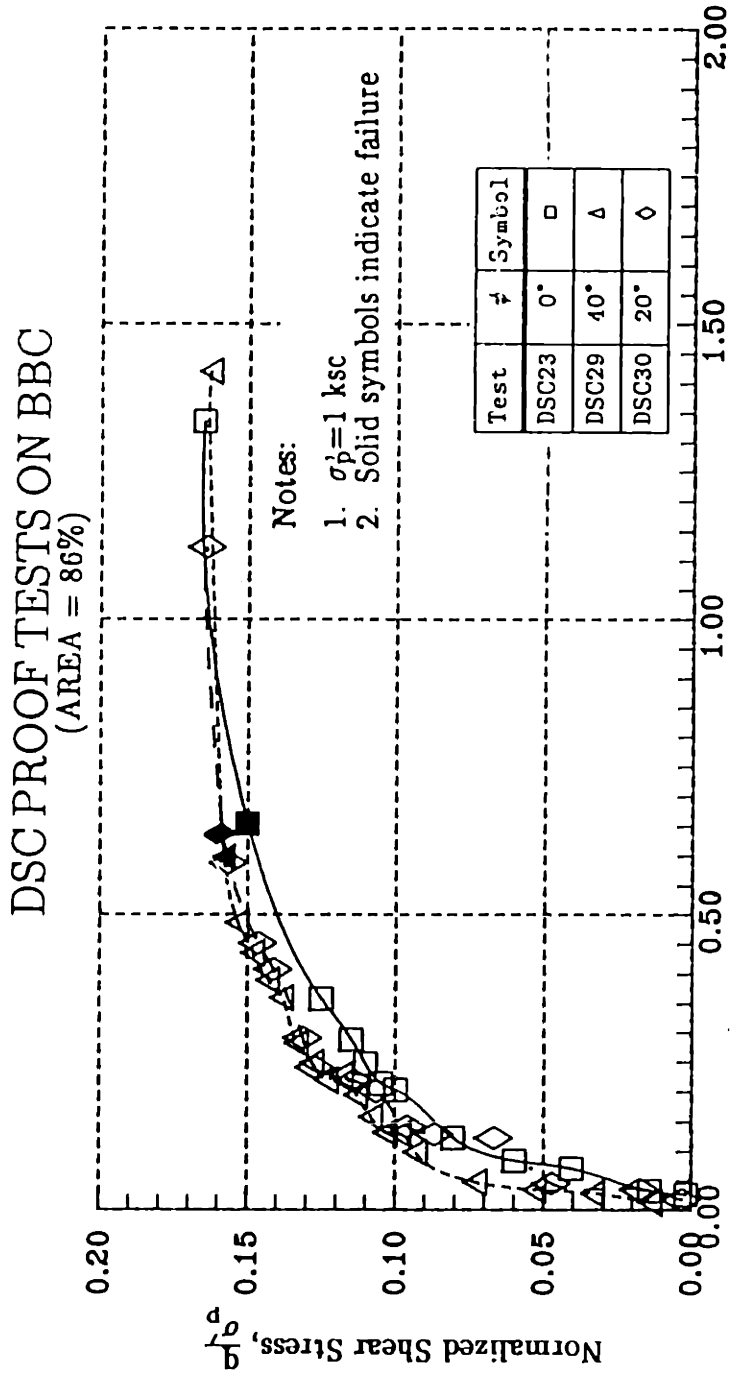

Figure 6.36b: Stress–Strain Relationships from DSC Proof Tests on OCR=4 BBC (Area No. 1).

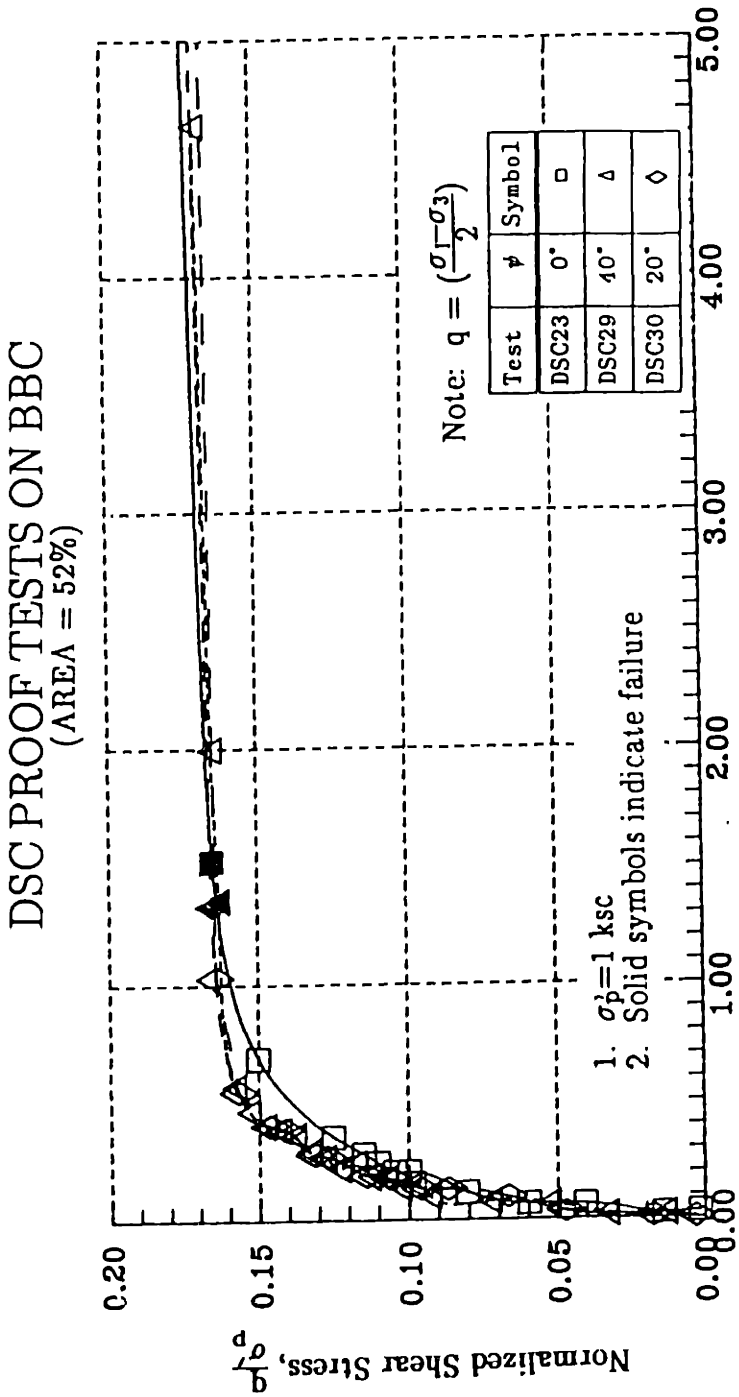

Figure 6.37: Stress–Strain Relationships from DSC Proof Tests on OCR=4 BBC (Area No. 2).

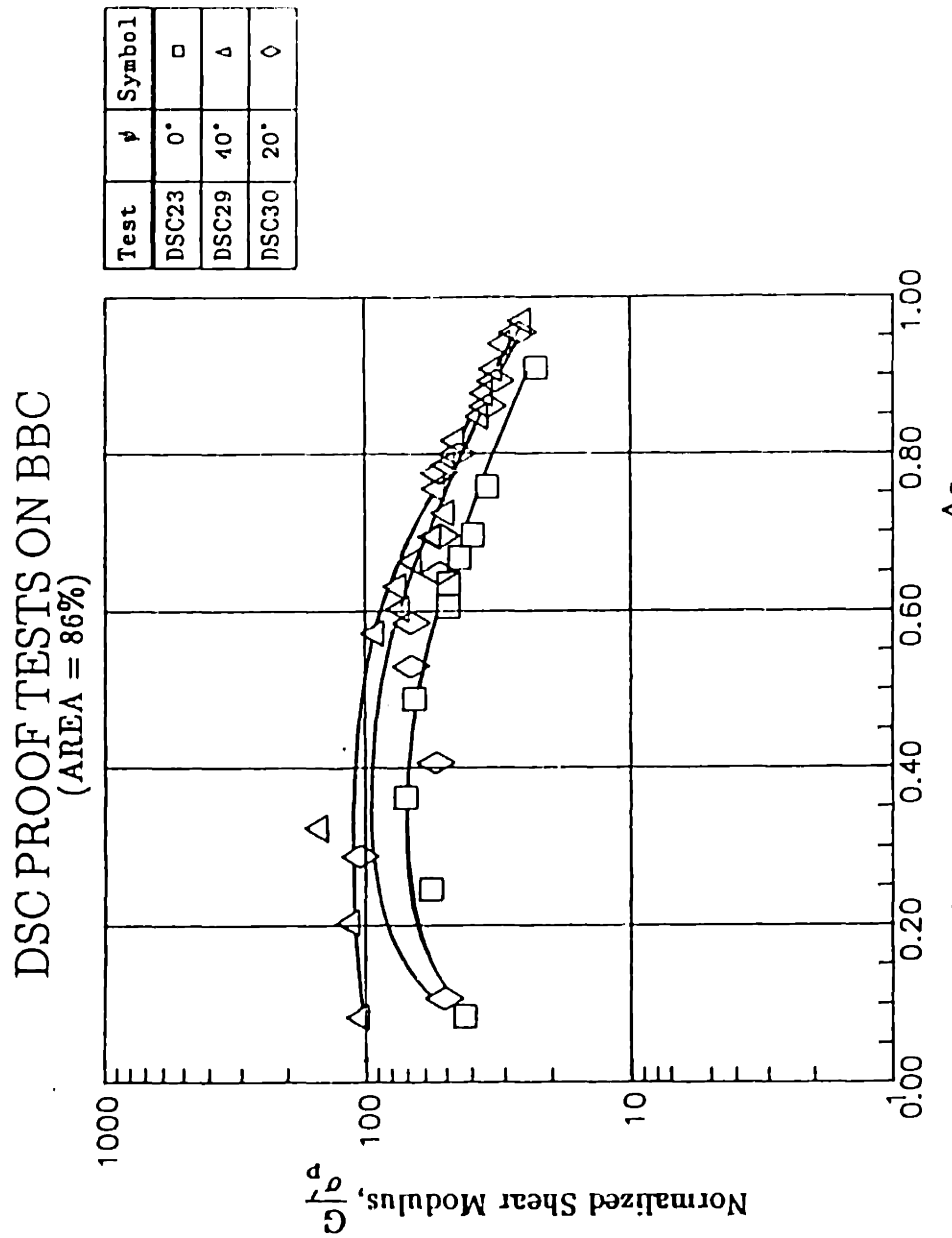

Figure 6.38: Variation of Normalized Shear Modulus with Applied Stress Level from DSC Proof Tests on OCR=4 BBC.

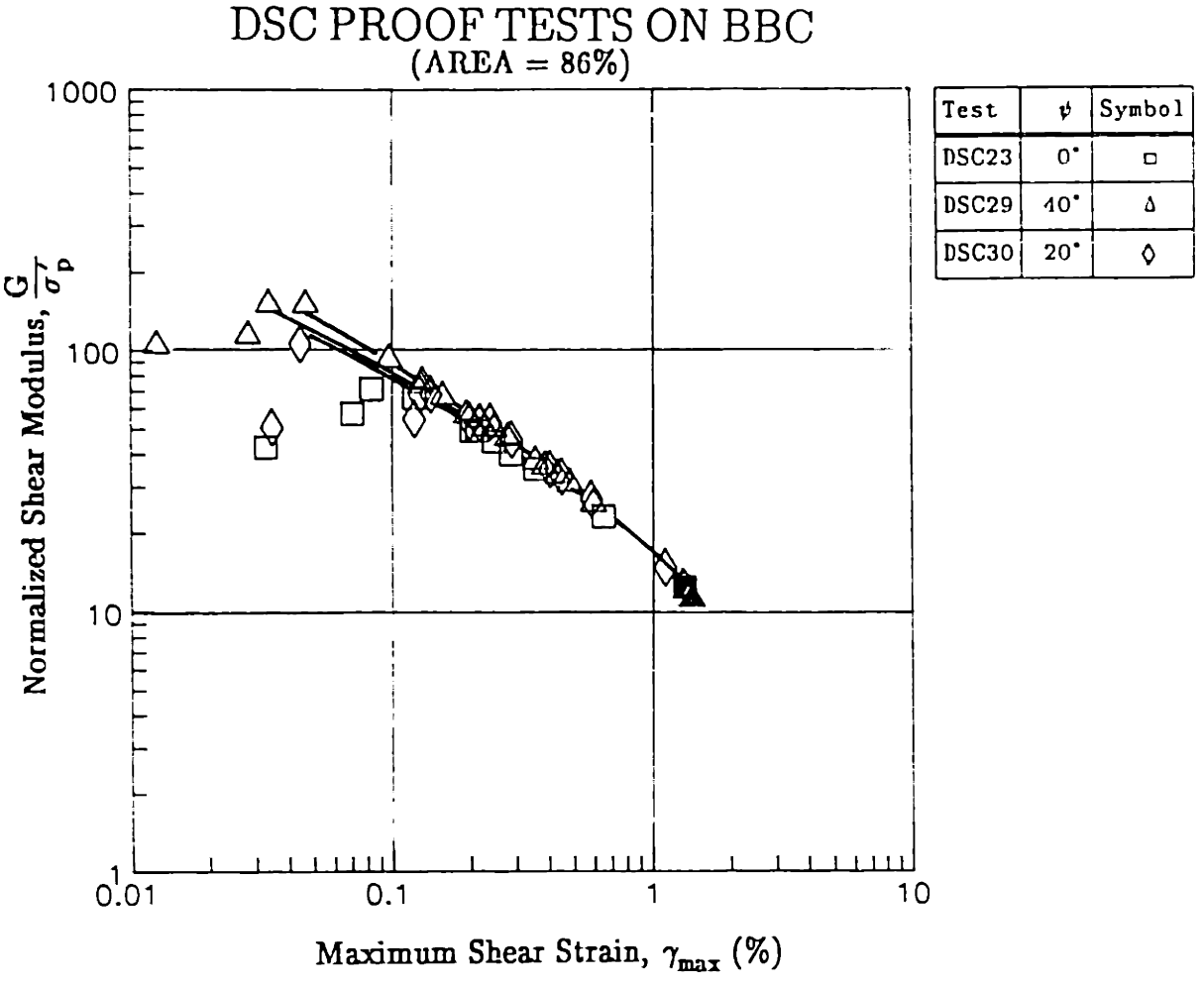

Figure 6.39: Variation of Normalized Shear Modulus with Maximum Shear Strain from DSC Proof Tests on OCR=4 BBC.

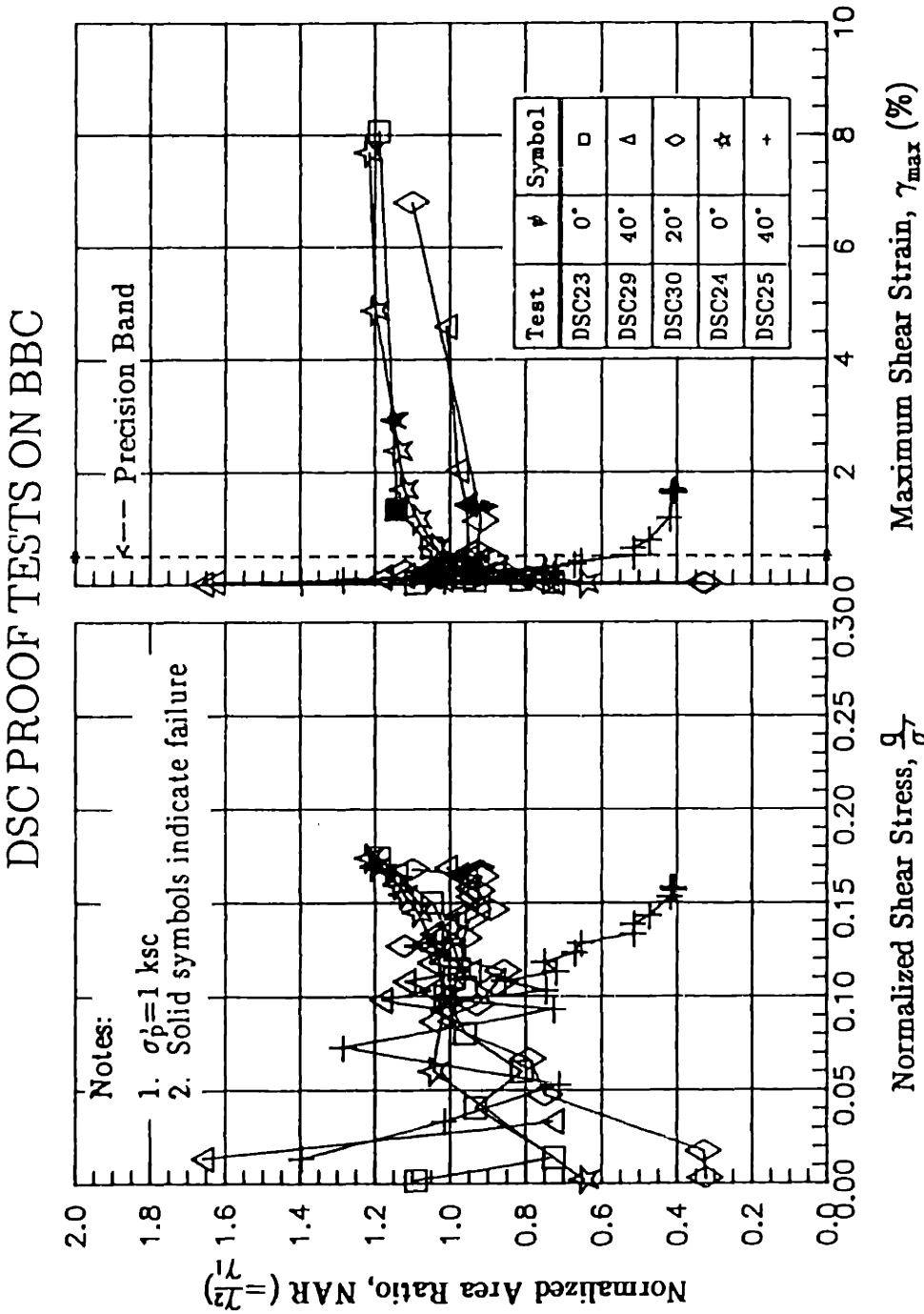

Figure 6.40: Variation of NAR with (a) Normalized Shear Stress and (b) Shear Strain from DSC Proof Tests on OCR=4 BBC.

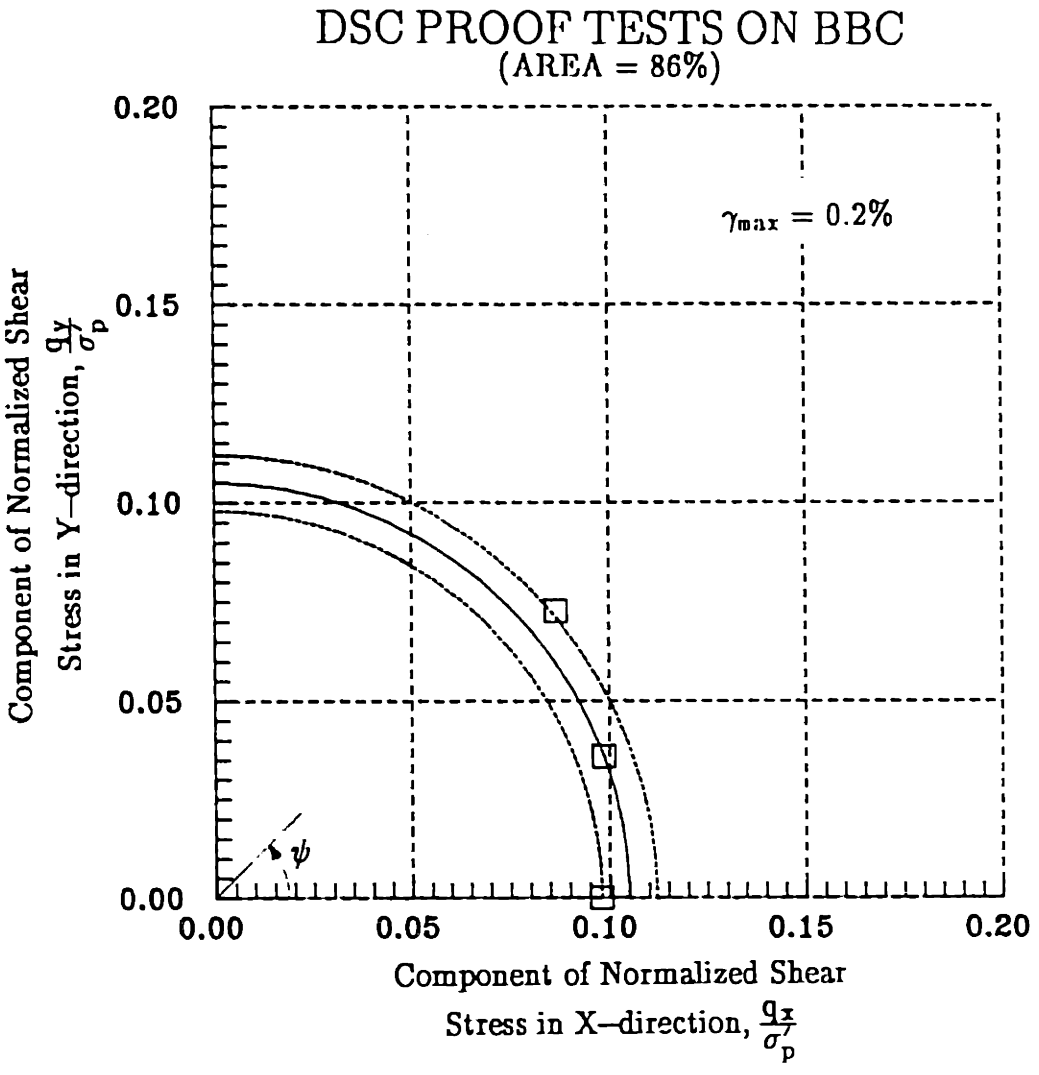

Figure 6.41: Variation of Shear Stress with ψ Angle at γ_{max}=0.2%.

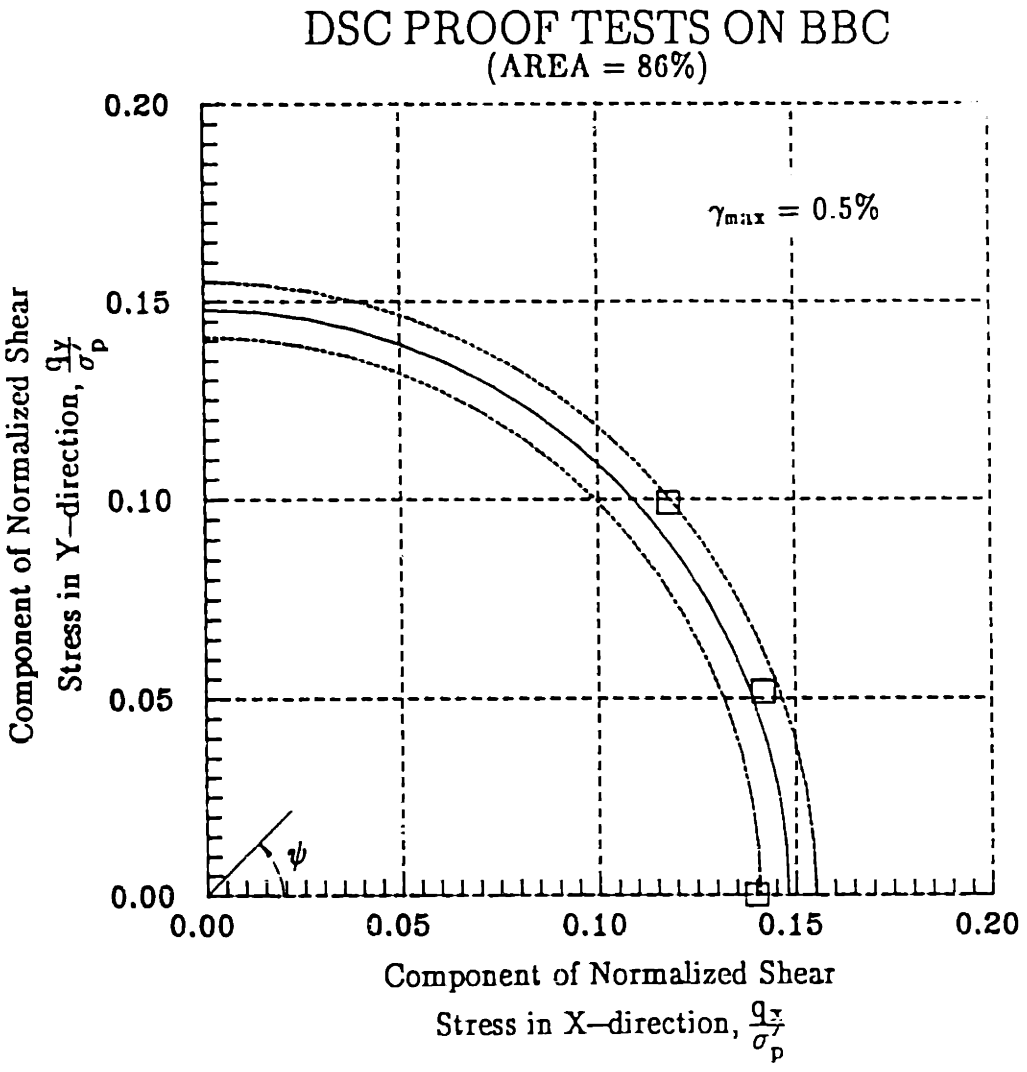

Figure 6.42: Variation of Shear Stress with ψ Angle at γ_{max}=0.5%.

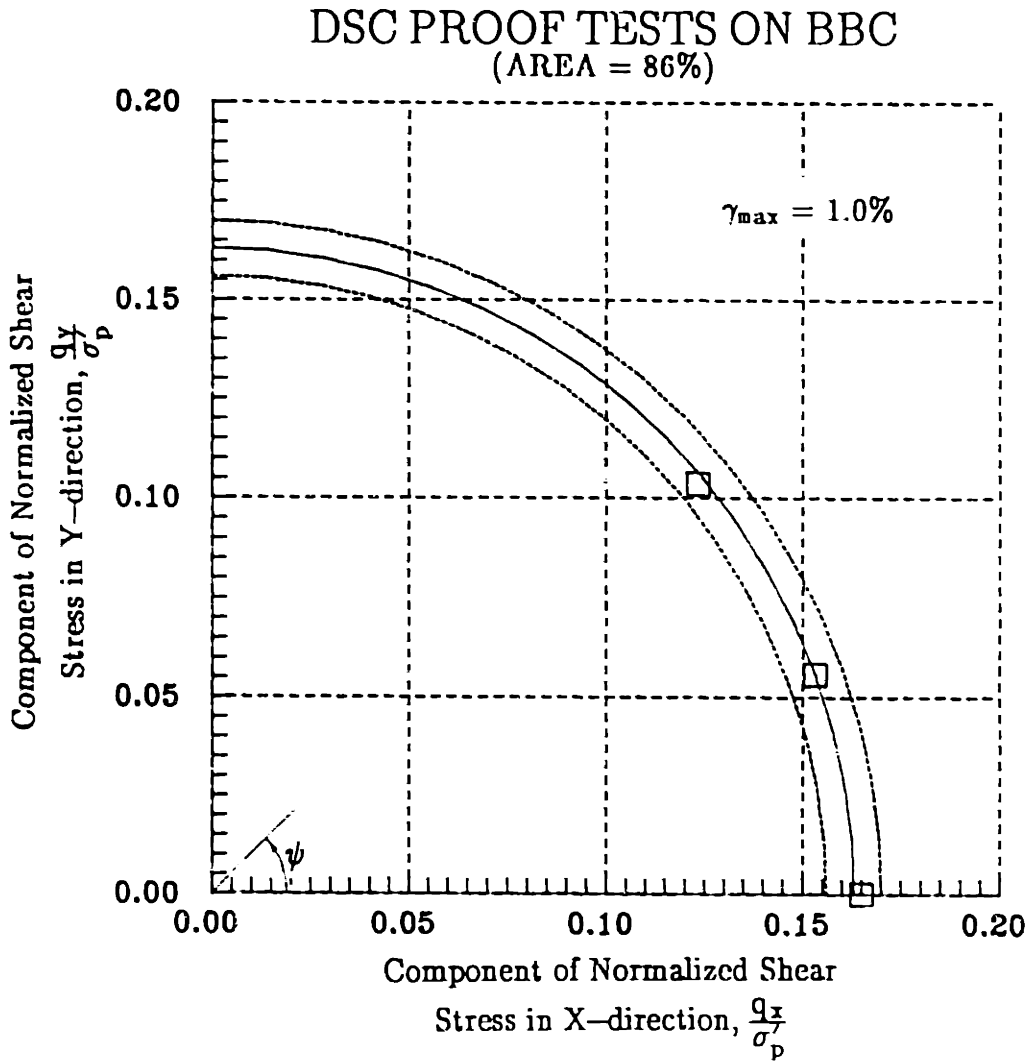

Figure 6.43: Variation of Shear Stress with ψ Angle at γ_{max}=1.0%.

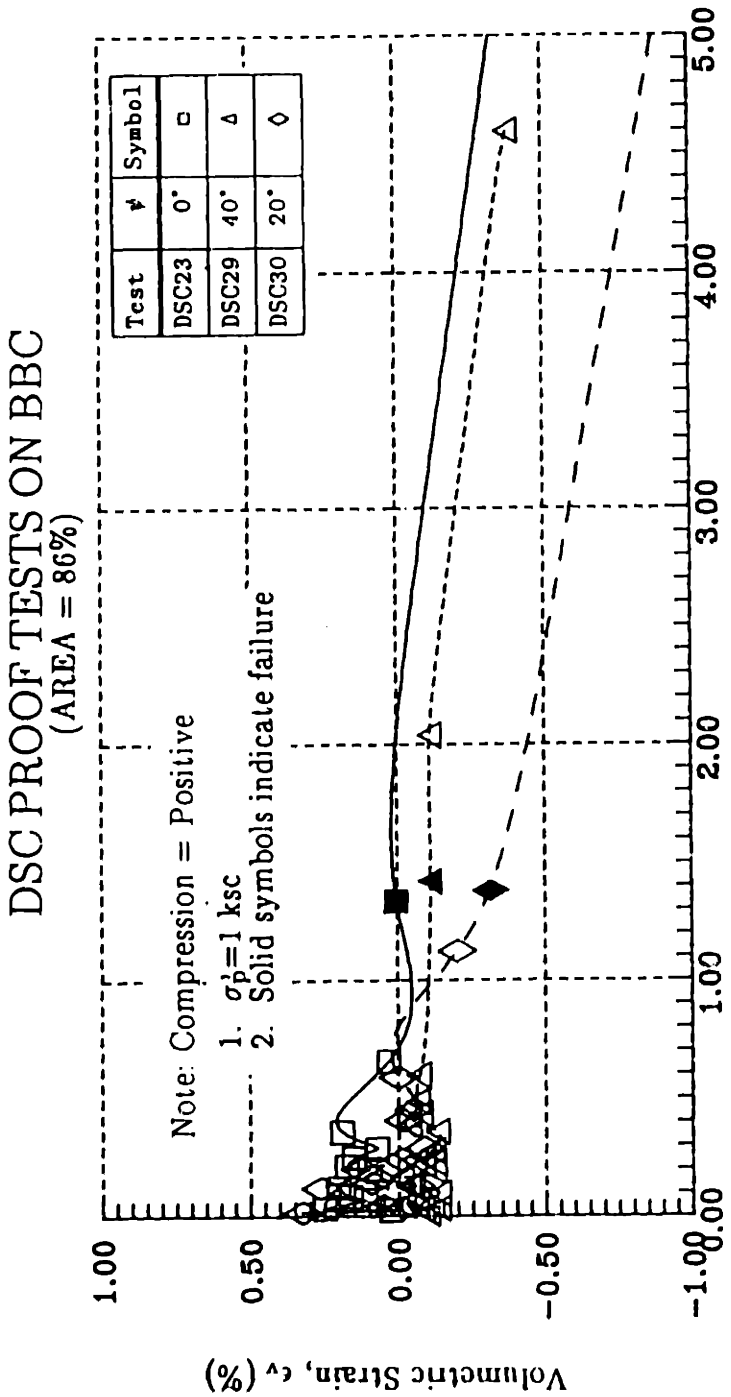

Figure 6.44: Volumetric Behavior of Proof Tests on OCR=4 BBC (Area No. 1).

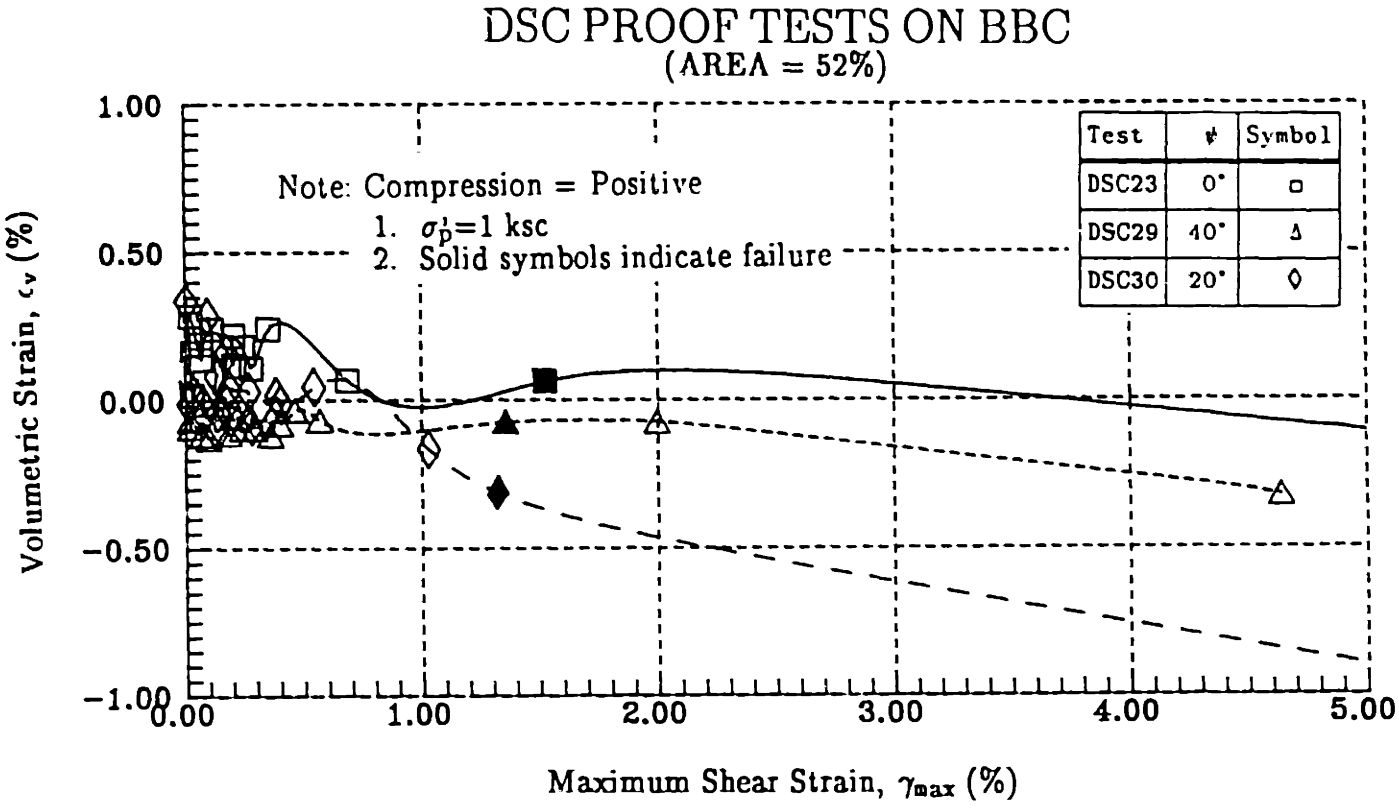

Figure 6.45: Volumetric Behavior of Proof Tests on OCR=4 BBC (Area No. 2).

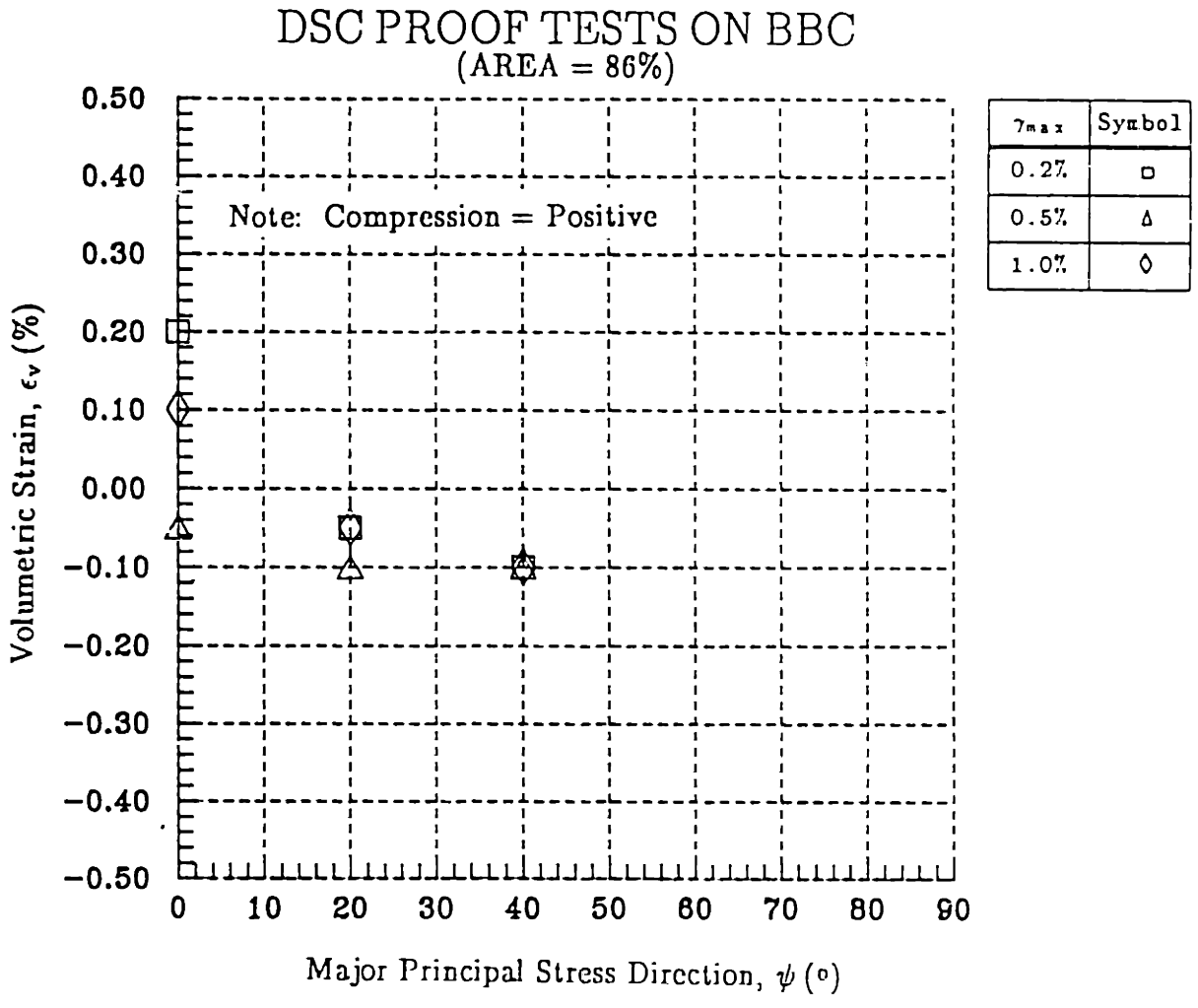

Figure 6.46: Volumetric Strain versus Major Principal Stress Direction for DSC Proof Tests on OCR=4 BBC at Given Levels of Strain.

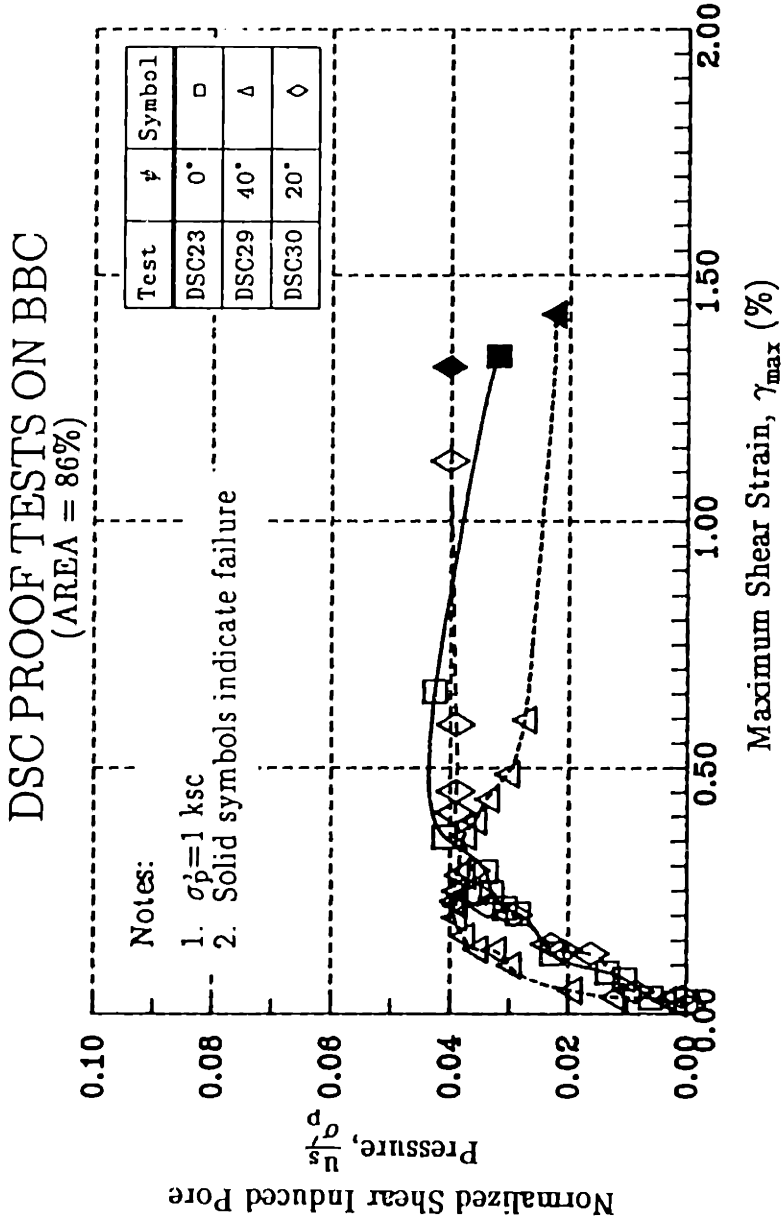

Figure 6.47: Normalized Shear Induced Pore Pressure versus Shear Strain for DSC Proof Tests on BBC (Area No. 1).

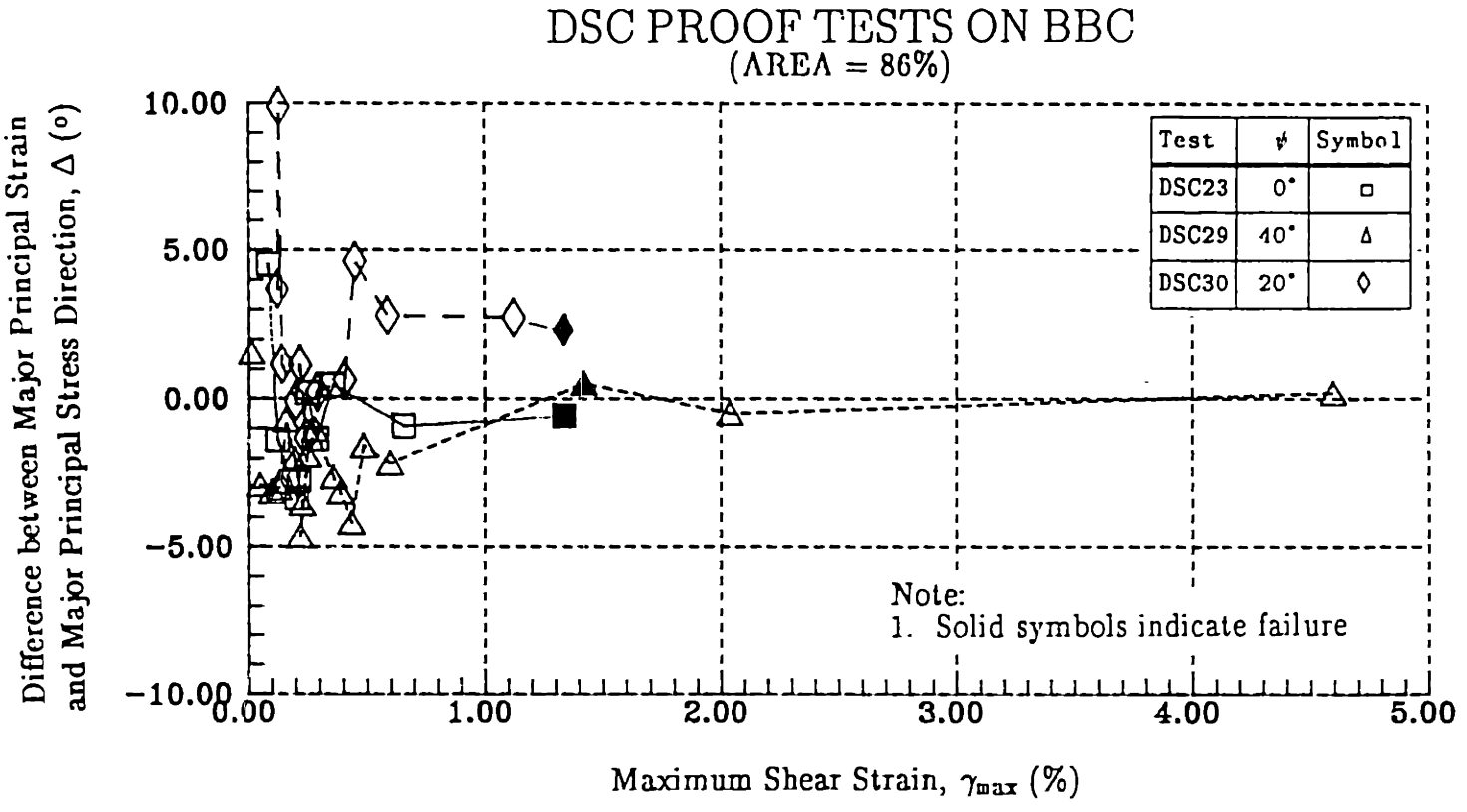

Figure 6.48: Strain–Stress Directions from DSC Proof Tests on OCR=4 BBC (Area No. 1).

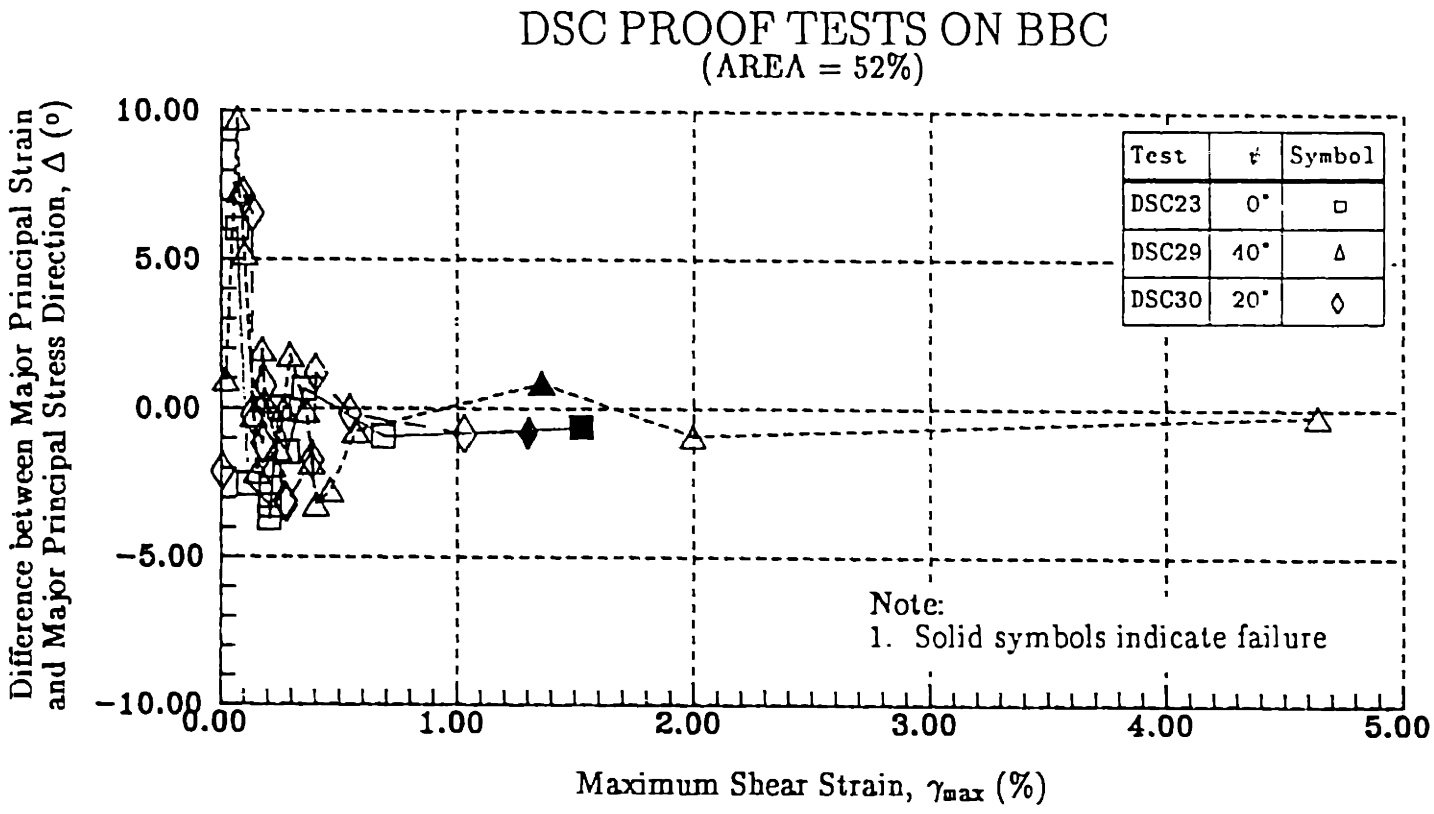

Figure 6.49: Strain–Stress Directions from DSC Proof Tests on OCR=4 BBC (Area No.2).

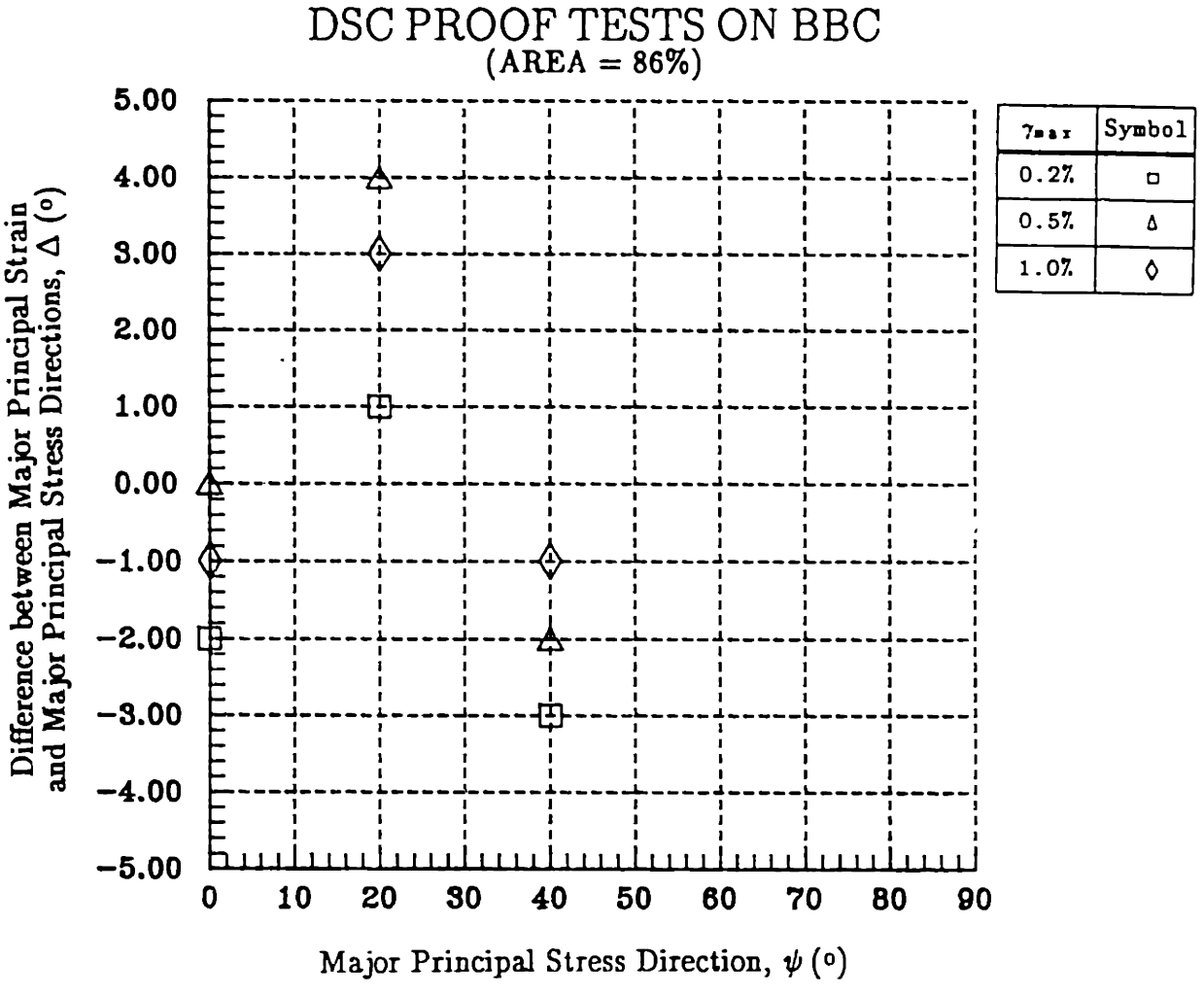

Figure 6.50: Δ versus ψ for Given Shear Strains.

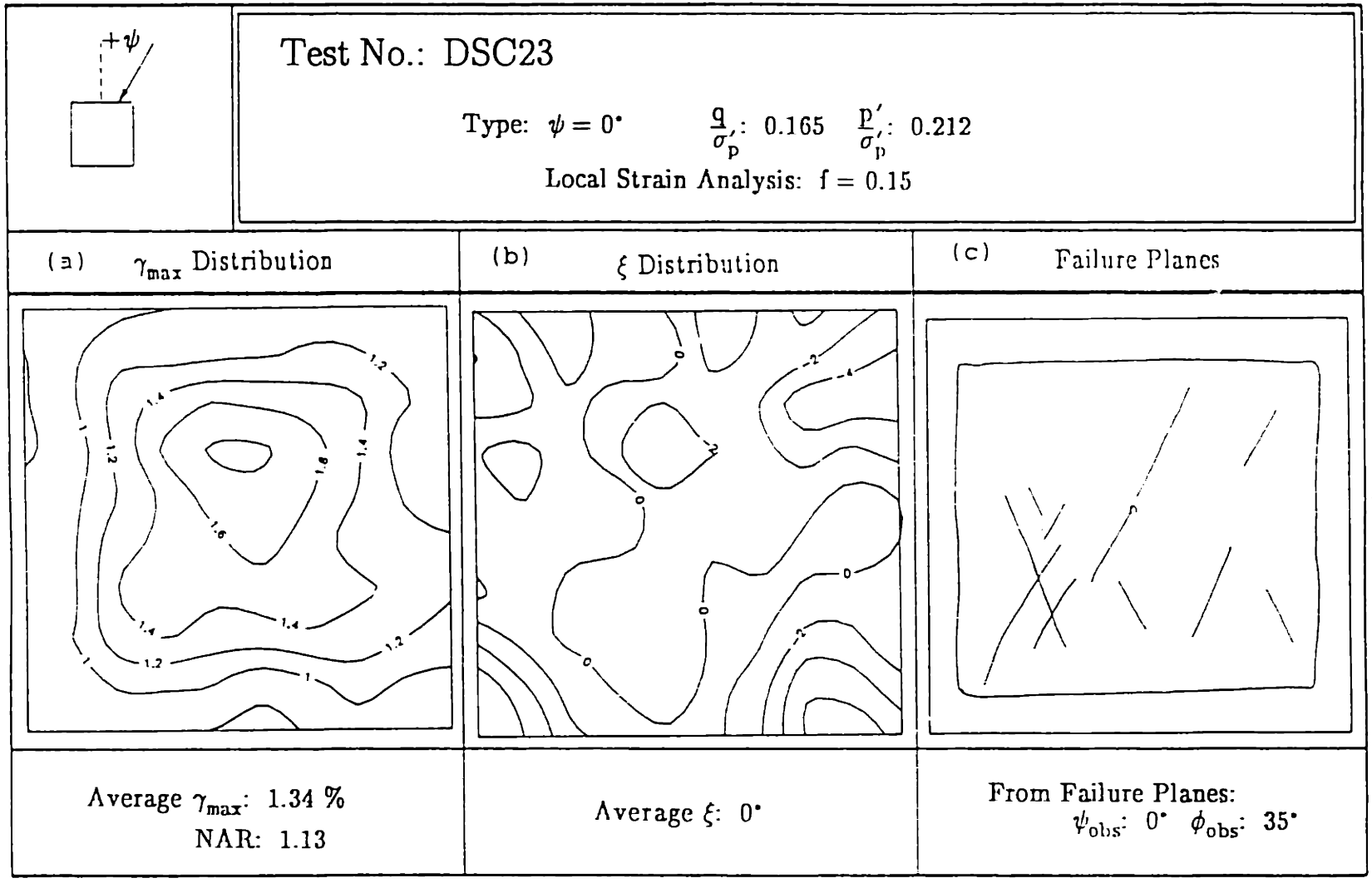

Figure 6.51: γ_{max}, ξ Distributions and Failure Planes for Test DSC23 on BBC.

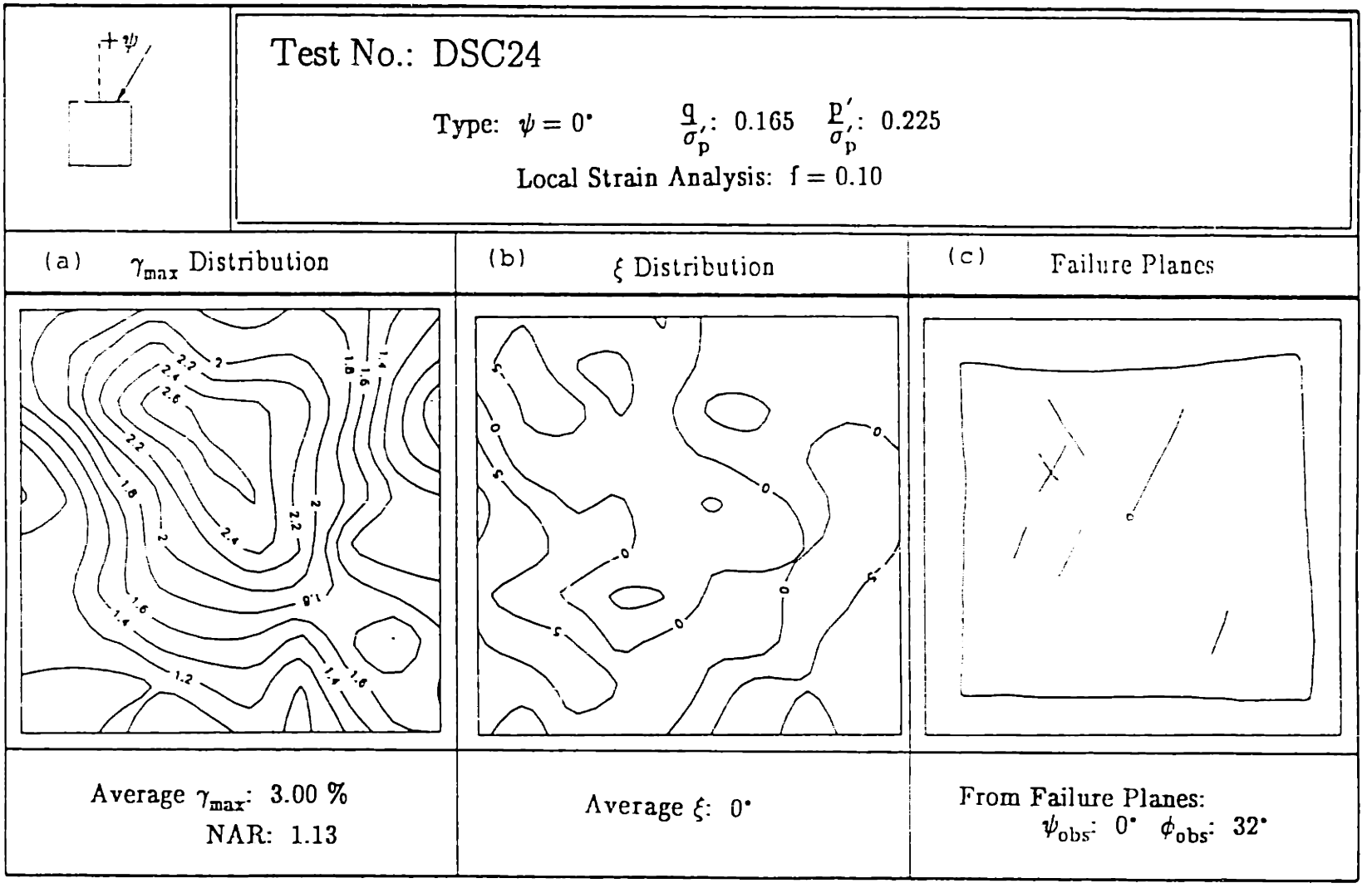

Figure 6.52: γ_{max}, ξ Distributions and Failure Planes for Test DSC24 on BBC.

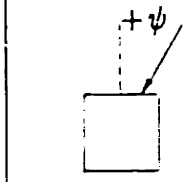

Test No.: DSC25

Type: $\psi = 40°$ $\frac{q}{\sigma'_p}$: 0.153 $\frac{p'}{\sigma'_p}$: 0.219

Local Strain Analysis: f = 0.05

(a) γ_{max} Distribution

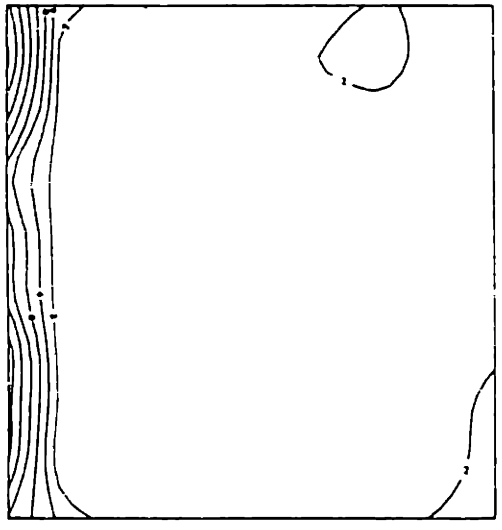

Average γ_{max}: 1.67 %

NAR: 0.41

(b) ξ Distribution

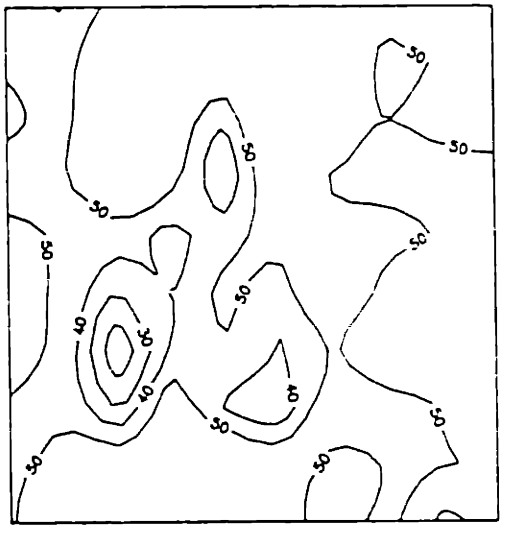

Average ξ: 42°

(c) Failure Planes

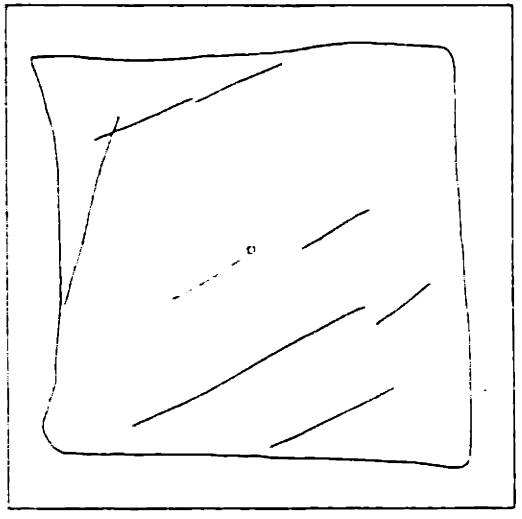

From Failure Planes:

ψ_{obs}: 43° ϕ_{obs}: 38°

Figure 6.53: γ_{max}, ξ Distributions and Failure Planes for Test DSC25 on BBC.

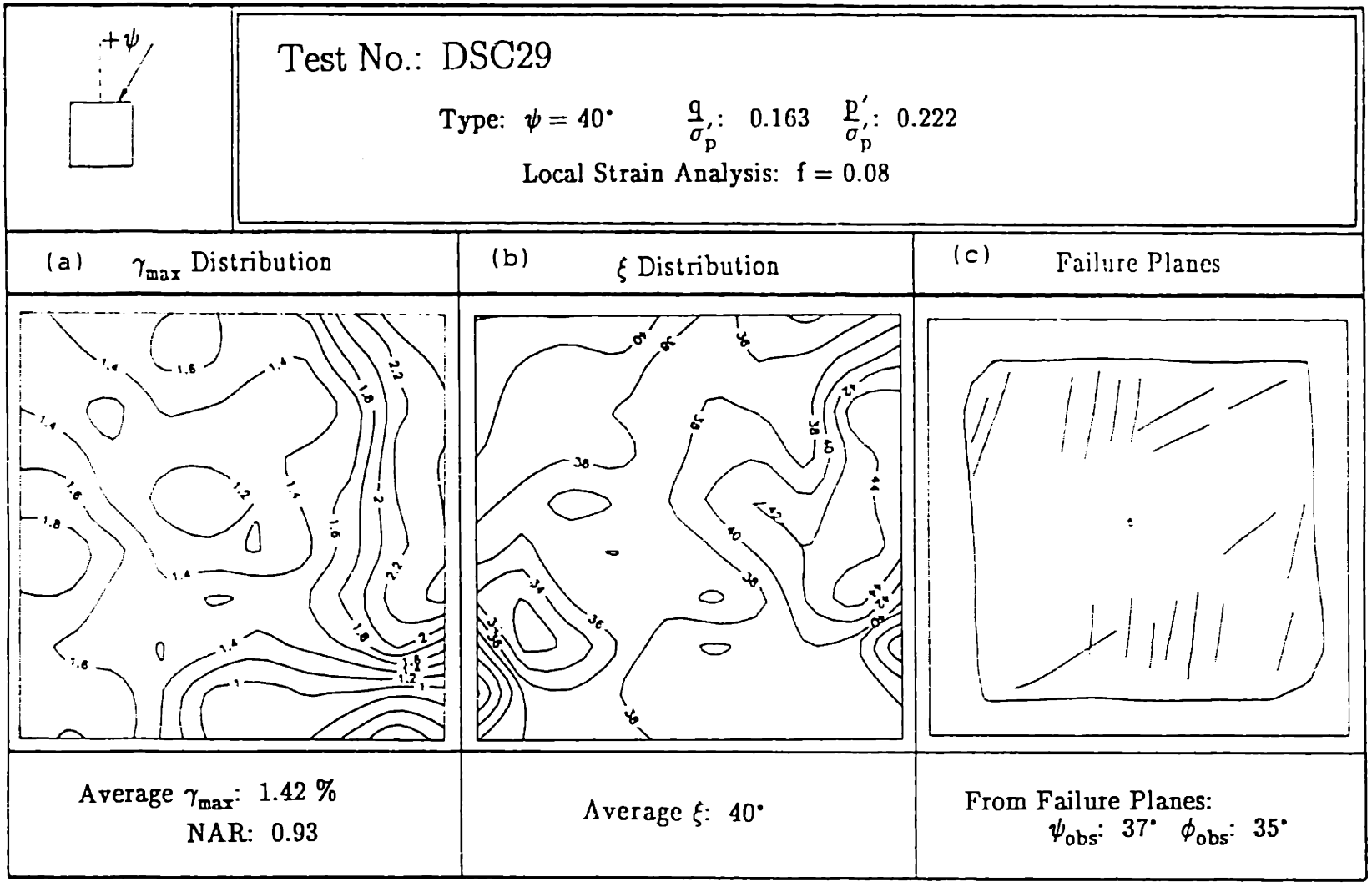

Figure 6.54: γ_{max}, ξ Distributions and Failure Planes for Test DSC29 on BBC.

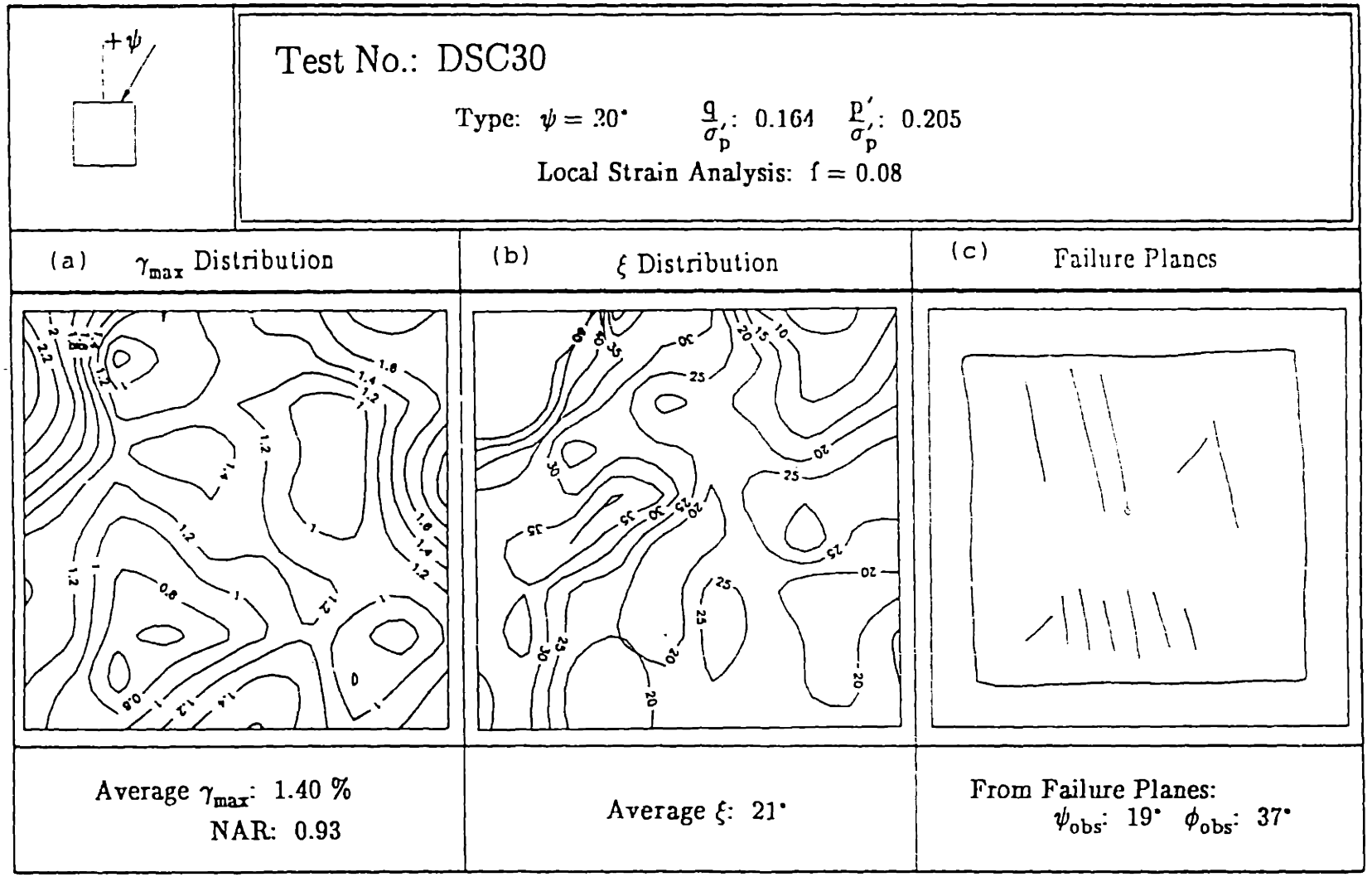

Figure 6.55: γ_{max}, ξ Distributions and Failure Planes for Test DSC30 on BBC.

Final Water Content Distribution of the DSC Sample: DSC23
Top Layer of the Sample
(all values in percent)

40.84	40.66	40.91
41.10	40.81	40.75
40.72	41.15	41.17

Initial Water Content:

w_i = 40.87 ± 1.06 % (2)

Final Water Content:

w_f = 40.90 ± 0.19 % (9)

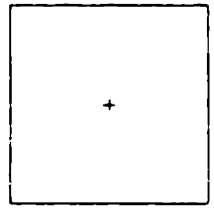

Figure 6.56: Final Water Content Distribution of the Sample from Test DSC23.

Final Water Content Distribution of the DSC Sample: DSC24
Top Layer of the Sample
(all values in percent)

41.05	41.34	41.10
41.52	41.59	41.73
40.83	41.52	41.88

Initial Water Content:

w_i = 41.20 ± 0.26 % (2)

Final Water Content:

w_f = 41.40 ± 0.34 % (9)

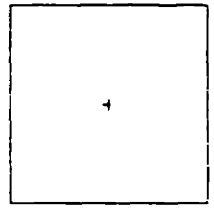

Figure 6.57: Final Water Content Distribution of the Sample from Test DSC24.

Final Water Content Distribution of the DSC Sample: DSC25
Top Layer of the Sample
(all values in percent)

40.32	40.75	40.13
40.17	40.37	40.65
40.35	40.42	40.15

Initial Water Content:

w_i = 40.56 ± 0.53 % (2)

Final Water Content:

w_f = 40.37 ± 0.22 % (9)

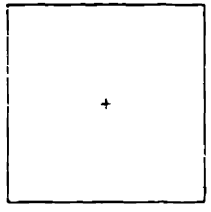

Figure 6.58: Final Water Content Distribution of the Sample from Test DSC25.

Final Water Content Distribution of the DSC Sample: DSC29
Top Layer of the Sample
(all values in percent)

40.56	40.51	40.68
40.61	39.92	40.20
40.94	40.36	40.13

Initial Water Content:

w_i = 40.70 ± 0.21 % (2)

Final Water Content:

w_f = 40.43 ± 0.31 % (9)

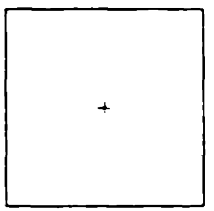

Figure 6.59: Final Water Content Distribution of the Sample from Test DSC29.

Final Water Content Distribution of the DSC Sample: DSC30
Top Layer of the Sample
(all values in percent)

40.81	41.81	40.49
40.84	40.75	40.75
40.34	40.51	41.20

Initial Water Content:

w_i = 40.68 ± 0.10 % (0)

Final Water Content:

w_f = 40.83 ± 0.42 % (0)

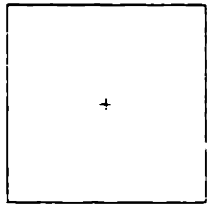

Figure 6.60: Final Water Content Distribution of the Sample from Test DSC30.

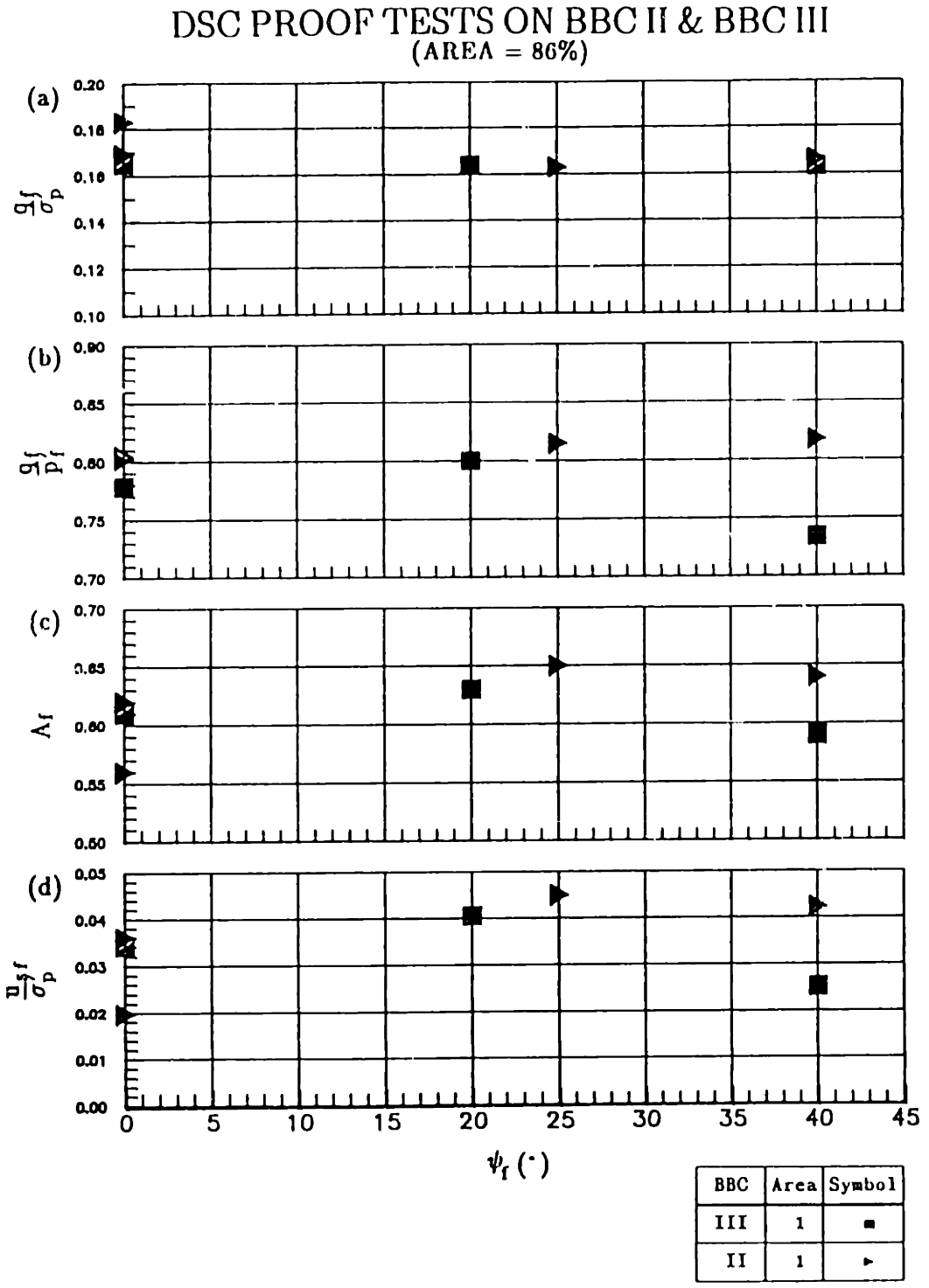

Figure 6.61: Comparisons between DSC Proof Tests on BBC II and BBC III.

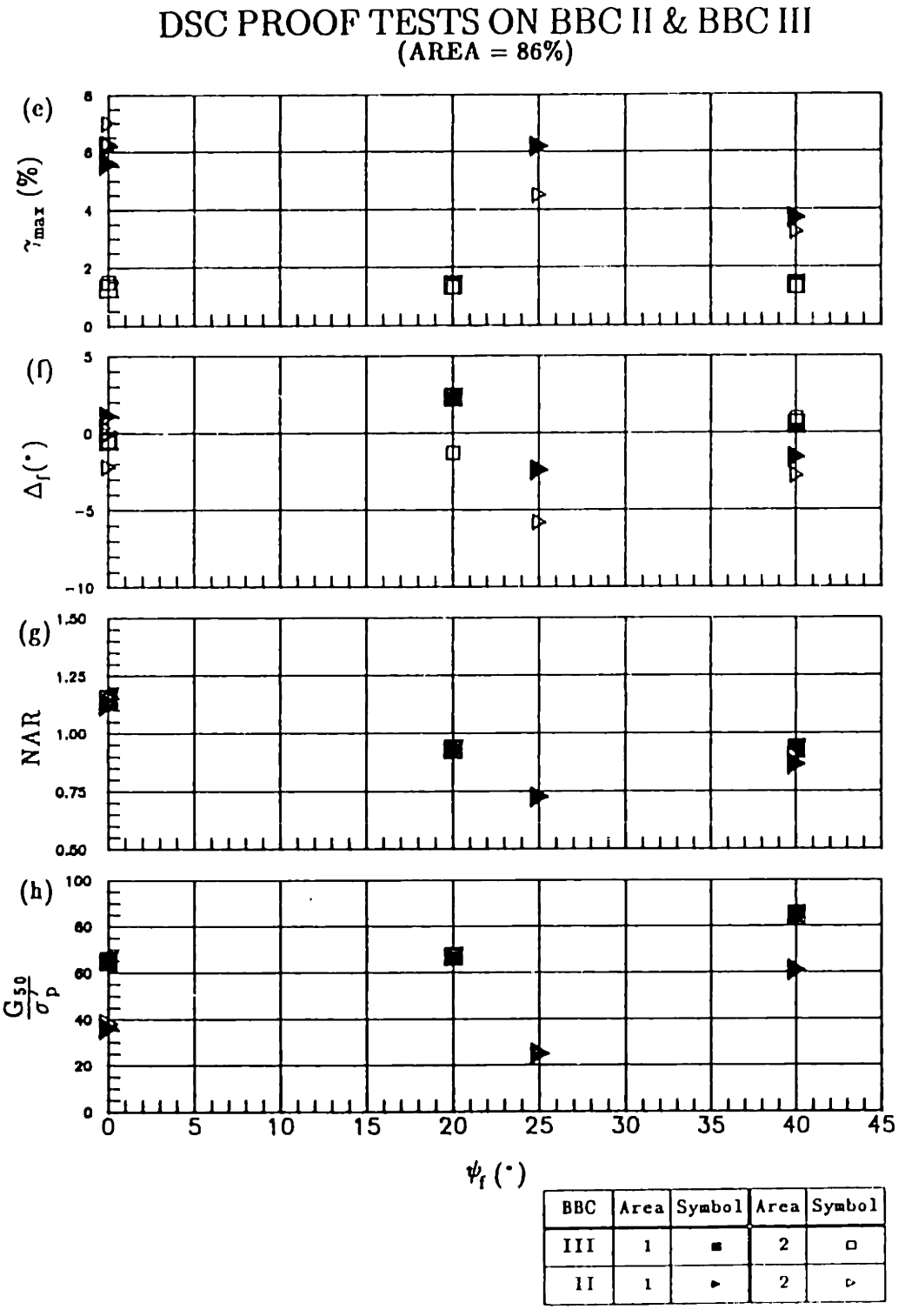

Figure 6.61: (Cont.)

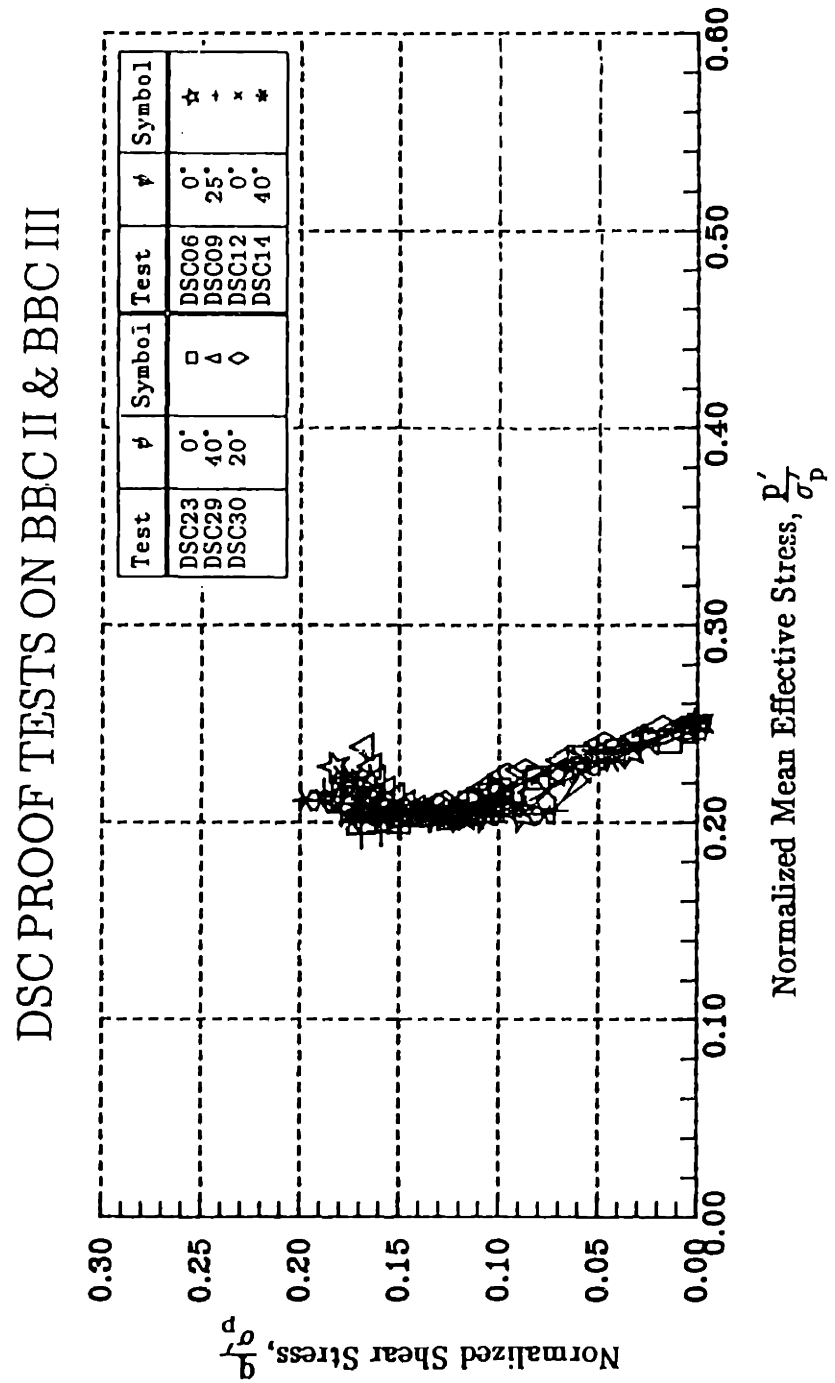

Figure 6.62: Effective Stress Paths from DSC Proof Tests on BBC II and BBC III at OCR=4 (Area No. 1).

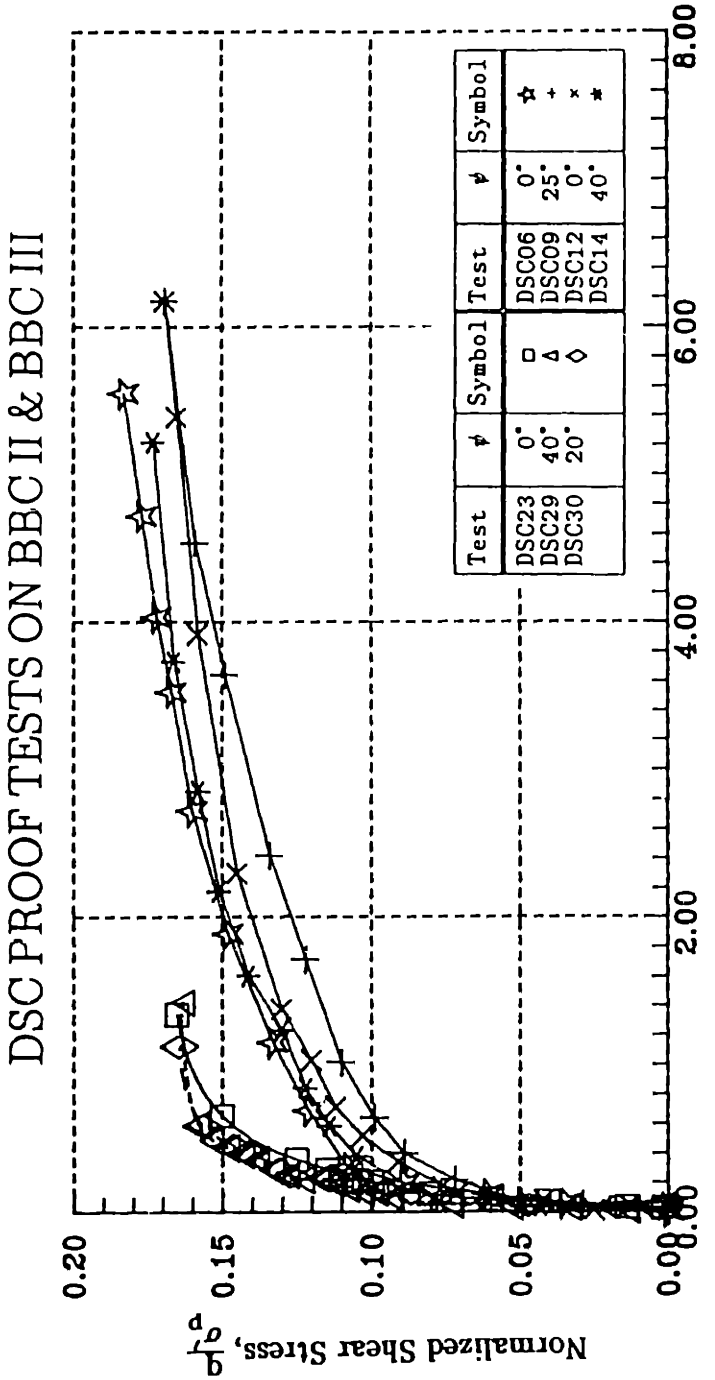

Figure 6.63: Stress–Strain Relationships from DSC Proof Tests on BBC II and BBC III at OCR=4. (Area No. 1).

CHAPTER 7

UNDRAINED STRESS–STRAIN–STRENGTH ANISOTROPY OF RESEDIMENTED BOSTON BLUE CLAY IN THE DIRECTIONAL SHEAR CELL

7.1 INTRODUCTION

An experimental program was conducted for this research with the objective of studying the undrained anisotropic behavior of resedimented Boston Blue Clay (BBC) in the context of rotation of the stress states using the Directional Shear Cell (DSC). An extensive test program has been performed by Germaine (1982) and O'Neill (1985) to investigate the undrained anisotropy of resedimented BBC, but only on overconsolidated BBC at an OCR of 4.

In this study, the clay samples were K_o–consolidated to overconsolidation ratios of either 4 or 1, then subjected to undrained shear until failure at a fixed major principal stress direction (δ) in the case of OCR=4 tests, and at a fixed incremental (applied) major principal stress direction (δ_{inc}) in the case of OCR=1 tests. The main emphasis in this research is to establish the undrained anisotropy for normally consolidated clay. Therefore, the DSC tests on samples at an OCR of 4 were used only for comparison with the previous DSC tests conducted by Germaine and O'Neill.

Section 7.2 describes the test program and the experimental procedure for the tests. For the DSC tests performed at OCR=4, the experimental procedure is essentially identical to that used by Germaine and O'Neill, except that new sets of normal pressure bags with position sensors, also referred to as Type B design, were used. A total of five DSC tests were performed at this OCR. The two of the tests at δ=30° suffered from boundary failures; the results are partially presented in this

chapter. The results of the remaining tests are also compared with the previous DSC tests in terms of the stress–strain–strength relationships. The quality of the tests is evaluated by examining the uniformity of the samples, e.g., using NAR values for each test and strain distributions. The intermediate principal stress was not measured in these tests.

An extensive test program was conducted on normally consolidated BBC in the DSC with fixed incremental major principal stress directions, δ_{inc}. Section 7.4 describes the setup of the tests on normally consolidated BBC, including the type of consolidation stress path, arrangement of the fabric used to separate the shear sheets and the pressure bags, the effect of additional filter strips on the dissipation of pore pressure during consolidation and measurement of the intermediate principal stress. A total of five DSC tests were conducted to study the undrained anisotropic behavior of normally consolidated BBC with δ_{inc} ranging from 0° to 90°. Sample uniformity was evaluated from both a strain analysis and a review of final water contents. For the DSC tests on samples with an OCR of 1, a correction factor was introduced to account for the effects of changes in the intermediate principal stress on deformation of the top rubber membrane (this affected measured values of volumetric strain).

The results of the DSC tests on both overconsolidated and normally consolidated BBC are presented in Sections 7.3 and 7.4, respectively, including the effective stress paths, stress–strain characteristics, stress–strain directions and the effect of intermediate principal stress.

Discussion of the experimental findings is given in Sections 7.4.4 and 7.5.

7.2 TEST PROGRAM

Ten DSC tests were conducted on resedimented Boston Blue Clay to investigate its undrained anisotropic behavior. Five of these tests were performed

at an OCR of 4, and the remaining five tests were carried out at an OCR of 1, as discussed in Sections 7.2.1 and 7.2.2, respectively.

7.2.1 Overconsolidated Resedimented Boston Blue Clay

Five DSC tests were conducted on resedimented BBC III at an OCR of 4 with three different δ directions, namely 0, 30 and 90 degrees. The primary objective in performing these tests was to obtain experimental data to be used as a basis for comparison with the undrained DSC tests conducted by Germaine (1982) and O'Neill (1985) on resedimented BBC II.

The DSC samples were obtained from several batches of resedimented BBC III with the general properties described in Chapter 4. All samples had a preconsolidation pressure (σ'_p) of 1 ksc.

The setup and test procedures are similar to the DSC proof tests on BBC and are summarized in Table 7.1. The samples are obtained from the humid room and trimmed to a 4"x4"x4" cube with the depositional direction clearly marked. Each sample is then enclosed in a sand–coated rubber membrane after the pore water pressure probe has been inserted. The intermediate principal stress was not measured in any of these tests. The detailed step–by–step procedure is given in Chapter 5.

The samples were consolidated in two hydrostatic stress increments, at 0.10 ksc and 0.25 ksc, with a duration of about 24 hours per increment. Once the samples were consolidated, they were ready to be sheared. Undrained shearing is done by increasing the deviatoric stress, $(\sigma_1-\sigma_3)$, in an incremental manner while maintaining zero pore water pressure in the middle of the sample by adjusting the mean stress, $(\frac{\sigma_1+\sigma_3}{2})$. The total stress path of these tests is identical to the effective stress path since the pore water pressure is zero.

Two of the DSC tests, designated as DSC21 and DSC27, were sheared at

δ=0° to check the reproducibility of the results. One DSC test, DSC22, was performed at δ=90°. A combination of these tests provided some basis for comparison with results from previous DSC tests on BBC II. These two types of tests are also referred to as Plane Strain Active (PSA) in the δ=0° case and Plane Strain Passive (PSP) in the δ=90° case. Two other DSC tests (DSC26 and DSC28) were sheared at δ=30°; unfortunately boundary failures were observed in both of these tests due to an interface problem between the sand–coated membrane and the clay. The results are considered unreliable, therefore less emphasis is placed on these tests. Detailed experimental data are presented in Appendix F.

7.2.2 Normally Consolidated Resedimented Boston Blue Clay

The main objective of this research is to establish experimental data on the undrained anisotropy of normally consolidated clay using the DSC. Unlike the DSC tests on clay with an OCR of 4, these samples must be K_o–consolidated to a vertical stress beyond the preconsolidation pressure in order to achieve normally consolidated behavior. During K_o–consolidation, the sample should not experience any lateral strain. Because the time required to compute the strains in a DSC test is at least a day, it is difficult to have a feedback loop that can estimate the horizontal stress (σ'_{hc}) to be applied to maintain zero lateral strain. Therefore, the approach adopted uses a consolidation stress path obtained from the results of a lateral stress oedometer and K_o–consolidation triaxial test performed by Sheahan (1988) on the same material with the same preconsolidation pressure. The results of these tests are discussed in Section 4.5.

A major problem foreseen in the DSC K_o–consolidation process is that the shear sheets used in the test will restrain the boundaries from straining freely. This problem was overcome by introducing a layer of fabric between the shear

sheets and the rubber membrane to reduce the friction between the surfaces during consolidation (see Section 5.4.3 and 5.5 for details). Since the sample is straining in one direction only (i.e., the depositional direction), the fabric was placed only on the two sample faces on which the applied horizontal stress is acting. The sample can slide freely on the top and bottom platens with the help of the silicone grease.

Five undrained DSC tests were performed on resedimented BBC with an OCR of 1. The intermediate principal stress was measured using the intermediate principal stress measuring device as described in Section 3.3. After the sample was K_o–consolidated to the required vertical stress (1.14 to 1.3 ksc), it was sheared at a fixed incremental major principal stress direction, δ_{inc}. Shear tests were conducted at a δ_{inc} of 0°, 45°, 60°, 75° and 90° under undrained conditions.

The setup and consolidation procedures were improved during the course of this investigation through study of a number of new variables. The improvements sometimes required a trial–and–error process to find the optimum procedure. The intermediate setups are described in Section 7.4. The revised setup used in this research is described in Sections 5.4.

7.3 RESULTS OF OVERCONSOLIDATED RESEDIMENTED BOSTON BLUE CLAY

Five DSC tests were conducted on overconsolidated resedimented BBC: tests DSC21, DSC22, DSC26, DSC27 and DSC28. The setups of these tests are summarized in Table 7.1. Two tests (DSC26 and DSC28) performed at δ=30° suffered from boundary slippages at different shear stresses, one (DSC26) at a shear stress of 0.18 ksc and the other (DSC28) at a much earlier stress level (about 0.08 ksc). Plots of strain distributions for these two tests, shown in Figures 7.13 and 7.15, indicate that severe boundary failures had occurred on the two surfaces having the lower normal stress. This problem is similar to the ψ test (DSC25)

performed at 40°. It is caused by poor bonding of the sand particles on the rubber membrane. This problem has been corrected by improving the technique for gluing the sand particles onto the rubber membrane. In fact, all the tests conducted after DSC28 show no sign of boundary failure. Therefore, the success rate in DSC testing is now almost 100 percent.

Failures in these tests are determined in the same manner as for the proof testing by observing the stability of the pore pressure reading and the rate of deformation from the signals of the position sensors on the pressure bags. The results have been confirmed by the existence of failure planes in all the samples tested. Most of the samples show multiple failure planes, oriented in two different directions, from which it is possible to estimate where the major principal stress is acting and the resulting friction angle. These results are tabulated in Table 7.3, with the direction of the major principal stress from this method compared with the prescribed direction of loading. This is discussed further in Section 7.3.4.

The following sections describe the experimental results of the DSC tests, which include the effective stress paths, the stress–strain behavior, strain–stress directions, sample uniformity. These data are summarized in Table 7.2. Note that the intermediate principal stress was not measured in any of these tests.

7.3.1 Effective Stress Paths

Tests DSC21 and DSC27 were performed at δ=0°. The normalized effective stress paths of these two tests are quite similar, as shown in Figure 7.1. The effective mean stress (p′) decreases at first, then increases for shear stresses (q) greater than 0.15 ksc. The effective stress path of DSC22, conducted at δ=90°, is also plotted in Figure 7.1. As seen, anisotropy causes a much lower p′ at higher shear stresses. The results of the two δ=30° tests (DSC26) are considered reliable only before the boundary slippages had taken place. Beyond this the results are

questionable, hence the results are not presented in the figure. One observation in this series of tests is that the initial portions of the effective stress paths for the δ=0° and δ=90° tests are almost vertical, implying the pore water pressure responses were stable. This did not happen in the tests performed by Germaine (1982) and O'Neill (1985).

7.3.2 Shear Stress and Strain Response

Figures 7.2 and 7.3 plot the shear stress–strain relationship for the three "good" tests using two different cross–sectional areas; Area No.1 (86% of the total sample area) and Area No.2 (52% of the total). It is more appropriate to consider the strains from a larger portion of the sample since it better represents the global behavior of the sample. Therefore, Area No.1 is used for most of the comparisons. The stress–strain parameters used in the plots are the normalized shear stress, $\frac{q}{\sigma'_p}$ ($=\frac{\sigma_1-\sigma_3}{2\,\sigma'_p}$), and maximum shear strain, γ_{max} ($=\epsilon_1-\epsilon_3$). The maximum shear strain is used because other strain parameters (e.g., ϵ_1) are affected by factors such as film shrinkage and the Poisson effect of the rubber membrane due to changes in the intermediate principal stress.

For the δ=0° tests, the normalized undrained shear strength ($\frac{q_f}{\sigma'_p}$) at an OCR of 4 is 0.22 at a maximum shear strain, as calculated from Area No.1, of about 1.3%. For the δ=90° test, the sample failed at a normalized undrained shear strength of 0.138. The strain at failure was approximately 10 percent. Figures with stress–strain relationships for different areas are given in Appendix F.

Section 5.3.4 describes the parameter NAR (Normalized Area Ratio), which is directly related to the NRS (Normalized Ring Standard) used by previous research to evaluate sample uniformity. These ratios have proven to be an extremely useful technique. For example, Figure 7.4 presents the NAR values

versus shear strain, where the results show that the NAR value plots below 0.8 at a shear stress of 0.18 ksc for Test DSC26 at δ=30°. This results from boundary slippage causing excessive straining near the boundaries. But the data for shear stresses below 0.18 ksc are still acceptable. In contrast, the NAR values for Test DSC28 with the same δ angle are extremely low, about 0.6 for shear stresses between 0.08 and 0.195 ksc, indicating that the boundary slippage must have occurred at an early stage. This test was abandoned due to its low value of NAR. The NAR values for Tests DSC21 and DSC22 have values greater than unity (about 1.2), meaning that the strains in the middle of the samples are higher. Test DSC27 at δ=0° had the most ideal conditions, with an NAR value close to 1.

A graph of the normalized shear modulus $(\frac{G}{\sigma'_p})$ versus applied shear stress ratio, as shown in Figure 7.5, reveals that the modulus decreases with increasing δ angle. Figure 7.6, a plot of the normalized shear modulus versus the shear strain, indicates that for a given shear strain, the modulus is higher at δ=0° than at δ=90°.

7.3.3 Volumetric Strain Behavior

No volume change should occur during undrained shear. The measured volumetric strain can be influenced by several factors, including: film shrinkage, the Poisson effect of the rubber membrane, and sample non–uniformity in the plane strain direction. Less emphasis has been placed on this parameter in these tests due to lack of critical experimental information, namely the magnitude of the intermediate principal stress.

The volumetric behavior of three tests is shown in Figures 7.7 and 7.8 for the two different cross–sectional areas. The volumetric strain in Test DSC21 decreases (i.e., more expansive) significantly compared to the other two tests. In general, the volumetric expansion was probably caused by non–uniformity of the

samples in the plane strain direction. The samples have a tendency to contract at mid–height and expand in the top and bottom sections. Germaine (1982) encountered the same problem of measuring negative volumetric strain (i.e., sample expansion) and concluded that it was attributable to the bowing of the non–plane strain sides of the samples. This is one of the tradeoffs of measuring strains on only one plane of the samples. Recommendations are given in Chapter 9 which may help to solve this problem.

7.3.4 Directions of Principal Strain and Stress

The difference (Δ angle) in major principal strain and major principal stress directions for two of the three good tests (i.e., at δ=0°, DSC21 and δ=90°, DSC22) was relatively small prior to failure, as shown in Figures 7.9 and 7.10. The other good test (DSC27) has a Δ value of about 2° at failure, partly due to the formation of the rupture surfaces which distort the global strain direction. Because of the inaccuracy in strain measurement at low strain levels (<0.5%), the results are quite scattered in this range. But the results improve for strains between 0.5% and failure.

The Δ value for Test DSC26 (δ=30°) computed from Area No.1 increases from about 0 to 8° at failure as tabulated in Table 7.3. The Δ value calculated from Area No.2 shows a smaller deviation at failure of 3°. The Δ value based on Area No. 2 is considered more reliable for this test because boundary slippage distorted the strain measurement for Area No.1. For Test DSC28 at δ=30°, Δ values at failure are 9° and 4° for Area No.1 and Area No.2, respectively.

Figures 7.11b through 7.15b show the major principal strain direction (ξ) distribution at failure. At low shear stress, the ξ distributions for all the tests are quite scattered due to errors in the strain measurement, therefore the results presented focus on the failure states of the samples. At high stress levels (in this

case at failure), the ξ distributions are much more uniform. Figure 7.11b shows the ξ distribution for Test DSC21 at δ=0°; one of the corners in this test had substantial rotation partly due the occurrence of rupture planes at that location. The ξ distribution for Test DSC22 at δ=90° is shown in Figure 7.12b. The distribution for this test is much better than the previous test because it shows the distribution at a higher strain level of 10 percent, where the error in measurement is less significant. Figure 7.14b presents the ξ distribution for Test DSC27 at δ=0°, which is as scattered as the distribution for Test DSC21, except that no distinct difference appeared at any corners. Figures 7.13b and 7.15b plot the ξ distributions for the two δ=30° tests. The distributions are as scattered as the two tests at δ=0°, with the mean ξ value about 35° to 40° in both cases. The ξ distribution plots do not provide much information because of the scatter. Therefore, an average ξ value from the global analysis is more useful for tests with low strains at failure.

The direction of applied stress can be roughly checked by determining the orientations of the failure planes in the sample. All of the samples had two sets of failure planes as shown in Figures 7.11c to 7.15c. The observed major principal stress direction (δ_{obs}) is assumed to be the angle between the line that bisects the acute angle of the two sets of failure planes and the depositional direction. The results tabulated in Table 7.3 indicate that the δ_{obs} values coincide with the applied δ values in all of the tests. This also implies that even though boundary failures had occurred in the δ=30° tests, the soil samples were "experiencing" the same applied major principal stress direction. The state of stress of the samples may not be affected by the localized boundary failure, therefore the effective stress paths for these tests may still be valid. The results are plotted in Appendix F.2.

7.3.5 Uniformity of Samples

There are three different ways of assessing uniformity of the samples: 1) water content distributions; 2) local strain analysis; and 3) global strain analysis using NAR values.

Once the shearing is completed, the DSC device is dismantled and the test specimen is cut into four layers along the plane of shearing so that the exposed surfaces can be studied. After this is completed, each layer is further divided into nine equal blocks, and the water content of each block is measured. The water content distributions of the top 1–inch layer (i.e., the layer closest to the top platen in the DSC tests) for the three tests are shown in Figures 7.16 to 7.18. The results from these water content distributions show no indication of non–uniformity since they are randomly distributed. The variation found in the measured water content is the same order of magnitude as the error for this technique of measurement. Therefore, this method provides very limited information.

The other two methods of evaluating sample uniformity are based on strain analysis. The local strain analysis provides visual information on the strain distribution by means of contour maps. The strain contour maps at failure for each test are shown in Figures 7.11a to 7.15a. For the two δ=0° tests, the strain distributions are rather non–uniform, partly due the inaccuracy in strain measurements at low strains. Figure 7.11a shows, from the strain distribution for DSC21, that larger strains occurred at one of the corners. The strain distribution for Test DSC27 (see Figure 7.14a) has a more uniform distribution of strain than Test DSC21, but this test also has larger strains at one of the corners. The distribution of strain for the δ=90° (DSC22) test is also non–uniform, with larger strains in the middle of the sample. This is probably caused by non–uniform boundary stress conditions which occurred at these very high strains.

The global strain analysis also provides some information on the uniformity of the samples by comparing the strain for different prescribed areas (NAR values). These results, as shown in Figure 7.4, indicate that the strains are higher in the middle of the samples for two of tests: DSC21 and DSC22. The NAR value for DSC27 is close to unity. The NAR values are also shown for the two tests at δ=30°, these having values of 0.74 and 0.70 at failure. According to the strain distribution standard set by Germaine in earlier DSC tests, Test DSC26 just qualifies to be a reasonable test since the NAR value is within the acceptable range of 1.00±0.26.

7.3.6 Discussion

The undrained strength of BBC decreases with increasing δ angle. The undrained anisotropic strength ratio, K_s, given by the ratio of $\frac{q_f(\delta=90^o)}{\sigma'_p}$ to $\frac{q_f(\delta=0^o)}{\sigma'_p}$, is 0.63 ($=\frac{0.138}{0.220}$).

Figures 7.19 and 7.20 show the relationship between the pore pressure parameter (A) and maximum shear strain for the two cross–sectional areas, 1 and 2. The results show that the A parameter for the δ=90° test increases with the strain from an initial value of 0.55 to 0.75 at failure. On the other hand, the A parameter for the two δ=0° tests show an opposite trend; the A value decreases with increasing strain from an initial value of about 0.6 to a failure value of about 0.40. The results clearly indicate that the A_f value increases with increasing δ. The shear induced pore water pressure (u_s) defined in Section 6.3.2.5 is calculated by assuming σ'_2=0.35 ($\sigma'_1+\sigma'_3$), increases initially, but the u_s value at failure increases with increasing δ angle as shown in Figure 7.21. Figures 7.22 and 7.23 present the stress ratio, ($\frac{q}{p'}$), versus the maximum shear strain. The stress ratio at failure is higher for the δ=0° tests than for the δ=90° test. The plot of strain rate versus applied shear stress level ($\frac{\Delta q}{q_f}$) presented in Figure 7.24 indicates

relatively low rates for all tests, ranging from 0.1%/hr to 1%/hr at applied stress levels below 0.8. Hence, the results confirm that the rates of loading chosen for these tests were appropriate.

The sample uniformity was evaluated by comparing the NAR values for each test (Figure 7.4). The NAR values are greater than unity in tests with the application of differential normal stresses only (i.e., δ=0° and δ=90°). Test DSC26 at δ=30° had much lower NAR values (down to 0.74) due to excessive boundary straining. The NAR values for Test DSC28 failed the strain distribution standard, having a value of about 0.7 at failure. Therefore, this test is considered unreliable.

Two sets of multiple rupture planes were observed in all the tested samples. With σ_1 assumed to be acting between the acute angle of the two sets of rupture planes, the friction angles were estimated from the orientation of these planes. The visibility of failure planes during a test depends on the strain level. Usually, it is difficult to spot the failure planes on a sample at low δ angle since the strain at failure is very small and there is no significant movement of the soil to reveal the rupture surfaces. Generally, in these cases the failure planes can only be identified from a cut sample surface. Failure planes were easily identified from the distortion of the top rubber membrane in the test at δ=90°, which exhibits a much softer behavior. Using data from stresses applied during the tests and failure planes observed after the tests, the results show that the directions of applied σ_1 coincide with the observed σ_1 directions.

7.3.7 Comparison of the New and the Old DSC Results on BBC at OCR=4

The BBC (designated as BBC II) used in previous research exhibited thixotropic behavior. That is, the behavior of the material depends on the storage time. Recompression shear tests performed on this material have to be corrected

for this effect, which sometimes can be very significant. To overcome this problem, a new batch of BBC (referred to as BBC III) was selected. The general properties of this new BBC are presented in Chapter 4. The primary difference, as discussed in Chapter 4, is that BBC III has a lower undrained shear strength at an OCR of 4 based on recompression and SHANSEP triaxial compression tests and some triaxial extension tests. Based on this observation, one would expect the behaviors of the two materials to be different in the plane strain DSC tests at OCR of 4. But the undrained shear strengths at an OCR of 1 for these two series do not differ very much.

Some of the results presented here for the DSC tests on BBC II performed by O'Neill (1985) do not agree with the results in her thesis, partly because of a difference in interpretation between the writer and O'Neill. But most of these differences are not significant and do not affect the global trend of the results.

Table 7.4 summarizes the results for both series of DSC tests on BBC at OCR=4 by Germaine (1982), O'Neill (1985) and this research. Figure 7.25 presents plots of several parameters versus the δ angles at failure for these two materials.

The variation of normalized undrained shear strength ($\frac{q_f}{\sigma'_p}$) with δ angle is presented in Figure 7.25a. The normalized shear strengths for these two materials differ by about 12% at δ=0° and 4% at δ=90°, with BBC III being weaker which is consistent with the above triaxial data. In order to compare the basic profile of the undrained shear strength versus δ angle, an alternative plot is presented in terms of the anisotropy ratio, K_s, which is defined as the ratio of normalized undrained shear strength at a given δ angle to the normalized undrained shear strength at δ=0°, as shown in Figure 7.25b. This plot shows that the profiles of the two series are very similar, with a $K_s(90°)$ value of 0.63 for BBC III and a $K_s(90°)$ value of 0.59 for BBC II. The values of pore pressure parameter, A_f, are

also compared as shown in Figure 7.25c. The A_f values are slightly higher for BBC III by about 0.07. The shear induced pore pressure at failure (Figure 7.25d) shows BBC III with a slightly higher u_s than the tests conducted on BBC II. One of the major differences in these two materials is that the strain at failure is much lower for BBC III at small δ angle (δ<45°), as shown in Figure 7.25e. This difference in strain at failure gives rise to a higher normalized shear modulus ($\frac{G_{50}}{\sigma'_p}$) for BBC III than BBC II at small δ angles (Figure 7.25h). At δ=90°, the strain at failure is almost identical, but the normalized modulus for BBC III is still slightly higher than BBC II. Figure 7.25f presents the Δ_f for different δ tests at failure; the Δ_f angle increases with δ angle to a peak value of about 5° at δ=65° and decreases sharply from δ=65° to δ=90° to a value close to 0°. Limited comparisons can be made between the two series of BBC regarding Δ_f angles because of an insufficient number of DSC tests performed on the BBC III at intermediate δ angles. The two BBC III tests at intermediate angles suffered from boundary failures. Although one of the δ=30° tests satisfied the strain distribution standard, it is still insufficient to make general comparisons about the Δ_f angle. The plot shown in Figure 7.25g, gives the NAR values for all the tests, and was used mainly to evaluate the uniformity of the samples. The NAR for all of these tests are within the acceptable range from 0.74 to 1.26, except for Test DSC28 with δ=30°. Those tests that have NAR values outside this range were disqualified.

In summary, the new BBC III is definitely weaker, and the strain at failure is lower (but only for low δ angle) than BBC II. Also, the normalized shear modulus is higher for BBC III than BBC II. The A_f and the u_s values are only slightly higher for BBC III. Generally though, the differences are not substantial and the basic trend is the same for both materials.

7.4 RESULTS OF NORMALLY CONSOLIDATED RESEDIMENTED BOSTON BLUE CLAY

7.4.1 Introduction and Test Procedure

There are a number of differences between the DSC testing procedures for K_o–normally consolidated clay and that for recompression testing at OCR of 4. These include the number of increments, and the duration, and the introduction of fabric between the shear sheets and the normal pressure bags, applying the minor principal stress (i.e., to reduce the interference from the shear sheets during K_o consolidation).

Five DSC undrained shear tests were conducted on normally consolidated BBC at δ_{inc} angles ranging from 0° to 90° (see Table 7.5). The parameter, δ_{inc}, is defined as the direction of the applied incremental major principal stress relative to the depositional direction during undrained shear (Figure 7.26).

One of the samples was K_o–consolidated to 1.15 ksc and sheared at δ_{inc}=0° (Test DSC34) to a shear strain of 2 to 3%, unloaded back to the initial consolidation stress, and then K_o–consolidated to a vertical stress of 1.3 ksc before it was sheared again at a δ_{inc} angle of 75° (Test DSC35). This was done because of the difficulty both in obtaining and in consolidating test specimens. It is believed that shearing at δ_{inc}=0° did not affect the behavior of the second test since the induced shear strain during first shear was not too large and the sample was reconsolidated to a higher stress.

As mentioned earlier, this was the first attempt to conduct undrained shear tests on normally consolidated clay in the DSC, and therefore no standard procedure for performing the tests existed. Better techniques and procedures have evolved in this research as the testing progressed. Table 7.5 summarizes the differences in the setups of the tests and the consolidation techniques used.

The initial effective stress of the samples was measured using a technique similar to the tests at OCR of 4. That is, the samples were hydrostatically

consolidated to 0.1 ksc and the pore water pressure in the middle of the samples was measured. The pore pressure at this stress is usually negative. The initial effective stress is the absolute sum of the hydrostatic stress and this negative pressure. The resulting effective stresses (values of σ'_s) are summarized in Table 7.11.

Three of the four samples had two pore water pressure probes (DSC31 had only one probe). One of the probes was placed in the middle of the sample and the other was placed midway between one of the corners and the center of the specimen. This provided a check on the distribution of pore pressure in the samples and some verification that the readings were reasonable.

In the first two DSC tests (DSC31 and DSC32), only four strips of filter paper were placed on the vertical edges of the specimens. It was discovered that the duration of consolidation was rather long. In order to speed up the consolidation process, eight more strips of filter paper were added to the remaining eight edges of the sample. These additional filter papers accelerated the consolidation process by a significant amount.

The fabric arrangement was modified during the course of the investigation. In the first three tests, the fabric was pulled out from the top. But in order to reduce the interference of the fabric on the strain measurement, the fabric was later pulled out from the bottom, shown in Figure 7.27.

The primary difference in performing the tests at OCR=1 occurs during the consolidation process. K_0–consolidation is achieved in the DSC by prescribing the vertical stress, σ_{vc}, and one of the horizontal stresses, σ_{hc}. The third stress (i.e., in the plane strain direction) is restrained and therefore has zero or very little lateral strain, as shown in Figure 7.29. Two different methods of applying stress increments were used. Tests DSC31 and DSC32 were performed using Method 1, and the other two samples (tests DSC33 and DSC34) were conducted using

Method 2, as shown in Figure 7.28. Method 1 applies the stresses for an increment in one step, whereas Method 2 divides the load increment into two sub–increments. First a hydrostatic stress is applied for an hour so that the sample can partially consolidate. Then the vertical stress is increased to the desired final stress. Method 2 reduces the adverse effects of undrained shear during consolidation. The fabric used to lubricate the sides of the samples was removed before imposing the last stress increment.

During the tenth consolidation increment of Test DSC32 (i.e., at a vertical stress of 1 ksc), one of the pressure bags was leaking. The sample shifted towards this defective bag, and distorted the rubber membrane. Therefore, the strain measurements for that increment are not reliable. After discovery of the leak, the pressure in the leaking bag was maintained with a constant supply of air from the compressor. This sample was consolidated to a maximum vertical stress of only 1.14 ksc, before it was sheared, to prevent further damage to the bag.

7.4.2 Consolidation Behavior

7.4.2.1 Poisson Effect of Rubber Membrane

The results of first three DSC tests (i.e., Tests DSC31, DSC32 and DSC33) initially indicated that the samples had undergone substantial negative horizontal strains (i.e., the samples expanded laterally in the y direction) as they followed the consolidation stress path A shown in Figure 7.30. It was first believed that the expansion was due to an underestimate of the correct applied horizontal stresses. The consolidation stress path (designated as Stress Path B shown in Figure 7.30) was slightly altered in Test DSC34 in an attempt to reduce this expansion, but results from this test showed a similar magnitude of strain in the horizontal direction.

It was later discovered that the above expansion was caused by the Poisson

effect of the rubber membrane on which the reference points or dots are placed. The increase in the intermediate principal stress causes the rubber membrane to expand, which leads to an increase in both normal strains, ϵ_x and ϵ_z. This obviously affects the horizontal, vertical and volumetric strains. The radial strain of the membrane does not affect the maximum shear strains since the Mohr circle of strain only shifted along the x–axis without altering the size of the circle. The strain due to the Poisson effect of the rubber membrane can be estimated, provided the normal stress in the plane strain direction and the properties of the rubber membrane are known. Fortunately, the normal stresses in the plane strain direction were measured in all tests except for DSC31 (due to a leak in the intermediate principal stress measuring device). The properties of the rubber are described in Appendix E.3. One of the problems encountered in estimating the radial strain was that the clay sample interacts with the sand particles on the rubber membrane, thus restricting the free motion of the membrane, and making the correction procedure rather complicated. A simple approach assumes an equivalent Poisson ratio (μ_r') of 0.25 for the rubber, which takes the effects of this restriction into account. A Poisson ratio of 0.5 would be more reasonable if there were no interaction between the clay sample and the rubber membrane at the top surface. Using a Poisson ratio of 0.25 and a Young's Modulus of 13 ksc for the rubber membrane, the strains in the horizontal direction due to the Poisson effect can be computed.

7.4.2.2 Stress and Strain Behavior

Corrections for the Poisson effect of the rubber membrane were made, as shown in Figures 7.31 to 7.35, and a substantial reduction in the magnitude of the horizontal strain in all tests resulted. In Test DSC34 with consolidation stress path B, the horizontal strain is slightly greater than zero (i.e., compression),

because the applied horizontal stresses are greater than the horizontal stresses at K_o–consolidation. Tables 7.6 to 7.10 summarize the applied and measured stresses and the corrected strains in the consolidation stages for all the tests.

Figures 7.36 to 7.38 present the consolidation curves based on the three corrected strains (i.e., maximum shear strain, vertical (axial) strain and the volumetric strain) identified above for all the tests . The results show that the curves for the tests fall within the limits from the oedometer tests. At vertical stresses less than the preconsolidation pressure the Recompression Ratios (RR) for these tests are close to the lowest limit from the oedometer. This is probably because the larger DSC samples experience less sample disturbance and there is no "seating" problem as in the oedometer tests. Therefore, it is not surprising that the behavior from the DSC tests reveal a stiffer response.

7.4.2.3 Pore Water Pressure Response

The pore pressure parameter B can be computed using the hydrostatic stress increment from 0.1 to 0.25 ksc during the consolidation process. Figure 7.39 shows a typical plot of the B ($=\frac{\Delta u}{\Delta \sigma_{oct}}$) response for the increment, that ends up at a hydrostatic stress of 0.25 ksc. Unlike the previous tests with no σ_2 measurement, this B value is calculated as the change in u over the change in octahedral normal stress, $\Delta\sigma_{oct}$. The B value is essentially equal to unity for most cases. If the change in the mean stress ($\Delta p=\frac{\Delta\sigma_a+\Delta\sigma_b}{2}$) is used, then this gives a lower B ($=\frac{\Delta u}{\Delta p}$) value because $\Delta\sigma_2$ was less than $\Delta\sigma_a=\Delta\sigma_b$.

In Tests DSC31 and DSC32, the pore water pressure dissipated slowly due to poor drainage conditions: filter strips had been placed only on the vertical edges of the samples. In subsequent tests, 12 filter strips were placed along all edges of the samples to improve the drainage conditions. This new technique accelerated the time of consolidation, and hence reduced the total testing time.

Consolidation Method 2 (with two sub–increments shown in Figure 7.28) was used for Tests DSC33 and DSC34, which allows the degree of saturation of the sample to be checked by comparing the change in the octahedral normal stress and the change in the pore water pressure in the middle of the sample. The results show that for most increments the pore pressure parameter B is equal to unity. When two pore water pressure probes were inserted into the sample, the results indicated that the dissipation of pore water pressure is slightly faster for Probe 2 (which is closer to the boundary) than for the probe (Probe 1) in the middle of the sample.

During the removal of the fabric at the end of the next to last increment, the pore water pressures showed a sharp increase of 0.1 ksc in some cases. This was probably caused by a decrease in the spacing between the normal pressure bags and the sample when the fabric is removed. The removal of the fabric may also introduce some shear stress to the sample, which could also cause the sample to experience some change in pore water pressure.

7.4.2.4 Intermediate Principal Stress Response

The intermediate principal stresses for each test were measured using the intermediate principal stress measuring device, except for Test DSC31 due to leakage in the water reservoir of the device during consolidation. Figure 7.40 shows the relationship between the measured intermediate principal stress and the average of the applied normal stresses (p). For vertical stresses less than 1.1 ksc, the intermediate stress is smaller than the applied horizontal stress (see Tables 7.6 to 7.10). The setup of the sample plays a role in this difference, in that there is a gap filled by the silicone grease between the sample and the two platens. This gap will result in a longer time period for the appropriate pressure to build up. The compliance of the intermediate principal stress measuring device can contribute to

this effect too. Similar observations were made in the lateral stress oedometer tests, where the measured horizontal stress in the initial recompression range generally has to be corrected based on the constant K_o value in the normally consolidated range (Dyvik et al, 1985).

Another factor in the intermediate principal stress response occurs when the fabric is removed. The intermediate stress increases, probably due to an increase in the applied horizontal stress when the fabric is pulled away from the pressure bags. Since the sample is on or close to the Virgin Compression line, a small increase in the mean stress can lead to significant deformation. Once the sample deforms, the stresses are redistributed, as evidenced by the sudden increase in intermediate principal stress.

In most tests, the measured intermediate principal stresses reached a value very close to the applied horizontal stresses just before shearing (see Table 7.11).

7.4.2.5 Uniformity of Samples

Figures 7.41 to 7.45 present the shear strain distributions of the samples at the end of consolidation (except for DSC32 which shows the strain distribution at a vertical consolidation stress of 0.878 ksc since the strains for the last two increments were unreliable). The maximum shear strain is chosen because it is not affected by the Poisson effect of the rubber membrane. In Test DSC31, the strains at two opposite corners are higher than the rest of the sample, but the overall uniformity is quite good. Figure 7.42 shows the strain distribution of Test DSC32 at an σ'_{vc} of 0.878 ksc, which indicates that the strain is higher at one of the corners; otherwise, the sample seems to be quite uniform. The strain distributions for Tests DSC33 and DSC34 also had reasonably good uniformity. In Test DSC35, the strain distribution demonstrates significantly higher strains in the middle of the sample; this non–uniformity is the result of the first shearing at $\delta_{inc}=0^{\circ}$.

The NAR values for these tests vary from 0.9 to 1.2 as shown in Figure 7.46. Test DSC31 consistently has NAR values very close to unity throughout the consolidation stage. Even at the final maximum shear strain of 3.7%, the NAR value is essentially equal to 1. The average NAR value for Test DSC32 is about 0.9, which is still better than any undrained shear test performed via the application of differential normal stress only. The final NAR value for Test DSC33 is about 1.1, therefore the strain is slightly higher in the middle than at the boundary of the soil sample. Test DSC34 has relatively good NAR values with a final value equal to 1. The last test (DSC35) has a final NAR value of 1.28, partly due to non–uniformity caused by the first shear at $\delta_{inc}=0^{\circ}$ since the same sample was used in Tests DSC34 and DSC35.

7.4.3 Undrained Shear Behavior

Once the specimen is consolidated to the required vertical stress, it is ready to be sheared. Two important issues have to be considered before the shearing takes place:

1) The amount of grease correction to be applied to the shear sheets. The correction for the grease resistance is determined experimentally, as described in Appendix E, and is expressed as a function of the maximum normal stress. The grease corrections for the tests with σ'_{vc} of 1.15 and 1.3 ksc are about 0.025 and 0.03 ksc respectively.

2) The rate of shearing. It is important to perform the tests at a rate as consistent as possible with that for other high quality CK_oU tests. If the deformation rate is too high, it might create non–uniform pore pressures in the sample. High quality CK_oU triaxial tests use an axial $\dot{\varepsilon}$ of 0.5 to 1.0% per hour. Figure 7.47 shows the strain rates

for the tests versus the applied shear stress ratio ($\frac{\Delta q}{\Delta q_f}$). The demonstrated strain rate is relatively low at low stress ratio, but it increases significantly as the stress ratio approaches 1.

All the samples were sheared to failure at a fixed applied incremental major principal stress direction, δ_{inc}, under undrained conditions. The results of these tests are tabulated in Tables 7.12 through 7.14.

Test DSC31 was sheared at δ_{inc}=90° with a maximum consolidation stress of 1.3 ksc, the shearing condition of this test is also known as plane strain passive. As mentioned earlier there was a leak in the intermediate stress measuring device during this test, but it was fixed just before shearing when the measured intermediate principal stress was only 0.51 ksc. This stress was then increased to the value of the horizontal stress, 0.677 ksc. This adjustment makes the intermediate stress measurement for this test less reliable than other tests.

Test DSC32 was sheared at δ_{inc}=45°. In this test, a different problem was encountered: one of the pressure bags (σ_a) had a leak. Fortunately, the compressor maintained the pressure at a constant value. This sample was consolidated to a vertical stress of only 1.14 ksc because of the potential for the leaking pressure bag to collapse at a higher stress level. At the end of the test, the pressure of the leaking pressure bag was checked by placing the bag on top of the intermediate principal stress measuring device. The measured pressure in the device agreed well with the applied pressure of the bag.

The third test (DSC33) was sheared at δ_{inc}=60°. This test went smoothly compared with the first two tests. The sample was consolidated to a vertical stress of 1.3 ksc before it was subjected to undrained shear.

Tests DSC34 and DSC35 were performed on one sample. The sample was consolidated to a vertical stress of 1.15 ksc, then sheared at δ_{inc}=0° until the peak

shear stress was reached (i.e., plane strain active). The stresses were then reduced to the initial consolidation stress. This was done to hopefully ensure that the strain was not large enough to alter the behavior of the material in the second shear test. To reduce the influence of the effects from the first shear, the sample was further consolidated to a vertical stress of 1.3 ksc before it was sheared at δ_{inc}=75°. One problem was encountered in this δ_{inc}=75° test. Halfway through the test, at γ=0.6%, the camera failed to function properly, leading to a loss of strain data in the latter part of the test. The final strain for this test is estimated from the final geometry of the tested sample, as shown in Figure 7.70c.

"Failure" is based on the stability of the samples at a given increment and the nature of the stress–strain curve. This requires a great deal of experience in DSC testing and a general knowledge of soil behavior. The interpretation of the failure condition depends on the researcher's judgment, therefore no definitive answer exists for this problem.

One very important observation from this testing program is the existence of failure planes in all of the samples. This fact suggests that the samples reached their peak strength. The interpretation of the friction angles and the direction of loading from these failure planes are discussed in Section 7.4.3.5.

The following sections present the undrained shear results of the tests, including effective stress paths, stress–strain relationships, volumetric behaviors (both corrected and uncorrected), and the directions of major principal stress and strain. Values of intermediate stress are also discussed.

7.4.3.1 Effective Stress Paths

The normalized effective stress paths of the five tests are shown in Figure 7.48. The effective stress paths for the δ_{inc}=0° and δ_{inc}=90° tests are typical of plane strain active and passive cases. But the effective stress paths for the other

three tests have unusual shapes, because of the nature of performing the tests with constant δ_{inc}. The friction angles as calculated from the failure values of p'_f and q_f are tabulated in Table 7.14.

Tests DSC32 to DSC35 were conducted with two pore water pressure probes. Figures 7.49 to 7.52 show the pore water pressure readings recorded using data acquisition system during the tests. Note that the pore pressure readings are slightly greater than zero. This is because the time required for the pore pressure to dissipate 100 percent during consolidation is extremely long. Therefore in most tests, shearing started when the pore water pressure decreased to about 0.003 ksc. The results indicate that the pore pressures at the two locations are essentially the same, which also confirms the uniformity of the stress state throughout the samples.

7.4.3.2 Shear Stress and Strain Response

The stress–strain relationships of the tests are presented in Figures 7.53 and 7.54 for different cross–sectional areas (Area No.1 includes 86% of the total cross–sectional area of the sample, and Area No.2 covers 52%). The parameter chosen to represent the stress in the specimen is the normalized maximum shear stress $(\frac{q}{\sigma'_{vc}})$, and the parameter used for strain is the maximum shear strain (γ_{max}). Based on the author's interpretation, the shear strain at failure ranged from 1.9% for the $\delta_{inc}=0^\circ$ test to 9.7% for the $\delta_{inc}=90^\circ$ test. The failure shear strain for Test DSC35 ($\delta_{inc}=75^\circ$) is about 6%, as estimated from the final geometry of the soil sample.

Plots of the normalized shear moduli for the tests are shown in Figures 7.55 and 7.56. The results indicate that the normalized shear modulus falls in a very narrow band in the plot of normalized modulus versus applied shear stress level (Figure 7.55). Figure 7.56 demonstrates that the modulus increases with

increasing δ_{inc} angle for a given strain level. The difference in the modulus for δ_{inc}=60°, 75° and 90° is not very significant.

7.4.3.3 Shear Induced Pore Water Pressure

Since the DSC tests are performed at a constant pore water pressure, the shear induced pore pressure is directly proportional to the change in the octahedral normal stress, $\Delta\sigma_{oct}$. Figure 7.57 shows that normalized shear induced pore water pressure increases with increase in the δ_{inc} angle. The normalized shear induced pore pressure at failure is summarized in Table 7.13, having a maximum value of 0.359 at δ_{inc}=90° and a minimum of 0.096 at δ_{inc}=0°.

7.4.3.4 Volumetric Strain Behavior

Figures 7.58 and 7.59 show the volumetric behavior for all tests without considering the Poisson effect of the rubber membrane. Tests DSC32 and DSC34 experienced some expansion, but the other tests (DSC31 and DSC33) had volumetric strains that were almost zero. From the discussion earlier in this chapter on the Poisson effect of the rubber membrane, corrections should be made if the change in the intermediate principal stress is significant, as was true for all five tests. Note that the σ_2 decreases during undrained shear, in contrast to the behavior during K_0–consolidation. Therefore, the membrane should have contracted. With the corrected volumetric behavior of the tests, as shown in Figures 7.60 and 7.61, all of the samples have apparently undergone some expansion. Since the samples were subjected to undrained shear, there should be no volumetric strain. The only explanation for the apparent change in the volumetric strain is probably due to the non–uniformity of the samples in the four vertical planes.

7.4.3.5 Directions of Principal Strain and Incremental Principal Stress

Figures 7.62 and 7.63 illustrate the changes in the major principal stress direction (δ) and the major principal strain direction (ξ) with strain. Alternative plots are shown in Figures 7.64 and 7.65 to demonstrate the differences between the major principal strain directions and major incremental principal stress directions (Δ_{inc}). The tests at δ_{inc}=0° and 90° (Tests DSC34 and DSC31) have coincidence of the two angular parameters because σ_1 acts in or perpendicular to the axis of the depositional direction. For the intermediate δ_{inc} angle Tests DSC32 and DSC33, the δ angle is always trailing behind the δ_{inc} angle. The ξ direction starts off close to the δ_{inc} direction, but it later moves towards the δ direction; this is due to the "elastic" nature of the material during the initial part of the shearing process. But as the strain increases, the BBC sample behaves like a plastic material, hence it strains in the direction towards the major principal stress direction. Test DSC35 at δ_{inc}=75° was incomplete due to a photographic failure, but for the initial results of strains up to 0.5%, the major principal strain direction also trailed behind the incremental major principal stress direction. The ξ_f angle was estimated from the final geometry of the sample to have a value of 63°, which was between the δ_{incf} and δ_f direction.

Figures 7.66b to 7.70b plot the ξ distributions at failure (except that Test DSC35 is shown for γ=0.5%). Test DSC31 at δ_{inc}=90° had a relatively small variation in ξ direction throughout the sample, except for significant rotation of one of the corners (Figure 7.66b). Figure 7.67b shows the ξ distribution for Test DSC32 at δ_{inc}=45°. This distribution is less than ideal on one face of the sample, where rotation occurred, but the rest of the sample is quite uniform. One of the best ξ distribution plots was at an intermediate δ_{inc}, as shown in Figure 7.68b for Test DSC33. ξ ranges from 40° to 60°, but for the most part, the sample has ξ values between 50° and 55°. The ξ distribution for Test DSC34 at δ_{inc}=0° in

Figure 7.69b shows an overall distribution that is reasonable, except for one face that experienced some rotation. The final plot, as shown in Figure 7.70b, gives the ξ distribution for Test DSC35 at δ_{inc}=75° for a normalized shear stress of 0.12 and a shear strain of 0.53%. ξ varies between 70° and 80°, which is very close to the applied δ_{inc} value of 75° at this small strain level.

As mentioned before, failure planes were found in all the tested samples. The failure planes were oriented in two different directions as shown in Figures 7.66c through 7.70c. Therefore, the direction of σ_1 and the friction angle could be computed. Table 7.14 summarizes the results, which show that the observed σ_1 direction is within a few degrees of the σ_1 direction, as calculated from the applied stresses. The observed friction angles are between 30° and 38°.

7.4.3.6 Intermediate Principal Stress Measurements

Figures 7.71 and 7.72 show the relationship between the relative magnitude of the intermediate principal stress, b, and the maximum shear strain. Tests DSC33 (δ_{inc}=60°), DSC32 (δ_{inc}=45°) and DSC34 (δ_{inc}=0°) had an increase of b from 0 to about 0.27. The b values in Tests DSC31 (δ_{inc}=90°) and DSC35 (δ_{inc}=75°) first decreased with the strain, then increased when the major principal stress direction (δ) was greater than 45° to a final value of 0.7 to 0.8. The normal strains in the plane strain direction, caused primarily by end plate contraction and by the squeezing of the top and bottom rubber membranes, are estimated to have maximum values of about 0.002% at failure. Table 7.12 shows the magnitudes of these estimated strains for the different tests. Although the positive normal strain in the plane strain direction is small, the intermediate principal stress measured presumably is too large, at least for the tests with δ_{inc}=75° and 90°.

7.4.3.7 Uniformity of Samples

Figures 7.66a to 7.70a show the strain distributions of the samples at failure for all tests except Test DSC35 (δ_{inc}=75°), where the strain distribution is at a shear stress of 0.156 ksc and a shear strain of 0.53 %. The strain for Test DSC31 (δ_{inc}=90°) was higher in the middle of the sample, as was the case in the OCR=4 test at δ=90° (DSC22). Test DSC32 (δ_{inc}=45°) had excessive strain at one corner of the sample, which was probably caused by the over–rotation of the shear sheets and backing plates on two adjacent faces. The strain distribution was quite good in Test DSC33 (δ_{inc}=60°), with strain varying from 1.5 to 3.5%. Test DSC34 at δ_{inc}=0° had significantly larger strains in the middle of the sample. The strain distribution for Test DSC35 at a shear stress of 0.156 ksc was relatively uniform with a maximum also in the middle of the soil sample.

The strain distributions for these tests are similar in terms of quality to the tests performed at an OCR of 4.

The NAR is used to evaluate the strains from different cross–sectional areas (for this research Areas No.1 and No.2). The NAR values shown in Figure 7.73 indicate that the strains were consistently higher in the middle of the samples for all the tests except DSC32, which had a NAR value of 1 at failure. The worst case was Test DSC34 at δ_{inc}=0°, where the NAR reached a value of 1.25 at failure. Note that the NAR values for most tests were above unity, which implies that there was no excessive boundary strain, and therefore the surface tractions were properly transmitted through the samples in the intermediate δ_{inc} tests.

Figures 7.74 to 7.76 show the final water content distributions for three of the four samples. Again, there is no clear indication of non–uniformity from these results; in other words, the distribution is random. The volumetric strain of a fully saturated sample is calculated from the water content, and the specific gravity, G_s, equal to 2.785. The calculated volumetric strain distributions are

shown in the same figures. These volumetric strains are either equal to or about 1 percent higher than the total volumetric strains during consolidation. This difference in volumetric strain may be due to swelling of the soil or an error in the assumed value of the effective Poisson ratio of the rubber membrane.

7.4.4 Summary and Discussion

The consolidation results have shown that the technique of consolidation used in this research works relatively well. They also demonstrate the importance of measuring the intermediate principal stress in this type of test so that any apparent radial strain can be computed. It is very difficult to assess the performance of the fabric in terms of reducing the friction between the rubber membrane and the shear sheets. The results from the strain distribution during consolidation have indicated that the samples were reasonably uniform, and that the compression curves for these five tests fall within the limits from oedometer tests on the same material. The pore pressure parameter B is about 1 in all the tests, which further confirmed that the samples were fully saturated.

The undrained shear results on normally consolidated clay show significance stress–strain anisotropy. The normalized undrained strength of the clay varies from a maximum of 0.332 at $\delta_{inc}=0^{\circ}$, to a minimum of 0.164 at $\delta_{inc}=90^{\circ}$ (Figure 7.53). It was found that the normalized modulus increases with the δ_{inc} angle for a given strain level. The normal strain in the plane strain direction was evaluated and found to be very small (<0.002%), but the intermediate principal stress measured is probably different from the plane strain values. Based on the corrected results, the volumetric strain decreases with shear strain, probably because of sample non–uniformity in the plane strain direction. Failure planes were encountered in all the tests, and the measured δ angles from the failure planes were within a few degrees of the applied δ angles. The observed friction angles

were also quite close to the friction angles computed from the applied stresses.

This discussion concentrates on the failure conditions of the samples. Two parameters are frequently used in the discussion; the major principal stress direction at failure (δ_f) and the applied incremental major principal stress direction at failure (δ_{incf}). The major principal stress direction at failure is computed from the total stresses (i.e., vector summation of the initial (K_o) and applied stresses. As a sample is sheared at a fixed intermediate δ_{inc} angle between 0° and 90°, the total major principal stress direction will tend towards the incremental major principal stress direction, δ_{inc}.

Figures 7.77a and 7.77b show the normalized undrained shear strength ($\frac{q_f}{\sigma'_{vc}}$) of the samples versus the δ_f and the δ_{incf} angles. The normalized undrained shear strength decreases with increases in both angles. The anisotropic strength ratio, $K_s(\delta)$, has been redefined as the ratio of the normalized undrained shear strength for a given δ angle to the normalized undrained strength at δ=0°. For δ=90°, the $K_s(90°)$ value is 0.49 ($=\frac{0.164}{0.332}$), which is typical for normally consolidated clay with a K_s of about 0.5.

The relationship between the normalized effective mean stress at failure ($\frac{p'_f}{\sigma'_{vc}}$) and the δ_f angle is shown in Figure 7.78a. Figure 7.78b presents the relationship of $\frac{p'_f}{\sigma'_{vc}}$ and the δ_{incf} angle. The profiles of the two curves are very similar to the undrained shear strength plots shown earlier. Graphs of the friction angle (ϕ) versus δ_f and δ_{incf} angles are shown in Figures 7.80a and 7.80b. The friction angles increase with δ_f and δ_{incf} angles from a value of 32° to a maximum of 35°, but the angles remain constant at δ_f greater than 20°. Since the shear induced pore pressure (u_s) is directly related to the change in octahedral normal stress, the profiles of normalized u_s (as shown in Figures 7.79a and 7.79b) are very similar to those in Figure 7.78.

Figures 7.81a and 7.81b give the relationship of the maximum shear strain

at failure (γ_f) with the two angles, δ_f and δ_{incf}. The strain at failure increases with increase in the δ_f and δ_{incf} angles from a value of 1.9% at δ=0° to a maximum of 9.6% at δ=90°.

The relationship of the difference between major principal stress direction (δ_f) and the incremental major principal stress direction at failure (δ_{incf}) is presented in Figure 7.82. The intermediate δ_f angle (i.e., $0° < \delta_f < 90°$) trails behind the δ_{incf} angle. The relationship between the incremental principal strain direction (ξ_f) versus the major principal stress direction at failure (δ_f) is shown in Figure 7.83, revealing the ξ_f leads the δ_f angle.

Two other interesting relationships are worth noting:

1) the difference in the principal strain–stress direction (Δ_f) and the major principal stress direction at failure (δ_f) (see Figure 7.84); and

2) the difference in the incremental principal strain–stress direction (Δ_{incf}) and the incremental major principal stress direction (δ_{incf}) (see Figure 7.85).

It is incomplete to only compare the stress–strain curves from the relationship of normalized shear stress versus strain. Therefore, an alternative method of presenting the results is shown in Figure 7.86, which uses the normalized applied shear stress ($\frac{\Delta q}{\sigma'_{vc}}$) and the maximum shear strain (γ_{max}). The normalized applied shear stress at failure increases with the δ_f and δ_{incf} angles (see Figures 7.87a and 7.87b).

Figure 7.88 shows the relationship between the measured intermediate principal stress (σ_2) and the average of the other two principal stresses ($\frac{\sigma'_1+\sigma'_3}{2}$). A graph of the relative magnitude of the intermediate principal stress at failure (b_f) versus the major principal stress at failure (δ_f) is shown in Figure 7.89. The profession has frequently assumed that the b_f value for plane strain lies between

0.2 to 0.5 for the entire range of δ_f angles. Experimental results show that b varies from 0.27 to 0.81. As discussed in Appendix E, the DSC test is not a true plane strain condition because the top and bottom platens of the device will bend when a stress is applied on the platens. The intermediate principal stress, as well as the applied normal stresses from the upper and lower faces of the pressure bags in contact with the platens all apply forces to the platens. The magnitude of the deflection at failure, expressed in terms of normal strain, ϵ_2, is estimated in Table 7.12. The value of this strain was estimated to be very small (0.002%). The high b values may be caused by the unloading of the stresses in the platens during shear resulting in higher σ_2.

Figures 7.90a and 7.90b give the relationship between the pore pressure parameter A_f and the δ_f angle at failure. The results indicate that A_f decreases with increasing δ_f angle from 1.286 at δ_f=0° to a minimum of 0.956 at δ_f=35°, but it increases again to a value of 1.085 at δ_f=90°.

A plot of the normalized shear modulus at 50% of the maximum applied shear stress ($\frac{\Delta q}{\Delta q_f}$) versus the δ angle, as presented in Figure 7.91, indicates that the modulus increases with the δ angle, except for the test at δ_{inc}=75°, which has a lower modulus. This is probably caused by the sample being slightly "disturbed" by the first shear at δ_{inc}=0°.

The NAR values at failure for the normally consolidated tests are shown in Figure 7.92. The tests at intermediate δ_{inc} do not suffer from any boundary failures. In fact, the NAR for these tests are very close to unity. The worst case was at δ_{inc}=0°, which had an NAR value of 1.28 at failure.

7.5 DISCUSSION OF THE EFFECT OF ROTATION OF MAJOR PRINCIPAL STRESS DIRECTION ON STRESS–STRAIN–STRENGTH PARAMETERS FOR BOSTON BLUE CLAY

One of the tasks in this discussion is to integrate the experimental results of

the DSC tests on normally consolidated BBC and on overconsolidated BBC at an OCR of 4. The test program conducted on BBC III in this research is inadequate to fully describe the undrained anisotropy at an OCR of 4 because the undrained shear tests were only performed at three δ angles. Therefore, it is necessary to incorporate the DSC data obtained by Germaine (1982) and O'Neill (1985) on BBC II at an OCR of 4. But as discussed in Section 7.3.7, the behavior of the BBC II is slightly different from the new material (BBC III) used in this research. BBC III has a lower undrained shear strength $(\frac{q_f}{\sigma'_p})$ than the previous BBC II at OCR of 4. The normalized undrained shear strength at δ=0° from the DSC test on BBC II with an OCR of 4 was about 0.246, whereas the normalized shear strength for the new material was 0.22. Furthermore, this new BBC has a higher modulus, shear induced pore pressure and A_f than BBC II (Figure 7.25). Still, from the information available the basic trend in the behavior of the materials are the same. Hence, the results from the tests on BBC II can be used for comparison with the DSC tests on normally consolidated BBC III, in terms of the general trend for the two different OCRs. The results obtained from the new DSC tests at OCR of 4 on BBC III can be used for comparison of absolute magnitudes to the normally consolidated DSC tests on the same material.

Figures 7.93 and 7.94 show the same parameters used in the comparison between the OCR=1 tests and the OCR=4 tests. Figure 7.93 presents a comparison of the tests on the same material at different OCRs, primarily used to compare the magnitudes of the parameters. Figure 7.94 reveals the differences between the OCR=1 tests and the OCR=4 tests on BBC II, for a comparison of basic trends at different OCRs. Emphasis is only placed on the results from the same material.

Figure 7.93a gives the normalized shear strength $(\frac{q_f}{\sigma'_p})$ of the new material at different OCRs. The $\frac{q_f}{\sigma'_p}$ values for OCR of 4 are much lower than the values

for an OCR of 1, with a difference of about 50% at δ=0°. But the magnitude of $\frac{q_f}{\sigma'_p}$ at δ=90° for OCR=4 is only about 18% lower than the value OCR=1. The $K_s(90°)$ value for the same material at OCR=4 is 0.63, as shown in Figure 7.93b . This means that K_s increases with OCR, which is also generally observed in sedimentary clays. The normalized undrained shear strength for normally consolidated BBC obtained from recent triaxial compression tests by Sheahan is 0.318±0.008. One triaxial extension test performed on normally consolidated BBC gave a normalized undrained strength of 0.135. The K_s from the triaxial tests of 0.42 is even lower than the results from the DSC tests at an OCR of 1. The profile of the normalized undrained shear strength versus the δ angle, as shown in Figure 7.93a, indicates the same trends at both OCRs. In Figure 7.93b, the K_s value versus δ angle for the two OCRs also indicates very similar profiles. Therefore, we conclude that an increase in OCR will shift the K_s curve upwards in a plot of K_s versus δ angle, which means that $K_s(90°)$ increases with increase in OCR.

Figure 7.93c plots the relationship between A_f and δ for two different OCR from the same material. The A_f value at δ=0° for an OCR of 4 is only 0.3, compared with a A_f value of 1.3 for OCR=1. The A_f values for an OCR of 4 increases with the δ angle. But the A_f values for an OCR of 1 do not change much with δ angle, ranging from 1.3 at δ=0° and 1.1 at δ=90°.

The results from Figure 7.93d show that the normalized u_s increases with increasing δ angles, regardless of the OCR. The magnitude of normalized u_s is about 0.16 higher in the OCR=1 test than for OCR=4 test at δ=0°; the largest deviation is at δ=90° which is about 0.3.

The strain at failure (γ_f) is very similar for both OCRs, as shown in Figure 7.93e, with a minimum value at δ=0° and a maximum value at δ=90°. For BBC III, the γ_f value for OCR=4 is slightly lower than the γ_f for the OCR=1 test.

Figure 7.93f is a plot of Δ_{incf} versus δ_f angles. The Δ_{incf} values are much

higher in the normally consolidated tests, with a maximum of 15° at δ_f=25°. For the tests at OCR=4, the maximum deviation is only 5° at δ_f around 65°. The results show that the overconsolidation ratio can influence the Δ_{incf} angles substantially.

Figure 7.93g presents the NAR values for the two OCRs. The NAR for the OCR of 1 tests are generally quite good, with values greater than unity. For the OCR of 4 tests, due to improper transferred of surface tractions, the NAR values at intermediate δ is less than unity. Therefore, we concluded that better uniformity is achieved in normally consolidated undrained shear tests, partly due to the improvement in the sand coating on the membrane.

Figure 7.93h presents a comparison of the normalized shear modulus (i.e., values normalized to σ'_p) for the different OCRs on the same material. At δ=0°, the normalized shear modulus does not change with OCR, but at δ=90° the modulus at an OCR of 4 is much lower than the modulus at an OCR of 1. The modulus for an OCR of 1 increases with increasing δ angle, whereas the opposite trend occurs for an OCR of 4.

In summary, anisotropy affects the undrained shear strength, the A_f parameter and the shear induced pore pressure more than the other parameters.

Figure 7.95 shows the normalized effective stress paths of three δ=0° DSC tests on BBC III, with two of the tests performed on the same clay at an OCR of 4 and one test performed on clay at an OCR of 1. Figure 7.96 presents the normalized effective stress paths of two δ=90° DSC tests on clay with an OCR of 4 and an OCR of 1.

Table 7.1: Summary of Setup of DSC Tests on OCR=4 Resedimented Boston Blue Clay.

Test Number	Batch Number	δ Angle (°)	Setup (Refer to Table 3.1)			
			Pressure Bag	Corner Design	Shear Sheet	Rubber Membrane
DSC21	200	0	Type B	-	-	No Coating
DSC22	200	90	Type B	-	-	No Coating
DSC26	202	30	Type B	Type C	Type C	Old Sand-Coating
DSC27	203	0	Type B	-	-	No Coating
DSC28	203	30	Type B	Type C	Type C	Old Sand-Coating

Table 7.2: Summary of DSC Undrained Shear Tests on OCR=4 Resedimented Boston Blue Clay III.

Test No.	Batch No.	δ Angle (°)	Shear Sheet	B * value	σ'_s* (ksc)	w_i/w_f (%)	At Failure							$\frac{G_{s0}}{\sigma'_p}$‡	Remarks
							$\frac{q_f}{\sigma'_p}$	$\frac{p'_f}{\sigma'_p}$	A_f	$\frac{\sigma'_{1f}}{\sigma'_{3f}}$	γ_1 ‡ (%)	γ_2 † (%)	$\frac{\gamma_2}{\gamma_1}$		
DSC21	200	0	No	-	-	41.12/ 40.44	0.220	0.295	0.40	6.87	1.40	1.68	1.20	80	
DSC22	200	90	No	0.70	0.12	41.10/ 40.01	0.138	0.191	0.75	6.20	10.15	11.84	1.17	45	
DSC27	203	0	No	0.86	0.12	40.72/ 40.24	0.220	0.297	0.40	6.71	1.23	1.23	0.96	62	
DSC26	202	30	Yes	1.00	0.13	41.06/ 40.68	0.200	0.256	0.51	8.14	2.51	1.86	0.74	53	Bound.Failure @ q/σ'_p=0.18
DSC28	203	30	Yes	0.92	0.13	40.62/ 40.21	0.200	0.263	0.47	7.35	~3.30	~2.30	0.70	77	Bound.Failure @ q/σ'_p=0.08

Notes:

* The pore pressure parameter B is computed from the change in Δu over the change in Δp for a mean stress of 0.1 to 0.25 ksc.
• Initial effective Stress, $\sigma'_s = \sigma_c - u$.
‡ Maximum Shear Strains taken from Area No.1 (86%).
† Maximum Shear Strains taken from Area No.2 (52%).

The preconsolidation pressure σ'_p=1 ksc.

Table 7.3: Summary of Angular Parameters for DSC Undrained Shear Tests on OCR=4 Resedimented Boston Blue Clay at Failure.

Test Number	δ_f from Applied Stress (°)	From Strain Analysis		Δ_{1f} ‡ (°)	Δ_{2f} ‡ (°)	From Failure Planes		Remarks
		ξ_{1f} * (°)	ξ_{2f} * (°)			δ_{obs} (°)	ϕ_{obs} (°)	
DSC21	0.0	-1.6	-2.5	-1.6	-2.5	0	38	
DSC27	0.0	2.6	2.3	2.6	2.3	0	38	
DSC22	90.0	89.7	89.9	-0.3	-0.1	0	35	
DSC26	30.0	37.7	33.1	7.7	3.1	30	30	Bound.Failure @ q/σ'_p=0.18
DSC28	30.0	38.6	34.1	8.6	4.1	30	31	Bound.Failure @ q/σ'_p=0.08

Notes:
* ξ_f is the major principal strain direction at failure.
‡ Δ_f is the difference between the major principal strain direction and the major principal stress direction.

Table 7.4: Summary of All DSC Undrained Shear Tests on OCR=4 Resedimented Boston Blue Clay at Failure.

Test Number	Reference Year (Series)	δ Angle (°)	At Failure								$\frac{G_{sn}}{\sigma'_p}$ ‡	Remarks
			q_f/σ'_p	p'_f/σ'_p	A_f	γ_1 (%) ‡	γ_2 (%) †	γ_2/γ_1	Δ_{1f}, %	Δ_{2f}, %		
DSC01	Germaine 1982 & O'Neill 1985 (BBC II)	0	0.237	0.318	0.36	2.3	2.1	0.91	3.7	4.2	30	
DSC03		0	0.254	0.337	0.33	2.4	2.2	0.92	-0.6	-2.3	32	
DSC15		20	0.225	0.305	0.38	4.0	3.6	0.90	-0.3	1.1	32	
DSC13		40	0.196	0.256	0.48	4.3	3.5	0.78	0.8	1.5	30	
DSC08		65	0.156	0.223	0.59	6.4	6.5	1.02	4.5	6.6	28	
DSC11		75	0.147	0.218	0.61	11.4	9.4	0.88	7.0	5.0	18	
DSC16		75	0.160	0.234	0.55	11.4	13.0	1.14	2.8	4.9	18	
DSC02		90	0.144	0.189	0.71	9.4	11.6	1.23	-0.2	0.1	30	
DSC21	This Research (BBC III)	0	0.220	0.295	0.40	1.4	1.7	1.20	-1.6	-2.5	80	
DSC27		0	0.220	0.297	0.40	1.3	1.2	0.96	2.6	2.3	62	
DSC22		90	0.138	0.191	0.75	10.2	11.9	1.17	-0.3	-0.1	45	
DSC26		30	0.200	0.256	0.51	2.5	1.9	0.74	7.7	3.1	53	B.F. @ q/σ'_p=0.18
DSC28		30	0.200	0.263	0.47	3.3	2.3	0.70	8.6	4.1	77	B.F. @ q/σ'_p=0.08

Notes: ‡ Maximum Shear Strain from Area No.1.
† Maximum Shear Strain from Area No.2.

Table 7.5: Summary of Setup of DSC Tests on Normally Consolidated Resedimented Boston Blue Clay III.

Test No.	Batch No.	δ_{inc} Angle (°)	SETUP		CONSOLIDATION					Remarks
			Number of Filter Strips used	Number of PVP Probes used	Type of Consolidation Stress Path•	Method of Consolid-ation‡	Number of Increments	Fabric remov.at Incr.No.	Fabric pulling from†	
DSC31	205	90	4	1	SP-A	M1	12	11	Top	
DSC32	205	45	4	2	SP-A	M1	11	10	Top	
DSC33	206	60	12	2	SP-A	M2	12	11	Top	
DSC34	206	0	12	2	SP-B	M2	11	10	Bottom	} Same Sample
DSC35		75					12			

Notes:
- • Refer to Figure 7.30.
- ‡ Refer to Figure 7.28.
- † Refer to Figure 7.27.

Table 7.6: DSC Consolidation Stresses and Strains for Test DSC31 (δ_{inc}=90°) on Resedimented Boston Blue Clay III.

Film Number	σ'_{vc} (ksc)	σ'_{hc} (ksc)	σ'_{2c}* (ksc)	ϵ_c* (%)	ϵ_{vol}† (%)	ϵ_a† (%)	γ_{max}† (%)	Remarks
1	0.102	0.100	0.079	0.00	0.00	0.00	0.00	σ_2 leaks
2	0.249	0.244	0.114	0.07	0.12	0.12	0.12	
3	0.301	0.261	0.124	0.09	0.24	0.21	0.18	
4	0.360	0.271	0.135	0.11	0.36	0.35	0.33	
5	0.429	0.290	0.150	0.14	0.49	0.49	0.49	
6	0.520	0.321	0.175	0.18	0.78	0.74	0.69	
7	0.619	0.351	0.205	0.24	0.86	0.89	0.93	
8	0.749	0.401	0.256	0.34	1.71	1.45	1.18	
9	0.879	0.469	0.327	0.48	1.98	1.71	1.44	
10	1.000	0.522	0.406	0.63	2.40	2.11	1.82	
11	1.136	0.595	0.525	0.86	3.26	3.26	3.25	Fabric removed
12	1.300	0.678	-	1.15	4.26	3.97	3.67	Assume $\sigma'_2=\sigma'_{hc}$

Notes: * Based on the results of three DSC consolidation tests.
$\sigma_2=10^{[0.537(\sigma_1+\sigma_3)-1.209]}$ (Figure 7.40)
* Apparent strain due to Poisson effect of the rubber membrane.
Assuming μ_r=0.25 and E_r=13 ksc, $\epsilon_c=1.923 \times \Delta \sigma_2$
† Corrected strains taken from Area No.1 (86%).

Table 7.7: DSC Consolidation Stresses and Strains for Test DSC32 (δ_{inc}=45°) on Resedimented Boston Blue Clay III.

Film Number	σ'_{vc} (ksc)	σ'_{hc} (ksc)	σ'_{2c}* (ksc)	ϵ_c* (%)	ϵ_{vol}‡ (%)	ϵ_a‡ (%)	γ_{max}† (%)	Remarks
1	0.102	0.101	0.116	0.00	0.00	0.00	0.00	
2	0.249	0.246	0.126	0.02	0.07	0.07	0.07	
3	0.302	0.261	0.109	-0.01	0.05	0.11	0.18	
4	0.360	0.271	0.121	0.01	0.28	0.32	0.36	
5	0.428	0.291	0.131	0.03	-	-	-	
6	0.520	0.322	0.157	0.08	0.35	0.45	0.55	
7	0.619	0.352	0.193	0.15	0.56	0.69	0.81	
8	0.748	0.401	0.244	0.25	0.78	0.94	1.10	
9	0.878	0.468	0.319	0.39	1.09	1.24	1.39	
10	1.000	0.522	0.408	0.56	~1.70	~1.70	~1.70	One σ_v bag leaks
11	1.135	0.595	0.595	0.90	3.05	2.95	2.85	

Notes: * Measured Intermediate Principal Stress.
* Assuming μ_r=0.25 and E_r=13 ksc,
ϵ_c=1.923 x Δ σ_2
‡ Corrected strains taken from Area No.1 (86%).
† Maximum Shear Strains taken from Area No.1 (86%).

Table 7.8: DSC Consolidation Stresses and Strains for Test DSC33 (δ_{inc}=60°) on Resedimented Boston Blue Clay III.

Film Number	σ'_{vc} (ksc)	σ'_{hc} (ksc)	σ'_{2c}* (ksc)	ϵ_c* (%)	ϵ_{vol}‡ (%)	ϵ_a‡ (%)	γ_{max}† (%)	Remarks
1	0.101	0.100	0.092	0.00	0.00	0.00	0.00	
2	0.250	0.247	0.138	0.09	0.11	0.12	0.12	
3	0.301	0.261	0.133	0.08	0.04	0.14	0.23	
4	0.361	0.271	0.159	0.13	0.24	0.28	0.32	
5	0.429	0.290	0.182	0.17	0.45	0.44	0.42	
6	0.521	0.321	0.211	0.23	0.59	0.59	0.59	
7	0.619	0.351	0.248	0.30	0.80	0.77	0.74	
8	0.750	0.401	0.304	0.41	1.16	1.08	1.00	
9	0.879	0.468	0.359	0.51	1.50	1.30	1.18	
10	1.000	0.522	0.409	0.61	1.78	1.69	1.60	
11	1.136	0.594	0.472	0.73	2.84	2.77	2.70	Fabric removed
12	1.300	0.677	0.680	1.13	3.30	3.24	3.18	

Notes: * Measured Intermediate Principal Stress.
• Assuming μ_r=0.25 and E_r=13 ksc,
ϵ_2=1.923 x $\Delta\ \sigma_2$
‡ Corrected strains taken from Area No.1 (86%).
† Maximum Shear Strains taken from Area No.1 (86%).

Table 7.9: DSC Consolidation Stresses and Strains for Test DSC34 (δ_{inc}=0°) on Resedimented Boston Blue Clay III.

Film Number	σ'_{vc} (ksc)	σ'_{hc} (ksc)	σ'_{2c}* (ksc)	ϵ_c* (%)	ϵ_{vol}‡ (%)	ϵ_a‡ (%)	γ_{max}† (%)	Remarks
1	0.102	0.100	0.069	0.00	0.00	0.00	0.00	
2	0.249	0.244	0.095	0.05	0.05	C.06	0.07	
3	0.301	0.261	0.091	0.04	-0.02	0.02	0.06	
4	0.360	0.271	0.107	0.07	0.09	0.14	0.15	
5	0.430	0.290	0.132	0.12	0.21	0.24	0.27	
6	0.520	0.321	0.159	0.17	0.40	0.39	0.39	
7	0.620	0.351	0.195	0.24	0.60	0.54	0.48	
8	0.750	0.401	0.234	0.32	0.86	0.81	0.75	
9	0.880	0.469	0.300	0.44	1.22	1.09	0.96	
10	1.000	0.522	0.451	0.73	1.58	1.44	1.30	Fabric removed
11	1.149	0.582	0.561	0.95	2.34	2.02	1.70	Error in σ'_{hc}(↓)

Notes: * Measured Intermediate Principal Stress.
• Assuming μ_r=0.25 and E_r=13 ksc,
ϵ_c=1.923 x Δ σ_2
‡ Corrected strains taken from Area No.1 (86%).
† Maximum Shear Strains taken from Area No.1 (86%).

Table 7.10: DSC Consolidation Stresses and Strains for Test DSC35 (δ_{inc}=75°) on Resedimented Boston Blue Clay III.

Film Number	σ'_{vc} (ksc)	σ'_{hc} (ksc)	σ'_{2c}* (ksc)	ϵ_c* (%)	ϵ_{vol}‡ (%)	ϵ_a‡ (%)	γ_{max}† (%)	Remarks
1	0.102	0.100	0.069	0.00	0.00	0.00	0.00	Same as DSC34
2	0.249	0.244	0.095	0.05	0.05	0.06	0.07	
3	0.301	0.261	0.091	0.04	-0.02	0.02	0.06	
4	0.360	0.271	0.107	0.07	0.09	0.14	0.15	
5	0.430	0.290	0.132	0.12	0.21	0.24	0.27	
6	0.520	0.321	0.159	0.17	0.40	0.39	0.39	
7	0.620	0.351	0.195	0.24	0.60	0.54	0.48	
8	0.750	0.401	0.234	0.32	0.86	0.81	0.75	
9	0.880	0.469	0.300	0.44	1.22	1.09	0.96	
10	1.000	0.522	0.451	0.73	1.58	1.44	1.30	
11	1.149	0.582	0.561	0.95	2.34	2.02	1.70	
12	1.299	0.676	0.676	1.17	2.39	3.24	4.09	

Notes: * Measured Intermediate Principal Stress.
• Assuming μ_r=0.25 and E_r=13 ksc,
$\epsilon_c = 1.923 \times \Delta \sigma_2$
‡ Corrected strains taken from Area No.1 (86%).
† Maximum Shear Strains taken from Area No.1 (86%).

Table 7.11: Summary of DSC Preshear Data on Normally Consolidated Resedimented Boston Blue Clay III at OCR=1.

Test No.	Batch No.	δ_{inc} Angle (°)	Shear Sheet	B* value	σ'_s* (ksc)	w_i (%)	Applied σ'_{vc} (ksc)	Applied σ'_{hc} (ksc)	Meas. σ'_{2c} (ksc)	Appl. K_c ‡	$\frac{\sigma'_{2c}}{\sigma'_{hc}}$	ϵ_{vol} (%)	ϵ_a (%)	Est. ϵ_2 † (%)	Remarks
DSC31	205	90	Yes	~1.00	0.13	40.21	1.300	0.678	-	0.522	-	4.26	3.97	-0.08	Leak in σ_2 device
DSC32	205	45	Yes	~1.00	0.17	40.10	1.135	0.595	0.585	0.524	0.98	3.05	2.95	-0.08	Leak in one Pressure bag
DSC33	206	60	Yes	~1.00	0.15	40.28	1.300	0.677	0.680	0.521	1.00	3.30	3.24	-0.08	
DSC34	206	0	Yes	~1.00	0.16	40.30	1.149	0.582	0.561	0.507	0.96	2.34	2.02	-0.08	} Same Sample
DSC35	203	75	Yes	~1.00	0.16	40.30	1.299	0.676	0.676	0.520	1.00	2.39	3.24	-0.08	

Notes:

* The Pore pressure parameter B is essentially equal to 1.

* Initial effective Stress, $\sigma'_s=\sigma_c-u$.

‡ $K_c=\sigma'_{hc}/\sigma'_{vc}$ see Figure 7.29.

† The normal strain (ϵ_2) in the plane strain direction is calculated from equation E.12. $\epsilon_2=\epsilon_{2p}+\epsilon_{2r}+\epsilon_{2g}$
Assuming E_{rubber}=13 ksc, t_{rubber}=0.02x2cm, H_s=10cm and the change in grease thickness of (0.01-0.05)x2 cm:
$\epsilon_{2p}=\epsilon_{2r}\simeq 0 \Rightarrow \epsilon_2=\epsilon_{2g}$

Table 7.12: Summary of DSC Anisotropic Undrained Shear Tests on Normally Consolidated Resedimented Boston Blue Clay III at Failure.

Test No.	Batch No.	δ_{1nc} Angle (°)	σ'_{vc} (ksc)	w_f (%)	At Failure								G_{sa} / σ'_{vc}	Remarks
					$\frac{q_f}{\sigma'_{vc}}$	$\frac{p'_f}{\sigma'_{vc}}$	A_f [1]	$\frac{\sigma'_{1f}}{\sigma'_{3f}}$	γ_1 [•] (%)	γ_2 [•] (%)	$\frac{\gamma_2}{\gamma_1}$	ϵ_2 [‡] (%)		
DSC34	206	0	1.149	-	0.332	0.619	1.286	3.31	1.86	2.41	1.29	0.000	60	
DSC32	205	45	1.135	37.07 ±0.38	0.295	0.526	1.056	3.56	3.17	3.20	1.01	0.001	60	
DSC33	206	60	1.300	36.18 ±0.55	0.276	0.486	0.956	3.63	~4.0	~4.2	1.05	0.002	74	
DSC35	206	75	1.299	38.34 ±0.29	0.195	0.345	1.076	3.60	~6.0†	-	-	0.002	50	Same Specimen as Test DSC34.
DSC31	205	90	1.300	36.49 ±0.37	0.164	0.288	1.085	3.65	9.62	11.24	1.17	0.002	80	

Notes:

[1] The pore pressure parameter at failure, $A_f = \frac{\Delta u_f - \Delta\sigma'_{3f}}{\Delta\sigma'_{1f} - \Delta\sigma'_{3f}}$

[•] Maximum Shear Strains taken from Area No.1 (86%).

[•] Maximum Shear Strains taken from Area No.2 (52%).

[‡] The normal strain (ϵ_2) in the plane strain direction is calculated from equation E.12. $\epsilon_2 = \epsilon_{2p} + \epsilon_{2r} + \epsilon_{2g}$
Assuming E_{rubber}=13 ksc, t_{rubber}=0.02x2cm, H_s=10cm and the change in grease thickness of 0 cm
$\epsilon_{2g}=0 \Rightarrow \epsilon_2 = \epsilon_{2p} + \epsilon_{2r}$

[†] Strain computed from the geometry of the sample at the end of the test:
ϵ_x=-2.14%; ϵ_y=2.10% and ϵ_{xy}=2.18%.

Table 7.13: Summary of DSC Anisotropic Undrained Shear Tests on Normally Consolidated Resedimented Boston Blue Clay III at Failure.

Test Number	δ_{inc} Angle (°)	δ_f Angle (°)	σ'_{vc} (ksc)	σ'_{hc} (ksc)	σ'_{2c} (ksc)	σ'_{1f} (ksc)	σ'_{3f} (ksc)	σ'_{2f} (ksc)	b_f •	$\frac{u_{sf}}{\sigma'_{vc}}$ ‡	$\frac{\Delta q_f}{\sigma'_{vc}}$ †	$\frac{\Delta p'_f}{\sigma'_{vc}}$ •
DSC34	0	0	1.149	0.582	0.561	1.093	0.330	0.538	0.27	0.096	0.085	-0.154
DSC32	45	18	1.135	0.595	0.587	0.932	0.162	0.436	0.26	0.202	0.172	-0.217
DSC33	60	36	1.300	0.677	0.678	0.991	0.273	0.474	0.28	0.235	0.300	-0.356
DSC35	75	56	1.299	0.676	0.676	0.701	0.195	0.535	0.67	0.313	0.362	-0.540
DSC31	90	90	1.300	0.678	0.677	0.588	0.161	0.506	0.81	0.359	0.404	-0.614

Notes:

- • The relative magnitude of intermediate principal stress at failure, $b_f = \frac{\sigma'_{2f} - \sigma'_{3f}}{\sigma'_{1f} - \sigma'_{3f}}$.
- ‡ Normalized Shear Induced Pore Pressure at failure, $\frac{u_{sf}}{\sigma'_{vc}} = -\Delta\sigma_{oct}$.
- † Normalized Applied Shear Stress, $\frac{\Delta q_f}{\sigma'_{vc}} = \frac{\Delta\sigma'_{1f} - \Delta\sigma'_{3f}}{2\,\sigma'_{vc}}$
- • Normalized Incremental Mean Stress, $\frac{\Delta p'_f}{\sigma'_{vc}} = \frac{\Delta\sigma'_{1f} + \Delta\sigma'_{3f}}{2\,\sigma'_{vc}}$

Table 7.14: Summary of Angular Parameters for DSC ndrained Shear Tests on Normally Consolidated Boston Blue Clay III at Failure.

Test Number	Stress Analysis			Strain Analysis		Δ_{1incf} ‡	Δ_{2incf} ‡	Δ_{1f} †	Δ_{2f} †	Failure Planes		Remarks
	δ_{incf} (°)	δ_f (°)	ϕ_f (°)	ζ_{1f} * (°)	ζ_{2f} * (°)	(°)	(°)	(°)	(°)	δ_{obs} (°)	ϕ_{obs} (°)	
DSC34	0	0.0	32.4	0.1	0.1	0.1	0.1	0.1	0.1	-	-	
DSC32	45	18.0	34.1	33.3	32.7	-11.7	-12.3	15.3	14.7	15	32	
DSC33	60	35.6	34.6	49.8	49.1	-10.2	-10.9	14.2	13.5	33	32	
DSC35	75	55.9	34.4	~63	-	-12	-	7.1	-	58	38	Same Specimen as Test DSC34.
DSC31	90	90.0	34.7	91.5	91.5	1.5	1.5	1.5	1.5	0	30	

* ζ_f is the major principal strain direction at failure.

‡ Δ_{incf} is the difference between the major principal strain and the incremental major principal stress directions at failure.

† Δ_f is the difference between the major principal strain and the major principal stress directions at failure.

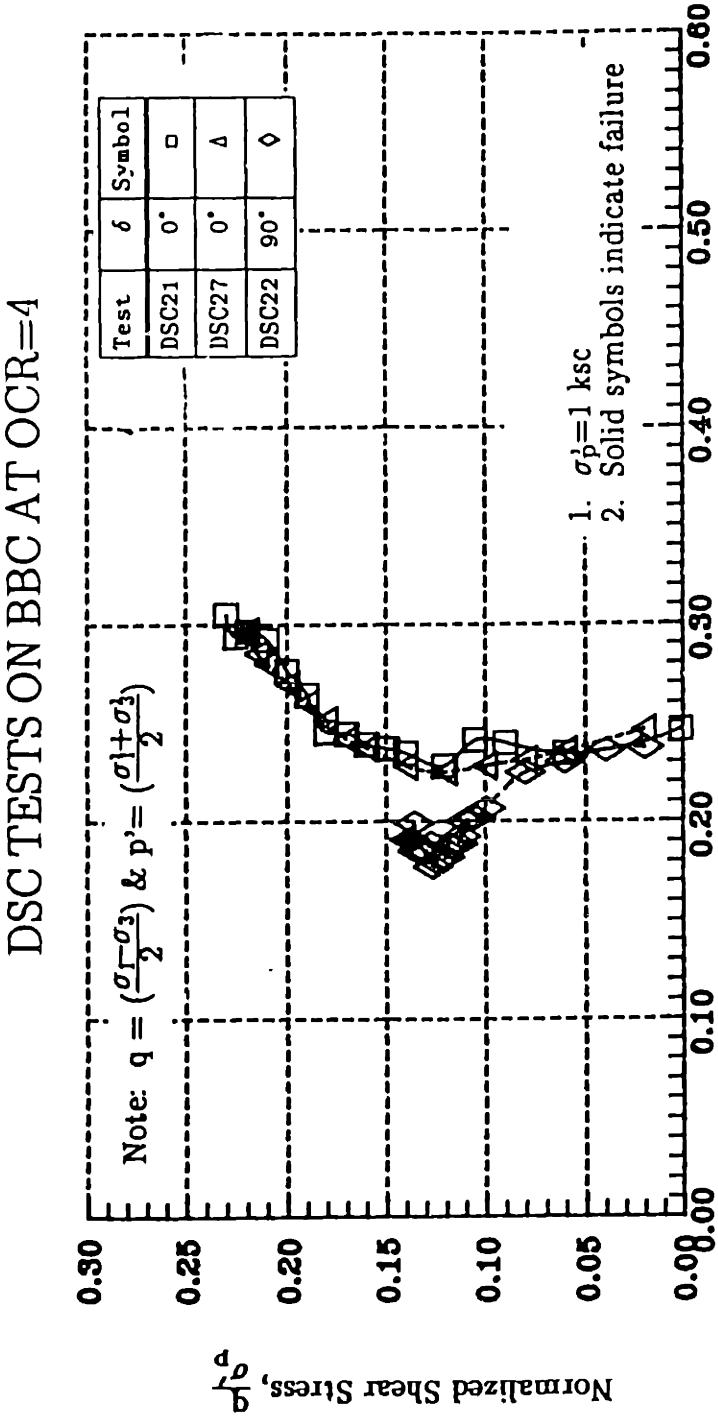

Figure 7.1: Effective Stress Paths from DSC Tests on BBC at OCR=4.

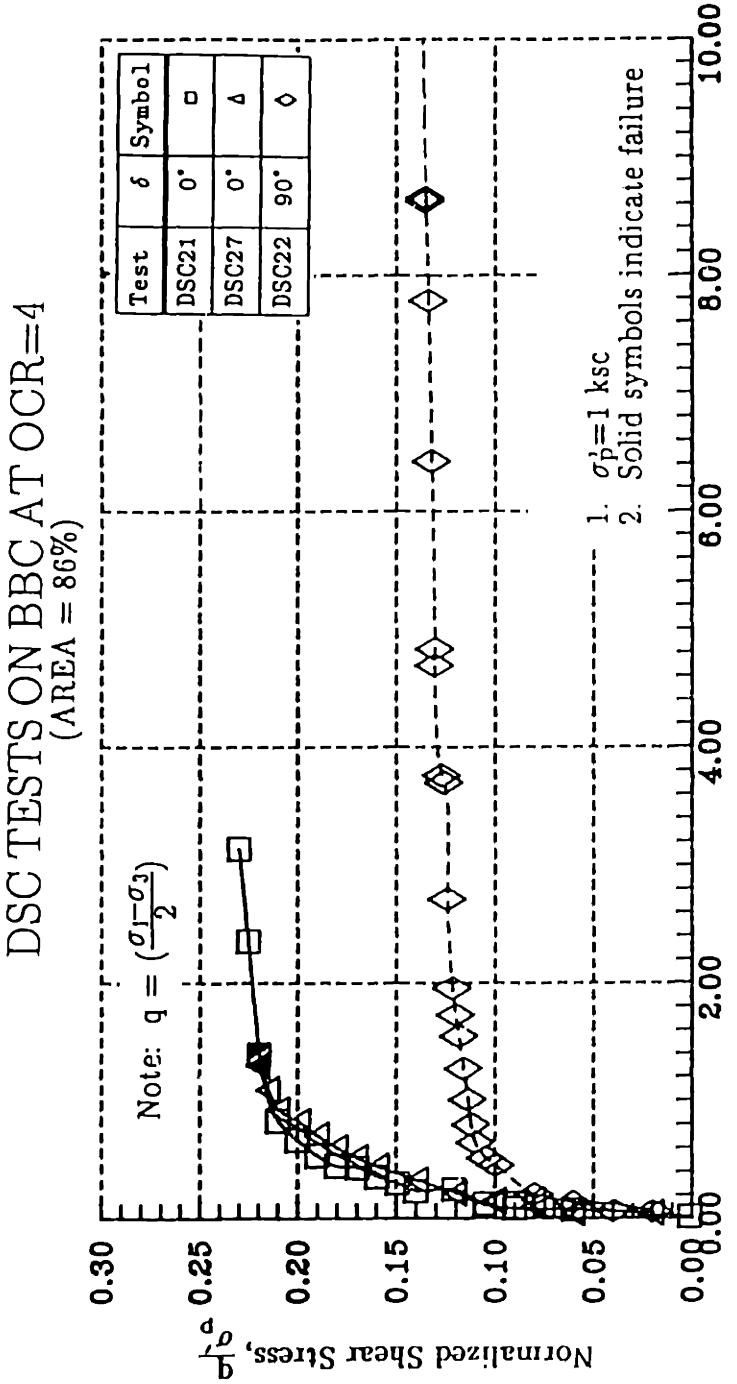

Figure 7.2a: Stress–Strain Relationships from DSC Tests on OCR=4 BBC (Area No. 1).

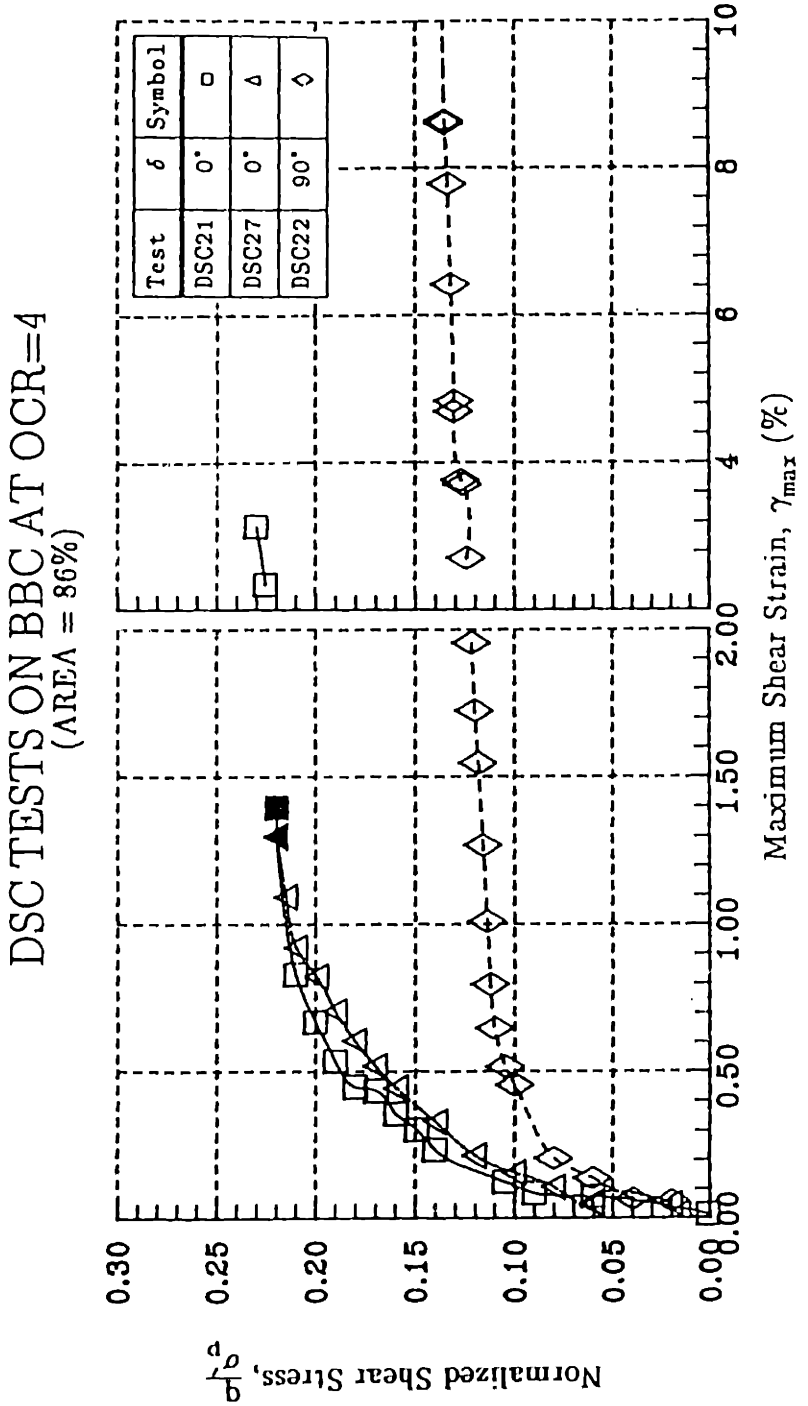

Figure 7.2b: Stress–Strain Relationships from DSC Tests on OCR=4 BBC (Area No. 1).

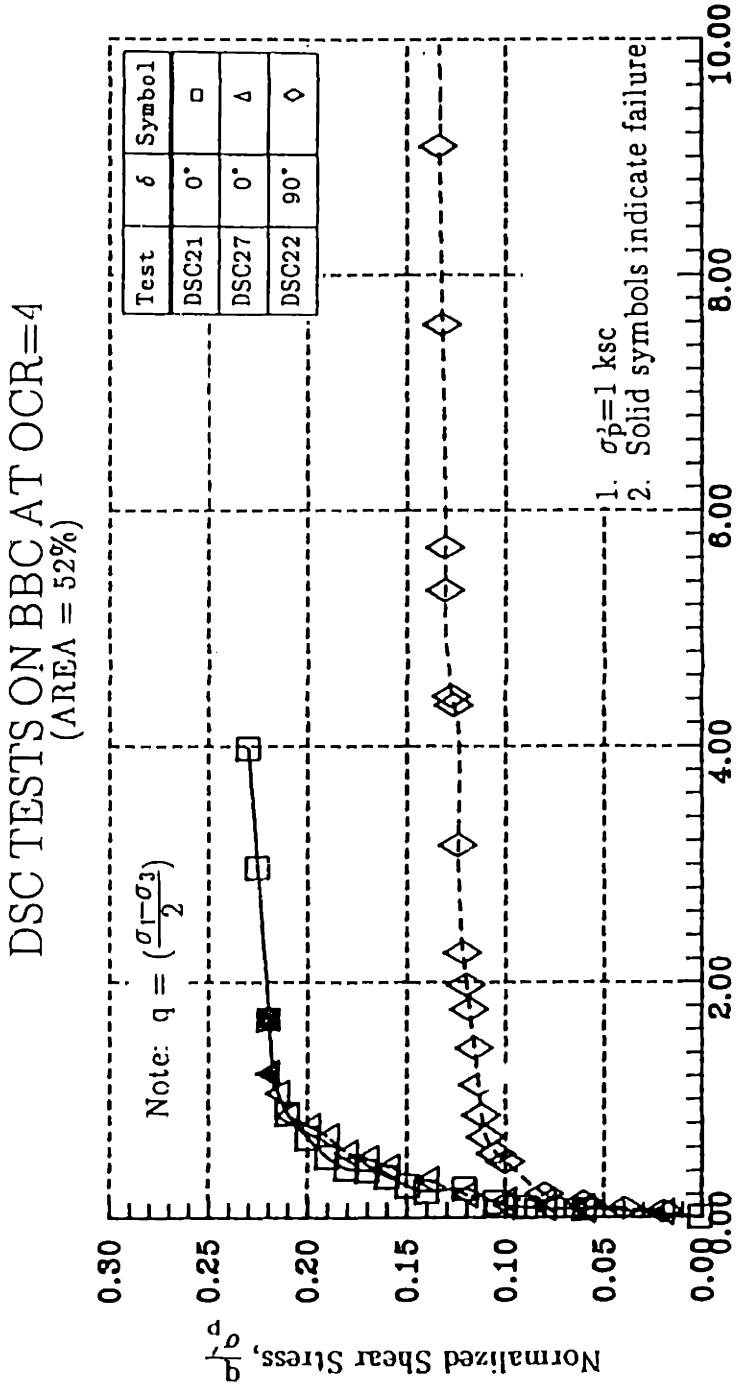

Figure 7.3: Stress–Strain Relationships from DSC Tests on OCR=4 BBC (Area No. 2).

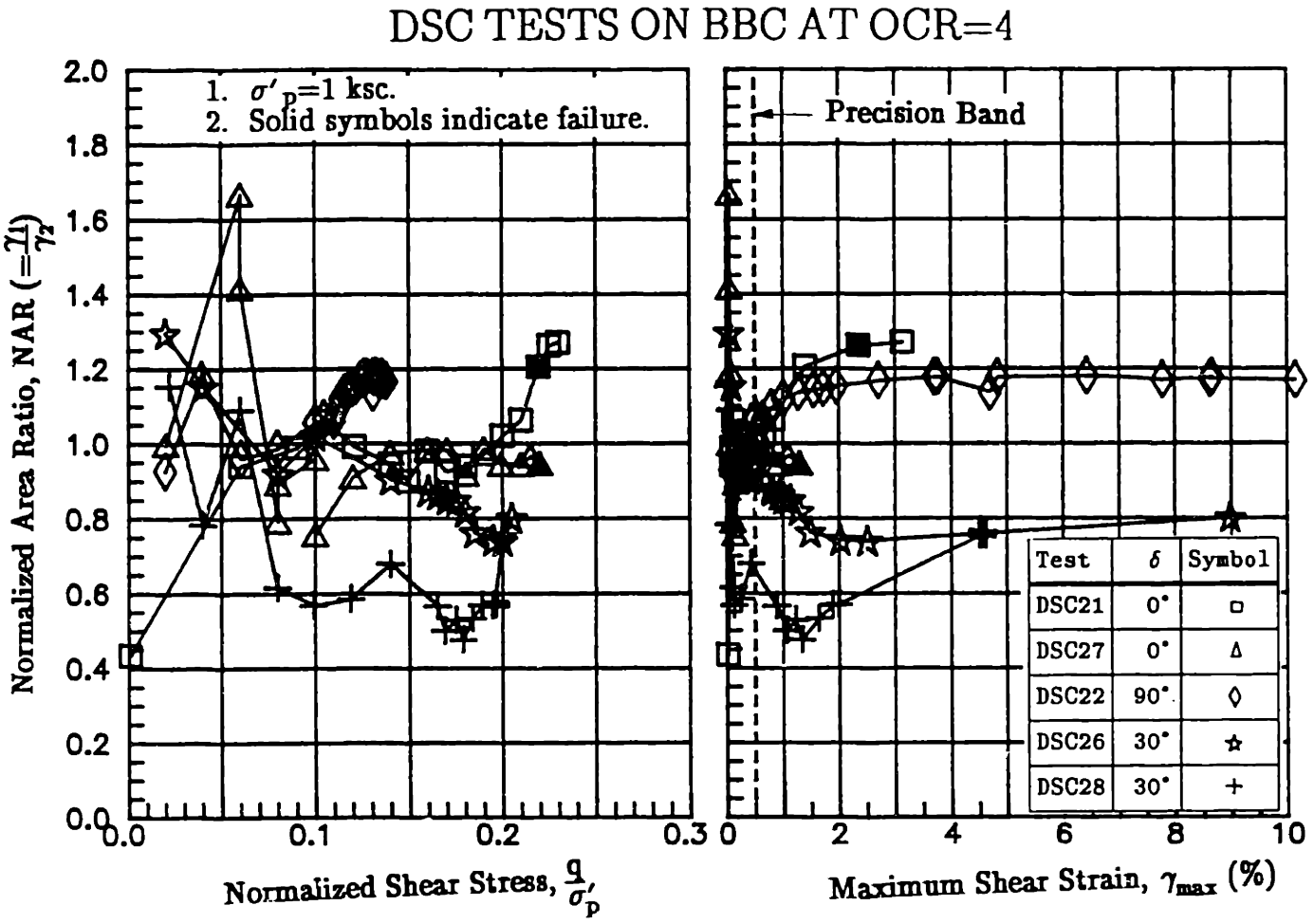

Figure 7.4: Variation of NAR with (a) Normalized Shear Stress and with (b) Maximum Shear Strain from DSC Tests on OCR=4 BBC.

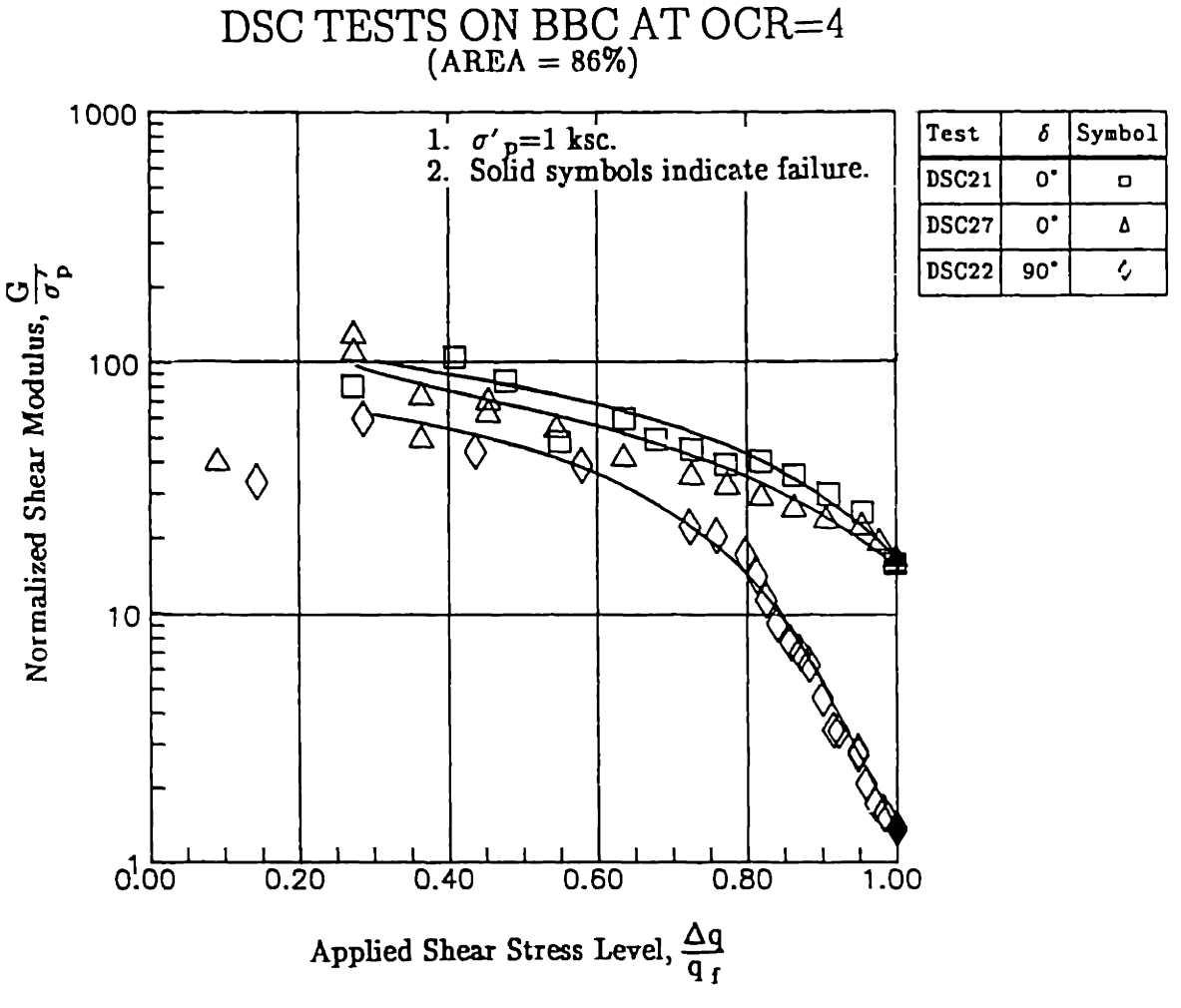

Figure 7.5: Normalized Shear Modulus versus Applied Shear Stress Level from DSC Tests on OCR=4 BBC.

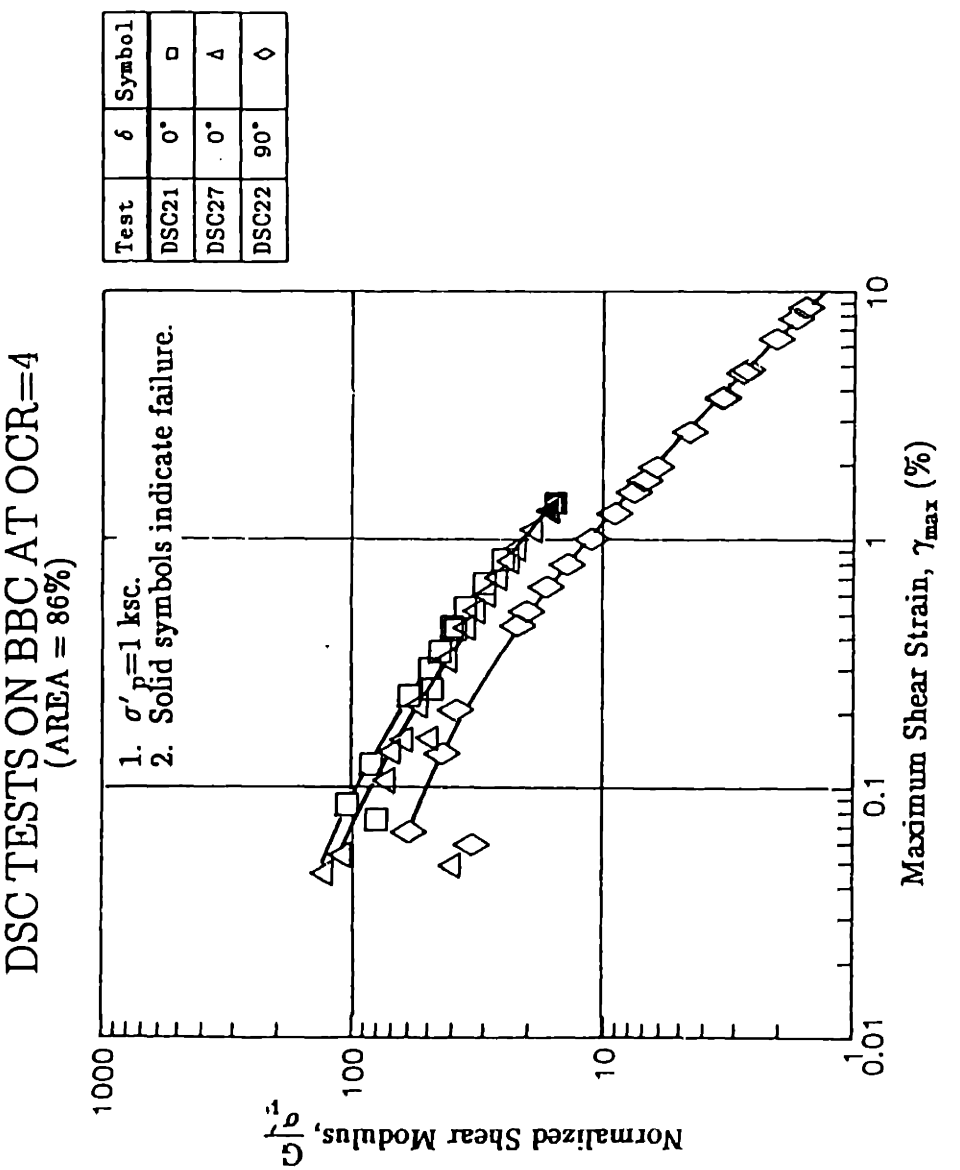

Figure 7.6: Variation of Normalized Shear Modulus with Maximum Shear Strain from DSC Tests on OCR=4 BBC.

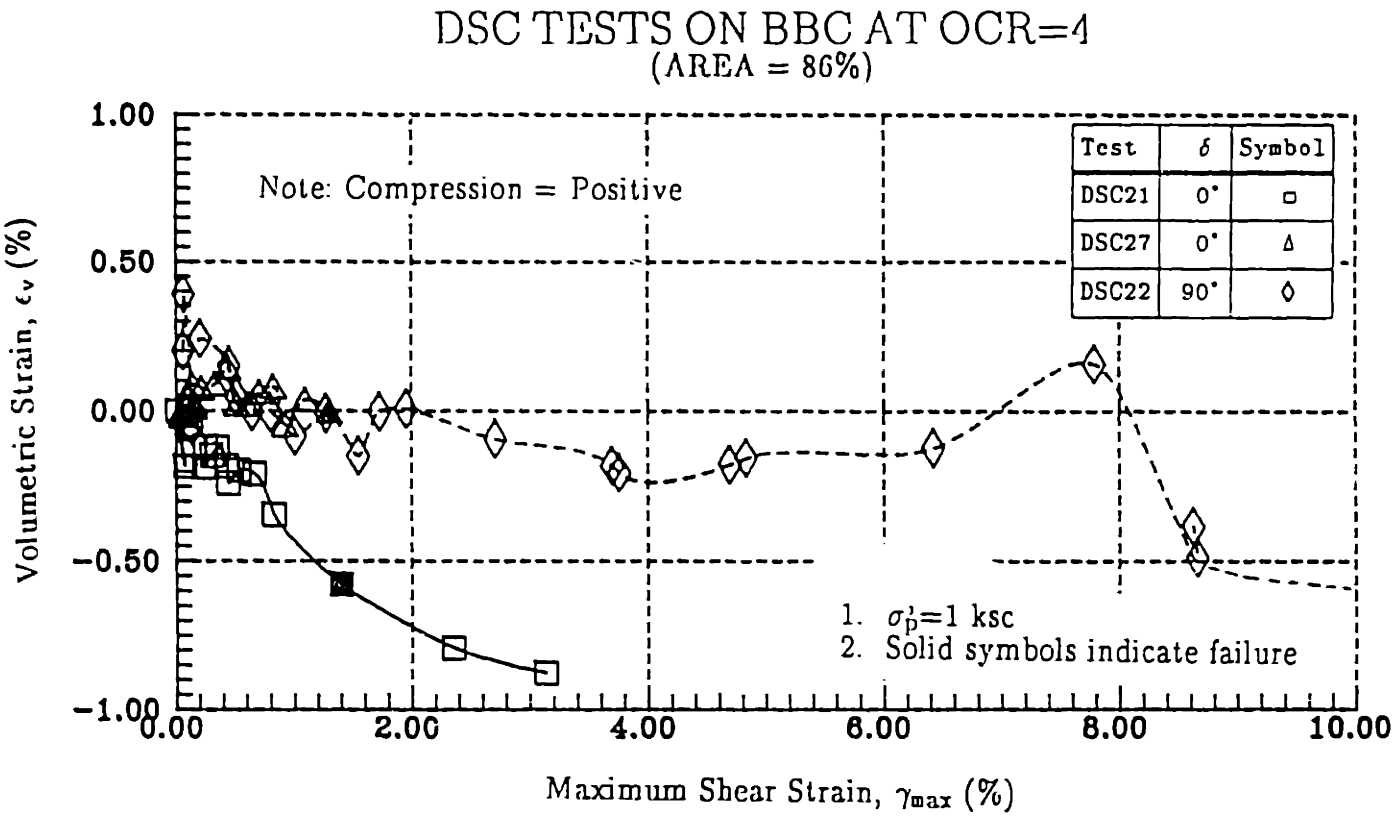

Figure 7.7: Volumetric Behavior of DSC Tests on OCR=4 BBC (Area No. 1).

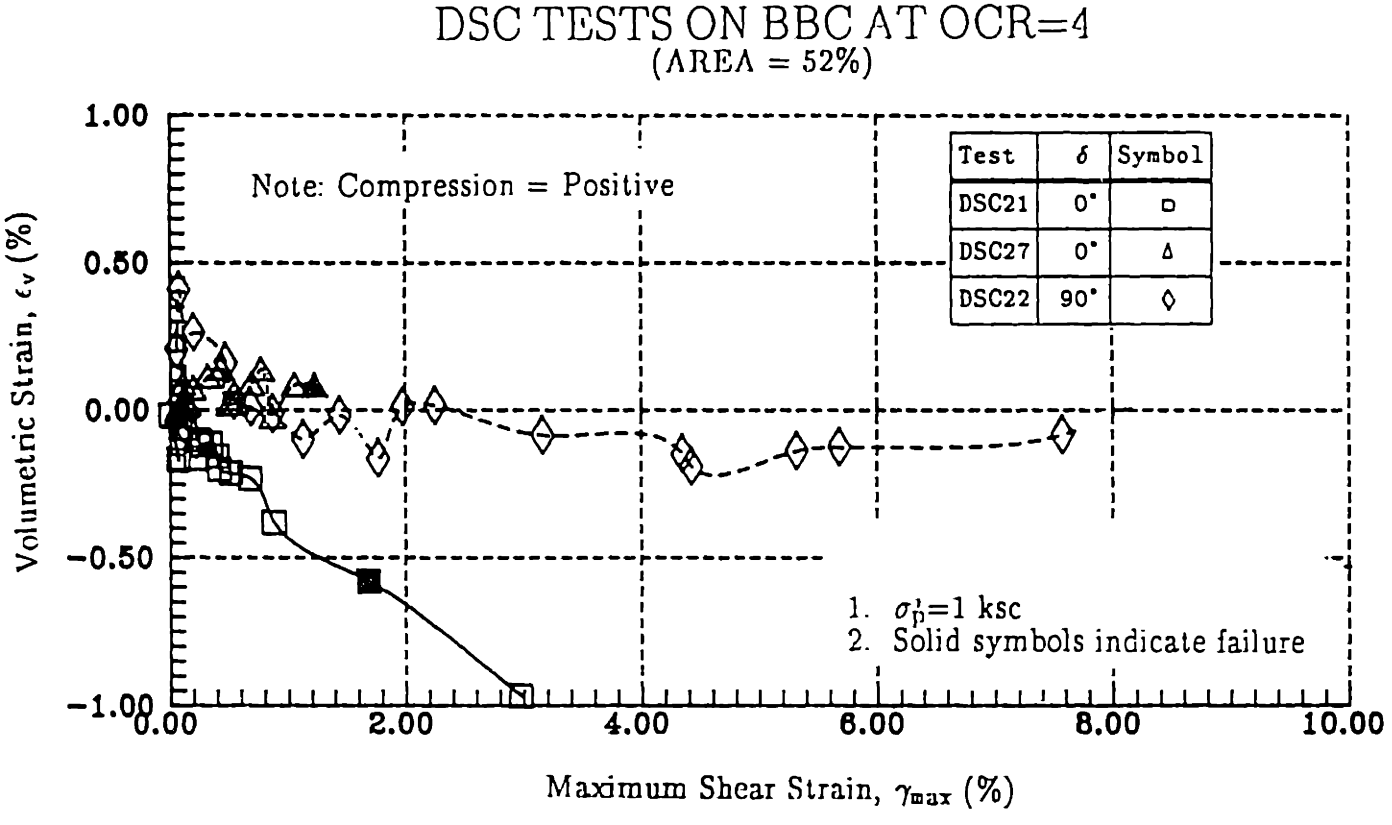

Figure 7.8: Volumetric Behavior of DSC Tests on OCR=4 BBC (Area No. 2).

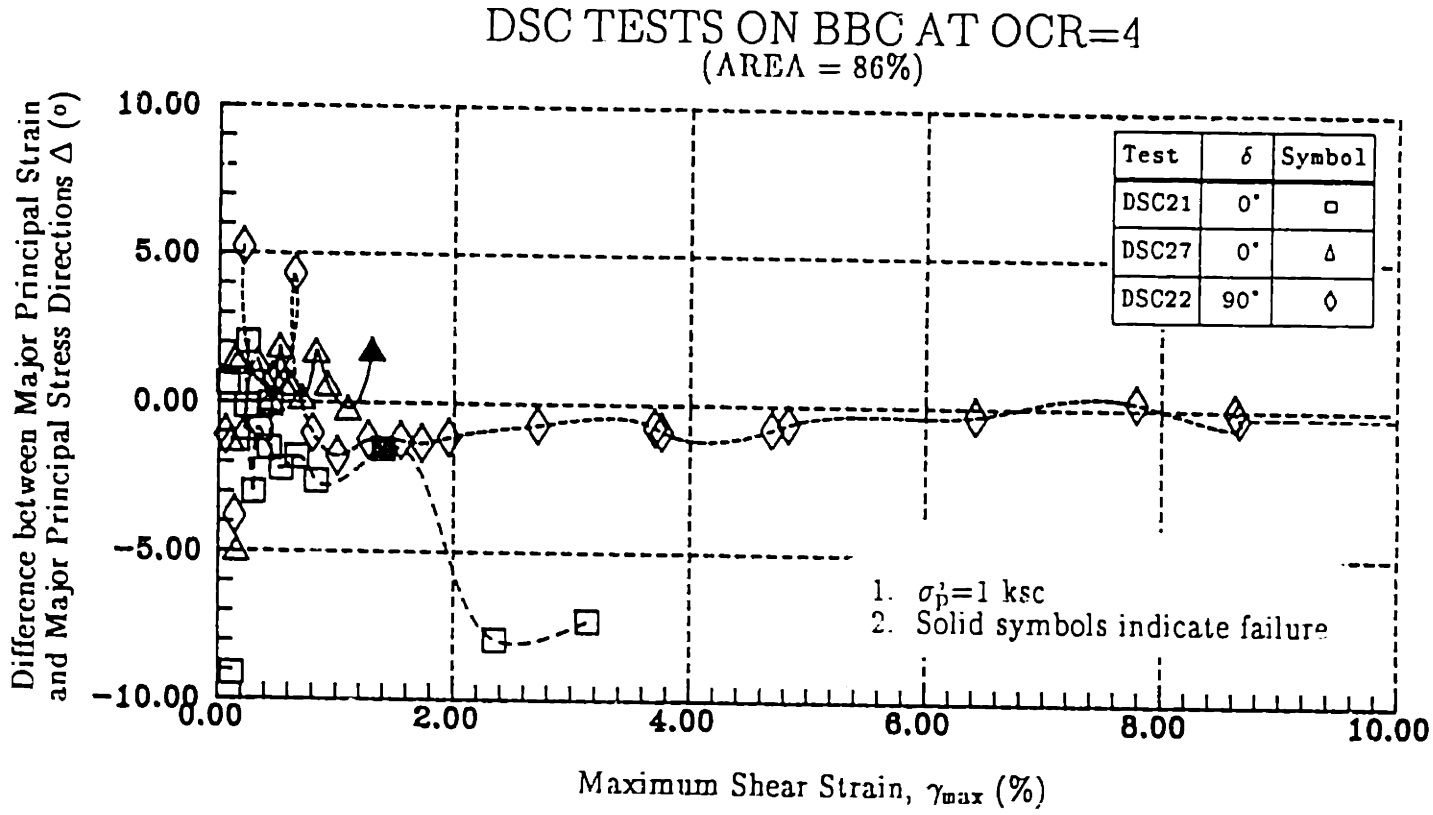

Figure 7.9: Δ versus Maximum Shear Strain for DSC Tests on OCR=4 BBC (Area No. 1).

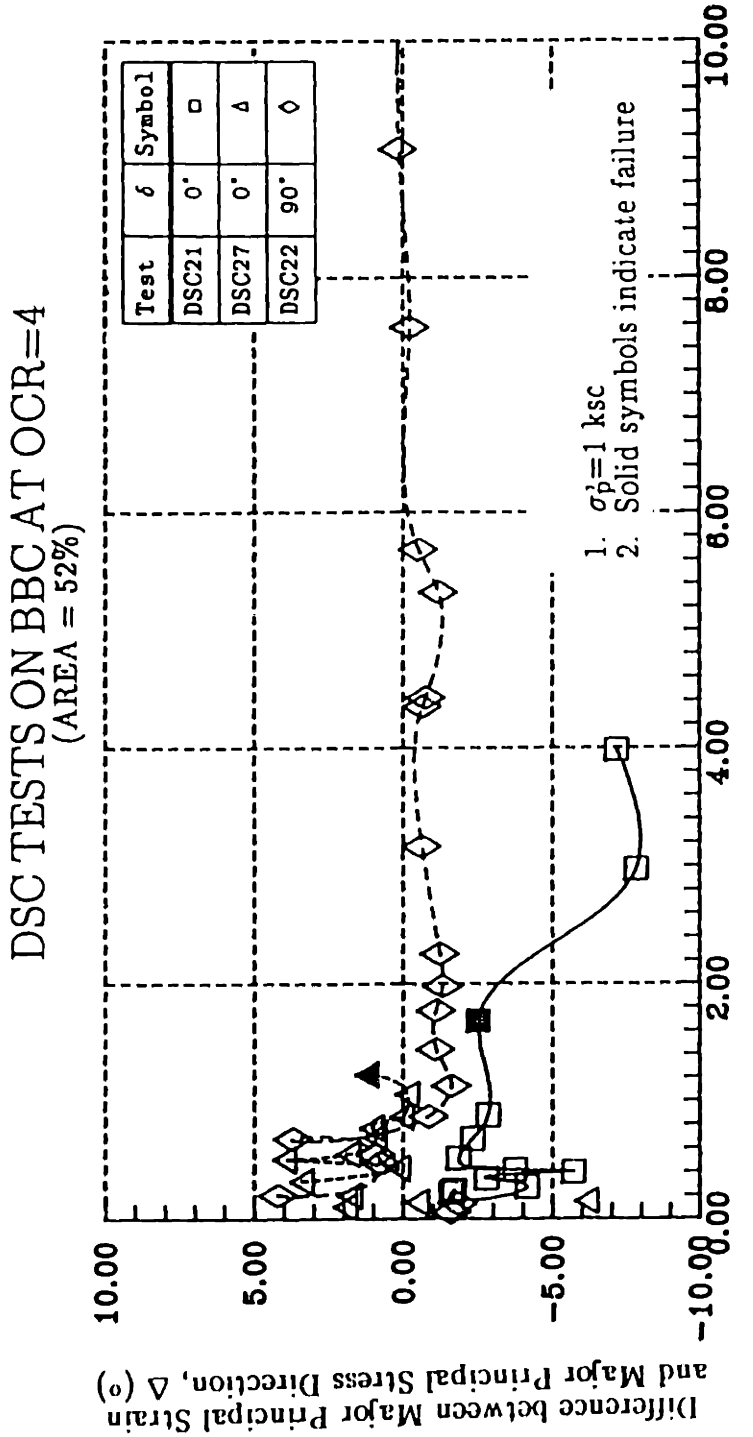

Figure 7.10: Δ versus Maximum Shear Strain for DSC Tests on OCR=4 BBC (Area No. 2).

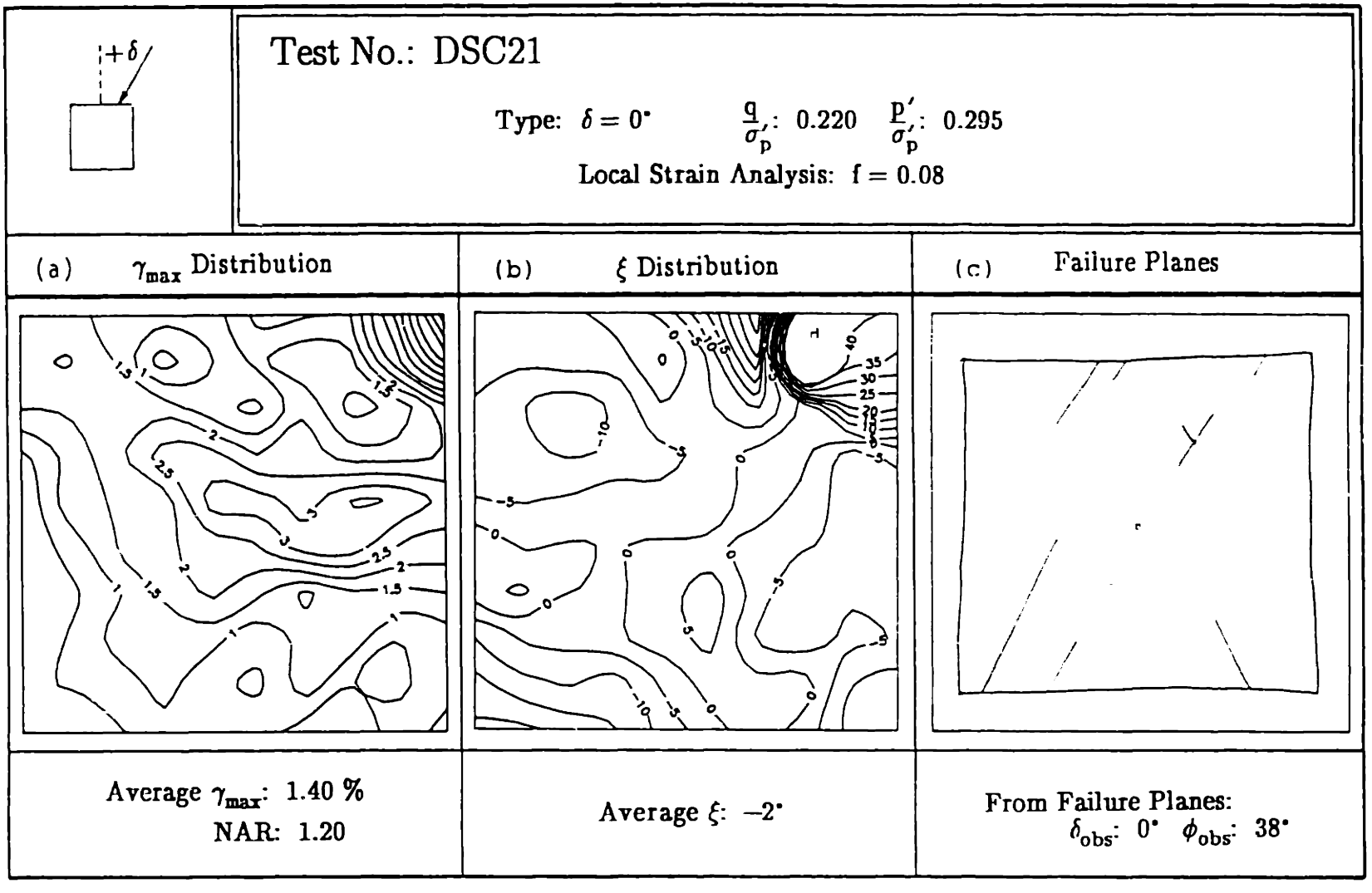

Figure 7.11: γ_{max}, ξ Distributions and Failure Planes for Test DSC21 on OCR=4 BBC.

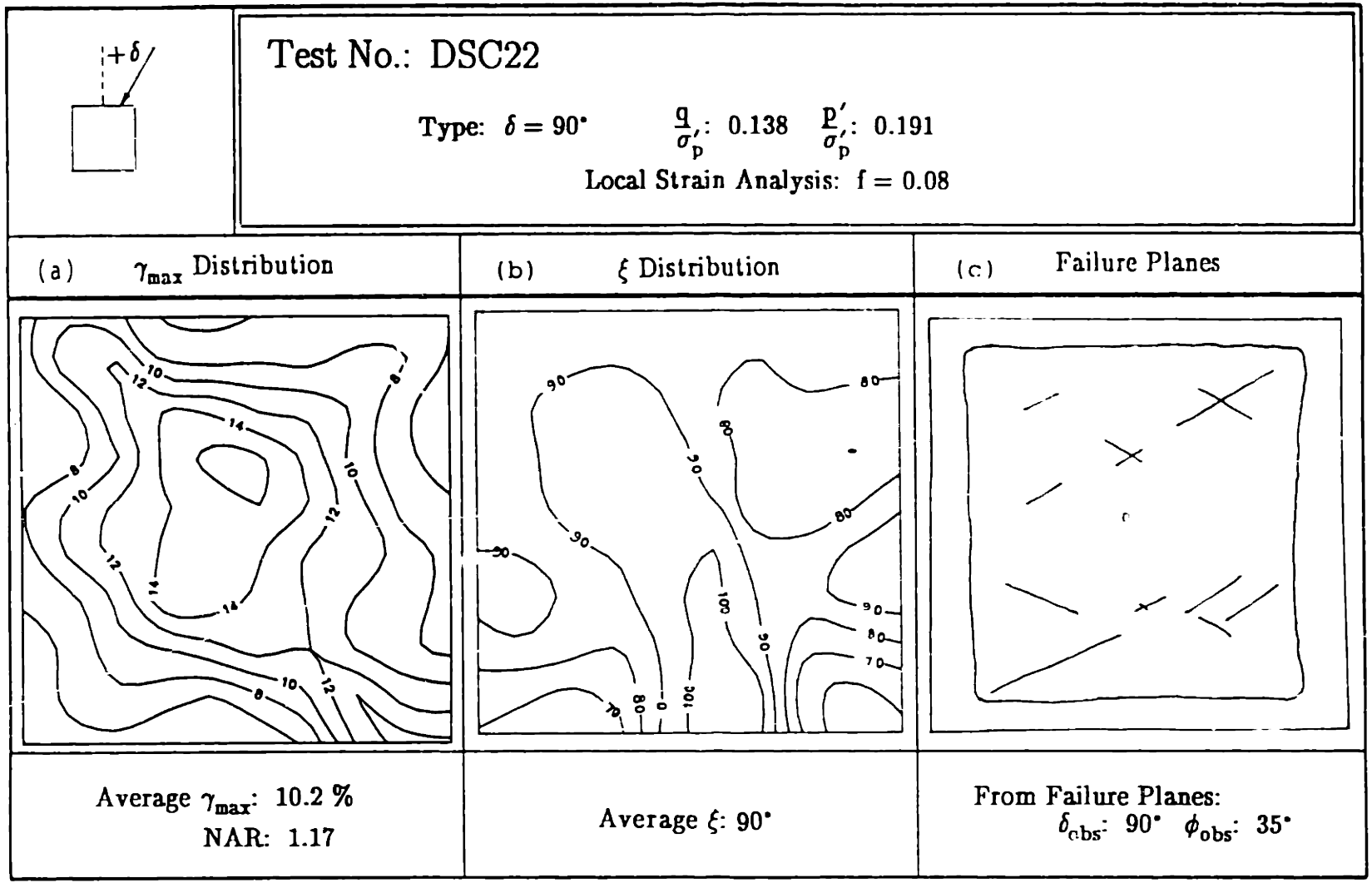

Figure 7.12: γ_{max}, ξ Distributions and Failure Planes for Test DSC22 on OCR=4 BBC.

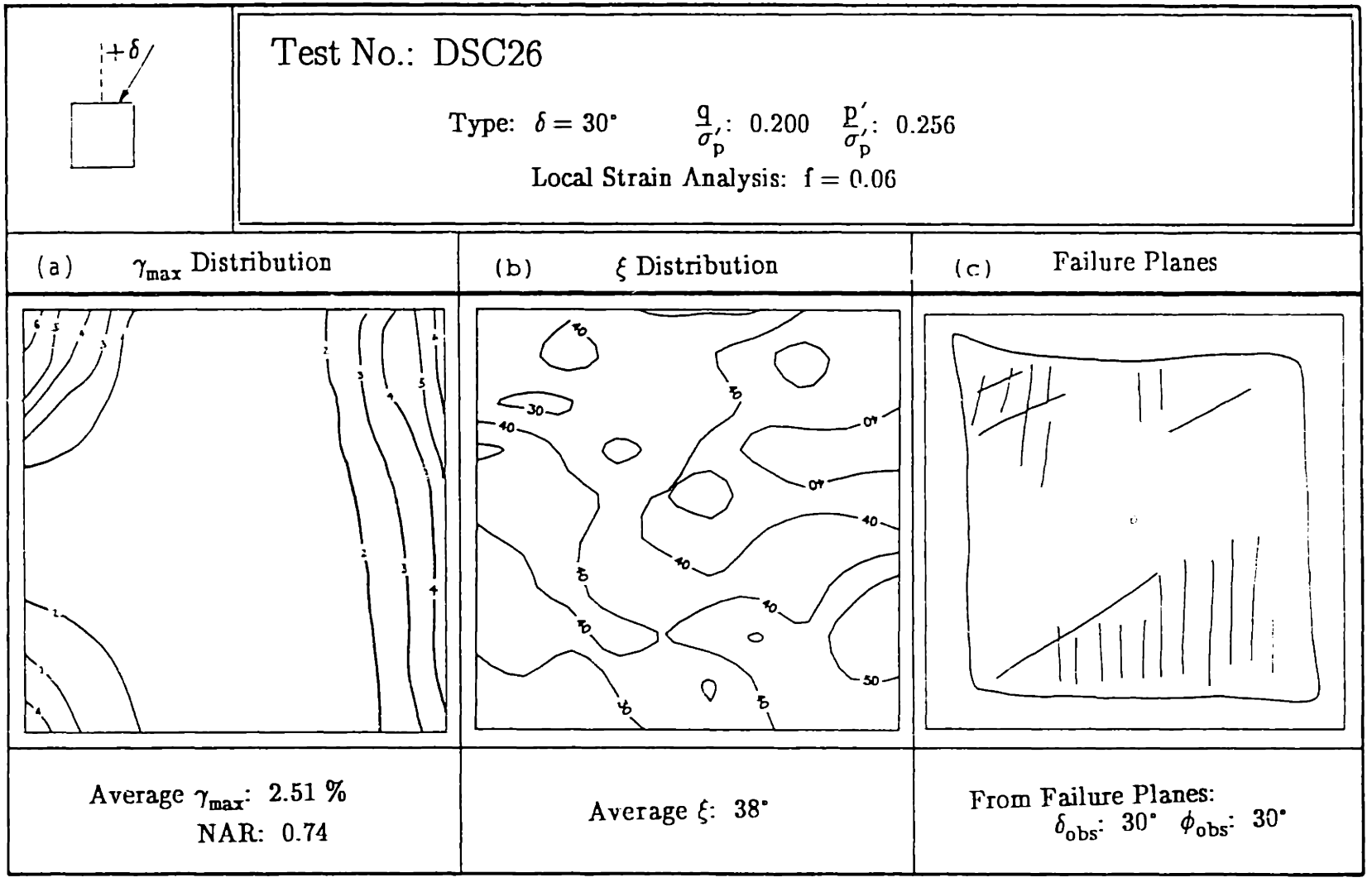

Figure 7.13: γ_{max}, ξ Distributions and Failure Planes for Test DSC26 on OCR=4 BBC.

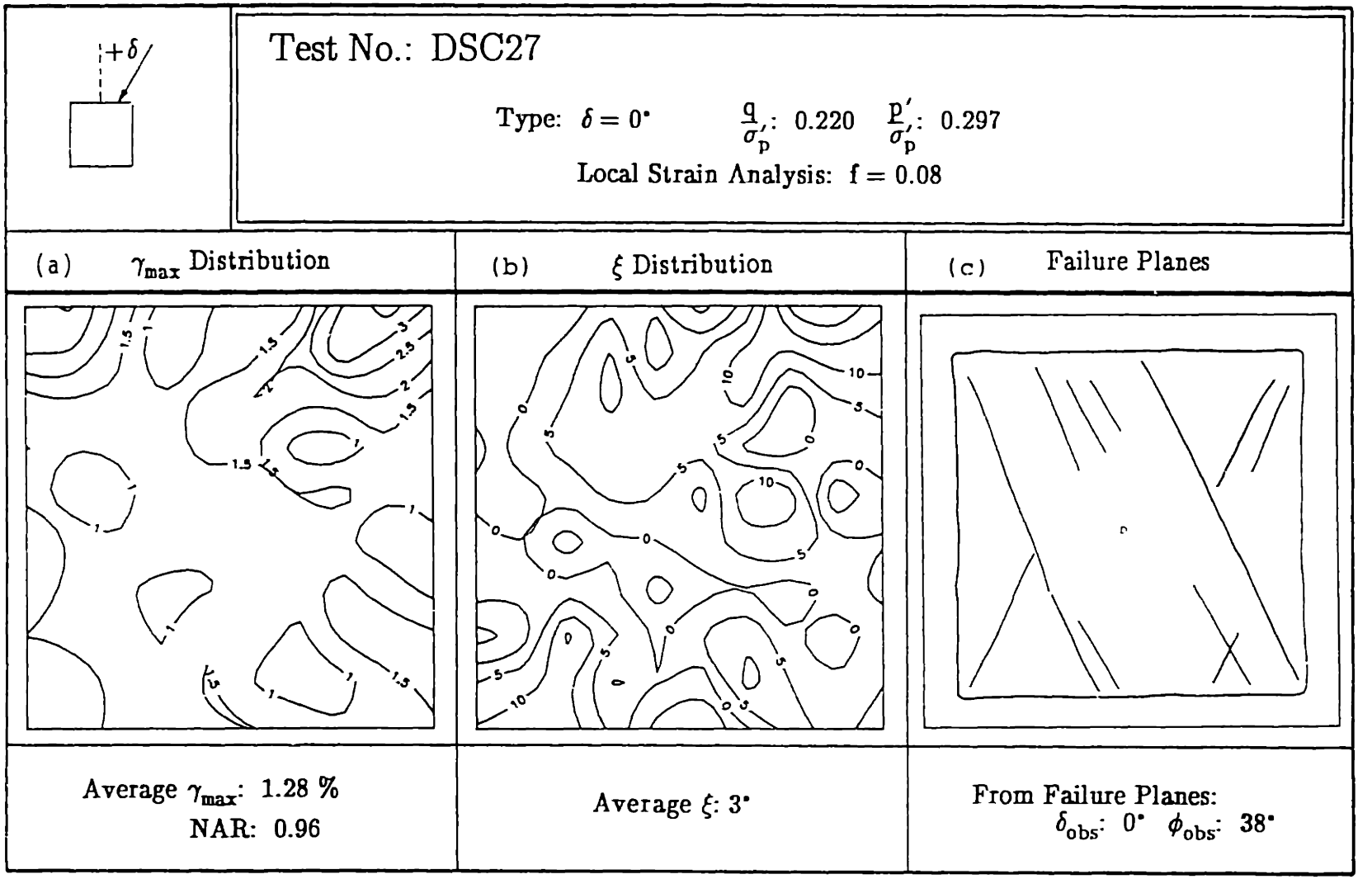

Figure 7.14: γ_{max}, ξ Distributions and Failure Planes for Test DSC27 on OCR=4 BBC.

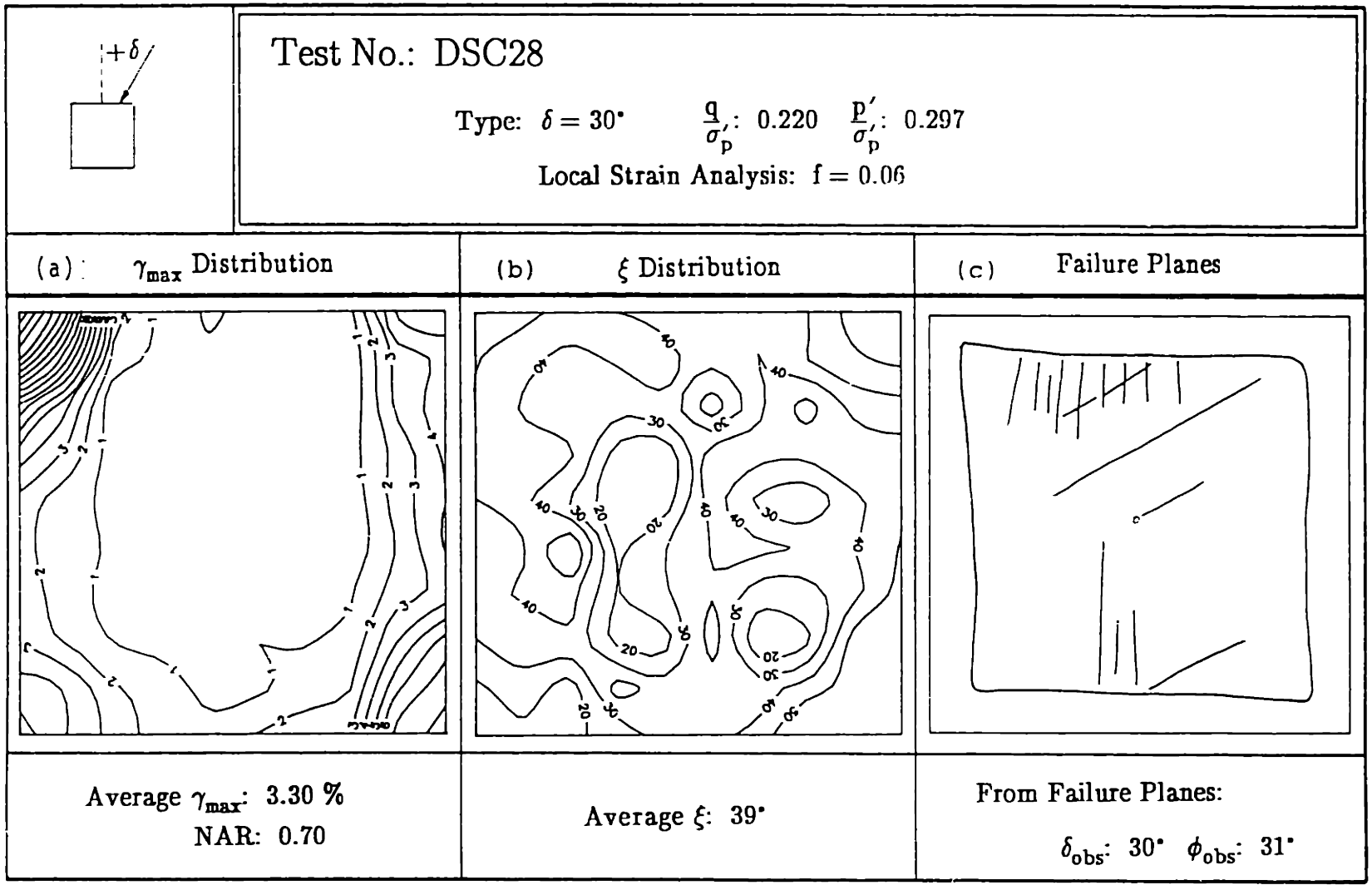

Figure 7.15: γ_{max}, ξ Distributions and Failure Planes for Test DSC28 on OCR=4 BBC.

Final Water Content Distribution of the DSC Sample: DSC27
Top Layer of the Sample
(all values in percent)

40.54	40.43	40.47
40.36	40.16	40.05
39.74	40.18	40.19

Initial Water Content:

w_i = 40.72 ± 0.11 % (2)

Final Water Content:

w_f = 40.24 ± 0.25 % (9)

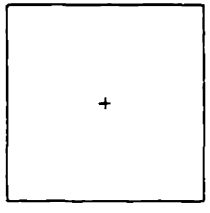

Figure 7.16: Final Water Content Distribution of the Sample from Test DSC21.

Final Water Content Distribution of the DSC Sample: DSC22
Top Layer of the Sample
(all values in percent)

39.79	40.35	40.14
40.19	40.12	40.28
39.56	39.86	39.79

Initial Water Content:

w_i = 41.10 ± 0.22 % (2)

Final Water Content:

w_f = 40.01 ± 0.27 % (9)

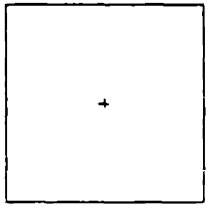

Figure 7.17: Final Water Content Distribution of the Sample from Test DSC22.

Final Water Content Distribution of the DSC Sample: DSC21
Top Layer of the Sample
(all values in percent)

40.09	40.67	40.18
40.17	40.70	40.74
40.38	40.49	40.58

Initial Water Content:

w_i = 41.12 ± 0.02 % (2)

Final Water Content:

w_f = 40.44 ± 0.25 % (9)

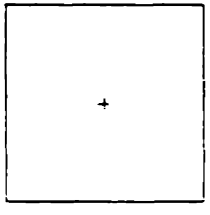

Figure 7.18: Final Water Content Distribution of the Sample from Test DSC27.

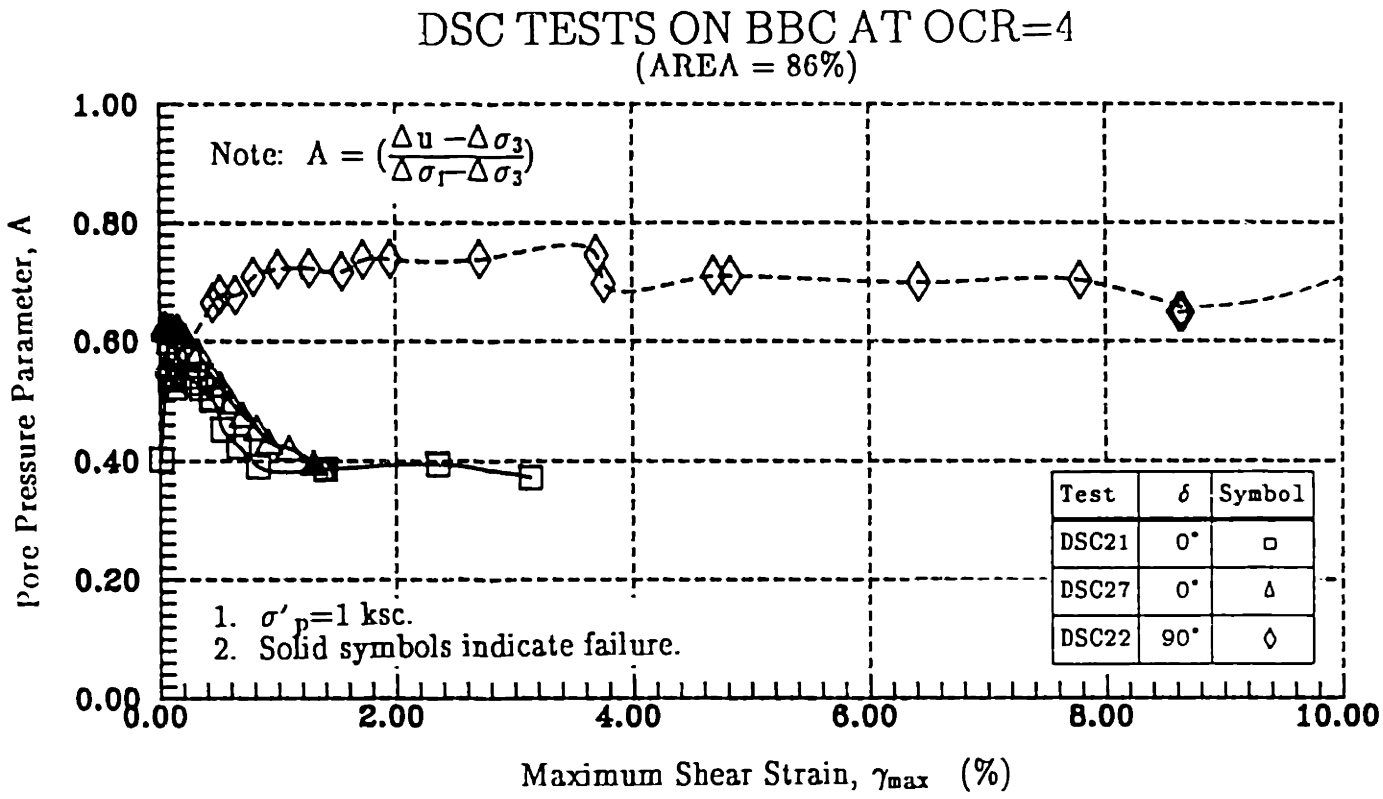

Figure 7.19a: Pore Pressure Parameter (A) versus Maximum Shear Strain for DSC Tests on OCR=4 BBC (Area No. 1).

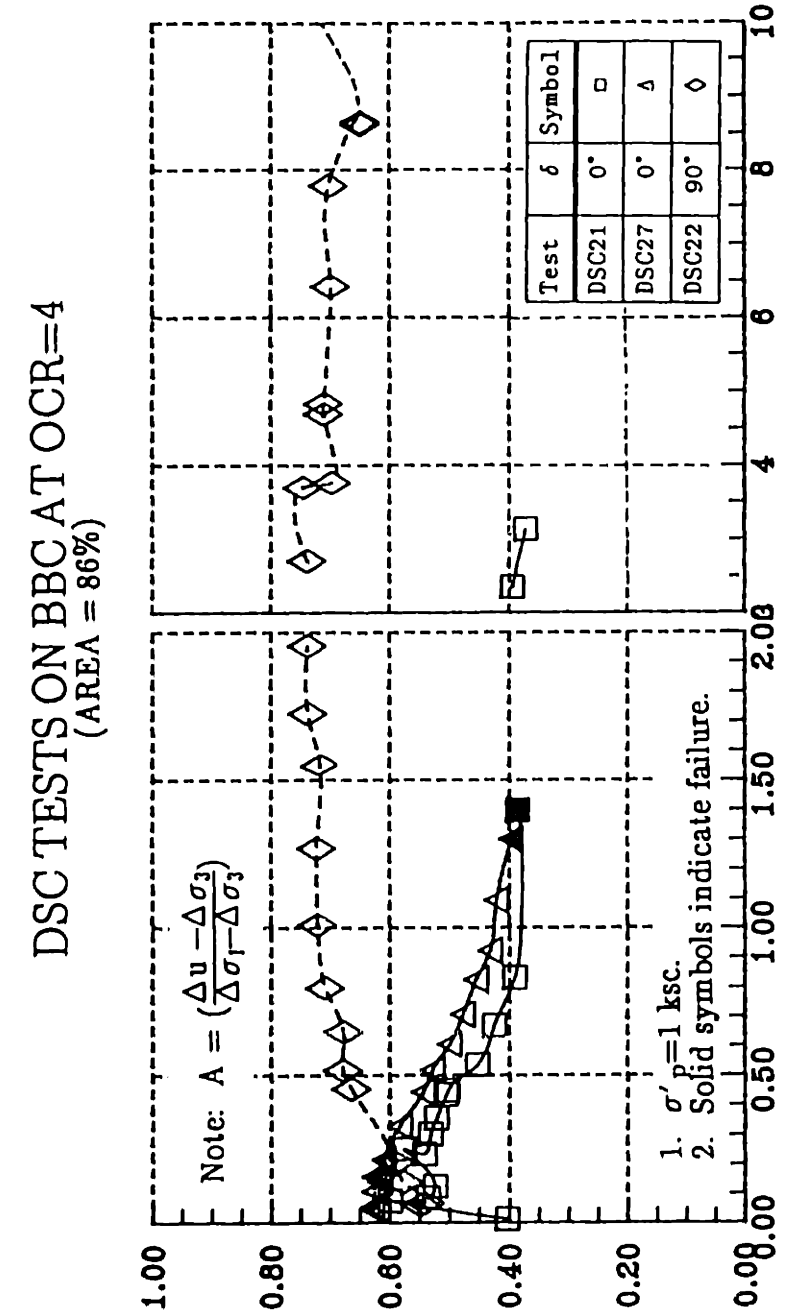

Figure 7.19b: Pore Pressure Parameter (A) versus Maximum Shear Strain for DSC Tests on OCR=4 BBC (Area No. 1).

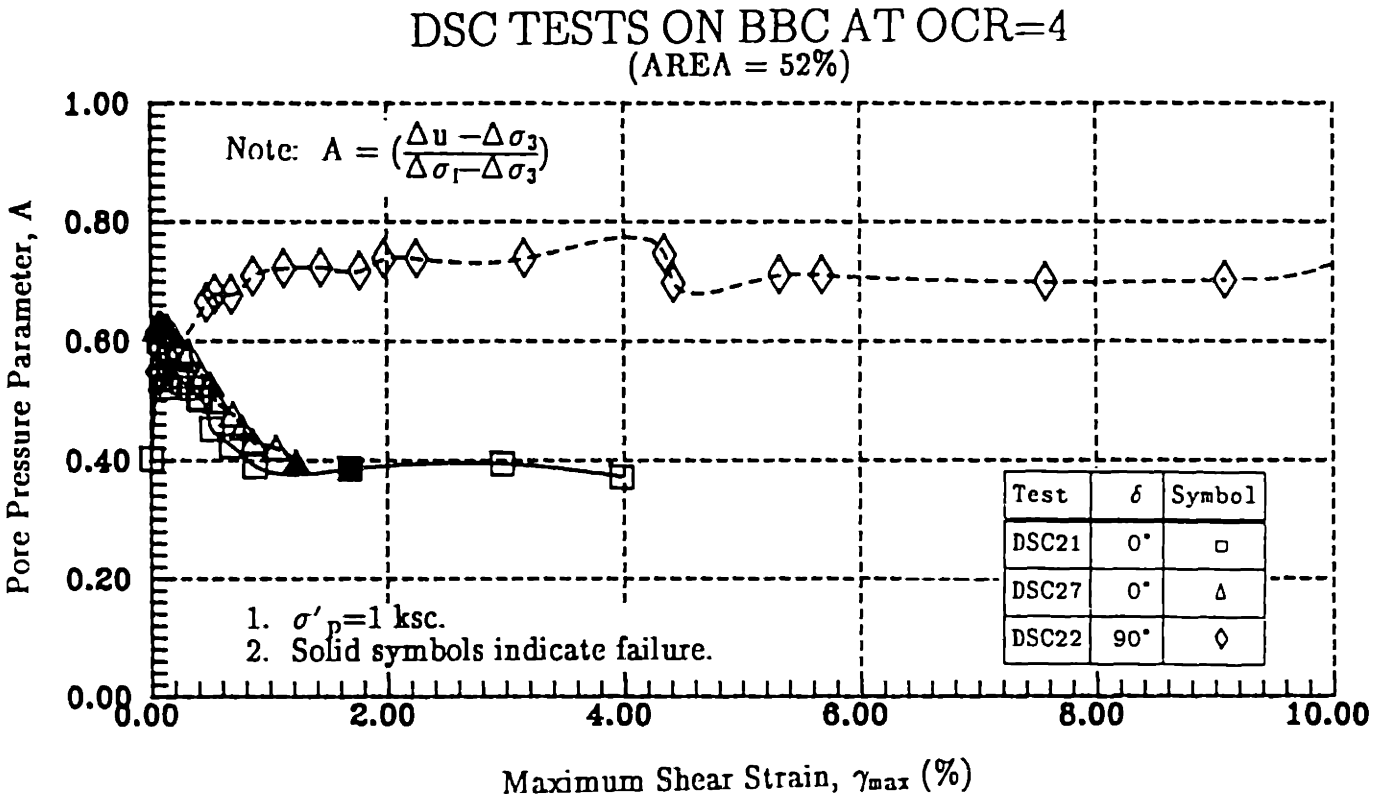

Figure 7.20a: Pore Pressure Parameter (A) versus Maximum Shear Strain for DSC Tests on OCR=4 BBC (Area No. 2).

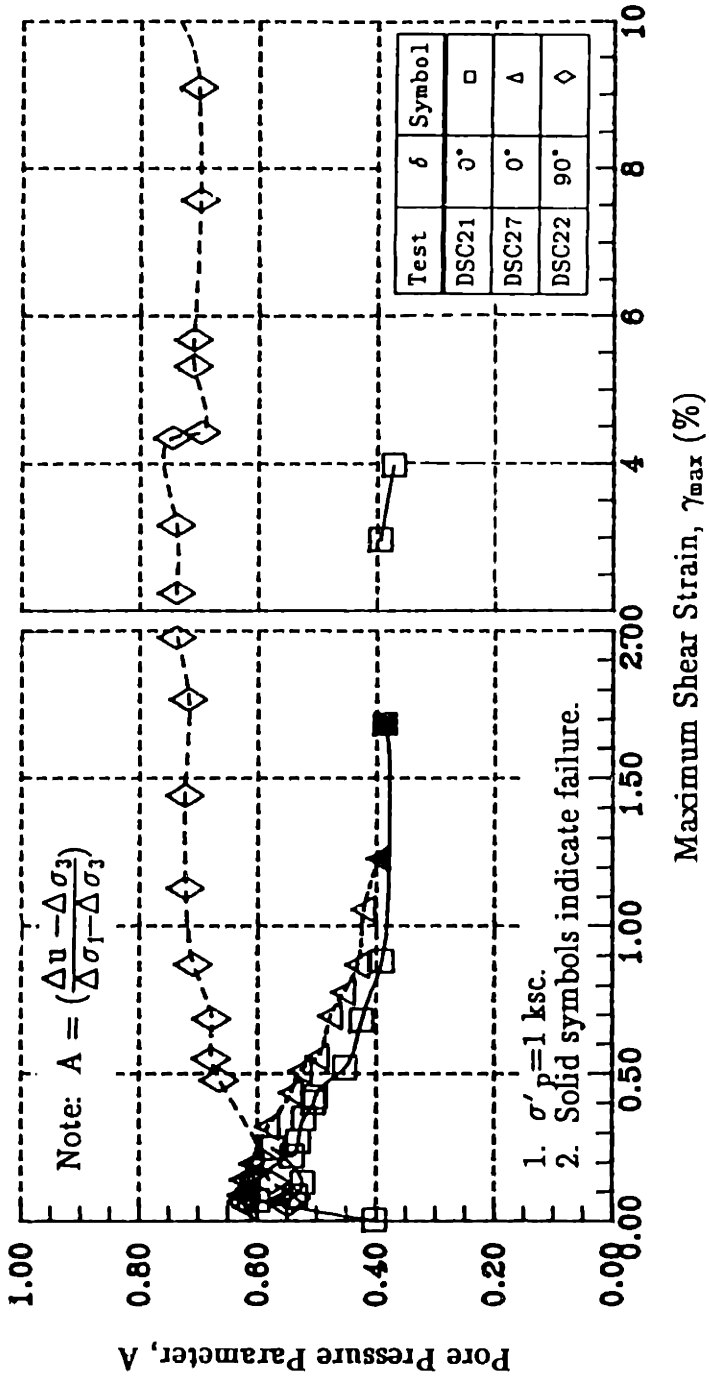

Figure 7.20b: Pore Pressure Parameter (A) versus Maximum Shear Strain for DSC Tests on OCR=4 BBC (Area No. 2).

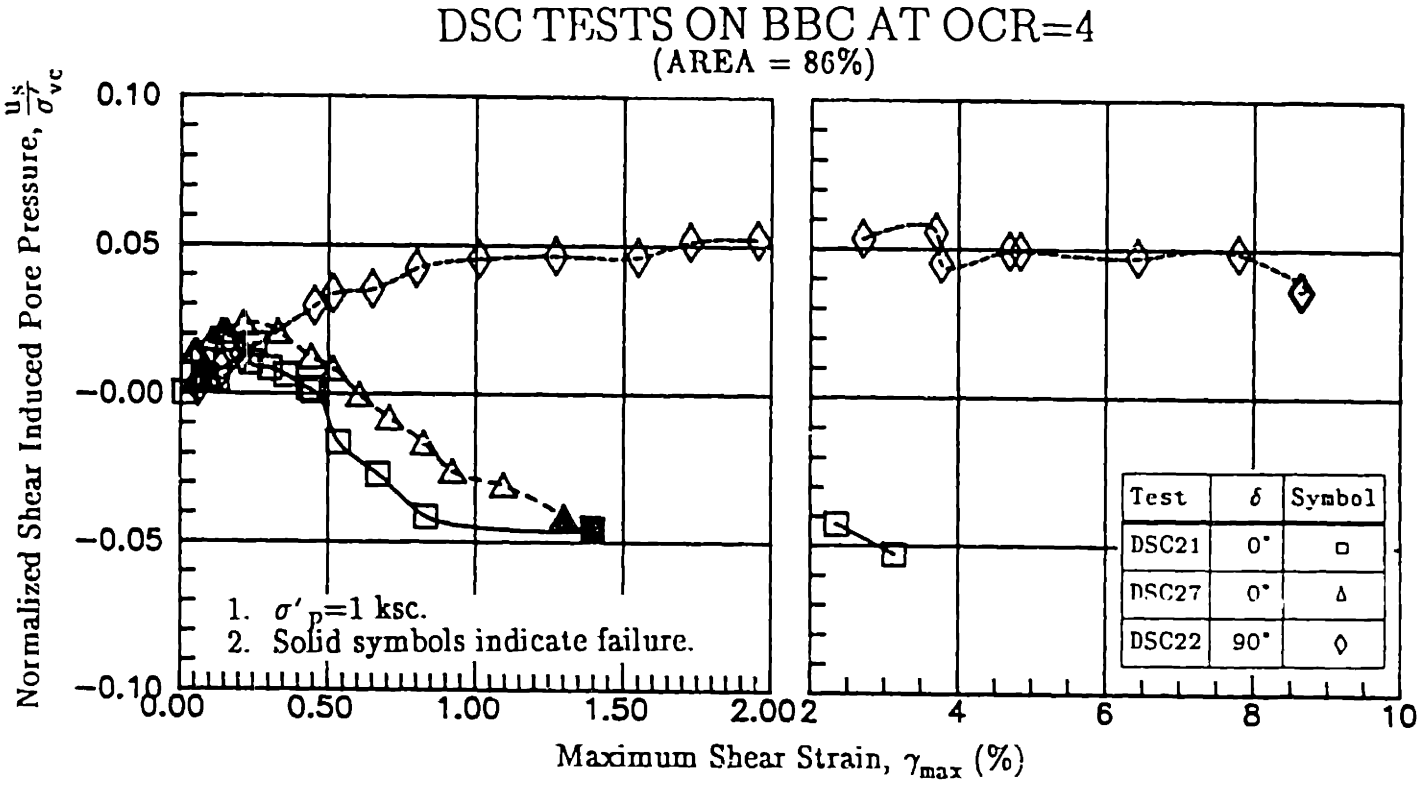

Figure 7.21: Normalized Shear Induced Pore Pressure versus Maximum Shear Strain for DSC Tests on OCR=4 BBC (Area No. 1).

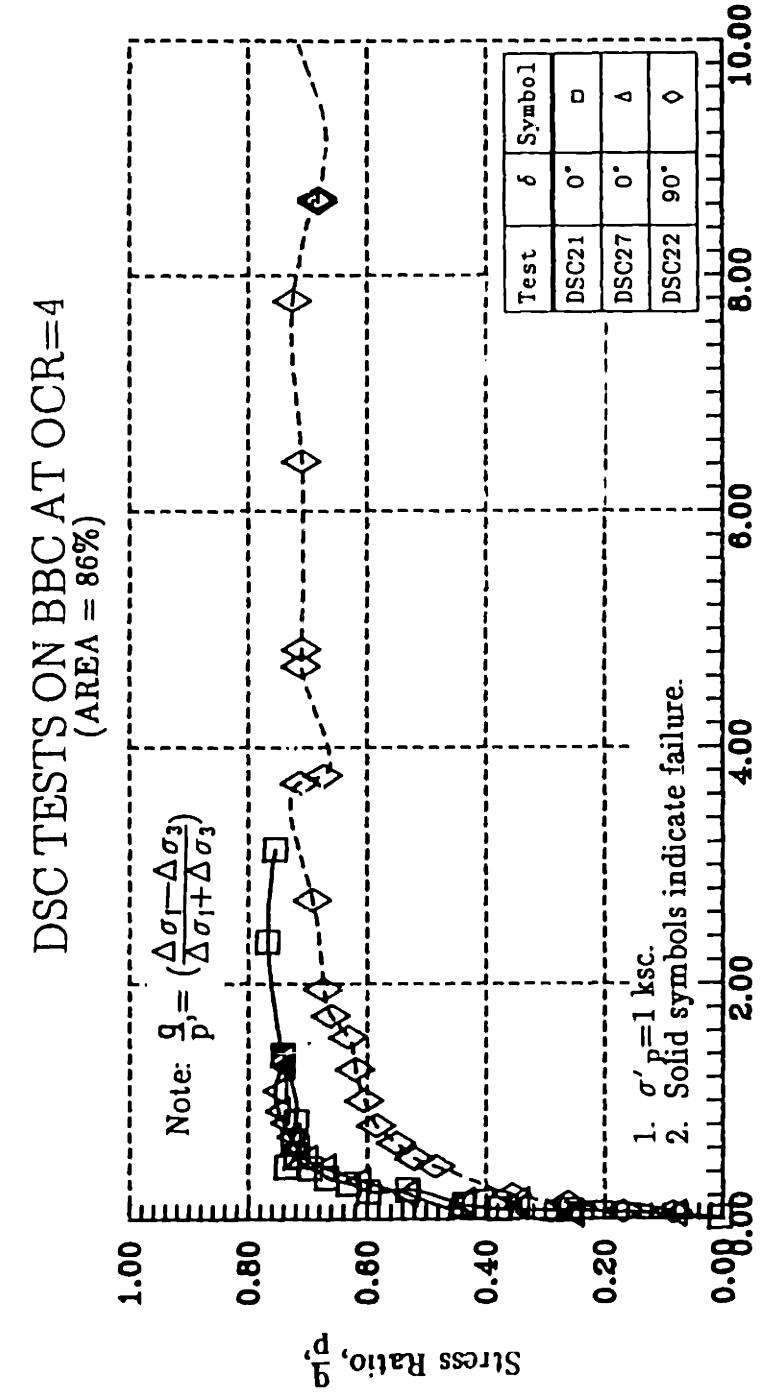

Figure 7.22: Stress Ratio versus Maximum Shear Strain for DSC Tests on OCR=4 BBC (Area No. 1).

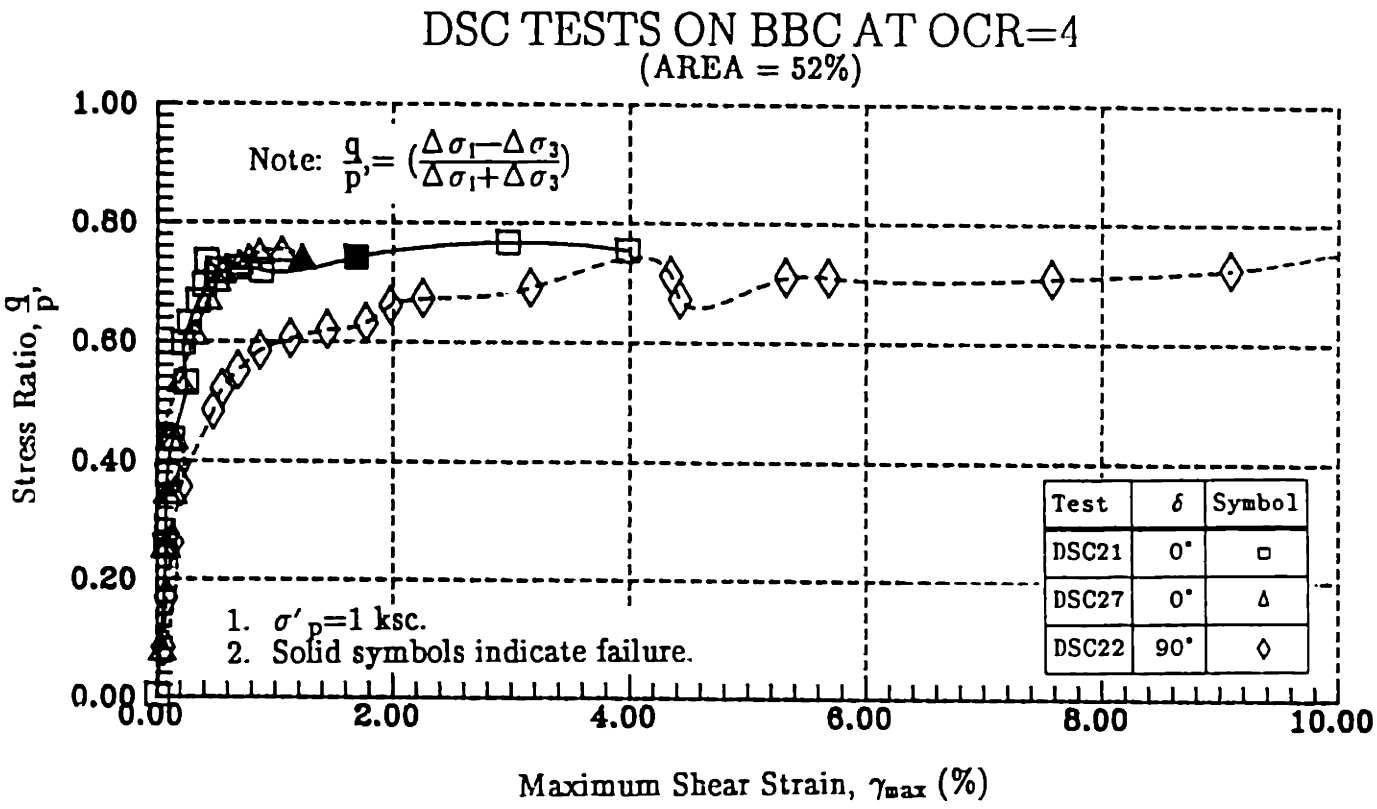

Figure 7.23: Stress Ratio versus Maximum Shear Strain for DSC Tests on OCR=4 BBC (Area No. 2).

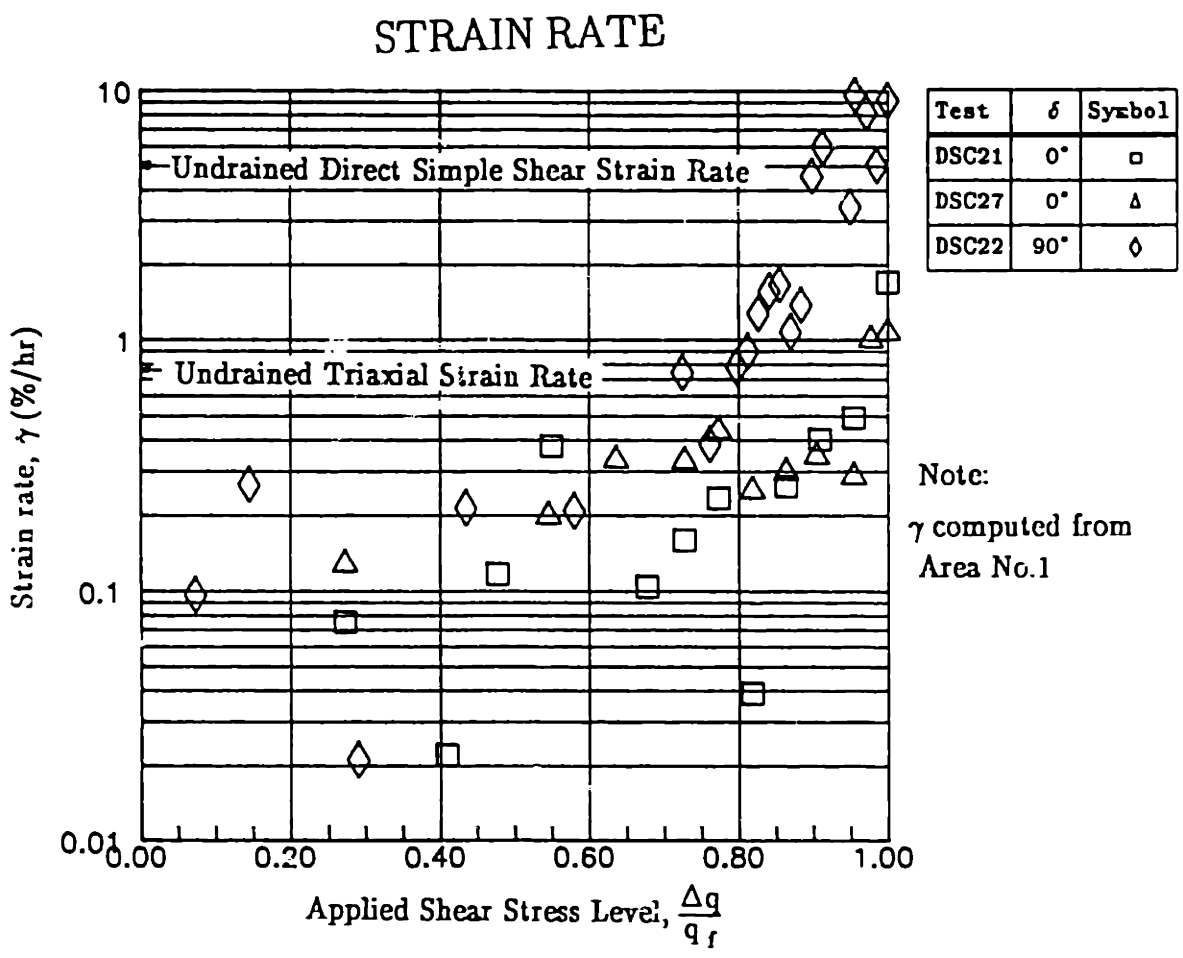

Figure 7.24: Shear Strain Rates from DSC Tests on OCR=4 BBC (Area No. 1).

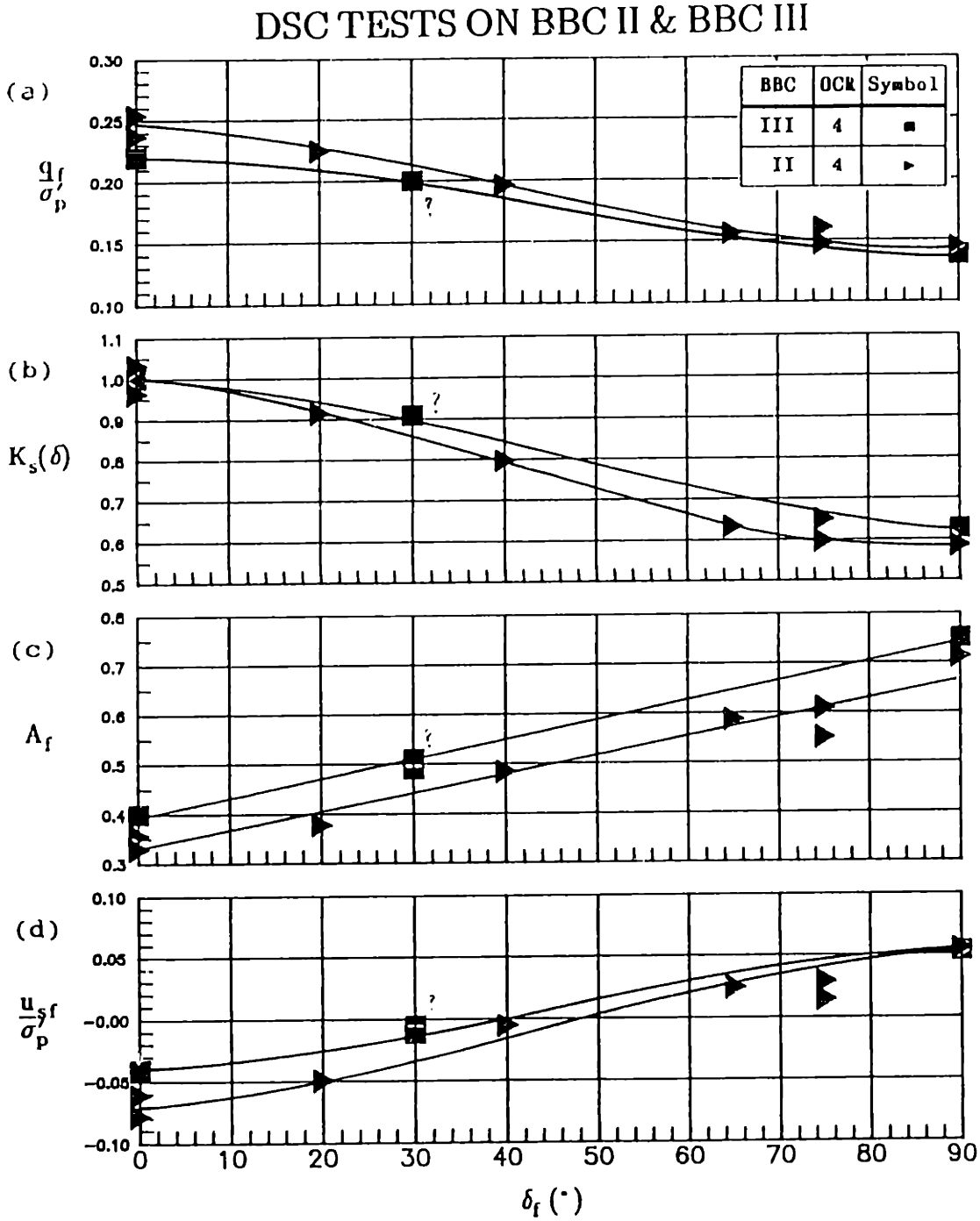

Figure 7.25: Comparisons of New and Old DSC Tests on BBC at OCR=4.

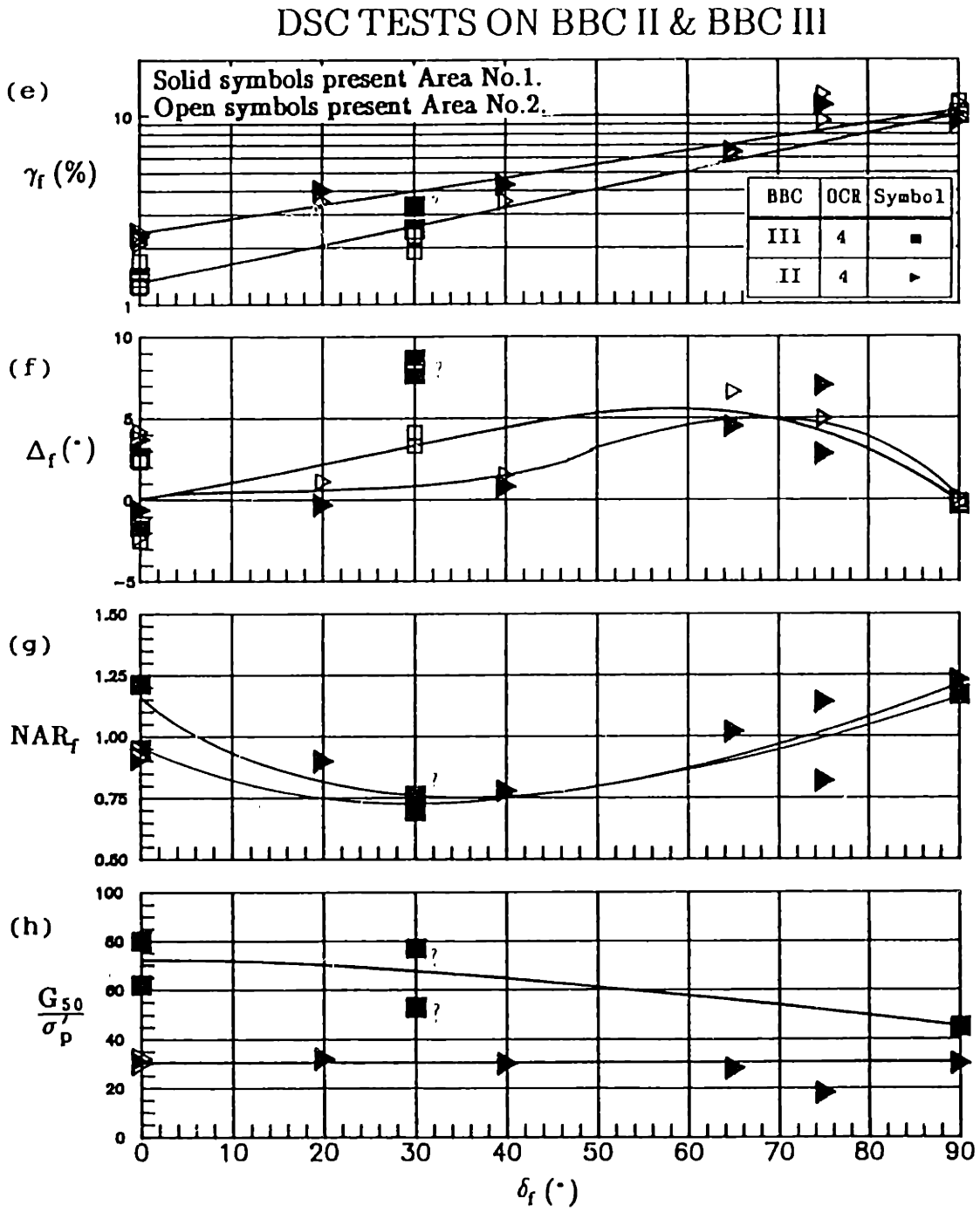

Figure 7.25: (Cont.)

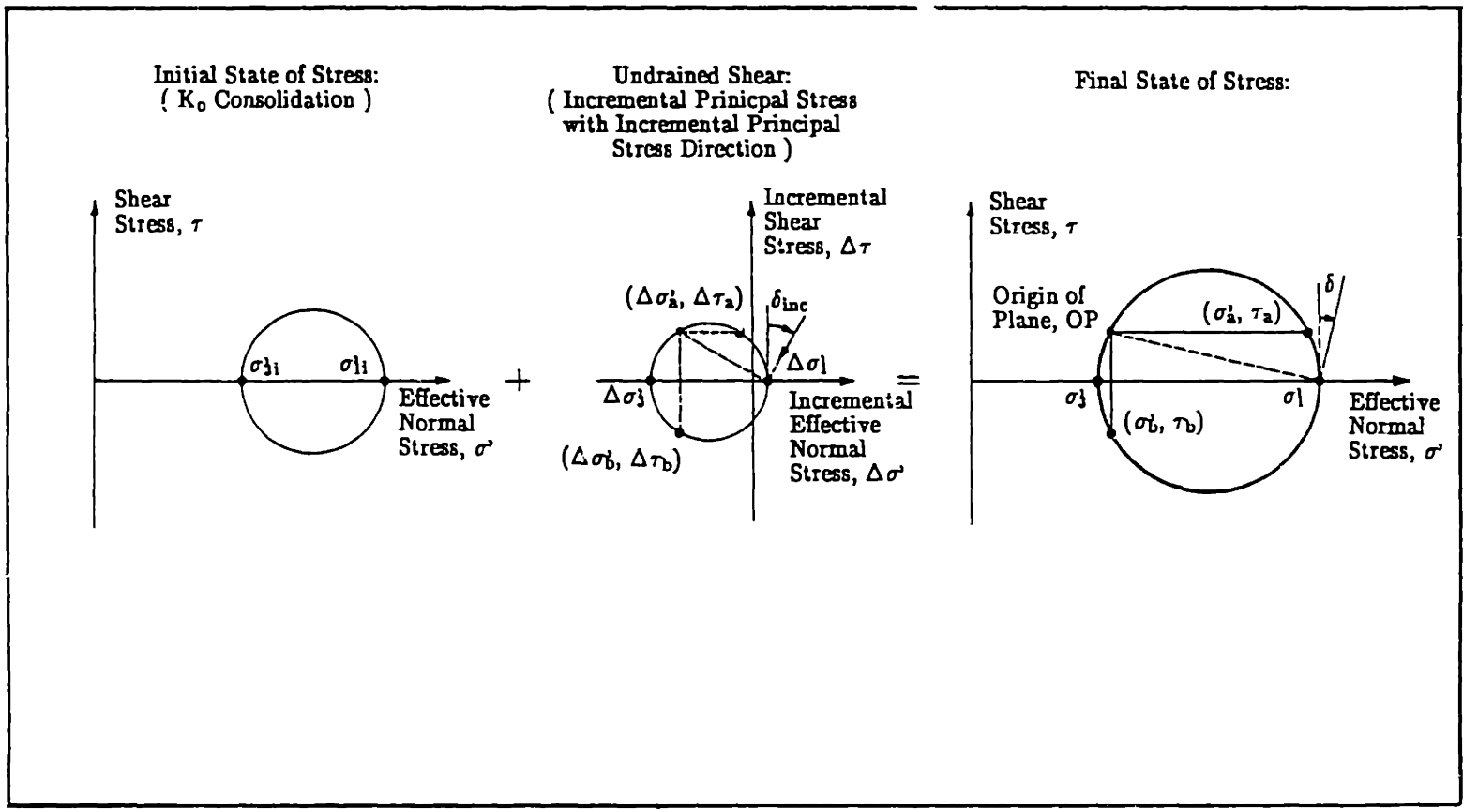

Figure 7.26: Stress State of a Fixed δ_{inc} DSC Test.

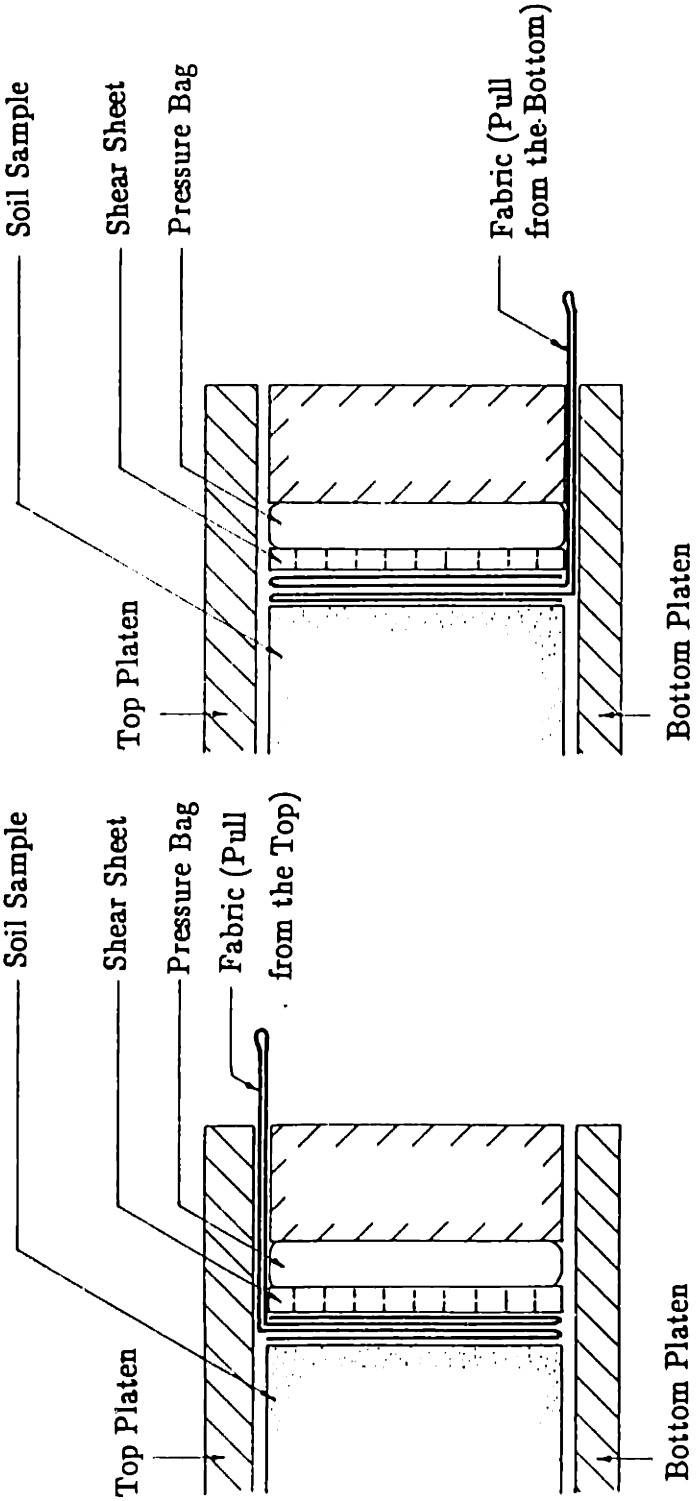

Figure 7.27: Fabric Arrangement for a Normally–Consolidated Clay Test: (a) Fabric is removed from the Top; (b) Fabric is removed from the Bottom.

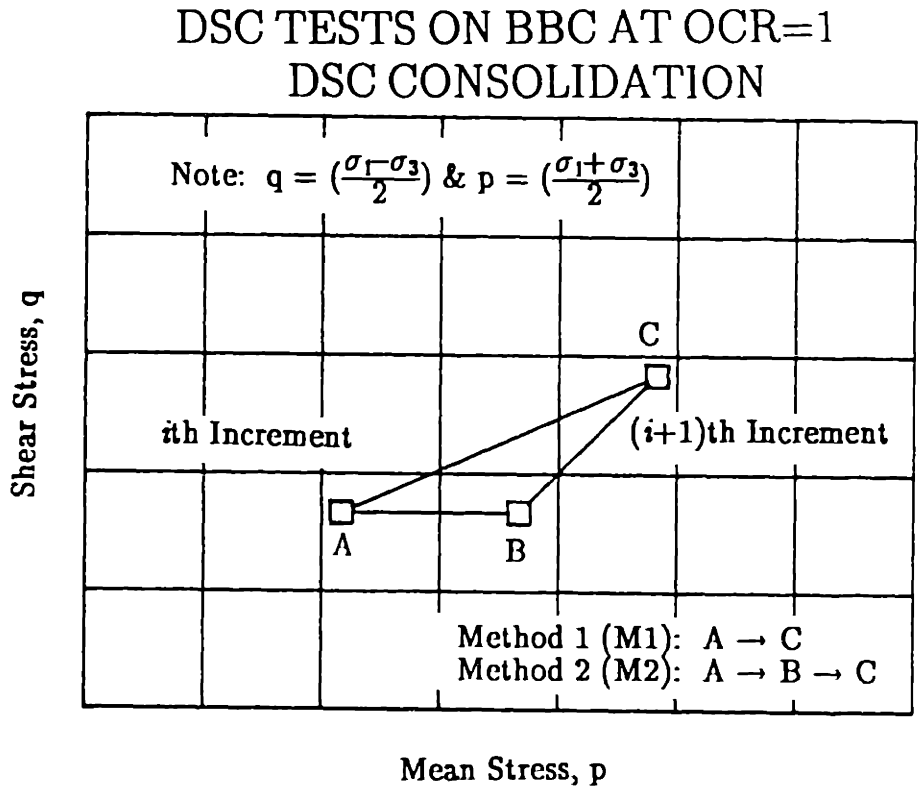

Figure 7.28: Different Method of Consolidating DSC Sample.

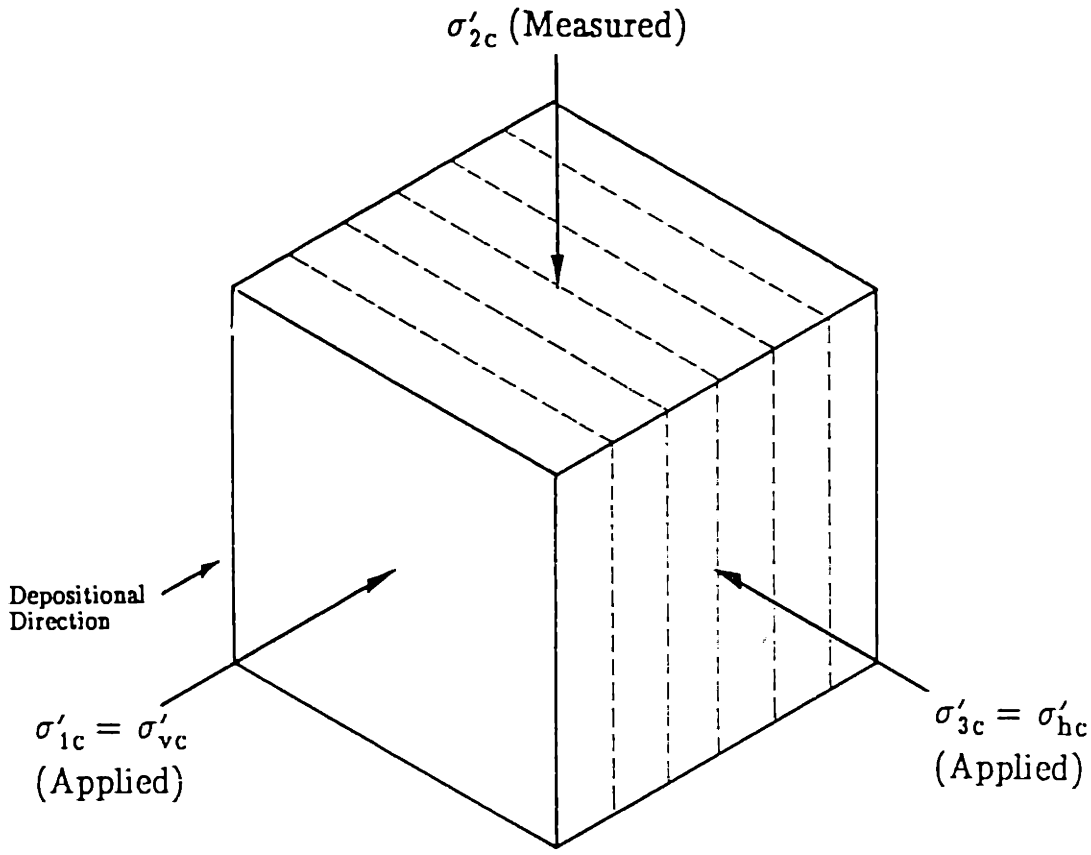

Figure 7.29: The Directions of Three Principal Consolidation Stresses.

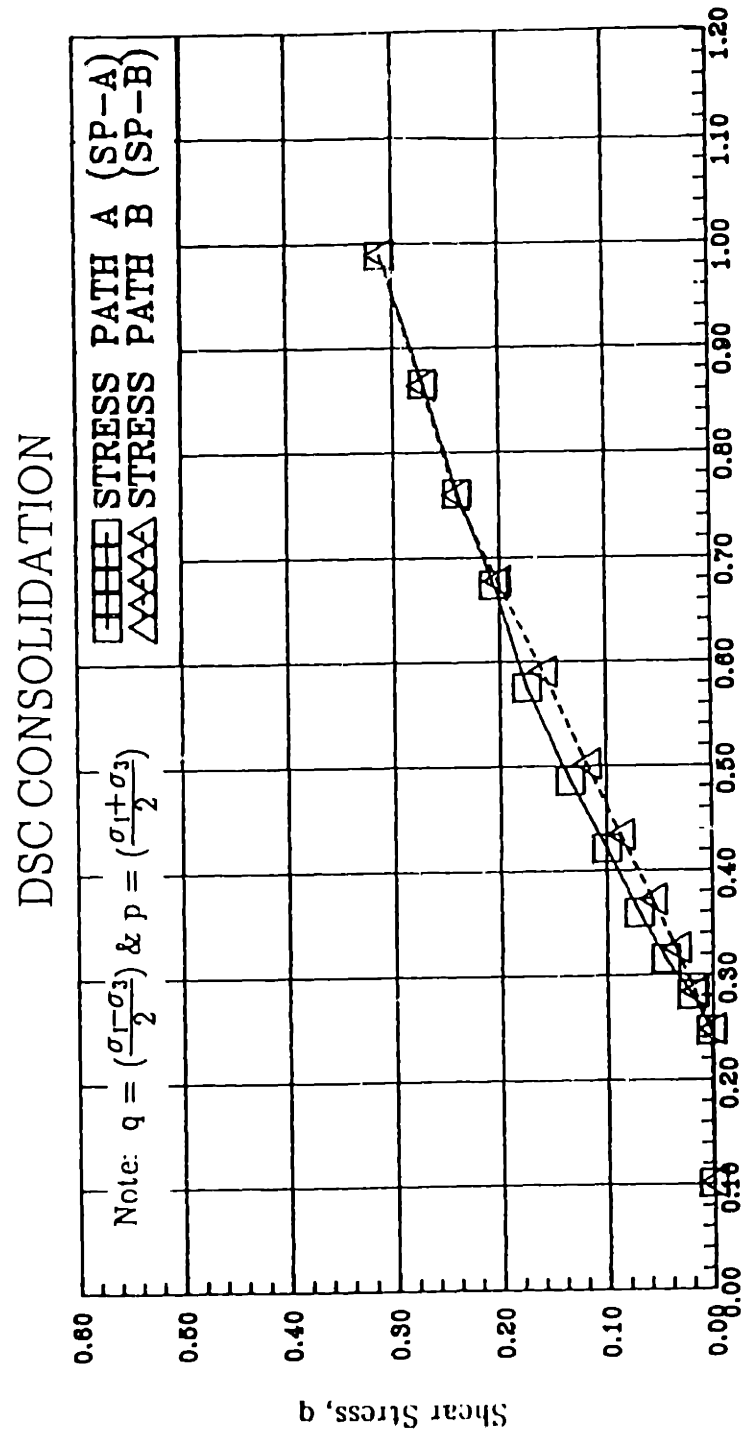

Figure 7.30: Different Stress Paths used for Consolidating DSC Sample.

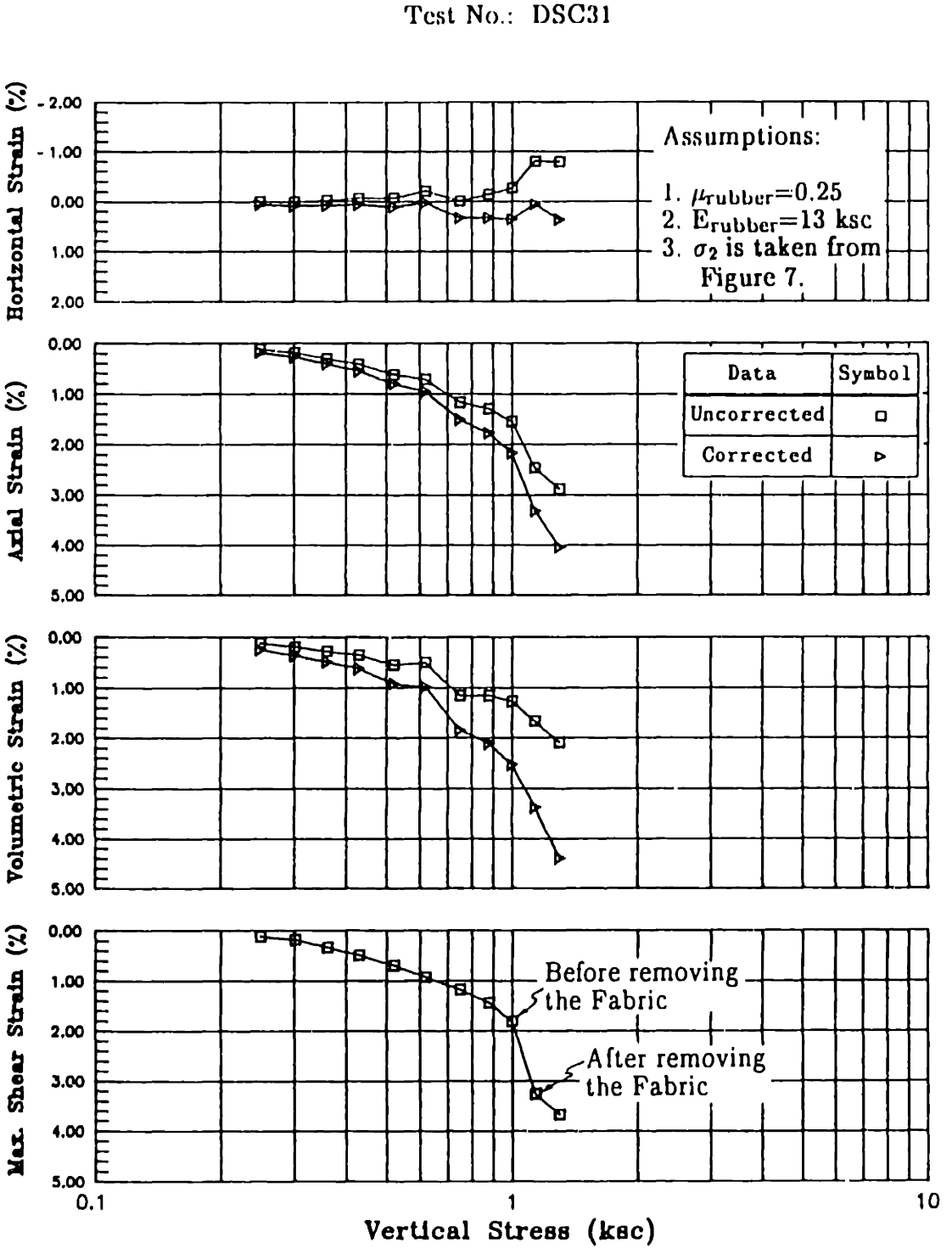

Figure 7.31: Compression Curves for Test DSC31.

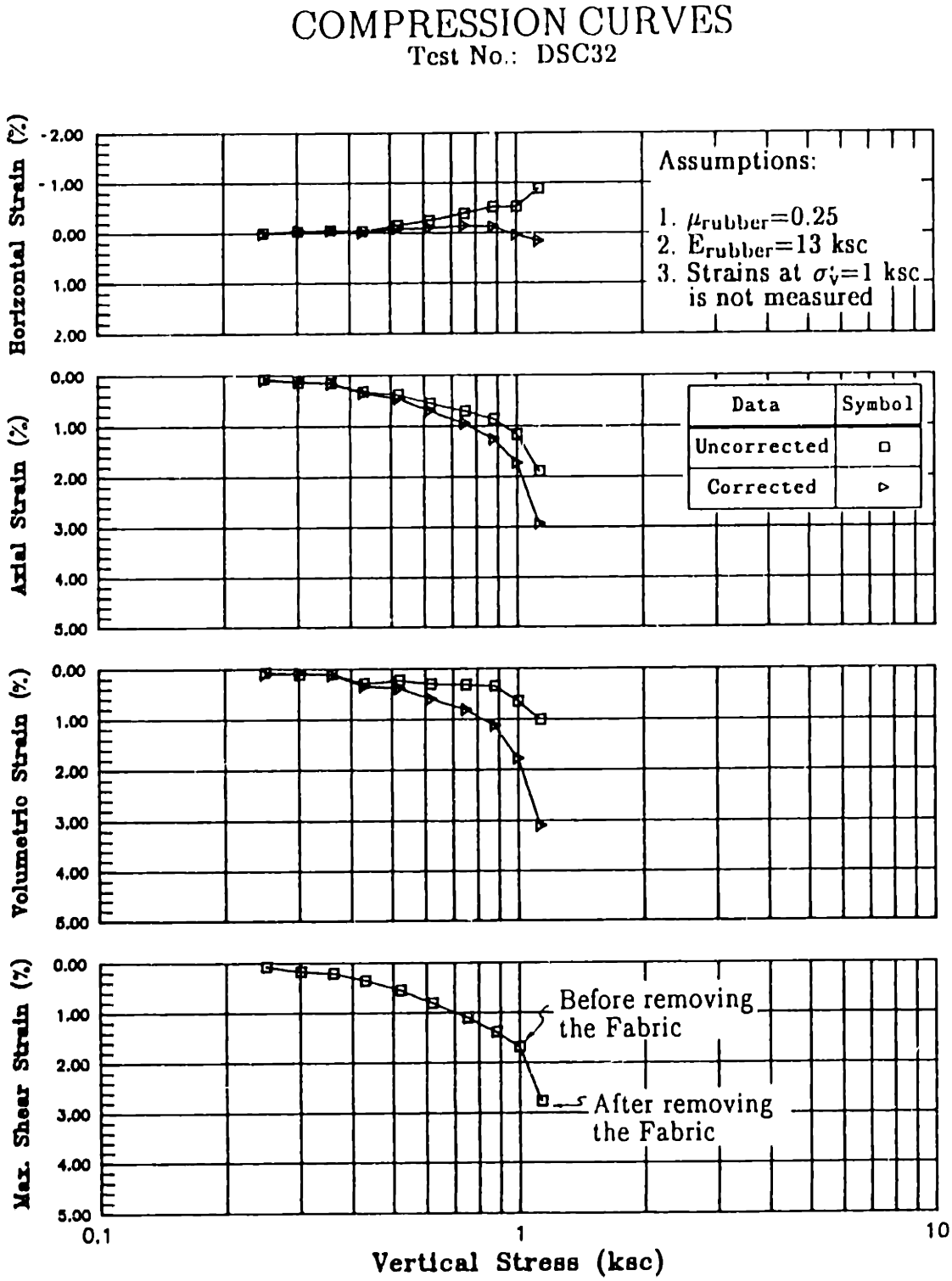

Figure 7.32: Compression Curves for Test DSC32.

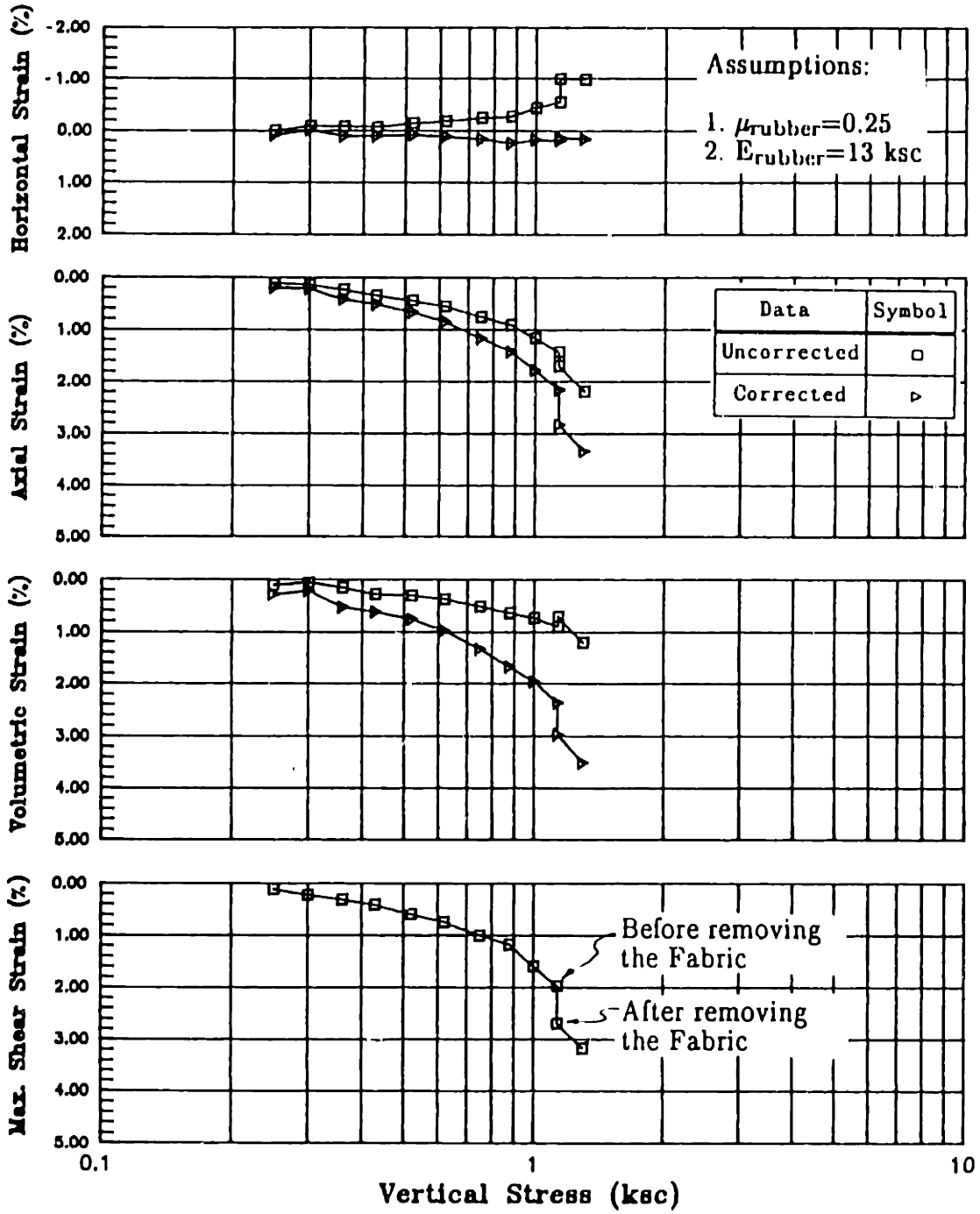

Figure 7.33: Compression Curves for Test DSC33.

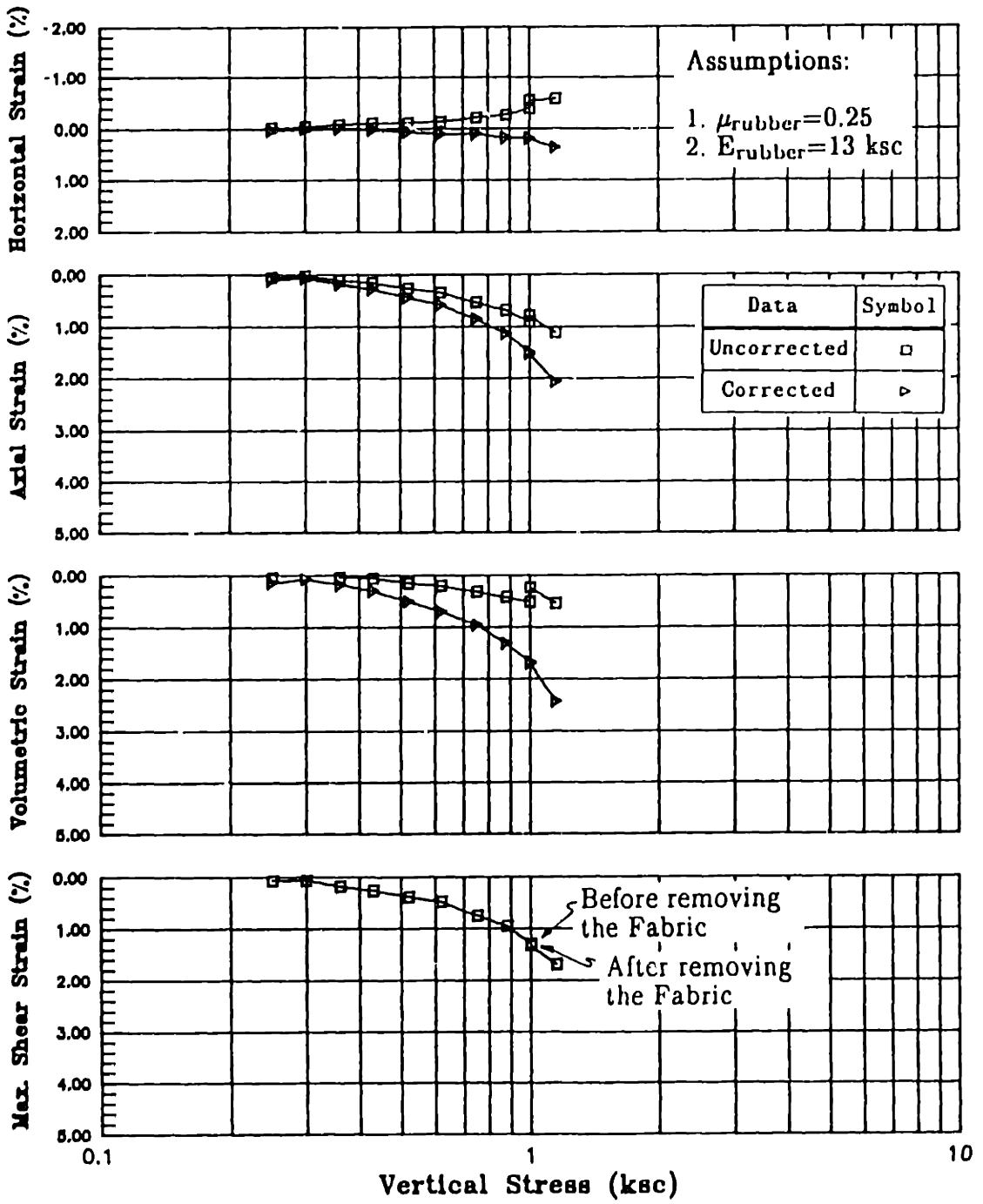

Figure 7.34: Compression Curves for Test DSC34.

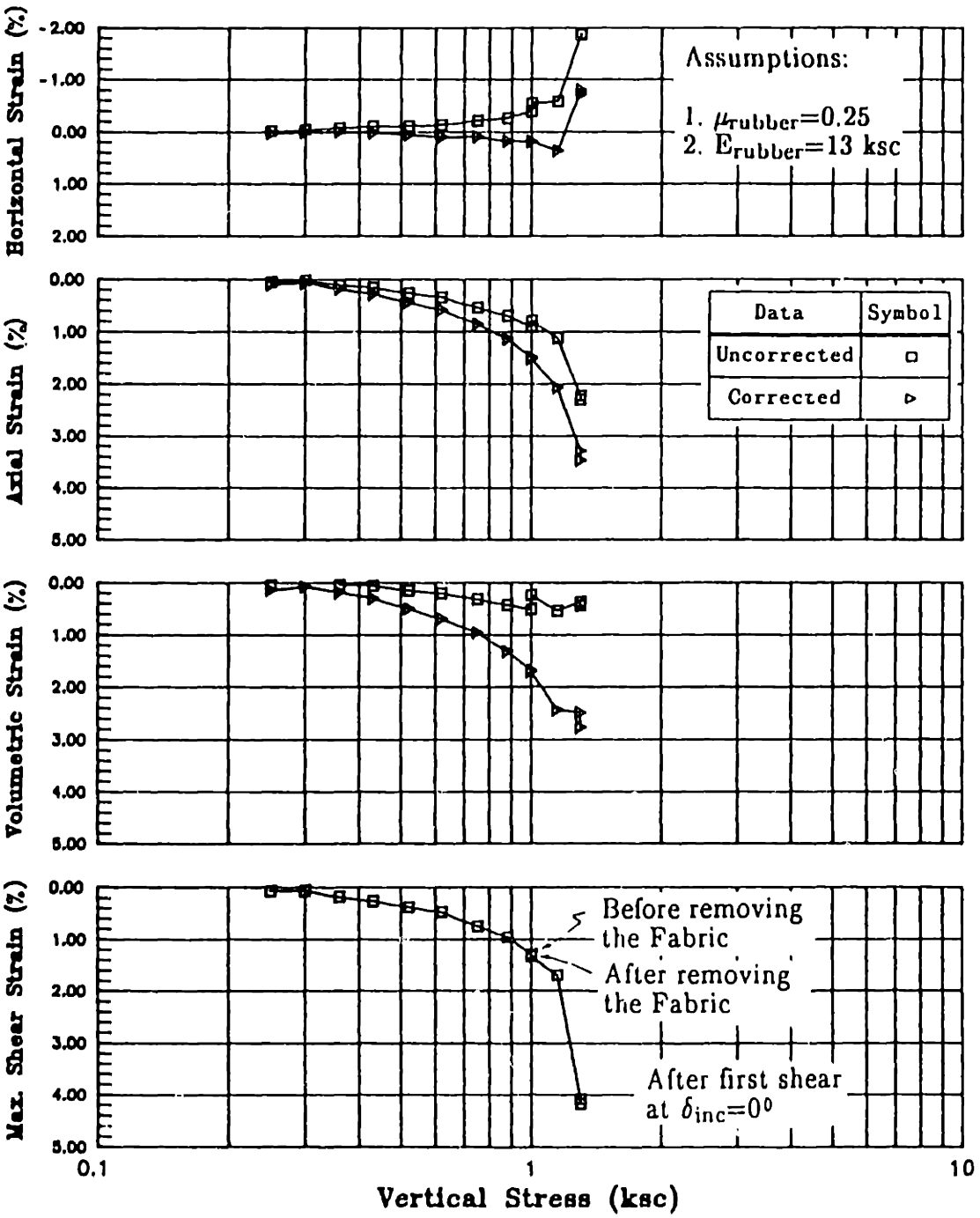

Figure 7.35: Compression Curves for Test DSC35.

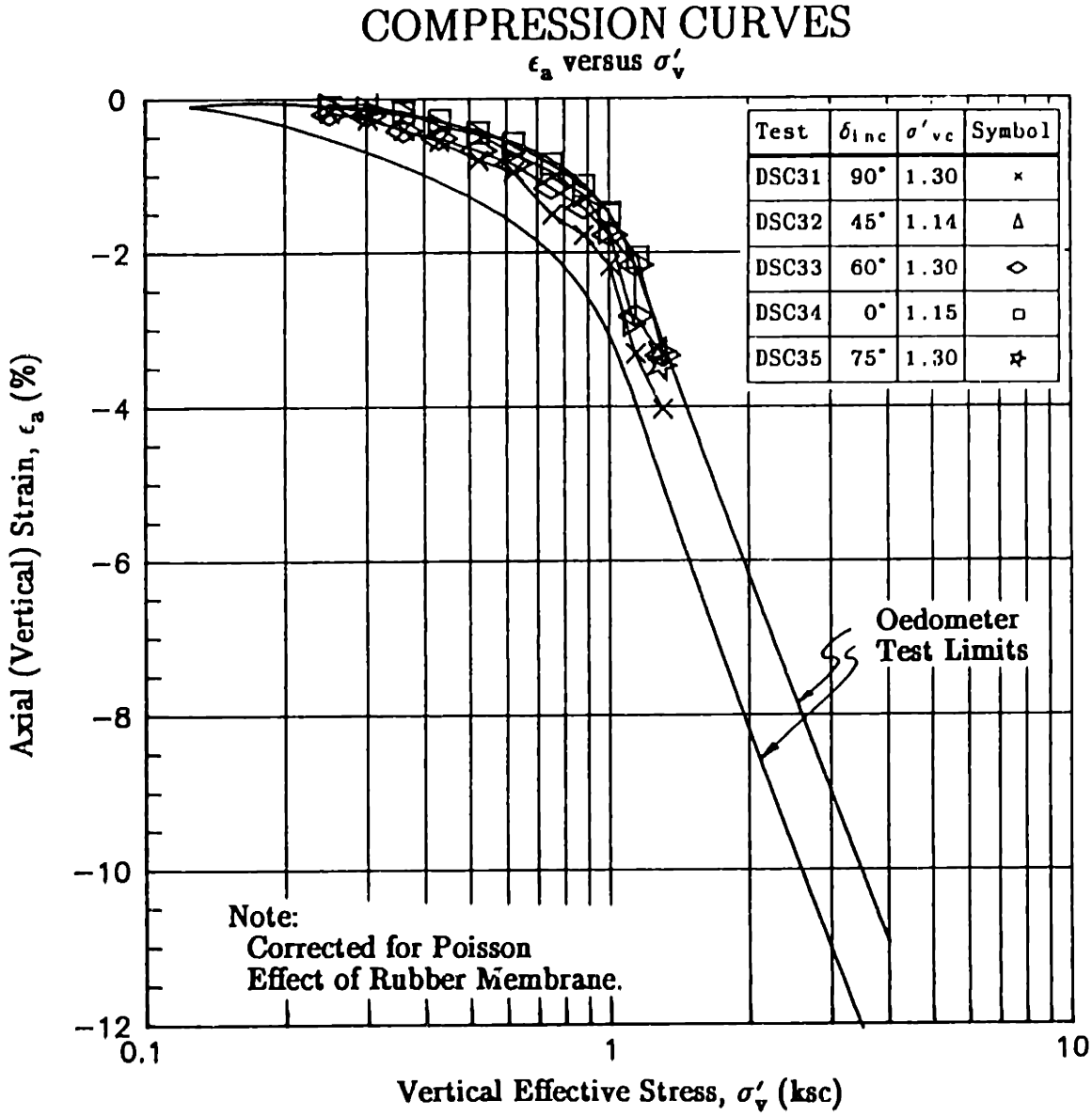

Figure 7.36: Axial Strain versus Vertical Effective Stress for DSC Tests on BBC and Ranges of Results from Oedometer Tests.

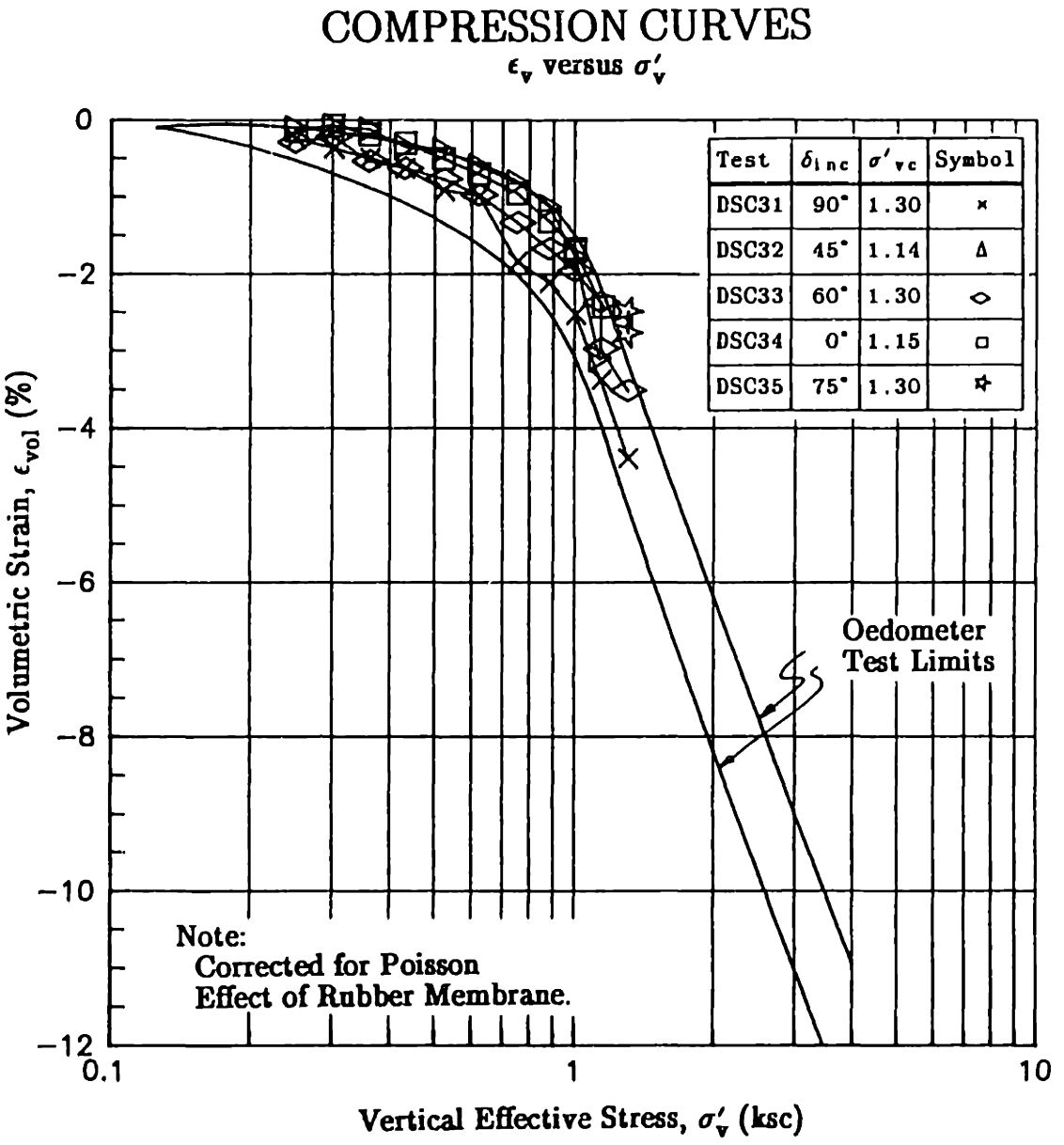

Figure 7.37: Volumetric Strain versus Vertical Effective Stress for DSC Tests on BBC and Ranges of Results from Oedometer Tests.

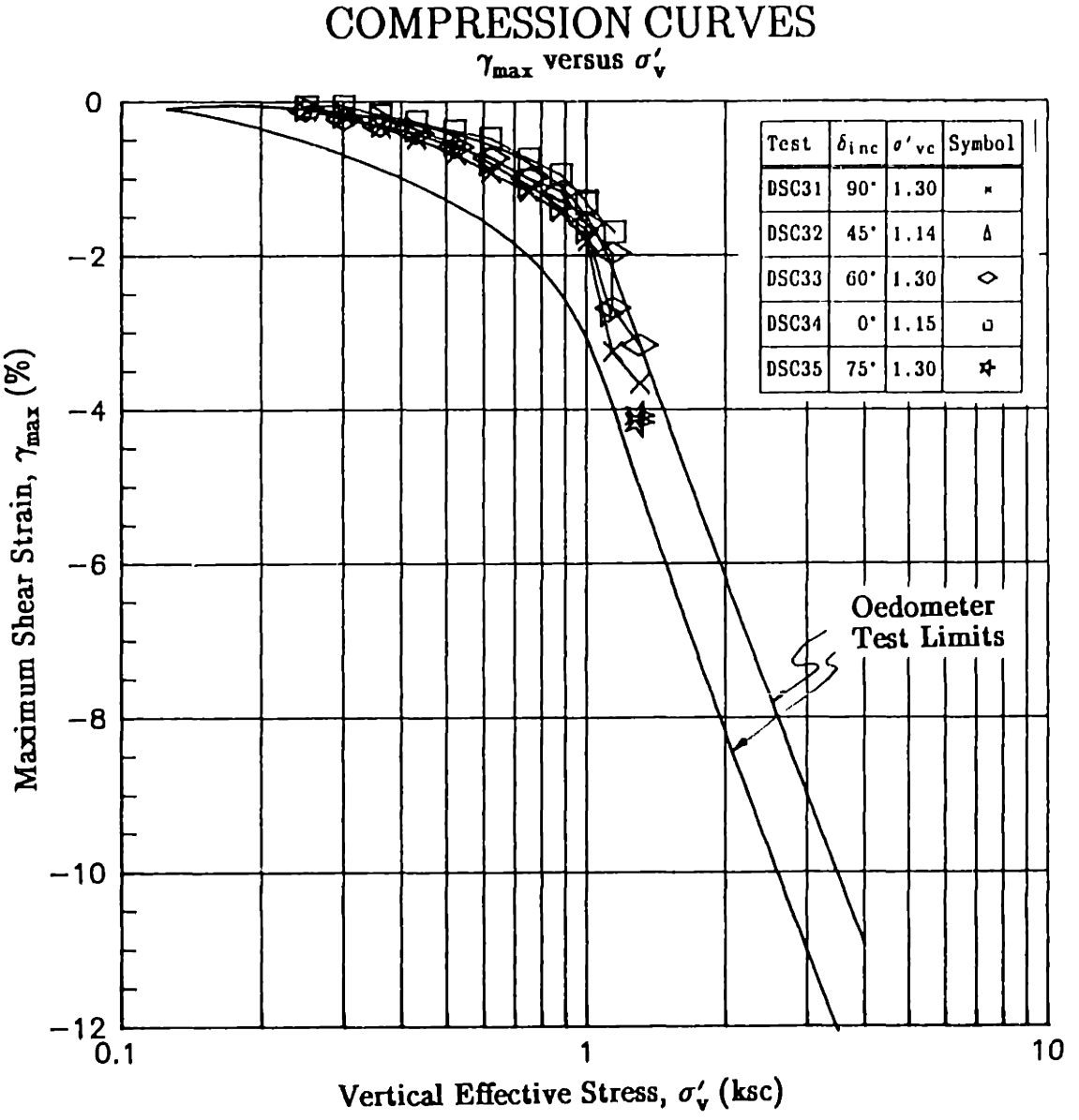

Figure 7.38: Maximum Shear Strain versus Vertical Effective Stress for DSC Tests on BBC and Ranges of Results from Oedometer Tests.

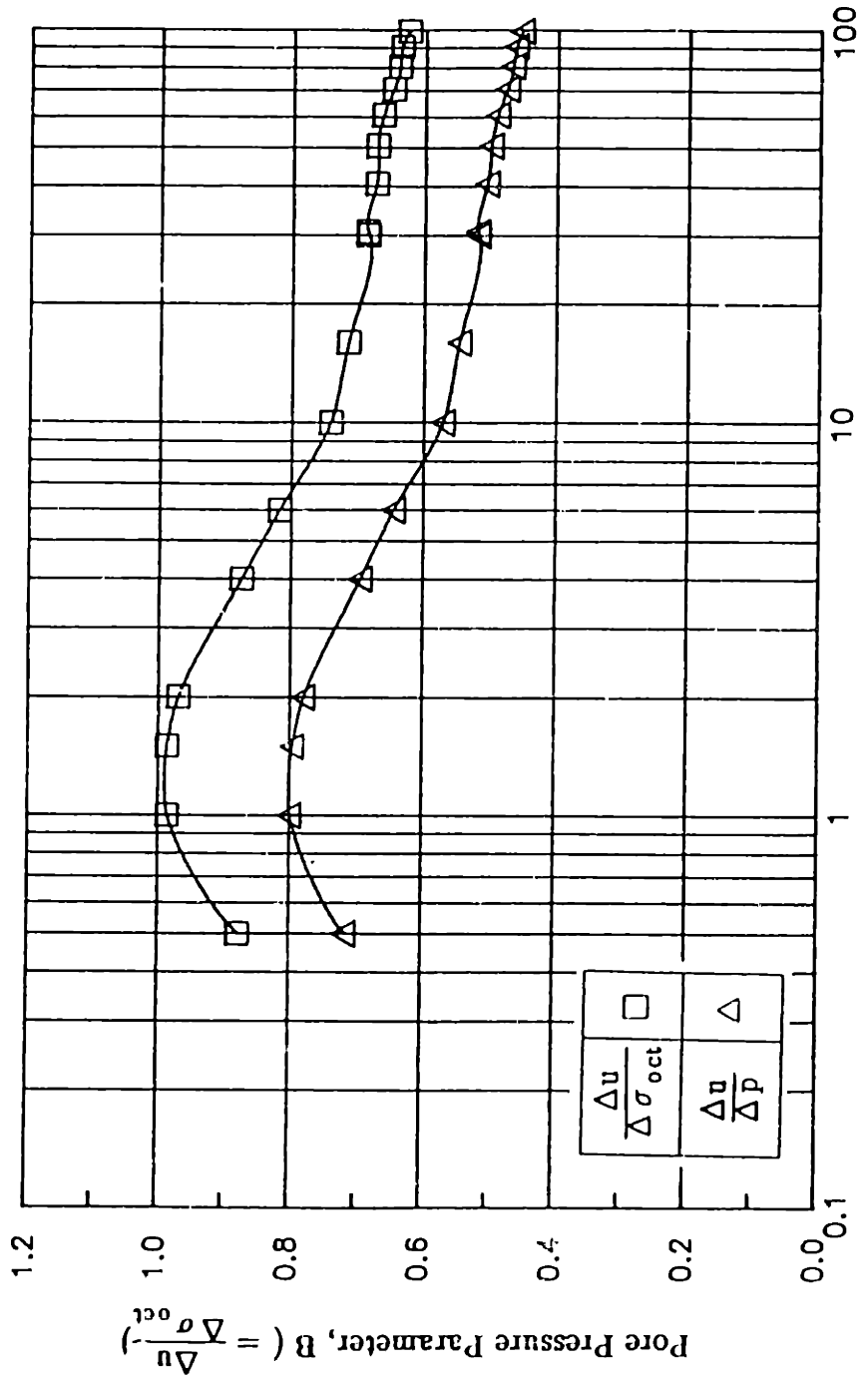

Figure 7.39: B Values computed from $\Delta\sigma_{oct}$ and $\Delta p'$ for Test DSC34 (same as Figure 6.34).

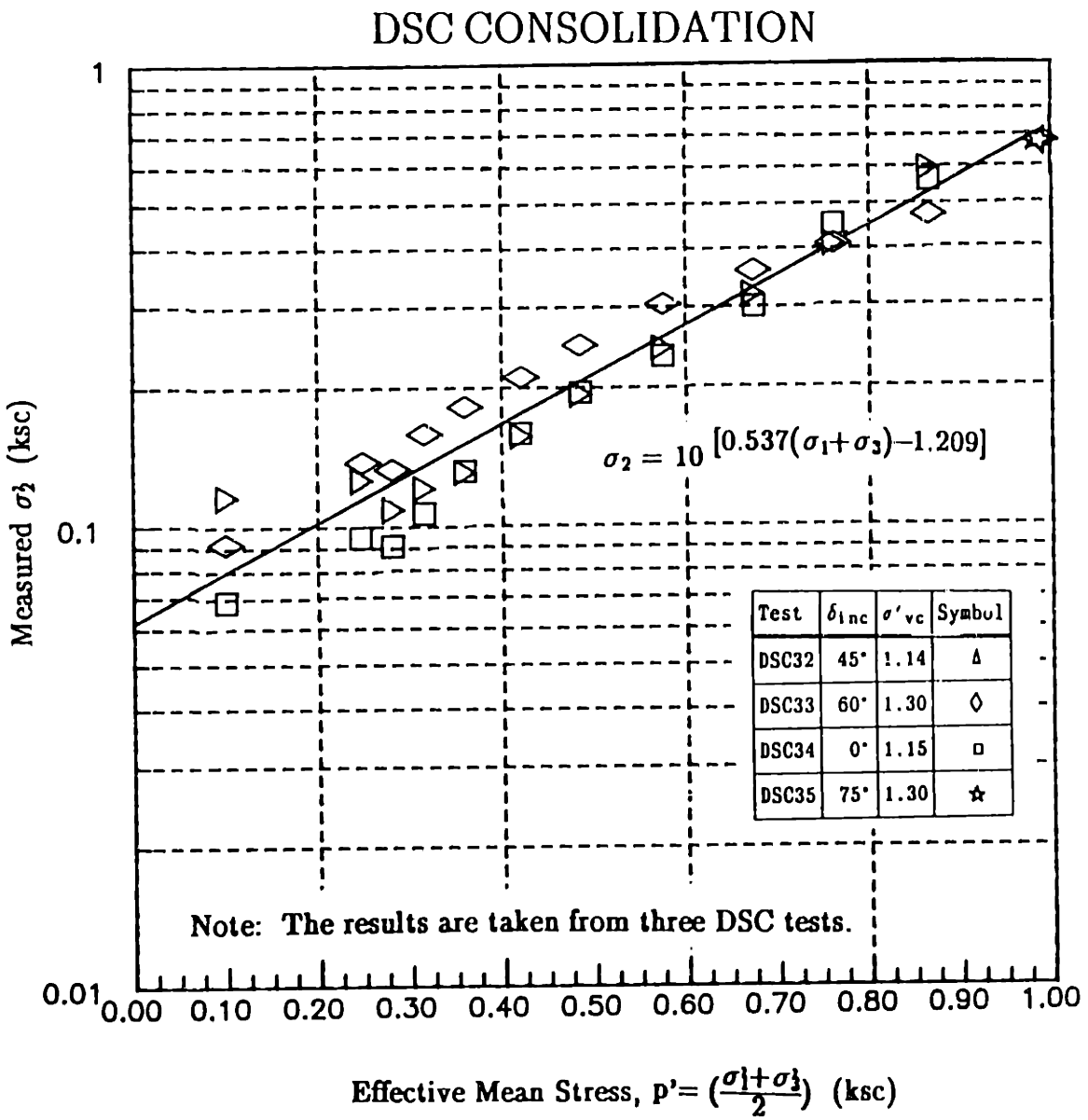

Figure 7.40: The Relationship Between Measured Intermediate Principal Stress and Mean Effective Stresses during Consolidation.

STRAIN DISTRIBUTION
Consolidation

Test No.: DSC31

Type : K_o-Consolidation
OCR : 1
σ'_{vc} : 1.300 ksc
σ_{hc} : 0.678 ksc

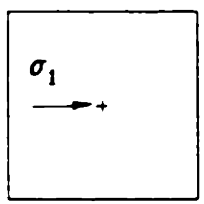

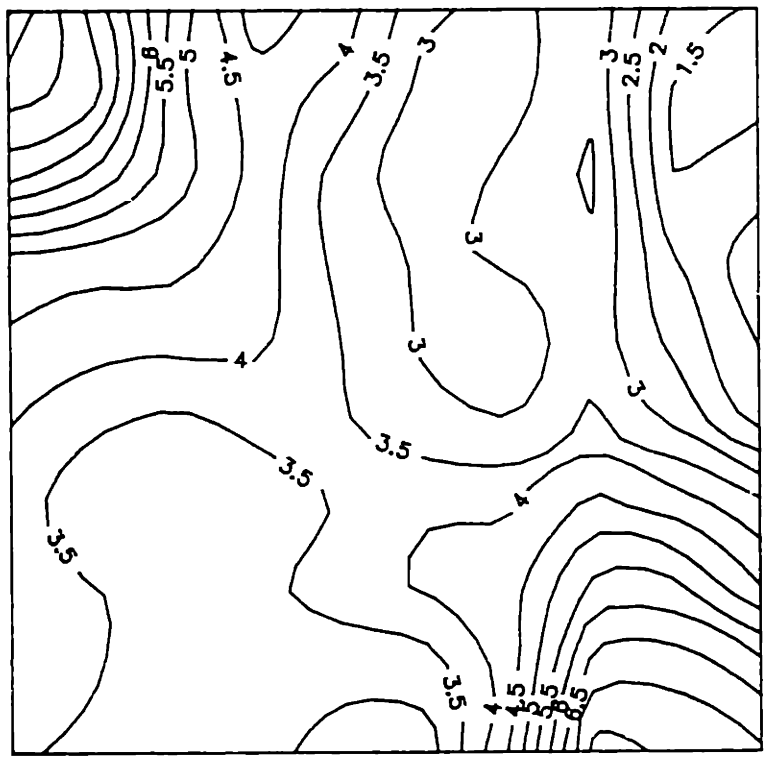

Local Strain Analysis

f = 0.08

Global Strain Analysis

γ = 3.67 ± 0.07 %

Figure 7.41: Shear Strain Distribution for Test DSC31 at the End of Consolidation.

STRAIN DISTRIBUTION
Consolidation

Test No.: DSC32

Type : K_o-Consolidation
OCR : 1
σ_{vc} : 0.878 ksc
σ_{hc} : 0.468 ksc

Local Strain Analysis

f = 0.08

Global Strain Analysis

γ = 1.39 ± 0.05 %

Figure 7.42: Shear Strain Distribution for Test DSC32 at σ'_{vc}=0.878 ksc.

STRAIN DISTRIBUTION
Consolidation

Test No.: DSC33

Type : K_o-Consolidation
OCR : 1
σ'_{vc} : 1.300 ksc
σ_{hc} : 0.677 ksc

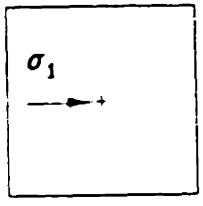

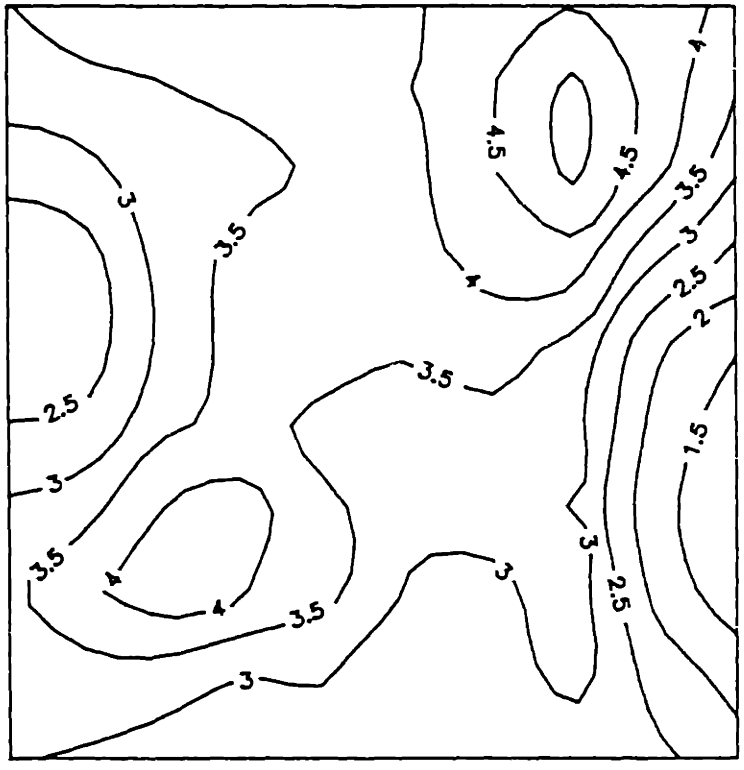

Local Strain Analysis

f = 0.08

Global Strain Analysis

γ = 3.18 ± 0.06 %

Figure 7.43: Shear Strain Distribution for Test DSC33 of the End of Consolidation.

STRAIN DISTRIBUTION
Consolidation

Test No.: DSC34

Type : K_o-Consolidation
OCR : 1
σ'_{vc} : 1.149 ksc
σ_{hc} : 0.582 ksc

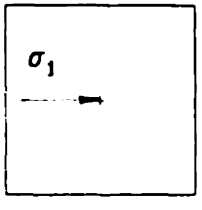

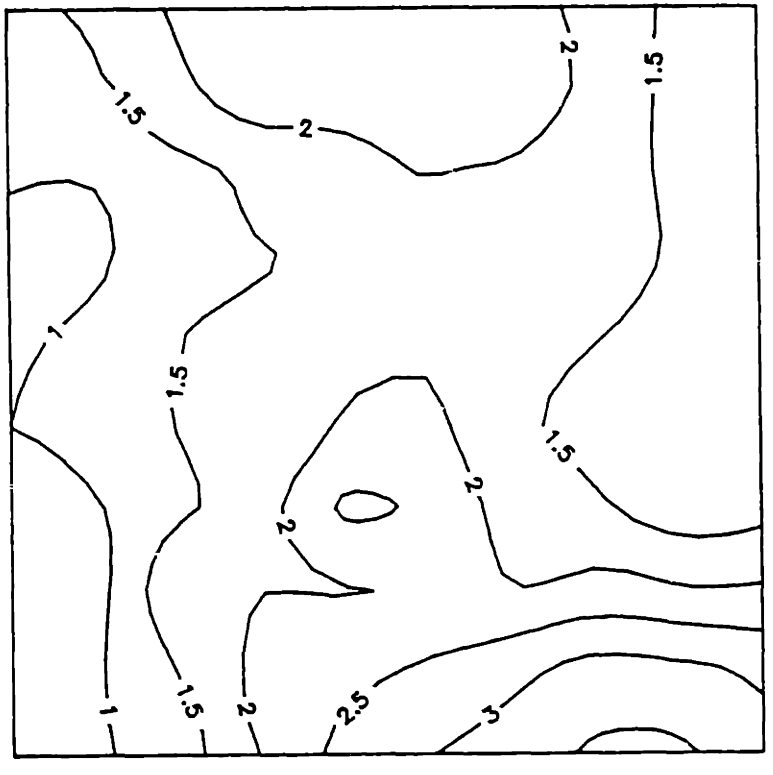

Local Strain Analysis

f = 0.08

Global Strain Analysis

γ = 1.70 ± 0.04 %

Figure 7.44: Shear Strain Distribution for Test DSC34 of the End of Consolidation.

STRAIN DISTRIBUTION
Consolidation

Test No.: DSC35

Type : K_o-Consolidation
OCR : 1
σ'_{vc} : 1.299 ksc
σ_{hc} : 0.676 ksc

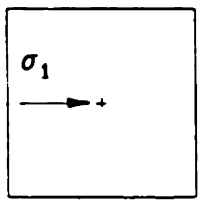

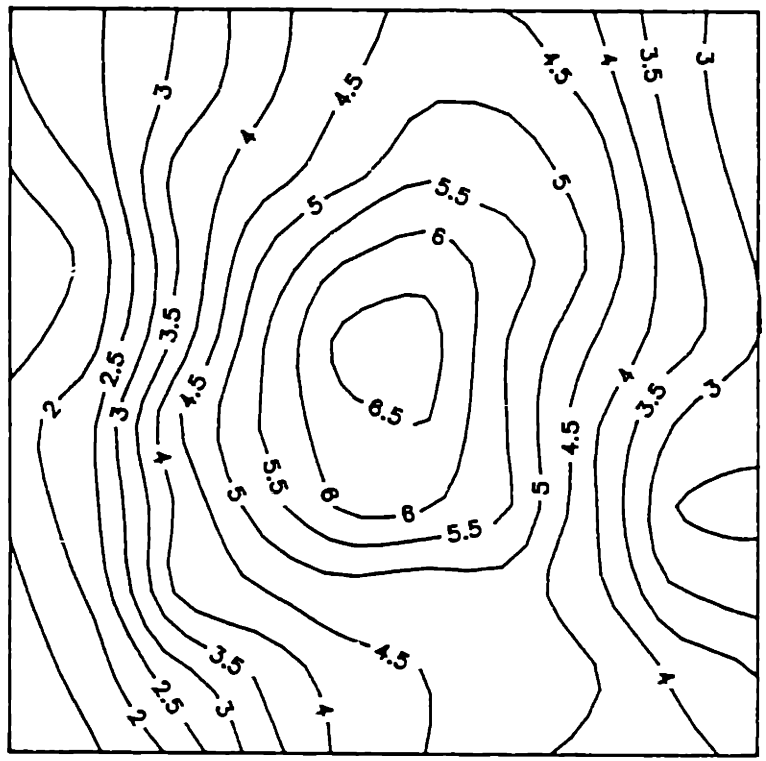

Local Strain Analysis

f = 0.08

Global Strain Analysis

γ = 4.09 ± 0.10 %

Figure 7.45: Shear Strain Distribution for Test DSC35 at the End of Consolidation.

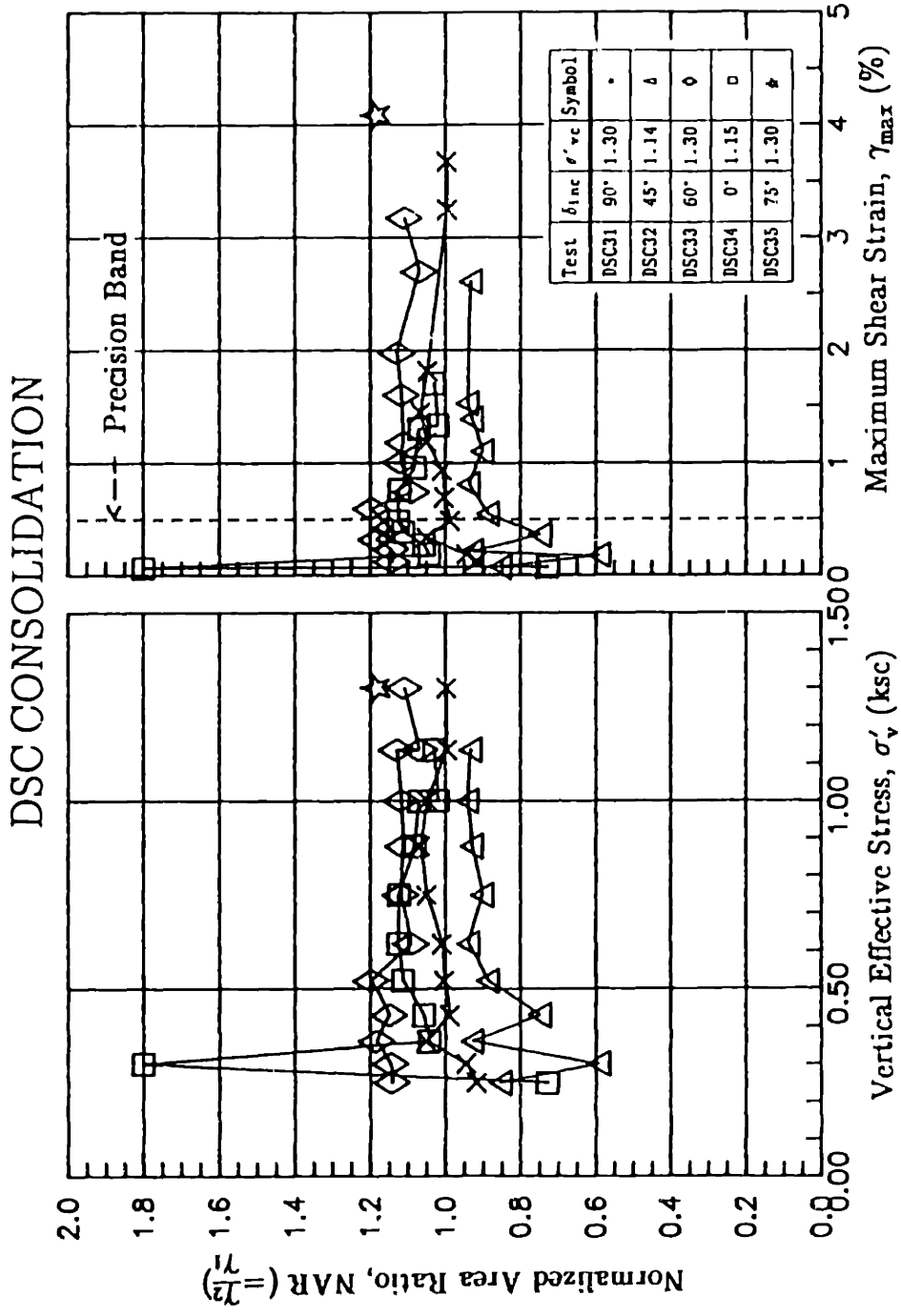

Figure 7.46: Variation of NAR with (a) Vertical Effective Stress and with (b) Maximum Shear Strain from DSC Tests during Consolidation.

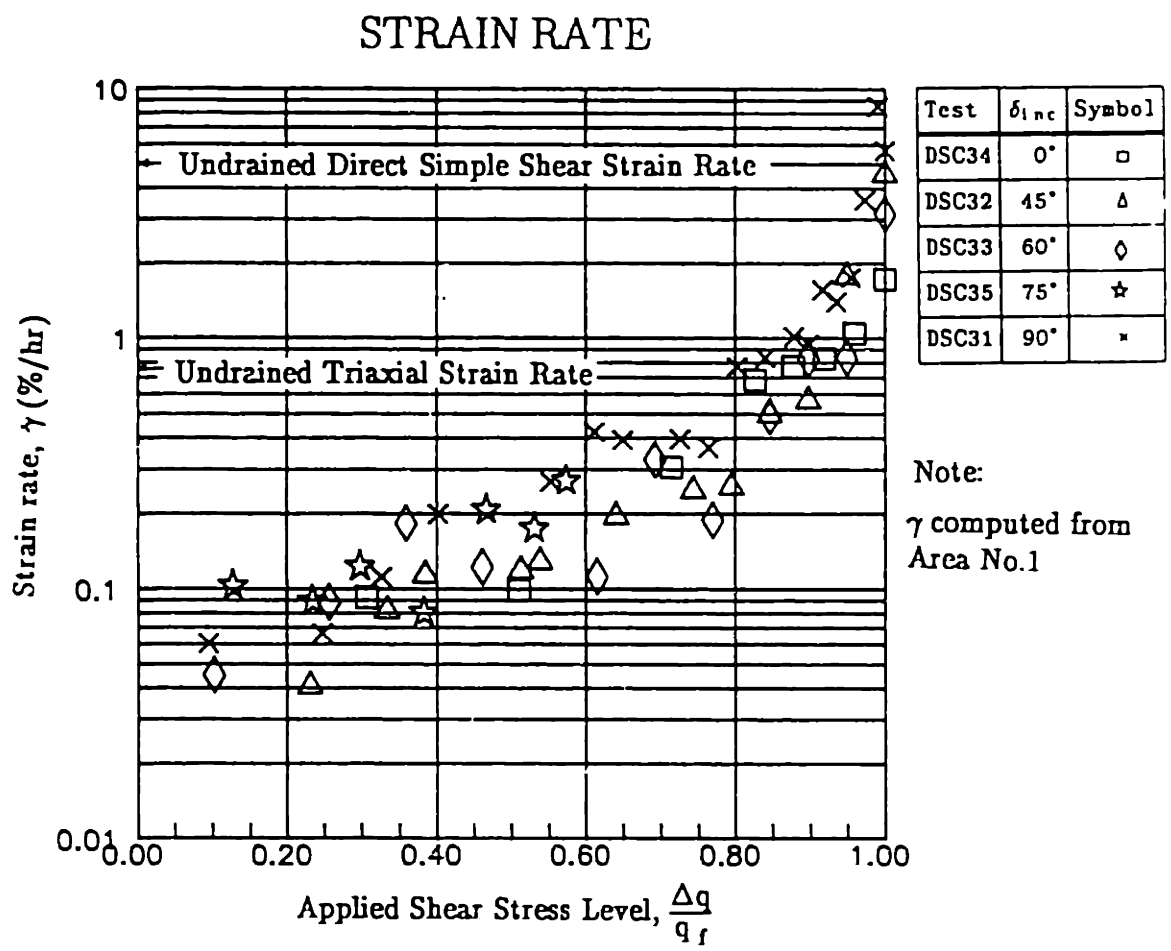

Figure 7.47: Shear Strain Rates from DSC Tests on BBC at OCR=1.

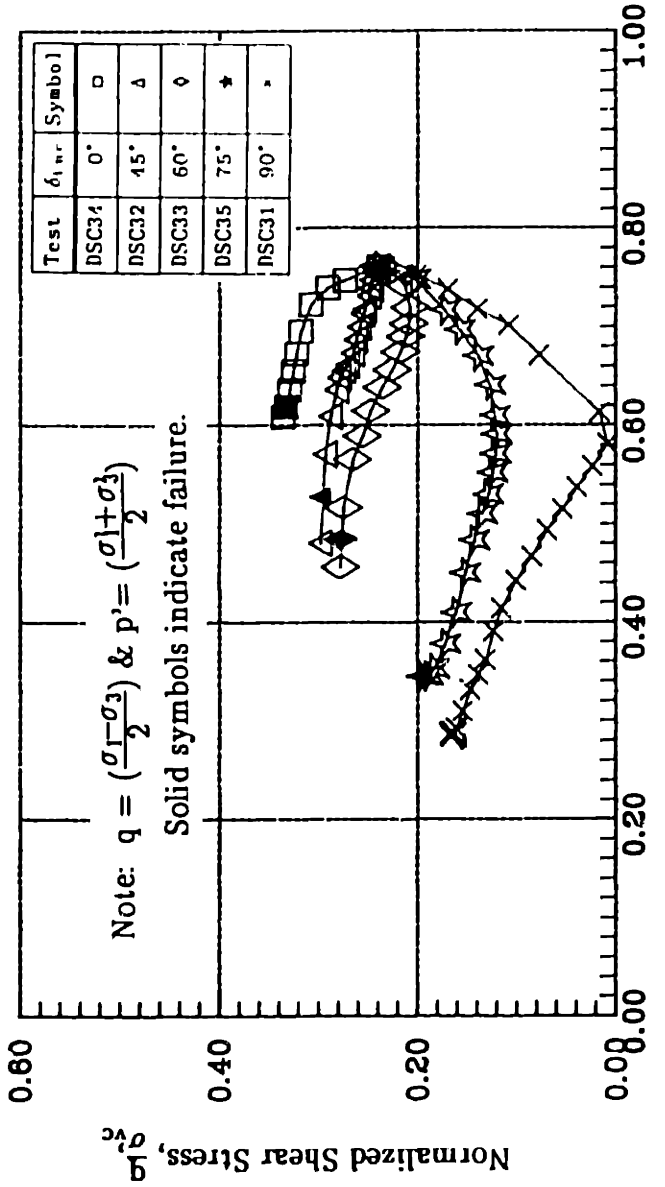

Figure 7.48: Normalized Effective Stress Paths for DSC Tests on BBC at OCR=1.

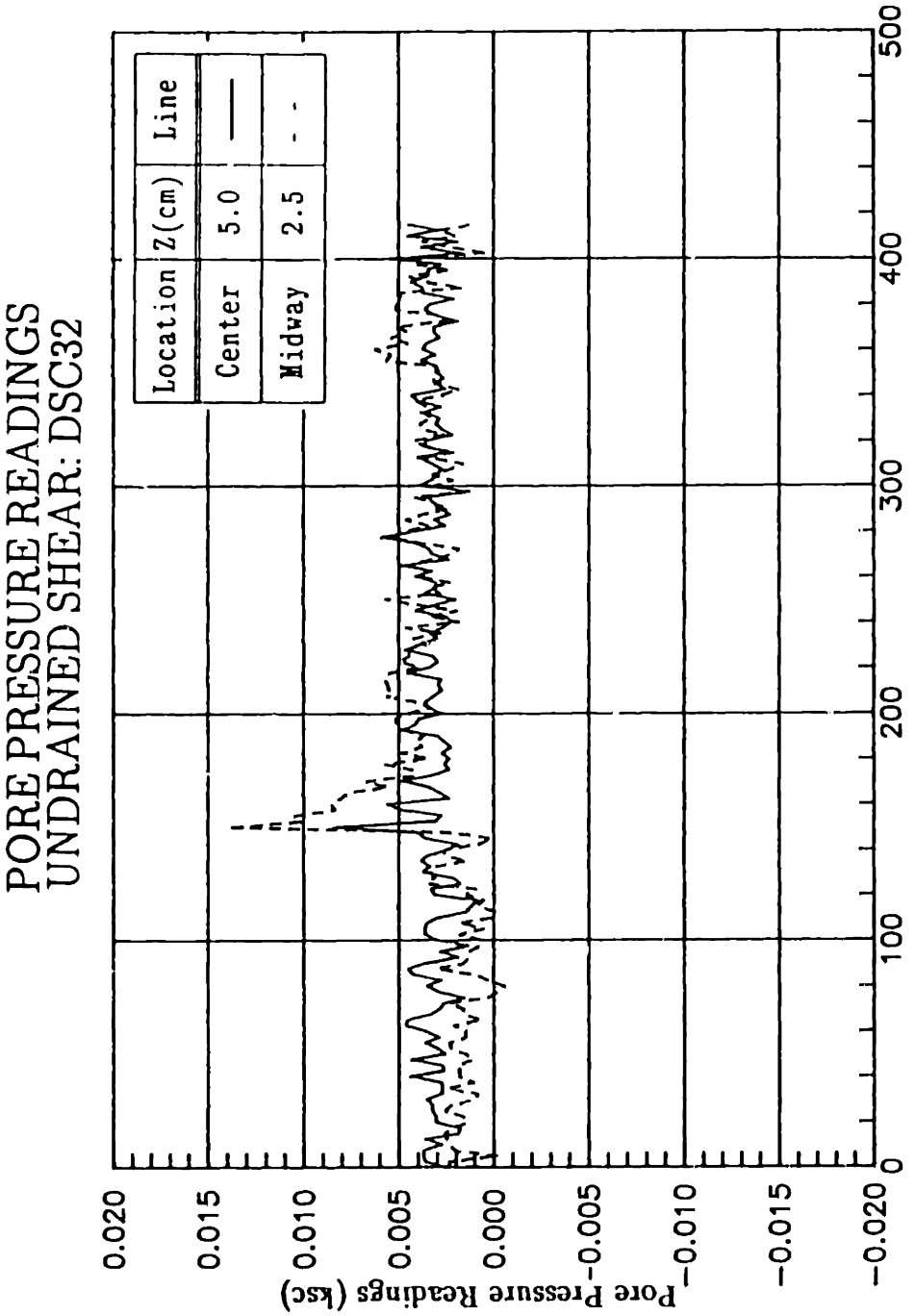

Figure 7.49: Pore Pressure Readings at Two Different Locations in the Sample from Test DSC32 During Undrained Shear.

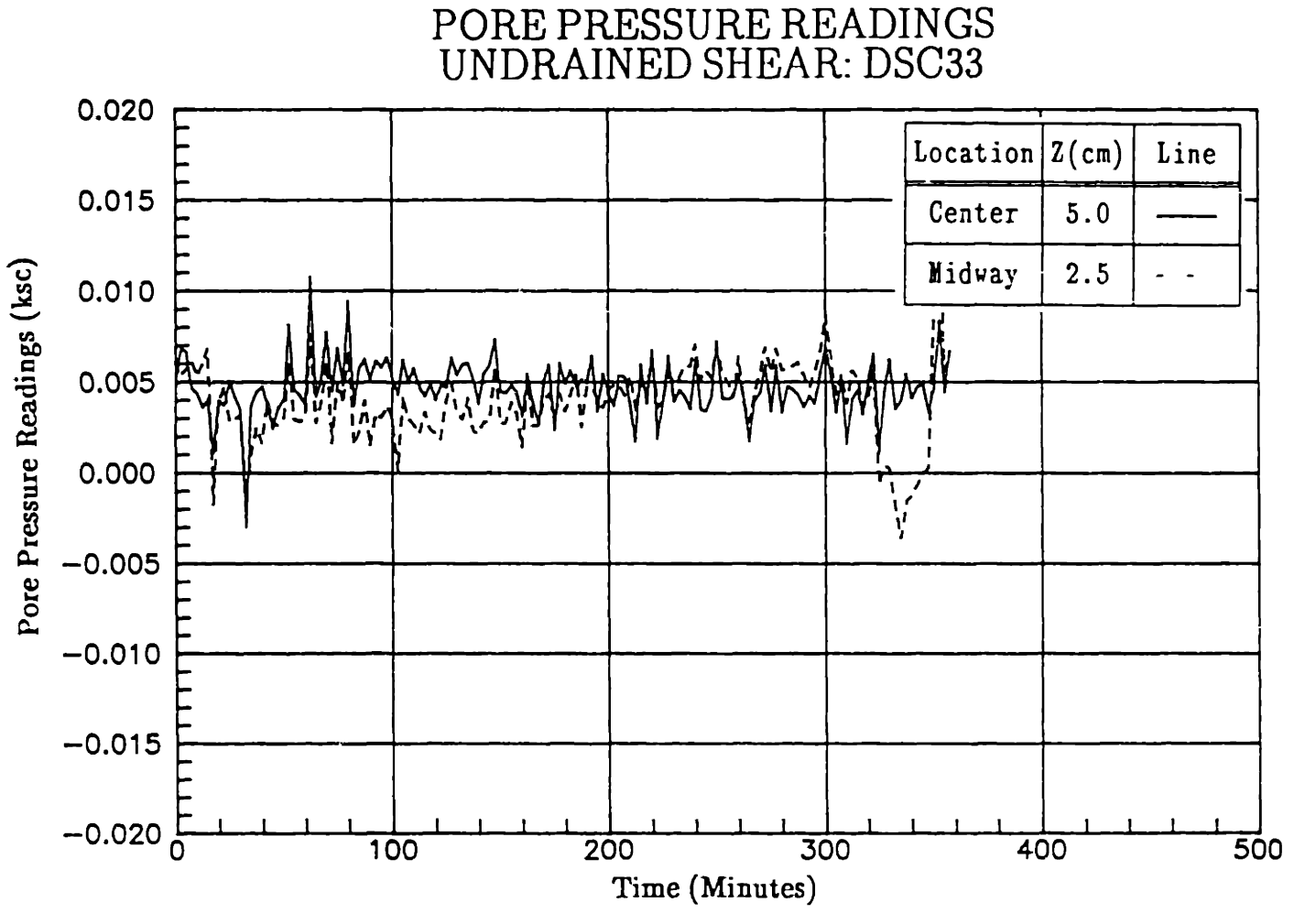

Figure 7.50: Pore Pressure Readings at Two Different Locations in the Sample from Test DSC33 During Undrained Shear.

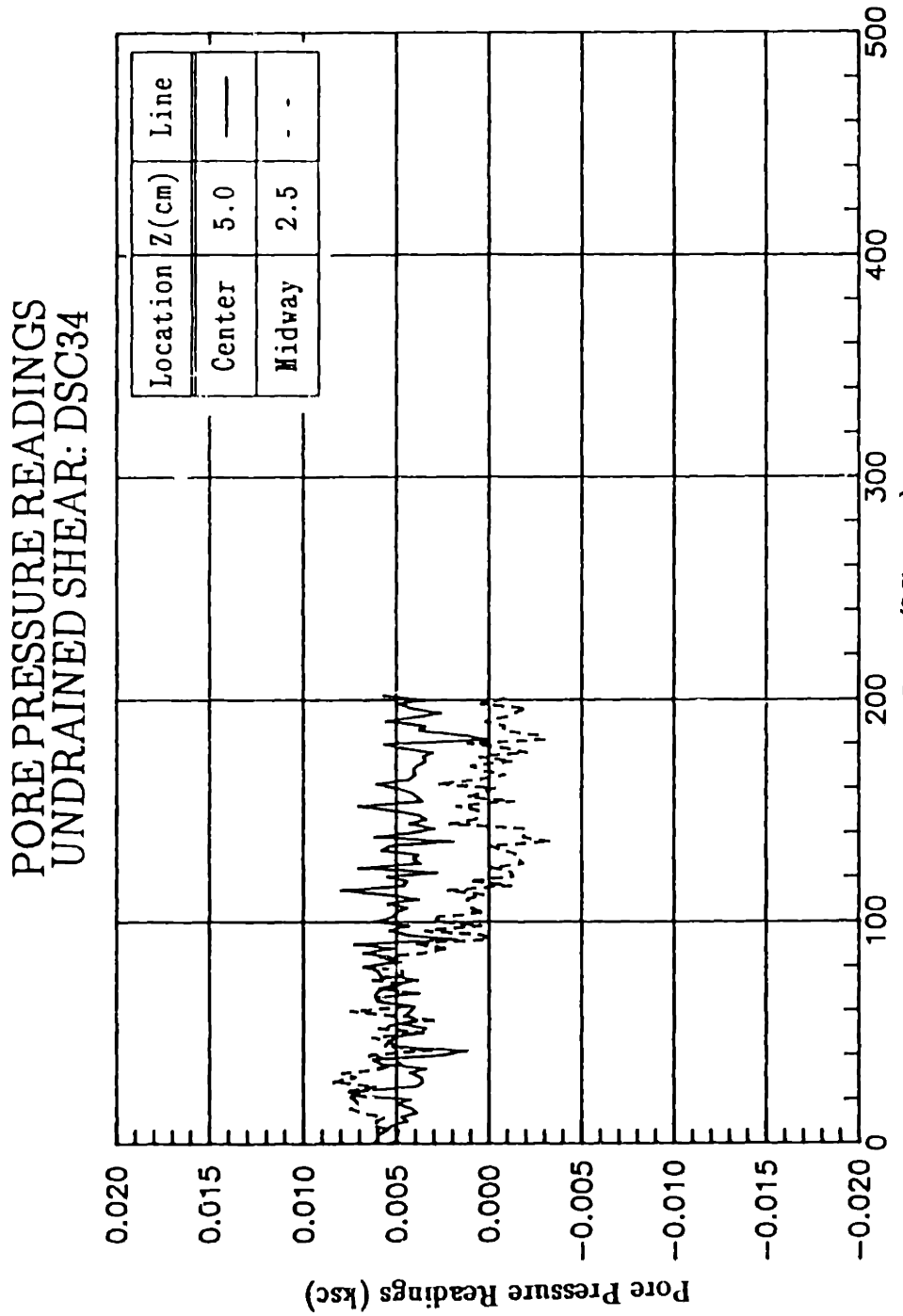

Figure 7.51: Pore Pressure Readings at Two Different Locations in the Sample from Test DSC34 During Undrained Shear.

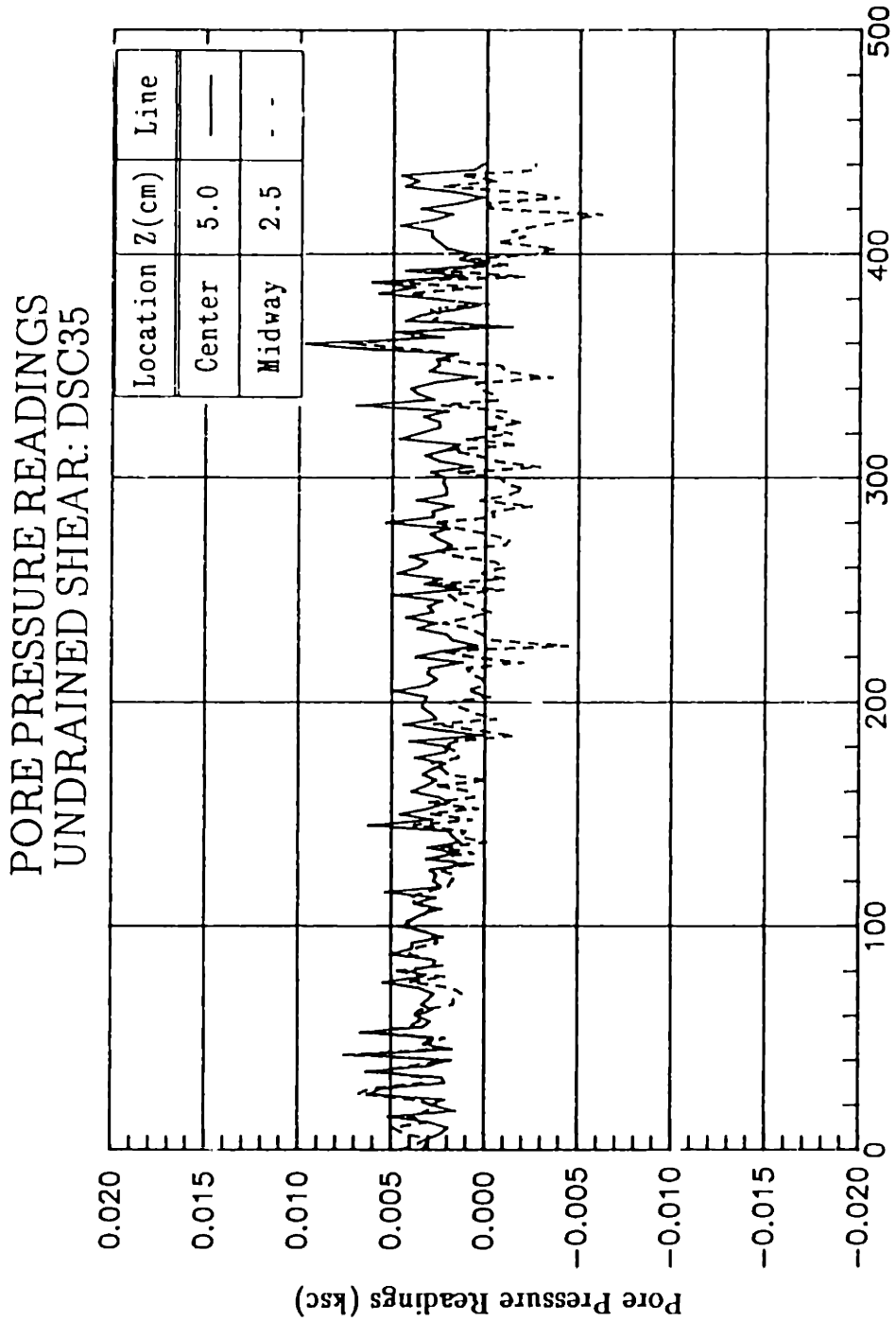

Figure 7.52: Pore Pressure Readings at Two Different Locations in the Sample from Test DSC35 During Undrained Shear.

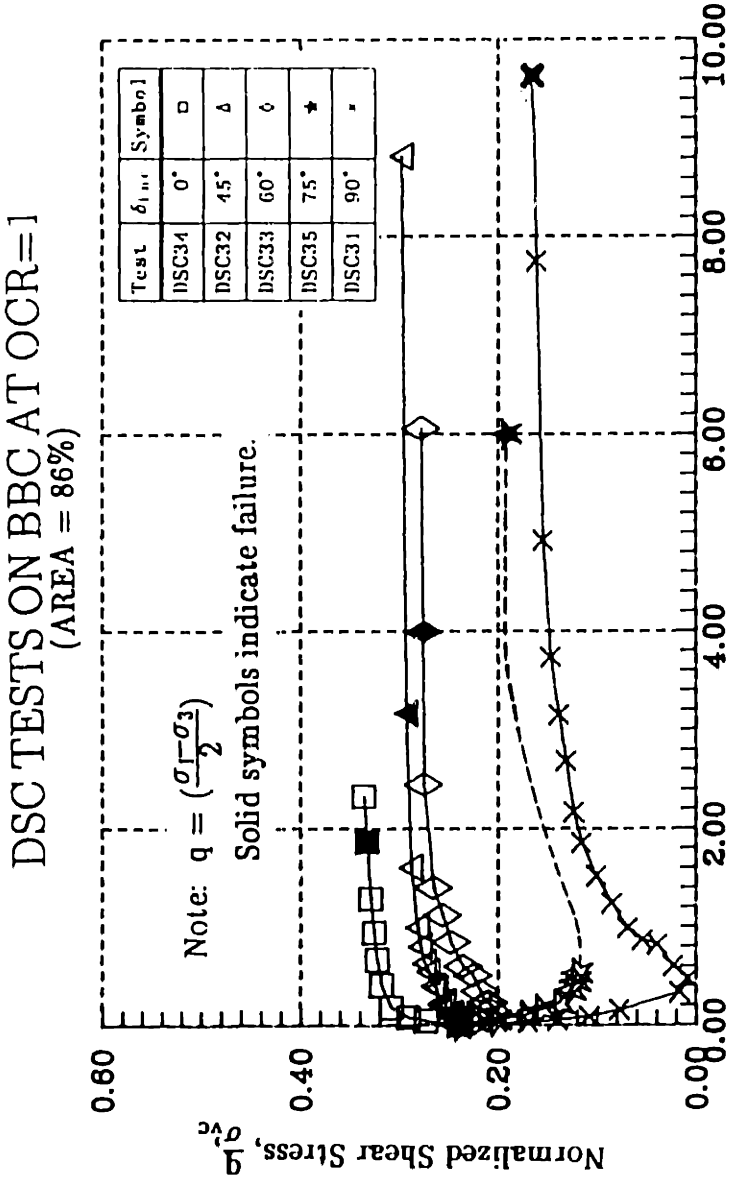

Figure 7.53a: Stress–Strain Relationships from DSC Tests on OCR=1 BBC (Area No. 1).

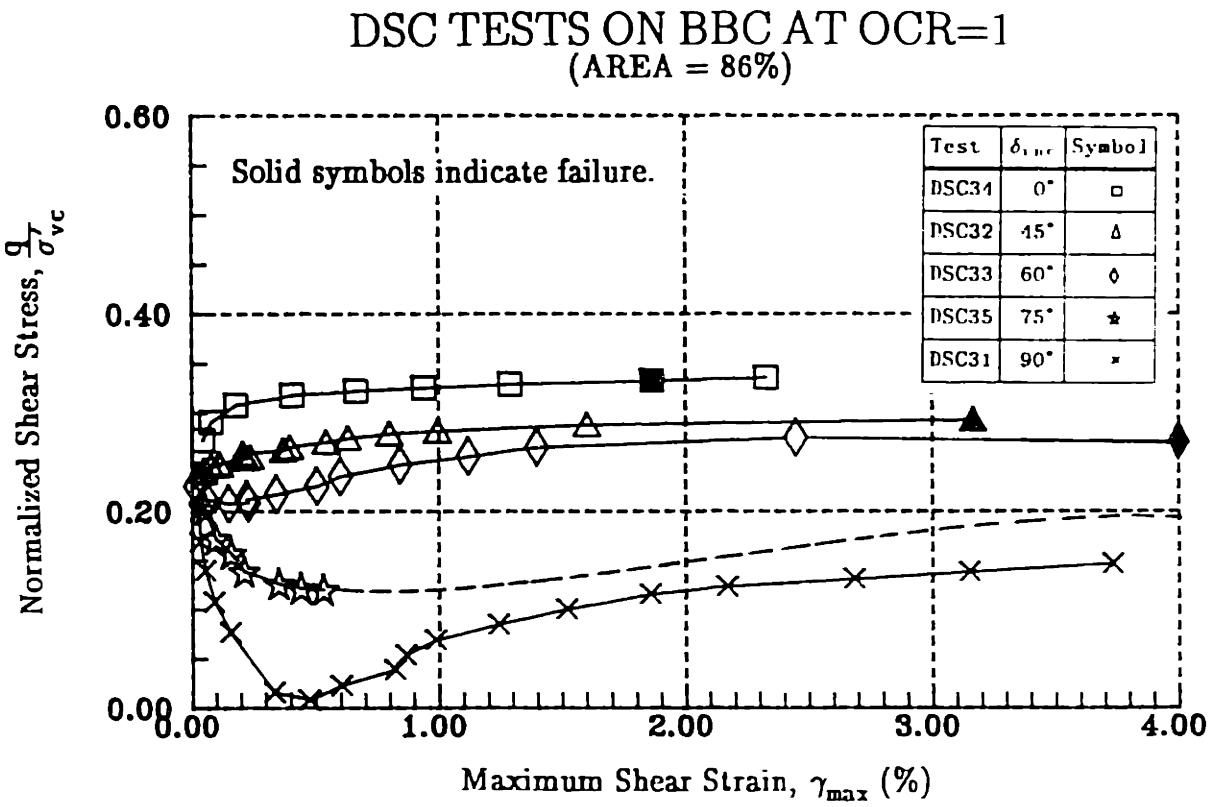

Figure 7.53b: Stress–Strain Relationships from DSC Tests on OCR=1 BBC (Area No. 1).

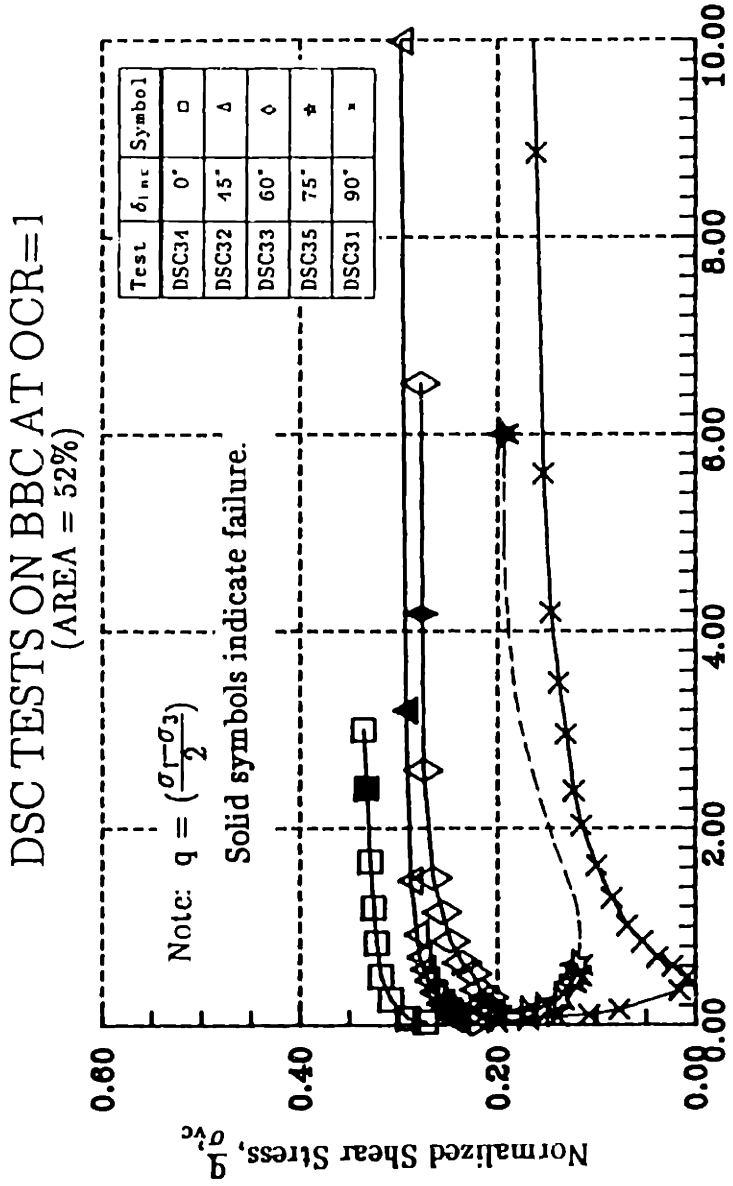

Figure 7.54a: Stress–Strain Relationships from DSC Tests on OCR=1 BBC (Area No. 2).

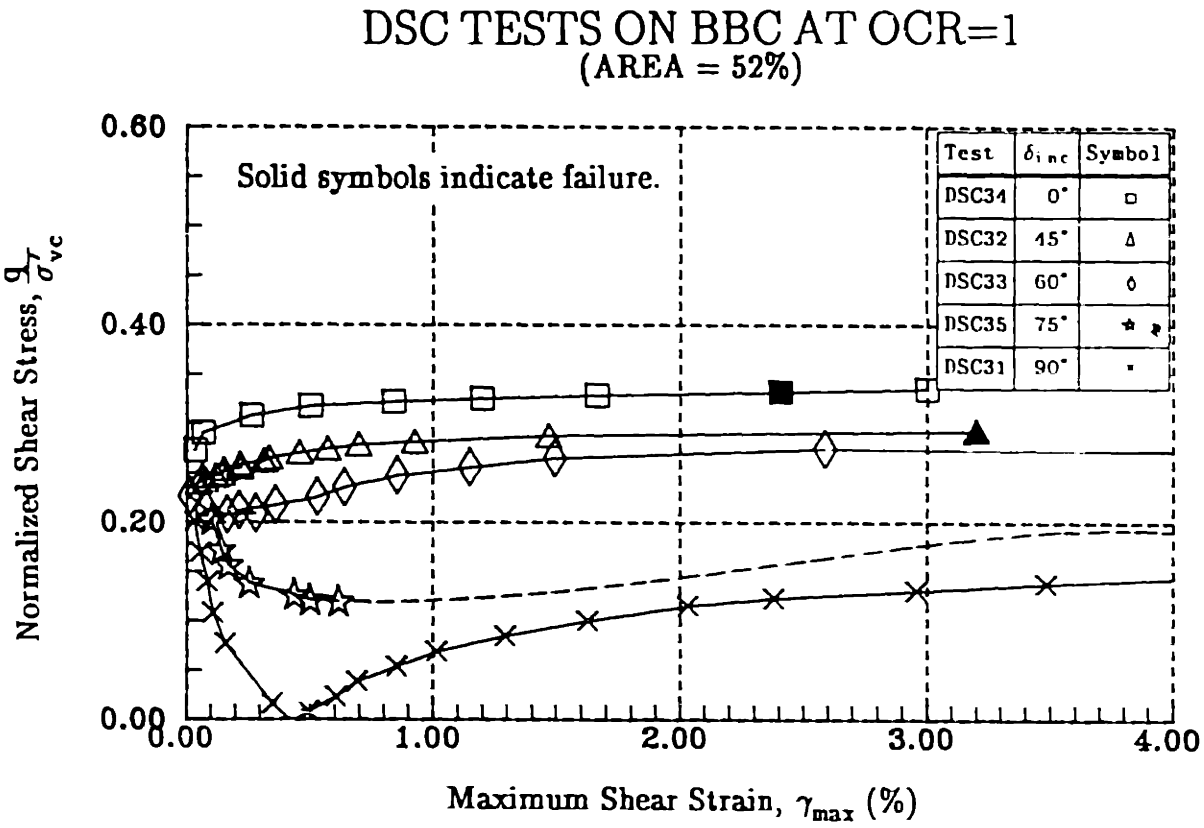

Figure 7.54b: Stress–Strain Relationships from DSC Tests on OCR=1 BBC (Area No. 2).

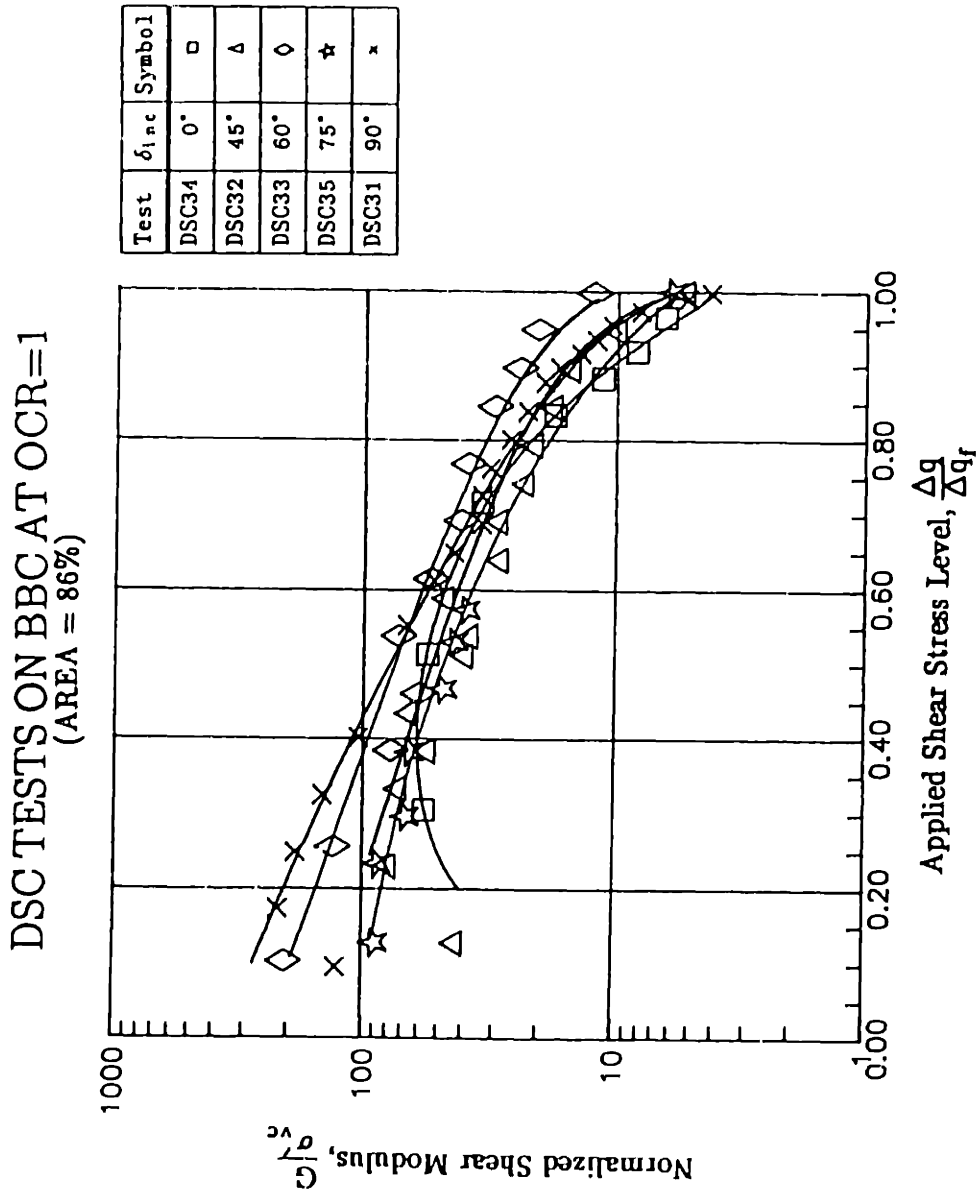

Figure 7.55: Variation of Normalized Shear Modulus with Applied Shear Stress Level from DSC Tests on OCR=1 BBC.

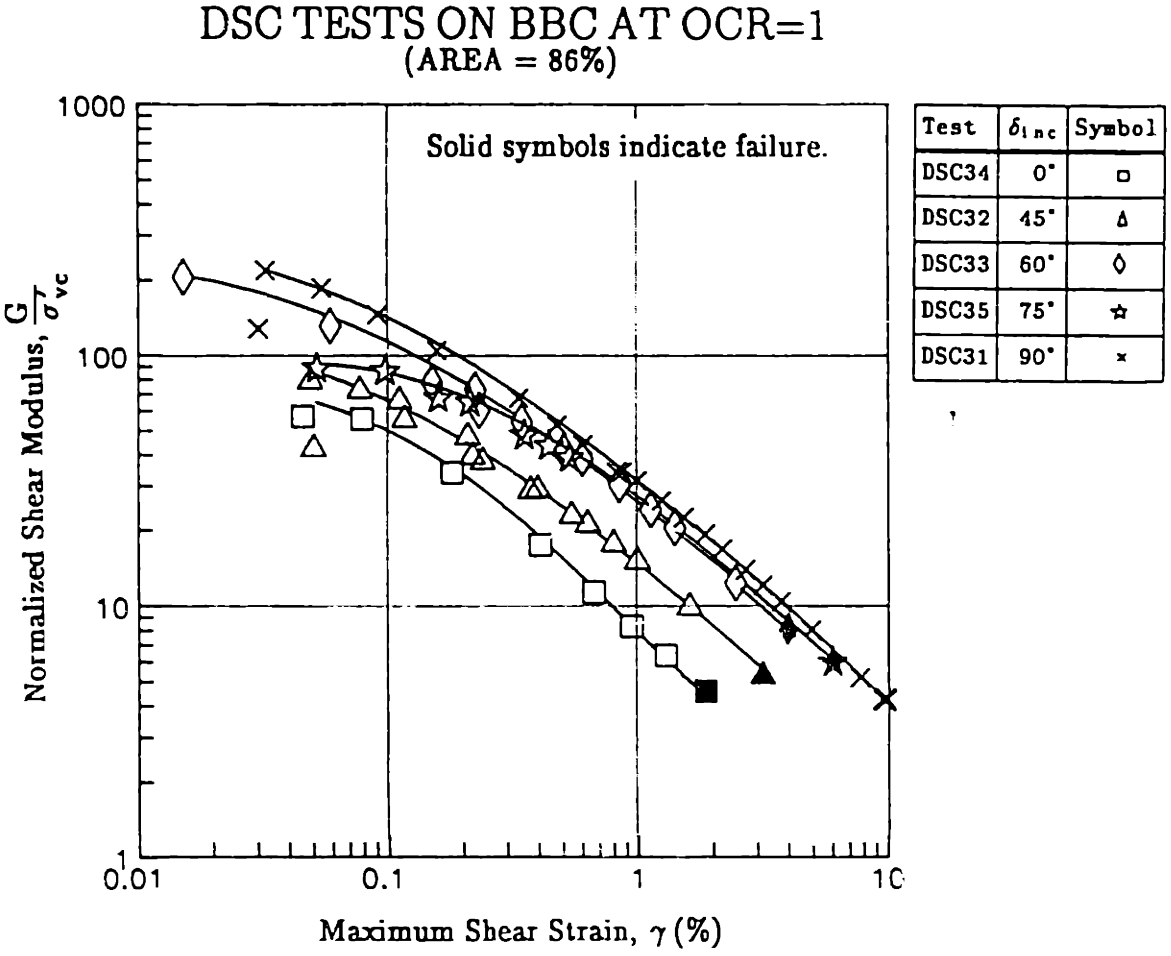

Figure 7.56: Variation of Normalized Shear Modulus with Maximum Shear Strain from DSC Tests on OCR=1 BBC.

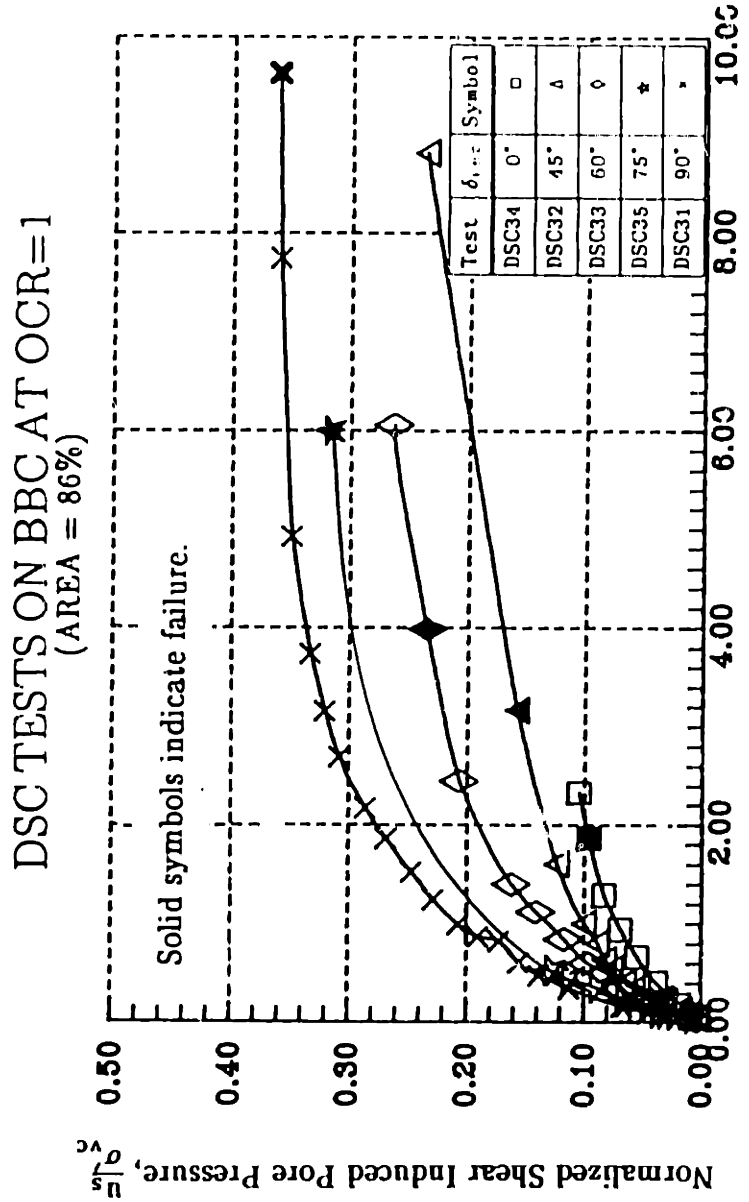

Figure 7.57a: Normalized Shear Induced Pore Pressure versus Maximum Shear Strain for DSC Tests on OCR=1 BBC (Area No. 1).

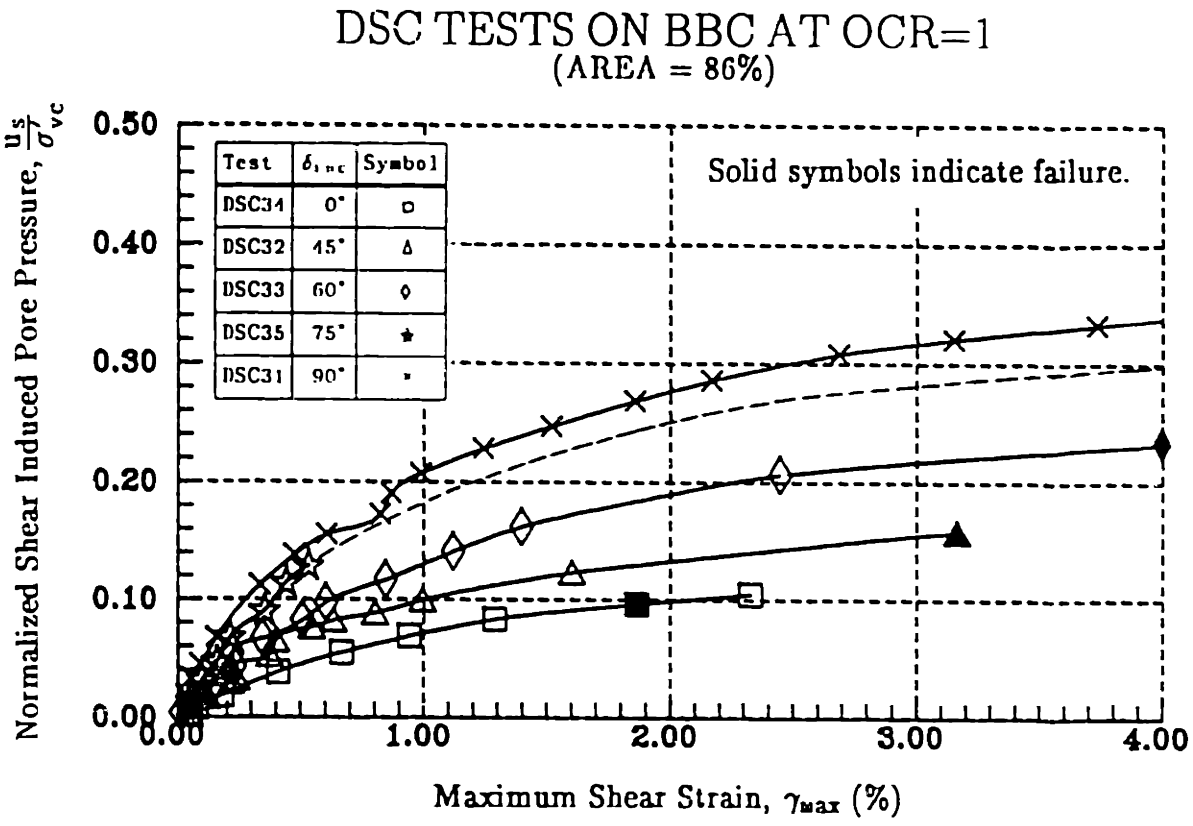

Figure 7.57b: Normalized Shear Induced Pore Pressure versus Maximum Shear Strain for DSC Tests on OCR=1 BBC (Area No. 1).

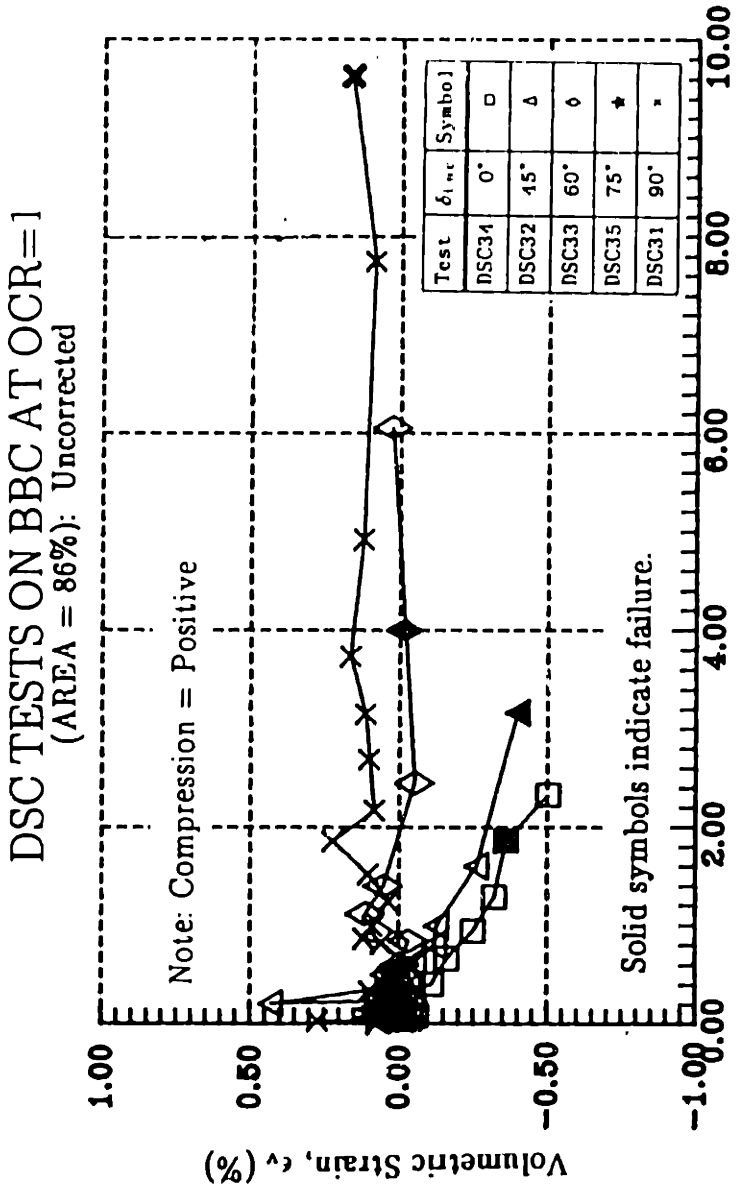

Figure 7.58: Uncorrected Volumetric Strain versus Maximum Shear Strain for DSC Tests on OCR=1 BBC (Area No. 1).

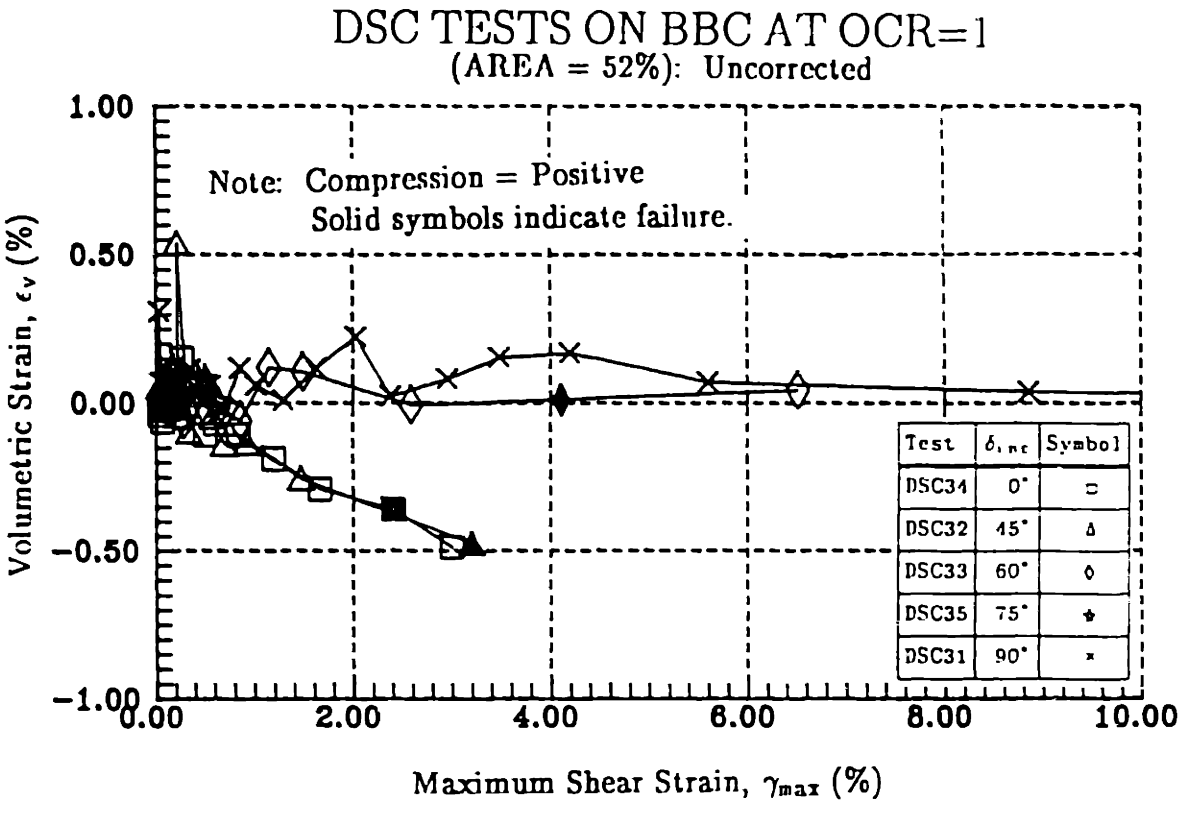

Figure 7.59: Uncorrected Volumetric Strain versus Maximum Shear Strain for DSC Tests on OCR=1 BBC (Area No. 2).

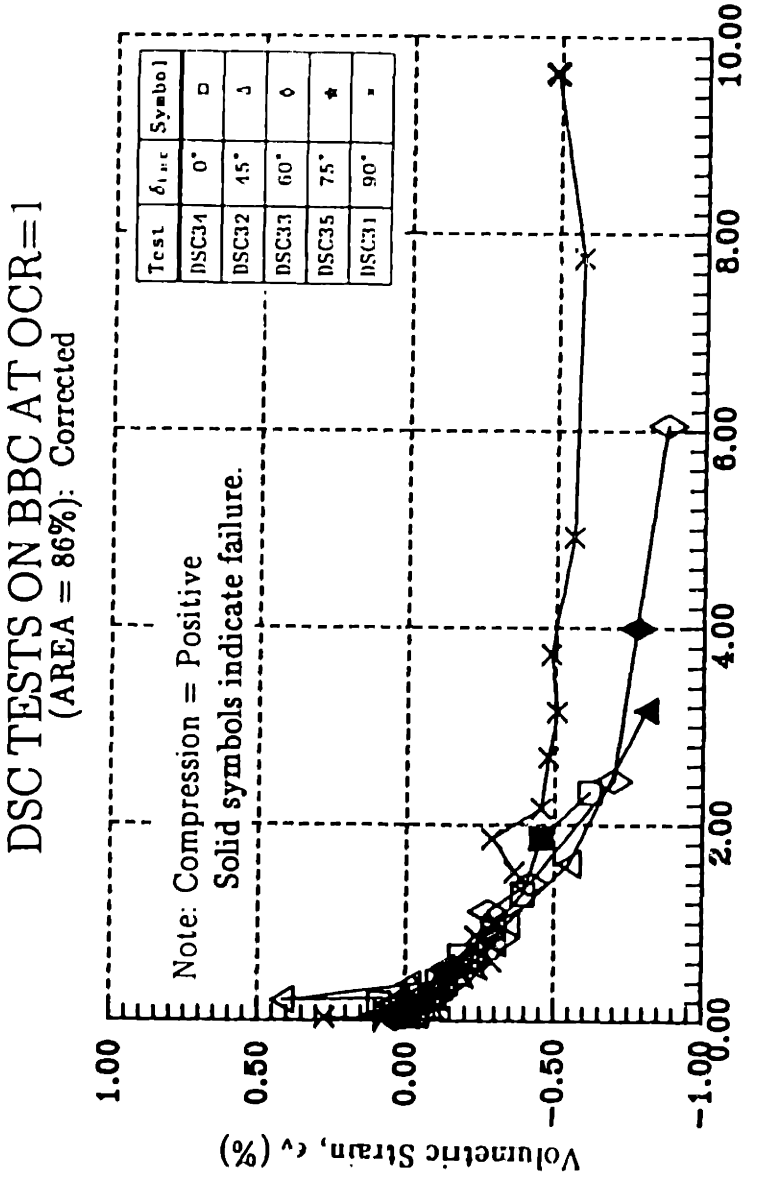

Figure 7.60: Corrected Volumetric Strain versus Maximum Shear Strain for DSC Tests on OCR=1 BBC (Area No. 1).

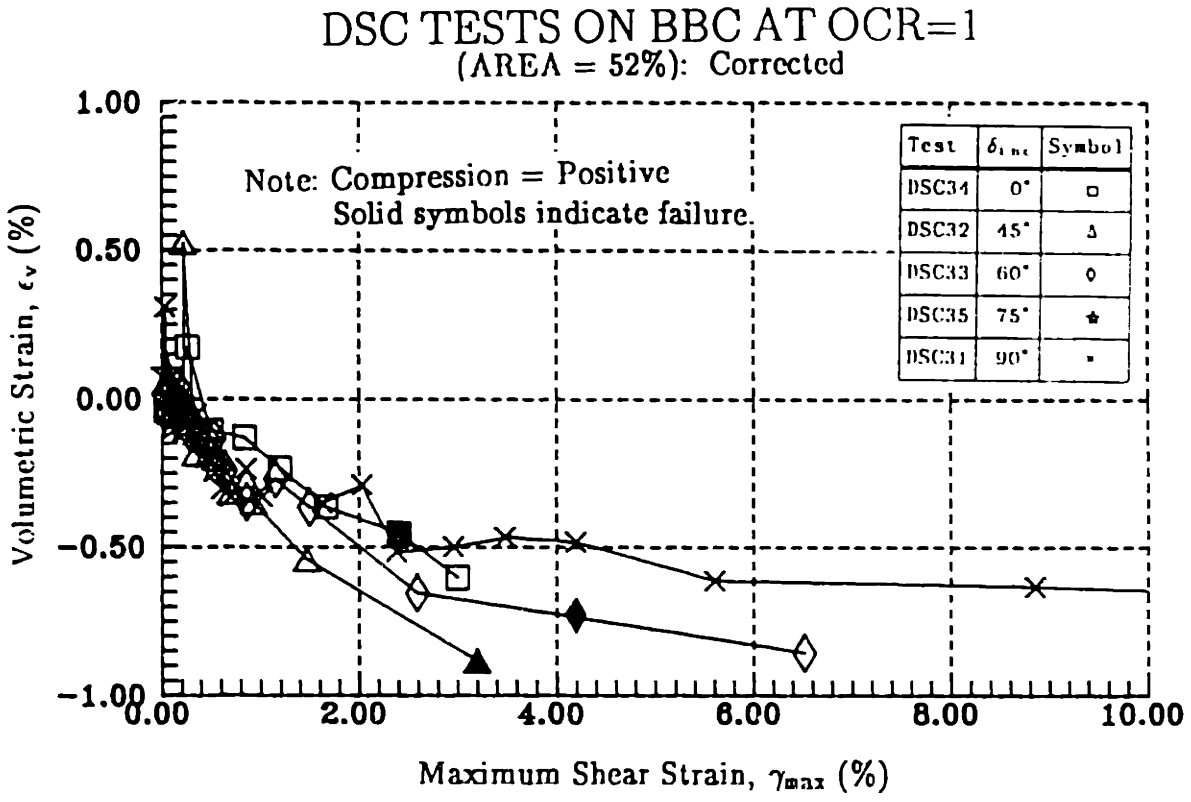

Figure 7.61: Corrected Volumetric Strain versus Maximum Shear Strain for DSC Tests on OCR=1 BBC (Area No. 2).

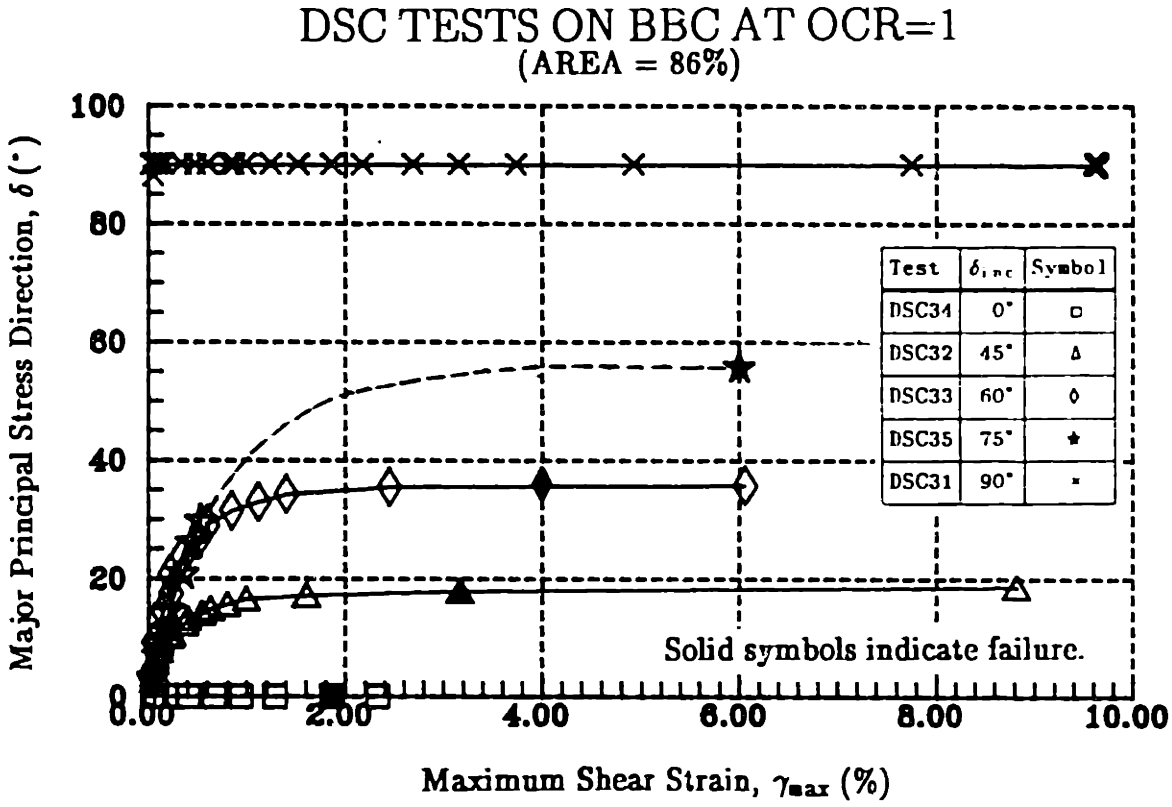

Figure 7.62: Major Principal Stress Direction (δ) versus Maximum Shear Strain for DSC Tests on OCR=1 BBC (Area No. 1).

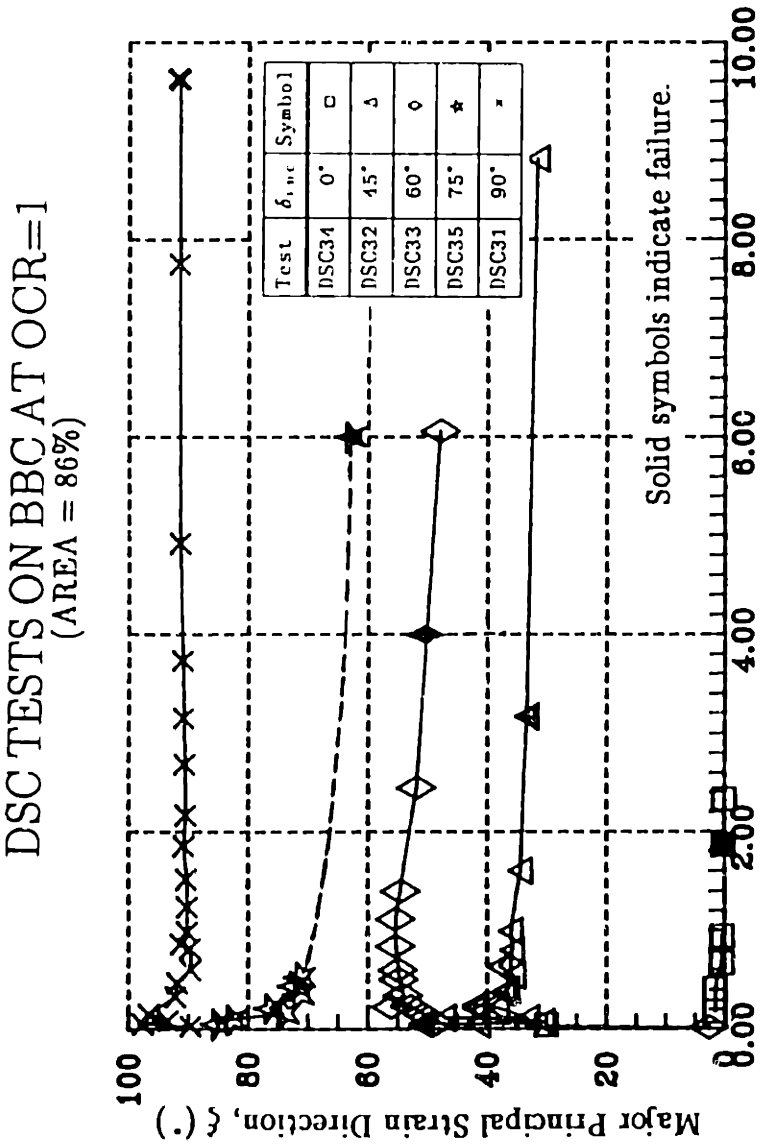

Figure 7.63: Major Principal Strain Direction (ξ) versus Maximum Shear Strain for DSC Tests on OCR=1 BBC (Area No. 2).

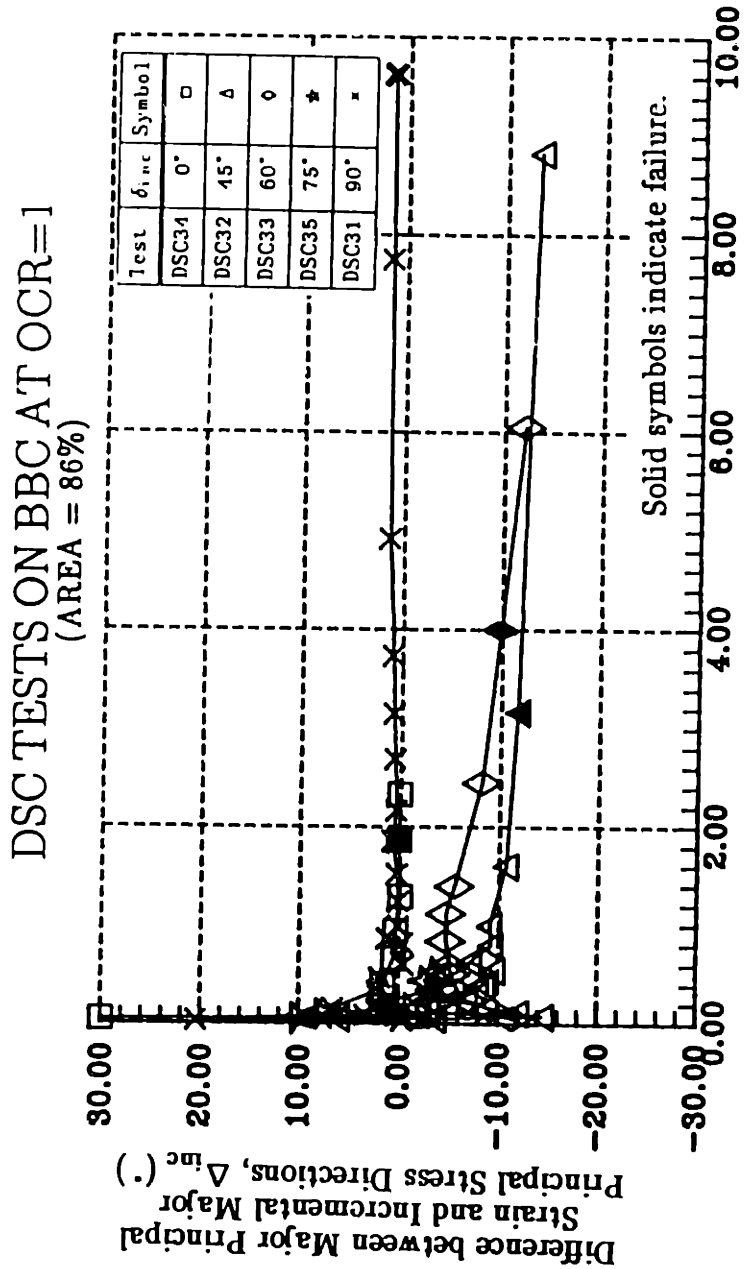

Figure 7.64a: Δ_{inc} versus Maximum Shear Strain for DSC Tests on OCR=1 BBC (Area No. 1).

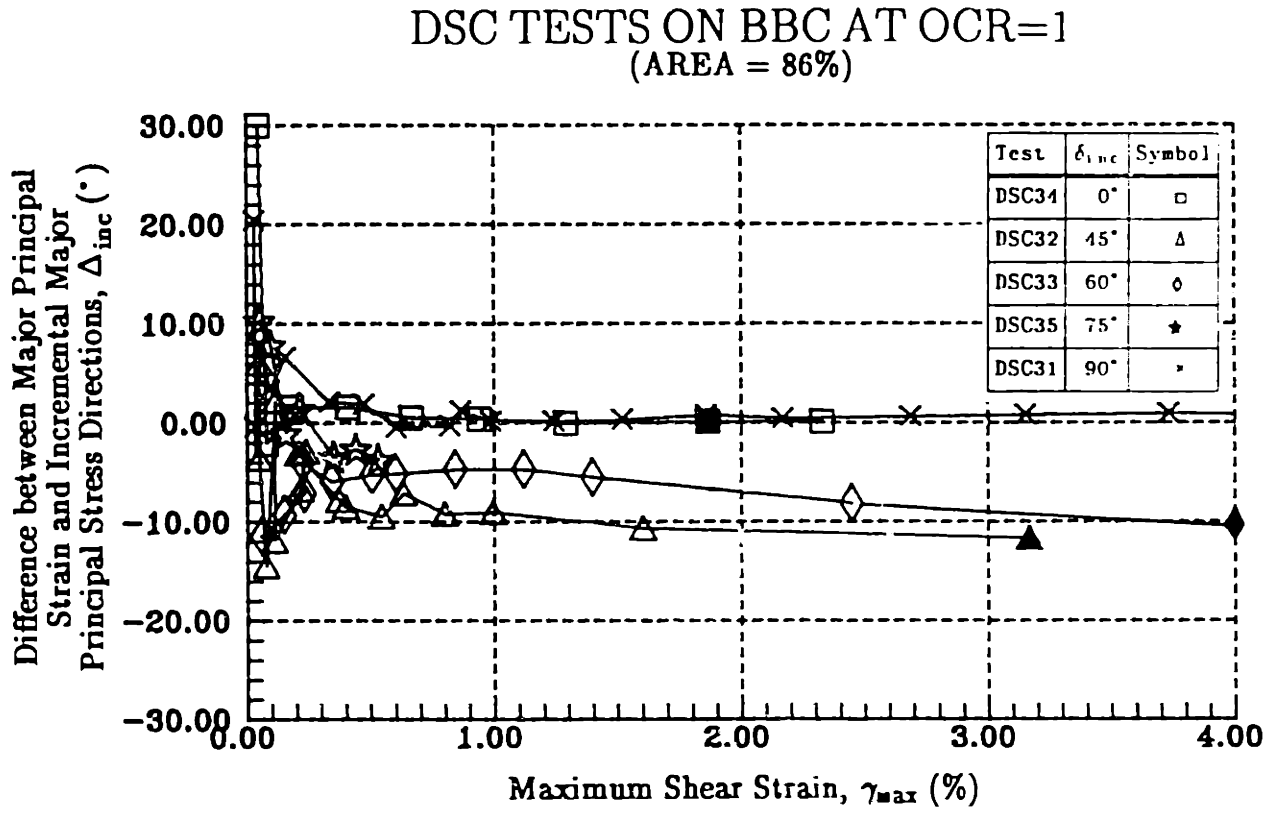

Figure 7.64b: Δ_{inc} versus Maximum Shear Strain for DSC Tests on OCR=1 BBC (Area No. 1).

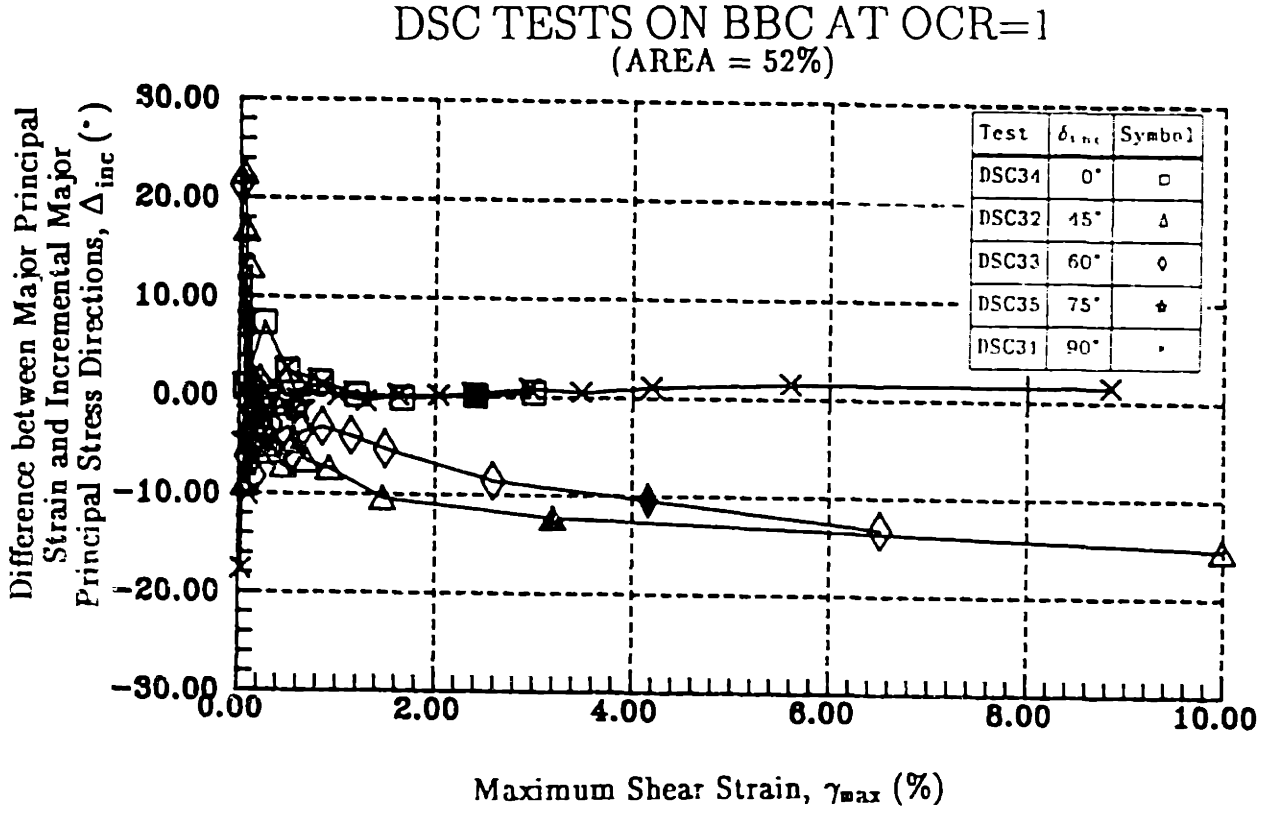

Figure 7.65a: Δ_{inc} versus Maximum Shear Strain for DSC Tests on OCR=1 BBC (Area No. 2).

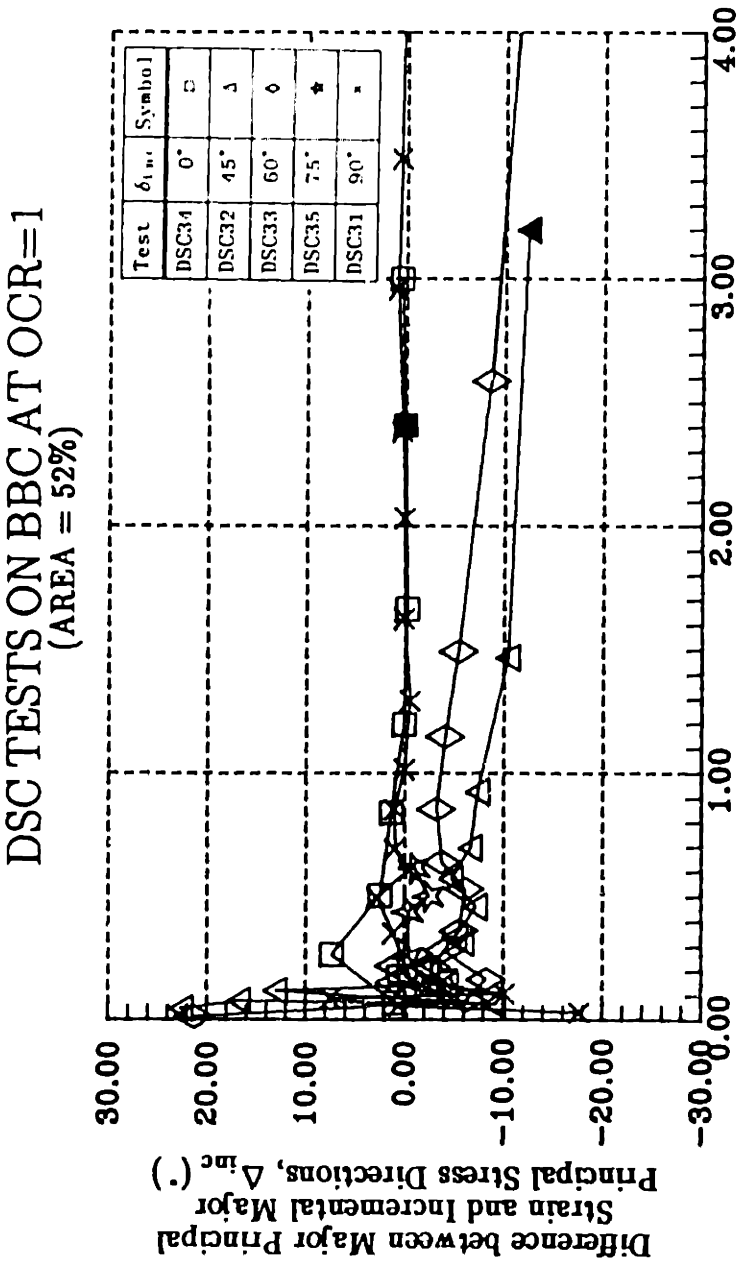

Figure 7.65b: Δ_{inc} versus Maximum Shear Strain for DSC Tests on OCR=1 BBC (Area No. 2).

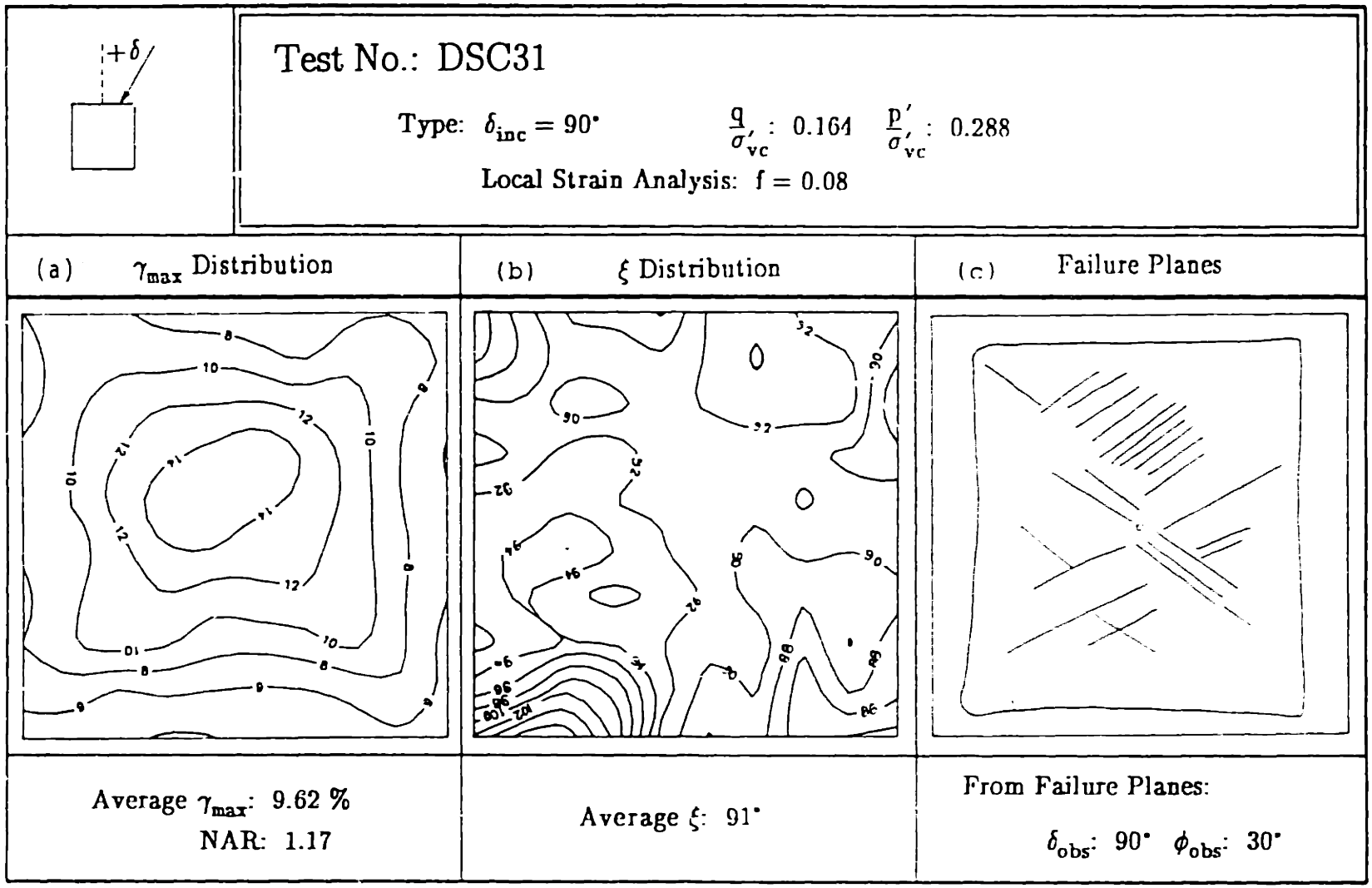

Figure 7.66: γ_{max}, ξ Distributions and Failure Planes for Test DSC31 on OCR=1 BBC.

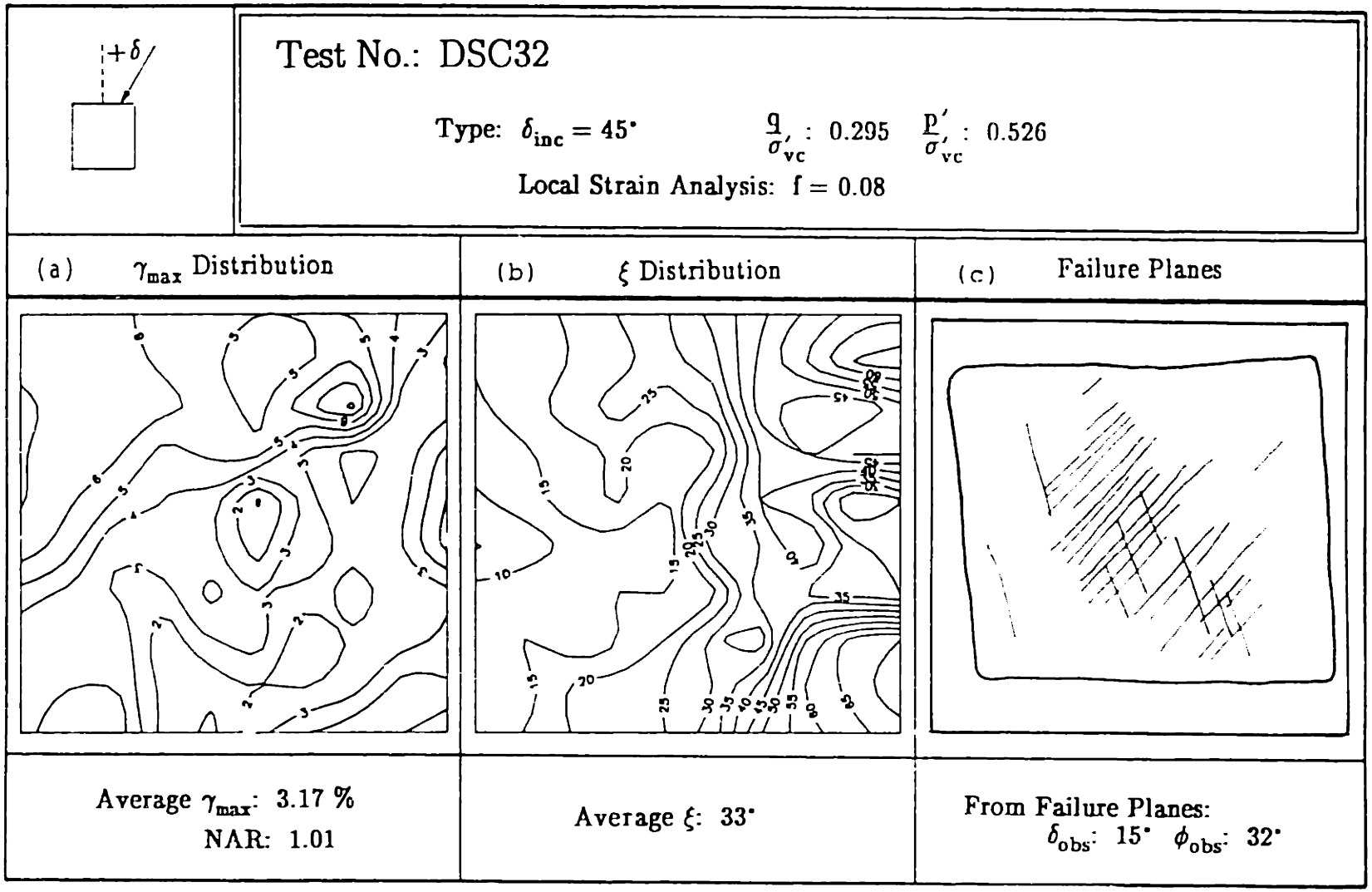

Figure 7.67: γ_{max}, ξ Distributions and Failure Planes for Test DSC32 on OCR=1 BBC.

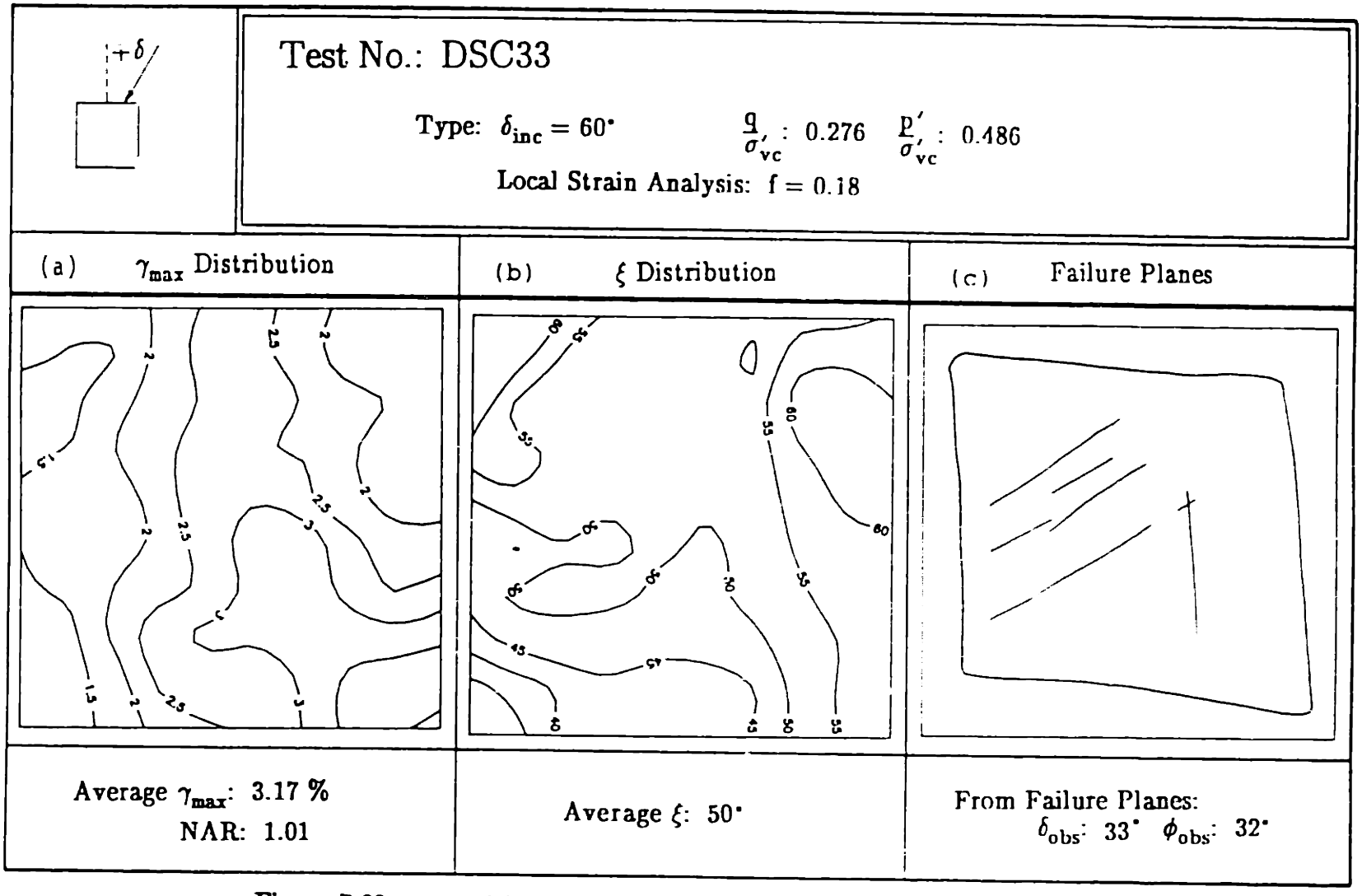

Figure 7.68: γ_{max}, ξ Distributions and Failure Planes for Test DSC33 on OCR=1 BBC.

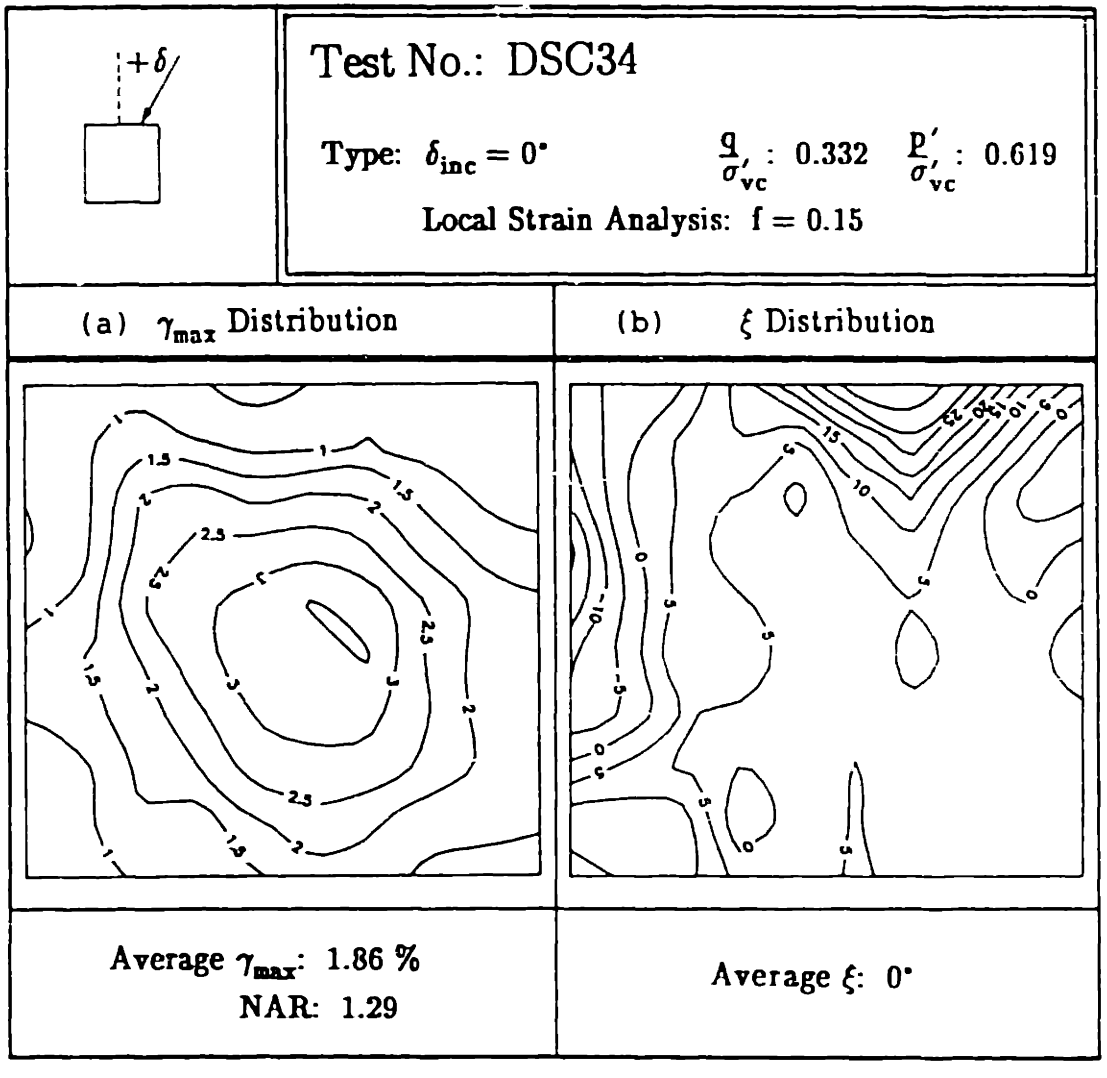

Figure 7.69: γ_{max} and ξ Distributions for Test DSC34 on OCR=1 BBC.

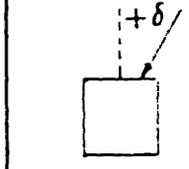

Test No.: DSC35

Type: $\delta_{inc} = 75°$ $\frac{q}{\sigma'_{vc}}$: 0.120 $\frac{p'}{\sigma'_{vc}}$: 0.591

Local Strain Analysis: f = 0.20

(a) γ_{max} Distribution

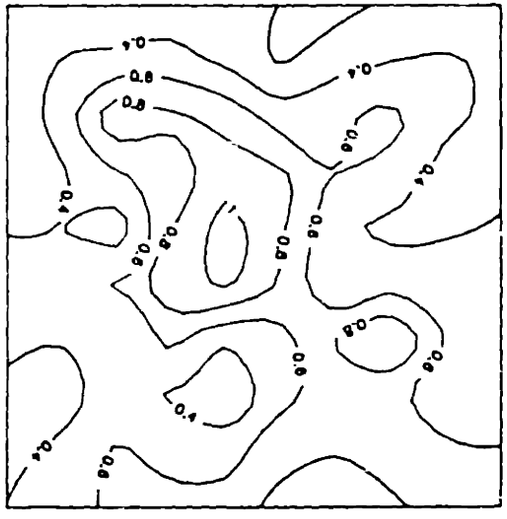

Average γ_{max}: 0.53 %

NAR: 1.16

(b) ξ Distribution

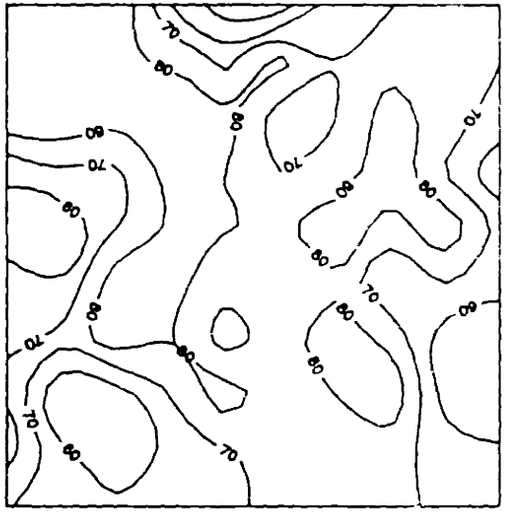

Average ξ: 71°

(c) Failure Planes

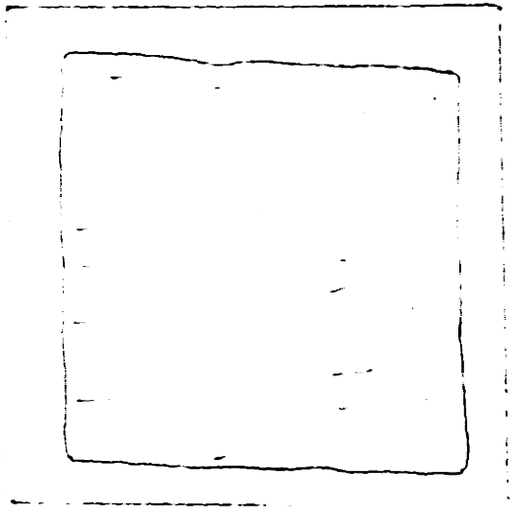

From Failure Planes:

δ_{obs}: 58° ϕ_{obs}: 38°

Figure 7.70: γ_{max}, ξ Distributions and Failure Planes for Test DSC35 on OCR=1 BBC.

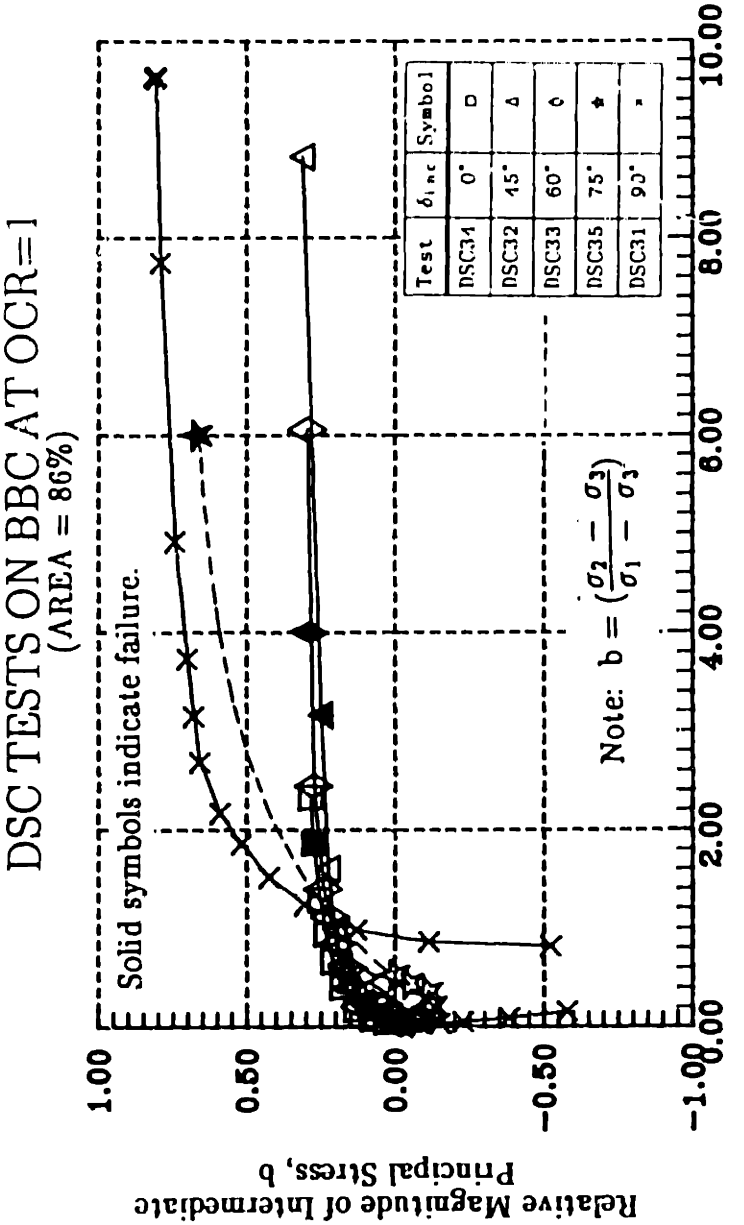

Figure 7.71: Relative Magnitude of Intermediate Principal Stress, b versus Maximum Shear Strain for DSC Tests on OCR=1 BBC (Area No. 1).

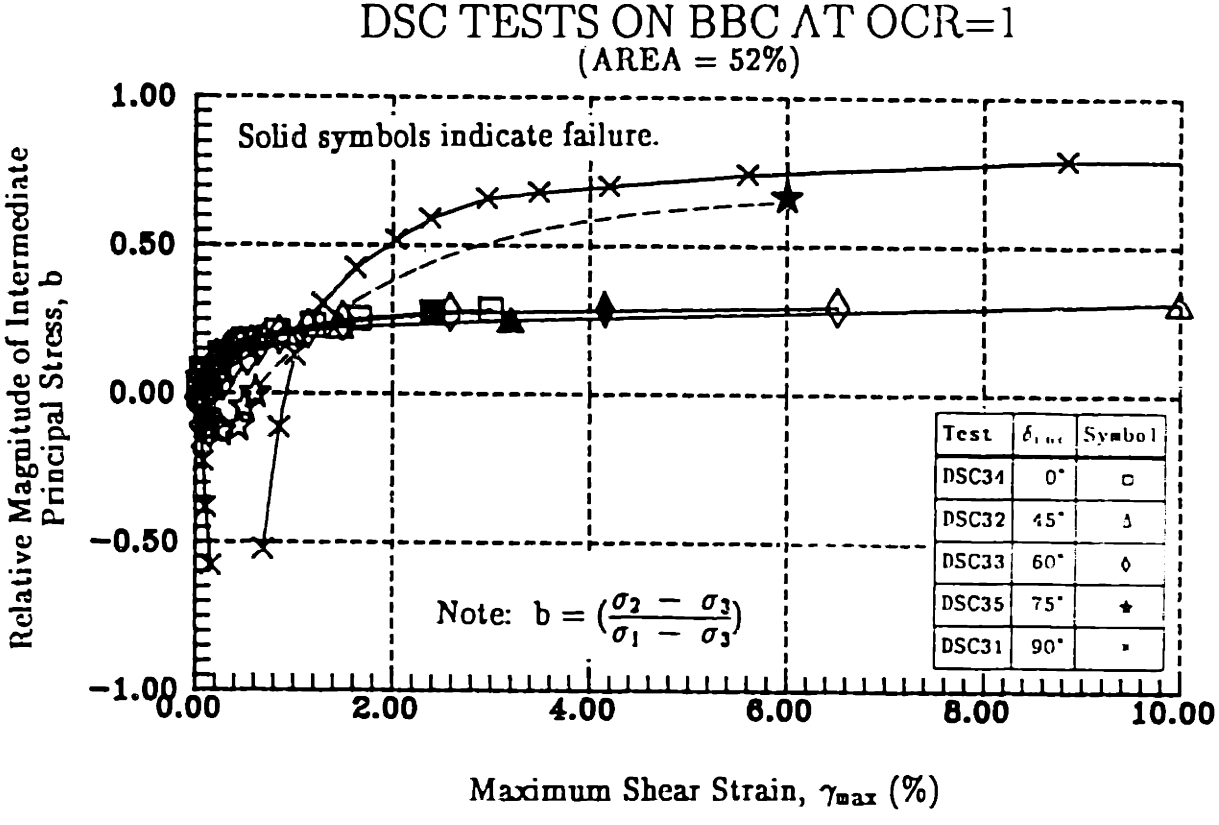

Figure 7.72: Relative Magnitude of Intermediate Principal Stress, b versus Maximum Shear Strain for DSC Tests on OCR=1 BBC (Area No. 2).

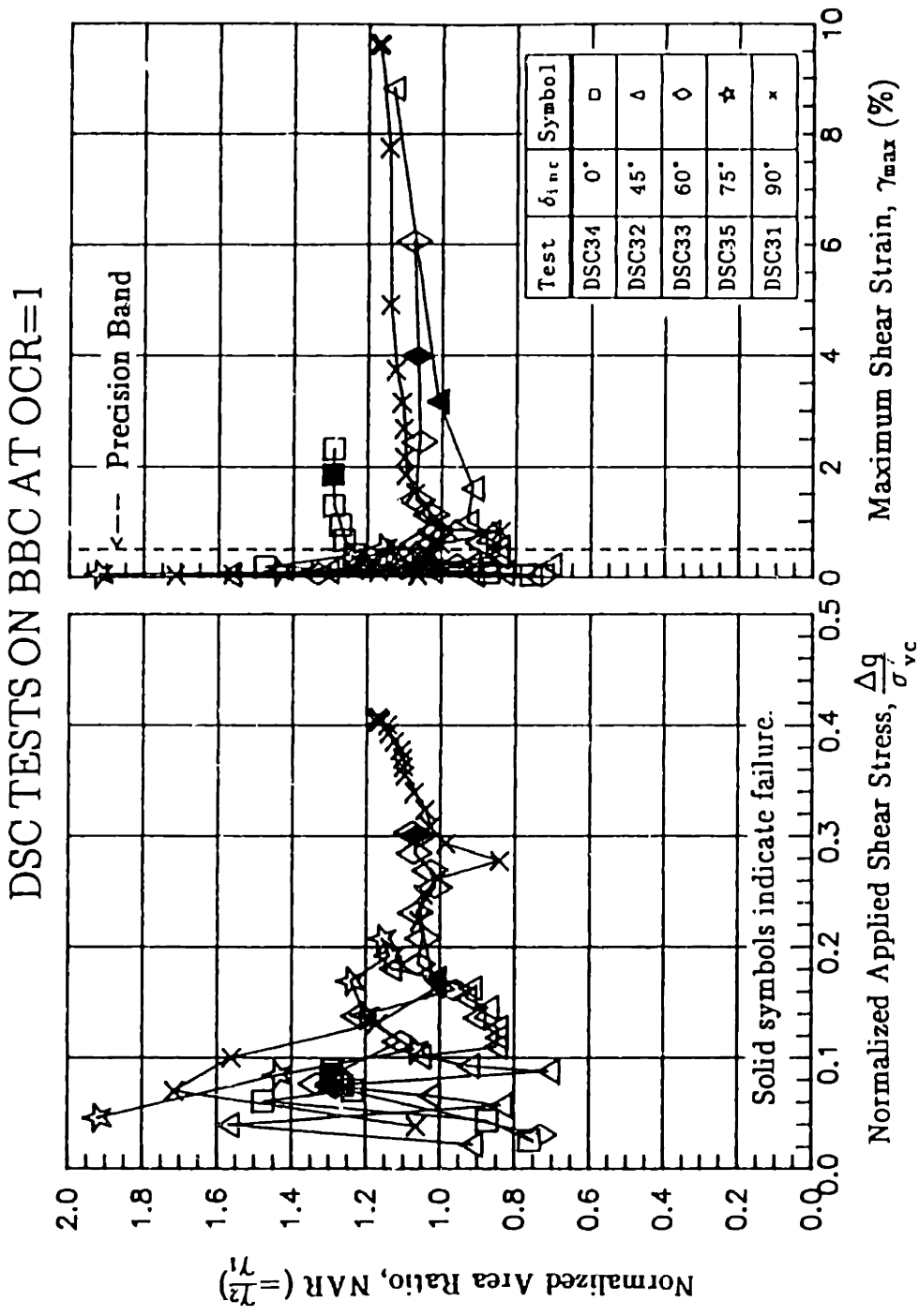

Figure 7.73: Variation of NAR with (a) Normalized Applied Shear Stress and with (b) Maximum Shear Strain from DSC Tests on OCR=1 BBC during Undrained Shear.

Final Water Content Distribution of the DSC Sample: DSC35
Top Layer of the Sample
(all values in percent)

38.12 (2.86)‡	38.54 (2.31)	38.23 (2.71)
38.73 (2.07)	38.68 (2.12)	38.51 (2.34)
38.03 (2.97)	38.31 (2.61)	37.91 (3.13)

Initial Water Content:

w_i = 40.30 ± 0.22 % (4)

Final Water Content:

w_f = 38.34 ± 0.29 % (9)

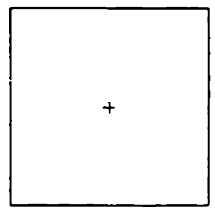

Note: ‡ Values in parentheses represent the volumetric strains (ϵ_v).

Figure 7.74 Final Water Content Distribution of the Sample from Test DSC32.

Final Water Content Distribution of the DSC Sample: DSC33
Top Layer of the Sample
(all values in percent)

36.28 (5.25)‡	36.25 (5.29)	35.70 (6.01)
37.05 (4.24)	36.97 (4.34)	36.24 (5.30)
35.57 (6.18)	35.97 (5.67)	35.56 (6.18)

Initial Water Content:

w_i = 40.28 ± 0.19 % (2)

Final Water Content:

w_f = 36.18 ± 0.55 % (9)

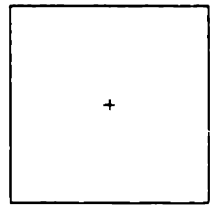

Note: ‡ Values in parentheses represent the volumetric strains (ϵ_v).

Figure 7.75: Final Water Content Distribution of the Sample from Test DSC33.

Final Water Content Distribution of the DSC Sample: DSC32
Top Layer of the Sample
(all values in percent)

36.35 (4.93)‡	36.57 (4.64)	37.02 (4.05)
37.06 (3.99)	37.23 (3.77)	37.35 (3.61)
37.23 (3.77)	37.49 (3.43)	37.30 (3.68)

Initial Water Content:

w_i = 40.10 ± 0.59 % (4)

Final Water Content:

w_f = 37.07 ± 0.38 % (9)

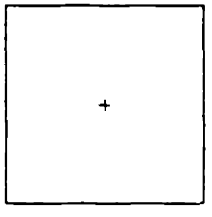

Note: ‡ Values in parentheses represent the volumetric strains (ϵ_v).

Figure 7.76: Final Water Content Distribution of the Sample from Test DSC35.

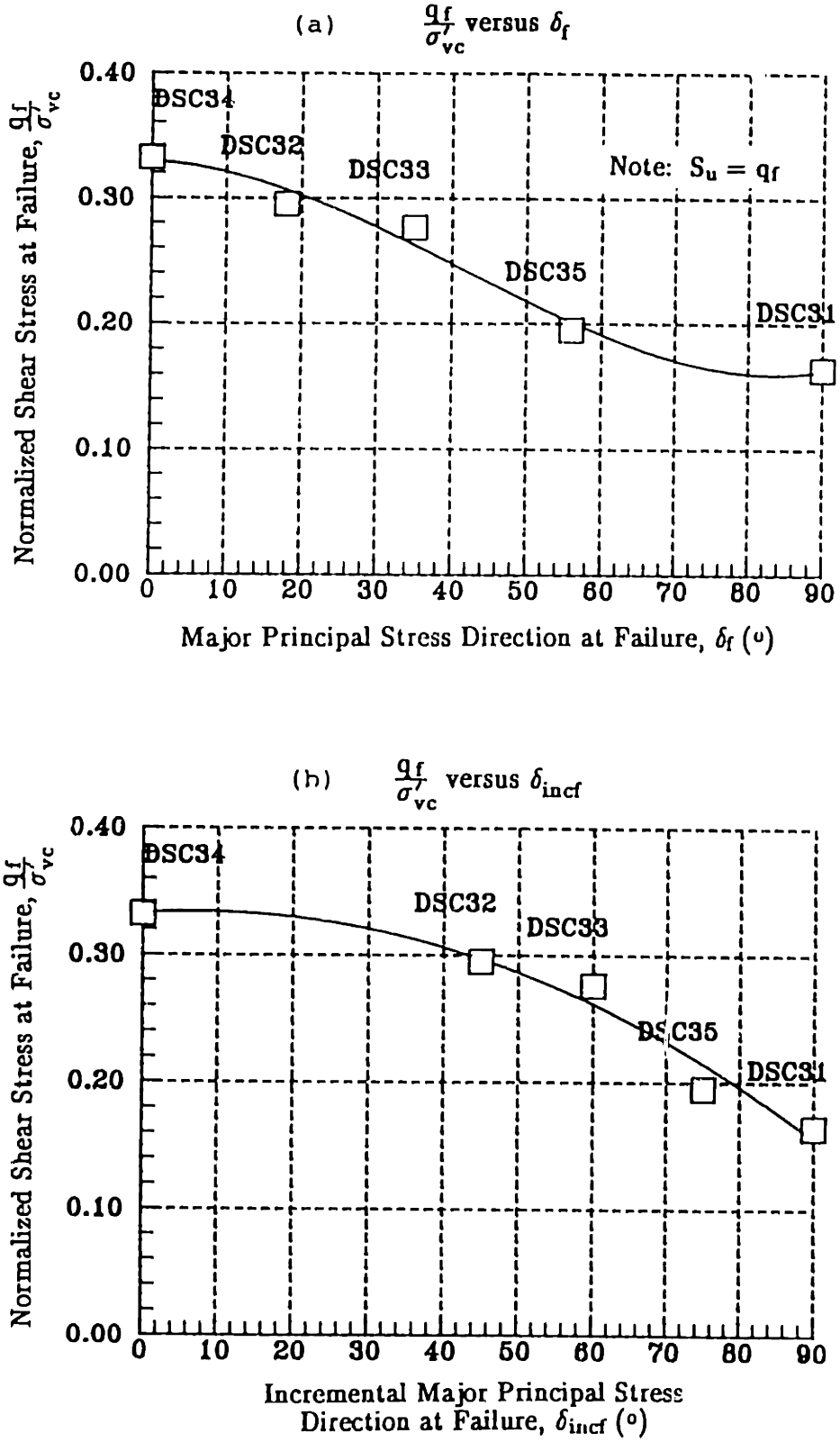

Figure 7.77: Normalized Shear Stress versus (a) Major Principal Stress Direction (δ_f); (b) Incremental Principal Stress Direction (δ_{incf}) at Failure.

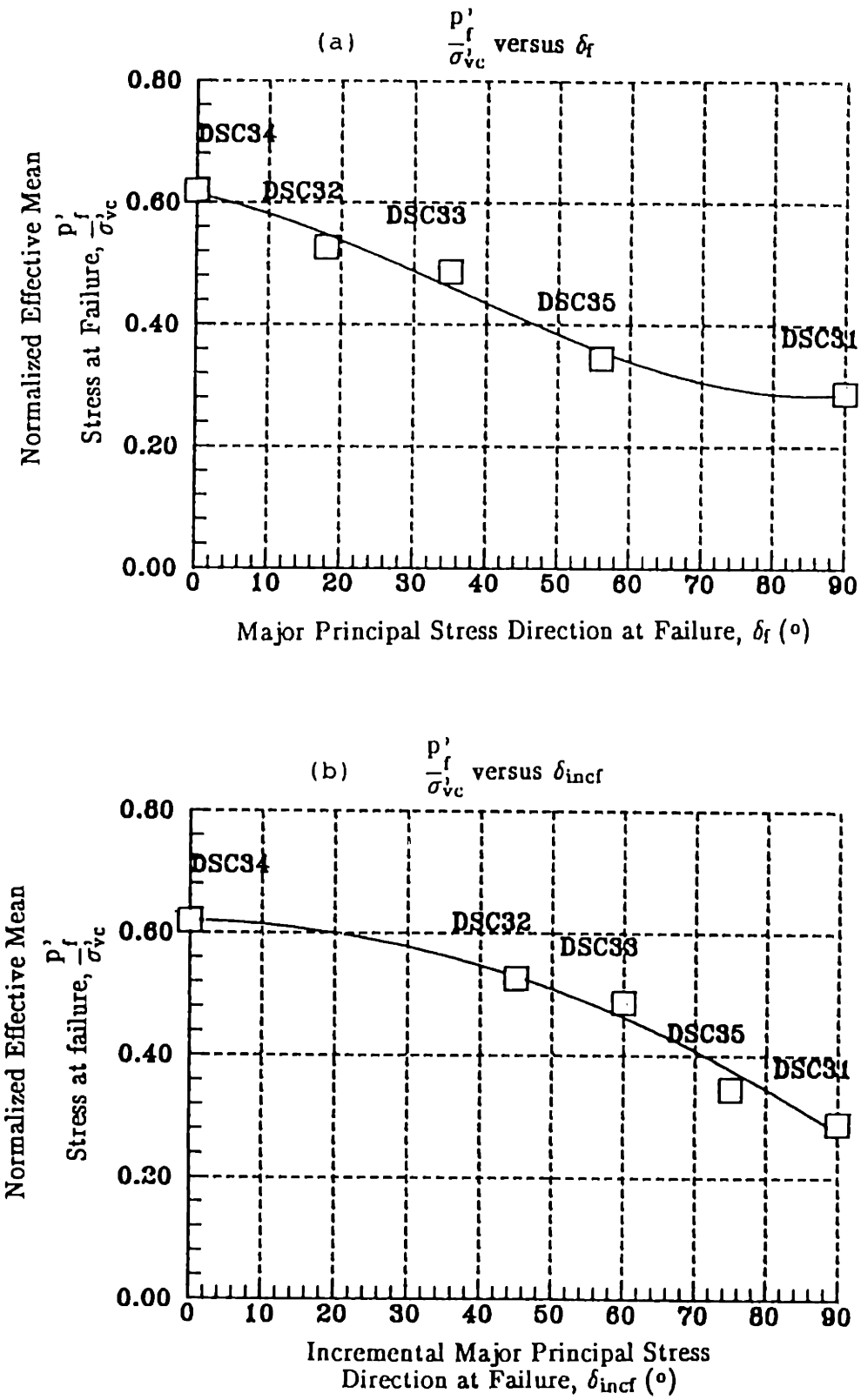

Figure 7.78: Normalized Mean Effective Stress versus (a) Major Principal Stress Direction (δ_f); (b) Incremental Principal Stress Direction (δ_{incf}) at Failure.

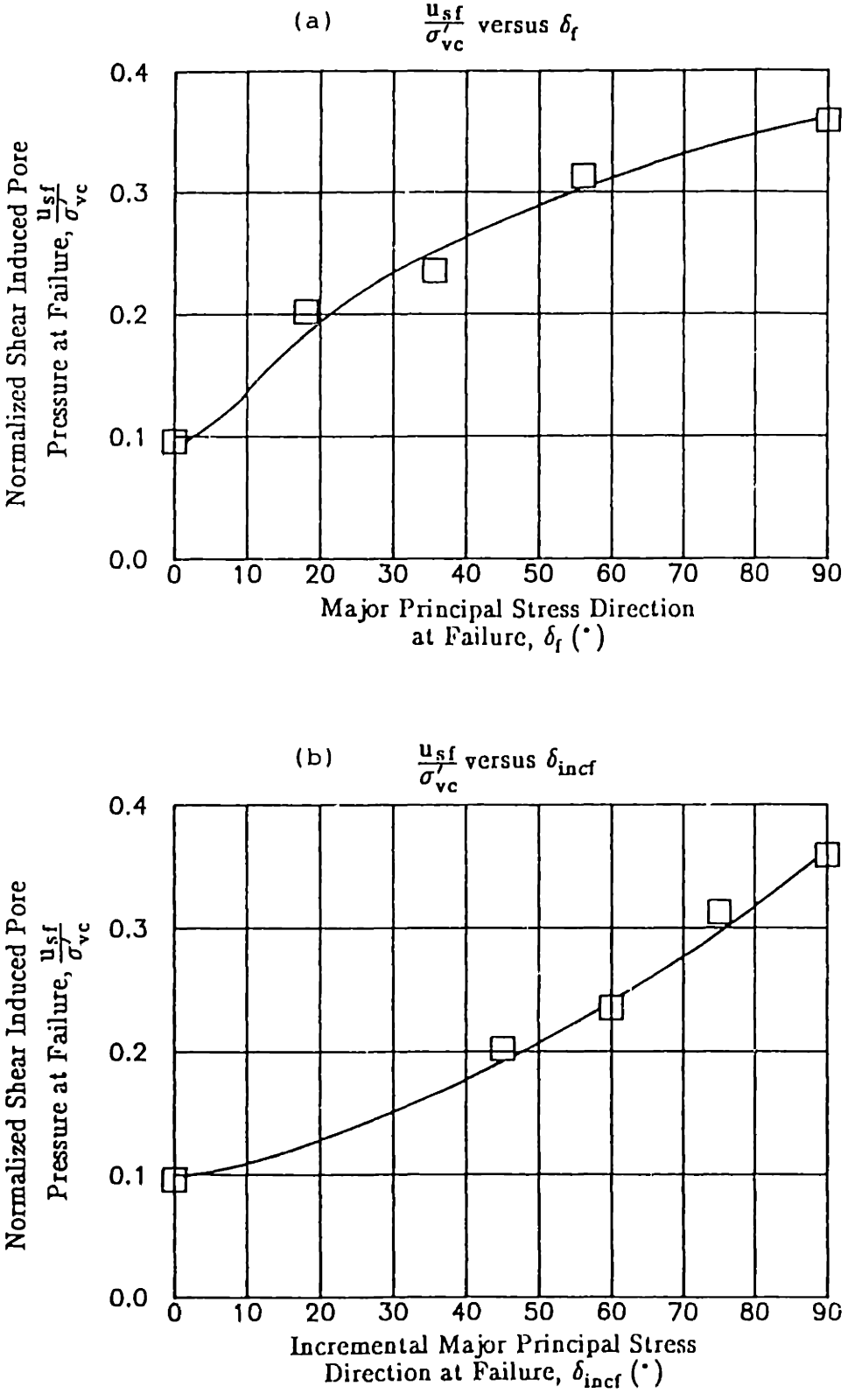

Figure 7.79: Normalized Shear Induced Pore Pressure versus (a) Major Principal Stress Direction (δ_f); (b) Incremental Principal Stress Direction (δ_{incf}) at Failure.

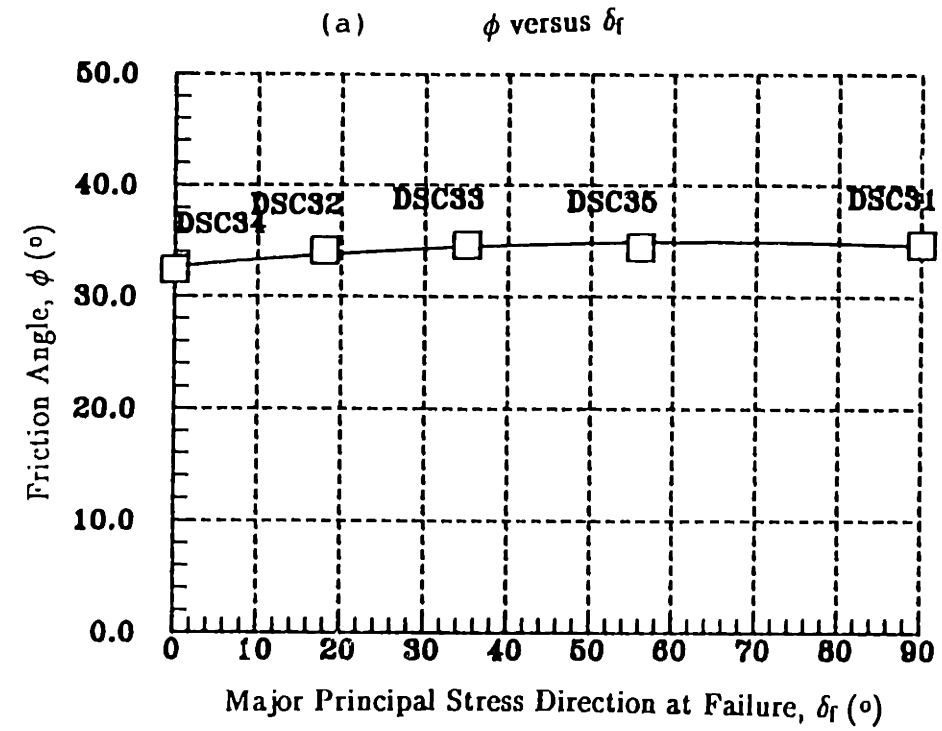

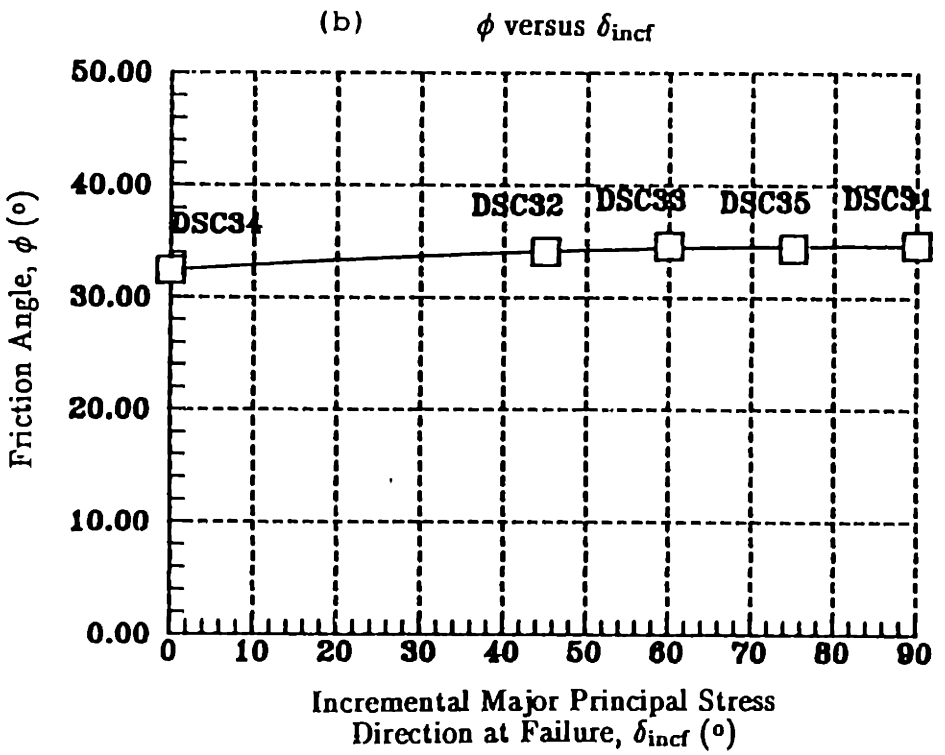

Figure 7.80: Friction Angle versus (a) Major Principal Stress Direction (δ_f); (b) Incremental Principal Stress Direction (δ_{incf}).

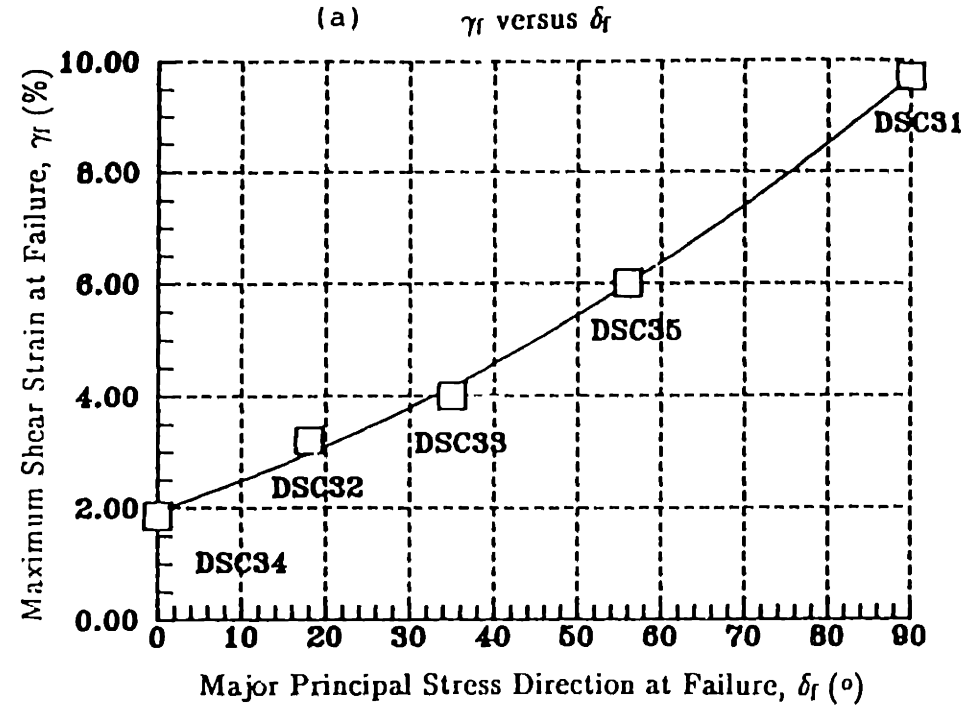

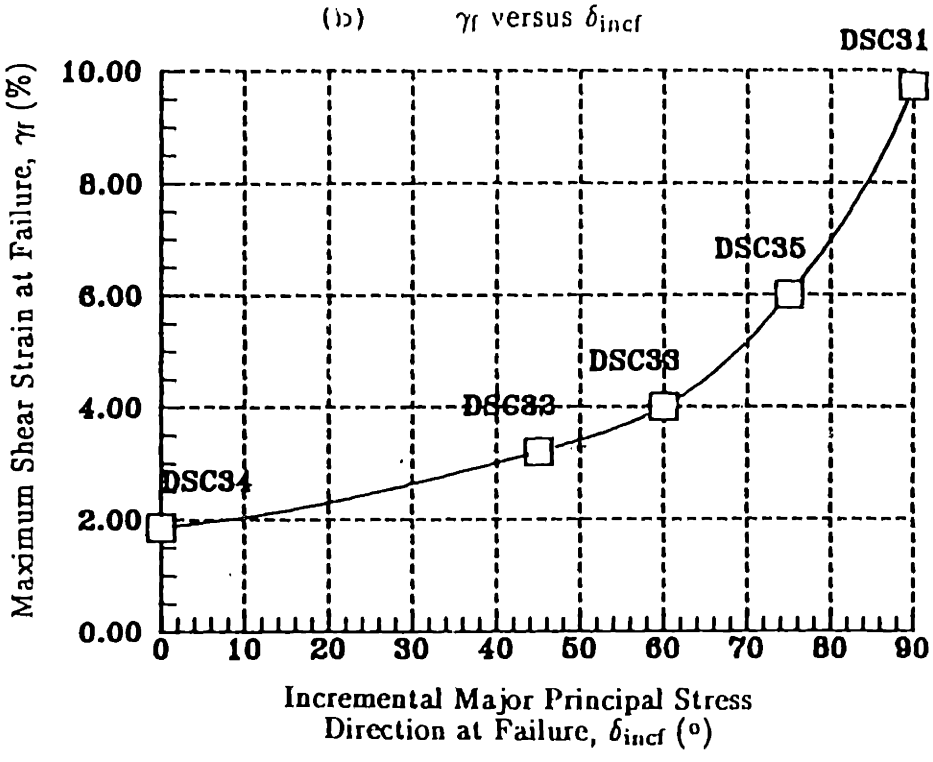

Figure 7.81: Maximum Shear Strain versus (a) Major Principal Stress Direction (δ_f); (b) Incremental Principal Stress Direction (δ_{incf}) at Failure.

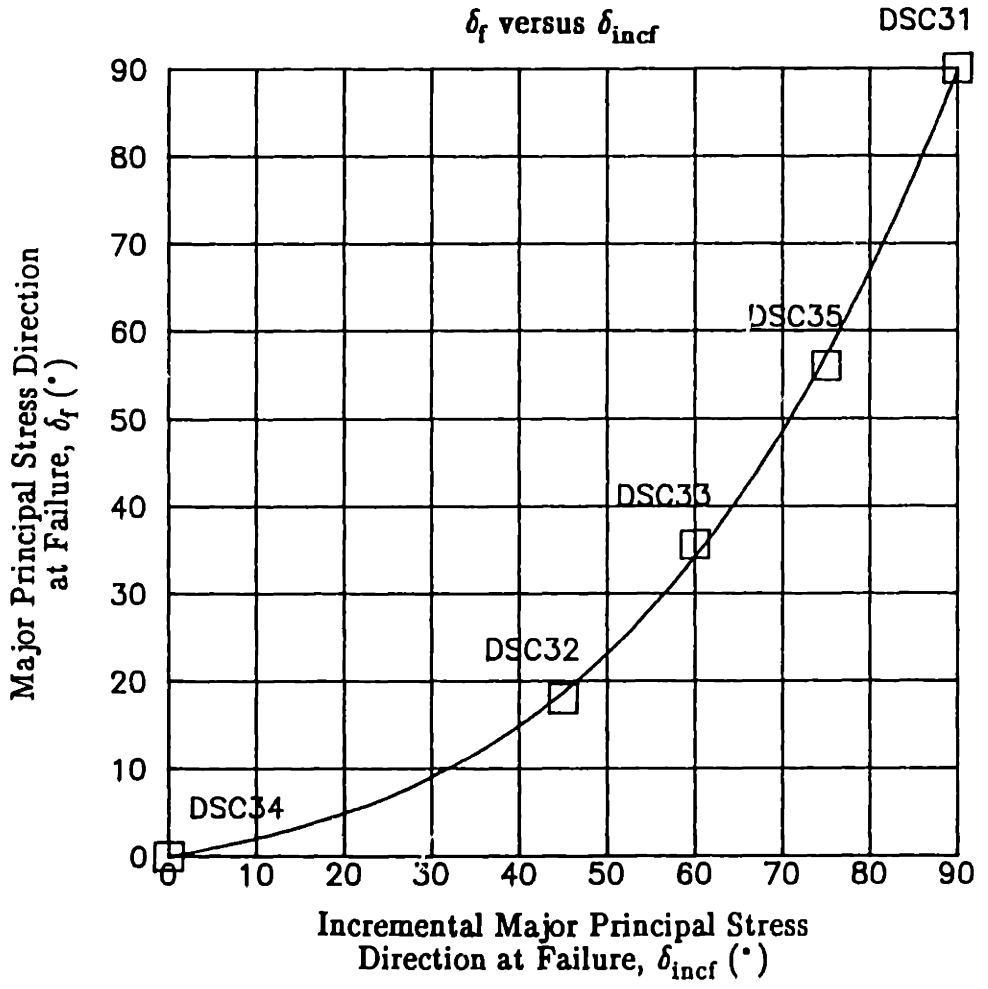

Figure 7.82: Major Principal Stress Direction (δ_f) versus Incremental Principal Stress Direction (δ_{incf}) at Failure.

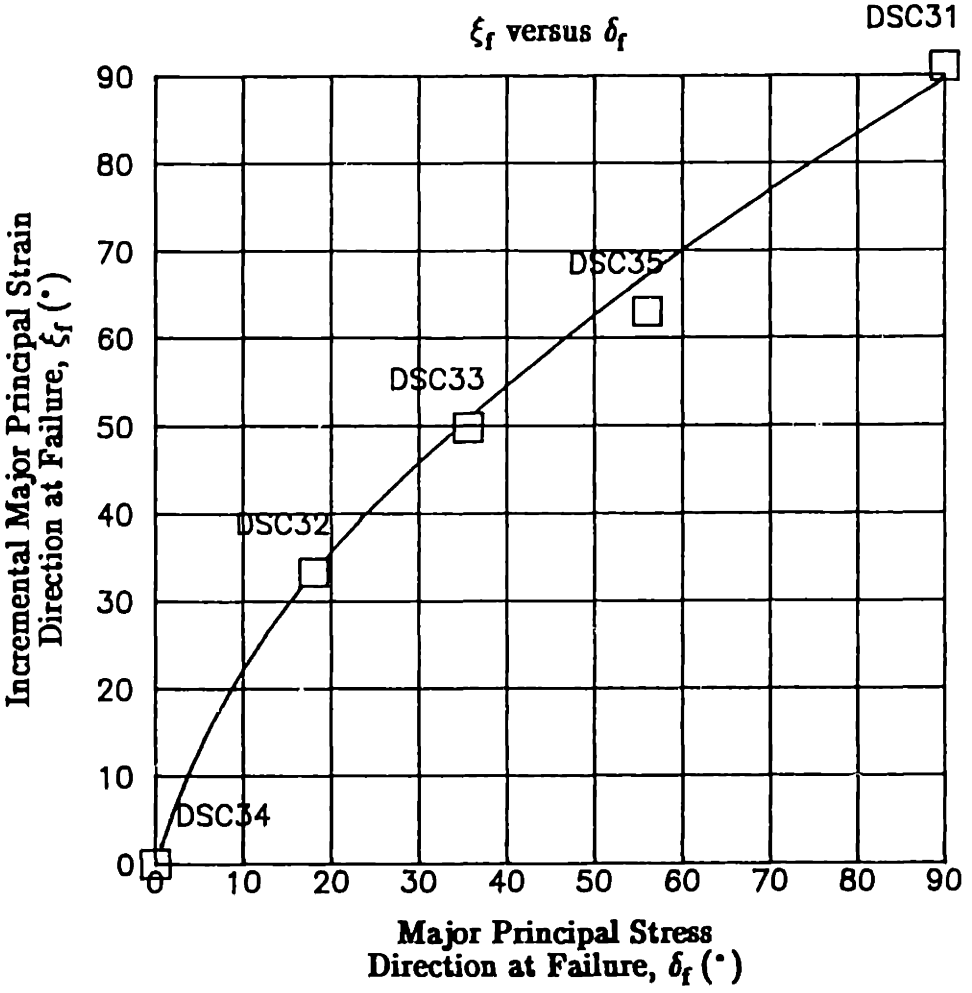

Figure 7.83: Incremental Major Principal Strain Direction (ξ_f) versus Major Principal Stress Direction (δ_f) at Failure.

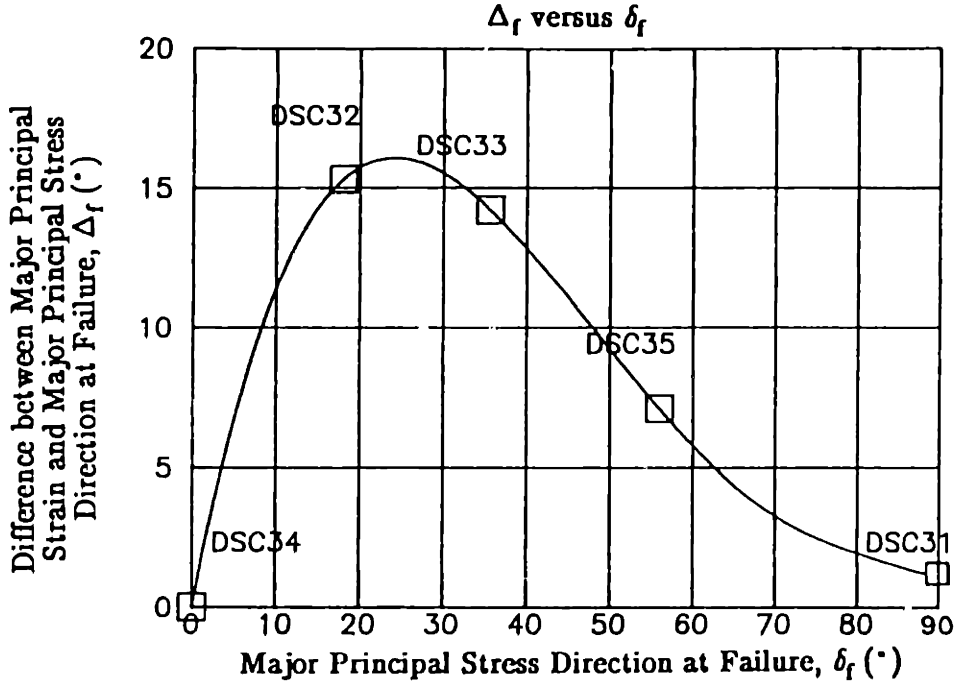

Figure 7.84: Relationship of Major Principal Strain and Major Principal Stress Directions (Δ_f) versus Major Principal Stress Direction (δ_f) at Failure.

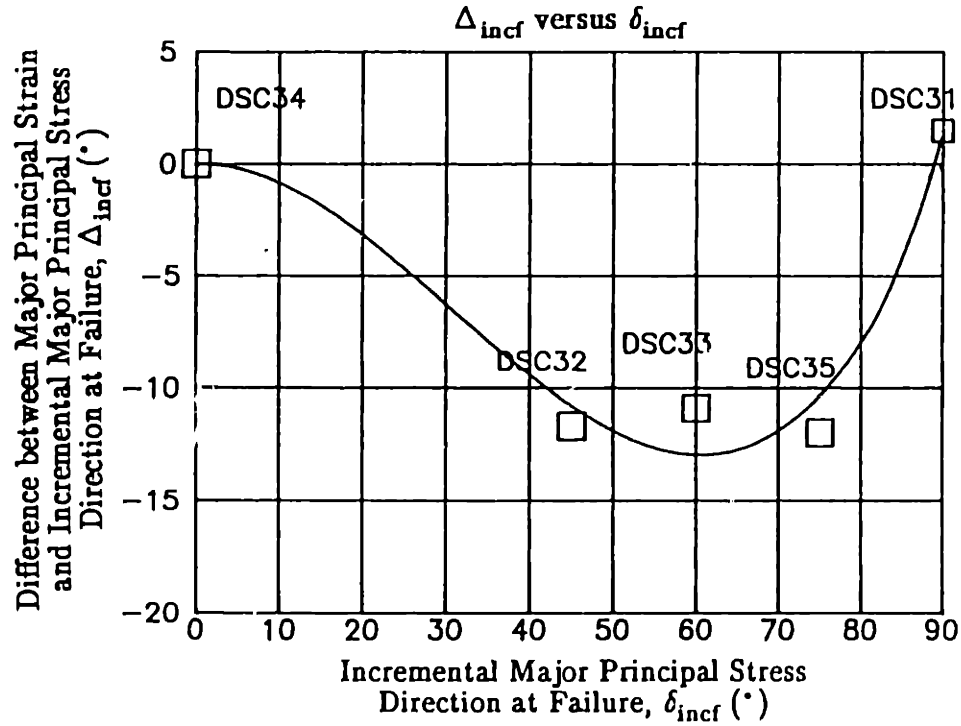

Figure 7.85: Relationship of Major Principal Strain and Incremental Major Principal Stress Directions (Δ_{incf}) versus Incremental Major Principal Stress Direction (δ_{incf}) at Failure.

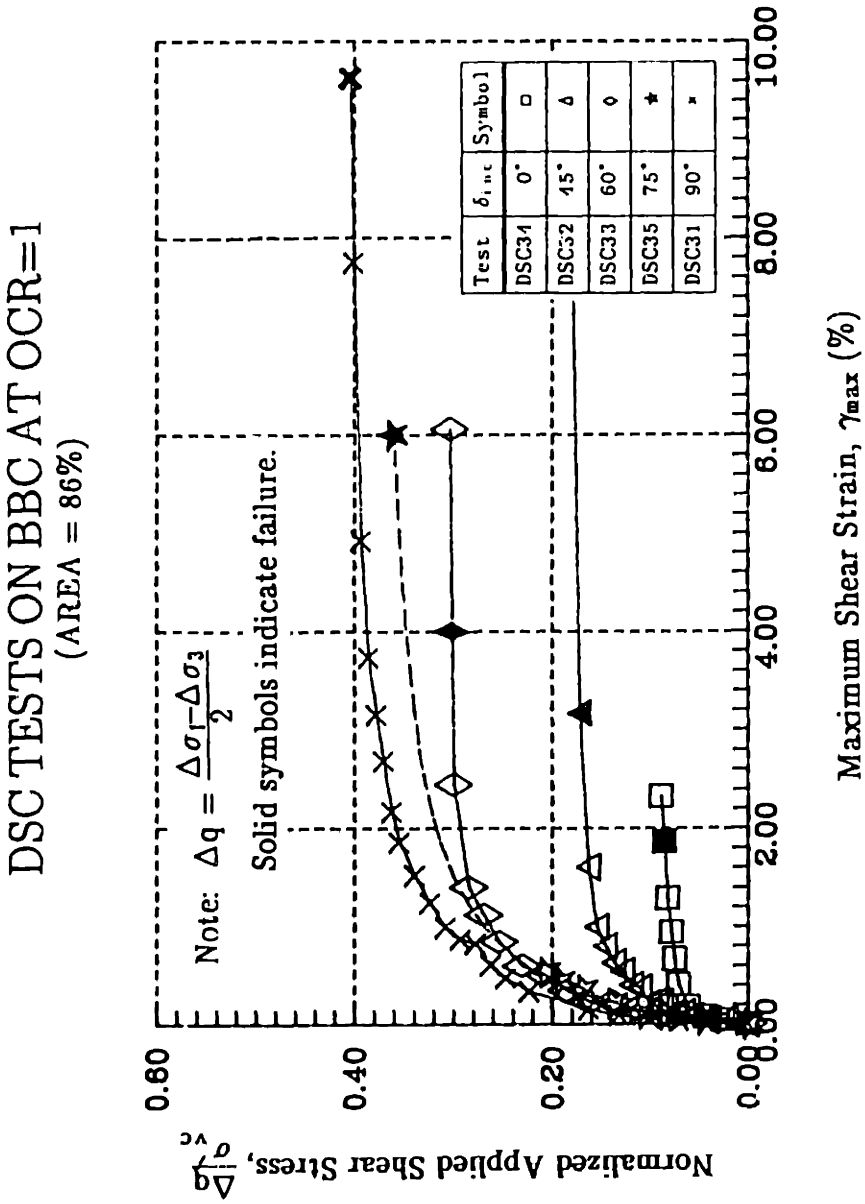

Figure 7.86a: Normalized Applied Shear Stress versus Maximum Shear Strain for DSC Tests on OCR=1 BBC (Area No. 1).

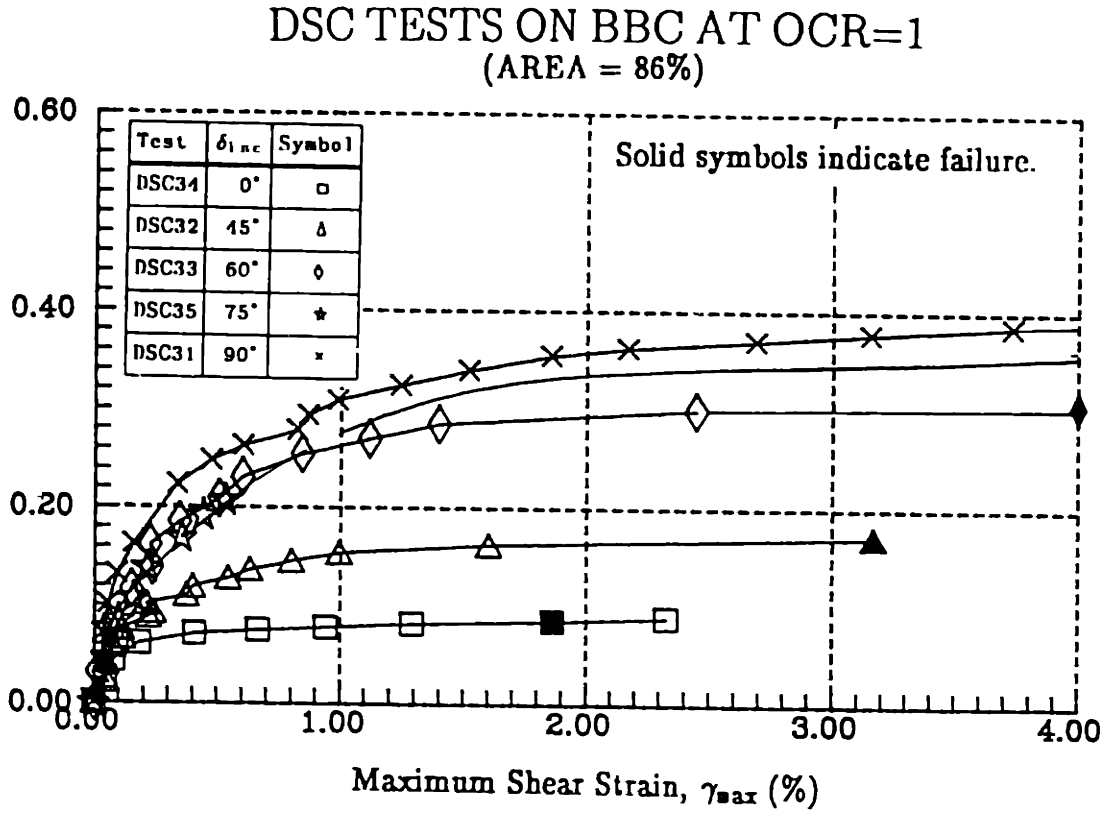

Figure 7.86b: Normalized Applied Shear Stress versus Maximum Shear Strain for DSC Tests on OCR=1 BBC (Area No. 1).

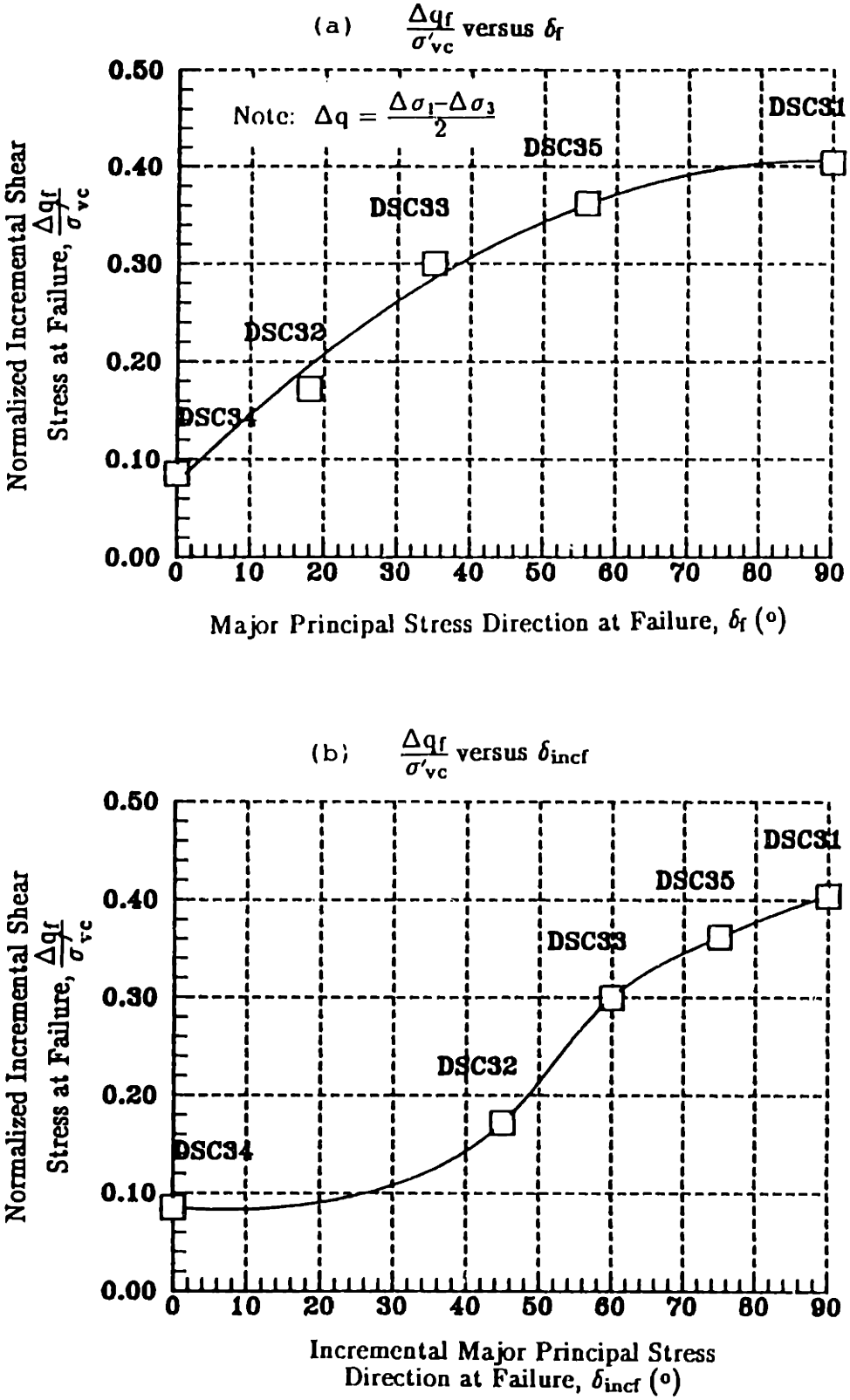

Figure 7.87: Normalized Applied Shear Stress versus (a) Major Principal Stress Direction (δ_f); (b) Incremental Principal Stress Direction (δ_{incf}) at Failure.

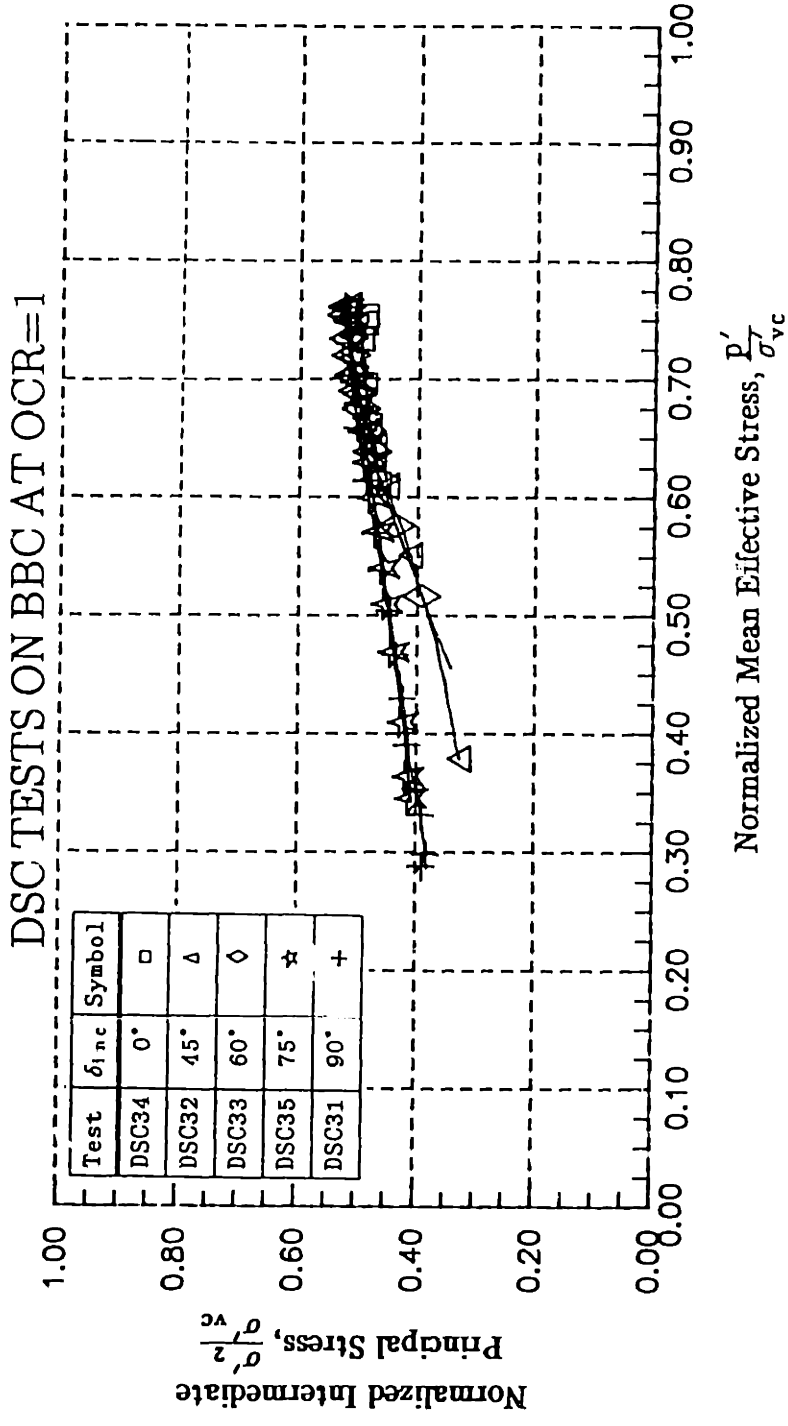

Figure 7.88: Relationship Between Measured Intermediate Principal Stress and Normalized Mean Effective Stress for DSC Tests on OCR=1 BBC.

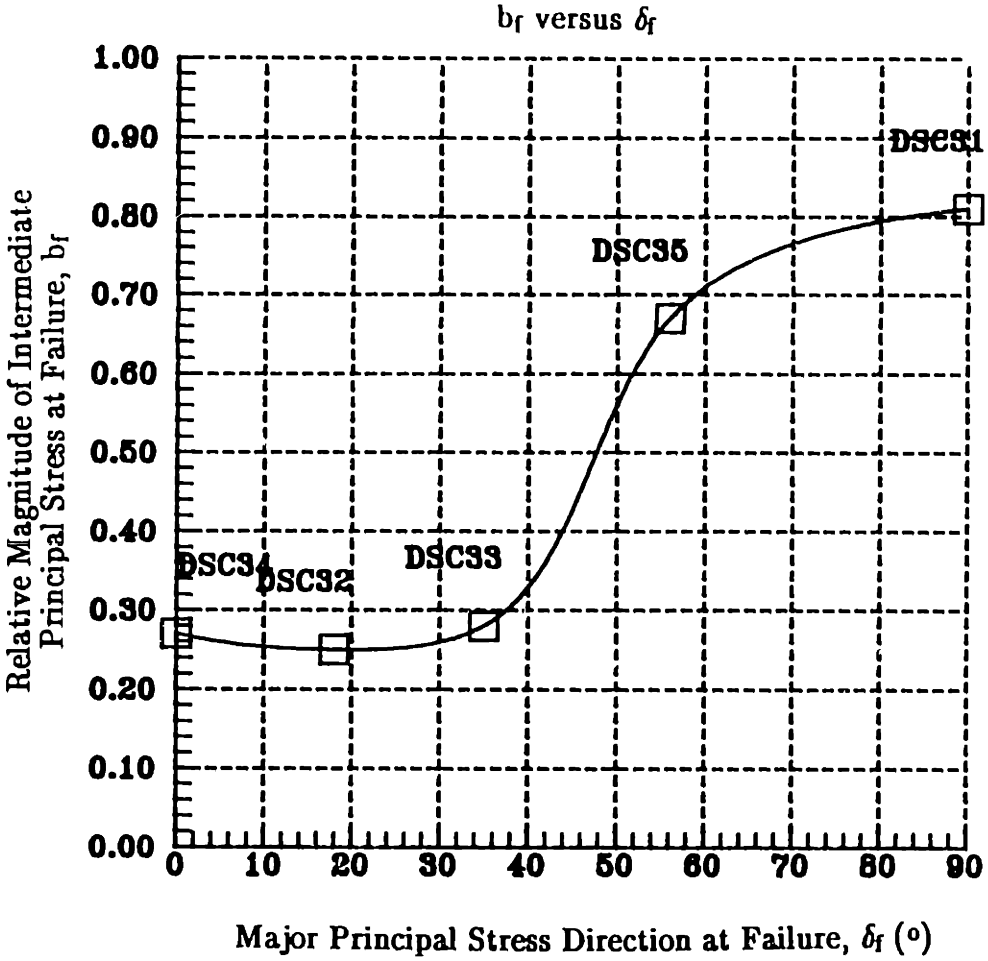

Figure 7.89: Relative Magnitude of Intermediate Principal Stress (b_f) versus Major Principal Stress Direction (δ_f) at Failure for DSC Tests on OCR=1 BBC.

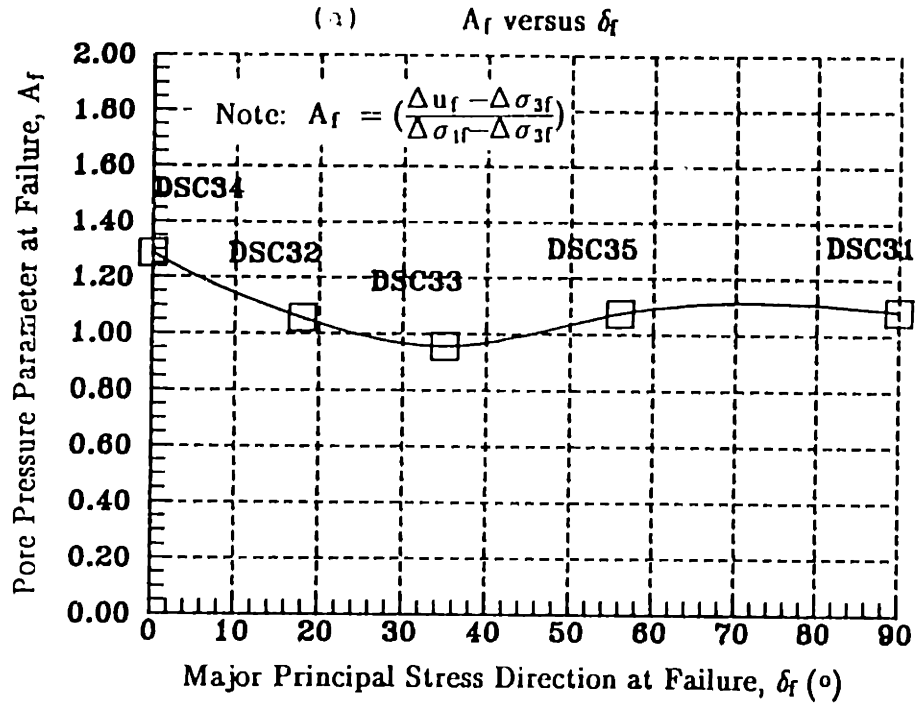

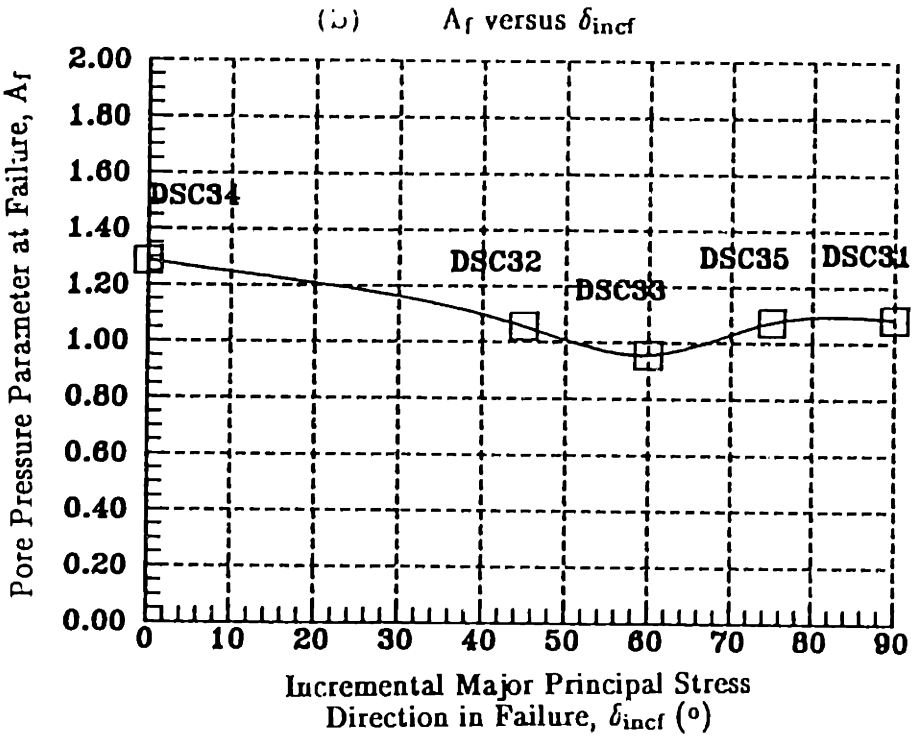

Figure 7.90: Pore Pressure Parameter A_f versus (a) Major Principal Stress Direction (δ_f); (b) Incremental Principal Stress Direction (δ_{incf}) at Failure.

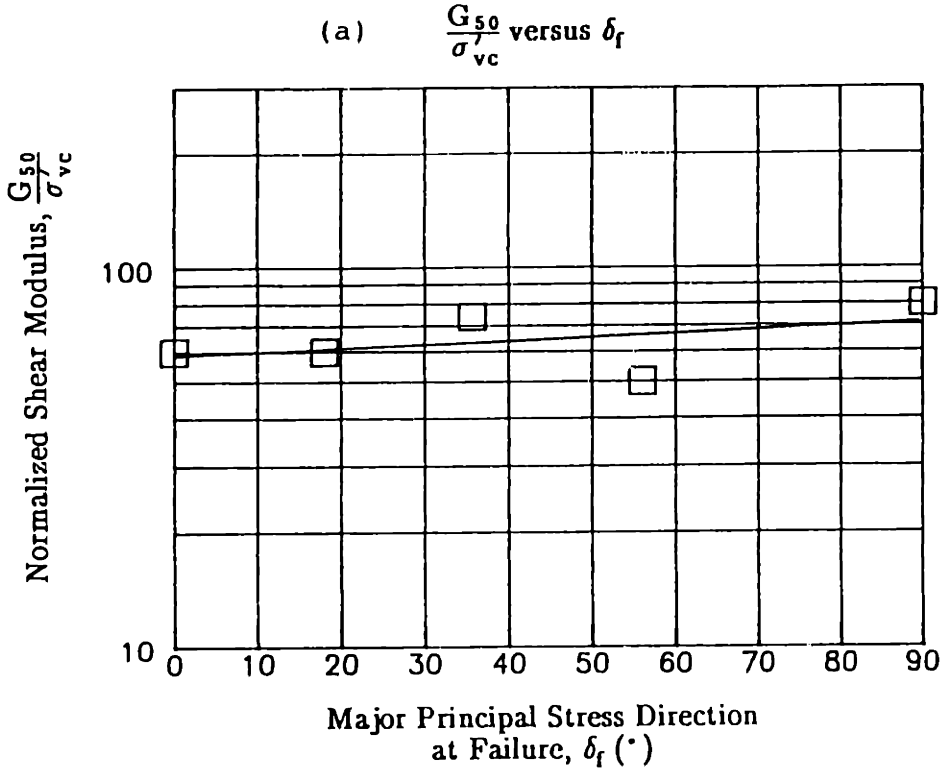

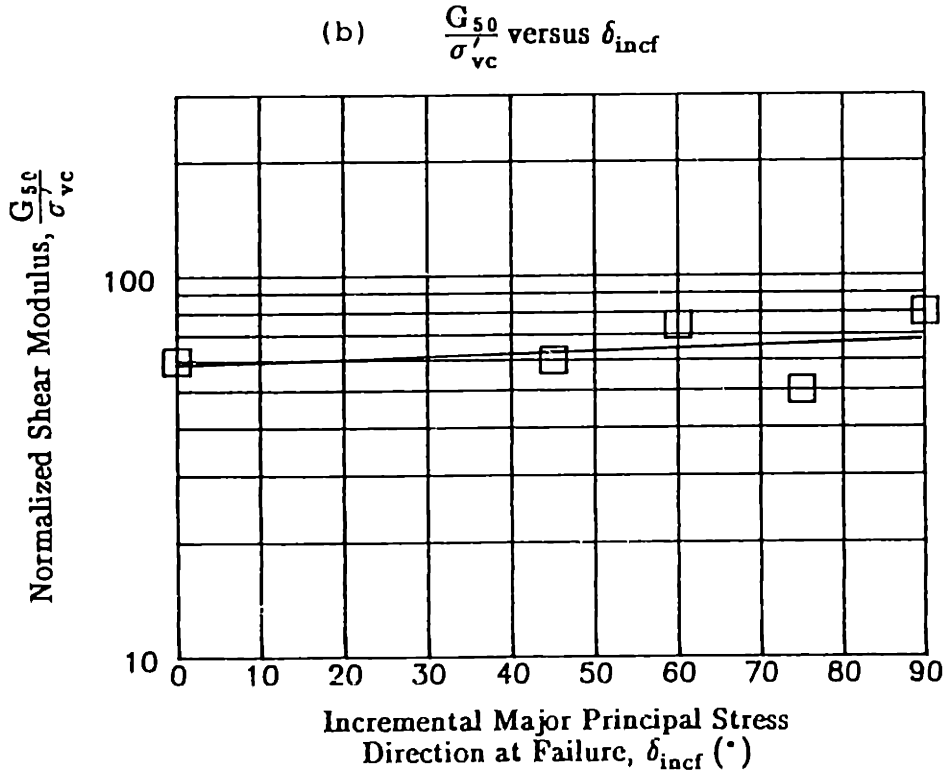

Figure 7.91: Normalized Shear Modulus at 50% of Maximum Applied Shear Stress versus (a) Major Principal Stress Direction (δ_f); (b) Incremental Principal Stress Direction (δ_{incf}).

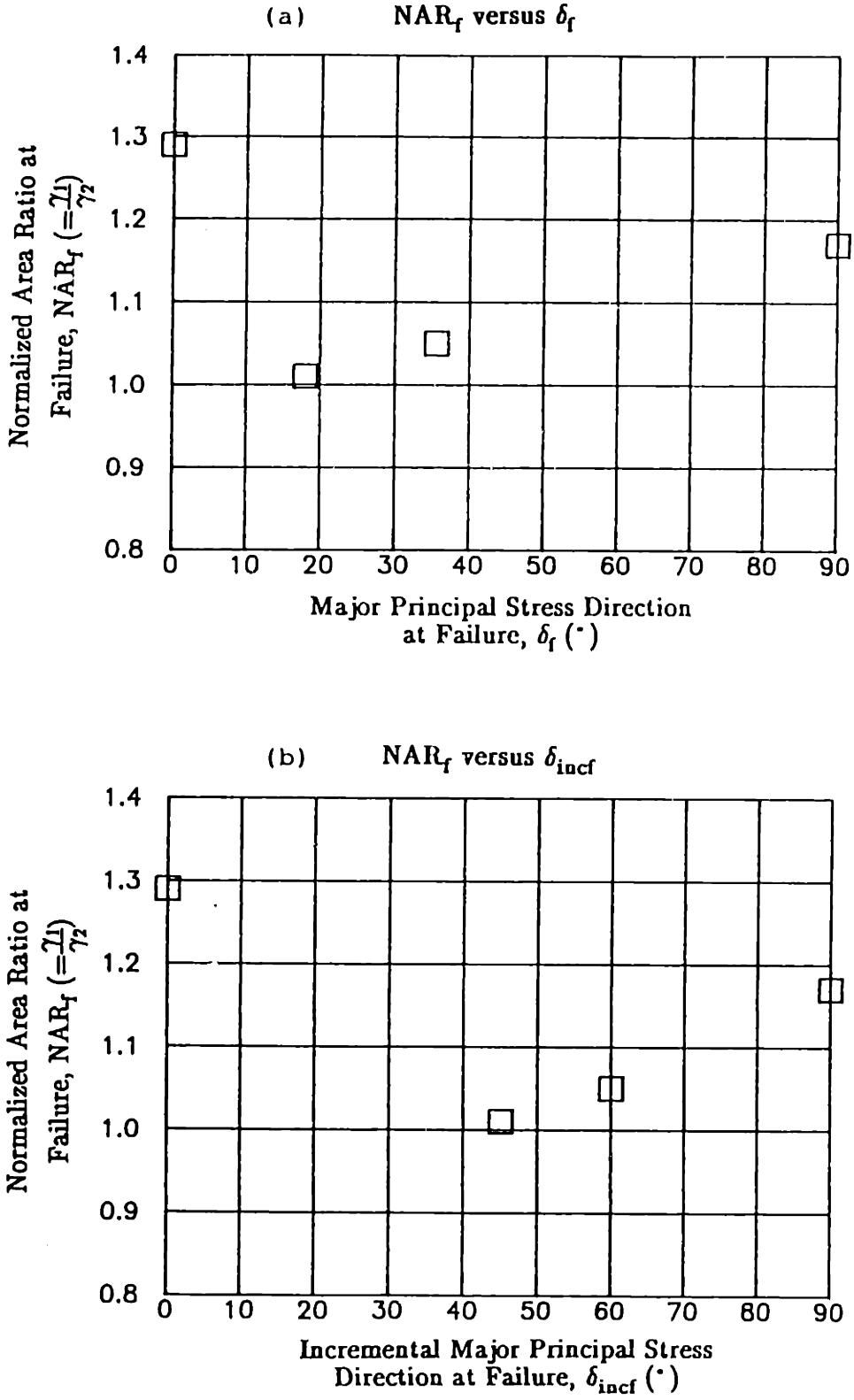

Figure 7.92: Normalized Area Ratio (NAR$_f$) versus (a) Major Principal Stress Direction (δ_f); (b) Incremental Principal Stress Direction (δ_{incf}) at Failure.

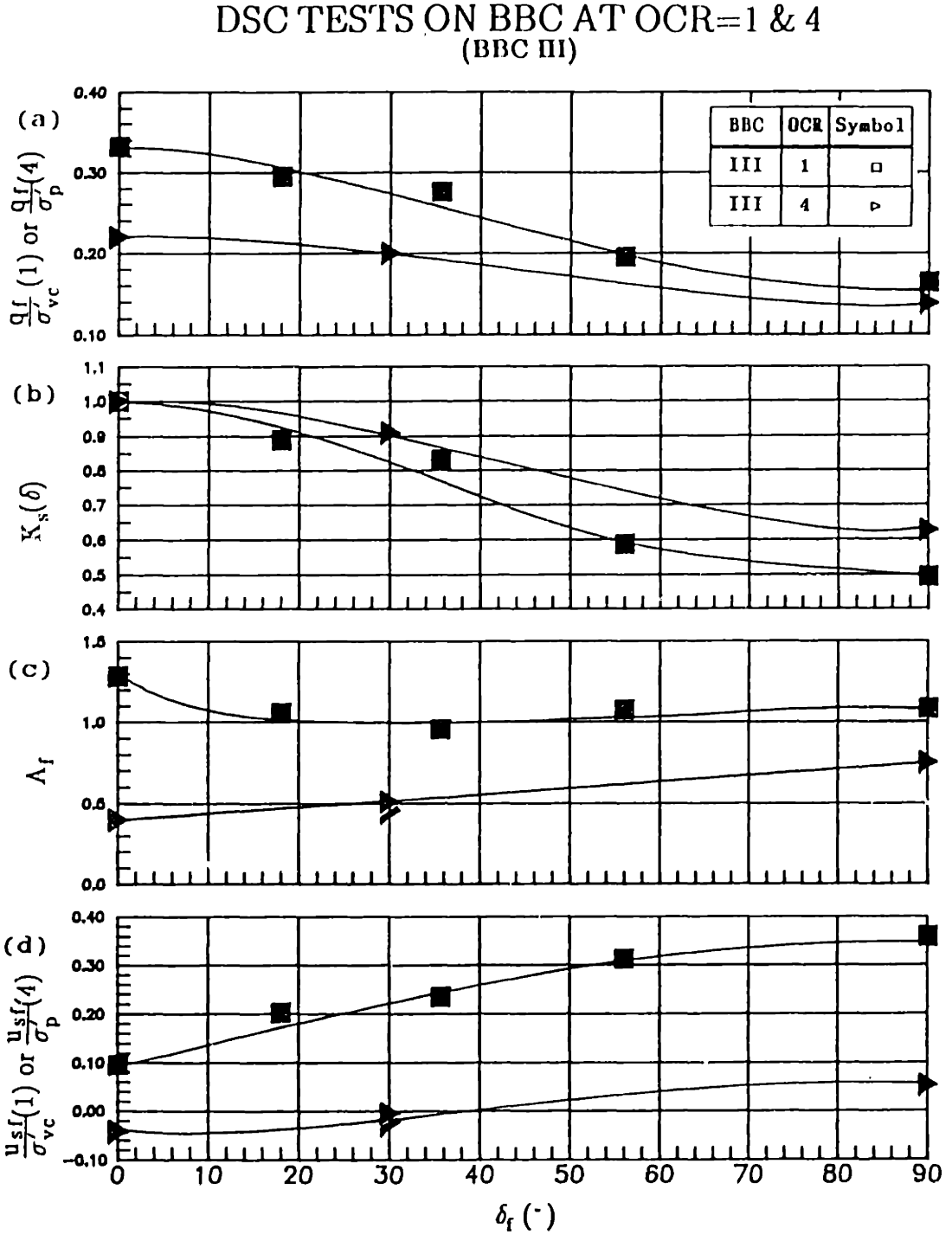

Figure 7.93: Comparison of DSC Tests on BBC III at OCR=1 and at OCR=4.

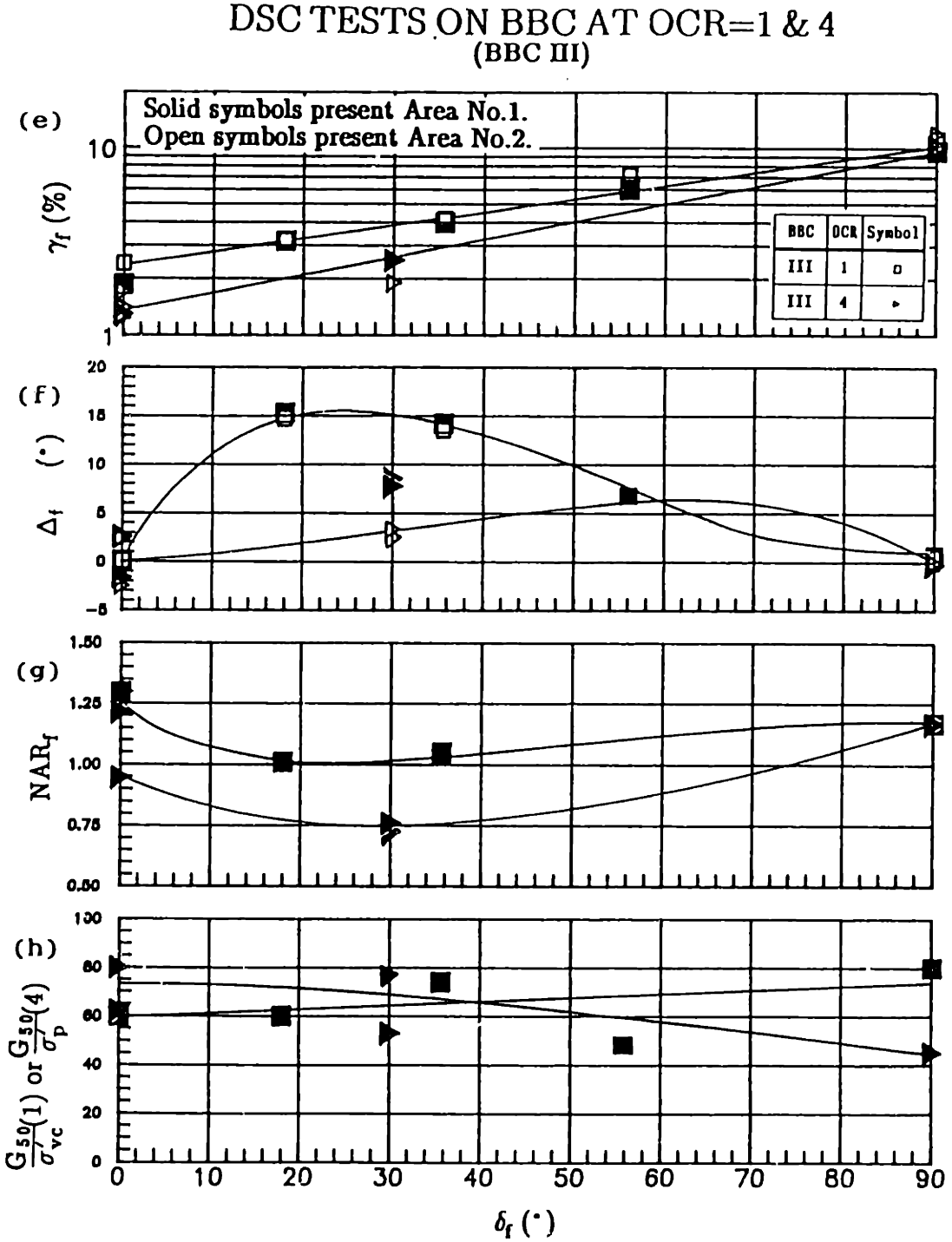

Figure 7.93: (Cont.)

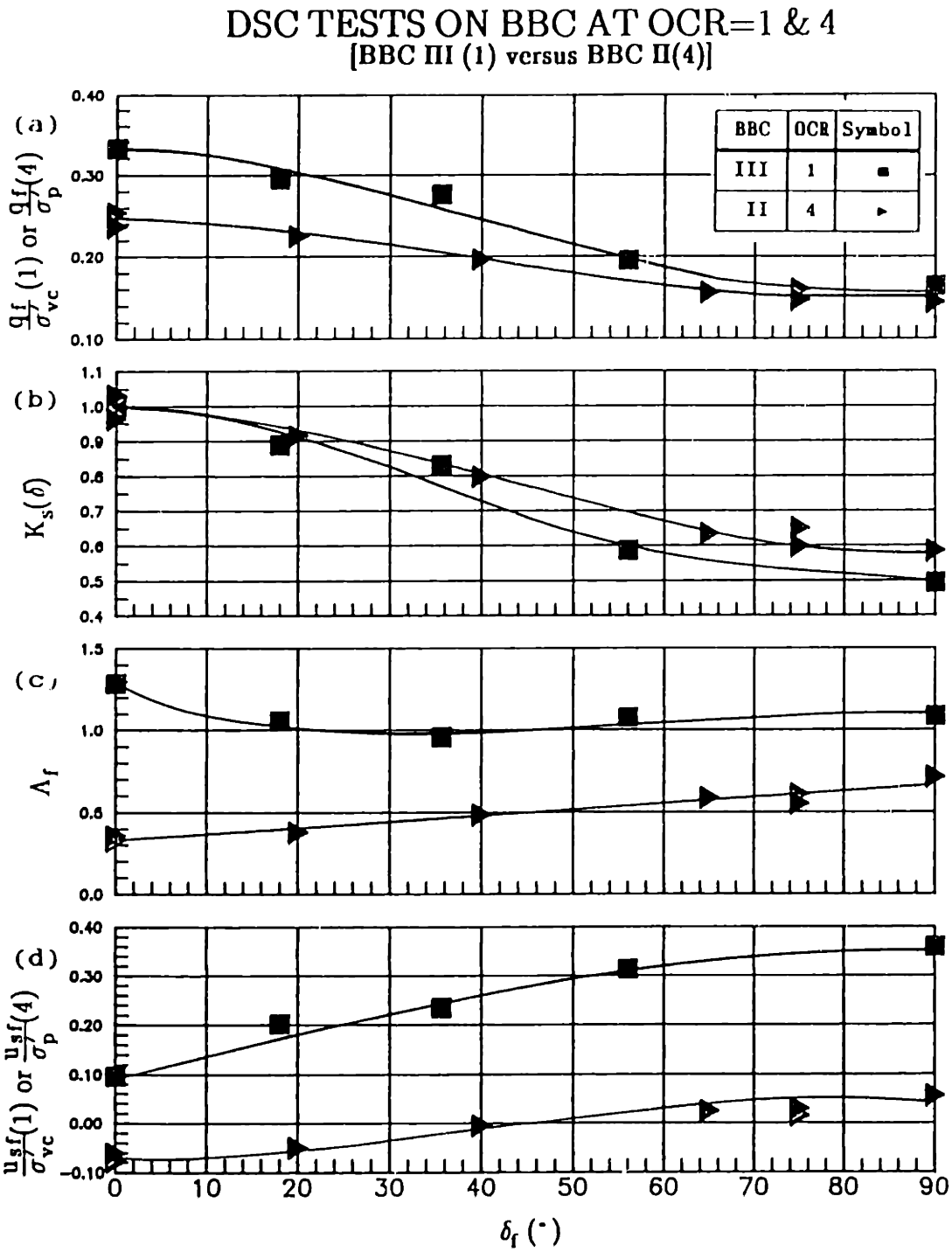

Figure 7.94: Comparison of DSC Tests on BBC III at OCR=1 and on BBC II at OCR=4.

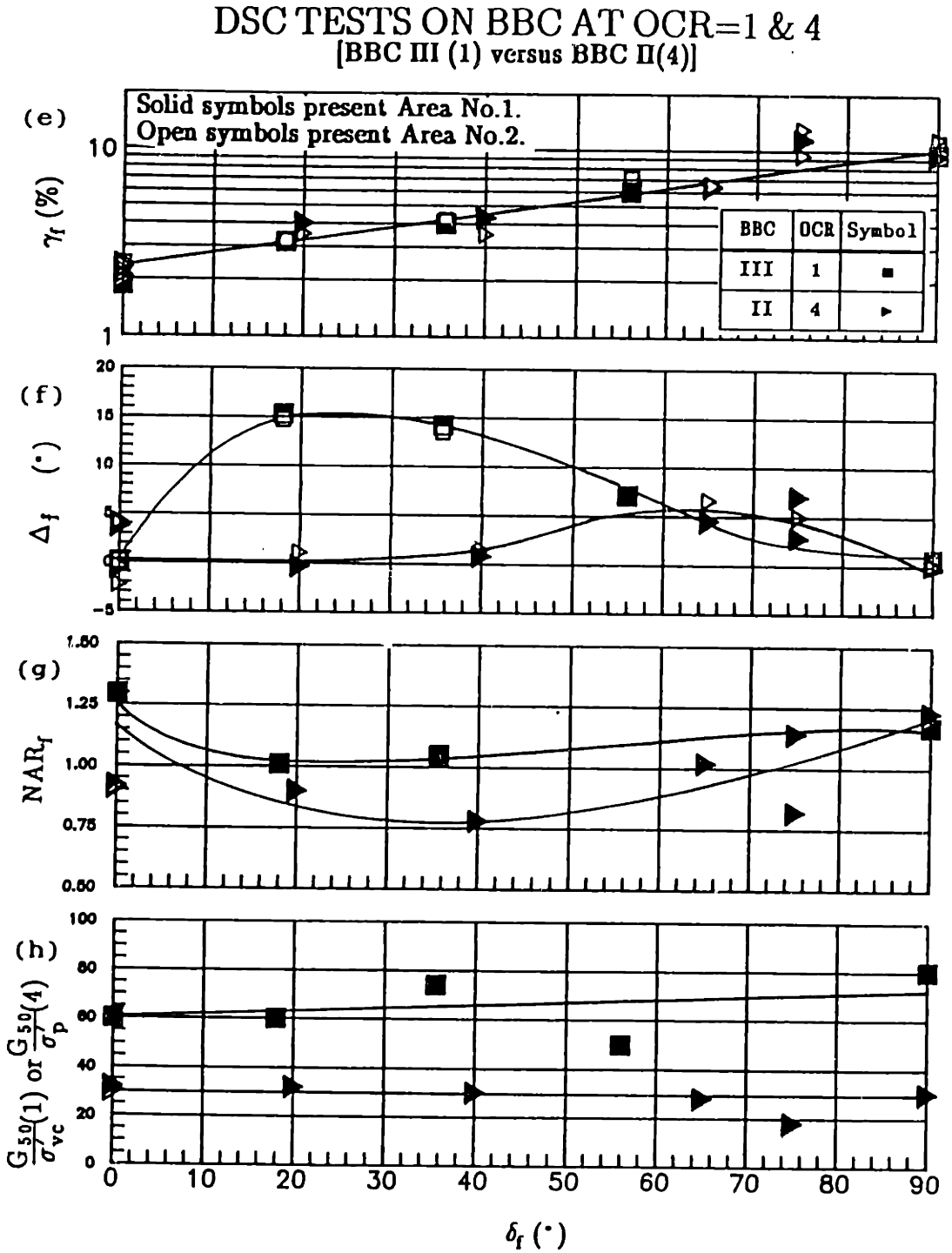

Figure 7.94: (Cont.)

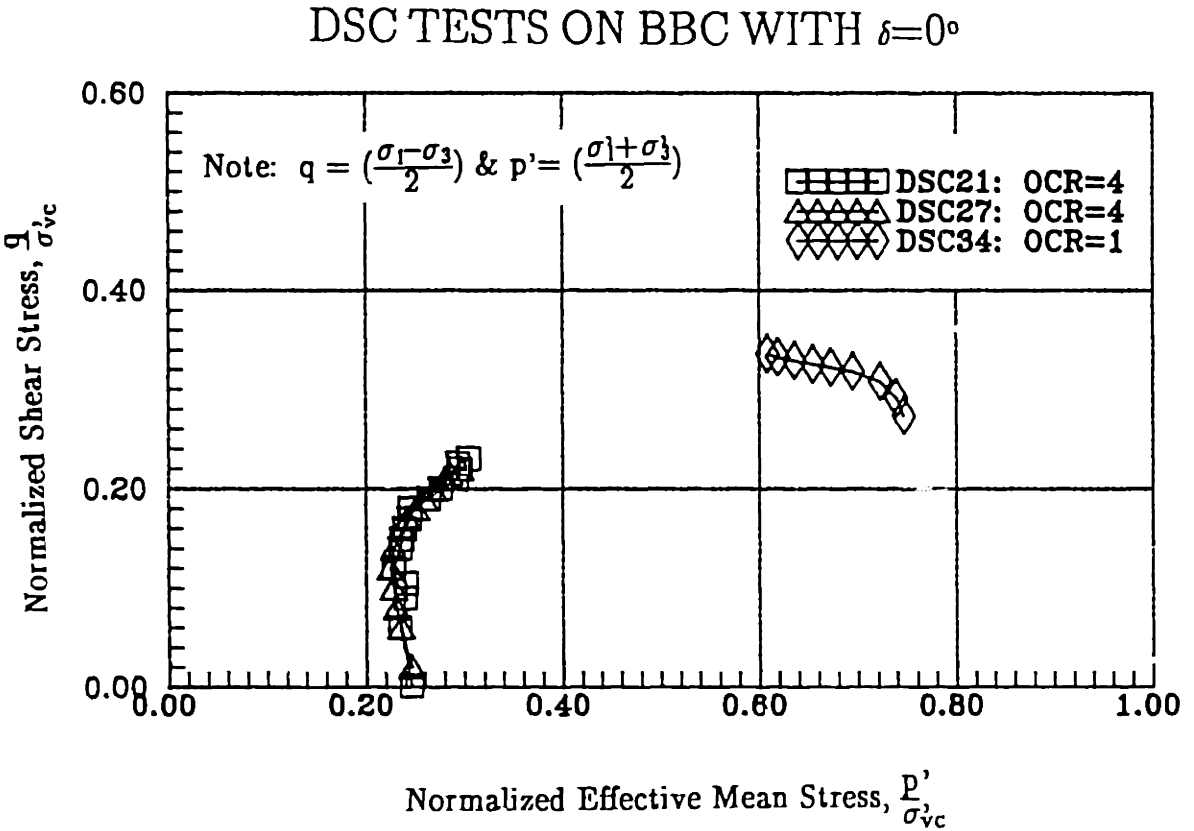

Figure 7.95: Normalized Effective Stress Paths from DSC Tests on BBC with δ=0°.

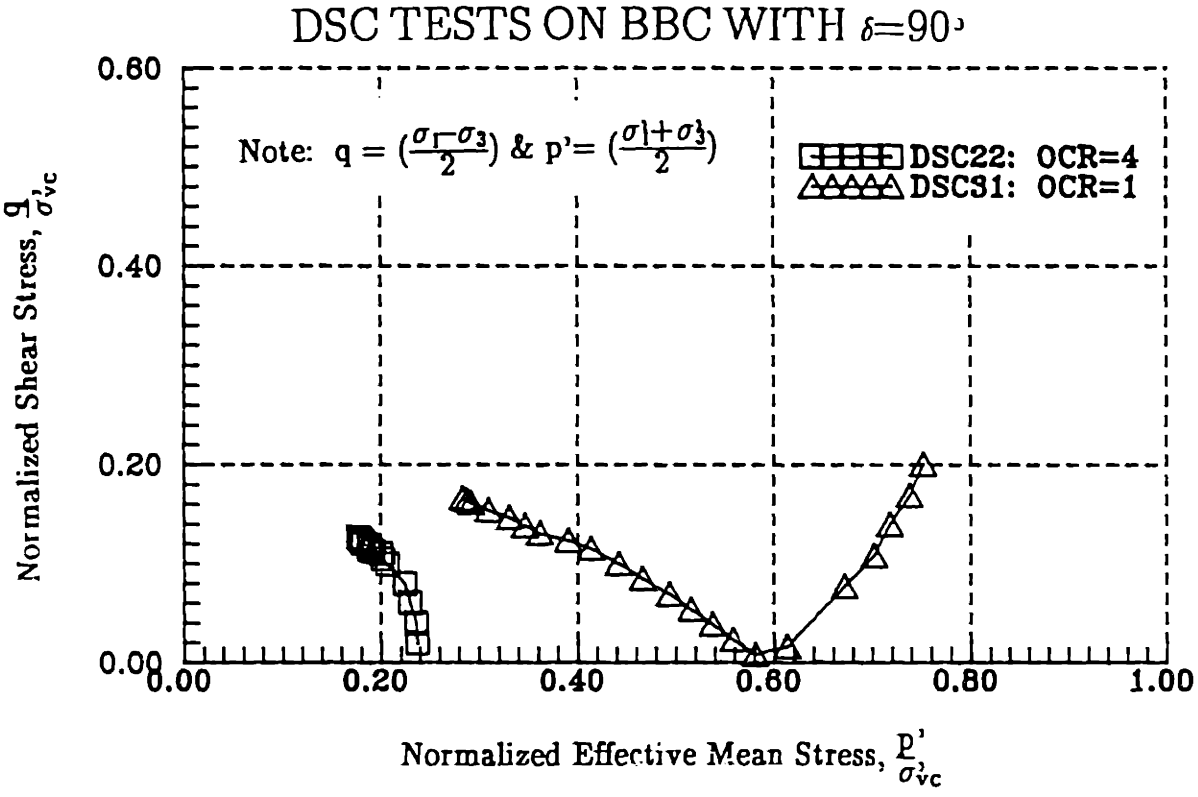

Figure 7.96: Normalized Effective Stress Paths from DSC Tests on BBC with δ=90°.

CHAPTER 8

COMPARISONS OF DSC DATA WITH RESULTS FROM OTHER TEST DEVICES AND MIT–E3 SOIL MODEL PREDICTIONS

8.1 INTRODUCTION

One objective of this chapter is to present comparisons between the DSC experimental data presented in Chapter 7 and existing laboratory data obtained from other shear tests. Such comparisons can be used as a tool to assess the performance of the DSC device and verify the DSC experimental data on BBC. Most of the available experimental data on BBC are restricted to triaxial and plane strain tests at δ=0° and δ=90°. Although extensive Direct Simple Shear tests also have been performed, the direction of the major principal stress and the state of stress of the soil in this device are not known. Hence, detailed comparisons at intermediate δ angles are not possible.

Another objective is to compare the DSC data with soil model predictions. A generalized effective soil model known as MIT–E3 is developed recently at MIT (Whittle, 1987) to describe the mechanical behavior of clays with varying overconsolidation. The model was evaluated extensively using laboratory data on BBC. The predictions from this model were found to be in good agreement with most experimental data for different modes of shearing such as triaxial, plane strain and direct simple shear. In addition, the model was used to predict the undrained shear behavior of overconsolidated BBC in the DSC mode of shear at different δ angles. Comparisons with measured stress–strain and effective stress paths from DSC tests performed by Germaine (1982) and O'Neill (1985) matched well. These results confirm the ability of the model to describe anisotropic

behavior caused by previous consolidation stress history. Therefore, it is appropriate to use predictions from this model to assess the results of the new DSC tests on normally consolidated BBC.

Section 8.4 of this chapter presents some of the "curve fitting" methods used to describe the variation in undrained strength with δ angle (Casagrande & Carillo, 1944, Bishop, 1966 and Davis & Christian, 1971). It is followed by comparison between these curves and the DSC experimental data.

8.2 COMPARISONS BETWEEN DSC RESULTS AND OTHER EXPERIMENTAL RESULTS

One of the advantages in performing shear tests on Boston Blue Clay (BBC) is that the extent of laboratory data available exceeds that of most clays used to study the strength–deformation behavior of cohesive soils. The experimental data include tests from K_o–consolidated triaxial tests (Sheahan, 1988), plane strain tests (Ladd et al., 1971), Direct Simple Shear tests (DeGroot, 1989 and Ladd & Edgers, 1972) and even DSC shear tests at an overconsolidation ratio of 4 (Germaine, 1982; O'Neill, 1985). Therefore, it is of interest to compare the DSC results at OCR=1 from this research with the results from other devices.

It should be noted that there are a number of differences between various shear devices like the triaxial, Direct Simple Shear, plane strain and DSC apparatuses, as discussed in Chapter 2. The differences include the boundary conditions (flexible versus rigid), the rate of deformation (strain–controlled versus stress–controlled), the magnitude of the intermediate principal stress (b) and the direction of the major principal stress (δ). Most of the existing data are from tests performed with the major principal stress acting in the direction of the depositional axis (δ=0°) or acting in the direction perpendicular to the depositional axis (δ=90°), except for DSS tests in which the direction of the major principal stress rotates continuously during shear.

The comparisons are limited based on the following:

1) Emphasis is placed on the results for normally consolidated resedimented BBC. Some comparisons of DSC test results at OCR=4 have been made with results from other devices (e.g. triaxial, plane strain and DSS) by Germaine (1982) and O'Neill (1982). Although this section focuses on the normally consolidated tests, the δ=0° and δ=90° results at OCR=4 are tabulated in Tables 8.1 and 8.2, respectively.

2) The experimental data should ideally be from the same series of resedimented BBC (i.e., BBC III). A number of CK_oUC triaxial tests were performed recently on BBC III (Sheahan, 1990) and his results are summarized in Table 4.11. The results for normally consolidated triaxial tests were remarkably similar, hence one representative test (from Sheahan, 1988) is presented in the comparison. Although a number of DSS tests were performed on this new resedimented BBC by DeGroot (1989), the tests chosen for the comparison were performed by the writer with a maximum vertical stress similar to that used for the new DSC tests at OCR=1. The results of the tests conducted using the MIT plane strain device are also compared with the DSC results. Although these tests were performed on a different series of BBC (i.e., BBC Ib), these are the only available data on BBC using the plane strain device.

8.2.1 Comparisons of Experimental Data at δ=0°

One of the most common modes of shearing imposes the major principal stress (σ_1) in the same direction as the depositional axis. There are a number of laboratory devices which are capable of the performing this mode of shearing,

including the conventional Triaxial apparatus (TX), the Plane Strain device (PS), the Directional Shear Cell (DSC) and the Torsional Shear Hollow Cylinder (TSHC). This shearing mode in conventional triaxial tests is referred to as a compression test. It is called the active case in plane strain tests, and in the DSC test is referred to as $\delta=0°$.

The results presented include experimental data on normally consolidated BBC from two plane strain active tests (PSA–6 and PSA–10) and one DSC test (DSC34) and three triaxial tests. One of triaxial test results was obtained from Sheahan (1988) on the new BBC (III). The results of two other triaxial tests performed by Sheahan recently are summarized in Table 8.3, but they are not presented in Figures 8.1 through 8.7. The plane strain data were collected from Ladd et al. (1971), and finally the DSC results were obtained from this research.

8.2.1.1 Conventional Stress–Strain Relationships

The first set of comparisons is made in terms of MIT's conventional format (as tabulated in Table 8.3), which excludes the effects of the intermediate principal stress (σ_2). The normalized shear stress is expressed as $\frac{q}{\sigma'_{vc}}$ $(=\frac{\sigma_1-\sigma_3}{2\sigma'_{vc}})$, and the normalized mean effective stress is given by $\frac{p'}{\sigma'_{vc}}$ $(=\frac{\sigma'_1+\sigma'_3}{2\sigma'_{vc}})$, where σ'_{vc} is the vertical consolidation stress for a normally consolidated clay. The variation in the K_c values for the different tests is not very significant, ranging from 0.46 to 0.55. Therefore, the comparison can be directly made without accounting for the effect of K_c.

The effective stress paths for the two plane strain tests are very similar to the DSC test as shown in Figure 8.1. Note that the results obtained from these two devices should be identical if the same material and similar strain rates are used. The plane strain tests produce a better defined curve because they include strain–softening behavior. The pore pressure parameter A_f for the DSC test of 1.3

is slightly higher than the plane strain tests of 0.9 as listed in Table 8.3. The magnitude of A_f in the triaxial tests is significantly lower than the plane strain tests (by approximately 50%). The effective stress path for the triaxial compression test differs significantly from the plane strain and DSC tests. The effective mean stress is fairly constant initially before the peak shear stress is reached, then decreases steadily after the peak. The difference in the shape of the effective stress paths from these devices (i.e., triaxial versus plane strain and DSC) is caused by the effects of σ_2. In the triaxial compression test, σ_2 is maintained at the same magnitude as the minor principal stress (σ_3). But in the plane strain tests, the magnitude of σ_2 is usually in between the two other principal stresses (σ_1 and σ_3). Therefore, for the purposes of comparisons, it is more appropriate to include the effect of the σ_2. Parameters which incorporate the three principal stresses are the octahedral normal stress (σ_{oct}) and shear stress (τ_{oct}), and the corresponding the octahedral shear strain (γ_{oct}). Further discussion of these parameters is presented in the next section.

The stress–strain relationships from the three devices are presented in Figure 8.2. The shear strains at failure (γ_f) in this mode of shearing are usually very small for normally consolidated BBC. The strains at failure for the two plane strain tests are 1.1 and 0.6%, and the corresponding normalized peak shear stresses are 0.334 and 0.32, respectively. The peak normalized shear stress of the DSC test falls between these plane strain results, but the shear strain at failure of γ_f=1.8% is higher than the plane strain tests. The stress–strain behavior obtained from the DSC test is almost identical to one of the plane strain tests (PSA–10). The stress–strain curve for the triaxial test is again very different from the other tests. It reaches a peak normal shear stress of 0.309 at an γ_f=0.20%, which is significantly lower than the plane strain tests. Two other triaxial tests (not shown in the figures, but given in Table 8.3) conducted by Sheahan (1990) on the same

series of BBC showed a slightly higher normalized shear strength of 0.322, but the strains at failure were in the same range (0.20–0.27%).

The normalized shear moduli ($\frac{G}{\sigma'_{vc}}$) for these tests are compared as shown in Figure 8.3. There is no significant difference in the modulus between the plane strain and the DSC tests, but the triaxial test shows a lower modulus at higher strain levels (γ>0.5%).

8.2.1.2 Octahedral Stress–Strain Relationships

The next series of comparisons are made in terms of octahedral stresses and octahedral strains which includes the effect of σ_2. The expressions for these parameters are given as follows:

Octahedral normal stress, $\sigma_{oct} = \frac{1}{3}(\sigma_1+\sigma_2+\sigma_3)$;

Octahedral shear stress, $\tau_{oct} = \frac{1}{3}\sqrt{(\sigma_1-\sigma_2)^2+(\sigma_2-\sigma_3)^2+(\sigma_3-\sigma_1)^2}$; and

Octahedral shear strain, $\gamma_{oct} = \frac{1}{3}\sqrt{(\epsilon_1-\epsilon_2)^2+(\epsilon_2-\epsilon_3)^2+(\epsilon_3-\epsilon_1)^2}$

The intermediate stress, σ_2, is measured in both the plane strain and DSC tests. Figure 8.4 plots the magnitude of the relative intermediate principal stress, b, versus the shear strain for both the plane strain and DSC tests. The magnitudes of b for DSC34 test is 0.23 at 1% strain, which is higher than the two plane strain tests of 0.18 and 0.12 at the same strain level. The difference in b is due to difficulty in measuring σ_2 on both devices. It should be noted that the σ_2 measured in the DSC is not necessarily equal to the actual σ_2 under a true plane strain condition due to deflections of the end platens (see Section 7.4.3.6).

The octahedral stress paths for the tests are shown in Figure 8.5. The

results are quite similar, apart from some discrepancy in the initial portion of the curve due to slightly different K_c values. The triaxial test results agree with the other tests quite well compared with the stress path shown earlier in the conventional format. There is some small variation in the post–peak portion of the triaxial and plane strain curves. This variation could be due to an error in the area correction of the triaxial test at large strains.

The stress–strain relationships of the different tests are presented in Figure 8.6. The shapes of the curves are almost identical, except that the DSC test has a slightly lower peak octahedral shear stress.

It is possible to evaluate the shear induced pore pressure ($u_s=\Delta u-\Delta\sigma_{oct}$) of these tests since σ_2 is measured; the u_s data are presented in Figure 8.7. The plot clearly indicates that the u_s value for the triaxial test is higher than the other tests at strains greater than 0.2%, but the u_s response below this strain level agrees well with the DSC test.

It is also of interest to compare the undrained strength ratio from the average of three triaxial tests (see Table 8.3) and the "plane strain" DSC test at $\delta=0^\circ$. The computed ratio is 0.96 ($=\frac{0.318}{0.332}$), which is almost the same as the value of 0.97 reported by Ladd et al. (1977) for BBC.

The comparisons at $\delta=0^\circ$ have demonstrated the validity of the results from the DSC, as the DSC data agree reasonably well with plane strain test results. Therefore, we conclude that the DSC device can definitely be used as a plane strain device in this mode of shearing.

8.2.2 Comparisons of Experimental Data at $\delta=90^\circ$

A total of four tests were selected for comparison: two plane strain passive tests (PSP–10 & PSP–11), one triaxial test and one DSC test (DSC31), all on normally consolidated BBC. A summary of the results is given in Table 8.4. The

plane strain results were obtained from Ladd et al. (1971) and the triaxial extension test was recently conducted by Sheahan at MIT, who kindly made the data available to the author for this comparison.

The parameters used in the comparison are similar to the δ=0° tests as described in the earlier section; the first set of parameters are expressed in the conventional MIT stress–strain format, and the octahedral stress–strain parameters are then employed to include the intermediate principal stress.

8.2.2.1 Conventional Stress–Strain Relationships

The definitions of normalized shear stress and effective mean stress used in the conventional form are as follows:

Normalized shear stress, $\frac{q}{\sigma'_{vc}} = \frac{1}{2}\left(\frac{\sigma_v - \sigma_h}{\sigma'_{vc}}\right)$; and

Normalized mean effective stress, $\frac{p'}{\sigma'_{vc}} = \frac{1}{2}\left(\frac{\sigma'_v + \sigma'_h}{\sigma'_{vc}}\right)$,

where the σ'_v and σ'_h designate the vertical effective stress and the horizontal effective stress.

Figure 8.8 displays the effective stress paths for the four tests. The stress paths show that the specimens experienced a jump rotation of 90° from δ=0° to δ=90° when the shear stress (q) reaches a value of zero. Strictly speaking, the specimens had undergone a δ=0° unloading to a shear stress of zero, then were subjected to a δ=90° loading as the shear stress decreases (i.e., becomes more negative). The stress path of the DSC matches very well with one of the plane strain tests (PSP–10), while the other plane strain test gives a higher mean effective stress. There is a significant deviation between the triaxial stress path

and the plane strain tests, as also observed in the δ=0° tests;, the triaxial test has a much lower mean effective stress for a given level of shear stress.

Figure 8.9 plots the stress–strain relationships for the tests. It is very difficult to pinpoint the strain at failure in the δ=90° tests because of the ductile behavior of the material. The change in the normalized shear stress between a shear strain of 2 and 10% is only about 0.1, compared with a change of 0.3 to 0.35 in the first 2% of straining (i.e.0<γ<2%). Furthermore, the strain at failure in a triaxial test depends on the type of area correction, since the sample is relatively non–uniform at large strains in a conventional triaxial apparatus with frictional ends. Therefore, it is more appropriate to compare the entire stress–strain curve instead of comparing the peak shear stress, unless rupture surfaces are clearly visible in the tested sample. The stress–strain curves for the DSC test (DSC31) and the plane strain test, PSP–10, are almost identical, with the other plane strain results also comparing relatively well. The triaxial results reveal a much softer behavior than the plane strain tests. In fact, the normalized shear stress of the triaxial test is about 0.06 lower than the average value of 0.11 in the other three tests at a strain of 2%. Therefore, without a doubt, the triaxial test yields a lower undrained shear strength than from plane strain and DSC tests in the δ=90° mode.

Figure 8.10 shows the relationship between the normalized shear modulus and the shear strain. The results all fall within a narrow band, and agree well even at very small shear strains (γ=0.1%).

8.2.2.2 Octahedral Stress–Strain Relationships

This section presents the results in terms of octahedral stress and strain for the same tests. Values of σ_2 were measured in both the plane strain and DSC tests, which allows the appropriate octahedral stresses to be computed. Figure 8.11 displays the measured b values versus the shear strain for the two plane strain

and DSC tests. The b value for the DSC test is exceptionally high, probably because of the influence of the top and bottom platens of the DSC device on the measured σ_2. When the sample is loaded during consolidation, strain energy is stored in the platens. But once the sample is subjected to undrained shear and the effective stresses decrease constantly, this strain energy is released, causing an increase in the measured σ_2. As a result, this increase in σ_2 yields a b value that is too high. It should be emphasized that the measured σ_2 is a correct measurement, but it does not correspond to the σ_2 under plane strain conditions.

The stress paths in the octahedral stress space as shown in Figure 8.12 indicate good agreement between the PSP–10 and DSC31 tests. The stress path for the triaxial test reaches a value of zero at $\frac{\sigma_{oct}}{\sigma'_{vc}}$=0.48, whereas the plane strain and DSC tests have a octahedral shear stress always greater than zero, due to non–zero deviatoric stress components. Unlike the δ=0° tests, the triaxial stress path for δ=90° is very different from the stress paths in plane strain.

The octahedral stress–strain relationships are shown in Figure 8.13, revealing excellent agreement between DSC31 and PSP–10. Both reach a minimum normalized octahedral shear stress of 0.05 at 0.3% strain, with increasing shear stresses thereafter. The other plane strain test (PSP–11) reaches a minimum shear stress of 0.09 at 0.4%. The stress–strain curve for the triaxial test is very different from the others, partly due to an abrupt change in the b value from 0 to 1 during shear.

Figure 8.14 presents the normalized shear induced pore pressure (u_s) versus the shear strain. The u_s value is somewhat higher in the DSC test at shear strains less than 2%, then somewhat lower at shear strains beyond 2%.

Ladd et al. (1977) reported that the ratio of the measured undrained shear strength at δ=90° from triaxial tests to plane strain tests had a value of 0.82 for BBC at OCR=1. This ratio based on the new DSC and triaxial results has an

identical value of 0.82 ($=\frac{0.135}{0.164}$).

The results presented at δ=90°, like those for δ=0°, show that the DSC data are in good agreement with the data from the plane strain tests.

8.2.3 Comparisons of Experimental Data at Intermediate Values of δ

One of the most commonly used shear devices at MIT is the Direct Simple Shear apparatus. A significant number of DSS tests have been performed at MIT on a variety of undisturbed cohesive soils as well as on resedimented BBC.

In the DSS test, the soil specimen is confined laterally with a wire–reinforced rubber membrane that allows only vertical deformation during consolidation. During shear, the sample deforms horizontally in a "simple shear" mode. One of the problems with the DSS test is the inability of the reinforced membrane to generate complementary shear stresses to those applied to the top and bottom of the specimen. In addition, the state of stress is unknown since only one shear stress and one normal stress are measured. It therefore poses a challenge to use the results from the DSC tests to predict soil behavior in a DSS mode of shearing.

There is one critical assumption used to compare the results from the DSC and DSS, which is related to the major principal strain direction (ξ). Since there is no vertical or horizontal normal strains induced during an undrained DSS shear test, it is reasonable to assume that ξ is 45° because the rigid body rotation is minimal for small shear strains. One can then compare the DSC tests at intermediate δ angles when ξ is approximately equal to 45°. This method of analysis is different from the comparisons made by Germaine (1982) and O'Neill (1985) at OCR=4. The magnitudes of the stress and strain from the DSS tests were compared directly with the DSC δ tests. Instead of comparing the results based on ξ=45°, they concluded that the rotation of σ_1 in the DSS tests at this

OCR begins with δ=50° at low shear strains and increases to δ=70° at high shear strains. However, the results presented here under the assumption of ξ=45° give a δ_f value of 43° at failure. More information on this topic will be given later in this section.

The DSC tests conducted in this test program have fixed δ_{inc} angles under undrained shear and the ξ direction is not controlled in the test. Therefore, the ξ=45° condition will have to be estimated from the DSC data. Figure 8.15a shows the effective stress paths (τ_h versus σ'_v) of two DSS tests (DSS06 and DSS07) and two DSC results performed on the same material. The DSS tests were performed at $\frac{\sigma'_{vc}}{\sigma'_p}$=1.12 and 1.30, which is the same as the final consolidation stress range of the DSC tests. The two DSC stress paths for δ_{inc}=45° and δ_{inc}=60° shown in this figure represent the horizontal shear stress and the vertical effective stress response on the plane normal to the depositional direction. This is done so that the magnitudes of the stresses can be compared directly with the DSS tests. The stress path for DSC32 at δ_{inc}=45° is very similar to the DSS stress paths, but it terminates at a peak shear stress (τ_{hmax}) of 0.172 at a normalized vertical effective stress of 0.8. The stress path for DSC33 at δ_{inc}=60° is very different from the the DSS tests, with a maximum horizontal shear stress of 0.26 at an effective vertical stress of 0.6. Figure 8.15b presents the ξ values for the two DSC tests. They do not follow a ξ =45° path; one test (δ_{inc}=45°) has ξ less than 45° and the other DSC test (δ_{inc}=60°) has ξ greater than 45°.

The stress–strain relationships for the four tests are shown in Figure 8.16a, and Figure 8.16b presents to the δ–γ relationship for the DSC tests. The normalized stress–strain relationships indicate that the DSS curves are in between the two DSC tests, as shown in Figure 8.16a. The results in Figure 8.16b, suggest that the δ–γ relationship for the DSS test should lie between the DSC tests with a δ≃25–30° at peak horizontal stress.

Figure 8.17a shows the change in normalized vertical effective stress $(-\frac{\Delta\sigma'_v}{\sigma'_{vc}})$ with strain for the DSS tests and the change in vertical effective stress with strain for the DSC tests. The same observation can be made from this figure: the DSS data fall between δ_{inc}=45° and δ_{inc}=60° tests, but with δ now closer to 35° at the peak horizontal shear stress.

Figure 8.18 displays the normalized shear modulus $(\frac{G}{\sigma'_{vc}})$ against the shear strain, γ, showing that the DSS data fall between the DSC tests.

There is another method to compare the results of the DSS and the DSC which considers the state of stress at failure; this also assumes that the DSS undrained shear tests follow a strain path of a ξ=45°. Figure 8.19 shows the relationship between ξ_f and δ_f obtained from the DSC tests at OCR=1. Based on this relationship, δ_f is 29° at ξ_f=45°, the q_f and p'_f values can be obtained from Figure 8.20. The results summarized in Table 8.6 (called "From DSC Data") indicate that the predicted shear strain at failure of 3.6% from the DSC data is fairly close to the measured DSS values. The predicted normalized horizontal shear stress (τ_f) and vertical effective stress (σ'_{vf}) are 0.237 and 0.579, respectively, at failure. The σ'_{vf} compares well with measured values, while the estimated τ_f is about 17% higher than the measured values.

A similar method of analysis using DSC results was employed for BBC at OCR=4 using a δ_f value of 43° at ξ_f=45° obtained from Figure 8.21 (compared with δ_f of 29° for normally consolidated BBC). The normalized stresses at failure are determined from Figure 8.22 for δ_f=43°. The results for OCR=4 from this method show τ_f higher than the measured DSS values as tabulated in the final row of Table 8.5. If the results from OCR=4 are compared with DSS tests, the method overestimates τ_f by 15% for recompression and 12% for SHANSEP type tests.

The discrepancy in the results between the predicted values of τ_f from the DSC and measured values from the DSS can be due to the following reasons:

1) The undrained strength variation (q_f–δ_f) is derived from five DSC data points. Error in drawing the profile may result in an overestimate of the undrained strength at intermediate δ angles, and a higher predicted horizontal stress. Another possible error could be in the ξ_f–δ_f relationship of the DSC data which may also influence the predictions.

2) The magnitude of the complementary shear stress on vertical planes of the DSS is not known, but it should be less than the applied horizontal shear stress. The stresses in the soil have to be redistributed in order to be in equilibrium, and this creates a non–uniformity of the stress in the soil. There is reason to believe that if the complementary shear stress was fully developed via rough boundaries, the peak horizontal shear stress would probably be higher, since more effort or energy would be required to shear the sample. This hypothesis might be checked by conducting DSS tests with a sand–coated wire–reinforced rubber membrane. Also, DeGroot (1989) hypothesized that the DSS device "induced reduction in σ'_v results in a corresponding decrease in the shear resistance and therefore a measured degree of strain softening which is greater than the true soil response."

One other method of checking the state of stress for the DSS is to conduct recompression DSS tests on BBC at an OCR of 4 with the depositional axis normal to the plane of shear, as shown Figure 8.23. Since the initial state of stress is approximately hydrostatic at this OCR (i.e., K_o near unity), such DSS undrained shear test performed should yield the same results as the ψ tests in the DSC since ξ and ψ would be equal to 45°. If the results are different from the ψ tests, i.e.,

the DSS produces a lower τ_f than from the DSC test, then this would support the hypothesis. According to O'Neill (1985), slippage between the soil and the top cap can occur in high OCR tests. Therefore, the recompression tests would have to be performed with pin–porous stones to prevent slippage during shear as described by O'Neill (1985).

8.3 PREDICTION OF DIRECTIONAL SHEAR CELL TEST RESULTS USING MIT–E3 SOIL MODEL

8.3.1 Description of the MIT–E3 Model (abstracted from Whittle, 1987)

8.3.1.1 Historical Perspective

The first generalized constitutive soil model was developed at Cambridge University in the 1960's. It was based on the concepts of critical state soil mechanics (Schofield and Wroth, 1968) and modeled the behavior of soil using plasticity theory. The work at Cambridge led to the development of the Modified Cam Clay (MCC) model (Roscoe and Burland, 1968) which is able to predict the behavior of hydrostatically consolidated triaxial compression tests during drained and undrained shear. However, the model is too simplistic for most natural clays since it does not take into account some important features of soil behavior such as anisotropy and strain softening. These issues were addressed by Kavvadas (1982) who developed the MIT–E1 soil model for describing the behavior of normally consolidated clays. It is based on the MCC model but is able to give more realistic predictions of soil anisotropy and strain softening. However, like the MCC model, the MIT–E1 model assumes that stress–strain behavior within the yield surface (i.e., overconsolidation states) is linear–elastic and therefore cannot realistically predict the behavior of overconsolidated soils. Using the MCC and MIT–E1 models as a framework, the MIT–E3 was developed to overcome these shortcomings so that it can provide realistic predictions for overconsolidated clays.

8.3.1.2 Description of the MIT–E3 Model

The MIT–E3 model describes the mechanical behavior of normally consolidated and overconsolidated clays using a formulation which consists of three distinct parts: 1) a Perfectly Hysteretic model; 2) an Elasto–Plastic model for normally consolidated clays and 3) a Bounding Surface Plasticity model. The basic assumptions used in the model consist of:

1. There is a distinction between unloading and reloading events such that the load history of a clay cannot be described fully by its overconsolidation ratio (i.e., new state variables are introduced to account for the past load history);

2. A load cycle in effective stress space always involves some plastic (irrecoverable) strain components. Thus, there is no purely elastic (reversible) range of behavior described by the model;

3. Coupling of the shear and volumetric behaviors is controlled by the bounding surface plasticity formulation;

4. The anisotropic behavior of the overconsolidated clay is related to the preferred directions of the normally consolidated clay via the bounding surface model; and

5. The perfectly hysteretic model controls the non–linearity at small strain levels.

The model is rate independent (i.e., creep effects are not considered) and applies to clays which exhibit normalized behavior. The three key components of the model can be summarized as:

(I) The Perfectly Hysteretic Model

This model describes a closed, symmetric hysteretic loop between stress reversal points. Non–linearity is related to the most recent stress reversal point as defined from the strain history imposed on the sample. As a result, the perfectly hysteretic model retains only a limited memory of the load history. Functions describing non–linearity are developed from the measured behavior in hydrostatic swelling and undrained shearing at small strain levels.

(II) Normally Consolidated Model

Normally consolidated behavior is described by a simplified version of the MIT–E1 model and includes:

1. A yield surface represented by a distorted ellipsoid. The surface can change in size homothetically, reflecting changes in the void ratio (density hardening) and also rotates in stress space to describe the evolving directions of anisotropy;

2. Critical state failure conditions are defined by a conical surface whose magnitude and orientation reflect the critical state strength anisotropy;

3. The model uses a non–associated flow rule such that all radial effective stress paths have the same virgin compression index.

The new version of the model improves predictions of the volumetric behavior of normally consolidated clay and also uses a smaller number of input parameters than its predecessor.

(III) Bounding Surface Plasticity Model

This model introduces plastic strains for overconsolidated stress states. The plastic behavior for a state inside the bounding surface is uniquely related to that of an image point on the surface (which is defined using a radial mapping rule). Functions are introduced to relate both the flow direction and the elasto–plastic modulus (at the current stress state) to the corresponding values at the image point. The model describes a smooth transition for stress paths approaching the bounding surface.

8.3.1.3 Input Parameters

The MIT–E3 model requires 15 input parameters as shown in Table 8.7. Most of the parameters can be determined from standard laboratory tests. Seven of the parameters are deterministic and eight are determined from predefined

parametric studies. Whittle (1987) recommends the following procedure for establishing the input parameters:

1. κ determines the elastic bulk modulus at small strain levels (i.e., those which occur immediately following a stress reversal). In concept, κ can be estimated from the modulus measured immediately after reversal of loading in an oedometer or triaxial test. However, practical difficulties due to inaccuracy of small strain measurements and secondary compression of clays invalidate this approach. Instead, it is recommended that κ be estimated from the results of either resonant column tests or from measurements of the in–situ elastic shear wave velocity using techniques such as crosshole or downhole techniques.

2. λ is the slope of the Virgin Compression Line (VCL) of a normally consolidated clay in e–$\log_e\sigma'$ space, which can also be determined directly from an oedometer test plotted in e–$\log_{10}\sigma'_v$ space.

3. (2G/K) is the ratio of the tangential elastic shear modulus to the bulk modulus, which is related to the Poisson's ratio, υ, of the soil skeleton:

$$2G/K = 3(1-2\upsilon)/(1+\upsilon)$$

For one–dimensional (K_o) swelling, it is assumed that the effective stress path is initially linear (assuming there are no plastic strains). If the OCR at $K_o = 1$ is known (OCR_1), then (2G/K) can be determined from the expression:

$$2G/K = \frac{(1 - K_{o\,nc})\,OCR_1}{(1/3)(1 + 2K_{onc})\,OCR_1 - 1}$$

4. ϕ'_{tc} and ϕ'_{te} are friction angles at the critical state condition measured in K_o consolidated triaxial compression and extension modes of shearing.

5. $(K_o)_{nc}$, the coefficient of lateral earth pressure at rest for normally consolidated clay, can be measured during K_o consolidation in either a triaxial test (with no lateral straining) or an oedometer with lateral stress measurement.

6. c, S_t are determined by a parametric study of the model behavior in undrained triaxial compression and extension tests for a K_o normally consolidated clay.

7. ψ_o is the parameter which controls the changes in anisotropy due to straining (i.e., rotational hardening of the model). There is limited experimental evidence giving the location of the yield surface for soils and almost no information on how yield surface rotates during subsequent loading. It is recommended that, until more data becomes available, ψ_o should be determined from parametric studies

such as those described in Whittle (1987).

8. C, n are the parameters used to describe the non–linearity in the volumetric response for the perfectly hysteretic formulation. Values of C and n are selected to match the swelling behavior in an oedometer or CRSC test.

9. ω, h and γ are used to complete the perfectly hysteretic formulation and to specify the mapping laws for the bounding surface plasticity. ω can be estimated from small strain measurements of the variation in secant modulus with strain level in undrained shear tests. However, in general, such data are not readily available, and in practice, all three constants must be estimated from parametric studies: Two types of tests are used to assess the parameters: a) hydrostatic or K_o unload and reload cycles and b) undrained shear tests in triaxial compression for overconsolidated clays.

Table 8.8 is a list of the input parameters selected by Whittle (1987) for Boston Blue Clay. These parameters were used to perform the MIT–E3 predictions of DSC tests on BBC in the following section.

8.3.2 MIT–E3 Predictions of DSC Test Results for Normally Consolidated BBC

Predictions of Directional Shear Cell behavior were reported by Whittle (1987) on resedimented BBC at OCRs of 1 and 4 using the input parameters given in Table 8.8. Comparisons of the experimental data and the model predictions at OCR=4 are described by Whittle. Therefore, this section will concentrate only on the results of normally consolidated BBC.

It should be noted that the properties of BBC III are slightly different from the previous series of BBC (mainly BBC II), which provided the basis for the model input parameters. These differences are less significant in normally consolidated behavior, as discussed in Chapter 4. Furthermore, there is insufficient laboratory data on the new material to justify selection of new parameters. Hence, under the circumstances it is reasonable to run the model with the same input parameters as used in previous studies.

The predictions of DSC behavior by Whittle (1987) were made by

simulating a fixed δ_{inc} undrained shear mode on normally consolidated BBC. The predictions were done with 15° increments from δ_{inc}=0° to δ_{inc}=90°. The results are presented through a comparison of the stress–strain–strength relationships and the stress–strain directions. Further evaluation focuses on the behavior at failure, and is discussed later in this section.

8.3.2.1 Predictions of DSC Undrained Shear Results

Five DSC tests were conducted at δ_{inc}=0°, 45°, 60°, 75° and 90° under an undrained shearing condition. The results of the model predictions are shown, along with the experimental data presented in Chapter 7, on normally consolidated BBC in Figures 8.24 to 8.31.

The effective stress paths (Figure 8.24) predicted by the model have the same trend in behavior as the five tests. The predicted stress paths for the δ_{inc}=0° and 90° agree very well with experimental data, but this is less so in the other three tests. The predicted stress–strain curves (Figure 8.25) are fairly similar to the experimental curves. The model has a distinct advantage over a DSC test: the ability to capture post peak behavior. It is not possible to measure strain–softening in the stress–controlled DSC device with current experimental procedure. The relationship between the applied shear stress (Δq) and shear strain is presented in Figure 8.26. The plot of Δq versus strain is easier to evaluate than the stress–strain curves. This applied shear stress is equal to the value of $\frac{\Delta\sigma_1-\Delta\sigma_3}{2}$ that is applied to the DSC specimen by application of normal and shear stress. Hence, for δ_{inc}=45°, Δq is equal to the stress applied via the shear sheets. The overall match is excellent. A log–log plot of normalized shear modulus versus shear strain is shown in Figure 8.27. These results were astonishing, showing exceptionally good agreement in terms of trend and magnitude. The only disagreement is at shear strain less than 0.2%, perhaps

because of the inability of the DSC to accurately measure small strains via the photographic technique.

Figure 8.28 displays the predicted and measured shear induced pore pressures ($u_s=\Delta u-\Delta\sigma_{oct}$) for the tests. The predicted u_s at low δ_{inc} is much higher than the measured values. However, the results of the other tests indicate good agreement.

One of the most interesting comparisons between the experimental data and the model prediction is the directions of principal stress and principal strain. Most of the comparisons made in previous research (except for the Multidirectional Direct Simple Shear tests conducted by DeGroot, 1989) do not include the rotation of principal stress and principal strain, partly due to insufficient laboratory tests with measured stress and strain rotations. Therefore, the comparison of these parameters can further evaluate the performance of the model in this respect.

Figure 8.29 presents the rotations of the major principal stress directions in the tests. The tests at $\delta_{inc}=0^\circ$ and 90° are a perfect match, which is expected since the principal stresses were acting in the depositional direction. More crucial are the comparisons of the results from the intermediate δ_{inc} tests. The predicted results for tests at $\delta_{inc}=45^\circ$ and $\delta_{inc}=75^\circ$ are in good agreement, while the model somewhat underpredicts the rotation of δ for the $\delta_{inc}=60^\circ$ test. In general, the predicted curves match well with the experimental curves.

The next comparison involves the rotation of the major principal strain direction, ξ, as shown in Figure 8.30. The experimental data show a significant amount of scatter at small strain levels ($\gamma<0.2\%$), but the trend is well defined at higher strain levels. The MIT–E3 predictions of major principal strain versus shear strain compare remarkably well once again for all the tests. For the intermediate δ_{inc} tests, the strain paths move away from the incremental major principal stress directions towards the major principal stress directions as the

shearing continues. The deviations from the δ_{inc} directions indicate that the soil has undergone plastic deformation, so that the sample tends to deform in the major principal stress direction. Both the experimental data and the predictions capture this behavior fairly well.

Figure 8.31 illustrates the measured and the predicted values of the intermediate principal stress, σ_2. The measured σ_2 value is clearly higher than the predicted results, especially at high δ angles. It is believed that the measured σ_2 does not represent a true plane strain value due to the deflection of the top and bottom platens. During undrained shear, the applied normal stresses were decreasing, leading to a reduction in the axial forces exerted on the top and bottom platens. As a result, the platens moved closer together, causing the measured intermediate principal stress to increase.

8.3.2.2 Evaluation of the MIT–E3 Predictions

This discussion concentrates on the behavior of the tests at failure. Some of the more important parameters are plotted against the δ and δ_{inc} angles so that comparisons can be made more easily. The results of the DSC test program and the MIT–E3 prediction are tabulated in Table 8.9, and are also presented in Figure 8.32 through 8.42.

The normalized undrained strength $(\frac{q_f}{\sigma'_{vc}})$ variation is given in Figure 8.32. The model predicts a very similar trend in behavior to that of the experimental data. However, the magnitudes of the predicted undrained strength are somewhat different from the measured values. The model overestimates the undrained shear strength at δ_f between 0° and 15°, then underestimates the strength for δ between 15° and 55°, and finally compares quite well in the last portion of the curve. Figure 8.32b shows the relationship between the normalized undrained strength and the prescribed δ_{inc} direction. Again the predicted results agree with the

experimental results quite well. The variation between the experimental and predicted mean effective stress at failure is also in very good agreement, as shown in Figure 8.33. The friction angle at the peak shear stress is related to the undrained shear strength and the mean effective stress at failure. These results are provided in Figure 8.34. The model predicts a higher friction angle at small δ angles, but the predicted friction angle is lower by about 2° at δ_f=55°. The span of the friction angle is between 32° and 35° in both the predicted and measured cases.

The shear strains at failure as a function of angle are illustrated in Figure 8.35. It is difficult to determine the shear strain at failure for the brittle behavior found at low δ angles in the DSC test. Figure 8.35 shows that the measured shear strain at failure for low δ angles is much higher than the predicted values. There is reason to believe that the measured strains are probably too high at small δ angles based on other experimental data, such as the triaxial and plane strain tests.

The plot of normalized applied shear stress at failure, $\frac{\Delta q_f}{\sigma'_{vc}}$, versus angle is shown in Figure 8.36, from which the predicted values agree well for δ<40°. There is a small difference at higher δ angles, with a maximum deviation of 0.03 at δ=90°. This good agreement is solely due to the difference in K_c values for the predictions and the applied values.

There is significant deviation between the model predictions and the measured normalized shear modulus at 50% of the maximum applied shear stress (Figure 8.37). The model predicts a very high normalized shear modulus at δ_f=0° and a minimum value of 50 at δ_f=50°. In contrast, the measured modulus does not change much with δ angle. One of the reasons for this poor agreement is that the error in the strain measurement in the DSC at small strains can be rather significant. Therefore, the measured modulus at this small shear strain is

correspondingly less reliable.

The pore pressure parameter, A_f, is compared in Figure 8.38; the predictions and measured values show similar trends and magnitudes with a maximum value at δ=0°.

The predicted shear induced pore pressure, u_s, at failure as shown in Figure 8.39 is also in reasonable agreement with the measured values, with u_s increasing steadily with δ angle.

Figures 8.40 and 8.41 display the relationships of ξ_f–δ_f and δ_f–δ_{incf}, respectively. Figure 8.40 shows exceptionally good agreement in the ξ_f–δ_f relationship between the predicted and the measured curves; the largest deviation is only on the order of 1°. The results of predicted δ_f versus δ_{incf} show a slightly larger difference, but the trends are identical.

Figure 8.42 presents the relationship between the relative magnitude of intermediate principal stress at failure, b_f, and the δ_f angle. The predicted b_f value decreases slightly with increasing δ_f angle. In contrast, the experimental results show a higher b_f, especially at δ_f values greater than 45°. These high values of b are believed to be due to the bending of the platens, which gives rise to excessive σ_2 values as explained earlier in this section.

There is one additional comment regarding the DSS test. The failure behavior in the DSS device can also be determined from the method described earlier using the model predictions for the DSC tests at failure. The results for an OCR of 1 are summarized in Table 8.6. The predicted τ_f for the DSS test is 0.211 at a vertical normal stress of 0.62. The predicted rotation from the model gives a δ_f value of 27° for ξ=45° as shown in Figure 8.40, compared with a δ_f of 29° using the DSC experimental data. These results are compared with the results predicted by MIT–E3 for direct simulation of the DSS shearing (Whittle, 1987). The predicted values of τ_f and σ'_{vf} are 0.207 and 0.64, respectively. The comparison

suggests that the technique of using DSC data to estimate DSS behavior at failure is reasonable.

8.4 ANISOTROPIC STRENGTH – CURVE FITTING METHODS

A number of curve fitting methods exist in the literature to represent the anisotropic strength for a given soil. Three methods of curve fitting are presented here. The first method was described by Casagrande and Carillo (1944), which uses a relationship between $S_u(\delta)$ and δ in the following form:

$$S_u(\delta) = S_u(\delta=90^\circ) + [S_u(\delta=0^\circ) - S_u(\delta=90^\circ)] \cos^2\delta$$

or it can be written as,

$$S_u(\delta) = S_u(\delta=90^\circ) \sin^2\delta + S_u(\delta=0^\circ) \cos^2\delta$$

The value of $S_u(\delta)$ is governed by the magnitudes of $S_u(\delta=0^\circ)$ and $S_u(\delta=90^\circ)$ only. The experimental results from the DSC at both OCRs (i.e., 1 and 4) are compared with the results obtained from this equation using known values of $S_u(\delta=0^\circ)$ and $S_u(\delta=90^\circ)$ from the DSC results, as shown in Figures 8.43 and 8.44 for the two different OCRs. This method seems to overestimate the S_u values at OCR of 1, but the fitted curve agrees rather well at OCR=4.

The second curve fitting method, described by Bishop (1966), is a modification of the original Casagrande–Carillo equation. The equation is given by:

$$S_u(\delta) = S_u(\delta=0^\circ) (1 - m \sin^2\delta) (1 - n \sin^2 2\delta)$$

The constants, m and n, have to be estimated based on known values of $S_u(\delta=0^\circ)$, $S_u(\delta=90^\circ)$ and an additional parameter $S_u(\delta)$ at an intermediate δ angle, say $S_u(\delta=45^\circ)$. In this problem, the $S_u(\delta=45^\circ)$ value is obtained from the plots of S_u versus δ_f (Figures 8.32 and 8.22) for $\delta_f=45^\circ$. The relationships for the different OCRs (1 and 4) are presented in Figures 8.43 and 8.44, showing remarkably good fit for these data sets.

The final method is the one proposed by Davis and Christian (1971) for use in bearing capacity analyses, which is known as the Elliptical Anisotropic Strength relationship. The form of the equation is as follows:

$$S_u(\delta)=\frac{M+\sqrt{M^2+L\,N}}{L}$$

where $M=\sqrt{a^2-N}\cos 2\delta$;

$a=\frac{1}{2}\left[S_u(\delta=0^\circ)+S_u(\delta=90^\circ)\right]$;

$N=S_u(\delta=0^\circ)\,S_u(\delta=90^\circ)$; and

$L=\cos^2 2\delta+\frac{N}{[S_u(\delta=45^\circ)]^2}\sin^2 2\delta$.

This equation also requires three S_u values, that is, $S_u(\delta=0^\circ)$, $S_u(\delta=90^\circ)$ and $S_u(\delta=45^\circ)$. For general comparison, the $S_u(\delta=45^\circ)$ is again obtained from the DSC experimental data, with the resulting fitted curves shown in Figures 8.43 to 8.46. The S_u–δ_f relationship from this method is identical to the curves from Bishop's method in both cases as shown in Figures 8.43 and 8.44, and the curves fit extremely well for this material.

One of the uncertainties in the last two methods lies in determining the $S_u(\delta=45^\circ)$ value. If $S_u(\delta=45^\circ)$ is assumed to equal to $\frac{1}{2}\left[S_u(\delta=0^\circ)+S_u(\delta=90^\circ)\right]$, then the curves for the three methods would be almost identical, and Bishop's

method will yield the same result as the first method, as shown in Figure 8.47. If one assumed that $S_u(\delta=45^\circ)$ is equal to the τ_f from DSS test, then $S_u(\delta=45^\circ)$ will be 0.20 at OCR=1 (from the DSS tests performed in this research), and $S_u(\delta=45^\circ)$ is approximately equal to 0.158 at OCR=4. The results using $S_u(\delta=45^\circ)$ of 0.20 at OCR=1 and $S_u(\delta=45^\circ)$ of 0.158 at OCR=4 are shown in Figures 8.48 and 8.49, along with the DSC data. Figures 8.50 and 8.51 display the results at OCR of 1 and 4 using the Bishop curve fitting method, indicating similar strength profiles as obtained from the Davis–Christian method. The new curves underestimate the undrained strength substantially at both OCRs. Therefore, in the author's opinion using $S_u(\delta=45^\circ)$ equal to $\frac{1}{2}[S_u(\delta=0^\circ)+S_u(\delta=90^\circ)]$ is a better approximation for this material than assuming $\tau_h(DSS)=S_u(\delta=45^\circ)$.

8.5 SUMMARY

The comparisons of results from DSC and other shear tests (e.g., plane strain and triaxial tests) were made. The results presented have shown exceptionally good agreement between the DSC and the plane strain tests at $\delta=0^\circ$ and $\delta=90^\circ$ on normally consolidated BBC in terms of the stress–strain–strength relationship. The difference in the results between the DSC and the triaxial is due to the difference in the intermediate principal stress. The ratios of undrained shear strength obtained from the triaxial tests and the DSC tests for $\delta=0^\circ$ and $\delta=90^\circ$ agree with the reported values by Ladd et al. (1977). The A_f values for the plane strain tests (including the DSC) are higher than the measured A_f value in the triaxial apparatus at $\delta=0^\circ$. The results also show that the strain at failure in the plane strain tests is substantially higher than the triaxial results. On the other hand, the variation of the A_f values at $\delta=90^\circ$ is very small between the different tests.

Comparisons were made between DSC and DSS data in an attempt to

unwrap the "mystery" behind the DSS state of stress. Unfortunately, the comparison led to more questions than answers. But all indications are that the rotation of the major principal stress in the DSS is about 29° at an OCR=1 and approximately equal to 43° at an OCR=4. For the analysis with ξ=45°, which only considered the strain condition at failure, the DSC data predict the following undrained strength ratios for failure in the DSS: $\frac{\tau_f}{\sigma'_p}$=0.24 at OCR of 1; $\frac{\tau_f}{\sigma'_p}$=0.19 at OCR of 4, whose τ_f is the peak τ_h. These predicted are about 17% higher at OCR=1 and 15% higher in the case of OCR=4.

The MIT–E3 constitutive soil model was developed at MIT to describe the mechanical behavior of clay with varying overconsolidation. This model consists of three components: 1) a Perfectly Hysteretic model; 2) an Elasto–Plastic model for normally consolidated clays; and 3) a Bounding Surface Plasticity model. Fifteen input parameters are required, that can be obtained mostly from standard laboratory tests. This model was shown (Whittle, 1987) to predict very well the significant effects of inherent anisotropy as measured by the DSC tests on BBC at OCR=4. Comparisons of the DSC shear behavior and MIT–E3 predictions at various δ_{inc} angles of normally consolidated clay were made in this chapter. The agreement is excellent between the experimental data and predicted values, in showing pronounced changes in clay behavior with δ angle. The most astonishing achievement was the agreement of q_f, Δq_f, ξ and δ directions between the experimental results and the model predictions, which supports the reliability of the experimental data and confirms the performance of the model in predicting the anisotropic behavior of normally consolidated clay.

Three methods of curve fitting to give anisotropic strength variations were described and evaluated. No one method shows superiority over the others for BBC at OCR=1 and 4, mainly due to the uncertainty in estimating $S_u(\delta$=45°). The former two methods offer more flexibility in the curve fitting process, but one

additional S_u value is required. If the $S_u(45^\circ)$ value is less than $\frac{1}{2}[S_u(0^\circ)+S_u(90^\circ)]$, which is commonly encountered in varved clays, then it will be more appropriate to use Bishop or Davis & Christian methods.

Table 8.1: Summary of δ=0° Undrained Shear Test Results on OCR=4 Resedimented Boston Blue Clay at Failure.

BBC Series (Ref.) Device	Test Number	Method of Consolidation • (OCR)	σ'_p(R) or σ'_{vm}(S) (ksc)	σ'_{vc} (ksc)	At Failure					$\frac{G_{sh}}{\sigma'_p}$	Remarks
					$\frac{q_f}{\sigma'_p}$	$\frac{p'_f}{\sigma'_p}$	γ_f (%)	$\frac{\sigma'_{1f}}{\sigma'_{3f}}$	A_f		
Ib Ladd (1971) PSD	PSA-5	S (4.0)	2.9	0.73	0.229	0.416	3.6	3.45	0.08	37	
	PSA-7	S (4.1)	6.0	1.46	0.243	0.372	3.8	4.77	0.18	23	
II O'Neill (1985) Triaxial	Average from 6 Recomp. Tests	R (4.0)‡	1.0	0.25	0.279	0.436	7.5	4.64	0.17	24	See Table 4.5
	TCSHAN	S (4.0)	2.46	0.62	0.252	0.449	3.8	3.56	0.06	67	
II Germaine (1982) DSC	DSC01	R (4.0)‡	1.0	0.25	0.237	0.318	2.2	6.85	0.36	30	
	DSC03	R (4.0)‡	1.0	0.25	0.254	0.337	2.4	7.12	0.33	32	
III Sheahan (1990) Triaxial		S (4.4)	6.2	1.42	0.206	0.395	5.4	3.18	0.13	-	
III This Research Triaxial	CIUC-1	R (4.0)	1.0	0.25	0.219	0.395	4.5	3.49	0.17	20	
	CIUC-2	R (4.1)	1.0	0.25	0.227	0.335	2.4	5.22	0.30	29	
III This Research DSC	DSC21	R (4.0)	1.0	0.25	0.220	0.295	1.4	6.87	0.40	80	
	DSC27	R (4.0)	1.0	0.25	0.220	0.297	1.2	6.71	0.40	62	

Notes: • S=SHANSEP, R=Recompression.
‡ All recompression values corrected for thixotropic effect.

Table 8.2: Summary of δ=90° Undrained Shear Test Results on OCR=4 Resedimented Boston Blue Clay at Failure.

BBC Series (Ref.) Device	Test Number	Method of Consolidation • (OCR)	σ'_p(R) or σ'_{vm}(S) (ksc)	σ'_{vc} (ksc)	At Failure					$\frac{G_{sn}}{\sigma'_p}$	Remarks
					$\frac{q_f}{\sigma'_p}$	$\frac{p'_f}{\sigma'_p}$	γ_f (%)	$\frac{\sigma'_{1f}}{\sigma'_{3f}}$	A_f		
Ib Ladd (1971) PSD	PSP-12H	S (4.0)	4.0	1.01	0.161	0.227	-10.6	5.9	0.51	16	
II O'Neill (1985) Triaxial	Average from 5 Recomp. Tests	R (4.0)‡	1.0	0.25	0.143	0.150	-16.4	22	0.86	11	See Table 4.6
II Germaine (1982) DSC	DSC02	R (4.0)‡	1.0	0.25	0.144	0.189	-9.4	7.4	0.71	30	
III This Research Triaxial	CIUE-1	R (4.2)	1.0	0.24	0.095	0.162	-9.6	3.83	0.93	30	
	CIUE-2	R (4.3)	1.0	0.23	>0.088	0.165	<-4.2	3.29	0.84	37	
III This Research DSC	DSC22	R (4.0)	1.0	0.25	0.138	0.191	-10.2	6.20	0.75	45	

Notes: • S=SHANSEP, R=Recompression.
‡ All recompression values corrected for thixotropic effect.

Table 8.3: Summary of δ=0° Undrained Shear Test Results on Normally Consolidated Resedimented Boston Blue Clay at Failure.

BBC Series (Ref.) Device	Test Number	Batch	K_c	σ'_{vc} (ksc)	At Failure					$\frac{G_{s0}}{\sigma'_{vc}}$	Remarks
					$\frac{q_f}{\sigma'_{vc}}$	$\frac{p'_f}{\sigma'_{vc}}$	γ_f (%)	$\frac{\sigma'_{1f}}{\sigma'_{3f}}$	A_f		
Ladd et al. (1971) PSD	PSA-6	I b	0.55	3.8	0.334	0.674	1.1	2.96	0.96	82	
	PSA-10		0.51	3.96	0.321	0.699	0.6	2.70	0.86	48	
Ladd et al. (1971)	Average from 4 Tests	I b	0.52	-	0.34	0.70	0.80	2.89	0.8	-	
Sheahan (1988) Triaxial	SPC7257	III	0.529	2.0	0.309	0.776	0.20	2.32	0.44	171	
Sheahan (1990) Triaxial	C(F)•	III	0.466	2.9	0.322	0.749	0.20	2.51	0.52	-	
	C(L)•		0.473	2.8	0.322	0.752	0.27	2.50	0.35	-	
This Research	DSC34	III	0.507	1.15	0.332	0.619	1.8	3.31	1.29	60	

Notes:

• F = Frictional end caps; L = Lubricated end caps.

Table 8.4: Summary of δ=90° Undrained Shear Test Results on Normally Consolidated Resedimented Boston Blue Clay at Failure.

BBC Series (Ref.) Device	Test Number	Batch	K_c	σ'_{vc} (ksc)	At Failure					$\frac{G_{s0}}{\sigma'_{vc}}$	Remarks
					$\frac{q_f}{\sigma'_{vc}}$	$\frac{p'_f}{\sigma'_{vc}}$	γ_f (%)	$\frac{\sigma'_{1f}}{\sigma'_{3f}}$	A_f		
Ladd et al. (1971) PSD	PSP-10	I b	0.497	3.98	0.185	0.266	-14.0	5.55	1.06	71	
	PSP-11		0.52	3.97	0.225	0.225	-12.0	∞	1.07	39	Criteria: σ'_v=0.0
Ladd et al. (1971)	Average from 4 Tests	I b	0.50	-	0.19	0.295	-8.6	4.62	1.02	-	
Sheahan (199) Triaxial	E(F)	III	0.464	2.8	0.135	0.220	-21.5	4.18	1.16	51	
This Research	DSC31	III	0.522	1.3	0.164	0.288	-9.6	3.65	1.17	80	

Notes:

Table 8.5: Summary of CK_oUDSS Test Results on OCR=4 Resedimented Boston Blue Clay at Failure.

Ref.	Test Number	Batch	Type of Consol	σ'_p(R) or σ'_{vm}(S) (ksc)	σ'_{vc} (ksc)	At Peak					$\frac{G_{s0}}{\sigma'_{vm}}$	Remarks
						γ_f (%)	$\frac{\tau_f}{\sigma'_{vm}}$	$\frac{\sigma'_{vf}}{\sigma'_{vm}}$	ϕ' (°)	δ_f (°)		
Ladd et al. (1972)	1002A	I	R	4.0	1.0	9.3	0.134	0.270	26.4	-		
	311		S	4.0	1.0	8.5	0.161	0.329	26.1	-		
	611		S	4.0	1.0	11.7	0.153	0.323	25.2	-		
	1304		S	4.0	1.0	7.7	0.139	0.307	24.3	-		
O'Neill (1985)	DSS	II	R	1.0	0.25	4.1	0.167	0.261	32.6	-		
	DSS		R	1.0	0.25	7.5	0.162	0.244	33.6	-		
	DSS7		S	2.0	0.5	10.5	0.167	0.331	26.8	-		
	DSS9		S	2.0	0.5	4.8	0.165	0.386	23.1	-		
	DSS15A		S	2.0	0.5	11.7	0.175	0.307	29.7	-		
Average	2 Tests	II	R	1.0	0.25	5.8 ±2.4	0.165 ±0.004	0.253 ±0.012	33.1	-		τ_f is 15% higher than DSC Pred.
Average	3 Tests	II	S	2.0	0.5	9.0 ±3.7	0.169 ±0.005	0.341 ±0.041	26.4	-		τ_f is 12% higher than DSC Pred.
Average	9 DSS Tests	I & II	R & S	1 to 4	-	8.4 ±2.7	0.158 ±0.014	0.306 ±0.043	27.3	-		
From DSC Data		II	R	0.25	1.0	4.1	0.189	0.274	35.8	43		Estimated for δ_f=43°.

Table 8.6: Summary of $C\bar{K}_oUDSS$ Test Results on Normally Consolidated Resedimented Boston Blue Clay at Failure.

Ref.	Test Number	Batch	σ'_{vc} (ksc)	At Peak					$\frac{G_{sa}}{\sigma'_{vc}}$	Remarks
				γ_f (%)	$\frac{\tau_f}{\sigma'_{vc}}$	$\frac{\sigma'_{vf}}{\sigma'_{vc}}$	ϕ' (°)	δ_f (°)		
DeGroot (1989)	G1 G2 G4	III	3.0 3.0 3.0	4.7 5.4 5.5	0.191 0.213 0.205	0.561 0.528 0.542	18.8 22.0 18.0	- - -	59 69 73	
This Research	DSS06 DSS07	III	1.12 1.30	2.5 3.1	0.201 0.202	0.667 0.606	16.8 18.5	-	62 59	
Average	2 Tests	III	1.12-1.30	2.8 ±0.4	0.202 ±0.001	0.637 ±0.043	17.6	-	61 ±2	γ_f is 17% higher than DSC Pred.
From DSC Data	-	III	1.14-1.30	3.6	0.237	0.579	22.3	29	62	Estimated for $\delta_f = 29°$.
MIT-E3 based on DSC Pred	-	-	-	2.8	0.211	0.621	18.8	27	58	Estimated for $\delta_f = 27°$.
MIT-E3 Predict. DSS	-	-	-	3.0	0.207	0.640	17.9	25	-	

Table 8.7: Input Parameters for MIT–E3 Soil Model (after Whittle, 1987).

Parameter	Role	How to Obtain
e_o	MIT-E3 NC clays	Void Ratio at reference state of Virgin Compression Line of normally consolidated clay.
κ		Determine small strain modulus from resonant column or in situ elastic shear wave velocity.
λ		Slope of Virgin Compression Line in e-$\log_e \sigma'$ space from oedometer.
2G/K		From K_o swelling in lateral stress oedometer.
ϕ'_{tc}		Critical state friction angles from CK_oUC/E tests on normally consolidated clay.
ϕ'_{te}		
$(K_o)_{nc}$		Measured in lateral stress oedometer or CK_oUC/E.
c		Parametric study of undrained strength in CK_oUC/E tests.
S_t		Parametric study of sensitivity in CK_oUC/E tests.
ψ_o		Rotation rate of yield surface.
C	Perfectly Hysteretic Model	Parametric study of swelling in oedometer tests.
n		
ω		Estimate stiffness at small strains in CK_oUC for overconsolidated clay.
γ	Bounding Surface Plasticity	Parametric study of CK_oUC test at OCR=2.
h		Parametric study of unload-reload cycles in hydrostatic or oedometer tests.

Table 8.8: MIT–E3 Input Parameters for Boston Blue Clay.

Parameter	Boston Blue Clay
e_o	1.12
κ	0.001
λ	0.184
2G/K	1.05
ϕ'_{tc}	33.4°
ϕ'_{te}	45.9°
$(K_o)_{nc}$	0.48
c	0.866
S_t	4.5
ψ_o	100.0
C	22.0
n	1.60
ω	0.07
γ	0.5
h	0.2

Table 8.9: Summary of Measured and Predicted Data of DSC Undrained Shear Tests on Resedimented Boston Blue Clay at OCR=1.

Source	Angles			Conventional Format					Octahedral Format						
	δ_{incf} (°)	δ_f (°)	ξ_f (°)	$\frac{q_f}{\sigma'_{vc}}$	$\frac{p'_f}{\sigma'_{vc}}$	$\frac{\Delta q_f}{\sigma'_{vc}}$	γ (%)	ϕ_f (°)	$\frac{\tau_{octf}}{\sigma'_{vc}}$	$\frac{\sigma_{octf}}{\sigma'_{vc}}$	γ_{oct} (%)	$\frac{u_{sf}}{\sigma'_{vc}}$	A_f	b_f	$\frac{G_{s0}}{\sigma'_{vc}}$
DSC Exper. Data	0	0.0	0.0	0.332	0.619	0.085	1.86	32.4	0.280	0.569	0.76	0.096	1.286	0.27	60
	45	18	33.3	0.295	0.526	0.172	3.20	34.1	0.280	0.449	1.31	0.202	1.056	0.25	60
	60	35.6	49.8	0.274	0.486	0.300	4.00	34.6	0.233	0.446	1.82	0.235	0.956	0.28	74
	75	56	63	0.195	0.345	0.362	6.00	34.4	0.162	0.367	2.44	0.313	1.074	0.67	50
	90	90	91.0	0.164	0.288	0.404	9.62	34.7	0.142	0.322	3.91	0.359	1.085	0.81	80
MIT-E3 Pred.	0	0.0	0.0	0.354	0.616	0.094	0.40	35.2	0.306	0.548	0.16	0.106	1.159	0.207	196
	45	15.8	32.2	0.304	0.548	0.159	1.32	33.7	0.263	0.488	0.54	0.165	1.098	0.200	74
	60	29.6	48.1	0.256	0.460	0.254	3.19	33.8	0.222	0.410	1.30	0.243	1.046	0.200	55
	75	55.1	68.3	0.203	0.379	0.380	6.20	32.3	0.176	0.337	2.53	0.316	0.972	0.181	49
	90	90.0	90.0	0.173	0.314	0.438	9.80	33.6	0.151	0.278	4.00	0.375	0.991	0.185	63

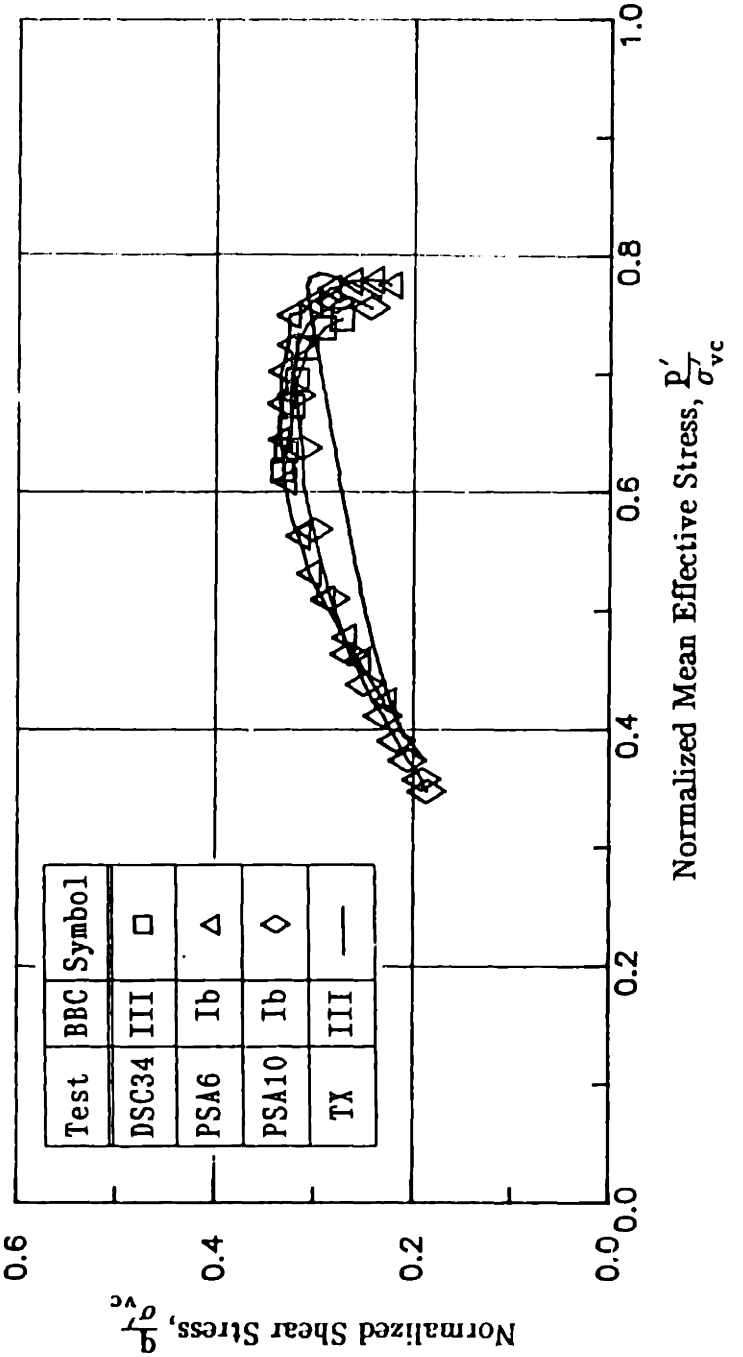

Figure 8.1: Normalized Effective Stress Paths from δ=0° Undrained Shear Tests on OCR=1 BBC.

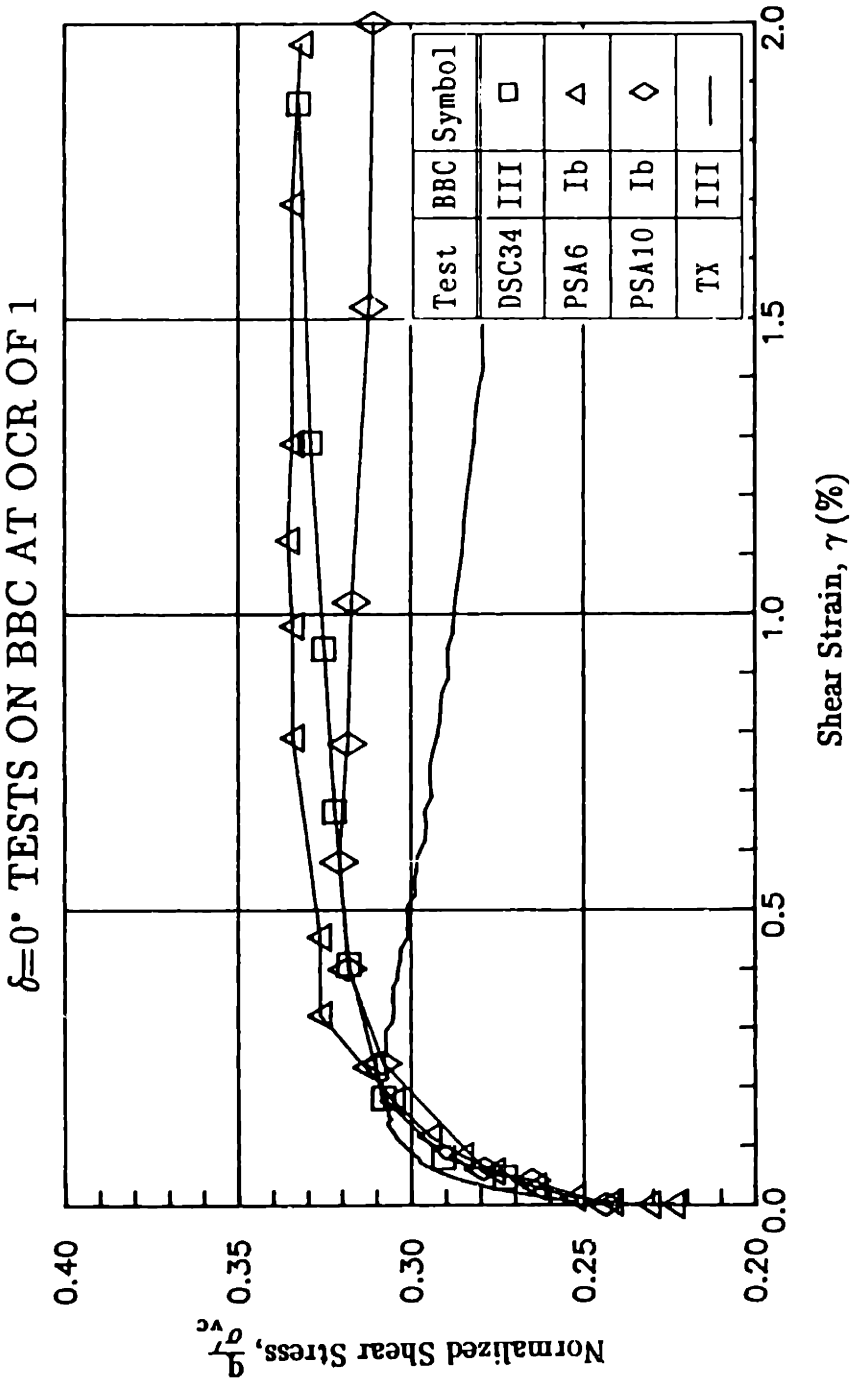

Figure 8.2: Normalized Stress–Strain Relationships from δ=0° Undrained Shear Tests on OCR=1 BBC.

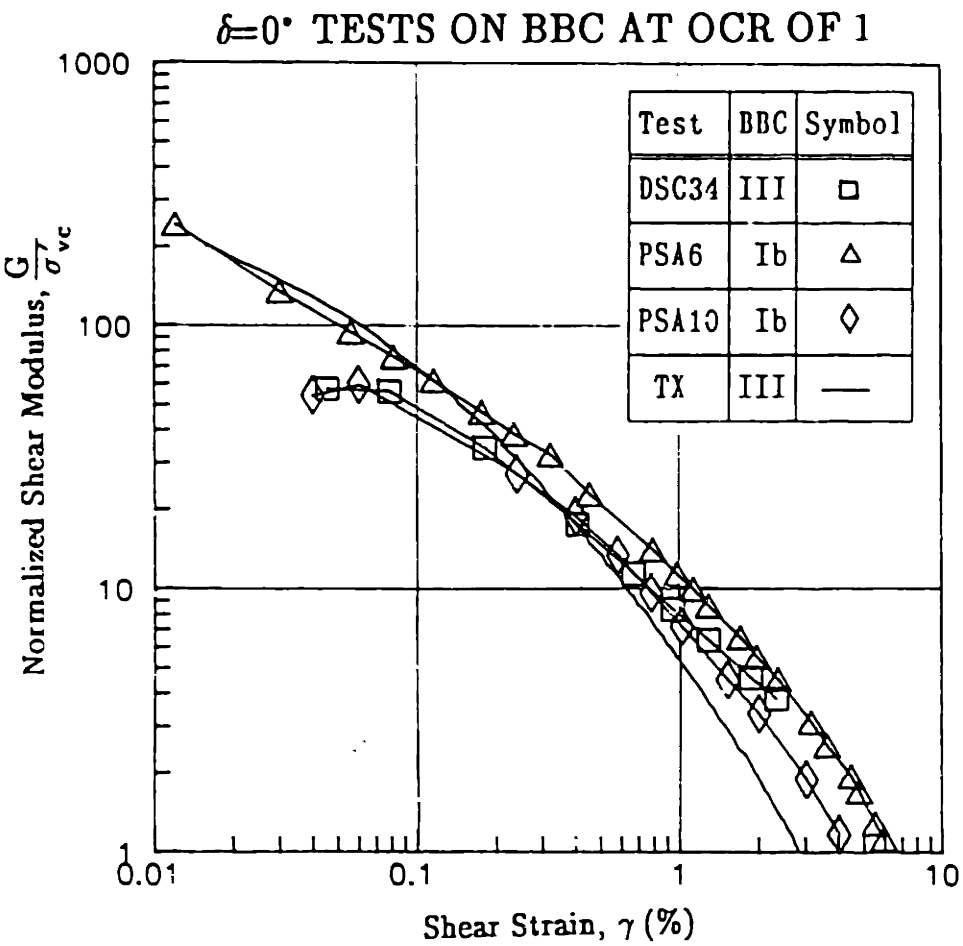

Figure 8.3: Normalized Shear Modulus versus Shear Strain for δ=0° Undrained Shear Tests on OCR=1 BBC.

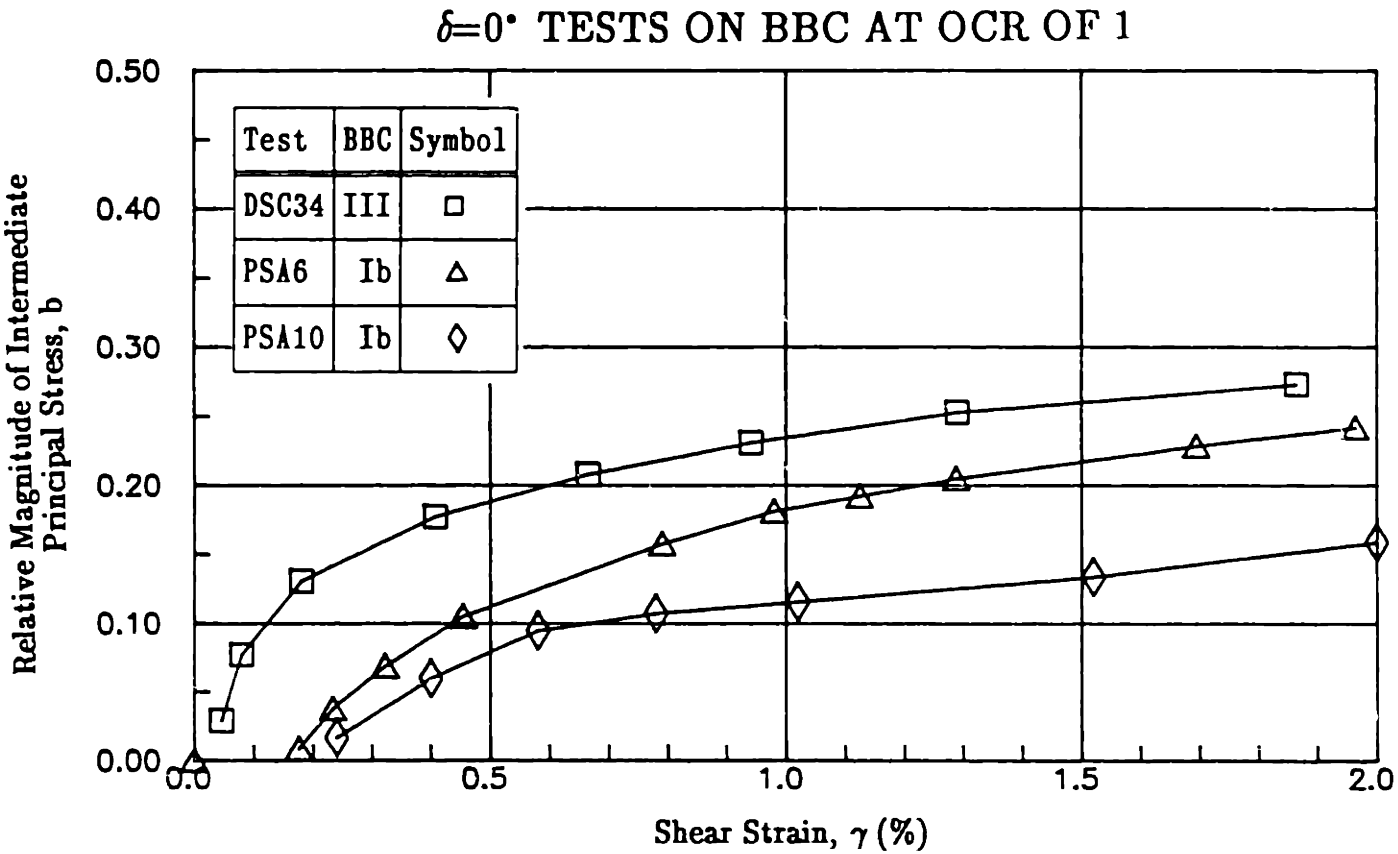

Figure 8.4: Relative Magnitude of Intermediate Principal Stress versus Shear Strain for δ=0° Undrained Shear Tests on OCR=1 BBC.

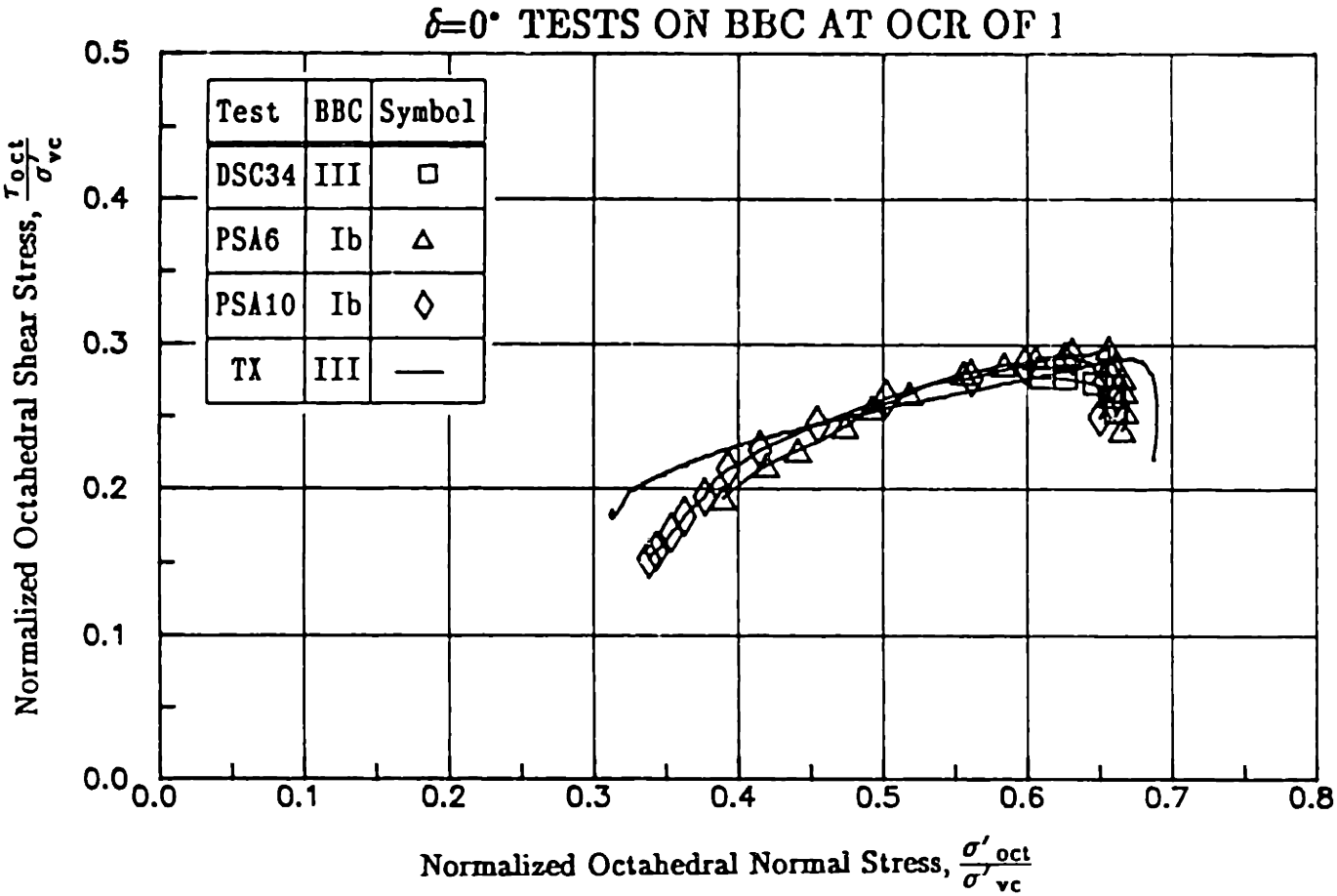

Figure 8.5: Normalized Octahedral Stress Paths from δ=0° Undrained Shear Tests on OCR=1 BBC.

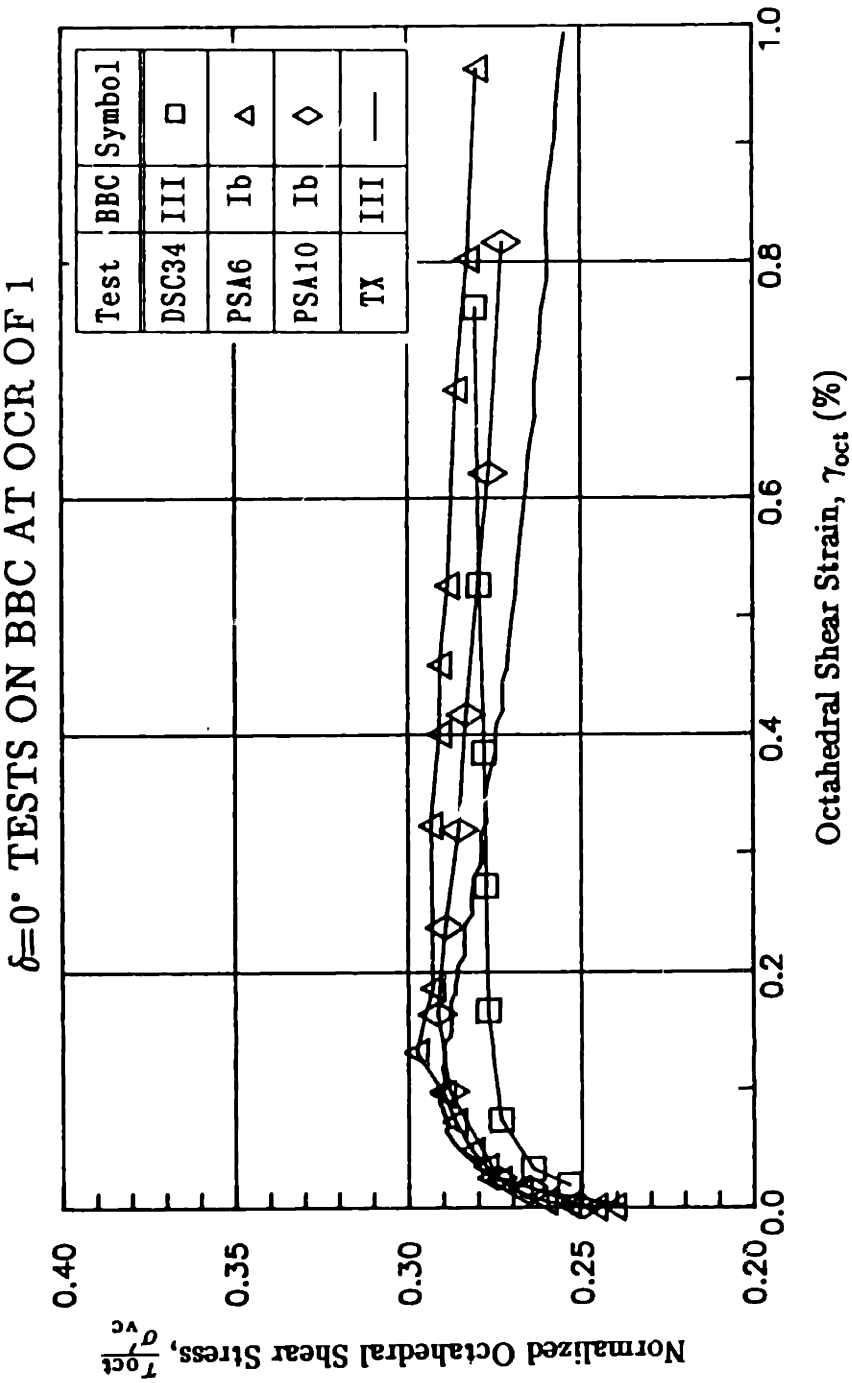

Figure 8.6: Normalized Octahedral Stress–Strain Relationships from δ=0° Undrained Shear Tests on OCR=1 BBC.

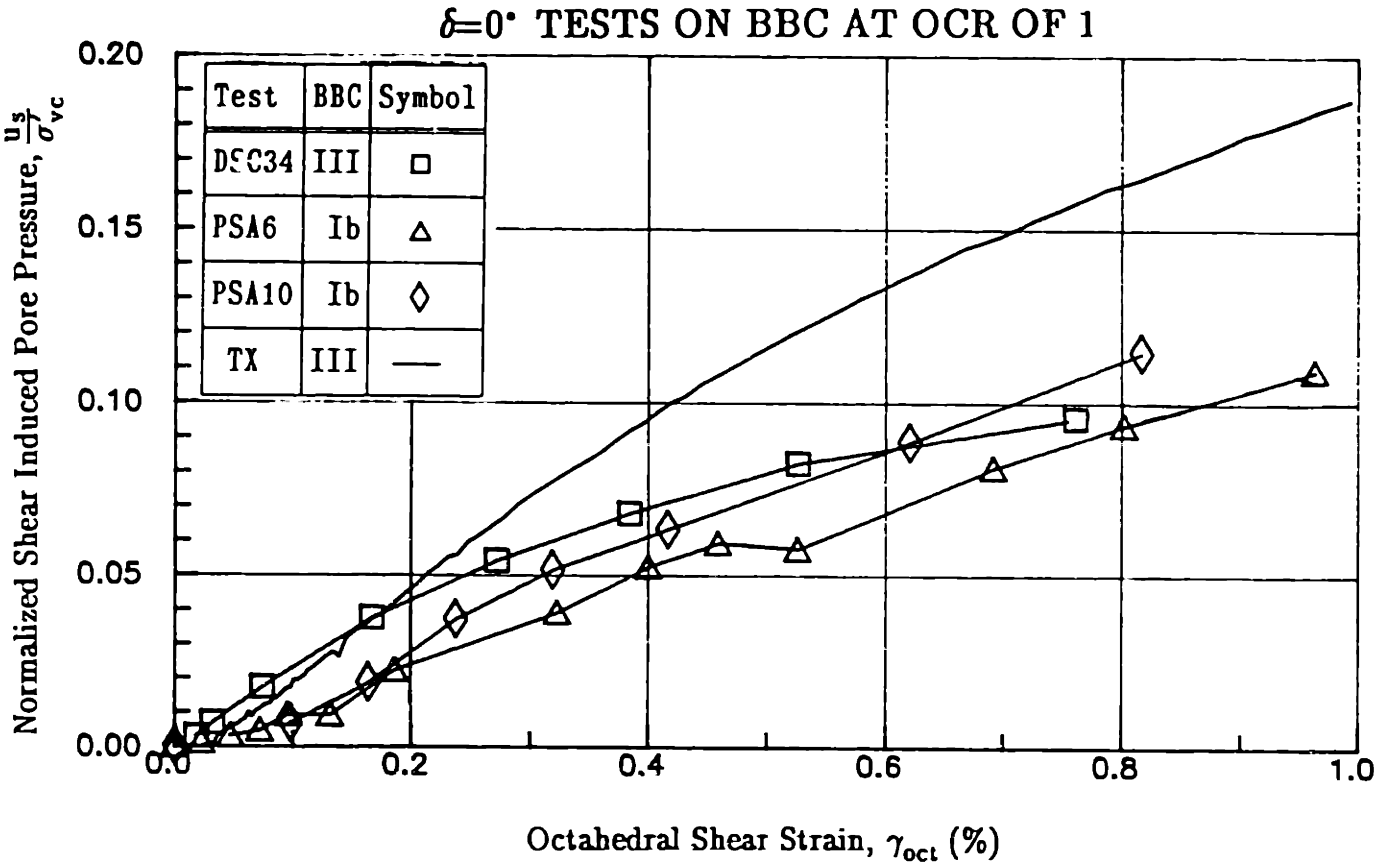

Figure 8.7: Normalized Shear Induced Pore Pressure versus Octahedral Shear Strain for δ=0° Undrained Shear Tests on OCR=1 BBC.

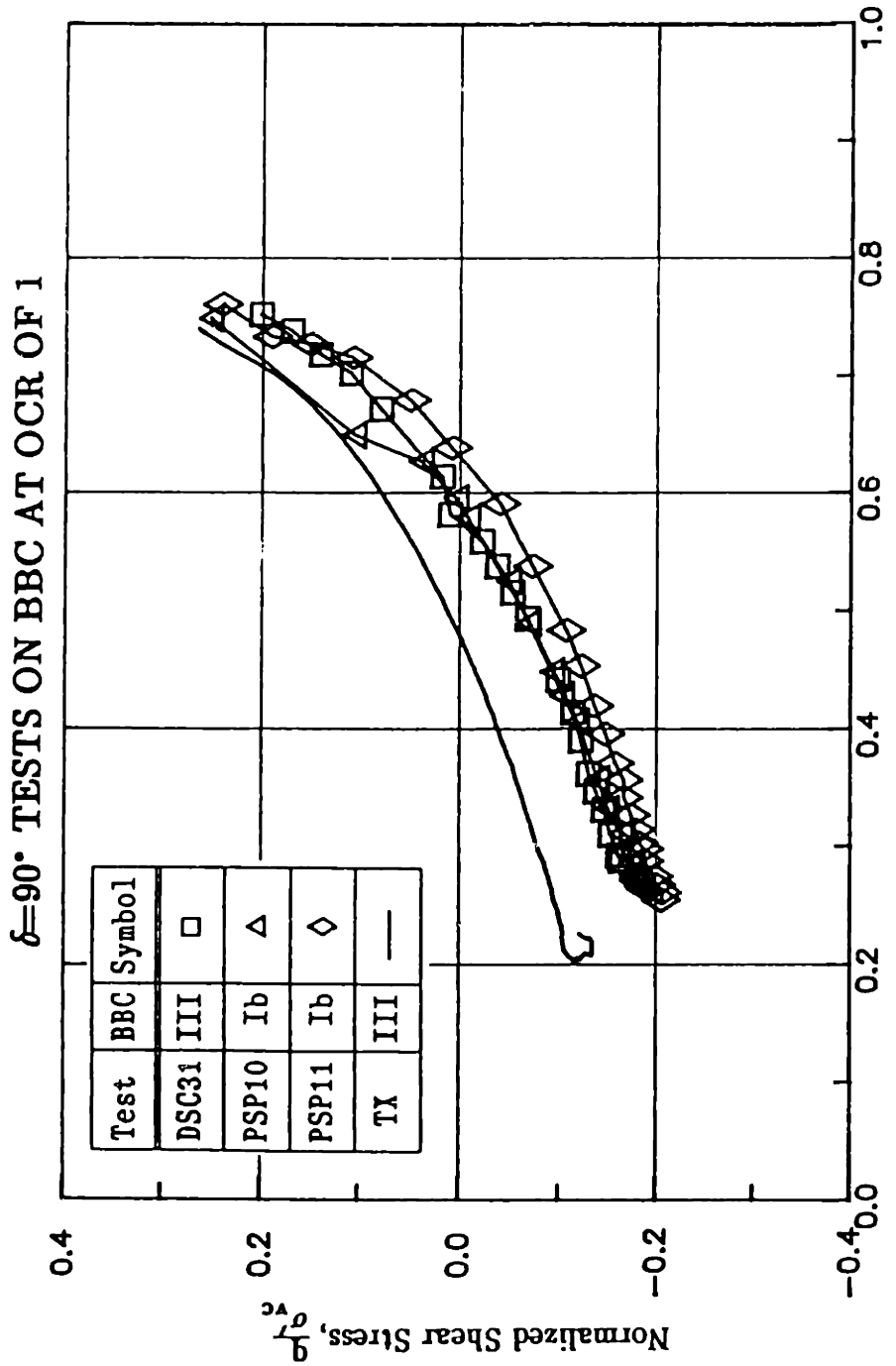

Figure 8.8: Normalized Effective Stress Paths from δ=90° Undrained Shear Tests on OCR=1 BBC.

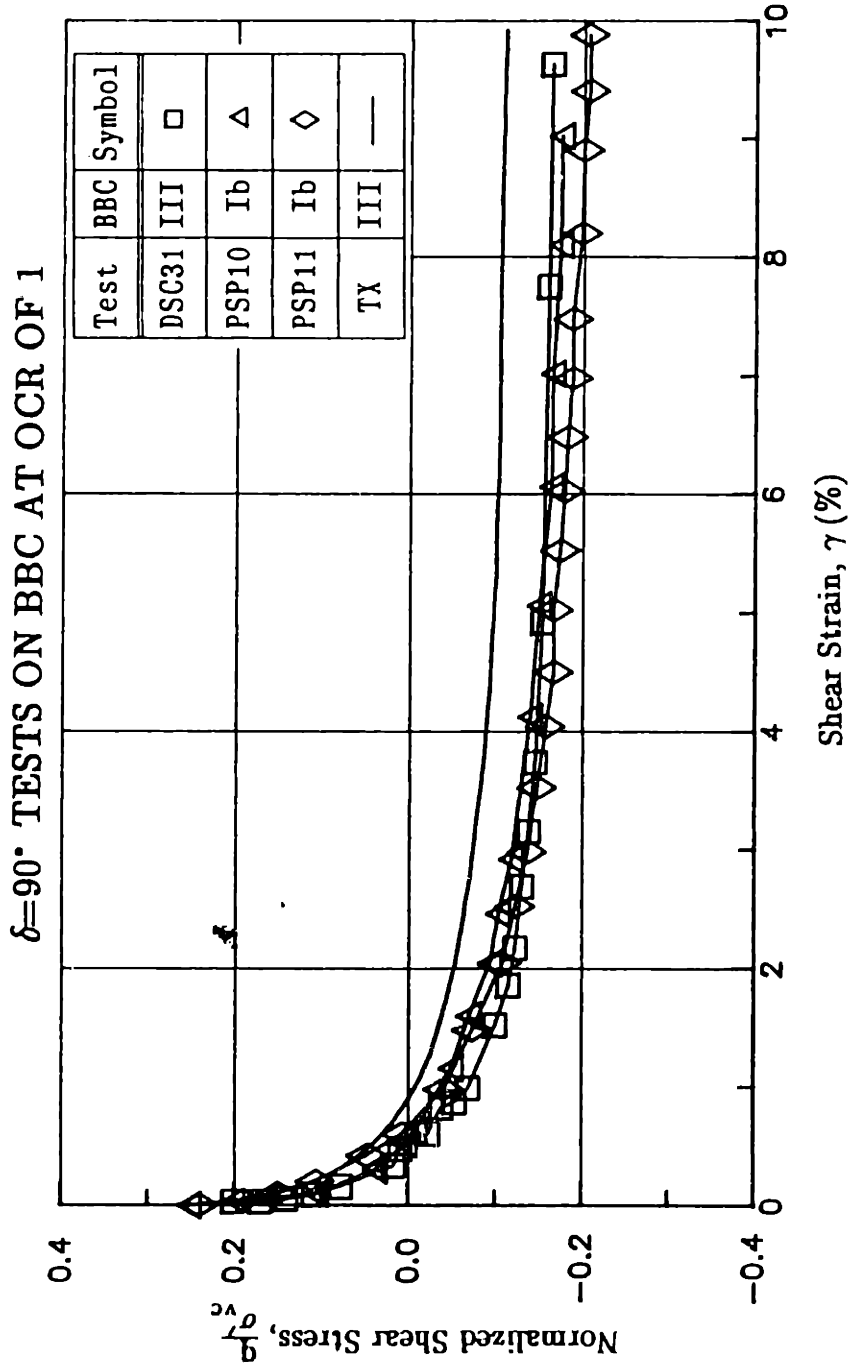

Figure 8.9: Normalized Stress–Strain Relationships from δ=90° Undrained Shear Tests on OCR=1 BBC.

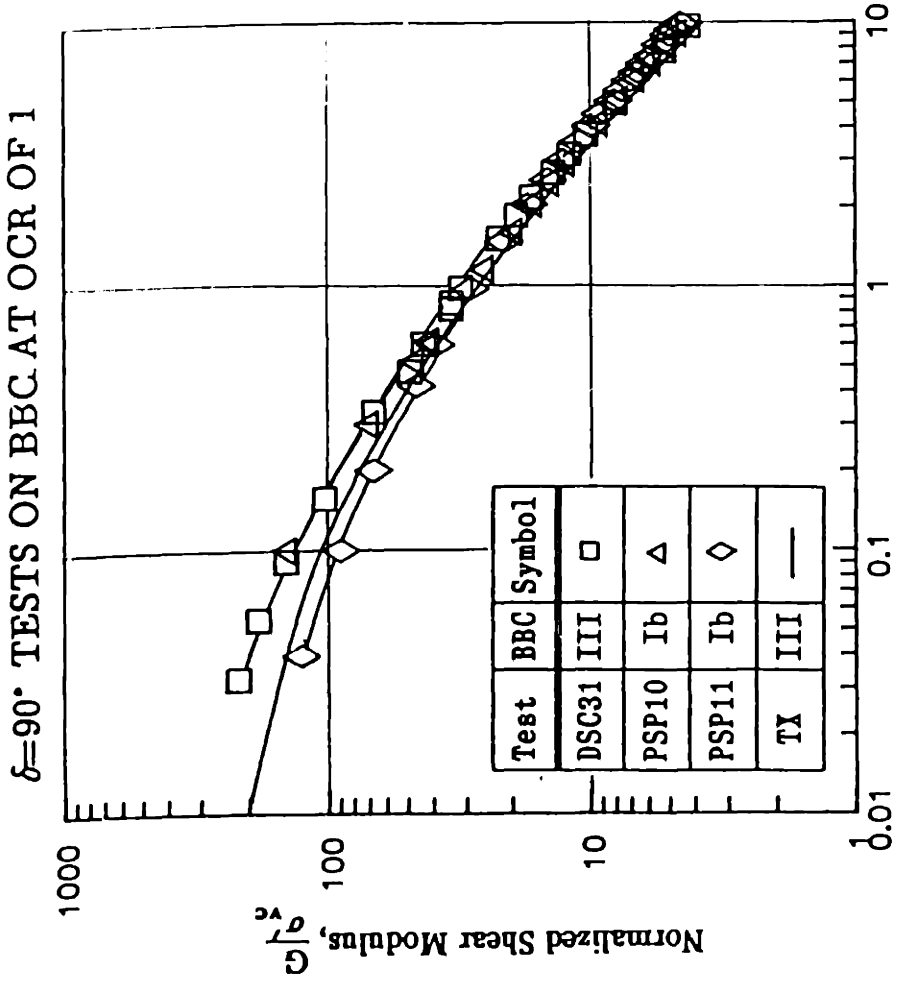

Figure 8.10: Normalized Shear Modulus versus Shear Strain for δ=90° Undrained Shear Tests on OCR=1 BBC.

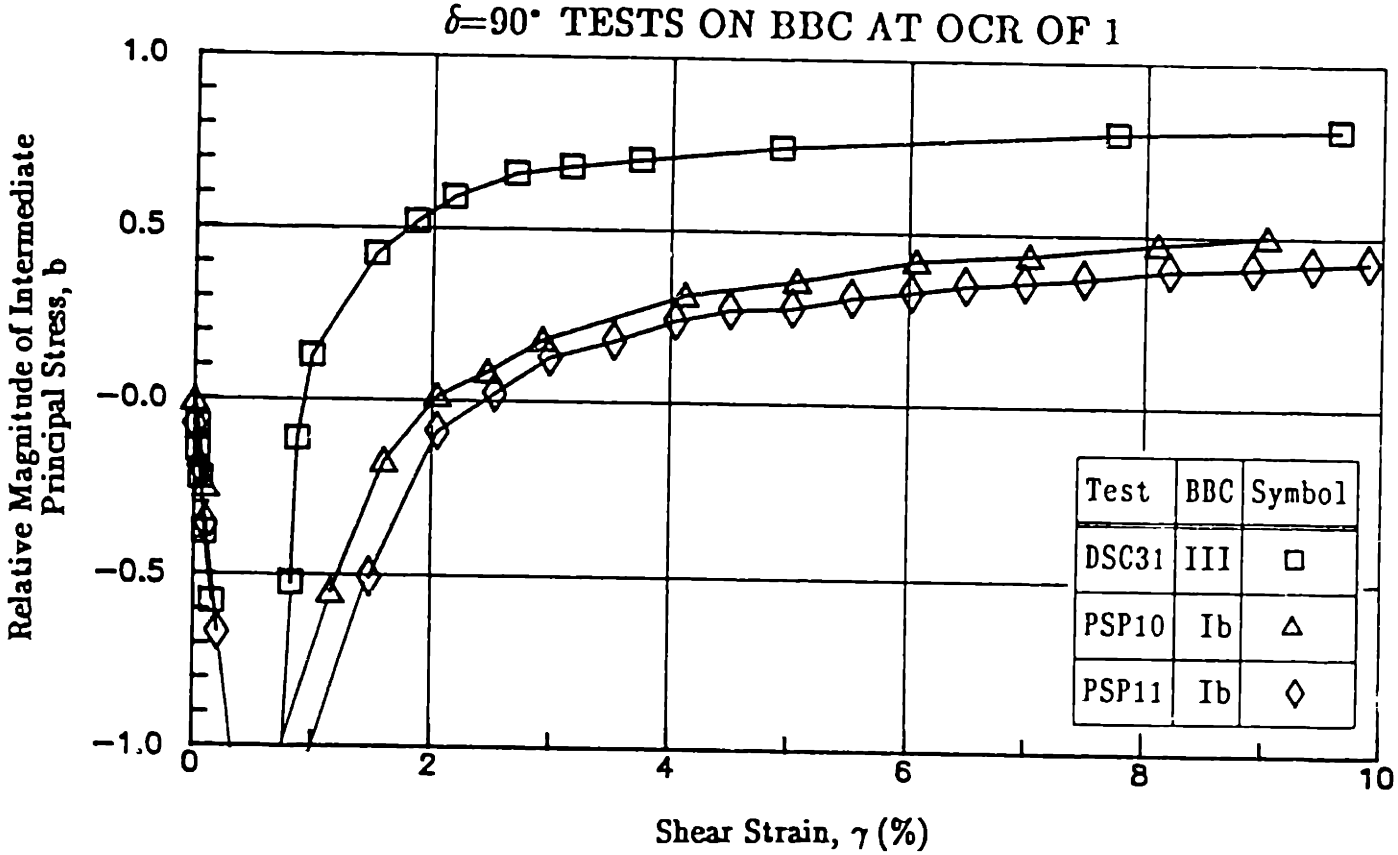

Figure 8.11: Relative Magnitude of Intermediate Principal Stress versus Shear Strain for δ=90° Undrained Shear Tests on OCR=1 BBC.

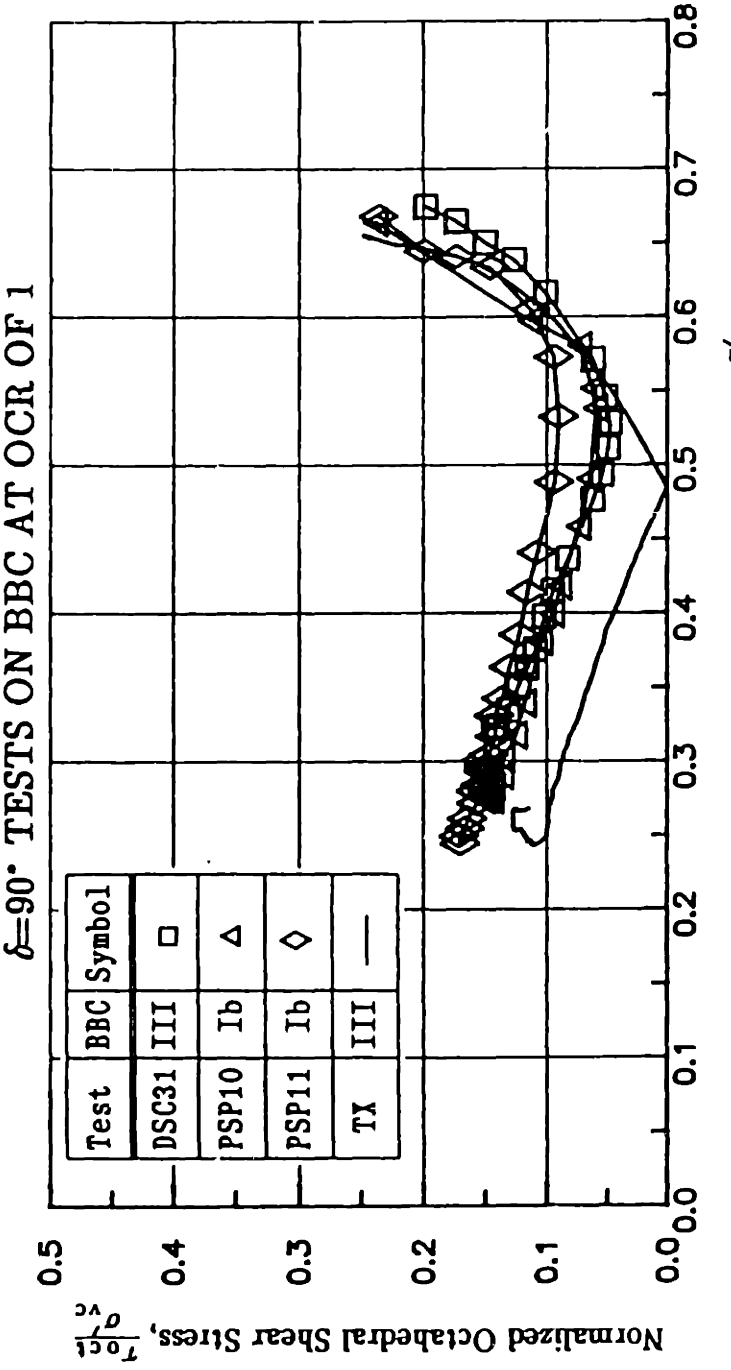

Figure 8.12: Normalized Octahedral Effective Stress Paths from δ=90° Undrained Shear Tests on OCR=1 BBC.

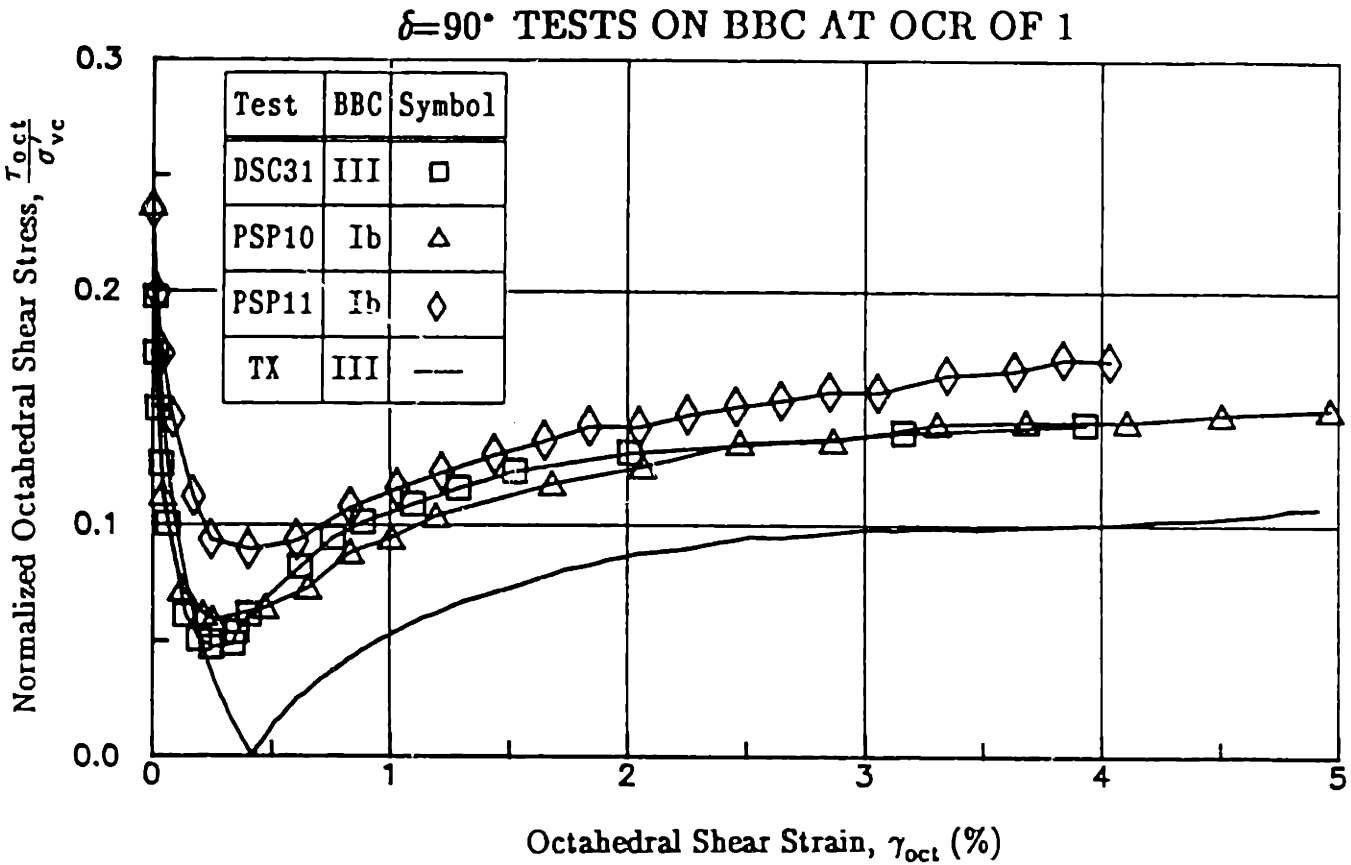

Figure 8.13: Normalized Octahedral Stress–Strain Relationships from δ=90° Undrained Shear Tests on OCR=1 BBC.

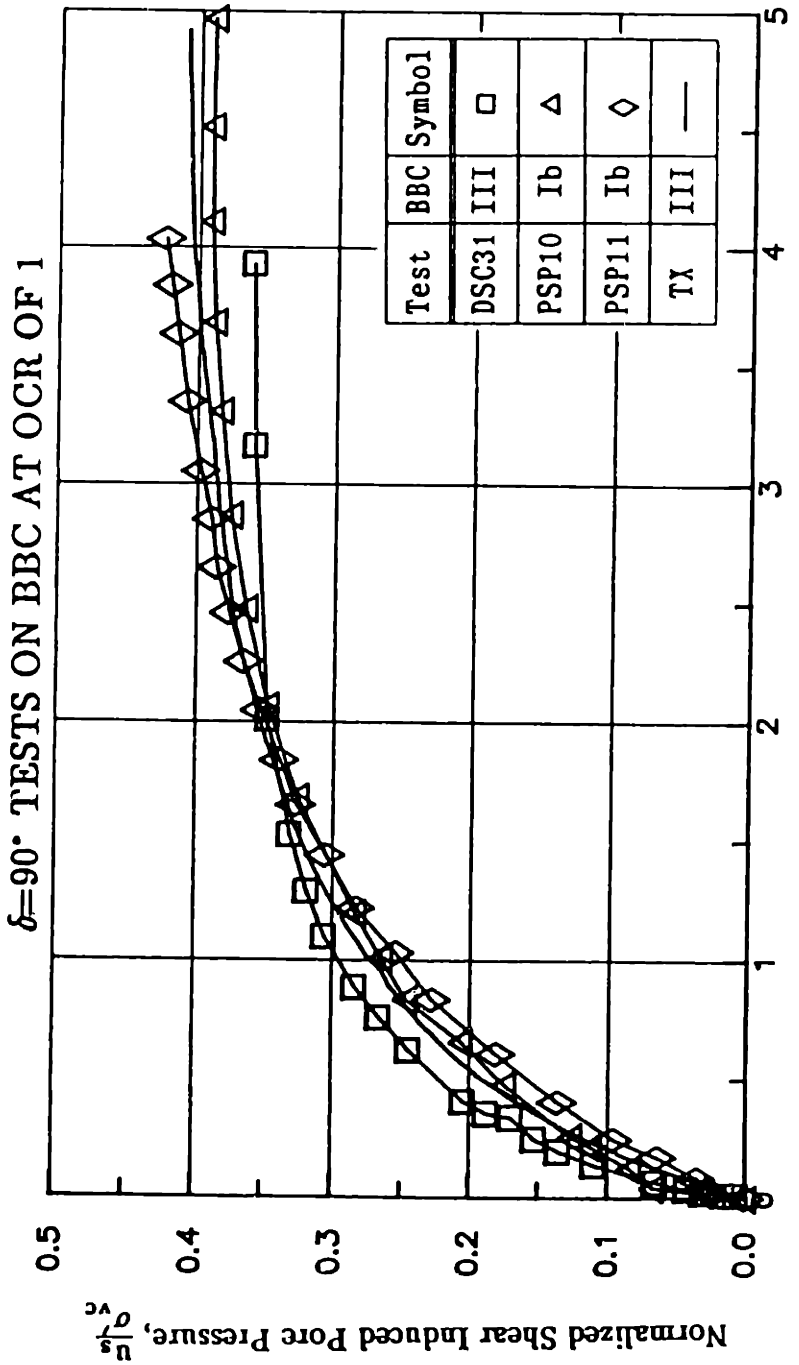

Figure 8.14: Normalized Shear Induced Pore Pressure versus Octahedral Shear Strain for δ=90° Undrained Shear Tests on OCR=1 BBC.

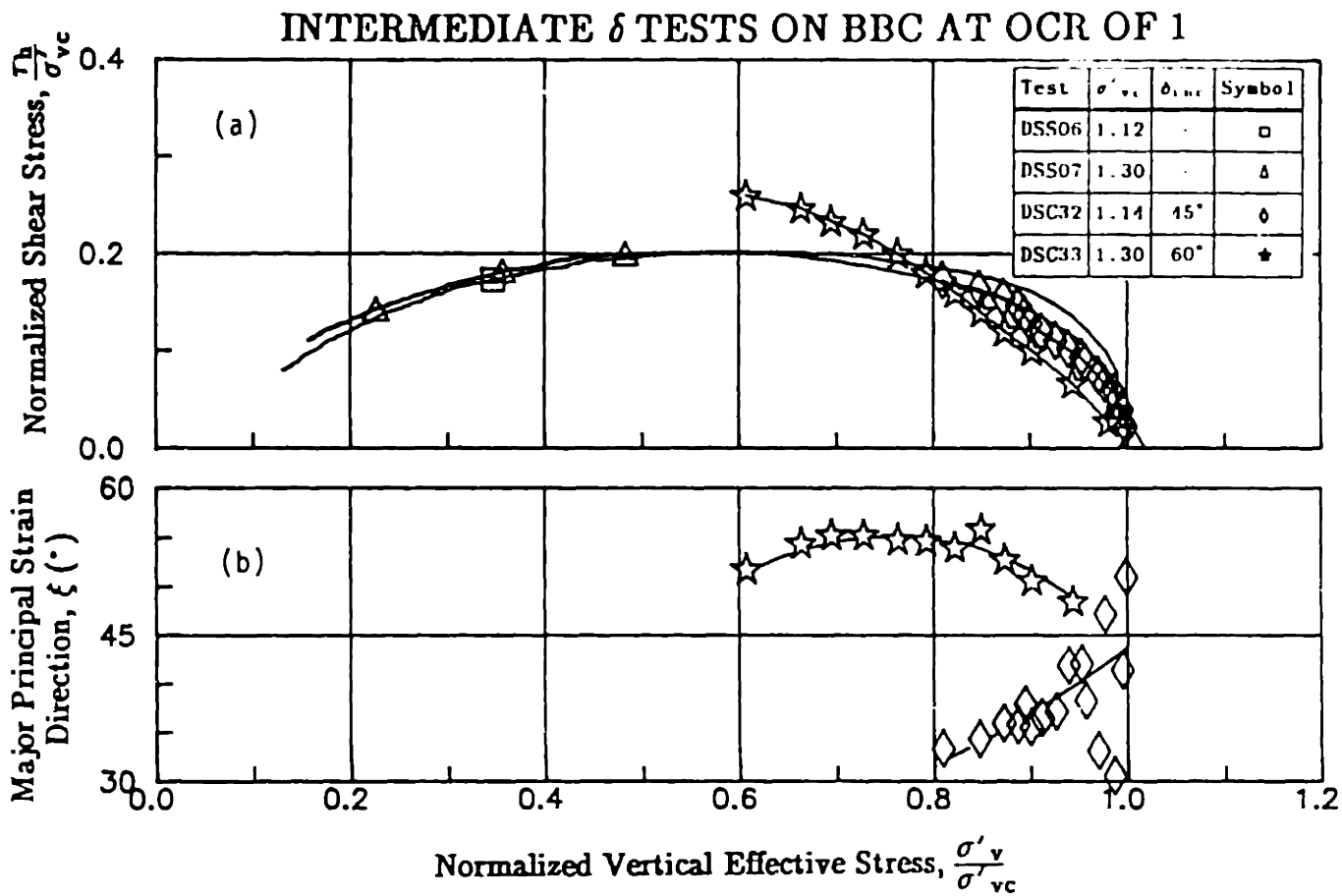

Figure 8.15: (a) Normalized Horizontal Shear Stress versus Normalized Vertical Effective Stress for DSC Undrained Shear Tests at Intermediate δ Angles and CK_0UDSS Tests on OCR=1 BBC; (b) Major Principal Strain Direction versus Normalized Vertical Effective Stress for DSC Undrained Shear Tests.

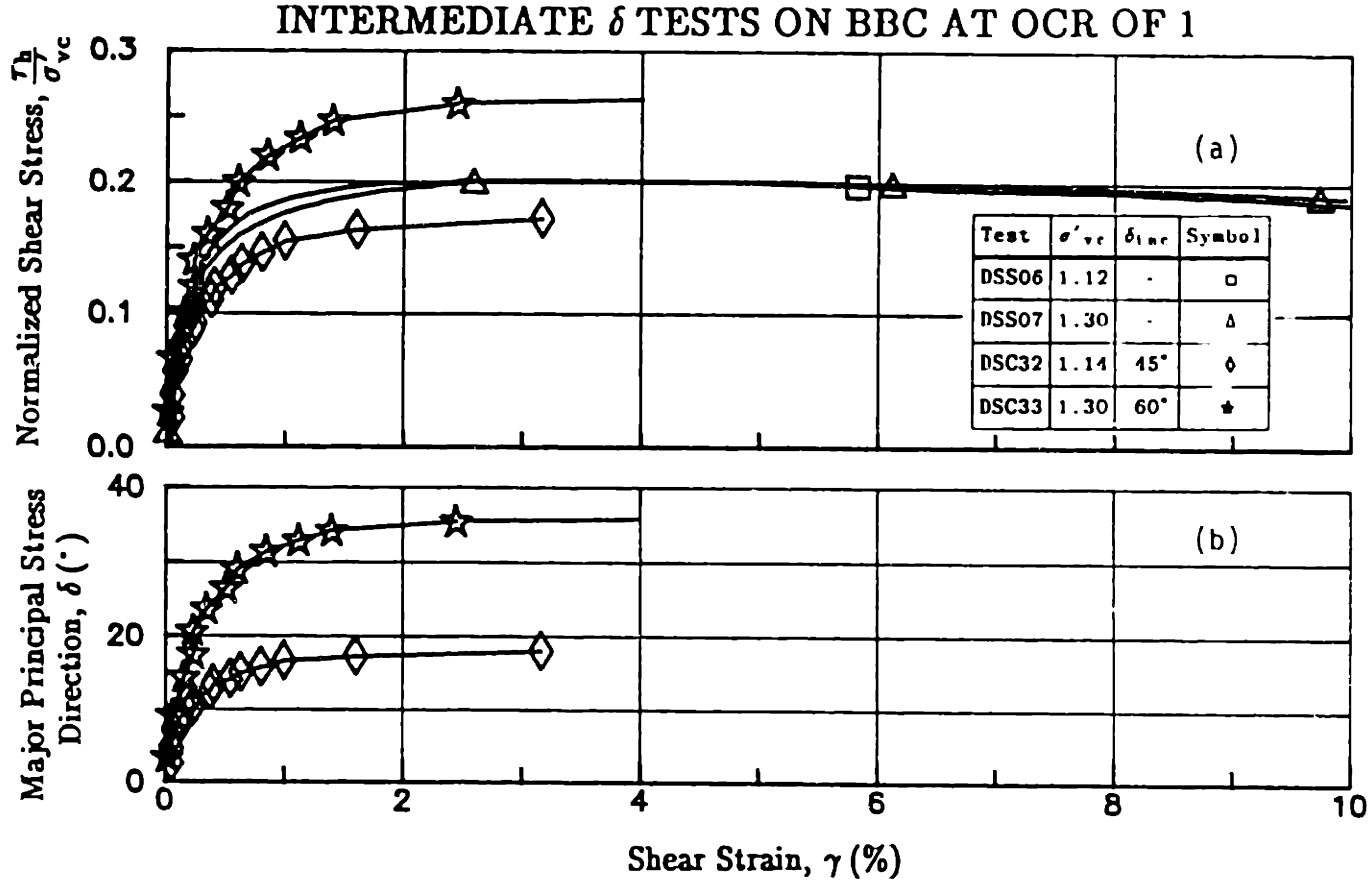

Figure 8.16: (a) Normalized Horizontal Shear Stress versus Shear Strain for DSC Undrained Shear Tests at Intermediate δ Angles and CK_oUDSS Tests on BBC at OCR=1 (b) Major Principal Stress Direction versus Shear Strain for DSC Undrained Shear Tests at Intermediate δ Angles on OCR=1 BBC.

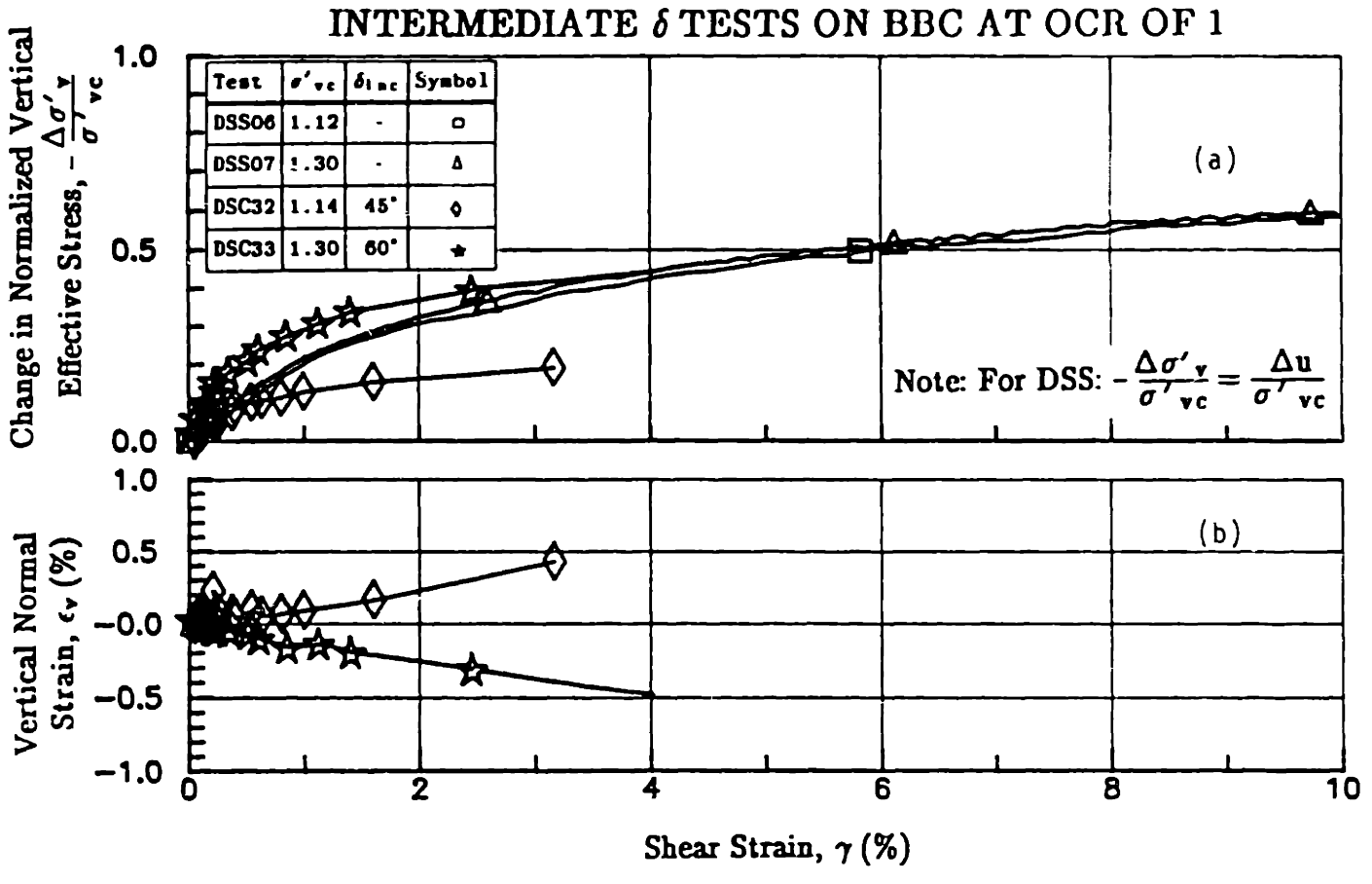

Figure 8.17: (a) Change in Normalized Vertical Effective Stress versus Shear Strain for DSC Undrained Shear Tests at Intermediate δ Angles and CK_oUDSS Tests at OCR=1. (b) Vertical Normal Strain versus Shear Strain for DSC Undrained Shear Tests at Intermediate δ Angles.

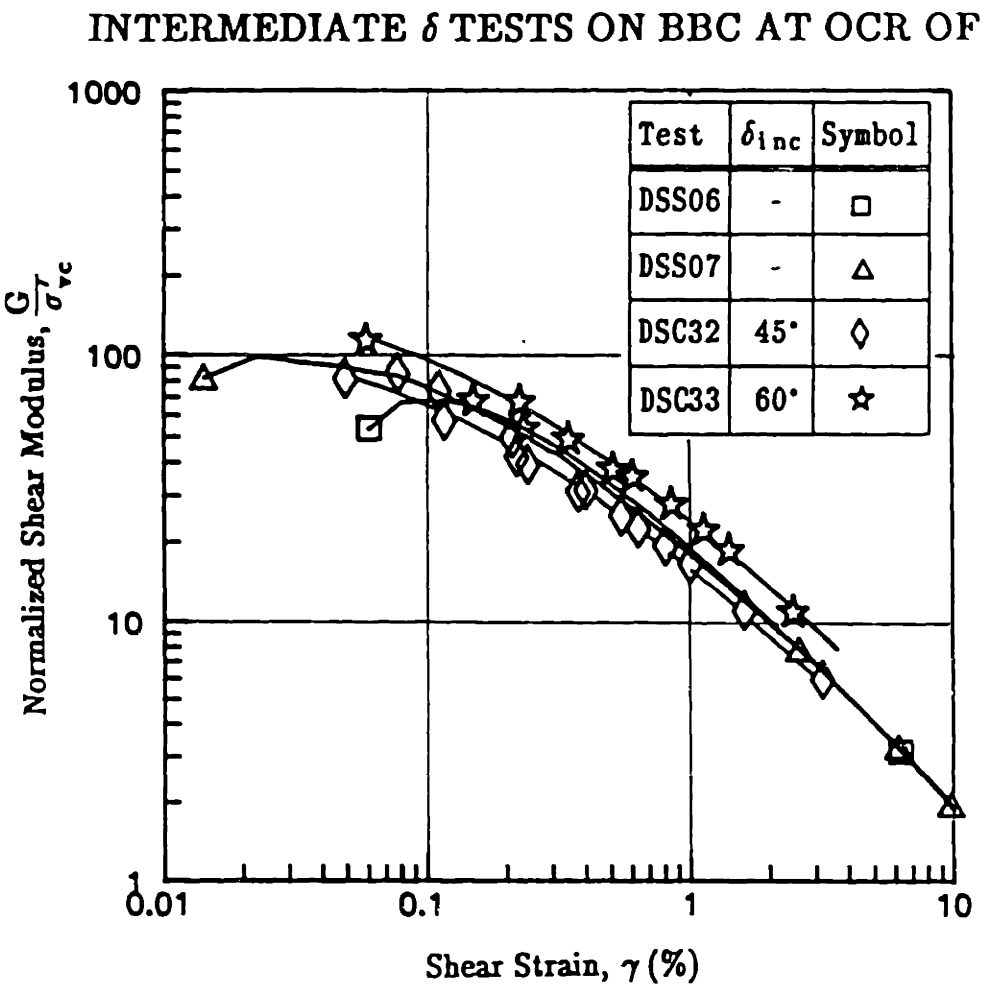

Figure 8.18: Normalized Shear Modulus versus Shear Strain for DSC Undrained Shear Tests at Intermediate δ Angles and CK_oUDSS Tests on OCR=1 BBC.

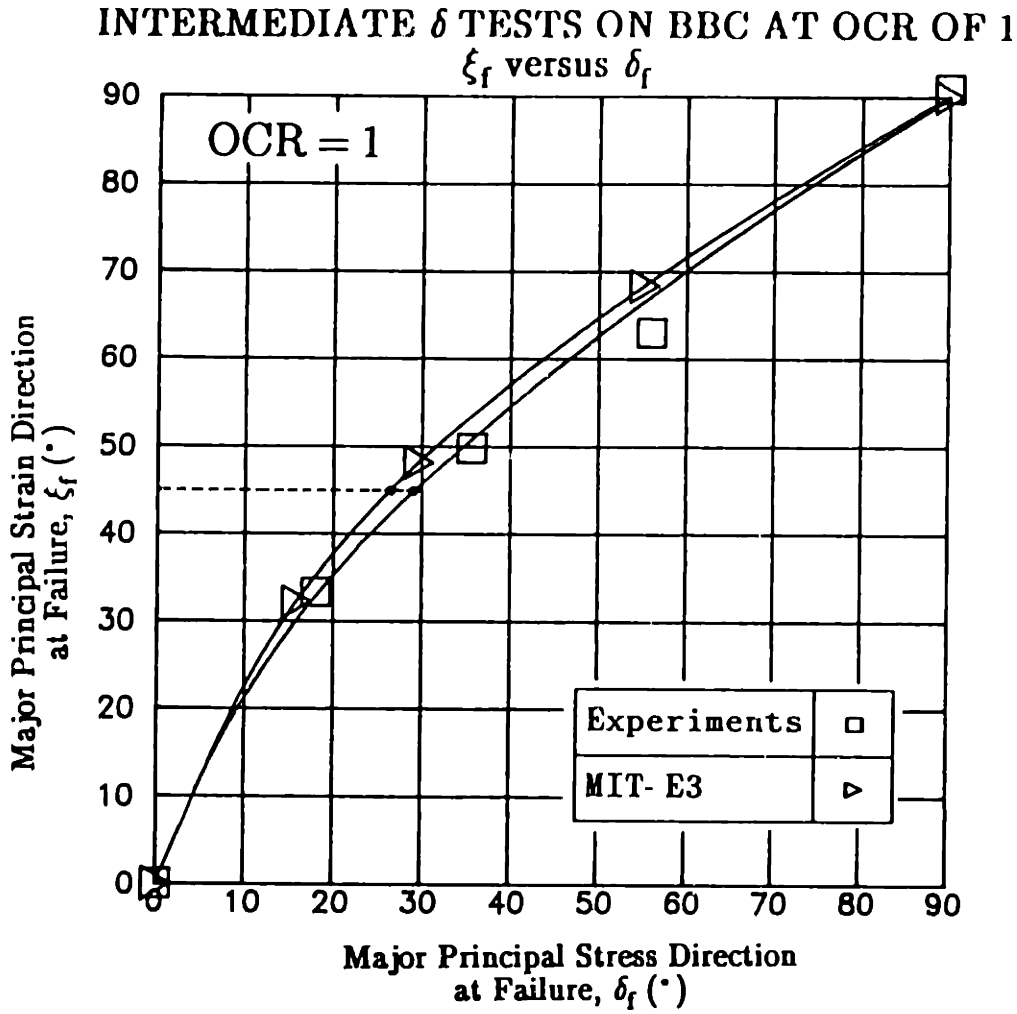

Figure 8.19: Major Principal Strain Direction versus Major Principal Stress Direction for DSC Undrained Shear Tests on OCR=1 BBC.

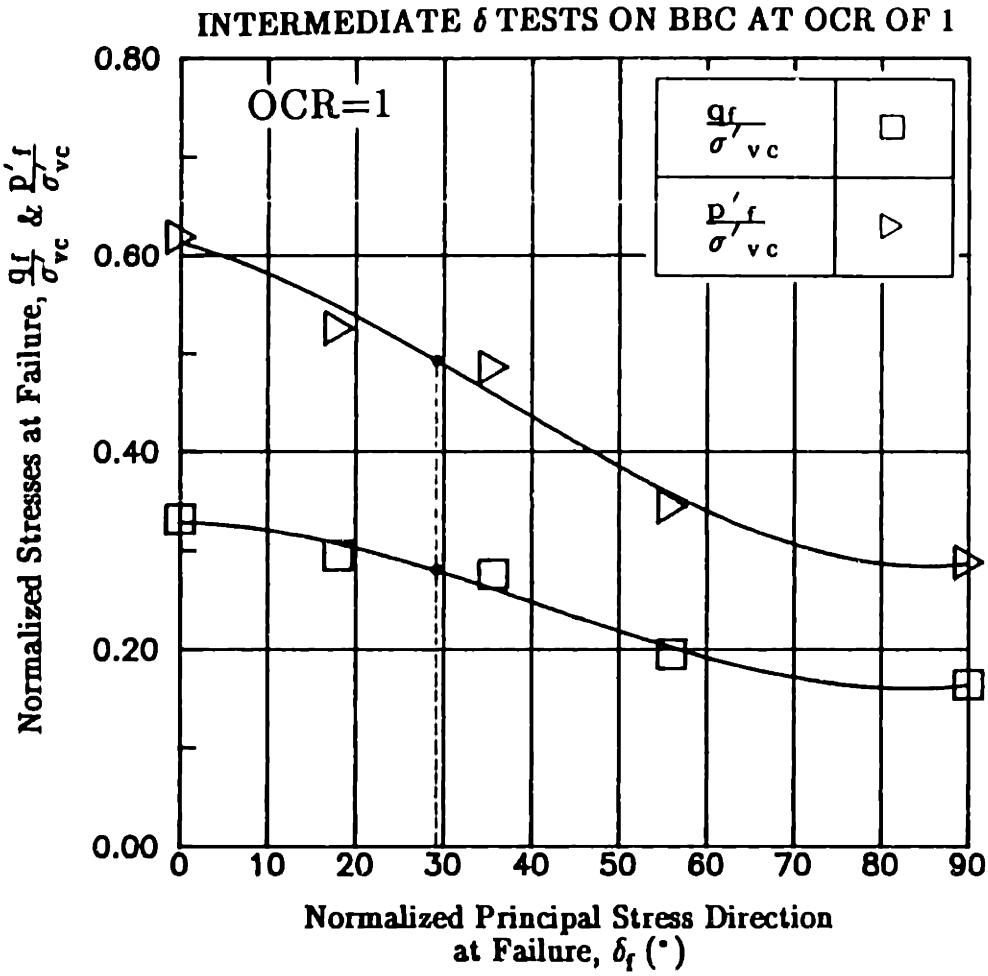

Figure 8.20: Normalized Stresses at Failure for DSC Undrained Shear Tests on OCR=1 BBC.

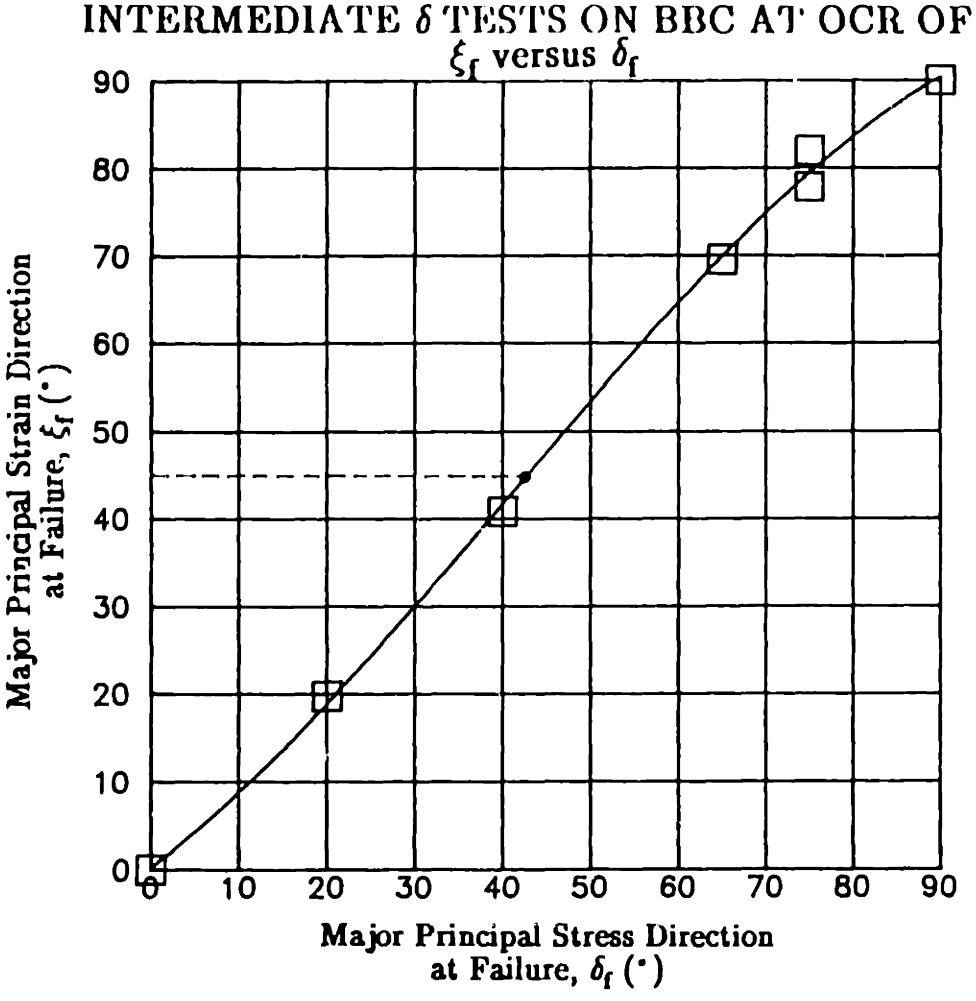

Figure 8.21: Major Principal Strain Direction versus Major Principal Stress Direction for DSC Undrained Shear Tests on OCR=1 BBC.

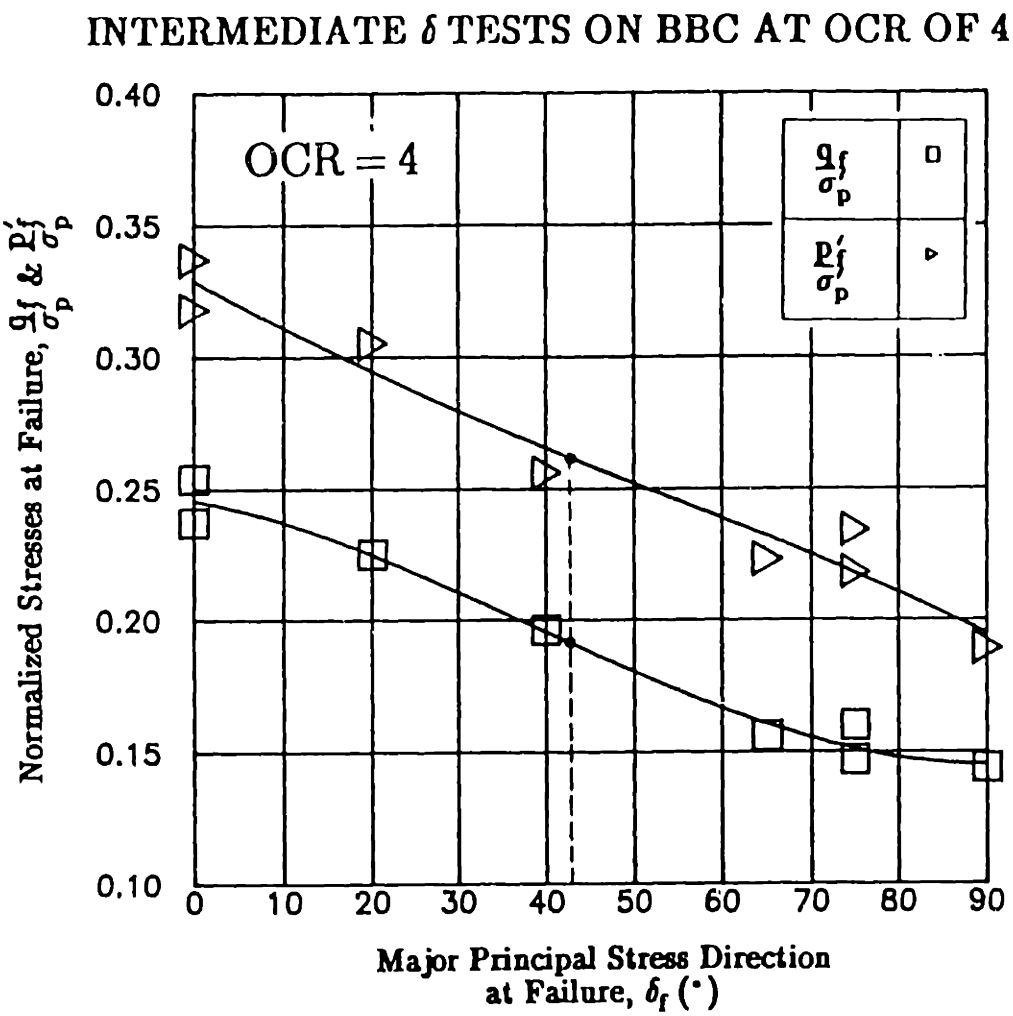

Figure 8.22: Normalized Stresses at Failure from DSC Undrained Shear Tests on OCR=1 BBC.

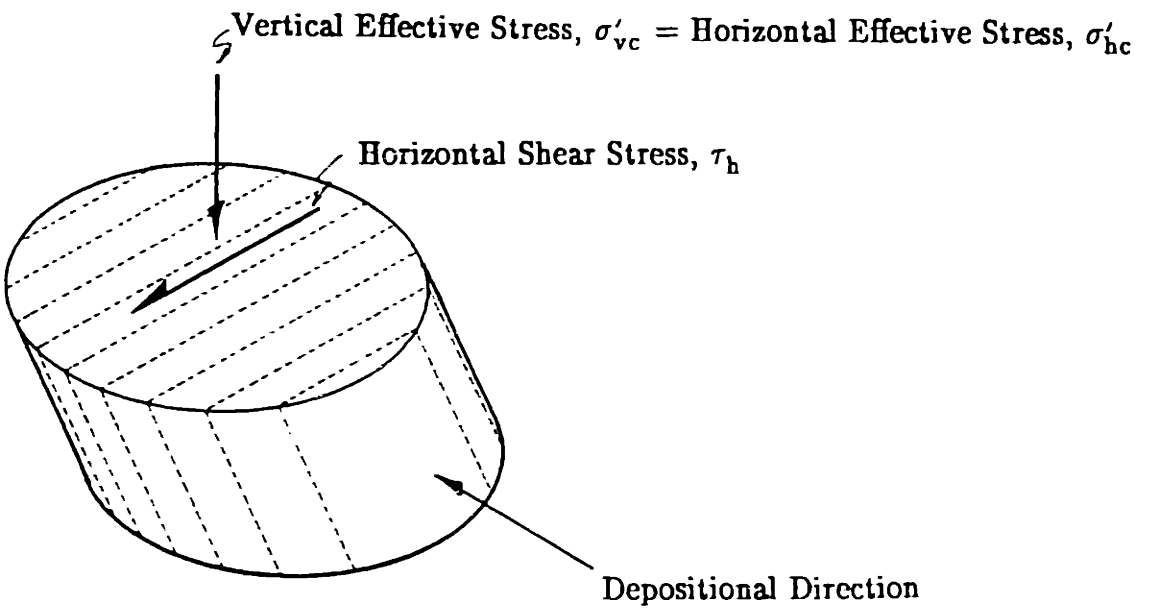

DSS ψ TEST ON BBC AT OCR=4

Figure 8.23: DSS Recompression ψ Tests on OCR=4 BBC.

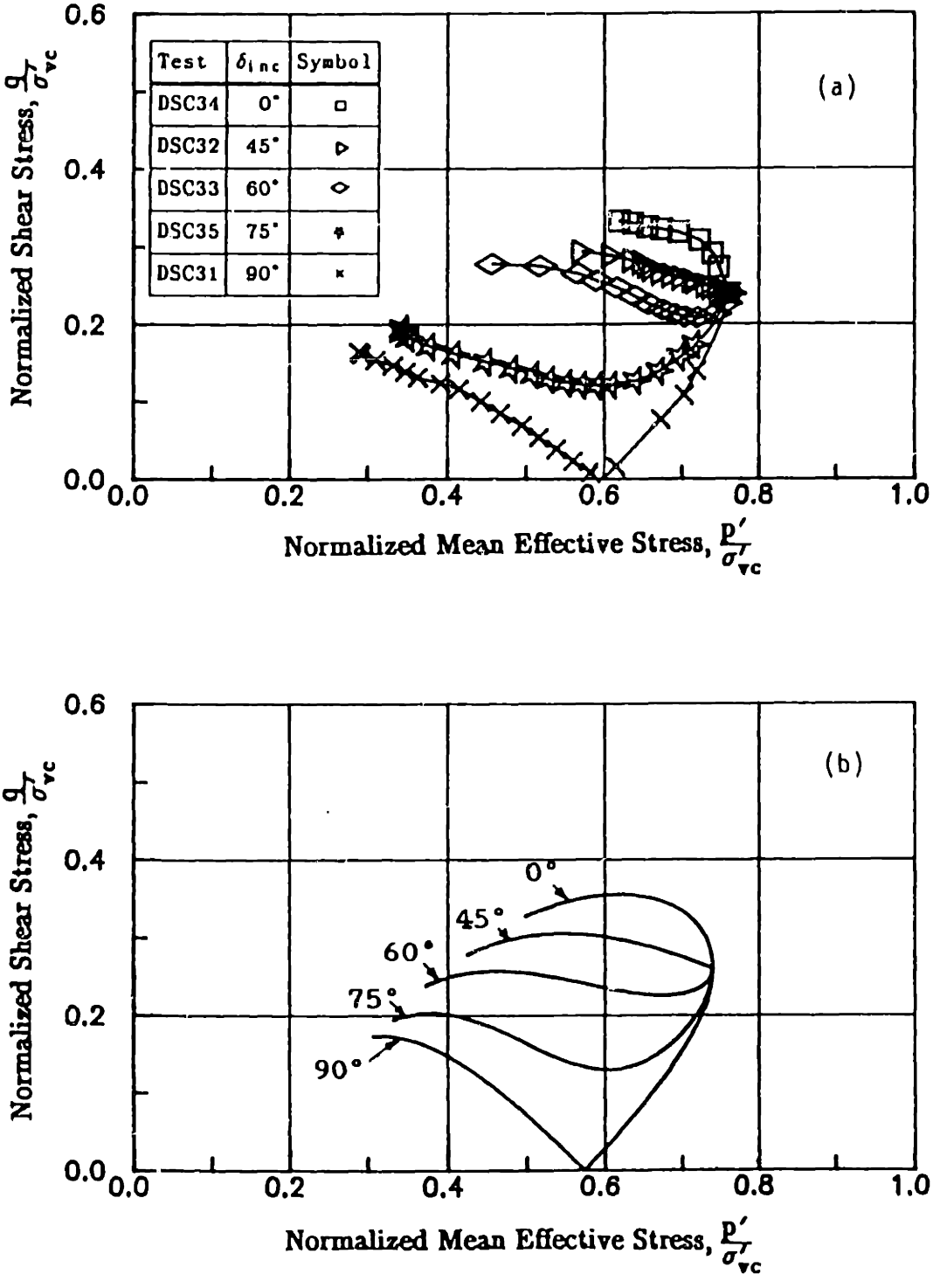

Figure 8.24: Normalized Effective Stress Paths from DSC Tests on OCR=1 BBC: (a) Experimental Results; (b) MIT–E3 Predictions.

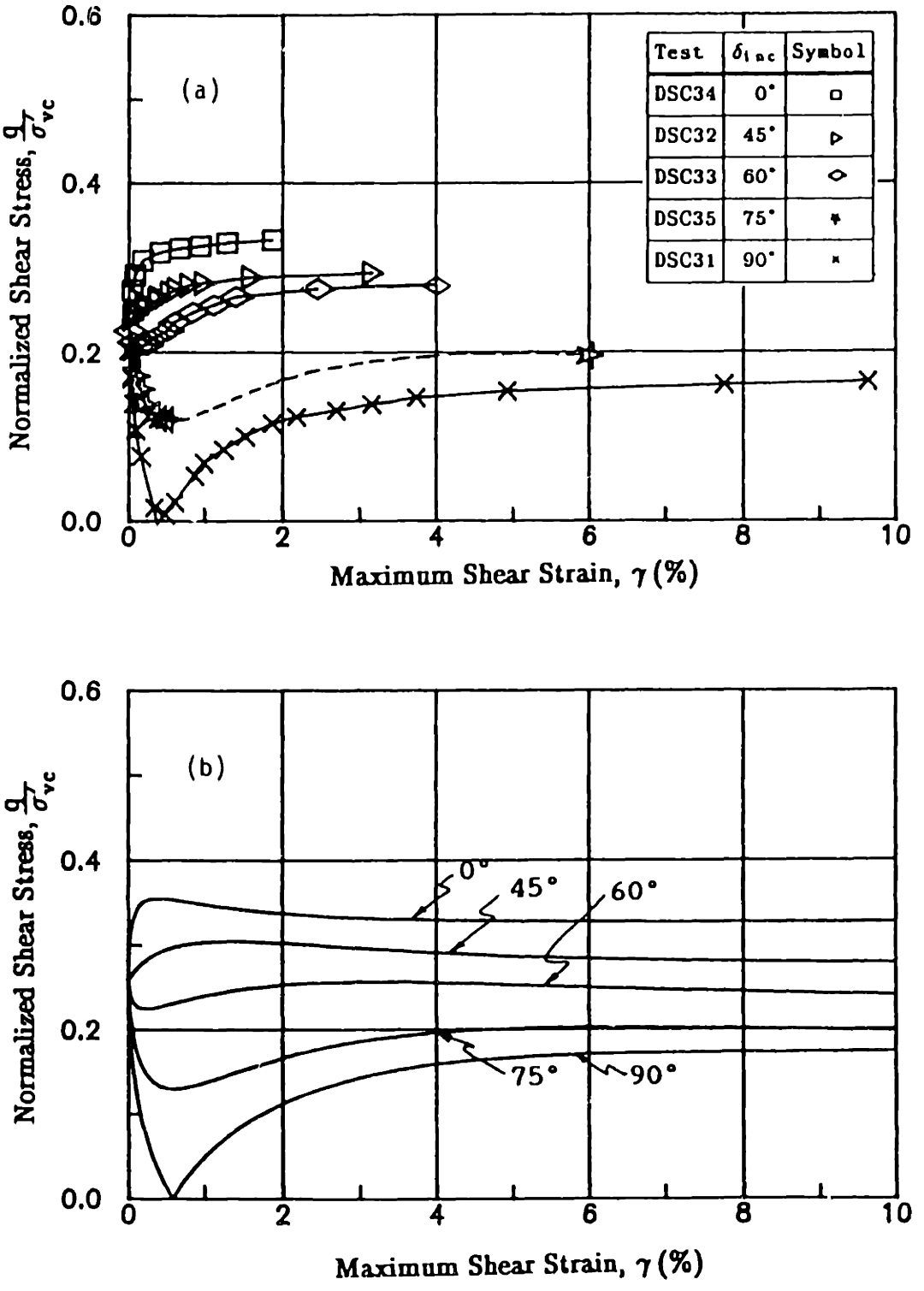

Figure 8.25: Normalized Stress–Strain Relationships from DSC Tests on OCR=1 BBC: (a) Experimental Results; (b) MIT–E3 Predictions.

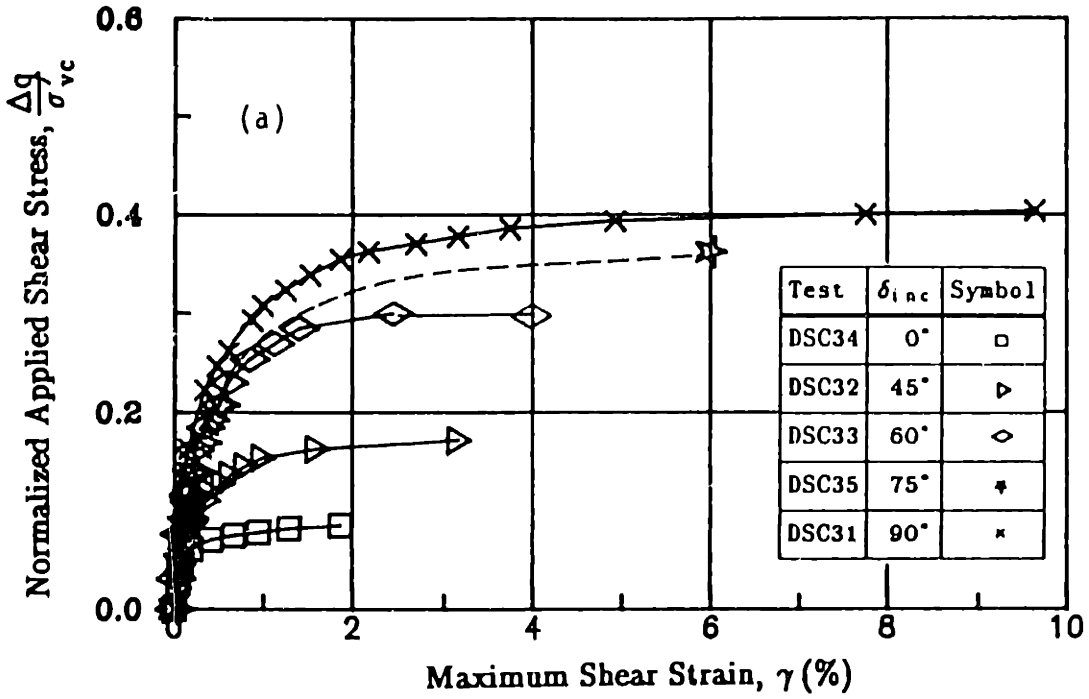

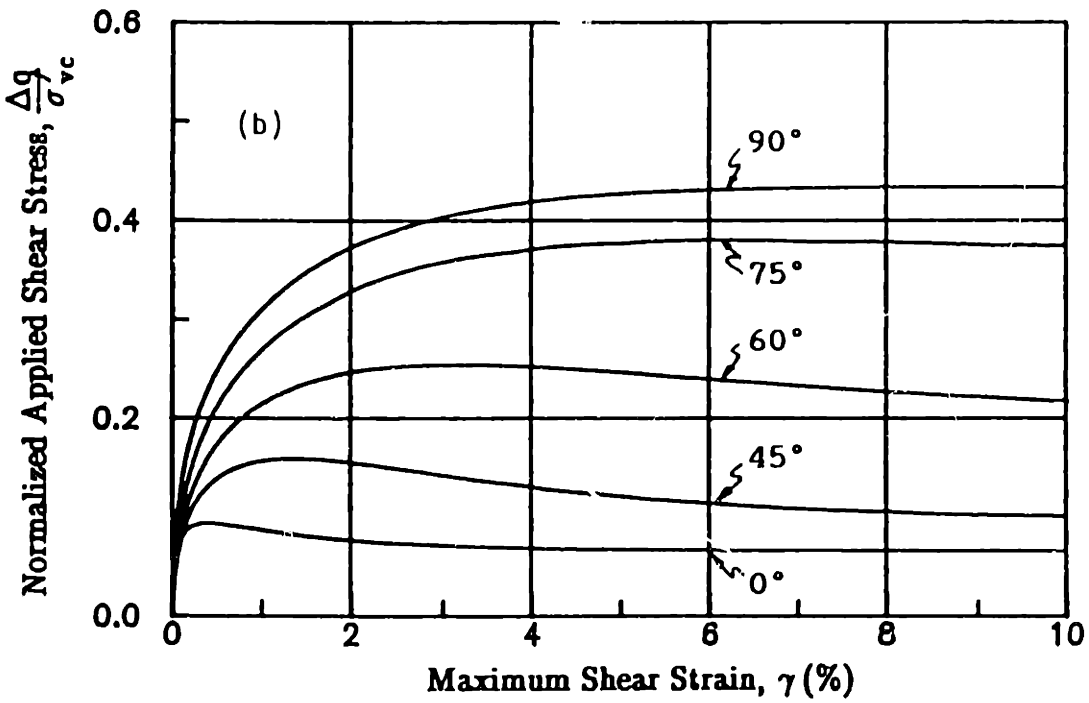

Figure 8.26: Normalized Applied Shear Stress versus Shear Strain for DSC Tests on OCR=1 BBC: (a) Experimental Results; (b) MIT–E3 Predictions.

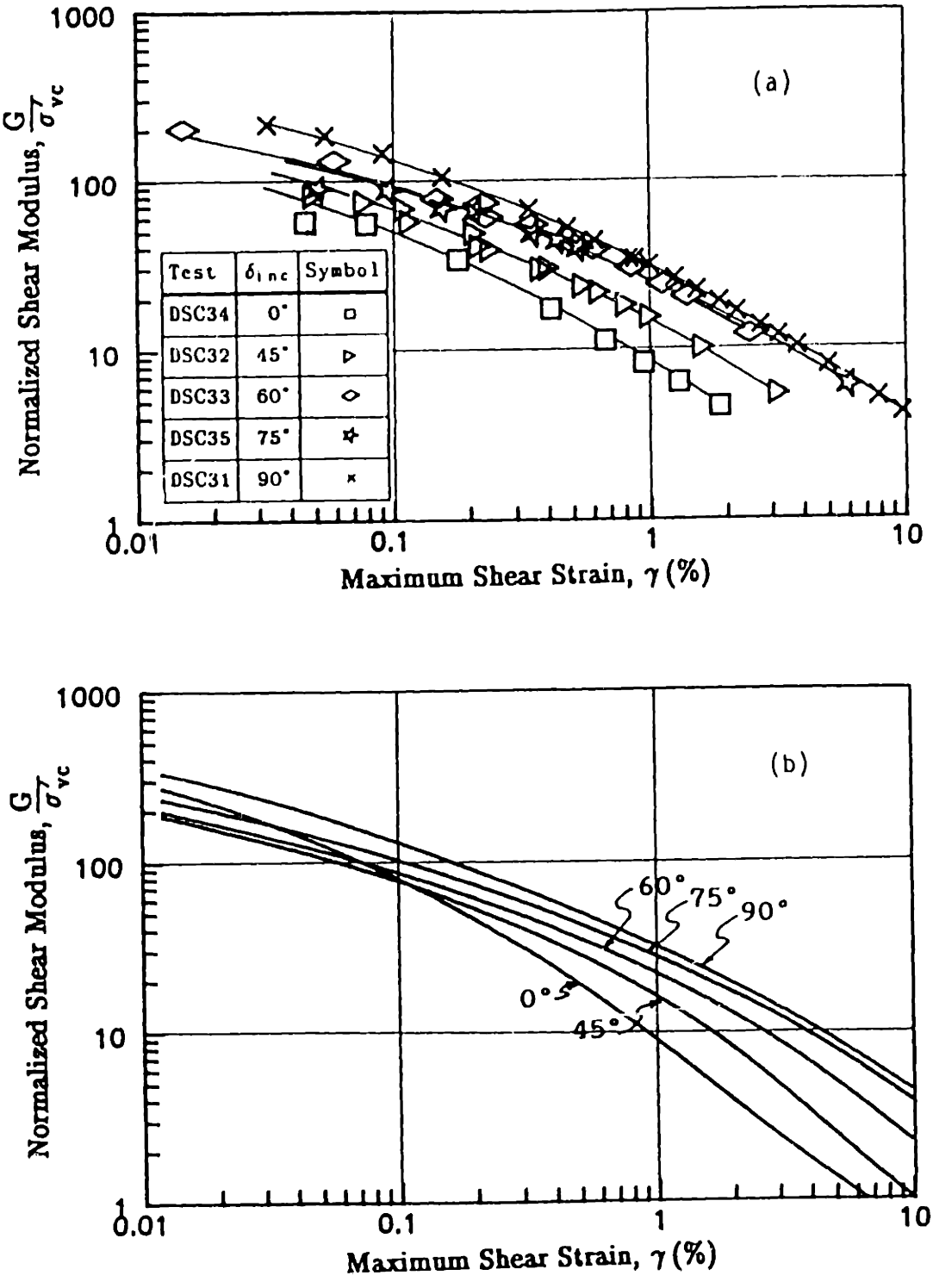

Figure 8.27: Normalized Shear Modulus Relationships from DSC Tests on OCR=1 BBC: (a) Experimental Results; (b) MIT–E3 Predictions.

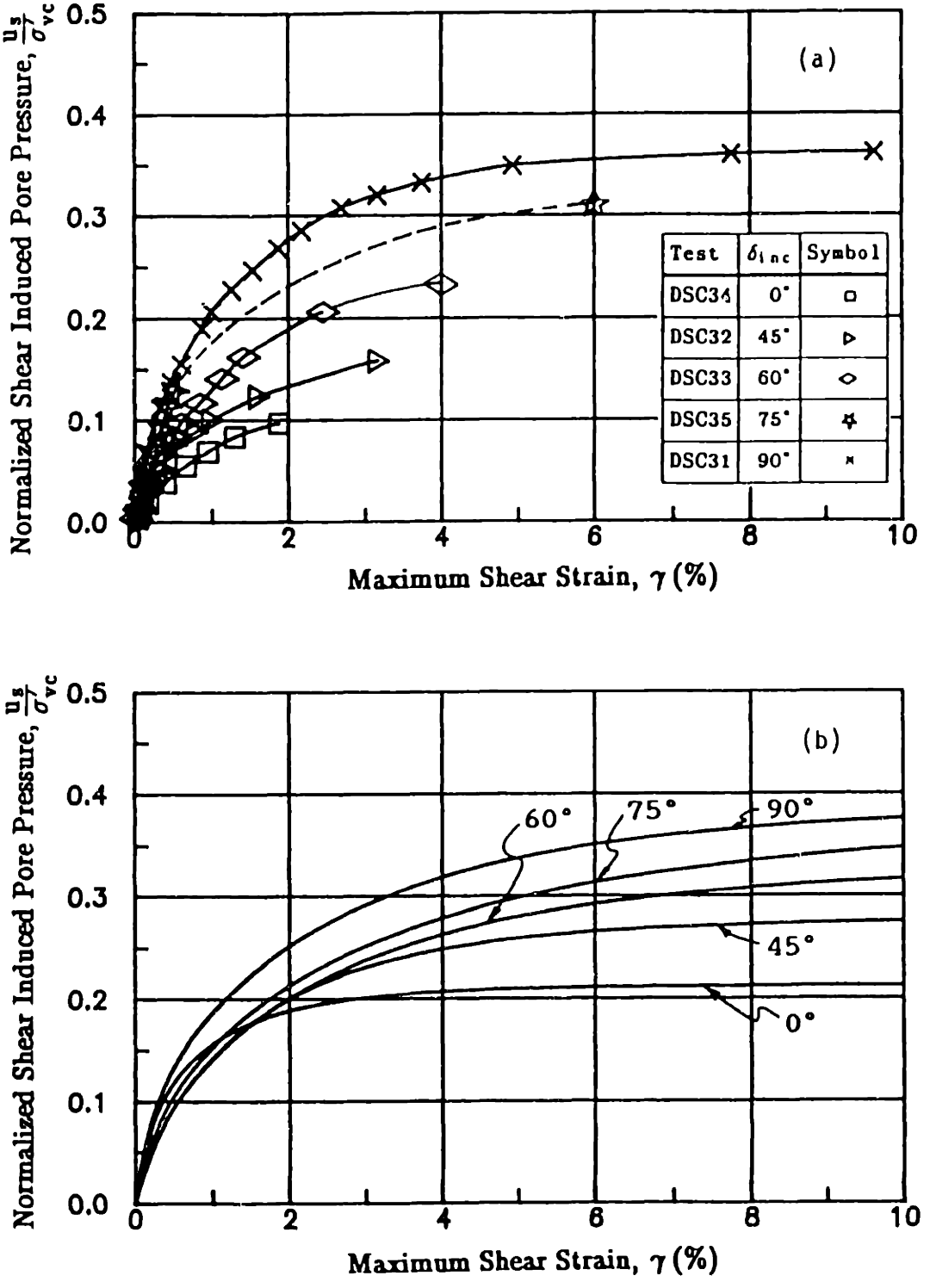

Figure 8.28: Normalized Shear Induced Pore Pressure versus Shear Strain for DSC Tests on OCR=1 BBC: (a) Experimental Results; (b) MIT–E3 Predictions.

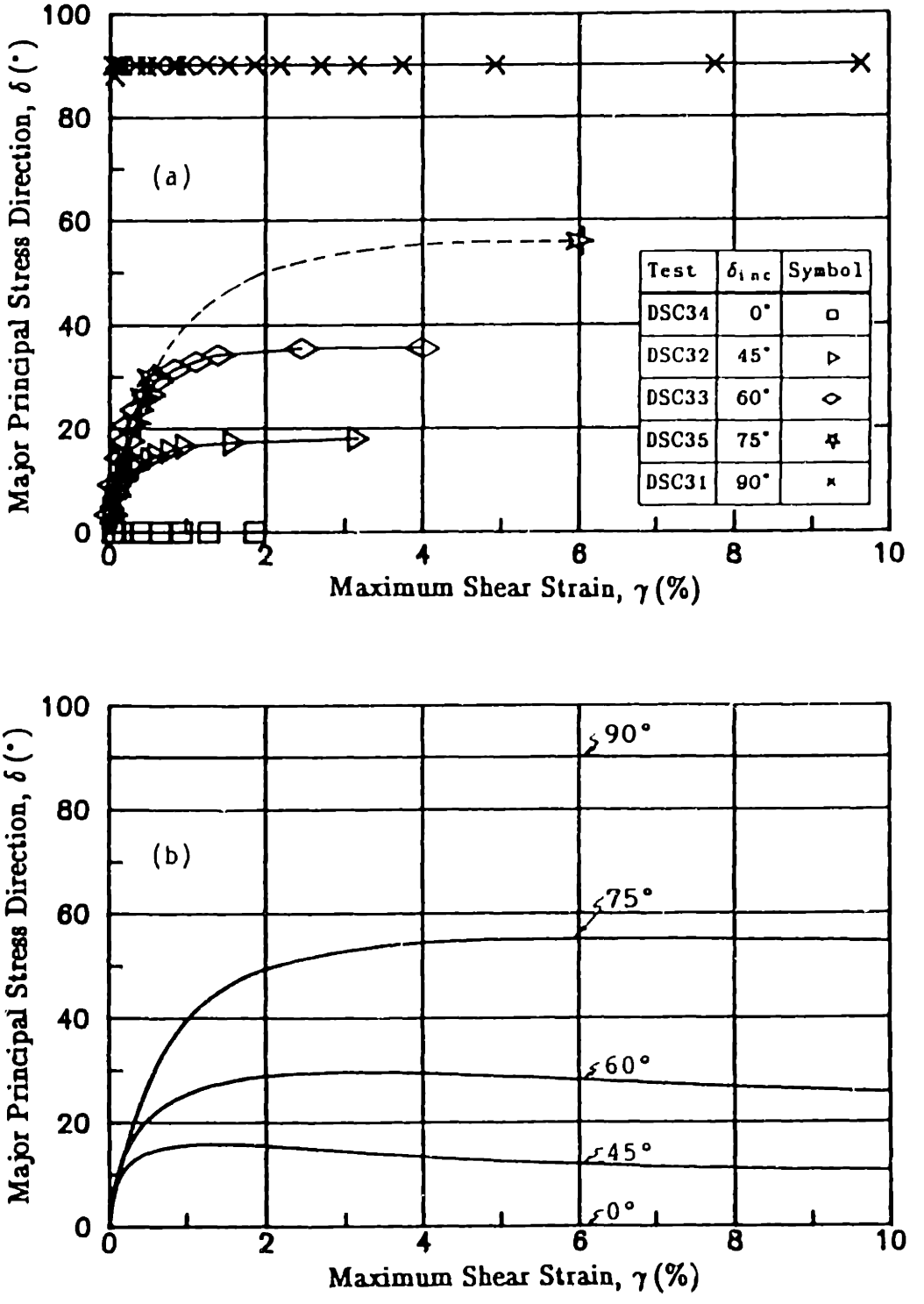

Figure 8.29: Major Principal Stress Direction versus Shear Strain for DSC Tests on OCR=1 BBC: (a) Experimental Results; (b) MIT–E3 Predictions.

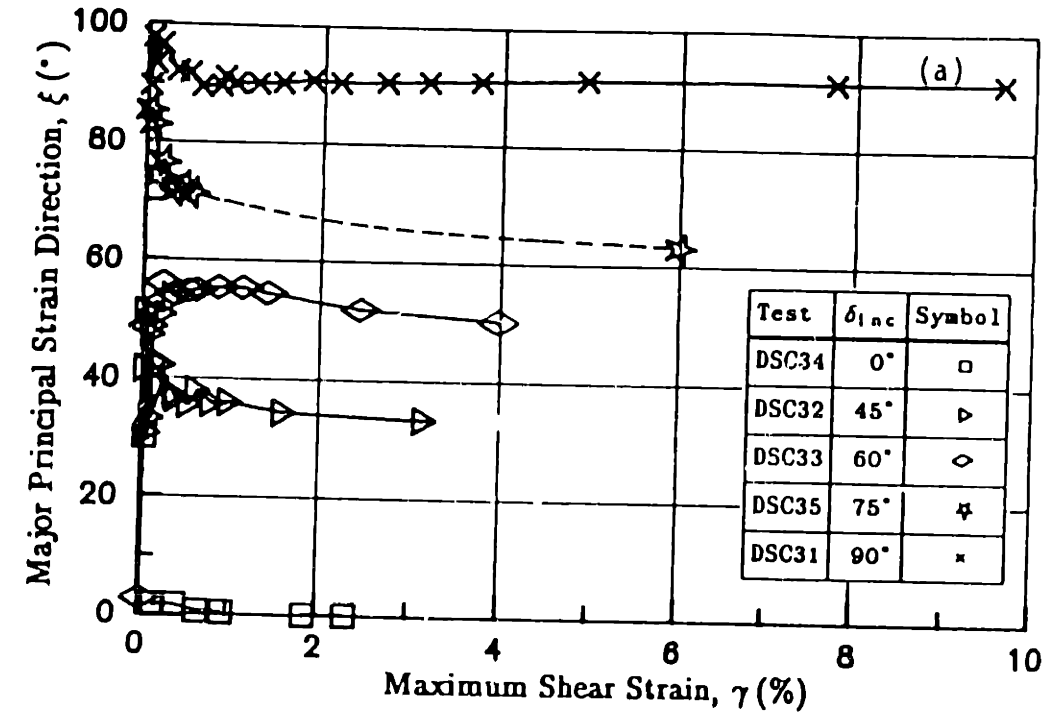

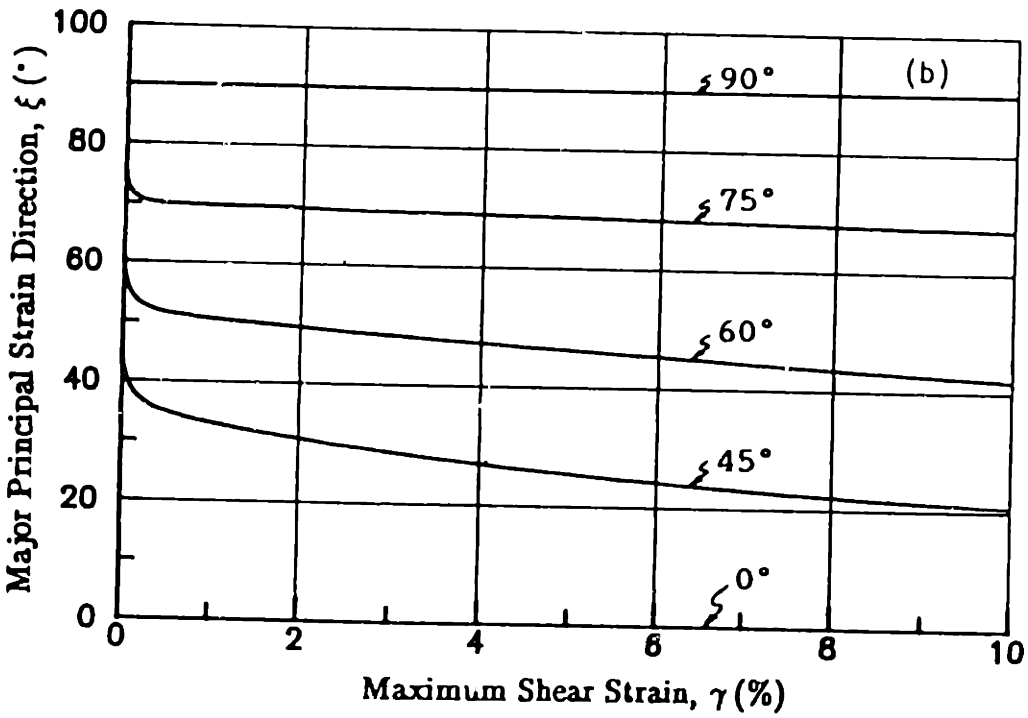

Figure 8.30: Major Principal Strain Direction versus Shear Strain for DSC Tests on OCR=1 BBC: (a) Experimental Results; (b) MIT–E3 Predictions.

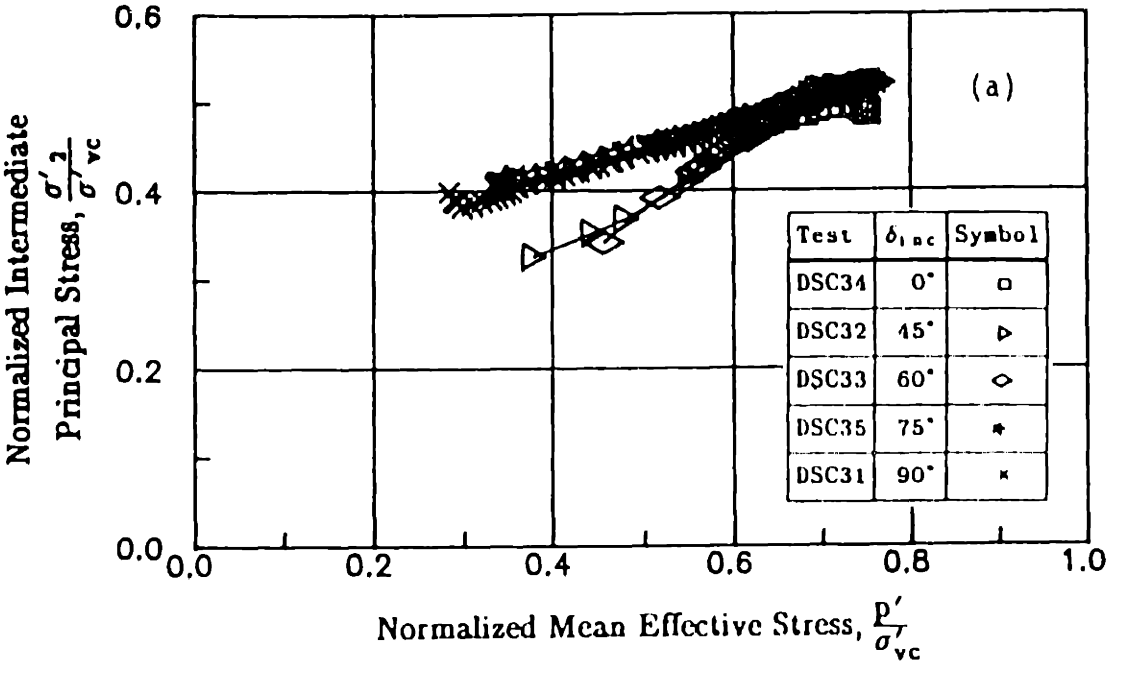

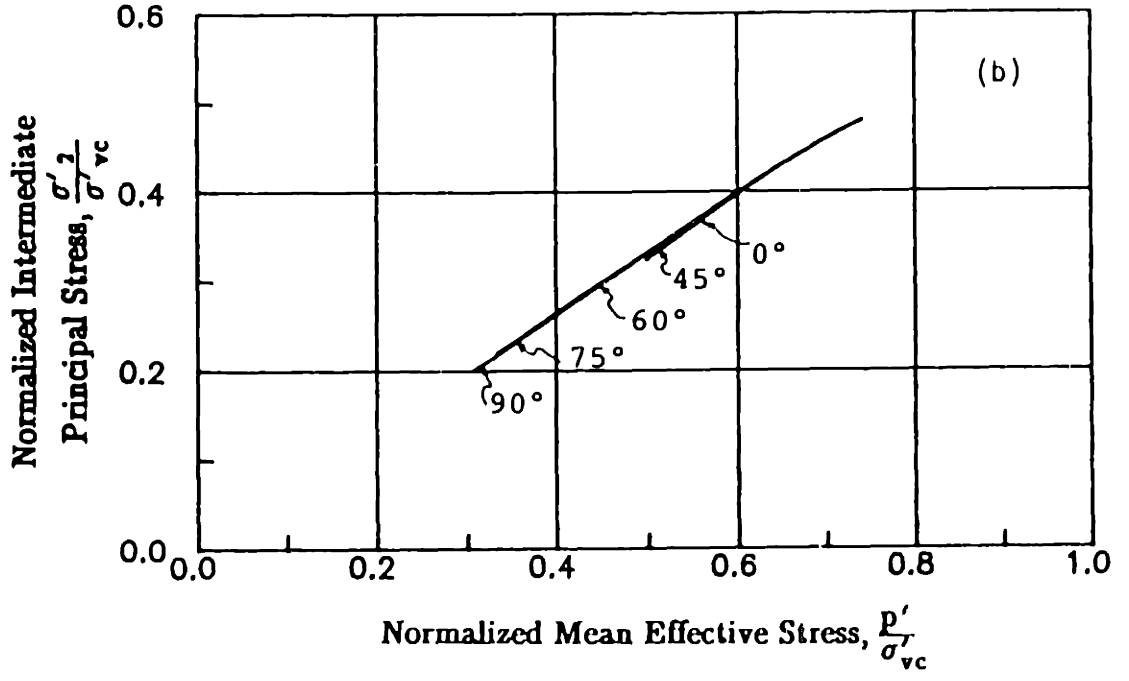

Figure 8.31: Normalized Intermediate Principal Stress versus Normalized Mean Effective Stress for DSC Tests on OCR=1 BBC: (a) Experimental Results; (b) MIT–E3 Predictions.

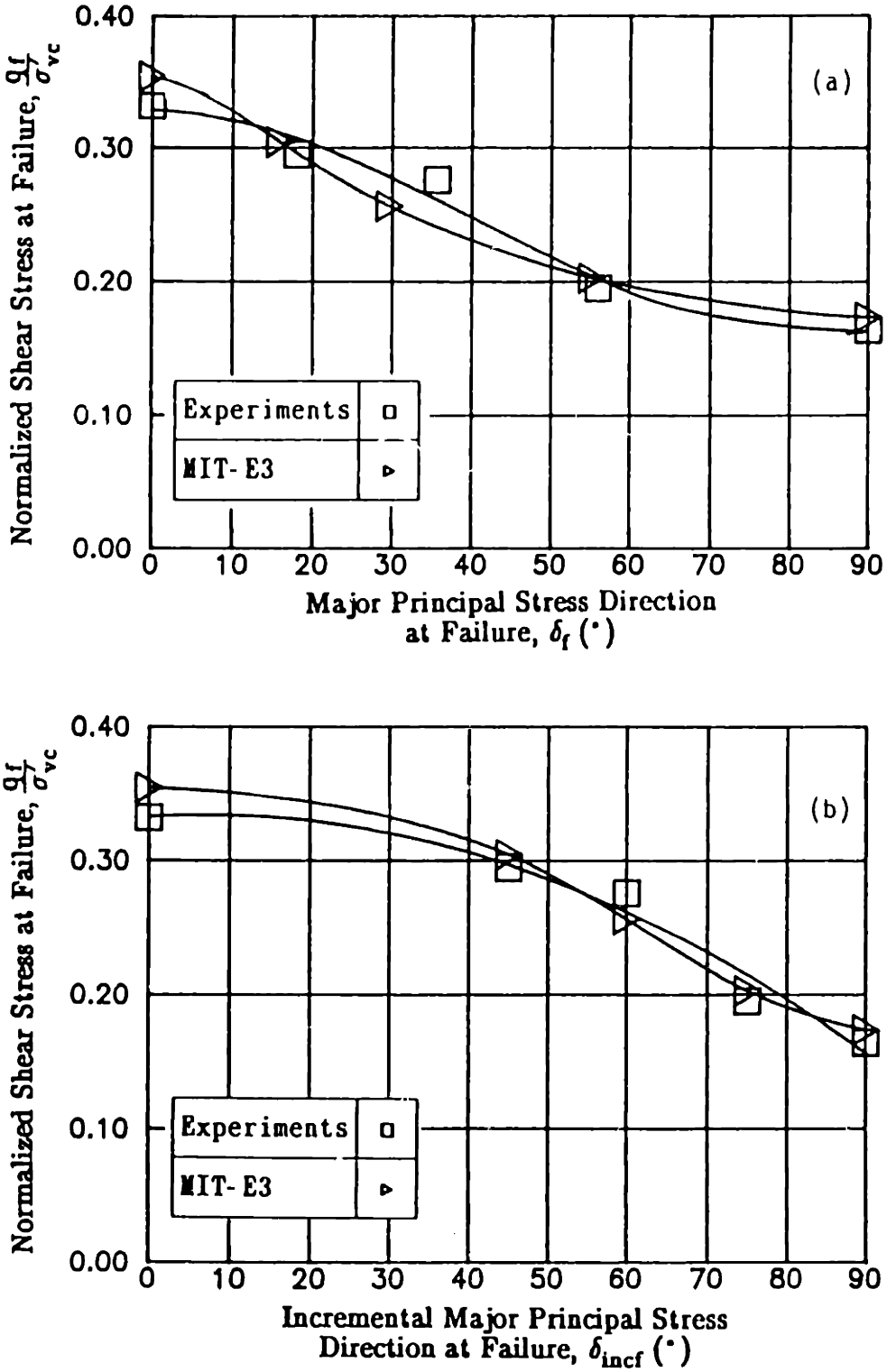

Figure 8.32: Measured and Predicted Normalized Shear Stress versus (a) Major Principal Stress Direction (δ_f); (b) Incremental Major Principal Stress Direction (δ_{incf}) at Failure.

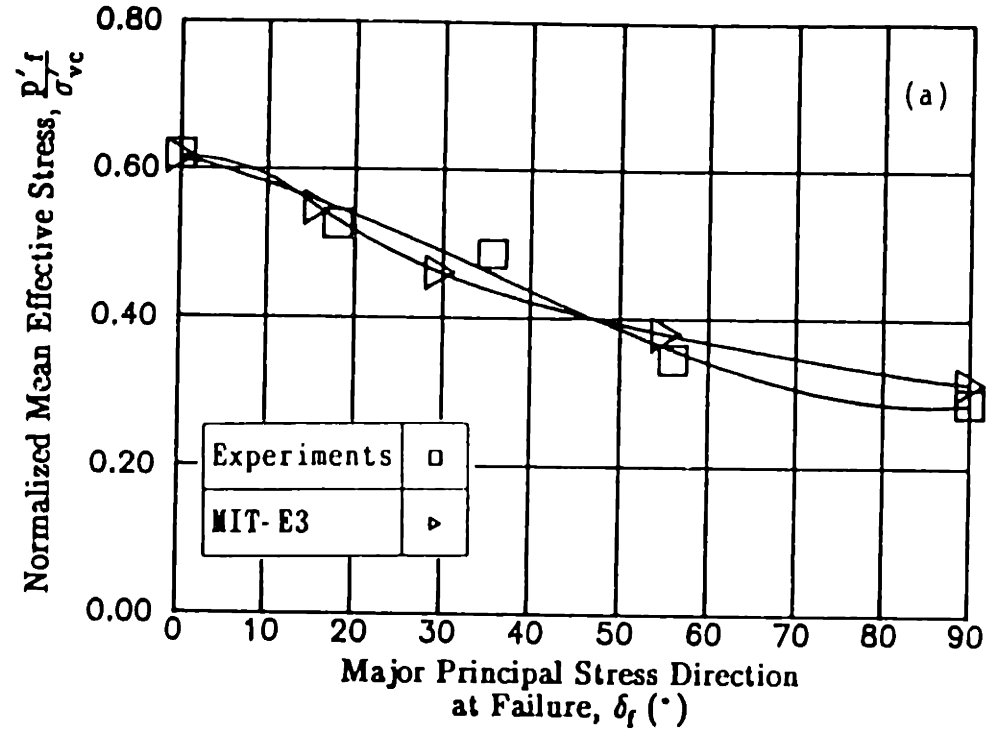

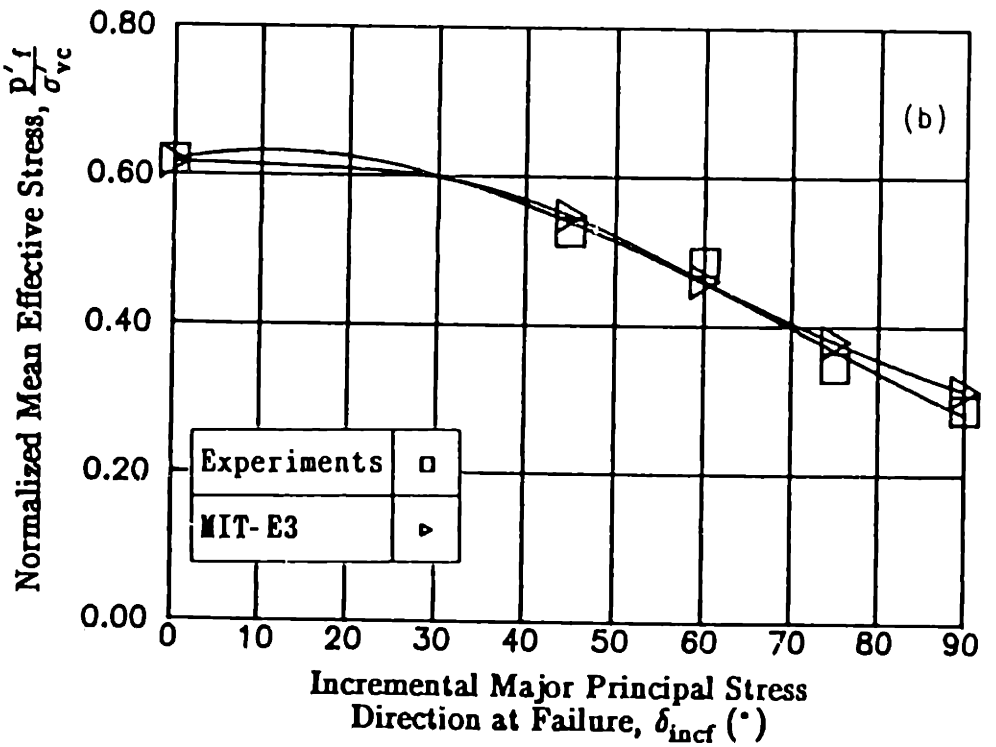

Figure 8.33: Measured and Predicted Normalized Mean Effective Stress versus (a) Major Principal Stress Direction (δ_f); (b) Incremental Major Principal Stress Direction (δ_{incf}) at Failure.

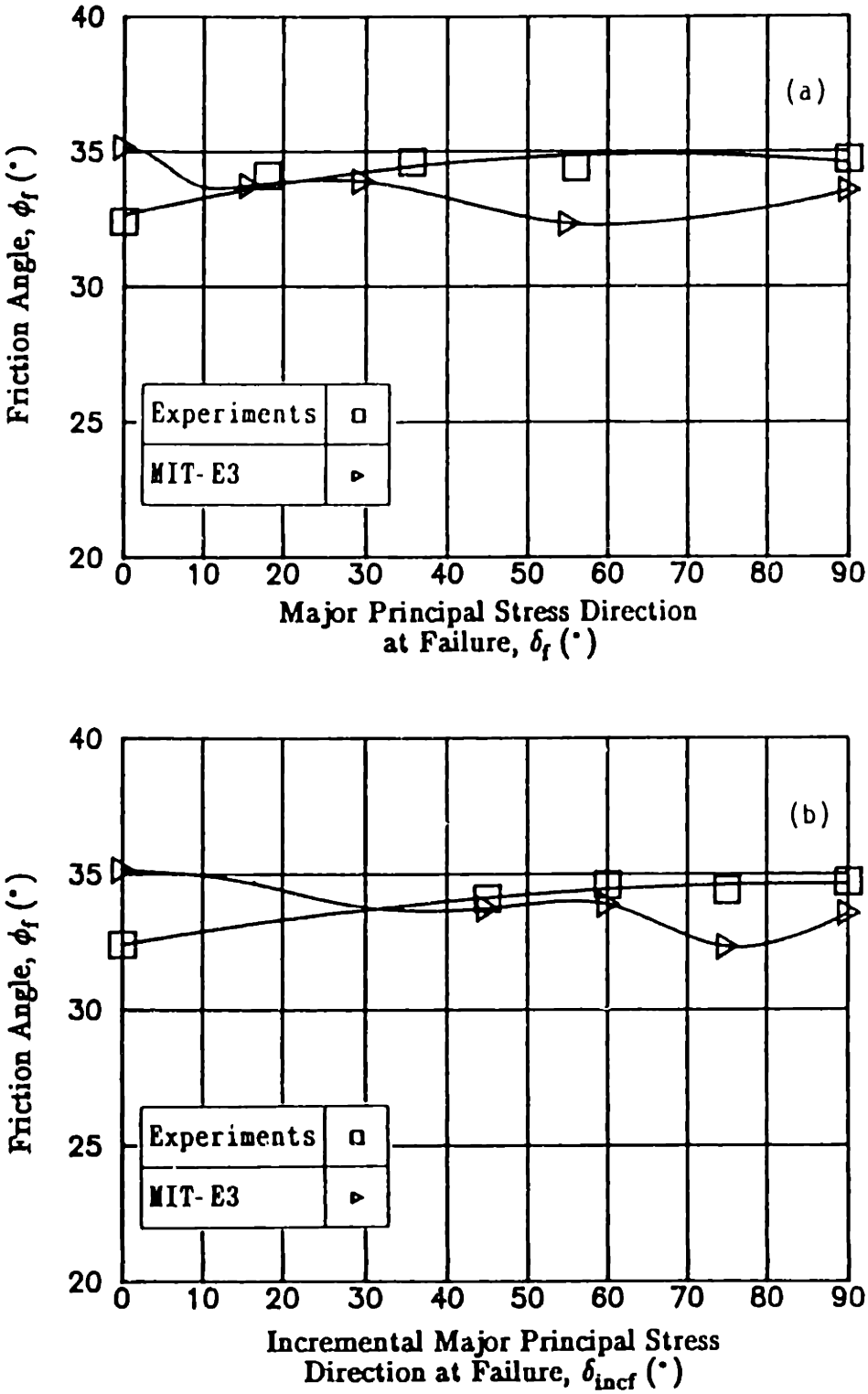

Figure 8.34: Measured and Predicted Friction Angle versus (a) Major Principal Stress Direction (δ_f); (b) Incremental Major Principal Stress Direction (δ_{incf}).

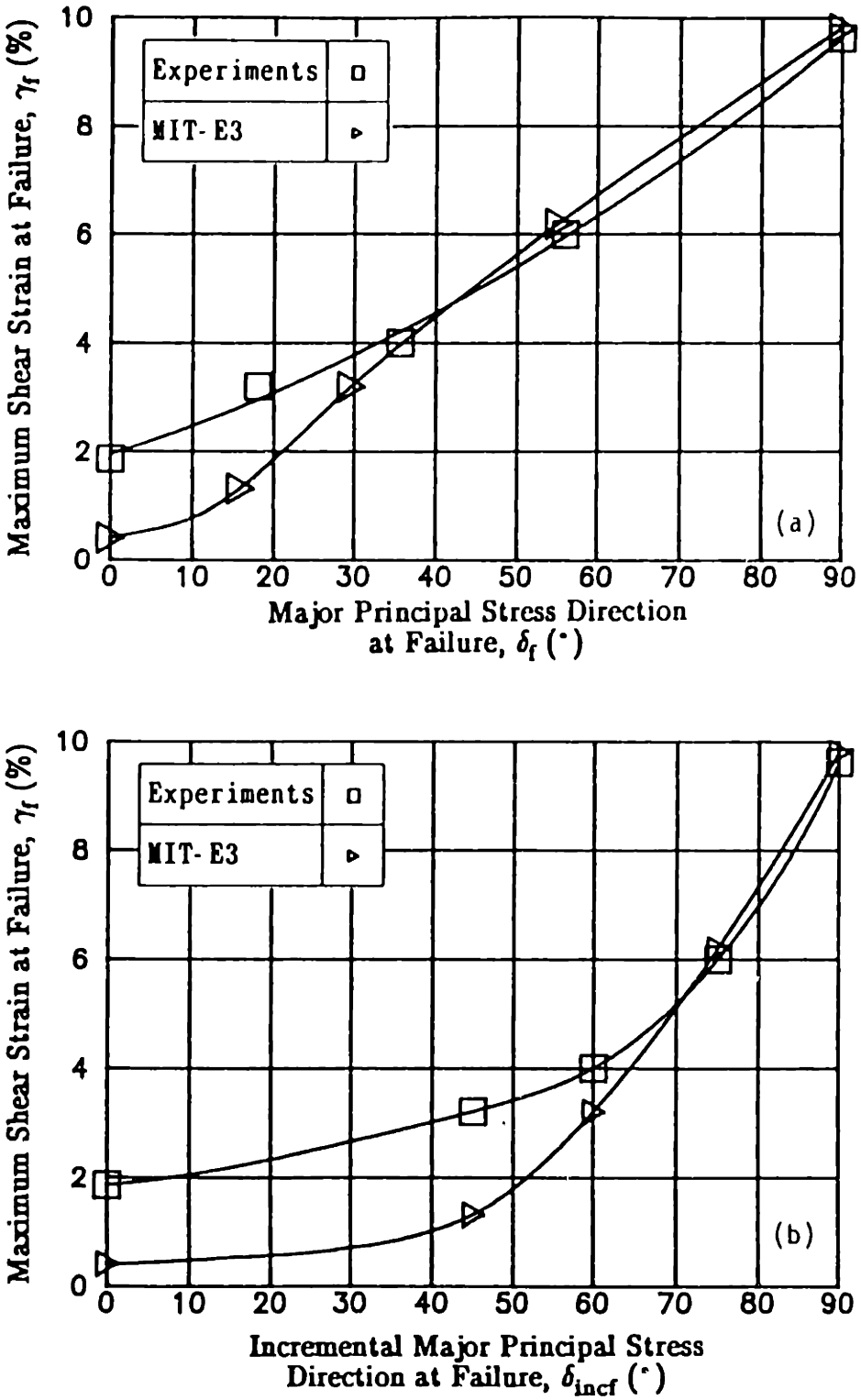

Figure 8.35: Measured and Predicted Maximum Shear Strain versus (a) Major Principal Stress Direction (δ_f); (b) Incremental Major Principal Stress Direction (δ_{incf}) at Failure.

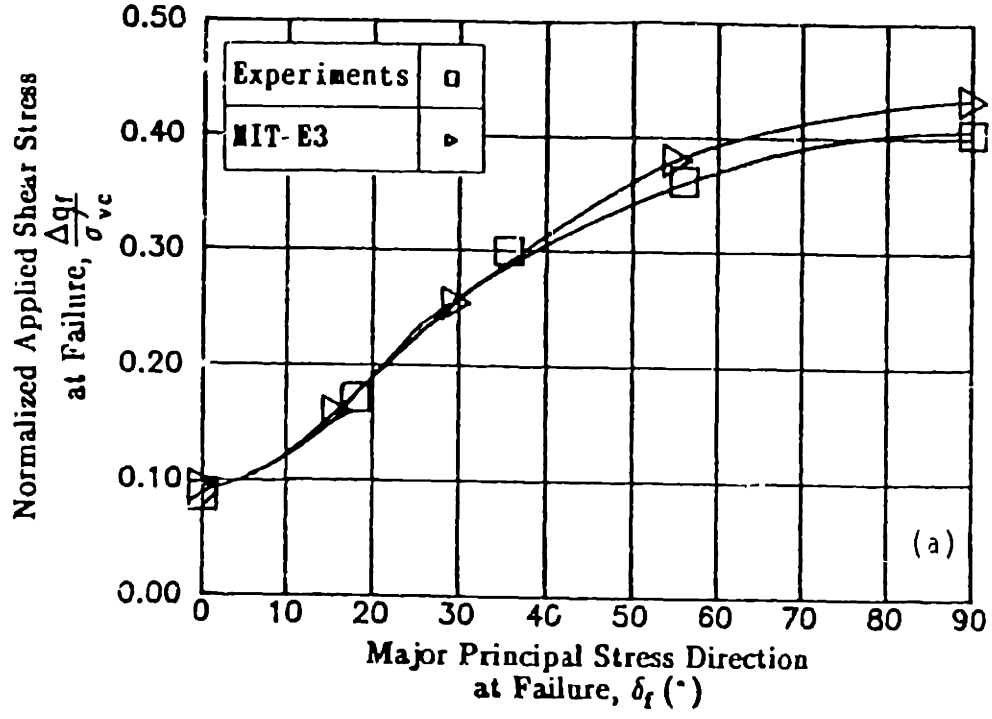

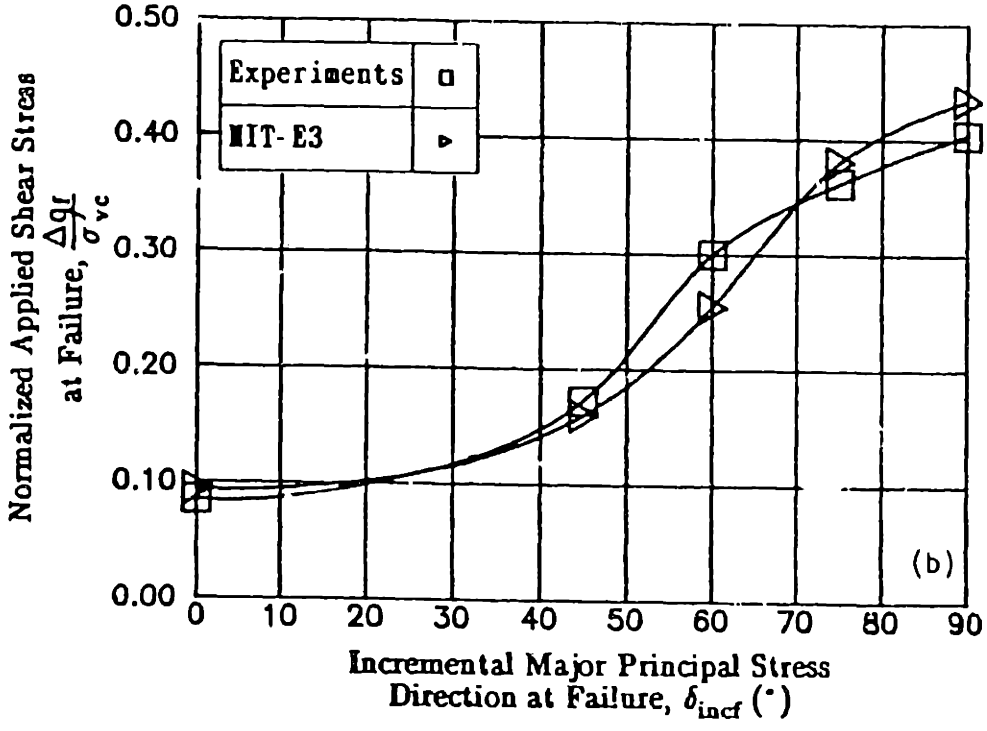

Figure 8.36: Measured and Predicted Normalized Applied Shear Stress versus (a) Major Principal Stress Direction (δ_f); (b) Incremental Major Principal Stress Direction (δ_{incf}) at Failure.

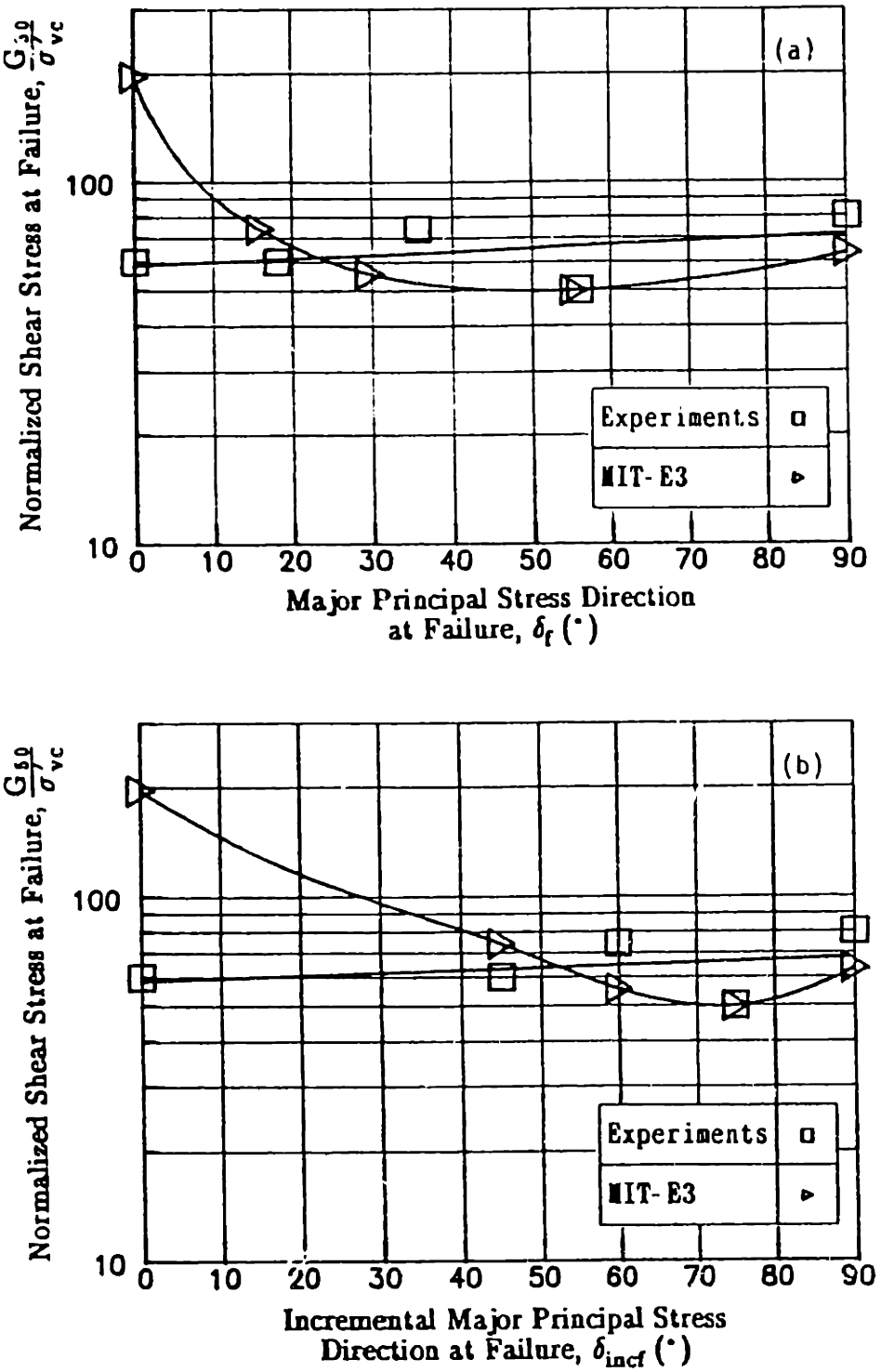

Figure 8.37: Measured and Predicted Normalized Shear Modulus at 50% of Maximum Applied Shear Stress versus (a) Major Principal Stress Direction (δ_f); (b) Incremental Major Principal Stress Direction (δ_{incf}).

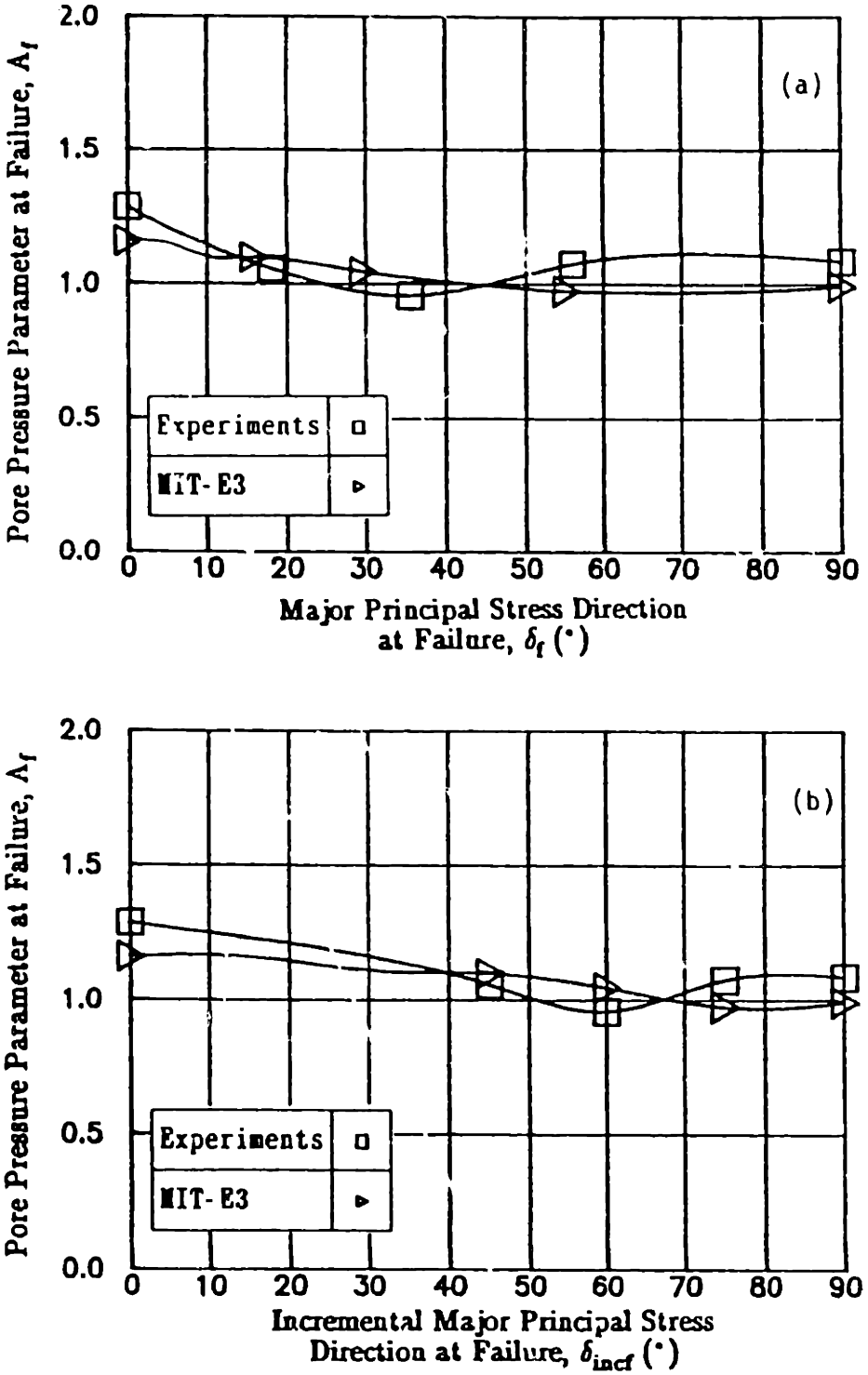

Figure 8.38: Measured and Predicted Pore Pressure Parameter (A_f) versus (a) Major Principal Stress Direction (δ_f); (b) Incremental Major Principal Stress Direction (δ_{incf}) at Failure.

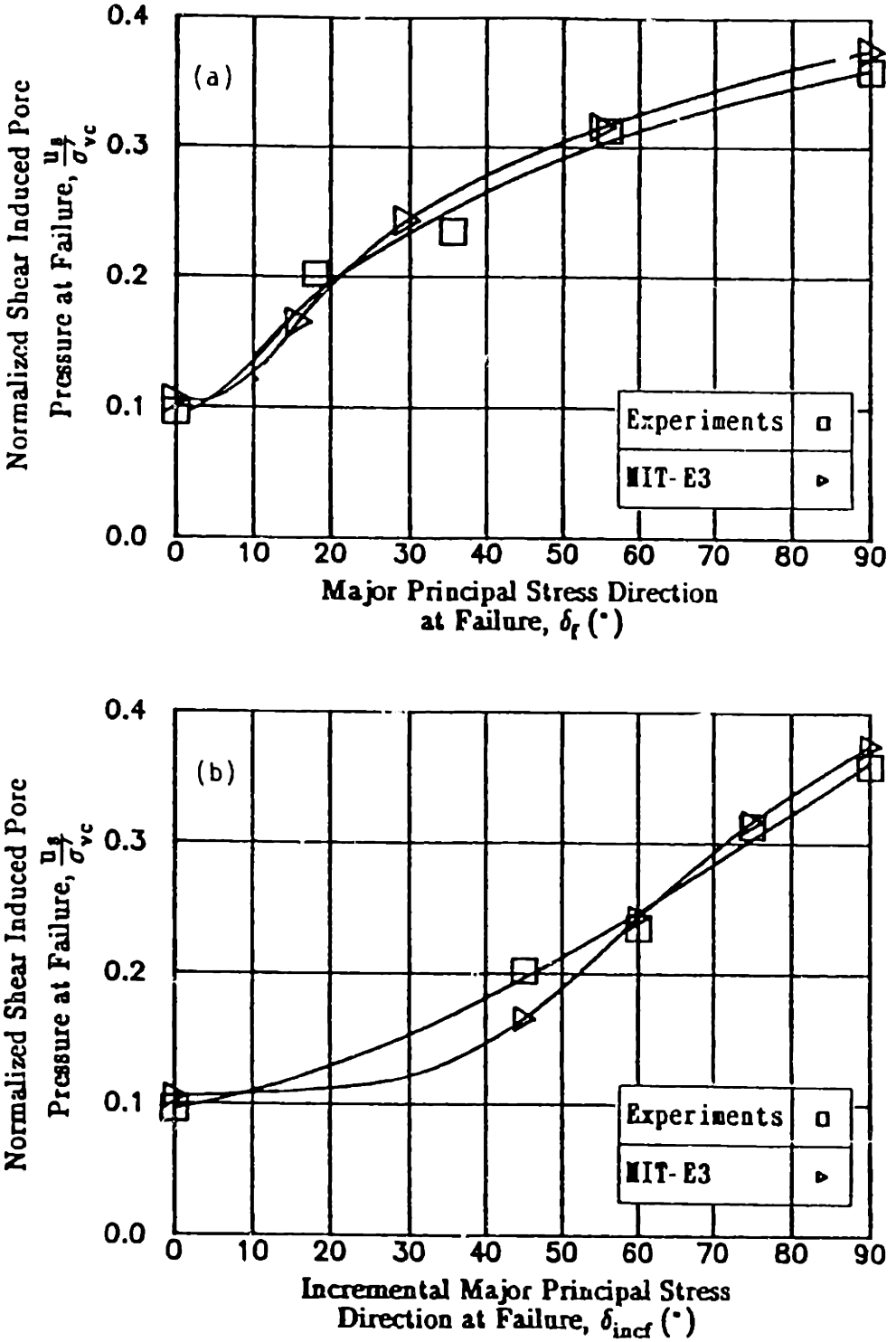

Figure 8.39: Measured and Predicted Normalized Shear Induced Pore Pressure versus (a) Major Principal Stress Direction (δ_f); (b) Incremental Major Principal Stress Direction (δ_{incf}) at Failure.

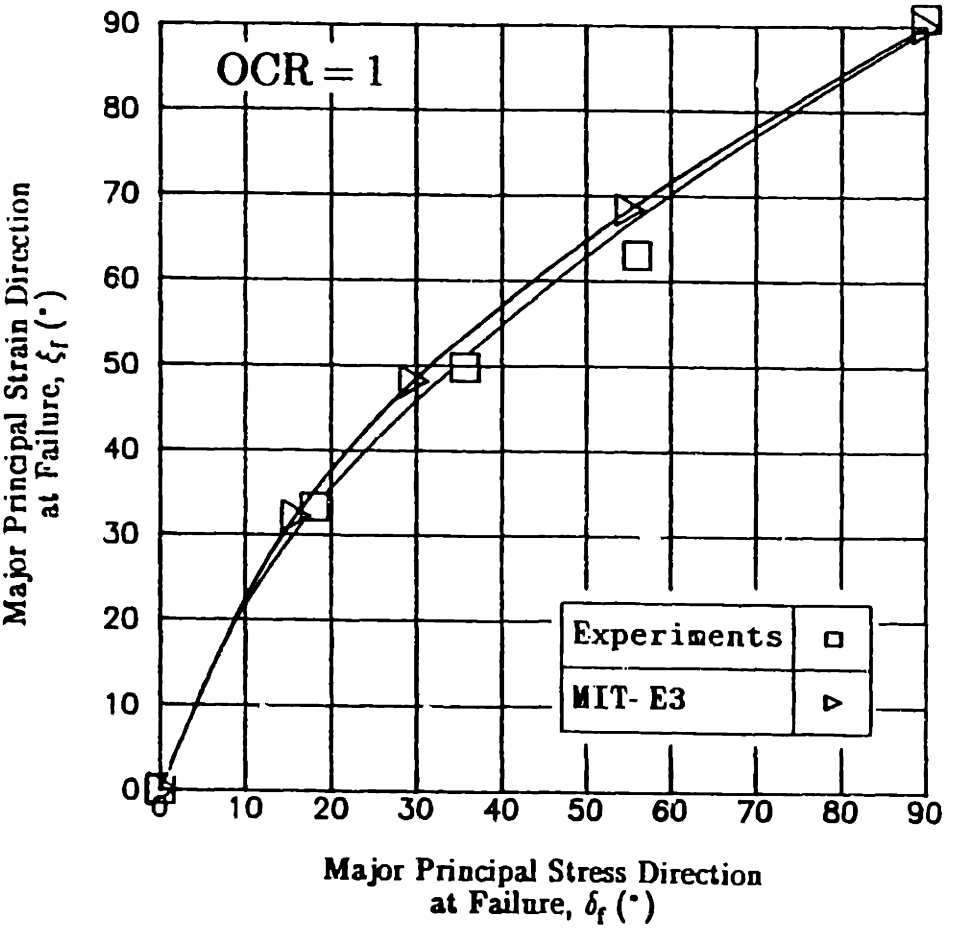

Figure 8.40: Measured and Predicted Major Principal Strain Direction versus Major Principal Stress Direction (δ_f) at Failure.

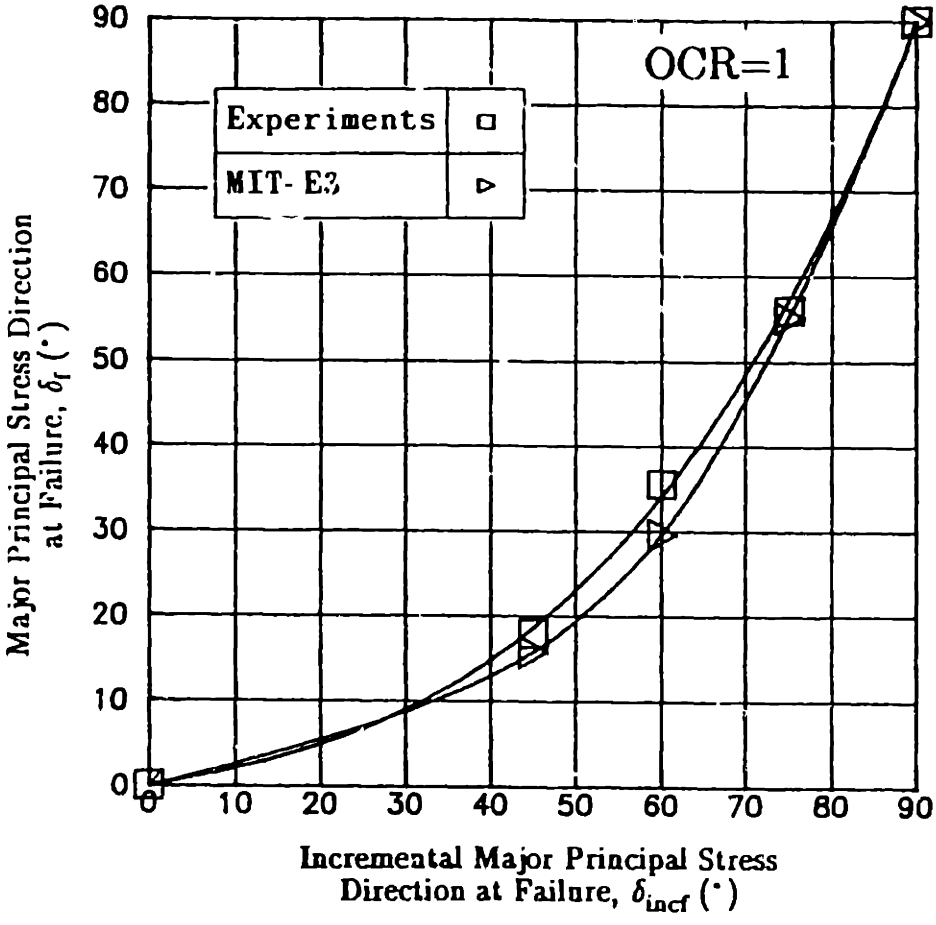

Figure 8.41: Measured and Predicted Major Principal Stress Direction (δ_f) versus Incremental Major Principal Stress Direction (δ_{incf}) at Failure.

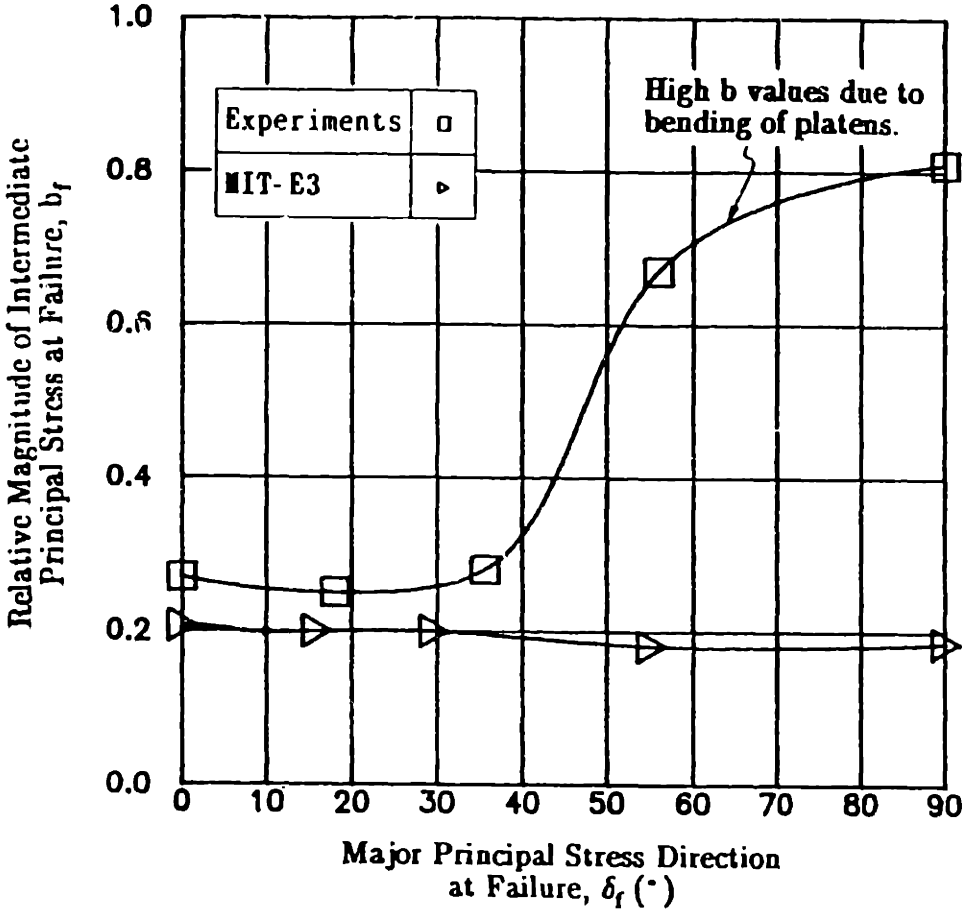

Figure 8.42: Measured and Predicted Relative Magnitude of Intermediate Principal Stress versus Major Principal Stress Direction (δ_f) at Failure.

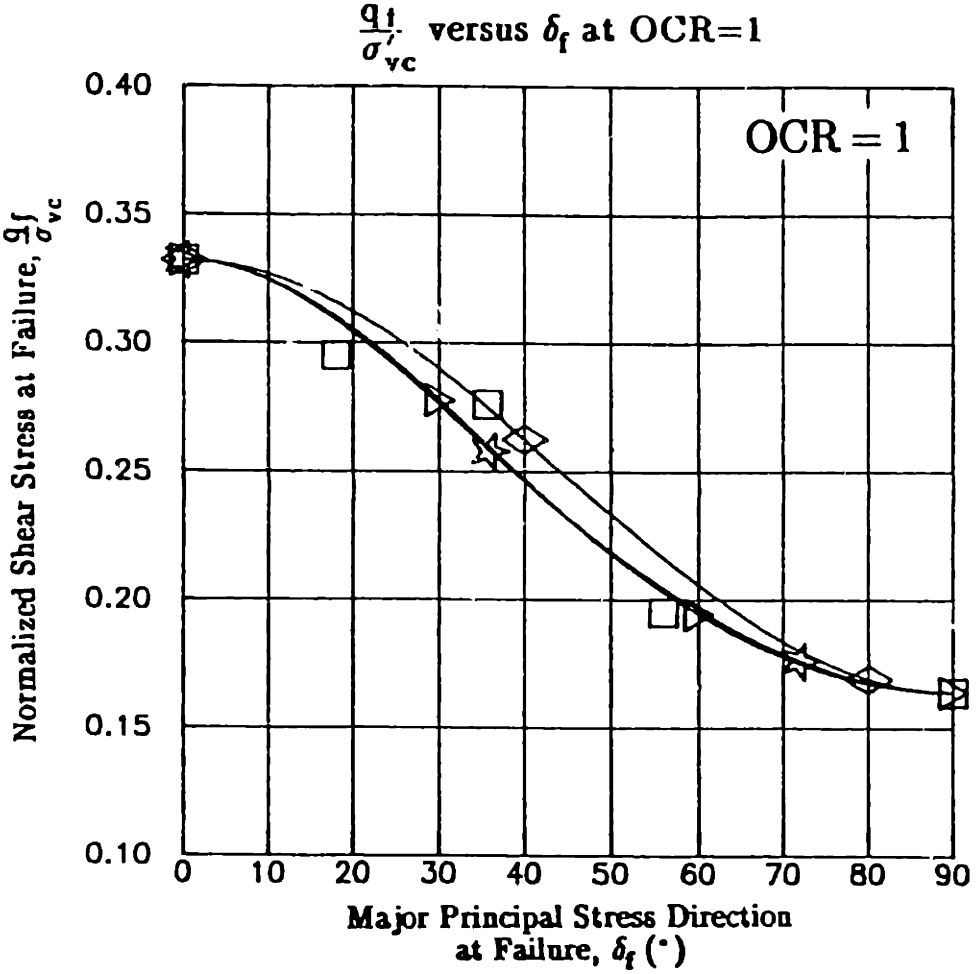

Symbol	$\frac{S_u(45°)}{\sigma'_{vc}}$	Source/Method
□	-	Experimental Data
◇	-	Casagrande-Carillo (1944)
☆	0.232	Bishop (1966)
▷	0.232	Davis-Christian (1971)

Figure 8.43: Normalized Shear Stress at Failure Curves of BBC at OCR=1 from Different Curve–Fitting Methods.

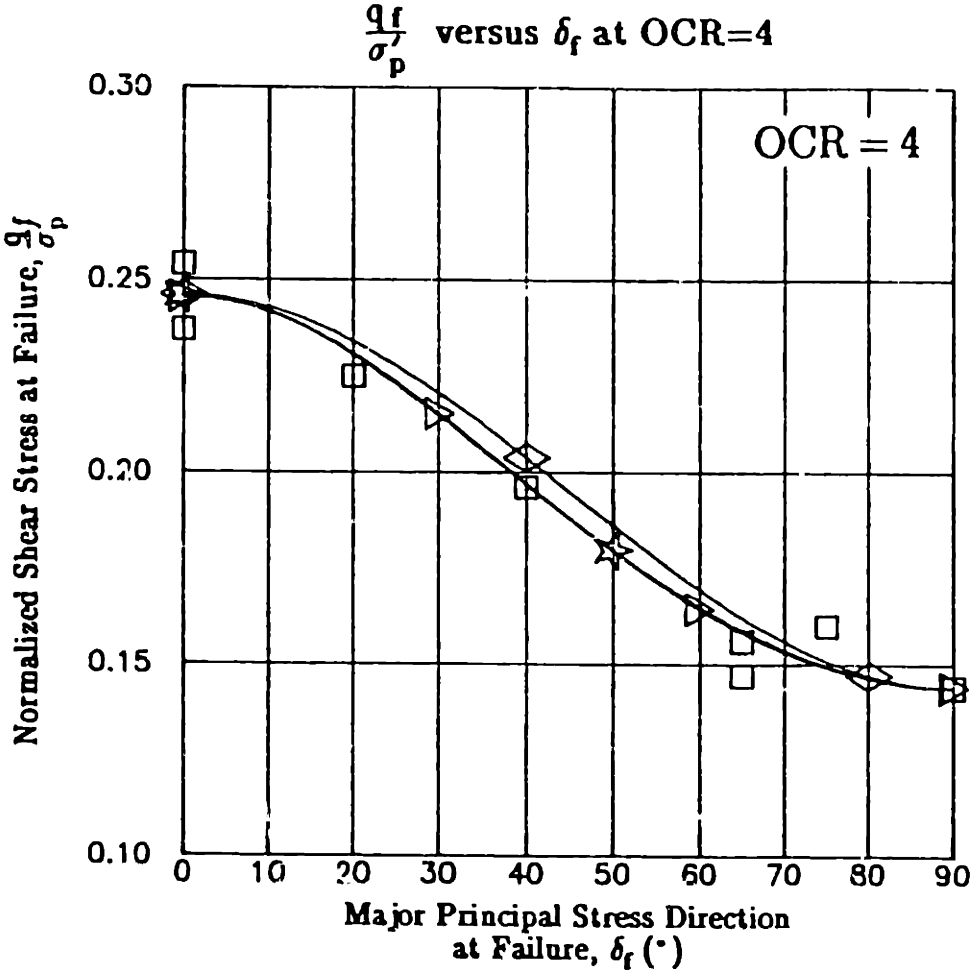

Symbol	$\frac{S_u(45°)}{\sigma'_{vc}}$	Source/Method
□	-	Experimental Data
◇	-	Casagrande-Carillo (1944)
☆	0.189	Bishop (1966)
▷	0.189	Davis-Christian (1971)

Figure 8.44: Normalized Shear Stress at Failure Curves of BBC at OCR=4 from Different Curve–Fitting Methods.

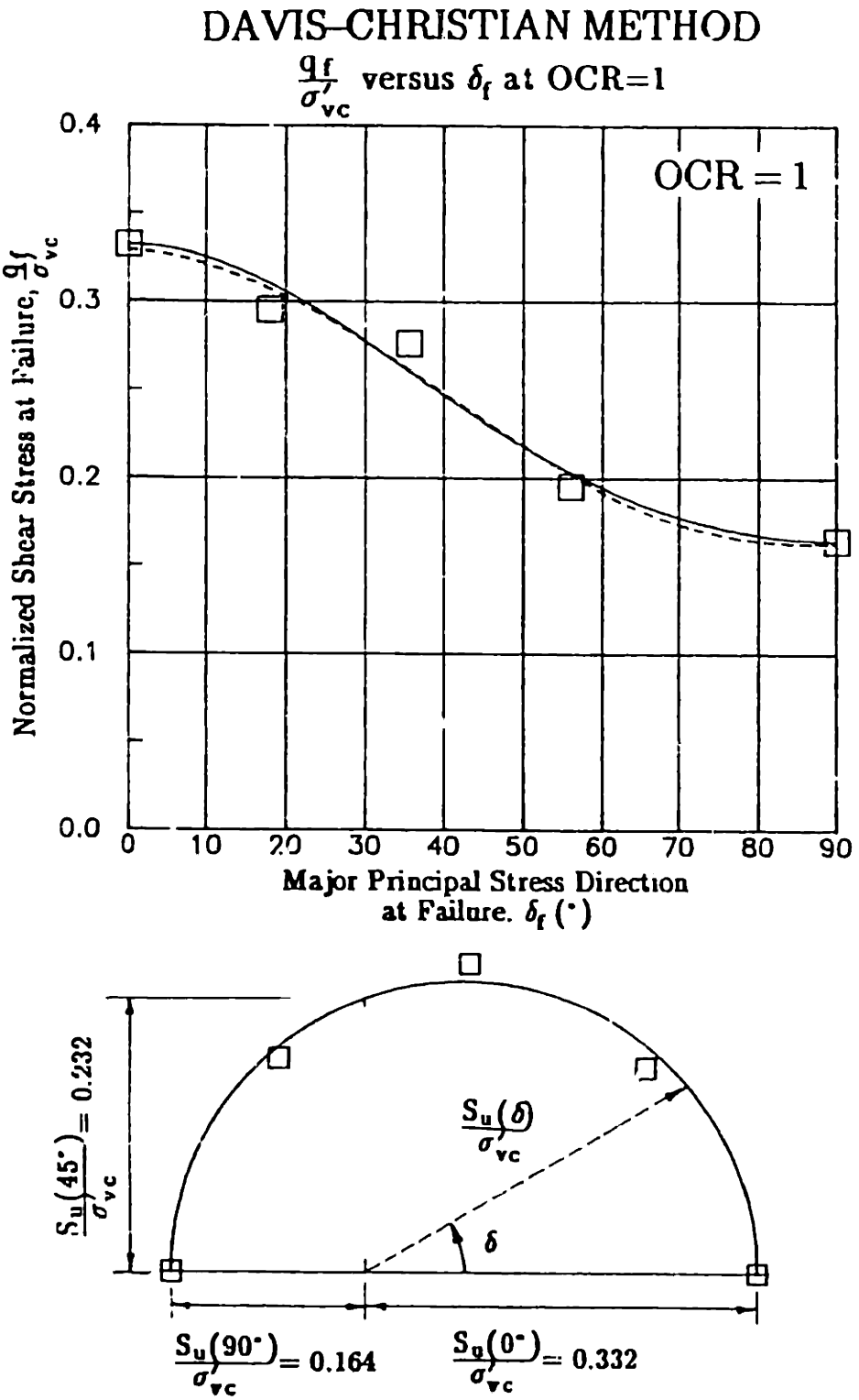

Figure 8.45: Normalized Shear Stress at Failure Curves of BBC at OCR=1 from Davis–Christian Method.

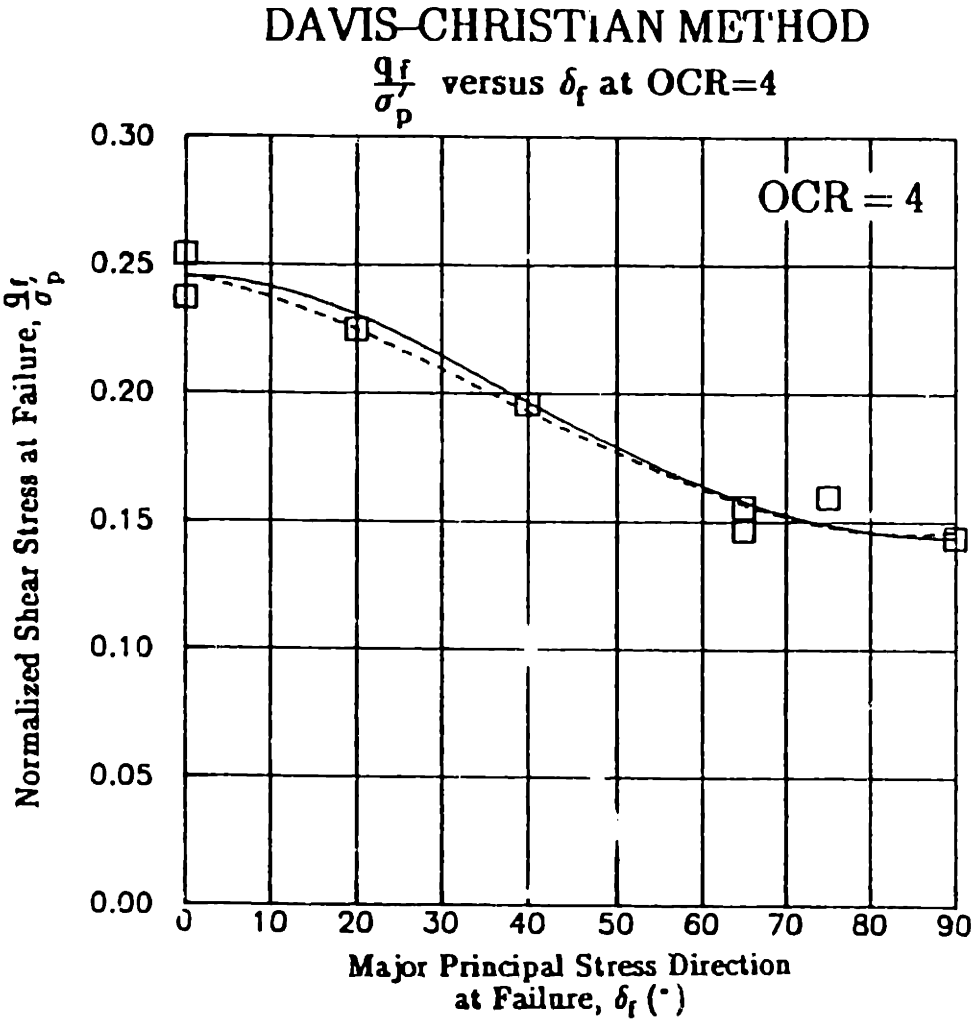

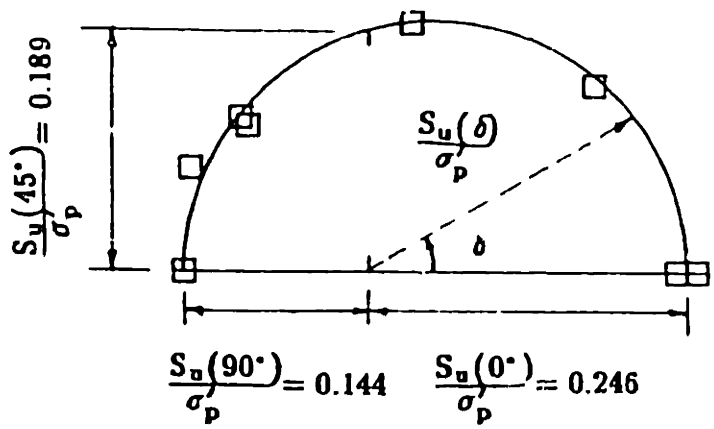

Figure 8.46: Normalized Shear Stress at Failure Curves of BBC at OCR=4 from Davis–Christian Method.

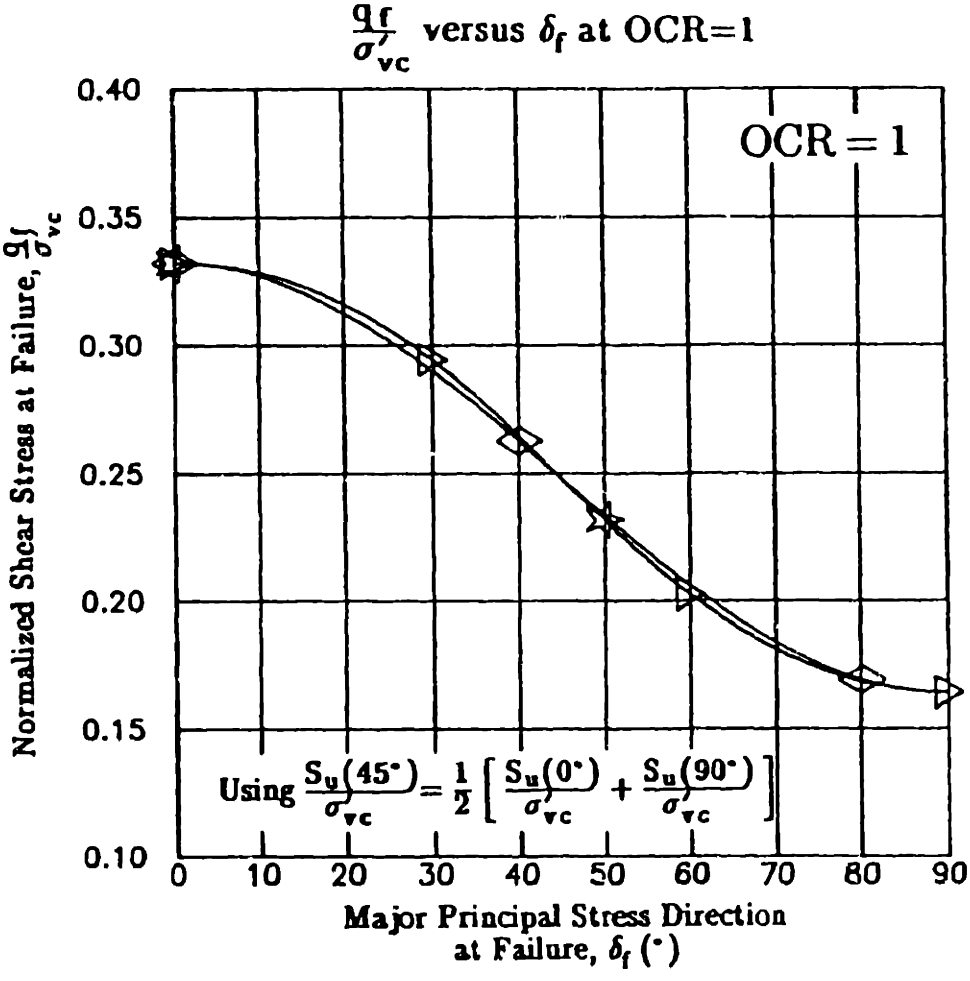

Symbol	Method
◇	Casagrande-Carillo (1944)
✡	Bishop (1966)
▷	Davis-Christian (1971)

Figure 8.47: Normalized Shear Stress at Failure Curves of BBC at OCR=1 from Different Curve–Fitting Methods using $S_u(45°)/\sigma'_{vc}=0.5[S_u(0°)/\sigma'_{vc}+S_u(90°)/\sigma'_{vc}]$.

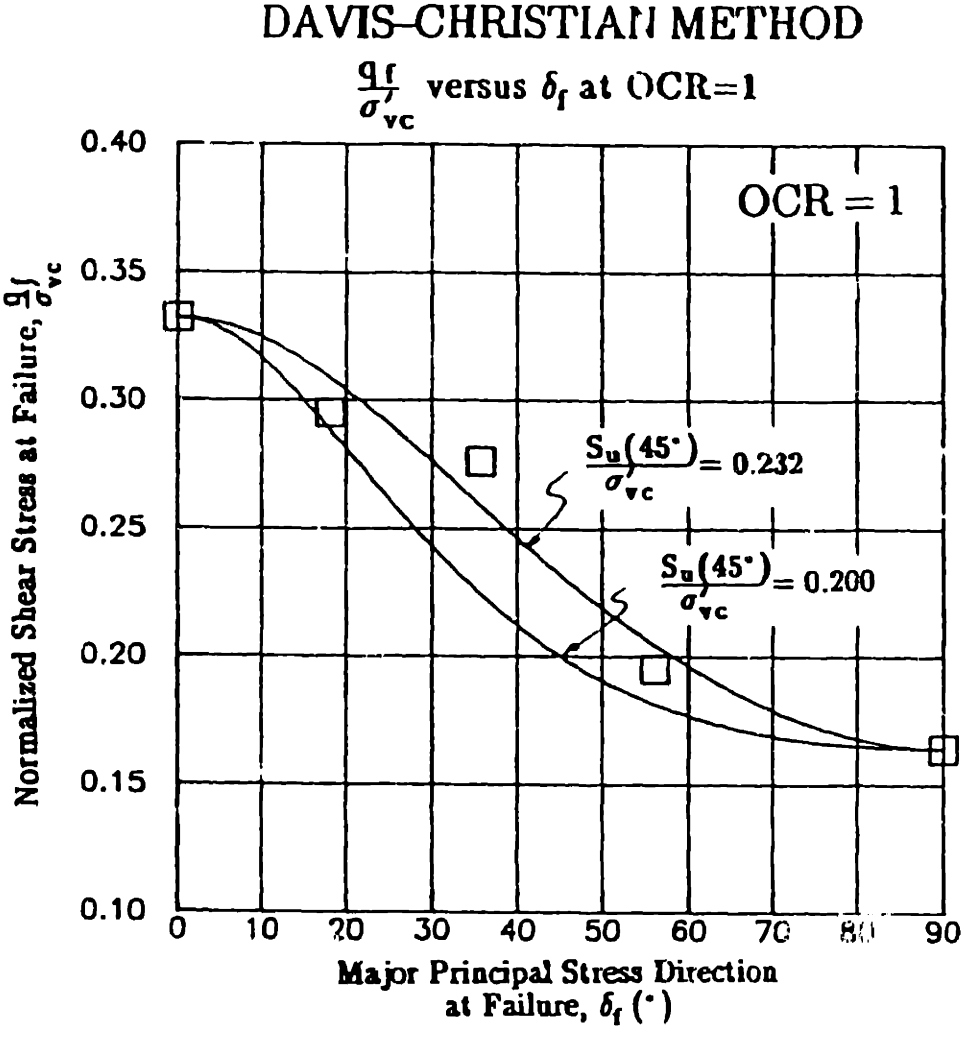

Figure 8.48: Normalized Shear Stress at Failure Curves of BBC at OCR=1 from Davis–Christian Method with $S_u(45^\circ)/\sigma'_{vc}$=0.232 and $S_u(45^\circ)/\sigma'_{vc}$=0.200.

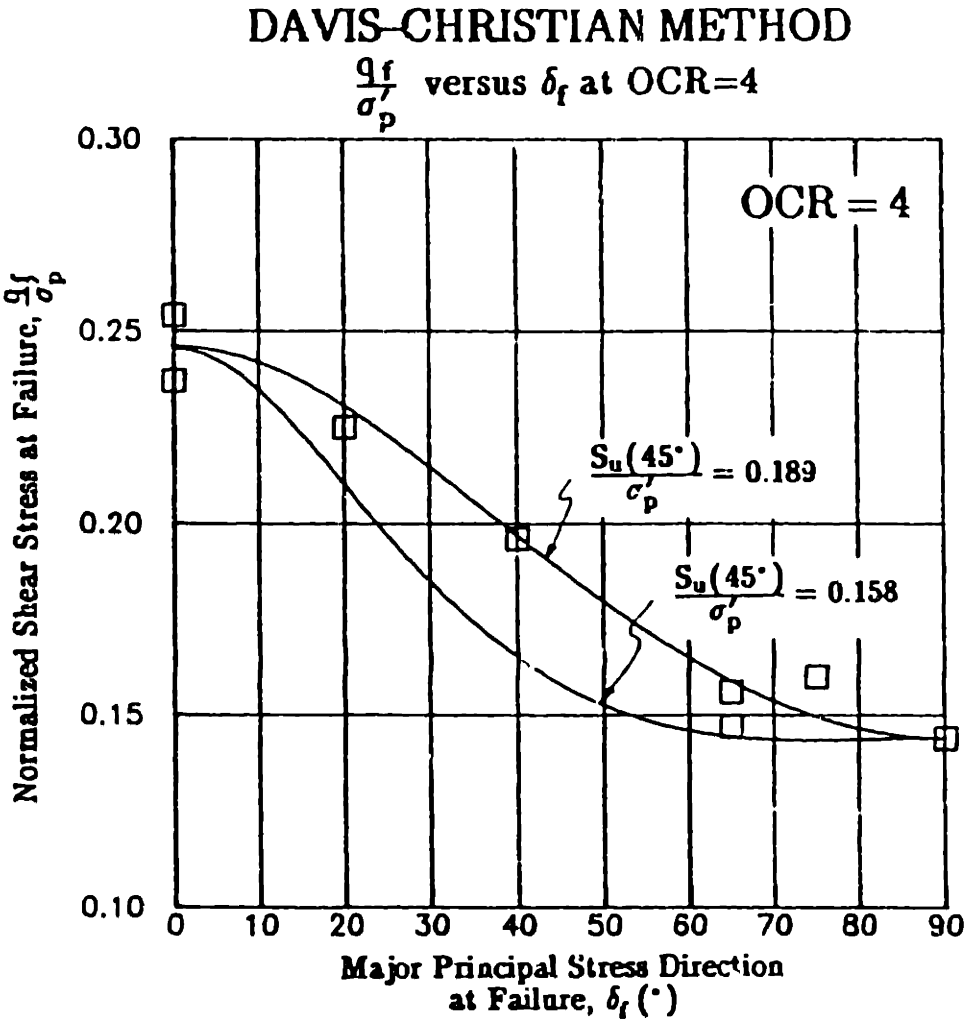

Figure 8.49: Normalized Shear Stress at Failure Curves of BBC at OCR=4 from Davis–Christian Method with $S_u(45^\circ)/\sigma'_p$=0.189 and $S_u(45^\circ)/\sigma'_p$=0.158.

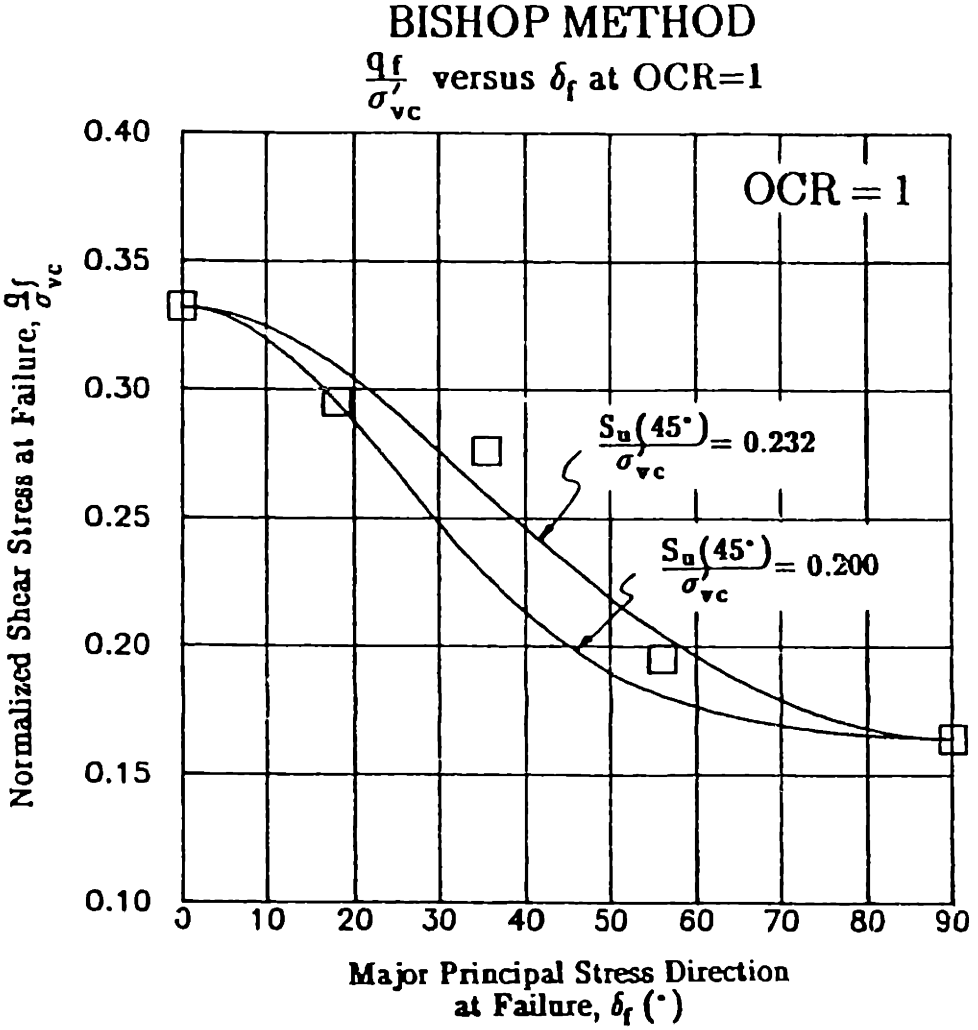

Figure 8.50: Normalized Shear Stress at Failure Curves of BBC at OCR=1 from Bishop Method with $S_u(45^\circ)/\sigma'_{vc}$=0.232 and $S_u(45^\circ)/\sigma'_{vc}$=0.200.

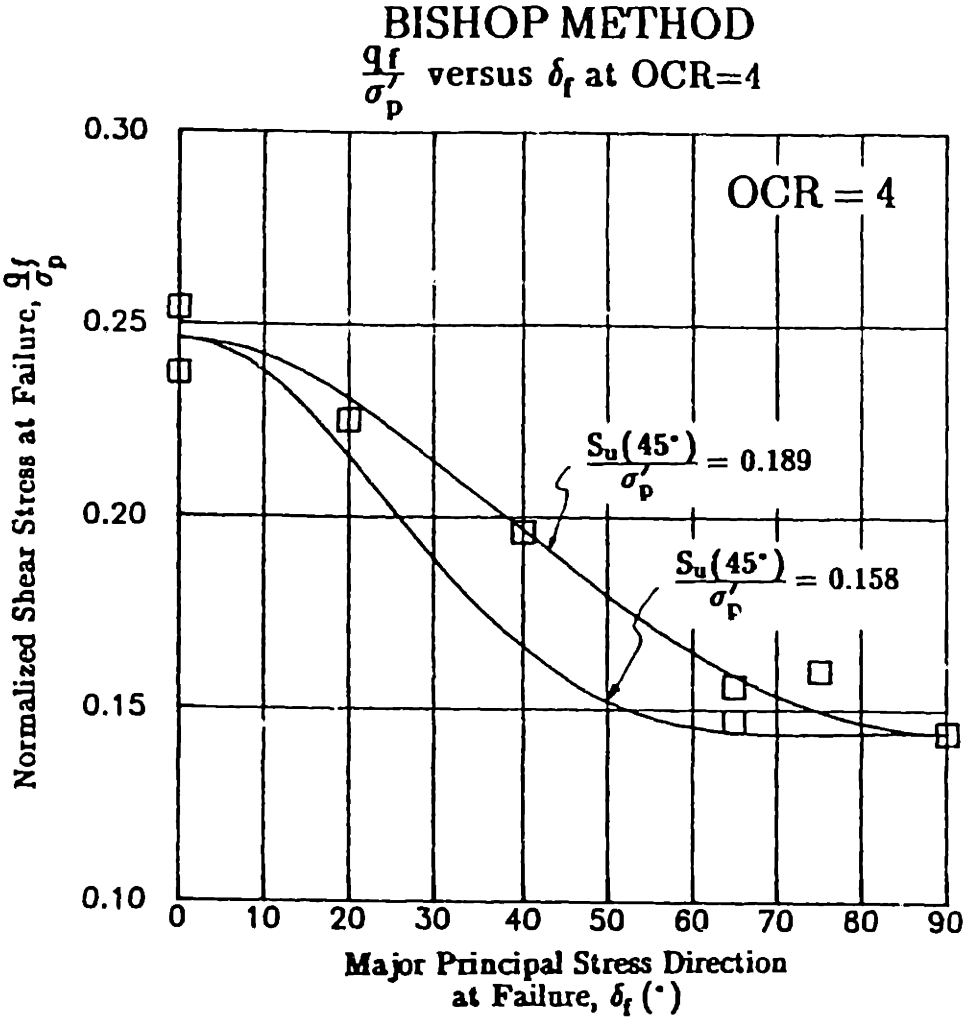

Figure 8.51: Normalized Shear Stress at Failure Curves of BBC at OCR=4 from Bishop Method with $S_u(45^\circ)/\sigma'_p$=0.189 and $S_u(45^\circ)/\sigma'_p$=0.158.

CHAPTER 9

SUMMARY, CONCLUSIONS AND RECOMMENDATIONS

9.1 INTRODUCTION

This research represents a contribution towards a better understanding of the undrained stress–strain–strength anisotropic behavior of resedimented Boston Blue Clay (BBC) using the Directional Shear Cell (DSC). The DSC has the unique ability to completely control the principal stress direction by varying the normal and shear stresses acting on a cubical specimen restrained by two end platens (Figure 6.2). The DSC was used to investigate both the inherent and combined anisotropy of BBC. Inherent anisotropy is defined as the material anisotropy caused by depositional environment and subsequent K_o–consolidation which characterizes the soil prior to the initiation of shear. This type of anisotropy was investigated by performing DSC recompression undrained shear tests on OCR=4 BBC starting from a hydrostatic initial stress state (since $K_o \simeq 1$ at this OCR). Combined anisotropy is defined as the anisotropy due to a combination of the inherent and initial shear stress components. The latter component produces directionally dependent clay properties whenever shearing starts from a $K_o \neq 1$ condition. The combined anisotropy was studied experimentally by conducting undrained DSC shear tests on K_o–normally consolidated BBC.

This chapter summarizes the experimental research and makes recommendations regarding further modification of the DSC device and future test programs.

9.2 THE DIRECTIONAL SHEAR CELL DEVICE

9.2.1 Description of the DSC

The normal stresses in the DSC are applied with flexible pressure bags and shear stresses are applied with shear sheets. The applied major principal stress in the DSC can thus be fixed in any desired direction, and/or continuously rotated during shear (Figure 5.1). The δ angle (Figure 2.1) is defined as the direction of the major principal stress relative to the depositional direction (taken as vertical). Another unique feature of the DSC is that its performance can be verified by performing tests in the isotropic plane of a specimen, which should have stress–strain relationships independent of the principal stress direction. Such tests are referred to as "proof" or ψ tests (Figure 2.1).

The strain distributions of the sample during consolidation and shearing are measured by either radiographic or photographic techniques. The photographic technique was adopted for this as well as prior DSC research by Germaine (1982), because it is impossible to embed tungsten balls (as used in Radiography) at mid–height without causing substantial disturbance to the clay sample.

The DSC was developed at University College London to study the effects of principal stress rotation on the strain induced anisotropy of dense sand (Arthur et al., 1977). The inherent anisotropy of sand was first studied in the DSC by Bekenstein (1980). Germaine (1982) then extended the capability of the DSC to enable the study of the undrained anisotropic behavior of clay when the initial stress of state was hydrostatic.

The DSC is considered to be the best plane strain device available for basic research into soil anisotropy because of its simplicity in both the application of stresses and the setup of the test compared with its counterpart, the Torsional Shear Hollow Cylinder. The latter requires a larger sample and much more extensive instrumentation.

9.2.2 Modifications of Directional Shear Cell Equipment

Modifications to the DSC device during this research included changes in the pressure bags, the shear sheets, the two end platens, the sample corner design and the pore water pressure probe. Better control of the position of the pressure bags was achieved with position sensors in the pressure bags. The intermediate principal stress can now be measured using the new flexible boundary measuring device flush–mounted on the bottom platen, as shown in Figure 3.8. The new sample corner design described in Section 3.3.5 enables the soil to strain more freely in the corners where the shear sheets were interweaved. A lighter and more versatile pore pressure probe helps to reduce sample disturbance during setup of the sample (Figure 3.10).

In addition, a data acquisition system was introduced to record readings of the pressure transducers during consolidation.

The testing technique was also greatly extended to enable measurement of the undrained anisotropy of normally consolidated clay. A layer of fabric was placed between the shear sheets and the rubber membrane to reduce friction between the surfaces of the rubber membrane on which the applied horizontal stresses are acting. This fabric is removed prior to shearing so that surface tractions from the shear sheets on these faces can then be transmitted to the soil sample. The resulting compression curves for the DSC tests on OCR=1 BBC fall within the limits from oedometer tests on the same material, indicating that this technique works relatively well.

9.2.3 Strain Measurement and Analysis

Due to potential uneven stress applications by the flexible pressure bags and shear sheets, the strains can be non–uniform. Determination of the strain

distribution is therefore extremely important to the evaluation of the quality of the tests, as well as for providing information on the stress–strain behavior of the material tested.

Strains are determined from displacements of reference dots or points on the top of the DSC specimens. Photographic images of these dots are taken at predetermined stress increments during both consolidation and shear tests, and superimposed to determine the displacement field of the sample from digitized images of the dots. The displacement field is then converted into a strain field via strain analysis.

A new strain analysis technique was developed in this research to further improve the representation of the strain field in two different forms: global and local (Section 5.3.3). The analysis uses a multiple linear regression method to estimate the strain from the displacement field. The global analysis presents an average strain for a representative area of the sample, whereas the local analysis enhances the visual information on the strain distributions by means of a strain contour map. The local analysis has proven to be a useful tool in identifying problems in DSC testing such as boundary slippage.

9.3 TESTED MATERIAL

The soil used in this study was resedimented Boston Blue Clay (BBC), which is a lean illitic glacio–marine clay of low–medium sensitivity. It was selected for two principal reasons: first, its availability and relevance to local engineering practice; second, that its behavior is significantly dependent on factors of interest, such as level of sample disturbance and mode of shearing (anisotropy).

The properties of the resedimented BBC used in this research (designated as BBC III) were compared to those from prior series of resedimented BBC. Chapter 4 summarizes the properties of three series of resedimented BBC,

including classification, index properties, consolidation characteristics, and undrained strength data from CK_oU Direct Simple Shear and CK_oU triaxial compression tests.

9.3.1 Preparation of Resedimented Boston Blue Clay

The preparation of the resedimented BBC used in this research and referred to as "batching" was first developed by Germaine (1982) for the study of undrained anisotropy in overconsolidated clay using the DSC. Each batch of clay yields only two DSC samples. The layout of the equipment (Figure A.4) and the procedure has been modified and improved in this research as described in Appendix A. The major specifications of the resedimented Boston Blue clay are: 1) a final OCR of 4 with a preconsolidation pressure of 1 ksc; 2) 100% saturation; and 3) identical properties from different batches. The most significant improvement in the preparation process was in the extrusion method: the soil cake was removed from the mold without any excavation in the new method. As a result, the uniformity of the soil sample has been improved, and less time and effort are required in this process.

9.3.2 Reference Tests

Eight batches of resedimented BBC (designated as BBC III) were prepared in this research. An extensive test program was conducted in conjunction with the batching to quantify the batch–to–batch variability of the resedimented clay. The program included measurement of salt concentration, index properties, and oedometer tests. Special unconsolidated–undrained triaxial tests were conducted to check the degree of saturation of the different batches of BBC.

The index properties indicate consistency between batches of resedimented BBC, in other words, the variability between batches is relatively small (Table

4.1). Typical indices are: LL=45.2%, PI=23.5% and LI=0.82. Hydrometer analyses were performed on resedimented clay cakes at different depths, with results indicating no sign of particle segregation in the clay (Figure 4.5). Therefore a salt concentration of 16 g/l was judged to be sufficient to prevent segregation. The oedometer tests on different batches of the clay (Figure 4.13) yielded very consistent results in terms of compressibilities (CR, SR and RR), with preconsolidation pressures close to the applied values from the large consolidometer tests indicating no sign of hardening due to thixotropic effects (Figure 4.15). These consolidation tests also provided a significant amount of data regarding the consolidation behavior of this clay (Table 4.4), which might be useful in other related research. The unconsolidated–undrained triaxial tests on the batches of clay show that the clay is fully saturated. Therefore, one can conclude that the technique of resedimentation produced very high quality samples with very little sample variability.

9.4 EXPERIMENTAL EVALUATION OF THE DSC DEVICE AND TESTING PROCEDURES

Proof testing has been the primary method used in evaluating the performance of the DSC and the operator's ability to perform DSC tests. DSC tests that are performed at different ψ angles by changing the relative magnitude of the normal and shear stress components on an isotropic material should, in theory, show identical behavior if the device and testing procedures operate as intended. Proof tests were conducted in the isotropic plane on two cross–anisotropic materials in this research: cross–anisotropic rubber foam (Section 6.3.1) and resedimented BBC.

The stress–strain curves of the tests performed on the rubber foam in the isotropic plane (Figure 6.10) were somewhat disappointing; they do not yield identical stress–strain curves primarily due to slightly anisotropic behavior in the

"isotropic" plane. Despite this problem, the overall results obtained from this study, including sample uniformity, are better than the results presented in previous proof tests on BBC.

The results of three good DSC proof tests were performed at ψ=0°, 20° and 40° on OCR=4 resedimented BBC in the isotropic plane show less scatter than the results of the rubber tests in terms of stress–strain relationships. But the stress–strain curves indicate that the ψ=0° sample has a slightly softer response than the other two tests (Figure 6.36). However, the effective stress paths are very consistent in the tests (Figure 6.35). In terms of matching the directions of major principal strain and stress, the deviation between the strain and stress directions is quite small (Figure 6.48). The measured directions of the major principal stress calculated from the orientation of the failure surfaces also agree well with what had been applied, as summarized in Table 6.6.

The results of the new proof tests performed on the OCR=4 resedimented BBC III were compared with the results obtained from previous studies by Germaine (1982) and O'Neill (1985) on BBC II. The comparisons indicate that the new material gives much lower strains at failure than BBC II (Figure 6.61). However, the effective stress paths of the two series of clay are very similar (Figure 6.62). The normalized undrained shear strength of BBC III is 0.164±0.001, which is slightly lower than BBC II with a mean strength of 0.170±0.009 (Table 6.5), BBC III is weaker because of a lower effective stress envelope. The collective results from the proof tests have shown that the technique of performing undrained DSC tests with different combination of normal and shear stresses (that is, different σ_1 directions) works well.

9.5 ANISOTROPIC BEHAVIOR OF BBC IN THE DSC

An extensive testing program was conducted with the objective of studying

the undrained anisotropic behavior of resedimented BBC using the Directional Shear Cell. Undrained DSC shear tests were performed at OCRs of 1 and 4. The main emphasis of this research was to develop new techniques for measuring the undrained anisotropy of BBC K_o consolidated into the normally consolidated range; the DSC tests at OCR of 4 were used only for comparison with previous DSC tests conducted by Germaine (1982) and O'Neill (1985).

9.5.1 Effects of Principal Stress Rotation on Properties of Overconsolidated BBC

A total of five DSC tests were performed on BBC III at an OCR of 4, but two of these tests (at δ=30°) suffered from boundary failures. Of the successful tests, two were carried out at δ=0° and one at δ=90°. The normalized undrained shear strength of the new BBC has a maximum of 0.22 at δ=0° and a minimum value of 0.138 at δ=90°, giving an undrained anisotropic ratio, K_s, as 0.63 (Figure 7.25). The effective stress paths of these tests presented in Figure 7.1, show that the paths are significantly influenced by the δ angle. The δ=0° tests show a much stiffer response and a very low strain at failure of 1.3% (Figure 7.2). The results of the two tests at δ=0° were almost identical, indicating that good reliability. For the δ=90° test, the behavior is much softer, with a strain at failure of about 10%.

Failure planes were observed in all five tests (Figures 7.11 to 7.15). The calculated σ_1 directions from the failure plane orientations agree with the applied σ_1 directions, confirming that the stresses are properly transmitted to the samples, as summarized in Table 7.3. The results show that the pore pressure parameter A_f and the shear induced pore pressure (u_{sf}) increase with increasing δ angle at failure (Figure 7.25).

The undrained shear strength of BBC III is somewhat lower than the shear strength of the BBC II, by 12% at δ=0° and 7% at δ=90° (Table 7.4), mainly due to a slightly lower effective stress envelope and lower p'_f value. A similar

observation was made from the DSC proof tests and the triaxial compression tests at OCR=4. Therefore, we conclude that the new BBC, in general, gives a lower undrained shear strength than BBC II at an overconsolidation ratio of 4.

9.5.2 Effect of Principal Stress Rotation on Properties of Normally Consolidated BBC

Five DSC tests were performed on normally consolidated BBC with fixed incremental (applied) major principal stress directions (δ_{inc}=0°, 45°, 60°, 75° and 90°). The samples were K_o–consolidated to a vertical consolidation stress slightly beyond the preconsolidation pressure (σ'_p) of the material (σ'_{vc}=1.15 and 1.3 ksc). The consolidation stress path was predetermined using the lateral stress oedometer and K_o consolidation triaxial to save both time and effort in the DSC consolidation process.

During the course of this research, it was discovered that the Poisson effect of the rubber membrane (on which the reference points are placed) can affect the strain measurement when there is a large change in σ_2. Corrections were made to adjust the strain data as described in Section 7.4.2.1. The corrected compression curves obtained from the DSC tests show very good agreement with the compression curves from the oedometer tests on the same BBC (Figures 7.36 to 7.38), indicating that the method of K_o consolidation of the DSC samples works well and the corrections were reasonable.

Four of the five tests were conducted with two pore pressure probes; one probe was placed in the middle of the sample and the second probe was inserted midway between one of the corners and the center of the sample. This is done both to check the state of stress of the sample during shearing, and to provide information on the distribution of the pore pressure during consolidation. The readings of the two pressure probes were almost identical during shear, indicating the state of stress of the sample was uniform, at least in the regions where the

probes are located (Figures 7.49 to 7.52).

The intermediate principal stress (σ_2) was measured in all the tests. This proved to be very useful in correcting for the Poisson effect of the rubber membrane, especially during consolidation. The σ_2 measurement was also needed to completely define the state of stress in the DSC tests.

The undrained DSC shear results on normally consolidated clay show significant anisotropy in the material, having a normalized undrained shear strength of 0.332 at δ_{inc}=0° with γ_f of 2% and a normalized value of 0.164 at δ_{inc}=90° with γ_f of 10% (Figure 7.53). The K_s ratio is 0.49 at OCR=1, compared with a value of 0.63 at OCR=4 (Figure 7.93). The effective stress paths are also affected by the change in δ_{inc} angle (Figure 7.48). The effective stress paths for the intermediate δ_{inc} angle tests have very unusual shapes because of the nature of performing tests with constant δ_{inc} angles. The magnitude of normalized shear induced pore pressure, u_s, increases steadily with increasing δ_{inc} angles, from a value of 0.10 at δ_{inc}=0° to a maximum value of 0.36 at δ_{inc}=90° (see Figure 7.57). The results show that the pore pressure parameter A_f does not change very much with δ_{inc} angle (Figure 7.93). For small δ_{inc} angles, the applied shear stress at failure (Δq_f) is small, giving an A_f value of 1.3 at δ_{inc}=0°. For larger δ_{inc} angles, the Δq_f is much larger and the decrease in mean effective stress is also much larger, having an A_f of 1.2 at δ_{inc}=90°. The friction angle at peak shear resistance varies very slightly, from 32° at δ_{inc}=0° to 35° at δ_{inc}=90° (Figure 7.80).

All the samples had multiple failure planes oriented in two distinct directions. These failure planes not only reveal that the samples have reached their ultimate strength, but more importantly imply that the stresses are uniform, since the orientation of the failure planes do not vary much within the soil samples (Table 7.14).

For intermediate δ_{inc} tests, the major principal strain directions coincide

with the δ_{inc} direction initially. But as the strain increases, the major principal strain directions move away from the δ_{inc} directions and towards the δ directions. This behavior indicates that the samples have experienced some plastic deformation at higher strain levels.

This study has demonstrated the significance of the effect of undrained anisotropy of normally consolidated clay. The behavior at this OCR is more pronounced than at OCR=4 (Figure 7.93).

9.6 COMPARISONS AND PREDICTIONS OF DIRECTIONAL SHEAR CELL TEST RESULTS

9.6.1 Comparisons of Normally Consolidated DSC Data from other Shear Devices

Comparisons between the DSC results and those of other shear devices are extremely important since disagreement could indicate problems in the DSC testing. Most of the available data on this material with a known stress state are restricted to triaxial and plane strain tests at δ=0° and δ=90°. The results presented show exceptionally good agreement between the DSC data and the plane strain tests at both δ angles on normally consolidated BBC (Tables 8.3 and 8.4). The DSC data also agree with triaxial compression data at δ=0° in the octahedral stress–strain space. The differences between the DSC data at δ=90° and the triaxial extension test are due to the difference in the magnitude of the intermediate principal stress. But the ratios of undrained shear strength obtained from the triaxial tests to the values from the plane strain DSC tests are identical to those reported by Ladd et al. (1977) at both δ=0° and δ=90°.

Comparisons between the DSC tests and Direct Simple Shear (DSS) tests were made in an attempt to determine the state of stress of the DSS at failure. From the results of the DSC, we concluded that the DSS tests on BBC experience a major principal stress rotation of about 29° for OCR=1 and a δ rotation of 43° for OCR=4 at failure (Tables 8.5 and 8.6). The maximum τ_h values computed

based on the DSC data are about 18% higher for OCR=1 and 12% higher for OCR=4 than the measured maximum τ_h in the DSS tests.

9.6.2 MIT–E3 Predictions

The MIT–E3 constitutive soil model developed at MIT (Whittle, 1987) has been shown to predict reliably the significance effects of inherent anisotropy as measured by the DSC tests on BBC at OCR=4. The predictions of the undrained behavior of normally consolidated BBC were made in 1987 (Whittle, 1987) before the experiments had been conducted.

Chapter 8 describes the comparisons between the model predictions and the measured DSC data on normally consolidated BBC. The predictions of DSC behavior were made by simulating a δ_{inc} undrained shear mode on normally consolidated BBC. The effective stress paths and stress–strain curves predicted by the model have the same trend in behavior as the experimental results (Figures 8.24 and 8.25). Although the predicts strain softening behavior at small δ_{inc} angles, this was measured in the DSC tests because of its stress–controlled technique of conducting tests. The results also indicate that the model is able to predict the rotation of the major principal stress direction and the direction of major principal strain very well (Figures 8.40 and 8.41). Figures 8.32 to 8.39 summarize the large changes in clay behavior with δ and δ_{inc} angles. The overall agreement between the predicted and measured values is considered excellent.

9.6.3 Anisotropic Strength Curve Fitting Techniques

Three methods of curve fitting for anisotropic strength variations were described in Chapter 8 and the DSC data were plotted along with fitted curves. Two methods (Davis–Christian and Bishop) show a very good fit with the DSC data, mainly because these methods require three S_u values from the experimental

data and pivot the curves on these three data points (Figures 8.43 and 8.44). If $S_u(\delta=45^\circ)$ is assumed equal to the maximum τ_h measured in the Direct Simple Shear test, the two methods will underpredict the strength variation of this clay.

9.7 RECOMMENDATIONS AND FUTURE RESEARCH

Recommendations for future research are divided into two categories, one related to modifying the DSC device, the other to suggested experimental programs on clay behavior:

9.7.1 The DSC Device

There are three phases of changes recommended for the DSC device:

Phase 1:

a) Redesign of the Strain Reference Points or Dots. Errors due to the Poisson effect of the rubber membrane can be eliminated by modifying the technique of placing reference dots, for example, by replacing the sand–coated top rubber membrane with a transparent uncoated rubber sheet, then inserting flat head needles (with diameter of 0.25 mm) used as reference points. Also, sprinkle the top of sample with fine black charcoal powder before the needles are placed to improve the contrast of the photographic images.

b) Redesign of the pressure bags. Leaks have occurred in the region between the ring connector and the backing plate during the tests, therefore it is necessary to redesign the connections between the ring connector and the backing plate of the normal pressure bag unit (Figure 4.27). One solution is to relocate the screws that are holding the rings such that the rings can be tightened during the test in case of leakage in that region.

Phase 2:

Reduce the size of the device to handle 3"x3"x3" cubical samples. One of the problems in DSC testing of clay is the difficulty in obtaining DSC samples. At present, it takes about three to four weeks to make two 4"x4"x4" cubical DSC samples. By reducing the sample size to a 3"x3"x3" cube, one can obtain as many as 12 DSC samples per batch of resedimented BBC without any modifications to the preparation apparatus. Other advantages include faster dissipation of pore pressure during consolidation and drained shear, and ease of handling since the sample is smaller and lighter. The accuracy in strain measurement should not be significantly affected because the photographic images of the reference points are governed by the position of the camera relative to the sample and the size of the film. Therefore, by lowering the camera (i.e., closer to the

sample), the size of photographic image can be produced similar to the 4"x4"x4" sample. If the radiography method is used, the x–ray images will have the same size as the prescribed grids (tungsten–Carbide shots). In this case, a smaller sample would result in poorer strain measurement.

Phase 3: Automation of the DSC device:

a) Automation of the strain measurement in the DSC. It is possible to replace the camera with an electronic scanner which can produce an image with 4000x4000 dot resolution. This image can be displayed on a black and white monitor with similar resolution. The information on the screen can be transformed into displacement or strain fields using a computer program. This type of system will eliminate the tedious process currently used in this research, and also provide strain data in less than a minute. The accuracy in strain measurement can be as good as the current method. This system can also extend the DSC capabilities to measure strain softening behavior since the strain data can be updated in a short period.

b) Automation of the stress applications in the DSC. The technology in controlling the stresses already exists (Sheahan, 1990). Combined with the instant strain measurement as described above, it would be possible to obtain stress–strain data during strain softening in a DSC test.

If further research is to continue using the DSC device, the author strongly recommends that the changes described in Phases 1 and 2 be made.

9.7.2 Experimental Programs

The following is a listing of test programs that can be performed using the DSC device to further investigate the anisotropic behavior of the clay:

1) Conduct undrained DSC tests on samples at an OCR of 2 to close the gap between the results obtained at OCR of 1 and 4. A minimum of four tests are recommended at $\delta_{inc}=0^{\circ}$, 45°, 70° and 90°.

2) Perform a test program focusing on the consolidated–drained behavior of BBC at various OCRs (i.e., 4 and 1). This will establish some experimental data needed for generalized behavior, and can help to better define the shape and location of the yield and failure envelopes. The duration of the test depends on the number of stress increments used and the size of test specimen. It will probably be between 4 to 8 days per test.

3) Perform strain induced anisotropy undrained DSC tests, similar to the DSC drained tests conducted by Bekenstein (1980) on Leighton Buzzard sand, to investigate whether the clay will behave in a fashion similar to sand. The samples should be sheared undrained at ψ=0° to about 80 to 90% of the undrained shear strength, then unloaded and reconsolidated and finally sheared undrained at other ψ angles (e.g. 0°, 40°, 70° and 90°). The MIT–E3 soil model can be used to first predict whether there will be noticeable change in the behavior for this type of tests.

4) Perform undrained DSC tests at δ=0° and 90° with different applied b values between 0.2 and 0.8. This is to investigate the influence of b on the undrained shear behavior. Tests can easily be performed at OCRs of 1, 2 and 4. Predictions from the MIT–E3 model can also be very useful here to indicate the magnitude of expected changes in behavior.

Arthur, J. R. F and Dunstan, T. (1988). "The Engineering application of direct and simple shear testing." XIth Géotechnique Symposium in Print, Géotechnique, Vol. 38, No. 4, pp. 651–652.

Arthur, J. R. F. and Menzies, B. K. (1972). "Inherent anisotropy in a sand." Géotechnique, Vol. 22, No. 1, pp. 115–128.

Arthur, J. R. F. and Phillips, A. B. (1975). "Homogeneous and layered sand in triaxial compression." Géotechnique, Vol. 25, No. 4, pp. 799–815.

ASTM (1988). "Standard test method for liquid limit, plastic limit, and plasticity index of soils." Annual book of ASTM Standards, Vol. 4.08, pp. 573–583.

Atkinson, J. H. (1975). "Anisotropic elastic deformations in laboratory tests on undisturbed London clay." Géotechnique, Vol. 25, No. 2, pp. 357–374.

Atkinson, J. H. (1981). Foundations and Slopes: An Introduction to Applications of Critical State Soil Mechanics. McGraw–Hill, 1st ed., London, England, 382 p.

Atkinson, J. H. and Bransby, P. L. (1978). The Mechanics of Soils: An Introduction to Critical State Soil Mechanics. McGraw–Hill, 1st ed., London, England, 375 p.

Atkinson, J. H., Evans J. S. and Ho, E. W. (1985). "Non–uniformity of triaxial samples due to consolidation with radial drainage." Géotechnique, Vol. 35, No. 3, pp. 353–355.

Atkinson, J. H. and Richardson, D. (1986). "The effect of local drainage in rupture zones on the undrained strength of overconsolidated clay." Géotechnique, Vol. 37, No. 3 pp. 393–403.

Bailey, W. A. (1961). "Effects of salt on the shear strength of Boston Blue clay." Thesis presented to the Department of Civil Engineering, Massachusetts Institute of Technology, at Cambridge, MA, in partial fulfillment of the requirements for the degree of Bachelor of Science.

Bekenstein, S. (1980). "Directional shear tests on Leighton Buzzard sand." Thesis presented to the Department of Civil Engineering, Massachusetts Institute of Technology, at Cambridge, MA, in partial fulfillment of the requirements for the degree of Master of Science, 307 p.

Bensari, J. E. (1984). "Stress–strain characteristics from undrained and drained triaxial tests on resedimented Boston blue clay." Thesis presented to the Department of Civil Engineering, Massachusetts Institute of Technology, at Cambridge, MA, in partial fulfillment of the requirements for the degree of Master of Science, 193 p.

Bishop, A. W. (1966). "The strength of soils as engineering materials." Géotechnique, Vol 16, pp. 89–132.

CHAPTER 10

REFERENCES

Notes:

ASCE	:	American Society of Civil Engineers
ASTM	:	American Society of Testing and Materials
FHWA	:	Federal Highway Administration
ICSMFE	:	International Conference on Soil Mechanics and Foundation Engineering
IUTAM	:	International Union for Theoretical and Applied Mechanics
JEMD	:	Journal of Engineering Mechanics Division
JGED	:	Journal of the Geotechnical Engineering Division
JSCE	:	Japanese Society of Civil Engineers
JSMFD	:	Journal of the Soil Mechanics and Foundations Division
MIT	:	Massachusetts Institute of Technology

Ahmed, I. (1990) Personal Communication.

Airey, D. W. and Wood, D. M. (1987). "An evaluation of direct simple shear tests on clay." Géotechnique, Vol. 37, No. 1, pp. 25–35.

Alawaji, H., Alawi, M., Ko, H. Y., Sture, S., Peters, J. F. and Wood, D. M. (1987). "Experimental observations of anisotropy in some stress controlled tests on dry sand." Cambridge University Research Report No. CUED/D–SOILS/TR198, Department of Engineering, Cambridge, England.

Arthur, J. R. F. and Assadi, A. (1977). "Ruptured sand sheared in plane strain." Proceedings of the 9th ICSMFE, Tokyo, Vol. 1, pp. 19–22.

Arthur, J. R. F, Bekenstein, S., Germaine, J. T. and Ladd, C. C. (1981). "Stress path tests with controlled rotation of principal stress directions." ASTM Symposium in Laboratory Shear Strength of Soil, Chicago, Il, STP 740, pp. 516–540.

Arthur, J. R. F., Chua, K. S. and Dunstan, T. (1977). "Induced anisotropy in a sand." Géotechnique, Vol. 27, No. 1, pp. 13–36.

Arthur, J. R. F., Chua, K. S., Dunstan, T. and Rodriguez del C., J. I. (1980). "Principal stress rotation, a missing parameter." JGED, ASCE, Vol. 106, No. GT4, pp. 419–433.

Arthur, J. R. F and Dunstan, T. (1988). "The Engineering application of direct and simple shear testing." XIth Géotechnique Symposium in Print, Géotechnique, Vol. 38, No. 4, pp. 651–652.

Arthur, J. R. F. and Menzies, B. K. (1972). "Inherent anisotropy in a sand." Géotechnique, Vol. 22, No. 1, pp. 115–128.

Arthur, J. R. F. and Phillips, A. B. (1975). "Homogeneous and layered sand in triaxial compression." Géotechnique, Vol. 25, No. 4, pp. 799–815.

ASTM (1988). "Standard test method for liquid limit, plastic limit, and plasticity index of soils." Annual book of ASTM Standards, Vol. 4.08, pp. 573–583.

Atkinson, J. H. (1975). "Anisotropic elastic deformations in laboratory tests on undisturbed London clay." Géotechnique, Vol. 25, No. 2, pp. 357–374.

Atkinson, J. H. (1981). Foundations and Slopes: An Introduction to Applications of Critical State Soil Mechanics. McGraw–Hill, 1st ed., London, England, 382 p.

Atkinson, J. H. and Bransby, P. L. (1978). The Mechanics of Soils: An Introduction to Critical State Soil Mechanics. McGraw–Hill, 1st ed., London, England, 375 p.

Atkinson, J. H., Evans J. S. and Ho, E. W. (1985). "Non–uniformity of triaxial samples due to consolidation with radial drainage." Géotechnique, Vol. 35, No. 3, pp. 353–355.

Atkinson, J. H. and Richardson, D. (1986). "The effect of local drainage in rupture zones on the undrained strength of overconsolidated clay." Géotechnique, Vol. 37, No. 3 pp. 393–403.

Bailey, W. A. (1961). "Effects of salt on the shear strength of Boston Blue clay." Thesis presented to the Department of Civil Engineering, Massachusetts Institute of Technology, at Cambridge, MA, in partial fulfillment of the requirements for the degree of Bachelor of Science.

Bekenstein, S. (1980). "Directional shear tests on Leighton Buzzard sand." Thesis presented to the Department of Civil Engineering, Massachusetts Institute of Technology, at Cambridge, MA, in partial fulfillment of the requirements for the degree of Master of Science, 307 p.

Bensari, J. E. (1984). "Stress–strain characteristics from undrained and drained triaxial tests on resedimented Boston blue clay." Thesis presented to the Department of Civil Engineering, Massachusetts Institute of Technology, at Cambridge, MA, in partial fulfillment of the requirements for the degree of Master of Science, 193 p.

Bishop, A. W. (1966). "The strength of soils as engineering materials." Géotechnique, Vol 16, pp. 89–132.

Bishop, A. W. and Henkel, D. J. (1957). The Measurement of Soil Properties in the Triaxial Test. Edward Arnold, 1st ed., London, 227 p.

Bjerrum, L. (1973). "Problems of soil mechanics and construction on soft clays." State–of–the–Art Report." Proceedings of the 8th ICSMFE, Moscow, Vol. 3, pp. 111–159.

Bjerrum, L. and Landva, A. (1966). "Direct simple shear tests on Norwegian quick clay." Géotechnique, Vol. 16, No. 1, pp. 1–20.

Bovee, R. and Ladd, C. C (1970) "MIT plane strain device." Phase Report No. 12, Research on Earth Physics, Department of Civil Engineering, MIT, Cambridge, MA, 121 p.

Braathen, N–F. (1966). "Investigation of effects of disturbance on undrained shear strength of Boston Blue Clay." Thesis presented to the Department of Civil Engineering, Massachusetts Institute of Technology, at Cambridge, MA, in partial fulfillment of the requirements for the degree of Master of Science.

Broms, B. B. and Ratnam, M. V. (1963). "Shear strength of an anisotropically consolidated clay." JSMFD, ASCE, Vol. 89, No. SM6, pp. 1–26.

Broms, B. B. and Casbarian, A. O. (1965). "Effects of rotation of the principal stress axes and the intermediate principal stress on the shear strength." Proceedings of the 6th ICSMFE, Montreal, Vol. 1, pp. 179–183.

Burland, J. B., Broms, B. B. and De Mello, V. F. B. (1977). "Behavior of foundations and structures: State–of–the–Art Report." Proceedings of the 9th ICSMFE, Tokyo, Vol. 2, pp. 495–546.

Casagrande, A. (1936). "The determination of the preconsolidation load and its practical significance." Proceedings of the 1st ICSMFE, Vol. 3, pp. 60–64.

Casagrande, A. and Carillo, N. (1944). "Shear failure of anisotropic materials." Proceedings of Boston Society of Civil Engineers, Vol. 31, pp. 74–87.

Cleveland, W. S. (1979). "Robust locally weighted regression and smoothing scatterplots." Journal of the American Statistical Association, Vol. 79, No. 368, pp.829–836.

DeGroot, D. J. (1989). "The multidirectional direct simple shear apparatus with application to design of offshore arctic structures." Thesis presented to the Department of Civil Engineering, Massachusetts Institute of Technology, at Cambridge, MA, in partial fulfillment of the requirements for the degree of Doctor of Science, 699 p.

Desai, C. S. and Siriwardene, H. J. (1984). Constitutive Laws for Engineering Materials. Prentice Hall, 1st ed., New Jersey.

Dickey, J. W. (1967). "A plane strain shear device for testing clays." Thesis presented to the Department of Civil Engineering, Massachusetts Institute of Technology, at Cambridge, MA, in partial fulfillment of the requirements for the degree of Master of Science.

Draper, N. and Smith, H. (1981). Applied Regression Analysis. John Wiley & Sons, New York.

Dyvik, R., Lacasse, S. and Martin, R. T. (1985). "Coefficient of lateral stress from oedometer cell." Proceedings of the 11th ICSMFE, San Francisco, CA, Vol. 2, pp. 1003–1006.

Fayad, P. H. (1986). "Aspects of the volumetric and undrained behavior of Boston blue clay." Thesis presented to the Department of Civil Engineering, Massachusetts Institute of Technology, at Cambridge, MA, in partial fulfillment of the requirements for the degree of Master of Science, 273 p.

Germaine, J. T. (1982). "Development of the directional shear cell for measuring Cross anisotropic Clay Properties." Thesis presented to the Department of Civil Engineering, Massachusetts Institute of Technology, at Cambridge, MA, in partial fulfillment of the requirements for the degree of Doctor of Science, 530 p.

Gibson, R. E. (1974). "The analytical method in soil mechanics: 14th Rankine Lecture." Géotechnique, Vol. 24, No. 2, pp. 115–140.

Gibson, R. E. and Henkel, D. J. (1954). "Influence of duration of tests at constant rate of strain on measured 'drained' strength", Géotechnique, Vol. 4, pp. 6–15.

Henkel, D. J. (1956). "The effect of overconsolidation on the behavior of clays, during Shear." Géotechnique, Vol. 6, pp. 138–150.

Henkel, D. J. (1960). "The relationships between the effective stresses and water content in saturated remoulded clays." Géotechnique, Vol. 10, No. 1, pp. 41–54.

Hicher, P–Y. and Lade, P. V. (1987). "Rotation of principal directions in K_o–consolidated clay." JGED, ASCE, Vol. 113, No. 7, pp. 774–788.

Hight, D. W., Gens, A. and Symes, M. J. (1983). " The development of a new hollow cylinder apparatus for investigating the effects of principal stress rotation in soils." Géotechnique, Vol. 33, No. 4, pp. 355–383.

Hight, D. W., Shibuya, S. and Symes, M. J. (1988). "The engineering application of direct and simple shear testing: Discussion." XIth Géotechnique Symposium in Print, Géotechnique, Vol. 38, No. 1, pp. 139–154.

Hvorslev, M. J (1960). "Physical components of the shear strength of saturated clays." Research Conference on Shear Strength of Cohesive Soils, ASCE, Boulder, pp. 168–273.

Jamiolkowski, M., Ladd, C. C., Germaine, J. T. and Lancellotta, R. (1985). "New developments in field and laboratory testing of soil: Theme Lecture 2." Proceedings of the 11th ICSMFE, San Francisco, CA, Vol. 1, pp. 57–153.

Janbu, N. (1985). "Soil models in offshore engineering: 25th Rankine Lecture." Géotechnique, Vol. 35, No. 3, pp. 241–281.

Jackson, W. T. (1963). "Stress paths and strains in a saturated clay." Thesis presented to the Department of Civil Engineering, Massachusetts Institute of Technology, at Cambridge, MA, in partial fulfillment of the requirements for the degree of Master of Science, 101 p.

Jordan, W. S. (1979). "Determination of negative pore pressure for embankment design." Thesis presented to the Department of Civil Engineering, Massachusetts Institute of Technology, at Cambridge, MA, in partial fulfillment of the requirements for the degree of Master of Science, 144 p.

Kavvadas, M. (1981). "Non–linear consolidation around driven piles clays." Thesis presented to the Department of Civil Engineering, Massachusetts Institute of Technology, at Cambridge, MA, in partial fulfillment of the requirements for the degree of Doctor of Science, 666 p.

Kinner, E. B. (1970). "Load–deformation behavior of saturated clay during undrained shear." Thesis presented to the Department of Civil Engineering, Massachusetts Institute of Technology, at Cambridge, MA, in partial fulfillment of the requirements for the degree of Doctor of Science.

Kinner, E. B. and Ladd, C. C. (1970). "Load deformation behavior of saturated clays during undrained shear." Research Report R70–27, No. 259, Department of Civil Engineering, MIT, Cambridge, MA, 302 p.

Ko. H. Y. and Scott, R. F. (1967). "A new soil testing apparatus." Géotechnique, Vol. 17, No. 1, pp. 40–57.

Ladd, C. C. (1964). "Stress–strain behavior of saturated clay and basic strength principles." Research Report R64–17, Research on Earth Physics, Department of Civil Engineering, MIT, Cambridge, MA, 112 p.

Ladd, C. C. (1965). "Stress–strain behavior of anisotropically consolidated clays during undrained shear." Proceedings of the 6th ICSMFE, Montreal, Vol. 1, pp. 282–286.

Ladd, C. C. (1973). "Estimating settlements of structures supported on cohesive soils." Metropolitan Section, ASCE, Foundations and Soil Mechanics, 99 p.

Ladd, C. C. (1988). "Stability evaluation during Staged Construction." 22nd Terzaghi Lecture, ASCE, draft version.

Ladd, C. C., Bovee, R. B., Edgers, L., and Rixner, J. J. (1971). "Consolidated–undrained plane strain shear tests on Boston blue clay." Research Report R71–13, No. 273, Department of Civil Engineering, MIT, Cambridge, MA, 243 p.

Ladd, C. C. and Edgers, L. (1972). "Consolidated–undrained direct simple shear tests on saturated clays." Research Report R72–82, No. 284, Department of Civil Engineering, MIT, Cambridge, MA, 354 p.

Ladd, C. C. and Foott, R. (1974). "New design procedure for stability of soft clays." JGED, ASCE, Vol. 100, No. GT7, pp. 763–786.

Ladd, C. C. and Foott, R. (1977a). "Foundation design of embankments constructed on varved clays." FHWA Report TS–77–214, U. S. Department of Transportation, 234 p.

Ladd, C. C. and Foott, R. (1977b). "The Behavior of embankments on clay foundations: Discussion." Canadian Geotechnical Journal, Vol. 17, No. 3, pp. 454–460.

Ladd, C. C., Foott, R., Ishihara, K., Schlosser, F. and Poulos, H. G. (1977). "Stress–deformation and strength characteristics: State–of–the–Art Report." Proceedings of the 9th ICSMFE, Tokyo, Vol. 2, pp. 421–494.

Ladd, C. C. and Germaine, J. T. (1985). "Initial and evolving stress–strain anisotropy of sedimented clay." National Science Foundation Proposal.

Ladd, C. C. and Luscher, U. (1965). "Engineering properties of the soils underlying the M.I.T. campus." Research Report R65–58, No. 185, Department of Civil Engineering, MIT, Cambridge, MA, 107 p.

Ladd, C. C. and Lambe, T. W. (1963). "The strength of undisturbed clay determined from undrained tests." NRC–ASTM Symposium on Laboratory Shear Testing of Soils, STP No. 361.

Ladd, C. C and Varallyay, J. (1965). "The influence of stress system on the behavior of saturated clays during undrained shear." Research Report R65–11, No. 177, Department of Civil Engineering, MIT, Cambridge, MA, 263 p.

Lade, P. V. (1975). "The stress–strain and strength characteristics of cohensionless soils." Ph.D. Thesis, University of California, Berkeley, 765 p.

Lade, P. V. (1978). "Cubical triaxial apparatus for soil testing." Geotechnical Testing Journal, ASTM, Vol. 1, No. 2, pp. 93–101.

Lade, P. V. and Musante, H. M. (1977). "Failure conditions in sand and remolded clay." Proceedings of the 9th ICSMFE, Tokyo, Vol. 1, pp. 181–186.

Lade, P. V. and Musante, H. M. (1978). "Three–dimensional behavior of remolded clay." JGED, ASCE, Vol. 104, No. GT2, pp. 193–209.

Malek, A. M. (1987). "Cyclic behavior of clay in undrained direct simple shear and application to offshore tension piles." Thesis presented to the Department of Civil Engineering, Massachusetts Institute of Technology, at Cambridge, MA, in partial fulfillment of the requirements for the degree of Doctor of Science, 381 p.

Marachi, N. D., Duncan, J. M., Chan, C. K. and Seed, H. B. (1981). "Plane strain testing of sand." Laboratory Shear Strength of Soil, ASTM, STP 740, R. N. Yong and F. C. Townsend, eds., pp. 294–302.

Martin, R. T. (1965). "Quantitative fabric of consolidated kaolinite." Research Report R65–47, No. 179, Department of Civil Engineering, MIT, Cambridge, MA, 79 p.

Martin, R. T. (1970). "Suggested method of test for determination for soluble salts in soil." Special Technical Publication 479, ASTM, pp. 288–290.

Martin, R. T. and Ladd, C. C. (1975). "Fabric of consolidated kaolinite." Clays and Clay Minerals, Vol. 23.

Matsuoka, H. (1974). "Stress strain relationships of sand based on the spatial mobilized plane." Soils and Foundations, Vol. 16, No. 2, pp. 47–61.

Matsuoka, H., Koyama, H. and Yamazaki, H. (1985). "A constitutive equation for sands and its application to analyses of rotational stress paths and liquefaction resistance." Soils and Foundations, Vol. 25, No. 1, pp. 27–42.

Matsuoka, H. and Nakai, T. (1974). "Stress deformation and strength characteristics under three different principal stresses." Proceedings of the JSCE, Vol. 232, pp. 59–70.

Matsuoka, H. and Nakai, T. (1982). "A new failure criterion for soils in three dimensional stresses. " Proceedings of IUTAM Conference on Deformation and Failure of Granular Materials, Delft, pp. 253–263.

Matsuoka, H. and Sakakibara, K. (1987). "A constitutive for sands and clays evaluating principal stress rotation." Soils and Foundations, Vol. 27, No. 4, pp. 73–88.

Menzies, B. K. (1970). "Stress–strain anisotropy in sands." Ph.D. Thesis, University of London, England.

Menzies, B. K. and Phillips, A. B. (1972). "On the making of rubber membranes." Géotechnique, Technical Note, Vol. 1, pp. 153–155.

Mesri, G. and Choi, Y. K. (1985). "The uniqueness of the end–of–primary (EOP) void ratio – effective stress relationships." Proceedings of the 11th ICSMFE, San Francisco, CA, pp. 587–590.

Mesri, G. and Olson, R.E. (1971). "Mechanisms controlling the permeability of clays." Clays and Clay Minerals, Vol. 19, pp. 151–158.

Mitchell, J. K. (1956). "Importance of structure to the engineering behavior of clay." Thesis presented to the Department of Civil Engineering, Massachusetts Institute of Technology, at Cambridge, MA, in partial fulfillment of the requirements for the degree of Doctor of Science, (unpublished).

Mitchell, J. K. (1976). Fundamentals of Soil Behavior. John Wiley and Sons, New York, 422 p.

Mitchell, R. J. (1972). "Some deviations from isotropy in a lightly overconsolidated clay." Géotechnique, Vol. 22, No. 3, pp. 459–467.

Mitchell, R. J. (1972). "An apparatus for plane strain and true triaxial testing of undisturbed soil samples." Canadian Geotechnical Journal, Vol. 10, No. 3, pp. 520–527.

Miura, K., Miura, S. and Toki, S. (1986). "Deformation behavior of anisotropic dense sand under principal stress axes rotation." Soils and Foundations, Vol. 26, No. 1, pp. 36–52.

Miura, K., Toki, S. and Miura, S. (1986). "Deformation prediction for anisotropic sand during the rotation of principal stress axes." Soils and Foundations, Vol. 26, No. 3, pp. 42–56.

Montgomery, D. C. and Peck, E. A. (1982). Introduction to Linear Regression Analysis. John Wiley & Sons, New York.

Moran, Proctor, Mueser and Rutledge, Consulting Engineers (1958). "Study of deep soil stabilization by vertical sand drains." Report prepared for U.S. Navy and available through U.S. Department of Commerce (Clearance house Code 410.14,Springfield, VA 22151).

Morgenstern, N. R. and Tchalenko, J. S. (1967a). "The optical determination of preferred orientation in clays and its application to the study of microstructure in consolidated kaolin. I." Proceedings of Royal Society, A300, pp. 218–234.

Morgenstern, N. R. and Tchalenko, J. S. (1967b). "The optical determination of preferred orientation in clays and its application to the study of microstructure in consolidated kaolin. II", Proceedings of Royal Society, A300, pp. 235–250.

Morgenstern, N. R. and Tchalenko, J. S. (1967c). "Microstructural observation of shear zones from slips in natural clays." Proceedings of Geotechnical Conference, Oslo, pp. 147–152.

Morgenstern, N. R. and Tchalenko, J. S. (1967d). "Microscopic structures in kaolin subjected to direct shear." Géotechnique, Vol. 17, pp. 309–328.

Nishida, Y. (1956). "A brief note on compression index of soil." JSMFD, ASCE, Vol. 82, No. SM3, Paper 1027.

Norman, L. E. J. (1958) "A comparison of values of liquid limit determined with apparatus having bases of different hardness." Géotechnique, Vol. 8, pp. 79–83.

Oda, M. and Koishikawa, I. (1977). "Anisotropic fabric of sands." Proceedings of the 9th ICSMFE, Tokyo, Vol. 1, pp.235–238.

Oda, M. and Konishi, J. (1974). "Rotation of Principal Stresses in Granular Materials during Simple Shear." Soils and Foundations, Vol. 14, pp. 39–53.

O'Neill, D. A. (1985). "Undrained strength anisotropy of an overconsolidated thixotropic clay." Thesis presented to the Department of Civil Engineering, Massachusetts Institute of Technology, at Cambridge, MA, in partial fulfillment of the requirements for the degree of Master of Science, 307 p. (incomplete).

Parry, R. H. G. (1960). "Triaxial compression and extension tests on remoulded clay." Géotechnique,, Vol. 10, pp. 166–180.

Phillips, A. B. (1972). "Strength and deformation of layered sand." Ph.D. Thesis, University of London, London, England, 339 p.

Preston, W. B. (1965). "The effects of sample disturbance on the undrained strength behavior of Boston Blue clay." Thesis presented to the Department of Civil Engineering, Massachusetts Institute of Technology, at Cambridge, MA, in partial fulfillment of the requirements for the degree of Master of Science, 193 p.

Prévost, J. H. (1978a). "Anisotropic undrained stress–strain behavior of clays." JGED, ASCE, Vol. 104, No. GT8, pp. 1075–1090.

Prévost, J. H. (1978b). "Plasticity theory for soil stress–strain behavior." JEMD, ASCE, Vol. 104, No. EM5, pp. 1177–1194.

Prévost, J. H. (1979). "Undrained shear tests on clays." JGED, ASCE, Vol. 105, No. GT1, pp. 49–64.

Prévost, J. H. and Hoeg, K. (1977). "Plasticity model for undrained stress–strain behavior." Proceedings of the 9th ICSMFE, Tokyo, Vol. 1, pp. 255–261.

Richardson, A. M. (1963). "The relationship of the effective stress–strain behavior of a saturated clay to the rate of strain." Thesis presented to the Department of Civil Engineering, Massachusetts Institute of Technology, at Cambridge, MA, in partial fulfillment of the requirements for the degree of Doctor of Science, 200 p.

Rodriguez del C., J. I. (1977). "Induced anisotropy in a loose sand." Ph.D. Thesis, University of London, London, England, 327 p.

Roscoe, K. H. (1953). "An apparatus for the application of simple shear to soil samples." Proceedings of the 3rd ICSMFE, Zurich, Vol. 1, pp. 186–191.

Roscoe, K. H. (1970). "The influence of strain in a loose sand." Géotechnique, Vol. 20, No. 2, pp. 129–170.

Roscoe, K. H., Arthur, J. R. F. and James, R. G. (1963). "The determination of strains in soils by an X–ray method." Civil Engineering and Public Works Review, July 1963, pp. 873–876; August 1963, pp. 1009–1012.

Roscoe, K. H., Bassett, R. H. and Cole, E. R. L. (1967). "Principal axes observed during simple shear of a sand." Proceedings of Geotechnical Conference, Vol. 1, Olso, pp. 231–237.

Roscoe, K. H. and Burland, J. B. (1968). "On the generalized stress–strain behavior of 'wet' clay." Engineering Plasticity, Cambridge University Press, Cambridge, England, pp. 535–609.

Roscoe, K. H., Schofield, A. N. and Wroth, C. P. (1958). "On the yielding of soils." Géotechnique, Vol. 8, pp. 22–53.

Roscoe, K. H., Schofield, A. N. and Thararajah, A. (1963). "Yielding of clays in states wetter than critical." Géotechnique, Vol. 13, No. 3, pp. 211–240.

Saada, A. S. (1970). "Testing of anisotropic clay soils." JSMFD, ASCE, Vol. 96, No. SM5, pp. 1847–1852.

Saada, A. S. (1977). "Closure to strength of one dimensionally consolidated clays." JGED, ASCE, Vol. 103, No. GT6, pp. 655–660.

Saada, A. S. and Bianchini, G. F. (1975). "Strength of one dimensionally consolidated clays." JGED, ASCE, Vol. 101, No. GT11, pp. 1151–1164.

Saada, A. S. and Ou, C. D. (1973). "Strain–stress relations and failure of anisotropic clays." JSMFD, ASCE, Vol. 99, No. SM12, pp. 1091–1111.

Saada, A. S. and Puccini, P. M. (1986). "Deformation behavior of anisotropic dense Sand under principal stress axes rotation: Discussions." Soils and Foundations, Vol. 26, No. 4, pp. 159–166.

Saada, A. S. and Townsend, F. C. (1981). "State of the art: Laboratory strength testing of soils." Laboratory Shear Strength of Soil, ASTM, STP 740, R. N. Yong and F. C. Townsend, eds., pp. 7–77.

Saada, A. S. and Zamani, K. K. (1969). "The mechanical behavior of cross anisotropic clays." Proceedings of the 7th ICSMFE, Mexico, Vol. 1, pp. 351–359.

Sambhandharaksa, S. (1977). "Stress–strain–strength anisotropy of varved clays." Thesis presented to the Department of Civil Engineering, Massachusetts Institute of Technology, at Cambridge, MA, in partial fulfillment of the requirements for the degree of Doctor of Science, 506 p.

Schofield, A.N. and Wroth, P.C. (1968). Critical State Soil Mechanics. McGraw–Hill Book Company, London, England, 310 p.

Sheahan, T. C. (1988). "Modification and implementation of a computer controlled triaxial apparatus." Thesis presented to the Department of Civil Engineering, Massachusetts Institute of Technology, at Cambridge, MA, in partial fulfillment of the requirements for the degree of Master of Science, 266 p.

Sheahan, T. C. (1990). Personal Communication.

Shibata, T. and Karube, D. (1965). "Influence of the variation of the intermediate principal stress on the mechanical properties of normally consolidated clays." Proceedings of the 6th ICSMFE, Montreal, Vol. 1, pp. 359–363.

Skempton, A. W. (1944). "Notes on the compressibility of clays." Quarterly Journal of Geological Society, Vol. 100, London, pp. 119.

Skempton, A. W. (1948). "A study of the immediate triaxial test on cohesive soils." Proceedings of the 2nd ICSMFE, Rotterdam, Vol. 1, pp. 192–196.

Skempton, A. W. (1954). "The pore–pressure coefficients A and B." Géotechnique, Vol. 4, No. 4, pp. 143–152.

Skempton, A.W. and Northey, R.D. (1953). "The sensitivity of clays." Géotechnique, Vol. 3, pp.30–53.

Sture. S. and Desai, C. S. (1979). "Fluid cushion truly triaxial or multiaxial testing device." Geotechnical Testing Journal, ASTM, Vol. 2, No. 1, pp. 20–33.

Sture, S., Ko, H. Y., Budiman, J. S. and Ontuna, A. K. (1985). "Development and application of a directional shear cell." Proceedings of the 11th ICSMFE, Vol. 2, San Francisco, CA, pp. 1061–1064.

Sture, S., Budiman, J. S., Ontuna, A. K. and Ko, H. Y. (1987). "Directional shear cell experiments on a dry cohesionless soil." Geotechnical Testing Journal, Vol. 10, No. 2, pp. 71–79.

Symes, M. J. P. R., Gens, A. and Hight, D. W. (1984). "Undrained anisotropy and principal stress rotation in saturated sand." Géotechnique, Vol. 34, No. 1, pp. 11–27.

Symes, M. J., Gens, A. and Hight, D. W. (1988). "Drained principal rotation in saturated sand." Géotechnique, Vol. 38, No. 1, pp. 59–81.

Tavenas, F. and Leroueil, S. (1977). "Effects of stresses and time on yielding of clays." Proceedings of the 9th ICSMFE, Tokyo, Vol. pp. 319–326.

Tavenas, F., Jean, P. Leblond, P. and Leroueil, S. (1983). "The permeability of natural soft clays. Part II: Permeability characteristics." Canadian Geotechnical Journal, No. 20, pp. 645–659.

Tavenas, F., Leblond, P., Jean, P. and Leroueil, S. (1983). "The permeability of natural soft clays. Part I: Permeability characteristics." Canadian Geotechnical Journal, No. 20, pp. 629–644.

Taylor, D. W. and Merchant, W. (1940). "A theory of clay consolidation accounting for secondary compressions." Journal of Math. Phys., Vol.19.

Taylor, D. W. (1948). Fundamentals of Soil Mechanics. John Wiley & Sons, New York, 700 p.

Terzaghi, K. and Peck, R. B. (1967). Soil Mechanics in Engineering Practice. John Wiley & Sons, New York, 729 p.

Vaid, Y. P. and Campanella, R. G. (1974). "Triaxial and plane strain behavior of natural clay", JGED, ASCE, Vol. 100, No. GT3, pp. 207–224.

Varallyay, J. (1964). "The effects of stress system variables on the undrained strength of Boston Blue clay." Thesis presented to the Department of Civil Engineering, Massachusetts Institute of Technology, at Cambridge, MA, in partial fulfillment of the requirements for the degree of Master of Science.

Vardoulakis, I. and Graf, B. (1985). "Calibration of constitutive models for granular materials using data from biaxial experiments." Géotechnique, Vol. 35, No. 3, pp. 299–317.

Walbaum, M. (1988) "Procedure for investigation of Sample disturbance using the Direct Simple Shear Apparatus." Thesis presented to the Department of Civil Engineering, Massachusetts Institute of Technology, at Cambridge, MA, in partial fulfillment of the requirements for the degree of Master of Science, 367 p.

Whittle, A. J. (1987). "A constitutive model for overconsolidated clays with application to the cyclic loading of friction piles." Thesis presented to the Department of Civil Engineering, Massachusetts Institute of Technology, at Cambridge, MA, in partial fulfillment of the requirements for the degree of Doctor of Science, 641 p.

Wissa, A. E. Z. (1961). "A study of the effects of environmental changes on the stress–strain properties of kaolinite." Thesis presented to the Department of Civil Engineering, Massachusetts Institute of Technology, at Cambridge, MA, in partial fulfillment of the requirements for the degree of Master of Science.

Wissa, A. E. Z., Christian, J. T., Davis, E. H. and Heiberg, S. (1971). "Analysis of consolidation at constant strain rate." JSMFD, ASCE, Vol. 97,No. SM10, pp. 1393–1413.

Wissa, A. E. Z. and Heiberg, S. A. (1969). "New one-dimensional consolidation test." Research Report 69–9, No. 229, MIT, Cambridge, MA, 161 p.

Wissa, A. E. Z., Martin, R. T. and Garlanger, J. E. (1975). "The piezometer probe." Proceedings of the ASCE Special Conference on In–Situ Measurement of Soil Properties, Raleigh, Vol. 1, pp. 536–545.

Wong, R. K. S. (1985). "Sand subjected to cyclic principal stress rotations." Ph.D. Thesis, University of London, London, England, 306 p.

Wong, R. K. S. and Arthur, J. R. F. (1985). "Induced and inherent anisotropy in sand." Géotechnique, Vol. 35, No. 4, pp. 471–481.

Wong, R. K. S. and Arthur, J. R. F. (1985). "Sand sheared by stresses with cyclic variations in direction." Géotechnique, Vol. 36, No. 2, pp. 215–226.

Wood, D. M. and Wroth, C. P. (1977). "Some laboratory experiments related to the results of pressuremeter tests." Géotechnique, Vol. 27, No. 2, pp. 181–201.

Wood, D. M. (1981). "True triaxial tests on Boston blue clay." Proceedings of the 10th ICSMFE, Stockholm, pp. 825–830.

Wroth, C. P. and Bassett, R. H. (1965). "A stress–strain relationship for shearing behaviour of a sand." Géotechnique, Vol. 15, No. 1, pp. 32–56.

Wroth, C. P. (1984). "The interpretation of in–situ soil tests: 24th Rankine Lecture." Géotechnique, Vol. 35, No. 4, pp. 449–489.

Wroth, C. P. (1987). "The behaviour of normally consolidated clay as observed in undrained direct shear tests." Géotechnique, Vol 37, No. 1, pp. 37–43.

Wu, T. H., Loh, A. K. and Malvern, L. E. (1963). "Study of failure envelopes of soils." JSMFD, ASCE, Vol. 89, No. SM1, pp. 145–181.

Wu, T. H., Loh, A. K. and Malvern, L. E. (1964). "Closure to study of failure envelopes of soils." JSMFD, ASCE, Vol. 90, No. SM2. pp. 165–166.

Yong, R. N. and McKyes, E. (1971). "Yield and failure of a clay under triaxial stresses." JSMFD, ASCE, Vol. 97, No. SM1, pp. 159–171.

APPENDIX A

SAMPLE PREPARATION AND BATCHING PROCEDURES

A.1 INTRODUCTION

Boston Blue Clay has been the primary soil used by MIT to develop an understanding of the behavior of clay. It has been shown that the properties of resedimented Boston Blue Clay are quite similar to the natural, undisturbed Boston Blue Clay. The process of resedimentation not only reduces the cost of laboratory testing, but improves the uniformity and consistency of the tests because it reduces variability of sample properties found in the natural clay.

The technique of resedimentation has been improved and modified over the years. Wissa (1961) first introduced the extrusion technique to obtain smaller test samples from a large consolidometer sample. Germaine (1982) developed a method to produce fully saturated resedimented Boston Blue Clay which is essential for undrained tests in the Directional Shear Cell.

The Appendix describes the layout of the batching equipment and the procedures for this resedimentation process. The technique is similar to Germaine's (1982), but the layout of the equipment and the procedures have been improved and simplified.

A.1.1 Resedimented Boston Blue Clay Specifications

The Boston Blue Clay used in this research was originally from Kendall Square in Cambridge, Massachusetts. It was oven–dried and crushed to form a powder in which 97% passed the No.100 sieve. The index properties of this material are described in Appendix B.

The specifications of the resedimented Boston Blue Clay for laboratory testing are:

a. a salt concentration of 16 gram/liter, *to control segregation of the soil particles;*
b. 100 % saturation, *which is essential for undrained tests in the Directional shear cell;*
c. K_o–consolidated to 1 ksc and rebound to 0.25 ksc at an overconsolidation ratio of 4 before extrusion and trimming, *at this ratio, the stress state of the soil is close to hydrostatic* ($\sigma'_v \simeq \sigma'_h$); and
d. a final water content of about 40 %, *to give a guideline to the consistency of the sample properties.*

A.1.2 Ingredients for Preparing the Resedimented Clay

The amounts of the ingredients required to make a batch of resedimented Boston Blue Clay are as follows:

a. 15 kg of oven–dried Boston Blue Clay powder (97% passed No.100 sieve);
b. 15 kg of distilled–deaired water;
c. a small quantity of salt, *required to make the 16 gram/liter salt concentration*; and
d. 2 ml of Phenol, *used to kill the bacteria in the soil which may otherwise alter the properties of the soil.*

Sometimes additional water may be added because the vacuum pump can draw significant amounts of water during batching.

A.2 EQUIPMENT DESCRIPTION

The resedimentation process can be divided into four stages: sedimentation, consolidation, extrusion and trimming. The following section describes the equipment used in each stage.

A.2.1 Mixing and Sedimentation Equipment

The basic concept of batching is to mix the dry soil, the distilled–deaired water and a known quantity of salt in the mixing chamber under a vacuum, the clay slurry is then allowed to cure in a sedimentation chamber where it will later be consolidated.

The mixing chamber consists of a Plexiglas cylinder with two aluminum platens attached to both ends of the cylinder by tie rods (Figure A.1). Several propellers and a soil breaker form the main mixing components. A variable speed motor is connected to the mixing shaft by two 45° gears. O–rings are used to seal all the joints and connections to prevent any leakage.

The dry soil is allowed to enter the chamber through a copper tube on the top aluminum platen. The other two connectors on the top platens are used for the entries of distilled–deaired water and the evacuation of the chamber. The clay slurry is dispatched to the sedimentation chamber through a connector mounted on the bottom platen.

The sedimentation chamber consists of a plastic free fall cylinder, a Plexiglas top platen, and a consolidometer (Figure A.2). O–rings are used to seal any leaks in the joints. There are two outlets in the chamber, one is located at the top platen and the other at the bottom, which serves as a drainage valve through the bottom porous base; both are connected to a vacuum pump. One inlet located at the top platen allows the clay slurry to enter this chamber from the mixing

chamber.

A.2.2 Batch Consolidometer

The consolidometer is formed by a 30cm diameter steel chamber and a porous base with a drainage valve. A piston with a porous disk is placed on top of the clay slurry during consolidation.

A.2.3 Extrusion Equipment

Once the sample is consolidated, it has to be removed from the consolidometer. The excavation technique used by Germaine (1982) is time consuming and involves a lot of manpower. A special excavation tool was designed to speed up the process (Figure A.3). This tool uses the liquefaction concept to excavate the soil. Water is injected into the soil through Tube No.1. A rotating wire at the tip helps to mix the soil and water together to form a slurry, which is then sucked up by a vacuum and trapped in a flask. This method reduces the excavation time from 6 to 3 hours.

A.2.4 Trimming Equipment

Since the clay sample produced is quite large, a special trimming device was designed to minimize sample disturbance and reduce the time spent in the trimming process.

The trimming equipment consists of a base plate with dimensions 46cm x 46cm x 1.3cm (Figure A.7). Four stainless steel posts were fixed at each corner, and four horizontally adjustable posts were attached to the sides of the plates. A Plexiglas disk is usually placed in the middle of the plate to raise the level of the soil cake for easy cutting.

A.3 SETUP PROCEDURE

This section describes the assembly of the mixing and sedimentation chambers.

A.3.1 Assembly of Mixing Chamber

a. Clean all parts.
b. Apply some high vacuum grease to the gloves and the O–rings.
c. Place the O–rings in the gloves of the bottom and top platens.
d. Put the Plexiglas cylinder on top of the O–ring of the bottom platen.
e. Install the mixing shaft in the cylinder.
f. Place the top platen to the other end of the cylinder.
g. Put 8 tie rods between the two platens.
h. Tighten the nuts on the tie rods until the cylinder is secured in place.
i. Attach a rubber hose to the copper tube on the top platen.
j. Place a 12 inch vibrating wire between the hose and the tube.
k. Connect a pipe to the other end of the hose.
l. Install a rubber stopper to the pipe for the soil flask.
m. Connect a 3–way valve to one of the outlet at the top platen.
n. Connect the other outlet to the vacuum pump.
o. Attach a tube to the outlet of the bottom platen.
p. The rest of the setup is shown in Figure A.4.

A.3.2 Assembly of Sedimentation Chamber

a. Clean all parts.
b. Apply some grease to all the O–rings.
c. Apply about 1mm thickness of vacuum grease to the inside wall of the steel chamber.
d. Place a filter paper on the top of the porous disk of the base.
e. Put a square steel plate below the base.
f. Place the O–rings between the porous base, the steel chamber,the free fall chamber and the top platen.
g. Place four tie rods between the porous base and the top platen.
h. Tighten the four nuts on the rods until the chamber is secured in place.
i. Connect one of the outlets of the top platen to the vacuum pump and the other to the tube which leads to mixing chamber.
j. Connect the drainage line of the porous base to the vacuum pump.
k. The rest of the setup is shown in Figure A.4.

A.4 BATCHING PROCEDURE

The following section describes the step by step procedure for the production of resedimented clay.

A.4.1 Evacuation of the Mixing Chamber

a. *Venting: (Setup mode)*
- Valve 1: Position A.
- Valve 2: Position C.
- Valve 3: Position B.

- Start Vacuum Pump No.1.

b. *Evacuating Flask No.1:*
- Valve 3: Position A.

Monitor the vacuum using Vacuum Tube No.1 for 30 seconds.

c. *Evacuating the mixing chamber:*
- Valve 4: Position A.
- Valve 5: Position A.
- Valve 2: Position A.
- Valve 1: Position B.
- Pinch Clamp in Close position.

Monitor the vacuum using Vacuum Tube No. 1 for 2 hours (< 800 mTorr).

If the reading is above 800 mTorr, then check all the connections.

A.4.2 Evacuation of the Sedimentation Chamber

a. *Venting:*
- Valve 10: Position C.
- Valve 11: Position B.
- Valve 13: Position B.

- Start Vacuum Pump No.2.

b. *Evacuating the Sedimentation Chamber:*
- Valve 11: Position A.
- Valve 10: Position B.

Monitor the vacuum using Bourdon Gauge No.2 for 20 min (<–29 feet of water).

- Turn Valve 10 to position C. Monitor the vacuum using Vacuum Tube No.2 for 2 hours (<400 mTorr).

If the reading is above 400 mTorr, then check all the connections.

A.4.3 Injection of Distilled/Deaired Water

a. *Venting:*
- Valve 7: Position A.

- Valve 9: Position B.
- Start Vacuum Pump No.3.

b. *Evacuating Flask No.2:*
- Valve 4: Position A.
- Valve 6: Position B.
- Valve 7: Position C.

Monitor the vacuum using Bourdon Gauge No.3 for 2 minutes (<–28 feet of water).

c. *Filling the tubes between Flask No.2 and No.3 with water:*
- Valve 4: Position B.

After the tubes are filled with water, turn Valve 4 to position A.

d. *Injecting water into the Mixing Chamber:*
- Valve 4: Position C.

When the water level in Flask No. 3 is 1cm above the bottom of the tube, turn Valve 4 to position A.

e. *Venting:*
- Valve 6: Position C.

f. *Refilling Flask No.3:*
- Remove Flask No.3.
- Refill Flask No.3.
- Place it back in position.
- Repeat Steps b to f till 90% of the water required is injected into the mixing chamber.

g. *Remaining Distilled/Deaired Water:*
- Add the last 10% of the water after all the soil is placed in the mixing chamber.

A.4.4 Soil Entry

a. Fill Flask No.5 with dry soil (≃2 kg).

b. Position Flask No.5 as shown in Figure A.4.

c. *Venting:*
- Valve 7: Position B.
- Valve 9: Position A.
- Valve 3: Position A.

- Start Vacuum Pump No.3.
- Start the propellers at 60 rpm.

d. *Evacuating Flasks No.4 and No.5:*

- Valve 7: Position B.
- Valve 8: Position B. Switch Valve No.8 from position A to B very slowly.

Monitor the vacuum using Bourdon Gauge No. 4 for 5 min (<–28 feet of water).

e. *Placing of dry soil:*
- Remove the Pinch Clamp.
- Switch on the vibrator (Mode: high or low).

The process takes about 20 to 45 minutes.

f. *Refilling Flask No.5 with Soil:*
- Switch off the vibrator.
- Clamp the rubber hose with the Pinch Clamp.

Venting:
- Valve 8: Position C. Switch Valve 8 from position B to C very slowly.

- Remove Flask No.5.
- Repeat Steps a, b, d, e and f until all the dry soil is placed in the mixing chamber.

g. *Final mixing stage:*
- Mix the slurry after all the ingredients have been added for 30 minutes at 60 rpm.

A.4.5 Sedimentation

a. Switch off the propellers.

- Valve 1: Position A.
- Valve 10: Position B.
- Valve 5: Position B.

The slurry will flow from the mixing chamber to the sedimentation chamber under its own weight.

- Close Valve 5 when the level of slurry in the mixing chamber is about 1 inch

b. *Curing Period:*
- Allow the slurry to settle down in the consolidometer from at least 12 hours.

A.4.6 Disassembly of the Equipment

a. *Venting:*
- Valve 2: Position C.
- Valve 3: Position B.

- Valve 7: Position A.
- Valve 9: Position B.
- Valve 12: Position A.
- Valve 10: Position C.
- Valve 11: Position B.

- Switch off all three vacuum pumps.

b. Dismantle the free fall chamber.

c. *Cleaning the equipment:*
- Clean all the valves and tubes which contain soil.
- Clean all the parts of the mixing chamber.

A.5 CONSOLIDATION PROCEDURE

After the free fall chamber is removed, the consolidation process begins. The instructions are as follows:

a. Place a filter paper on top of the porous disk of the piston.

b. Screw four 14–inch screw rods to the square steel plate.

c. Place the piston through the guide bushing.

d. Clamp the piston.

e. Put the guide bushing and the piston in the consolidometer.

f. Tighten the four nuts on the screw rods.

g. Connect a funnel to the bottom drainage line.

h. Open the valve to that drainage line.

i. *See Figure A.5.*

Stage 1: *Consolidation for vertical stress between 0 and 0.013 ksc.*
- Connect a hook to the end of the piston shaft.
- Attach a steel wire to the hook over two pulleys and counterbalance the piston by weights.
- Push the piston down slowly until it touches the slurry.
- Measure the depth of the piston relative to the top of the steel chamber.
- Attach a displacement transducer to guide bushing to measure the displacement of the piston during consolidation.
- Place two dial gauges to the far end of the guide bushing to check the alignment of the piston.
- Calculate the amount of counterweight required for a given stress.
- Record the readings using the data acquisition.

j. Stage 2: *Consolidation for vertical stress between 0.013 and 0.125 ksc.*
- Remove the hook and the wire cable.
- Place the weight adapter on top of the piston.
- Put the required weights on the adapter.
- Record the displacement using the data acquisition.

k. Stage 3: *Consolidation for vertical stress between 0.125 and 1.0 ksc.*
- Remove the weights and the adapter.
- Move the consolidometer to the loading frame.
- Place the load cell adapter between the piston and the pressure chamber.
- Adjust the pressure in the pressure chamber using the control valve.
- Record the readings using the data acquisition.

A.6 EXTRUSION PROCEDURE

After consolidation, the sample is ready to be extruded and trimmed. The procedure for extrusion is as follows (Figure A.6):

a. Close the drainage valve to the bottom porous base.

b. Remove the excess water on top of the piston.

c. Measure the depth of the piston relative to the steel chamber.

d. Reduce the pressure in the chamber to zero.

e. Move the consolidometer to the floor.

f. Remove the tie rods and guide bushing.

g. Move the consolidometer to the humid room.

h. Tilt the consolidometer.

i. Replace the porous base with a Plexiglas base.

j. Follow Method A or Method B for extrusion depending on the amount of grease on the side wall of the steel chamber.

k. Method A:
- Put the consolidometer in the upright position.
- Remove the piston.
- Connect the outlets excavation trimming tool to a flask of distilled–deaired water and a vacuum pump through a trapping flask.
- Excavate the side of the soil cake.
- Remove the steel chamber when the excavation is done.

or Method B:

- Put the consolidometer in the upright position.
- Remove the piston.
- Remove the steel chamber.
- Scrap off the grease on the side of the soil cake.

A.7 TRIMMING PROCEDURE

After extrusion, the soil cake is trimmed and cut using the wire saw technique as described below (Figure A.7):

a. Place the soil cake together with the Plexiglas base on top of the trimming device.

b. Cover the top of the soil cake with plastic wrap.

c. Mark the positions of the cuts (Figure A.8).

d. Align the adjustable posts to the markings.

e. *Cutting the cake using the wire saw:*

- Cut along Line 1 by moving the saw vertically downwards until it reaches the base, move the saw horizontally away from the center of the cake.
- Pull Sample A away from the main cake.
- Cut Sample A into four equal size pieces for water content distribution.
- Repeat the same process on the other side.
- Cut along Line 2 by moving the saw vertically downwards until it reaches the base, move the saw horizontally away from the center of the cake.
- Place a glass plate with wax paper vertically along Line 1.
- Tilt the whole trimming base until Sample B begins to separate from the main cake.
- Hold Sample B with the glass plate.
- Repeat the same process on the other side.
- Cut along Line 3 by moving the saw vertically downwards until it reaches the base, move the saw horizontally away from the center of the cake.
- Pull Sample C away from the main cake.
- Repeat the same process on the other side.
- Cut along Line 4 by moving the saw vertical downwards till it reaches the base, move the saw horizontally away from the center of the cake.
- Place two glass plates vertically on the same side along Line 2.
- Tilt the whole base until the both pieces of Samples C are resting on the glass plates.
- Separate the samples by pulling the glass plates apart.

f. *Waxing all the pieces:*
   - Mix equal amounts of wax and petroleum jelly in a heating bath.
   - Allow the wax to melt.
   - Apply a layer of the wax to each piece of soil.
   - Wrap the soil with plastic wrap.
   - Coat aluminum foil with a layer of wax.
   - Wrap the soil with the aluminum foil.
   - Wax the outside of the foil until it is air–tied.
   - Put it in the humid for storage.

A number of test samples are made from each batch of resedimented clay. A typical number soil samples are listed as follows:

a. Two Directional Shear Cell samples.

b. Four 1.4"ϕ Triaxial test samples.

c. Twelve to sixteen oedometer or Direct Simple Shear test samples.

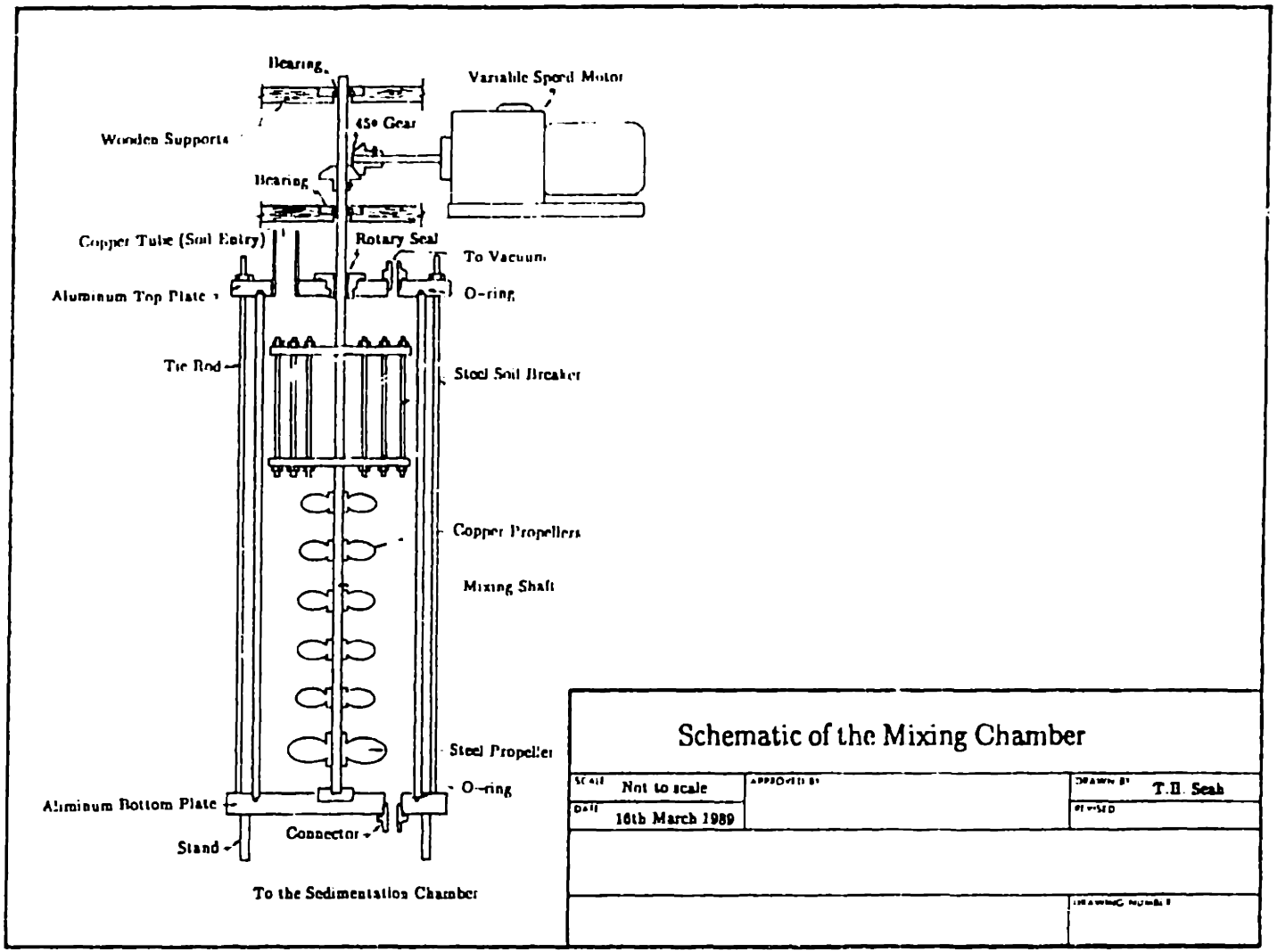

Figure A.1: Schematic of Mixing Chamber.

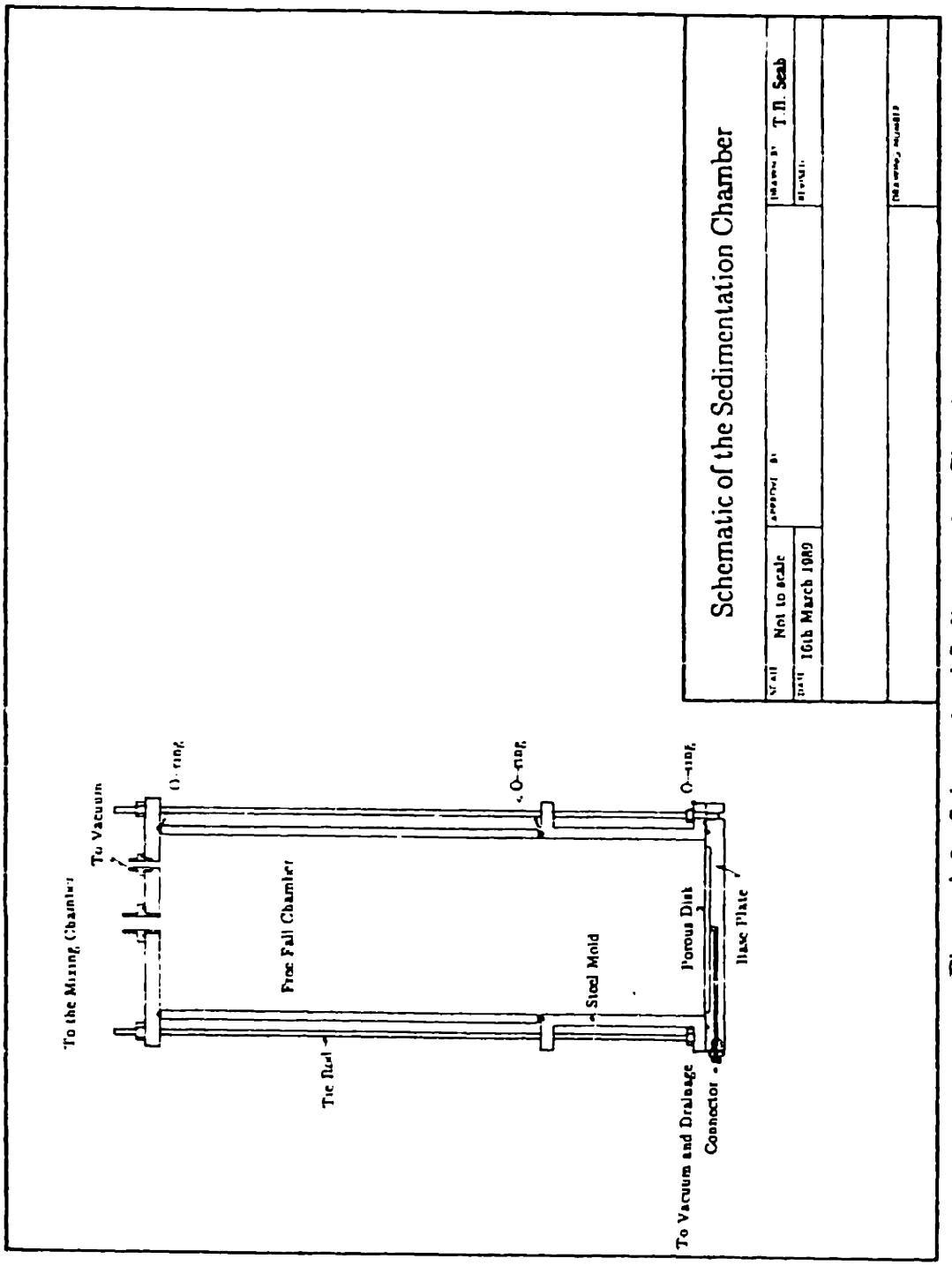

Figure A.2: Schematic of Sedimentation Chamber.

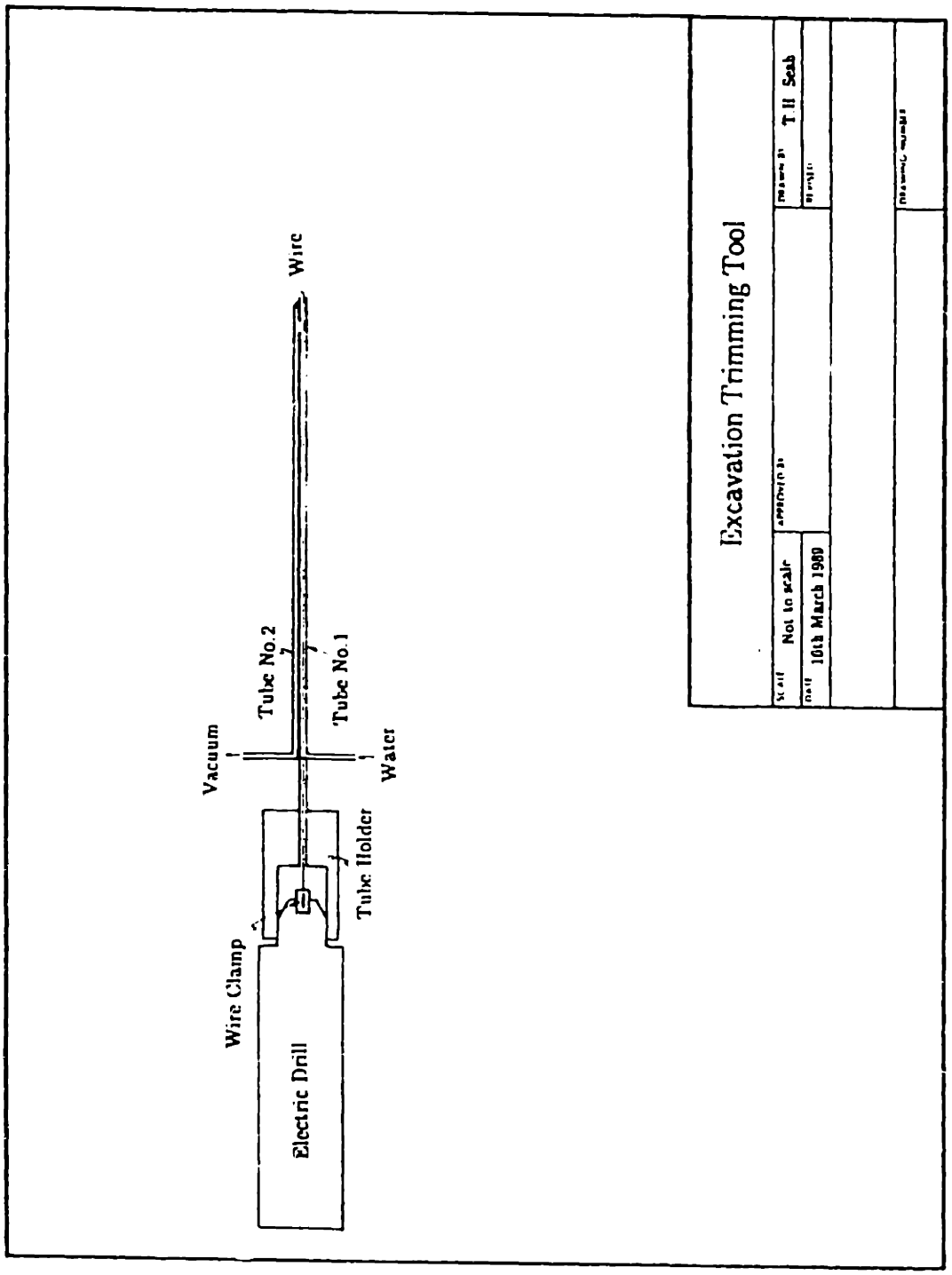

Figure A.3: Schematic of Excavation Trimming Tool.

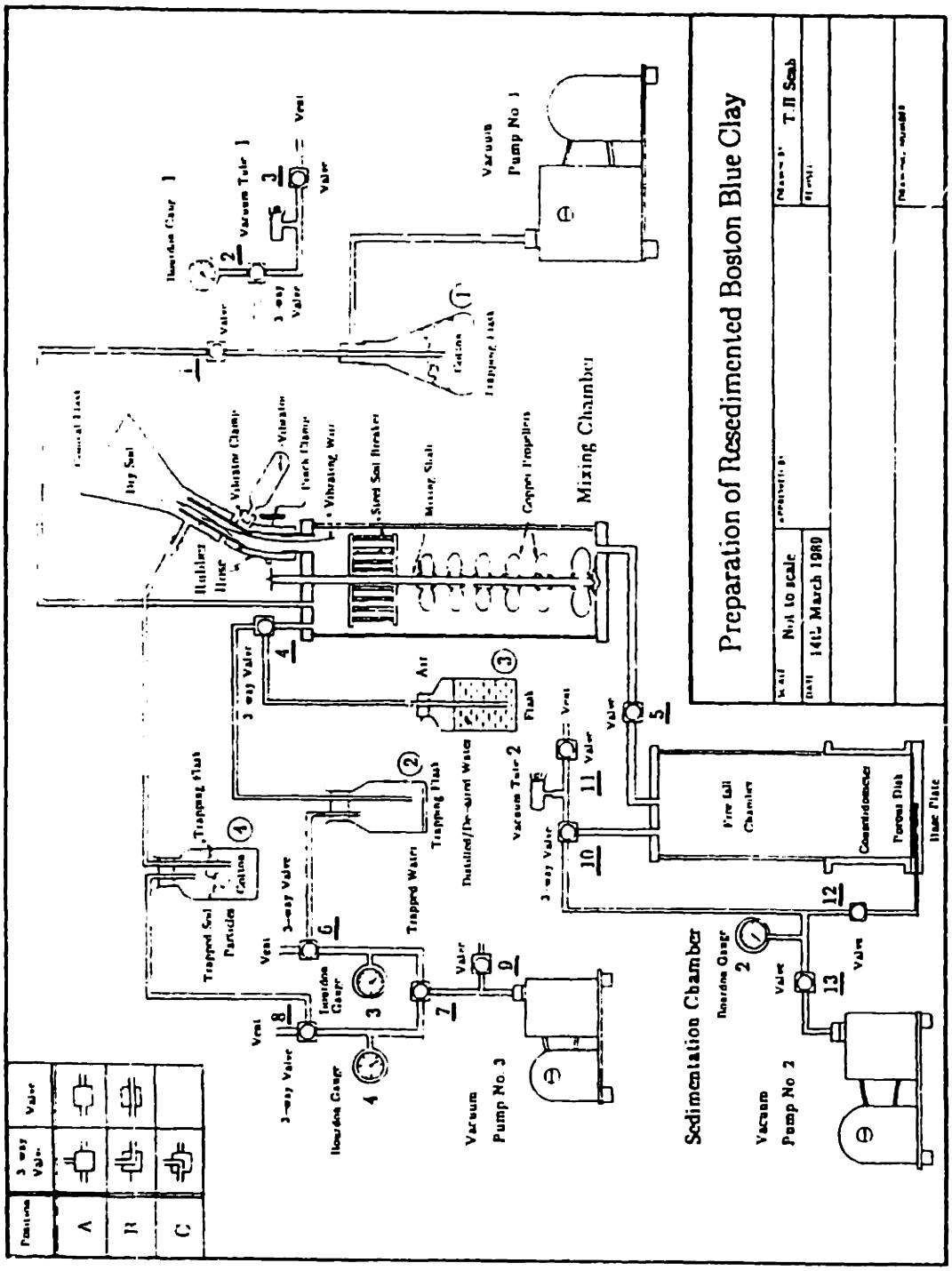

Figure A.4: Schematic of General Layout.

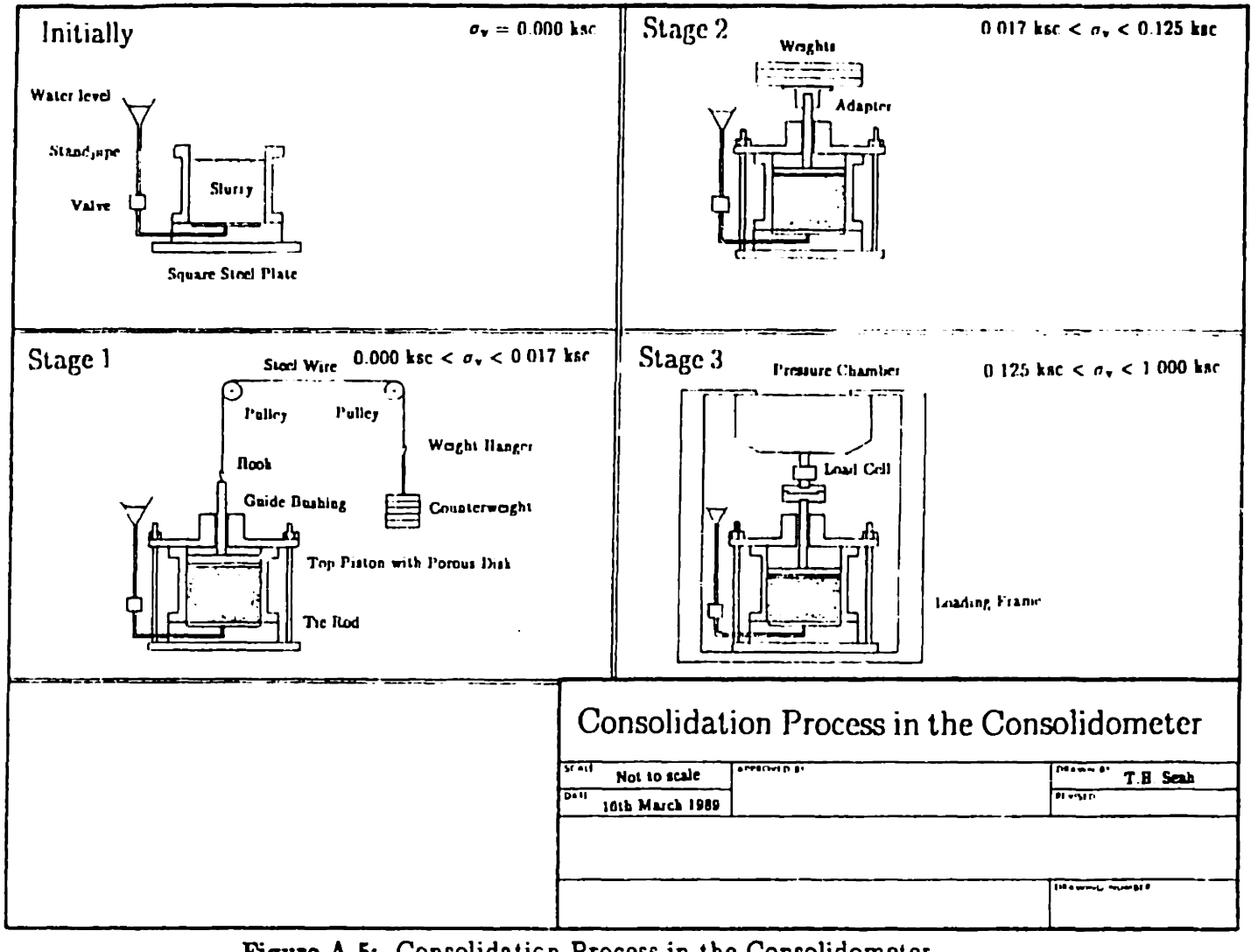

Figure A.5: Consolidation Process in the Consolidometer.

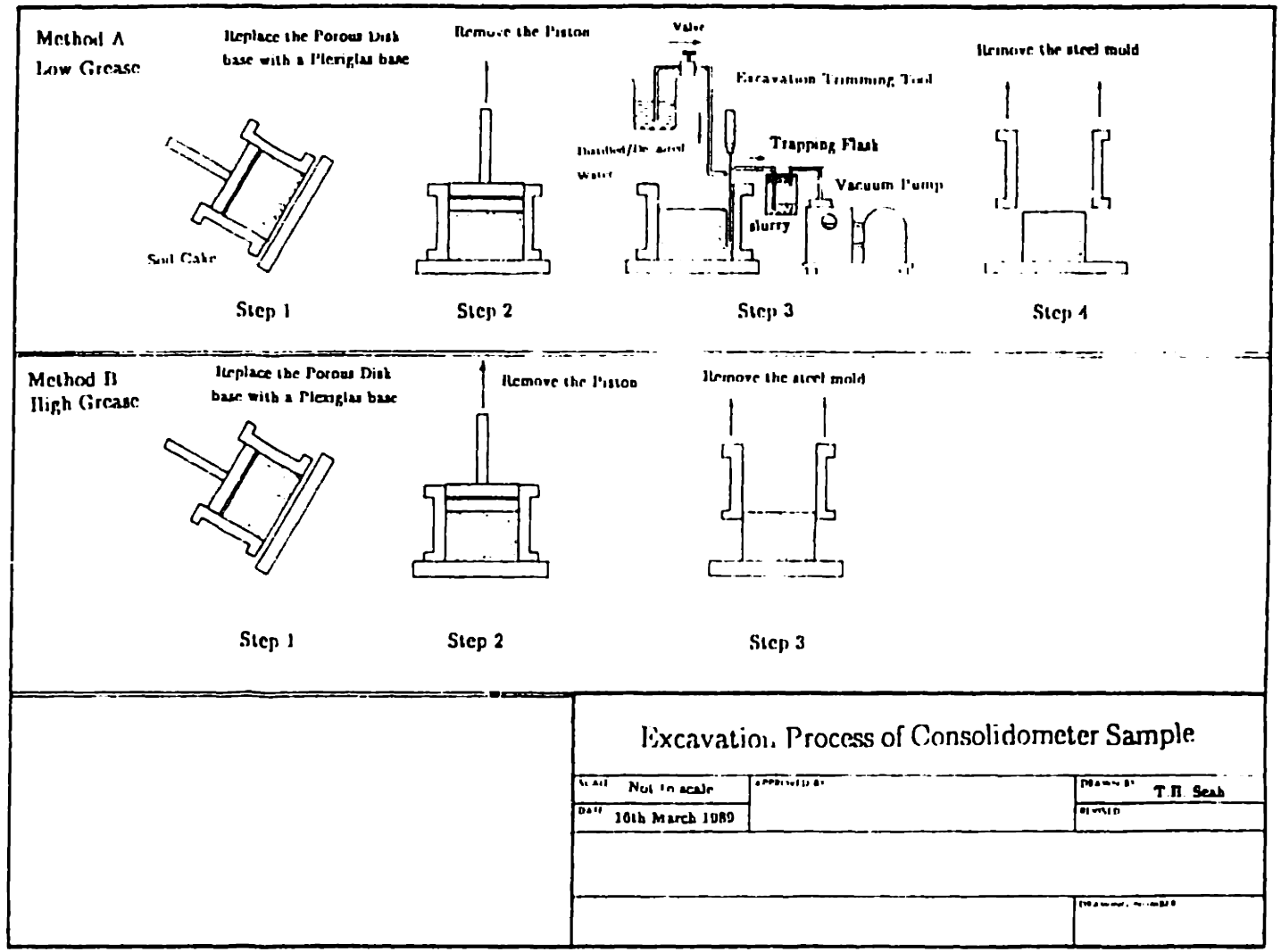

Figure A.6: Excavation Process of the Consolidometer.

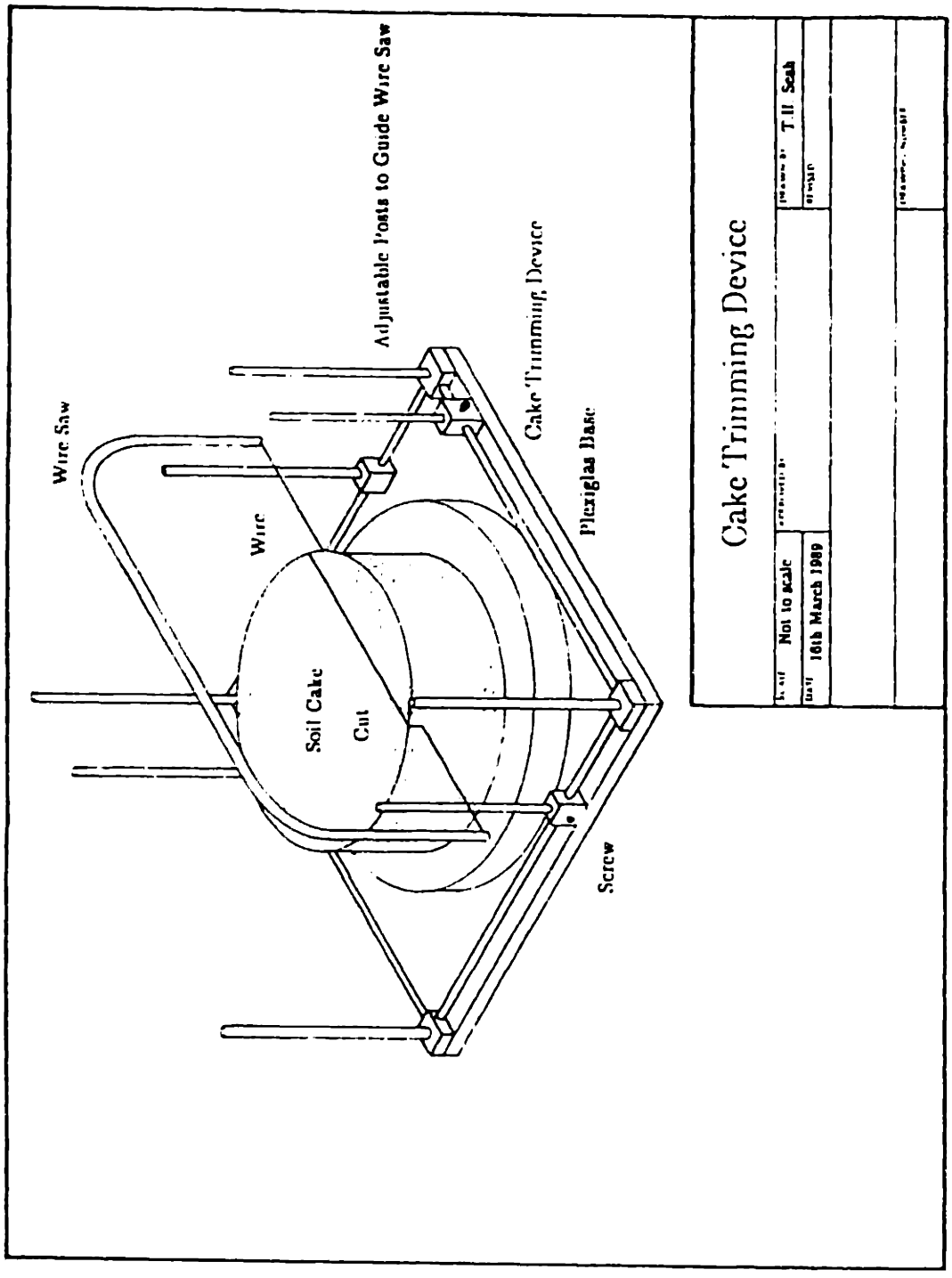

Figure A.7: Cake Trimming Device.

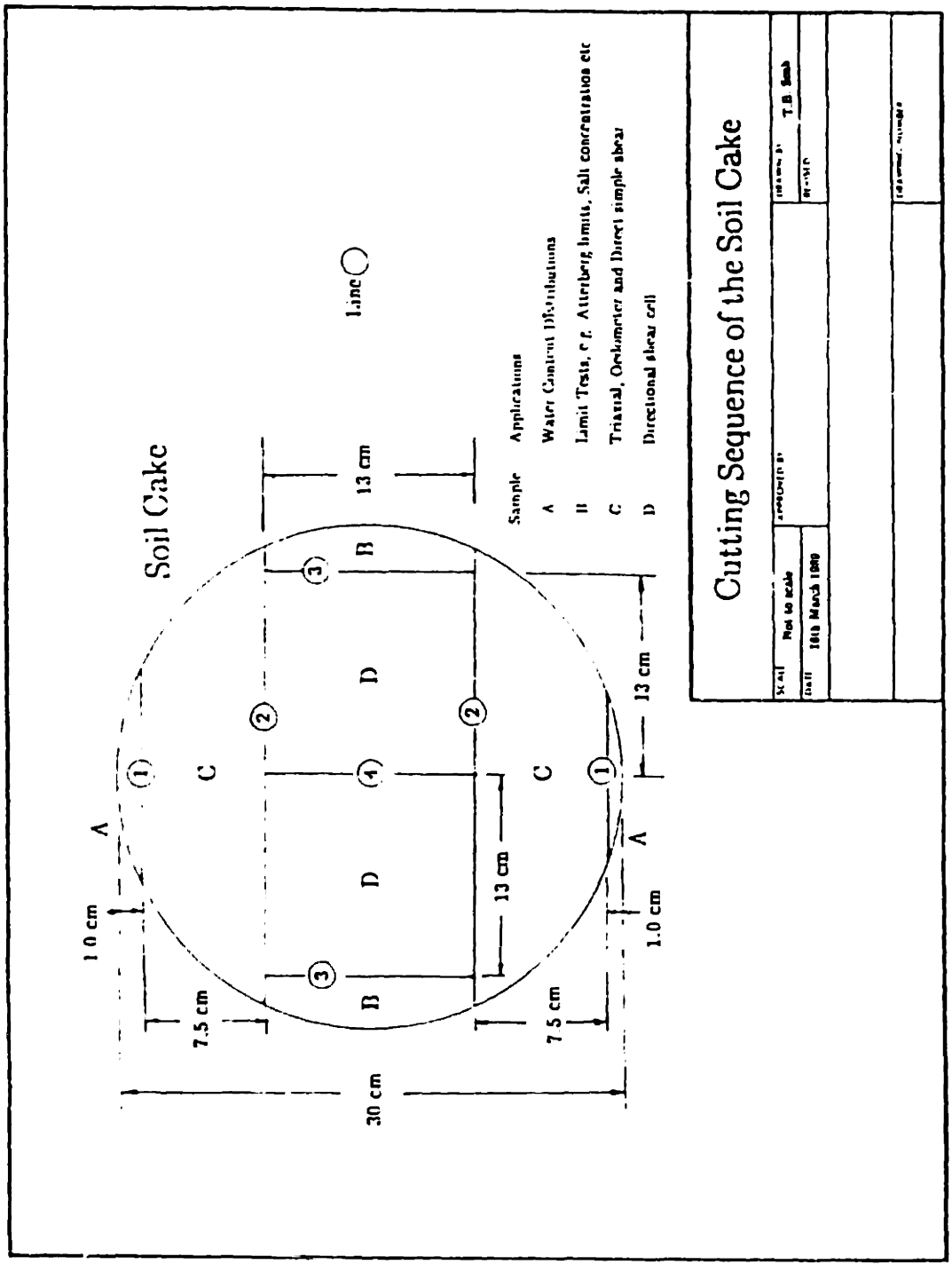

Figure A.8: Cutting Sequence of the Soil Cake.

APPENDIX B

REFERENCE TESTS FOR RESEDIMENTED BOSTON BLUE CLAY

B.1 INTRODUCTION

The aim of performing reference tests is to check the batch–to–batch sample variability. This appendix provides comprehensive data on index properties and consolidation behavior of resedimented Boston Blue Clay III. The results include Atterberg limits, salt concentration and consolidation tests on all 8 batches of resedimented Boston Blue Clay III. The compression parameters from the consolidation tests are compared with several empirical correlations. Section B.4.7 describes the coefficients of permeability computed based on Terzaghi one–dimensional consolidation theory and data from incremental consolidation tests. These results are compared with the results from constant rate of strain consolidation tests performed by Walbaum (1988).

Other experimental data, including specific gravity, particle size distribution, and unconsolidated undrained tests are given in Chapter 4, and therefore are not discussed here.

B.2 ATTERBERG LIMITS

Atterberg limit tests have been performed on the batches of resedimented Boston Blue Clay to check the index properties of the clay. The test procedure is described in the American Society for Testing and Materials Standard, D4318–84 (1988). The liquid limits were obtained using the Casagrande liquid limit apparatus. The results of the Atterberg limit tests are presented in Table B.1. The variation among the batches is relatively small; the mean (±standard

deviation) of the liquid limit is 45.20±0.44% and the mean plastic limit is 21.74±0.44%. The average results are plotted on the plasticity chart shown in Figure B.1. The data point falls between the "A " and "C" lines, which is classified as "CL" soil.

B.3 SALT CONCENTRATION DETERMINATION

The salt concentrations of the batches were determined using the electrolysis method suggested by Martin (1970). The equivalent concentrations expressed in terms of sodium chloride (NaCl) vary between 14 and 22 g/l for the batches, as shown in Table B.1. The intended salt concentration was 16 g/l as described in Appendix A. Due to evaporation during batch consolidometer tests, there is a tendency for the salt concentration to be higher than the prescribed value. Salt concentration of the processed clay powder was found to have a value of about 2 g/kg of dry soil. Atterberg limits were obtained for this low salt concentration clay and a comparison was made between this clay and the resedimented clay with a concentration of about 16 g/l. The liquid and plastic limits change negligibly with salt concentration. The conclusion is that the Atterberg limits of the clay are not sensitive to changes in salt concentration.

B.4 CONSOLIDATION TESTS

There are basically two stages of consolidation; the first occurs during batching in the large consolidometer, and the second occurs during oedometer tests on smaller samples. Both stages were conducted with incremental loading; details are given below.

B.4.1 Batch Consolidometer Tests

After the clay slurry with initial water content of 100% was introduced into

the consolidometer under vacuum, the consolidation process was started with a very low vertical consolidation stress (about 0.003 ksc). A load increment ratio of one was chosen for the tests, with a 48–hour duration for each increment. For the first few loading increments, the time to reach the end–of–primary consolidation is extremely long (several days); therefore the increments have to be placed before the end–of–primary consolidation is reached in order to reduce the time of consolidation. At a vertical consolidation stress greater than 0.06 ksc, the end–of–primary consolidation is usually reached in less than 48 hours and a full settlement–time curve could then be analyzed. The batch is consolidated to a maximum vertical stress, σ'_p of 1 ksc and unloaded to a vertical stress, σ'_{vc} of 0.25 ksc, where the effective horizontal to vertical stress ratio is about 1 (determined experimentally, see Chapter 4). The batch is removed and trimmed to smaller sizes, which are wrapped and stored for subsequent tests.

The measured mean water content at the end of batch consolidation, as tabulated in Table B.1, was used with measured heights to "back–calculate" the water content at the end of each prior increment. The void ratio is calculated based on the assumption of 100% saturation, which is verified by conducting unconsolidated undrained tests as described in Chapter 4. The specific gravity of the soil is measured and has an average value of 2.785. For each increment, the coefficient of consolidation, c_v, was determined using two different methods: the Casagrande log–time method and the Taylor & Merchant (1940) root–time construction. The coefficient of permeability, k_v, was calculated based on Terzaghi's one–dimensional consolidation theory:

$$k_v = c_v \gamma_w m_v \quad \text{cm/s}$$

where c_v (cm^2/s) is the average value computed between the two methods;

γ_w is the unit weight of water (0.001 kg/cm³); and

m_v is the coefficient of volume compressibility which is equal to $\frac{\Delta \epsilon}{\Delta \sigma_v}$. cm²/kg.

Since the height of the sample changes quite substantially during consolidation, m_v is redefined as,

$$m_v = \frac{(H_1 - H_2)}{H_{ave}(\sigma_2 - \sigma_1)}$$

where

H_1 is the sample height at the end–of–primary consolidation under a vertical stress of σ_1;

H_2 is the sample height at the end–of–primary consolidation under a vertical stress of σ_2; and

H_{ave} is the average sample height, which is equal to $\frac{H_1+H_2}{2}$.

The results of the consolidometer tests are tabulated in Tables B.7 to B.14. Table B.2 summarizes the consolidation characteristics of the batches.

B.4.2 Oedometer Tests

Eleven incremental oedometer tests and two DSS consolidation tests (DeGroot, 1986) were performed on the batches of resedimented Boston Blue Clay. Several oedometer tests were run to the check thixotropic effects (discussed in Section B.4.2.2 and Section 4.4.5), the variation of preconsolidation pressure with depth in the large consolidometer, and the repeatability of the tests. At least one consolidation test was performed on each batch of clay. For Batch 203, the only consolidation data are from a DSS consolidation to a maximum vertical stress of 3

ksc (DeGroot, 1989).

The oedometer tests were carried out with a load increment ratio of one, and with increment durations of 24 hours in most tests. All the samples were loaded to 8 ksc, unloaded to 2 ksc, and reloaded to a maximum of 16 ksc before they were unloaded to 1 ksc.

The results from each test are tabulated in Tables B.15 to B.28. Table B.3 summarizes the oedometer and DSS consolidation characteristics.

B.4.2.1 The Preconsolidation Pressure

The preconsolidation pressure (σ'_p) of each sample of resedimented Boston Blue Clay was determined from the compression curves of the oedometer tests using the Casagrande (1936) construction method. The construction method is only accurate to 5 percent of the true value of σ'_p. The results are tabulated in Table B.3. There are a number of factors which can affect the preconsolidation pressure in an oedometer test, including:

1) sample disturbance; this effect will lower the measured σ'_p in an oedometer test;
2) side friction; sometimes the side friction of the wall on the oedometer ring can affect the stress distribution of the sample. This effect is more significant when the ratio of sample height to sample diameter is large. The ratio in most of the tests is about 0.4, therefore the side friction is assumed to be negligible; and
3) thixotropic effects; O'Neill (1985) discovered that the effects of thixotropy have the tendency to increase the apparent σ'_p.

It is very difficult to evaluate these factors independently. The measured σ'_p from the oedometer test represents the net effect. If the measured σ'_p is close to the maximum applied vertical stress from the consolidometer test, these effects can

be ignored.

B.4.2.2 Aging or Thixotropic Effect

The oedometer tests were performed with a storage time, t_s, ranging from 1 to 248 days. The storage time is defined as the time during which the specimens are stored before testing. A graph of the apparent preconsolidation pressure from the Casagrande construction method versus storage time is shown in Figure 4.12, which indicates no change in preconsolidation pressure with storage time. The conclusion is that the resedimented BBC is non–thixotropic.

B.4.2.3 The Effect of Side Friction on the Preconsolidation Pressure

In the consolidometer test, uniformity of the batch sample depends on the magnitude of the side friction of the wall. This side friction will affect the preconsolidation pressure of the soil at different locations along the depth of the sample; this effect might give rise to lower preconsolidation pressures at the bottom of the consolidometer. Two DSS–CRS tests were conducted on samples obtained from different locations of the consolidometer (the top 1 inch and the bottom 1 inch) on batch 201 by Walbaum (1988). He discovered that the preconsolidation pressure of the sample from the top of the consolidometer had a higher value than the one from the bottom, the difference being about 0.1 ksc. Two oedometer tests were also performed to investigate this effect on batch 204 (Figure B.3); the difference was less significant. In Batch number 206, a significant amount of grease was used to lubricate the side of the consolidometer in an attempt to reduce this side friction. Two oedometer tests were performed with samples obtained from the top and the bottom of the batch. The results were astonishing: the grease not only helped to reduce the side friction, which resulted in the same preconsolidation pressure for both tests (Figure B.4), it also eliminated

the "extrusion" process previously used.

B.4.3 Compression Curves

B.4.3.1 Experiment Results

Figure B.13 shows the compression curves for all of the consolidometer tests. The slope of the virgin compression line is concave upwards, in other words, the slope decreases with increases in consolidation stress (Table B.2). The results of the batch consolidometer tests were combined with the results from the oedometer tests. The combined compression curve for each batch of clay is plotted in Figures B.5 to B.12. Comparisons of experimental results with empirical correlations are made below.

B.4.3.2 Empirical Correlations with Compression Indices from the Literature

There are a number of empirical methods for estimating the compression index, C_c, based on the Atterberg limits and initial void ratio. The following section describes four empirical methods.

(I) Skempton Empirical Correlation between the Compression Index and Liquid Limit

Skempton (1944) found that for 25 different clays, the value of the compression index (C_c) can be correlated with the liquid limit (Figure B.14a). He reported the following relationship:

$$C_c' = 0.0076\ [\ LL - 11.5\ \%\ ]$$

where C_c' is the compression index in the remolded state, and LL is the liquid limit. Of the 25 soils, 11 were tested at the British Building Research Station (BRS) and the rest were performed mostly by American research groups.

Presumably, the liquid limits of the soils done by Building Research Station were carried out with the British Standard (BS) apparatus and the others were obtained with the ASTM apparatus.

Norman (1958) conducted liquid limit tests on five different British clays using both the British Standard and ASTM apparatus; the results are plotted in Figure B.15. Using linear regression, the correlation is:

$$LL(USA) = 0.941\ LL(BS)$$

where LL(USA) and LL(BS) are the liquid limits obtained from the British Standard and ASTM apparatus, respectively. Appropriate corrections were made on the results of 11 soils obtained with the BS apparatus, with the corrected results shown in Figure B.14b. Linear regression was applied to these data, and the goodness of fit, r^2, increased from 0.951 (uncorrected) to 0.964 (corrected). The new relationship is:

$$C_c' = 0.0078\ [\ LL(USA) - 11.2\ \%] \qquad \text{Eq.B.1}$$

The relationship between C_c (corresponding to the undisturbed field virgin compression line on natural clay) and C_c' is given by Terzaghi & Peck (1967),

$$C_c \simeq 1.30\ C_c'$$

Substituting $C_c = 1.30\ C_c'$ in Equation B.1 gives,

$$C_c = 0.010\ [\ LL(USA) - 11.2\%\ ] \qquad \text{Eq.B.2}$$

(II) Nishida's Correlation between the Compression Index and Initial Void Ratio

Nishida (1956) related the compression index, C_c, with the initial void ratio, e_o. The relationship is as follows:

$$C_c = 0.54 \, (\, e_o - 0.35 \,) \qquad \text{Eq.B.3}$$

The initial void ratio is taken as the void ratio at the average value of C_c between the plastic limit and liquid limit on the compression curve for each batch of clay. The C_c values are then computed from the equation above.

(III) Moran, Proctor, Mueser and Rutledge (MPMR) Correlation between the Compression Index, Initial void ratio and Liquid limit (1950)

Figure B.16 shows the relationship between the virgin compression index, C_c, the initial void ratio, e_o, and the liquid limit, LL. The compression index can be determined from this graph if the void ratio and liquid limit of the soil are known.

(IV) Schofield & Wroth (1968) Correlation between the Compression Index and Plasticity Index

Skempton and Northey (1953) found that for four different types of clay, the ratio of undrained strength at the plastic limit and the liquid limit is approximately 100. In critical state soil mechanics, it is assumed that the slope of the virgin compression line (or normal consolidation line) is parallel to the critical state line (CSL). Based on these above conditions, Schofield and Wroth (1968) derived the following equation,

$$C_c' = 0.005 \, G_s \, PI(BS) \quad \text{or}$$

$$\Rightarrow \quad C_c' = 0.005 \, G_s \, [\, 1.06 \, LL(USA) - PL \,]$$

where C_c' is the compression index of the remolded soil; G_s is the specific gravity of the soil; PI(BS) is the plasticity index (British); and PL is the plastic limit of the soil. Using the relationship between C_c and C_c' given by Terzaghi and Peck (1967) gives,

$$C_c = 0.0065\ G_s\ PI(BS) \text{ or} \qquad \text{Eq.B.4}$$

$$C_c = 0.0065\ G_s\ [\ 1.06\ LL(USA) - PL] \qquad \text{Eq.B.5}$$

Schofield and Wroth also obtained an empirical relationship between the plasticity index and the liquid limit, which is as follows:

$$PI(BS) = 0.615\ [\ LL(BS) - 9\%\ ] \qquad \text{Eq.B.6}$$

Combining the Equations B.4 and B.6, gives,

$$C_c = 0.004\ G_s\ [\ 1.06\ LL(USA) - 9\%\ ]$$

Assuming G_s is 2.7, the above equation becomes,

$$C_c = 0.011\ [\ LL(USA) - 10\%\ ] \qquad \text{Eq.B.7}$$

This equation is basically identical to Skempton's empirical relationship for natural clay,

$$C_c' = 0.010\ [\ LL(USA) - 11.2\%\ ]$$

(V) Summary

The four empirical correlations are given as follows:

1) Skempton: $C_c = 0.010 [LL(USA) - 11.2\%]$

2) Nishida: $C_c = 0.54 (e_o - 0.35)$

3) MPMR: See Figure B.16

4) S & W: $C_c = 0.011 [LL(USA) - 10\%]$

B.4.3.3 Comparison between Experimental Results and Empirical Correlations

The average compression index was obtained for each batch of resedimented Boston Blue Clay, and compared with empirical correlations based on the Atterberg limits and void ratio as shown in Table B.4. Figure B.17 graphically shows the experimental results versus the empirical estimates. MPMR and Schofield & Wroth's methods compared well with the experimental results; Nishida's and Skempton's correlations give lower C_c values.

B.4.4 Recompression Ratio and Swelling Ratio

The recompression ratio (RR) and the swelling ratio (SR) are defined as shown in Figure B.18. Ladd (1973) reported that the RR at an overconsolidation ratio (OCR) of 5 has a value close to the SR value at an OCR of 10 for the same clay. This was investigated in these oedometer tests. The samples were first loaded to a vertical stress of 8 ksc, unloaded to 2 ksc (OCR of 4), then reloaded to 16 ksc before finally being unloaded to 1 ksc (OCR of 16). Based on Ladd's work, it is reasonable to compare the RR at an OCR of 4 and the SR at OCR of 8 for this series of tests. The ratio of RR/SR for each test is shown in Table B.3. The mean ratio for all the tests is 0.92 with a standard deviation of 0.51.

B.4.5 Compression Ratio and Recompression Ratio

Ladd (1973) has shown that in most clays, the compression ratio (CR) is about 5 to 10 times recompression ratio (RR) of the same soil. The ratios of CR to RR for all oedometer tests are tabulated in Table B.3; CR is the value taken from the increment from 4 to 8 ksc. The recompression ratio is given at an overconsolidation ratio of 4. The mean value for the tests is 11.8±3.4.

B.4.6 Rate of Secondary Compression Versus Compression Ratio

Mesri and Choi (1985) reported that for most clays, the ratio of the rate of secondary compression ($C_{\alpha\epsilon}$) to the compression ratio (CR) is 0.04±0.01. The rate of secondary compression in our oedometer tests is given from the change in strain after the end–of–primary consolidation over the change in the logarithm of time. For most increments, the slope of the curve in the secondary compression range was not a straight line (Figure B.19). Therefore, in our tests, the minimum slopes of the strain versus the logarithm of time plots are taken as the rate of secondary compression. The $C_{\alpha\epsilon}$ and the ratio of $C_{\alpha\epsilon}$/CR for each increment of the test is reported in Tables B.15 to B.28. The mean ratio is lower than the values reported by Mesri & Choi because of the non–linear relationship between the strain and the logarithm of time in the secondary compression range. Table B.5 shows the variation in the results depending on where the tangent to the point on the secondary compression time curve is being taken (Figure B.19). As a results, the computed $C_{\alpha\epsilon}$ values range from 0.26 to 0.60.

B.4.7 Coefficient of Permeability

The results presented here include all consolidation tests done on the 200 series Resedimented BBC by this research group. They consist of three CRS, eleven oedometer, two DSS consolidation and 8 large consolidometer tests.

The Coefficient of Permeability in the CRS test can be calculated directly based on the rate of deformation (Wissa et al., 1971), as follows:

$$k = \frac{1}{2} \frac{\dot{\epsilon} \; H^2 \; \gamma_w}{u_b}$$

where $\dot{\epsilon}$ is the strain rate;

H is the drainage path length;

U_b is the excess pore water pressure on the bottom undrained boundary; and γ_w is the unit weight of water.

The void ratio is calculated based on the $G_s \; w = S \; e$ relationship. The degree of saturation (S) is 100%, the specific gravity of soil is 2.785 and w is water content of the soil.

The coefficient of permeability is usually expressed as a function of the void ratio. There are two relationships commonly used by the profession, which are described below.

Taylor (1948) suggested an empirical linear relationship between the logarithm of k and the void ratio,

$$\log k = \log k_0 - \frac{e_0 - e}{C} \qquad \text{Eq.B.8}$$

where C is a constant, which is later defined as permeability change index, C_k, k_0 and e_0 are the in–situ values of the natural clay.

Equation B.8 can also be expressed as,

$$C_k = \frac{e_o - e}{\log(k_o) - \log(k)}$$

$$\text{or } C_k = \frac{\Delta e}{\Delta \log(k)} \qquad \text{Eq.B.9}$$

For engineering practice, C_k is usually assumed to be constant over the typical range void ratios. Tavenas et al. (1983) shows that $C_k = 0.5\ e_0$ is a reasonable approximation (Figure B.20).

An alternative relationship is given by Mesri and Olson (1971). They assumed a linear relationship between logarithm of k and logarithm of e,

$$\log k = A \log e + B \qquad \text{Eq.B.10}$$

where A and B are constants.

Equation B.10 can be written in terms of e, as follows,,

$$\log_e e = \frac{2.303}{A} (\log k - B) \qquad \text{Eq.B.11}$$

By differentiating with respect to the logarithm of k, the equation becomes:

$$\frac{de}{d(\log k)} = \frac{2.303}{A} e \qquad \text{Eq.B.12}$$

But $C_k = \frac{\Delta e}{\Delta \log k} \simeq \frac{de}{d(\log k)}$ is the slope of e vs. log k from Equation B.9, therefore, Equation B.12 becomes

$$C_k = \frac{2.303}{A} e \qquad \text{Eq.B.13}$$

This implies that C_k is a function of e, for a log e–log k relationship.

Equation B.11 can be rewritten as,

$$\left[\frac{e}{e_0}\right] = \left[\frac{k}{k_0}\right]^{1/A} \qquad \text{Eq.B.14}$$

Graphs of e versus log k, and log e versus log k were plotted for all incremental consolidation tests. Figures B.21 and B.22 show that the e–log k and log e–log k relationships for oedometer and DSS consolidation tests have an initial void ratio of about 1.15. Linear regression was used to compute the constants C_k and A from Equations B.9 and B.11. The results are shown in Table B.6. Figures B.23 and B.24 show the e–log k and log e–log k relationships for the large consolidometer tests from batches 200–207. Linear regression was used to determine the constants for all consolidation tests, which include oedometer tests and batch tests with e_0 ranging from 1.1 to 2. Figures B.25 and B.26 compare the incremental oedometer tests with the three CRS tests (from Walbaum, 1988) on Batch 201 specimens with an initial void ratio of 1.1. Figures B.27 and B.28 show the results of both the oedometer and consolidometer tests on Batch 201. The results indicate that the incremental consolidation tests give a lower k value than the CRS tests (a difference of about 20%). One explanation for the lower k value is that no compressibility correction is made on the CRS results, which means the actual void ratio is higher than the void ratio reported. Further discussion is provided by Ahmed (1990).

Figure B.29 shows the C_k–initial void ratio relationship for all incremental consolidation tests. The permeability change index, C_k, is calculated based on Equations B.9 (e–log k) and B.13 (log e–log k) for each individual test. For a high initial void ratio, C_k computed from e–log k does not agree very well with the $C_k=0.5e_0$ relationship very well. The C_k value computed from Equation B.13 (log e–log k) gives a better correlation with $C_k=0.5e$. The conclusion is that for this

resedimented BBC, the C_k is a function of the current void ratio, e, rather than a function of initial void ratio, e_o.

Table B.1: Index Properties of Resedimented Boston Blue Clay III.

Batch (Source)	G_s	w_c (%)	σ'_{max} (ksc)	LL (%)	PL (%)	PI (%)	LI	Clay Fr. $<2\mu$, (%)	Salt Conc. g/l	Remarks
(Ground)	2.785			44.90 ±0.14	22.45 ±0.07	22.45			1.98 ±0.10g/kg	97% passed Sieve No.100
200		41.10 ±0.80	1.000	45.90	21.95 ±0.35	23.95	0.80		22.13 ±2.02	
201		39.42 ±1.90	1.000	44.82	21.19 ±0.35	23.63	0.77	57.6 ±1.1	14.53 ±1.43	
202		40.67 ±0.40	1.032	45.46	22.27 ±0.62	23.19	0.79		15.05 ±0.95	
203		40.70	1.002	44.50	21.18 ±0.58	23.32	0.84		15.90 ±3.20	
204		40.19	1.005	45.60	21.47 ±0.58	24.13	0.78		13.63 ±3.02	
205		40.66	1.000	45.0'	21.62 ±0.63	23.39	0.81		15.69 ±3.65	
206		41.24	0.977	45.17	22.10 ±0.64	23.07	0.83		17.38 ±2.52	
207		40.75	1.000	45.12	22.15 ±0.57	22.97	0.81		16.25 ±1.73	
Mean S.D		40.59 ±0.57		45.20 ±0.44	21.74 ±0.44	23.46 ±0.42	0.82 -		16.34 ±2.60	

Note: ' Maximum applied vertical stress in the consolidometer.
No Standard Deviation means one measurement only.

Table B.2: Results of Consolidometer Tests for Resedimented Boston Blue Clay III.

Batch No.	H_c[1] (cm)	w_c[2] (%)	e_c[3]	σ'_{vm}[4] (ksc)	C_c (stress range, ksc)			C_s (stress range, ksc)		C_h from e-lgk	Remarks
					0.125-0.25	0.25-0.50	0.50-1.00	1.00-0.50	0.50-0.25		
200	10.272	41.10	1.145	1.00	0.482	0.509	0.409		0.010	0.686	
201	13.490	39.42	1.100	1.00	0.641	0.419	0.522	0.010	0.020	0.748	low w_c
202	13.822	40.67	1.132	1.03	0.508	0.453	0.453	0.011	0.006	0.813	
203	13.757	40.70	1.133	1.00	0.568	0.608	0.518			0.928	
204	13.238	40.10	1.119	1.01	0.512	0.487	0.463			0.676	
205	13.682	40.66	1.132	1.00	0.661	0.508	0.402			0.772	
206	11.646	41.24	1.148	0.98	0.548	0.439	0.416	0.023	0.025	0.728	
207	14.624	40.75	1.135	1.00	0.477	0.412	0.409	0.023	0.023	0.659	
Mean S.D.					0.557 ±0.068	0.479 ±0.064	0.449 ±0.049	0.017 ±0.007	0.017 ±0.008	0.751 ±0.088	

Notes:
1. Final sample height.
2. Final water content from Table B.1.
3. Final void ratio.
4. Maximum applied vertical stress.

Table B.3: Results of Oedometer Tests on Samples from Batches of Resedimented Boston Blue Clay III.

Test No.	Batch Label	Age t_s (days)	e_i	w_i (%)	σ'_p (ksc)	CR (stress range, ksc)			RR	SR	RR/SR	CR/RR for ΔCR=4	C_c from e-lgt
						1-2	2-4	4-8	2-8-2	16-2			
1	200-1[1]	23	1.127	40.47	1.05	0.187	0.162	0.141	0.012	0.015	0.76	11.8	0.44
2	200-2	24	1.179	42.33	1.08	0.152	0.173	0.139	0.010	0.018	0.54	13.9	0.49
3	200-3	79	1.160	41.66	1.00	0.187*	0.154	0.138	0.015	0.015	1.06	9.2	0.43
4	201	1	1.168	41.94	0.98	0.147*	0.165	0.138	0.012	0.016	0.77	11.5	0.57
5	202	9	1.164	41.80	0.98	0.159*	0.165	0.154	0.012	0.018	0.67	12.8	0.50
6	202-B[2]		1.133	40.70	1.00		0.169[7]						0.30
7	203-B		1.139	40.90	1.00		0.183[7]						0.33
8	204-T[3]	61	1.135	40.76	0.98	0.176*	0.156	0.152	0.025	0.010	2.45	6.1	0.45
9	204-B[4]	61	1.127	40.47	0.95	0.182*	0.155	0.165	0.008	0.015	0.55	20.6	0.55
10	205-T	248	1.115	40.03	1.00	0.156*	0.159	0.142	0.012	0.013	0.93	11.8	0.49
	205LSO[5]	257	1.115	40.04	1.00	0.172*	0.164	0.135	0.011	0.020	0.55	12.5	0.49

Test No.	Batch Label	Age t_s (days)	e_i	w_i (%)	σ'_p (ksc)	CR (stress range, ksc)			RR	SR	RR/SR	CR/RR for ΔCR=4	C_c from e-lgt
						1-2	2-4	4-8	2-8-2	16-2			
11	206-T	1	1.147	41.18	0.98	0.134	0.150	0.145	0.013	0.015	0.88	11.2	0.47
12	206-B	1	1.145	41.11	0.98	0.139	0.156	0.155	0.014	0.016	0.88	11.1	0.57
13	207-T	40	1.114	40.00	1.00	0.132*	0.159	0.152	0.016	0.017	0.96	9.5	0.50
Mean S.D						0.160 ±0.020	0.164 ±0.011	0.146 ±0.009	0.013 ±0.004	0.016 ±0.002	0.92 ±0.51	11.8 ±3.4	0.47 ±0.08

Note:
[1] Test Number on the Batch.
[2] Results obtained from DSS consolidation.
[3] Specimen taken at the top of the Consolidometer.
[4] Specimen taken at the bottom of the Consolidometer.
[5] CR taken from 4-8 ksc load increment.
[7] CR taken from 1.2-2 ksc load increment.
[*] CR taken from 1.5-3 ksc load increment.

Table B.4: Experimental Results versus Empirical Methods for Determining Virgin Compression Index.

Source (Batch)		LL (%)	PL (%)	C_c obtained experimentally			Void Ratio at average C_c, e_{ave}	C_c determined from empirical methods				
				at LL	at PL	Average value		Skempton[1]	Nishida[2]	MPMR[3]	Schofield & Wroth[4]	Average
1	200	45.90	22.45	0.46	0.30	0.38	0.95	0.35	0.38	0.41	0.40	0.39
2	201	44.82	21.19	0.47	0.36	0.42	0.92	0.34	0.31	0.39	0.38	0.36
3	202	45.46	22.27	0.45	0.31	0.38	0.94	0.34	0.32	0.40	0.39	0.36
4	203	44.50	21.18	0.56	0.30	0.43	0.91	0.33	0.30	0.39	0.38	0.35
5	204	45.60	21.47	0.48	0.31	0.40	0.93	0.34	0.31	0.40	0.39	0.36
6	205	45.01	21.62	0.46	0.27	0.37	0.93	0.34	0.31	0.40	0.39	0.36
7	206	45.17	22.10	0.43	0.32	0.38	0.94	0.34	0.32	0.40	0.39	0.36
8	207	45.12	22.15	0.41	0.32	0.37	0.94	0.34	0.32	0.40	0.39	0.36

Notes:

Specific Gravity of the soil, $G_s = 2.785$

[1] Skempton(1944) $C_c = 0.010 (LL - 11.2 \%)$

[2] Nishida (1956) $C_c = 0.54 (e_o - 0.35)$ assuming $e_o = e_{ave}$

[3] MPMR (1958) From Figure B.16

[4] Schofield & Wroth (1968) $C_c = 0.011 (LL - 10 \%)$

See Figure B.17 for comparison.

Table B.5: Interpretation of ϵ_{100} from a Typical Oedometer Load Increment (refer to Figure B.19, Batch 207: σ'_{vc}=4 to 8 ksc).

Tangent to point at time t (minutes)	Time at EOP, t_{100} (minutes)	Strain at EOP, ϵ_{100} (%)	Rate of 2nd. Compression $C_{\alpha\epsilon}$	Compression Ratio, CR	Ratio of $C_{\alpha\epsilon}$/CR
30	6.1	15.06	0.600	13.32	0.045
100	7.2	15.17	0.483	13.69	0.035
1000	12.0	15.62	0.260	15.18	0.017

Notes:

1. EOP: End of Primary
2. CR is assumed to be, $CR = \frac{\epsilon_{100} - 11.05\%}{\log (8/4)} / 100$

Table B.6: Linear Regression Results for e–k Relationship.

Source	Type of Relation	Number of Observations	Constants				r^2	Initial Void Ratio, e_i
			e_o	k_o (cm/s)	A	$C_k(c)$		
Oedometer	e vs lg(k)	79	0.90	4.0×10^{-8}		0.425	0.73	≈ 1.1
Oedometer	lg(e) vs lg(k)	79	0.90	4.1×10^{-8}	5.056	0.455c	0.73	≈ 1.1
Oedometer & Batch	e vs lg(k)	111	1.00	6.1×10^{-8}		0.565	0.91	≈ 1.1-2
Oedometer & Batch	lg(e) vs lg(k)	111	1.00	6.5×10^{-8}	4.855	0.474c	0.94	≈ 1.1-2

Table B.7: Results of Consolidometer Test for Batch 200.

CONSOLIDATION TEST DATA SHEET : Batch 200 DATE: 04/04/1987 DONE BY : CPA/TBS

Incr Number	Scale Load (kg)	σ'_{vc} (ksc)	Height of Sample			Water Content, %		Void Ratio , e		
			H_{50} ,cm	H_{100},cm	H_f ,cm	W_{c100},%	W_{cf}, %	e_{50}	e_{100}	e_f
5		0.055			13.749		61.17			1.871
6		0.130	13.014	12.278	12.271	56.14	56.09	1.717	1.563	1.562
7		0.249	11.948	11.624	11.263	51.24	48.53	1.495	1.427	1.352
8		0.500	11.076	10.889	10.878	45.73	45.64	1.313	1.273	1.271
9		1.000	10.588	10.297	10.244	41.29	40.89	1.211	1.150	1.139
10		0.500			10.256		40.98			1.141
11		0.250	10.263	10.270	10.272	41.09	41.10	1.142	1.144	1.145

Incr. Number	σ'_{vc} (ksc)	Time (min)			Coef. of Consolidation cm^2/s			C_c	a_v cm^2/kg	k x 10^{-6} cm^2/s
		Duration (hours)	t_{50} (√t)	t_{50} (log)	√t	log t	Average			
5	0.055									
6	0.130	50	201	95	0.00300	0.00146	0.00223	0.824	1.511	337.6
7	0.249	45	734	162	0.00069	0.00073	0.00071	0.482	0.458	32.5
8	0.500	25	470	107	0.00092	0.00094	0.00093	0.509	0.265	24.7
9	1.000	52	296	67	0.00134	0.00137	0.00135	0.409	0.111	13.5
10	0.500	25								
11	0.250	650	36.2	12	0.01028	0.00720	0.00874	0.010	0.006	4.9

Table B.8: Results of Consolidometer Test for Batch 201.

CONSOLIDATION TEST DATA SHEET . Batch 201 DATE: 06/30/1987 DONE BY : CPA/TRS

Incr Number	Scale Load (kg)	σ'_{vc} (ksc)	Height of Sample			Water Content, %		Void Ratio , e		
			$H_{t_{50}}$,cm	$H_{t_{100}}$,cm	H_f ,cm	$w_{c_{100}}$,%	w_{cf}, %	$e_{t_{50}}$	$e_{t_{100}}$	e_f
4		0.0313			19.89		75.14			2.096
5		0.0625	18.735	17.58	17.33	62.25	60.86	1.916	1.736	1.697
6		0.125	16.925	16.52	16.52	56.34	56.34	1.634	1.571	1.571
7		0.250	15.90	15.28	15.24	49.42	49.19	1.475	1.376	1.372
8		0.500	14.86	14.47	14.43	44.90	44.67	1.312	1.252	1.246
9		1.000	13.95	13.46	13.42	39.26	39.04	1.171	1.095	1.089
10		0.500	13.43	13.44	13.43	39.15	39.20	1.091	1.092	1.093
11		0.250	13.46	13.46	13.45	39.37	39.42	1.092	1.096	1.100

Height of Solids, H_s = 6.425 cm

Incr Number	σ'_{vc} (ksc)	Time (min)			Coef. of Consolidation cm^2/s			C_c	m_v cm^2/kg	k x 10^{-6} cm^2/s
		Duration (hours)	t_{50} (√t)	t_{50} (log)	√t	log t	Average			
4	0.0313									
5	0.0625	50	2783	631	0.00045	0.00046	0.00046	1.199	3.957	182.0
6	0.125	22	1565	355	0.00065	0.00056	0.00066	0.548	1.002	66.2
7	0.250	46	1135	199	0.00079	0.00104	0.00092	0.641	0.624	57.4
8	0.500	27	608	158	0.0012.	0.00115	0.00122	0.419	0.218	26.6
9	1.000	50	533	120	0.00129	0.00133	0.00131	0.522	0.145	18.9
10	0.500	23	16.6	6.3	0.03839	0.02350	0.03095	-0.001	-0.003	
11	0.250	110	47.3	20	0.01353	0.00744	0.01049	0.020	0.011	12.0

Table B.9: Results of Consolidometer Test for Batch 202.

CONSOLIDATION TEST DATA SHEET : Batch 202 DATE: 07/07/1987 DONE BY : CPA/TBS

Incr. Number	Scale Load (kg)	σ'_{vc} (kgf/cm²)	Height of Sample			Water Content, %		Void Ratio , e		
			H_{ss} ,cm	H_{100},cm	H_f ,cm	W_{c100},%	W_{cf}, %	e_{ss}	e_{100}	e_f
3		0.016			22.669		89.83			2.502
4		0.031	21.320	19.971	19.71	74.72	74.72	2.292	2.081	2.081
5		0.063	19.005	18.038	18.035	64.01	64.01	1.932	1.783	1.783
6		0.127	17.371	17.032	16.643	56.62	56.28	1.680	1.577	1.567
7		0.246	16.163	15.682	15.653	50.96	50.80	1.493	1.414	1.415
8		0.499	15.195	14.744	14.650	45.76	45.30	1.345	1.275	1.262
9		1.032	14.240	13.819	13.782	40.64	40.44	1.197	1.132	1.126
10		0.535	13.792	13.631	13.812	40.54	40.60	1.128	1.129	1.131
11		0.250	13.816	13.820	13.822	40.66	40.67	1.131	1.131	1.132

Height of Solids, H_s = 6.482 cm

Incr. Number	σ'_{vc} (kgf/cm²)	Time (min)			Coef. of Consolidation cm²/s			C_c	m_v cm²/kg	k x 10^{-4} cm²/s
		Duration (hours)	t_{sc} (√t)	t_{sc} (log)	√t	log t	Average			
3	0.016									
4	0.031	71		955		0.00039	0.00039	1.466	8.526	332.5
5	0.063	46	2704	524	0.00047	0.00057	0.00052	0.968	3.176	165.2
6	0.127	52	1646	288	0.00065	0.00086	0.00076	0.677	1.201	91.3
7	0.246	50	833	209	0.00111	0.00103	0.00107	0.568	0.549	58.8
8	0.499	40	758	155	0.00108	0.00122	0.00115	0.453	0.234	26.9
9	1.032	54	615	112	0.00117	0.00149	0.00133	0.453	0.122	16.2
10	0.535	40	16.6	6.3	0.04049	0.02478	0.03264	-0.011	-0.003	
11	0.250	142	69	22	0.00977	0.00699	0.00838	0.006	0.003	2.8

Table B.10: Results of Consolidometer Test for Batch 203.

CONSOLIDATION TEST DATA SHEET Batch 203 DATE: 10/11/1987 DONE BY : CPA/TRS

Incr. Number	Scale Load (kg)	σ'_{vc} (ksc)	Height of Sample			Water Content, %		Void Ratio , e		
			H_{to} ,cm	H_{100},cm	H_f ,cm	W_{c100},%	W_{cf}, %	e_{to}	e_{100}	e_f
5		0.059			18.070		64.72			1.802
6		0.125			16.988		58.69			1.635
7		0.280	16.286	15.709	15.569	51.57	50.79	1.526	1.436	1.415
8		0.519	15.059	14.647	14.499	45.71	44.83	1.335	1.273	1.249
9		1.002	14.110	13.705	13.673	40.41	40.23	1.189	1.125	1.120
10		0.500			13.704		40.40			1.125
11		0.250			13.757		40.70			1.133

Incr Number	σ'_{vc} (ksc)	Time (min)			Coef. of Consolidation cm^2/s			C_c	m_v cm^2/kg	k $\times 10^{-6}$ cm^2/s
		Duration (hours)	t_{50} (√t)	t_{50} (log)	√t	log t	Average			
5	0.059									
6	0.125	22	1924		0.00053		0.00053			
7	0.280	26	1276	257	0.00073	0.00085	0.00079	0.568	0.508	40.2
8	0.519	47	889	186	0.00090	0.00100	0.00095	0.608	0.292	27.7
9	1.002	49	591	126	0.00119	0.00130	0.00125	0.518	0.140	17.5
10	0.500	24								
11	0.250	64								

Table B.11: Results of Consolidometer Test for Batch 204.

CONSOLIDATION TEST DATA SHEET : Batch 204 DATE: 11/27/1987 DONE BY : CPA/TRS

Incr Number	Scale Load (kg)	σ'_{vc} (ksc)	Height of Sample			Water Content, %		Void Ratio , e		
			H_{so} ,cm	H_{100},cm	H_f ,cm	W_{c100},%	W_{cf} , %	e_{so}	e_{100}	e_f
5		0.062			17.051		62.11			1.730
6		0.125			15.903		55.51			1.549
7		0.250	15.429	15.590	14.910	50.09	49.60	1.470	1.395	1.387
8		0.506	14.465	14.032	13.970	44.75	44.40	1.316	1.246	1.236
9		1.003	13.553	13.165	13.134	39.76	39.53	1.170	1.106	1.103
10		0.500			13.175		39.83			1.109
11		0.250			13.235		40.15			1.119

Incr Number	σ'_{vc} (ksc)	Time (min)			Coef. of Consolidation cm^2/s			C_c	m_v cm^2/kg	k x 10^{-6} cm^2/s
		Duration (hours)	t_{50} (√t)	t_{50} (log)	√t	log t	Average			
5	0.062									
6	0.125	96								
7	0.250	46	1088	251	0.00077	0.00078	0.00078	0.512	0.499	38.9
8	0.506	25	681	169	0.00109	0.00102	0.00106	0.487	0.251	26.6
9	1.003	51	539	145	0.00120	0.00104	0.00112	0.463	0.127	14.3
10	0.500	25								
11	0.250	96								

Table B.12: Results of Consolidometer Test for Batch 205.

CONSOLIDATION TEST DATA SHEET : Batch 205 DATE: 05/02/1988 DONE BY : CPA/TKS

Incr. Number	Scale Load (kg)	σ'_{vc} (ksc)	Height of Sample			Water Content, %		Void Ratio , e		
			H_{50} ,cm	H_{100},cm	H_f ,cm	W_{c100},%	W_{cf}, %	e_{50}	e_{100}	e_f
4		0.0312			20.206		76.77			2.134
5		0.063			18.088		64.96			1.809
6		0.125	17.427	16.750	16.750	57.94	57.49	1.706	1.601	1.601
7		0.250	16.124	15.466	15.428	50.33	50.12	1.504	1.402	1.396
8		0.500	14.965	14.481	14.439	44.84	44.61	1.324	1.249	1.242
9		1.000	14.064	13.706	13.653	40.52	40.23	1.184	1.128	1.120
10		0.500	13.671	13.682	13.685	40.39	40.40	1.123	1.125	1.125
11		0.250			13.731		40.66			1.132

Incr Number	σ'_{vc} (ksc)	Time (min)			Coef. of Consolidation cm^2/s			C_c	m_v cm^2/kg	k x 10^{-4} cm^2/s
		Duration (hours)	t_{50} (√t)	t_{50} (log)	√t	log t	Average			
4	0.0312									
5	0.0625	48	3340	692	0.00039	0.00044	0.00042	1.078	3.297	138.5
6	0.125	45	1900	338	0.00056	0.00063	0.00060	0.899	1.240	74.4
7	0.250	25	1397	269	0.00066	0.00079	0.00073	0.661	0.636	46.4
8	0.500	45	732	190	0.00106	0.00097	0.00103	0.508	0.263	27.1
9	1.000	43	557	138	0.00125	0.00118	0.00122	0.402	0.111	13.5
10	0.500	43		8.5						
11	0.250	96								

Table B.13: Results of Consolidometer Test for Batch 206.

CONSOLIDATION TEST DATA SHEET . Batch 206 DATE. 11/12/1986 DONE BY : T.H. Seah

Incr Number	Scale Load (kg)	σ'_{vc} (ksc)	Height of Sample			Water Content, %		Void Ratio , e		
			H_{so} ,cm	H_{100},cm	H_f ,cm	W_{c100},%	W_{cf}, %	e_{so}	e_{100}	e_f
4		0.0317	16.334	15.643	15.622	67.72	67.574	2.013	1.886	1.882
5		0.0618	15.164	14.706	14.674	61.50	61.297	1.797	1.713	1.707
6		0.1246	14.271	13.869	13.844	55.95	55.794	1.633	1.558	1.554
7		0.2492	13.409	12.974	12.949	50.05	49.863	1.474	1.393	1.389
8		0.4650	12.639	12.328	12.291	45.75	45.508	1.332	1.274	1.267
9		0.9770	11.945	11.598	11.565	40.92	40.969	1.204	1.140	1.133
10		0.4650	11.583	11.600	11.630	40.93	40.930	1.137	1.140	1.140
11		0.265	11.617	11.633	11.646	41.140	41.235	1.143	1.146	1.148

Height of Solids, H_s = 5.4208 cm

Incr Number	σ'_{vc} (ksc)	Time (min)			Coef. of Consolidation cm^2/s			C_c	m_v cm^2/kg	k x 10^{-4} cm^2/s
		Duration (hours)	t_{50} (√t)	t_{50} (log)	√t	log t	Average			
3	0.0156									
4	0.0317	48	1776	407	0.00053	0.00054	0.00054			
5	0.0618	48	1225	363	0.00066	0.00052	0.00059	0.597	2.055	121.2
6	0.1246	48	841	209	0.00086	0.00080	0.00083	0.509	0.937	77.8
7	0.2492	48	506	123	0.00126	0.00120	0.00123	0.548	0.535	65.8
8	0.4650	48	400	100	0.00141	0.00131	0.00136	0.439	0.236	31.2
9	0.9770	48	298	71	0.00169	0.00166	0.00168	0.416	0.119	19.9
10	0.4650	48	17.1	6.3	0.02772	0.01745	0.02259	0.000	0.000	
11	0.2650	96	43	20	0.01109	0.00555	0.00832	0.025	0.014	11.6

Table B.14: Results of Consolidometer Test for Batch 207.

CONSOLIDATION TEST DATA SHEET : Batch 207 DATE 12/13/1988 DONE BY : T.B. Seah

Incr Number	Scale Load (kg)	σ'_{vc} (ksc)	Height of Sample			Water Content, %		Void Ratio , e		
			H_{ic} ,cm	H_{100},cm	H_f ,cm	W_{c100},%	W_{cf}, %	e_{s0}	e_{100}	e_f
1		0.017			21.130		74.860			2.085
2		0.0316	20.432	19.734	19.716	67.54	67.461	1.983	1.881	1.879
3		0.0616	19.028	18.330	18.303	60.18	60.039	1.778	1.676	1.672
4		0.1259	17.772	17.241	17.166	54.47	54.269	1.595	1.517	1.511
5		0.250	16.717	16.265	16.204	49.37	49.039	1.443	1.375	1.366
6		0.500	15.812	15.419	15.368	44.92	44.653	1.309	1.251	1.244
7		1.000	14.972	14.576	14.530	40.50	40.263	1.186	1.126	1.121
8		0.500	14.546	14.562	14.565	40.43	40.444	1.124	1.126	1.126
9		0.250	14.585	14.610	14.624	40.69	40.754	1.130	1.133	1.135

Height of Solids, H_s = 6.84965cm

Incr Number	σ'_{vc} (ksc)	Time (min)			Coef. of Consolidation cm^2/s			C_c	a_v cm^2/kg	k x 10^{-6} cm^2/s
		Duration (hours)	t_{50} (√t)	t_{50} (log)	√t	log t	Average			
S	0.0000									
1	0.0172	96								
2	0.0316	48	2370	543	0.00062	0.00063	0.00062	0.772	4.749	294.4
3	0.0616	48	2078	450	0.00062	0.00066	0.00064	0.707	2.460	157.4
4	0.1259	48	1551	336	0.00072	0.00077	0.00075	0.693	0.917	68.8
5	0.250	48	931	233	0.00106	0.00099	0.00102	0.477	0.468	47.8
6	0.500	48	621	150	0.00142	0.00137	0.00139	0.412	0.215	29.9
7	1.000	48	489	116	0.00162	0.00159	0.00161	0.409	0.113	18.1
8	0.500	48	40.3	7.8	0.01855	0.02226	0.02041	-0.007	-0.002	
9	0.250	96	71.9	28	0.01046	0.00624	0.00835	0.023	0.013	11.0

Table B.15: Results of Oedometer Test No. 1 for Batch 200.

CONSOLIDATION TEST DATA SHEET : Batch 200 1 DATE: 06/23/1987 DONE BY CPA/TMS

Incr Number	Scale Load (kg)	σ'_{vc} (ksc)	Height of Sample			Vertical Strain, %		Void Ratio , e		
			H_{so} ,cm	H_{100},cm	H_f ,cm	ε_{100}, %	ε_f , %	e_{so}	e_{100}	e_f
1	3.93	0.125			2.4160		0.00			1.127
2	7.86	0.25	2.4157	2.4141	2.3926	0.07	0.93	1.127	1.125	1.107
3	15.72	0.50	2.3929	2.3887	2.3845	1.13	1.30	1.105	1.103	1.099
4	31.44	1.00	2.3729	2.3627	2.3492	2.21	2.76	1.089	1.080	1.068
5	62.88	2.00	2.2610	2.2265	2.2155	7.84	8.30	0.991	0.960	0.950
6	125.76	4.00	2.1360	2.1089	2.0955	12.72	13.26	0.850	0.656	0.845
7	251.52	8.00	2.0233	2.0063	1.9915	16.96	17.57	0.781	0.766	0.753
8	125.76	4.00	1.9925	1.9934	1.9976	17.49	17.31	0.754	0.755	0.759
9	62.88	2.00	2.0016	2.0056	2.0102	16.99	16.79	0.763	0.766	0.770
10	125.76	4.00	2.0083	2.0064	2.0022	16.93	17.13	0.746	0.766	0.763
11	251.76	8.00	1.9944	1.9865	1.9788	17.78	18.09	0.756	0.749	0.742
12	502.04	16.00	1.9429	1.9069	1.8845	21.07	22.00	0.711	0.679	0.659
13	251.76	8.00	1.8865	1.8885	1.8927	21.85	21.66	0.661	0.663	0.666
14	125.76	4.00	1.8953	1.8976	1.9063	21.45	21.10	0.669	0.671	0.678
15	31.44	1.00	1.9219	1.9375	1.9392	19.80	19.73	0.692	0.706	0.707

Height of Solids H_s =1.13589 cm

Incr Number	σ'_{vc} (ksc)	Time (min)			Coef. of Consolidation cm^2/s			k $\times 10^{-4}$ cm^2/s	C_R (%)	C_c (%)	C_c/C_R
		Duration (hours)	t_{90} ($\sqrt{t}$)	t_{50} (log)	$\sqrt{t}$	log t	Average				
0	0.00										
1	0.125	24	1.32		0.0156						
2	0.25	24	2.89	0.514	0.0071		0.0071	4.3	0.23		
3	0.50	24	1.32	0.452	0.0151	0.0102	0.0127	5.3	3.52	0.006	0.003
4	1.00	24	2.40	1.93	0.0081	0.0023	0.0052	6.7	3.60	0.028	0.008
5	2.00	24	16.82	4.57	0.0012	0.0009	0.0011	6.3	18.70	0.210	0.019
6	4.00	24	9.00	2.78	0.0018	0.0013	0.0016	4.2	16.21	0.210	0.012
7	8.00	24	5.76	2.32	0.0025	0.0015	0.0020	2.4	14.09	0.330	0.022
8	4.00	24		4.60		0.0007				0.230	0.016
9	2.00	24		0.70		0.0045			1.69		
10	4.00	24	1.00	0.25	0.0145	0.0128	0.0137	1.9	-0.10		
11	8.00	24	1.25	0.79	0.0109	0.0040	0.0075	1.9	2.49		
12	16.00	24	4.00	1.22	0.0032	0.0025	0.0029	1.5	10.93	0.110	0.016
13	8.00	24		0.29		0.0099				0.230	0.021
14	4.00	24		0.36		0.0080			1.43		
15	1.00	24		1.81		0.0016			2.74		

Table B.16: Results of Oedometer Test No. 2 for Batch 200.

CONSOLIDATION TEST DATA SHEET Batch 200 2 DATE: 06/25/1987 DONE BY CPA/TWS

Incr Number	Scale Load (kg	σ'_{vc} (ksc)	Height of Sample			Vertical Strain, %		Void Ratio, e		
			H_{to}, cm	H_{tcc}, cm	H_f, cm	ϵ_{tac}, %	ϵ_f, %	e_{to}	e_{tcc}	e_f
1	3.95	0.125			2.0167	0.00				1.179
2	7.90	0.25	2.1062	2.0141	2.0079	0.13	0.44	1.178	1.176	1.169
3	15.81	0.50	2.0060	2.0045	2.0013	0.60	0.77	1.168	1.166	1.162
4	31.61	1.00	1.9966	1.9701	1.9543	2.31	3.10	1.145	1.129	1.111
5	63.22	2.00	1.9069	1.8777	1.8592	6.69	7.81	1.002	1.035	1.009
6	126.44	4.00	1.8136	1.7725	1.7592	12.11	12.77	0.959	0.915	0.901
7	252.89	8.00	1.7247	1.6955	1.6737	16.26	17.01	0.863	0.824	0.806
8	126.44	4.00			1.6512		16.64			0.816
9	63.22	2.00	1.6839	1.6870	1.6913	16.35	16.13	0.819	0.823	0.827
10	126.44	4.00			1.6544		16.46			0.820
11	252.89	8.00	1.6655	1.6760	1.6681	16.69	17.35	0.815	0.811	0.800
12	505.78	16.00	1.6423	1.5935	1.5917	20.99	21.07	0.774	0.722	0.720
13	252.89	8.00			1.5959		20.72			0.727
14	126.44	4.00			1.6055		20.15			0.739
15	31.61	1.00			1.6407		18.64			0.773

Incr Number	σ'_{vc} (ksc)	Time (min)			Coef. of Consolidation cm^2/s			k x 10^{-6} cm^2/s	CR (%)	Ce (%)	Ce/CR
		Duration (hours)	t_{90} ($\sqrt{t}$)	t_{50} (log)	$\sqrt{t}$	log t	average				
1	0.125										
		24							0.43		
2	0.25										
3	0.50	24	5.76	0.83	0.0025	0.0040	0.0033	6.3	1.56		
		24	3.80	1.90	0.0037	0.0017	0.0027	9.3	5.65	0.049	0.014
4	1.00	24	12.25	4.60	0.0011	0.0007	0.0009	4.2	15.21	0.370	0.035
5	2.00	24	8.41	2.00	0.0014	0.0014	0.0014	3.9	17.34	0.210	0.013
6	4.00	24	3.90	1.30	0.0027	0.0019	0.0022	2.6	13.85	0.310	0.020
7	8.00									0.210	0.015
8	4.00	24									
		24							1.20		
9	2.00										
10	4.00	24	1.05		0.0096		0.0096	2.0	0.43		
		24	0.77	0.25	0.0132	0.0116	0.0124	1.5	1.36		
11	8.00	24	3.06	1.00	0.0030	0.0022	0.0026	1.6	13.62	0.104	0.014
12	16.00									0.192	0.014
13	8.00	24									
14	4.00	24									
15	1.00	24									

Table B.17: Results of Oedometer Test No. 3 for Batch 200.

CONSOLIDATION TEST DATA SHEET : Batch 200-3 DATE: 07/27/1987 DONE BY : CPA/THS

Incr. Number	Scale Load (kg)	σ'_{vc} (ksc)	Height of Sample			Vertical Strain,%		Void Ratio , e		
			H_{s0} ,cm	H_{t100},cm	H_f ,cm	ϵ_{100}, %	ϵ_f , %	e_{s0}	e_{t100}	e_f
1	3.95	0.125			2.3765		0.00			1.166
2	7.90	0.25	2.3726	2.3688	2.3646	0.33	0.50	1.162	1.159	1.155
3	25.27	0.80	2.3473	2.3301	2.3194	1.95	2.41	1.139	1.124	1.114
4	37.91	1.20	2.2988	2.2781	2.2687	4.14	4.54	1.095	1.076	1.068
5	63.18	2.00	2.2242	2.1797	2.1708	8.28	8.67	1.027	0.987	0.978
6	126.36	4.00	2.1203	2.0697	2.0562	12.91	13.50	0.935	0.886	0.874
7	252.72	8.00	2.0136	1.9709	1.9709	17.07	17.66	0.835	0.796	0.784
8	126.36	4.00			1.9680		17.22			0.794
9	63.18	2.00	1.9748	1.9817	1.9822	16.64	16.62	0.800	0.806	0.807
10	126.36	4.00			1.9806		16.68			0.805
11	252.72	8.00	1.9712	1.9618	1.9514	17.48	17.92	0.797	0.788	0.778
12	505.44	16.00	1.9156	1.8798	1.8656	20.93	21.53	0.746	0.713	0.700
13	252.72	8.00	1.8660	1.8663	1.8681	21.501	21.45	0.701	0.701	0.703
14	126.36	4.00			1.8811		20.88			0.714
15	31.59	1.00	1.8968	1.9124	1.9147	19.56	19.56	0.729	0.743	0.743

Height of Solids, H_s = 1.09728 cm

Incr. Number	σ'_{vc} (ksc)	Time (min)			Coef. of Consolidation cm^2/s			k x 10^{-4}	CR (%)	Ca (%)	Ca/CR
		Duration (hours)	t_{90} ($\sqrt{t}$)	t_{50} (log)	$\sqrt{t}$	log t	Average				
1	0.125										
2	0.25	24	3.06	0.60	0.0065	0.0077	0.0071	18.4	1.10		
3	0.80	24	4.49	1.55	0.0043	0.0029	0.0036	10.4	3.21		
4	1.20	24	20 25	13.80	0.0009	0.0003	0.0006	3.3	12.44	0.175	0.022
5	2.00	24	18.06	7.07	0.0010	0.0006	0.0008	4.3	18.66	0.350	0.023
6	4.00	24	10.24	3.20	0.0016	0.0012	0.0014	3.7	15.38	0.266	0.016
7	8.00	24	5.66	2.00	0.0025	0.0017	0.0021	2.5	13.82	0.282	0.019
8	4.00	24								0.210	0.015
9	2.00	24									
10	4.00	24							0.13		
11	8.00	24	1.44	0.32	0.0094	0.0100	0.0097	2.3	2.66		
12	16.00	24	3.04	1.48	0.0043	0.0021	0.0032	1.7	11.46	0.195	0.028
13	8.00	24								0.196	0.017
14	4.00	24									
15	1.00	24									

Table B.18: Results of Oedometer Test No. 4 for Batch 201.

CONSOLIDATION TEST DATA SHEET : Batch 201 DATE: 06/22/1987 DONE BY : CPA/THS

Incr. Number	Scale Load (kg)	σ'_{vc} (ksc)	Height of Sample			Vertical Strain,%		Void Ratio , e		
			H_{s0} ,cm	H_{100},cm	H_f ,cm	ϵ_{100}, %	ϵ_f , %	e_{s0}	e_{100}	e_f
1	3.94	0.125			2.3820		0.00			1.172
2	7.88	0.25			2.3736		0.35			1.165
3	15.76	0.50	2.3694	2.3652	2.3576	0.71	1.02	1.161	1.157	1.150
4	25.21	0.80	2.3513	2.3446	2.3328	1.57	2.07	1.144	1.138	1.127
5	37.81	1.20	2.3242	2.2922	2.2848	3.77	4.08	1.120	1.090	1.084
6	63.02	2.00	2.2449	2.2043	2.1952	7.46	7.84	1.047	1.010	1.002
7	126.04	4.00	2.1376	2.0858	2.0793	12.44	12.71	0.949	0.902	0.896
8	252.08	8.00	2.0353	1.9870	1.9686	16.58	17.36	0.856	0.812	0.795
9	126.04	4.00			1.9762		17.03			0.802
10	63.02	2.00	1.9808	1.9860	1.9919	16.62	16.38	0.806	0.811	0.817
11	126.04	4.00	1.9901	1.9873	1.9830	16.57	16.75	0.815	0.812	0.808
12	252.08	8.00	1.9766	1.9689	1.9578	17.34	17.81	0.803	0.796	0.785
13	504.16	16.00	1.9212	1.8814	1.8327	21.02	23.00	0.752	0.716	0.671
14	252.08	8.00	1.8674	1.8694	1.8755	21.52	21.26	0.703	0.705	0.710
15	126.04	4.00	1.8801	1.8859	1.8885	20.83	20.72	0.715	0.720	0.722
16	31.51	1.00	1.8938	1.9204	1.9228	19.38	19.28	0.727	0.751	0.754

Height of Solids, H_s = 1.09652 cm

Incr. Number	σ'_{vc} (ksc)	Time (min)			Coef. of Consolidation cm^2/s			k x 10^{-4} cm^2/s	CR (%)	Ca (%)	Ca/CR
		Duration (hours)	t_{90} ($\sqrt{t}$)	t_{50} (log)	$\sqrt{t}$	log t	Average				
1	0.125										
2	0.25	24	4.62		0.0043				1.16		
3	0.50	24	2.89	1.55	0.0069	0.0080	0.0075	10.6	2.00		
4	0.80	24	5.57	2.00	0.0035	0.0022	0.0029	8.5	4.21		
5	1.20	24	20.25	10.00	0.0010	0.0004	0.0007	5.2	12.50	0.230	0.017
6	2.00	24	18.06	5.62	0.0010	0.0007	0.0009	4.3	14.71	0.250	0.016
7	4.00	24	7.56	2.95	0.0021	0.0013	0.0017	4.6	16.50	0.270	0.018
8	8.00	24	5.29	1.58	0.0028	0.0022	0.0025	3.1	13.75	0.275	0.020
9	4.00	24									
10	2.00	24		0.50		0.0064					
11	4.00	24	0.67	0.40	0.0021	0.0082	0.0052	0.6	-0.16	0.010	0.008
12	8.00	24	2.25	0.63	0.0062	0.0051	0.0057	1.3	2.56	0.095	0.013
13	16.00	24	3.45	1.20	0.0038	0.0024	0.0031	1.7	12.22	0.147	0.012
14	8.00	24		0.28		0.0102					
15	4.00	24							2.29		
16	1.00	24							2.41		

Table B.19: Results of Oedometer Test No. 5 for Batch 202.

CONSOLIDATION TEST DATA SHEET : Batch 202 - Top DATE: 08/08/1987 DONE BY : CPA/THS

Incr. Number	Scale Load (kg)	σ'_{vc} (ksc)	Height of Sample			Vertical Strain,%		Void Ratio , e		
			H_{s0} ,cm	H_{100},cm	H_f ,cm	ϵ_{100}, %	ϵ_f , %	e_{s0}	e_{100}	e_f
1	3.96	0.125			1.9870		0.00			1.164
2	7.92	0.25	1.9829	1.9788	1.9729	0.41	0.49	1.160	1.155	1.153
3	15.84	0.50		1.9655		1.08			1.141	
4	25.34	0.80	1.9624	1.9474	1.9373	1.99	2.50	1.137	1.121	1.110
5	38.02	1.20	1.9210	1.9046	1.8999	4.14	4.38	1.092	1.074	1.069
6	63.36	2.00	1.8673	1.8348	1.8255	7.66	8.13	1.034	0.998	0.988
7	126.72	4.00	1.7807	1.7360	1.7257	12.63	13.15	0.939	0.891	0.879
8	252.44	8.00	1.6848	1.6439	1.6332	17.27	17.81	0.839	0.790	0.779
9	126.72	4.00	1.6360	1.6388	1.6408	17.52	17.42	0.782	0.785	0.787
10	63.36	2.00	1.6444	1.6481	1.6517	17.05	16.87	0.791	0.795	0.709
11	126.72	4.00	1.6493	1.6470	1.6448	17.11	17.22	0.796	0.794	0.791
12	252.44	8.00	1.6397	1.6346	1.6270	17.73	18.12	0.786	0.780	0.772
13	504.88	16.00	1.5927	1.5583	1.5466	21.57	22.16	0.735	0.697	0.684
14	252.44	8.00			1.5533		21.83			0.692
15	126.72	4.00	1.5571	1.5610	1.5647	21.44	21.25	0.696	0.700	0.704
16	31.68	1.00	1.5805	1.5963	1.5993	19.66	19.51	0.721	0.739	0.742

Height of Solids, H_s = 0.91821 cm

Incr. Number	σ'_{vc} (ksc)	Time (min)			Coef. of Consolidation cm^2/s			k x 10^{-6} cm^2/s	CR (%)	C_α (%)	C_α/CR
		Duration (hours)	t_{90} ($\sqrt{t}$)	t_{50} (log)	$\sqrt{t}$	log t	Average				
1	0.125										
2	0.25	24	2.33	0.60	0.0060	0.0054	0.0057	18.8	1.36	0.071	0.040
3	0.50	24	1.96		0.0070		0.0070	18.8	2.23		
4	0.80	24	2.56	1.44	0.0053	0.0022		11.7	4.46	0.230	0.028
5	1.20	24	12.25	8.50	0.0011	0.0004	0.0008	4.5	12.21	0.185	0.013
6	2.00	24	11.90	4.07	0.0010	0.0007	0.0009	4.1	15.87	0.277	0.017
7	4.00	24	5.06	1.74	0.0021	0.0015	0.0018	4.9	16.51	0.278	0.017
8	8.00	24	3.06	1.07	0.0032	0.0022	0.0027	3.6	15.41	0.243	0.016
9	4.00	24		0.15		0.0147					
10	2.00	24		0.32		0.0084			1.56		
11	4.00	24	0.86	0.17	0.0112	0.0132	0.0122	4.1	0.20	0.025	0.022
12	8.00	24	0.64	0.16	0.0148	0.0139	0.0144	2.7	2.06	0.119	0.016
13	16.00	24	1.56	0.78	0.0056	0.0027	0.0042	2.5	12.76	0.275	0.022
14	8.00	24									
15	4.00	24		0.21		0.0095			1.30		
16	1.00	24		1.25		0.0016			5.91		

Table B.20: Results of Oedometer Test No. 6 for Batch 202.

GEOTECHNICAL LABORATORY - DEPARTMENT OF CIVIL ENGINEERING, KIT

CONSOLIDATION TEST DATA SHEET : Batch 202 DATE: 11/28/1987 DONE BY : DJD/TWS

Incr. Number	Scale Load (kg)	σ_{vc} (ksc)	Height of Sample			Vertical Strain, %		Void Ratio , e		
			H_{so} ,cm	H_{100},cm	H_f ,cm	ϵ_{100}, %	ϵ_f , %	e_{so}	e_{100}	e_f
1	4.38	0.125	2.2472	2.2456	2.2453	0.14	0.153	1.132	1.131	1.130
2	9.75	0.25	2.2410	2.2389	2.2382	0.44	0.465	1.126	1.124	1.124
3	17.50	0.50	2.2302	2.2248	2.2230	1.06	1.143	1.116	1.111	1.109
4	31.50	0.90	2.2095	2.2030	2.1972	2.03	2.290	1.096	1.090	1.085
5	52.50	1.50	2.1616	2.1260	2.1185	5.456	5.790	1.051	1.017	1.010
6	105.00	3.00	2.0525	1.9980	1.9890	11.15	11.549	0.947	0.896	0.887

Incr. Number	σ_{vc} (ksc)	Time (min)			Coef. of Consolidation cm^2/s			k $\times 10^{-4}$ cm^2/s	CR (%)	Cα (%)	Cα/CR
		Duration (hours)	t_{50} ($\sqrt{t}$)	t_{50} (log)	$\sqrt{t}$	log t	Average				
0	0.00										
1	0.125	0.3	8.23		0.0022					0.011	
2	0.25	0.6	1.76	0.56	0.0101	0.0073	0.0087	20.8	1.002	0.032	0.021
3	0.50	2.6	2.29	0.70	0.0083	0.0059	0.0071	17.9	2.076	0.058	0.020
4	0.90	3.6	3.78	0.75	0.0046	0.0053	0.0050	12.4	3.798	0.174	0.018
5	1.50	12.5	17.18	6.49	0.0010	0.0006	0.0008	4.8	15.43	0.360	0.021
6	3.00	28.0	10.14	3.21	0.0015	0.0011	0.0013	5.2	18.91	0.200	0.011

Table B.21: Results of Oedometer Test No. 7 for Batch 203.

GEOTECHNICAL LABORATORY · DEPARTMENT OF CIVIL ENGINEERING, MIT

CONSOLIDATION TEST DATA SHEET : Batch 203 DATE: 01/29/1988 DONE BY : DJD/THS

Incr. Number	Scale Load (kg)	σ_{vc} (ksc)	Height of Sample			Vertical Strain,%		Void Ratio , e		
			H_{s0} ,cm	H_{100},cm	H_f ,cm	ϵ_{100}, %	ϵ_f , %	e_{s0}	e_{100}	e_f
1	4.38	0.125	2.3078	2.3065	2.3063	0.11	0.120	1.137	1.136	1.136
2	9.75	0.25	2.3020	2.2983	2.2972	0.46	0.513	1.132	1.129	1.127
3	17.50	0.50	2.2884	2.2812	2.2793	1.20	1.284	1.119	1.113	1.111
4	31.50	0.90	2.2687	2.2600	2.2553	2.12	2.326	1.101	1.093	1.089
5	52.50	1.50	2.2197	2.1870	2.1805	5.28	5.565	1.056	1.025	1.019
6	105.00	3.00	2.1180	2.0600	2.0523	10.78	11.118	0.962	0.908	0.901

Incr. Number	σ_{vc} (ksc)	Time (min)			Coef. of Consolidation cm^2/s			k x 10^{-4} cm^2/s	CR (%)	Cα (%)	Cα/CR
		Duration (hours)	t_{50} (√t)	t_{50} (log)	√t	log t	Average				
0	0.00										
1	0.125	0.3	4.27	1.00	0.0044	0.0044	0.0044			0.022	
2	0.25	0.9	3.27	0.86	0.0057	0.0051	0.0054	15.4	1.180	0.027	0.015
3	0.50	1.9	3.56	1.08	0.0052	0.0040	0.0046	13.7	2.464	0.068	0.022
4	0.90	1.7	3.14	0.89	0.0059	0.0047	0.0053	12.3	3.597	0.174	0.019
5	1.50	14.4	17.25	6.49	0.0010	0.0056	0.0033	17.8	14.25	0.280	0.017
6	3.00	24.0	12.54	3.34	0.0013	0.0010	0.0012	4.6	18.27	0.200	0.011

Table B.22: Results of Oedometer Test No. 8 for Batch 204.

CONSOLIDATION TEST DATA SHEET : Batch 204 - Top DATE: 01/26/1988 DONE BY : CPA/THS

Incr. Number	Scale Load (kg)	σ'_{vc} (ksc)	Height of Sample			Vertical Strain,%		Void Ratio , e		
			H_{50} ,cm	H_{100},cm	H_f ,cm	ϵ_{100}, %	ϵ_f , %	e_{50}	e_{100}	e_f
1	3.94	0.125			2.3401		0.03			1.159
2	7.88	0.25			2.3320		0.31			1.151
3	15.76	0.50	2.3246	2.3171	2.3072	0.95	1.38	1.144	1.138	1.128
4	25.22	0.80	2.2996	2.2921	2.2849	2.02	2.33	1 121	1.115	1.108
5	37.82	1.20	2.2666	2.2484	2.2420	3.89	4.16	1.091	1.074	1.068
6	63.04	2.00	2.1995	2.1570	2.1513	7.79	8.04	1.029	0.990	0.985
7	126.08	4.00	2.0994	2.0474	2.0344	12.49	13.03	0.937	0.889	0.877
8	252.16	8.00	1.9872	1.9400	1.9299	17.07	17.50	0.833	0.790	0.780
9	126.08	4.00	1.9335	1.9372	1.9379	17.19	17.16	0.784	0.787	0.788
10	63.04	2.00	1.9501	1.9623	1.9509	16.12	16.60	0.799	0.810	0.800
11	126.08	4.00	1.9474	1.9439	1.9432	16.91	16.93	0.796	0.793	0.793
12	252.16	8.00	1.9344	1.9255	1.9206	17.69	17.90	0.764	0.776	0.772
13	504.32	16.00	1.8816	1.8426	1.8330	21.23	21.65	0.736	0.700	0.691
14	252.16	8.00								
15	126.08	4.00								
16	31.52	1.00								

Height of Solids, H_s = 1.0840 cm

Incr. Number	σ'_{vc} (ksc)	Time (min)			Coef. of Consolidation cm^2/s			k x 10^{-4} cm^2/s	CR (%)	Ca (%)	Ca/CR
		Duration (hours)	t_{90} ($\sqrt{t}$)	t_{50} (log)	$\sqrt{t}$	log t	Average				
1	0.125										
		24									
2	0.25										
		24	3.80	1.05	0.0050	0.0042	0.0046	11.8	2.13		
3	0.50									0.044	0.012
		24	3.24	1.44	0.0058	0.0030	0.0044	12.8	5.24		
4	0.80									0.165	0.021
		24	10.60	8.04	0.0017	0.0005	0.0013	8.3	10.62		
5	1.20									0.296	0.021
		24	14.10	5.01	0.0012	0.0008	0.0010	5.1	17.58		
6	2.00									0.281	0.018
		24	7.29	2.40	0.0022	0.0015	0.0018	4.6	15.61		
7	4.00									0.296	0.019
		24	4.84	1.48	0.0034	0.0022	0.0018	2.4	15.21		
8	8.00									0.296	0.019
		24		0.17		0.0185					
9	4.00										
		24		0.85		0.0037			3.55		
10	2.00										
		24	0.95	0.25	0.0141	0.0217	0.0179	8.4	2.62		
11	4.00									0.020	0.008
		24	0.68	0.24	0.0195	0.0128	0.0161	3.8	2.59		
12	8.00									0.103	0.014
		24	4.31	0.85	0.0029	0.0026	0.0028	1.6	11.76		
13	16.00									0.265	0.023
		24									
14	8.00										
		24									
15	4.00										
		24									
16	1.00										

Table B.23: Results of Oedometer Test No. 9 for Batch 204.

CONSOLIDATION TEST DATA SHEET : Batch 204 - Bottom DATE: 02/18/1988 DONE BY : CPA/THS

Incr. Number	Scale Load (kg)	σ'_{vc} (ksc)	Height of Sample			Vertical Strain,%		Void Ratio , e		
			H_{so} ,cm	H_{100},cm	H_f ,cm	ϵ_{100}, %	ϵ_f , %	e_{so}	e_{100}	e_f
1	3.94	0.125			2.3459		0.08			1.129
2	7.88	0.25			2.3400		0.18			1.123
3	15.76	0.50	2.3377	2.3353	2.3274	0.37	0.71	1.121	1.119	1.112
4	25.22	0.80	2.3252	2.3230	2.3139	0.90	1.28	1.110	1.108	1.100
5	37.82	1.20	2.2990	2.2840	2.2725	2.56	3.05	1.087	1.073	1.062
6	63.04	2.00	2.2309	2.1892	2.1755	6.60	7.19	1.025	0.987	0.974
7	126.08	4.00	2.1278	2.0800	2.0592	11.26	12.15	0.931	0.887	0.869
8	252.16	8.00	2.0115	1.9637	1.9528	16.23	16.69	0.826	0.782	0.772
9	126.08	4.00	1.9537	1.9545	1.9591	16.62	16.42	0.773	0.774	0.778
10	63.04	2.00	1.9623	1.9655	1.9693	16.15	15.99	0.781	0.784	0.787
11	126.08	4.00	1.9679	1.9665	1.9634	16.11	16.24	0.786	0.784	0.782
12	252.16	8.00	1.9594	1.9553	1.9408	16.58	17.20	0.778	0.774	0.761
13	504.32	16.00	1.8975	1.8542	1.8494	20.90	21.10	0.722	0.683	0.678
14	252.16	8.00	1.8500	1.8506	1.8552	21.05	20.85	0.679	0.679	0.683
15	126.08	4.00	1.8590	1.8628	1.8664	20.53	20.38	0.687	0.690	0.694
16	31.52	1.00	1.8826	1.8987	1.9035	19.00	18.79	0.709	0.723	0.727

Height of Solids, H_s = 1.1020 cm

Incr. Number	σ'_{vc} (ksc)	Time (min)			Coef. of Consolidation cm^2/s			k x 10^{-4} cm^2/s	CR (%)	Cc (%)	Cc/CR
		Duration (hours)	t_{90} ($\sqrt{t}$)	t_{50} (log)	$\sqrt{t}$	log t	Average				
1	0.125										
		24									
2	0.25										
		24	5.06	1.00	0.00382	0.00449	0.00415	3.3	0.56		
3	0.50										
		24	5.06	1.26	0.00377	0.00352	0.00365	6.4	2.60		
4	0.80										
		24	23.58	6.03	0.00079	0.00072	0.00076	3.2	9.43		
5	1.20									0.179	0.013
		24	16.36	4.37	0.00107	0.00094	0.00101	5.2	18.21		
6	2.00									0.385	0.023
		24	6.84	2.24	0.00234	0.00166	0.00200	5.0	15.48		
7	4.00									0.295	0.018
		24	6.15	1.95	0.00232	0.00170	0.00201	2.8	16.51		
8	8.00									0.256	0.016
		24	3.06	0.73	0.00441	0.00429	0.00435	0.5			
9	4.00										
		24	2.49	0.85	0.00546	0.00372	0.00459	1.3	1.56		
10	2.00										
		24	1.01	0.33	0.01355	0.00837	0.01096	0.8	-0.13		
11	4.00									0.014	0.020
		24	1.56	0.32	0.00870	0.00985	0.00927	1.3	1.56		
12	8.00									0.116	0.015
		24	3.26	1.07	0.00390	0.00276	0.00333	2.2	14.32		
13	16.00									0.193	0.013
		24	1.32	0.25	0.00916	0.01237	0.01020	0.8			
14	8.00										
		24	1.56	0.42	0.00783	0.00675	0.00729	1.2			
15	4.00										
		24	5.53	1.32	0.00226	0.00220	0.00223	1.4			
16	1.00										

Table B.24: Results of Oedometer Test No. 10 for Batch 205.

CONSOLIDATION TEST DATA SHEET : Batch 205 - Top DATE: 01/06/1989 DONE BY : T.H. Seah

Incr. Number	Scale Load (kg)	σ'_{vc} (ksc)	Height of Sample			Vertical Strain,%		Void Ratio , e		
			H_{50} ,cm	H_{100},cm	H_f ,cm	ϵ_{100}, %	ϵ_f , %	e_{50}	e_{100}	e_f
1	7.94	0.25	2.0130	2.0101	2.0080	0.30	0.395	1.112	1.109	1.107
2	15.88	0.50	2.0079	2.0039	1.9998	0.81	1.047	1.102	1.098	1.093
3	25.40	0.80	1.9874	1.9781	1.9766	1.88	1.953	1.085	1.075	1.074
4	38.10	1.20	1.9583	1.9378	1.9327	3.88	4.132	1.054	1.033	1.028
5	63.50	2.00	1.8792	1.8678	1.8564	7.35	7.919	0.972	0.960	0.947
6	127.00	4.00	1.8176	1.7715	1.7611	17.13	12.643	0.907	0.858	0.848
7	254.00	8.00	1.7269	1.6852	1.6789	16.41	16.722	0.812	0.768	0.761
8	127.00	4.00	1.6815	1.6846	1.6853	16.44	16.404	0.764	0.767	0.768
9	63.50	2.00	1.6882	1.6930	1.6944	16.02	15.955	0.771	0.776	0.778
10	127.00	4.00	1.6928	1.6896	1.6888	16.19	16.233	0.776	0.773	0.772
11	254.00	8.00	1.6838	1.6775	1.6702	16.79	17.154	0.766	0.760	0.752
12	508.00	16.00	1.6436	1.6092	1.6024	20.18	20.515	0.724	0.688	0.681
13	254.00	8.00	1.6033	1.6090	1.6102	20.19	20.130	0.682	0.688	0.689
14	127.00	4.00	1.6112	1.6152	1.6170	19.88	19.794	0.690	0.695	0.696
15	63.50	2.00	1.6207	1.6263	1.6290	19.33	19.198	0.700	0.706	0.709
16	31.75	1.00	1.6322	1.6384	1.6412	18.72	18.593	0.712	0.719	0.722

Incr. Number	σ'_{vc} (ksc)	Time (min)			Coef. of Consolidation cm^2/s			k x 10^{-4} cm^2/s	CR (%)	Cα (%)	Cα/CR
		Duration (Hours)	t_{50} ($\sqrt{t}$)	t_{50} (log)	$\sqrt{t}$	log t	Average				
0	0.00										
1	0.25	24	1.09	0.30	0.0131	0.0111	0.0121		0.999[a]	0.044	0.033
2	0.50	24	2.63	0.65	0.0054	0.0051	0.0053	9.8	1.694	0.099	0.029
3	0.80	24	3.10	5.48	0.0045	0.0006	0.0025	10.7	5.242	0.077	0.009
4	1.20	24	13.96	17.63	0.0010	0.0002	0.0006	3.1	11.36	0.396	0.029
5	2.00	24	17.61	5.47	0.0007	0.0005	0.0006	2.7	15.64	0.552	0.035
6	4.00	24	6.31	2.18	0.0019	0.0012	0.0016	4.1	15.88	0.275	0.018
7	8.00	24	3.88	1.53	0.0027	0.0016	0.0022	2.7	14.22	0.167	0.012
8	4.00	24	0.56	0.21	0.0178	0.0111	0.0145	1.2	-0.10		
9	2.00	24	1.49	0.62	0.0068	0.0038	0.0056	1.4	1.395		
10	4.00	24	0.87	0.28	0.0116	0.0084	0.0100	1.0	0.565	0.012	0.009
11	8.00	24	0.95	0.26	0.0105	0.0090	0.0098	1.8	1.993	0.127	0.019
12	16.00	24	1.30	1.00	0.0073	0.0022	0.0048	2.4	11.26	0.176	0.016
13	8.00	24	1.18	0.43	0.0077	0.0049	0.0063	0.3	-0.03		
14	4.00	24	1.00	0.50	0.0092	0.0043	0.0068	0.5	1.030		
15	2.00	24	2.21	1.07	0.0042	0.0020	0.0031	1.1	1.827		
16	1.00	24	4.30	2.51	0.0022	0.0009	0.0016	1.2	2.026		

Table B.25: Results of LSO Test for Batch 205.

CONSOLIDATION TEST DATA SHEET : Batch 205 - Top (LSO) DATE: 07/07/1989 DONE BY : T.H. Seah

Incr. Number	Scale Load (kg)	σ'_{vc} (ksc)	Height of Sample			Vertical Strain,%		Void Ratio , e		
			H_{so} ,cm	H_{100},cm	H_f ,cm	ϵ_{100}, %	ϵ_f , %	e_{so}	e_{100}	e_f
1		0.25	2.6671	2.6615	2.6594	0.30	0.38	1.113	1.108	1.107
2		0.50	2.6588	2.6521	2.6481	0.65	0.80	1.106	1.101	1.098
3		0.80	2.6428	2.6383	2.6303	1.17	1.47	1.094	1.090	1.084
4		1.20	2.6105	2.5867	2.5867	3.10	3.10	1.068	1.049	1.049
5		2.00	2.5376	2.4850	2.4760	6.91	7.25	1.010	0.969	0.962
6		4.00	2.4159	2.3526	2.3385	11.87	12.40	0.914	0.864	0.853
7		8.00	2.2926	2.2445	2.2317	15.92	16.40	0.816	0.776	0.768
8		4.00	2.2317	2.2352	2.2360	16.27	16.24	0.768	0.771	0.771
9		2.00	2.2408	2.2469	2.2493	15.83	15.74	0.775	0.780	0.782
10		4.00	2.2467	2.2432	2.2424	15.97	16.00	0.780	0.777	0.776
11		8.00	2.2365	2.2269	2.2149	16.56	17.03	0.772	0.764	0.755
12		12.00	2.1954	2.1730	2.1623	18.60	19.00	0.739	0.721	0.713
13		16.00	2.1375	2.1257	2.1190	20.37	20.62	0.693	0.684	0.679
14		14.00	2.1190	2.1190	2.1190	20.62	20.62	0.679	0.679	0.679
15		12.00	2.1193	2.1193	2.1193	20.61	20.61	0.679	0.679	0.679
16		10.00	2.1196	2.1207	2.1288	20.56	20.54	0.679	0.680	0.687

Incr. Number	Scale Load (kg)	σ'_{vc} (ksc)	Height of Sample			Vertical Strain,%		Void Ratio , e		
			H_{so} ,cm	H_{100},cm	H_f ,cm	ϵ_{100}, %	ϵ_f , %	e_{so}	e_{100}	e_f
17		6.00	2.1228	2.1260	2.1276	20.36	20.30	0.682	0.684	0.686
18		4.00	2.1295	2.1329	2.1348	20.10	20.03	0.687	0.690	0.691
19		2.00	2.1412	2.1492	2.1436	19.49	19.70	0.696	0.703	0.704
20		1.00	2.1588	2.1679	2.1703	18.79	18.70	0.710	0.717	0.719

Height of Solids, Hs = 1.26227 cm

Incr. Number	σ'_{vc} (ksc)	Time (min)			Coef. of Consolidation cm^2/s			k x 10^{-4} cm^2/s	CR (%)	Cα (%)	Cα/CR
		Duration (Hours)	t_{50} ($\sqrt{t}$)	t_{50} (log)	$\sqrt{t}$	log t	Average				
0	0.00									0.045	
1	0.25	4	0.40	0.71	0.0628	0.0082	0.0355	42.6	0.300	0.013	0.018
2	0.50	4	4.29	1.00	0.0058	0.0058	0.0058	8.1	1.163	0.018	0.010
3	0.80	8	6.77	2.31	0.0036	0.0025	0.0031	5.4	2.548		
4	1.20	4	5.57	11.09	0.0044	0.0005	0.0024	11.6	10.96	0.717	0.051
5	2.00	4	11.07	7.57	0.0021	0.0007	0.0014	6.7	17.17	0.368	0.022
6	4.00	16	11.34	3.77	0.0018	0.0013	0.0015	3.7	16.48	0.447	0.029
7	8.00	4	8.40	2.57	0.0022	0.0017	0.0019	1.9	13.45		
8	4.00	4	0.90	0.29	0.0196	0.0141	0.0158	0.6	0.432		
9	2.00	20	1.87	0.66	0.0095	0.0062	0.0079	1.7	1.462		
10	4.00	4	0.63	0.33	0.0270	0.0126	0.0198	0.5	0.465		
11	8.00	26	0.55	0.40	0.0321	0.0103	0.0212	3.2	2.026	0.023	0.018
12	12.00	17	6.30	3.39	0.0027	0.0012	0.0019	1.0	11.47	0.181	0.027
13	16.00	11	16.27	15.85	0.0009	0.0002	0.0006	0.3	14.17	0.283	0.022
14	14.00										
15	12.00										
16	10.00										

Table B.26: Results of Oedometer Test No. 11 for Batch 206.

CONSOLIDATION TEST DATA SHEET : Batch 206 - Top DATE: 11/12/1988 DONE BY : T.H. Seah

Incr. Number	Scale Load (kg)	σ'_{vc} (ksc)	Height of Sample			Vertical Strain,%		Void Ratio , e		
			H_{50} ,cm	H_{100},cm	H_f ,cm	ϵ_{100}, %	ϵ_f , %	e_{50}	e_{100}	e_f
1	7.94	0.25	2.0098	2.0045	2.0030	0.56	0.633	1.141	1.135	1.133
2	15.88	0.50	1.9971	1.9914	1.9892	1.21	1.318	1.127	1.121	1.1186
3	31.75	1.00	1.9740	1.9600	1.9529	2.77	3.116	1.102	1.088	1.080
4	63.50	2.00	1.9155	1.8787	1.8369	6.80	7.386	1.040	1.001	0.988
5	127.00	4.00	1.8280	1.7880	1.7756	11.30	11.912	0.947	0.904	0.891
6	254.00	8.00	1.7234	1.7002	1.6870	15.65	16.307	0.836	0.811	0.797
7	127.00	4.00		1.6942	1.6942	15.95	15.953		0.804	0.804
8	63.50	2.00		1.7017	1.7019	15.58	15.588		0.812	0.813
9	127.00	4.00	1.6936	1.6981	1.6973	15.76	15.796	0.810	0.808	0.808
10	254.00	8.00	1.6890	1.6842	1.6745	16.45	16.927	0.799	0.794	0.783
11	508.00	16.00	1.6440	1.6141	1.6016	19.90	20.547	0.751	0.719	0.706
12	254.00	8.00		1.6084	1.6092	20.21	20.170		0.713	0.714
13	127.00	4.00		1.6178	1.6193	19.74	19.668		0.723	0.725
14	63.50	2.00		1.6257	1.6318	19.18	19.045		0.735	0.738
15	31.75	1.00		1.6416	1.6458	18.56	18.353		0.748	0.753
16	15.88	0.50		1.6594	1.6592	17.68	17.686		0.767	0.767

Incr. Number	σ'_{vc} (ksc)	Time (min)			Coef. of Consolidation cm^2/s			k x 10^{-4} cm^2/s	CR (%)	Ca (%)	Ca/CR
		Duration (hours)	t_{90} (√t)	t_{50} (log)	√t	log t	Average				
0	0.00										
1	0.25	4	1.00	0.10	0.0142	0.0332	0.0237		1.860*	0.011	0.005
2	0.50	4	2.89	0.50	0.0049	0.0066	0.0058	15.2	2.159	0.061	0.017
3	1.00	4	2.56	1.13	0.0054	0.0028	0.0041	12.9	5.182	0.240	0.026
4	2.00	4	4.20	2.00	0.0031	0.0015	0.0023	9.5	13.39	0.380	0.027
5	4.00	4	3.61	1.40	0.0032	0.0020	0.0026	6.3	14.95	0.465	0.032
6	8.00	4	2.89	1.00	0.0036	0.0024	0.0030	3.7	14.45	0.440	0.030
7	4.00	24									
8	2.00	4									
9	4.00	4	0.90	0.50	0.0113	0.0047	0.0080	0.8	0.598	0.020	0.014
10	8.00	4	0.64	0.18	0.0157	0.0130	0.0144	2.9	2.292	0.188	0.027
11	16.00	4	1.56	0.75	0.0061	0.0030	0.0046	2.4	11.46	0.320	0.028
12	8.00	4									
13	4.00	24									
14	2.00	4									
15	1.00	4									

Table B.27: Results of Oedometer Test No. 12 for Batch 206.

CONSOLIDATION TEST DATA SHEET : Batch 206 Bottom DATE: 11/12/1988 DONE BY : T.H. Seah

Incr. Number	Scale Load (kg)	σ'_{vc} (ksc)	Height of Sample			Vertical Strain,%		Void Ratio , e		
			H_{50} ,cm	H_{100},cm	H_f ,cm	ϵ_{100}, %	ϵ_f , %	e_{50}	e_{100}	e_f
1	7.92	0.25	1.984	1.9782	1.9767	0.57	0.644	1.139	1.133	1.131
2	15.85	0.50	1.972	1.9672	1.9646	1.12	1.252	1.126	1.121	1.118
3	31.69	1.00	1.951	1.9348	1.9279	2.75	3.095	1.103	1.086	1.079
4	63.38	2.00	1.892	1.8512	1.8414	6.95	7.447	1.040	0.996	0.985
5	126.76	4.00	1.803	1.7597	1.7488	11.55	12.100	0.944	0.897	0.885
6	253.52	8.00	1.708	1.6702	1.6567	16.05	16.728	0.841	0.800	0.786
7	126.76	4.00		1.6640	1.6644	16.36	16.341		0.794	0.794
8	63.38	2.00		1.6724	1.6735	15.94	15.885		0.803	0.804
9	126.76	4.00	1.670	1.6692	1.6683	16.10	16.147	0.800	0.799	0.799
10	253.52	8.00	1.660	1.6539	1.6446	16.67	17.326	0.790	0.783	0.773
11	507.04	16.00	1.612	1.5737	1.5682	20.90	21.177	0.738	0.697	0.691
12	253.52	8.00			1.5751		20.830			0.698
13	126.76	4.00		1.5846	1.5863	20.35	20.2267		0.708	0.710
14	63.38	2.00		1.5974	1.5997	19.71	19.592		0.722	0.725
15	31.69	1.00		1.6107	1.6146	19.04	18.845		0.737	0.741
16	15.85	0.50		1.6284	1.6285	18.15	18.144		0.756	0.756

Incr. Number	σ'_{vc} (ksc)	Time (min)			Coef. of Consolidation cm^2/s			k x 10^{-4} cm^2/s	CR (%)	Ca (%)	Ca/CR
		Duration (hours)	t_{50} ($\sqrt{t}$)	t_{50} (log)	$\sqrt{t}$	log t	Average				
0	0.00										
1	0.25	4	1.00	0.30	0.0138	0.0108	0.0123		1.893[a]	0.011	0.006
2	0.50	4	2.72	0.65	0.0050	0.0049	0.0050	11.1	1.827	0.060	0.018
3	1.00	4	3.24	1.00	0.0041	0.0031	0.0036	11.8	4.684	0.240	0.026
4	2.00	4	5.06	1.96	0.0025	0.0015	0.0020	8.6	13.92	0.380	0.026
5	4.00	4	3.43	1.25	0.0033	0.0020	0.0027	6.7	15.55	0.465	0.030
6	8.00	4	2.41	0.85	0.0042	0.0024	0.0033	4.4	15.45	0.440	0.028
7	4.00	24									
8	2.00	4									
9	4.00	4	0.43	0.20	0.0229	0.0115	0.0172	1.6	0.897	0.024	0.014
10	8.00	4	0.85	0.18	0.0114	0.0126	0.0120	2.8	2.491	0.188	0.023
11	16.00	4	1.96	0.50	0.0045	0.0043	0.0044	2.7	14.12	0.322	0.023
12	8.00	24									
13	4.00	4									
14	2.00	4									
15	1.00	4									

Table B.28: Results of Oedometer Test No. 13 for Batch 207.

CONSOLIDATION TEST DATA SHEET : Batch 207 - Top DATE: 01/06/1989 DONE BY : T.H. Seah

Incr. Number	Scale Load (kg)	σ'_{vc} (ksc)	Height of Sample			Vertical Strain,%		Void Ratio , e		
			H_{50} ,cm	H_{100},cm	H_f ,cm	ϵ_{100}, %	ϵ_f , %	e_{50}	e_{100}	e_f
1	7.94	0.25	1.9880	1.9860	1.9861	0.20	0.196	1.112	1.110	1.110
2	15.88	0.50	1.9815	1.9775	1.9766	0.63	0.673	1.105	1.101	1.100
3	25.40	0.80	1.9680	1.9596	1.9576	1.53	1.620	1.091	1.082	1.080
4	38.10	1.20	1.9420	1.9235	1.9223	3.34	3.403	1.063	1.043	1.042
5	63.50	2.00	1.8971	1.8654	1.8563	6.26	6.718	1.015	0.982	0.972
6	127.00	4.00	1.8149	1.7701	1.7581	11.05	11.656	0.928	0.880	0.868
7	[illegible]	8.00	1.7210	1.6792	1.6692	15.62	16.119	0.828	0.784	0.773
8	127.00	4.00	1.6726	1.6752	1.6763	15.95	15.763	0.777	0.780	0.781
9	63.50	2.00	1.6821	1.6869	1.6890	15.23	15.126	0.787	0.792	0.794
10	127.00	4.00	1.6816	1.6788	1.6771	15.64	15.726	0.786	0.783	0.782
11	254.00	8.00	1.6720	1.6658	1.6570	16.29	16.733	0.776	0.770	0.760
12	508.00	16.00	1.6236	1.5894	1.5793	20.13	20.639	0.724	0.688	0.676
13	254.00	8.00	1.5874	1.5910	1.5924	20.05	19.978	0.686	0.690	0.692
14	127.00	4.00	1.5934	1.5978	1.6000	19.71	19.600	0.693	0.697	0.700
15	63.50	2.00	1.6037	1.6095	1.6128	19.12	18.954	0.704	0.710	0.713
16	31.75	1.00	1.6143	1.6213	1.6249	18.53	18.347	0.715	0.722	0.726

Incr. Number	σ'_{vc} (ksc)	Time (min)			Coef. of Consolidation cm^2/s			k x 10^{-8} cm^2/s	CR (%)	Ca (%)	Ca/CR
		Duration (Hours)	t_{50} (√t)	t_{50} (log)	√t	log t	Average				
0	0.00										
1	0.25	24	-	11.12	-	0.0003			0.664[a]		
2	0.50	24	1.64	0.70	0.0085	0.0046	0.0066	11.3	1.415	0.029	0.010
3	0.80	24	1.55	7.27	0.0088	0.0004	0.0046	13.9	4.429	0.121	0.016
3	1.20	24	3.88	13.00	0.0034	0.0002	0.0018	8.3	10.28	0.235	0.020
4	2.00	24	7.77	3.10	0.0016	0.0010	0.0013	4.9	13 16	0.405	0.028
5	4.00	24	4.62	1.58	0.0025	0.0017	0.0021	5.4	15.91	0.326	0.021
6	8.00	24	2.58	1.13	0.0041	0.0022	0.0032	4.1	15.18	0.260	0.017
7	4.00	24	0.60	0.18	0.0165	0.0125	0.0145	0.9	-0.66		
8	2.00	24	0.79	0.38	0.0127	0.0061	0.0094	3.3	1.959		
9	4.00	24	0.79	0.15	0.0126	0.0155	0.0141	3.4	1.362	0.029	0.016
10	8.00	24	0.87	0.17	0.0114	0.0136	0.0125	2.4	2.159	0.136	0.018
11	16.00	24	2.03	0.84	0.0046	0.0026	0.0036	2.2	12.76	0.392	0.031
12	8.00	24	0.60	0.14	0.0148	0.0148	0.0148	1.4	0.266		
13	4.00	24	1.21	0.35	0.0074	0.0060	0.0067	0.7	1.129		
14	2.00	24	2.92	0.78	0.0031	0.0027	0.0029	1.0	1.960		
15	1.00	24	5.93	1.89	0.0016	0.0011	0.0014	1.0	1.960		

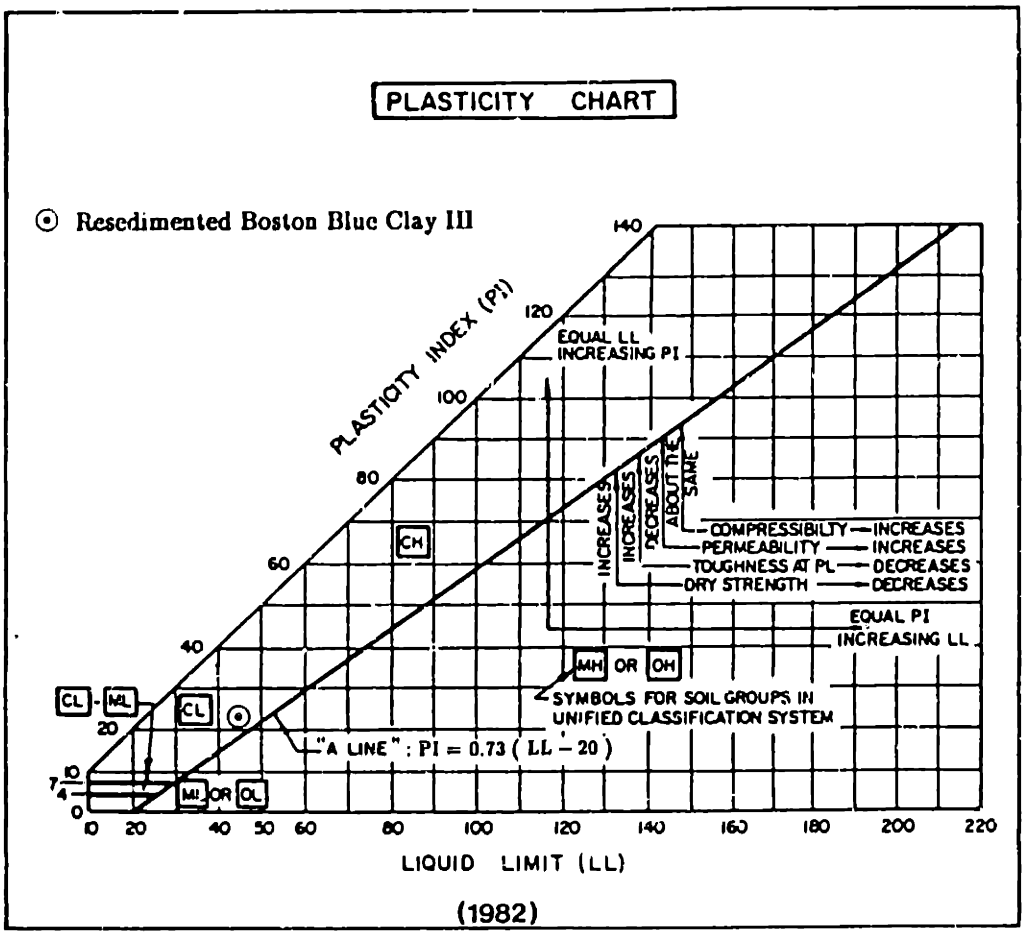

Plasticity Chart (from NAVFAC DM – 7.1, p1δ)

Figure B.1: Plasticity Chart (from NAVFAC DM–7.1 (1982), pp.18).

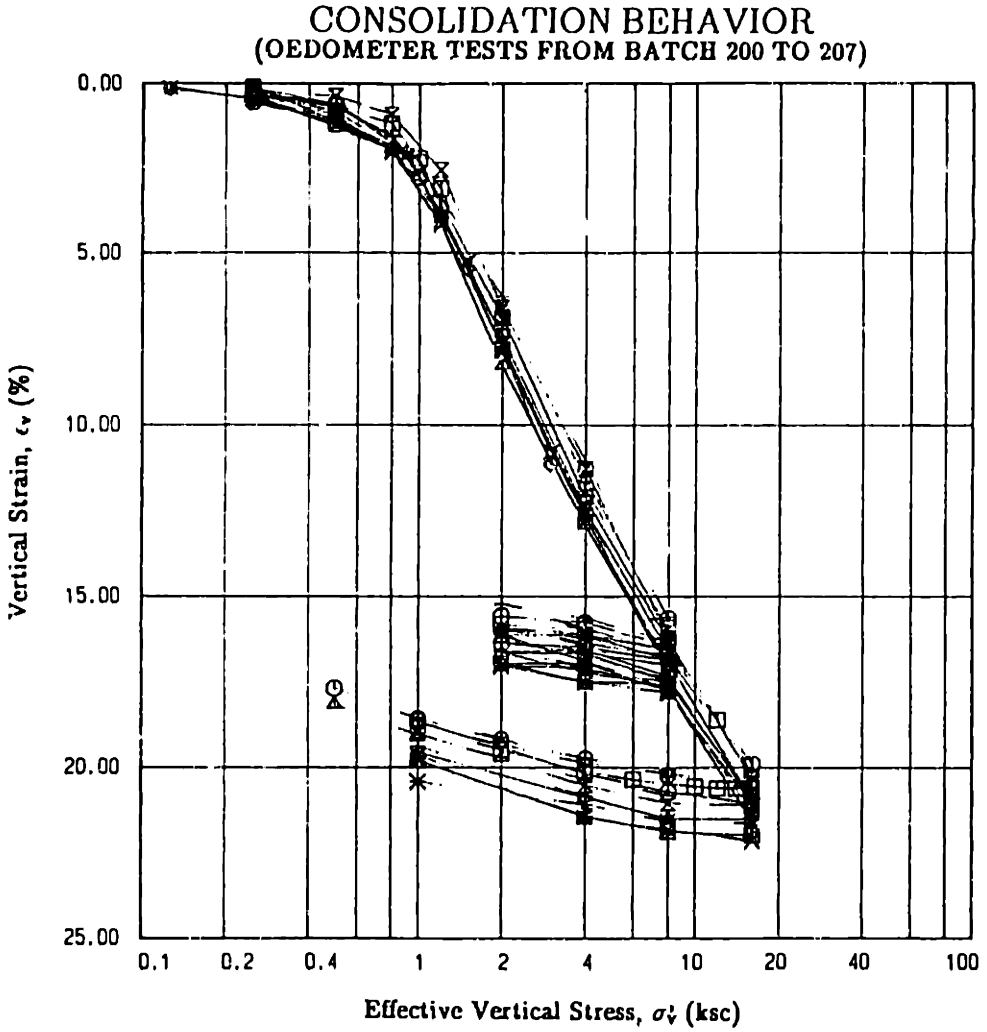

Figure B.2: Compression Curves of Oedometer Tests (Batch 200 to 207).

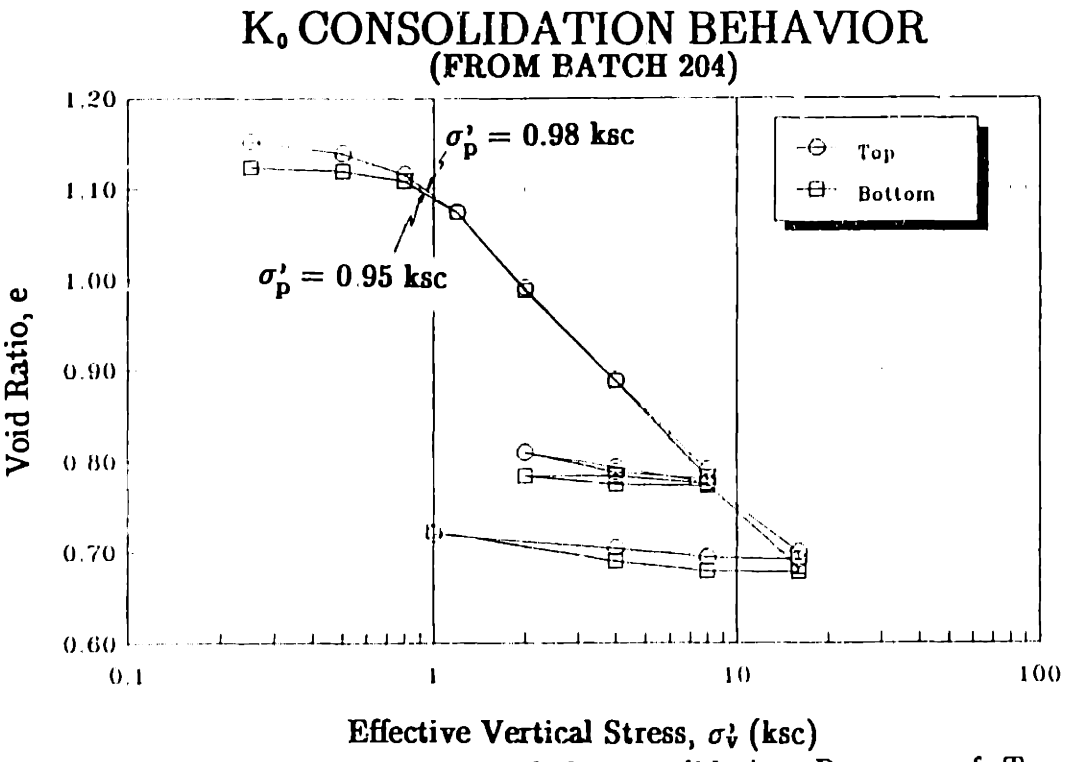

Figure B.3: Determination of Preconsolidation Pressure of Two Oedometer Samples taken from the Top and Bottom of the Consolidometer (Batch 204).

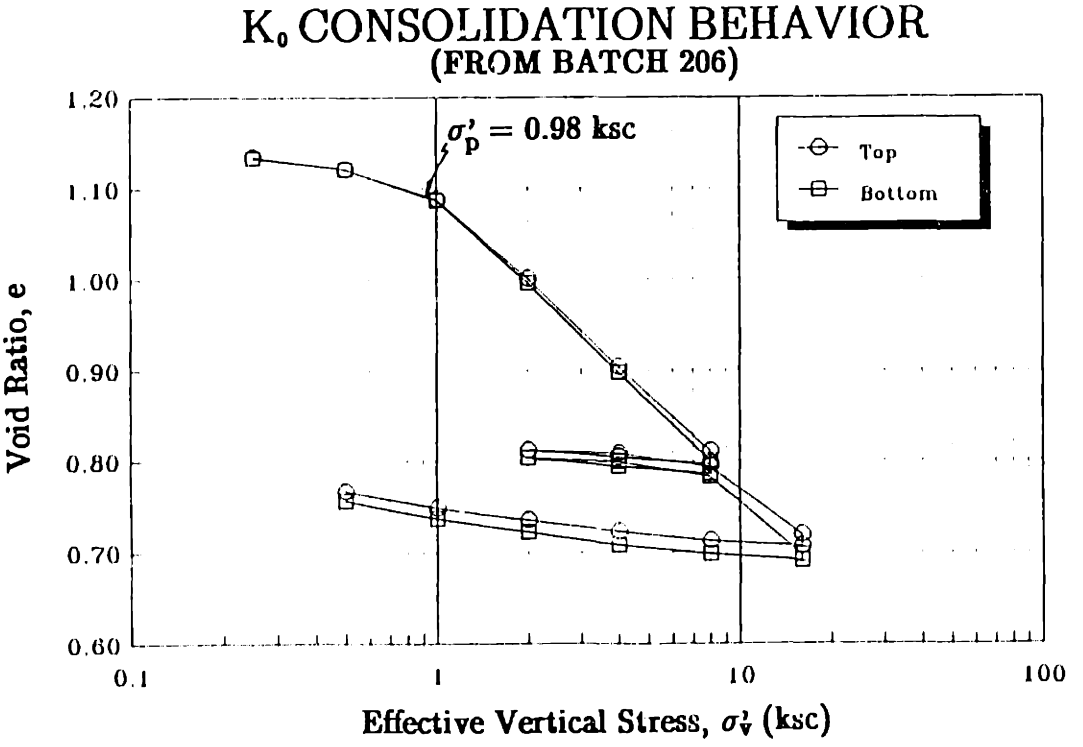

Figure B.4: Determination of Preconsolidation Pressure of Two Oedometer Samples taken from the Top and Bottom of the Consolidometer (Batch 206).

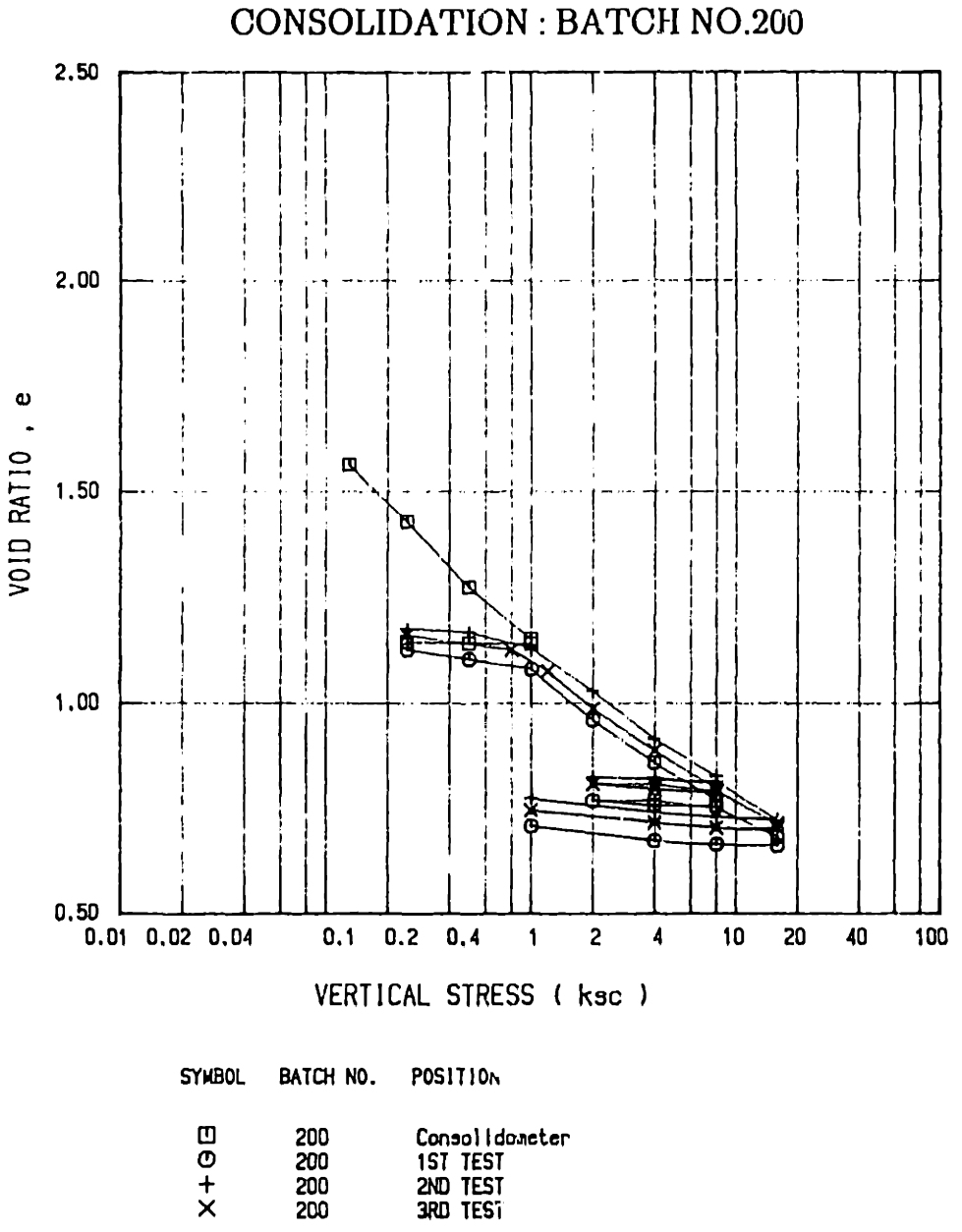

Figure B.5: Void Ratio versus Vertical Effective Stress for Batch 200 (Results from the Consolidometer & Oedometer Tests).

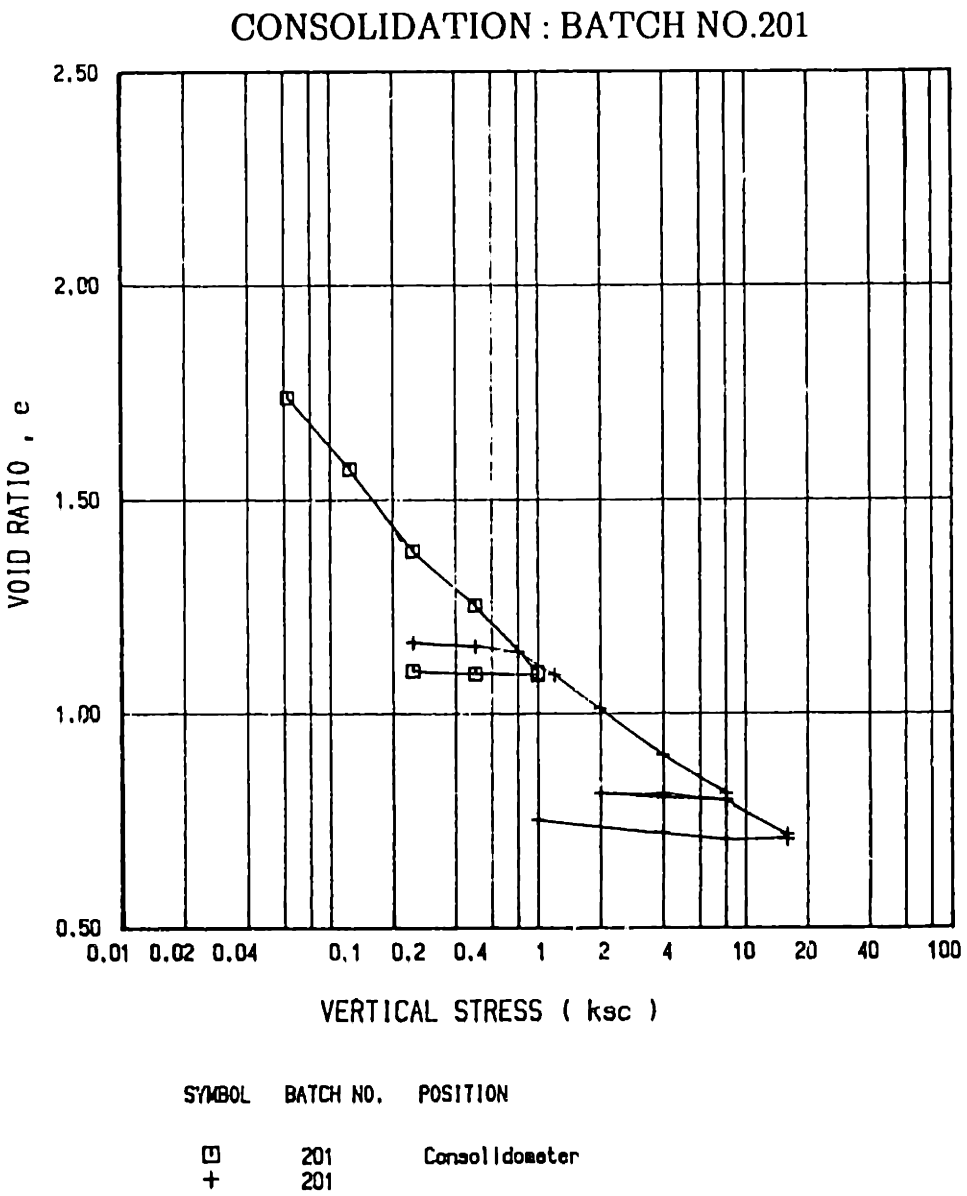

Figure B.6: Void Ratio versus Vertical Effective Stress for Batch 201 (Results from the Consolidometer & Oedometer Tests).

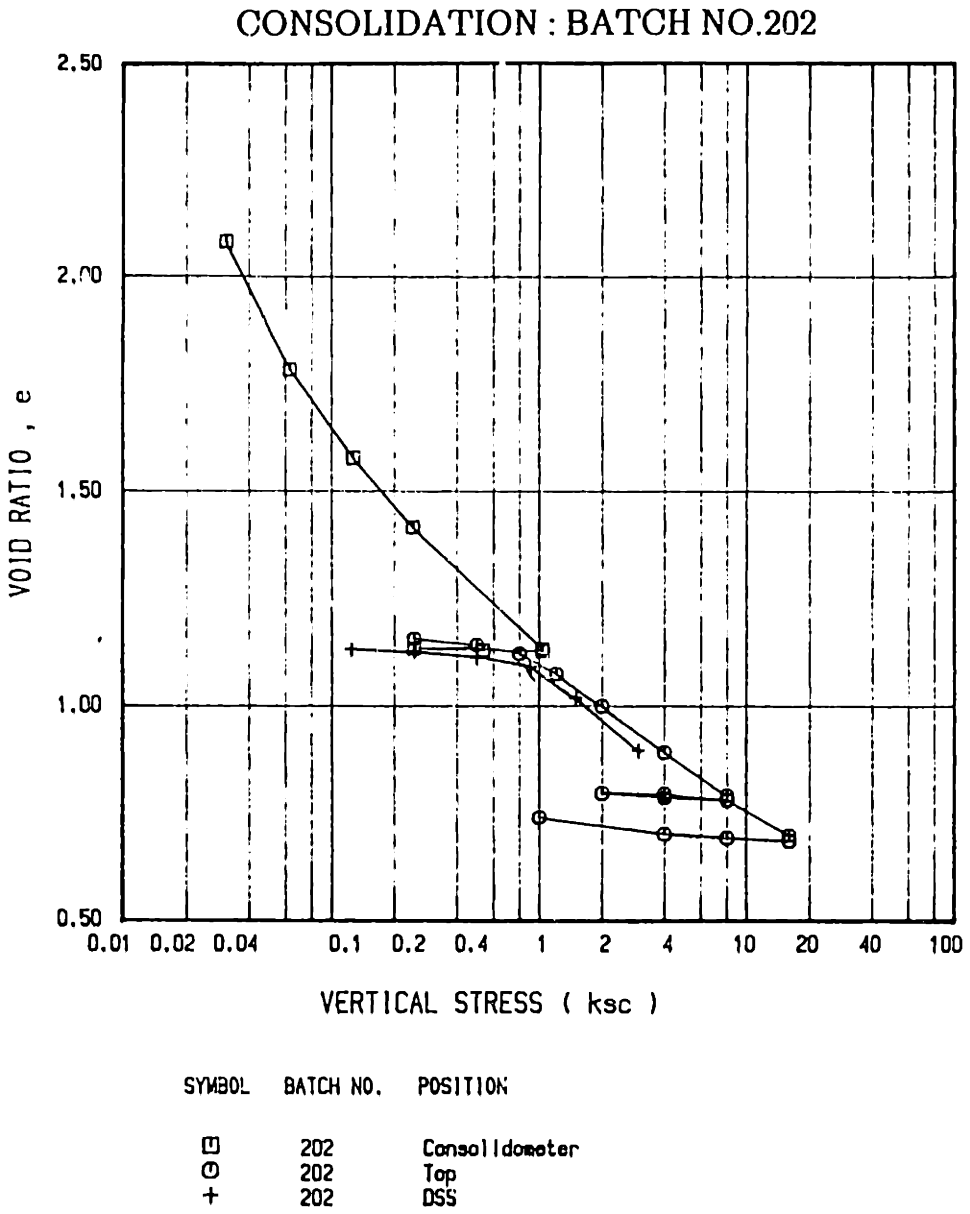

Figure B.7: Void Ratio versus Vertical Effective Stress for Batch 202 (Results from the Consolidometer & Oedometer Tests).

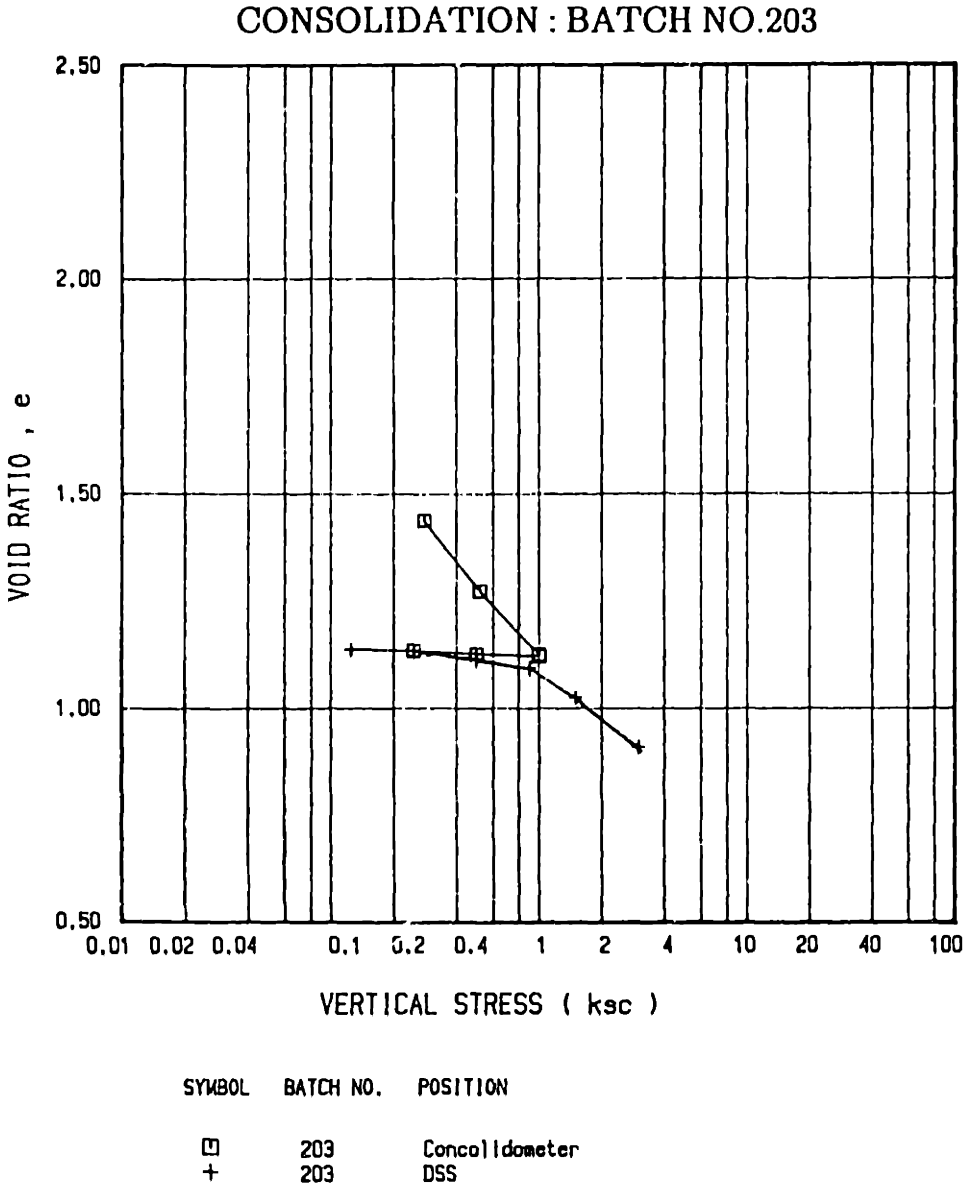

Figure B.8: Void Ratio versus Vertical Effective Stress for Batch 203 (Results from the Consolidometer & Oedometer Tests).

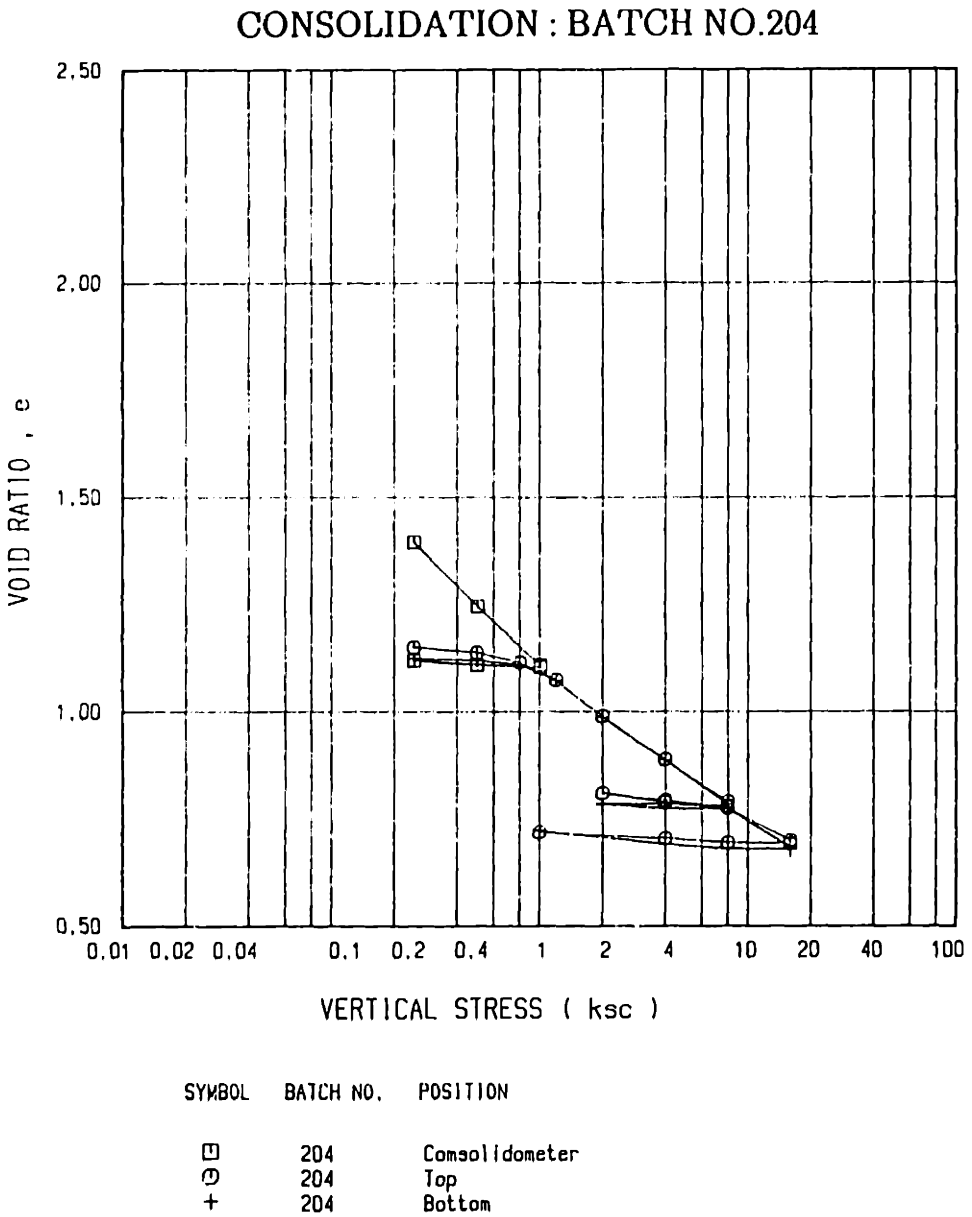

Figure B.9: Void Ratio versus Vertical Effective Stress for Batch 204 (Results from the Consolidometer & Oedometer Tests).

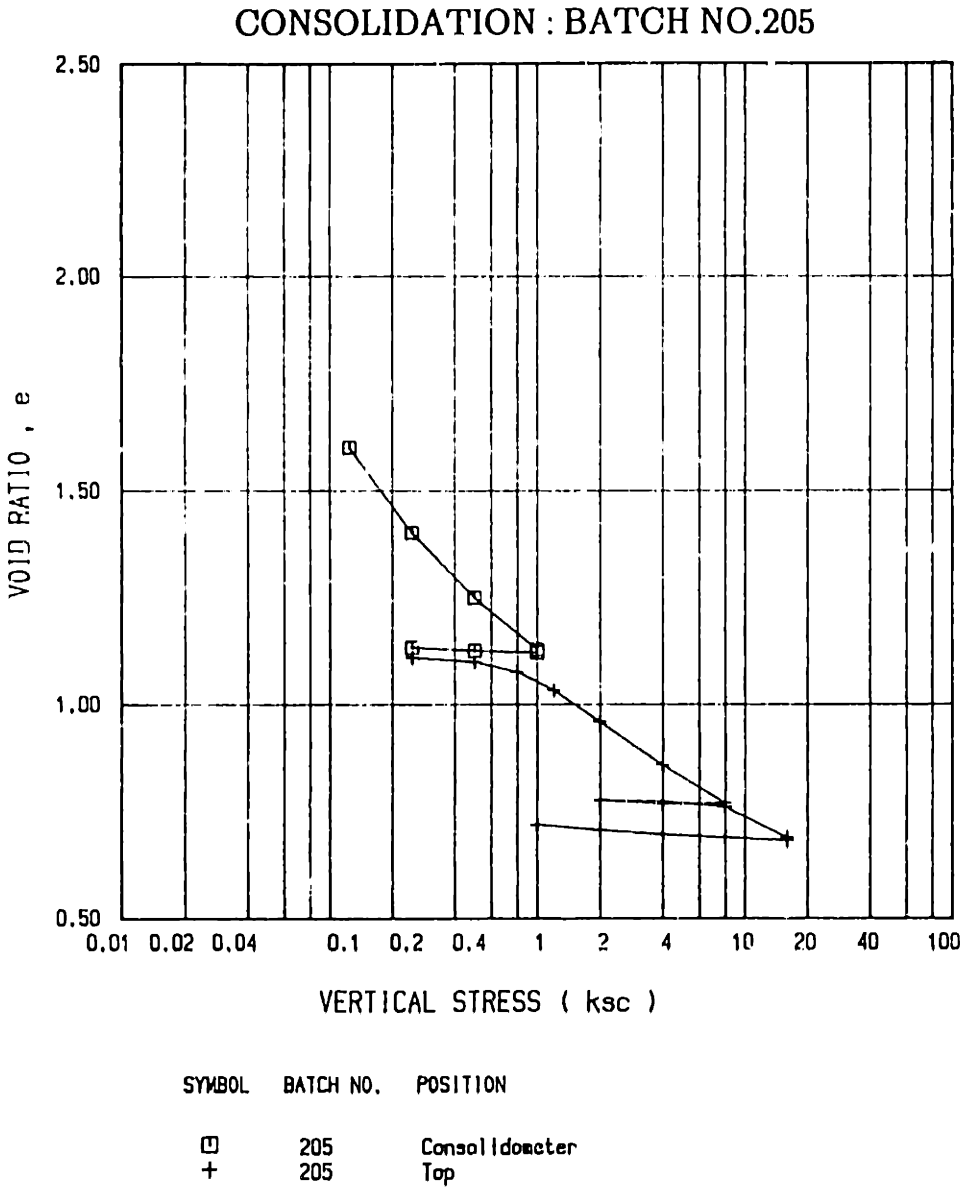

Figure B.10: Void Ratio versus Vertical Effective Stress for Batch 205 (Results from the Consolidometer & Oedometer Tests).

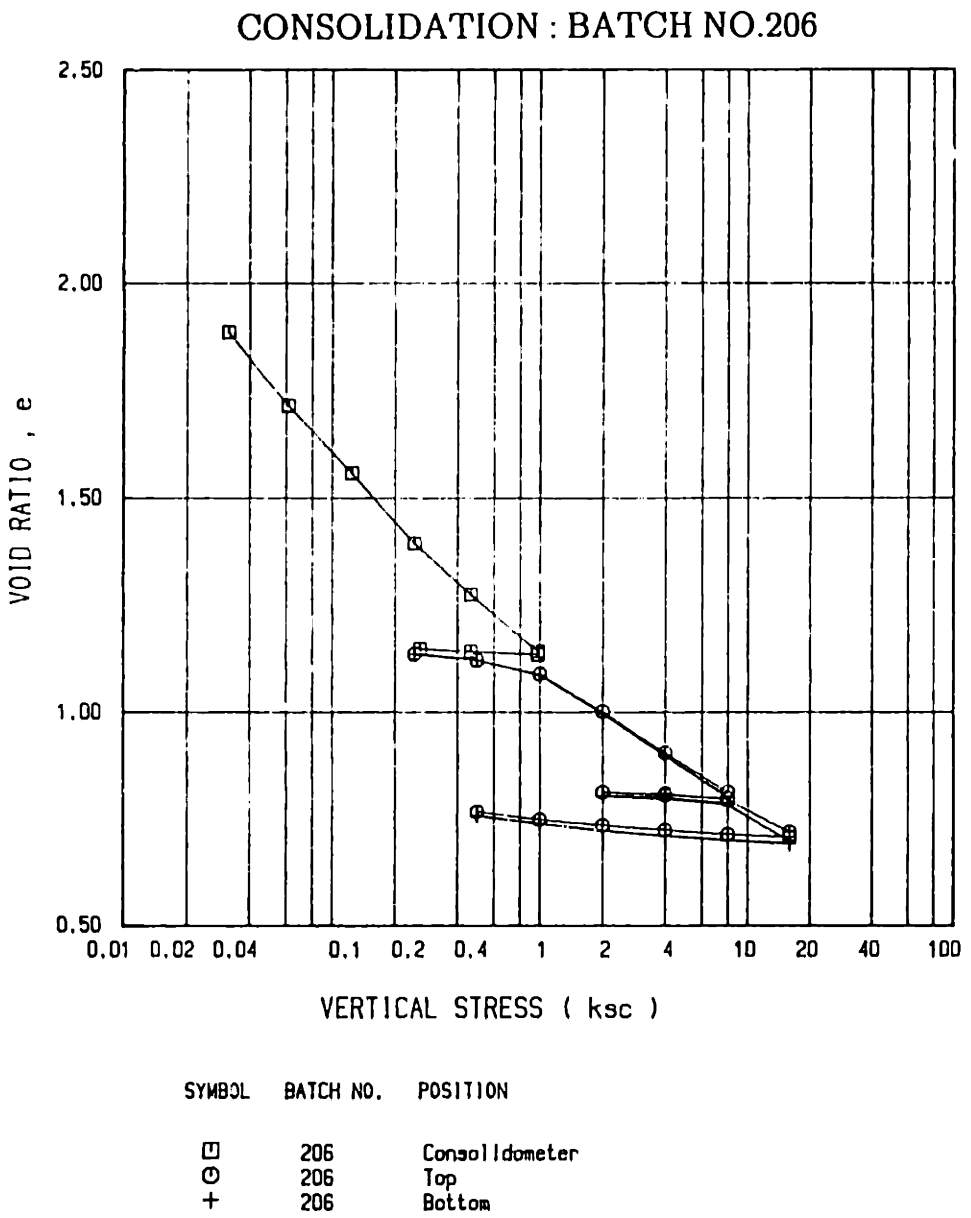

Figure B.11: Void Ratio versus Vertical Effective Stress for Batch 206 (Results from the Consolidometer & Oedometer Tests).

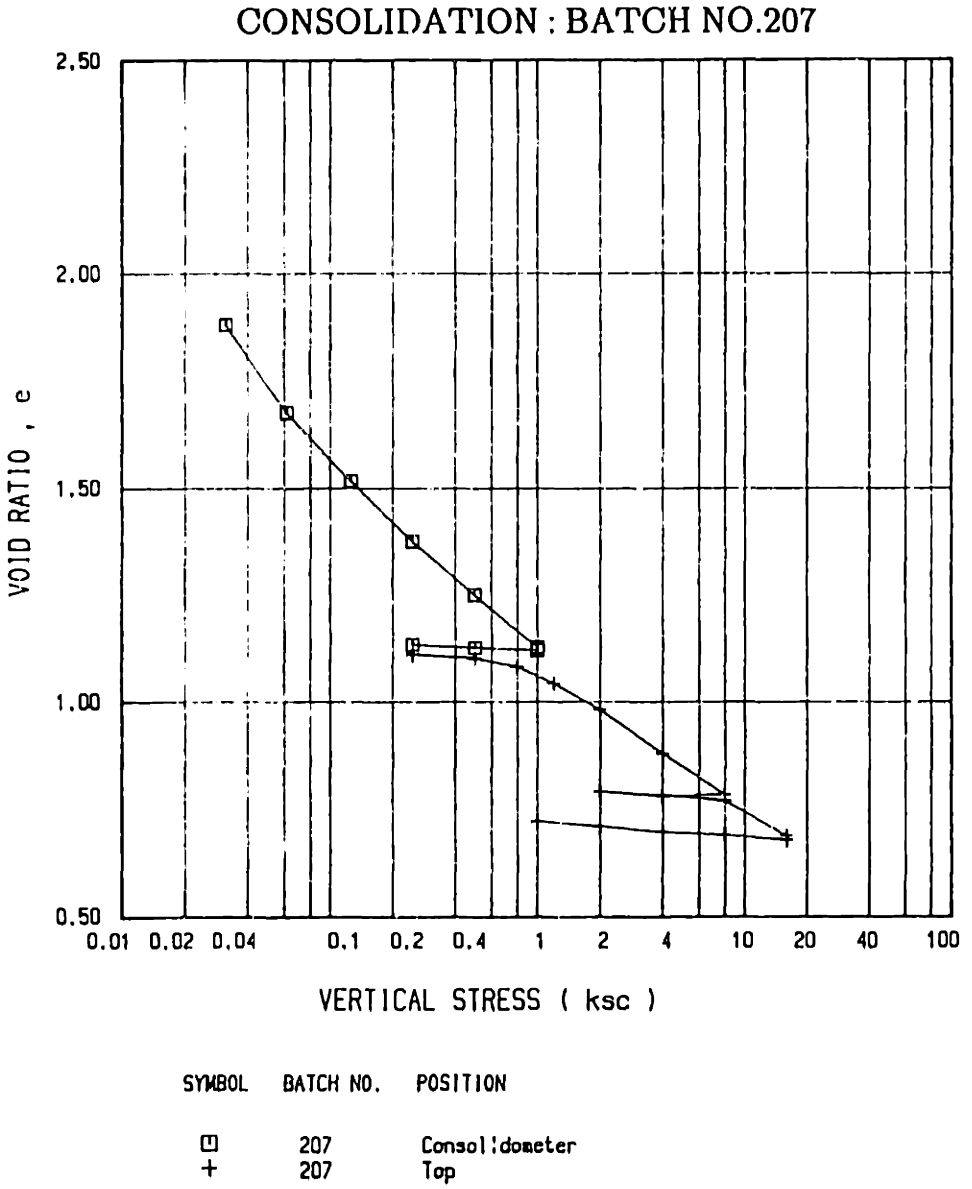

Figure B.12: Void Ratio versus Vertical Effective Stress for Batch 207 (Results from the Consolidometer & Oedometer tests).

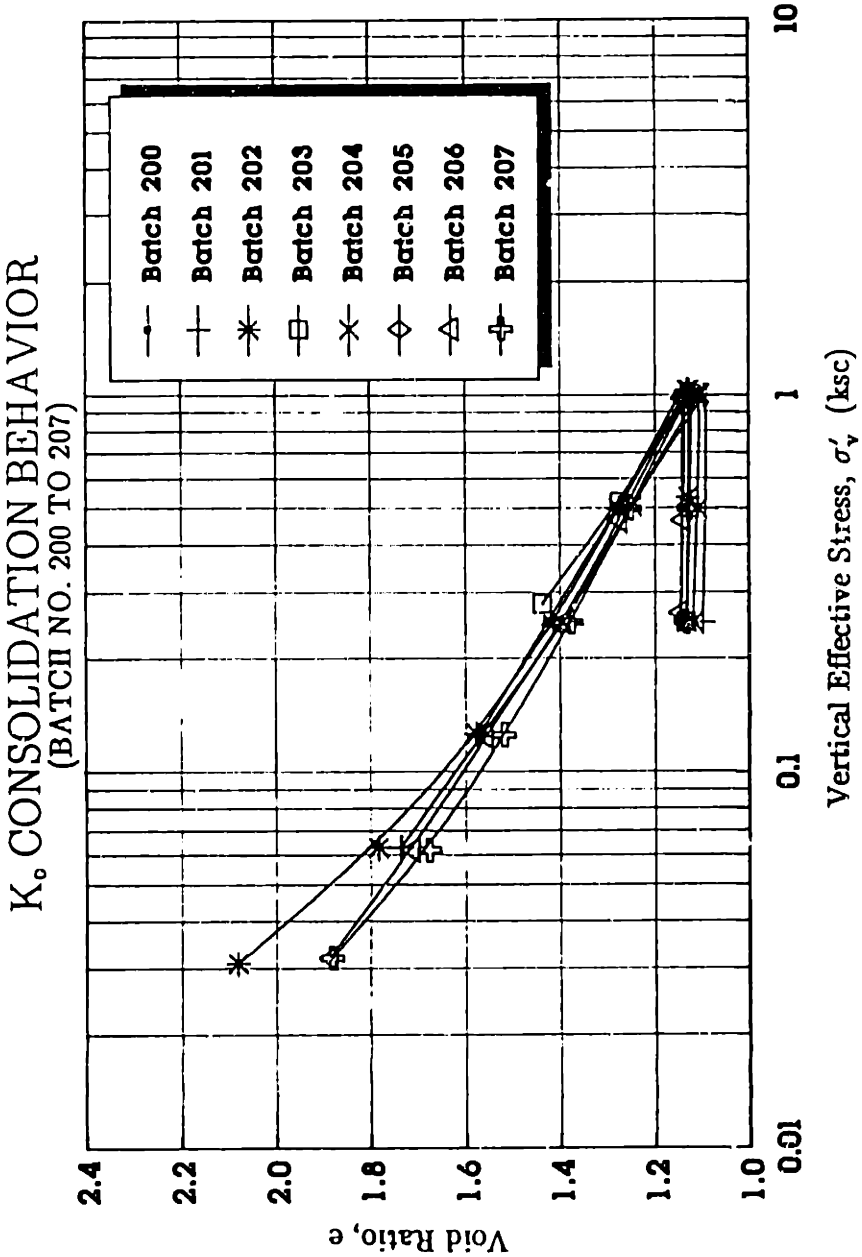

Figure B.13: Compression Curves of the Consolidometer Tests (Batch 200 to 207).

Relationship between Compression Index &
Liquid Limit (Skempton, 1944)

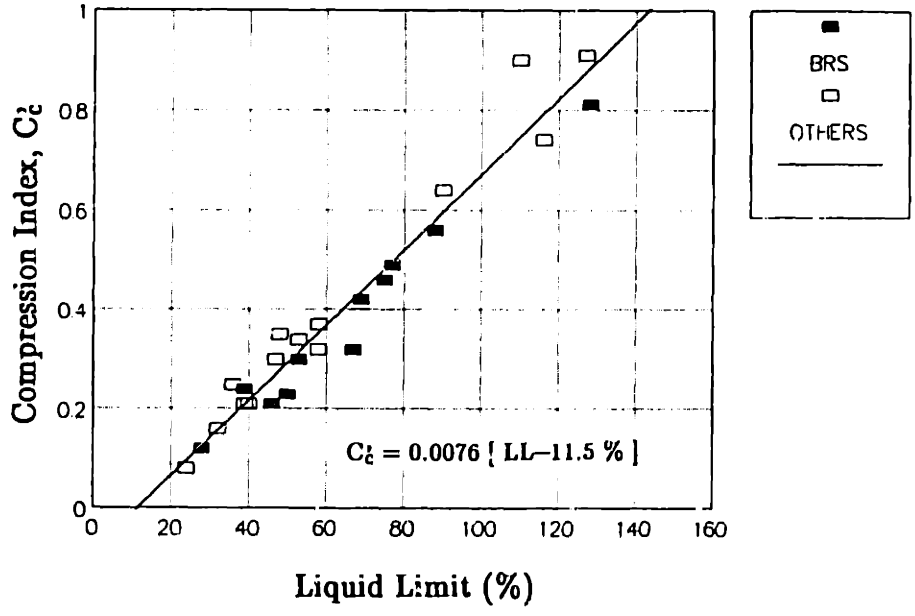

Figure B.14a: Compression Index versus Uncorrected Liquid Limit (after Skempton, 1944).

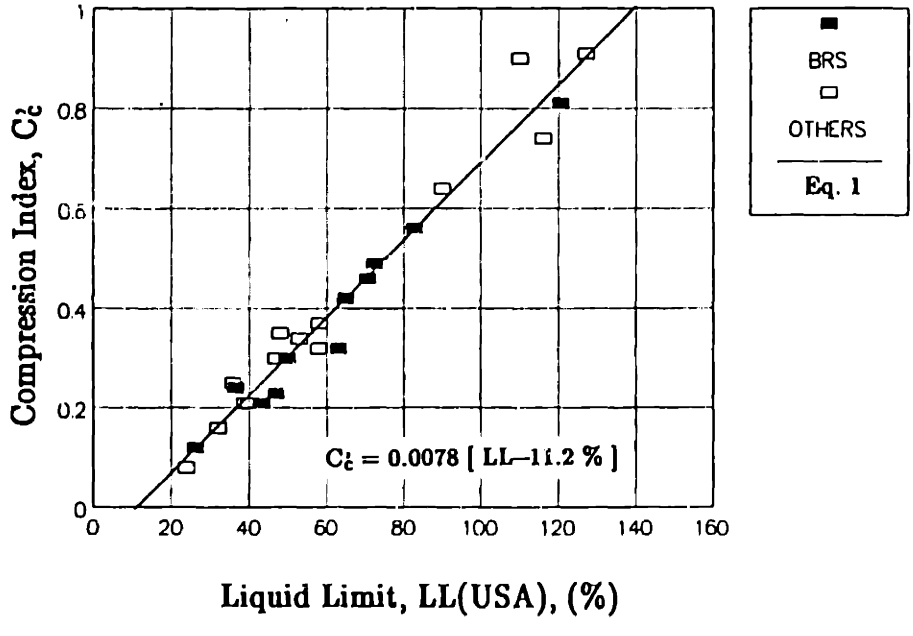

Figure B.14b: Compression Index versus Corrected Liquid Limit [LL(USA)].

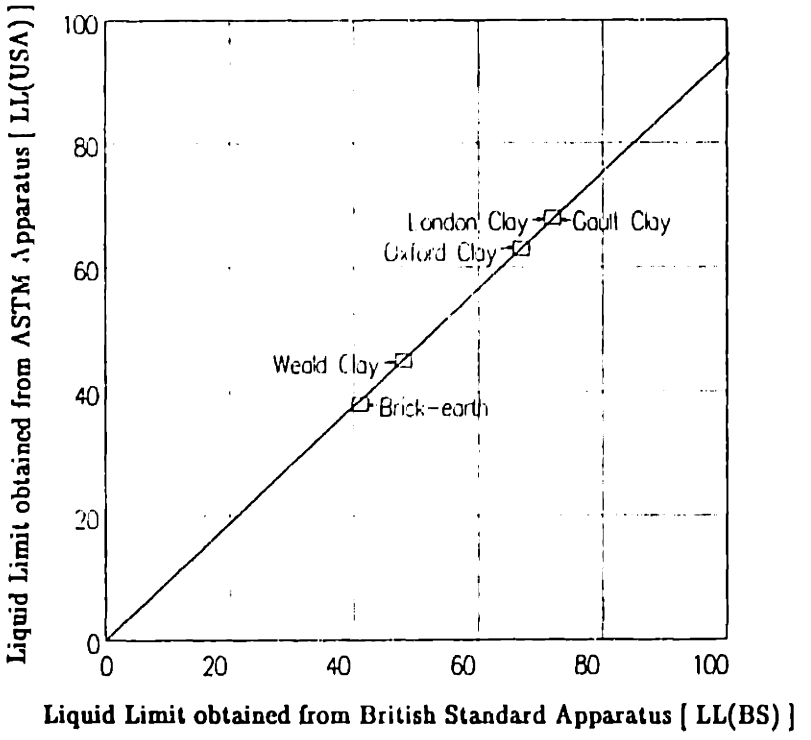

The equation of the line is LL(USA) = 0.941 LL(BS)

The Goodness of Fit, $r^2 = 0.99997$

Figure B.15: Comparison Between the Liquid Limits (LL) obtained from British Standard and ASTM Apparatuses for Five Different Soils (Data obtained from Norman, 1958).

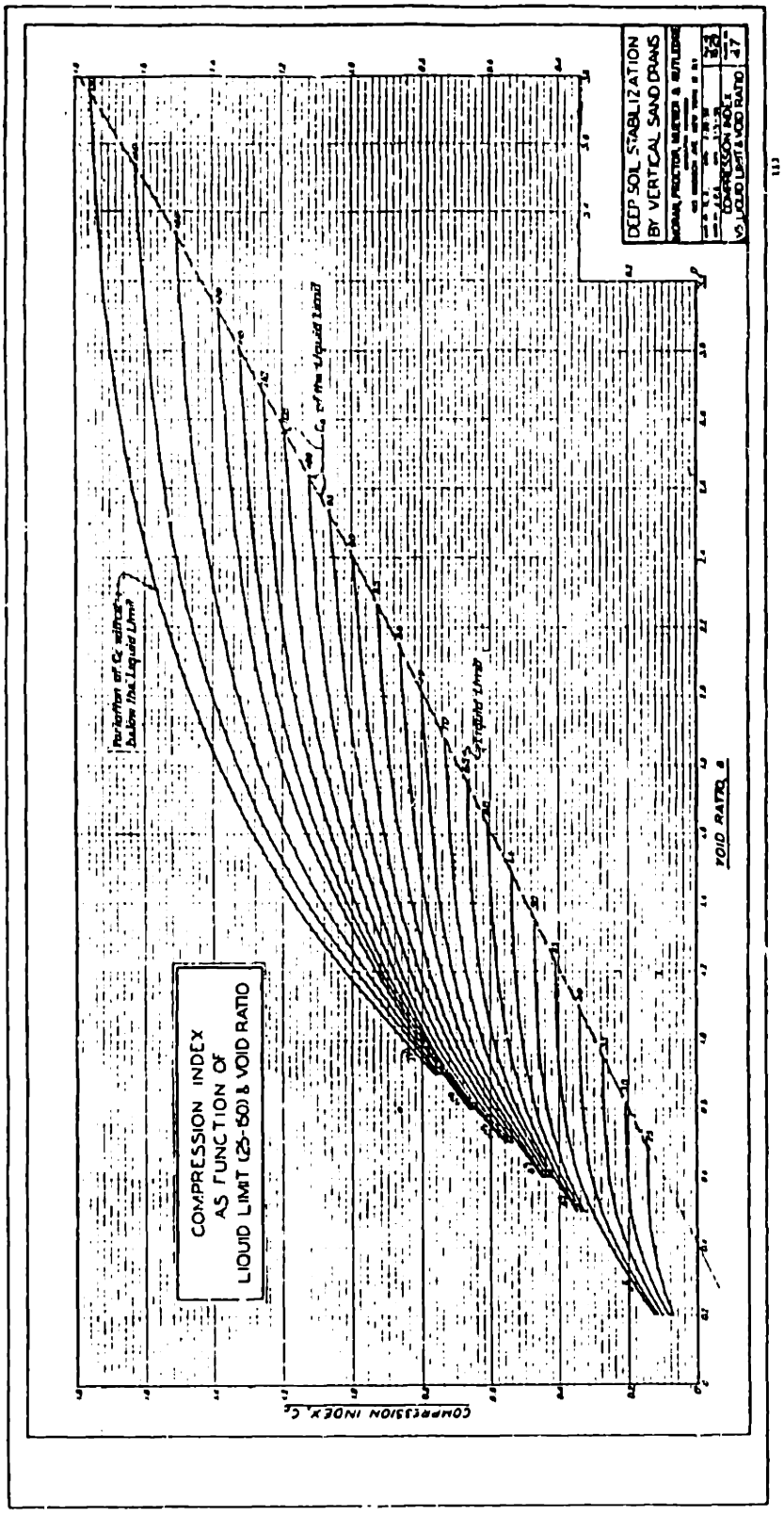

Figure B.16: Virgin Compression Index as Function of Liquid Limit and Void Ratio (from MPMR, 1958).

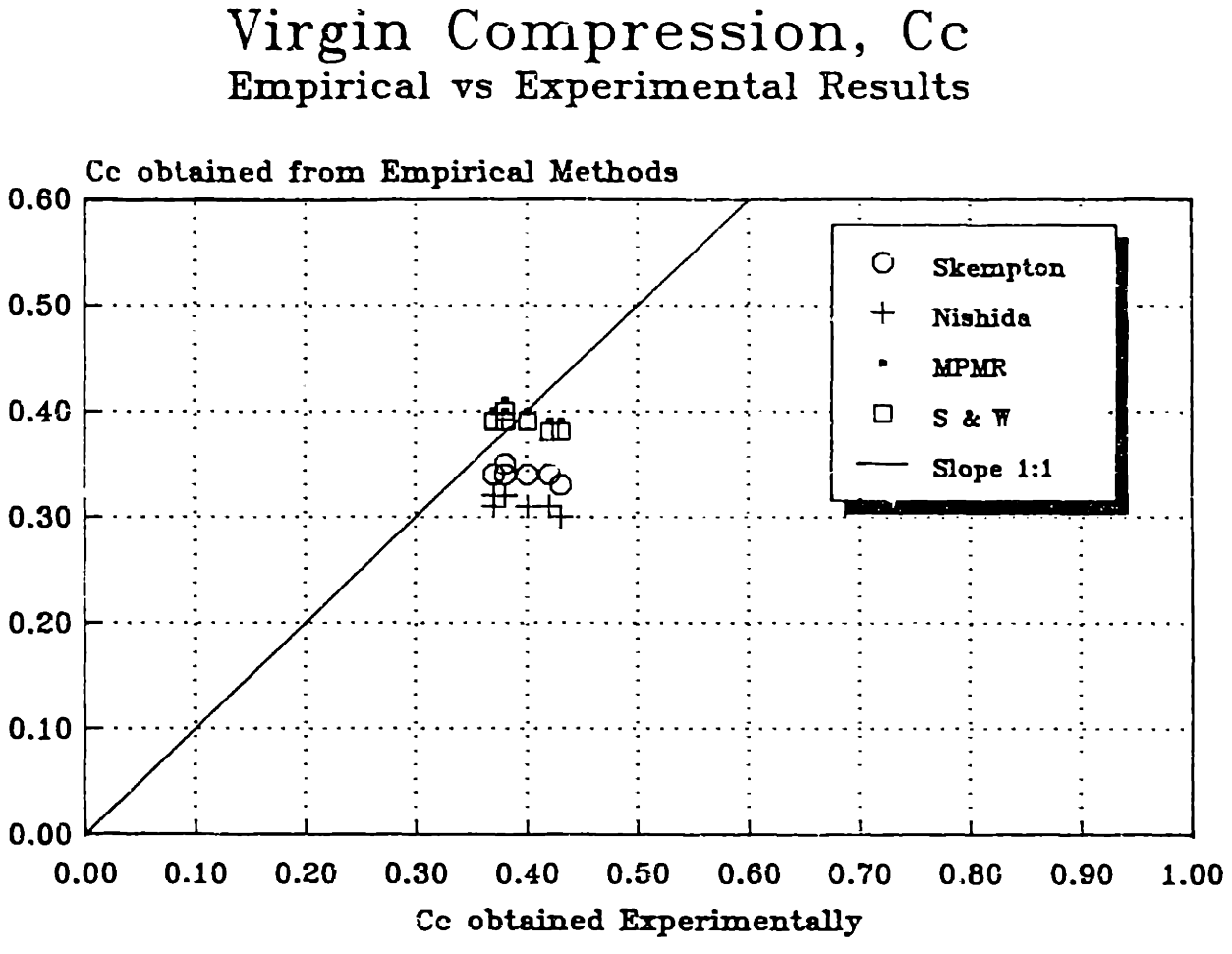

Figure B.17: Empirical Results versus Experimental Results of Compression Index.

Definitions of Recompression Ratio (RR) and Swelling Ratio (SR)

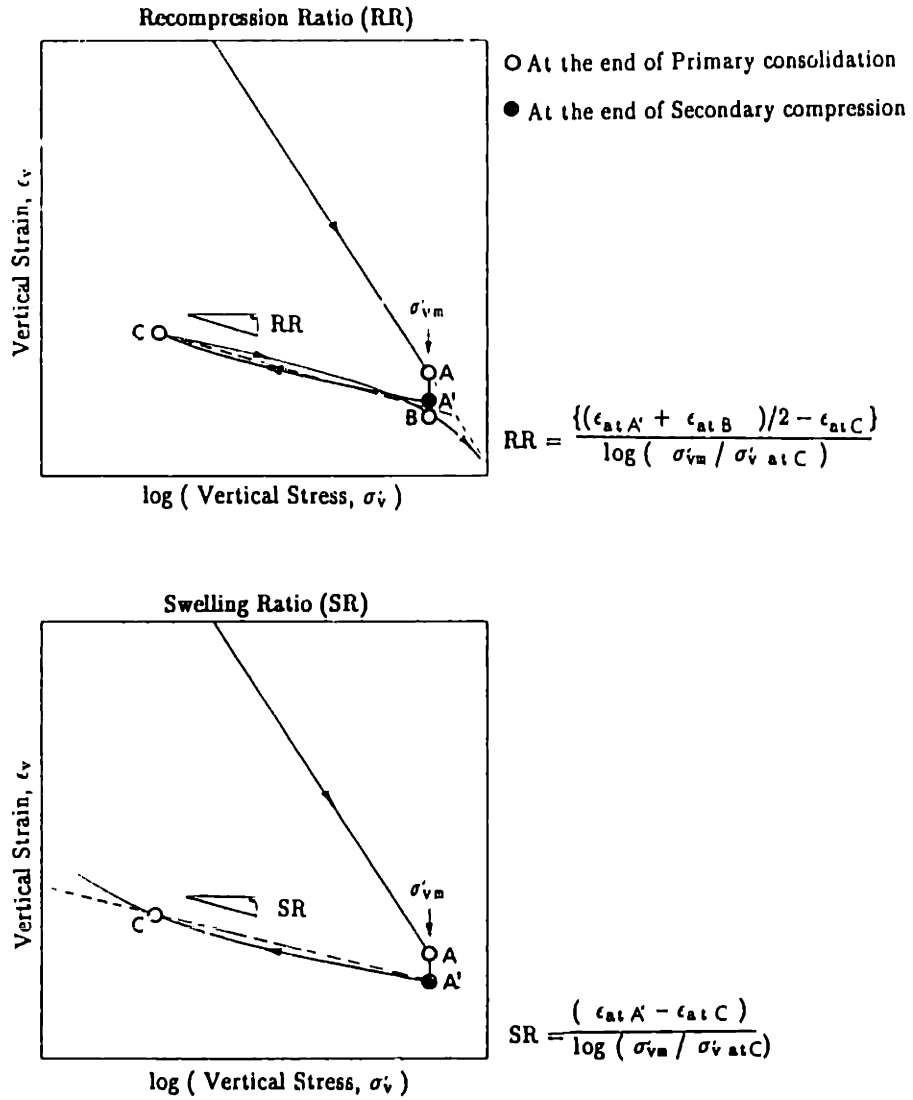

Figure B.18: Definitions of Recompression Ratio (RR) and Swelling Ratio (SR).

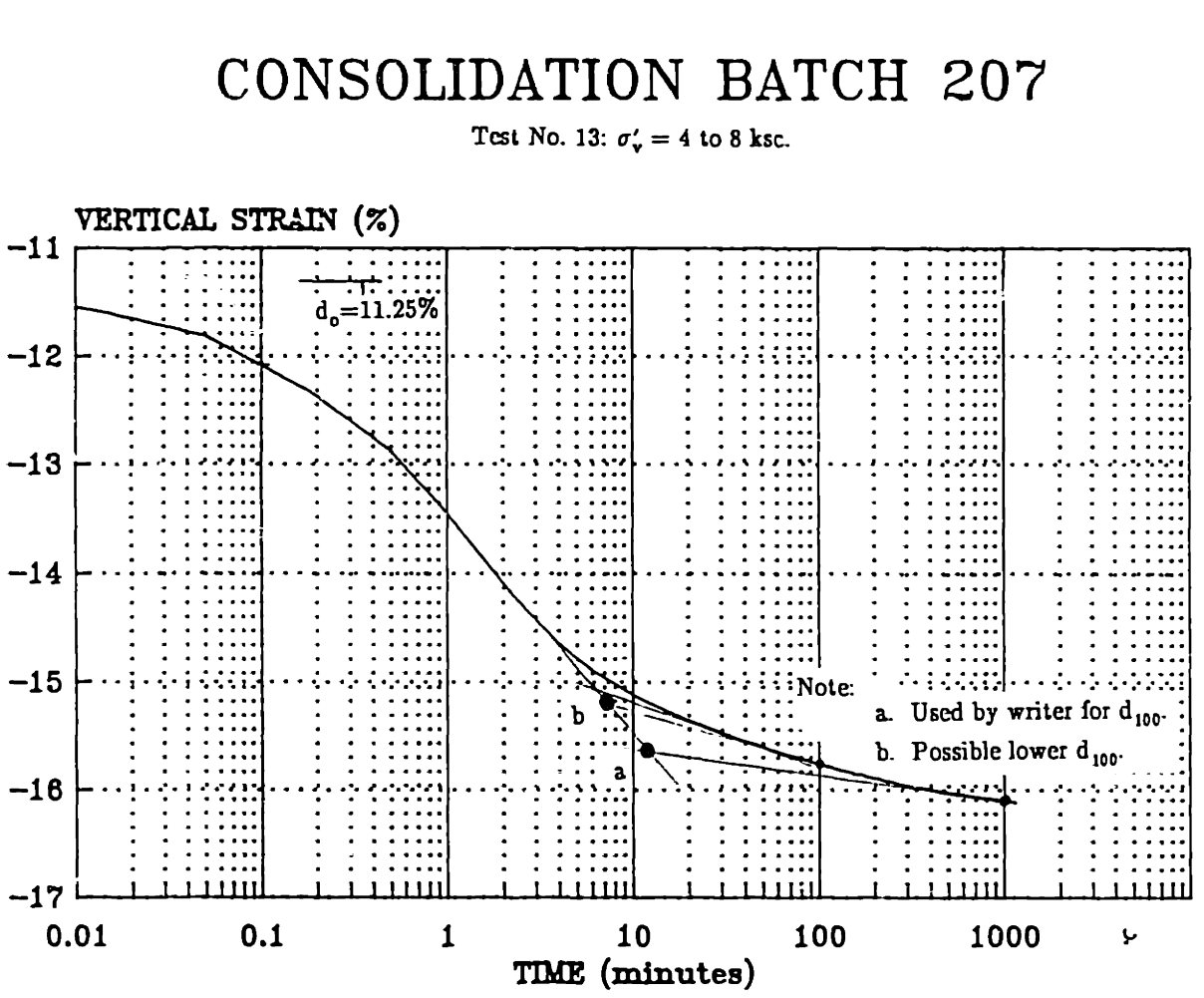

Figure B.19: Typical Settlement–Time Curve of a Consolidation Increment in the Oedometer Test.

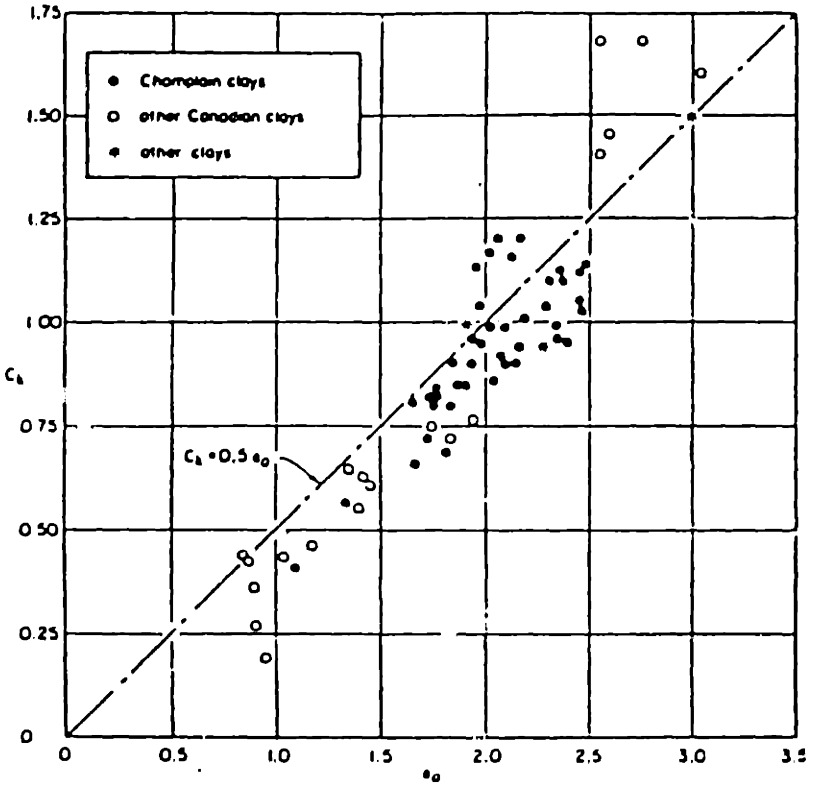

Figure B.20: Relation Between Permeability Change Index, C_k, and Initial Void Ratio, e_o, for All Clays Tested (From Tavernas et al., 1983).

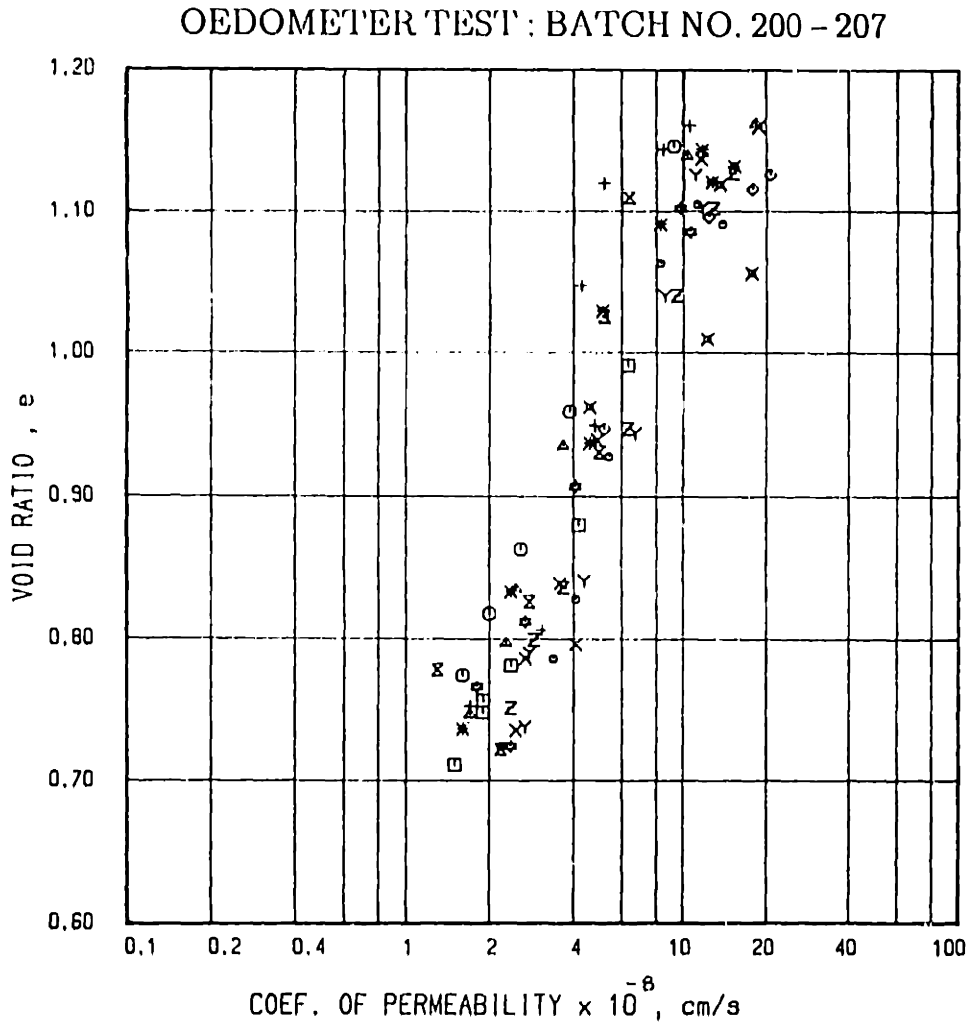

SYMBOL	BATCH NO.	POSITION	SYMBOL	BATCH NO.	POSITION
⊡	200	1ST TEST	✳	204	Top
⊙	200	2ND TEST	⧖	204	Bottom
△	200	3RD TEST	✡	205	Top
+	201	1ST TEST	Z	206	Top
×	202	Top	Y	206	Bottom
◈	202	DSS	•	207	Top
✳	203	DSS			

Figure B.21: Graph of Void Ratio versus Logarithm of Coefficient of Permeability for the Oedometer and DSS Consolidation Tests.

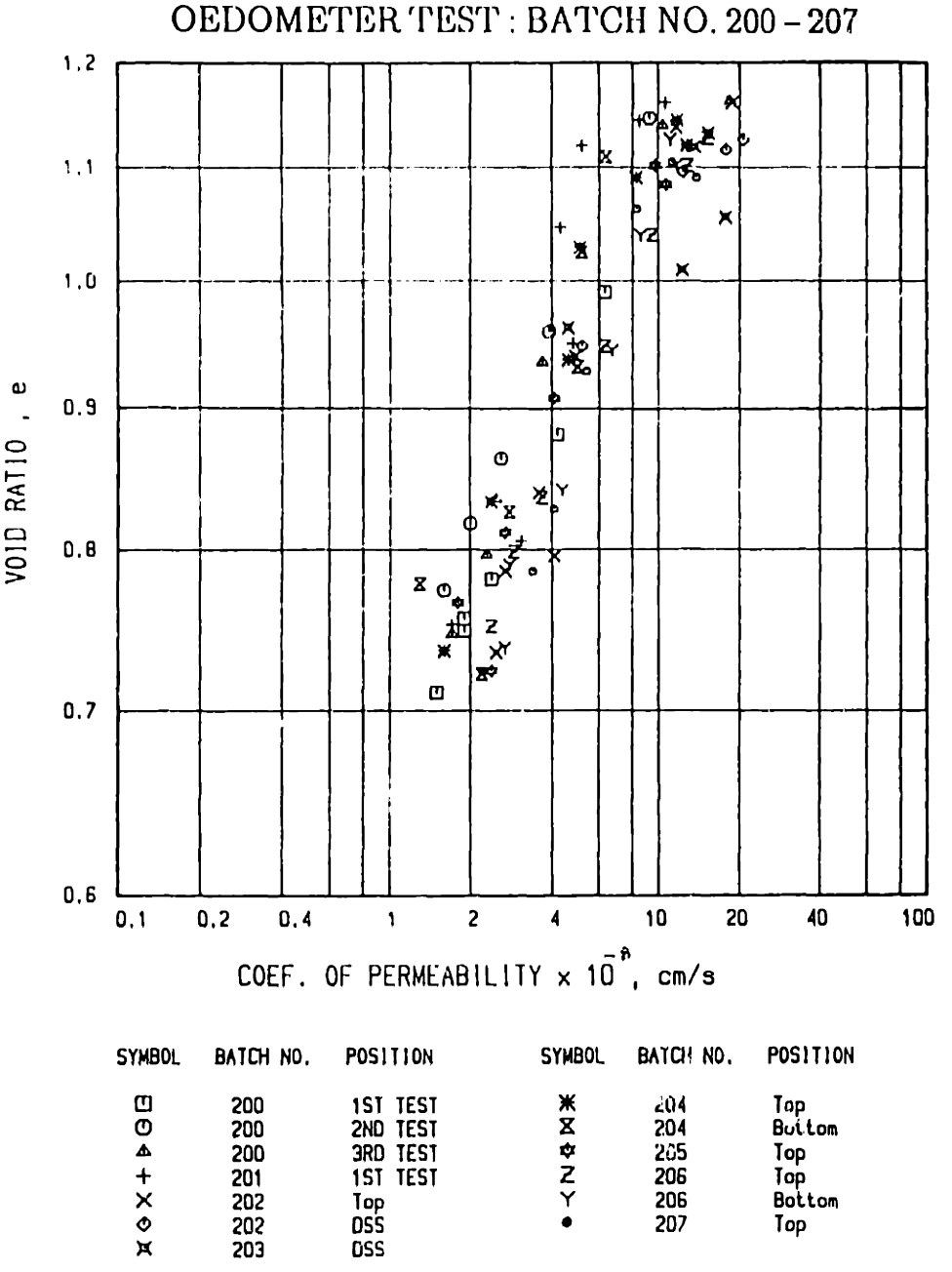

Figure B.22: Graph of Logarithm of Void Ratio versus Logarithm of Coefficient of Permeability for the Oedometer and DSS Consolidation Tests.

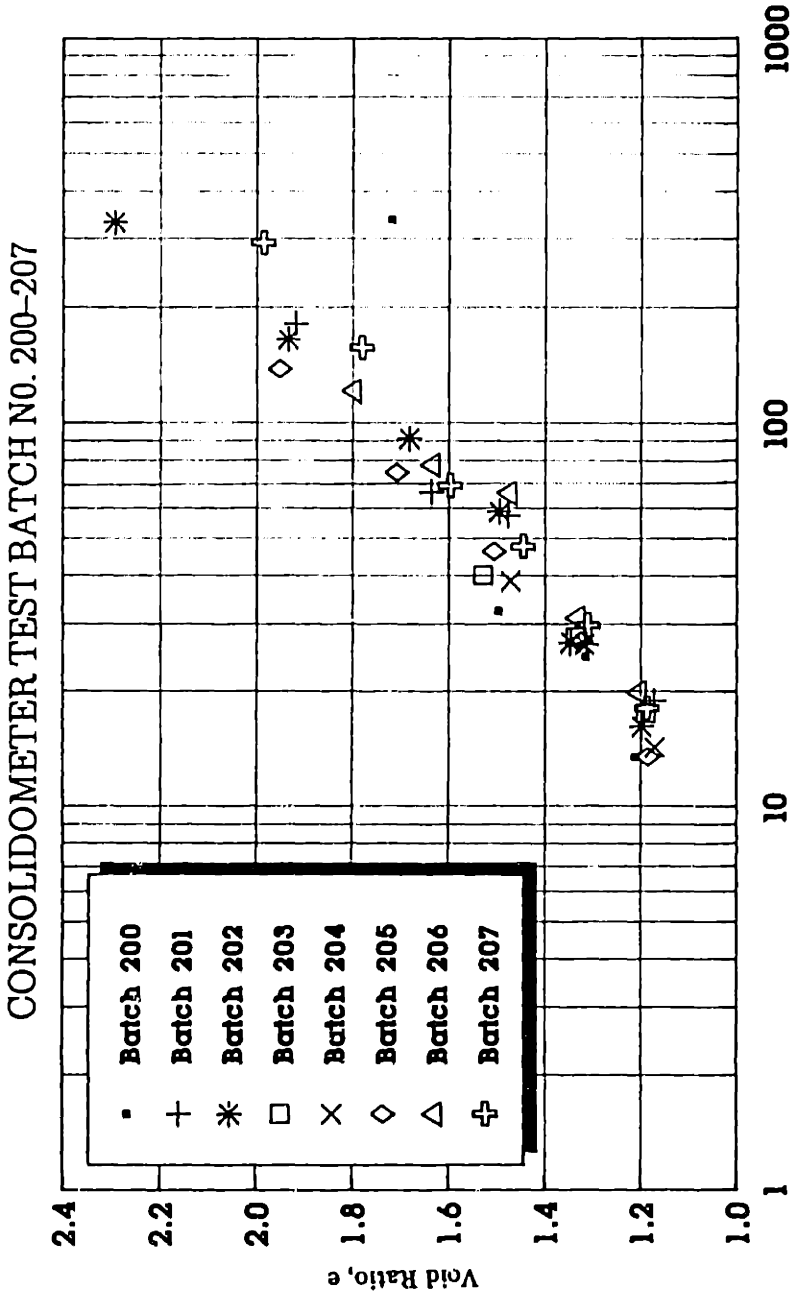

Figure B.23: Graph of Void Ratio versus Logarithm of Coefficient of Permeability for the Consolidometer Tests.

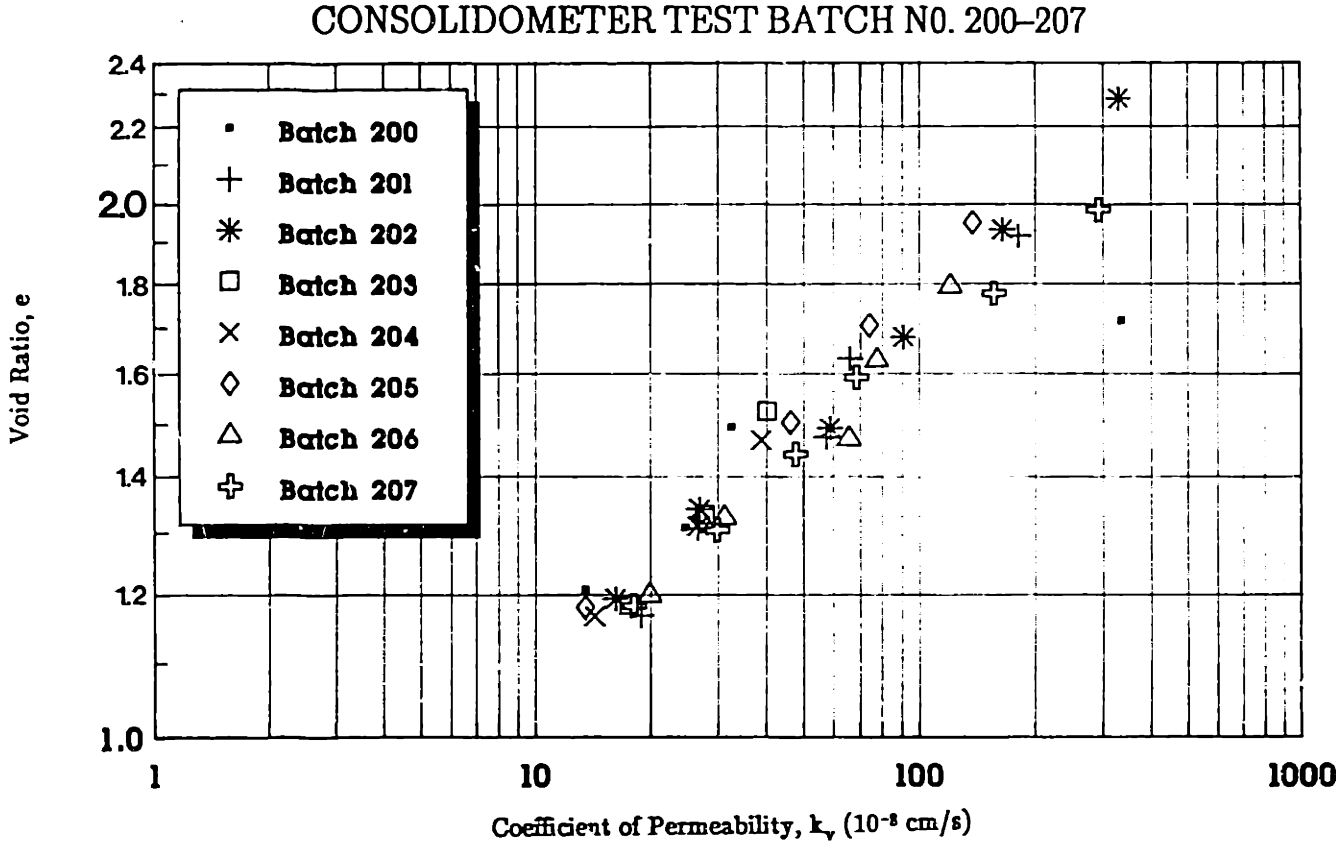

Figure B.24: Graph of Logarithm of Void Ratio versus Logarithm of Coefficient of Permeability for the Consolidometer Tests.

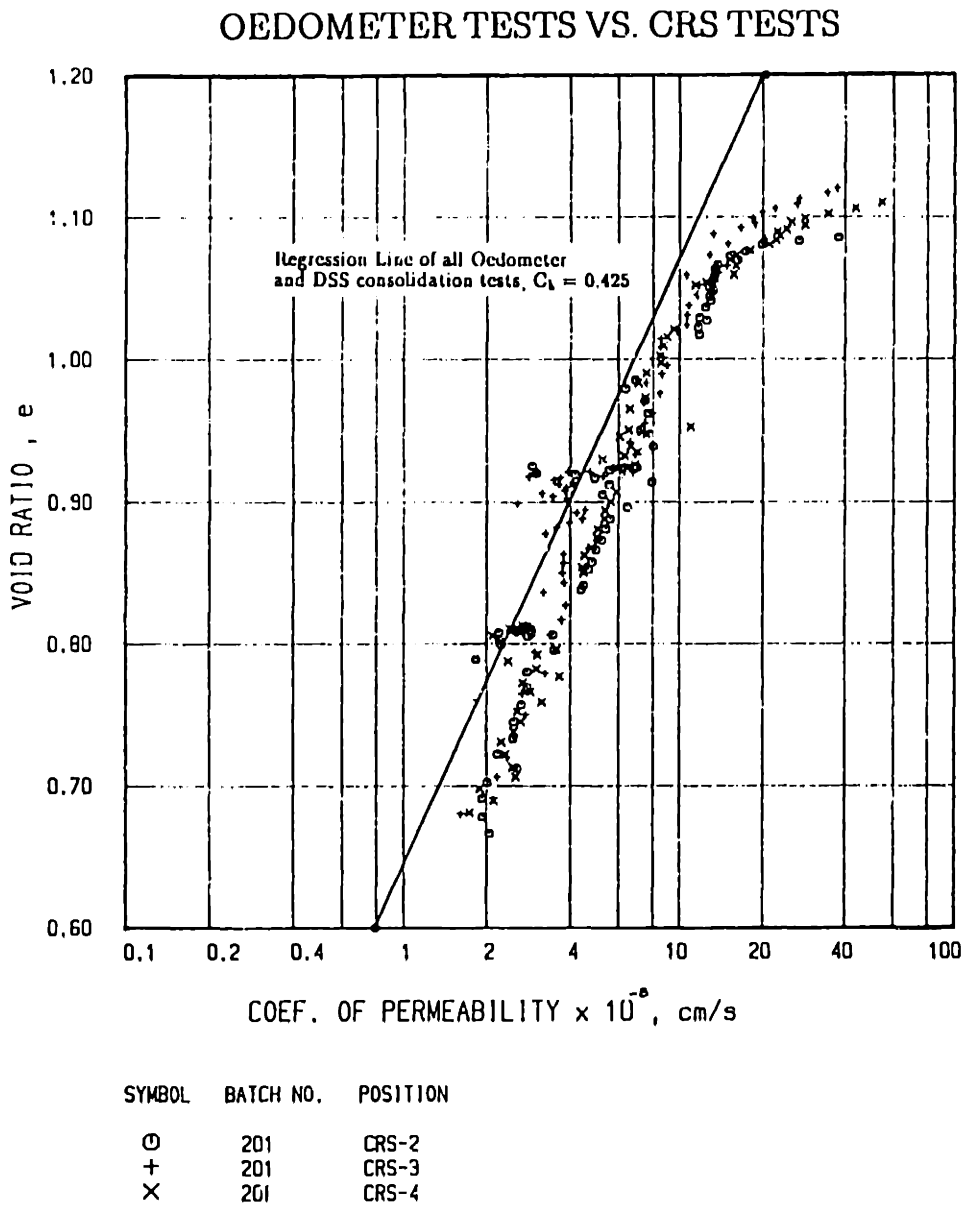

Figure B.25: Graph of Void Ratio versus Logarithm of Coefficient of Permeability for the Oedometer, DSS consolidation and CRS tests.

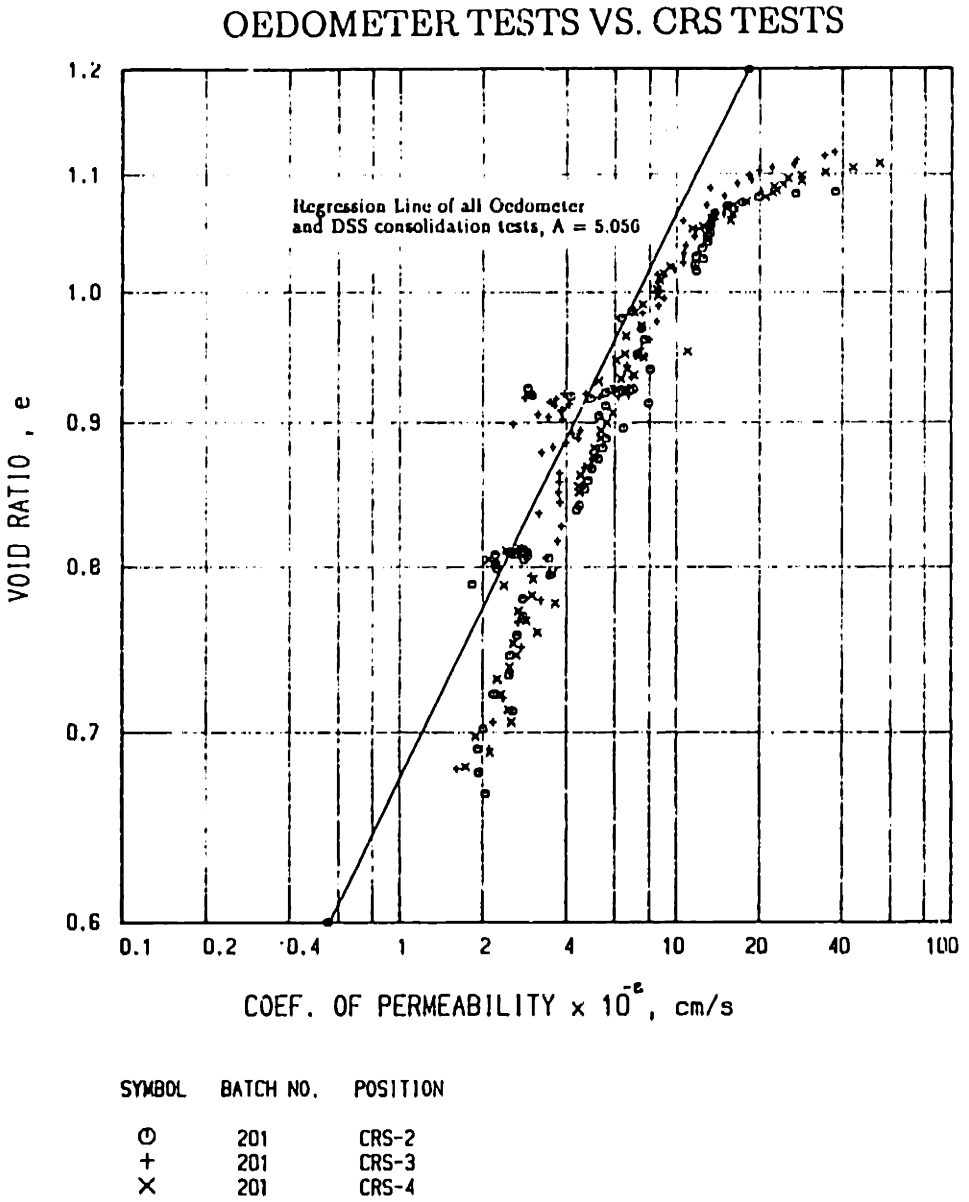

Figure B.26: Graph of Logarithm of Void Ratio versus Logarithm of Coefficient of Permeability for the Oedometer, DSS Consolidation and CRS Tests.

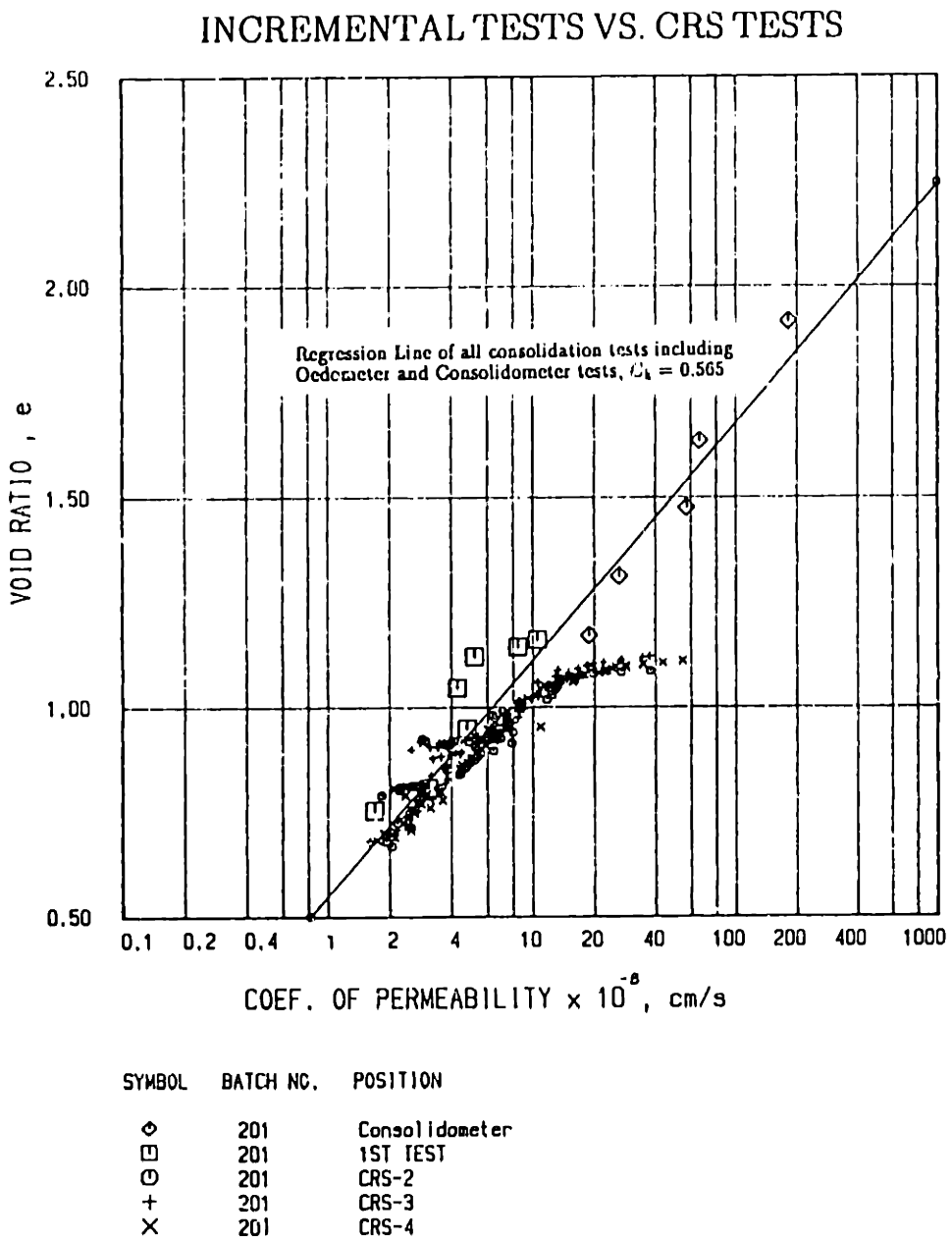

Figure B.27: Graph of Void Ratio versus Logarithm of Coefficient of Permeability for the Incremental Consolidation and CRS Tests.

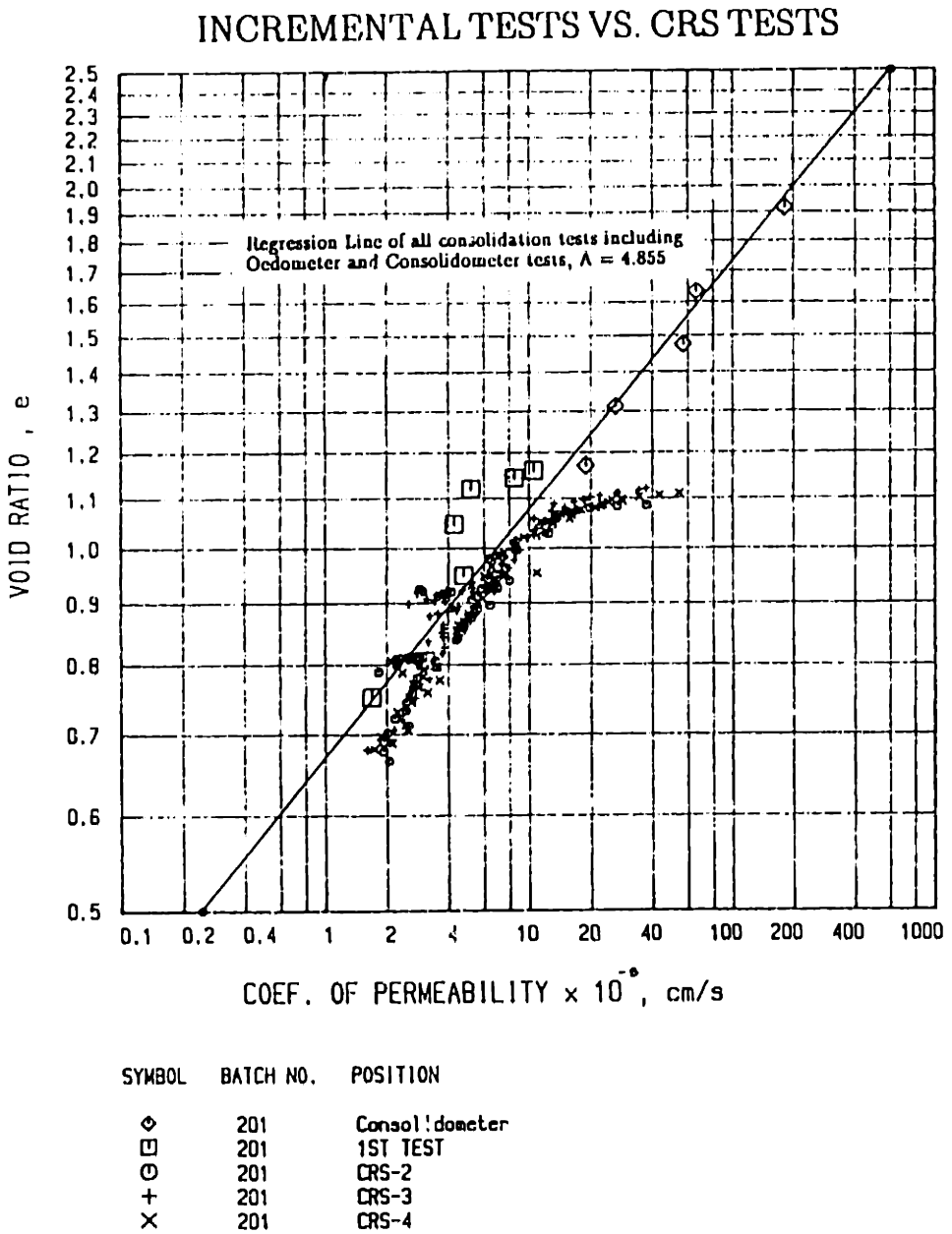

Figure B.28: Graph of Logarithm of Void Ratio versus Logarithm of Coefficient of Permeability for the Incremental Consolidation and CRS Tests.

Coefficient of Permeability

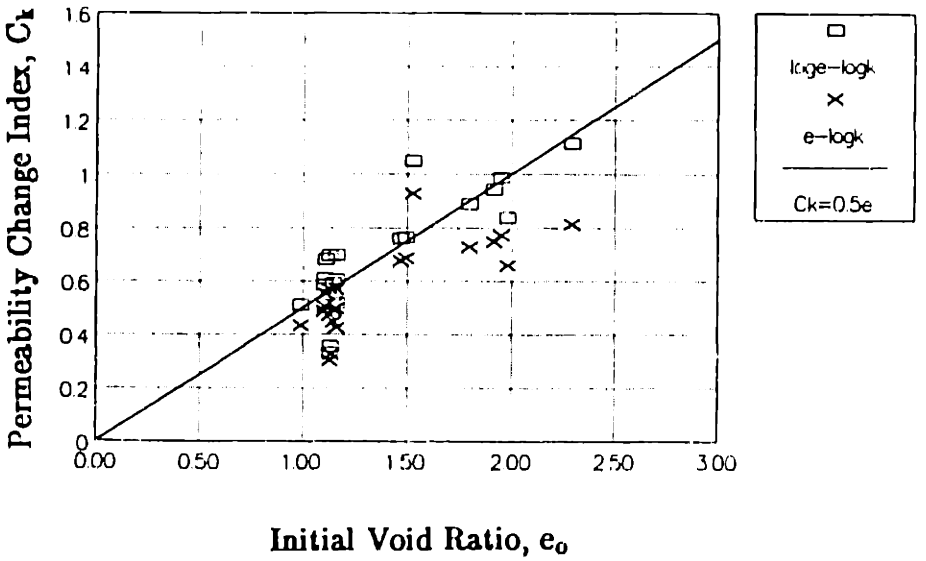

Figure B.29: Graph of Permeability Change Index, C_k, versus Initial Void Ratio, e_o.

APPENDIX C

RESULTS OF PREVIOUS DSC TESTS ON RESEDIMENTED BOSTON BLUE CLAY

C.1 INTRODUCTION

This appendix summarizes the experimental results of the DSC tests on OCR=4 resedimented Boston Blue Clay performed by Germaine (1982) and O'Neill (1985).

Sixteen DSC tests were performed, eleven of which were the tests conducted to investigate the undrained anisotropy of overconsolidated clay. Three of these tests suffered from boundary failures, and the results of the three tests were disregarded by O'Neill (1985). Five proof tests were also conducted to check the performance of the DSC device on OCR=4 BBC. Two out of five tests were disqualified due to boundary slippage. The results of the remaining three tests are discussed in Section 6.2.2.

The resedimented BBC used (designated as BBC II) was found to be thixotropic (O'Neill, 1985). This thixotropic behavior causes an increase in the preconsolidation pressure and the undrained shear strength. A correction procedure was developed by O'Neill (1985) to remove the discrepancy due to this effect based on the results from triaxial compression and triaxial extension tests on the same material at OCR=4.

A plot of Δq_y and $\Delta(\Delta u_s)$ versus storage time (t_s) from the triaxial data was established which is used as basis for correction in the DSC data. The Δq_y is defined as the thixotropic strength gain and the $\Delta(\Delta u_s)$ is the change in shear induced pore pressure, for a given storage time (t_s). The storage time is defined as the time elapsed between application of the last batch consolidation increment and

the recompression in the DSC test. The correction procedure is discussed in the next section (Table C.1).

C.2 PROCEDURE TO CORRECT FOR THIXOTROPIC EFFECT

The shear stresses (q) in the DSC tests were corrected for thixotropic effects using the Δq_y versus t_s relationship obtained from triaxial tests. The mean effective stresses (p′) of the DSC tests were also modified for thixotropy by assuming the intermediate principal stress (σ'_2) equals to $0.35(\sigma'_1+\sigma'_3)$, which can then be expressed in terms of Δu_s. Table C.1 summarizes the correction procedure which consists of two parts:

a) Shear Stress Correction:

The shear stress correction procedure is as follows:

1) Determine the elapsed storage time (t_s) for a given test.

2) Refer to Figure C.1 to estimate the strength increase, Δq_y, due to thixotropy.

3) Determine the measured yield stress, q_y, from the uncorrected stress–strain curve using either the Strain Energy Method (Tavenas et al., 1979) or another suitable construction.

4) Calculate q_t (i.e., q at "t_s=0") for all shear stress levels less than or equal to q_y ($t=t_s$) as follows:

$$q_t = \left(\frac{q}{q_y}\right) \times [\, q_y(t=t_s) - \Delta q_y \,] = q - \Delta q_y\left(\frac{q}{q_y}\right)$$

5) Calculate q_t for all shear stress levels greater than $q_y(t=t_s)$ as follows:

$$q_t = q - \Delta q_y.$$

b) Mean Effective Stress Correction:

The procedure for correcting the mean effective stress is as follows:

1) Determine the shear stress level at which the stress–strain curve first deviates from its initial shear modulus. Refer, then, to the accompanying stress path to ascertain the p' associated with this level of shear stress. Call these values q_e and p'_e respectively, using the subscript $_e$ to denote the elastic behavior.

2) For the given shear test, the full correction effect is applied at the shear strain levels at which essentially constant Δu_s values are reached. The shear stress level for these strains are determined from the appropriate stress–strain curves and, subsequently, one can obtain the pertinent value of p' from the effective stress for the test. Call these q_p and p'_p respectively, in this case using the subscript $_p$ to denote the more plastic behavior at this point in the test. It is slightly more difficult to determine q_p and p'_p for stress–controlled type tests, such as the DSC tests, since nearly constant values of Δu_s are not so readily achieved. For these cases, the stress–strain curve is once again consulted for the shear stress level, q, at which the yielded modulus, G_y, is reached.

3) Determine $\Delta(\Delta u_s)$ from Figure C.1 based on the same time of storage, t_s, used to determine Δq_y. Convert $\Delta(\Delta u_s)$ to $\Delta(\Delta p')$ relevant to the test conditions under consideration.

4) For values of $q<q_e$, do not alter p' (therefore $p'_t=p'$).

5) For values of $q>q_p$, subtract $\Delta(\Delta p')$ from p' to obtain the corrected value, p'_t.

6) For intermediate values of q (which are also intermediate values of p', i.e., $p'_e<p'<p'_p$ and $q_e<q<q_p$) subtract a proportional amount of $\Delta(\Delta p')$ from p' according to the following equation:

$$p'_t = p' - \Delta(\Delta p') \times \left(\frac{p' - p'_p}{p'_p - p'_e}\right)$$

C.3 SUMMARY OF RESULTS

Table C.2 presents the estimated parameters needed in correcting the thixotropic effects for all the sixteen DSC tests on BBC II. Summary of the corrected results at failure are tabulated in Table C.3.

The uncorrected and corrected stress values together with strain data for each test are summarized in Tables C.4 through C.19. These data are also presented in Figures C.2 to C.17, which include plots of the effective stress paths, the stress–strain relationships and the volumetric behaviors.

Figures C.18 to C.33 plot the NAR (Normalized Area Ratio=$\frac{\gamma_2}{\gamma_1}$) versus the corrected normalized shear stress and shear strain for each test to show if the test has qualified the strain distribution standard, i.e., within the acceptable range of $0.84<NAR<1.26$. DSC tests with NAR falling outside this range usually suffered from boundary failures.

Table C.1: Correction Method for Effect of Thixotropy on Undrained Shear Strength Tests (after O'Neill, 1985).

Correction for Thixotropic Effect		Triaxial Compression $\sigma_1 > \sigma_2 = \sigma_3$	Triaxial Extension $\sigma_1 = \sigma_2 > \sigma_3$	DSC (Plane Strain) $\sigma_1 > \sigma_2 > \sigma_3$, $\sigma'_2 = 0.35\ (\sigma'_1 + \sigma'_3)$
Correction of Shear Stress, $q = \frac{(\sigma_1 - \sigma_3)}{2}$	General	• Determine elapse storage time, t_s. [t_s (days)=date test recompressed-date batch unloaded to 0.25 ksc -5]. • Find Δq_y using t_s from Figure C.1.		
	$q \leq q_y$	$q_t = q - \Delta q_y\ (q/q_y)$		
	$q > q_y$	$q_t = q - \Delta q_y$		
Correction of Average Effective Stress, $p' = \frac{(\sigma'_1 + \sigma'_3)}{2}$	General	• Using t_s, find $\Delta(\Delta u_s)$ from Figure C.1.		
	Convert $\Delta(\Delta u_s) = \Delta(\Delta p')$	$\Delta(\Delta p') = \Delta q_y/3 - \Delta(\Delta u_s)$	$\Delta(\Delta p') = -[\Delta q_y/3 + \Delta(\Delta u_s)]$	$\Delta(p') = -1.1\ \Delta(\Delta u_s)$
	$q \leq q_e$	$p'_t = p'$		
	$q > q_p$	$p'_t = p' - \Delta(\Delta p')$		
	$q_e < q < q_p$ and $p_e < p' < p_p$	$p'_t = p' - \Delta(\Delta p') \left[\frac{p' - p'_e}{p'_p - p'_e} \right]$		

Table C.2: Summary of Parameters used in DSC Tests for Correction of Thixotropic Effect.

Test Number	Batch Number	Age, t_s • (days)	Type of Test	Δq_y • (ksc)	q_y (ksc)	q_e ‡ (ksc)	q_p ‡ (ksc)	p'_e ‡ (ksc)	p'_p ‡ (ksc)	Δu_s • (ksc)
DSC1	101	29	δ=0°	0.018	0.202	0.125	0.278	0.208	0.392	-0.030
DSC2	101	44	δ=90°	0.020	0.116	0.060	0.102	0.238	0.208	-0.033
DSC3	102	60	δ=0°	0.021	0.225	0.120	0.288	0.224	0.392	-0.035
DSC4	102	71	δ=45°	0.022	-	-	-	-	-	-0.020
DSC5	103	34	δ=45°	0.018	0.166	0.090	0.228	0.255	0.337	-0.028
DSC6	103	48	ϕ=0°	0.020	0.163	0.095	0.180	0.203	0.240	-0.034
DSC7	104	15	ϕ=45°	0.015	0.163	0.136	0.212	0.223	0.255	-0.025
DSC8	104	167	δ=65°	0.046	0.144	0.113	0.175	0.242	0.268	-0.070
DSC9	105	169	ϕ=25°	0.046	0.166	0.085	0.132	0.209	0.270	-0.071
DSC10	105	207	δ=20°	0.054	-	-	-	-	-	-
DSC11	106	71	δ=75°	0.022	0.118	0.065	0.108	0.260	0.242	-0.036
DSC12	106	91	ϕ=0°	0.023	0.155	0.085	0.140	0.203	0.252	-0.039
DSC13	107	39	δ=40°	0.019	0.160	0.105	0.197	0.215	0.311	-0.032
DSC14	109	79	ϕ=40°	0.022	0.153	0.090	0.130	0.204	0.243	-0.037
DSC15	109	92	δ=20°	0.023	0.188	0.100	0.215	0.215	0.318	-0.039
DSC16	110	105	δ=75°	0.027	0.122	0.074	0.120	0.253	0.236	-0.040

Notes: • Refer to Figure C.1.
‡ Refer to Table C.1.

Table C.3: Summary of DSC Tests on OCR=4 Resedimented Boston Blue Clay II at Failure.

Test No.	Batch No.	Type of Test (°)	Shear Sheet / Prism	B * value	u_c* (ksc)	w_i/w_f (%)	At Failure							$G_{s,0}$‡ / σ'_p	Remarks
							$\frac{q_f}{\sigma'_p}$	$\frac{p'_f}{\sigma'_p}$	A_f	$\frac{\sigma'_{1f}}{\sigma'_{3f}}$	γ_1 ‡ (%)	γ_2 † (%)	$\frac{\gamma_2}{\gamma_1}$		
DSC01	101	δ=0	No /No	0.86	0.14	40.6 /39.4	0.237	0.318	0.36	6.85	2.3	2.1	0.9	30	
DSC02	101	δ=90	No /No	1.00	0.08	40.8 /40.3	0.144	0.189	0.71	7.40	9.4	11.6	1.2	30	
DSC03	102	δ=0	Yes /No	0.85	0.11	39.7 /39.4	0.254	0.337	0.33	7.12	2.4	2.2	0.9	32	Sheared at δ=45° but membrane slipped
DSC04	102	δ=45	Yes /No	0.92	0.09	39.8 /39.8	-	-	-	-	-	-	-	-	Lost sides to progressive failure
DSC05	103	δ=45	Yes /Yes	0.99	0.07	40.1 /40.0	-	-	-	-	-	-	-	-	Anamalous pore pressure behavior
DSC06	103	δ=0	No /No	0.85	0.15	40.2 /39.6	0.183	0.228	0.56	9.32	5.6	6.9	1.2	65	
DSC07	104	δ=45	Yes /Yes	0.91	0.07	39.6 /39.9	-	-	-	-	-	-	-		
DSC08	104	δ=65	Yes /Yes	0.85	0.15	40.6 /40.4	0.156	0.223	0.59	5.66	6.4	6.5	1.0	28	

Notes:
- * The pore pressure parameter B is computed from the change in Δu over the change in $\Delta\sigma$ from a mean consolidation stress of 0.1 to 0.25 ksc.
- • Initial effective Stress.
- ‡ Maximum Shear Strains taken from Area No.1 (86%).
- † Maximum Shear Strains taken from Area No.2 (52%).

The preconsolidation pressure, σ'_p=1 ksc.

Table C.3: (Cont.)

Test No.	Batch No.	Type of Test (*)	Shear Sheet / Prism	B * value	u_c* (ksc)	w_i/w_f (%)	At Failure							$\frac{G_{s,0}}{\sigma'_p}$ ‡	Remarks
							$\frac{q_f}{\sigma'_p}$	$\frac{p'_f}{\sigma'_p}$	A_f	$\frac{\sigma'_{1f}}{\sigma'_{3f}}$	γ_1 ‡ (%)	γ_2 † (%)	$\frac{\gamma_2}{\gamma_1}$		
DSC09	105	ϕ=25	Yes /Yes	0.84	0.12	40.9 /40.8	0.163	0.200	0.65	9.81	6.2	4.5	0.7	35	
DSC10	105	δ=20	Yes /Yes	0.90	0.12	41.1 /40.9	-	-	-	-	-	-	-	-	Lost two corners to progressive yield
DSC11	106	δ=75	Yes /Yes	0.97	0.10	40.9 /40.6	0.147	0.218	0.61	4.82	11.4	9.4	0.8	18	
DSC12	106	ϕ=0	Yes /Yes	0.76	0.15	40.6 /40.8	0.169	0.210	0.62	9.24	6.2	7.0	1.1	45	
DSC13	107	δ=40	Yes /Yes	0.97	0.09	40.9 /40.6	0.196	0.256	0.48	7.53	4.3	3.5	0.8	30	
DSC14	109	ϕ=40	Yes /Yes	0.71	0.13	42.1 /42.1	0.166	0.203	0.64	9.97	3.7	3.2	0.9	60	Reconsolidated due to bag leak
DSC15	109	δ=20	Yes /Yes	0.85	0.13	41.6 /41.9	0.225	0.305	0.38	6.63	4.0	3.6	1.1	32	Deleted corners with prisms from strain cal
DSC16	110	δ=75	Yes /Yes	0.77	0.15	40.3 /40.0	0.160	0.234	0.55	5.32	11.3	13.0	1.1	18	New chervon-shaped prisms (Type B)

Notes:
- * The pore pressure parameter B is computed from the change in Δu over the change in $\Delta\sigma$ from a mean consolidation stress of 0.1 to 0.25 ksc.
- • Initial effective Stress.
- ‡ Maximum Shear Strains taken from Area No.1 (86%).
- † Maximum Shear Strains taken from Area No.2 (52%).
- The preconsolidation pressure, σ'_p=1 ksc.

Table C.4: Summary of Stress and Strain Data for Test DSC01.

DSC01: $\delta = 0°$

Film No.	Max.Shear Strain (%)		Volumetric Strain (%)		Uncorrected		Corrected	
					q	p'	qc	p'c
	(Area 1)	(Area 2)	(Area 1)	(Area 2)	(ksc)			
4	0.000	0.000	0.000	0.000	0.000	0.252	0.000	0.252
5	0.077	0.101	0.012	-0.005	0.051	0.223	0.046	0.223
6	0.247	0.212	-0.105	-0.096	0.085	0.207	0.077	0.207
7	0.476	0.432	-0.019	-0.037	0.139	0.208	0.127	0.208
8	0.689	0.641	-0.393	-0.419	0.163	0.216	0.149	0.215
9	0.984	0.908	0.007	-0.020	0.195	0.247	0.178	0.240
10	1.262	1.203	0.145	0.112	0.215	0.273	0.197	0.261
11	1.564	1.465	0.098	0.098	0.235	0.311	0.217	0.293
12	2.266	2.073	0.082	0.082	0.255	0.341	0.237	0.317

Notes:

1. Area No. 1 represents 86% of cross–sectional area.
2. Area No. 2 represents 52% of cross–sectional area.
3. Volumetric Strain: Contraction is positive.
4. Corrected values have been adjusted for thixotropic effect.

Table C.5: Summary of Stress and Strain Data for Test DSC02.

DSC02: $\delta = 90°$

Film No.	Max.Shear Strain (%)		Volumetric Strain (%)		Uncorrected		Correct	
					q	p′	qc	p′c
	(Area 1)	(Area 2)	(Area 1)	(Area 2)	(ksc)			
3	0.000	0.000	0.000	0.000	0.000	0.251	0.000	0.251
4	0.004	0.051	0.251	0.229	0.030	0.246	0.027	0.246
5	0.080	0.107	0.363	0.417	0.060	0.242	0.055	0.242
6	0.302	0.318	0.289	0.331	0.090	0.231	0.082	0.222
7	0.637	0.634	0.291	0.321	0.105	0.220	0.096	0.184
8	0.972	1.045	0.302	0.333	0.115	0.215	0.105	0.179
9	1.310	1.447	0.313	0.328	0.120	0.214	0.102	0.178
10	1.842	2.127	0.248	0.248	0.124	0.208	0.106	0.172
11	2.558	3.027	0.334	0.334	0.130	0.210	0.112	0.174
12	3.550	4.335	0.218	0.263	0.136	0.211	0.118	0.175
13	4.462	5.558	0.284	0.226	0.142	0.215	0.124	0.179
14	5.825	7.215	0.143	0.115	0.146	0.217	0.128	0.181
15	6.700	8.322	0.150	0.100	0.152	0.217	0.134	0.181
16	7.658	9.511	0.142	0.071	0.158	0.223	0.140	0.187
17	8.071	10.007	0.189	0.091	0.160	0.223	0.142	0.187
18	9.444	11.612	0.014	-0.144	0.162	0.225	0.144	0.189
19	10.872	13.128	-0.080	-0.292	0.164	0.230	0.146	0.194

Notes:

1. Area No. 1 represents 86% of cross–sectional area.
2. Area No. 2 represents 52% of cross–sectional area.
3. Volumetric Strain: Contraction is positive.
4. Corrected values have been adjusted for thixotropic effect.

Table C.6: Summary of Stress and Strain Data for Test DSC03.

DSC03: $\delta = 0°$

Film No.	Max.Shear Strain (%)		Volumetric Strain (%)		Uncorrected		Corrected	
					q	p'	qc	p'c
	(Area 1)	(Area 2)	(Area 1)	(Area 2)	(ksc)			
13	0.000	0.000	0.000	0.000	0.000	0.250	0.000	0.250
14	0.052	0.016	-0.102	-0.124	0.050	0.234	0.046	0.234
15	0.186	0.121	0.066	0.077	0.100	0.224	0.091	0.224
16	0.370	0.140	0.359	0.219	0.135	0.225	0.123	0.225
17	0.547	0.399	-0.014	-0.021	0.160	0.241	0.146	0.237
18	0.732	0.570	0.059	0.022	0.183	0.250	0.167	0.244
19	0.978	0.788	0.038	-0.007	0.205	0.270	0.187	0.259
20	1.187	0.979	0.140	0.101	0.220	0.298	0.200	0.281
21	1.367	1.162	0.151	0.061	0.235	0.304	0.214	0.286
22	1.577	1.369	0.140	0.115	0.250	0.325	0.229	0.302
23	1.864	1.697	0.021	-0.027	0.265	0.349	0.244	0.320
24	2.347	2.193	0.058	-0.012	0.275	0.369	0.254	0.336

Notes:

1. Area No. 1 represents 86% of cross–sectional area.
2. Area No. 2 represents 52% of cross–sectional area.
3. Volumetric Strain: Contraction is positive.
4. Corrected values have been adjusted for thixotropic effect.

Table C.7: Summary of Stress and Strain Data for Test DSC04.

DSC04: $\delta = 45°$

Film No.	Max. Shear Strain (%)		Volumetric Strain (%)		Uncorrected		Corrected	
					q	p'	qc	p'c
	(Area 1)	(Area 2)	(Area 1)	(Area 2)	(ksc)			
3	0.000	0.000	0.000	0.000	0.000	0.253		
4	0.046	0.015	0.016	0.025	0.031	0.261		
5	0.109	0.020	0.060	0.104	0.059	0.254		
6	0.156	0.060	0.048	0.077	0.080	0.247		
7	0.277	0.124	-0.053	-0.020	0.103	0.238		
8	1.280	0.226	0.041	-0.001	0.124	0.236		
9	0.658	0.327	0.015	0.127	0.136	0.240		
10	0.806	0.373	-0.103	0.034	0.145	0.245		
11	1.017	0.421	-0.065	0.098	0.155	0.254		
12	1.292	0.565	-0.183	0.002	0.163	0.259		
13	1.556	0.675	-0.166	0.077	0.170	0.264		
14	1.823	0.763	-0.185	0.099	0.178	0.269		
15	2.130	0.903	-0.238	0.111	0.185	0.275		
16	2.622	1.107	-0.286	0.104	0.193	0.285		
17	3.019	1.250	-0.324	0.126	0.200	0.292		
18	3.460	1.480	-0.369	0.096	0.207	0.298		

Notes:

1. Area No. 1 represents 86% of cross–sectional area.
2. Area No. 2 represents 52% of cross–sectional area.
3. Volumetric Strain: Contraction is positive.
4. Corrected values have been adjusted for thixotropic effect.

Table C.6: Summary of Stress and Strain Data for Test DSC05.

DSC05: $\delta = 45°$

Film No.	Max.Shear Strain (%)		Volumetric Strain (%)		Uncorrected		Corrected	
					q	p'	qc	p'c
	(Area 1)	(Area 2)	(Area 1)	(Area 2)	(ksc)			
4	0.000	0.000	0.000	0.000	0.000	0.252	0.000	0.252
5	0.071	0.070	-0.042	-0.055	0.040	0.277	0.033	0.277
6	0.130	0.119	-0.060	-0.029	0.070	0.272	0.058	0.272
7	0.196	0.200	-0.097	-0.096	0.090	0.259	0.075	0.250
8	0.303	0.274	-0.006	0.014	0.113	0.251	0.094	0.243
9	0.506	0.457	-0.072	-0.049	0.133	0.250	0.111	0.242
10	0.786	0.666	-0.085	-0.026	0.150	0.262	0.125	0.252
11	1.081	0.883	-0.134	-0.063	0.164	0.273	0.136	0.261
12	1.782	1.424	-0.173	-0.066	0.180	0.286	0.152	0.272
13	2.492	1.908	-0.234	-0.063	0.190	0.299	0.162	0.282
14	3.423	2.618	-0.348	-0.124	0.198	0.307	0.170	0.289
15	4.090	3.190	-0.449	-0.238	0.205	0.313	0.177	0.294
16	4.890	3.901	-0.386	-0.115	0.213	0.321	0.185	0.300
17	5.882	4.771	-0.550	-0.281	0.220	0.325	0.192	0.30[illegible]
18	7.427	6.208	-0.603	-0.180	0.228	0.337	0.200	0.3[illegible]

Notes:

1. Area No. 1 represents 86% of cross–sectional area.
2. Area No. 2 represents 5[illegible]% of cross–sectional area.
3. Volumetric Strain: Contraction is positive.
4. Corrected values have been adjusted for thixotropic effect.

Table C.9: Summary of Stress and Strain Data for Test DSC06.

DSC06: $\psi = 0°$

Film No.	Max. Shear Strain (%)		Volumetric Strain (%)		Uncorrected		Corrected	
					q	p'	qc	p'c
	(Area 1)	(Area 2)	(Area 1)	(Area 2)	(ksc)			
2	0.000	0.000	0.000	0.000	0.000	0.250	0.000	0.250
3	0.054	0.060	0.052	0.027	0.040	0.235	0.035	0.235
5	0.122	0.103	0.034	0.033	0.070	0.229	0.061	0.229
6	0.195	0.191	0.081	0.049	0.101	0.219	0.089	0.203
7	0.404	0.349	0.399	0.017	0.123	0.205	0.108	0.203
8	0.688	0.626	-0.042	-0.116	0.138	0.203	0.121	0.203
9	1.145	1.075	0.025	0.030	0.152	0.207	0.133	0.203
10	1.887	1.887	0.081	0.099	0.168	0.227	0.148	0.203
11	2.723	2.837	-0.057	-0.027	0.180	0.240	0.160	0.203
12	3.524	3.821	-0.122	-0.127	0.187	0.246	0.167	0.209
13	4.031	4.471	-0.103	-0.099	0.192	0.256	0.172	0.219
14	4.722	5.293	-0.190	-0.199	0.197	0.258	0.177	0.221
15	5.554	6.261	-0.118	-0.157	0.203	0.265	0.183	0.228

Notes:

1. Area No. 1 represents 86% of cross–sectional area.
2. Area No. 2 represents 52% of cross–sectional area.
3. Volumetric Strain: Contraction is positive.
4. Corrected values have been adjusted for thixotropic effect.

Table C.10: Summary of Stress and Strain Data for Test DSC07.

DSC07: $\psi = 45°$

Film No.	Max.Shear Strain (%)		Volumetric Strain (%)		Uncorrected		Corrected	
					q	p'	qc	p'c
	(Area 1)	(Area 2)	(Area 1)	(Area 2)	(ksc)			
3	0.000	0.000	0.000	0.000	0.000	0.252	0.000	0.252
4	0.060	0.044	-0.163	-0.152	0.030	0.267	0.027	0.267
5	0.047	0.033	-0.147	-0.199	0.061	0.259	0.055	0.259
6	0.110	0.104	-0.077	-0.073	0.090	0.244	0.082	0.244
7	0.278	0.239	0.046	0.093	0.117	0.233	0.106	0.233
8	0.548	0.455	0.019	0.119	0.136	0.223	0.124	0.223
9	0.918	0.728	-0.107	-0.018	0.153	0.224	0.139	0.223
10	1.478	1.178	-0.245	-0.107	0.167	0.234	0.152	0.225
11	2.058	1.656	-0.150	0.077	0.180	0.237	0.165	0.225
12	2.712	2.194	-0.258	0.023	0.186	0.239	0.171	0.225
13	3.422	2.781	-0.407	-0.114	0.193	0.243	0.178	0.226
14	4.128	3.439	-0.572	-0.198	0.197	0.248	0.182	0.227
15	4.814	4.064	-0.692	-0.278	0.203	0.248	0.188	0.227
16	5.707	4.960	-0.674	-0.215	0.208	0.251	0.193	0.227
17	7.123	6.431	-0.861	-0.322	0.212	0.255	0.197	0.228
18	8.338	7.638	-1.162	-0.561	0.216	0.255	0.201	0.228

Notes:

1. Area No. 1 represents 86% of cross–sectional area.
2. Area No. 2 represents 52% of cross–sectional area.
3. Volumetric Strain: Contraction is positive.
4. Corrected values have been adjusted for thixotropic effect.

Table C.11: Summary of Stress and Strain Data for Test DSC08.

DSC08: $\delta = 65°$

Film No.	Max.Shear Strain (%)		Volumetric Strain (%)		Uncorrected		Corrected	
					q	p'	qc	p'c
	(Area 1)	(Area 2)	(Area 1)	(Area 2)	(ksc)			
2	0.000	0.000	0.000	0.000	0.000	0.250	0.000	0.250
4	0.072	0.075	-0.109	-0.165	0.030	0.257	0.020	0.257
5	0.074	0.083	-0.146	-0.153	0.060	0.263	0.041	0.263
6	0.210	0.173	-0.107	-0.173	0.090	0.249	0.061	0.249
7	0.276	0.231	-0.169	-0.202	0.113	0.246	0.077	0.246
8	0.415	0.368	-0.090	-0.100	0.135	0.244	0.092	0.244
9	0.643	0.589	-0.020	0.003	0.150	0.248	0.104	0.236
10	1.009	0.890	-0.079	-0.063	0.160	0.254	0.114	0.223
12	2.100	1.835	-0.263	-0.141	0.175	0.268	0.129	0.191
14	3.026	2.822	-0.416	-0.224	0.185	0.276	0.139	0.199
16	4.815	4.732	-0.460	-0.195	0.198	0.283	0.152	0.206
18	6.427	6.523	-0.512	-0.205	0.208	0.293	0.162	0.216
20	8.387	8.743	-0.881	-0.562	0.218	0.303	0.172	0.226
22	11.734	12.448	-1.182	-0.728	0.228	0.322	0.182	0.245
24	13.819	15.235	-1.365	-0.913	0.228	0.317	0.182	0.240

Notes:

1. Area No. 1 represents 86% of cross–sectional area.
2. Area No. 2 represents 52% of cross–sectional area.
3. Volumetric Strain: Contraction is positive.
4. Corrected values have been adjusted for thixotropic effect.

Table C.12: Summary of Stress and Strain Data for Test DSC09.

DSC09: $\psi = 25°$

Film No.	Max.Shear Strain (%)		Volumetric Strain (%)		Uncorrected		Corrected	
					q	p'	qc	p'c
	(Area 1)	(Area 2)	(Area 1)	(Area 2)	(ksc)			
1	0.000	0.000	0.000	0.000	0.000	0.252	0.000	0.252
2	0.071	0.091	0.211	0.268	0.000	0.250	0.000	0.250
4	0.055	0.038	0.121	-0.071	0.040	0.240	0.029	0.240
5	0.073	0.082	0.078	0.118	0.070	0.236	0.051	0.236
6	0.218	0.197	0.150	0.213	0.100	0.218	0.072	0.206
7	0.401	0.304	0.186	0.248	0.123	0.209	0.089	0.209
8	0.641	0.438	0.042	0.156	0.137	0.209	0.099	0.209
9	1.016	0.759	-0.075	0.119	0.152	0.217	0.110	0.207
10	1.714	1.123	-0.017	0.302	0.168	0.222	0.122	0.205
11	2.417	1.679	-0.153	0.251	0.180	0.234	0.134	0.202
13	3.640	2.662	-0.370	0.157	0.195	0.250	0.149	0.198
15	4.540	3.370	-0.360	0.254	0.205	0.259	0.159	0.195
17	6.177	4.516	-0.625	0.115	0.215	0.272	0.169	0.194
19	8.407	6.937	-0.887	-0.084	0.225	0.283	0.179	0.205
21	11.961	11.120	-1.318	-0.550	0.230	0.291	0.184	0.213
22	14.032	13.949	-1.601	-0.875	0.234	0.293	0.188	0.215

Notes:

1. Area No. 1 represents 86% of cross–sectional area.
2. Area No. 2 represents 52% of cross–sectional area.
3. Volumetric Strain: Contraction is positive.
4. Corrected values have been adjusted for thixotropic effect.

Table C.13: Summary of Stress and Strain Data for Test DSC10.

DSC10: $\delta = 20°$

Film No.	Max.Shear Strain (%)		Volumetric Strain (%)		Uncorrected		Corrected	
					q	p'	qc	p'c
	(Area 1)	(Area 2)	(Area 1)	(Area 2)	(ksc)			
2	0.028	0.019	0.040	0.034	0.000	0.252	0.000	
4	0.083	0.071	-0.081	-0.102	0.051	0.246	0.032	
5	0.174	0.168	0.036	0.025	0.088	0.236	0.055	
6	0.317	0.315	-0.064	-0.111	0.120	0.221	0.075	
7	0.563	0.569	0.006	0.002	0.151	0.223	0.095	
8	1.093	0.890	-0.101	-0.057	0.175	0.235	0.110	
9	2.759	1.286	-0.459	0.000	0.198	0.261	0.130	
10	3.253	1.623	-0.487	-0.005	0.213	0.281	0.145	
11	4.916	2.157	-0.537	-0.002	0.228	0.305	0.160	
12	5.111	2.773	-0.684	-0.175	0.240	0.321	0.172	
13	5.761	4.174	-0.661	-0.119	0.248	0.341	0.180	
14	6.012	4.477	-0.599	-0.083	0.251	0.397	0.183	
15	6.406	4.949	-0.659	0.143	0.253	0.352	0.185	
16	7.066	5.658	-0.735	-0.196	0.258	0.361	0.190	
17	8.630	7.496	-0.782	-0.185	0.264	0.366	0.196	
18	9.703	8.763	-0.880	-0.318	0.265	0.367	0.197	

Notes:

1. Area No. 1 represents 86% of cross–sectional area.
2. Area No. 2 represents 52% of cross–sectional area.
3. Volumetric Strain: Contraction is positive.
4. Corrected values have been adjusted for thixotropic effect.

Table C.14: Summary of Stress and Strain Data for Test DSC11.

DSC11: $\delta = 75°$

Film No.	Max. Shear Strain (%)		Volumetric Strain (%)		Uncorrected		Corrected	
					q	p'	qc	p'c
	(Area 1)	(Area 2)	(Area 1)	(Area 2)	(ksc)			
2	0.050	0.029	0.041	0.054	0.000	0.251	0.000	0.252
4	0.010	0.020	0.088	0.104	0.010	0.253	0.008	0.253
5	0.004	0.023	-0.053	-0.005	0.020	0.255	0.016	0.255
6	0.028	0.014	0.008	0.013	0.031	0.259	0.025	0.259
7	0.114	0.141	0.023	0.047	0.060	0.260	0.049	0.260
8	0.426	0.412	0.070	0.101	0.090	0.252	0.073	0.234
9	0.754	0.753	0.042	0.087	0.107	0.244	0.087	0.209
10	1.436	1.535	0.031	0.050	0.123	0.243	0.101	0.203
11	2.143	2.314	0.057	0.038	0.131	0.242	0.109	0.202
12	3.727	4.351	0.010	0.076	0.141	0.241	0.119	0.201
13	6.177	6.611	0.356	-0.113	0.150	0.248	0.128	0.208
14	7.166	8.678	-0.217	-0.236	0.158	0.250	0.136	0.210
15	8.311	10.123	-0.285	-0.324	0.163	0.256	0.141	0.216
16	9.739	11.882	-0.276	-0.374	0.168	0.258	0.146	0.218
17	11.441	14.059	-0.467	-0.656	0.173	0.263	0.151	0.223
18	12.730	15.651	-0.638	-0.839	0.176	0.266	0.154	0.226
19	13.706	16.909	-0.750	-1.021	0.178	0.266	0.156	0.226

Notes:

1. Area No. 1 represents 86% of cross–sectional area.
2. Area No. 2 represents 52% of cross–sectional area.
3. Volumetric Strain: Contraction is positive.
4. Corrected values have been adjusted for thixotropic effect.

Table C.15: Summary of Stress and Strain Data for Test DSC12.

DSC12: $\psi = 0°$

Film No.	Max.Shear Strain (%)		Volumetric Strain (%)		Uncorrected		Corrected	
					q	p'	qc	p'c
	(Area 1)	(Area 2)	(Area 1)	(Area 2)	(ksc)			
2	0.013	0.016	-0.088	-0.036	0.000	0.250	0.000	0.250
4	0.014	0.063	-0.118	-0.072	0.030	0.239	0.025	0.239
5	0.081	0.064	-0.036	0.006	0.050	0.233	0.042	0.233
6	0.111	0.096	-0.041	-0.029	0.070	0.225	0.059	0.225
7	0.171	0.192	-0.057	0.008	0.090	0.216	0.076	0.216
8	0.342	0.307	-0.024	0.012	0.108	0.208	0.091	0.208
9	0.519	0.447	-0.041	0.018	0.123	0.205	0.103	0.205
10	0.713	0.662	-0.098	-0.005	0.133	0.203	0.112	0.203
11	1.028	0.958	0.007	0.066	0.143	0.204	0.120	0.203
12	1.373	1.369	-0.048	0.045	0.153	0.210	0.130	0.204
13	2.296	2.418	-0.062	0.079	0.168	0.224	0.145	0.206
14	3.916	4.324	-0.327	-0.197	0.181	0.234	0.158	0.207
15	5.390	6.071	-0.449	-0.337	0.188	0.250	0.165	0.209
16	6.177	7.028	-0.462	-0.379	0.192	0.253	0.169	0.210
17	10.197	12.010	-0.832	-0.799	0.198	0.257	0.175	0.214
18	13.641	16.387	-1.180	-1.202	0.203	0.261	0.180	0.218

Notes:

1. Area No. 1 represents 86% of cross–sectional area.
2. Area No. 2 represents 52% of cross–sectional area.
3. Volumetric Strain: Contraction is positive.
4. Corrected values have been adjusted for thixotropic effect.

Table C.16: Summary of Stress and Strain Data for Test DSC13.

DSC13: $\delta = 40°$

Film No.	Max. Shear Strain (%)		Volumetric Strain (%)		Uncorrected		Corrected	
					q	p'	qc	p'c
	(Area 1)	(Area 2)	(Area 1)	(Area 2)	(ksc)			
3	0.000	0.000	0.000	0.000	0.000	0.250	0.000	0.250
5	0.107	0.044	0.009	-0.111	0.010	0.249	0.009	0.249
6	0.032	0.049	-0.121	-0.133	0.030	0.245	0.026	0.245
7	0.026	0.040	-0.062	-0.042	0.051	0.238	0.045	0.238
8	0.116	0.128	-0.109	-0.106	0.071	0.228	0.063	0.228
9	0.142	0.188	-0.006	0.016	0.090	0.221	0.079	0.221
10	0.229	0.254	-0.030	-0.062	0.105	0.213	0.093	0.214
11	0.319	0.357	-0.078	-0.056	0.120	0.207	0.106	0.211
12	0.658	0.637	-0.444	-0.466	0.135	0.211	0.119	0.213
13	0.666	0.650	-0.012	0.002	0.145	0.215	0.128	0.215
14	0.887	0.838	-0.089	-0.041	0.155	0.229	0.137	0.221
15	1.046	0.970	-0.082	-0.015	0.165	0.237	0.146	0.225
16	1.287	1.147	0.002	0.093	0.175	0.249	0.156	0.231
17	1.600	1.429	-0.003	0.123	0.185	0.260	0.166	0.236
18	2.170	1.852	-0.095	0.060	0.192	0.271	0.173	0.241
19	2.921	2.465	-0.237	-0.028	0.200	0.284	0.181	0.249
20	3.496	2.871	-0.222	0.048	0.208	0.283	0.189	0.248
21	4.318	3.460	-0.140	0.163	0.215	0.291	0.196	0.256
22	5.362	4.320	-0.401	-0.078	0.223	0.294	0.204	0.259
23	7.027	5.889	-0.501	-0.133	0.230	0.300	0.211	0.265
24	9.977	8.905	-0.666	-0.236	0.238	0.311	0.219	0.276
25	13.011	12.710	-0.702	-0.260	0.241	0.309	0.222	0.274
26	13.934	13.147	-0.694	-0.227	0.241	0.307	0.222	0.272

Notes:

1. Area No. 1 represents 86% of cross–sectional area.
2. Area No. 2 represents 52% of cross–sectional area.
3. Volumetric Strain: Contraction is positive.
4. Corrected values have been adjusted for thixotropic effect.

Table C.17: Summary of Stress and Strain Data for Test DSC14.

DSC14: $\psi = 40^{\circ}$

Film No.	Max.Shear Strain (%)		Volumetric Strain (%)		Uncorrected		Corrected	
					q	p'	qc	p'c
	(Area 1)	(Area 2)	(Area 1)	(Area 2)	(ksc)			
2	0.058	0.010	-0.032	-0.014	0.000	0.250	0.000	0.250
5	0.037	0.036	0.367	0.445	0.050	0.231	0.043	0.231
7	0.061	0.155	0.344	0.464	0.090	0.215	0.077	0.204
9	0.380	0.452	0.408	0.585	0.123	0.205	0.105	0.204
10	0.583	0.640	0.272	0.442	0.133	0.204	0.114	0.204
11	0.841	0.846	0.218	-0.019	0.142	0.204	0.122	0.204
12	1.228	1.178	-0.041	0.091	0.152	0.207	0.130	0.204
13	1.605	1.514	0.184	0.441	0.163	0.218	0.141	0.203
14	2.175	1.974	-0.119	0.114	0.173	0.223	0.151	0.203
15	2.852	2.555	0.000	0.594	0.180	0.227	0.158	0.203
16	3.730	3.163	0.034	0.570	0.188	0.236	0.166	0.203
17	5.218	4.322	-0.204	0.416	0.195	0.242	0.173	0.201
19	8.845	7.195	0.008	0.510	0.211	0.252	0.189	0.211
20	11.481	9.503	-0.682	0.380	0.219	0.252	0.197	0.211

Notes:

1. Area No. 1 represents 86% of cross–sectional area.
2. Area No. 2 represents 52% of cross–sectional area.
3. Volumetric Strain: Contraction is positive.
4. Corrected values have been adjusted for thixotropic effect.

Table C.18: Summary of Stress and Strain Data for Test DSC15.

DSC15: $\delta = 20°$

Film No.	Max.Shear Strain (%)		Volumetric Strain (%)		Uncorrected		Corrected	
					q	p'	qc	p'c
	(Area 1)	(Area 2)	(Area 1)	(Area 2)	(ksc)			
2	0.126	0.074	0.288	0.423	0.000	0.251	0.000	0.251
4	0.106	0.070	0.248	0.338	0.031	0.236	0.027	0.236
5	0.070	0.077	-0.059	-0.052	0.060	0.221	0.053	0.221
6	0.144	0.180	-0.051	-0.008	0.090	0.217	0.079	0.217
7	0.301	0.314	0.011	0.048	0.120	0.216	0.105	0.216
8	0.535	0.524	-0.007	0.025	0.145	0.221	0.127	0.219
9	0.753	0.737	0.022	0.090	0.168	0.239	0.147	0.229
10	1.050	0.989	0.007	0.077	0.190	0.263	0.167	0.243
11	1.360	1.284	0.287	0.458	0.205	0.288	0.182	0.258
12	1.937	1.701	0.018	0.168	0.220	0.310	0.197	0.270
13	2.441	2.110	0.144	0.362	0.228	0.324	0.205	0.281
14	2.930	2.579	0.502	0.785	0.235	0.337	0.212	0.294
15	3.458	3.039	0.502	0.801	0.243	0.343	0.220	0.300
16	4.022	3.580	0.469	0.786	0.248	0.348	0.225	0.305
17	5.739	5.265	0.247	0.601	0.253	0.358	0.230	0.315
18	6.375	5.951	0.272	0.627	0.256	0.360	0.233	0.317

Notes:

1. Area No. 1 represents 86% of cross–sectional area.
2. Area No. 2 represents 52% of cross–sectional area.
3. Volumetric Strain: Contraction is positive.
4. Corrected values have been adjusted for thixotropic effect.

Table C.19: Summary of Stress and Strain Data for Test DSC16.

DSC16: $\delta = 75^{\circ}$

Film No.	Max.Shear Strain (%)		Volumetric Strain (%)		Uncorrected		Corrected	
					q	p'	qc	p'c
	(Area 1)	(Area 2)	(Area 1)	(Area 2)	(ksc)			
2	0.034	0.020	-0.012	-0.006	0.000	0.252	0.000	0.251
4	0.107	0.085	-0.668	-0.750	0.032	0.254	0.025	0.254
5	0.194	0.153	-0.612	-0.722	0.061	0.255	0.048	0.255
6	0.287	0.211	0.102	0.104	0.090	0.247	0.070	0.231
7	0.668	0.515	-0.109	-0.131	0.115	0.244	0.090	0.221
8	1.226	1.028	-0.634	-0.721	0.135	0.238	0.108	0.194
9	2.132	2.079	-0.719	-0.799	0.150	0.244	0.123	0.200
10	3.759	4.088	-0.616	-0.642	0.160	0.254	0.133	0.210
11	5.443	6.046	-0.805	-0.795	0.167	0.258	0.140	0.214
12	7.017	8.048	-0.881	-0.947	0.175	0.261	0.148	0.217
13	8.499	9.786	-0.940	-1.029	0.182	0.267	0.155	0.223
14	11.289	13.043	-1.108	-1.164	0.190	0.277	0.163	0.233
15	12.439	14.569	-1.122	-1.211	0.195	0.278	0.168	0.234

Notes:

1. Area No. 1 represents 86% of cross–sectional area.
2. Area No. 2 represents 52% of cross–sectional area.
3. Volumetric Strain: Contraction is positive.
4. Corrected values have been adjusted for thixotropic effect.

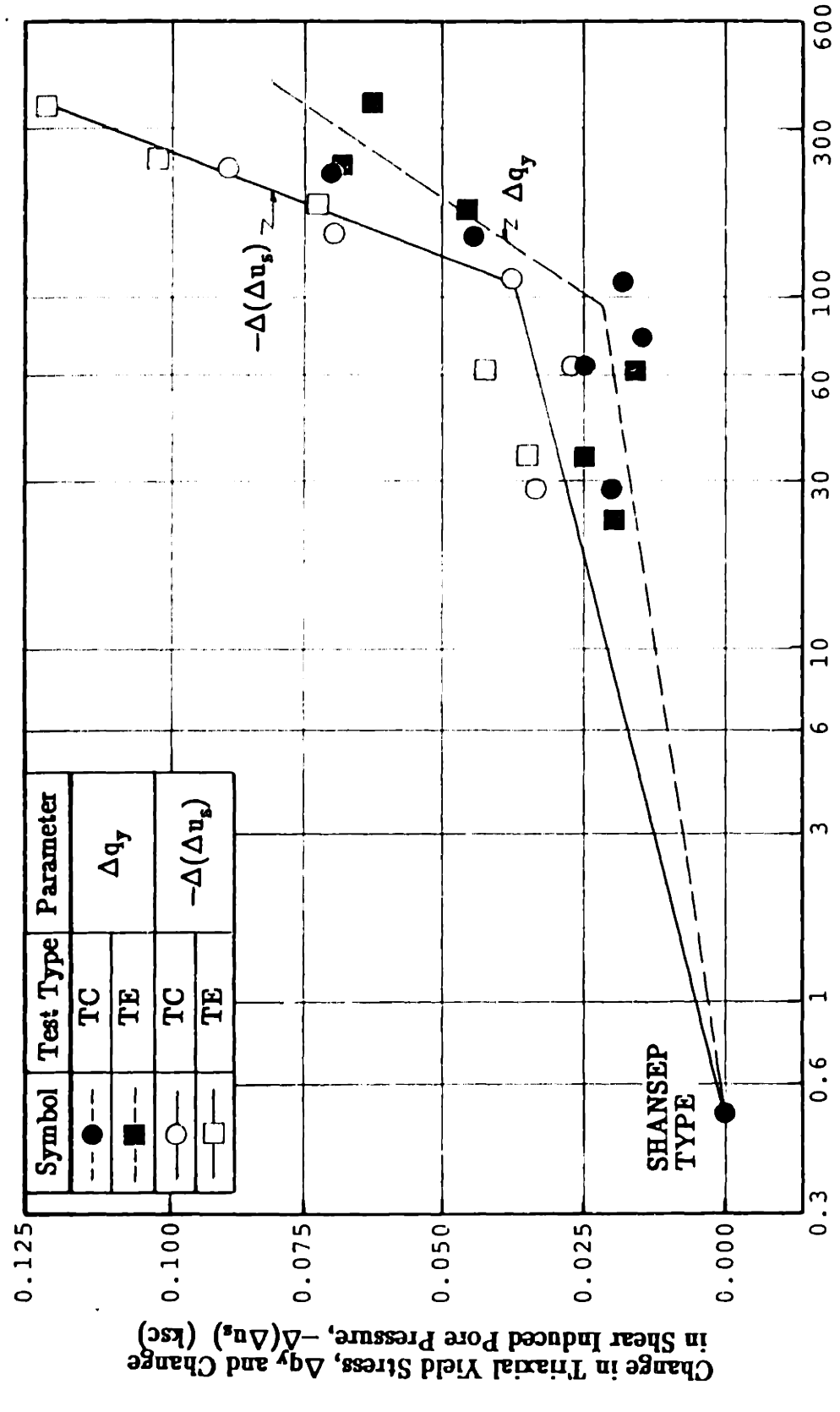

Figure C.1: Summary Plot of Effect of Storage Time on Undrained Shear Yield Stress and Shear Induced Pore Pressure for Resedimented BBC at OCR=4 (after O'Neill, 1985).

DSC01: $\delta = 0°$

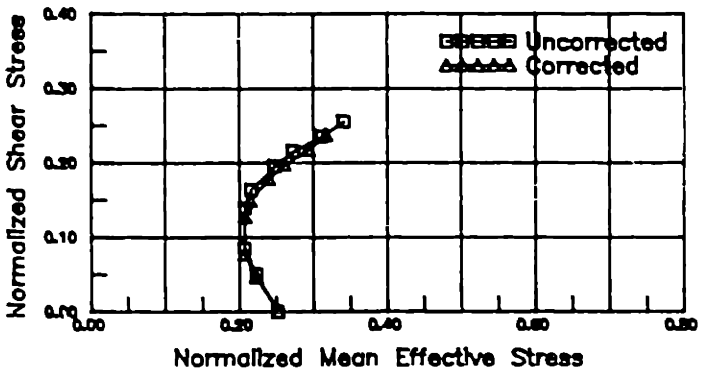

(a) q versus p'

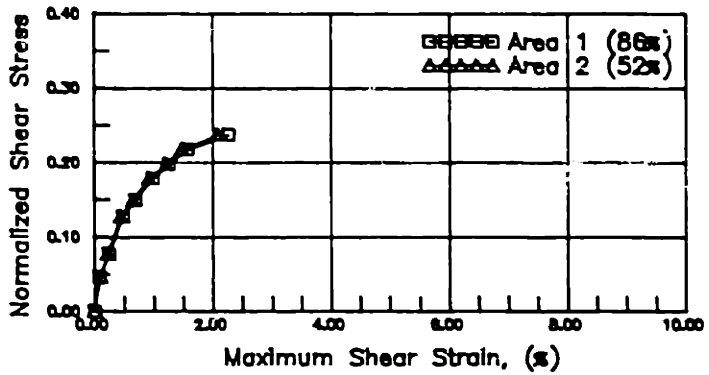

(b) Shear Stress versus Shear Strain (Corrected for Thixotropic Effects)

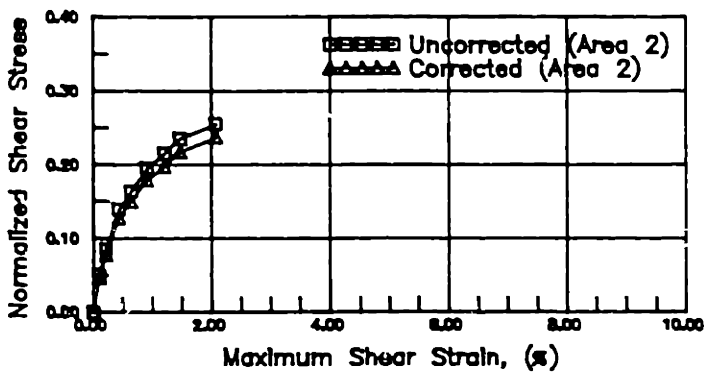

(b) Shear Stress versus Shear Strain

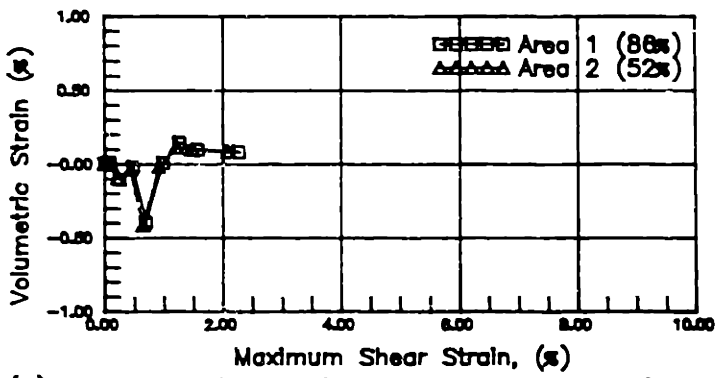

(c) Volumetric Strain versus Shear Strain

Figure C.2: Results of Test DSC01.

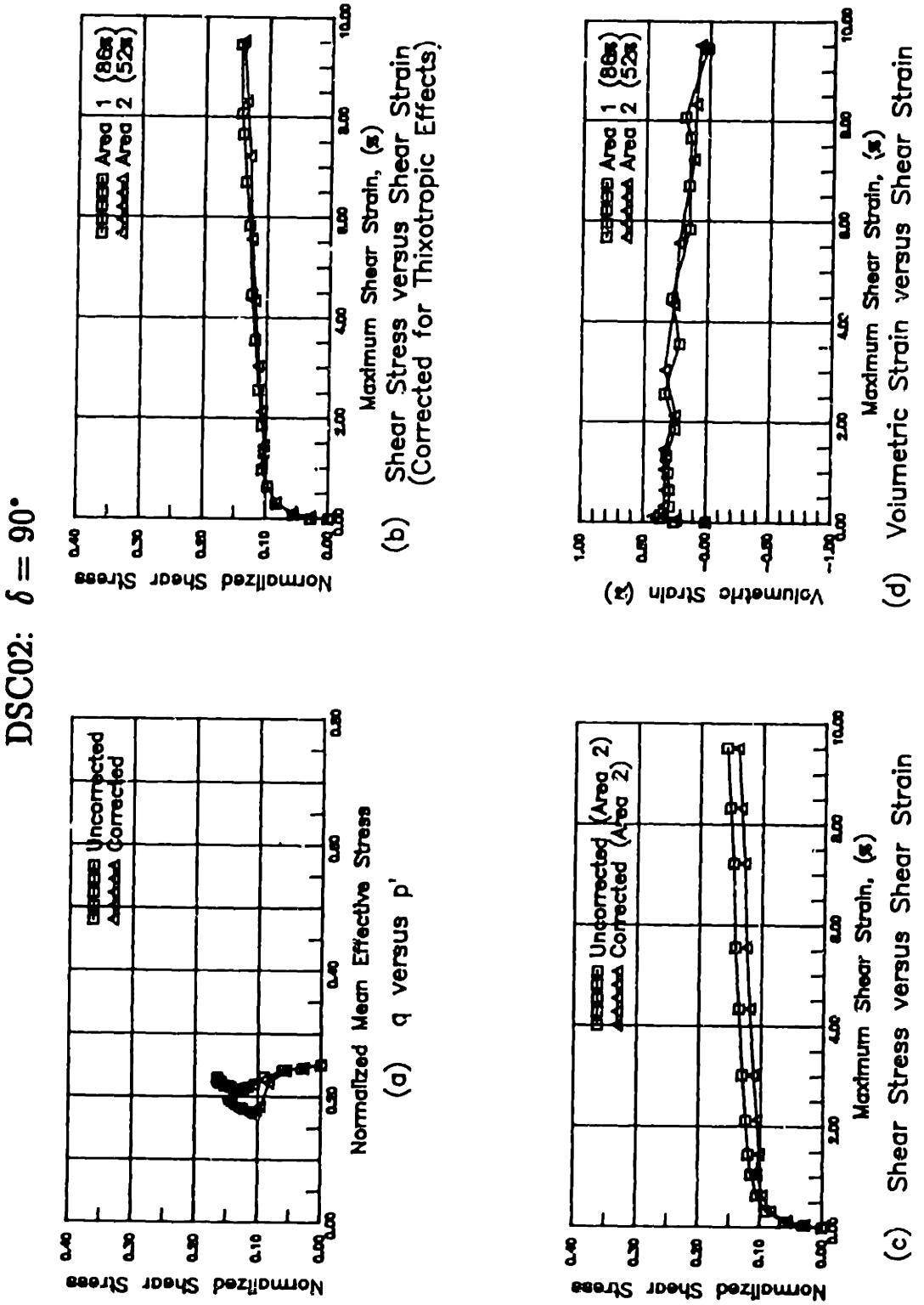

Figure C.3: Results of Test DSC02.

DSC03: $\delta = 0°$

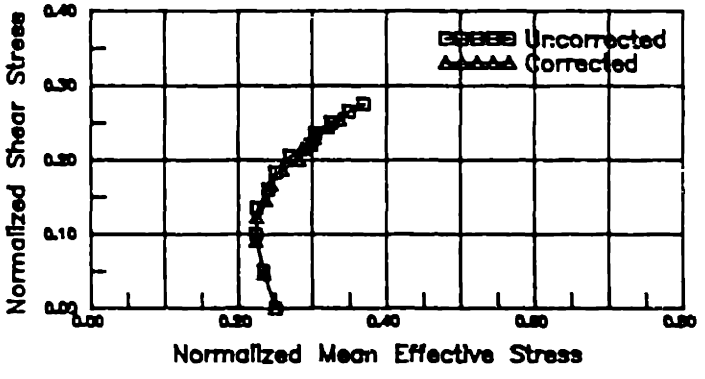

(a) q versus p'

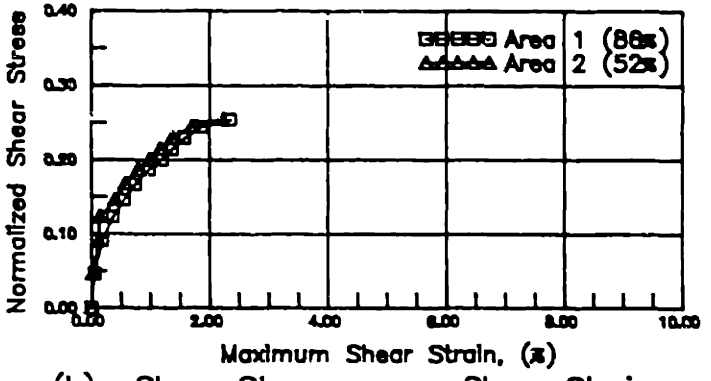

(b) Shear Stress versus Shear Strain (Corrected for Thixotropic Effects)

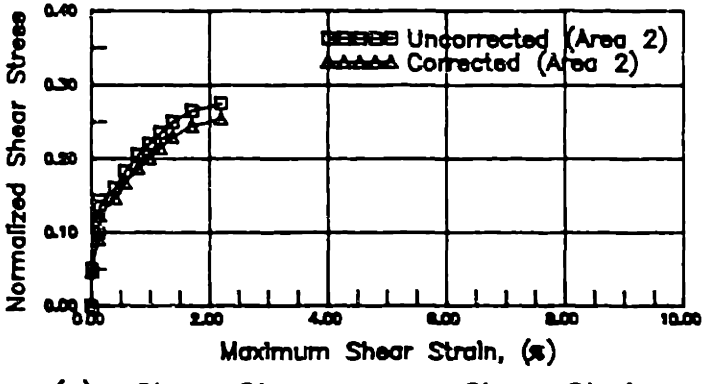

(c) Shear Stress versus Shear Strain

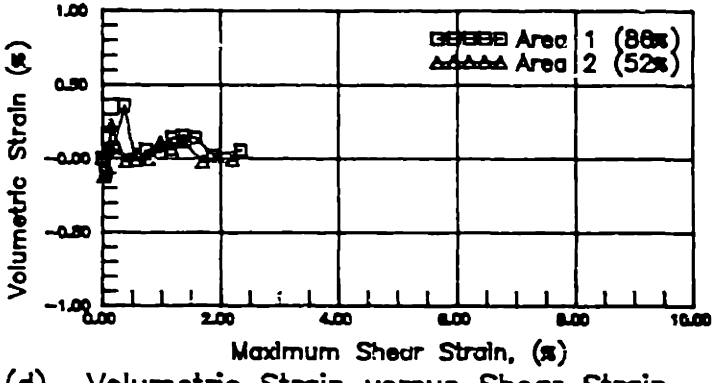

(d) Volumetric Strain versus Shear Strain

Figure C.4: Results of Test DSC03.

DSC04: $\delta = 45°$

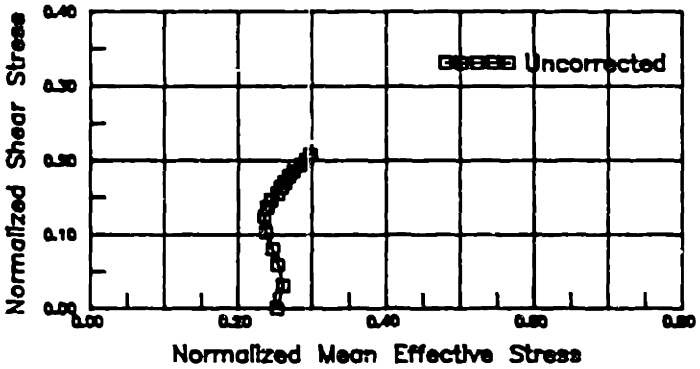

(a) q versus p'

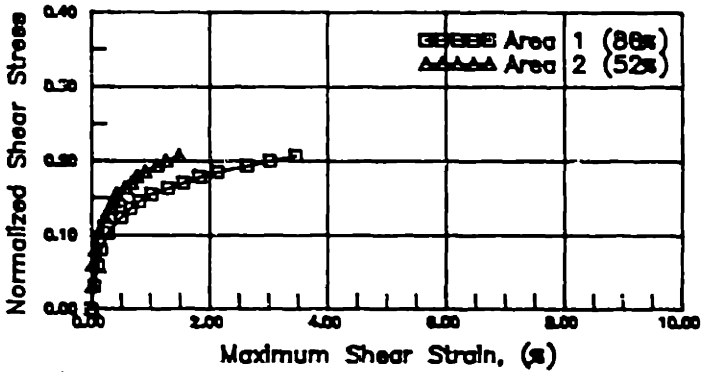

(b) Shear Stress versus Shear Strain (Uncorrected for Thixotropic Effects)

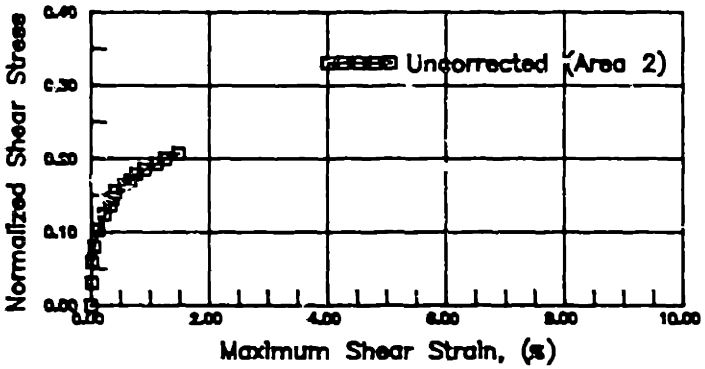

(c) Shear Stress versus Shear Strain

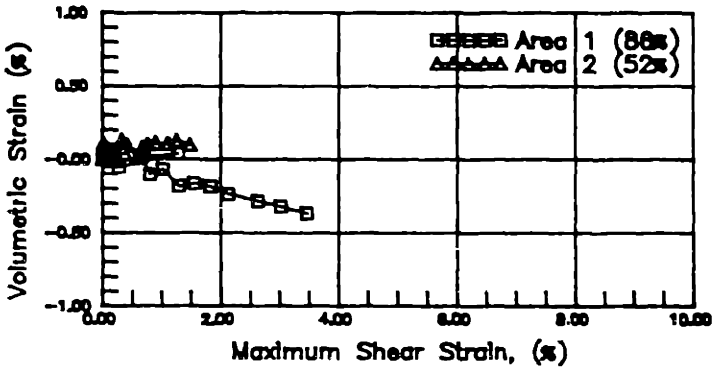

(d) Volumetric Strain versus Shear Strain

Figure C.5: Results of Test DSC04.

DSC05: $\delta = 45°$

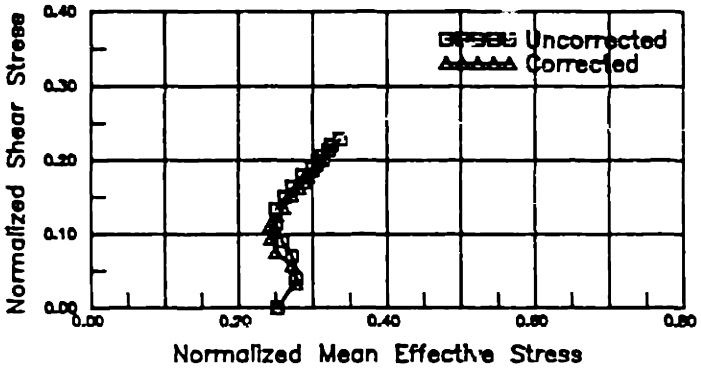

(a) q versus p'

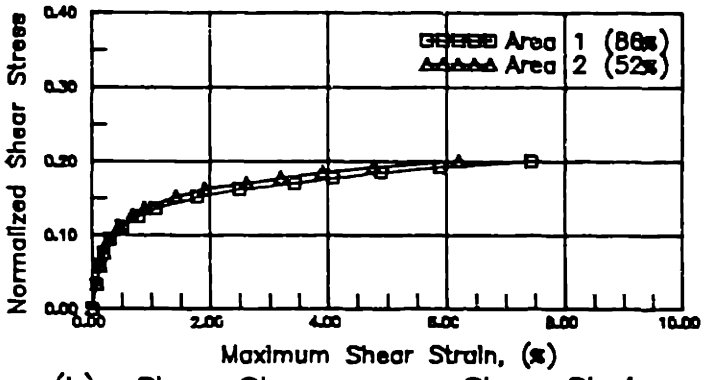

(b) Shear Stress versus Shear Strain (Corrected for Thixotropic Effects)

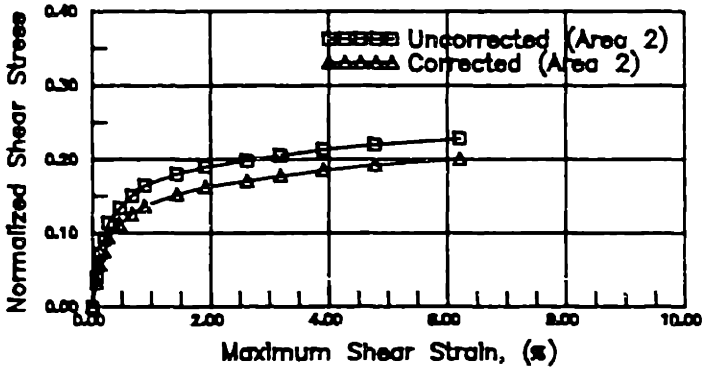

(c) Shear Stress versus Shear Strain

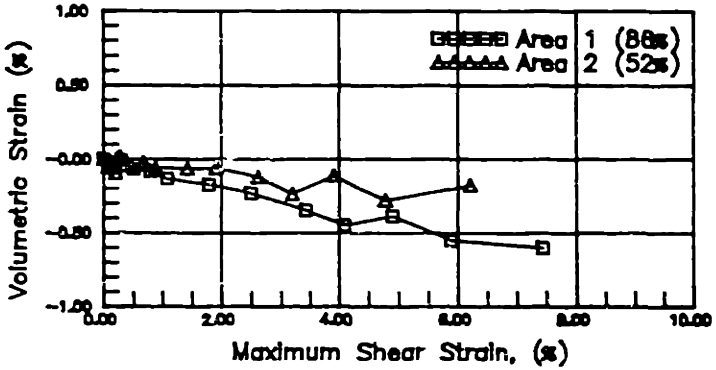

(d) Volumetric Strain versus Shear Strain

Figure C.6: Results of Test DSC05.

DSC06: $\psi = 0°$

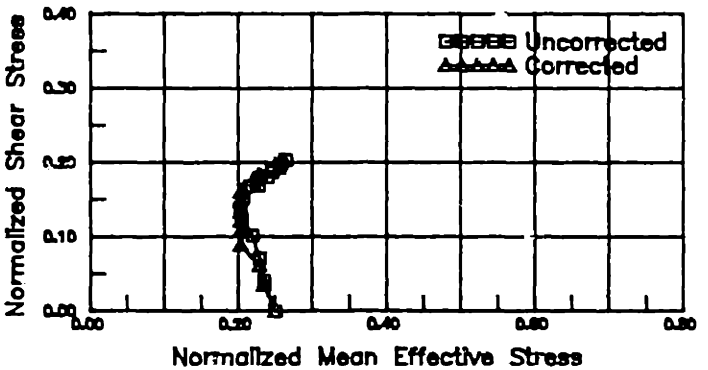

(a) q versus p'

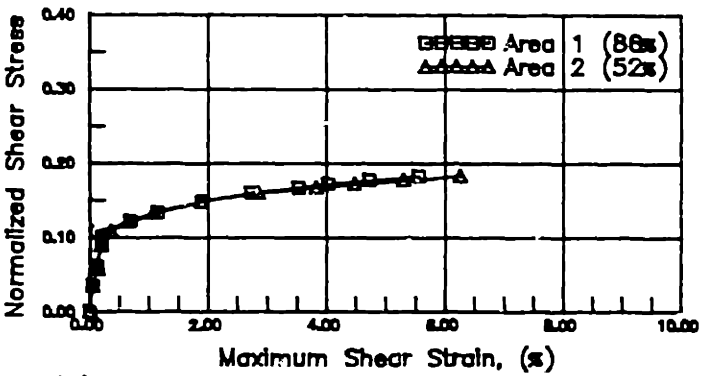

(b) Shear Stress versus Shear Strain (Corrected for Thixotropic Effects)

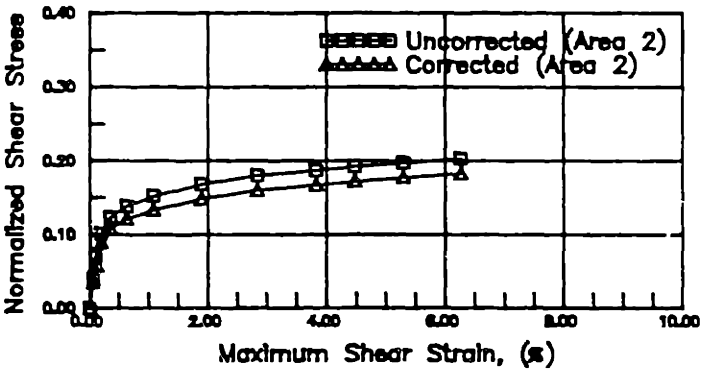

(c) Shear Stress versus Shear Strain

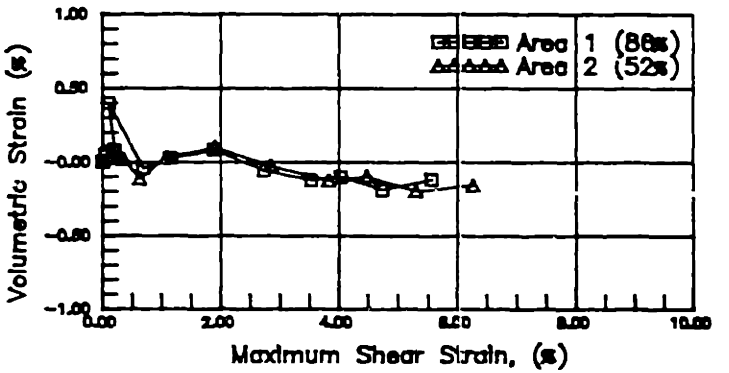

(d) Volumetric Strain versus Shear Strain

Figure C.7: Results of Test DSC06.

DSC07: $\psi = 45°$

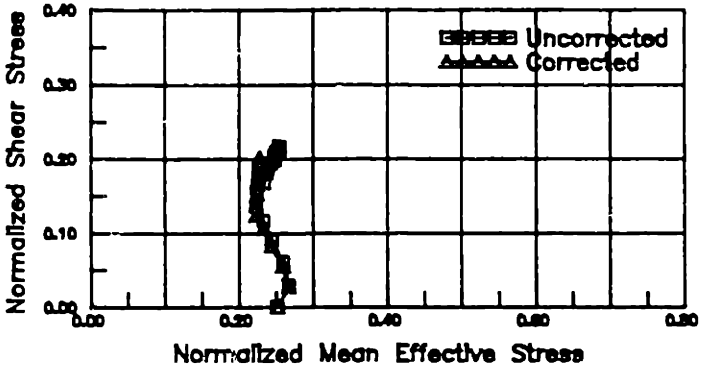

(a) q versus p'

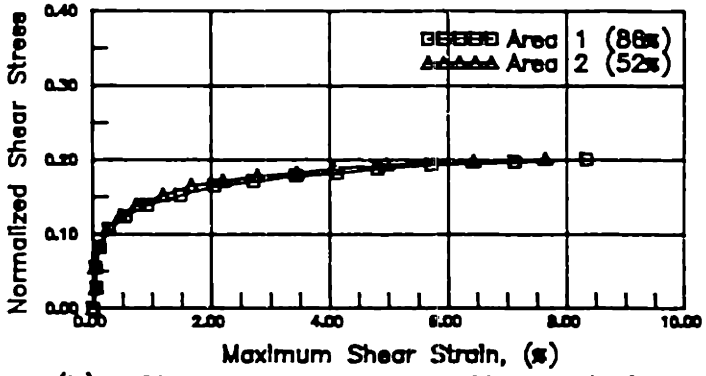

(b) Shear Stress versus Shear Strain (Corrected for Thixotropic Effects)

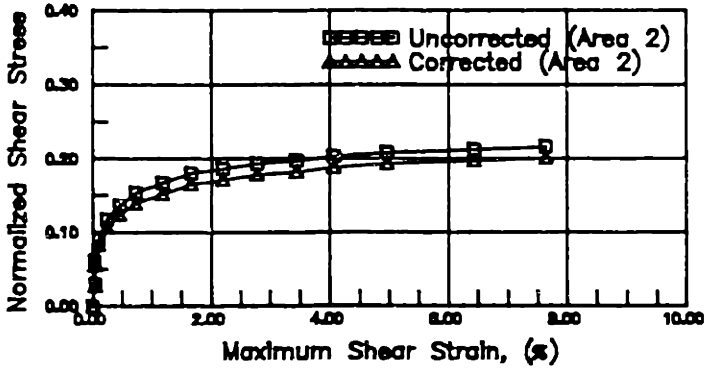

(c) Shear Stress versus Shear Strain

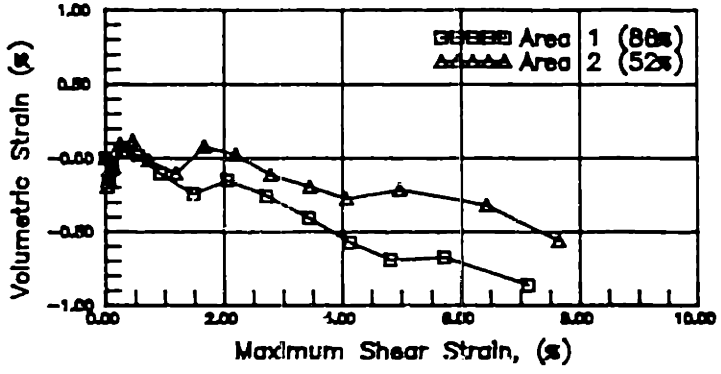

(d) Volumetric Strain versus Shear Strain

Figure C.8: Results of Test DSC07.

DSC08: $\delta = 65°$

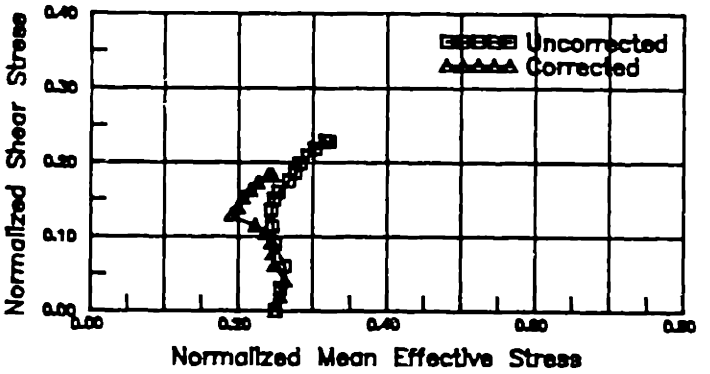

(a) q versus p'

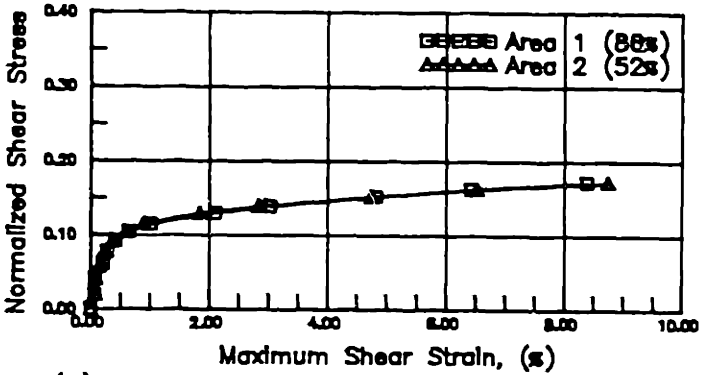

(b) Shear Stress versus Shear Strain (Corrected for Thixotropic Effects)

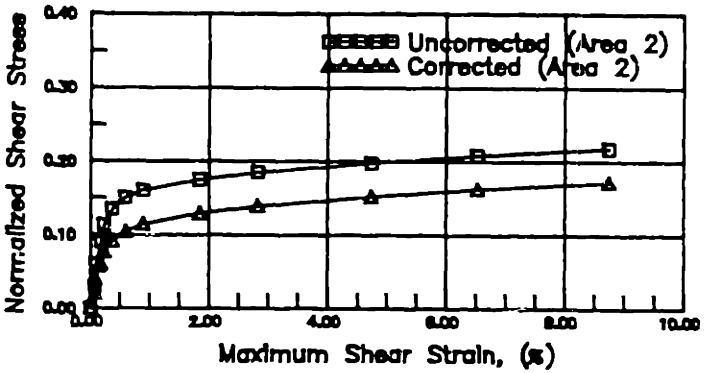

(c) Shear Stress versus Shear Strain

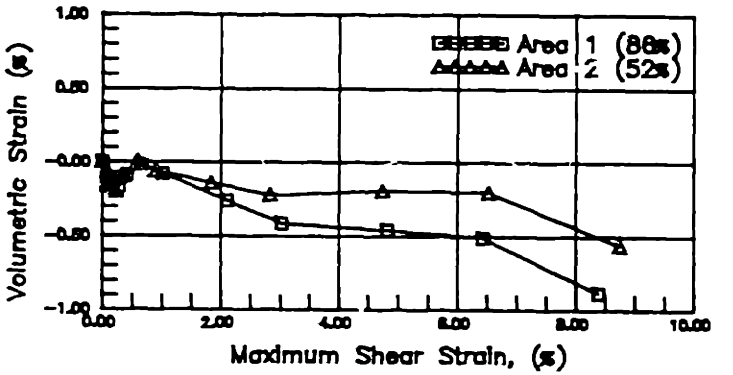

(d) Volumetric Strain versus Shear Strain

Figure C.9: Results of Test DSC08.

DSC09: $\psi = 25°$

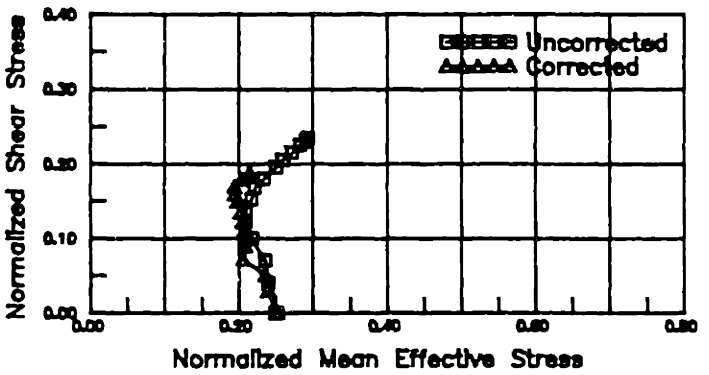

(a) q versus p'

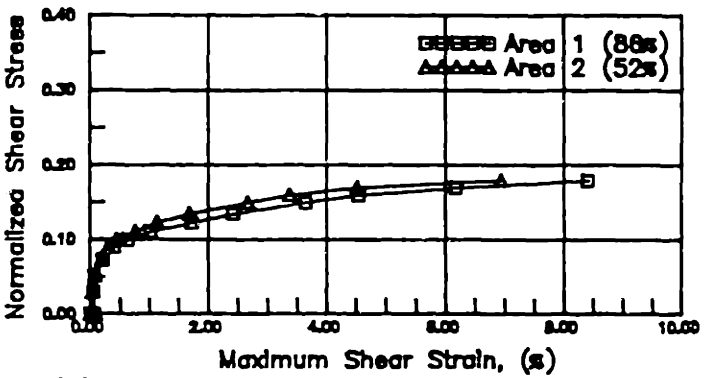

(b) Shear Stress versus Shear Strain (Corrected for Thixotropic Effects)

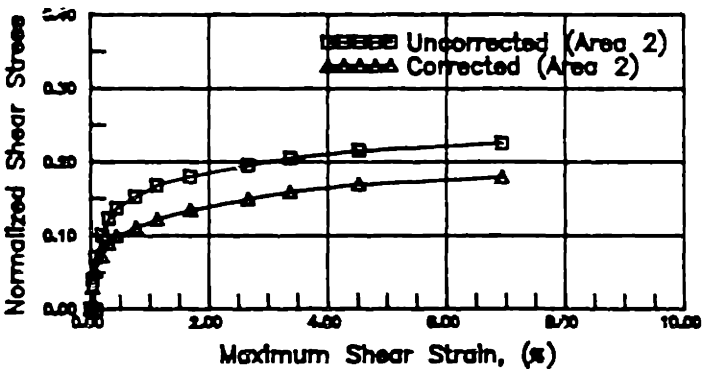

(c) Shear Stress versus Shear Strain

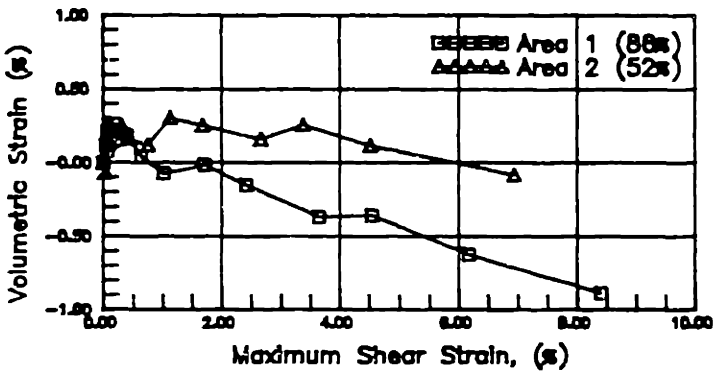

(d) Volumetric Strain versus Shear Strain

Figure C.10: Results of Test DSC09.

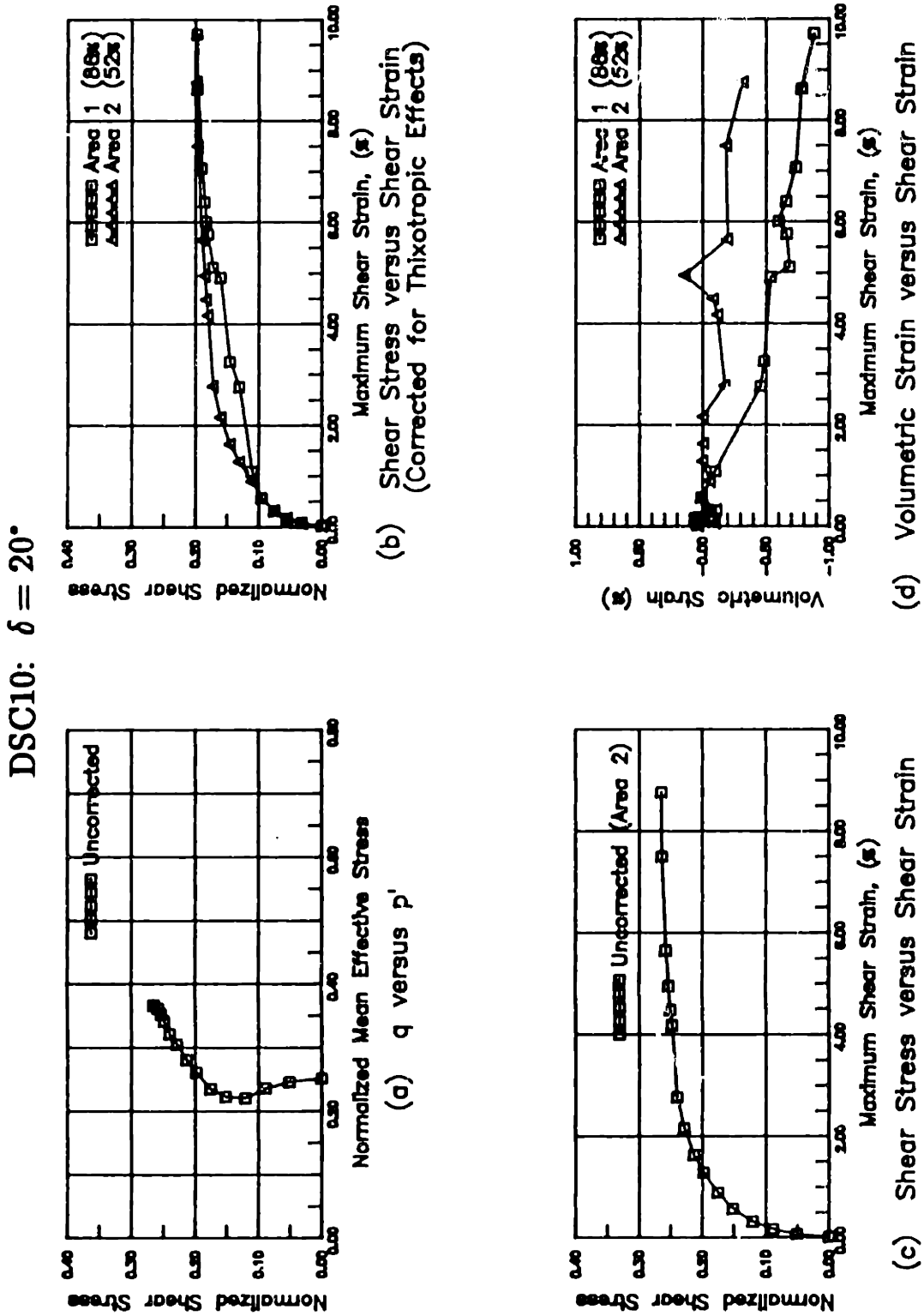

Figure C.11: Results of Test DSC10.

DSC11: $\delta = 75°$

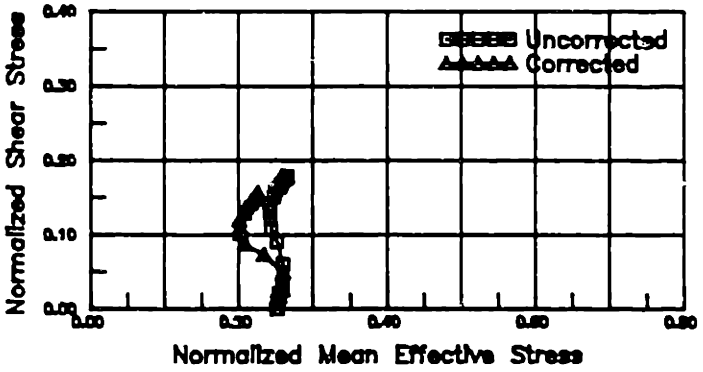

(a) q versus p'

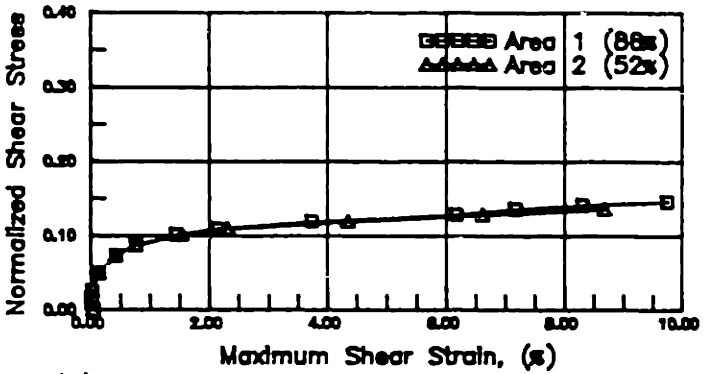

(b) Shear Stress versus Shear Strain (Corrected for Thixotropic Effects)

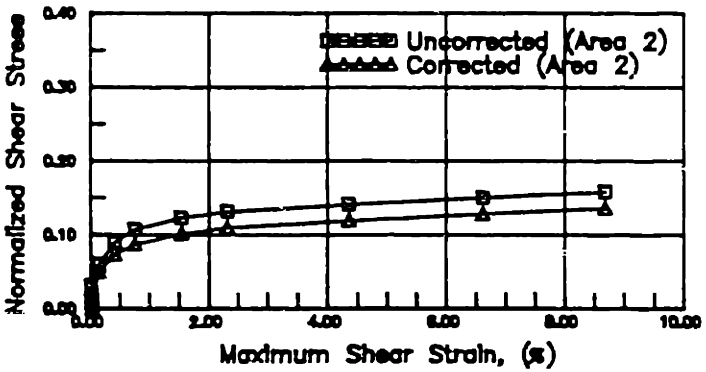

(c) Shear Stress versus Shear Strain

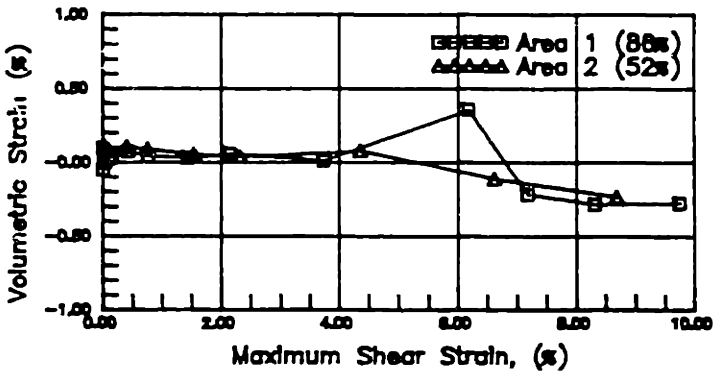

(d) Volumetric Strain versus Shear Strain

Figure C.12: Results of Test DSC11.

DSC12: $\psi = 0°$

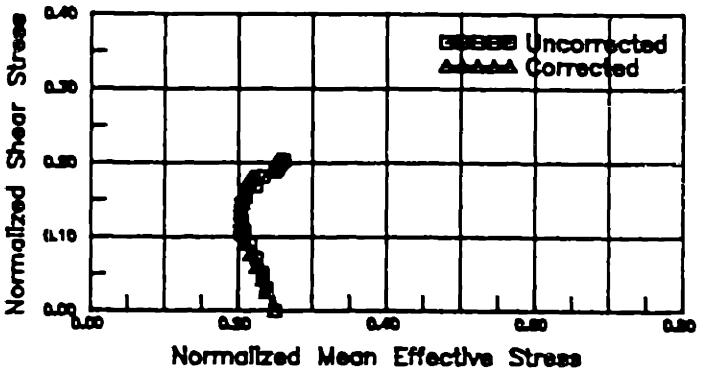

(a) q versus p'

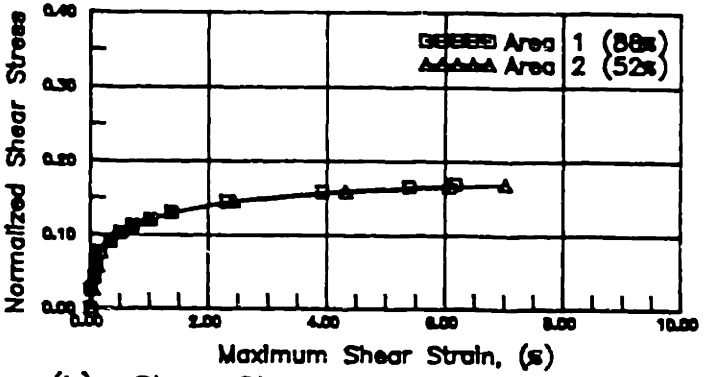

(b) Shear Stress versus Shear Strain (Corrected for Thixotropic Effects)

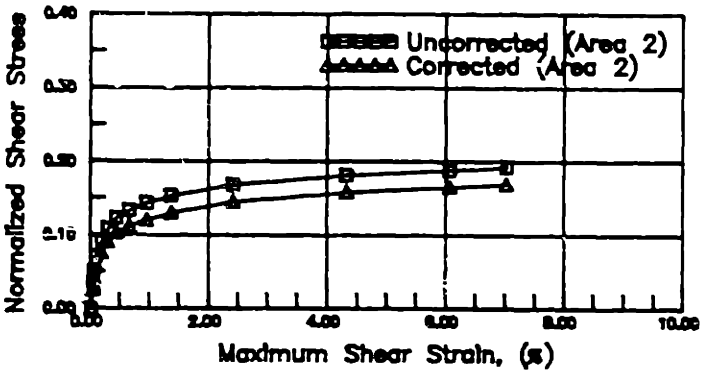

(c) Shear Stress versus Shear Strain

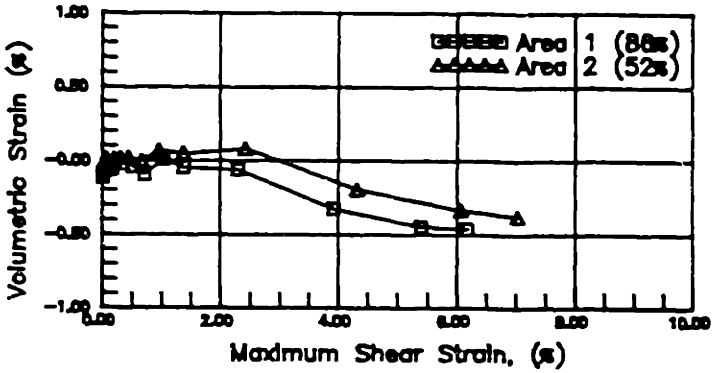

(d) Volumetric Strain versus Shear Strain

Figure C.13: Results of Test DSC12.

DSC13: $\delta = 40°$

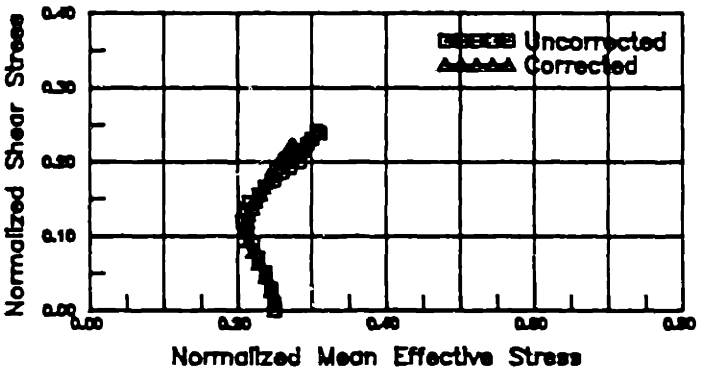

(a) q versus p'

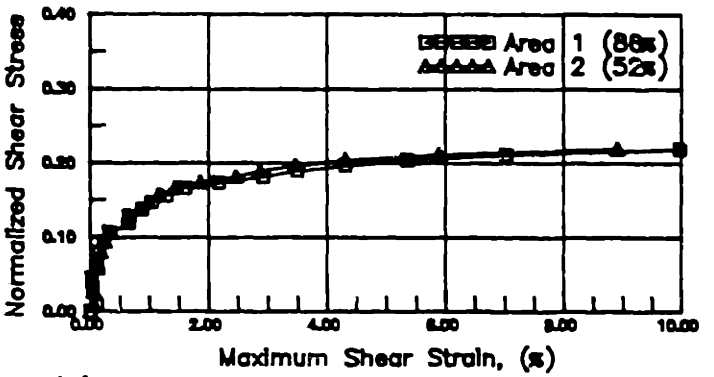

(b) Shear Stress versus Shear Strain (Corrected for Thixotropic Effects)

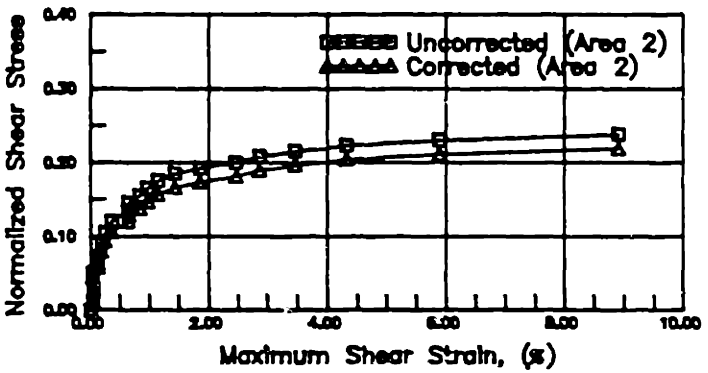

(c) Shear Stress versus Shear Strain

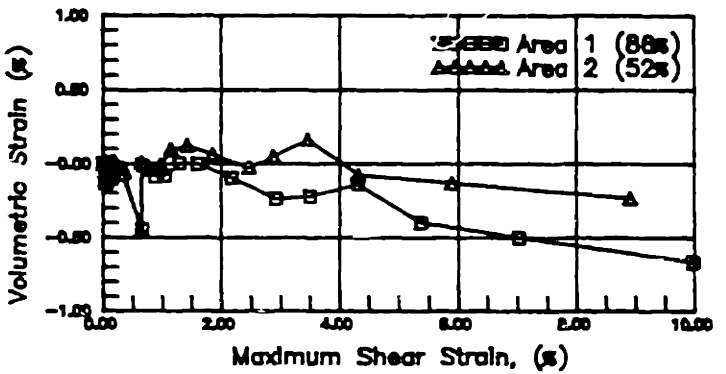

(d) Volumetric Strain versus Shear Strain

Figure C.14: Results of Test DSC13.

DSC14: $\psi = 40°$

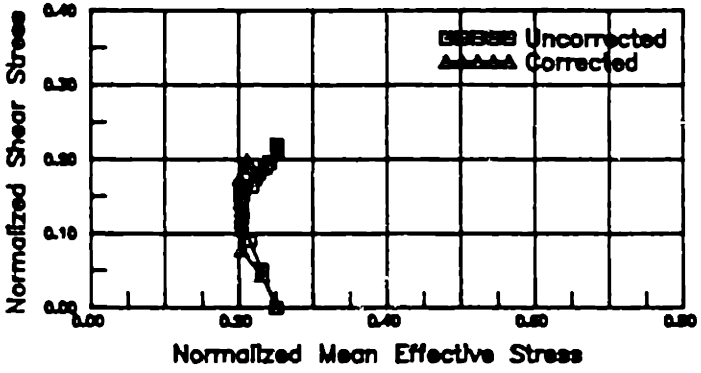

(a) q versus p'

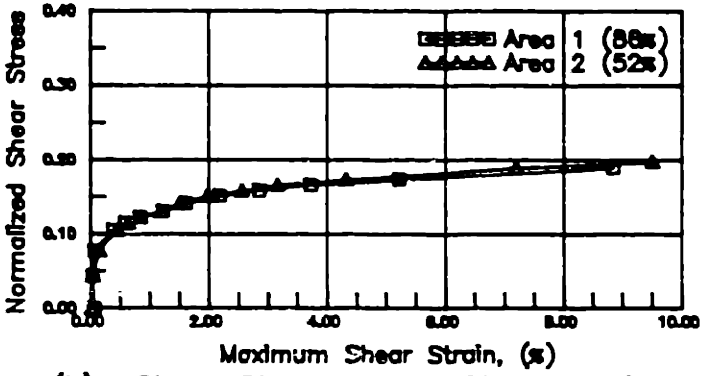

(b) Shear Stress versus Shear Strain (Corrected for Thixotropic Effects)

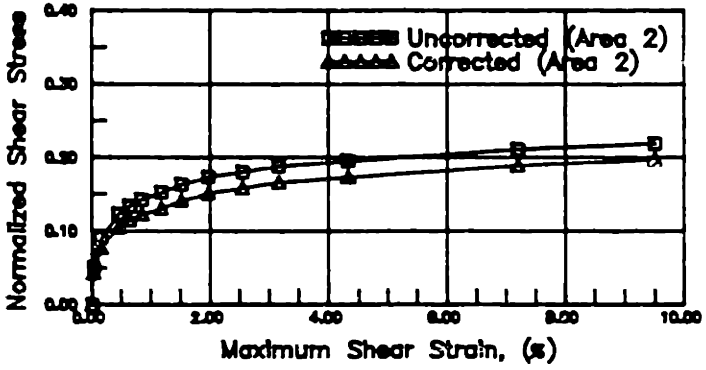

(c) Shear Stress versus Shear Strain

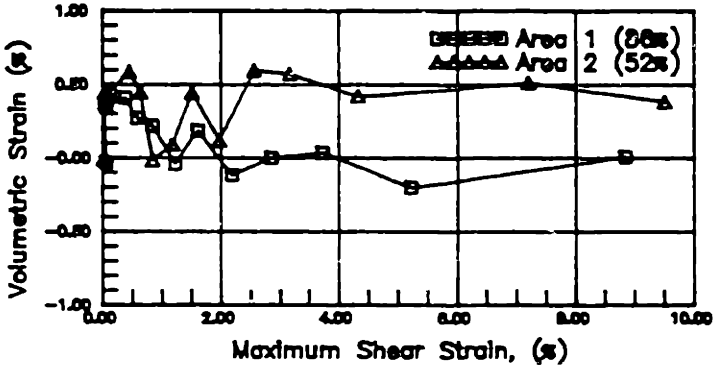

(d) Volumetric Strain versus Shear Strain

Figure C.15: Results of Test DSC14.

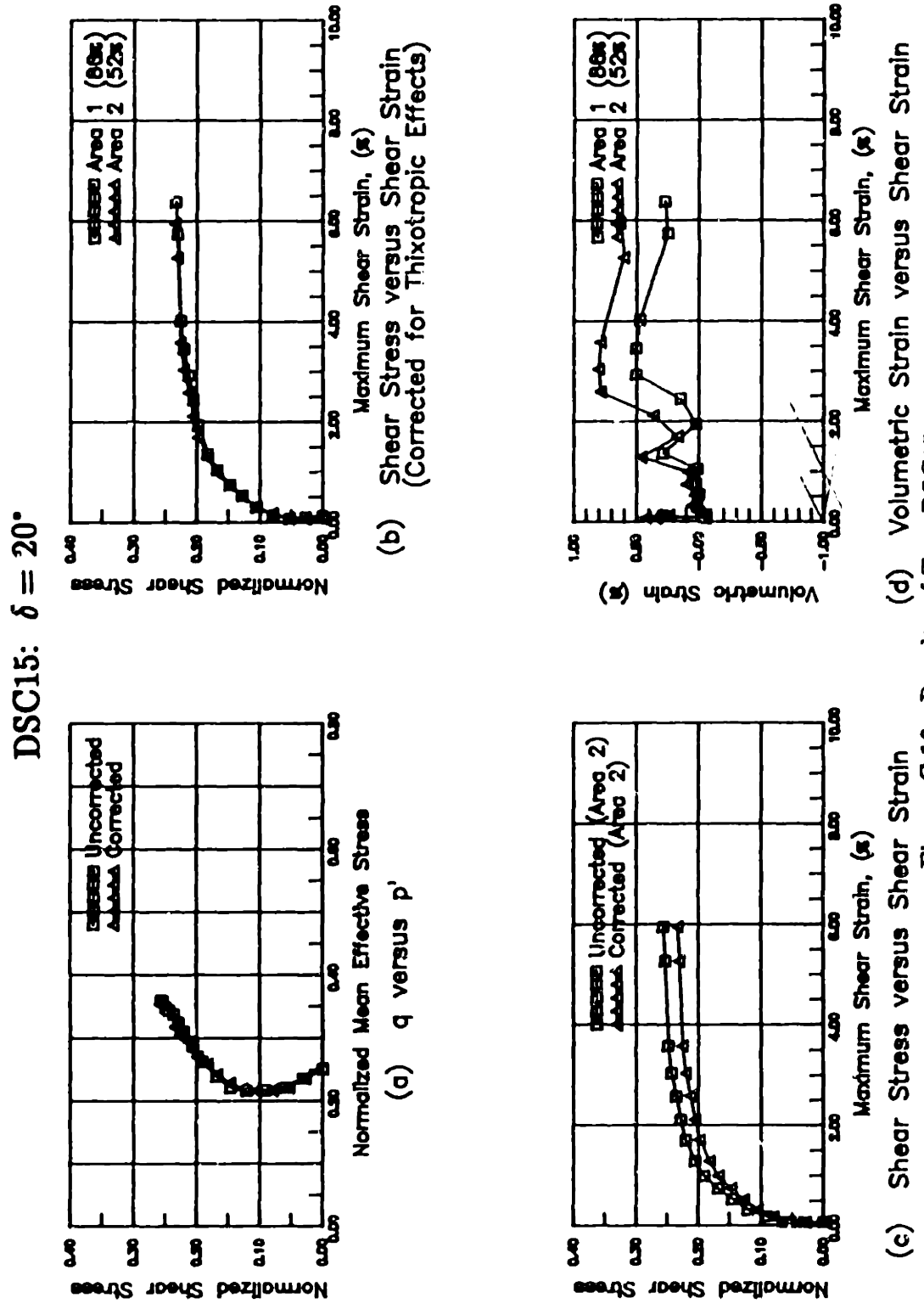

Figure C.16: Results of Test DSC15.

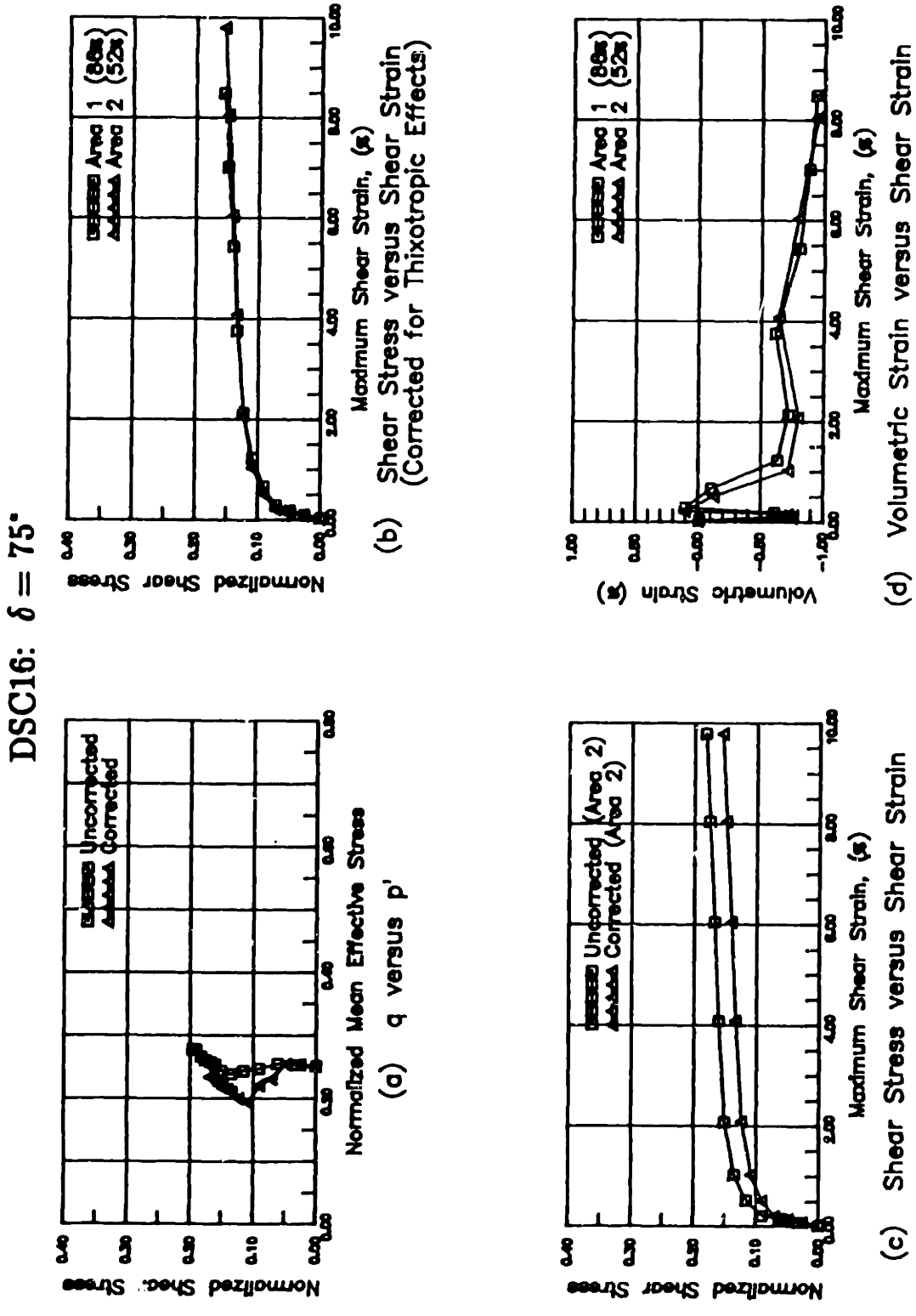

Figure C.17: Results of Test DSC16.

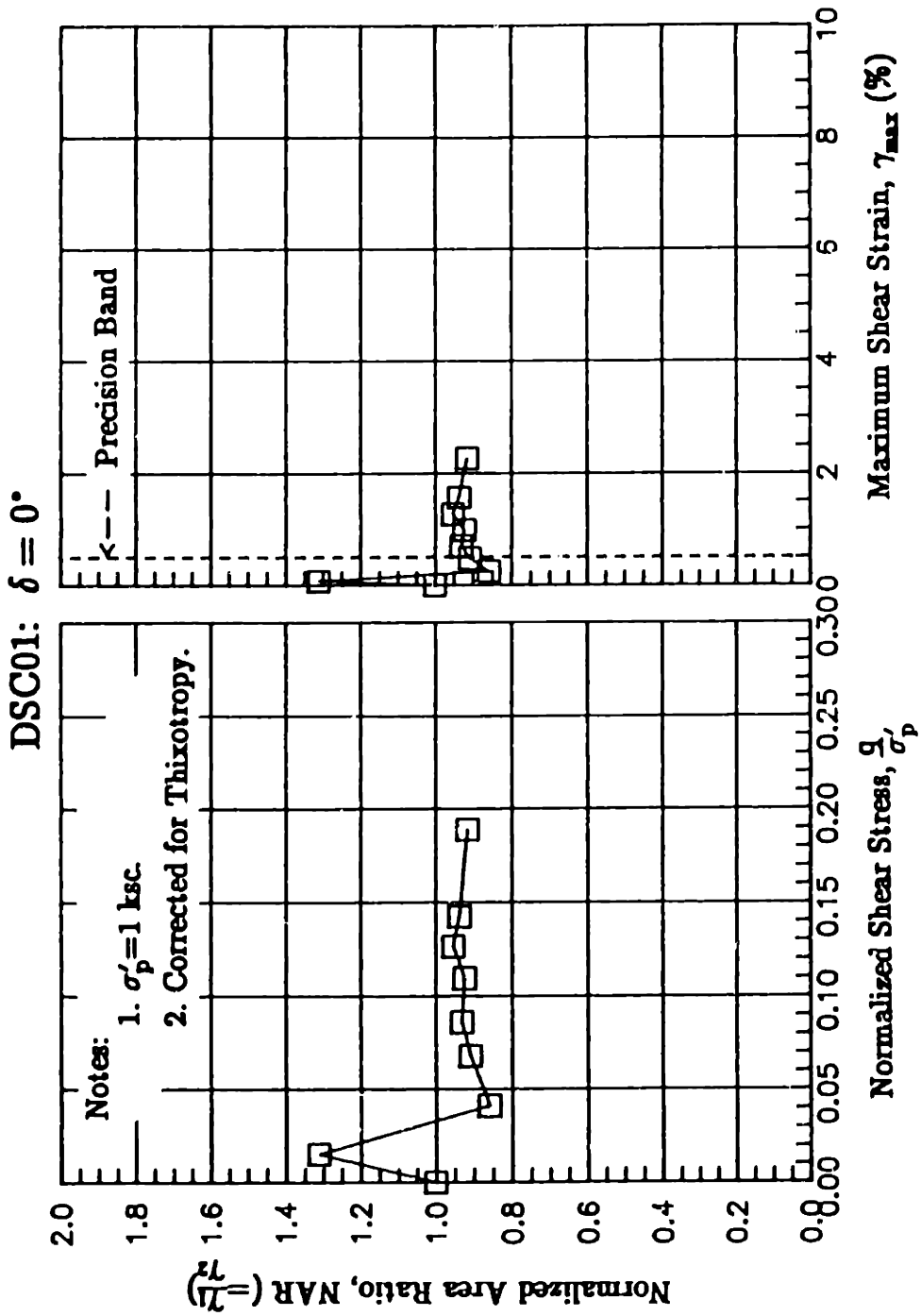

Figure C.18: Variation of NAR with (a) Normalized Shear Stress and with (b) Maximum Shear Strain from Test DSC01.

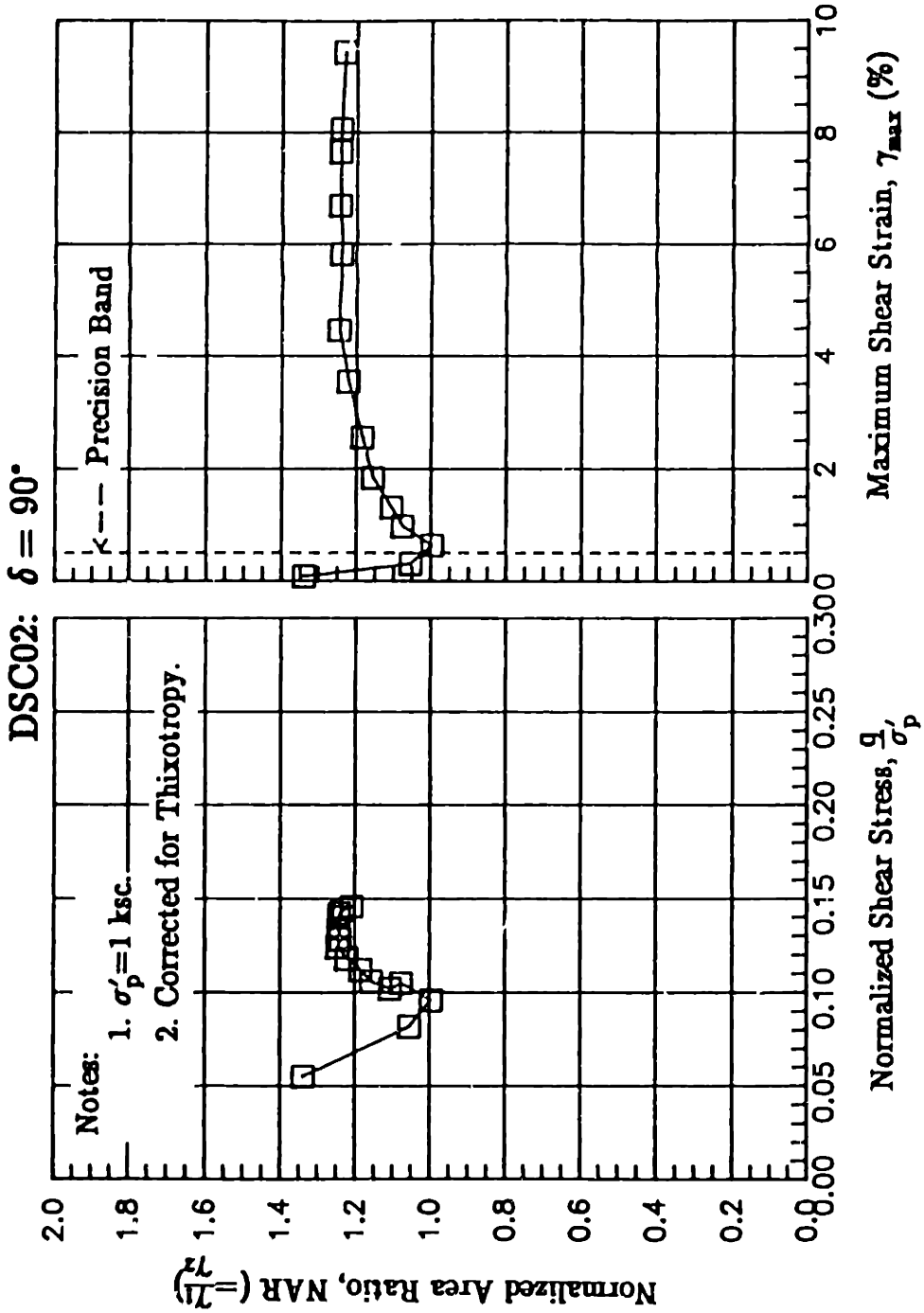

Figure C.19: Variation of NAR with (a) Normalized Shear Stress and with (b) Maximum Shear Strain from Test DSC02.

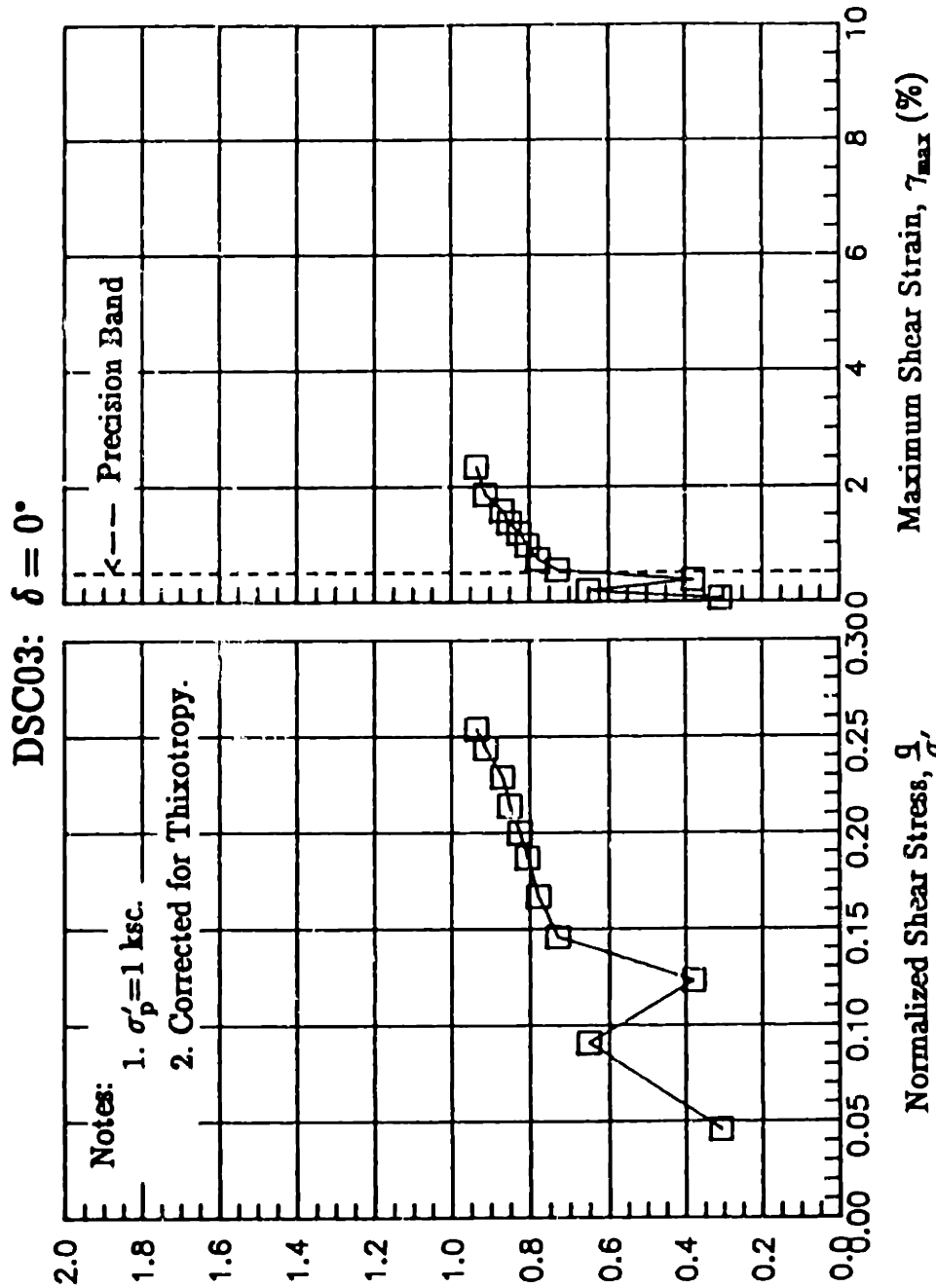

Figure C.20: Variation of NAR with (a) Normalized Shear Stress and with (b) Maximum Shear Strain from Test DSC03.

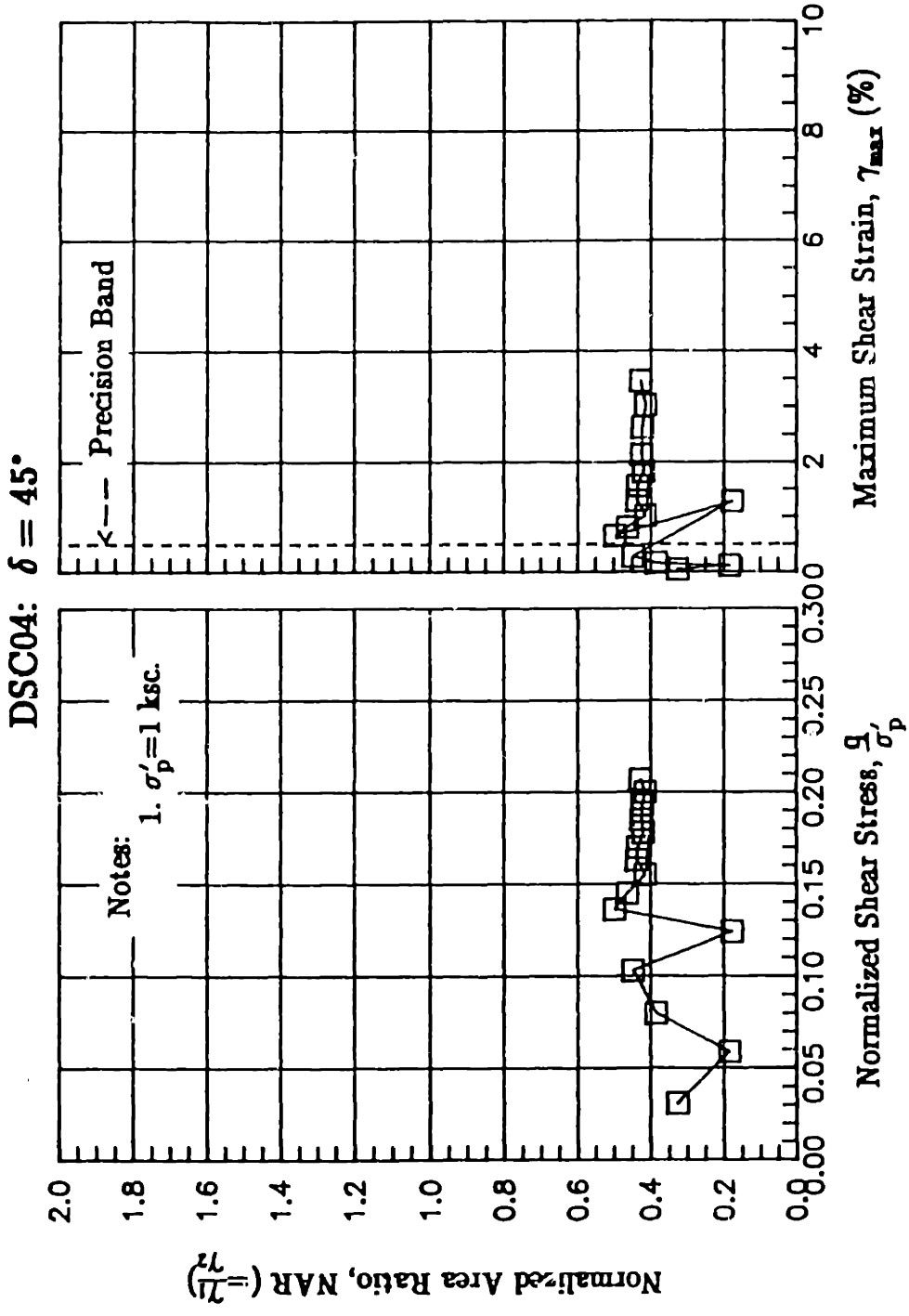

Figure C.21: Variation of NAR with (a) Normalized Shear Stress and with (b) Maximum Shear Strain from Test DSC04.

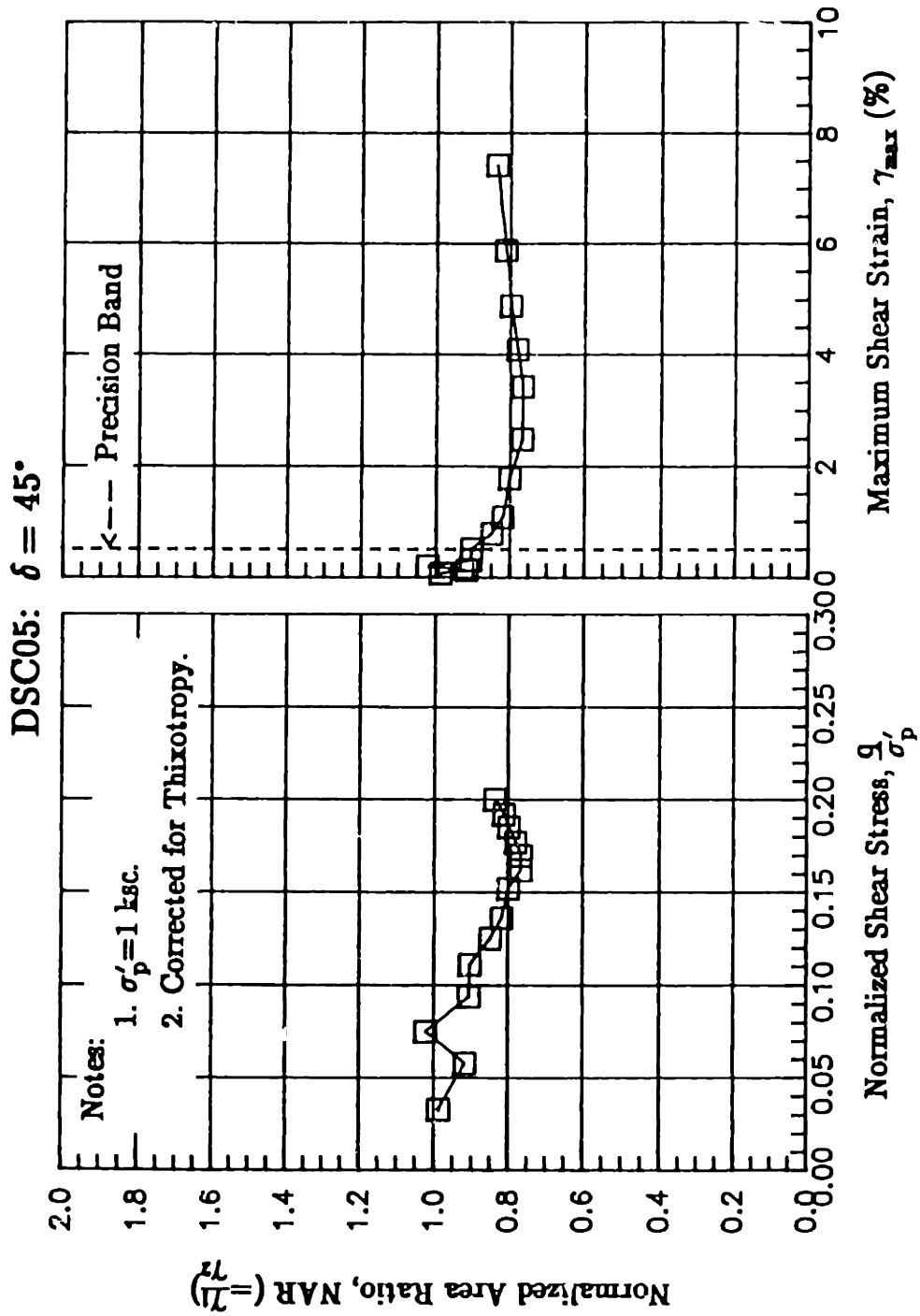

Figure C.22: Variation of NAR with (a) Normalized Shear Stress and with (b) Maximum Shear Strain from Test DSC05.

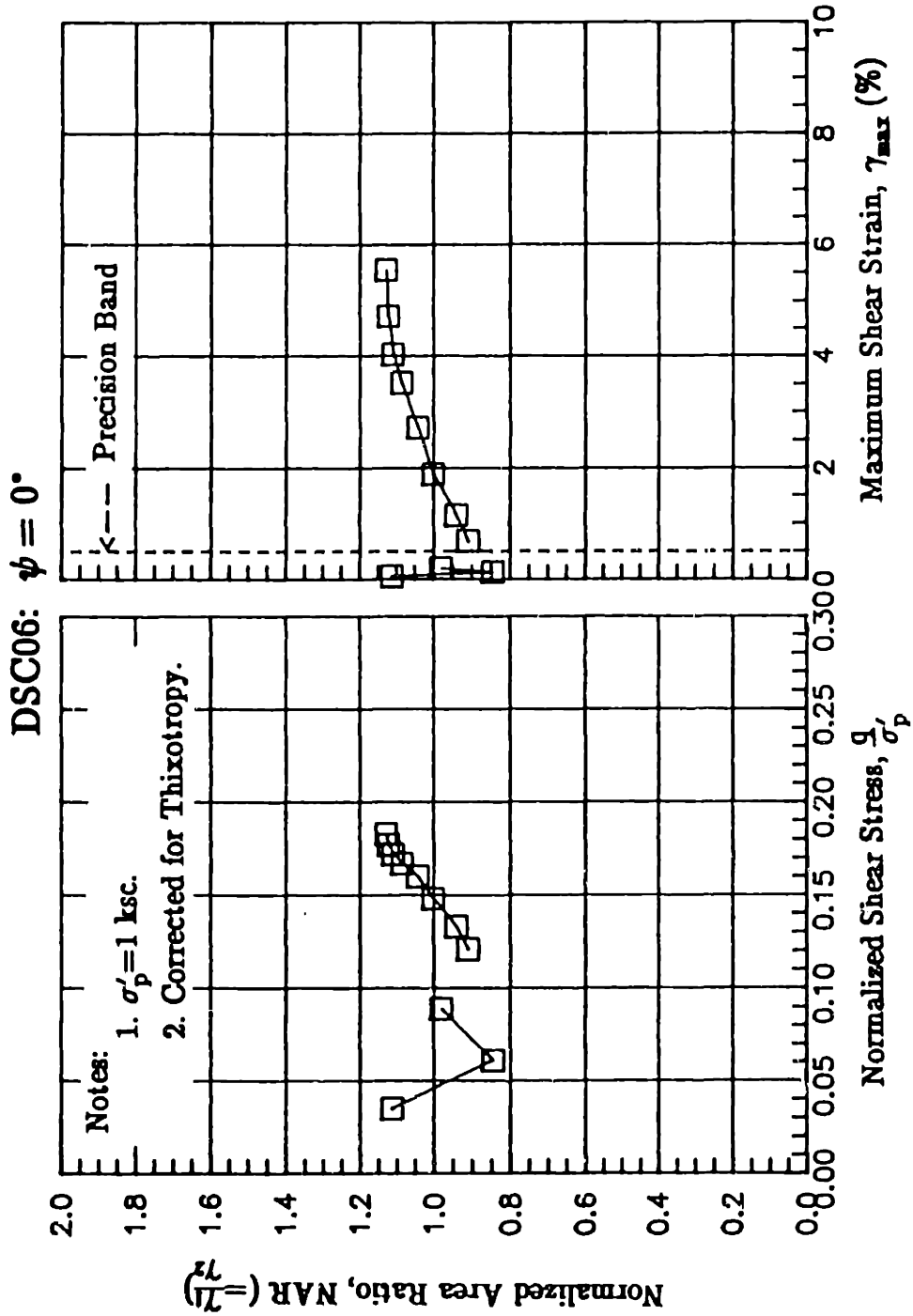

Figure C.23: Variation of NAR with (a) Normalized Shear Stress and with (b) Maximum Shear Strain from Test DSC06.

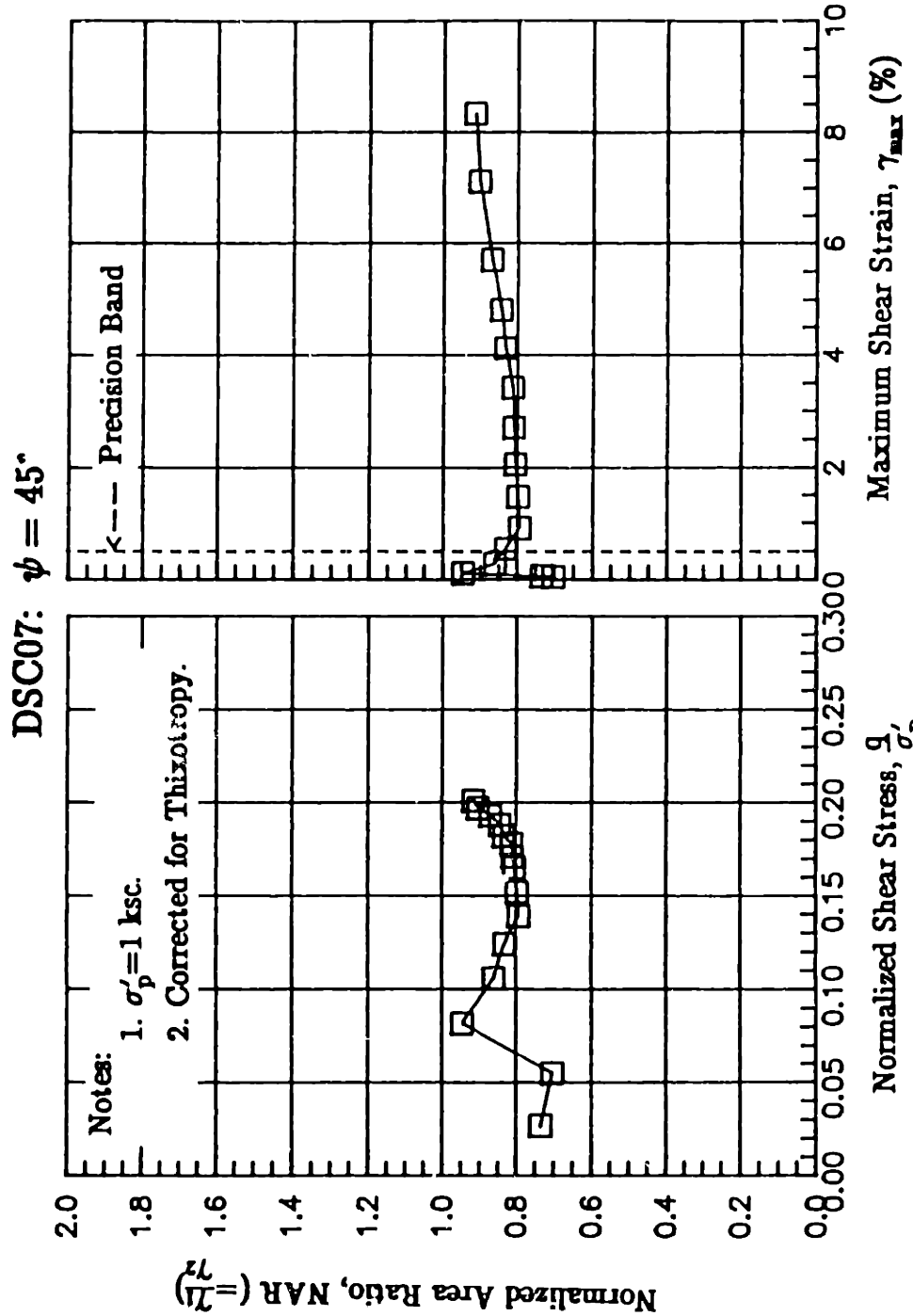

Figure C.24: Variation of NAR with (a) Normalized Shear Stress and with (b) Maximum Shear Strain from Test DSC07.

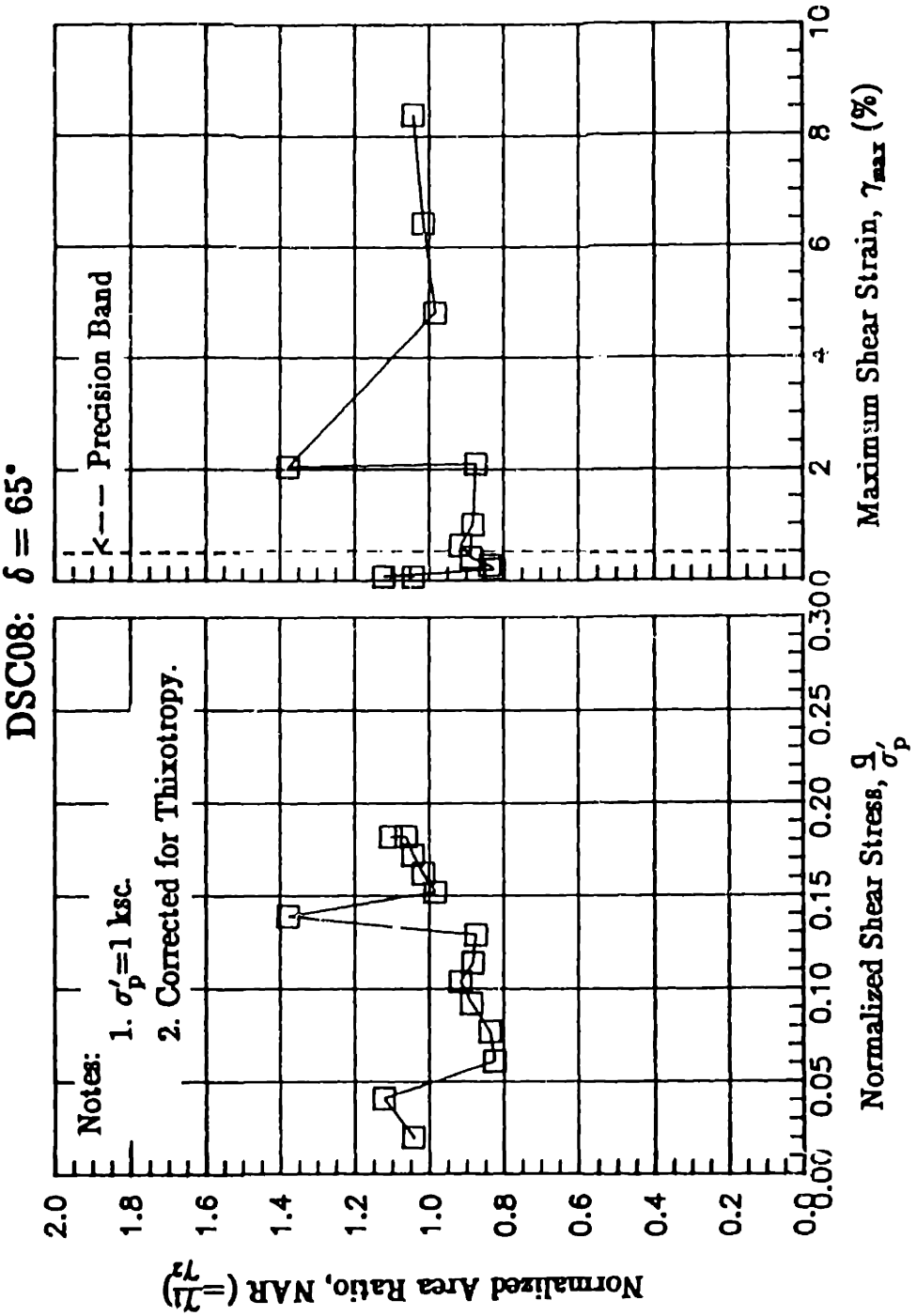

Figure C.25: Variation of NAR with (a) Normalized Shear Stress and with (b) Maximum Shear Strain from Test DSC08.

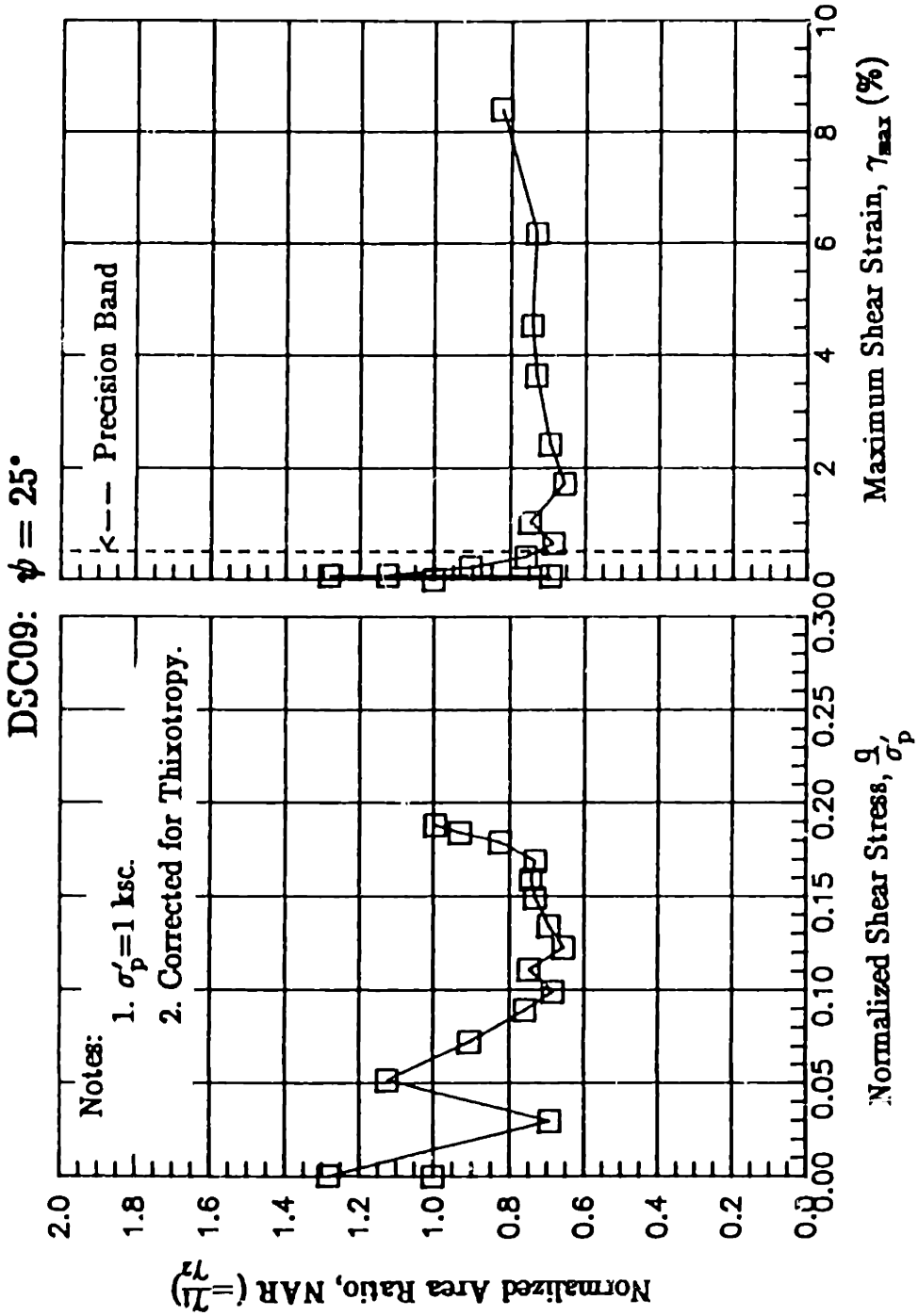

Figure C.26: Variation of NAR with (a) Normalized Shear Stress and with (b) Maximum Shear Strain from Test DSC09.

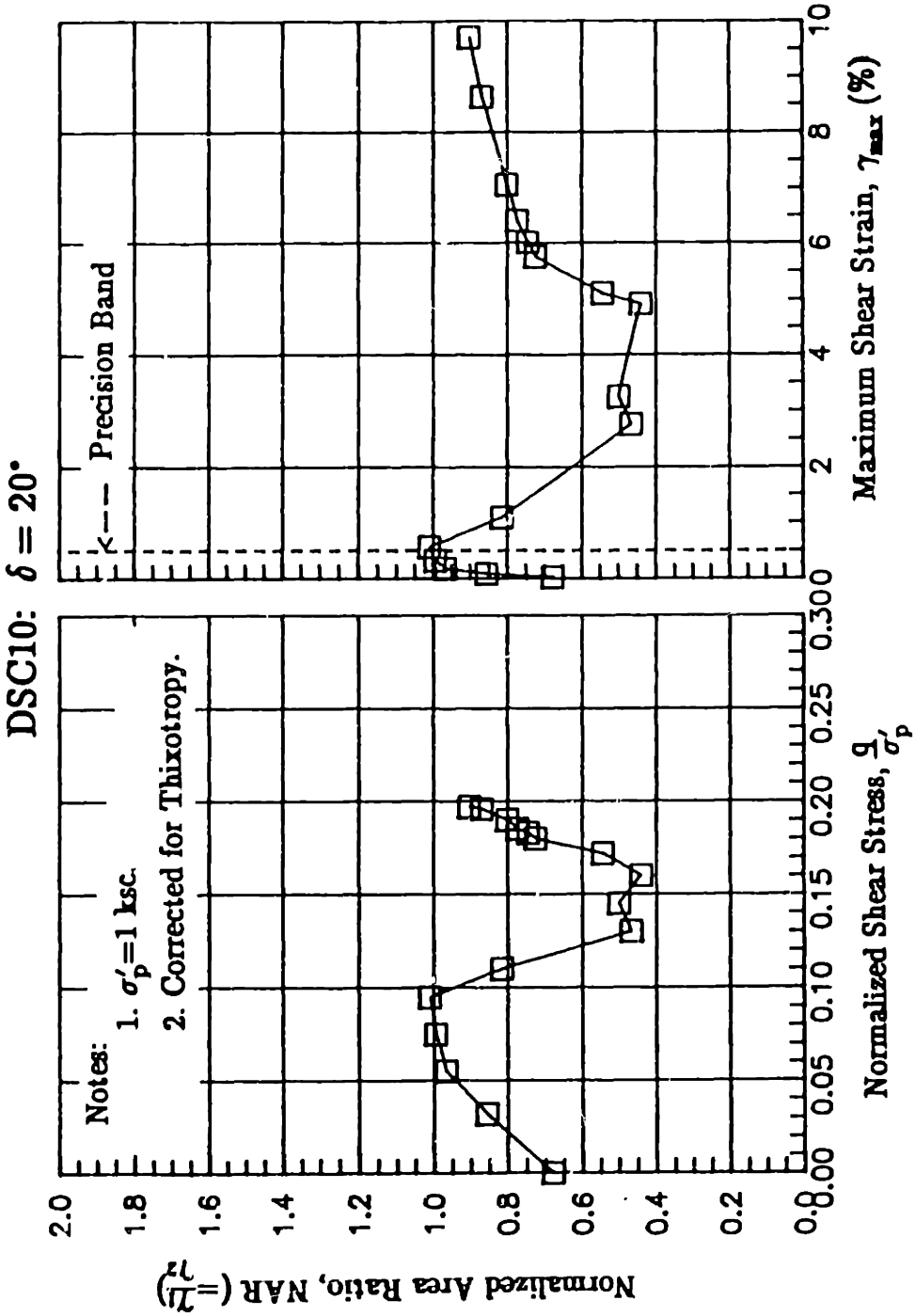

Figure C.27: Variation of NAR with (a) Normalized Shear Stress and with (b) Maximum Shear Strain from Test DSC10.

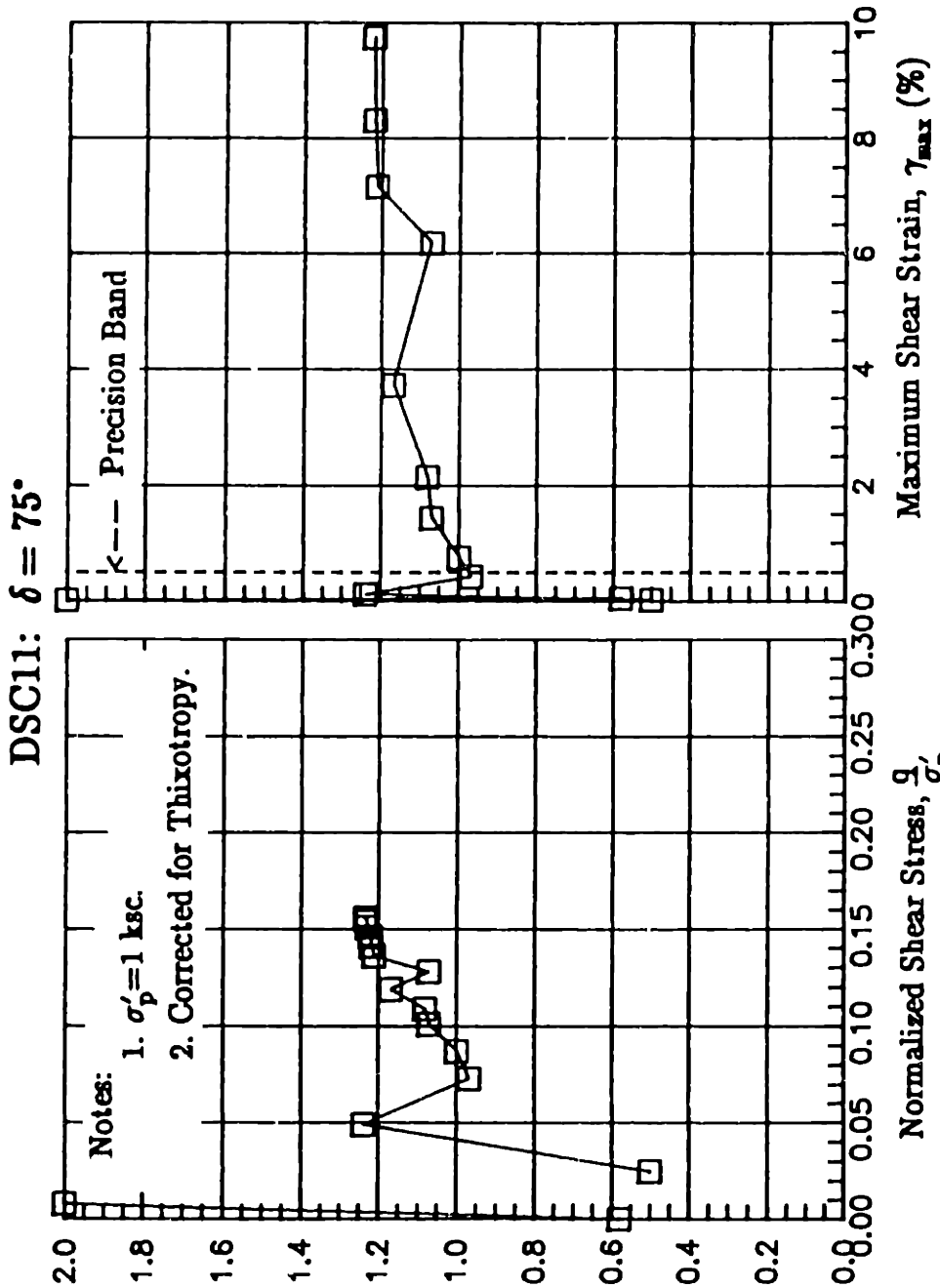

Figure C.28: Variation of NAR with (a) Normalized Shear Stress and with (b) Maximum Shear Strain from Test DSC11.

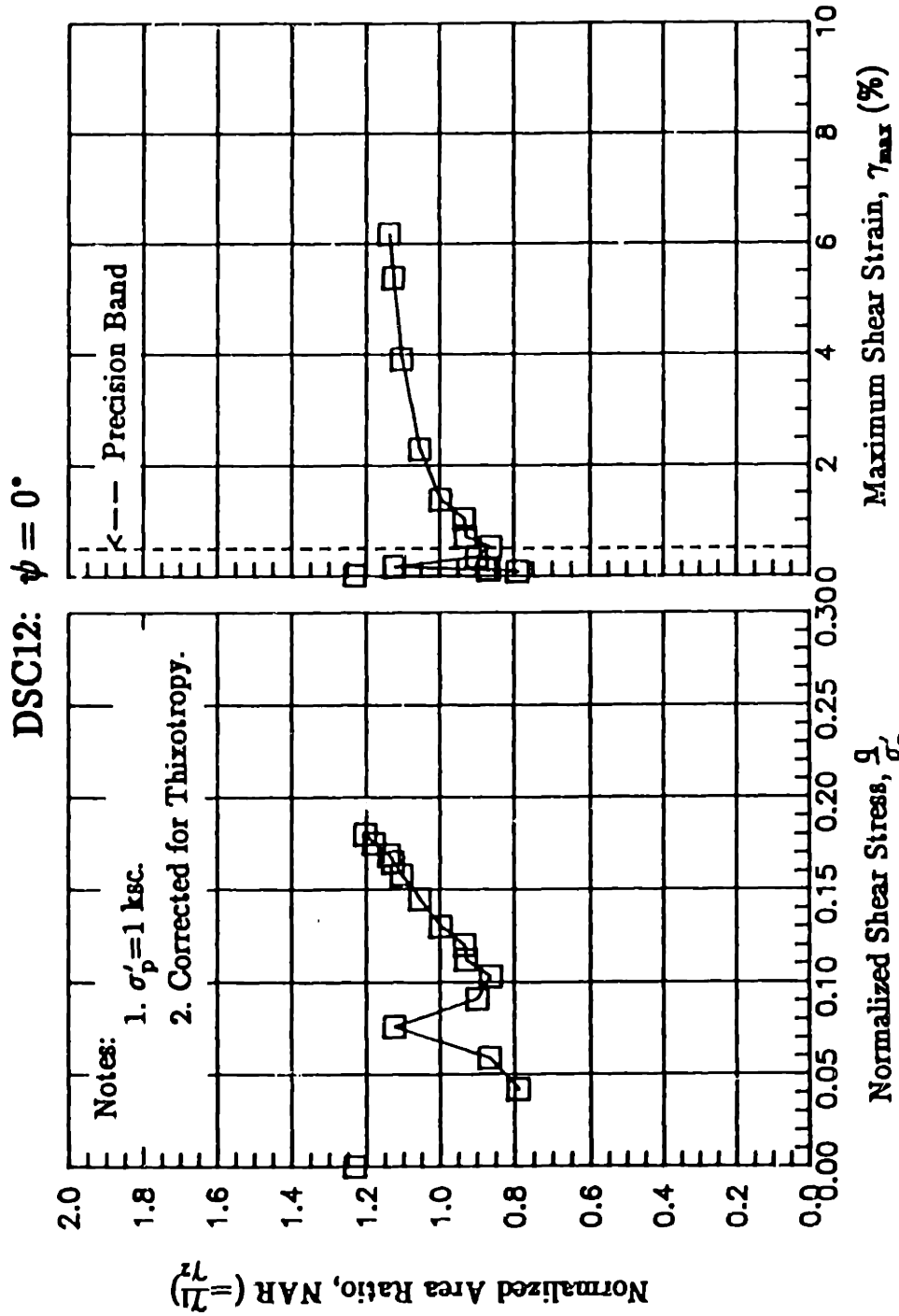

Figure C.29: Variation of NAR with (a) Normalized Shear Stress and with (b) Maximum Shear Strain from Test DSC12.

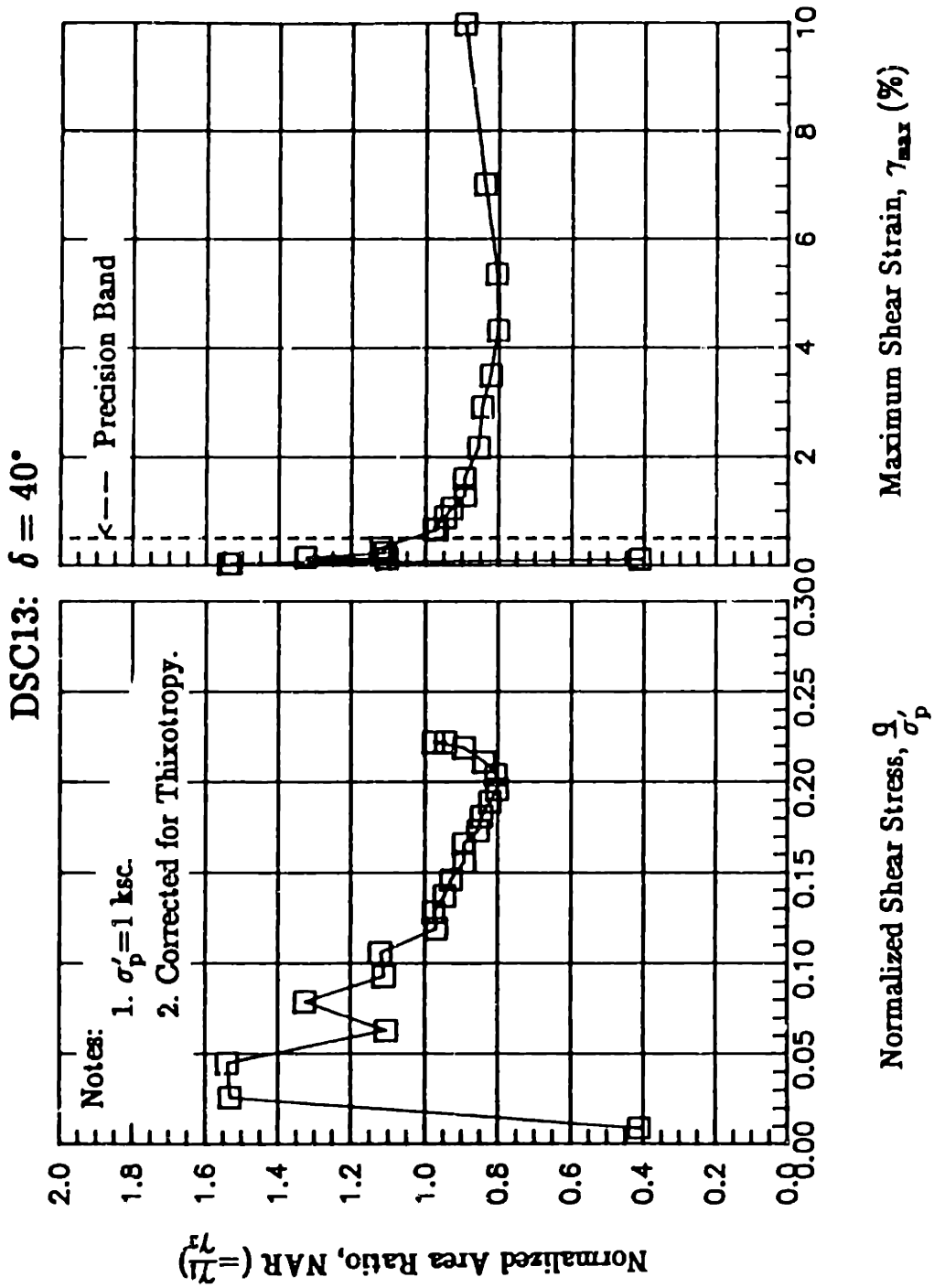

Figure C.30: Variation of NAR with (a) Normalized Shear Stress and with (b) Maximum Shear Strain from Test DSC13.

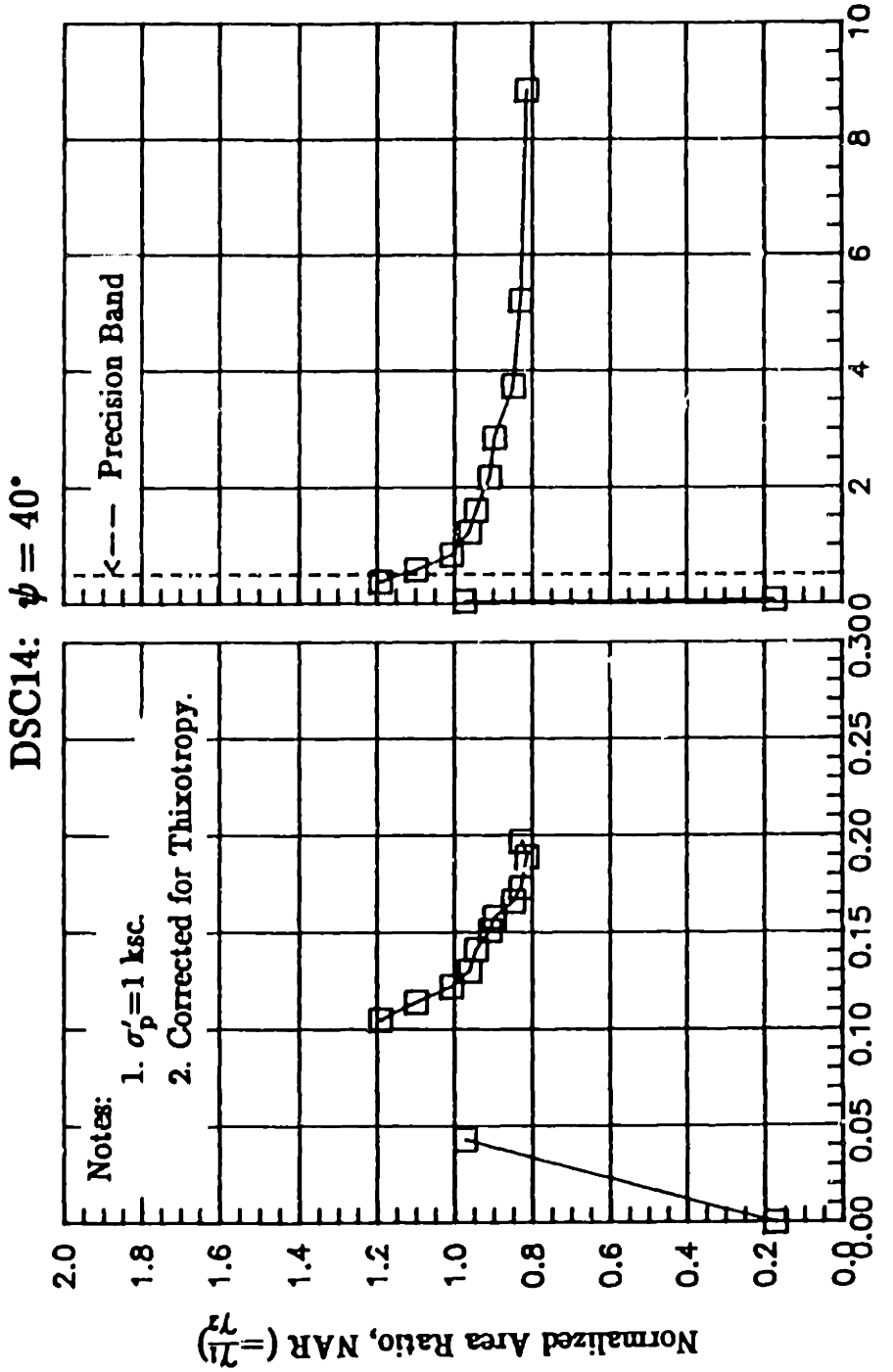

Figure C.31: Variation of NAR with (a) Normalized Shear Stress and with (b) Maximum Shear Strain from Test DSC14.

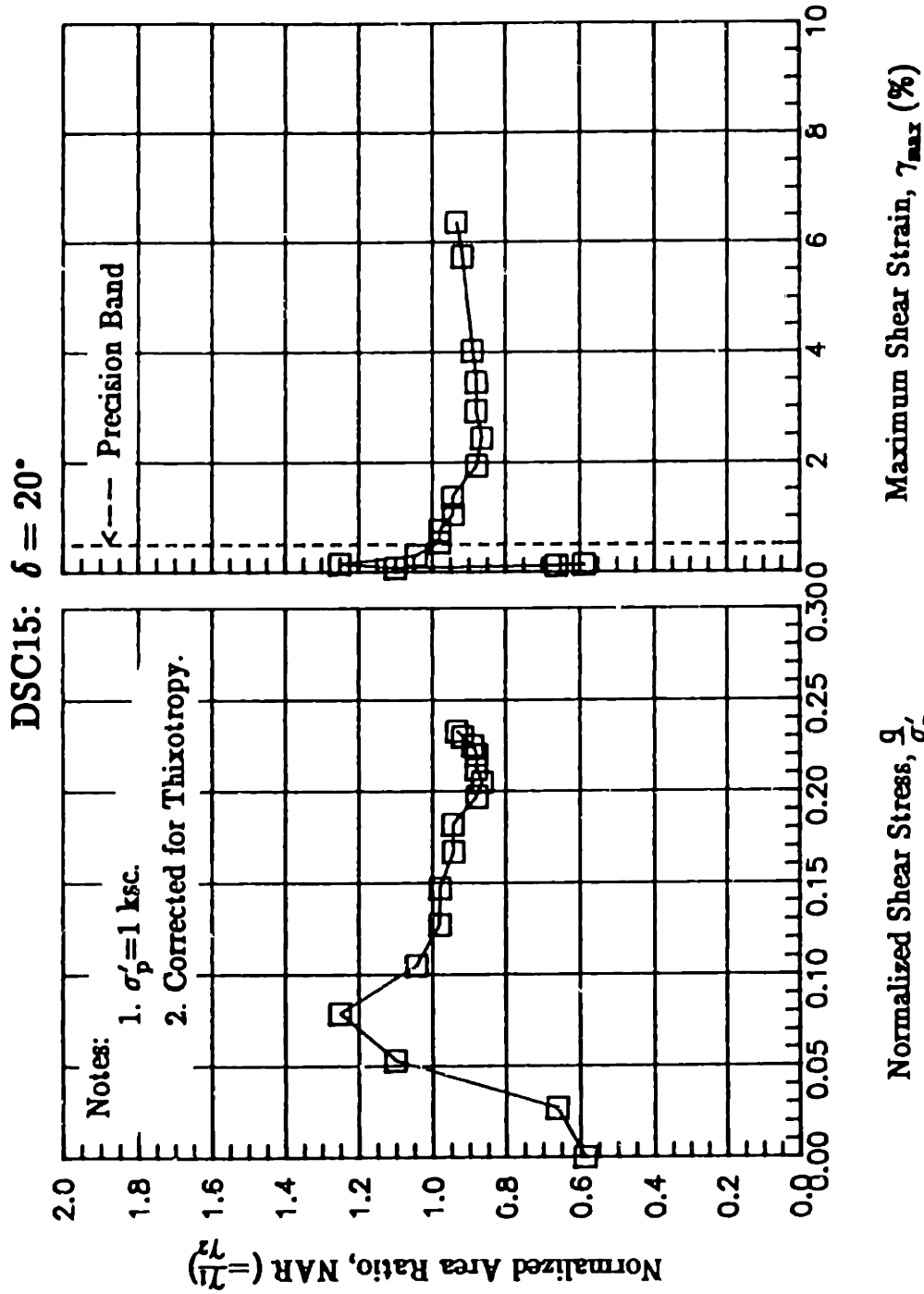

Figure C.32: Variation of NAR with (a) Normalized Shear Stress and with (b) Maximum Shear Strain from Test DSC15.

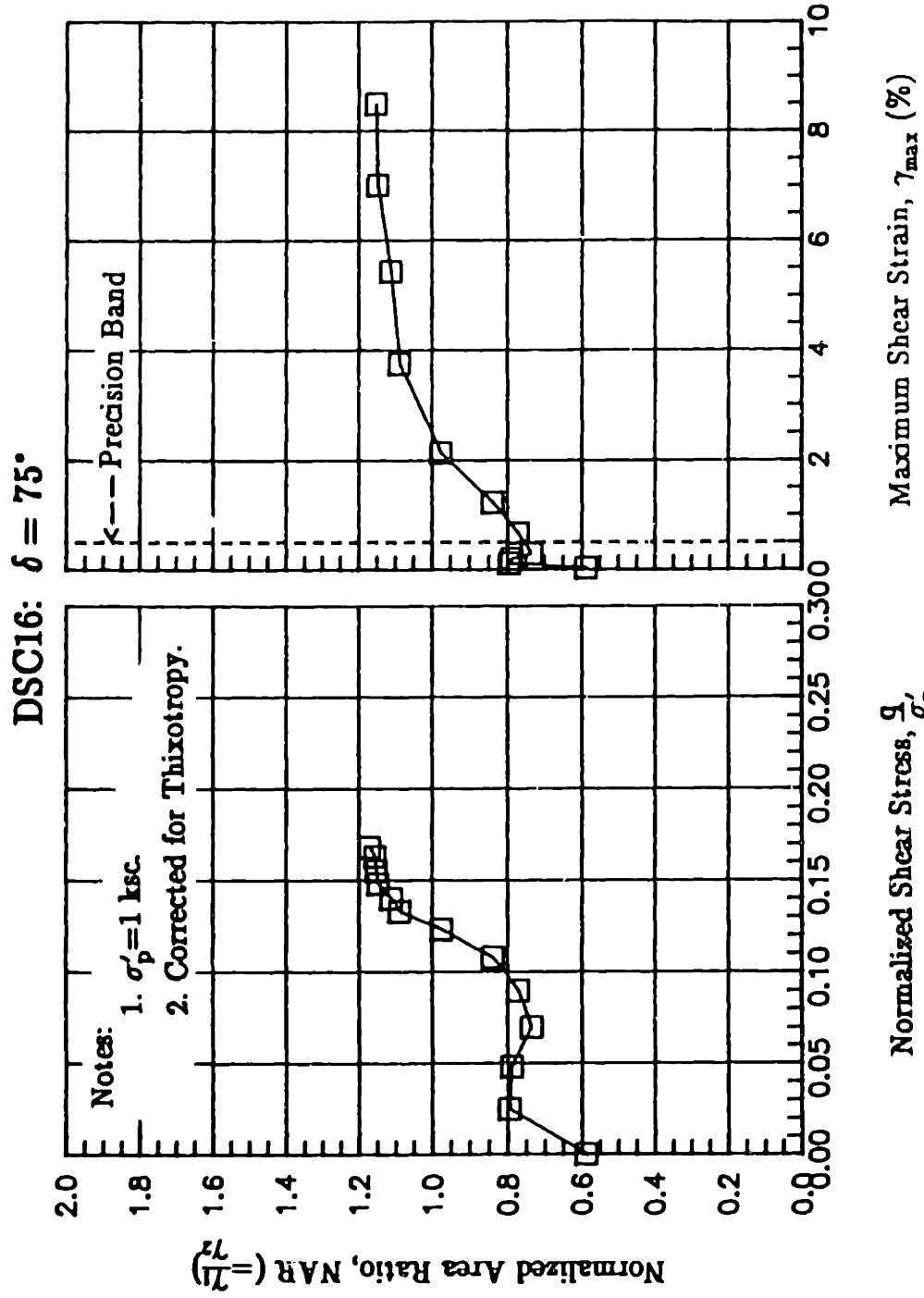

Figure C.33: Variation of NAR with (a) Normalized Shear Stress and with (b) Maximum Shear Strain from Test DSC16.

APPENDIX D

CONSTRUCTION OF INDIVIDUAL COMPONENTS OF THE DIRECTIONAL SHEAR CELL

D.1 SAMPLE MEMBRANE CONSTRUCTION

D.1.1 Introduction

The sample membrane for the Directional Shear Cell test has to be made in the laboratory due to its unusual size and specifications. The membrane helps to apply normal stress to the specimen from the pressure bags and is essential for application of surface traction forces (shear stresses) from the shear sheets. Another vital feature of the membrane is that it provides the background on which displacement markers are located on the top surface. By assuming that the strain of the sample is uniform in the plane strain direction, the displacement of the markers can be used to calculate the actual strain of the soil sample.

This section describes the construction of a rubber membrane, including the material and the procedures.

D.1.2 Ingredients for Preparing the Rubber Membrane

Two major components are used in the manufacturing process: the coagulant and the rubber latex with a whitening agent. The coagulant is used to coagulate the rubber latex to achieve a uniform membrane thickness. The chemicals required for preparing the coagulant are as follows:

a. 19 kg of Methanol (CH_3OH).
b. 12.6 kg of Calcium Nitrate Solution ($Ca(NO_3)_2.4H_2O$).

These chemicals are mixed together in a bucket, and stirred continuously

for 10 minutes. The above amounts of chemicals will produce 5 gallons of coagulant. The solution can be stored at room temperature, but should be covered when not in use to prevent any evaporation.

The rubber latex has to be whitened in order to produce a high contrast photography image for strain reduction; therefore, a whitening agent (Rutile) is added to the natural latex. The quantities of chemicals required for preparing 5 gallons of white latex are:

a. 18.5 kg (5 U.S. gallons) of natural rubber latex.

b. Coloring agent: 370 g of Tetra Sodium Polyphosphate, 370 g of distilled water and 1.85 g of Rutile.

The procedure for preparing the white latex is as follows: the whitening agent, Rutile (TiO_2) is mixed with the water along with some Tetra Sodium–Polyphosphate (TSPP) to act as a dispersant. This mixture is stirred in a blender for 30 minutes. It is then poured into the rubber latex, and the solution is stirred for another 20 minutes. This solution should be stored at room temperature in a bucket with a lid when it is not in use.

D.1.3 Procedure for Preparing the Rubber Membrane

This section describes the step by step procedure for constructing the rubber membrane (Figure D.1):

a. *Cleaning the form:*
   - Clean the form with an abrasive detergent (e.g., Ajax or Soft Scrub).
   - Wash it thoroughly under warm water.
   - Dry it with cotton balls.
   - Place it under the ventilating hood.
   - Clean it with Acetone.

Caution: Do not inhale Acetone vapor.

b. *Coating the form with the coagulant:*
- Dip the cleaned form in the Methanol–Calcium Nitrate solution for 20 seconds. Make sure the form is uniformly coated with the coagulant.
- Tilt the form at an angle to remove any excess coagulant.

c. *Drying the coagulant:*
- Place the form in the oven at 60° C for 2 to 4 hours until the coagulant is completely dried.

d. *Dipping in the Rubber Latex:*
- Allow the form to cool to about 40° C.
- Dip the form in the white latex at an angle.
- Rotate the form 360°.
- Remove the form from the latex.
- Place it in a upright position.

Note: the dipping process should take no more than 5 seconds, otherwise the membrane will be too thick.

e. *Removing the excess latex:*
- Immediately squeeze off any excess latex on the sides of the membrane using a glass rod.
- Allow the membrane to cure for 24 hours at room temperature.

f. *Wrapping the membrane with plastic wrap:*
- Cut four 4"x5" pieces of plastic wrap.
- Wrap the vertical sides of the membrane with the plastic.

g. *Marking the reference points:*
- Mark 10 rows of 10 points on the top face of the membrane using a black ball–point pen.
- Allow the ink to dry for at least an hour.

Note: Try out the pen on a piece of rubber first to ensure the dot is circular. The diameter of the dot should be in range of 1.0–1.5 mm.

h. *Coating the top face with Silicone Spray:*
- Place the form in the ventilating hood.
- Spray the top face of the membrane with a layer of silicone (Krylon Crystal Clear).
- Dry the silicone for 30 minutes.

Caution: Do not inhale the vapor; reports have associated repeated and prolonged occupational overexposure to solvents with permanent brain, nervous system and other internal organ damage.

i. *Removing the membrane from the form:*
- Cut the lower edges of the membrane.
- Pull the corners of the membrane away from the form as shown in Figure D.1a.

- Stop the process when the membrane is in the upright position.

j. *Wrapping the vertical faces of the membrane with plastic wrap:*
- Place a 3.5"x3.5"x3.5" rubber foam on top of the membrane.
- Cut 4 4"x5" pieces of plastic wrap.
- Attach the wrap around the vertical sides of the membrane.
- Pull the membrane away from the form.

k. *Flipping the membrane:*
- Flip the membrane over, so that the pen dots are on the outside face.

The plastic wrap should prevent the rubber from sticking to itself.

l. *Placing the membrane in the membrane stretcher:*
- Remove the plastic wrap on the outside faces.
- Place the membrane in the membrane stretcher.
- Connect the stretcher to a vacuum pump.
- Position the membrane with the stretcher.
- Turn on the vacuum.
- Place a glass plate on top of the stretcher to seal any leakage.
- Tape the edges of the membrane to the stretcher.
- Remove the glass plate and the interior plastic wrap.

m. *Leaching the membrane:*
- Disconnect the vacuum pump.
- Fill the membrane with water a few times.
- Dry the membrane with cotton balls.
- Clean the inside with Acetone under the ventilating hood.

n. *Attaching the fabric reinforcement:*
- Apply vacuum to the stretcher.
- Apply some rubber cement to the fabric.
- Place two pieces of 1.4"x4" cheese cloth on opposite corners of the membrane.

Be sure the fabric is glued to the corners tightly.

o. *Placing the brass reinforcement:*
- Cut four 0.25"x3.5" strips of brass sheet (thickness of 0.10").
- Round the edges of the brass strips.
- Clean the strips with Acetone.
- Apply some 5–minute epoxy to one face of the strip.
- Glue the strips to the fabric reinforcement.
- Press the strips firmly to the fabric for a few minutes until the epoxy is set.
- Place some plastic (coffee) stirrers to hold the strips in place as shown in Figure D.1b.
- Allow the epoxy to cure for additional 6 hours.

p. *Coating the membrane with sand:*
- Prepare 300 g of Sieve No.30–40 sand.
- Clean the sand by washing with water.

- Apply a layer of rubber cement on the inner faces of the membrane.
- Pour the sand in the membrane immediately.
- Place a glass plate on top of the membrane.
- Shake the stretcher thoroughly for 1 minute.
- Remove the glass plate and the excess sand.
- Allow the rubber cement to dry for 24 hours.

q. *Coating with additional layer of rubber cement:*
- Prepare 100 ml of 1:1 ratio of rubber cement–water solution.
- Pour the solution in a spray container.
- Turn the stretcher upside down.
- Spray the inside of the membrane with the diluted solution.
- Allow the excess solution to drip off the membrane.

r. *Drying and storing the membrane:*
- Dry the membrane for another 24 hours at room temperature.
- Rub the coated sand – if the sand falls apart, then repeat step q.
- Leave the membrane in the stretcher.

The membrane is ready for use (Figure D.2). The membrane should be stored in a refrigerator to prolong its life.

D.2 RUBBER BAG CONSTRUCTION

D.2.1 Introduction

The normal stresses, σ_a and σ_b, in the DSC are applied to four faces of the test specimen using two sets of pressurized flexible rubber bags. Each bag is attached to a backing plate unit and two retaining vanes. The rubber bag has to be manufactured in the laboratory. Due to the nature of the natural rubber, the rubber bags have to be replaced regularly, depending on the usage and the storing environment.

D.2.2 Ingredients for Preparing the Rubber Bag

The chemicals used in the construction of the the rubber bag are similar to those of the sample membrane except that white latex is not required. Therefore, only the coagulant and the natural rubber latex are used.

D.2.3 Procedure for Preparing the Rubber Bag

The procedure for making the rubber bag is as follows (Figure D.3):

a. *Cleaning the form:*
- Clean the form with an abrasive detergent (e.g., Ajax or Soft Scrub).
- Wash it thoroughly under warm water.
- Dry it with cotton balls.
- Place it under the ventilating hood.
- Clean it with Acetone.

Caution: Do not inhale Acetone vapor.

b. *Coating the form with coagulant:*
- Dip the cleaned form in the Methanol–Calcium Nitrate solution. Make sure the form is properly coated with the coagulant.
- Tilt the form at an angle to remove any excess coagulant.

c. *Drying the coagulant:*
- Place the form in the oven at 60° C for 2 to 4 hours until the coagulant is completely dried.

d. *Dipping in the Rubber Latex:*
- Allow the form to cool to about 40° C.
- Dip the form in the latex at an angle.
- Rotate the form in the latex for 2 minutes.
- Remove the form from the latex.
- Place it in a upright position.
- Remove any excess latex using a glass rod.
- Allow the latex to cure for 24 hours at room temperature.

e. *Placing the fabric reinforcement:*
- Place a 5.5"x5.5" cheese cloth at the center of cured rubber.
- Glue the cloth to the rubber using rubber latex.
- Dry it for 4 hours.

f. *Folding the fabric:*
- Fold one side of the fabric under the form.
- Apply latex to the folded edge.
- Fold the adjacent side of the fabric.
- Apply latex to this folded fabric.
- Fold the corner of the folded sides under the form.
- Glue the corner with the latex.
- Fold the other sides and corners of the fabric. Make sure the fabric is glued properly to the rubber.
- Dry it for 24 hours.

g. *Dipping in the latex:*
- Dip the form in latex for 1 minute.
- Dry the latex for 24 hours..
- Repeat the above two steps until the total thickness of the rubber plus fabric is about 0.100".

h. *Marking a ring:*
- Mark a 1.8 inch diameter ring on the underside of the rubber around the form handle.

i. *Cutting the ring:*
- Cut along the marked circle.
- Remove the centered rubber disc.
- Remove the rubber bag from the form.

j. *Attaching additional reinforcement:*
- Prepare an 0.100"x4"x4.2" fabric reinforced rubber sheet.
- Cut a 1.8–inch diameter ring in the middle of the rubber sheet.
- Clean the rubber sheet with acetone.
- Apply latex to one face of the rubber sheet.
- Glue the sheet to the rubber bag.
- Press it with a glass plate and some weights.
- Allow it to dry for 24 hours.

k. *Punching some holes:*
- Mark the positions of the 9 holes for the bag connector as shown in Figure D.4.
- Punch the holes using a 1/8" hole puncher.

l. *Attaching the aluminum disc:*
- Cut a 1" diameter piece of aluminum foil.
- Clean the foil with acetone.
- Apply some rubber cement to one of the faces.
- Place the glued face to the inner face of the rubber bag.
- Dry the cement for 24 hours.

The rubber bag is ready for use.

D.3 ASSEMBLY OF THE PRESSURE BAG

D.3.1 Introduction

This section of the Appendix describes the individual components of the pressure bag, and the assembly process. The major components of the pressure bag are the position sensors, the rubber bag, the backing plate unit, the bag

connector and two retaining vanes, as shown in Figures D.4 to D.8. The complete unit is shown in Figure D.10.

D.3.2 Assembly and Operation of the Position Sensor

The position sensor is designed to control the relative position of the pressure bag during the test. It consists of two strips of 1 in long brass sheets mounted on one face of the backing plate (A) with plastic screws and nuts (Figure D.9a). A brass screw is connected to one end of the upper metal strip. Three electric wires are connected to the two metal strips and the aluminum disc on the rubber bag. These three wires are then soldered to three separate steel rods on the backing plate (A). The rods are inserted into a hole on the backing plate (A) and sealed in place using epoxy as shown in Figure D.9b.

Figure D.9c illustrates the electric circuit diagram of the position sensor. When the brass screw comes in contact with aluminum disc, Switch 1 will be closed and the red light will appear on the control panel. The bag is considered to be at neutral position where the differential displacement of the rubber bag at the center and the edges is zero; therefore, no action is taken. When the bag is overinflated, the brass screw will be separated from the aluminum disc, Switch 1 will be opened, and no light will be on. The bag will have to move towards the sample until the red light is turned on again at the neutral position. This control sensor also takes care of underinflation of the pressure bag. If the bag is underinflated, the aluminum disc will force the brass screw to come in contact with the adjacent metal strip. Switches 1 and 2 will be closed, and red and green lights will appear simultaneously; the bag would then have to be moved away from the soil sample, until it is in the neutral position. Hence, the position sensor helps to keep the bag at the neutral position in order to maintain a constant bag pressure.

D.3.3 Assembly of the Rubber Bag and the Backing Plate Unit

After the position sensor is assembled, the next step is to assemble the whole pressure bag. The following steps describe the procedure (Figure D.10):

a. Place the bag connector in the rubber bag with the dowels inserted into the three holes on the bag.

b. Align the dowels in the bag with the holes on the back plate (A).

c. Place six 6–40 1–1/2" flat head screws through the middle six holes on the backing plate (A) from the opposite face.

d. Tighten the screws.

The rubber bag should be held in place by the bag connector and the screws.

e. Place the backing plate (B) behind the backing plate (A).

f. Place eight 8–32 3/4" flat head screws through the eight holes on the backing plate (B).

g. Tighten all the screws.

h. Place the O–ring sealed connector (for the air pressure, Figure D.9) through the middle hole on the backing plate (B).

i. Tighten the connector.

j. Place the two retaining vanes on the opposite faces of the backing plate (A).

k. Secure the vanes in place with four 8–32 1/4" round head screws.

The pressure bag is fully assembled.

D.4 ASSEMBLY OF THE INTERMEDIATE PRINCIPAL STRESS MEASURING DEVICE

D.4.1 Introduction

The intermediate principal stress measuring device is designed to measure the intermediate principal stress in the Directional Shear Cell test. The device consists of a 6"x6" aluminum base plate with a circular central depression of 0.04" and 3.5" diameter (Figure D.11) which is filled with de–aired water. The water reservoir is enclosed by a rubber disc with a thickness of 0.06 in and a 4.5 in diameter ring (Figure D.12) which is flush mounted to the base plate. A pressure transducer is connected to the reservoir of water so that the pressure of the water can be monitored. This device is placed on the bottom platen during the test. The lower face of the test specimen will cover the entire rubber bag during the test. As the normal and shear stresses in the lateral faces vary, the change in the intermediate principal stress exerted by the soil can be measured from the water pressure in the reservoir.

D.4.2 Assembly of the Intermediate Principal Stress Measuring Device

The procedure for assembly of the device is as follows (Figure D.13):

a. Screw the transducer adapter to the base plate.

b. Prepare 2 gallons of de–aired water.

c. Place the water in a 8"x8"x8" tank.

d. Submerge the base plate in the water with the depression side facing up.

e. Remove any trapped air bubbles around the depression zone and in the transducer adapter.

f. Submerge the rubber disc and the ring.

g. Remove any trapped air bubbles on the rubber disc and the ring.

h. Place the ring in the slot on the base plate with the rubber disc sandwiched between the two.

i. Place the eight 4–40 0.40" flat head screws in the holes on the ring.

j. Tighten the screws.

k. Turn the base plate over.

l. Submerge the pressure transducer and transducer nut.

m. Remove any trapped air bubbles around the transducer and the nuts.

n. Position the transducer and the nuts with the transducer adapter.

o. Tighten the nuts by hand.

p. Turn the base plate over.

If the rubber bag is bulging, then:

- Unscrew the screws.
- Remove some water in the reservoir.
- Tighten the screws.
- Repeated this step until the rubber bag is almost flat.

q. Remove the base plate from the tank.

The measuring device is ready for use in a DSC test.

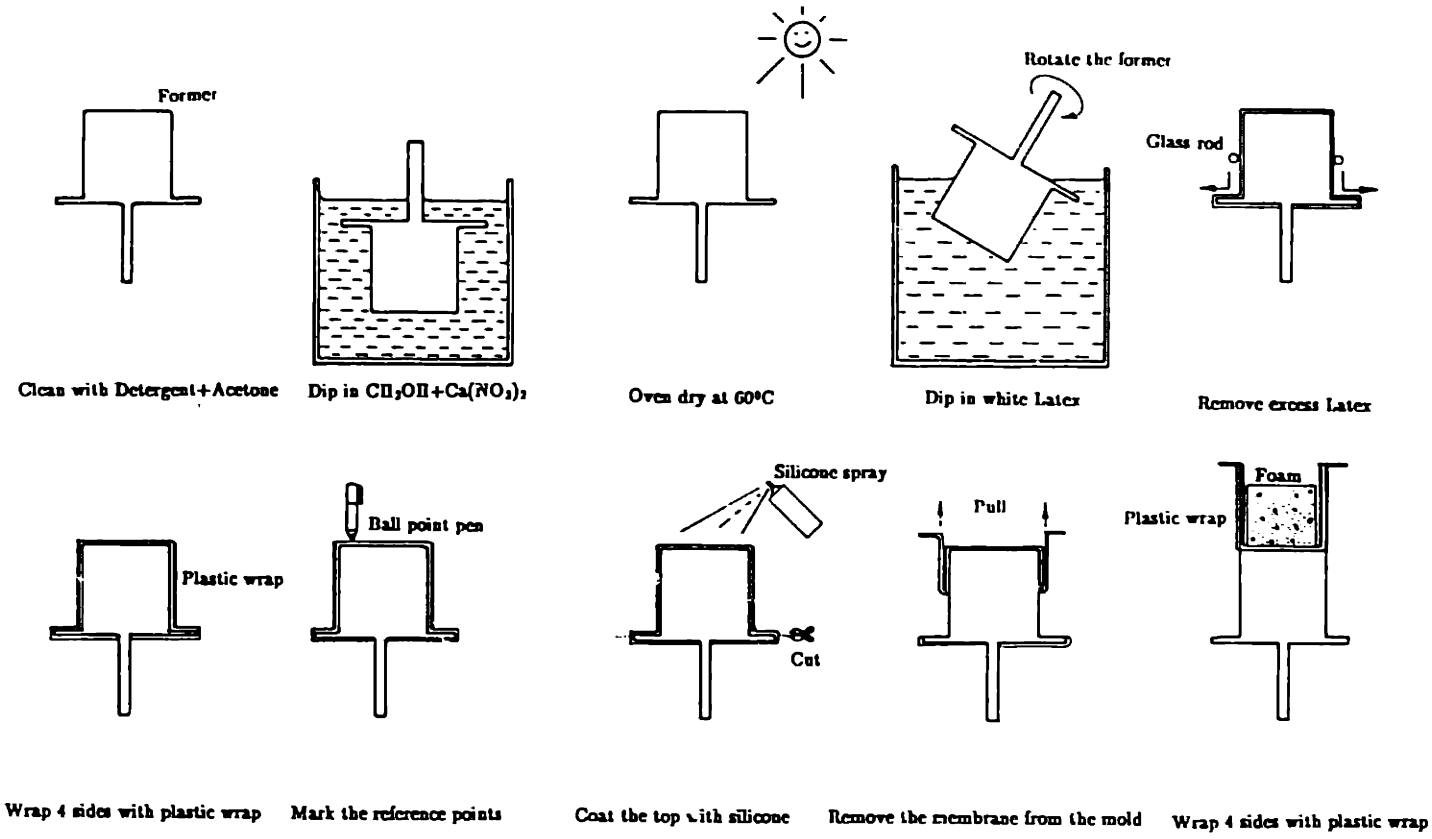

Figure D.1: Preparation of Directional Shear Cell Rubber Membrane.

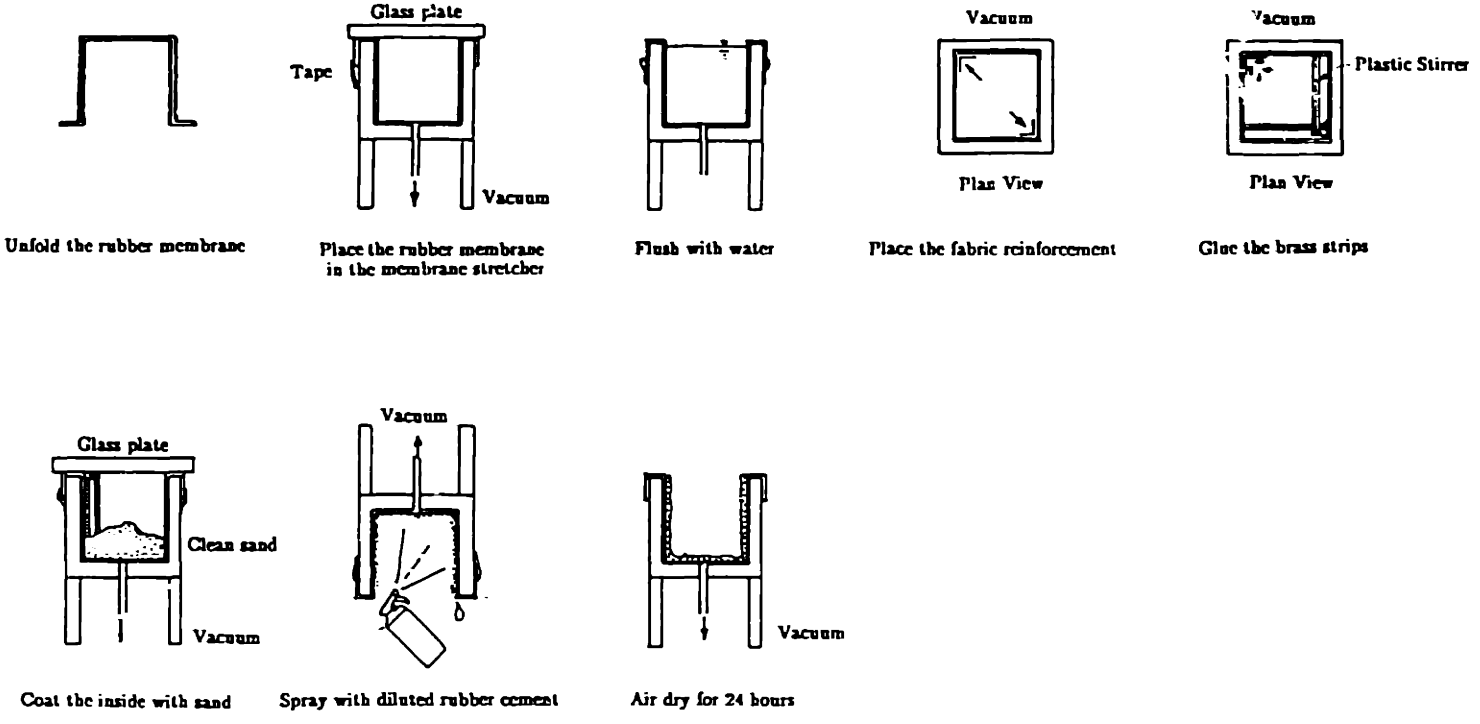

Figure D.1: (Cont.)

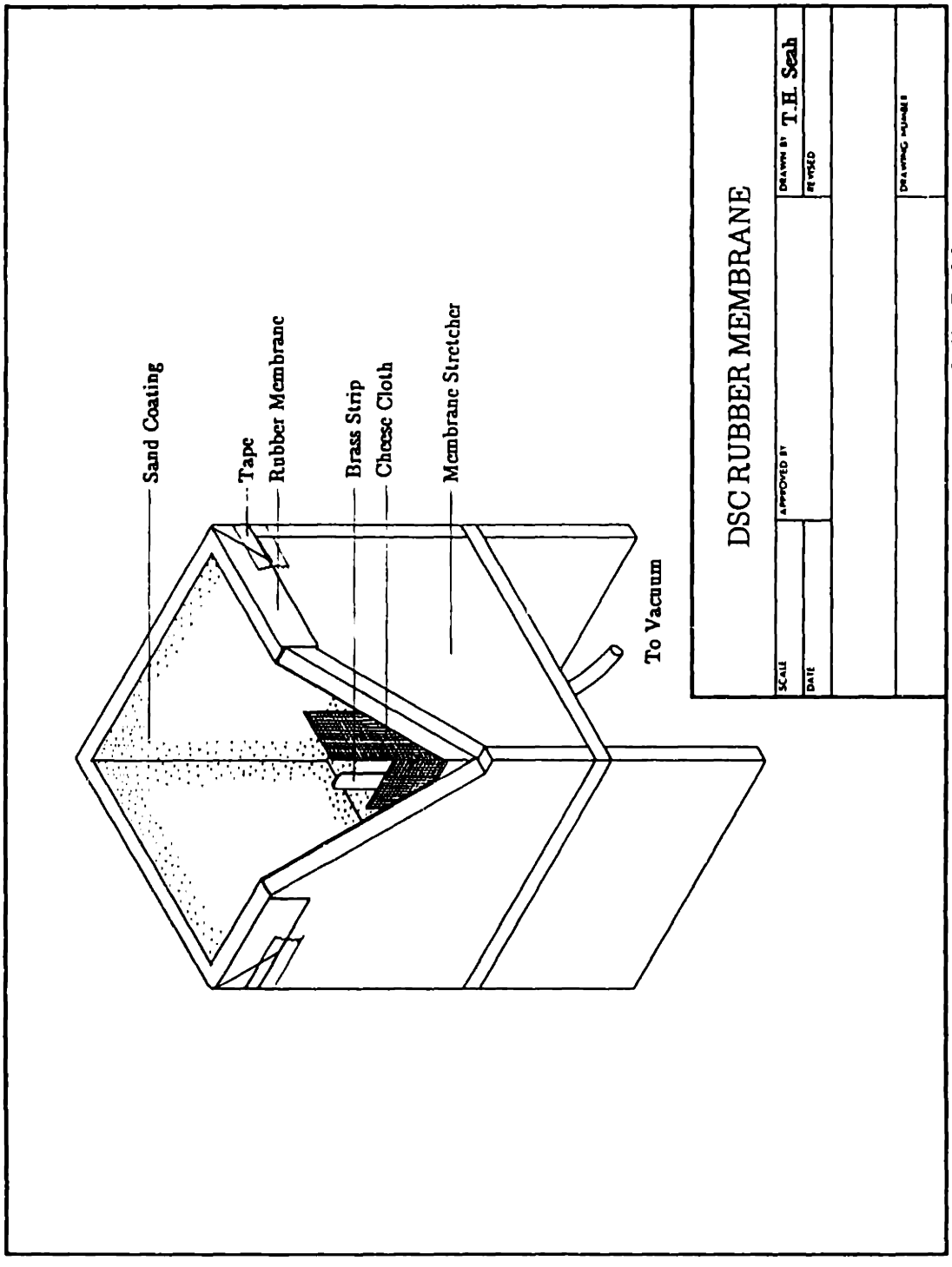

Figure D.2: Schematic of the Directional Shear Cell Rubber Membrane.

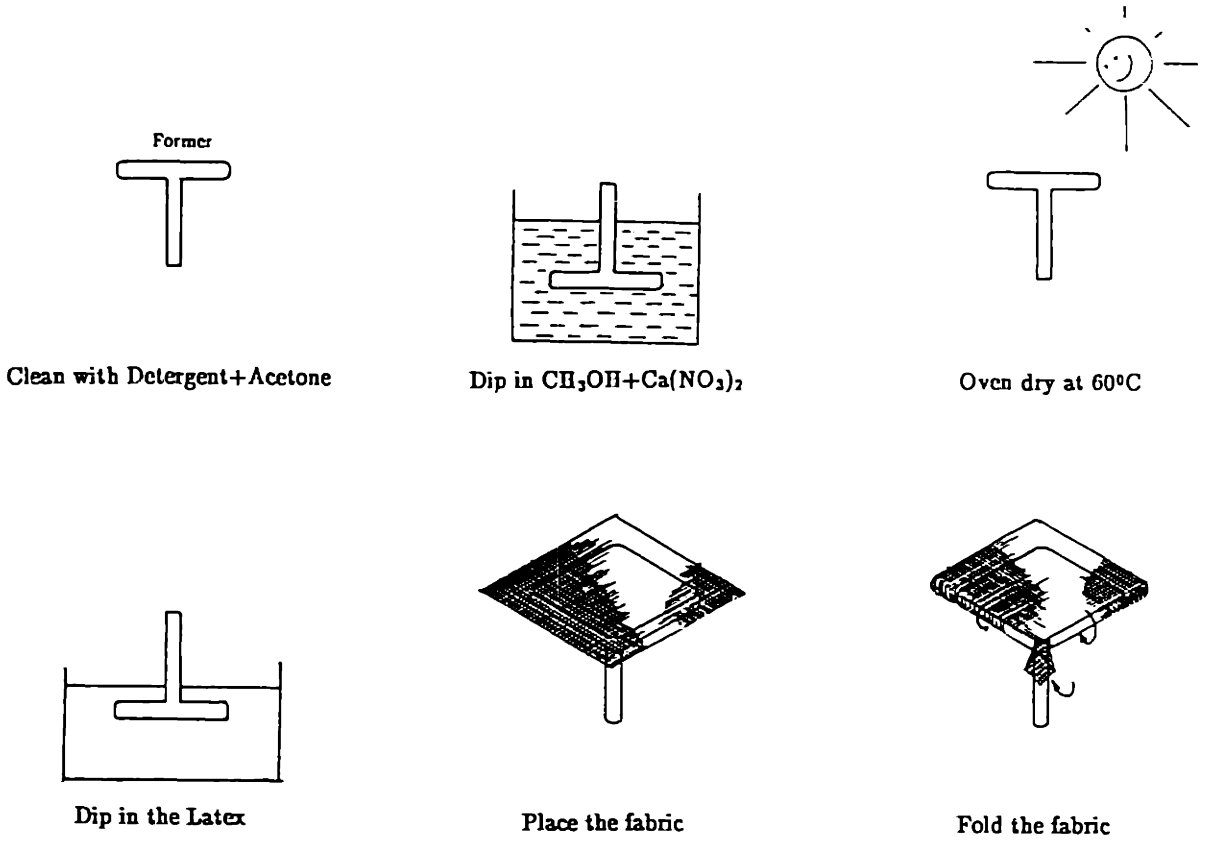

Figure D.3: Preparation of the Rubber Bag.

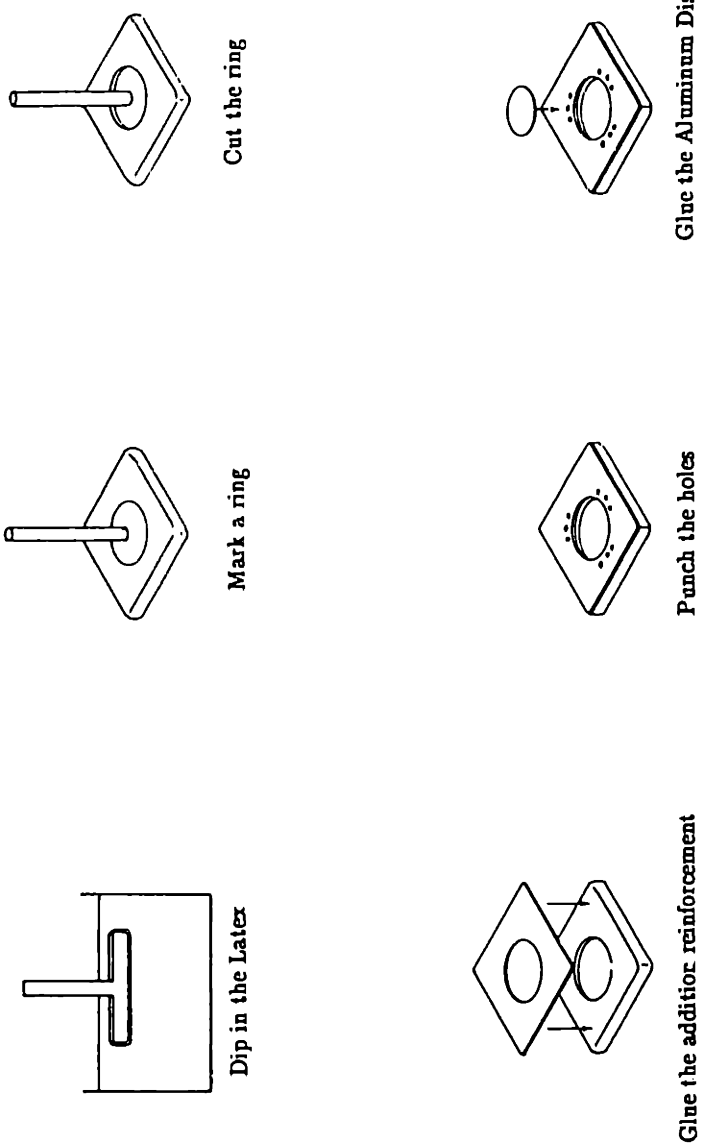

Figure D.3: (Cont.)

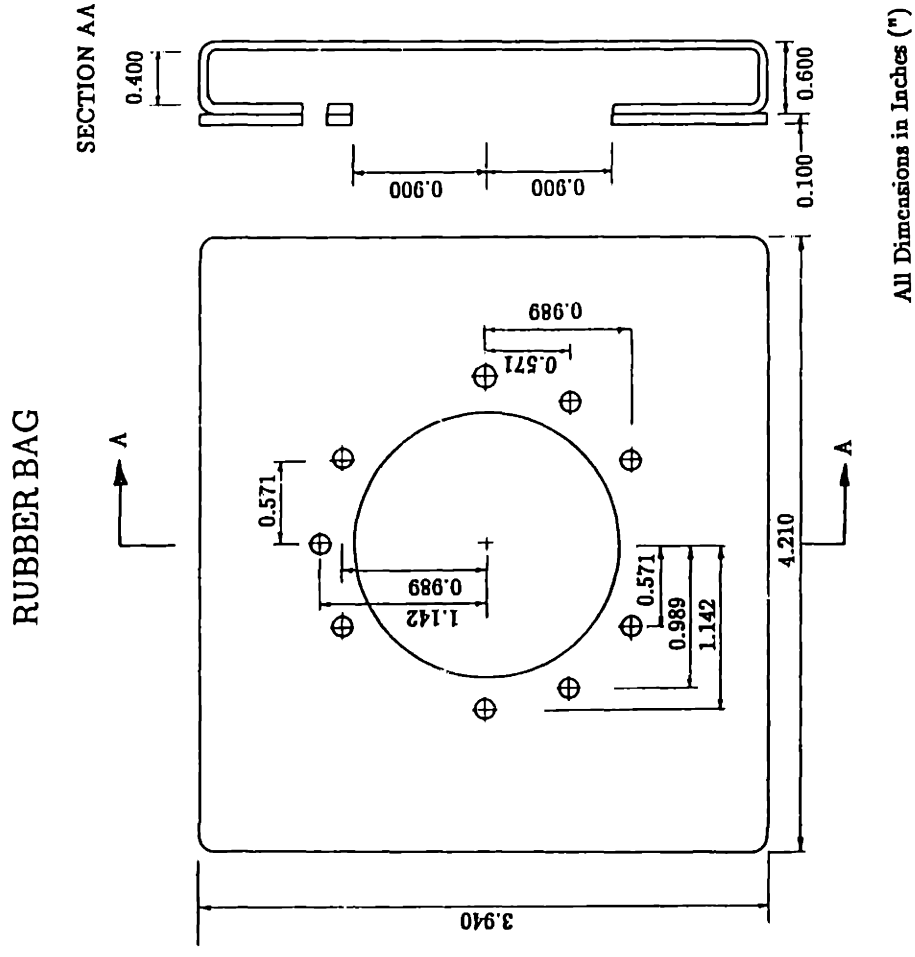

Figure D.4: Schematic of the Rubber Bag.

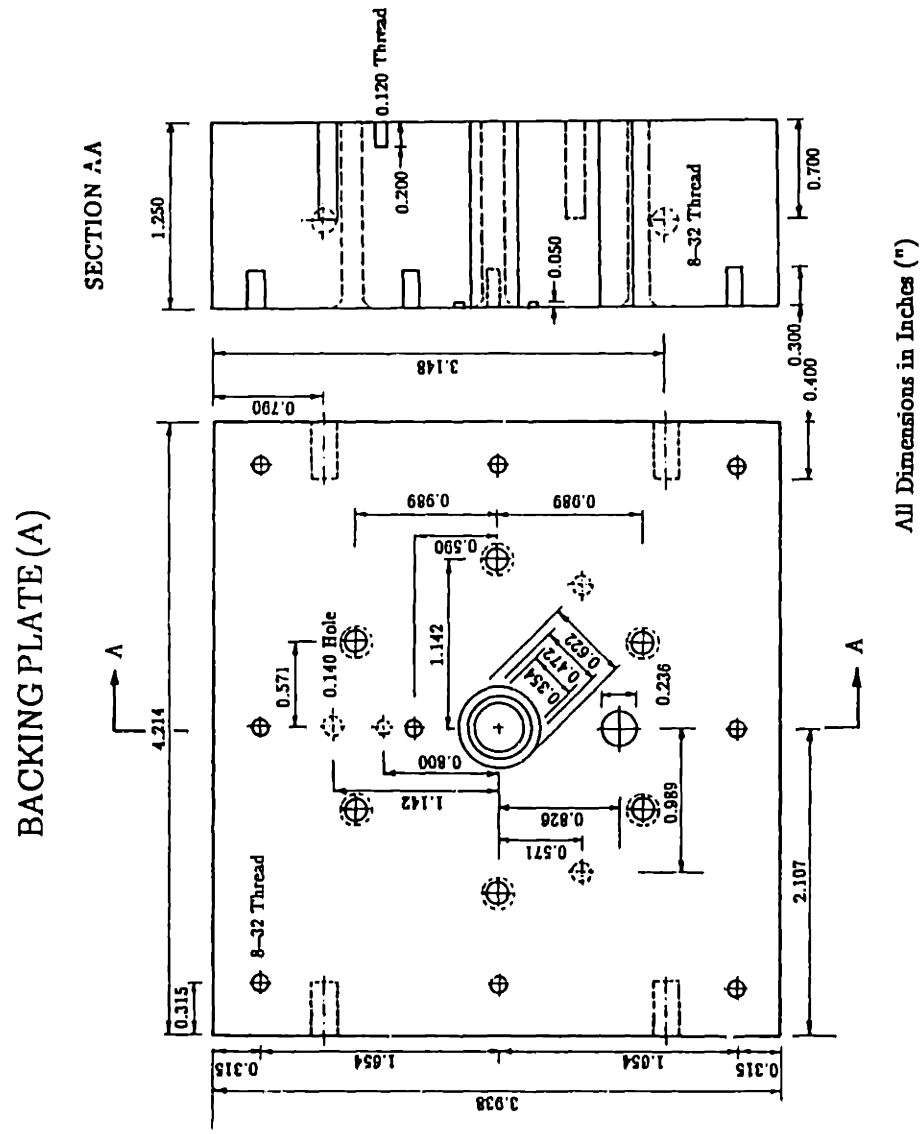

Figure D.5: Schematic of the Backing Plate (A).

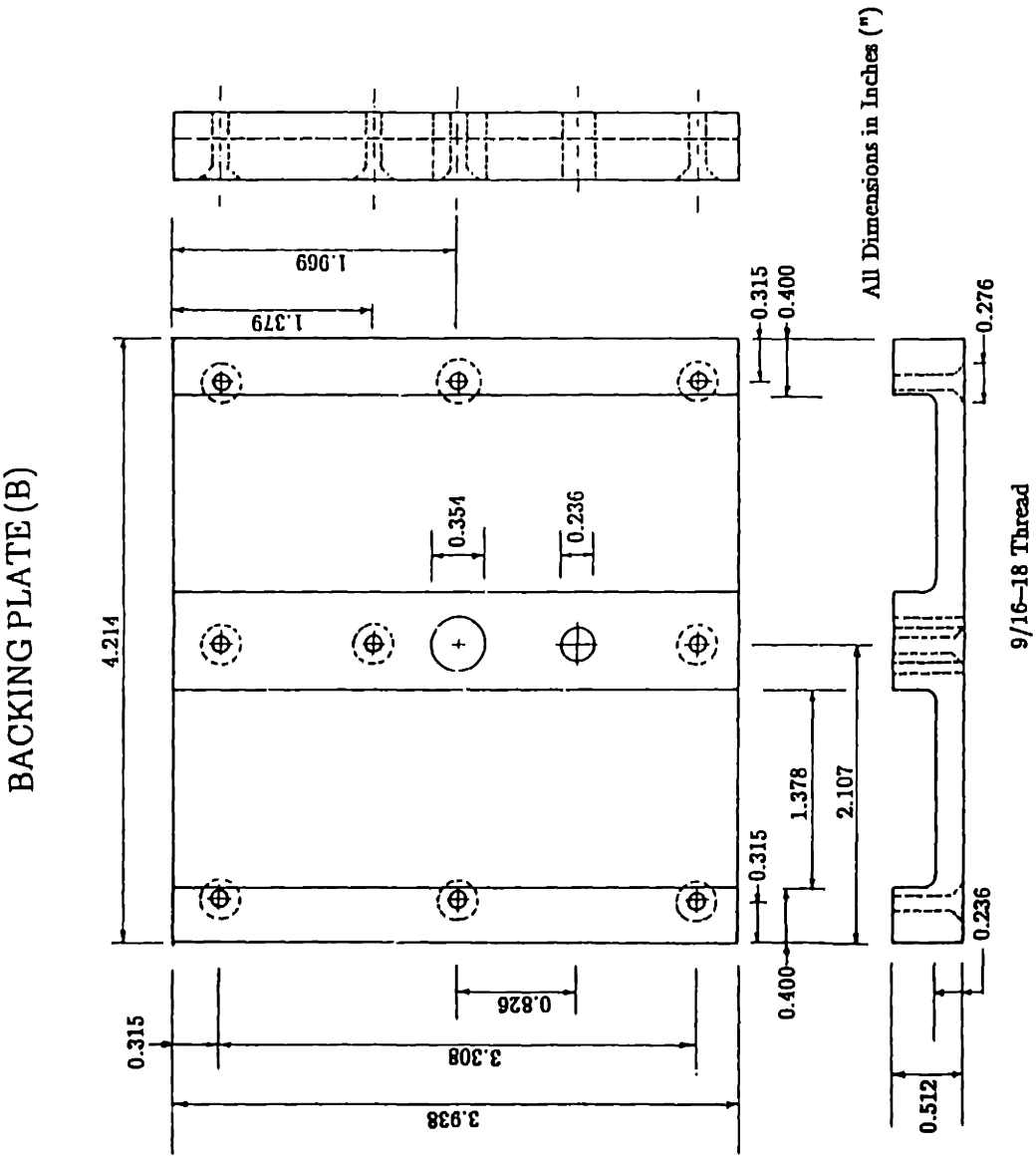

Figure D.6: Schematic of the Backing Plate (B).

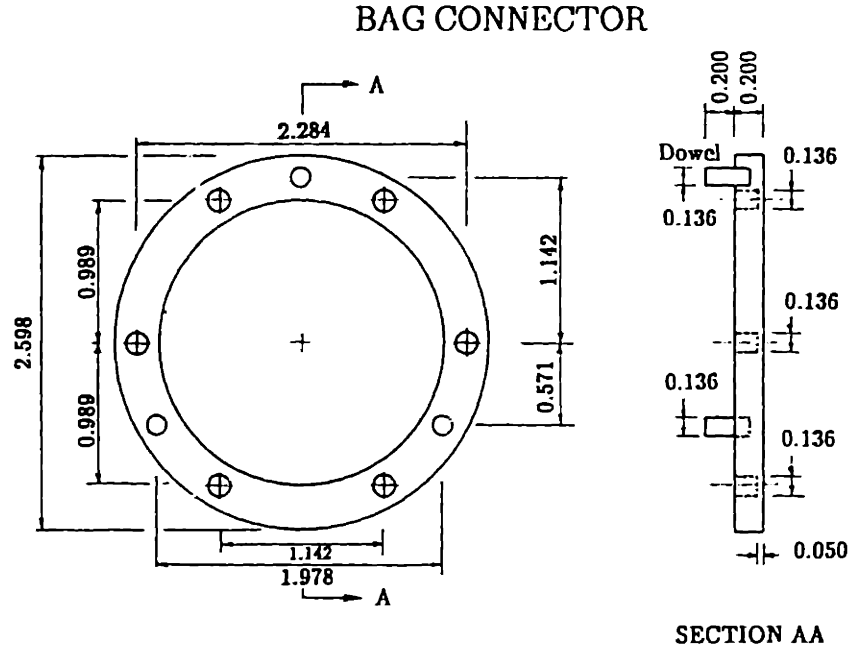

Figure D.7: Schematic of the Bag Connector.

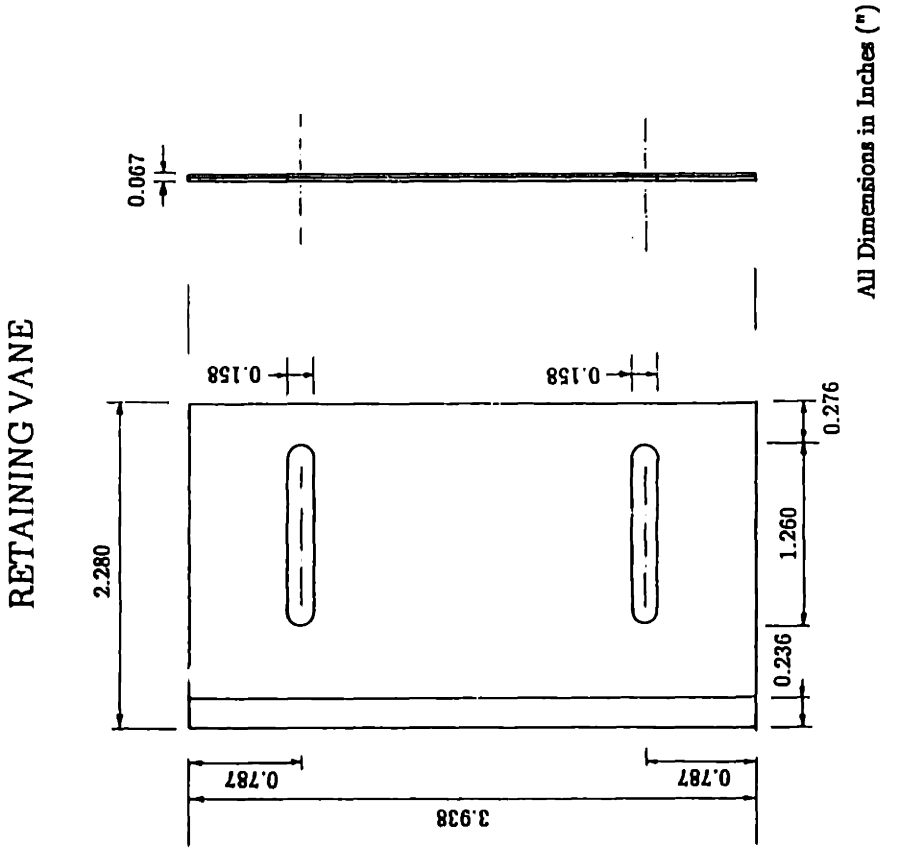

Figure D.8: Schematic of the Retaining Vane.

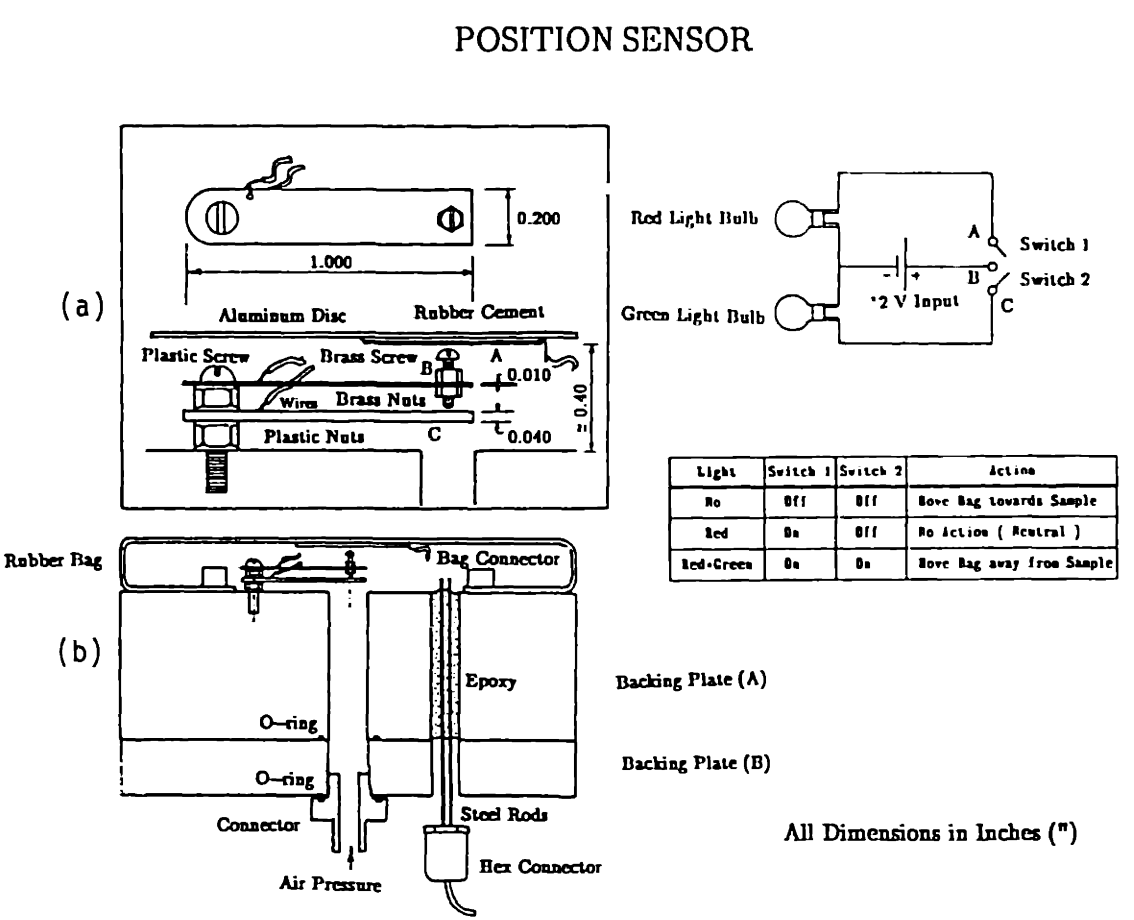

Figure D.9: Assembly of the Pressure Bag Position Sensor.

ASSEMBLY OF THE PRESSURE BAG

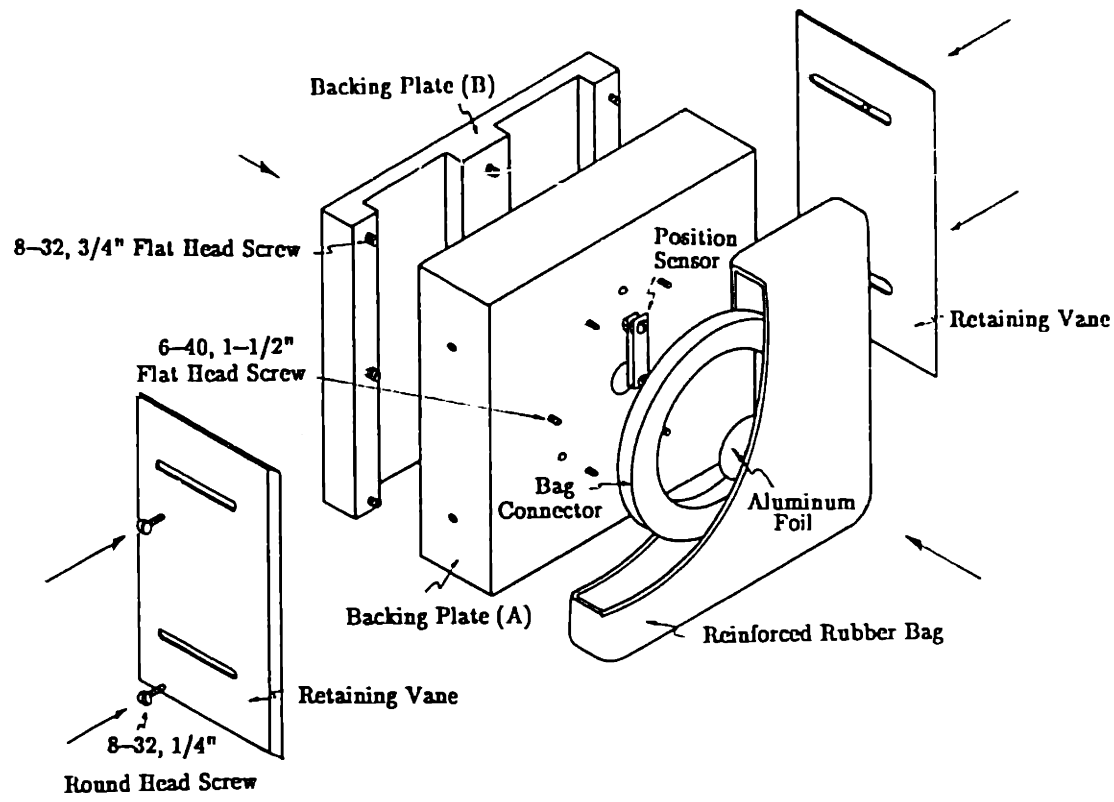

Figure D.10: Assembly of the Pressure Bag.

INTERMEDIATE PRINCIPAL STRESS
MEASURING DEVICE - BASE PLATE

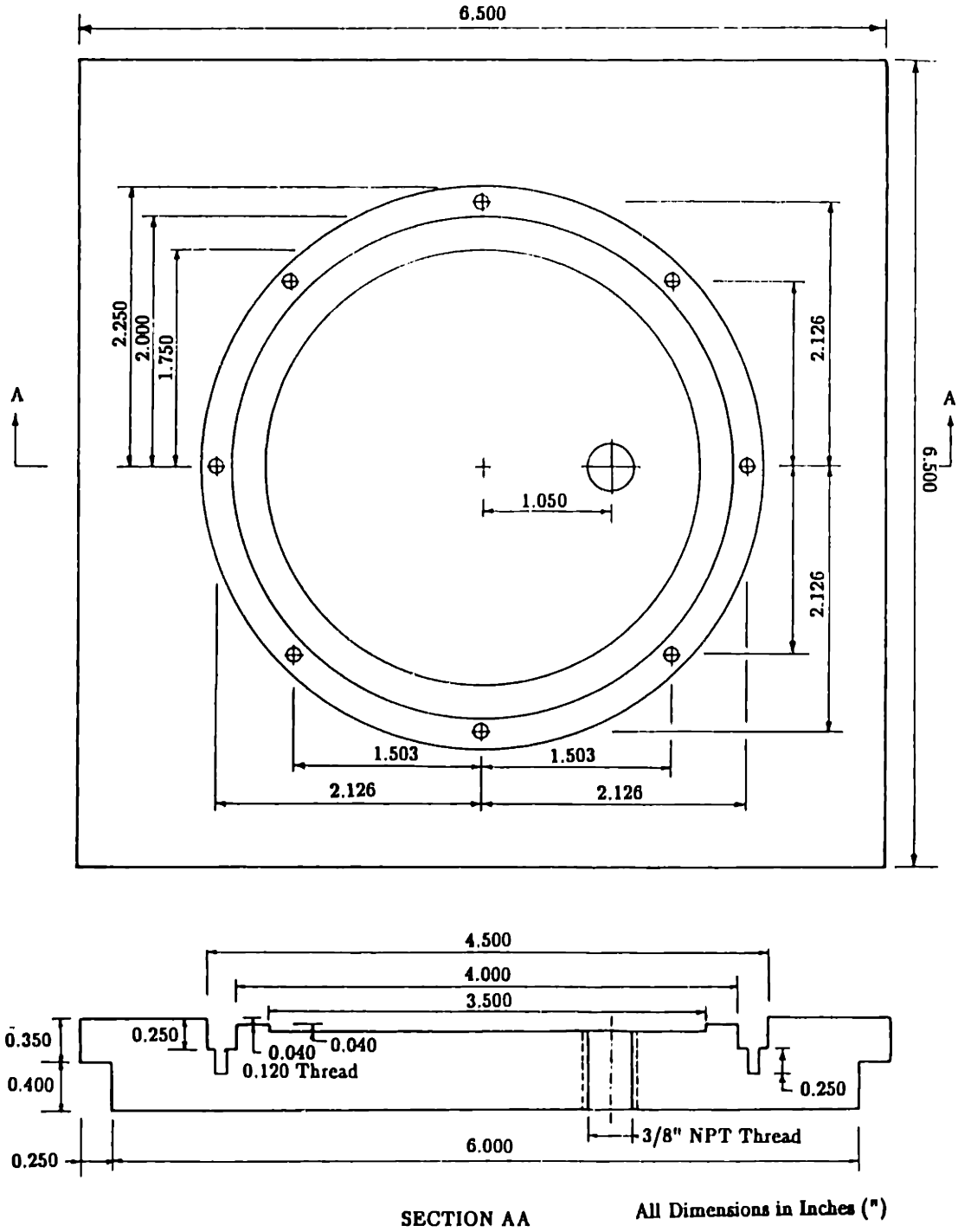

Figure D.11: Schematic of the Intermediate Principal Stress Measuring Device: Base Plate.

INTERMEDIATE PRINCIPAL STRESS
MEASURING DEVICE - RING

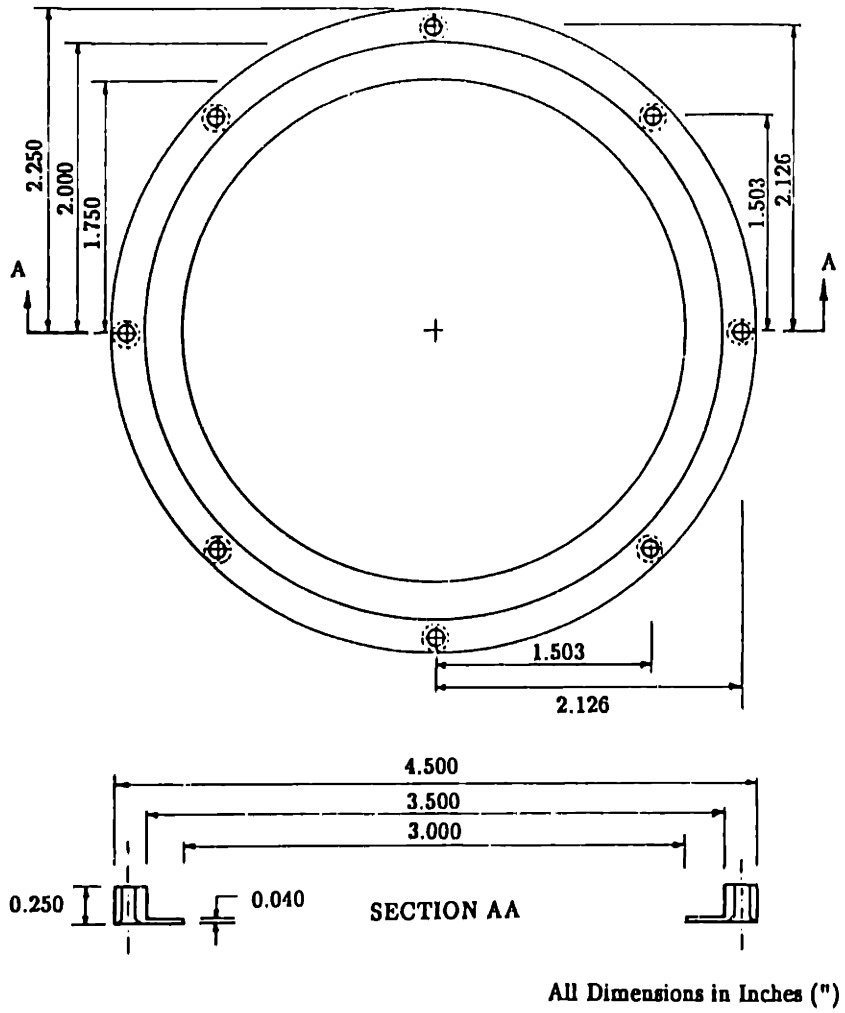

Figure D.12: Schematic of the Intermediate Principal Stress Measuring Device: Ring.

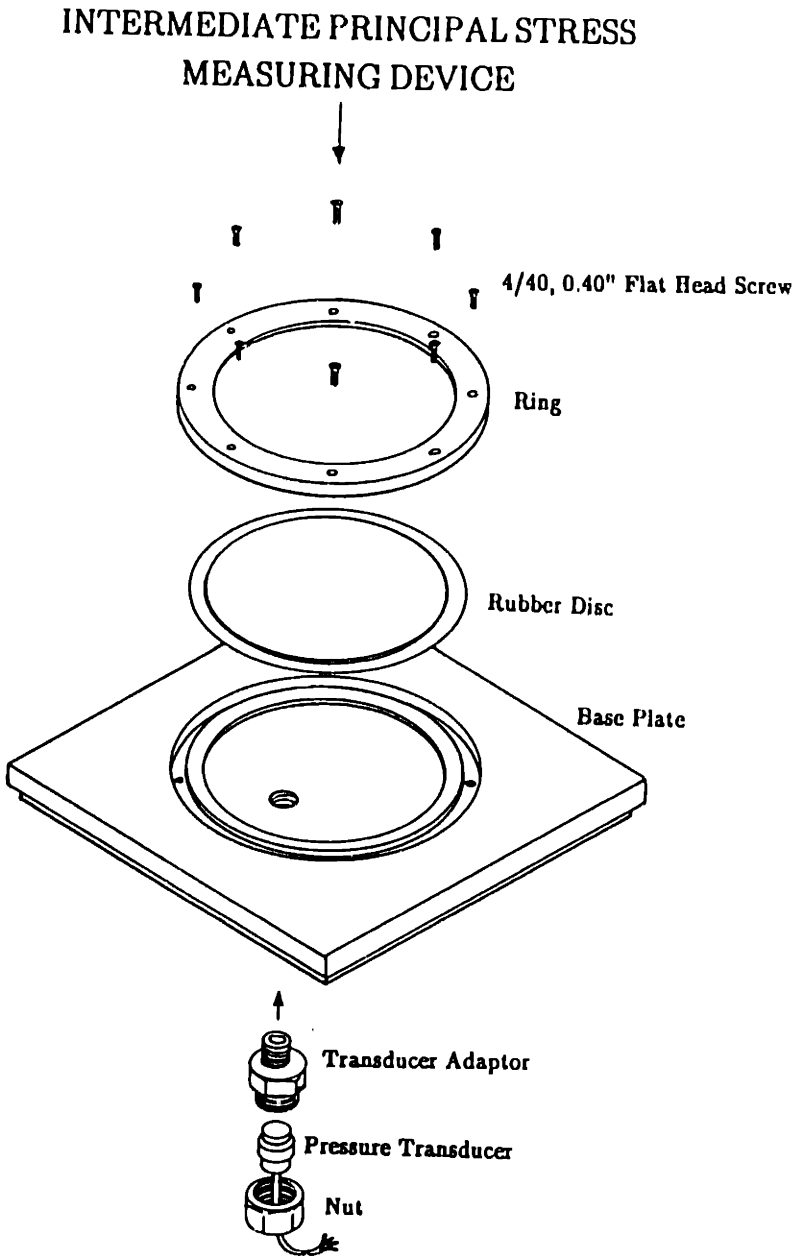

Figure D.13: Assembly of the Intermediate Principal Stress Measuring Device.

APPENDIX E

CALIBRATION OF THE DIRECTIONAL SHEAR CELL DEVICE

E.1 CALIBRATION OF THE SHEAR SHEET

E.1.1 Introduction

The shear stresses in the Directional Shear Cell cannot be computed simply from the applied pressure to the pistons because of frictional effects on the shear piston diaphragms and frictional losses due to the grease between the pressure bags and the shear sheets. A technique of calibration has been developed by Rodriguez (1977) and Bekenstein (1980) to determine the relation between the applied piston stress and shear stress acting on the sample face; this method is described in Germaine (1982). In this research, the pressure bags have been redesigned, being filled with air instead of water; thus, the above method is no longer valid. Therefore, the indirect approach described below was adopted.

The shear stresses, τ_a and τ_b, that are applied to the sample faces can be expressed in terms of the shear piston force, F_{piston}, and the frictional losses, τ_{grease}, due to the grease, as:

$$\tau\,(\tau_a, \tau_b) = f(F_{piston}) - f(\tau_{grease}) \qquad \text{Eq.E.1}$$

The relationship between the shear piston force and the shear piston pressure, σ_{piston}, can be determined experimentally. Special direct shear tests on the grease were conducted to measure the frictional losses.

E.1.2 Calibration of the Shear Pistons

The shear pistons are used to apply pulling forces to the rubber shear sheets. Each piston is connected to the rubber shear sheet by tie rods. Water pressure is applied to the piston cylinder which in turn causes tie rod to pull on the shear sheet. This pulling action of the shear sheet develops a shear stress to a sample face. Since the effective area of the piston and friction losses of the diaphragm are unknowns, calibration is required.

E.1.2.1 Experimental Setup

The shear piston is connected to a load cell by a tie rod. The load cell is aligned with the axis of the piston to ensure the loading is concentric, as shown in Figure E.1. The water pressure in the piston is increased from 0.1 to 2.4 ksc, and the corresponding load cell readings are recorded. The process is repeated for the other three pistons.

E.1.2.2 Experimental Results

Figure E.2 shows the relationship between the measured load (the force on the shear piston force, F_{piston}) and the shear piston pressure, σ_{piston}, for all four shear pistons. Linear regression was applied to the experimental data. The slope of the line represents the "effective area of the shear piston" which is 14.13 cm^2, compared with the design area of 15.21 cm^2. The intercept on the x–axis is the threshold pressure required to overcome frictional forces of the piston diaphragm. The relationship is:

$$F_{piston} = 14.134 \times \sigma_{piston} - 0.657 \text{ (kg)} \qquad \text{Eq. E.2}$$

where

σ_{piston} is the applied piston pressure in ksc, and

F_{piston} is the force on the piston.

E.1.3 Grease Friction

The grease is used to lubricate the shear sheets and normal pressure bag interface in order to reduce the friction between the end platens and the rubber membrane. This lubricant is made up of 30% Dow Corning No.7 compound grease and 70% Dow Corning Molykote III compound grease, which provides reasonable lubrication and stability in long duration tests. In previous research, 10 % of Dupont Teflon Powder was added to the mix, but there is no evidence to show that the powder improves the lubrication. Furthermore, this powder reduces the photography quality due to its opaque nature, and therefore the powder was omitted. The grease friction between the shear sheets and the pressure bags is a function of the normal stress; the following section describes the experimental program in determining this magnitude, in order to make an appropriate correction to the results.

E.1.3.1 Experimental Setup and Test Program

In order to determine the grease friction, a special adapter for the Geonor Direct Simple Shear (DSS) apparatus was made. It consists of a aluminum cap with a rubber sheet glued to its flat surface with epoxy and a aluminum base with a rubber sheet attached to its face in the same manner (Figure E.3). The cap is held by the top platen of the DSS apparatus, and the base rests on top of the DSS bottom base. A layer of grease is spread between the two rubber sheets with initial thickness greater than 2 mm. A constant vertical stress is then applied, and the vertical displacement is recorded.

E.1.3.2 Grease Thickness Versus Time Under Constant Normal Stress

Seven grease thickness tests were conducted with different normal (vertical) stresses. Figure E.4 shows the change in the thickness of the grease with normal stress at different time intervals. The grease thickness decreases with increasing time and normal stress.

E.1.3.3 Shear Stress versus Displacement

Four shear tests were conducted with normal vertical stress ranging from 0.25 to 1.3 ksc. All the tests were subject to a vertical stress for 100 minutes, then sheared at a speed of 1 mm per hour. This speed is close to the average rate of shearing for Directional Shear Cell tests on clay. The results of these tests are shown in Figure E.5. The shear stress for all tests reached peak values at about 0.1 mm and remained almost constant thereafter. Figure E.6a shows the relationship between the shear strength (shear resistance) and the normal stress acting on the grease. The final thickness of the grease is governed by the normal stress; the larger the normal stress, the smaller the thickness of the grease. Therefore, as long as the initial thickness of the grease is larger than 2 mm, there is a unique relationship between the final grease thickness and the normal stress. The relationship between the shear strength and the thickness of the grease is presented in Figure E.6b. Essentially the smaller the thickness, the higher the shear resistance.

E.1.3.4 Effects of Strain Rate

Two shear tests were conducted at the same normal stress but with different shearing speeds, 1 mm per hour and 2 mm per hour, with a grease thickness of 0.1 mm both before and after shear. The results, shown in Figures E.7a and E.7b, indicate that the shear resistance of the grease increases with rate

of displacement.

E.1.3.5 Conclusion

The direct shear tests on the grease show that the shear resistance is a function of the normal stress, the grease thickness and the rate of shearing. O'Neill (1985) concluded that the resistance is governed by the grease thickness rather than the normal stress, but the thickness of the grease can be related to the maximum applied normal stress, $\sigma_{n\text{-}max}$. Therefore, the grease resistance will be expressed as,

$$\text{Grease Resistance, } \tau_{grease} = 0.025(\sigma_{n\text{-}max}) \qquad \text{Eq. E.3}$$

E.1.4 Results of Calibration

From the calibration of the pistons and the grease friction tests, Equation E.1 can be rewritten as,

$$\tau = \frac{F_{piston}}{A_s} - \tau_{grease}$$

where A_s is the average contact area of the vertical faces of the test specimen.

Substituting Equations E.2 and E.3 into the above equation, gives,

$$\tau = \frac{14.134}{A_s}\sigma_{piston} - \frac{0.657}{A_s} - 0.025(\sigma_{n\text{-}max}) \qquad \text{Eq. E.4}$$

The first component of the equation presents the direct relationship

between the shear stress and the piston stress. The second and third components are the frictional losses due to the piston diaphragm and the grease resistance.

The results from Equation E.4 are compared with the results obtained by Rodriguez and Bekenstein in Figure E.8. The grease frictions for σ_n=0.25 ksc and σ_n=1.30 ksc are 0.007 ksc and 0.030 ksc respectively. The difference in results between the two methods is relatively small. Therefore, Equation E.4 is used as the calibration curve for the Directional Shear Cell tests on clay.

E.2 CALIBRATIONS OF THE INTERMEDIATE PRINCIPAL STRESS MEASURING DEVICE AND THE PRESSURE BAGS

E.2.1 Introduction

The pressure bags are used to apply the normal stresses to the soil sample. A method of calibration was carried out by Germaine (1982) using a load cell and a rigid platen, but the results were not very satisfactory due to the uncertainty in measuring the "effective area" of the pressure bag. Hence, the calibration done was performed by a different method.

The intermediate principal stress measuring device is a new component of the DSC, designed to measure the normal stress in the plane strain direction. The design of the device is described in Appendix D.4, and calibration is described below.

E.2.2 Experimental Setup

A simple way to calibrate both the pressure bags and the intermediate principal stress measuring device is shown in Figure E.9. The pressure bag is placed on top of the intermediate principal stress measuring device and held in place by the tie rods and restraining bars. A known pressure is applied to the pressure bag, and the position of the pressure bag is adjusted with the help of the

position sensor. The pressure in the intermediate principal stress measuring device is measured. The sensitivity of the position sensor is checked by adjusting the position of the pressure bag relative to the intermediate principal stress measuring device under a constant pressure. The bag is moved away from the measuring device by about 1 mm (no light will be shown in the panel) and moved 1 mm closer to the measuring device relative to the neutral position (green and red light will appear), with stress measured in both positions.

E.2.3 Experimental Results

The results of the calibration are plotted as shown in Figure E.10a. Linear regression is applied to the data points, which gives a slope of 1.007 and a goodness of fit equal to 0.99993. This result shows that the pressure in the bag is the same as the stress on the measuring device and indicates that the pressure in the pressure bag is the same as the normal stress applied to the sample.

Figure E.10b shows the variation in measured stress recorded on the intermediate principal stress measuring device due to the change in the positions of the pressure bag. For a 1 mm change in displacement of the pressure bag, the corresponding change in stress is only 0.007 ksc. The position sensor can control the position of the bag to ±0.5 mm. Thus the maximum error in applied normal stress is, in theory, at most 0.007 ksc with the help of the position sensor.

E.3 STRAIN MEASUREMENTS IN THE INTERMEDIATE PRINCIPAL STRESS DIRECTION

E.3.1 Introduction

When a DSC sample is subject to a change in the boundary stresses, there will be some axial strain in the intermediate principal stress (or plane strain) direction, even though the sample is restrained in this direction. The strain occurs

due to deflections (δ_p) on the platens, axial deformations (δ_r) of the rubber membrane, and the change in grease thicknesses (δ_g), due to the change in the stress. The axial strain, ϵ_2, can be expressed as,

$$\epsilon_2 = [\, f(\delta_p) + f(\delta_r) + f(\delta_g) \,] \,/\, H_s \qquad \text{Eq.E.5}$$

where H_s is the height of the soil sample.

Each of the above components can be determined theoretically or experimentally. The deformation of the rubber membrane can be estimated if the thickness of the membrane and its Young's modulus are known. The thickness of grease is related to the normal stress as described in Appendix E.1.3.2. The deflection of the platens can be measured experimentally. The following section describes the technique used to determine the axial strain due to three components as described above.

E.3.2 Axial Strain due to Deflection of the Top and Bottom Platens

The magnitude of the platen deflection in the plane strain direction is dependent on the vertical forces acting on the platens. These result both from the intermediate normal stress on the sample and the stresses in the pressure bags, since the top and bottom sides of the bags are in contact with the platens. Experiments were carried out to measure the axial strain due to the deflection of the top and bottom platens. The setup and results are discussed in the next section.

E.3.2.1 Experimental Setup

The setup of the experiment was the same as for DSC tests on dense Leighton Buzzard sand (Bekenstein,1980), but now the Directional Shear Cell has

the intermediate principal stress measuring device. Two displacement transducers are attached to the supporting frame of the DSC to independently measure the deflections of the centers of the platens, where the deflections are maximum, as shown in Figure E.11. Hydrostatic stresses ($\sigma_a=\sigma_b$) are applied to the sample, and the change in displacements and stress in the plane strain direction are recorded. The sample was loaded from 0 to 1.2 ksc with 1 minute intervals, then unloaded back to 0 ksc.

E.3.2.2 Experimental Results

Stress versus displacement is plotted for the top and bottom platens in Figures E.12 and E.13, respectively. As the hydrostatic stress increases, the stress in the plane strain direction increases too, and the platens move apart due to this change in stress. During unloading of the hydrostatic stress, the stress in the plane strain direction increases at first, then decreases with the hydrostatic stress. The results show that the magnitude of the separation of the platens depends both on the stresses in the pressure bags and the stress in the plane strain direction. This behavior is best expressed in terms of the resultant force acting on the platens. This resultant force, F_p, is defined as,

$$F_p = A_s \times \sigma_2 + 2 \times A_a \times \sigma_a + 2 \times A_b \times \sigma_b \qquad \text{Eq.E.6}$$

where

A_s is the cross–sectional area of the sample;

A_a is the area of the Pressure Bag A in contact with the platen;

A_a is the area of the Pressure Bag B in contact with the platen;

σ_2 is the measured stress acting in the plane strain direction;

σ_a is the stress on the Pressure Bag A; and

σ_b is the stress on the Pressure Bag B.

In most of the DSC tests, A_s is about 100 cm^2, and A_a and A_b are 13 cm^2; hence Equation E.6 can be rewritten as,

$$F_p = 100 \times \sigma_2 + 2 \times 13 \times \sigma_a + 2 \times 13 \times \sigma_b \text{ (kg)} \qquad \text{Eq.E.7}$$

where σ_2, σ_a and σ_b are in ksc.

A graph of force versus displacement is shown in Figure E.14 using Equation E.7. The relationship is almost linear in the range of interest for both platens. The results also indicate that the bottom platen is stiffer than the top platen. This is expected since the bottom platen is solid aluminum, whereas the center 6x6 inch portion of the top platen is glass with a thickness of 0.35 inches.

The experiment provides the relationship between the resultant force and the displacements at the centers of the platens, but the average axial strain of the sample due to the separation of the platens is unknown. There are two approaches to determine this average axial strain. One is to measure the displacements at different locations on the platens during testing so that a displacement profile can be plotted, and an average axial strain can be calculated. One of the problems is the top displacement transducer will be blocking the camera for horizontal strain measurement. Furthermore, more displacement transducers are needed if a displacement profile is required, which in turn makes the whole process impractical. The second approach is to use finite element analysis to predict the strain profile, which is much simpler than the other method.

E.3.2.3 Finite Element Analysis

A finite element analysis was used to model the deflections of the platens

under varying loading conditions. The geometry of the actual platen is quite complex, there are slots and joints in each platen which makes modeling very difficult. Therefore, some assumptions were made to simplify the problem. The problem is treated as a simply supported beam instead of a plate. This representation and associated input parameters are shown in Figure E.15.

The computed deflection at the center of the platen (δ_{center}) is compared with the experimental results in Figure E.14. They agree relatively well except for the bottom platen, where the difference between the experimental and predicted results is 60%. This level of error, given the assumptions, is reasonable. Since the analysis also gives the displacement profile, the average axial strain of the soil sample can be determined. Figure E.15b shows the profile of the relative displacement along the soil sample. The average displacement of the soil sample, δ_{ave}, is found to be,

$$\delta_{ave} = 0.92\ \delta_{center} \qquad \text{Eq.E.8}$$

Since δ_{center} is a function of the resultant force, the average strain of the soil sample can then be determined.

The average axial strain, ϵ_{2p}, due to the platen separation is,

$$\epsilon_{2p} = 0.92 \times \frac{\left(\delta^{top}_{center} + \delta^{bottom}_{center} \right)}{H_s} \qquad \text{Eq.E.9}$$

where

δ^{top}_{center} is the deflection at the center of the top platen;

δ^{bottom}_{center} is the deflection at the center of the bottom platen; and

H_s is the height of the soil sample.

The deflections at the centers of the platens can be determined based on the three known normal stresses (σ_a, σ_b and σ_2) by using Equation E.7 and the experimental results in Figure E.14. The axial strain due to the platen separation can be estimated from Equation E.4.

E.3.3 Strains due to the Deformation of the Rubber Membrane

E.3.3.1 Introduction

As the stress in the plane strain direction changes, the top and bottom portions of the rubber membrane between the soil sample and the platens are undergoing some deformation. There is some axial strain in the plane strain direction as well as radial strain in the orthogonal direction. The axial strain is attributed to the overall strain in the plane strain direction. The radial strain on the top portion of the membrane distorts the strain measurement of the soil in the orthogonal direction. Therefore, corrections on the photography strain measurement are made in regard to this radial strain.

E.3.3.2 Experimental Setup

The procedure for determining the Young's modulus (E_r) of the rubber membrane is described in Bishop and Henkel (1957). A cylindrical white rubber membrane was made with 0.2 mm thickness, and prepared for testing as shown in Figure E.16. The rubber membrane was loaded to an axial strain of about 1 ksc and the axial strain was measured.

E.3.3.3 Experimental Results

The Young's modulus, E_r, of the rubber is compared with the published data from O'Neill (1985) and Bishop & Henkel. The results are plotted in Figure

E.17. From this relationship, the axial strain (ϵ_{2r}) of the sample in the DSC due to the deformation of rubber membrane can be estimated if the initial thickness of rubber membrane (t_r) is known, with the equation:

$$\epsilon_{2r} = \frac{2 \text{ x } \sigma_2 \text{ x } t_r}{E_r \text{ x } H_s} \qquad \text{Eq. E.10}$$

where

σ_2 is the axial stress in the plane strain direction; and

H_s is the height of the soil sample.

The radial strain (ϵ_r) of the rubber membrane can be calculated based on a Poisson ratio of 0.5, and is given by:

$$\epsilon_r = -0.5 \frac{\sigma_2}{E_r} \qquad \text{Eq. E.11}$$

Figure E.18 shows the relationship between the axial stress and the radial strain.

E.3.3.4 Discussion

The Young's modulus of the rubber membrane depends on the duration of curing and the conditions of testing, for example, the wetness of the rubber membrane. There is also some uncertainty in measuring the thickness of the rubber cylinder during the test.

In the DSC test, the inner surface of the rubber membrane is coated with a layer of sand. These sand particles are eventually embedded in the top surface of the clay sample. This restricts the movement of the rubber membrane laterally, and reduces the radial strain of the rubber membrane in the DSC test compared to

the value calculated from Equation E.11. This makes the radial strain correction more complicated.

E.3.4 Conclusion

The axial strain in the plane strain given in Equation E.5 can also be expressed as,

$$\epsilon_2 = [\, f(\delta_p) + f(\delta_r) + f(\delta_g)] \,/\, H_s \qquad \text{Eq. E.5}$$

$$\epsilon_2 = \epsilon_{2p} + \epsilon_{2r} + \epsilon_{2g} \qquad \text{Eq. E.12}$$

The magnitudes of ϵ_{2g} and ϵ_{2p} are determined from the Figures E.6 and E.14, respectively. The value of ϵ_{2r} is given by Equation E.10, with an average value of E_r of 13 ksc.

E.4 CLAY–RUBBER MEMBRANE INTERFACE TESTS

E.4.1 Introduction

During the evaluation of the previous DSC tests by Germaine (1982) and the first few tests in this research that used shear sheets, boundary failures occurred due to the surface traction applied by the shear sheets. This led to an investigation of boundary interface between the clay sample and the rubber membrane as described in this section.

E.4.2 Experimental Setup

The arrangement of the interface test is shown in Figure E.19. A 4"x4" resedimented Boston Blue Clay sample (σ'_p = 1 ksc, σ'_{vc} = 0.25 ksc) with 0.7" thickness was placed on a coarse porous stone in a wooden frame. A sand–coated rubber membrane was placed on the top surface of the clay sample. A

displacement transducer was connected to the non–stressed end of the rubber sheet by means of a string to measure horizontal displacement. The shear sheet and pressure bag rest on top of the rubber membrane, and the pressure bag is held in place by restraining bars and tie rods.

The sample was subjected to both normal and shear stresses. The stress path used is similar to one of the DSC tests at δ=30°. This stress path and the relationship of the stress ratio to the horizontal displacement on the top of the soil sample is shown in Figure E.20.

E.4.3 Experimental Results

Three interface tests were conducted with different conditions. In Test No.1, the rubber membrane was coated with a layer of No. 40–50 mesh sand using the technique described by Germaine (1982). The clay sample was sheared at 3 minute stress intervals until boundary failure occurred. When the apparatus was disassembled, it was found that the sand particles on the rubber sheet were torn from the sheet during shearing indicating a sand bonding problem. To improve the bonding between the rubber membrane and the sand particles, an extra layer of rubber cement was coated on the rubber membrane after the sand particles are glued in place. Furthermore, the size of the sand particles are larger than previous tests in order to increase the traction further. The new coating was used in Test Nos. 2 and 3. The results were remarkably different. There was no slippage at the sand–rubber boundary, and the samples failed by shear with about 5 mm of shear zone in the region next to the rubber membrane. The maximum obliquity angles also increased to a value closer to the friction angle of the clay.

E.4.4 Summary

The new technique for bonding sand particles to the sample rubber

membrane improves the interface conditions and therefore reduces the likelihood of boundary failures. The size of the sand particles used was somewhat arbitrary. The particle size should not be so large as to cause excessive disturbance of the clay boundary, nor be so small that the roughness of the coating will be reduced below that necessary for good sand–clay adhesion. By trial and error, the sand particle size between 425μm and 600μm (Sieve No.30–40) was found to give satisfactory results; hence, this size range was chosen for DSC testing for this research.

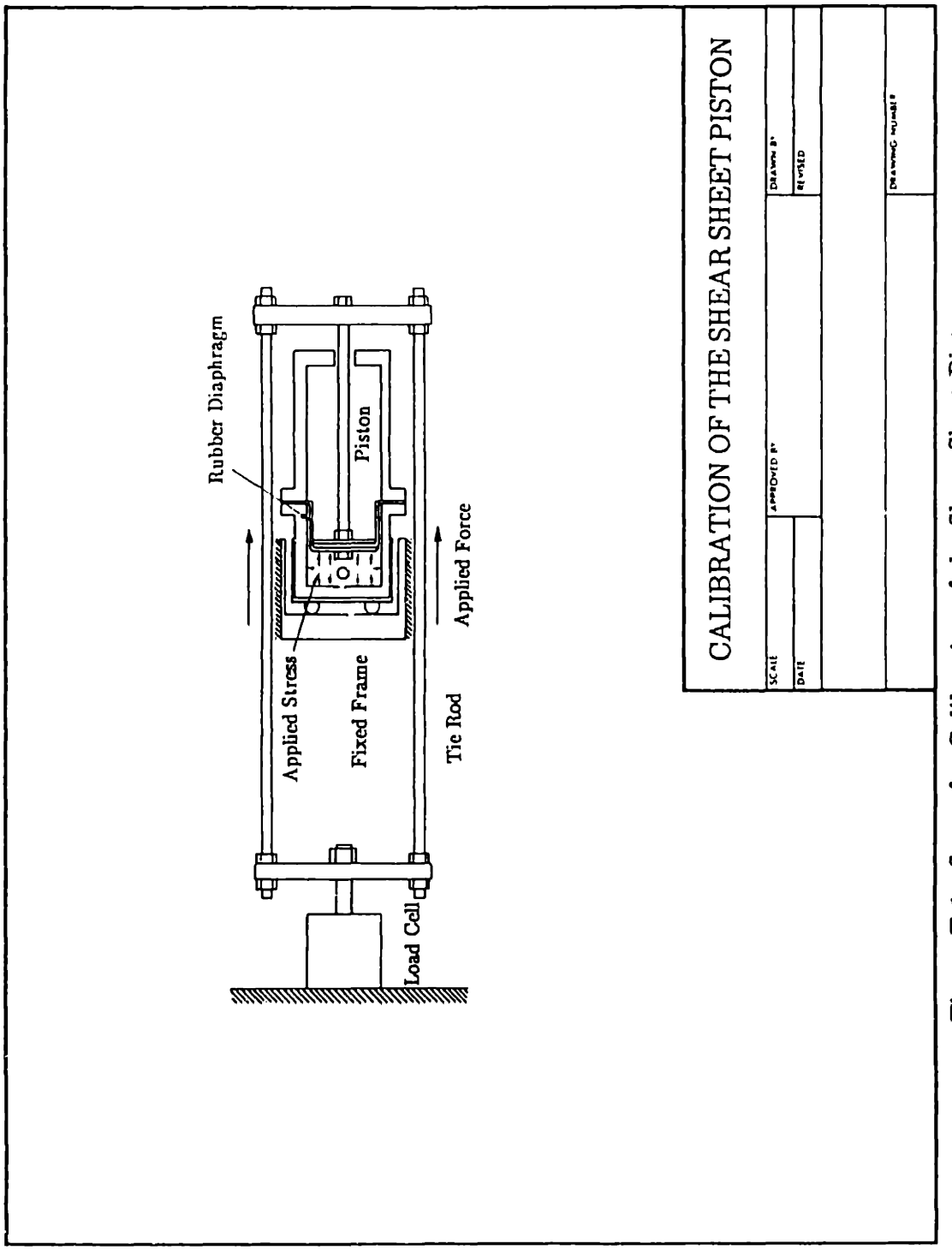

Figure E.1: Setup for Calibration of the Shear Sheet Piston.

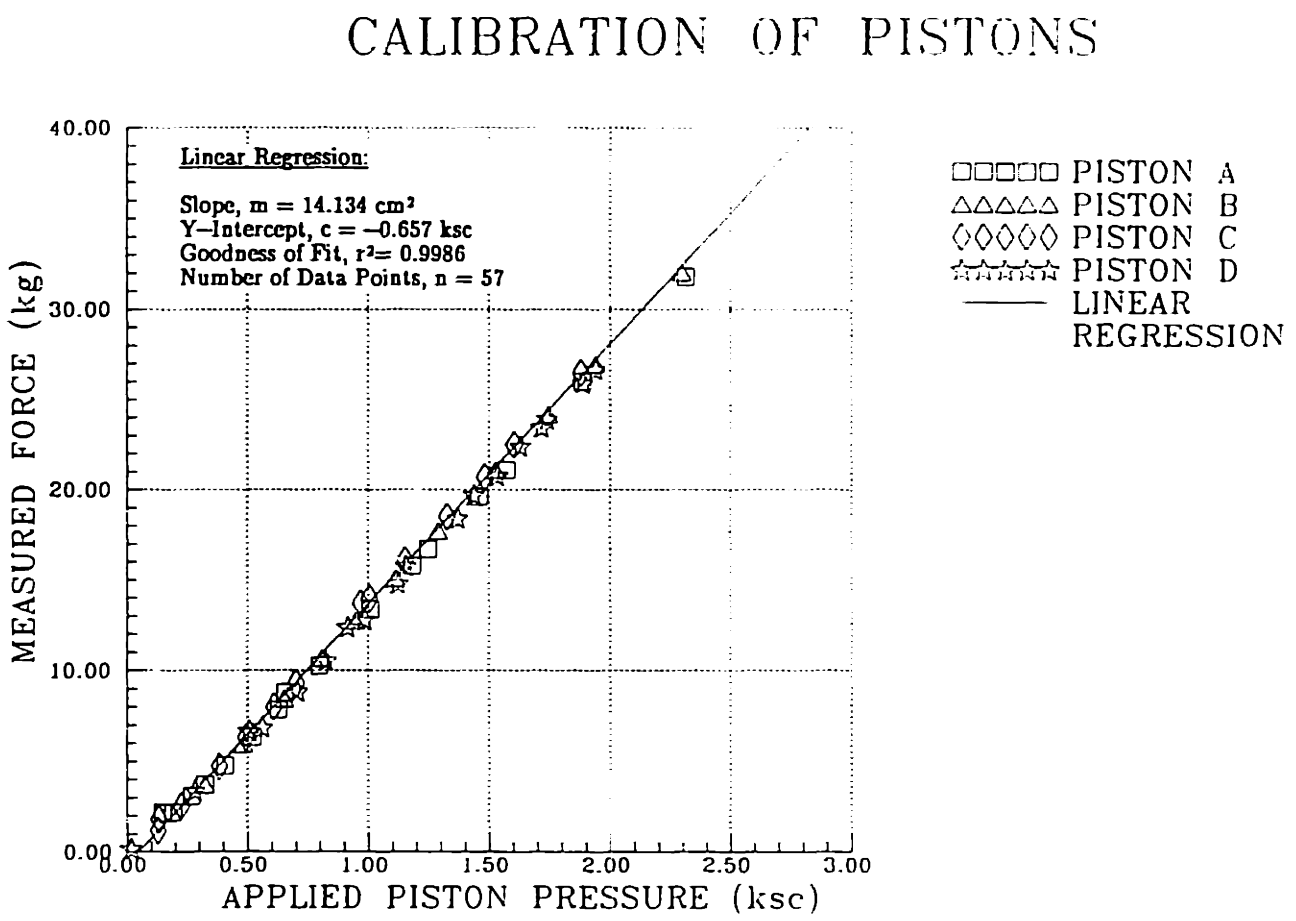

Figure E.2: Calibration Curve of the Shear Piston.

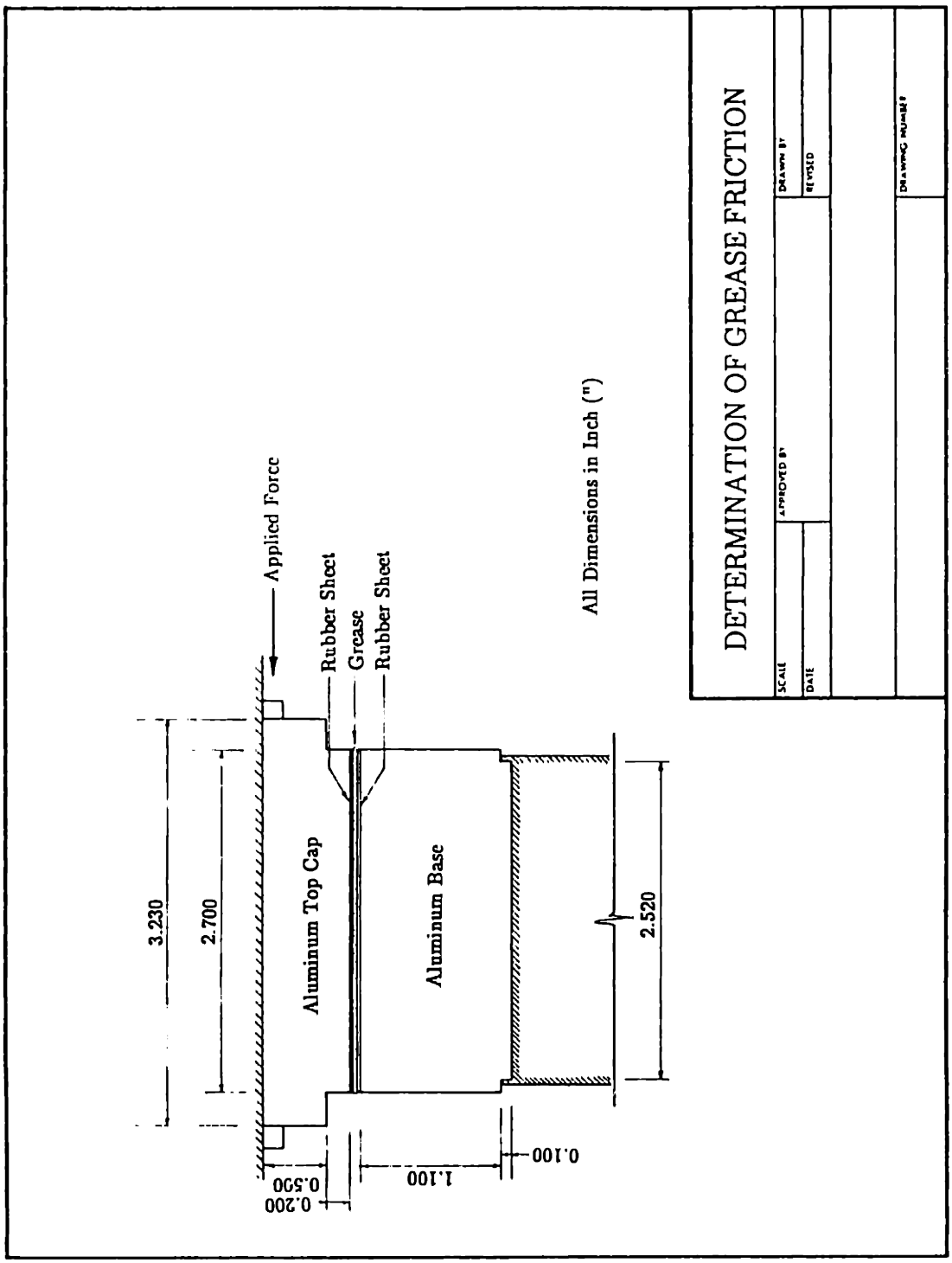

Figure E.3: Setup for Determination of the Grease Friction.

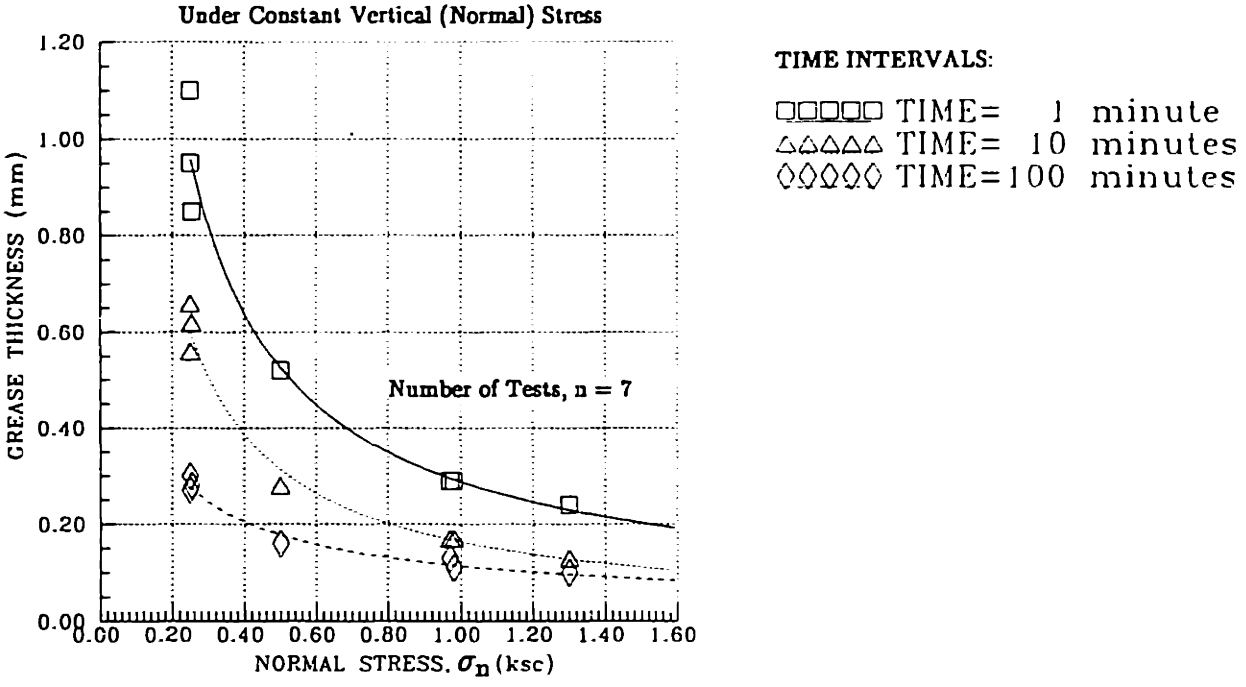

Figure E.4: "Squeezing" Curves of Silicone Grease.

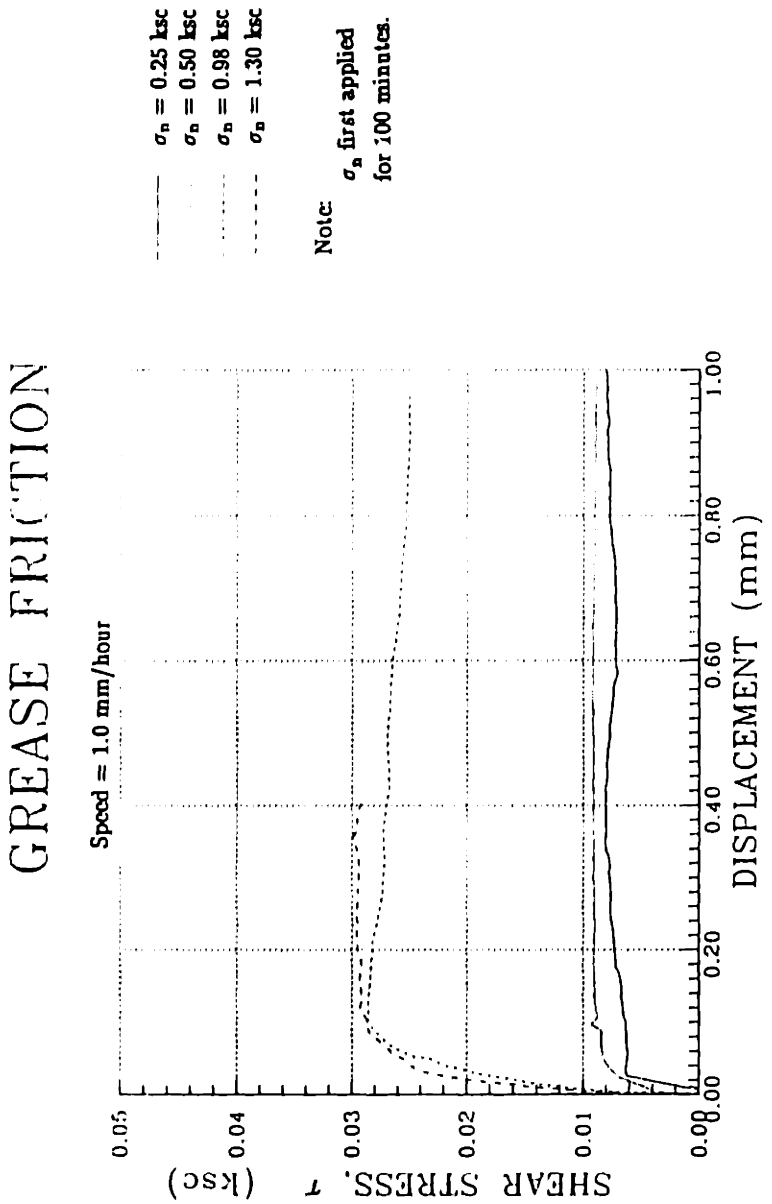

Figure E.5: Shear Stress versus Horizontal Displacement for the Grease Tests.

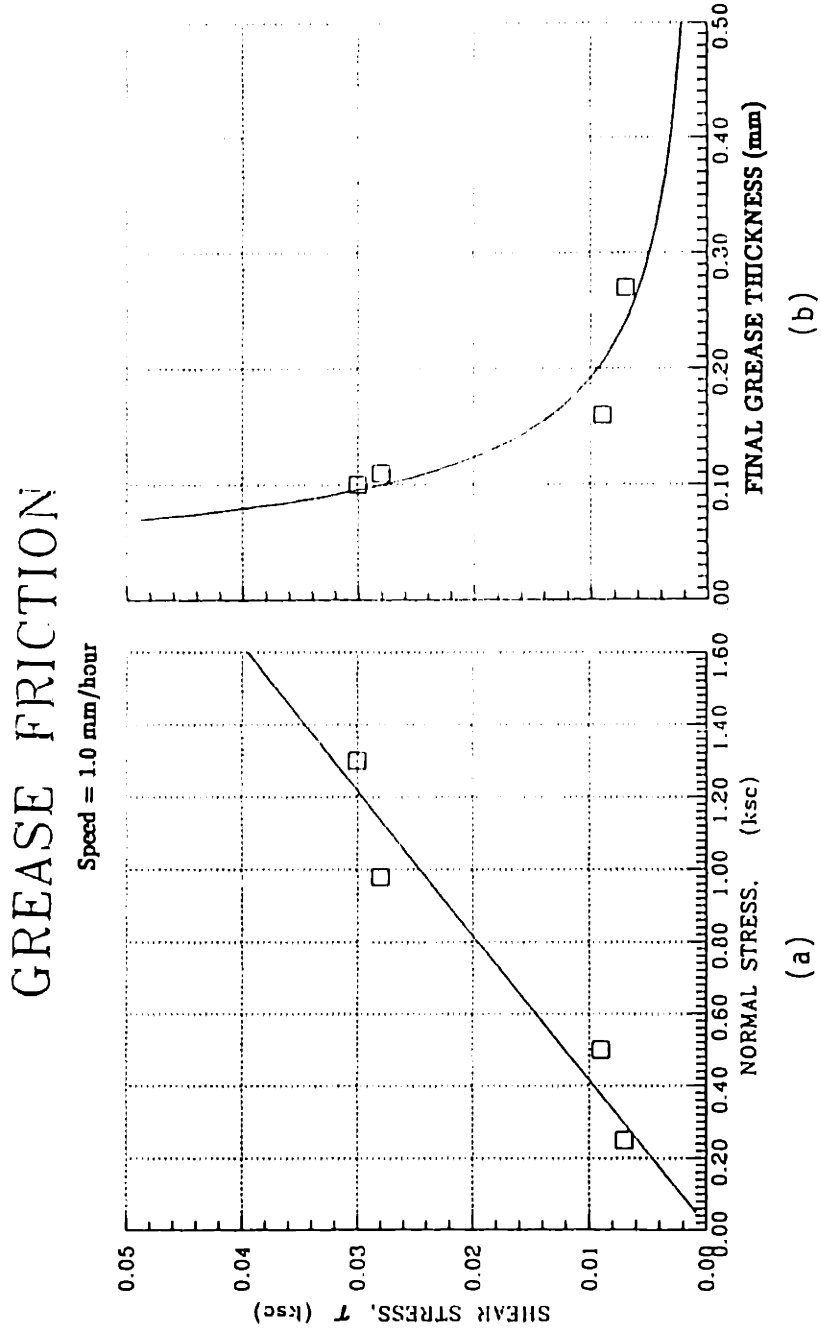

Figure E.6: Generalized Behavior of the Silicone Grease.

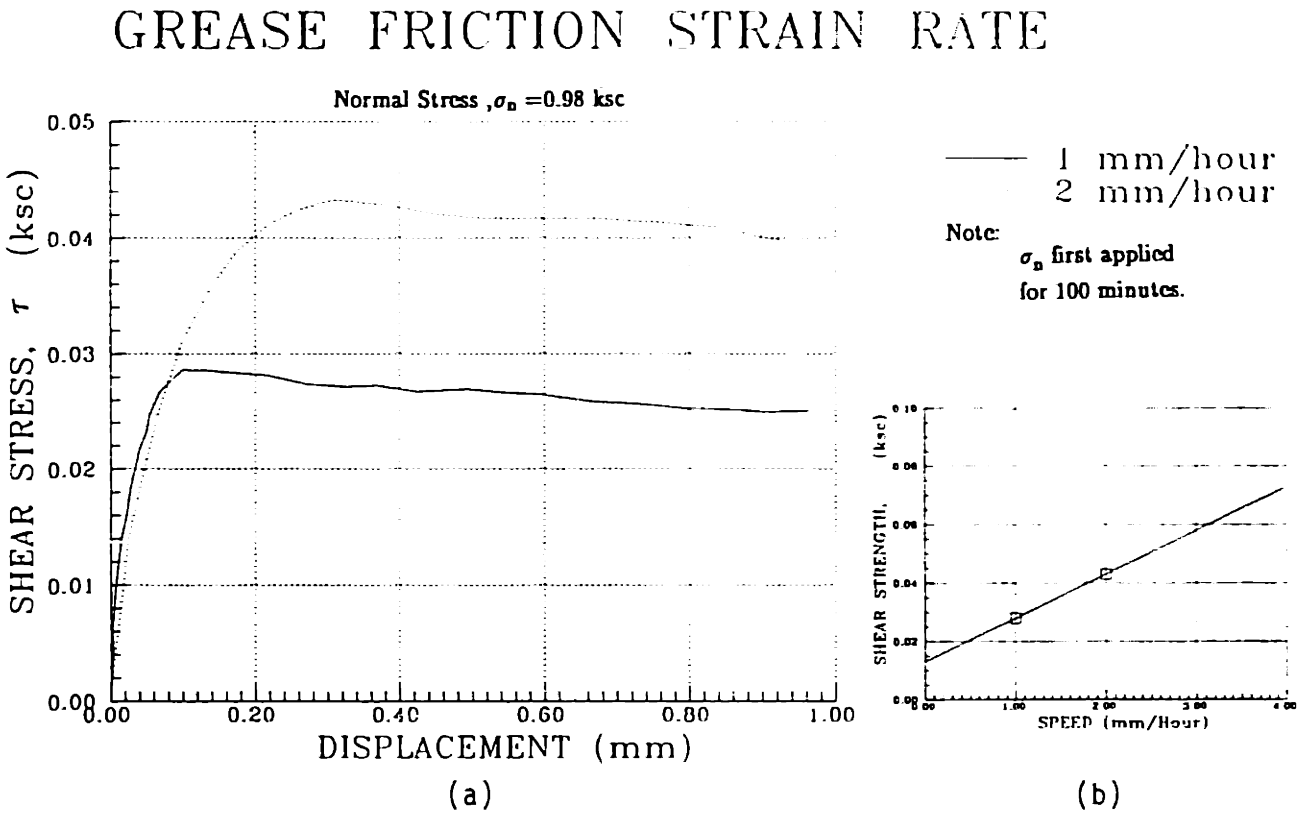

Figure E.7: Rate Effects on the Silicone Grease.

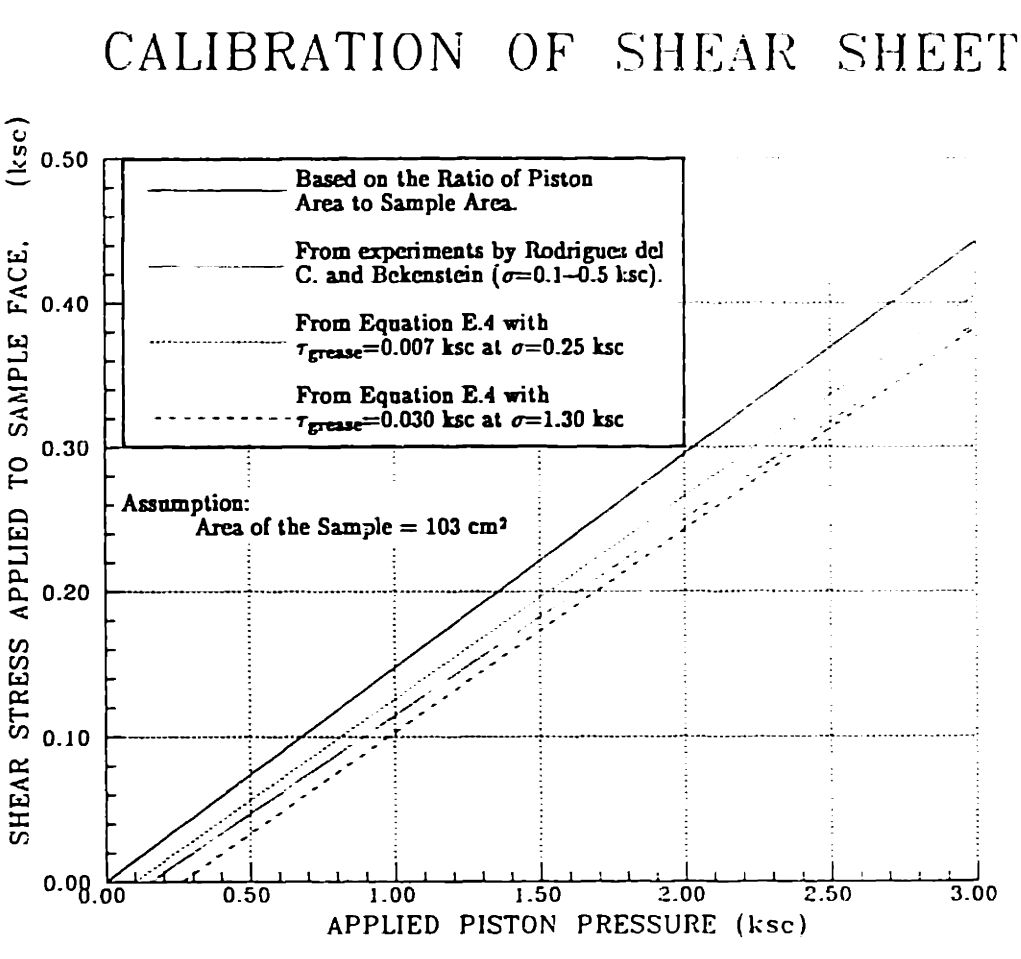

Figure E.8: Different Calibration Curves for the Shear Sheet.

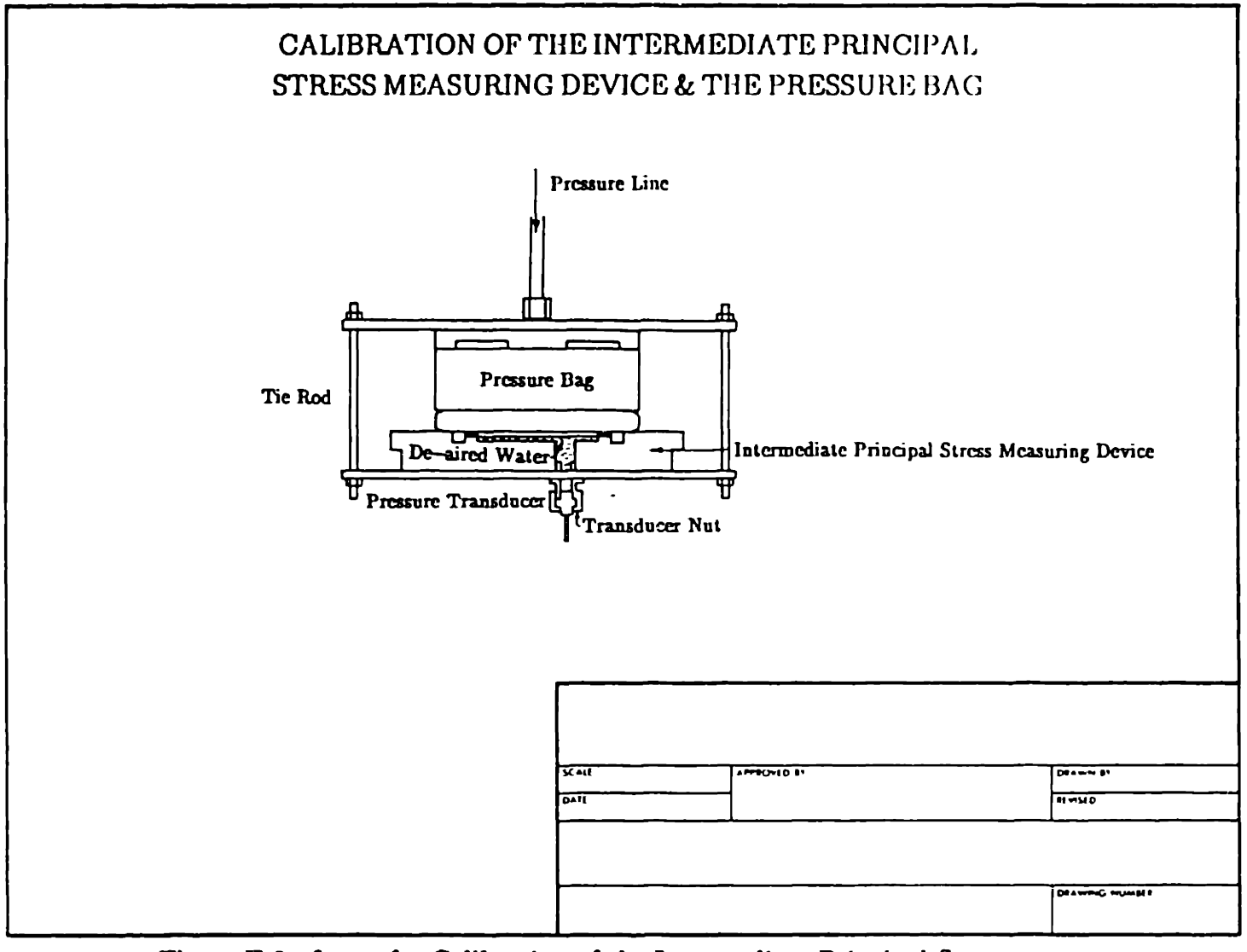

Figure E.9: Setup for Calibration of the Intermediate Principal Stress Measuring Device and the Pressure Bag.

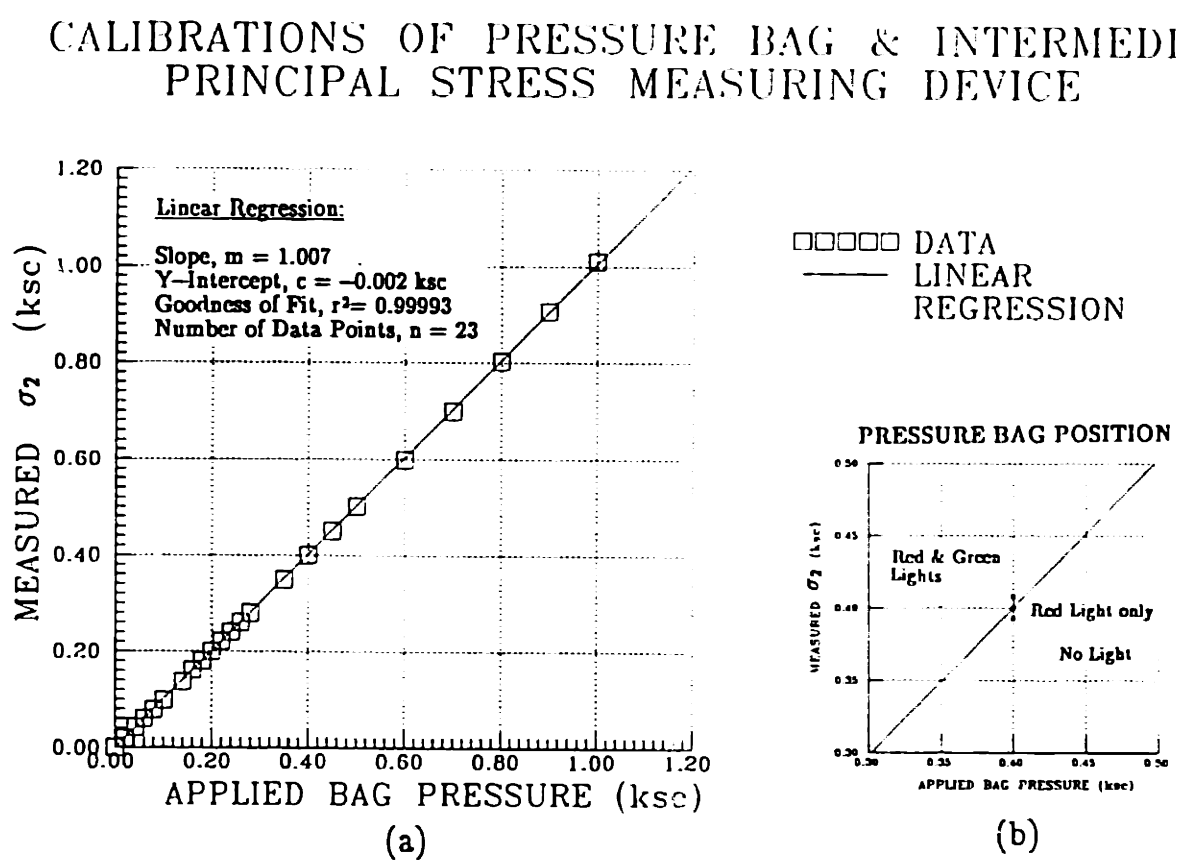

Figure E.10: Calibration of the Pressure Bag and the Intermediate Principal Stress Measuring Device.

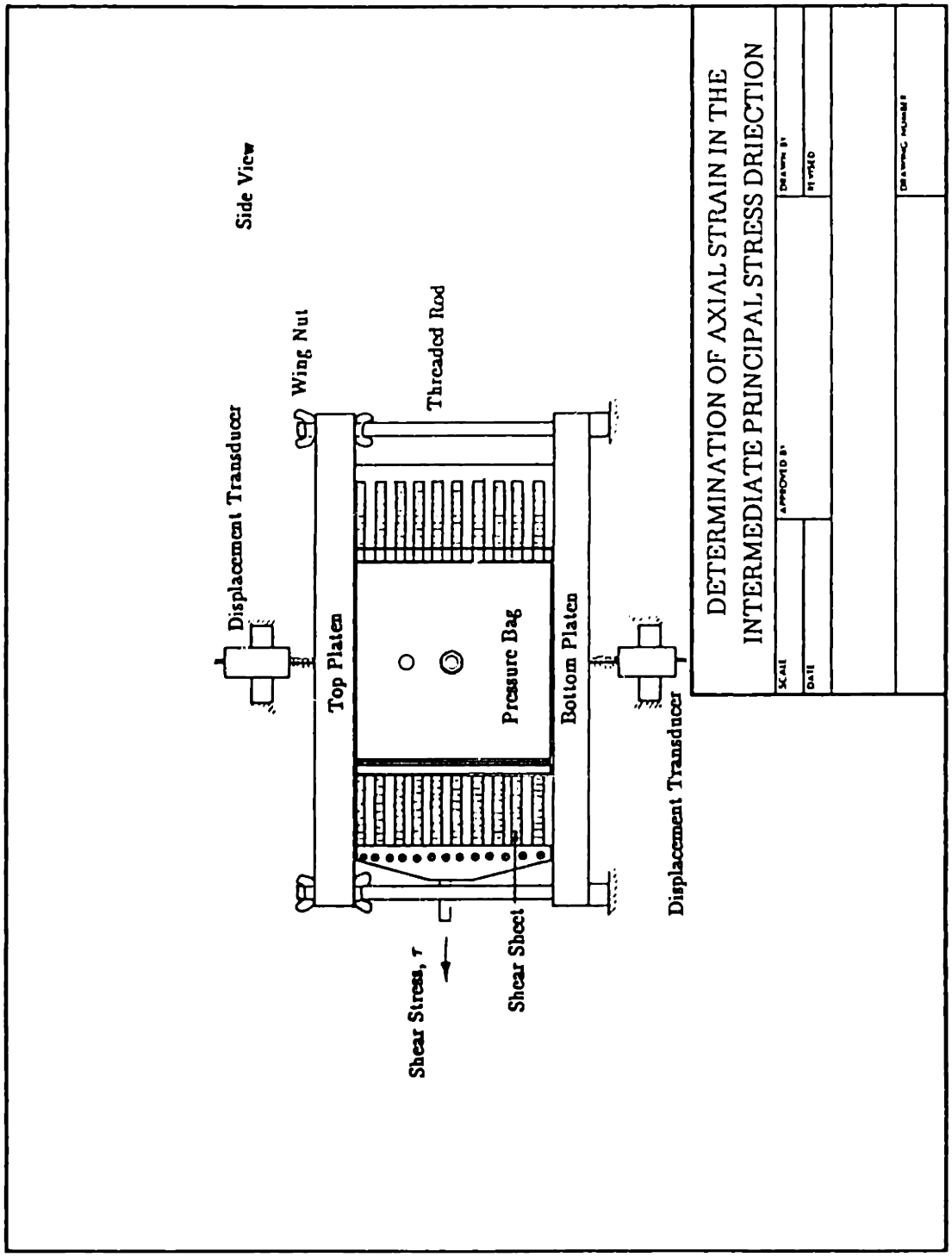

Figure E.11: Setup for Determination of the Axial Strain in the Intermediate Principal Stress Direction.

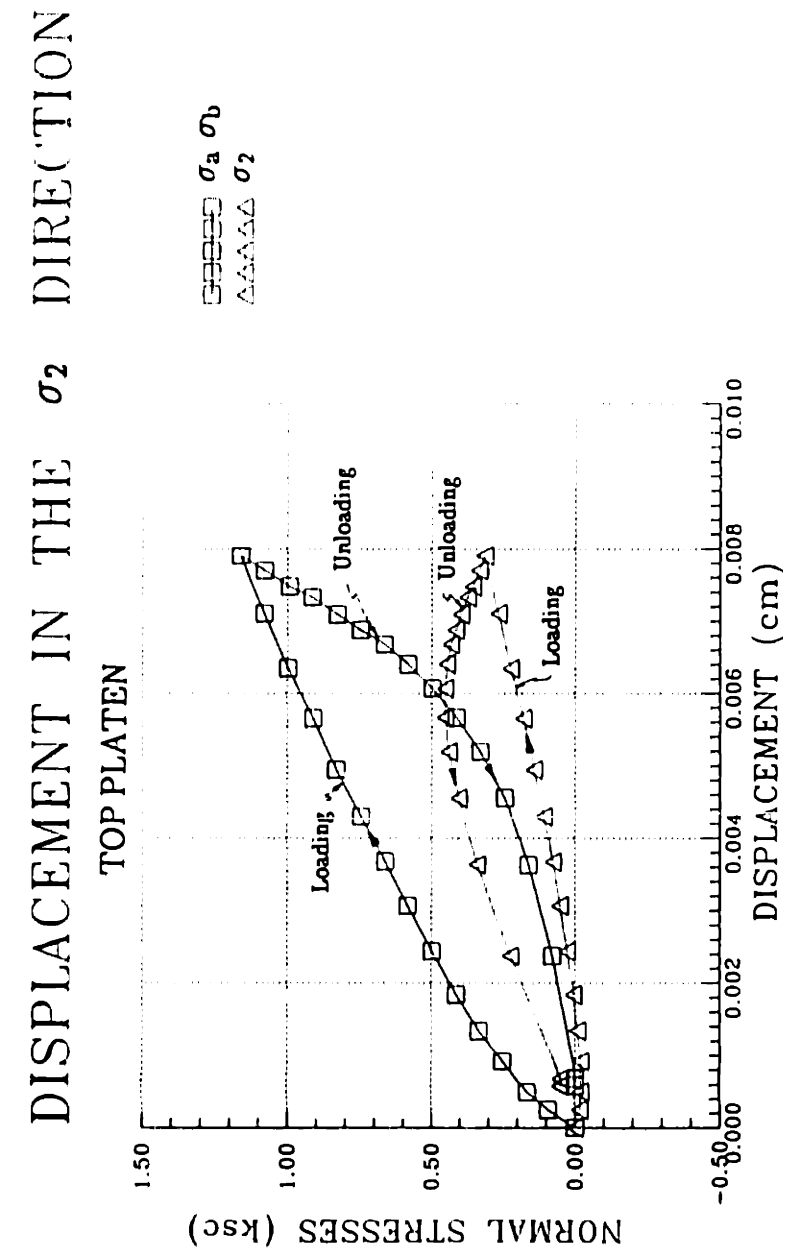

Figure E.12: Normal Stresses versus Displacement of the Top Platen.

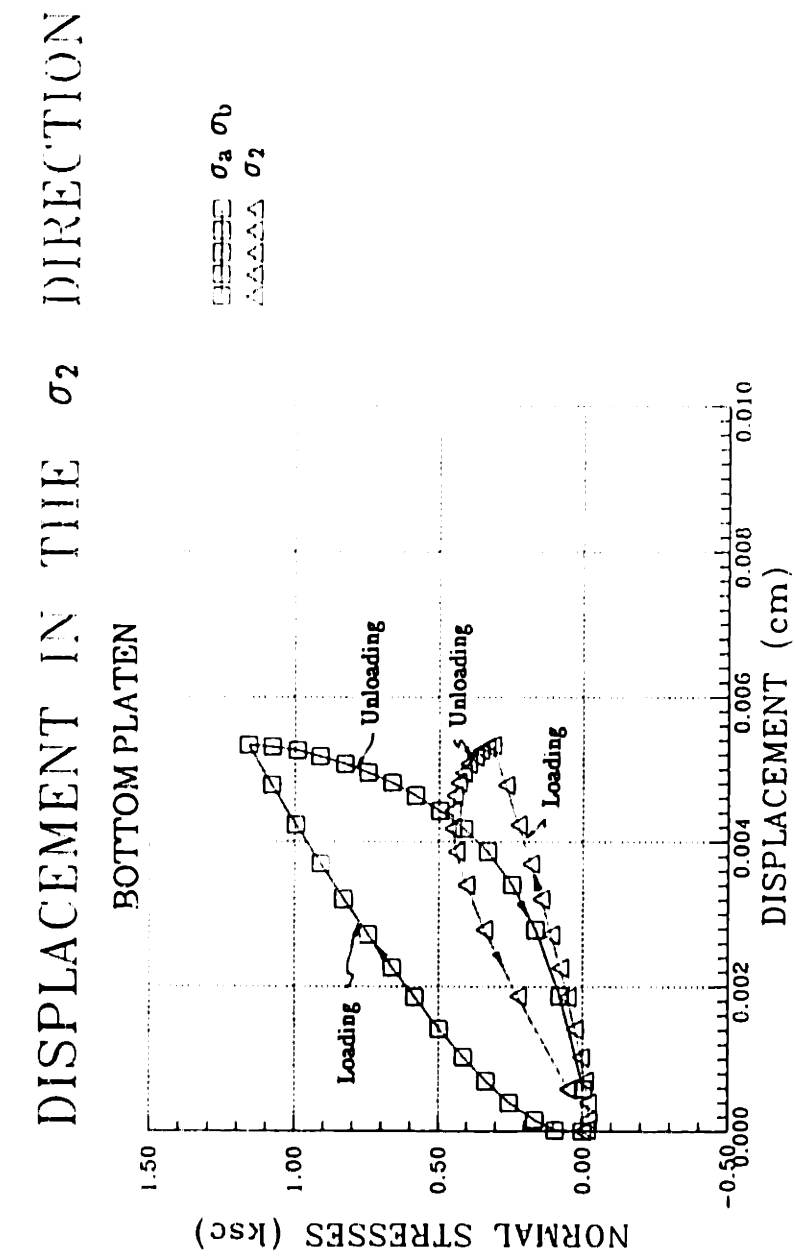

Figure E.13: Normal Stresses versus Displacement of the Bottom Platen.

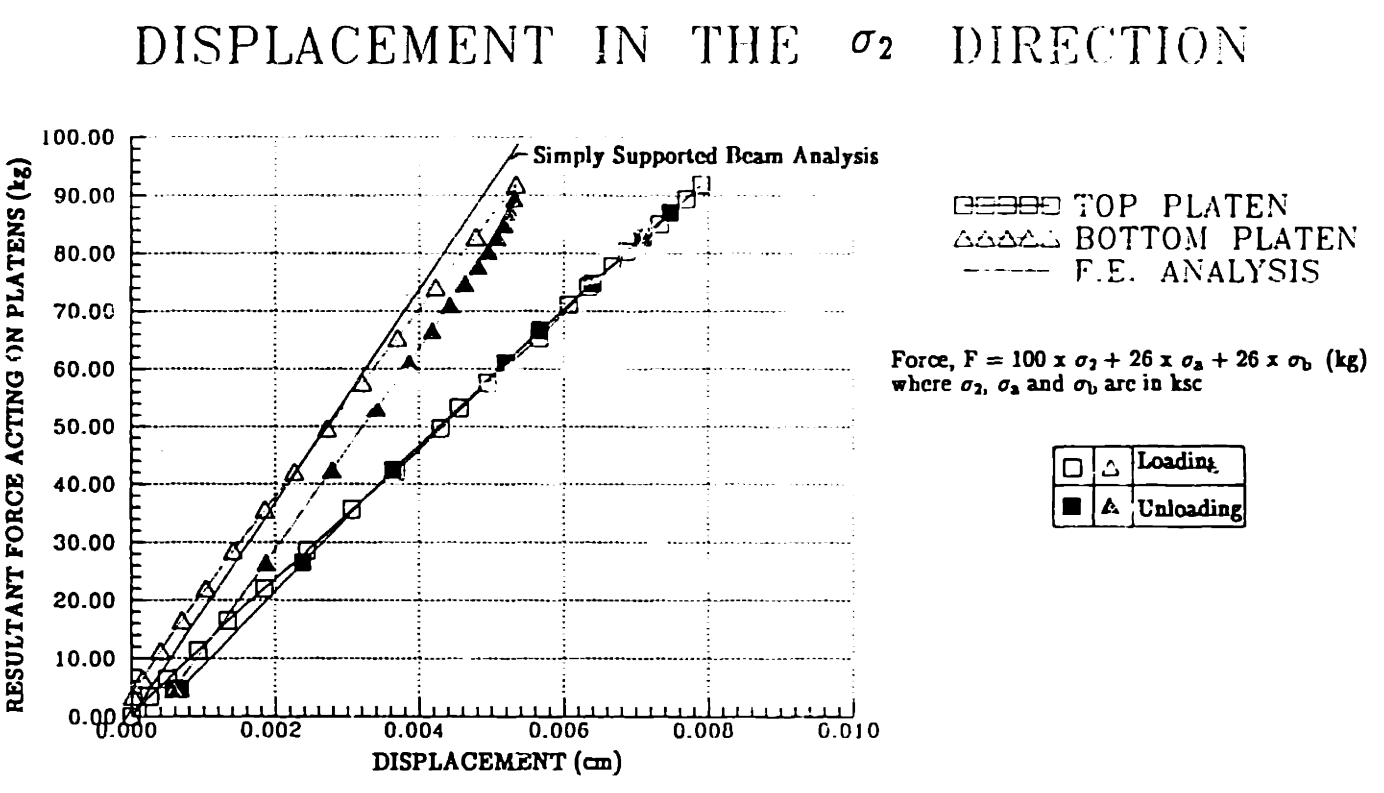

Figure E.14: Resultant Force versus Displacements at the Center of the Top and Bottom Platens.

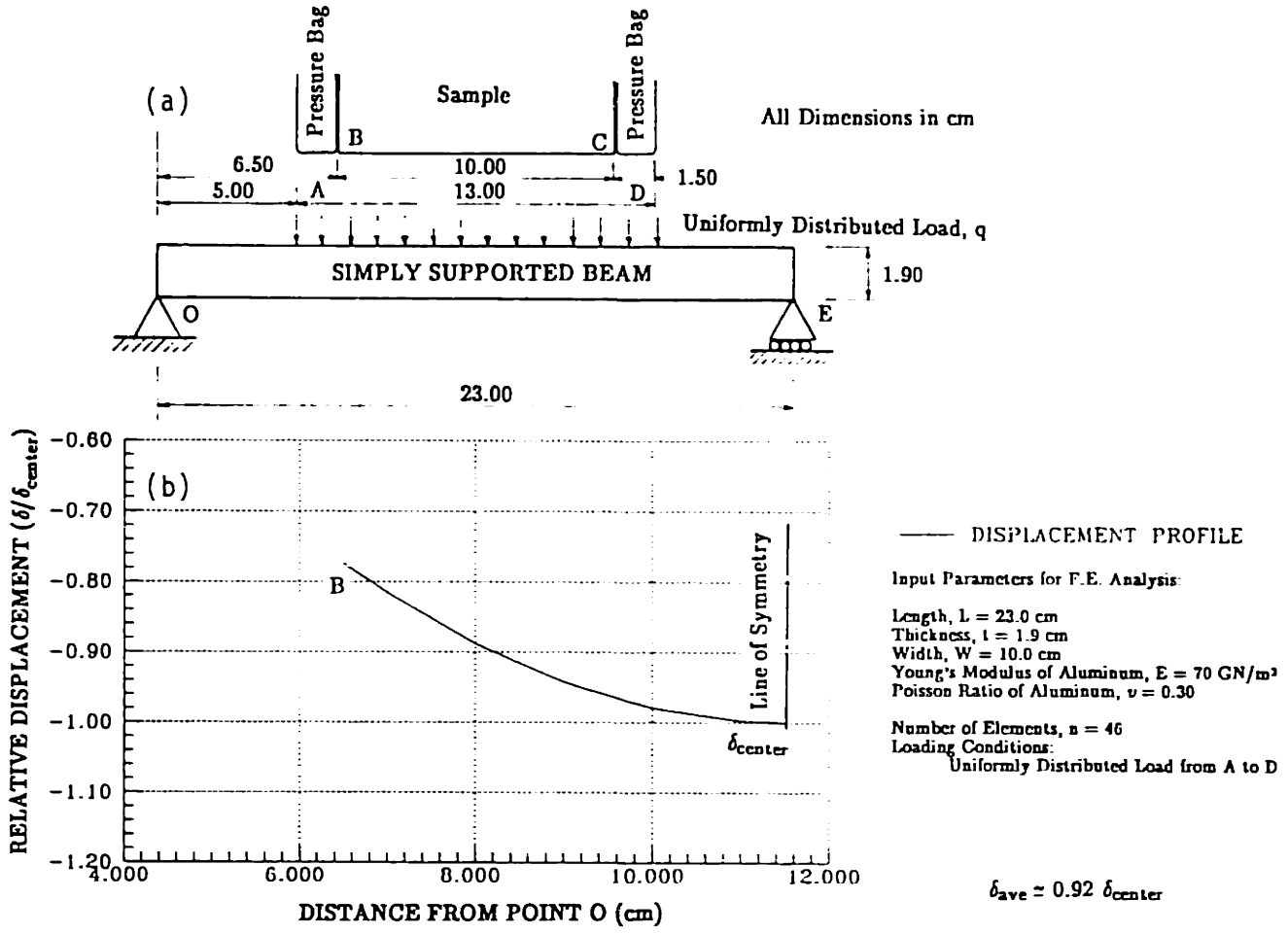

Figure E.15: Finite Element Analysis on Simply Supported Beam.

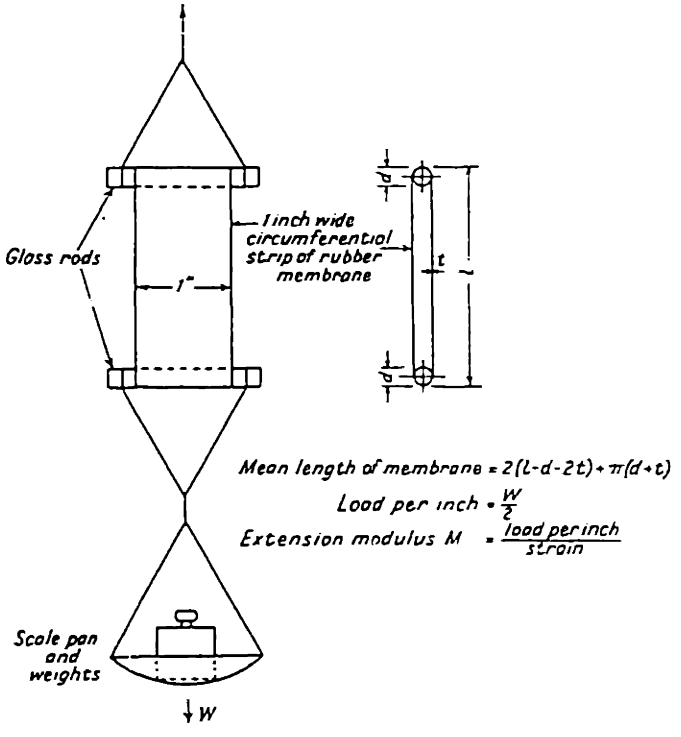

Figure E.16: Setup for Determining Young's Modulus of Rubber (from Bishop and Henkel, 1957).

AXIAL STRESS VERSUS AXIAL STRAIN
RUBBER

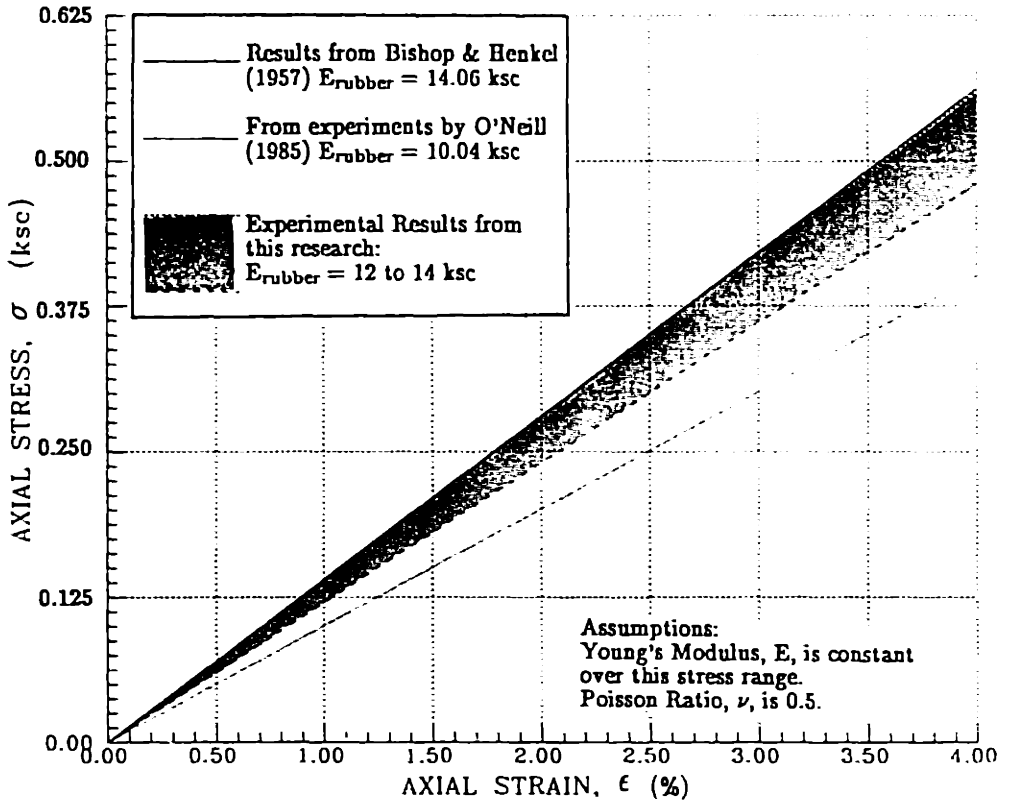

Figure E.17: Axial Stress versus Axial Strain for Rubber.

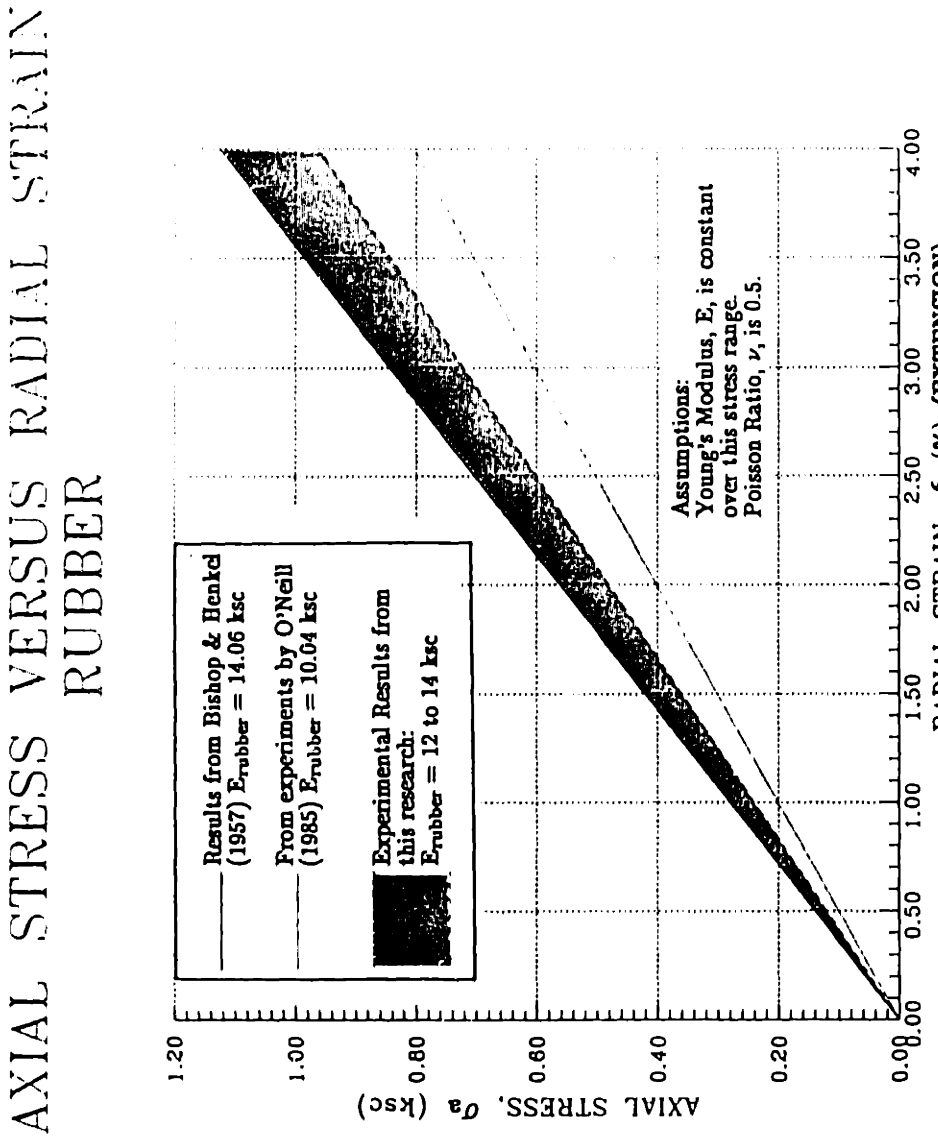

Figure E.18: Axial Stress versus Radial Strain for Rubber.

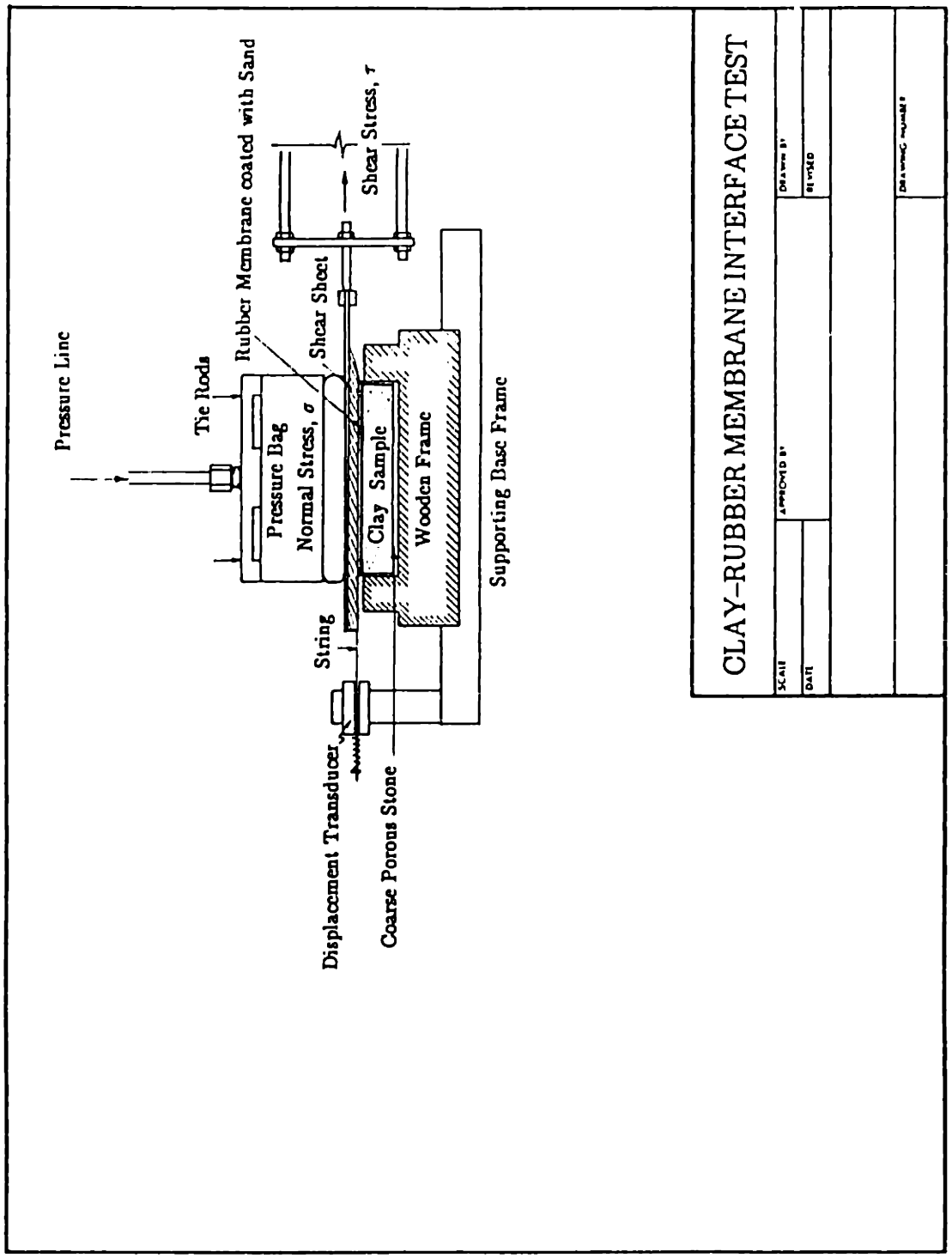

Figure E.19: Setup for the Clay–Rubber Membrane Interface Test.

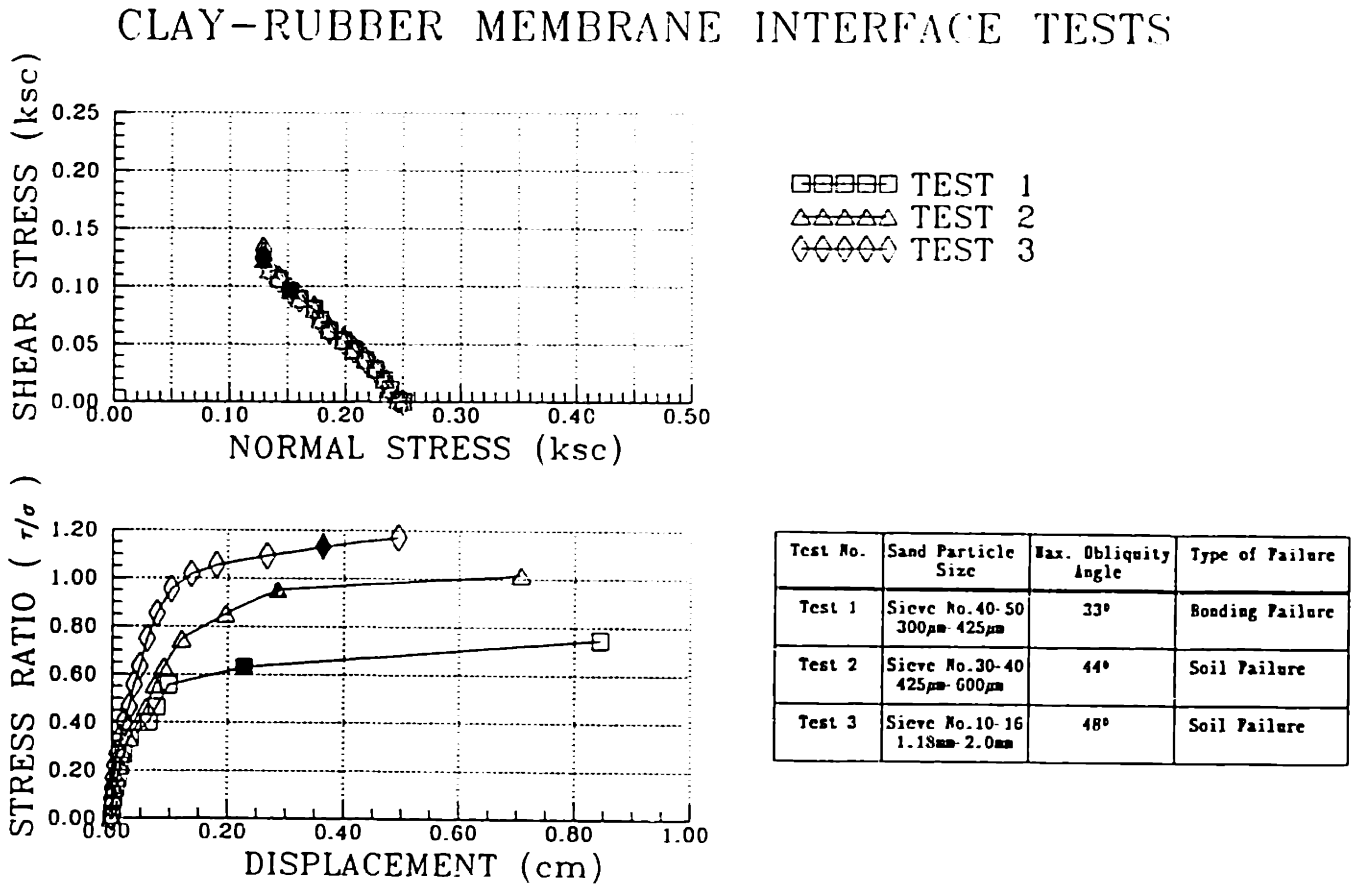

Test No.	Sand Particle Size	Max. Obliquity Angle	Type of Failure
Test 1	Sieve No.40-50 300μm-425μm	33°	Bonding Failure
Test 2	Sieve No.30-40 425μm-600μm	44°	Soil Failure
Test 3	Sieve No.10-16 1.18mm-2.0mm	48°	Soil Failure

Figure E.20: Results of the Clay–Rubber Membrane Interface Tests.

APPENDIX F

CONSOLIDATION AND UNDRAINED SHEAR DATA FROM DSC TESTS ON RUBBER FOAM AND BBC

F.1 RESULTS OF DSC TESTS ON RUBBER FOAM

This section contains:

- Computer printouts of stress data for DSC tests on rubber foam.
- Computer printouts of strain data for DSC tests on rubber foam.
- Plots of results from DSC tests on rubber foam.

RUBBER2

FILM No.	DELTA deg	ALFA deg	P ksc	Q ksc	P' ksc	U ksc	Sig.a mV	Sig.b mV	T a mV	T b mV	U mV	Sig.a ksc	Sig.b ksc	T a ksc	T b ksc	Input V Volts
0	0.000	0.000	0.000	0.000	0.000	0.000	0.890	0.380	-0.354	-0.352	0.000	0.000	0.000	0.000	0.000	0.000
1	-0.177	-0.091	0.199	0.002	0.199	0.000	5.730	5.300	0.000	0.000	0.000	0.201	0.197	-0.000	-0.000	10.000
2	-0.034	-0.018	0.200	0.010	0.200	0.000	5.950	5.130	0.000	0.000	0.000	0.210	0.190	-0.000	-0.000	10.000
3	-0.017	-0.009	0.200	0.020	0.200	0.000	6.200	4.890	0.000	0.000	0.000	0.220	0.180	-0.000	-0.000	10.000
4	-0.011	-0.006	0.200	0.030	0.200	0.000	6.440	4.620	0.000	0.000	0.000	0.230	0.170	-0.000	-0.000	10.000
5	-0.008	-0.004	0.200	0.040	0.200	0.000	6.670	4.370	0.000	0.000	0.000	0.240	0.160	-0.000	-0.000	10.000
6	-0.007	-0.003	0.200	0.050	0.200	0.000	6.910	4.120	0.000	0.000	0.000	0.250	0.150	-0.000	-0.000	10.000
7	-0.006	-0.003	0.200	0.060	0.200	0.000	7.150	3.880	0.000	0.000	0.000	0.260	0.140	-0.000	-0.000	10.000
8	-0.005	-0.002	0.200	0.070	0.200	0.000	7.390	3.630	0.000	0.000	0.000	0.270	0.130	-0.000	-0.000	10.000
9	-0.004	-0.002	0.200	0.080	0.200	0.000	7.630	3.380	0.000	0.000	0.000	0.280	0.120	-0.000	-0.000	10.000
10	-0.004	-0.002	0.200	0.090	0.200	0.000	7.880	3.130	0.000	0.000	0.000	0.290	0.110	-0.000	-0.000	10.000
11	-0.003	-0.002	0.200	0.100	0.200	0.000	8.120	2.880	0.000	0.000	0.000	0.300	0.100	-0.000	-0.000	10.000
12	-0.161	-0.082	0.199	0.002	0.199	0.000	5.730	5.290	0.000	0.000	0.000	0.201	0.196	-0.000	-0.000	10.000

RUBBER3

FILM No.	DELTA deg	ALFA deg	P ksc	Q ksc	P' ksc	U ksc	Sig.a mV	Sig.b mV	T a mV	T b mV	U mV	Sig.a ksc	Sig.b ksc	T a ksc	T b ksc	Input V Volts
0	90.000	0.000	0.000	0.000	0.000	0.000	0.890	0.380	-0.354	-0.352	0.000	0.000	0.000	0.000	0.000	0.000
1	-0.200	-0.102	0.198	0.002	0.198	0.000	5.710	5.290	0.000	0.000	0.000	0.200	0.196	-0.000	-0.000	10.000
2	0.034	0.018	0.200	0.010	0.200	0.000	5.480	5.630	0.000	0.000	0.000	0.190	0.210	-0.000	-0.000	10.000
3	0.017	0.009	0.200	0.020	0.200	0.000	5.240	5.880	0.000	0.000	0.000	0.180	0.220	-0.000	-0.000	10.000
4	0.011	0.006	0.200	0.030	0.200	0.000	4.990	6.130	0.000	0.000	0.000	0.170	0.230	-0.000	-0.000	10.000
5	0.008	0.004	0.200	0.040	0.200	0.000	4.750	6.390	0.000	0.000	0.000	0.160	0.241	-0.000	-0.000	10.000
6	0.007	0.003	0.200	0.050	0.200	0.000	4.510	6.640	0.000	0.000	0.000	0.150	0.251	-0.000	-0.000	10.000
7	0.006	0.003	0.200	0.060	0.200	0.000	4.270	6.880	0.000	0.000	0.000	0.140	0.260	-0.000	-0.000	10.000
8	0.005	0.002	0.200	0.070	0.200	0.000	4.020	7.130	0.000	0.000	0.000	0.130	0.270	-0.000	-0.000	10.000
9	0.004	0.002	0.200	0.081	0.200	0.000	3.760	7.390	0.000	0.000	0.000	0.119	0.281	-0.000	-0.000	10.000
10	0.004	0.002	0.200	0.090	0.200	0.000	3.550	7.640	0.000	0.000	0.000	0.110	0.291	-0.000	-0.000	10.000
11	0.003	0.002	0.200	0.100	0.200	0.000	3.310	7.880	0.000	0.000	0.000	0.100	0.300	-0.000	-0.000	10.000
12	-0.199	-0.102	0.199	0.002	0.199	0.000	5.720	5.300	0.000	0.000	0.000	0.200	0.197	-0.000	-0.000	10.000

RUBBER4

FILM No.	DELTA deg	ALFA deg	P ksc	Q ksc	P' ksc	U ksc	Sig.a mV	Sig.b mV	T a mV	T b mV	U mV	Sig.a ksc	Sig.b ksc	T a ksc	T b ksc	Input V Volts
0	0.000	0.000	0.000	0.000	0.000	0.000	0.890	0.380	-0.354	-0.352	0.000	0.000	0.000	0.000	0.000	0.000
1	-0.262	-0.134	0.198	0.001	0.198	0.000	5.700	5.300	0.000	0.000	0.000	0.199	0.197	-0.000	-0.000	10.000
2	-0.035	-0.018	0.201	0.010	0.201	0.000	5.960	5.150	0.000	0.000	0.000	0.210	0.191	-0.000	-0.000	10.000
3	-0.017	-0.009	0.200	0.020	0.200	0.000	6.180	4.870	0.000	0.000	0.000	0.219	0.180	-0.000	-0.000	10.000
4	-0.011	-0.006	0.200	0.030	0.200	0.000	6.440	4.640	0.000	0.000	0.000	0.230	0.170	-0.000	-0.000	10.000
5	-0.009	-0.004	0.200	0.040	0.200	0.000	6.670	4.380	0.000	0.000	0.000	0.240	0.160	-0.000	-0.000	10.000
6	-0.007	-0.003	0.200	0.050	0.200	0.000	6.930	4.130	0.000	0.000	0.000	0.250	0.150	-0.000	-0.000	10.000
7	-0.006	-0.003	0.200	0.060	0.200	0.000	7.170	3.890	0.000	0.000	0.000	0.260	0.140	-0.000	-0.000	10.000
8	-0.005	-0.002	0.200	0.070	0.200	0.000	7.410	3.640	0.000	0.000	0.000	0.270	0.130	-0.000	-0.000	10.000
9	-0.004	-0.002	0.200	0.080	0.200	0.000	7.640	3.380	0.000	0.000	0.000	0.280	0.120	-0.000	-0.000	10.000
10	-0.004	-0.002	0.200	0.090	0.200	0.000	7.880	3.130	0.000	0.000	0.000	0.290	0.110	-0.000	-0.000	10.000
11	-0.003	-0.002	0.200	0.100	0.200	0.000	8.120	2.880	0.000	0.000	0.000	0.300	0.100	-0.000	-0.000	10.000
12	-0.199	-0.102	0.199	0.002	0.199	0.000	5.720	5.300	0.000	0.000	0.000	0.200	0.197	-0.000	-0.000	10.000

RUBBER5

FILM No.	DELTA deg	ALFA deg	P ksc	Q ksc	P' ksc	U ksc	Sig.a mV	Sig.b mV	T a mV	T b mV	U mV	Sig.a ksc	Sig.b ksc	T a ksc	T b ksc	Input V Volts
0	45.000	0.000	0.000	0.000	0.000	0.000	0.900	0.370	-1.250	-0.120	0.000	0.000	0.000	0.000	0.000	0.000
1	0.000	0.000	0.198	0.000	0.198	0.000	5.710	5.290	-0.895	0.232	0.000	0.199	0.197	0.000	0.000	10.000
2	35.637	12.553	0.198	0.003	0.198	0.000	5.710	5.300	-0.400	0.750	0.000	0.199	0.197	0.003	0.003	10.000
3	43.121	27.572	0.199	0.014	0.199	0.000	5.720	5.320	0.110	1.280	0.000	0.200	0.198	0.013	0.014	10.000
4	43.630	-5.827	0.199	0.023	0.199	0.000	5.720	5.310	0.600	1.710	0.000	0.200	0.198	0.023	0.023	10.000
5	44.041	-4.599	0.199	0.033	0.199	0.000	5.720	5.310	1.090	2.200	0.000	0.200	0.198	0.033	0.033	10.000
6	44.678	15.872	0.199	0.043	0.199	0.000	5.700	5.320	1.600	2.730	0.000	0.199	0.198	0.043	0.044	10.000
7	-44.979	52.984	0.200	0.053	0.200	0.000	5.720	5.367	2.081	3.190	0.000	0.200	0.200	0.053	0.053	10.000
8	44.772	9.615	0.199	0.063	0.199	0.000	5.720	5.340	2.580	3.700	0.000	0.200	0.199	0.063	0.063	10.000
9	44.719	-22.687	0.200	0.072	0.200	0.000	5.730	5.340	3.060	4.140	0.000	0.200	0.199	0.073	0.072	10.000
10	44.822	-28.211	0.200	0.082	0.200	0.000	5.730	5.350	3.540	4.620	0.000	0.200	0.199	0.082	0.082	10.000
11	44.780	-19.334	0.200	0.092	0.200	0.000	5.730	5.340	4.040	5.120	0.000	0.200	0.199	0.092	0.092	10.000

RUBBER6

FILM No.	DELTA deg	ALFA deg	P ksc	Q ksc	P' ksc	U ksc	Sig.a mV	Sig.b mV	T a mV	T b mV	U mV	Sig.a ksc	Sig.b ksc	T a ksc	T b ksc	Input V Volts
0	90.000	0.000	0.000	0.000	0.000	0.000	0.860	0.380	-0.354	-0.352	0.000	0.000	0.000	0.000	0.000	0.000
1	-0.374	-0.191	0.199	0.001	0.199	0.000	5.680	5.340	0.000	0.000	0.000	0.200	0.198	-0.000	-0.000	10.000
2	0.034	0.017	0.200	0.010	0.200	0.000	5.440	5.630	0.000	0.000	0.000	0.190	0.210	-0.000	-0.000	10.000
3	0.017	0.009	0.200	0.020	0.200	0.000	5.200	5.890	0.000	0.000	0.000	0.180	0.221	-0.000	-0.000	10.000
4	0.011	0.006	0.200	0.030	0.200	0.000	4.980	6.130	0.000	0.000	0.000	0.171	0.230	-0.000	-0.000	10.000
5	0.008	0.004	0.201	0.040	0.201	0.000	4.730	6.390	0.000	0.000	0.000	0.161	0.241	-0.000	-0.000	10.000
6	0.007	0.003	0.200	0.050	0.200	0.000	4.470	6.630	0.000	0.000	0.000	0.150	0.250	-0.000	-0.000	10.000
7	0.006	0.003	0.200	0.060	0.200	0.000	4.220	6.880	0.000	0.000	0.000	0.139	0.260	-0.000	-0.000	10.000
8	0.005	0.002	0.200	0.071	0.200	0.000	3.980	7.140	0.000	0.000	0.000	0.129	0.271	-0.000	-0.000	10.000
9	0.004	0.002	0.200	0.081	0.200	0.000	3.730	7.390	0.000	0.000	0.000	0.119	0.281	-0.000	-0.000	10.000
10	0.004	0.002	0.199	0.090	0.199	0.000	3.490	7.620	0.000	0.000	0.000	0.109	0.290	-0.000	-0.000	10.000
11	0.003	0.002	0.200	0.100	0.200	0.000	3.260	7.830	0.000	0.000	0.000	0.100	0.300	-0.000	-0.000	10.000
12	-0.484	-0.247	0.199	0.001	0.199	0.000	5.680	5.340	0.000	0.000	0.000	0.200	0.198	-0.000	-0.000	10.000

RUBBER7

FILM No.	DELTA deg	ALFA deg	P ksc	Q ksc	P' ksc	U ksc	Sig.a mV	Sig.b mV	T a mV	T b mV	U mV	Sig.a ksc	Sig.b ksc	T a ksc	T b ksc	Input V Volts
0	45.000	0.000	0.000	0.000	0.000	0.000	0.880	0.380	-1.180	-0.050	0.000	0.000	0.000	0.000	0.000	0.000
1	24.702	-49.403	0.200	0.002	0.200	0.000	5.750	5.350	-0.300	0.300	0.000	0.202	0.199	0.004	0.000	10.000
2	33.588	6.179	0.199	0.003	0.199	0.000	5.720	5.330	-0.330	0.810	0.000	0.201	0.198	0.003	0.003	10.000
3	42.605	3.389	0.200	0.013	0.200	0.000	5.720	5.340	0.180	1.310	0.000	0.201	0.198	0.013	0.013	10.000
4	43.615	4.576	0.200	0.023	0.200	0.000	5.730	5.350	0.670	1.800	0.000	0.201	0.199	0.023	0.023	10.000
5	43.845	0.523	0.200	0.033	0.200	0.000	5.730	5.340	1.150	2.270	0.000	0.201	0.198	0.033	0.033	10.000
6	44.116	1.587	0.200	0.043	0.200	0.000	5.740	5.350	1.660	2.780	0.000	0.202	0.199	0.043	0.043	10.000
7	44.282	6.936	0.200	0.053	0.200	0.000	5.740	5.350	2.150	3.280	0.000	0.202	0.199	0.053	0.053	10.000
8	44.487	4.299	0.200	0.063	0.200	0.000	5.740	5.360	2.650	3.770	0.000	0.202	0.199	0.063	0.063	10.000
9	44.475	4.649	0.201	0.073	0.201	0.000	5.750	5.360	3.140	4.260	0.000	0.202	0.199	0.073	0.073	10.000
10	44.539	5.682	0.201	0.083	0.201	0.000	5.750	5.360	3.640	4.760	0.000	0.202	0.199	0.083	0.083	10.000
11	44.652	7.902	0.200	0.093	0.200	0.000	5.740	5.360	4.130	5.250	0.000	0.202	0.199	0.093	0.093	10.000

RUBBER8

FILM No.	DELTA deg	ALFA deg	P ksc	Q ksc	P' ksc	U ksc	Sig.a mV	Sig.b mV	T a mV	T b mV	U mV	Sig.a ksc	Sig.b ksc	T a ksc	T b ksc	Input V Volts
0	15.000	0.000	0.000	0.000	0.000	0.000	0.870	0.350	-1.250	-0.120	0.000	0.000	0.000	0.000	0.000	0.000
1	0.000	0.000	0.200	0.001	0.200	0.000	5.700	5.320	-0.895	0.232	0.000	0.200	0.199	0.000	0.000	10.000
2	0.000	0.000	0.200	0.009	0.200	0.000	5.910	5.110	-0.640	0.500	0.000	0.209	0.190	0.000	0.000	10.000
3	5.513	0.795	0.200	0.018	0.200	0.000	6.110	4.900	-0.390	0.760	0.000	0.217	0.182	0.003	0.004	10.000
4	8.942	-0.549	0.200	0.027	0.200	0.000	6.320	4.700	-0.120	0.980	0.000	0.226	0.174	0.009	0.008	10.000
5	10.348	-0.381	0.201	0.038	0.201	0.000	6.560	4.470	0.130	1.230	0.000	0.236	0.165	0.014	0.013	10.000
6	11.402	0.236	0.199	0.047	0.199	0.000	6.730	4.250	0.350	1.490	0.000	0.243	0.156	0.018	0.018	10.000
7	12.066	-0.012	0.200	0.057	0.200	0.000	6.930	4.050	0.600	1.720	0.000	0.251	0.148	0.023	0.023	10.000
8	12.437	0.286	0.200	0.067	0.200	0.000	7.160	3.820	0.840	1.990	0.000	0.261	0.139	0.028	0.029	10.000
9	12.765	0.010	0.200	0.077	0.200	0.000	7.360	3.620	1.090	2.210	0.000	0.269	0.131	0.033	0.033	10.000
10	12.965	-0.204	0.200	0.087	0.200	0.000	7.570	3.390	1.350	2.440	0.000	0.278	0.122	0.038	0.038	10.000
11	13.283	-0.042	0.200	0.097	0.200	0.000	7.770	3.180	1.600	2.710	0.000	0.286	0.113	0.043	0.043	10.000

RUBBER9

FILM No.	DELTA deg	ALFA deg	P ksc	Q ksc	P' ksc	U ksc	Sig.a mV	Sig.b mV	T a mV	T b mV	U mV	Sig.a ksc	Sig.b ksc	T a ksc	T b ksc	Input V Volts
0	30.000	0.000	0.000	0.000	0.000	0.000	0.870	0.350	-1.250	-0.140	0.000	0.000	0.000	0.000	0.000	0.000
1	0.000	0.000	0.200	0.001	0.200	0.000	5.700	5.320	-0.895	0.232	0.000	0.200	0.199	0.000	0.000	10.000
2	8.948	0.435	0.200	0.005	0.200	0.000	5.820	5.230	-0.470	0.640	0.000	0.205	0.195	0.002	0.002	10.000
3	23.373	-0.827	0.200	0.014	0.200	0.000	5.930	5.100	-0.020	1.070	0.000	0.210	0.190	0.011	0.010	10.000
4	25.822	0.303	0.200	0.024	0.200	0.000	6.070	4.980	0.400	1.510	0.000	0.216	0.185	0.019	0.019	10.000
5	27.031	0.288	0.200	0.034	0.200	0.000	6.170	4.840	0.820	1.930	0.000	0.220	0.180	0.028	0.028	10.000
6	27.735	0.278	0.200	0.044	0.200	0.000	6.300	4.720	1.260	2.370	0.000	0.225	0.175	0.036	0.037	10.000
7	28.298	0.080	0.200	0.054	0.200	0.000	6.410	4.610	1.680	2.780	0.000	0.230	0.170	0.045	0.045	10.000
8	28.335	-0.063	0.200	0.064	0.200	0.000	6.540	4.460	2.120	3.210	0.000	0.235	0.164	0.054	0.054	10.000
9	28.690	-0.026	0.200	0.074	0.200	0.000	6.650	4.350	2.540	3.630	0.000	0.240	0.160	0.062	0.062	10.000
10	28.805	-0.126	0.200	0.084	0.200	0.000	6.780	4.230	2.97.	4.050	0.000	0.245	0.155	0.071	0.071	10.000
11	28.913	-0.089	0.200	0.094	0.200	0.000	6.900	4.100	3.400	4.480	0.000	0.250	0.150	0.080	0.079	10.000

RUBBER2

AREA	Ex	Ex(SD)	Ey	Ey(SD)	Exy	Exy(SD)	E3	E3(SD)	E1	E1(SD)	GAMMA	G(SD)	EV	EV(SD)	PS.	PS(SD)
		P' =	0.199	ksc			Q =	0.002	ksc							
1	0.205	0.010	-0.173	0.012	0.025	0.008	-0.175	0.012	0.207	0.010	0.382	0.015	0.032	0.015	3.71	1.15
2	0.182	0.016	-0.214	0.017	0.068	0.012	-0.226	0.017	0.194	0.016	0.419	0.023	-0.032	0.023	9.45	1.58
3	0.151	0.028	-0.269	0.033	0.093	0.022	-0.289	0.032	0.170	0.028	0.459	0.043	-0.118	0.043	11.92	2.68
4	0.038	0.077	-0.223	0.086	0.185	0.058	-0.319	0.083	0.134	0.078	0.453	0.115	-0.185	0.115	27.35	7.27
5	0.151	0.367	-0.690	0.756	0.110	0.434	-0.704	0.751	0.166	0.377	0.870	0.841	-0.538	0.840	7.35	28.49
		P' =	0.200	ksc			Q =	0.010	ksc							
1	0.047	0.009	0.017	0.009	0.008	0.006	0.015	0.009	0.049	0.009	0.035	0.013	0.064	0.013	14.50	10.40
2	0.045	0.013	-0.006	0.014	0.013	0.010	-0.009	0.014	0.048	0.013	0.057	0.019	0.040	0.019	12.96	9.52
3	0.040	0.023	-0.047	0.022	0.024	0.016	-0.053	0.022	0.046	0.023	0.099	0.032	-0.007	0.032	14.24	9.22
4	-0.011	0.067	0.019	0.048	0.082	0.041	-0.079	0.060	0.087	0.056	0.166	0.082	0.008	0.083	-39.83	14.25
5	-0.074	0.141	-0.126	0.121	0.150	0.093	-0.252	0.129	0.052	0.132	0.304	0.185	-0.200	0.186	40.03	17.48
		P' =	0.200	ksc			Q =	0.020	ksc							
1	0.032	0.010	-0.066	0.008	0.009	0.007	-0.067	0.008	0.033	0.010	0.099	0.013	-0.034	0.013	5.03	3.77
2	0.034	0.015	-0.089	0.014	0.018	0.010	-0.091	0.014	0.037	0.015	0.128	0.020	-0.055	0.020	8.16	4.58
3	0.046	0.027	-0.111	0.026	0.034	0.019	-0.118	0.026	0.053	0.027	0.171	0.038	-0.065	0.038	11.73	6.30
4	-0.043	0.058	-0.077	0.063	0.127	0.043	-0.188	0.061	0.068	0.060	0.256	0.085	-0.120	0.085	41.15	9.55
5	0.000	0.001	-0.371	0.101	0.209	0.053	-0.465	0.093	0.095	0.043	0.560	0.104	-0.371	0.101	24.22	5.28
		P' =	0.200	ksc			Q =	0.030	ksc							
1	0.135	0.009	-0.054	0.007	-0.000	0.006	-0.054	0.007	0.135	0.009	0.190	0.011	0.081	0.011	-0.04	1.72
2	0.116	0.014	-0.074	0.012	0.010	0.009	-0.075	0.012	0.116	0.014	0.191	0.018	0.041	0.018	3.11	2.71
3	0.079	0.027	-0.091	0.022	0.020	0.017	-0.094	0.022	0.082	0.027	0.175	0.035	-0.012	0.035	6.73	5.70
4	0.038	0.072	-0.043	0.048	0.092	0.043	-0.103	0.056	0.098	0.065	0.200	0.086	-0.005	0.086	33.00	12.36
5	0.328	0.303	0.229	0.203	0.280	0.179	-0.006	0.246	0.563	0.264	0.569	0.359	0.557	0.365	40.00	18.37
		P' =	0.200	ksc			Q =	0.040	ksc							
1	0.156	0.009	-0.132	0.009	0.019	0.006	-0.133	0.009	0.158	0.009	0.290	0.013	0.025	0.013	3.81	1.25
2	0.161	0.013	-0.159	0.015	0.034	0.010	-0.163	0.015	0.164	0.013	0.307	0.020	0.001	0.020	5.93	1.76
3	0.169	0.023	-0.185	0.026	0.040	0.018	-0.189	0.026	0.173	0.023	0.362	0.035	-0.017	0.035	6.33	2.76
4	0.098	0.046	-0.044	0.050	0.135	0.034	-0.125	0.049	0.179	0.047	0.304	0.068	0.054	0.068	31.10	6.44
5	0.630	0.009	0.050	0.041	0.109	0.022	0.030	0.041	0.650	0.012	0.620	0.043	0.680	0.042	10.31	2.03
		P' =	0.200	ksc			Q =	0.050	ksc							
1	0.211	0.010	-0.187	0.010	0.005	0.007	-0.187	0.010	0.211	0.010	0.398	0.014	0.024	0.014	0.78	0.99
2	0.212	0.015	-0.211	0.016	0.021	0.011	-0.212	0.016	0.213	0.015	0.424	0.022	0.001	0.022	2.77	1.45
3	0.192	0.031	-0.246	0.029	0.011	0.021	-0.246	0.029	0.193	0.031	0.439	0.043	-0.054	0.043	1.41	2.79
4	0.178	0.094	-0.149	0.054	0.056	0.054	-0.158	0.055	0.168	0.093	0.346	0.109	0.029	0.108	9.40	8.97
5	0.215	0.320	-0.068	0.408	-0.156	0.263	-0.137	0.397	0.284	0.338	0.421	0.523	0.148	0.518	-23.89	35.53
		P' =	0.200	ksc			Q =	0.060	ksc							
1	0.280	0.008	-0.225	0.009	-0.013	0.006	-0.226	0.009	0.281	0.008	0.506	0.012	0.055	0.012	-1.47	0.65
2	0.271	0.012	-0.260	0.013	0.000	0.009	-0.260	0.013	0.271	0.012	0.531	0.017	0.011	0.017	0.03	0.93
3	0.265	0.023	-0.299	0.020	0.010	0.015	-0.299	0.020	0.265	0.023	0.564	0.030	-0.034	0.030	0.97	1.54
4	0.143	0.044	-0.221	0.032	0.047	0.027	-0.227	0.032	0.149	0.044	0.376	0.055	-0.078	0.055	7.28	4.17
5	-0.071	0.069	-0.284	0.116	0.039	0.069	-0.291	0.114	-0.064	0.071	0.227	0.135	-0.355	0.135	10.10	17.34

AREA	Ex	Ex(SD)	Ey	Ey(SD)	Exy	Exy(SD)	E3	E3(SD)	E1	E1(SD)	GAMMA G(SD)	EV	EV(SD)	PS.	PS(SD)
		P' =	0.200 ksc				Q =	0.070 ksc							
1	0.329	0.010	-0.325	0.011	0.005	0.007	-0.325	0.011	0.329	0.010	0.654 0.015	0.004	0.015	0.45	0.65
2	0.345	0.015	-0.384	0.015	0.020	0.011	-0.385	0.015	0.346	0.015	0.730 0.021	-0.039	0.021	1.57	0.83
3	0.318	0.027	-0.429	0.025	0.052	0.018	-0.433	0.025	0.322	0.027	0.755 0.036	-0.111	0.036	3.93	1.37
4	0.279	0.057	-0.404	0.062	0.103	0.042	-0.419	0.062	0.294	0.057	0.713 0.084	-0.125	0.085	8.37	3.39
5	0.278	0.099	-0.218	0.062	0.148	0.057	-0.259	0.065	0.319	0.097	0.578 0.117	0.060	0.117	15.41	5.73
		P' =	0.200 ksc				Q =	0.080 ksc							
1	0.460	0.008	-0.432	0.011	0.011	0.007	-0.433	0.011	0.460	0.008	0.892 0.014	0.027	0.014	0.70	0.45
2	0.472	0.011	-0.478	0.015	0.040	0.009	-0.480	0.015	0.474	0.011	0.954 0.018	-0.006	0.018	2.43	0.54
3	0.466	0.019	-0.527	0.027	0.041	0.017	-0.529	0.027	0.468	0.019	0.997 0.033	-0.061	0.033	2.38	0.95
4	0.375	0.045	-0.461	0.053	0.110	0.035	-0.475	0.053	0.389	0.045	0.864 0.069	-0.086	0.069	7.40	2.30
5	0.318	0.035	-0.686	0.180	0.248	0.096	-0.744	0.176	0.376	0.055	1.120 0.185	-0.369	0.183	13.15	4.86
		P'_a =	0.200 ksc				Q =	0.090 ksc							
1	0.538	0.010	-0.535	0.012	0.012	0.008	-0.535	0.012	0.538	0.010	1.073 0.016	0.003	0.016	0.63	0.43
2	0.572	0.015	-0.594	0.016	0.037	0.011	-0.595	0.016	0.573	0.015	1.169 0.022	-0.022	0.022	1.80	0.53
3	0.574	0.025	-0.664	0.026	0.054	0.018	-0.666	0.026	0.576	0.025	1.243 0.036	-0.090	0.036	2.51	0.84
4	0.469	0.053	-0.612	0.041	0.137	0.034	-0.629	0.041	0.486	0.053	1.116 0.068	-0.143	0.068	7.09	1.73
5	0.694	0.157	-0.435	0.097	0.105	0.091	-0.444	0.098	0.704	0.157	1.148 0.185	0.260	0.185	5.26	4.53
		P' =	0.200 ksc				Q =	0.100 ksc							
1	0.658	0.010	-0.613	0.012	-0.004	0.008	-0.613	0.012	0.658	0.010	1.271 0.016	0.045	0.016	-0.18	0.35
2	0.693	0.014	-0.675	0.015	0.031	0.010	-0.676	0.015	0.694	0.014	1.370 0.021	0.018	0.021	1.31	0.43
3	0.693	0.025	-0.755	0.023	0.071	0.017	-0.758	0.023	0.696	0.025	1.454 0.034	-0.062	0.034	2.81	0.67
4	0.608	0.059	-0.713	0.046	0.195	0.038	-0.742	0.046	0.637	0.059	1.378 0.075	-0.105	0.075	8.24	1.56
5	0.826	0.415	-0.660	0.294	0.151	0.251	-0.675	0.295	0.841	0.414	1.515 0.509	0.166	0.509	5.73	9.50

RUBBER3

AREA	Ex	Ex(SD)	Ey	Ey(SD)	Exy	Exy(SD)	E3	E3(SD)	E1	E1(SD)	GAMMA	G(SD)	EV	EV(SD)	PS.	PS(SD)
			P' = 0.199 ksc				Q = 0.002 ksc									
1	-0.232	0.012	0.331	0.012	0.009	0.008	-0.232	0.012	0.331	0.012	0.562	0.017	0.099	0.017	-0.90	0.87
2	-0.250	0.017	0.366	0.016	0.004	0.012	-0.250	0.017	0.366	0.016	0.616	0.023	0.116	0.023	-0.41	1.08
3	-0.279	0.027	0.372	0.029	0.020	0.020	-0.280	0.027	0.373	0.029	0.653	0.039	0.094	0.039	-1.76	1.73
4	-0.208	0.065	0.281	0.072	0.018	0.049	-0.209	0.065	0.282	0.072	0.490	0.097	0.073	0.097	-2.09	5.68
5	0.171	0.372	-0.169	0.513	-0.232	0.322	-0.287	0.491	0.289	0.409	0.576	0.641	0.002	0.634	-26.90	31.74
			P' = 0.200 ksc				Q = 0.010 ksc									
1	-0.003	0.041	0.090	0.020	0.012	0.023	-0.004	0.040	0.091	0.021	0.095	0.045	0.087	0.045	-7.15	13.61
2	0.016	0.079	0.111	0.038	-0.004	0.044	0.016	0.079	0.111	0.038	0.095	0.088	0.127	0.088	2.16	26.30
3	0.117	0.190	0.107	0.087	-0.039	0.104	0.073	0.142	0.151	0.153	0.079	0.207	0.224	0.209	-41.60	75.96
4	0.779	0.640	0.194	0.295	-0.280	0.351	0.081	0.364	0.891	0.606	0.810	0.701	0.972	0.704	-21.87	24.80
5	0.322	0.283	0.153	0.081	-0.007	0.141	0.153	0.082	0.322	0.282	0.170	0.294	0.475	0.294	-2.37	47.77
			P' = 0.200 ksc				Q = 0.020 ksc									
1	-0.073	0.010	0.142	0.010	0.002	0.007	-0.073	0.010	0.142	0.010	0.215	0.013	0.070	0.013	-0.52	1.79
2	-0.073	0.015	0.156	0.013	-0.003	0.010	-0.073	0.015	0.156	0.013	0.229	0.020	0.083	0.020	0.78	2.49
3	-0.078	0.025	0.157	0.021	-0.001	0.016	-0.078	0.025	0.157	0.021	0.235	0.033	0.078	0.033	0.14	3.96
4	0.045	0.063	0.100	0.049	0.019	0.040	0.039	0.061	0.105	0.050	0.066	0.079	0.144	0.079	-17.17	34.28
5	0.346	0.195	0.317	0.196	0.112	0.139	0.219	0.195	0.444	0.195	0.225	0.277	0.662	0.277	41.25	35.17
			P' = 0.200 ksc				Q = 0.030 ksc									
1	-0.117	0.010	0.215	0.011	0.001	0.007	-0.117	0.010	0.215	0.011	0.332	0.015	0.098	0.015	-0.09	1.25
2	-0.147	0.015	0.236	0.017	-0.009	0.011	-0.147	0.015	0.236	0.017	0.383	0.022	0.089	0.022	1.40	1.66
3	-0.156	0.030	0.194	0.034	0.017	0.022	-0.156	0.030	0.195	0.034	0.352	0.045	0.039	0.045	-2.77	3.64
4	-0.241	0.064	0.107	0.099	0.017	0.059	-0.242	0.064	0.108	0.099	0.349	0.118	-0.134	0.118	-2.78	9.71
5	-0.097	0.161	0.131	0.366	-0.060	0.207	-0.112	0.181	0.145	0.359	0.257	0.402	0.034	0.400	13.81	45.71
			P' = 0.200 ksc				Q = 0.040 ksc									
1	-0.137	0.010	0.363	0.011	-0.006	0.008	-0.137	0.010	0.363	0.011	0.500	0.015	0.226	0.015	0.63	0.86
2	-0.148	0.017	0.383	0.017	0.001	0.012	-0.148	0.017	0.383	0.017	0.530	0.025	0.235	0.025	-0.05	1.32
3	-0.129	0.034	0.383	0.028	0.001	0.022	-0.129	0.034	0.383	0.028	0.512	0.044	0.253	0.044	-0.12	2.46
4	-0.146	0.092	0.377	0.077	0.038	0.060	-0.148	0.092	0.379	0.077	0.527	0.120	0.231	0.120	-4.08	6.51
5	0.624	0.097	0.200	0.251	0.063	0.139	0.191	0.249	0.633	0.103	0.443	0.269	0.824	0.269	8.23	17.96
			P' = 0.200 ksc				Q = 0.050 ksc									
1	-0.262	0.010	0.375	0.010	0.002	0.007	-0.262	0.010	0.375	0.010	0.636	0.014	0.113	0.014	-0.14	0.62
2	-0.275	0.015	0.396	0.014	-0.008	0.010	-0.276	0.015	0.396	0.014	0.672	0.021	0.121	0.021	0.69	0.88
3	-0.299	0.028	0.413	0.026	-0.017	0.019	-0.299	0.028	0.413	0.026	0.713	0.038	0.114	0.038	1.39	1.52
4	-0.351	0.063	0.449	0.077	0.035	0.050	-0.352	0.063	0.451	0.077	0.803	0.100	0.098	0.100	-2.51	3.55
5	-0.071	0.029	0.334	0.023	0.347	0.018	-0.271	0.028	0.533	0.024	0.804	0.037	0.263	0.037	-24.86	1.32
			P' = 0.200 ksc				Q = 0.060 ksc									
1	-0.323	0.009	0.469	0.012	0.009	0.007	-0.323	0.009	0.469	0.012	0.792	0.015	0.145	0.015	-0.65	0.53
2	-0.360	0.012	0.515	0.014	0.007	0.009	-0.360	0.012	0.516	0.014	0.876	0.018	0.155	0.018	-0.46	0.60
3	-0.389	0.021	0.545	0.021	0.014	0.015	-0.390	0.021	0.545	0.021	0.934	0.030	0.155	0.030	-0.86	0.93
4	-0.457	0.040	0.553	0.056	0.027	0.034	-0.457	0.040	0.554	0.056	1.011	0.069	0.097	0.069	-1.51	1.94
5	-0.344	0.470	0.396	0.183	0.125	0.244	-0.364	0.464	0.417	0.195	0.781	0.502	0.053	0.505	-9.34	17.93

AREA	Ex	Ex(SD)	Ey	Ey(SD)	Exy	Exy(SD)	E3	E3(SD)	E1	E1(SD)	GAMMA	G(SD)	EV	EV(SD)	PS.	PS(SD)
		P' =	0.200	ksc			Q =	0.070	ksc							
1	-0.376	0.011	0.550	0.012	-0.002	0.008	-0.376	0.011	0.550	0.012	0.926	0.016	0.174	0.016	0.11	0.50
2	-0.404	0.018	0.595	0.014	0.003	0.012	-0.404	0.018	0.595	0.014	0.999	0.023	0.192	0.023	-0.17	0.67
3	-0.382	0.031	0.578	0.023	0.033	0.019	-0.384	0.031	0.579	0.023	0.963	0.039	0.196	0.039	-1.97	1.14
4	-0.355	0.071	0.621	0.058	0.082	0.046	-0.362	0.070	0.628	0.058	0.990	0.091	0.266	0.091	-4.79	2.64
5	-0.169	0.581	0.616	0.438	0.125	0.360	-0.189	0.577	0.636	0.441	0.824	0.726	0.447	0.727	-8.84	25.01
		P' =	0.200	ksc			Q =	0.081	ksc							
1	-0.477	0.010	0.668	0.011	0.002	0.007	-0.477	0.010	0.668	0.011	1.145	0.015	0.191	0.015	-0.09	0.37
2	-0.518	0.014	0.727	0.013	-0.002	0.010	-0.518	0.014	0.727	0.013	1.245	0.020	0.209	0.020	0.08	0.45
3	-0.550	0.026	0.764	0.024	0.005	0.018	-0.550	0.026	0.764	0.024	1.313	0.035	0.214	0.035	-0.22	0.77
4	-0.524	0.058	0.756	0.045	0.041	0.037	-0.525	0.058	0.758	0.045	1.283	0.074	0.232	0.074	-1.81	1.64
5	-0.030	0.214	0.514	0.005	-0.043	0.102	-0.034	0.214	0.517	0.017	0.551	0.214	0.484	0.214	4.53	10.66
		P' =	0.200	ksc			Q =	0.090	ksc							
1	-0.537	0.010	0.780	0.015	-0.005	0.009	-0.537	0.010	0.780	0.015	1.317	0.018	0.243	0.018	0.22	0.38
2	-0.591	0.012	0.860	0.018	-0.012	0.011	-0.591	0.012	0.860	0.018	1.451	0.022	0.269	0.022	0.47	0.43
3	-0.624	0.021	0.929	0.027	-0.013	0.017	-0.624	0.021	0.929	0.027	1.554	0.035	0.305	0.035	0.48	0.64
4	-0.630	0.049	0.926	0.053	0.028	0.036	-0.630	0.049	0.926	0.053	1.557	0.072	0.295	0.072	-1.04	1.33
5	-0.469	0.061	1.052	0.063	0.007	0.044	-0.469	0.061	1.052	0.063	1.521	0.088	0.583	0.088	-0.28	1.65
		P' =	0.200	ksc			Q =	0.100	ksc							
1	-0.598	0.011	0.941	0.015	0.001	0.009	-0.598	0.011	0.941	0.015	1.539	0.019	0.344	0.019	-0.05	0.35
2	-0.647	0.016	1.027	0.017	0.009	0.012	-0.647	0.016	1.027	0.017	1.675	0.023	0.380	0.023	-0.32	0.39
3	-0.643	0.028	1.088	0.028	-0.001	0.020	-0.643	0.028	1.088	0.028	1.731	0.039	0.445	0.039	0.02	0.65
4	-0.638	0.039	1.097	0.072	-0.011	0.041	-0.638	0.039	1.097	0.072	1.736	0.081	0.459	0.081	0.36	1.35
5	-0.406	0.097	1.111	0.012	0.242	0.047	-0.443	0.096	1.149	0.019	1.592	0.097	0.706	0.098	-8.84	1.69

RUBBER4

AREA	Ex	Ex(SD)	Ey	Ey(SD)	Exy	Exy(SD)	E3	E3(SD)	E1	E1(SD)	GAMMA	G(SD)	EV	EV(SD)	PS.	PS(SD)
		P' =	0.199	ksc			Q =	0.002	ksc							
1	0.239	0.010	-0.144	0.009	-0.014	0.007	-0.145	0.009	0.240	0.010	0.385	0.014	0.095	0.014	-2.11	1.03
2	0.243	0.016	-0.145	0.016	-0.021	0.011	-0.146	0.016	0.245	0.016	0.391	0.022	0.098	0.022	-3.06	1.62
3	0.281	0.032	-0.136	0.027	-0.030	0.021	-0.138	0.027	0.283	0.032	0.421	0.042	0.145	0.042	-4.08	2.83
4	0.286	0.081	-0.072	0.070	0.009	0.053	-0.072	0.070	0.286	0.081	0.358	0.107	0.214	0.107	1.48	8.53
5	-0.070	0.108	0.067	0.173	0.087	0.104	-0.112	0.124	0.110	0.163	0.222	0.207	-0.003	0.204	-25.87	26.60
		P' =	0.201	ksc			Q =	0.010	ksc							
1	0.069	0.008	0.038	0.008	0.009	0.005	0.035	0.008	0.071	0.008	0.035	0.011	0.107	0.011	14.85	8.69
2	0.055	0.012	0.045	0.012	0.016	0.008	0.033	0.012	0.067	0.012	0.034	0.017	0.099	0.017	36.47	14.18
3	0.092	0.021	-0.005	0.023	0.005	0.015	-0.005	0.023	0.092	0.021	0.097	0.031	0.087	0.031	2.91	9.05
4	0.218	0.041	-0.008	0.058	0.019	0.036	-0.009	0.058	0.220	0.042	0.229	0.072	0.211	0.072	4.66	8.98
5	0.450	0.142	0.285	0.161	0.170	0.108	0.179	0.156	0.557	0.148	0.378	0.216	0.736	0.215	32.08	16.30
		P' =	0.200	ksc			Q =	0.020	ksc							
1	0.056	0.009	-0.047	0.008	0.010	0.006	-0.048	0.008	0.057	0.009	0.105	0.012	0.010	0.012	5.38	3.40
2	0.069	0.016	-0.026	0.012	0.004	0.010	-0.026	0.012	0.069	0.016	0.095	0.020	0.043	0.020	2.42	5.97
3	0.109	0.027	0.005	0.021	-0.033	0.017	-0.004	0.022	0.118	0.026	0.123	0.034	0.114	0.034	-16.20	7.94
4	0.075	0.056	0.035	0.051	0.032	0.038	0.017	0.052	0.093	0.054	0.075	0.075	0.110	0.075	29.34	28.65
5	0.231	0.342	0.133	0.164	0.211	0.184	-0.035	0.244	0.399	0.283	0.434	0.369	0.364	0.380	38.50	25.05
		P' =	0.200	ksc			Q =	0.030	ksc							
1	0.117	0.010	-0.088	0.008	0.000	0.006	-0.088	0.008	0.117	0.010	0.204	0.013	0.029	0.013	0.02	1.76
2	0.137	0.016	-0.104	0.012	0.012	0.010	-0.105	0.012	0.137	0.016	0.242	0.020	0.032	0.020	2.85	2.38
3	0.152	0.028	-0.083	0.022	0.007	0.018	-0.084	0.022	0.152	0.028	0.236	0.036	0.069	0.036	1.80	4.34
4	0.281	0.050	-0.044	0.061	0.062	0.039	-0.055	0.060	0.293	0.050	0.348	0.079	0.237	0.079	10.47	6.47
5	0.373	0.378	0.150	0.057	0.133	0.182	0.088	0.162	0.435	0.340	0.347	0.373	0.522	0.382	25.04	31.06
		P' =	0.200	ksc			Q =	0.040	ksc							
1	0.190	0.008	-0.112	0.007	0.005	0.006	-0.112	0.007	0.190	0.008	0.302	0.011	0.078	0.011	0.87	1.05
2	0.198	0.013	-0.104	0.012	-0.006	0.009	-0.104	0.012	0.198	0.013	0.303	0.018	0.094	0.018	-1.09	1.68
3	0.237	0.024	-0.090	0.021	-0.019	0.016	-0.091	0.021	0.238	0.024	0.329	0.032	0.148	0.032	-3.32	2.77
4	0.318	0.050	-0.077	0.053	-0.020	0.037	-0.078	0.053	0.319	0.050	0.397	0.073	0.240	0.073	-2.91	5.27
5	0.161	0.056	-0.018	0.225	0.035	0.121	-0.024	0.221	0.168	0.070	0.192	0.233	0.144	0.231	10.64	35.84
		P' =	0.200	ksc			Q =	0.050	ksc							
1	0.284	0.011	-0.149	0.009	-0.007	0.007	-0.150	0.009	0.284	0.011	0.433	0.014	0.134	0.014	-0.89	0.92
2	0.293	0.018	-0.146	0.014	0.006	0.011	-0.146	0.014	0.293	0.018	0.439	0.023	0.146	0.023	0.73	1.47
3	0.330	0.034	-0.125	0.027	-0.005	0.022	-0.125	0.027	0.330	0.034	0.455	0.043	0.205	0.043	-0.57	2.71
4	0.468	0.063	-0.019	0.073	0.107	0.048	-0.042	0.073	0.491	0.063	0.533	0.097	0.449	0.097	11.89	5.19
5	0.515	0.270	0.169	0.203	0.039	0.167	0.165	0.204	0.519	0.269	0.354	0.338	0.684	0.338	6.32	27.09
		P' =	0.200	ksc			Q =	0.060	ksc							
1	0.350	0.010	-0.202	0.009	0.006	0.007	-0.202	0.009	0.350	0.010	0.552	0.013	0.148	0.013	0.62	0.70
2	0.358	0.017	-0.228	0.013	0.013	0.011	-0.228	0.013	0.358	0.017	0.586	0.022	0.130	0.022	1.25	1.05
3	0.383	0.028	-0.265	0.023	0.015	0.018	-0.265	0.023	0.383	0.028	0.648	0.036	0.119	0.036	1.32	1.60
4	0.454	0.051	-0.291	0.072	0.037	0.044	-0.293	0.072	0.456	0.051	0.749	0.088	0.163	0.088	2.80	3.39
5	0.170	0.137	-0.354	0.013	-0.070	0.066	-0.363	0.021	0.179	0.136	0.542	0.137	-0.184	0.138	-7.50	6.93

AREA	Ex	Ex(SD)	Ey	Ey(SD)	Exy	Exy(SD)	E3	E3(SD)	E1	E1(SD)	GAMMA	G(SD)	EV	EV(SD)	PS.	PS(SD)
		P' =	0.200	ksc			Q =	0.070	ksc							
1	0.396	0.011	-0.367	0.009	-0.006	0.007	-0.367	0.009	0.396	0.011	0.763	0.015	0.028	0.015	-0.41	0.55
2	0.420	0.017	-0.408	0.014	-0.001	0.011	-0.408	0.014	0.420	0.017	0.828	0.022	0.013	0.022	-0.06	0.75
3	0.446	0.030	-0.430	0.026	-0.005	0.020	-0.430	0.026	0.446	0.030	0.875	0.040	0.016	0.040	-0.31	1.32
4	0.415	0.036	-0.338	0.041	0.079	0.027	-0.346	0.041	0.423	0.036	0.769	0.055	0.077	0.055	5.93	2.03
5	0.409	0.096	-0.090	0.246	0.090	0.137	-0.106	0.243	0.424	0.104	0.530	0.265	0.319	0.264	9.86	14.73
		P' =	0.200	ksc			Q =	0.080	ksc							
1	0.495	0.027	-0.442	0.012	-0.010	0.015	-0.442	0.012	0.495	0.027	0.937	0.029	0.053	0.029	-0.63	0.90
2	0.556	0.049	-0.480	0.019	-0.010	0.026	-0.480	0.019	0.556	0.049	1.036	0.052	0.076	0.052	-0.58	1.44
3	0.727	0.106	-0.516	0.035	-0.019	0.055	-0.516	0.035	0.727	0.106	1.243	0.111	0.211	0.111	-0.89	2.54
4	1.163	0.323	-0.511	0.105	-0.054	0.169	-0.513	0.105	1.164	0.323	1.677	0.339	0.652	0.340	-1.84	5.79
5	0.162	0.375	-0.392	0.870	-0.046	0.491	-0.396	0.868	0.166	0.382	0.562	0.949	-0.230	0.947	-4.74	49.99
		P' =	0.200	ksc			Q =	0.090	ksc							
1	0.622	0.013	-0.524	0.012	0.004	0.008	-0.524	0.012	0.622	0.013	1.146	0.017	0.097	0.017	0.19	0.43
2	0.670	0.018	-0.568	0.015	0.009	0.012	-0.568	0.015	0.670	0.018	1.238	0.024	0.102	0.024	0.42	0.55
3	0.719	0.025	-0.608	0.026	-0.012	0.018	-0.608	0.026	0.719	0.025	1.327	0.036	0.111	0.036	-0.50	0.78
4	0.753	0.059	-0.690	0.058	0.070	0.041	-0.694	0.058	0.757	0.059	1.450	0.083	0.063	0.083	2.76	1.64
5	0.848	0.363	-0.437	0.236	0.200	0.213	-0.468	0.239	0.878	0.360	1.346	0.432	0.411	0.433	8.67	9.06
		P' =	0.200	ksc			Q =	0.100	ksc							
1	0.732	0.013	-0.604	0.013	-0.009	0.009	-0.604	0.013	0.732	0.013	1.336	0.018	0.128	0.018	-0.38	0.38
2	0.792	0.016	-0.665	0.017	0.008	0.012	-0.665	0.017	0.792	0.016	1.458	0.024	0.127	0.024	0.33	0.46
3	0.871	0.024	-0.734	0.029	0.024	0.019	-0.734	0.029	0.872	0.024	1.606	0.038	0.137	0.038	0.86	0.68
4	0.972	0.058	-0.688	0.077	0.038	0.048	-0.689	0.077	0.973	0.058	1.662	0.096	0.284	0.096	1.29	1.66
5	0.687	0.017	-0.252	0.083	0.317	0.044	-0.349	0.080	0.784	0.030	1.133	0.086	0.435	0.085	17.00	2.21

RUBBER5

AREA	Ex	Ex(SD)	Ey	Ey(SD)	Exy	Exy(SD)	E3	E3(SD)	E1	E1(SD)	GAMMA G(SD)	EV	EV(SD)	PS.	PS(SD)
		P' =	0.198 ksc				Q =	0.003 ksc							
1	0.097	0.018	0.070	0.009	0.037	0.010	0.044	0.013	0.123	0.016	0.080 0.020	0.167	0.020	34.87	7.29
2	0.111	0.033	0.072	0.015	0.034	0.018	0.053	0.021	0.131	0.029	0.078 0.036	0.183	0.036	29.88	13.21
3	0.194	0.073	0.066	0.027	0.082	0.039	0.026	0.040	0.235	0.067	0.209 0.078	0.260	0.078	26.14	10.74
4	0.500	0.192	0.037	0.061	0.103	0.100	0.015	0.072	0.522	0.188	0.506 0.202	0.537	0.201	12.06	11.38
5	0.918	0.718	0.695	0.361	0.744	0.391	0.054	0.536	1.559	0.587	1.505 0.783	1.613	0.804	40.74	15.28
		P' =	0.199 ksc				Q =	0.014 ksc							
1	0.044	0.012	0.065	0.012	0.109	0.008	-0.055	0.012	0.164	0.012	0.219 0.017	0.109	0.017	47.78	2.21
2	0.048	0.021	0.080	0.021	0.114	0.015	-0.051	0.021	0.179	0.021	0.230 0.029	0.128	0.029	49.08	3.65
3	0.005	0.044	0.081	0.044	0.143	0.031	-0.105	0.044	0.191	0.044	0.296 0.063	0.086	0.063	52.46	6.05
4	0.036	0.118	0.196	0.138	0.182	0.091	-0.083	0.124	0.315	0.132	0.398 0.181	0.232	0.181	56.87	13.06
5	0.317	0.143	1.249	0.883	0.793	0.467	-0.137	0.472	1.703	0.780	1.840 0.923	1.566	0.895	60.21	14.06
		P' =	0.199 ksc				Q =	0.023 ksc							
1	0.055	0.012	0.074	0.009	0.151	0.007	-0.087	0.011	0.216	0.010	0.303 0.015	0.129	0.015	46.73	1.41
2	0.059	0.020	0.090	0.015	0.159	0.013	-0.080	0.018	0.239	0.018	0.319 0.025	0.159	0.025	46.81	2.27
3	0.069	0.046	0.101	0.032	0.177	0.028	-0.093	0.040	0.262	0.039	0.355 0.055	0.169	0.056	47.57	4.49
4	0.026	0.151	0.112	0.088	0.249	0.087	-0.184	0.128	0.321	0.118	0.505 0.174	0.137	0.175	49.91	9.89
5	0.479	0.342	0.331	0.473	0.841	0.297	-0.439	0.423	1.249	0.411	1.688 0.593	0.810	0.583	42.49	9.91
		P' =	0.199 ksc				Q =	0.033 ksc							
1	-0.022	0.013	0.014	0.011	0.217	0.008	-0.222	0.012	0.214	0.012	0.436 0.017	-0.008	0.017	47.33	1.12
2	-0.018	0.023	0.037	0.017	0.222	0.014	-0.214	0.020	0.233	0.020	0.447 0.028	0.019	0.028	48.54	1.82
3	-0.052	0.046	0.066	0.031	0.249	0.028	-0.248	0.041	0.263	0.037	0.511 0.055	0.014	0.055	51.65	3.10
4	-0.057	0.144	0.075	0.068	0.307	0.079	-0.305	0.119	0.323	0.104	0.628 0.158	0.018	0.159	51.04	7.24
5	0.874	0.466	0.287	0.069	0.763	0.226	-0.237	0.263	1.398	0.382	1.635 0.453	1.161	0.472	34.47	8.20
		P' =	0.199 ksc				Q =	0.043 ksc							
1	-0.018	0.014	0.019	0.012	0.271	0.009	-0.271	0.013	0.272	0.013	0.543 0.019	0.001	0.019	46.95	0.97
2	0.018	0.023	0.035	0.020	0.273	0.015	-0.247	0.022	0.299	0.022	0.546 0.031	0.053	0.031	45.92	1.61
3	0.001	0.050	0.044	0.035	0.290	0.030	-0.269	0.043	0.314	0.042	0.583 0.061	0.045	0.061	47.11	2.98
4	-0.028	0.164	0.032	0.089	0.325	0.093	-0.324	0.135	0.329	0.128	0.653 0.187	0.004	0.187	47.64	8.21
5	0.216	0.777	-0.094	0.534	0.856	0.465	-0.809	0.642	0.931	0.685	1.740 0.930	0.122	0.943	39.87	15.51
		P' =	0.200 ksc				Q =	0.053 ksc							
1	0.046	0.013	0.049	0.010	0.326	0.008	-0.279	0.012	0.373	0.012	0.652 0.016	0.094	0.016	45.14	0.71
2	0.064	0.023	0.071	0.016	0.346	0.014	-0.279	0.020	0.413	0.020	0.692 0.028	0.134	0.028	45.29	1.17
3	0.022	0.050	0.092	0.032	0.363	0.029	-0.308	0.042	0.422	0.041	0.729 0.059	0.114	0.059	47.75	2.32
4	-0.099	0.144	0.102	0.072	0.405	0.080	-0.416	0.121	0.419	0.105	0.835 0.160	0.003	0.161	51.96	5.51
5	0.461	0.145	0.333	0.136	0.748	0.099	-0.353	0.140	1.147	0.141	1.501 0.198	0.794	0.198	42.54	3.78
		P' =	0.199 ksc				Q =	0.063 ksc							
1	0.054	0.013	0.077	0.012	0.373	0.009	-0.307	0.012	0.438	0.012	0.745 0.017	0.131	0.017	45.86	0.67
2	0.074	0.022	0.109	0.020	0.385	0.015	-0.294	0.021	0.477	0.021	0.770 0.030	0.183	0.030	46.32	1.11
3	0.055	0.046	0.110	0.032	0.395	0.028	-0.313	0.040	0.478	0.039	0.791 0.056	0.165	0.056	47.00	2.02
4	-0.007	0.143	0.108	0.084	0.420	0.082	-0.373	0.120	0.474	0.112	0.847 0.165	0.101	0.165	48.89	5.59
5	0.458	0.360	0.523	0.196	0.744	0.200	-0.255	0.290	1.236	0.283	1.490 0.400	0.981	0.409	46.27	7.87

AREA	Ex	Ex(SD)	Ey	Ey(SD)	Exy	Exy(SD)	E3	E3(SD)	E1	E1(SD)	GAMMA	G(SD)	EV	EV(SD)	PS.	PS(SD)
		P' =	0.200	ksc			Q =	0.072	ksc							
1	0.000	0.014	0.013	0.010	0.430	0.009	-0.423	0.012	0.437	0.012	0.859	0.017	0.014	0.017	45.43	0.58
2	0.014	0.024	0.027	0.017	0.455	0.015	-0.435	0.021	0.475	0.021	0.910	0.030	0.041	0.030	45.41	0.93
3	-0.057	0.050	0.036	0.030	0.485	0.029	-0.498	0.042	0.477	0.040	0.975	0.058	-0.021	0.058	47.74	1.72
4	-0.092	0.148	0.016	0.055	0.551	0.079	-0.591	0.115	0.516	0.107	1.107	0.157	-0.076	0.158	47.79	4.08
5	0.649	0.458	0.304	0.259	1.161	0.257	-0.697	0.354	1.650	0.383	2.348	0.515	0.953	0.526	40.78	6.41
		P' =	0.200	ksc			Q =	0.082	ksc							
1	0.012	0.013	0.008	0.013	0.529	0.009	-0.519	0.013	0.539	0.013	1.058	0.018	0.020	0.018	44.89	0.50
2	0.038	0.021	0.036	0.020	0.548	0.015	-0.511	0.021	0.585	0.021	1.095	0.029	0.074	0.029	44.96	0.76
3	0.011	0.045	0.044	0.038	0.586	0.029	-0.559	0.042	0.614	0.041	1.173	0.059	0.055	0.059	45.80	1.44
4	-0.053	0.121	0.064	0.087	0.583	0.075	-0.580	0.107	0.591	0.103	1.171	0.149	0.011	0.149	47.87	3.65
5	0.922	0.082	0.452	0.471	0.947	0.250	-0.289	0.382	1.663	0.306	1.951	0.498	1.374	0.478	38.03	7.04
		P' =	0.200	ksc			Q =	0.092	ksc							
1	0.030	0.015	0.034	0.012	0.572	0.010	-0.540	0.014	0.604	0.014	1.144	0.019	0.064	0.019	45.09	0.48
2	0.029	0.026	0.052	0.018	0.605	0.016	-0.565	0.022	0.646	0.022	1.211	0.031	0.081	0.032	45.54	0.74
3	-0.018	0.053	0.040	0.035	0.649	0.032	-0.639	0.045	0.661	0.045	1.299	0.064	0.022	0.064	46.27	1.41
4	-0.026	0.171	0.077	0.068	0.688	0.092	-0.665	0.133	0.716	0.126	1.381	0.183	0.051	0.184	47.14	3.81
5	0.676	0.074	0.108	0.018	0.992	0.037	-0.640	0.046	1.424	0.059	2.064	0.073	0.784	0.076	37.02	1.05

RUBBER6

AREA	Ex	Ex(SD)	Ey	Ey(SD)	Exy	Exy(SD)	E3	E3(SD)	E1	E1(SD)	GAMMA G(SD)	EV	EV(SD)	PS.	PS(SD)
		P' =	0.199 ksc				Q =	0.001 ksc							
1	-0.033	0.010	0.461	0.013	0.027	0.008	-0.035	0.010	0.463	0.013	0.498 0.017	0.428	0.017	-3.16	0.96
2	-0.013	0.016	0.525	0.015	0.054	0.011	-0.019	0.016	0.531	0.015	0.549 0.022	0.512	0.022	-5.63	1.15
3	-0.053	0.028	0.579	0.026	0.049	0.019	-0.057	0.028	0.583	0.026	0.640 0.038	0.526	0.038	-4.45	1.69
4	-0.094	0.061	0.495	0.057	0.061	0.042	-0.101	0.061	0.501	0.057	0.602 0.084	0.401	0.084	-5.82	3.98
5	-0.225	0.181	0.345	0.407	0.071	0.230	-0.234	0.187	0.354	0.404	0.588 0.448	0.120	0.446	-7.01	22.46
		P' =	0.200 ksc				Q =	0.010 ksc							
1	0.004	0.011	0.095	0.009	-0.022	0.007	-0.001	0.011	0.100	0.009	0.101 0.014	0.099	0.014	12.85	4.03
2	0.006	0.019	0.100	0.014	-0.016	0.012	0.003	0.019	0.103	0.014	0.100 0.023	0.106	0.023	9.63	6.75
3	-0.011	0.042	0.109	0.026	-0.038	0.025	-0.022	0.041	0.120	0.028	0.142 0.050	0.098	0.050	16.34	10.02
4	-0.075	0.122	0.001	0.061	-0.104	0.068	-0.148	0.107	0.074	0.087	0.222 0.137	-0.074	0.137	34.99	17.69
5	-1.005	1.011	-0.627	0.203	-0.627	0.494	-1.470	0.814	-0.161	0.613	1.309 0.995	-1.632	1.032	36.62	22.58
		P' =	0.200 ksc				Q =	0.020 ksc							
1	0.012	0.008	0.227	0.008	0.004	0.006	0.012	0.008	0.227	0.008	0.215 0.011	0.238	0.011	-1.10	1.47
2	0.013	0.011	0.258	0.011	0.014	0.008	0.013	0.011	0.258	0.011	0.246 0.016	0.271	0.016	-3.18	1.84
3	0.000	0.017	0.285	0.021	0.003	0.013	0.000	0.017	0.285	0.021	0.285 0.027	0.285	0.027	-0.65	2.70
4	-0.036	0.041	0.231	0.047	0.015	0.031	-0.037	0.041	0.232	0.047	0.269 0.063	0.194	0.063	-3.19	6.67
5	-0.266	0.059	0.087	0.118	-0.339	0.068	-0.472	0.081	0.293	0.107	0.765 0.135	-0.179	0.132	31.28	4.95
		P' =	0.200 ksc				Q =	0.030 ksc							
1	-0.040	0.009	0.284	0.008	0.011	0.006	-0.040	0.009	0.284	0.008	0.324 0.013	0.244	0.013	-1.92	1.11
2	-0.048	0.013	0.322	0.011	0.030	0.009	-0.050	0.013	0.324	0.011	0.375 0.017	0.274	0.017	-4.58	1.31
3	-0.087	0.023	0.355	0.018	0.014	0.015	-0.088	0.023	0.356	0.018	0.443 0.029	0.268	0.029	-1.82	1.89
4	-0.118	0.058	0.286	0.040	0.015	0.035	-0.119	0.058	0.287	0.040	0.405 0.070	0.168	0.070	-2.13	4.97
5	-0.054	0.123	0.595	0.049	-0.101	0.064	-0.070	0.122	0.610	0.052	0.680 0.132	0.541	0.132	8.63	5.43
		P' =	0.201 ksc				Q =	0.040 ksc							
1	-0.114	0.008	0.315	0.010	0.001	0.007	-0.114	0.008	0.315	0.010	0.429 0.013	0.201	0.013	-0.12	0.87
2	-0.130	0.012	0.356	0.012	0.014	0.008	-0.131	0.012	0.357	0.012	0.487 0.017	0.226	0.017	-1.59	1.01
3	-0.150	0.023	0.382	0.021	0.003	0.016	-0.150	0.023	0.382	0.021	0.532 0.032	0.233	0.032	-0.37	1.70
4	-0.188	0.062	0.369	0.047	0.033	0.039	-0.190	0.062	0.371	0.047	0.561 0.078	0.182	0.078	-3.38	3.98
5	-0.250	0.468	0.304	0.347	-0.145	0.288	-0.286	0.463	0.340	0.356	0.625 0.582	0.055	0.583	13.85	26.50
		P' =	0.200 ksc				Q =	0.050 ksc							
1	-0.106	0.010	0.448	0.011	-0.001	0.007	-0.106	0.010	0.448	0.011	0.553 0.015	0.342	0.015	0.08	0.75
2	-0.111	0.015	0.512	0.014	0.009	0.010	-0.111	0.015	0.512	0.014	0.623 0.020	0.401	0.020	-0.80	0.93
3	-0.149	0.024	0.550	0.020	-0.009	0.016	-0.149	0.024	0.551	0.020	0.700 0.031	0.401	0.031	0.73	1.28
4	-0.143	0.054	0.568	0.044	-0.044	0.035	-0.146	0.054	0.571	0.044	0.717 0.070	0.425	0.070	3.55	2.79
5	-0.215	0.245	0.328	0.013	-0.071	0.117	-0.224	0.244	0.337	0.033	0.561 0.246	0.113	0.246	7.35	12.04
		P' =	0.200 ksc				Q =	0.060 ksc							
1	-0.182	0.012	0.554	0.012	0.011	0.008	-0.182	0.012	0.554	0.012	0.737 0.017	0.372	0.017	-0.86	0.66
2	-0.188	0.018	0.619	0.017	0.014	0.012	-0.189	0.018	0.620	0.017	0.808 0.025	0.431	0.025	-0.98	0.88
3	-0.245	0.030	0.681	0.025	0.003	0.019	-0.245	0.030	0.681	0.025	0.927 0.039	0.436	0.039	-0.19	1.19
4	-0.297	0.061	0.664	0.055	-0.035	0.041	-0.298	0.061	0.665	0.055	0.963 0.082	0.367	0.082	2.10	2.43
5	-0.248	0.077	0.697	0.252	-0.399	0.137	-0.394	0.116	0.844	0.241	1.237 0.266	0.450	0.263	20.11	6.20

AREA	Ex	Ex(SD)	Ey	Ey(SD)	Exy	Exy(SD)	E3	E3(SD)	E1	E1(SD)	GAMMA G(SD)	EV	EV(SD)	PS.	PS(SD)
		P' =	0.200 ksc				Q =	0.071 ksc							
1	0.068	0.015	0.968	0.019	-0.024	0.012	0.067	0.015	0.969	0.019	0.9[illegible]	0.024	1.036	0.024	1.54	0.77
2	0.067	0.019	1.066	0.021	0.016	0.014	0.067	0.019	1.066	0.021	0.999	0.028	1.133	0.028	-0.89	0.81
3	0.072	0.033	1.176	0.031	0.009	0.023	0.072	0.033	1.176	0.031	1.104	0.045	1.247	0.045	-0.45	1.18
4	0.036	0.086	1.124	0.068	0.095	0.055	0.028	0.086	1.132	0.068	1.104	0.109	1.160	0.109	-4.93	2.83
5	-0.234	0.300	1.360	0.198	0.064	0.177	-0.236	0.299	1.363	0.198	1.599	0.359	1.127	0.359	-2.29	6.32
		P' =	0.200 ksc				Q =	0.081 ksc							
1	-0.366	0.011	0.692	0.016	0.024	0.010	-0.367	0.011	0.693	0.016	1.059	0.019	0.326	0.019	-1.30	0.52
2	-0.393	0.017	0.798	0.017	0.046	0.012	-0.395	0.017	0.800	0.017	1.195	0.023	0.405	0.023	-2.23	0.56
3	-0.412	0.029	0.859	0.026	0.074	0.019	-0.417	0.029	0.863	0.026	1.280	0.039	0.446	0.039	-3.33	0.86
4	-0.316	0.054	0.894	0.065	0.075	0.042	-0.320	0.054	0.898	0.065	1.219	0.084	0.578	0.084	-3.55	1.98
5	-0.610	0.645	0.781	0.306	-0.068	0.162	-0.614	0.047	0.785	0.306	1.398	0.309	0.171	0.309	2.78	6.62
		P' =	0.199 ksc				Q =	0.090 ksc							
1	-0.406	0.011	0.815	0.017	0.019	0.010	-0.407	0.011	0.816	0.017	1.222	0.021	0.409	0.021	-0.87	0.48
2	-0.444	0.016	0.916	0.019	0.031	0.013	-0.445	0.016	0.917	0.019	1.362	0.025	0.472	0.025	-1.29	0.53
3	-0.468	0.024	1.009	0.024	0.002	0.017	-0.468	0.024	1.009	0.024	1.478	0.034	0.541	0.034	-0.09	0.65
4	-0.453	0.048	0.991	0.054	-0.009	0.036	-0.453	0.048	0.991	0.054	1.443	0.072	0.538	0.072	0.35	1.43
5	-0.319	0.004	1.299	0.296	0.096	0.155	-0.325	0.019	1.305	0.295	1.630	0.297	0.980	0.296	-3.37	5.46
		P' =	0.200 ksc				Q =	0.100 ksc							
1	-0.464	0.012	0.936	0.020	0.030	0.012	-0.465	0.012	0.936	0.020	1.401	0.023	0.472	0.023	-1.23	0.48
2	-0.494	0.016	1.065	0.024	0.051	0.014	-0.496	0.016	1.067	0.024	1.563	0.029	0.571	0.029	-1.87	0.53
3	-0.456	0.030	1.195	0.034	0.042	0.023	-0.457	0.030	1.196	0.034	1.653	0.045	0.739	0.045	-1.46	0.79
4	-0.448	0.066	1.199	0.077	0.108	0.051	-0.455	0.066	1.206	0.077	1.662	0.101	0.751	0.101	-3.72	1.75
5	-0.539	0.011	1.274	0.049	0.006	0.026	-0.539	0.011	1.274	0.049	1.813	0.050	0.735	0.050	-0.18	0.83

RUBBER7

AREA	Ex	Ex(SD)	Ey	Ey(SD)	Exy	Exy(SD)	E3	E3(SD)	E1	E1(SD)	GAMMA	G(SD)	EV	EV(SD)	PS.	PS(SD)
		P' =	0.199	ksc			Q =	0.003	ksc							
1	0.012	0.011	0.050	0.010	0.013	0.007	0.009	0.011	0.054	0.010	0.045	0.015	0.062	0.015	72.97	9.37
2	-0.012	0.020	0.066	0.015	0.023	0.012	-0.018	0.020	0.072	0.015	0.090	0.025	0.053	0.025	74.83	7.89
3	-0.015	0.034	0.080	0.027	0.057	0.022	-0.042	0.033	0.107	0.028	0.149	0.043	0.065	0.043	64.90	8.32
4	0.064	0.085	0.141	0.060	0.082	0.052	0.012	0.078	0.194	0.068	0.182	0.104	0.205	0.104	57.41	16.41
5	-0.271	0.263	-0.257	0.310	0.406	0.205	-0.669	0.287	0.142	0.287	0.812	0.410	-0.527	0.406	45.49	14.34
		P' =	0.200	ksc			Q =	0.013	ksc							
1	0.005	0.010	0.044	0.009	0.036	0.007	-0.017	0.010	0.065	0.009	0.082	0.014	0.049	0.014	59.31	4.78
2	-0.002	0.017	0.063	0.014	0.046	0.011	-0.026	0.017	0.086	0.015	0.112	0.022	0.061	0.022	62.76	5.62
3	-0.017	0.033	0.074	0.020	0.055	0.019	-0.043	0.031	0.100	0.023	0.142	0.038	0.057	0.038	64.74	7.67
4	0.042	0.077	0.092	0.044	0.049	0.045	0.011	0.069	0.122	0.055	0.111	0.089	0.134	0.089	58.48	22.95
5	-0.481	0.472	0.055	0.047	0.023	0.226	-0.482	0.471	0.056	0.050	0.538	0.473	-0.425	0.474	87.56	24.02
		P' =	0.200	ksc			Q =	0.023	ksc							
1	0.003	0.013	0.050	0.010	0.066	0.008	-0.044	0.012	0.097	0.011	0.140	0.016	0.053	0.016	54.65	3.25
2	0.001	0.020	0.059	0.016	0.066	0.013	-0.042	0.019	0.102	0.018	0.144	0.026	0.059	0.026	56.90	5.19
3	0.014	0.036	0.072	0.027	0.081	0.022	-0.043	0.033	0.129	0.030	0.171	0.044	0.086	0.044	54.83	7.43
4	0.144	0.091	0.143	0.049	0.070	0.052	0.074	0.072	0.214	0.073	0.140	0.103	0.288	0.103	44.79	21.19
5	0.147	0.069	-0.091	0.003	-0.071	0.033	-0.110	0.018	0.166	0.067	0.277	0.068	0.056	0.069	-15.33	6.86
		P' =	0.200	ksc			Q =	0.033	ksc							
1	-0.019	0.011	0.022	0.011	0.112	0.008	-0.113	0.011	0.116	0.011	0.228	0.016	0.003	0.016	50.10	1.95
2	-0.045	0.018	0.050	0.017	0.119	0.013	-0.125	0.018	0.131	0.017	0.257	0.025	0.006	0.025	55.90	2.79
3	0.003	0.032	0.093	0.029	0.116	0.022	-0.076	0.031	0.172	0.030	0.248	0.043	0.096	0.043	55.57	4.99
4	0.086	0.066	0.121	0.048	0.117	0.041	-0.015	0.058	0.222	0.056	0.236	0.081	0.207	0.082	49.29	9.89
5	-0.011	0.378	0.185	0.198	0.114	0.208	-0.064	0.350	0.237	0.235	0.301	0.419	0.174	0.426	65.27	40.03
		P' =	0.200	ksc			Q =	0.043	ksc							
1	0.052	0.013	0.051	0.010	0.159	0.008	-0.108	0.012	0.211	0.012	0.319	0.017	0.103	0.017	44.89	1.49
2	0.032	0.022	0.068	0.016	0.164	0.013	-0.115	0.019	0.214	0.018	0.329	0.027	0.100	0.027	48.17	2.31
3	0.034	0.040	0.109	0.026	0.190	0.024	-0.122	0.035	0.265	0.033	0.387	0.048	0.142	0.048	50.59	3.57
4	0.060	0.097	0.144	0.064	0.206	0.058	-0.108	0.084	0.312	0.078	0.420	0.116	0.203	0.116	50.75	7.89
5	-0.117	0.450	0.405	0.180	0.071	0.234	-0.127	0.446	0.415	0.187	0.542	0.483	0.288	0.485	82.43	24.79
		P' =	0.200	ksc			Q =	0.053	ksc							
1	0.046	0.015	0.062	0.013	0.228	0.010	-0.174	0.014	0.282	0.014	0.456	0.020	0.108	0.020	45.95	1.26
2	0.022	0.026	0.105	0.018	0.257	0.016	-0.197	0.023	0.323	0.022	0.520	0.032	0.127	0.032	49.58	1.74
3	0.056	0.042	0.121	0.031	0.284	0.026	-0.198	0.037	0.375	0.036	0.573	0.052	0.177	0.052	48.29	2.61
4	0.131	0.089	0.097	0.076	0.299	0.058	-0.186	0.082	0.414	0.082	0.600	0.117	0.227	0.117	43.39	5.58
5	-0.312	0.653	0.104	0.020	0.586	0.311	-0.726	0.522	0.518	0.363	1.244	0.623	-0.208	0.653	54.75	14.91
		P' =	0.201	ksc			Q =	0.073	ksc							
1	0.060	0.017	0.063	0.015	0.337	0.011	-0.276	0.016	0.398	0.016	0.674	0.023	0.123	0.023	45.15	0.96
2	0.008	0.028	0.067	0.022	0.351	0.018	-0.315	0.025	0.390	0.025	0.705	0.035	0.075	0.036	47.38	1.44
3	0.023	0.059	0.038	0.039	0.397	0.035	-0.367	0.050	0.428	0.050	0.795	0.071	0.061	0.071	45.53	2.55
4	0.038	0.143	0.299	0.082	0.458	0.082	-0.308	0.124	0.644	0.107	0.952	0.165	0.337	0.165	52.97	4.96
5	-0.664	0.548	0.255	0.308	0.789	0.307	-1.117	0.494	0.709	0.376	1.826	0.616	-0.409	0.629	60.10	9.79

AREA	Ex	Ex(SD)	Ey	Ey(SD)	Exy	Exy(SD)	E3	E3(SD)	E1	E1(SD)	GAMMA	G(SD)	EV	EV(SD)	PS.	PS(SD)
		P' =	0.201	ksc			Q =	0.083	ksc							
1	0.051	0.015	0.068	0.013	0.445	0.010	-0.385	0.014	0.504	0.014	0.890	0.020	0.119	0.020	45.54	0.63
2	0.053	0.021	0.094	0.019	0.477	0.014	-0.404	0.020	0.551	0.020	0.955	0.028	0.147	0.028	46.23	0.84
3	0.124	0.036	0.132	0.031	0.525	0.024	-0.397	0.034	0.653	0.034	1.050	0.048	0.256	0.048	45.22	1.30
4	0.241	0.098	0.125	0.067	0.561	0.059	-0.381	0.082	0.747	0.085	1.128	0.119	0.366	0.119	42.05	3.01
5	0.590	0.090	-0.207	0.078	0.555	0.059	-0.492	0.080	0.874	0.087	1.366	0.119	0.382	0.119	27.16	2.49
		P' =	0.200	ksc			Q =	0.093	ksc							
1	0.025	0.016	0.031	0.014	0.578	0.011	-0.551	0.015	0.606	0.015	1.156	0.021	0.055	0.021	45.15	0.53
2	0.029	0.024	0.056	0.017	0.619	0.015	-0.577	0.021	0.661	0.021	1.238	0.030	0.085	0.030	45.62	0.69
3	0.082	0.037	0.070	0.032	0.654	0.024	-0.578	0.034	0.730	0.034	1.308	0.049	0.152	0.049	44.72	1.07
4	0.011	0.070	0.049	0.058	0.743	0.046	-0.713	0.064	0.773	0.064	1.487	0.091	0.060	0.091	45.74	1.76
5	-0.139	0.635	0.203	0.085	0.889	0.306	-0.873	0.481	0.937	0.396	1.810	0.611	0.064	0.641	50.45	10.11

RUBBER8

AREA	Ex	Ex(SD)	Ey	Ey(SD)	Exy	Exy(SD)	E3	E3(SD)	E1	E1(SD)	GAMMA G(SD)	EV	EV(SD)	PS.	PS(SD)
		P' =	0.200 ksc				Q =	0.009 ksc							
1	0.018	0.011	-0.027	0.009	0.022	0.007	-0.035	0.009	0.027	0.011	0.062 0.014	-0.008	0.014	22.02	6.50
2	0.000	0.018	-0.046	0.015	0.034	0.012	-0.064	0.016	0.018	0.017	0.081 0.024	-0.046	0.024	27.71	8.27
3	0.001	0.033	-0.060	0.031	0.025	0.023	-0.069	0.031	0.009	0.032	0.078 0.045	-0.059	0.045	19.50	16.57
4	0.082	0.082	-0.096	0.077	0.001	0.056	-0.096	0.077	0.082	0.082	0.178 0.112	-0.015	0.112	0.24	18.05
5	0.234	0.050	-0.183	0.495	-0.202	0.261	-0.265	0.465	0.316	0.200	0.581 0.513	0.051	0.497	-22.00	25.33
		P' =	0.200 ksc				Q =	0.018 ksc							
1	0.018	0.013	-0.097	0.009	0.044	0.008	-0.112	0.009	0.033	0.013	0.144 0.016	-0.079	0.016	18.53	3.16
2	-0.011	0.020	-0.104	0.013	0.044	0.012	-0.121	0.014	0.006	0.019	0.128 0.024	-0.115	0.024	21.64	5.45
3	0.040	0.041	-0.133	0.027	0.025	0.025	-0.137	0.027	0.043	0.041	0.180 0.050	-0.094	0.049	7.95	7.88
4	0.158	0.104	-0.141	0.056	0.050	0.059	-0.149	0.058	0.166	0.103	0.315 0.118	0.017	0.118	9.14	10.73
5	0.033	1.123	-0.128	0.179	0.224	0.543	-0.285	0.638	0.190	0.905	0.475 1.097	-0.095	1.137	35.09	68.47
		P' =	0.200 ksc				Q =	0.027 ksc							
1	0.108	0.012	-0.120	0.012	0.047	0.008	-0.129	0.012	0.117	0.012	0.246 0.017	-0.012	0.017	11.11	1.95
2	0.114	0.020	-0.141	0.019	0.057	0.014	-0.153	0.019	0.126	0.019	0.279 0.027	-0.027	0.027	12.13	2.78
3	0.135	0.032	-0.159	0.036	0.052	0.024	-0.168	0.036	0.144	0.032	0.313 0.048	-0.024	0.048	9.76	4.37
4	0.154	0.079	-0.140	0.086	0.000	0.058	-0.140	0.086	0.154	0.079	0.293 0.117	0.014	0.117	0.09	11.42
5	0.515	0.336	-0.040	0.223	0.283	0.198	-0.159	0.240	0.634	0.319	0.792 0.401	0.475	0.403	22.75	14.50
		P' =	0.201 ksc				Q =	0.038 ksc							
1	0.090	0.012	-0.187	0.011	0.085	0.008	-0.211	0.011	0.114	0.012	0.325 0.016	-0.097	0.016	15.67	1.41
2	0.064	0.018	-0.207	0.016	0.099	0.012	-0.239	0.016	0.096	0.018	0.335 0.024	-0.143	0.024	18.04	2.08
3	0.096	0.037	-0.293	0.030	0.110	0.024	-0.322	0.030	0.125	0.037	0.447 0.048	-0.197	0.048	14.76	3.07
4	0.120	0.075	-0.301	0.065	0.057	0.050	-0.308	0.065	0.128	0.075	0.436 0.099	-0.181	0.099	7.64	6.53
5	0.305	0.439	-0.053	0.561	-0.122	0.361	-0.091	0.554	0.343	0.454	0.434 0.717	0.252	0.712	-17.18	47.60
		P' =	0.199 ksc				Q =	0.047 ksc							
1	0.175	0.011	-0.211	0.010	0.123	0.008	-0.246	0.010	0.211	0.011	0.457 0.015	-0.035	0.015	16.23	0.96
2	0.161	0.018	-0.234	0.016	0.139	0.012	-0.278	0.016	0.205	0.018	0.483 0.024	-0.073	0.024	17.55	1.43
3	0.194	0.032	-0.260	0.031	0.138	0.022	-0.299	0.031	0.233	0.032	0.532 0.045	-0.066	0.045	15.68	2.40
4	0.197	0.083	-0.247	0.052	0.137	0.049	-0.286	0.054	0.236	0.081	0.522 0.098	-0.050	0.098	15.82	5.38
5	0.046	0.677	-0.481	0.008	0.315	0.323	-0.628	0.274	0.193	0.605	0.822 0.663	-0.435	0.677	25.07	23.32
		P' =	0.200 ksc				Q =	0.057 ksc							
1	0.170	0.012	-0.351	0.010	0.148	0.008	-0.390	0.010	0.209	0.012	0.599 0.015	-0.180	0.015	14.79	0.74
2	0.152	0.018	-0.403	0.014	0.169	0.011	-0.450	0.014	0.200	0.017	0.650 0.023	-0.251	0.023	15.66	1.00
3	0.173	0.032	-0.448	0.025	0.183	0.020	-0.498	0.025	0.223	0.032	0.720 0.041	-0.275	0.041	15.26	1.62
4	0.226	0.069	-0.401	0.050	0.198	0.043	-0.458	0.051	0.283	0.068	0.742 0.086	-0.175	0.085	16.14	3.30
5	0.050	0.134	-0.473	0.308	0.101	0.174	-0.492	0.304	0.068	0.144	0.561 0.336	-0.424	0.336	10.56	17.63
		P' =	0.200 ksc				Q =	0.067 ksc							
1	0.297	0.014	-0.336	0.011	0.161	0.009	-0.375	0.012	0.336	0.013	0.710 0.018	-0.039	0.018	13.44	0.71
2	0.289	0.020	-0.369	0.015	0.182	0.013	-0.416	0.016	0.336	0.020	0.752 0.025	-0.080	0.025	14.49	0.96
3	0.304	0.037	-0.422	0.027	0.176	0.023	-0.462	0.028	0.344	0.037	0.807 0.046	-0.118	0.046	12.97	1.64
4	0.295	0.093	-0.374	0.048	0.126	0.052	-0.397	0.050	0.318	0.091	0.715 0.105	-0.079	0.105	10.28	4.19
5	0.182	0.393	-0.505	0.235	0.134	0.224	-0.530	0.241	0.207	0.388	0.737 0.458	-0.323	0.458	10.63	17.52

AREA	Ex	Ex(SD)	Ey	Ey(SD)	Exy	Exy(SD)	E3	E3(SD)	E1	E1(SD)	GAMMA	G(SD)	EV	EV(SD)	PS.	PS(SD)
			P' = 0.200 ksc				Q = 0.077 ksc									
1	0.322	0.012	-0.426	0.010	0.200	0.008	-0.476	0.010	0.372	0.012	0.848	0.016	-0.104	0.016	14.04	0.52
2	0.315	0.018	-0.466	0.013	0.213	0.011	-0.521	0.013	0.370	0.018	0.890	0.023	-0.151	0.023	14.28	0.73
3	0.296	0.030	-0.517	0.026	0.210	0.020	-0.568	0.026	0.348	0.030	0.916	0.040	-0.221	0.040	13.66	1.25
4	0.424	0.059	-0.518	0.025	0.170	0.032	-0.548	0.026	0.453	0.058	1.001	0.064	-0.095	0.064	9.91	1.84
5	0.290	0.245	-0.469	0.191	0.219	0.154	-0.546	0.194	0.347	0.241	0.894	0.311	-0.200	0.311	14.69	9.91
			P' = 0.200 ksc				Q = 0.087 ksc									
1	0.386	0.013	-0.481	0.012	0.233	0.009	-0.540	0.012	0.445	0.013	0.985	0.018	-0.095	0.018	14.13	0.52
2	0.400	0.018	-0.543	0.019	0.254	0.013	-0.607	0.018	0.464	0.018	1.071	0.02[illegible]	-0.143	0.026	14.18	0.69
3	0.379	0.032	-0.635	0.030	0.271	0.022	-0.703	0.031	0.447	0.032	1.150	0.045	-0.256	0.045	14.06	1.11
4	0.491	0.072	-0.644	0.066	0.217	0.049	-0.684	0.066	0.531	0.072	1.215	0.098	-0.154	0.098	10.45	2.30
5	0.569	0.050	-0.416	0.644	0.351	0.339	-0.528	0.614	0.681	0.209	1.210	0.653	0.153	0.646	17.73	15.70
			P' = 0.200 ksc				Q = 0.097 ksc									
1	0.489	0.012	-0.577	0.014	0.261	0.009	-0.638	0.014	0.549	0.012	1.187	0.018	-0.089	0.018	13.03	0.43
2	0.500	0.017	-0.656	0.017	0.295	0.012	-0.727	0.017	0.571	0.017	1.298	0.024	-0.156	0.024	13.52	0.53
3	0.511	0.032	-0.735	0.031	0.311	0.022	-0.808	0.031	0.585	0.032	1.393	0.045	-0.224	0.045	13.25	0.92
4	0.618	0.068	-0.775	0.075	0.276	0.050	-0.828	0.074	0.671	0.068	1.500	0.101	-0.157	0.101	10.82	1.92
5	0.558	0.660	-0.298	0.608	0.267	0.448	-0.374	0.610	0.634	0.654	1.008	0.897	0.260	0.898	15.97	25.49

RUBBER9

AREA	Ex	Ex(SD)	Ey	Ey(SD)	Exy	Exy(SD)	E3	E3(SD)	E1	E1(SD)	GAMMA	G(SD)	EV	EV(SD)	PS.	PS(SD)
		P' =	0.200	ksc			Q =	0.005	ksc							
1	0.042	0.013	0.006	0.010	0.063	0.008	-0.041	0.011	0.089	0.012	0.131	0.017	0.048	0.017	37.05	3.64
2	0.062	0.024	0.004	0.016	0.065	0.014	-0.038	0.019	0.104	0.022	0.142	0.029	0.066	0.029	32.90	5.80
3	0.117	0.044	-0.028	0.027	0.114	0.026	-0.091	0.031	0.180	0.041	0.271	0.052	0.089	0.052	28.74	5.45
4	-0.002	0.075	-0.020	0.029	0.048	0.040	-0.060	0.053	0.038	0.060	0.098	0.081	-0.022	0.081	39.98	23.61
5	0.490	0.326	-0.191	0.043	-0.010	0.157	-0.191	0.043	0.490	0.326	0.681	0.328	0.299	0.328	-0.83	13.20
		P' =	0.200	ksc			Q =	0.014	ksc							
1	0.065	0.014	-0.012	0.008	0.081	0.008	-0.064	0.010	0.117	0.012	0.180	0.016	0.053	0.016	32.36	2.53
2	0.065	0.024	-0.005	0.014	0.090	0.014	-0.067	0.018	0.126	0.021	0.193	0.028	0.060	0.028	34.27	4.11
3	0.132	0.048	-0.009	0.026	0.111	0.027	-0.069	0.032	0.193	0.043	0.262	0.054	0.124	0.054	28.72	5.91
4	0.021	0.083	-0.053	0.048	0.069	0.048	-0.094	0.059	0.062	0.075	0.156	0.096	-0.032	0.096	30.78	17.69
5	0.245	0.679	0.269	0.001	0.302	0.324	-0.045	0.475	0.559	0.456	0.604	0.648	0.514	0.679	-43.88	32.16
		P' =	0.200	ksc			Q =	0.024	ksc							
1	0.099	0.015	-0.070	0.011	0.114	0.009	-0.127	0.012	0.157	0.014	0.284	0.018	0.029	0.018	26.81	1.85
2	0.132	0.025	-0.065	0.017	0.120	0.015	-0.122	0.019	0.189	0.024	0.310	0.030	0.067	0.030	25.41	2.80
3	0.212	0.045	-0.063	0.030	0.171	0.027	-0.145	0.033	0.294	0.043	0.439	0.054	0.149	0.054	25.60	3.55
4	0.094	0.101	-0.045	0.054	0.105	0.057	-0.101	0.067	0.150	0.092	0.251	0.115	0.050	0.114	28.18	13.10
5	0.567	0.587	0.090	0.201	-0.038	0.300	0.087	0.206	0.570	0.586	0.484	0.619	0.657	0.621	-4.50	35.45
		P' =	0.200	ksc			Q =	0.034	ksc							
1	0.169	0.015	-0.043	0.009	0.159	0.009	-0.128	0.011	0.255	0.014	0.383	0.017	0.127	0.017	28.19	1.28
2	0.210	0.025	-0.047	0.015	0.173	0.015	-0.134	0.017	0.297	0.023	0.431	0.029	0.163	0.029	26.77	1.94
3	0.255	0.046	-0.053	0.029	0.225	0.027	-0.172	0.033	0.374	0.043	0.545	0.055	0.202	0.055	27.78	2.87
4	0.201	0.080	-0.019	0.062	0.189	0.050	-0.128	0.066	0.310	0.075	0.438	0.101	0.181	0.101	29.92	6.60
5	0.679	0.490	0.512	0.276	0.438	0.275	0.150	0.371	1.041	0.410	0.892	0.551	1.191	0.562	39.60	18.07
		P' =	0.200	ksc			Q =	0.044	ksc							
1	0.130	0.014	-0.126	0.011	0.213	0.009	-0.247	0.012	0.251	0.014	0.498	0.018	0.004	0.018	29.49	1.04
2	0.170	0.024	-0.134	0.018	0.229	0.015	-0.256	0.019	0.293	0.023	0.549	0.030	0.036	0.030	28.23	1.57
3	0.253	0.043	-0.167	0.034	0.270	0.027	-0.299	0.036	0.385	0.041	0.685	0.055	0.086	0.055	26.05	2.28
4	0.135	0.078	-0.241	0.059	0.236	0.049	-0.355	0.062	0.249	0.074	0.603	0.097	-0.106	0.097	25.74	4.63
5	0.385	0.929	-0.264	0.160	0.423	0.451	-0.472	0.419	0.594	0.825	1.066	0.923	0.121	0.942	26.25	25.09
		P' =	0.200	ksc			Q =	0.054	ksc							
1	0.193	0.015	-0.139	0.009	0.237	0.009	-0.263	0.011	0.316	0.014	0.579	0.018	0.054	0.018	27.49	0.88
2	0.245	0.025	-0.132	0.015	0.263	0.014	-0.267	0.017	0.380	0.023	0.647	0.029	0.114	0.029	27.17	1.27
3	0.315	0.041	-0.156	0.022	0.323	0.023	-0.321	0.027	0.479	0.038	0.800	0.046	0.158	0.046	26.97	1.66
4	0.198	0.076	-0.198	0.045	0.307	0.044	-0.365	0.053	0.365	0.070	0.731	0.088	-0.000	0.088	28.61	3.47
5	-0.112	0.427	-0.533	0.301	0.219	0.258	-0.626	0.321	-0.018	0.407	0.608	0.520	-0.645	0.523	23.10	24.54
		P' =	0.200	ksc			Q =	0.064	ksc							
1	0.212	0.015	-0.191	0.010	0.309	0.009	-0.358	0.012	0.379	0.014	0.738	0.018	0.021	0.018	28.48	0.71
2	0.245	0.025	-0.207	0.017	0.324	0.015	-0.376	0.019	0.414	0.023	0.790	0.030	0.038	0.030	27.57	1.10
3	0.316	0.041	-0.216	0.030	0.356	0.025	-0.394	0.032	0.494	0.039	0.889	0.051	0.100	0.051	26.63	1.63
4	0.227	0.095	-0.224	0.047	0.367	0.053	-0.429	0.062	0.432	0.086	0.861	0.106	0.003	0.106	29.20	3.54
5	1.310	0.510	-0.014	0.232	0.380	0.272	-0.116	0.256	1.412	0.493	1.527	0.558	1.296	0.560	14.94	10.31

AREA	Ex	Ex(SD)	Ey	Ey(SD)	Exy	Exy(SD)	E3	E3(SD)	E1	E1(SD)	GAMMA	G(SD)	EV	EV(SD)	PS.	PS(SD)
		P' =	0.200	ksc			Q =	0.074	ksc							
1	0.261	0.017	-0.204	0.011	0.350	0.010	-0.392	0.013	0.449	0.016	0.841	0.020	0.057	0.020	28.21	0.68
2	0.290	0.028	-0.216	0.018	0.360	0.017	-0.403	0.020	0.477	0.026	0.880	0.033	0.074	0.033	27.43	1.09
3	0.353	0.056	-0.202	0.037	0.402	0.033	-0.413	0.041	0.564	0.052	0.977	0.067	0.151	0.067	27.70	1.96
4	0.415	0.146	-0.159	0.082	0.282	0.084	-0.275	0.093	0.531	0.138	0.805	0.168	0.256	0.167	22.25	5.97
5	0.403	1.055	0.641	0.440	0.482	0.554	0.026	0.857	1.018	0.719	0.992	1.107	1.044	1.143	-38.06	32.87
		P' =	0.200	ksc			Q =	0.084	ksc							
1	0.278	0.017	-0.264	0.013	0.404	0.011	-0.480	0.014	0.494	0.016	0.974	0.021	0.014	0.021	28.10	0.63
2	0.296	0.027	-0.278	0.022	0.441	0.017	-0.517	0.023	0.535	0.026	1.052	0.035	0.019	0.035	28.49	0.94
3	0.392	0.050	-0.274	0.042	0.512	0.032	-0.552	0.043	0.670	0.048	1.222	0.065	0.118	0.065	28.48	1.52
4	0.400	0.107	-0.190	0.109	0.512	0.076	-0.486	0.108	0.696	0.107	1.182	0.152	0.210	0.152	30.04	3.69
5	0.404	0.092	0.487	0.548	0.824	0.290	-0.380	0.390	1.271	0.408	1.651	0.581	0.892	0.556	-43.56	9.65
		P' =	0.200	ksc			Q =	0.094	ksc							
1	0.319	0.018	-0.315	0.011	0.453	0.011	-0.551	0.013	0.555	0.017	1.105	0.021	0.004	0.021	27.48	0.54
2	0.345	0.028	-0.328	0.019	0.484	0.017	-0.581	0.021	0.598	0.026	1.179	0.033	0.017	0.033	27.61	0.81
3	0.474	0.046	-0.369	0.030	0.540	0.027	-0.632	0.033	0.738	0.044	1.370	0.055	0.105	0.055	26.00	1.15
4	0.361	0.107	-0.355	0.058	0.511	0.061	-0.621	0.071	0.627	0.098	1.248	0.122	0.006	0.122	27.51	2.80
5	0.407	0.058	-0.418	0.187	0.468	0.102	-0.630	0.172	0.618	0.095	1.248	0.199	-0.012	0.195	24.31	4.53

RUBBER2

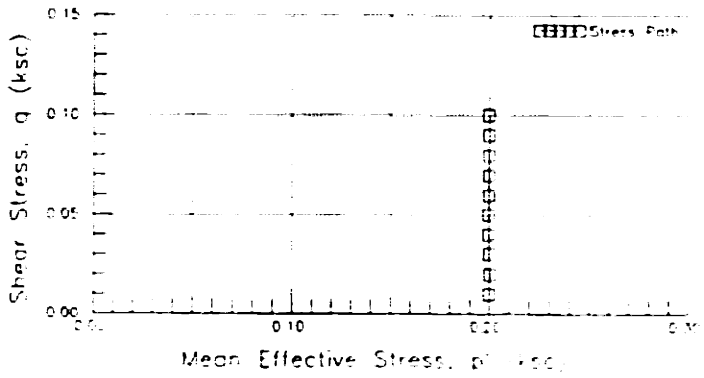

(a) q versus p'

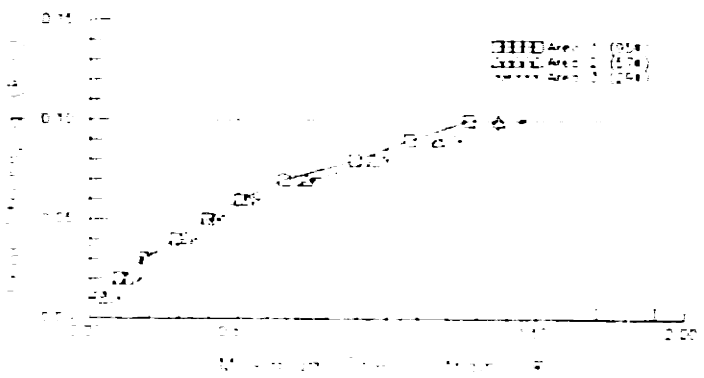

(b) Shear Stress versus Shear Strain

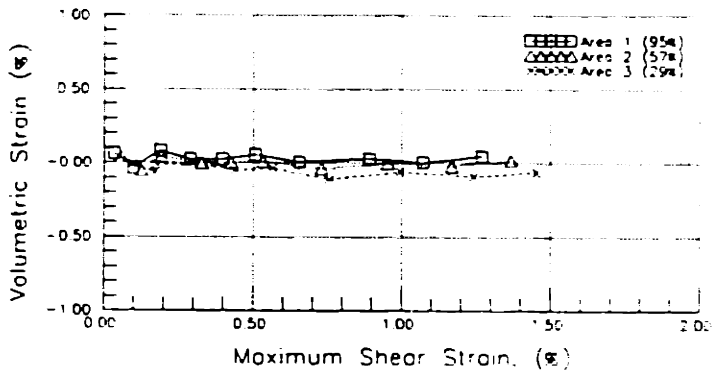

(c) Volumetric Strain versus Shear Strain

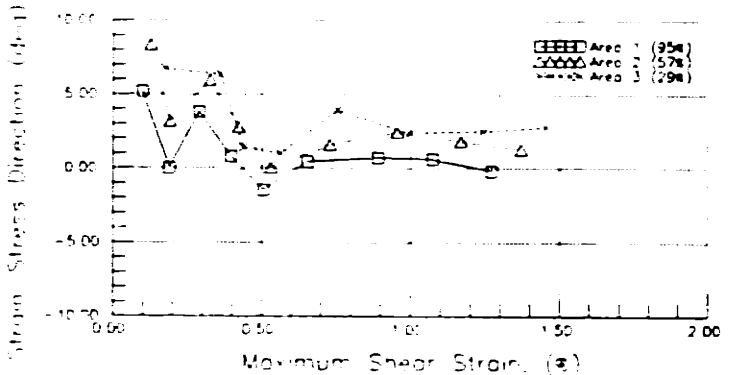

(d) Strain-Stress Direction versus Shear Strain

RUBBER3

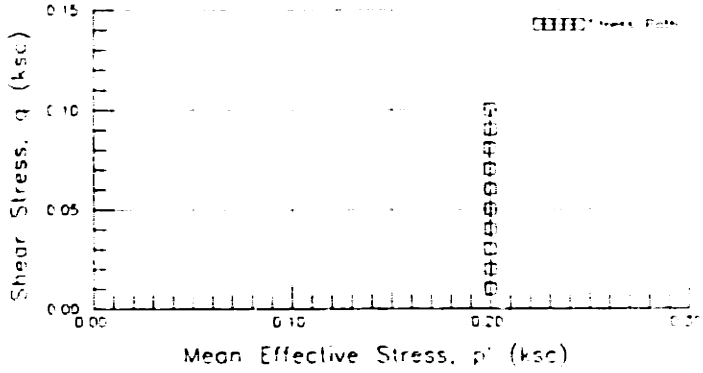

(a) q versus p'

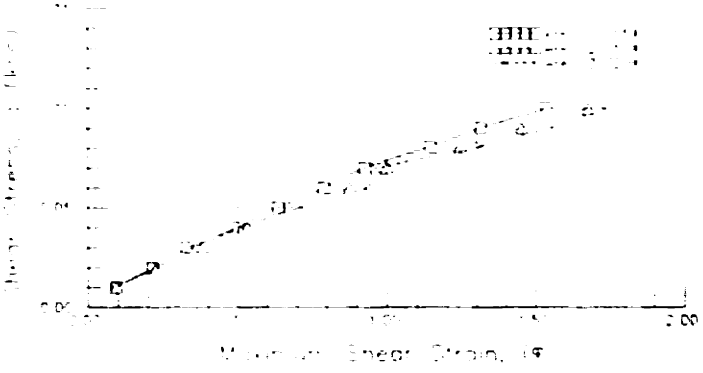

(b) Shear Stress versus Shear Strain

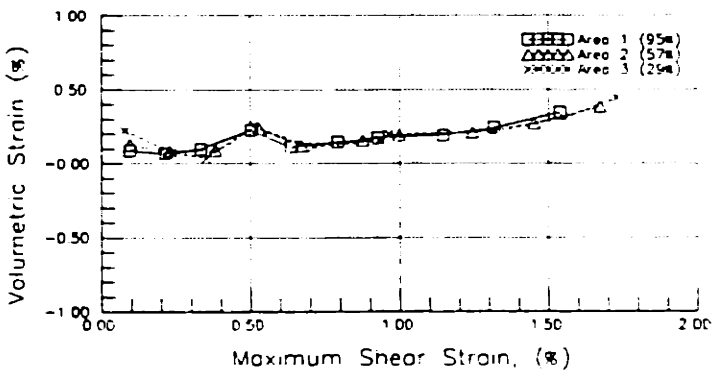

(c) Volumetric Strain versus Shear Strain

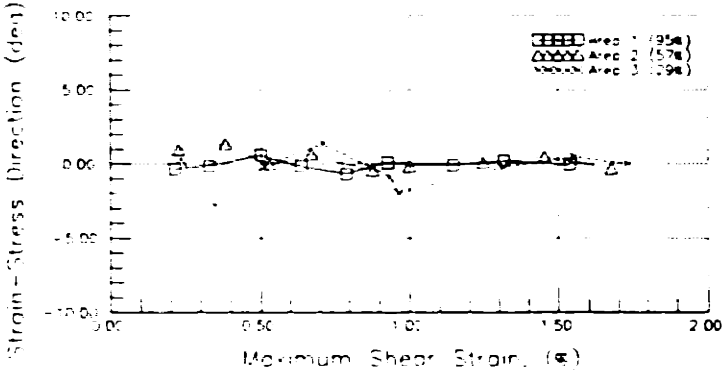

(d) Strain-Stress Direction versus Shear Strain

RUBBER4

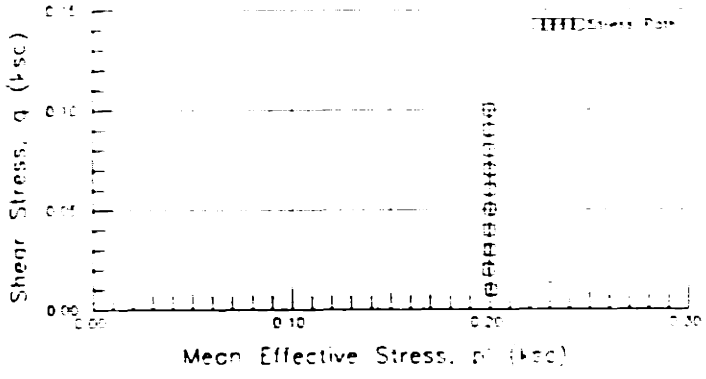

(a) q versus p'

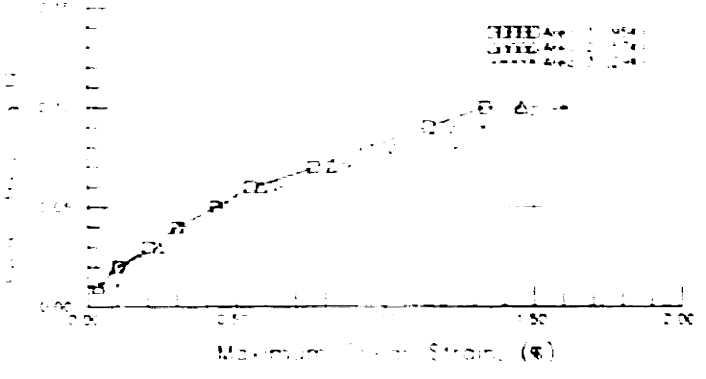

(b) Shear Stress versus Shear Strain

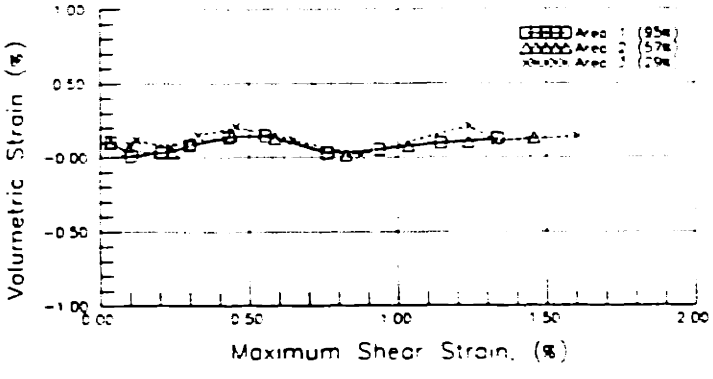

(c) Volumetric Strain versus Shear Strain

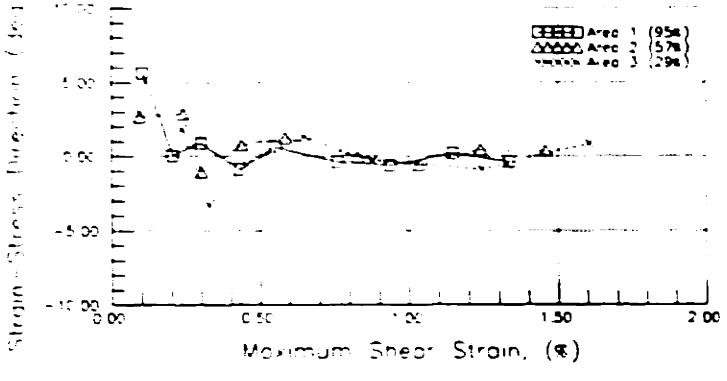

(d) Strain–Stress Direction versus Shear Strain

RUBBER5

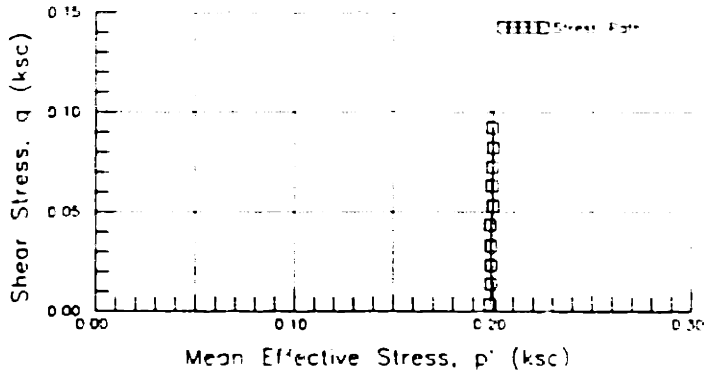

(a) q versus p'

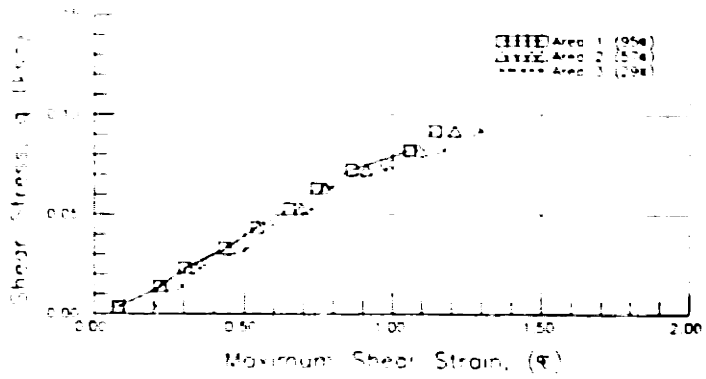

(b) Shear Stress versus Shear Strain

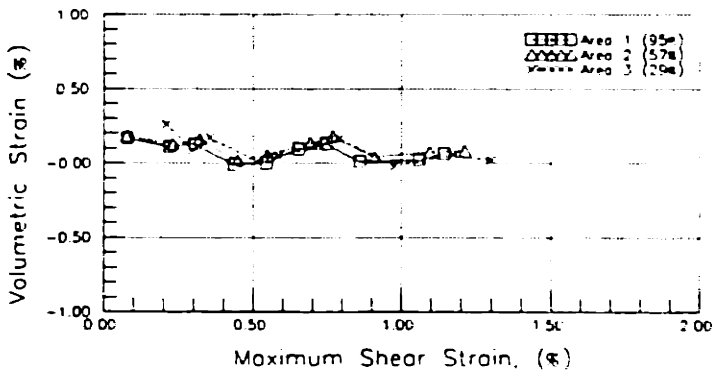

(c) Volumetric Strain versus Shear Strain

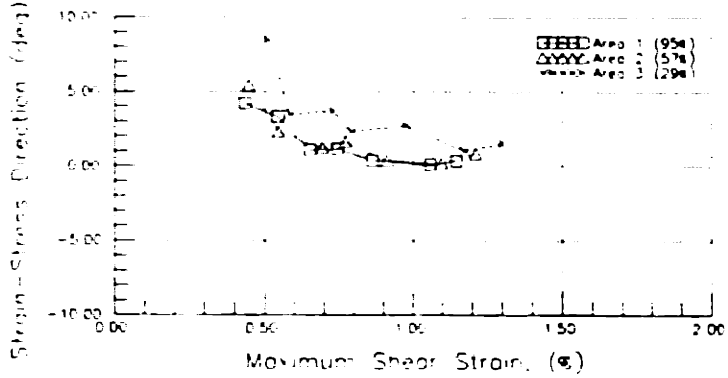

(d) Strain-Stress Direction versus Shear Strain

RUBBER6

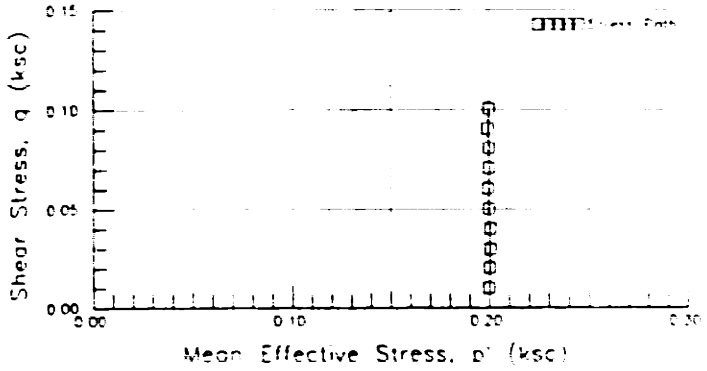

(a) q versus p'

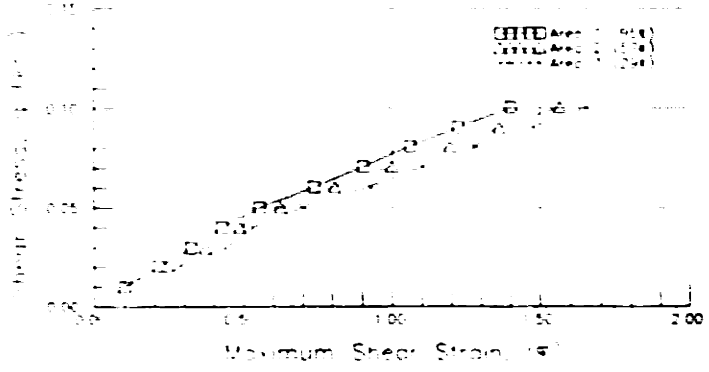

(b) Shear Stress versus Shear Strain

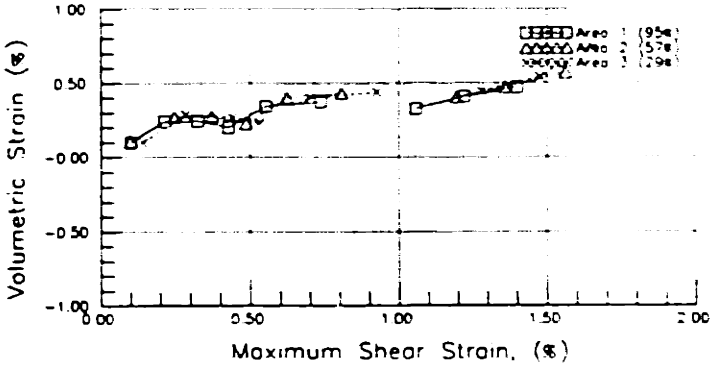

(c) Volumetric Strain versus Shear Strain

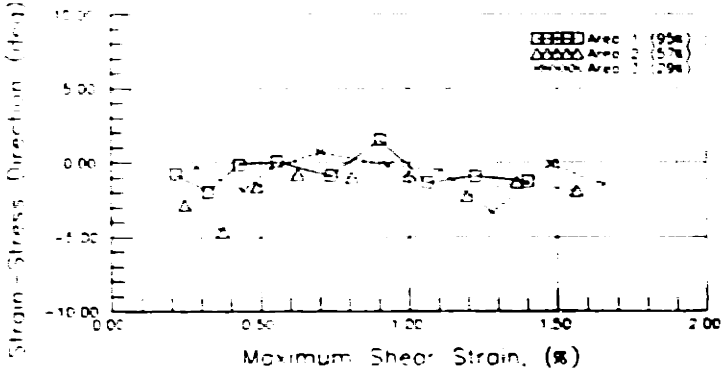

(d) Strain-Stress Direction versus Shear Strain

RUBBER7

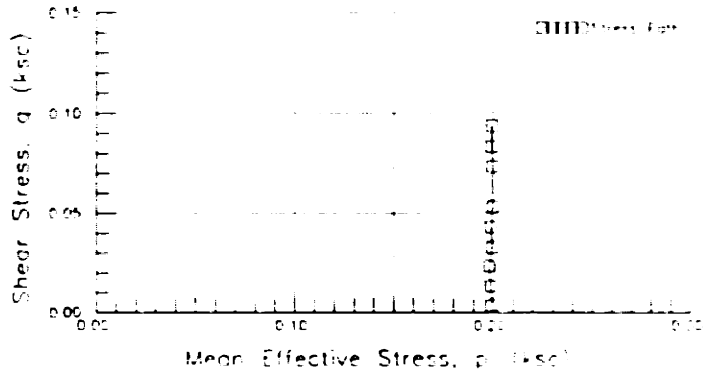

(a) q versus p

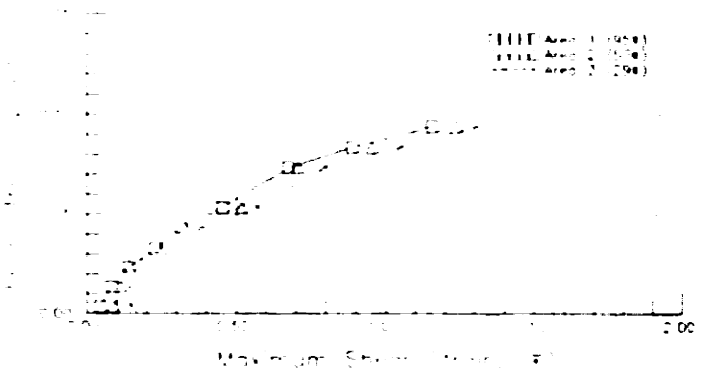

(b) Shear Stress versus Shear Strain

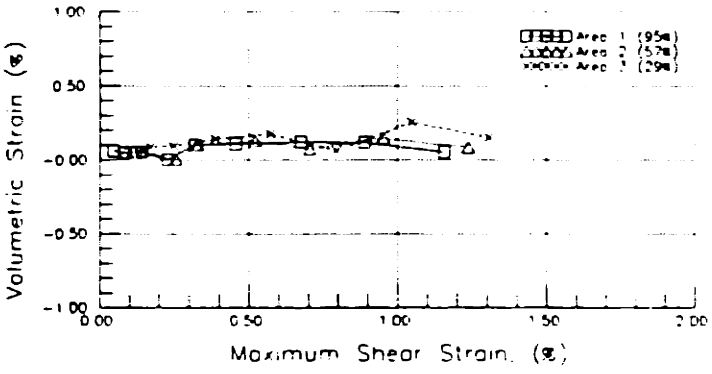

(c) Volumetric Strain versus Shear Strain

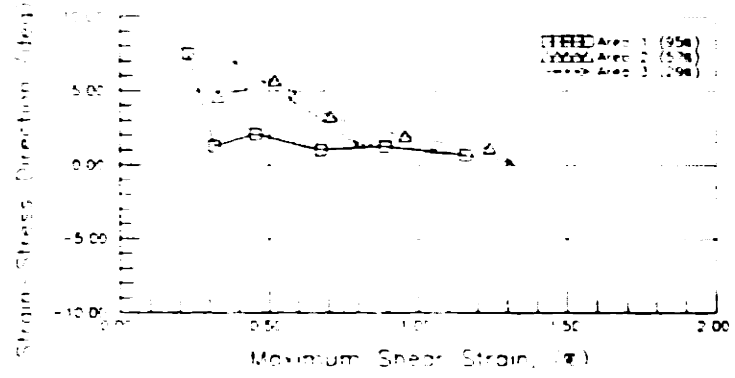

(d) Strain-Stress Direction versus Shear Strain

RUBBER8

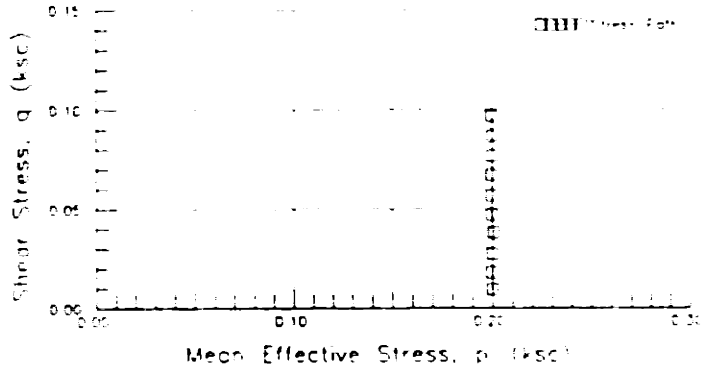

(a) q versus p

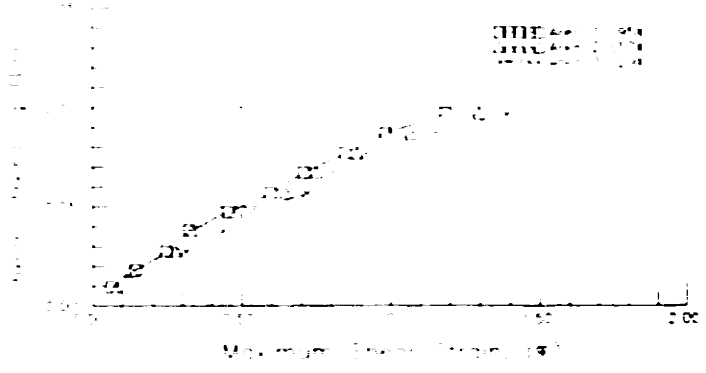

(b) Shear Stress versus Shear Strain

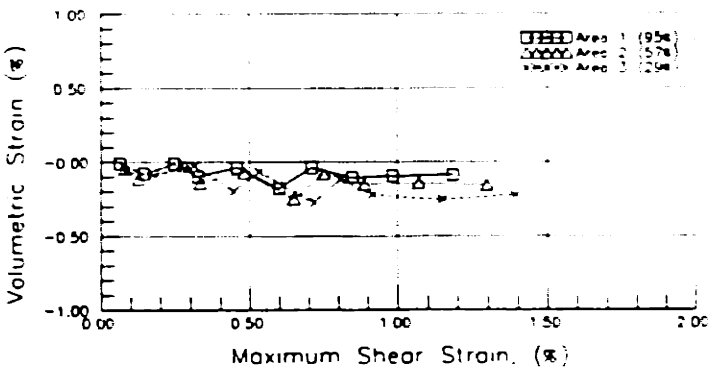

(c) Volumetric Strain versus Shear Strain

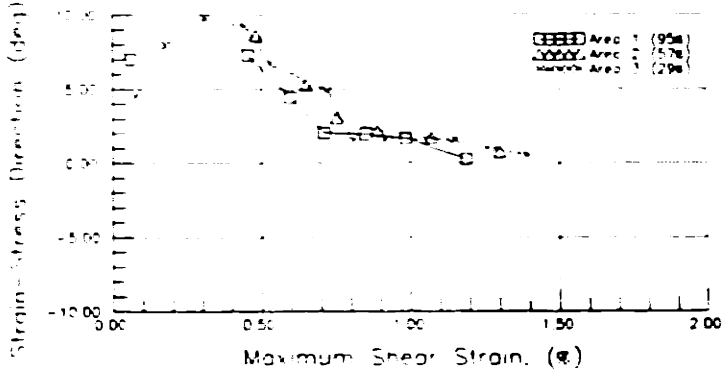

(d) Strain-Stress Direction versus Shear Strain

RUBBER9

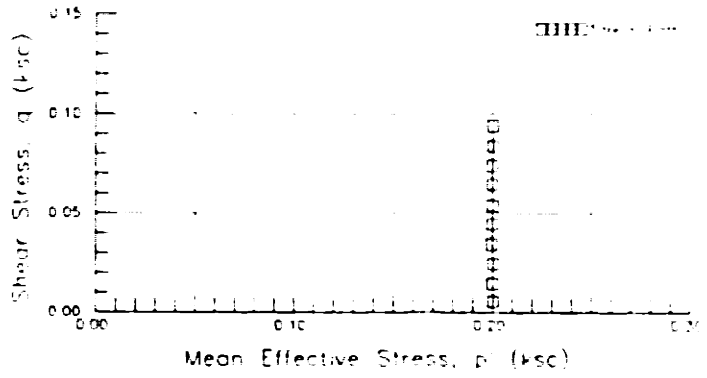

(a) q versus p'

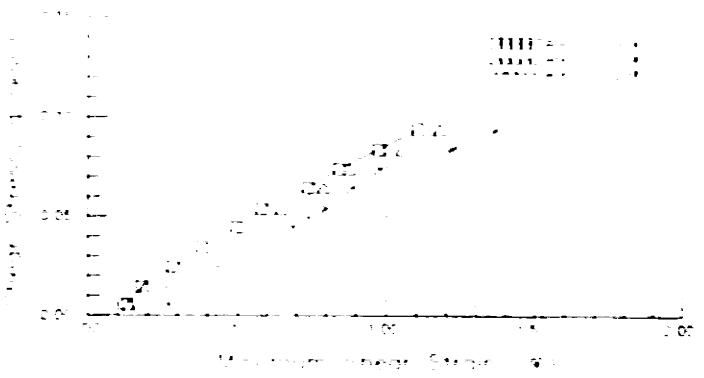

(b) [illegible]

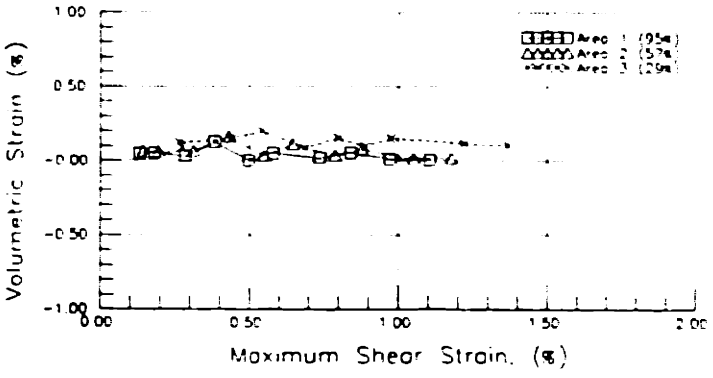

(c) Volumetric Strain versus Shear Strain

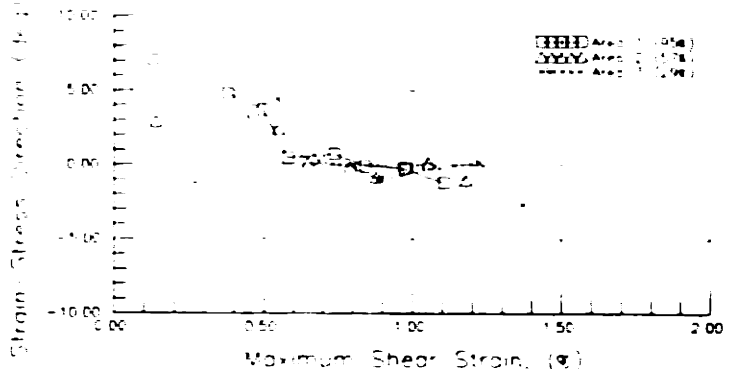

(d) Strain-Stress Direction versus Shear Strain

F.2 UNDRAINED SHEAR RESULTS OF DSC TESTS ON OCR=4 BBC

This section contains:

- Computer printouts of stress data for DSC tests on OCR=4 BBC.
- Computer printouts of strain data for DSC tests on OCR=4 BBC.
- Plots of pore pressure dissipations during consolidation.
- Plots of undrained shear results from DSC tests on OCR=4 BBC.

DSC21

FILM No.	DELTA deg	ALFA deg	P ksc	Q ksc	P' ksc	U ksc	Sig.a mV	Sig.b mV	T a mV	T b mV	U mV	Sig.a ksc	Sig.b ksc	T a ksc	T b ksc	Input V Volts
0	90.000	0.000	0.000	0.000	0.000	0.000	0.820	0.360	-0.354	-0.352	-110.800	0.000	0.000	0.000	0.000	0.000
0	-0.541	-0.277	0.092	0.001	0.092	0.000	3.060	2.650	0.000	0.000	-110.800	0.093	0.092	-0.000	-0.000	10.000
0	0.307	0.157	0.246	0.001	0.246	0.000	6.730	6.540	0.000	0.000	-110.000	0.245	0.247	-0.000	-0.000	10.000
3	0.307	0.157	0.246	0.001	0.246	0.000	6.730	6.540	0.000	0.000	-110.800	0.245	0.247	-0.000	-0.000	10.000
0	0.041	0.021	0.252	0.008	0.252	0.000	6.690	6.860	0.000	0.000	-111.300	0.243	0.260	-0.000	-0.000	10.000
0	0.017	0.009	0.244	0.020	0.244	0.000	6.220	6.970	0.000	0.000	-111.300	0.224	0.265	-0.000	-0.000	10.000
4	0.011	0.006	0.242	0.030	0.242	0.000	5.920	7.160	0.000	0.000	-111.300	0.212	0.272	-0.000	-0.000	10.000
0	0.008	0.004	0.247	0.040	0.247	0.000	5.800	7.520	0.000	0.000	-110.300	0.207	0.287	-0.000	-0.000	10.000
0	0.007	0.003	0.245	0.050	0.245	0.000	5.510	7.730	0.000	0.000	-111.300	0.195	0.295	-0.000	-0.000	10.000
5	0.006	0.003	0.234	0.060	0.234	0.000	5.020	7.710	0.000	0.000	-11.300	0.174	0.294	-0.000	-0.000	10.000
0	0.005	0.002	0.235	0.070	0.235	0.000	4.790	7.970	0.000	0.000	-111.300	0.165	0.305	-0.000	-0.000	10.000
0	0.004	0.002	0.238	0.080	0.238	0.000	4.630	8.310	0.000	0.000	-111.300	0.158	0.318	-0.000	-0.000	10.000
6	0.004	0.002	0.240	0.090	0.240	0.000	4.430	8.600	0.000	0.000	-111.800	0.150	0.330	-0.000	-0.000	10.000
0	0.003	0.002	0.241	0.100	0.241	0.000	4.210	8.880	0.000	0.000	-111.300	0.141	0.341	-0.000	-0.000	10.000
7	0.003	0.002	0.241	0.105	0.241	0.000	4.100	9.010	0.000	0.000	-111.300	0.136	0.346	-0.000	-0.000	10.000
0	0.003	0.002	0.240	0.110	0.240	0.000	3.960	9.090	0.000	0.000	-111.300	0.130	0.349	-0.000	-0.000	10.000
8	0.003	0.001	0.228	0.121	0.228	0.000	3.400	9.080	0.000	0.000	-111.800	0.107	0.349	-0.000	-0.000	10.000
0	0.003	0.001	0.228	0.130	0.228	0.000	3.170	9.300	0.000	0.000	-111.300	0.097	0.358	-0.000	-0.000	10.000
9	0.002	0.001	0.235	0.140	0.235	0.000	3.100	9.720	0.000	0.000	-111.800	0.095	0.375	-0.000	-0.000	10.000
10	0.002	0.001	0.237	0.149	0.237	0.000	2.930	10.010	0.000	0.000	-111.300	0.088	0.386	-0.000	-0.000	10.000
0	0.002	0.001	0.237	0.155	0.237	0.000	2.800	10.160	0.000	0.000	-111.300	0.082	0.392	-0.000	-0.000	10.000
11	0.002	0.001	0.239	0.160	0.239	0.000	2.740	10.330	0.000	0.000	-111.300	0.080	0.399	-0.000	-0.000	10.000
0	0.002	0.001	0.242	0.166	0.242	0.000	2.650	10.570	0.000	0.000	-111.300	0.076	0.409	-0.000	-0.000	10.000
12	0.002	0.001	0.244	0.170	0.244	0.000	2.620	10.710	0.000	0.000	-111.300	0.075	0.414	-0.000	-0.000	10.000
0	0.002	0.001	0.244	0.175	0.244	0.000	2.490	10.830	0.000	0.000	-111.300	0.069	0.419	-0.000	-0.000	10.000
13	0.002	0.001	0.245	0.180	0.245	0.000	2.390	10.990	0.000	0.000	-111.300	0.065	0.425	-0.000	-0.000	10.000
0	0.002	0.001	0.259	0.185	0.259	0.000	2.600	11.440	0.000	0.000	-111.300	0.074	0.443	-0.000	-0.000	10.000
14	0.002	0.001	0.264	0.190	0.264	0.000	2.610	11.710	0.000	0.000	-111.300	0.074	0.454	-0.000	-0.000	10.000
0	0.002	0.001	0.274	0.196	0.274	0.000	2.710	12.090	0.000	0.000	-111.300	0.078	0.469	-0.000	-0.000	10.000
15	0.002	0.001	0.276	0.200	0.276	0.000	2.660	12.260	0.000	0.000	-111.300	0.076	0.476	-0.000	-0.000	10.000

0	0.002	0.001	0.285	0.205	0.285	0.000	2.760	12.600	0.000	0.000-111.300	0.080	0.490	-0.000	-0.000	10.000
16	0.002	0.001	0.292	0.210	0.292	0.000	2.800	12.910	0.000	0.000-111.300	0.082	0.502	-0.000	-0.000	10.000
0	0.002	0.00.	0.295	0.215	0.295	0.000	2.750	13.110	0.000	0.000-111.300	0.080	0.510	-0.000	-0.000	10.000
17	0.002	0.001	0.296	0.220	0.296	0.000	2.670	13.250	0.000	0.000-111.300	0.077	0.516	-0.000	-0.000	10.000
18	0.002	0.001	0.294	0.225	0.294	0.000	2.470	13.330	0.000	0.000-111.300	0.068	0.519	-0.000	-0.000	10.000
19	0.001	0.001	0.305	0.230	0.305	0.000	2.630	13.730	0.000	0.000-111.300	0.075	0.535	-0.000	-0.000	10.000

DSC22

FILM No.	DELTA deg	ALFA deg	P ksc	Q ksc	P' ksc	U ksc	Sig.a mV	Sig.b mV	T a mV	T b mV	U mV	Sig.a ksc	Sig.b ksc	T a ksc	T b ksc	Input V Volts
0	90.000	0.000	0.000	0.000	0.000	0.000	0.870	0.340	-0.354	-0.352	0.130	0.000	0.000	0.000	0.000	0.000
0	5.889	3.049	0.092	0.001	0.092	0.000	3.060	2.650	0.000	0.000	0.130	0.091	0.092	-0.000	-0.000	10.000
0	0.039	0.020	0.239	0.002	0.239	0.000	6.730	6.300	0.000	0.000	0.130	0.238	0.241	-0.000	-0.000	10.000
1	0.504	0.258	0.239	0.010	0.239	0.000	6.400	6.550	0.000	0.000	0.130	0.229	0.248	-0.000	-0.000	10.000
2	0.244	0.125	0.237	0.020	0.237	0.000	6.110	6.760	0.000	0.000	0.130	0.217	0.257	-0.000	-0.000	10.000
0	0.162	0.083	0.236	0.030	0.236	0.000	5.840	6.980	0.000	0.000	0.130	0.206	0.266	-0.000	-0.000	10.000
3	0.122	0.062	0.236	0.040	0.236	0.000	5.600	7.220	0.000	0.000	0.130	0.196	0.275	-0.000	-0.000	10.000
0	0.097	0.049	0.235	0.050	0.235	0.000	5.330	7.460	0.000	0.000	0.130	0.185	0.285	-0.000	-0.000	10.000
4	0.080	0.041	0.230	0.060	0.230	0.000	4.960	7.590	0.000	0.000	0.130	0.170	0.290	-0.000	-0.000	10.000
0	0.069	0.035	0.230	0.070	0.230	0.000	4.720	7.840	0.000	0.000	0.130	0.160	0.300	-0.000	-0.000	10.000
5	0.061	0.031	0.225	0.080	0.225	0.000	4.360	7.950	0.000	0.000	0.130	0.145	0.305	-0.000	-0.000	10.000
0	0.053	0.027	0.212	0.090	0.212	0.000	3.810	7.910	0.000	0.000	0.130	0.122	0.303	-0.000	-0.000	10.000
6	0.048	0.025	0.206	0.100	0.206	0.000	3.440	7.990	0.000	0.000	0.130	0.107	0.306	-0.000	-0.000	10.000
7	0.046	0.024	0.202	0.105	0.202	0.000	3.210	8.000	0.000	0.000	0.130	0.097	0.307	-0.000	-0.000	10.000
8	0.044	0.022	0.200	0.110	0.200	0.000	3.040	8.090	0.000	0.000	0.130	0.090	0.310	-0.000	-0.000	10.000
9	0.043	0.022	0.192	0.112	0.192	0.000	2.800	7.950	0.000	0.000	0.130	0.080	0.305	-0.000	-0.000	10.000
10	0.042	0.022	0.189	0.114	0.189	0.000	2.670	7.900	0.000	0.000	0.130	0.075	0.303	-0.000	-0.000	10.000
11	0.042	0.021	0.187	0.116	0.187	0.000	2.590	7.920	0.000	0.000	0.130	0.071	0.303	-0.000	-0.000	10.000
12	0.041	0.021	0.188	0.118	0.188	0.000	2.540	7.990	0.000	0.000	0.130	0.069	0.306	-0.000	-0.000	10.000
13	0.040	0.021	0.182	0.120	0.182	0.000	2.360	7.890	0.000	0.000	0.130	0.062	0.302	-0.000	-0.000	10.000
14	0.040	0.020	0.181	0.122	0.181	0.000	2.300	7.910	0.000	0.000	0.130	0.059	0.303	-0.000	-0.000	10.000
15	0.039	0.020	0.180	0.124	0.180	0.000	2.210	7.940	0.000	0.000	0.130	0.056	0.304	-0.000	-0.000	10.000
16	0.038	0.020	0.177	0.126	0.177	0.000	2.100	7.920	0.000	0.000	0.130	0.051	0.303	-0.000	-0.000	10.000
17	0.038	0.019	0.189	0.127	0.189	0.000	2.360	8.240	0.000	0.000	0.130	0.062	0.316	-0.000	-0.000	10.000
18	0.037	0.019	0.184	0.131	0.184	0.000	2.160	8.210	0.000	0.000	0.130	0.053	0.315	-0.000	-0.000	10.000
19	0.037	0.019	0.187	0.132	0.187	0.000	2.180	8.310	0.000	0.000	0.130	0.054	0.319	-0.000	-0.000	10.000
20	0.036	0.018	0.185	0.134	0.185	0.000	2.100	8.310	0.000	0.000	0.130	0.051	0.319	-0.000	-0.000	10.000
21	0.036	0.018	0.199	0.136	0.199	0.000	2.400	8.700	0.000	0.000	0.130	0.063	0.335	-0.000	-0.000	10.000
22	0.035	0.018	0.191	0.138	0.191	0.000	2.140	8.550	0.000	0.000	0.130	0.053	0.329	-0.000	-0.000	10.000

DSC23

FILM No.	DELTA deg	ALFA deg	P ksc	Q ksc	P' ksc	U ksc	Sig.a mV	Sig.b mV	T a mV	T b mV	U mV	Sig.a ksc	Sig.b ksc	T a ksc	T b ksc	Input V Volts
0	90.000	0.000	0.000	0.000	0.000	0.000	0.890	0.370	-0.354	-0.352		0.000	0.000	0.000	0.000	0.000
0	43.461	78.109	0.101	0.001	0.101	0.000	3.300	2.868	0.000	0.000	0.230	0.100	0.100	-0.000	-0.000	10.000
1	-2.727	-1.397	0.247	0.002	0.247	0.000	6.900	6.510	0.000	0.000	0.230	0.249	0.246	-0.000	-0.000	10.000
0	0.479	0.244	0.244	0.010	0.244	0.000	6.540	6.730	0.000	0.000	0.230	0.234	0.255	-0.000	-0.000	10.000
2	0.344	0.176	0.241	0.014	0.241	0.000	6.360	6.740	0.000	0.000	0.230	0.227	0.255	-0.000	-0.000	10.000
0	0.160	0.082	0.240	0.030	0.240	0.000	5.940	7.110	0.000	0.000	0.230	0.209	0.270	-0.000	-0.000	10.000
3	0.119	0.061	0.236	0.041	0.236	0.000	5.600	7.280	0.000	0.000	0.230	0.195	0.277	-0.000	-0.000	10.000
0	0.097	0.049	0.235	0.050	0.235	0.000	5.350	7.490	0.000	0.000	0.230	0.185	0.285	-0.000	-0.000	10.000
4	0.081	0.041	0.233	0.060	0.233	0.000	5.060	7.680	0.000	0.000	0.230	0.173	0.293	-0.000	-0.000	10.000
0	0.069	0.035	0.230	0.070	0.230	0.000	4.740	7.850	0.000	0.000	0.230	0.160	0.299	-0.000	-0.000	10.000
5	0.060	0.031	0.222	0.081	0.222	0.000	4.310	7.940	0.000	0.000	0.230	0.142	0.303	-0.000	-0.000	10.000
0	0.054	0.027	0.220	0.090	0.220	0.000	4.020	8.120	0.000	0.000	0.230	0.130	0.310	-0.000	-0.000	10.000
6	0.048	0.025	0.216	0.100	0.216	0.000	3.690	8.260	0.000	0.000	0.230	0.116	0.316	-0.000	-0.000	10.000
7	0.046	0.024	0.213	0.105	0.213	0.000	3.510	8.320	0.000	0.000	0.230	0.109	0.318	-0.000	-0.000	10.000
8	0.044	0.022	0.211	0.110	0.211	0.000	3.320	8.390	0.000	0.000	0.230	0.101	0.321	-0.000	-0.000	10.000
9	0.042	0.022	0.210	0.115	0.210	0.000	3.180	8.480	0.000	0.000	0.230	0.095	0.325	-0.000	-0.000	10.000
10	0.040	0.021	0.203	0.120	0.203	0.000	2.890	8.440	0.000	0.000	0.230	0.083	0.323	-0.000	-0.000	10.000
11	0.039	0.020	0.202	0.125	0.202	0.000	2.750	8.540	0.000	0.000	0.230	0.077	0.327	-0.000	-0.000	10.000
12	0.037	0.019	0.202	0.130	0.202	0.000	2.620	8.660	0.000	0.000	0.230	0.072	0.332	-0.000	-0.000	10.000
13	0.036	0.018	0.202	0.135	0.202	0.000	2.500	8.780	0.000	0.000	0.230	0.067	0.337	-0.000	-0.000	10.000
14	0.035	0.018	0.202	0.140	0.202	0.000	2.380	8.910	0.000	0.000	0.230	0.062	0.342	-0.000	-0.000	10.000
15	0.033	0.017	0.201	0.145	0.201	0.000	2.240	9.000	0.000	0.000	0.230	0.056	0.345	-0.000	-0.000	10.000
16	0.032	0.016	0.200	0.150	0.200	0.000	2.100	9.120	0.000	0.000	0.230	0.050	0.350	-0.000	-0.000	10.000
17	0.031	0.016	0.203	0.155	0.203	0.000	2.050	9.320	0.000	0.000	0.230	0.048	0.358	-0.000	-0.000	10.000
18	0.030	0.015	0.205	0.160	0.205	0.000	1.970	9.480	0.000	0.000	0.230	0.045	0.365	-0.000	-0.000	10.000
19	0.029	0.015	0.212	0.165	0.212	0.000	2.020	9.790	0.000	0.000	0.230	0.047	0.377	-0.000	-0.000	10.000
20	0.029	0.015	0.213	0.170	0.213	0.000	1.950	9.940	0.000	0.000	0.230	0.044	0.383	-0.000	-0.000	10.000
21	0.028	0.014	0.215	0.172	0.215	0.000	1.920	10.050	0.000	0.000	0.230	0.043	0.387	-0.000	-0.000	10.000
22	0.028	0.014	0.215	0.174	0.215	0.000	1.880	10.090	0.000	0.000	0.230	0.041	0.389	-0.000	-0.000	10.000
23	0.027	0.014	0.211	0.176	0.211	0.000	1.730	10.050	0.000	0.000	0.230	0.035	0.387	-0.000	-0.000	10.000

DSC24

FILM No.	DELTA deg	ALFA deg	P ksc	Q ksc	P' ksc	U ksc	Sig.a mV	Sig.b mV	T a mV	T b mV	U mV	Sig.a ksc	Sig.b ksc	T a ksc	T b ksc	Input V Volts
0	90.000	0.000	0.000	0.000	0.000	0.000	0.890	0.370	-0.354	-0.352	0.090	0.000	0.000	0.000	0.000	0.000
0	-2.096	-1.072	0.243	0.002	0.243	0.000	6.810	6.390	0.000	0.000	0.090	0.246	0.241	-0.000	-0.000	10.000
1	-2.096	-1.072	0.243	0.002	0.243	0.000	6.810	6.390	0.000	0.000	0.090	0.246	0.241	-0.000	-0.000	10.000
0	0.479	0.244	0.244	0.010	0.244	0.000	6.540	6.730	0.000	0.000	0.090	0.234	0.255	-0.000	-0.000	10.000
2	0.250	0.128	0.239	0.019	0.239	0.000	6.190	6.830	0.000	0.000	0.090	0.220	0.259	-0.000	-0.000	10.000
0	0.163	0.083	0.236	0.030	0.236	0.000	5.870	7.010	0.000	0.000	0.090	0.207	0.266	-0.000	-0.000	10.000
3	0.119	0.061	0.231	0.041	0.231	0.000	5.470	7.150	0.000	0.000	0.090	0.190	0.271	-0.000	-0.000	10.000
0	0.103	0.053	0.238	0.047	0.238	0.000	5.500	7.490	0.000	0.000	0.090	0.191	0.285	-0.000	-0.000	10.000
0	0.098	0.050	0.229	0.049	0.229	0.000	5.220	7.330	0.000	0.000	0.090	0.180	0.279	-0.000	-0.000	10.000
4	0.124	0.063	0.226	0.060	0.226	0.000	4.890	7.500	0.000	0.000	0.090	0.166	0.285	-0.000	-0.000	10.000
0	0.069	0.035	0.222	0.070	0.222	0.000	4.540	7.660	0.000	0.000	0.090	0.151	0.292	-0.000	-0.000	10.000
5	0.069	0.035	0.222	0.070	0.222	0.000	4.550	7.660	0.000	0.000	0.090	0.152	0.292	-0.000	-0.000	10.000
0	0.054	0.027	0.213	0.090	0.213	0.000	3.850	7.950	0.000	0.000	0.090	0.123	0.303	-0.000	-0.000	10.000
6	0.048	0.025	0.212	0.100	0.212	0.000	3.590	8.160	0.000	0.000	0.090	0.112	0.312	-0.000	-0.000	10.000
0	0.048	0.025	0.212	0.100	0.212	0.000	3.590	8.170	0.000	0.000	0.090	0.112	0.312	-0.000	-0.000	10.000
7	0.046	0.024	0.211	0.105	0.211	0.000	3.440	8.260	0.000	0.000	0.090	0.106	0.316	-0.000	-0.000	10.000
8	0.044	0.022	0.209	0.110	0.209	0.000	3.270	8.340	0.000	0.000	0.090	0.099	0.319	-0.000	-0.000	10.000
9	0.042	0.021	0.208	0.115	0.208	0.000	3.130	8.440	0.000	0.000	0.090	0.093	0.323	-0.000	-0.000	10.000
10	0.040	0.021	0.205	0.120	0.205	0.000	2.930	8.480	0.000	0.000	0.090	0.085	0.325	-0.000	-0.000	10.000
11	0.039	0.020	0.205	0.125	0.205	0.000	2.830	8.610	0.000	0.000	0.090	0.080	0.330	-0.000	-0.000	10.000
12	0.037	0.019	0.205	0.130	0.205	0.000	2.700	8.740	0.000	0.000	0.090	0.075	0.335	-0.000	-0.000	10.000
13	0.036	0.018	0.205	0.135	0.205	0.000	2.570	8.860	0.000	0.000	0.090	0.070	0.340	-0.000	-0.000	10.000
14	0.035	0.018	0.206	0.140	0.206	0.000	2.480	9.020	0.000	0.000	0.090	0.066	0.346	-0.000	-0.000	10.000
15	0.033	0.017	0.209	0.145	0.209	0.000	2.440	9.220	0.000	0.000	0.090	0.064	0.354	-0.000	-0.000	10.000
16	0.032	0.016	0.212	0.150	0.212	0.000	2.390	9.410	0.000	0.000	0.090	0.062	0.362	-0.000	-0.000	10.000
17	0.031	0.016	0.217	0.155	0.217	0.000	2.400	9.660	0.000	0.000	0.090	0.063	0.372	-0.000	-0.000	10.000
18	0.030	0.015	0.228	0.160	0.228	0.000	2.530	10.060	0.000	0.000	0.090	0.068	0.388	-0.000	-0.000	10.000
19	0.029	0.015	0.239	0.165	0.239	0.000	2.690	10.460	0.000	0.000	0.090	0.075	0.404	-0.000	-0.000	10.000
20	0.029	0.015	0.233	0.169	0.233	0.000	2.430	10.430	0.000	0.000	0.090	0.064	0.403	-0.000	-0.000	10.000
21	0.028	0.014	0.190	0.174	0.190	0.000	1.270	9.460	0.000	0.000	0.090	0.016	0.364	-0.000	-0.000	10.000

DSC25

FILM No.	DELTA deg	ALFA deg	P ksc	Q ksc	P' ksc	U ksc	Sig.a mV	Sig.b mV	T a mV	T b mV	U mV	Sig.a ksc	Sig.b ksc	T a ksc	T b ksc	Input V Volts
0	40.000	0.000	0.000	0.000	0.000	0.000	0.890	0.370	-1.210	0.430	0.220	0.000	0.000	0.000	0.000	0.000
1	0.000	0.000	0.253	0.000	0.253	0.000	7 000	6.690	-0.840	0.780	0.220	0.253	0.253	0.000	0.000	10.000
0	29.210	-7.263	0.252	0.004	0.252	0.000	7.010	6.610	-0.330	1.280	0.220	0.254	0.250	0.004	0.003	10.000
2	36.694	2.483	0.248	0.013	0.248	0.000	6.980	6.490	0.120	1.770	0.220	0.253	0.245	0.013	0.013	10.000
0	38.320	11.945	0.245	0.025	0.245	0.000	7.060	6.480	0.620	2.370	0.220	0.256	0.245	0.023	0.025	10.000
3	38.561	0.866	0.245	0.033	0.245	0.000	6.990	6.320	1.100	2.740	0.220	0.253	0.238	0.032	0.033	10.000
0	38.931	-1.060	0.246	0.043	0.246	0.000	7.020	6.270	1.590	3.200	0.220	0.254	0.236	0.042	0.042	10.000
4	39.206	0.313	0.244	0.053	0.244	0.000	7.030	6.200	2.070	3.700	0.220	0.255	0.233	0.052	0.052	10.000
0	39.313	-1.013	0.244	0.063	0.244	0.000	7.040	6.120	2.580	4.180	0.220	0.255	0.230	0.062	0.062	10.000
5	39.530	0.019	0.240	0.073	0.240	0.000	7.020	6.030	3.050	4.670	0.220	0.254	0.227	0.072	0.072	10.000
0	39.500	-0.260	0.240	0.083	0.240	0.000	7.050	5.960	3.550	5.160	0.220	0.255	0.224	0.082	0.082	10.000
6	39.607	0.172	0.235	0.093	0.235	0.000	6.980	5.810	4.030	5.650	0.220	0.253	0.218	0.091	0.092	10.000
0	39.607	0.172	0.235	0.093	0.235	0.000	6.980	5.810	4.030	5.650	0.220	0.253	0.218	0.091	0.092	10.000
7	39.660	-0.116	0.232	0.098	0.232	0.000	6.920	5.710	4.280	5.890	0.220	0.250	0.214	0.096	0.096	10.000
8	39.766	-0.077	0.227	0.103	0.227	0.000	6.820	5.580	4.520	6.130	0.220	0.246	0.209	0.101	0.101	10.000
9	39.590	0.533	0.223	0.108	0.223	0.000	6.780	5.460	4.750	6.380	0.220	0.244	0.204	0.106	0.106	10.000
10	39.741	-0.003	0.221	0.113	0.221	0.000	6.720	5.380	5.010	6.620	0.220	0.242	0.200	0.111	0.111	10.000
11	39.572	0.027	0.220	0.118	0.220	0.000	6.730	5.310	5.250	6.860	0.220	0.242	0.198	0.116	0.116	10.000
12	39.701	0.057	0.220	0.123	0.220	0.000	6.740	5.300	5.500	7.110	0.220	0.243	0.197	0.121	0.121	10.000
13	39.681	0.817	0.218	0.128	0.218	0.000	6.760	5.270	5.730	7.370	0.220	0.243	0.196	0.126	0.126	10.000
14	39.627	0.340	0.216	0.133	0.216	0.000	6.710	5.160	5.980	7.600	0.220	0.241	0.192	0.131	0.131	10.000
15	39.692	0.585	0.216	0.138	0.216	0.000	6.740	5.160	6.220	7.850	0.220	0.243	0.192	0.136	0.136	10.000
16	39.738	0.596	0.217	0.143	0.217	0.000	6.790	5.180	6.450	8.080	0.220	0.245	0.192	0.140	0.141	10.000
17	39.762	0.174	0.218	0.148	0.218	0.000	6.810	5.160	6.710	8.320	0.220	0.246	0.192	0.145	0.146	10.000
18	39.702	0.601	0.219	0.153	0.219	0.000	6.890	5.180	6.950	8.580	0.220	0.249	0.192	0.150	0.151	10.000
19	39.732	0.609	0.226	0.158	0.226	0.000	7.080	5.340	7.190	8.820	0.220	0.257	0.199	0.155	0.156	10.000
20	39.809	0.622	0.229	0.163	0.229	0.000	7.160	5.400	7.430	9.060	0.220	0.260	0.201	0.160	0.161	10.000
21	39.764	1.197	0.239	0.165	0.239	0.000	7.450	5.670	7.510	9.170	0.220	0.272	0.212	0.162	0.163	10.000
22	39.787	1.197	0.252	0.167	0.252	0.000	7.780	6.000	7.610	9.270	0.220	0.286	0.225	0.164	0.165	10.000

DSC26

FILM No.	DELTA deg	ALFA deg	P ksc	Q ksc	P' ksc	U ksc	Sig.a mV	Sig.b mV	T a mV	T b mV	U mV	Sig.a ksc	Sig.b ksc	T a ksc	T b ksc	Input V Volts
0	30.000	0.000	0.000	0.000	0.000	0.000	0.890	0.370	-1.130	-0.140	0.230	0.000	0.000	0.000	0.000	0.000
1	-0.028	0.411	0.240	0.002	0.240	0.000	6.710	6.310	-0.775	0.212	0.400	0.241	0.238	0.000	-0.000	10.000
0	30.849	-1.635	0.241	0.010	0.241	0.000	6.820	6.270	-0.330	0.670	0.400	0.246	0.236	0.009	0.009	10.000
2	30.253	-1.498	0.241	0.020	0.241	0.000	6.960	6.160	0.090	1.100	0.400	0.252	0.232	0.017	0.018	10.000
0	30.775	-1.120	0.243	0.030	0.243	0.000	7.100	6.080	0.540	1.550	0.400	0.258	0.229	0.027	0.027	10.000
3	30.335	-0.296	0.247	0.040	0.247	0.000	7.320	6.060	0.940	1.930	0.400	0.267	0.228	0.035	0.035	10.000
0	29.429	-0.708	0.247	0.051	0.247	0.000	7.480	5.890	1.360	2.370	0.400	0.273	0.221	0.043	0.044	10.000
4	30.060	-0.079	0.246	0.060	0.246	0.000	7.540	5.770	1.800	2.780	0.400	0.276	0.216	0.052	0.052	10.000
0	30.020	-0.102	0.247	0.070	0.247	0.000	7.680	5.660	2.230	3.210	0.400	0.282	0.212	0.061	0.061	10.000
5	29.983	0.026	0.245	0.080	0.245	0.000	7.770	5.500	2.660	3.630	0.400	0.28[illegible]	0.205	0.069	0.069	10.000
0	30.081	-0.004	0.244	0.090	0.244	0.000	7.860	5.360	3.090	4.060	0.400	0.285	0.200	0.078	0.078	10.000
6	30.029	-0.027	0.243	0.100	0.243	0.000	7.960	5.210	3.510	4.480	0.400	0.293	0.194	0.086	0.086	10.000
0	29.977	0.059	0.243	0.110	0.243	0.000	8.080	5.070	3.950	4.910	0.400	0.298	0.188	0.095	0.095	10.000
7	29.487	0.125	0.206	0.121	0.206	0.000	7.360	3.950	4.390	5.340	0.400	0.268	0.143	0.104	0.104	10.000
0	29.930	0.102	0.201	0.130	0.201	0.000	7.300	3.750	4.810	5.760	0.400	0.266	0.135	0.113	0.112	10.000
8	30.026	0.078	0.202	0.140	0.202	0.000	7.440	3.670	5.240	6.190	0.400	0.272	0.132	0.121	0.121	10.000
0	30.048	0.134	0.204	0.150	0.204	0.000	7.610	3.600	5.680	6.620	0.400	0.279	0.129	0.130	0.130	10.000
9	30.040	0.038	0.210	0.160	0.210	0.000	7.870	3.620	6.100	7.050	0.400	0.289	0.130	0.139	0.138	10.000
10	29.925	-0.026	0.211	0.165	0.211	0.000	7.970	3.560	6.312	7.270	0.400	0.294	0.128	0.143	0.143	10.000
11	29.994	0.158	0.223	0.170	0.223	0.000	8.300	3.800	6.540	7.470	0.400	0.307	0.137	0.147	0.147	10.000
12	29.965	-0.381	0.228	0.175	0.228	0.000	8.530	3.900	6.720	7.730	0.400	0.317	0.141	0.151	0.152	10.000
13	29.968	-0.378	0.228	0.180	0.228	0.000	8.580	3.830	6.930	7.940	0.400	0.319	0.138	0.155	0.156	10.000
14	29.920	-0.497	0.230	0.185	0.230	0.000	8.710	3.830	7.120	8.150	0.400	0.324	0.138	0.159	0.161	10.000
15	29.999	-0.554	0.241	0.190	0.241	0.000	9.030	4.060	7.340	8.380	0.400	0.338	0.148	0.164	0.165	10.000
16	30.025	-0.785	0.247	0.195	0.247	0.000	9.260	4.180	7.540	8.620	0.400	0.347	0.152	0.168	0.170	10.000
17	30.027	-0.713	0.256	0.200	0.256	0.000	9.530	4.330	7.770	8.840	0.400	0.358	0.158	0.172	0.175	10.000
18	30.023	-0.928	0.274	0.205	0.274	0.000	10.030	4.730	7.950	9.060	0.400	0.379	0.174	0.176	0.179	10.000
19	30.001	-0.855	0.299	0.210	0.299	0.000	10.700	5.290	8.170	9.270	0.400	0.407	0.197	0.180	0.183	10.000
20	29.970	-1.483	0.313	0.215	0.313	0.000	11.140	5.610	8.320	9.540	0.550	0.425	0.210	0.183	0.189	10.000

DSC27

FILM No.	DELTA deg	ALFA deg	P ksc	Q ksc	P' ksc	U ksc	Sig.a mV	Sig.b mV	T a mV	T b mV	U mV	Sig.a ksc	Sig.b ksc	T a ksc	T b ksc	Input V Volts
0	0.000	0.000	0.000	0.000	0.000	0.000	0.890	0.370	-0.354	-0.352	0.400	0.000	0.000	0.000	0.000	0.000
1	-0.152	-0.078	0.251	0.002	0.251	0.000	7.000	6.590	0.000	0.000	0.600	0.253	0.249	-0.000	-0.000	10.000
0	-0.035	-0.018	0.249	0.010	0.249	0.000	7.140	6.360	0.000	0.000	0.600	0.259	0.240	-0.000	-0.000	10.000
2	-0.017	-0.009	0.246	0.020	0.246	0.000	7.310	6.020	0.000	0.000	0.600	0.266	0.226	-0.000	-0.000	10.000
0	-0.011	-0.006	0.243	0.030	0.243	0.000	7.480	5.700	0.000	0.000	0.600	0.273	0.213	-0.000	-0.000	10.000
3	-0.009	-0.004	0.240	0.040	0.240	0.000	7.640	5.370	0.000	0.000	0.600	0.280	0.200	-0.000	-0.000	10.000
0	-0.007	-0.003	0.238	0.050	0.238	0.000	7.820	5.060	0.000	0.000	0.600	0.287	0.188	-0.000	-0.000	10.000
4	-0.006	-0.003	0.235	0.060	0.235	0.000	8.020	4.750	0.000	0.000	0.600	0.296	0.175	-0.000	-0.000	10.000
0	-0.005	-0.002	0.233	0.070	0.233	0.000	8.190	4.450	0.000	0.000	0.600	0.303	0.163	-0.000	-0.000	10.000
5	-0.004	-0.002	0.231	0.080	0.231	0.000	8.390	4.140	0.000	0.000	0.600	0.311	0.151	-0.000	-0.000	10.000
0	-0.004	-0.002	0.229	0.090	0.229	0.000	8.590	3.840	0.000	0.000	0.600	0.319	0.139	-0.000	-0.000	10.000
6	-0.003	-0.002	0.228	0.100	0.228	0.000	8.800	3.570	0.000	0.000	0.600	0.328	0.128	-0.000	-0.000	10.000
7	-0.003	-0.001	0.225	0.120	0.225	0.000	9.210	2.990	0.000	0.000	0.600	0.345	0.105	-0.000	-0.000	10.000
0	-0.003	-0.001	0.227	0.130	0.227	0.000	9.500	2.780	0.000	0.000	0.600	0.357	0.096	-0.000	-0.000	10.000
8	-0.002	-0.001	0.228	0.140	0.228	0.000	9.760	2.570	0.000	0.000	0.600	0.368	0.088	-0.000	-0.000	10.000
0	-0.002	-0.001	0.231	0.150	0.231	0.000	10.070	2.400	0.000	0.000	0.600	0.381	0.081	-0.000	-0.000	10.000
9	-0.002	-0.001	0.237	0.160	0.237	0.000	10.460	2.310	0.000	0.000	0.600	0.397	0.078	-0.000	-0.000	10.000
10	-0.002	-0.001	0.242	0.170	0.242	0.000	10.820	2.160	0.000	0.000	0.600	0.412	0.072	-0.000	-0.000	10.000
0	-0.002	-0.001	0.247	0.175	0.247	0.000	11.070	2.170	0.000	0.000	0.600	0.422	0.072	-0.000	-0.000	10.000
11	-0.002	-0.001	0.251	0.180	0.251	0.000	11.300	2.150	0.000	0.000	0.600	0.432	0.071	-0.000	-0.000	10.000
0	-0.002	-0.001	0.255	0.185	0.255	0.000	11.500	2.130	0.000	0.000	0.600	0.440	0.070	-0.000	-0.000	10.000
12	-0.002	-0.001	0.260	0.190	0.260	0.000	11.740	2.120	0.000	0.000	0.600	0.450	0.070	-0.000	-0.000	10.000
0	-0.002	-0.001	0.265	0.195	0.265	0.000	11.970	2.120	0.000	0.000	0.600	0.460	0.070	-0.000	-0.000	10.000
13	-0.002	-0.001	0.269	0.199	0.269	0.000	12.190	2.120	0.000	0.000	0.600	0.469	0.070	-0.000	-0.000	10.000
0	-0.002	-0.001	0.276	0.205	0.276	0.000	12.480	2.140	0.000	0.000	0.600	0.481	0.071	-0.000	-0.000	10.000
14	-0.002	-0.001	0.280	0.210	0.280	0.000	12.700	2.120	0.000	0.000	0.600	0.490	0.070	-0.000	-0.000	10.000
15	-0.002	-0.001	0.285	0.215	0.285	0.000	12.950	2.120	0.000	0.000	0.600	0.500	0.070	-0.000	-0.000	10.000
16	-0.002	-0.001	0.297	0.220	0.297	0.000	13.350	2.290	0.000	0.000	0.600	0.517	0.077	-0.000	-0.000	10.000
0	-0.002	-0.001	0.310	0.222	0.310	0.000	13.710	2.560	0.000	0.000	0.600	0.532	0.088	-0.000	-0.000	10.000
17	-0.002	-0.001	0.313	0.225	0.313	0.000	13.870	2.580	0.000	0.000	0.600	0.538	0.088	-0.000	-0.000	10.000

DSC28

FILM No.	DELTA deg	ALFA deg	P ksc	Q ksc	P' ksc	U ksc	Sig.a mV	Sig.b mV	T a mV	T b mV	U mV	Sig.a ksc	Sig.b ksc	T a ksc	T b ksc	Input V Volts
0	30.000	0.000	0.000	0.000	0.000	0.000	0.370	0.890	-1.320	-0.160	0.390	0.000	0.000	0.000	0.000	0.000
0	0.307	4.501	0.249	0.000	0.249	0.000	6.590	6.900	-0.965	0.192	0.390	0.249	0.249	0.000	-0.000	10.000
2	0.307	4.501	0.249	0.000	0.249	0.000	6.590	6.900	-0.965	0.192	0.390	0.249	0.249	0.000	-0.000	10.000
0	30.576	0.458	0.248	0.010	0.248	0.000	6.680	6.750	-0.540	0.620	0.390	0.253	0.243	0.009	0.009	10.000
3	31.671	0.977	0.247	0.022	0.247	0.000	6.780	6.610	-0.020	1.150	0.390	0.257	0.237	0.019	0.019	10.000
0	30.196	-0.474	0.246	0.030	0.246	0.000	6.870	6.450	0.330	1.470	0.390	0.260	0.231	0.026	0.026	10.000
4	30.114	-0.000	0.243	0.040	0.243	0.000	6.950	6.280	0.760	1.910	0.390	0.263	0.224	0.035	0.035	10.000
0	30.159	0.047	0.239	0.050	0.239	0.000	6.960	6.060	1.180	2.330	0.390	0.264	0.214	0.043	0.043	10.000
5	30.131	-0.116	0.235	0.060	0.235	0.000	6.980	5.840	1.610	2.750	0.390	0.265	0.205	0.052	0.052	10.000
0	30.333	-0.068	0.230	0.069	0.230	0.000	6.950	5.610	2.020	3.160	0.390	0.263	0.196	0.060	0.060	10.000
6	29.972	-0.171	0.224	0.080	0.224	0.000	6.970	5.330	2.470	3.600	0.390	0.264	0.184	0.069	0.069	10.000
0	30.374	0.003	0.221	0.089	0.221	0.000	6.970	5.160	2.890	4.030	0.390	0.264	0.177	0.078	0.078	10.000
7	30.157	-0.443	0.220	0.099	0.220	0.000	7.080	4.990	3.340	4.440	0.390	0.269	0.170	0.087	0.086	10.000
0	30.067	0.152	0.213	0.110	0.213	0.000	7.060	4.710	3.750	4.900	0.390	0.268	0.158	0.095	0.095	10.000
8	30.136	-0.035	0.210	0.119	0.210	0.000	7.090	4.520	4.180	5.310	0.390	0.269	0.151	0.104	0.104	10.000
0	29.945	-0.281	0.206	0.130	0.206	0.000	7.120	4.270	4.610	5.710	0.390	0.270	0.140	0.112	0.112	10.000
9	29.940	0.005	0.202	0.140	0.202	0.000	7.170	4.060	5.050	6.180	0.390	0.272	0.131	0.121	0.121	10.000
0	30.103	0.021	0.202	0.150	0.202	0.000	7.290	3.980	5.480	6.610	0.390	0.277	0.128	0.130	0.130	10.000
10	30.230	-0.039	0.207	0.159	0.207	0.000	7.510	4.000	5.900	7.020	0.390	0.286	0.129	0.138	0.138	10.000
11	30.114	-0.171	0.212	0.165	0.212	0.000	7.690	4.010	6.140	7.240	0.390	0.293	0.129	0.143	0.143	10.000
12	30.088	-0.022	0.220	0.169	0.220	0.000	7.970	4.160	6.330	7.450	0.390	0.304	0.136	0.147	0.147	10.000
13	30.000	0.118	0.225	0.175	0.225	0.000	8.180	4.210	6.540	7.680	0.390	0.313	0.138	0.151	0.152	10.000
14	30.124	-0.008	0.229	0.179	0.229	0.000	8.320	4.270	6.760	7.880	0.390	0.318	0.140	0.156	0.156	10.000
15	30.173	-0.064	0.236	0.184	0.236	0.000	8.550	4.390	6.980	8.090	0.390	0.327	0.145	0.160	0.160	10.000
16	30.162	1.056	0.241	0.189	0.241	0.000	8.810	4.520	7.100	8.390	0.390	0.338	0.151	0.163	0.166	10.000
17	29.809	1.005	0.245	0.196	0.245	0.000	9.050	4.490	7.330	8.620	0.390	0.347	0.149	0.167	0.171	10.000
18	29.934	0.939	0.281	0.200	0.281	0.000	9.960	5.300	7.540	8.820	0.390	0.384	0.183	0.171	0.175	10.000
19	30.057	1.327	0.280	0.205	0.280	0.000	10.010	5.270	7.730	9.080	0.420	0.386	0.182	0.175	0.180	10.000

DSC29

FILM No.	DELTA deg	ALFA deg	P ksc	Q ksc	P' ksc	U ksc	Sig.a mV	Sig.b mV	T a mV	T b mV	U mV	Sig.a ksc	Sig.b ksc	T a ksc	T b ksc	Input V Volts
0	40.000	0.000	0.000	0.000	0.000	0.000	0.850	0.360	-0.590	0.030	0.470	0.000	0.000	0.000	0.000	0.000
2	0.000	0.000	0.250	0.002	0.250	0.000	6.920	6.560	-0.235	0.382	0.470	0.252	0.248	0.000	0.000	10.000
0	29.048	1.192	0.250	0.004	0.250	0.000	6.920	6.550	0.270	0.890	0.470	0.252	0.248	0.003	0.003	10.000
3	37.339	1.046	0.247	0.014	0.247	0.000	6.900	6.450	0.760	1.380	0.470	0.251	0.244	0.013	0.013	10.000
0	38.850	-0.141	0.244	0.023	0.244	0.000	6.840	6.320	1.240	1.850	0.470	0.248	0.239	0.023	0.023	10.000
4	39.121	-0.759	0.243	0.033	0.243	0.000	6.860	6.250	1.730	2.330	0.470	0.249	0.236	0.033	0.032	10.000
0	39.249	-1.120	0.242	0.043	0.242	0.000	6.860	6.160	2.210	2.800	0.470	0.249	0.232	0.042	0.042	10.000
5	39.515	-0.245	0.233	0.053	0.233	0.000	6.710	5.930	2.690	3.290	0.470	0.243	0.223	0.052	0.052	10.000
0	39.402	-0.090	0.229	0.063	0.229	0.000	6.670	5.780	3.180	3.780	0.470	0.241	0.217	0.062	0.062	10.000
6	39.552	-0.401	0.225	0.073	0.225	0.000	6.600	5.630	3.670	4.260	0.470	0.238	0.211	0.072	0.072	10.000
0	39.611	0.105	0.220	0.083	0.220	0.000	6.530	5.470	4.160	4.760	0.470	0.236	0.205	0.082	0.082	10.000
7	39.598	0.172	0.214	0.093	0.214	0.000	6.430	5.270	4.650	5.250	0.470	0.231	0.196	0.091	0.092	10.000
8	39.535	-0.113	0.211	0.098	0.211	0.000	6.380	5.160	4.900	5.490	0.470	0.229	0.192	0.096	0.096	10.000
9	39.688	0.229	0.207	0.103	0.207	0.000	6.320	5.080	5.130	5.730	0.470	0.227	0.189	0.101	0.101	10.000
10	39.734	0.255	0.205	0.108	0.205	0.000	6.280	5.000	5.380	5.980	0.470	0.225	0.186	0.106	0.106	10.000
11	39.668	-0.003	0.203	0.113	0.203	0.000	6.260	4.920	5.630	6.220	0.470	0.224	0.182	0.111	0.111	10.000
12	39.690	-0.239	0.203	0.118	0.203	0.000	6.260	4.880	5.870	6.450	0.470	0.224	0.181	0.116	0.116	10.000
13	39.764	-0.201	0.204	0.123	0.204	0.000	6.290	4.880	6.120	6.700	0.470	0.226	0.181	0.121	0.121	10.000
14	39.738	-0.164	0.203	0.128	0.203	0.000	6.310	4.850	6.360	6.940	0.470	0.226	0.180	0.126	0.126	10.000
15	39.719	-0.129	0.204	0.133	0.204	0.000	6.350	4.840	6.610	7.190	0.470	0.228	0.179	0.131	0.131	10.000
16	39.650	-0.096	0.205	0.138	0.205	0.000	6.410	4.840	6.850	7.430	0.470	0.231	0.179	0.136	0.136	10.000
17	39.743	-0.069	0.207	0.143	0.207	0.000	6.470	4.880	7.090	7.670	0.470	0.233	0.181	0.141	0.141	10.000
18	39.717	-0.254	0.209	0.148	0.209	0.000	6.540	4.900	7.340	7.910	0.470	0.236	0.182	0.146	0.145	10.000
19	39.764	0.401	0.213	0.153	0.213	0.000	6.690	5.020	7.580	8.180	0.470	0.242	0.186	0.151	0.151	10.000
20	39.688	0.405	0.217	0.158	0.217	0.000	6.800	5.070	7.810	8.410	0.470	0.247	0.188	0.155	0.156	10.000
21	39.832	0.823	0.222	0.163	0.222	0.000	6.960	5.230	8.050	8.670	0.470	0.253	0.195	0.160	0.161	10.000
22	39.737	0.807	0.228	0.165	0.228	0.000	7.130	5.360	8.150	8.770	0.470	0.260	0.200	0.162	0.163	10.000
23	39.751	1.379	0.230	0.167	0.230	0.000	7.230	5.450	8.230	8.880	0.470	0.265	0.204	0.164	0.165	10.000
24	39.815	1.769	0.238	0.169	0.238	0.000	7.440	5.670	8.310	8.980	0.470	0.273	0.213	0.165	0.167	10.000
25	39.772	3.050	0.243	0.171	0.243	0.000	7.680	5.890	8.360	9.100	0.470	0.283	0.221	0.166	0.170	10.000

DSC30

FILM No.	DELTA deg	ALFA deg	P ksc	Q ksc	P' ksc	U ksc	Sig.a mV	Sig.b mV	T a mV	T b mV	U mV	Sig.a ksc	Sig.b ksc	T a ksc	T b ksc	Input V Volts
0	20.000	0.000	0.000	0.000	0.000	0.000	0.850	0.360	-0.590	0.030	0.470	0.000	0.000	0.000	0.000	0.000
1	0.000	0.000	0.103	0.001	0.103	0.000	3.360	2.900	-0.285	0.472	-1.100	0.104	0.102	0.000	0.000	10.000
2	0.000	0.000	0.249	0.003	0.249	0.000	6.940	6.510	-0.285	0.472	-0.950	0.253	0.246	0.000	0.000	10.000
3	2.908	5.817	0.249	0.008	0.249	0.000	7.050	6.380	0.070	0.810	-0.940	0.257	0.241	0.000	0.002	10.000
4	10.998	5.498	0.249	0.018	0.249	0.000	7.250	6.180	0.360	1.130	-0.940	0.265	0.233	0.005	0.008	10.000
5	14.951	3.379	0.247	0.027	0.247	0.000	7.390	5.970	0.710	1.460	-0.940	0.271	0.225	0.012	0.015	10.000
0	16.123	3.297	0.242	0.037	0.242	0.000	7.470	5.660	1.000	1.790	-0.940	0.275	0.212	0.018	0.021	10.000
6	17.259	2.374	0.240	0.047	0.240	0.000	7.600	5.410	1.360	2.130	-0.940	0.280	0.202	0.025	0.028	10.000
0	17.741	2.958	0.235	0.058	0.235	0.000	7.690	5.090	1.660	2.510	-0.940	0.284	0.189	0.031	0.036	10.000
7	17.783	1.415	0.231	0.067	0.231	0.000	7.760	4.810	1.970	2.710	-0.940	0.287	0.178	0.037	0.040	10.000
8	18.099	1.448	0.230	0.076	0.230	0.000	7.910	4.600	2.270	3.030	-0.940	0.293	0.170	0.043	0.047	10.000
9	18.327	1.211	0.226	0.087	0.226	0.000	8.010	4.300	2.610	3.360	-0.940	0.297	0.158	0.050	0.053	10.000
10	18.335	0.655	0.224	0.096	0.224	0.000	8.120	4.050	2.910	3.600	-0.940	0.302	0.148	0.056	0.058	10.000
11	18.664	1.068	0.221	0.101	0.221	0.000	8.140	3.910	3.070	3.820	-0.940	0.302	0.142	0.060	0.063	10.000
12	18.560	1.015	0.217	0.106	0.217	0.000	8.150	3.690	3.220	3.970	-0.940	0.303	0.133	0.063	0.066	10.000
13	18.704	0.848	0.214	0.111	0.214	0.000	8.160	3.520	3.400	4.130	-0.940	0.303	0.126	0.066	0.069	10.000
14	19.159	0.714	0.212	0.114	0.212	0.000	8.140	3.450	3.560	4.270	-0.940	0.302	0.124	0.069	0.072	10.000
15	18.787	0.851	0.211	0.121	0.211	0.000	8.270	3.260	3.700	4.440	-0.940	0.308	0.116	0.072	0.075	10.000
16	18.638	0.811	0.210	0.127	0.210	0.000	8.380	3.110	3.860	4.600	-0.940	0.312	0.110	0.076	0.078	10.000
17	18.835	0.850	0.209	0.131	0.209	0.000	8.420	3.020	4.010	4.760	-0.940	0.314	0.106	0.079	0.082	10.000
18	18.801	0.820	0.207	0.137	0.207	0.000	8.480	2.860	4.170	4.920	-0.940	0.316	0.100	0.082	0.085	10.000
19	18.920	0.800	0.206	0.141	0.206	0.000	8.530	2.750	4.330	5.080	-0.940	0.319	0.096	0.085	0.088	10.000
20	18.931	0.675	0.206	0.146	0.206	0.000	8.630	2.650	4.500	5.230	-0.940	0.323	0.092	0.088	0.091	10.000
21	18.964	0.657	0.206	0.151	0.206	0.000	8.720	2.550	4.660	5.390	-0.940	0.326	0.088	0.092	0.094	10.000
22	18.972	0.639	0.206	0.157	0.206	0.000	8.820	2.450	4.820	5.550	-0.940	0.331	0.084	0.095	0.098	10.000
23	19.064	0.627	0.206	0.161	0.206	0.000	8.890	2.370	4.970	5.700	-0.940	0.333	0.080	0.098	0.101	10.000
24	19.072	0.661	0.205	0.164	0.205	0.000	8.930	2.280	5.070	5.810	-0.940	0.335	0.077	0.100	0.103	10.000
25	18.992	0.652	0.205	0.166	0.205	0.000	8.980	2.230	5.120	5.860	-0.940	0.337	0.075	0.101	0.104	10.000
26	19.089	0.605	0.205	0.168	0.205	0.000	9.000	2.200	5.200	5.930	-0.940	0.338	0.074	0.103	0.105	10.000
27	19.129	0.558	0.205	0.170	0.205	0.000	9.030	2.180	5.260	5.980	-0.940	0.339	0.073	0.104	0.106	10.000

DSC21

AREA	Ex	Ex(SD)	Ey	Ey(SD)	Exy	Exy(SD)	E3	E3(SD)	E1	E1(SD)	GAMMA G(SD)	EV	EV(SD)	PS.	PS(SD)
		P' = 0.246 ksc					Q = 0.001 ksc								
1	0.006	0.005	-0.008	0.004	0.001	0.003	-0.008	0.004	0.006	0.005	0.014 0.006	-0.002	0.006	3.81	12.55
2	-0.007	0.006	-0.013	0.005	-0.001	0.004	-0.013	0.005	-0.007	0.006	0.006 0.008	-0.019	0.008	-8.54	37.87
3	-0.007	0.011	-0.001	0.008	-0.001	0.007	-0.007	0.011	-0.000	0.008	0.007 0.014	-0.008	0.014	8.93	57.35
4	0.030	0.022	0.001	0.015	-0.018	0.013	-0.008	0.017	0.039	0.021	0.046 0.027	0.030	0.027	-25.48	16.51
5	-0.066	0.034	-0.036	0.033	0.019	0.023	-0.075	0.034	-0.027	0.033	0.047 0.047	-0.102	0.047	-25.56	28.21
		P' = 0.234 ksc					Q = 0.060 ksc								
1	-0.055	0.017	-0.130	0.021	0.000	0.014	-0.130	0.021	-0.055	0.017	0.075 0.027	-0.184	0.027	0.06	10.46
2	-0.055	0.009	-0.115	0.009	-0.019	0.006	-0.120	0.009	-0.050	0.009	0.071 0.013	-0.170	0.013	-16.10	5.08
3	-0.038	0.015	-0.125	0.012	-0.019	0.010	-0.129	0.012	-0.034	0.015	0.095 0.019	-0.163	0.019	-11.92	5.84
4	-0.025	0.044	-0.158	0.021	0.024	0.024	-0.162	0.022	-0.021	0.044	0.141 0.049	-0.183	0.049	9.94	9.88
5	-0.087	0.119	-0.192	0.204	0.064	0.119	-0.222	0.193	-0.057	0.139	0.165 0.238	-0.279	0.236	25.20	41.16
		P' = 0.240 ksc					Q = 0.090 ksc								
1	0.010	0.008	-0.061	0.009	-0.024	0.006	-0.069	0.009	0.017	0.008	0.086 0.012	-0.051	0.012	-17.21	4.12
2	0.002	0.008	-0.063	0.010	-0.027	0.006	-0.073	0.010	0.012	0.008	0.085 0.013	-0.061	0.013	-19.89	4.20
3	0.003	0.012	-0.066	0.014	-0.019	0.009	-0.070	0.014	0.008	0.012	0.078 0.019	-0.062	0.019	-14.33	6.76
4	0.038	0.028	-0.052	0.025	-0.008	0.019	-0.053	0.025	0.039	0.028	0.092 0.037	-0.015	0.037	-5.19	11.59
5	0.101	0.056	-0.030	0.096	0.137	0.056	-0.116	0.088	0.188	0.071	0.304 0.113	0.072	0.111	32.29	10.54
		P' = 0.241 ksc					Q = 0.105 ksc								
1	0.037	0.007	-0.082	0.007	-0.019	0.005	-0.085	0.007	0.039	0.007	0.125 0.010	-0.046	0.010	-8.82	2.30
2	0.030	0.007	-0.093	0.009	-0.026	0.006	-0.098	0.009	0.035	0.007	0.132 0.011	-0.063	0.011	-11.34	2.44
3	0.031	0.012	-0.097	0.013	-0.029	0.009	-0.104	0.013	0.037	0.012	0.141 0.017	-0.067	0.017	-12.19	3.49
4	0.088	0.027	-0.138	0.029	-0.015	0.020	-0.139	0.029	0.088	0.027	0.227 0.040	-0.051	0.040	-3.16	5.04
5	0.131	0.061	-0.143	0.081	-0.066	0.051	-0.158	0.080	0.146	0.062	0.304 0.101	-0.012	0.101	-12.90	9.58
		P' = 0.228 ksc					Q = 0.121 ksc								
1	0.066	0.018	-0.185	0.014	0.009	0.012	-0.185	0.014	0.066	0.018	0.251 0.023	-0.119	0.023	2.05	2.63
2	0.073	0.010	-0.175	0.011	-0.007	0.008	-0.175	0.011	0.073	0.010	0.249 0.015	-0.102	0.015	-1.68	1.77
3	0.085	0.014	-0.175	0.016	-0.003	0.011	-0.175	0.016	0.085	0.014	0.259 0.021	-0.090	0.021	-0.76	2.34
4	0.066	0.041	-0.154	0.038	0.030	0.028	-0.158	0.038	0.070	0.041	0.228 0.056	-0.089	0.056	7.53	7.01
5	0.115	0.120	-0.119	0.170	-0.068	0.105	-0.137	0.166	0.134	0.124	0.271 0.208	-0.004	0.208	-15.12	22.02
		P' = 0.235 ksc					Q = 0.140 ksc								
1	0.025	0.011	-0.210	0.011	-0.001	0.008	-0.210	0.011	0.025	0.011	0.235 0.015	-0.184	0.015	-0.12	1.86
2	0.029	0.007	-0.193	0.010	-0.006	0.006	-0.193	0.010	0.029	0.007	0.222 0.012	-0.164	0.012	-1.59	1.60
3	0.027	0.011	-0.189	0.012	0.005	0.008	-0.189	0.012	0.027	0.011	0.216 0.016	-0.161	0.016	1.26	2.09
4	0.041	0.020	-0.190	0.026	-0.008	0.016	-0.190	0.026	0.041	0.020	0.231 0.033	-0.149	0.033	-1.91	4.07
5	0.015	0.013	-0.071	0.076	0.148	0.039	-0.182	0.062	0.126	0.048	0.308 0.078	-0.056	0.077	36.95	7.19
		P' = 0.237 ksc					Q = 0.149 ksc								
1	0.077	0.011	-0.224	0.014	-0.016	0.009	-0.225	0.014	0.078	0.011	0.303 0.018	-0.147	0.018	-3.00	1.71
2	0.075	0.013	-0.194	0.011	-0.020	0.008	-0.196	0.011	0.076	0.013	0.272 0.017	-0.119	0.017	-4.15	1.75
3	0.091	0.015	-0.213	0.014	-0.006	0.010	-0.213	0.014	0.091	0.015	0.304 0.020	-0.122	0.020	-1.21	1.89
4	0.073	0.035	-0.190	0.023	0.036	0.021	-0.194	0.023	0.078	0.035	0.273 0.042	-0.116	0.042	7.57	4.39
5	0.114	0.090	-0.251	0.117	0.057	0.074	-0.260	0.117	0.123	0.091	0.383 0.148	-0.137	0.148	8.68	11.09

AREA	Ex	Ex(SD)	Ey	Ey(SD)	Exy	Exy(SD)	E3	E3(SD)	E1	E1(SD)	GAMMA	G(SD)	EV	EV(SD)	PS.	PS(SD)
		P' =	0,239	ksc			Q =	0,160	ksc							
1	0,117	0,014	-0,238	0,012	-0,006	0,009	-0,238	0,012	0,117	0,014	0,356	0,018	-0,121	0,018	-0,92	1,45
2	0,117	0,008	-0,230	0,010	-0,017	0,006	-0,231	0,010	0,117	0,008	0,348	0,013	-0,114	0,013	-2,79	1,03
3	0,119	0,011	-0,249	0,013	-0,019	0,008	-0,250	0,013	0,120	0,011	0,370	0,017	-0,131	0,017	-2,87	1,32
4	0,162	0,031	-0,221	0,020	-0,019	0,018	-0,222	0,020	0,163	0,031	0,385	0,037	-0,059	0,037	-2,78	2,73
5	0,167	0,135	-0,149	0,181	0,001	0,113	-0,149	0,181	0,167	0,135	0,316	0,226	0,019	0,226	0,10	20,53
		P' =	0,244	ksc			Q =	0,170	ksc							
1	0,126	0,012	-0,308	0,021	-0,012	0,012	-0,308	0,021	0,126	0,012	0,434	0,024	-0,182	0,024	-1,54	1,61
2	0,119	0,012	-0,275	0,013	-0,040	0,009	-0,279	0,013	0,123	0,012	0,401	0,018	-0,156	0,018	-5,71	1,27
3	0,098	0,017	-0,294	0,016	-0,025	0,012	-0,295	0,016	0,100	0,017	0 395	0,023	-0,196	0,023	-3,63	1,66
4	0,095	0,043	-0,261	0,022	0,013	0,024	-0,261	0,022	0,096	0,043	0,357	0,048	-0,166	0,048	2,16	3,81
5	0,070	0,166	-0,148	0,169	-0,027	0,118	-0,151	0,168	0,074	0,166	0,225	0,237	-0,077	0,237	-6,95	30,18
		P' =	0,245	ksc			Q =	0,180	ksc							
1	0,104	0,017	-0,344	0,019	-0,001	0,013	-0,344	0,019	0,104	0,017	0,447	0,025	-0,240	0,025	-0,07	1,60
2	0,108	0,015	-0,309	0,016	-0,027	0,011	-0,310	0,016	0,110	0,015	0,420	0,022	-0,201	0,022	-3,75	1,49
3	0,122	0,013	-0,351	0,015	-0,032	0,010	-0,353	0,015	0,124	0,013	0,477	0,020	-0,229	0,020	-3,90	1,18
4	0,109	0,029	-0,316	0,030	-0,017	0,021	-0,316	0,030	0,110	0,028	0,426	0,042	-0,207	0,042	-2,33	2,80
5	0,023	0,112	-0,208	0,096	-0,082	0,073	-0,234	0,097	0,049	0,110	0,283	0,147	-0,185	0,147	-17,76	14,86
		P' =	0,264	ksc			Q =	0,190	ksc							
1	0,168	0,009	-0,365	0,013	-0,021	0,008	-0,365	0,013	0,169	0,009	0,534	0,015	-0,197	0,015	-2,21	0,83
2	0,152	0,009	-0,366	0,014	-0,017	0,008	-0,367	0,014	0,152	0,009	0,519	0,017	-0,214	0,017	-1,85	0,93
3	0,162	0,009	-0,391	0,015	-0,012	0,009	-0,391	0,015	0,162	0,009	0,553	0,018	-0,229	0,018	-1,24	0,93
4	0,172	0,024	-0,454	0,024	0,013	0,017	-0,455	0,024	0,172	0,024	0,627	0,034	-0,283	0,034	1,21	1,57
5	0,091	0,045	-0,332	0,109	0,020	0,060	-0,333	0,109	0,092	0,046	0,426	0,118	-0,241	0,118	2,67	8,06
		P' =	0,276	ksc			Q =	0,200	ksc							
1	0,229	0,011	-0,438	0,017	-0,021	0,010	-0,439	0,017	0,230	0,011	0,668	0,020	-0,209	0,020	-1,82	0,86
2	0,224	0,011	-0,455	0,020	-0,028	0,011	-0,456	0,020	0,225	0,011	0,681	0,023	-0,231	0,023	-2,32	0,94
3	0,241	0,014	-0,498	0,024	-0,030	0,014	-0,499	0,024	0,242	0,014	0,741	0,028	-0,257	0,028	-2,35	1,06
4	0,265	0,024	-0,540	0,046	-0,032	0,026	-0,541	0,046	0,266	0,024	0,807	0,052	-0,274	0,052	-2,24	1,87
5	0,228	0,041	-0,322	0,097	-0,080	0,054	-0,333	0,097	0,239	0,043	0,572	0,106	-0,094	0,106	-8,07	5,35
		P' =	0,292	ksc			Q =	0,210	ksc							
1	0,241	0,015	-0,586	0,022	-0,038	0,013	-0,589	0,022	0,243	0,015	0,831	0,026	-0,345	0,026	-2,63	0,91
2	0,248	0,021	-0,629	0,029	-0,044	0,018	-0,632	0,029	0,250	0,021	0,882	0,035	-0,381	0,035	-2,84	1,15
3	0,300	0,023	-0,736	0,036	-0,050	0,021	-0,738	0,036	0,302	0,023	1,041	0,043	-0,436	0,043	-2,76	1,17
4	0,313	0,049	-0,824	0,042	-0,019	0,032	-0,824	0,042	0,313	0,049	1,137	0,064	-0,511	0,064	-0,93	1,61
5	0,106	0,198	-0,615	0,041	-0,059	0,100	-0,619	0,043	0,111	0,197	0,730	0,203	-0,508	0,202	-4,62	7,84
		P' =	0,296	ksc			Q =	0,220	ksc							
1	0,409	0,040	-0,987	0,046	-0,038	0,030	-0,988	0,046	0,410	0,040	1,398	0,060	-0,578	0,060	-1,57	1,24
2	0,549	0,046	-1,129	0,048	-0,074	0,033	-1,132	0,048	0,552	0,046	1,684	0,066	-0,580	0,066	-2,51	1,13
3	0,672	0,066	-1,381	0,073	-0,071	0,049	-1,383	0,073	0,674	0,066	2,057	0,098	-0,709	0,098	-1,97	1,37
4	0,821	0,142	-1,655	0,111	-0,029	0,090	-1,656	0,111	0,821	0,142	2,477	0,180	-0,835	0,180	-0,67	2,08
5	1,111	0,871	-1,379	0,593	-0,290	0,524	-1,412	0,597	1,144	0,866	2,556	1,056	-0,268	1,054	-6,57	11,77

AREA	Ex	Ex(SD)	Ey	Ey(SD)	Exy	Exy(SD)	E3	E3(SD)	E1	E1(SD)	GAMMA	G(SD)	EV	EV(SD)	PS.	PS(SD)
		P' =	0.294	ksc			Q =	0.225	ksc							
1	0.736	0.076	-1.528	0.053	-0.323	0.046	-1.573	0.054	0.781	0.075	2.354	0.093	-0.792	0.093	-7.96	1.13
2	0.947	0.112	-1.915	0.078	-0.401	0.067	-1.970	0.075	1.002	0.111	2.973	0.134	-0.968	0.134	-7.83	1.29
3	1.213	0.189	-2.476	0.107	-0.537	0.109	-2.553	0.110	1.290	0.188	3.843	0.217	-1.263	0.217	-8.12	1.62
4	1.784	0.410	-3.191	0.181	-0.665	0.223	-3.279	0.187	1.871	0.406	5.149	0.449	-1.408	0.448	-7.48	2.49
5	2.570	2.318	-3.329	0.453	-1.354	1.164	-3.625	0.656	2.866	2.256	6.491	2.371	-0.759	2.362	-12.32	10.37
		P' =	0.305	ksc			Q =	0.230	ksc							
1	1.079	0.112	-1.956	0.068	-0.396	0.065	-2.006	0.069	1.130	0.112	3.136	0.131	-0.876	0.131	-7.31	1.19
2	1.378	0.168	-2.479	0.095	-0.494	0.097	-2.541	0.097	1.441	0.167	3.982	0.193	-1.101	0.193	-7.18	1.39
3	1.772	0.291	-3.235	0.138	-0.663	0.162	-3.321	0.142	1.859	0.290	5.179	0.323	-1.462	0.322	-7.42	1.79
4	2.636	0.623	-4.232	0.249	-0.839	0.334	-4.333	0.258	2.737	0.618	7.070	0.672	-1.596	0.671	-6.86	2.71
5	4.510	3.990	-4.987	0.717	-1.942	1.997	-5.369	1.031	4.892	3.901	10.260	4.070	-0.477	4.054	-11.12	11.25

DSC22

AREA	Ex	Ex(SD)	Ey	Ey(SD)	Exy	Exy(SD)	E3	E3(SD)	E1	E1(SD)	GAMMA	G(SD)	EV	EV(SD)	PS.	PS(SD)
		P' =	0.239	ksc			Q =	0.010	ksc							
1	0.006	0.003	-0.008	0.003	-0.004	0.002	-0.009	0.003	0.007	0.003	0.016	0.004	-0.003	0.004	-15.62	7.73
2	0.006	0.004	-0.012	0.005	-0.003	0.003	-0.012	0.005	0.007	0.004	0.019	0.007	-0.005	0.007	-8.21	9.83
3	0.003	0.008	-0.020	0.008	-0.001	0.006	-0.020	0.008	0.003	0.008	0.023	0.012	-0.018	0.012	-2.93	14.86
4	0.005	0.020	-0.026	0.020	0.005	0.014	-0.027	0.020	0.006	0.020	0.033	0.028	-0.022	0.028	9.33	24.73
5	0.059	0.034	0.087	0.066	0.088	0.037	-0.016	0.056	0.163	0.061	0.179	0.072	0.146	0.074	-40.46	11.61
		P' =	0.237	ksc			Q =	0.020	ksc							
1	0.129	0.005	0.070	0.005	0.005	0.004	0.070	0.005	0.129	0.005	0.060	0.007	0.199	0.007	4.75	3.34
2	0.129	0.006	0.074	0.007	0.004	0.005	0.074	0.007	0.129	0.006	0.055	0.009	0.203	0.009	4.26	4.92
3	0.122	0.011	0.061	0.014	0.010	0.009	0.060	0.014	0.123	0.011	0.064	0.018	0.182	0.018	8.80	8.11
4	0.112	0.026	0.061	0.028	0.005	0.019	0.061	0.028	0.117	0.026	0.052	0.038	0.172	0.038	5.19	21.16
5	0.073	0.131	0.082	0.110	0.173	0.086	-0.096	0.136	0.250	0.136	0.347	0.172	0.154	0.171	-44.25	14.13
		P' =	0.236	ksc			Q =	0.040	ksc							
1	0.211	0.008	0.177	0.008	0.029	0.006	0.161	0.008	0.228	0.008	0.067	0.011	0.389	0.011	29.63	4.77
2	0.223	0.010	0.183	0.008	0.034	0.006	0.164	0.009	0.243	0.009	0.078	0.013	0.407	0.013	29.78	4.67
3	0.218	0.016	0.180	0.012	0.027	0.010	0.166	0.013	0.232	0.016	0.066	0.020	0.398	0.020	27.76	8.75
4	0.232	0.043	0.146	0.026	0.027	0.025	0.139	0.028	0.240	0.042	0.101	0.049	0.379	0.050	15.95	14.05
5	0.341	0.198	0.140	0.095	0.048	0.112	0.129	0.108	0.352	0.206	0.222	0.205	0.481	0.220	12.73	26.69
		P' =	0.230	ksc			Q =	0.060	ksc							
1	0.041	0.004	-0.095	0.005	-0.008	0.003	-0.096	0.005	0.042	0.004	0.138	0.006	-0.054	0.006	-3.32	1.33
2	0.037	0.005	-0.095	0.006	-0.003	0.004	-0.096	0.006	0.037	0.005	0.132	0.008	-0.059	0.008	-1.34	1.82
3	0.039	0.011	-0.101	0.011	0.002	0.008	-0.101	0.011	0.039	0.011	0.140	0.016	-0.062	0.016	0.77	3.19
4	0.016	0.023	-0.105	0.024	0.017	0.017	-0.107	0.024	0.019	0.023	0.126	0.033	-0.089	0.033	7.93	7.52
5	0.021	0.024	-0.079	0.144	0.110	0.072	-0.150	0.135	0.092	0.089	0.242	0.157	-0.058	0.146	32.81	18.83
		P' =	0.225	ksc			Q =	0.080	ksc							
1	0.222	0.006	0.018	0.006	0.019	0.004	0.017	0.006	0.224	0.006	0.207	0.008	0.240	0.008	5.37	1.11
2	0.231	0.007	0.030	0.008	0.015	0.005	0.029	0.008	0.233	0.007	0.204	0.011	0.261	0.011	4.35	1.53
3	0.245	0.011	0.026	0.013	0.020	0.009	0.024	0.013	0.247	0.011	0.223	0.017	0.271	0.017	5.11	2.23
4	0.243	0.027	0.020	0.027	0.013	0.019	0.019	0.027	0.244	0.027	0.225	0.038	0.263	0.038	3.41	4.83
5	0.282	0.119	0.265	0.112	0.007	0.081	0.263	0.121	0.284	0.128	0.022	0.161	0.547	0.163	19.72	13.19
		P' =	0.206	ksc			Q =	0.100	ksc							
1	0.301	0.006	-0.152	0.005	0.006	0.004	-0.152	0.005	0.301	0.006	0.453	0.008	0.149	0.008	0.73	0.50
2	0.319	0.007	-0.158	0.007	0.007	0.005	-0.158	0.007	0.319	0.007	0.477	0.010	0.161	0.010	0.85	0.61
3	0.317	0.014	-0.172	0.011	0.012	0.009	-0.172	0.011	0.318	0.014	0.490	0.018	0.146	0.018	1.36	1.03
4	0.290	0.032	-0.205	0.023	0.012	0.020	-0.205	0.023	0.291	0.032	0.496	0.040	0.086	0.040	1.33	2.31
5	0.253	0.105	-0.214	0.005	0.071	0.054	-0.224	0.017	0.264	0.106	0.488	0.097	0.040	0.105	8.52	5.80
		P' =	0.202	ksc			Q =	0.105	ksc							
1	0.281	0.005	-0.235	0.006	0.009	0.004	-0.235	0.006	0.281	0.005	0.517	0.008	0.046	0.008	0.97	0.42
2	0.291	0.007	-0.260	0.008	0.009	0.005	-0.260	0.008	0.291	0.007	0.550	0.011	0.031	0.011	0.97	0.55
3	0.305	0.013	-0.280	0.012	0.017	0.008	-0.280	0.012	0.305	0.013	0.585	0.017	0.025	0.017	1.68	0.83
4	0.311	0.032	-0.284	0.020	0.034	0.019	-0.286	0.020	0.313	0.032	0.599	0.038	0.028	0.038	3.24	1.83
5	0.294	0.056	-0.293	0.043	0.127	0.036	-0.319	0.046	0.320	0.058	0.639	0.069	0.002	0.071	11.66	3.10

AREA	Ex	Ex(SD)	Ey	Ey(SD)	Exy	Exy(SD)	E3	E3(SD)	E1	E1(SD)	GAMMA G(SD)	EV	EV(SD)	PS,	PS(SD)
		P' =	0.200 ksc				Q =	0.110 ksc							
1	0.318	0.008	-0.322	0.006	0.049	0.005	-0.325	0.006	0.322	0.008	0.647 0.010	-0.004	0.010	4.38	0.44
2	0.345	0.009	-0.336	0.008	0.045	0.006	-0.339	0.008	0.348	0.009	0.686 0.012	0.009	0.012	3.76	0.49
3	0.355	0.015	-0.377	0.012	0.041	0.009	-0.380	0.012	0.357	0.015	0.736 0.019	-0.023	0.019	3.22	0.73
4	0.350	0.035	-0.410	0.022	0.020	0.021	-0.410	0.022	0.350	0.035	0.761 0.041	-0.060	0.041	1.52	1.58
5	0.466	0.008	-0.525	0.035	0.079	0.018	-0.532	0.035	0.473	0.009	1.004 0.037	-0.059	0.036	4.55	1.04
		P' =	0.192 ksc				Q =	0.112 ksc							
1	0.395	0.007	-0.402	0.008	-0.014	0.005	-0.402	0.008	0.395	0.007	0.797 0.010	-0.006	0.010	-0.99	0.38
2	0.429	0.009	-0.442	0.009	-0.012	0.006	-0.442	0.009	0.429	0.009	0.871 0.013	-0.013	0.013	-0.81	0.42
3	0.439	0.016	-0.479	0.014	-0.007	0.011	-0.479	0.014	0.439	0.016	0.919 0.021	-0.040	0.021	-0.46	0.66
4	0.482	0.034	-0.499	0.026	0.012	0.021	-0.499	0.026	0.482	0.034	0.981 0.042	-0.017	0.042	0.69	1.25
5	0.557	0.023	-0.539	0.064	0.091	0.033	-0.547	0.065	0.564	0.024	1.111 0.070	0.017	0.068	4.72	1.78
		P' =	0.189 ksc				Q =	0.114 ksc							
1	0.462	0.008	-0.546	0.011	-0.031	0.007	-0.547	0.011	0.463	0.008	1.009 0.014	-0.084	0.014	-1.76	0.39
2	0.514	0.010	-0.613	0.012	-0.031	0.008	-0.614	0.012	0.515	0.010	1.129 0.016	-0.099	0.016	-1.57	0.41
3	0.553	0.019	-0.673	0.018	-0.034	0.013	-0.674	0.017	0.554	0.019	1.228 0.026	-0.120	0.026	-1.58	0.60
4	0.611	0.034	-0.749	0.023	-0.031	0.021	-0.750	0.023	0.612	0.034	1.362 0.041	-0.138	0.041	-1.31	0.88
5	0.689	0.027	-0.803	0.043	0.006	0.025	-0.803	0.043	0.689	0.027	1.491 0.051	-0.114	0.051	0.24	0.97
		P' =	0.187 ksc				Q =	0.116 ksc							
1	0.630	0.011	-0.639	0.014	-0.027	0.009	-0.639	0.014	0.630	0.011	1.269 0.018	-0.009	0.018	-1.21	0.40
2	0.711	0.012	-0.729	0.014	-0.027	0.009	-0.730	0.014	0.712	0.012	1.441 0.018	-0.018	0.018	-1.05	0.37
3	0.775	0.019	-0.783	0.020	-0.021	0.014	-0.783	0.020	0.776	0.019	1.559 0.027	-0.008	0.027	-0.77	0.50
4	0.837	0.042	-0.829	0.041	-0.018	0.029	-0.829	0.041	0.837	0.042	1.666 0.059	0.008	0.059	-0.61	1.01
5	1.123	0.194	-0.843	0.077	0.050	0.106	-0.845	0.078	1.124	0.195	1.969 0.206	0.279	0.209	1.46	3.05
		P' =	0.188 ksc				Q =	0.118 ksc							
1	0.698	0.015	-0.847	0.018	-0.033	0.012	-0.848	0.018	0.698	0.015	1.546 0.023	-0.150	0.023	-1.24	0.43
2	0.801	0.017	-0.965	0.017	-0.033	0.012	-0.966	0.017	0.802	0.017	1.767 0.024	-0.164	0.024	-1.06	0.39
3	0.887	0.028	-1.059	0.020	-0.035	0.017	-1.059	0.020	0.888	0.028	1.947 0.034	-0.172	0.034	-1.03	0.50
4	0.964	0.053	-1.165	0.030	-0.040	0.031	-1.166	0.030	0.964	0.053	2.130 0.060	-0.202	0.060	-1.06	0.83
5	1.207	0.087	-1.151	0.075	-0.043	0.058	-1.152	0.075	1.200	0.087	2.360 0.115	0.056	0.115	-1.05	1.40
		P' =	0.182 ksc				Q =	0.120 ksc							
1	0.859	0.018	-0.864	0.018	-0.040	0.013	-0.865	0.018	0.860	0.018	1.725 0.026	-0.004	0.026	-1.32	0.42
2	0.992	0.019	-0.982	0.018	-0.044	0.013	-0.983	0.018	0.993	0.019	1.977 0.026	0.010	0.026	-1.28	0.38
3	1.098	0.031	-1.085	0.022	-0.050	0.019	-1.087	0.022	1.099	0.031	2.185 0.038	0.012	0.038	-1.31	0.49
4	1.204	0.062	-1.186	0.034	-0.060	0.036	-1.187	0.034	1.206	0.062	2.393 0.071	0.019	0.071	-1.44	0.86
5	1.507	0.189	-1.259	0.060	0.021	0.101	-1.259	0.060	1.507	0.190	2.766 0.198	0.248	0.198	0.43	2.09
		P' =	0.181 ksc				Q =	0.122 ksc							
1	0.979	0.021	-0.973	0.021	-0.038	0.015	-0.974	0.021	0.980	0.021	1.954 0.030	0.006	0.030	-1.12	0.44
2	1.132	0.023	-1.118	0.021	-0.047	0.015	-1.118	0.021	1.133	0.023	2.252 0.031	0.015	0.031	-1.19	0.39
3	1.266	0.033	-1.239	0.025	-0.048	0.021	-1.240	0.025	1.267	0.033	2.506 0.041	0.027	0.041	-1.10	0.47
4	1.380	0.057	-1.368	0.037	-0.077	0.034	-1.370	0.037	1.382	0.056	2.752 0.068	0.013	0.068	-1.60	0.72
5	1.793	0.126	-1.426	0.019	-0.044	0.065	-1.427	0.019	1.793	0.126	3.220 0.128	0.367	0.128	-0.77	1.17

AREA	Ex	Ex(SD)	Ey	Ey(SD)	Exy	Exy(SD)	E3	E3(SD)	E1	E1(SD)	GAMMA	G(SD)	EV	EV(SD)	PS.	PS(SD)
		P' =	0.180	ksc			Q =	0.124	ksc							
1	1.308	0.033	-1.401	0.034	-0.032	0.024	-1.402	0.034	1.308	0.033	2.710	0.047	-0.093	0.047	-0.68	0.50
2	1.540	0.035	-1.625	0.034	-0.033	0.024	-1.625	0.034	1.540	0.035	3.165	0.049	-0.085	0.049	-0.59	0.44
3	1.755	0.048	-1.818	0.039	-0.021	0.031	-1.818	0.039	1.755	0.048	3.574	0.062	-0.063	0.062	-0.34	0.49
4	1.976	0.075	-2.002	0.057	-0.041	0.048	-2.002	0.057	1.976	0.075	3.978	0.095	-0.026	0.095	-0.58	0.69
5	2.518	0.162	-2.162	0.093	-0.018	0.095	-2.162	0.093	2.518	0.162	4.680	0.187	0.355	0.187	-0.22	1.16
		P' =	0.177	ksc			Q =	0.126	ksc							
1	1.757	0.050	-1.939	0.051	-0.046	0.036	-1.939	0.051	1.758	0.050	3.697	0.071	-0.182	0.071	-0.72	0.55
2	2.100	0.052	-2.247	0.054	-0.046	0.038	-2.247	0.054	2.100	0.052	4.348	0.075	-0.147	0.075	-0.61	0.50
3	2.440	0.064	-2.547	0.062	-0.040	0.045	-2.547	0.062	2.440	0.064	4.988	0.089	-0.107	0.089	-0.45	0.51
4	2.788	0.094	-2.829	0.090	-0.050	0.065	-2.829	0.090	2.788	0.094	5.618	0.130	-0.041	0.130	-0.51	0.66
5	3.455	0.095	-3.050	0.077	0.047	0.062	-3.051	0.077	3.455	0.096	6.506	0.122	0.404	0.123	0.41	0.54
		P' =	0.189	ksc			Q =	0.127	ksc							
1	1.776	0.050	-1.981	0.052	-0.056	0.036	-1.982	0.052	1.777	0.050	3.759	0.073	-0.205	0.073	-0.86	0.55
2	2.116	0.054	-2.306	0.055	-0.056	0.039	-2.306	0.055	2.117	0.054	4.423	0.077	-0.189	0.077	-0.72	0.50
3	2.458	0.065	-2.617	0.064	-0.043	0.046	-2.617	0.063	2.458	0.065	5.076	0.091	-0.159	0.091	-0.48	0.51
4	2.813	0.095	-2.899	0.090	-0.045	0.066	-2.899	0.090	2.814	0.095	5.713	0.131	-0.086	0.131	-0.46	0.66
5	3.448	0.088	-3.089	0.178	0.164	0.098	-3.093	0.179	3.452	0.089	6.545	0.200	0.359	0.199	1.43	0.87
		P' =	0.184	ksc			Q =	0.131	ksc							
1	2.338	0.066	-2.493	0.069	-0.047	0.048	-2.493	0.069	2.338	0.066	4.832	0.096	-0.155	0.096	-0.56	0.57
2	2.779	0.071	-2.903	0.073	-0.048	0.051	-2.904	0.073	2.780	0.071	5.684	0.102	-0.124	0.102	-0.48	0.51
3	3.239	0.081	-3.303	0.082	-0.022	0.058	-3.303	0.082	3.239	0.081	6.542	0.116	-0.064	0.116	-0.19	0.51
4	3.726	0.096	-3.650	0.124	0.009	0.078	-3.650	0.124	3.726	0.096	7.376	0.157	0.076	0.157	0.07	0.60
5	4.312	0.091	-3.722	0.181	0.143	0.100	-3.724	0.182	4.314	0.092	8.038	0.204	0.590	0.203	1.02	0.72
		P' =	0.187	ksc			Q =	0.132	ksc							
1	3.150	0.089	-3.272	0.093	-0.026	0.065	-3.272	0.093	3.150	0.089	6.422	0.129	-0.122	0.129	-0.23	0.58
2	3.744	0.094	-3.827	0.099	-0.025	0.068	-3.827	0.099	3.744	0.094	7.571	0.137	-0.083	0.137	-0.19	0.52
3	4.348	0.103	-4.353	0.114	0.003	0.077	-4.353	0.114	4.348	0.103	8.701	0.154	-0.005	0.154	0.02	0.51
4	4.943	0.112	-4.877	0.150	0.051	0.093	-4.877	0.150	4.943	0.112	9.820	0.187	0.066	0.187	0.30	0.54
5	5.593	0.054	-5.052	0.177	0.295	0.091	-5.060	0.178	5.601	0.055	10.661	0.187	0.541	0.185	1.59	0.49
		P' =	0.185	ksc			Q =	0.134	ksc							
1	3.970	0.110	-3.813	0.106	0.035	0.076	-3.813	0.106	3.970	0.110	7.783	0.153	0.157	0.153	0.26	0.56
2	4.683	0.112	-4.408	0.116	0.029	0.081	-4.408	0.116	4.683	0.112	9.091	0.162	0.275	0.162	0.18	0.51
3	5.402	0.115	-5.006	0.132	0.056	0.088	-5.006	0.132	5.403	0.115	10.409	0.175	0.396	0.175	0.31	0.48
4	6.110	0.122	-5.521	0.155	0.100	0.098	-5.522	0.155	6.111	0.122	11.632	0.197	0.589	0.197	0.49	0.48
5	6.606	0.116	-5.539	0.143	0.284	0.092	-5.546	0.144	6.613	0.117	12.158	0.185	1.067	0.184	1.34	0.43
		P' =	0.199	ksc			Q =	0.136	ksc							
1	4.118	0.118	-4.501	0.119	0.000	0.084	-4.501	0.119	4.118	0.118	8.619	0.168	-0.384	0.168	-0.00	0.56
2	4.898	0.120	-5.192	0.128	0.021	0.088	-5.192	0.128	4.898	0.120	10.089	0.175	-0.294	0.175	0.12	0.50
3	5.674	0.118	-5.869	0.141	0.075	0.093	-5.870	0.141	5.675	0.118	11.544	0.184	-0.195	0.184	0.37	0.46
4	6.381	0.148	-6.377	0.161	0.140	0.109	-6.379	0.161	6.383	0.148	12.761	0.219	0.004	0.219	0.63	0.49
5	6.982	0.232	-6.204	0.030	0.385	0.120	-6.215	0.031	6.994	0.234	13.209	0.230	0.778	0.234	1.67	0.51

AREA	Ex	Ex(SD)	Ey	Ey(SD)	Exy	Exy(SD)	E3	E3(SD)	E1	E1(SD)	GAMMA G(SD)	EV	EV(SD)	PS.	PS(SD)
		P' =	0.191	ksc			Q =	0.138	ksc						
1	4.760	0.136	-5.385	0.139	-0.056	0.097	-5.385	0.139	4.760	0.136	10.145 0.194	-0.625	0.194	-0.32	0.55
2	5.647	0.134	-6.195	0.147	-0.013	0.100	-6.195	0.147	5.647	0.134	11.842 0.199	-0.548	0.199	-0.06	0.48
3	6.528	0.122	-6.964	0.159	0.059	0.101	-6.964	0.159	6.528	0.122	13.492 0.200	-0.436	0.200	0.25	0.43
4	7.181	0.200	-7.395	0.162	0.195	0.130	-7.398	0.162	7.184	0.200	14.582 0.257	-0.214	0.257	0.77	0.51
5	7.506	0.446	-7.030	0.025	0.356	0.228	-7.038	0.027	7.515	0.449	14.553 0.441	0.477	0.447	1.40	0.89

DSC23

AREA	Ex	Ex(SD)	Ey	Ey(SD)	Exy	Exy(SD)	E3	E3(SD)	E1	E1(SD)	GAMMA G(SD)	EV	EV(SD)	PS.	PS(SD)
		P' =	0,247 ksc				Q =	0,002 ksc							
1	0,014	0,003	0,011	0,004	0,013	0,002	-0,001	0,003	0,026	0,003	0,027 0,005	0,025	0,005	42,03	5,20
2	0,008	0,005	0,011	0,005	0,015	0,004	-0,005	0,005	0,024	0,005	0,029 0,007	0,019	0,007	-42,53	6,91
3	0,017	0,011	0,016	0,007	0,018	0,006	-0,001	0,009	0,034	0,009	0,035 0,013	0,033	0,013	44,33	10,26
4	0,049	0,020	0,035	0,016	-0,010	0,013	0,029	0,017	0,054	0,019	0,025 0,025	0,084	0,025	-27,45	29,35
5	-0,013	0,083	-0,025	0,029	-0,111	0,047	-0,129	0,063	0,092	0,066	0,221 0,094	-0,038	0,088	-43,41	11,37
		P' =	0,241 ksc				Q =	0,014 ksc							
1	0,140	0,005	0,109	0,006	0,005	0,004	0,108	0,006	0,141	0,005	0,033 0,008	0,248	0,008	9,42	6,84
2	0,154	0,007	0,131	0,008	0,005	0,005	0,131	0,008	0,154	0,007	0,024 0,010	0,285	0,010	11,15	12,34
3	0,192	0,008	0,154	0,012	0,013	0,008	0,150	0,012	0,196	0,009	0,046 0,015	0,346	0,015	17,06	9,39
4	0,220	0,019	0,182	0,024	0,002	0,015	0,182	0,024	0,220	0,019	0,038 0,030	0,402	0,030	2,54	23,27
5	0,150	0,040	-0,003	0,010	-0,037	0,022	-0,012	0,014	0,158	0,039	0,170 0,042	0,146	0,041	-12,90	7,37
		P' =	0,236 ksc				Q =	0,041 ksc							
1	0,088	0,005	0,023	0,004	0,015	0,003	0,020	0,004	0,091	0,005	0,071 0,007	0,111	0,007	12,38	2,70
2	0,101	0,006	0,038	0,006	0,011	0,004	0,036	0,006	0,103	0,006	0,066 0,008	0,139	0,008	9,39	3,58
3	0,122	0,010	0,053	0,009	0,007	0,007	0,053	0,009	0,122	0,010	0,070 0,014	0,175	0,014	5,73	5,58
4	0,153	0,022	0,087	0,024	-0,004	0,017	0,087	0,024	0,153	0,022	0,067 0,033	0,240	0,033	-3,66	14,17
5	0,110	0,009	-0,075	0,035	-0,028	0,017	-0,079	0,035	0,115	0,010	0,193 0,036	0,036	0,036	-8,55	5,04
		P' =	0,233 ksc				Q =	0,060 ksc							
1	0,123	0,005	0,040	0,005	0,007	0,003	0,039	0,005	0,123	0,005	0,084 0,006	0,162	0,006	4,98	2,19
2	0,129	0,006	0,062	0,006	0,008	0,004	0,061	0,006	0,130	0,006	0,068 0,009	0,191	0,009	6,51	3,68
3	0,151	0,011	0,094	0,010	-0,003	0,007	0,094	0,010	0,151	0,011	0,057 0,015	0,245	0,015	-2,47	7,38
4	0,169	0,023	0,120	0,029	-0,019	0,019	0,114	0,028	0,176	0,023	0,062 0,037	0,289	0,037	-18,73	17,05
5	0,108	0,068	0,029	0,028	-0,052	0,039	0,003	0,041	0,133	0,064	0,130 0,076	0,136	0,074	-26,30	16,59
		P' =	0,222 ksc				Q =	0,081 ksc							
1	0,163	0,005	0,040	0,005	-0,002	0,004	0,040	0,005	0,163	0,005	0,123 0,007	0,203	0,007	-1,05	1,69
2	0,178	0,007	0,061	0,006	-0,005	0,005	0,060	0,006	0,178	0,007	0,118 0,009	0,239	0,009	-2,19	2,25
3	0,205	0,012	0,089	0,009	-0,005	0,008	0,089	0,009	0,206	0,012	0,116 0,015	0,295	0,015	-2,62	3,73
4	0,238	0,025	0,130	0,017	-0,022	0,015	0,126	0,018	0,242	0,025	0,116 0,031	0,368	0,031	-11,03	7,58
5	0,152	0,054	0,046	0,056	-0,039	0,039	0,034	0,056	0,165	0,054	0,132 0,078	0,199	0,078	-18,21	16,93
		P' =	0,216 ksc				Q =	0,100 ksc							
1	0,150	0,006	-0,053	0,005	-0,011	0,004	-0,053	0,005	0,151	0,006	0,204 0,008	0,097	0,008	-3,19	1,10
2	0,161	0,008	-0,044	0,007	-0,011	0,005	-0,044	0,007	0,162	0,008	0,206 0,011	0,118	0,011	-3,11	1,49
3	0,180	0,013	-0,030	0,012	-0,011	0,009	-0,031	0,012	0,181	0,013	0,211 0,017	0,150	0,017	-3,03	2,36
4	0,204	0,023	0,010	0,023	-0,018	0,016	0,008	0,023	0,206	0,023	0,198 0,033	0,214	0,033	-5,25	4,71
5	0,185	0,005	-0,155	0,032	-0,030	0,015	-0,157	0,032	0,188	0,005	0,345 0,032	0,030	0,032	-4,94	2,49
		P' =	0,213 ksc				Q =	0,105 ksc							
1	0,194	0,006	-0,020	0,006	-0,010	0,004	-0,020	0,006	0,194	0,006	0,214 0,008	0,174	0,008	-2,63	1,11
2	0,212	0,008	0,008	0,007	-0,013	0,006	0,007	0,007	0,213	0,008	0,205 0,011	0,220	0,011	-3,58	1,55
3	0,236	0,013	0,036	0,011	-0,011	0,008	0,036	0,011	0,236	0,013	0,200 0,017	0,272	0,017	-3,08	2,43
4	0,265	0,026	0,055	0,029	-0,042	0,019	0,047	0,028	0,273	0,026	0,227 0,039	0,320	0,039	-10,83	4,90
5	0,273	0,083	-0,124	0,092	-0,132	0,062	-0,164	0,092	0,313	0,084	0,477 0,124	0,149	0,124	-16,82	7,44

AREA	Ex	Ex(SD)	Ey	Ey(SD)	Exy	Exy(SD)	E3	E3(SD)	E1	E1(SD)	GAMMA	G(SD)	EV	EV(SD)	PS.	PS(SD)
	P' = 0.211 ksc						Q = 0.110 ksc									
1	0.199	0.006	-0.049	0.005	0.001	0.004	-0.049	0.005	0.199	0.006	0.247	0.007	0.150	0.007	0.28	0.85
2	0.212	0.007	-0.032	0.006	0.001	0.005	-0.032	0.006	0.212	0.007	0.244	0.009	0.180	0.009	0.11	1.07
3	0.230	0.011	-0.010	0.009	0.005	0.007	-0.010	0.009	0.231	0.011	0.240	0.014	0.221	0.014	1.27	1.68
4	0.256	0.015	0.044	0.019	-0.005	0.012	0.044	0.019	0.256	0.015	0.212	0.025	0.300	0.025	-1.39	3.31
5	0.202	0.038	-0.073	0.037	-0.057	0.027	-0.084	0.038	0.213	0.038	0.297	0.053	0.129	0.053	-11.19	5.18
	P' = 0.210 ksc						Q = 0.115 ksc									
1	0.180	0.005	-0.108	0.005	-0.006	0.004	-0.109	0.005	0.180	0.005	0.288	0.007	0.071	0.007	-1.27	0.73
2	0.195	0.006	-0.086	0.007	-0.007	0.005	-0.086	0.007	0.195	0.006	0.281	0.009	0.108	0.009	-1.39	0.94
3	0.208	0.012	-0.060	0.009	-0.003	0.007	-0.060	0.009	0.208	0.012	0.268	0.015	0.148	0.015	-0.66	1.57
4	0.248	0.023	-0.016	0.020	-0.016	0.015	-0.017	0.020	0.249	0.023	0.266	0.030	0.231	0.030	-3.35	3.26
5	0.143	0.114	-0.065	0.115	-0.132	0.081	-0.130	0.116	0.207	0.115	0.336	0.162	0.077	0.162	-25.90	13.81
	P' = 0.202 ksc						Q = 0.125 ksc									
1	0.273	0.006	-0.085	0.007	0.003	0.005	-0.085	0.007	0.273	0.006	0.358	0.009	0.188	0.009	0.53	0.74
2	0.297	0.007	-0.057	0.008	0.004	0.005	-0.057	0.008	0.297	0.007	0.353	0.010	0.240	0.010	0.72	0.84
3	0.325	0.011	-0.037	0.010	0.004	0.007	-0.037	0.010	0.325	0.011	0.362	0.014	0.288	0.014	0.64	1.14
4	0.368	0.020	-0.026	0.023	-0.010	0.015	-0.026	0.022	0.368	0.020	0.394	0.030	0.342	0.030	-1.52	2.17
5	0.347	0.015	-0.062	0.031	-0.100	0.017	-0.085	0.031	0.371	0.016	0.456	0.034	0.286	0.035	-13.08	2.10
	P' = 0.200 ksc						Q = 0.150 ksc									
1	0.342	0.009	-0.312	0.011	-0.010	0.007	-0.312	0.011	0.343	0.009	0.654	0.014	0.031	0.014	-0.85	0.62
2	0.376	0.012	-0.310	0.012	-0.010	0.008	-0.310	0.012	0.376	0.012	0.686	0.017	0.066	0.017	-0.86	0.70
3	0.438	0.015	-0.308	0.015	-0.006	0.011	-0.308	0.015	0.438	0.015	0.746	0.021	0.129	0.021	-0.47	0.82
4	0.490	0.022	-0.298	0.031	-0.017	0.019	-0.298	0.031	0.491	0.022	0.789	0.038	0.193	0.038	-1.20	1.36
5	0.434	0.116	-0.424	0.027	-0.023	0.064	-0.425	0.027	0.434	0.116	0.859	0.119	0.010	0.119	-1.50	4.28
	P' = 0.212 ksc						Q = 0.165 ksc									
1	0.670	0.019	-0.666	0.022	-0.012	0.015	-0.666	0.022	0.670	0.019	1.336	0.029	0.003	0.029	-0.52	0.62
2	0.793	0.022	-0.731	0.026	-0.015	0.017	-0.731	0.026	0.793	0.022	1.524	0.034	0.063	0.034	-0.57	0.64
3	0.907	0.026	-0.802	0.031	-0.008	0.020	-0.802	0.031	0.907	0.026	1.709	0.040	0.106	0.040	-0.27	0.68
4	1.047	0.037	-0.906	0.038	-0.009	0.026	-0.906	0.038	1.047	0.037	1.953	0.053	0.141	0.053	-0.27	0.77
5	0.989	0.183	-1.151	0.005	0.112	0.099	-1.157	0.012	0.995	0.183	2.152	0.183	-0.162	0.183	2.99	2.65
	P' = 0.215 ksc						Q = 0.174 ksc									
1	3.649	0.162	-4.341	0.110	-0.560	0.098	-4.380	0.111	3.688	0.162	8.068	0.196	-0.693	0.196	-3.99	0.70
2	4.521	0.180	-5.027	0.129	-0.456	0.111	-5.049	0.129	4.542	0.180	9.591	0.222	-0.506	0.222	-2.73	0.66
3	5.261	0.237	-5.571	0.208	-0.257	0.158	-5.577	0.208	5.267	0.237	10.844	0.315	-0.310	0.315	-1.36	0.83
4	5.673	0.580	-5.996	0.396	-0.242	0.351	-6.001	0.396	5.678	0.579	11.679	0.702	-0.322	0.702	-1.19	1.72
5	5.692	2.254	-5.374	1.746	-0.217	1.465	-5.379	1.747	5.696	2.254	11.075	2.851	0.318	2.851	-1.12	7.58

DSC24

AREA	Ex	Ex(SD)	Ey	Ey(SD)	Exy	Exy(SD)	E3	E3(SD)	E1	E1(SD)	GAMMA	G(SD)	EV	EV(SD)	PS.	PS(SD)
		P' =	0.243	ksc			Q =	0.002	ksc							
1	0.002	0.004	-0.005	0.005	0.005	0.003	-0.008	0.004	0.005	0.004	0.013	0.006	-0.004	0.006	29.26	13.41
2	-0.003	0.005	-0.005	0.007	0.004	0.005	-0.008	0.007	0.000	0.006	0.008	0.009	-0.008	0.009	35.11	31.22
3	-0.003	0.009	-0.009	0.011	0.008	0.007	-0.015	0.010	0.003	0.010	0.018	0.014	-0.012	0.014	35.06	22.86
4	-0.018	0.024	-0.017	0.020	-0.006	0.016	-0.024	0.022	-0.011	0.022	0.013	0.031	-0.035	0.031	43.75	70.04
5	-0.014	0.047	0.016	0.008	-0.094	0.024	-0.094	0.036	0.096	0.031	0.190	0.049	0.002	0.048	40.47	7.23
		P' =	0.226	ksc			Q =	0.060	ksc							
1	0.102	0.009	-0.031	0.011	-0.005	0.007	-0.032	0.011	0.102	0.009	0.134	0.014	0.071	0.014	-2.08	2.90
2	0.132	0.011	-0.007	0.013	-0.006	0.008	-0.007	0.013	0.132	0.011	0.140	0.017	0.125	0.017	-2.30	3.51
3	0.161	0.020	0.054	0.015	0.002	0.013	0.054	0.015	0.161	0.020	0.107	0.025	0.214	0.025	1.06	6.87
4	0.155	0.038	0.059	0.040	0.008	0.028	0.058	0.040	0.156	0.038	0.098	0.055	0.214	0.055	4.89	16.05
5	0.133	0.041	-0.034	0.013	0.042	0.022	-0.045	0.016	0.143	0.040	0.187	0.043	0.098	0.043	13.44	6.60
		P' =	0.212	ksc			Q =	0.100	ksc							
1	0.202	0.007	-0.130	0.007	-0.017	0.005	-0.131	0.007	0.203	0.007	0.333	0.010	0.072	0.010	-2.98	0.85
2	0.229	0.008	-0.107	0.010	-0.013	0.006	-0.108	0.010	0.230	0.008	0.337	0.013	0.122	0.013	-2.12	1.09
3	0.234	0.015	-0.101	0.014	-0.006	0.010	-0.101	0.014	0.234	0.015	0.335	0.020	0.133	0.020	-1.01	1.75
4	0.208	0.035	-0.099	0.040	-0.002	0.027	-0.099	0.040	0.208	0.035	0.307	0.053	0.108	0.053	-0.34	4.98
5	0.244	0.118	-0.189	0.131	-0.047	0.088	-0.194	0.130	0.249	0.118	0.444	0.176	0.055	0.176	-6.12	11.36
		P' =	0.205	ksc			Q =	0.125	ksc							
1	0.289	0.007	-0.360	0.008	-0.011	0.005	-0.360	0.008	0.289	0.007	0.650	0.011	-0.071	0.011	-0.97	0.48
2	0.309	0.009	-0.366	0.011	-0.005	0.007	-0.366	0.011	0.309	0.009	0.675	0.014	-0.057	0.014	-0.45	0.61
3	0.312	0.012	-0.389	0.017	-0.003	0.010	-0.389	0.017	0.312	0.012	0.701	0.020	-0.076	0.020	-0.21	0.82
4	0.238	0.022	-0.420	0.037	-0.028	0.021	-0.422	0.037	0.239	0.022	0.660	0.043	-0.183	0.043	-2.41	1.86
5	0.161	0.069	-0.363	0.093	-0.057	0.058	-0.369	0.093	0.167	0.069	0.536	0.116	-0.202	0.116	-6.15	6.16
		P' =	0.209	ksc			Q =	0.145	ksc							
1	0.563	0.013	-0.589	0.016	-0.027	0.010	-0.590	0.016	0.564	0.013	1.154	0.021	-0.026	0.021	-1.33	0.51
2	0.617	0.017	-0.636	0.022	-0.020	0.014	-0.636	0.022	0.617	0.017	1.253	0.028	-0.019	0.028	-0.90	0.63
3	0.654	0.026	-0.720	0.031	-0.028	0.020	-0.721	0.031	0.655	0.026	1.375	0.041	-0.066	0.041	-1.16	0.85
4	0.641	0.065	-0.827	0.070	-0.063	0.048	-0.830	0.070	0.644	0.065	1.474	0.095	-0.186	0.095	-2.46	1.85
5	0.867	0.162	-0.727	0.235	0.061	0.142	-0.729	0.235	0.870	0.162	1.599	0.285	0.141	0.285	2.19	5.08
		P' =	0.217	ksc			Q =	0.155	ksc							
1	0.792	0.022	-0.898	0.023	-0.016	0.016	-0.898	0.023	0.792	0.022	1.690	0.032	-0.106	0.032	-0.54	0.53
2	0.896	0.026	-1.000	0.030	-0.020	0.020	-1.000	0.030	0.896	0.026	1.896	0.040	-0.105	0.040	-0.60	0.60
3	0.990	0.030	-1.118	0.046	-0.041	0.027	-1.119	0.046	0.991	0.030	2.109	0.055	-0.128	0.055	-1.11	0.73
4	1.035	0.050	-1.267	0.072	-0.097	0.044	-1.271	0.072	1.039	0.051	2.310	0.088	-0.232	0.088	-2.40	1.09
5	1.057	0.016	-1.455	0.240	-0.201	0.118	-1.471	0.239	1.073	0.024	2.545	0.240	-0.398	0.240	-4.55	2.65
		P' =	0.228	ksc			Q =	0.160	ksc							
1	1.090	0.034	-1.298	0.034	0.012	0.024	-1.298	0.034	1.090	0.034	2.388	0.048	-0.208	0.048	0.28	0.58
2	1.250	0.040	-1.466	0.043	0.014	0.030	-1.466	0.043	1.250	0.040	2.715	0.059	-0.216	0.059	0.30	0.62
3	1.450	0.047	-1.678	0.058	0.023	0.037	-1.678	0.058	1.450	0.047	3.129	0.074	-0.228	0.074	0.42	0.68
4	1.616	0.043	-1.944	0.080	0.003	0.045	-1.944	0.080	1.617	0.043	3.561	0.091	-0.327	0.091	0.04	0.73
5	1.684	0.168	-2.205	0.203	-0.054	0.131	-2.206	0.203	1.685	0.168	3.890	0.263	-0.521	0.263	-0.80	1.93

AREA	Ex	Ex(SD)	Ey	Ey(SD)	Exy	Exy(SD)	E3	E3(SD)	E1	E1(SD)	GAMMA	G(SD)	EV	EV(SD)	PS.	PS(SD)
		P' =	0.233	ksc				Q =	0.169	ksc						
1	2.232	0.090	-2.642	0.085	0.019	0.062	-2.642	0.085	2.232	0.090	4.875	0.124	-0.410	0.124	0.22	0.73
2	2.704	0.105	-3.142	0.107	0.003	0.075	-3.142	0.107	2.704	0.105	5.847	0.150	-0.438	0.150	0.03	0.73
3	3.225	0.121	-3.712	0.148	-0.039	0.095	-3.712	0.148	3.226	0.121	6.938	0.191	-0.487	0.191	-0.32	0.78
4	3.729	0.140	-4.404	0.201	-0.094	0.122	-4.405	0.201	3.730	0.140	8.135	0.245	-0.675	0.245	-0.66	0.86
5	4.076	0.201	-4.957	0.248	-0.251	0.159	-4.964	0.248	4.083	0.201	9.048	0.319	-0.881	0.319	-1.59	1.01
		P' =	0.190	ksc				Q =	0.174	ksc						
1	3.531	0.167	-4.152	0.147	0.196	0.111	-4.157	0.147	3.536	0.167	7.693	0.223	-0.620	0.223	1.46	0.83
2	4.343	0.212	-4.997	0.187	0.216	0.142	-5.002	0.187	4.348	0.212	9.350	0.283	-0.655	0.283	1.32	0.87
3	5.279	0.286	-5.898	0.276	0.128	0.199	-5.900	0.276	5.281	0.286	11.180	0.397	-0.619	0.397	0.65	1.02
4	6.001	0.440	-6.757	0.386	-0.000	0.293	-6.757	0.386	6.001	0.440	12.758	0.585	-0.756	0.585	-0.00	1.32
5	5.895	0.023	-6.724	0.158	-0.136	0.078	-6.725	0.157	5.896	0.023	12.622	0.159	-0.829	0.159	-0.62	0.35

DSC25

AREA	Ex	Ex(SD)	Ey	Ey(SD)	Exy	Exy(SD)	E3	E3(SD)	E1	E1(SD)	GAMMA	G(SD)	EV	EV(SD)	PS.	PS(SD)
		P' =	0,248	ksc			Q =	0,013	ksc							
1	-0,003	0,013	0,024	0,010	-0,022	0,008	-0,014	0,012	0,036	0,010	0,051	0,016	0,022	0,016	29,10	8,95
2	-0,022	0,020	0,012	0,014	-0,031	0,013	-0,041	0,019	0,030	0,016	0,071	0,025	-0,010	0,025	30,62	10,09
3	0,018	0,034	0,001	0,027	-0,036	0,022	-0,027	0,030	0,046	0,031	0,073	0,043	0,019	0,043	-38,47	16,89
4	-0,098	0,087	0,002	0,062	-0,040	0,054	-0,112	0,084	0,017	0,065	0,128	0,107	-0,095	0,107	19,40	23,86
5	0,244	0,375	-0,217	0,110	-0,003	0,193	-0,217	0,110	0,244	0,374	0,461	0,390	0,027	0,390	-0,36	23,93
		P' =	0,245	ksc			Q =	0,033	ksc							
1	-0,022	0,011	0,005	0,009	-0,032	0,007	-0,044	0,010	0,026	0,009	0,070	0,014	-0,017	0,014	33,79	5,72
2	-0,041	0,016	-0,015	0,011	-0,033	0,010	-0,064	0,014	0,007	0,013	0,071	0,019	-0,056	0,019	34,28	7,84
3	-0,041	0,025	-0,047	0,019	-0,038	0,016	-0,082	0,022	-0,006	0,023	0,076	0,032	-0,088	0,032	-42,82	12,04
4	-0,068	0,064	-0,081	0,042	-0,022	0,038	-0,098	0,051	-0,051	0,057	0,047	0,077	-0,149	0,076	-36,57	46,88
5	0,268	0,040	-0,101	0,181	-0,120	0,094	-0,136	0,173	0,304	0,064	0,440	0,184	0,167	0,185	-16,55	12,07
		P' =	0,244	ksc			Q =	0,053	ksc							
1	-0,007	0,011	-0,004	0,010	-0,038	0,007	-0,044	0,011	0,033	0,010	0,077	0,015	-0,011	0,015	43,68	5,54
2	-0,035	0,016	-0,034	0,014	-0,027	0,011	-0,062	0,015	-0,007	0,015	0,055	0,021	-0,069	0,021	44,19	11,22
3	-0,031	0,025	-0,074	0,021	-0,034	0,016	-0,092	0,022	-0,013	0,024	0,080	0,033	-0,105	0,033	-28,80	11,84
4	-0,015	0,052	-0,094	0,042	-0,035	0,034	-0,107	0,043	-0,002	0,051	0,105	0,067	-0,108	0,067	-20,65	18,32
5	-0,021	0,090	-0,338	0,023	-0,238	0,046	-0,466	0,046	0,107	0,079	0,573	0,093	-0,359	0,093	-28,19	4,69
		P' =	0,240	ksc			Q =	0,073	ksc							
1	-0,017	0,016	-0,029	0,012	-0,042	0,010	-0,066	0,014	0,020	0,014	0,085	0,020	-0,046	0,020	-40,77	6,57
2	-0,063	0,021	-0,029	0,016	-0,052	0,013	-0,101	0,020	0,008	0,018	0,110	0,027	-0,093	0,027	35,93	6,96
3	-0,016	0,031	-0,081	0,027	-0,059	0,021	-0,116	0,028	0,019	0,030	0,135	0,041	-0,097	0,041	-30,51	8,73
4	-0,104	0,070	-0,144	0,057	-0,008	0,045	-0,145	0,057	-0,102	0,069	0,043	0,090	-0,248	0,090	-11,19	59,98
5	-0,210	0,302	-0,324	0,038	0,064	0,150	-0,353	0,127	-0,182	0,278	0,171	0,298	-0,534	0,304	24,04	50,01
		P' =	0,235	ksc			Q =	0,093	ksc							
1	-0,042	0,014	-0,003	0,012	-0,070	0,009	-0,096	0,013	0,050	0,012	0,146	0,018	-0,045	0,018	37,32	3,50
2	-0,068	0,019	-0,015	0,015	-0,046	0,012	-0,094	0,018	0,012	0,016	0,106	0,024	-0,083	0,024	29,86	6,48
3	-0,077	0,025	-0,036	0,027	-0,053	0,018	-0,113	0,025	0,000	0,026	0,114	0,036	-0,113	0,036	34,39	9,15
4	-0,077	0,047	-0,097	0,052	0,001	0,035	-0,097	0,052	-0,077	0,047	0,020	0,070	-0,174	0,070	3,07	99,62
5	-0,154	0,001	-0,123	0,153	0,064	0,078	-0,204	0,097	-0,073	0,122	0,131	0,155	-0,277	0,153	-38,33	33,39
		P' =	0,232	ksc			Q =	0,098	ksc							
1	-0,069	0,012	-0,037	0,011	-0,093	0,008	-0,147	0,011	0,041	0,011	0,189	0,016	-0,106	0,016	40,14	2,43
2	-0,101	0,018	-0,069	0,017	-0,092	0,012	-0,178	0,017	0,008	0,017	0,186	0,024	-0,170	0,024	40,08	3,76
3	-0,113	0,028	-0,100	0,032	-0,094	0,021	-0,201	0,030	-0,012	0,030	0,189	0,043	-0,213	0,043	43,09	6,44
4	-0,267	0,061	-0,221	0,062	-0,084	0,043	-0,331	0,061	-0,157	0,061	0,174	0,087	-0,487	0,087	37,34	14,25
5	-0,156	0,162	-0,404	0,222	0,035	0,138	-0,409	0,221	-0,151	0,164	0,258	0,275	-0,560	0,275	7,78	30,73
		P' =	0,227	ksc			Q =	0,103	ksc							
1	-0,054	0,016	-0,034	0,012	-0,109	0,010	-0,153	0,014	0,066	0,014	0,219	0,020	-0,087	0,020	42,40	2,62
2	-0,067	0,022	-0,043	0,018	-0,081	0,014	-0,137	0,020	0,026	0,020	0,163	0,028	-0,110	0,028	40,85	5,01
3	-0,088	0,034	-0,074	0,030	-0,105	0,023	-0,186	0,032	0,024	0,032	0,210	0,045	-0,161	0,045	43,08	6,17
4	-0,130	0,062	-0,046	0,072	-0,051	0,047	-0,154	0,063	-0,022	0,070	0,132	0,095	-0,176	0,095	25,26	20,60
5	-0,005	0,070	-0,349	0,185	0,007	0,100	-0,349	0,185	-0,005	0,070	0,344	0,198	-0,354	0,198	1,15	16,69

AREA	Ex	Ex(SD)	Ey	Ey(SD)	Exy	Exy(SD)	E3	E3(SD)	E1	E1(SD)	GAMMA G(SD)	EV	EV(SD)	PS.	PS(SD)
		P' =	0,223 ksc				Q =	0,108 ksc							
1	-0,083	0,014	-0,038	0,011	-0,124	0,009	-0,186	0,013	0,065	0,012	0,252 0,018	-0,121	0,018	39,80	2,00
2	-0,133	0,021	-0,058	0,015	-0,101	0,013	-0,203	0,019	0,012	0,017	0,215 0,026	-0,192	0,026	34,85	3,39
3	-0,136	0,032	-0,104	0,028	-0,118	0,021	-0,239	0,030	-0,001	0,030	0,238 0,042	-0,239	0,042	41,14	5,10
4	-0,153	0,073	-0,239	0,049	-0,078	0,045	-0,285	0,056	-0,107	0,068	0,178 0,089	-0,392	0,088	-30,67	14,26
5	-0,093	0,057	-0,045	0,180	0,127	0,096	-0,197	0,125	0,060	0,146	0,258 0,190	-0,137	0,189	-39,65	20,92
		P' =	0,221 ksc				Q =	0,113 ksc							
1	-0,046	0,015	0,018	0,013	-0,151	0,010	-0,168	0,014	0,140	0,014	0,308 0,020	-0,028	0,020	38,95	1,84
2	-0,090	0,021	-0,030	0,014	-0,107	0,013	-0,171	0,019	0,051	0,017	0,222 0,026	-0,120	0,026	37,13	3,30
3	-0,090	0,035	-0,076	0,027	-0,114	0,022	-0,197	0,031	0,031	0,031	0,228 0,044	-0,165	0,044	43,28	5,52
4	-0,141	0,060	-0,131	0,061	-0,018	0,043	-0,154	0,060	-0,118	0,060	0,037 0,085	-0,272	0,085	37,15	66,65
5	-0,128	0,150	-0,154	0,093	0,002	0,088	-0,154	0,094	-0,128	0,150	0,026 0,176	-0,282	0,177	4,81	190,49
		P' =	0,220 ksc				Q =	0,118 ksc							
1	-0,035	0,011	0,001	0,014	-0,141	0,009	-0,160	0,013	0,125	0,013	0,285 0,018	-0,034	0,018	41,36	1,83
2	-0,056	0,017	-0,006	0,012	-0,104	0,011	-0,138	0,016	0,076	0,014	0,214 0,021	-0,061	0,021	38,21	2,83
3	-0,029	0,029	-0,035	0,023	-0,108	0,019	-0,140	0,026	0,076	0,026	0,217 0,037	-0,064	0,037	-44,15	4,89
4	-0,104	0,051	-0,065	0,046	-0,043	0,035	-0,132	0,050	-0,038	0,048	0,094 0,069	-0,169	0,069	32,79	21,07
5	0,093	0,181	-0,154	0,002	-0,061	0,089	-0,168	0,041	0,108	0,175	0,276 0,182	-0,061	0,181	-13,22	18,74
		P' =	0,220 ksc				Q =	0,123 ksc							
1	-0,041	0,011	-0,004	0,018	-0,176	0,011	-0,200	0,015	0,154	0,015	0,354 0,021	-0,046	0,021	41,97	1,73
2	-0,072	0,019	-0,017	0,012	-0,115	0,011	-0,163	0,017	0,074	0,015	0,237 0,022	-0,088	0,022	38,27	2,70
3	-0,044	0,032	-0,041	0,023	-0,119	0,020	-0,161	0,028	0,076	0,028	0,237 0,040	-0,085	0,039	44,67	4,75
4	-0,117	0,048	-0,044	0,042	-0,045	0,032	-0,139	0,046	-0,022	0,043	0,116 0,063	-0,161	0,063	25,42	15,60
5	0,000	0,001	-0,078	0,075	0,053	0,038	-0,105	0,067	0,027	0,035	0,132 0,076	-0,078	0,075	27,01	16,43
		P' =	0,218 ksc				Q =	0,128 ksc							
1	-0,039	0,012	0,002	0,024	-0,205	0,013	-0,225	0,018	0,188	0,019	0,413 0,026	-0,037	0,026	42,13	1,82
2	-0,057	0,018	-0,006	0,013	-0,132	0,011	-0,167	0,016	0,103	0,015	0,270 0,022	-0,064	0,022	39,56	2,35
3	-0,034	0,028	-0,034	0,025	-0,124	0,019	-0,158	0,027	0,090	0,027	0,248 0,038	-0,068	0,038	-44,99	4,36
4	-0,111	0,042	-0,071	0,057	-0,027	0,035	-0,125	0,045	-0,057	0,054	0,068 0,071	-0,182	0,071	26,86	29,98
5	0,027	0,099	-0,139	0,031	-0,083	0,051	-0,173	0,047	0,061	0,091	0,234 0,104	-0,112	0,104	-22,44	12,71
		P' =	0,216 ksc				Q =	0,133 ksc							
1	-0,068	0,012	-0,013	0,035	-0,250	0,019	-0,291	0,025	0,211	0,027	0,502 0,037	-0,080	0,037	41,87	2,12
2	-0,077	0,018	-0,030	0,015	-0,127	0,012	-0,183	0,016	0,076	0,016	0,258 0,023	-0,107	0,023	39,72	2,54
3	-0,076	0,030	-0,068	0,025	-0,122	0,019	-0,195	0,027	0,050	0,027	0,245 0,039	-0,145	0,039	44,05	4,54
4	-0,158	0,056	-0,144	0,052	-0,067	0,038	-0,218	0,054	-0,084	0,054	0,134 0,077	-0,302	0,077	42,23	16,37
5	-0,045	0,384	-0,269	0,125	-0,056	0,199	-0,282	0,149	-0,032	0,373	0,250 0,406	-0,314	0,404	-13,27	46,19
		P' =	0,216 ksc				Q =	0,138 ksc							
1	-0,114	0,013	-0,076	0,049	-0,322	0,025	-0,412	0,035	0,232	0,036	0,644 0,051	-0,180	0,051	43,72	2,25
2	-0,096	0,019	-0,052	0,014	-0,165	0,012	-0,240	0,017	0,092	0,016	0,332 0,023	-0,147	0,023	41,23	2,02
3	-0,070	0,028	-0,081	0,024	-0,136	0,019	-0,211	0,026	0,061	0,026	0,271 0,037	-0,150	0,037	-43,83	3,90
4	-0,159	0,058	-0,129	0,052	-0,048	0,039	-0,195	0,055	-0,094	0,054	0,100 0,078	-0,289	0,078	36,32	22,13
5	-0,046	0,085	-0,043	0,089	-0,063	0,062	-0,107	0,086	0,019	0,086	0,126 0,123	-0,089	0,123	44,25	28,05

AREA	Ex	Ex(SD)	Ey	Ey(SD)	Exy	Exy(SD)	E3	E3(SD)	E1	E1(SD)	GAMMA	G(SD)	EV	EV(SD)	PS,	PS(SD)
		P' =	0.217	ksc			Q =	0.143	ksc							
1	-0.180	0.015	-0.114	0.063	-0.389	0.032	-0.537	0.044	0.243	0.047	0.780	0.065	-0.294	0.065	42.60	2.38
2	-0.137	0.018	-0.072	0.015	-0.182	0.012	-0.290	0.017	0.081	0.016	0.370	0.023	-0.209	0.023	40.00	1.79
3	-0.113	0.026	-0.109	0.028	-0.166	0.019	-0.277	0.027	0.055	0.027	0.332	0.038	-0.222	0.038	44.62	3.29
4	-0.191	0.051	-0.160	0.050	-0.085	0.036	-0.262	0.050	-0.089	0.050	0.172	0.072	-0.351	0.072	39.85	11.92
5	-0.078	0.079	-0.217	0.108	-0.124	0.067	-0.290	0.101	-0.005	0.087	0.285	0.134	-0.295	0.134	-30.41	13.44
		P' =	0.219	ksc			Q =	0.153	ksc							
1	-0.364	0.033	-0.168	0.138	-0.827	0.071	-1.099	0.094	0.567	0.105	1.666	0.142	-0.532	0.142	41.62	2.45
2	-0.212	0.026	-0.073	0.019	-0.332	0.016	-0.481	0.023	0.197	0.022	0.678	0.032	-0.284	0.032	39.09	1.35
3	-0.132	0.031	-0.121	0.028	-0.288	0.021	-0.415	0.029	0.162	0.029	0.576	0.042	-0.253	0.042	44.42	2.07
4	-0.139	0.052	-0.176	0.069	-0.217	0.043	-0.376	0.061	0.060	0.060	0.436	0.086	-0.316	0.086	-42.56	5.66
5	-0.144	0.210	-0.178	0.108	-0.109	0.117	-0.271	0.157	-0.051	0.172	0.220	0.235	-0.322	0.236	-40.64	30.86

DSC26

AREA	Ex	Ex(SD)	Ey	Ey(SD)	Exy	Exy(SD)	E3	E3(SD)	E1	E1(SD)	GAMMA	G(SD)	EV	EV(SD)	PS.	PS(SD)
Q = 0.020																
1	0.026	0.106	0.008	0.089	0.021	0.069	-0.006	0.096	0.040	0.103	0.046	0.138	0.034	0.139	33.46	1.51
2	0.019	0.118	0.018	0.093	0.030	0.074	-0.011	0.107	0.048	0.108	0.059	0.148	0.037	0.150	44.59	1.26
3	0.037	0.189	0.004	0.158	0.026	0.124	-0.010	0.166	0.052	0.182	0.062	0.247	0.042	0.247	28.86	2.00
4	0.048	0.244	0.038	0.283	0.136	0.187	-0.093	0.265	0.179	0.264	0.272	0.373	0.086	0.374	43.99	0.69
5	0.030	0.375	-0.666	0.263	-0.068	0.230	-0.672	0.263	0.036	0.372	0.709	0.460	-0.636	0.458	-5.57	0.33
Q = 0.040																
1	0.032	0.102	-0.037	0.096	0.021	0.070	-0.043	0.098	0.038	0.103	0.080	0.140	-0.005	0.140	15.33	0.87
2	0.027	0.119	-0.038	0.096	0.033	0.076	-0.052	0.102	0.041	0.118	0.093	0.152	-0.011	0.154	22.89	0.82
3	0.016	0.180	-0.087	0.130	0.017	0.111	-0.090	0.132	0.019	0.179	0.109	0.222	-0.071	0.222	9.15	1.02
4	0.102	0.283	-0.056	0.154	0.078	0.162	-0.088	0.179	0.134	0.269	0.221	0.323	0.046	0.322	22.33	0.73
5	0.558	0.017	-0.423	0.354	-0.115	0.175	-0.436	0.349	0.572	0.043	1.008	0.349	0.136	0.354	-6.57	0.17
Q = 0.080																
1	0.011	0.104	-0.086	0.089	0.046	0.068	-0.105	0.092	0.030	0.104	0.134	0.137	-0.075	0.137	21.75	0.51
2	-0.005	0.122	-0.079	0.082	0.050	0.071	-0.103	0.093	0.020	0.117	0.123	0.144	-0.083	0.148	26.64	0.59
3	-0.015	0.166	-0.109	0.110	0.018	0.100	-0.112	0.113	-0.012	0.164	0.101	0.200	-0.124	0.199	10.55	0.99
4	0.043	0.283	-0.101	0.161	0.063	0.164	-0.125	0.181	0.066	0.272	0.191	0.326	-0.058	0.326	20.51	0.86
5	0.202	0.357	-0.298	0.092	-0.124	0.186	-0.327	0.120	0.231	0.344	0.558	0.376	-0.095	0.368	-13.19	0.34
Q = 0.100																
1	0.061	0.110	-0.061	0.089	0.072	0.071	-0.094	0.095	0.095	0.108	0.189	0.141	0.001	0.142	24.84	0.37
2	0.065	0.127	-0.052	0.086	0.076	0.074	-0.090	0.097	0.102	0.122	0.192	0.150	0.012	0.154	26.30	0.39
3	0.093	0.170	-0.075	0.137	0.074	0.109	-0.103	0.141	0.121	0.167	0.224	0.219	0.017	0.218	20.79	0.49
4	0.098	0.278	-0.013	0.175	0.123	0.165	-0.093	0.211	0.178	0.252	0.271	0.329	0.085	0.328	32.81	0.61
5	0.416	0.592	-0.112	0.085	0.079	0.302	-0.123	0.122	0.428	0.591	0.552	0.589	0.305	0.598	8.37	0.54
Q = 0.140																
1	0.132	0.122	-0.125	0.106	0.158	0.081	-0.200	0.111	0.207	0.121	0.408	0.161	0.007	0.162	25.49	0.20
2	0.119	0.127	-0.107	0.091	0.146	0.077	-0.178	0.101	0.190	0.122	0.368	0.154	0.012	0.157	26.11	0.21
3	0.096	0.143	-0.147	0.121	0.125	0.094	-0.200	0.125	0.149	0.140	0.349	0.188	-0.052	0.188	22.94	0.27
4	0.046	0.214	-0.084	0.178	0.184	0.140	-0.215	0.191	0.177	0.203	0.391	0.279	-0.038	0.279	35.25	0.36
5	-0.429	0.573	-0.124	0.055	0.233	0.290	-0.555	0.517	0.002	0.285	0.556	0.593	-0.553	0.575	-28.41	0.53
Q = 0.160																
1	0.176	0.534	-0.202	0.213	0.363	0.287	-0.422	0.336	0.397	0.476	0.819	0.568	-0.026	0.574	31.28	0.35
2	0.196	0.451	-0.164	0.120	0.308	0.212	-0.341	0.238	0.373	0.394	0.715	0.427	0.032	0.466	29.85	0.31
3	0.152	0.182	-0.190	0.168	0.196	0.124	-0.279	0.170	0.241	0.180	0.520	0.248	-0.038	0.248	24.46	0.24
4	0.222	0.234	-0.176	0.306	0.272	0.192	-0.314	0.292	0.360	0.250	0.674	0.384	0.047	0.385	26.90	0.29
5	0.164	0.502	-0.481	0.293	0.056	0.292	-0.486	0.297	0.169	0.503	0.655	0.579	-0.317	0.581	4.88	0.44

AREA	Ex	Ex(SD)	Ey	Ey(SD)	Exy	Exy(SD)	E3	E3(SD)	E1	E1(SD)	GAMMA	G(SD)	EV	EV(SD)	PS.	PS(SD)
Q = 0.165																
1	0.137	0.675	-0.237	0.253	0.433	0.360	-0.521	0.433	0.421	0.590	0.943	0.713	-0.100	0.721	33.31	0.38
2	0.191	0.531	-0.201	0.133	0.357	0.249	-0.413	0.282	0.402	0.460	0.815	0.499	-0.010	0.547	30.62	0.32
3	0.156	0.163	-0.184	0.152	0.228	0.112	-0.299	0.154	0.270	0.161	0.569	0.223	-0.029	0.223	26.67	0.20
4	0.208	0.240	-0.136	0.168	0.278	0.147	-0.290	0.188	0.363	0.225	0.653	0.294	0.072	0.293	29.11	0.22
5	0.283	0.408	-0.069	0.397	0.441	0.285	-0.368	0.411	0.582	0.415	0.950	0.569	0.215	0.570	34.14	0.30
Q = 0.170																
1	0.172	0.751	-0.241	0.254	0.461	0.396	-0.539	0.467	0.471	0.655	1.010	0.783	-0.069	0.792	32.93	0.39
2	0.241	0.590	-0.185	0.124	0.373	0.272	-0.401	0.301	0.457	0.511	0.858	0.548	0.057	0.602	30.11	0.34
3	0.183	0.183	-0.184	0.176	0.236	0.127	-0.300	0.177	0.299	0.181	0.599	0.254	-0.001	0.254	26.04	0.21
4	0.265	0.310	-0.100	0.199	0.225	0.185	-0.207	0.224	0.373	0.293	0.580	0.369	0.165	0.368	25.51	0.32
5	0.299	0.065	-0.126	0.202	0.033	0.105	-0.128	0.202	0.301	0.067	0.429	0.214	0.173	0.212	4.40	0.25
Q = 0.175																
1	0.170	0.863	-0.262	0.279	0.522	0.453	-0.610	0.541	0.519	0.745	1.129	0.897	-0.092	0.907	33.77	0.40
2	0.261	0.658	-0.210	0.130	0.417	0.302	-0.454	0.334	0.504	0.569	0.958	0.609	0.051	0.670	30.27	0.34
3	0.210	0.165	-0.187	0.154	0.234	0.113	-0.295	0.156	0.318	0.163	0.612	0.226	0.023	0.226	24.84	0.18
4	0.271	0.198	-0.015	0.187	0.255	0.136	-0.164	0.190	0.420	0.196	0.584	0.273	0.256	0.272	30.33	0.23
5	0.270	0.373	-0.040	0.929	0.276	0.497	-0.202	0.842	0.431	0.580	0.633	1.013	0.230	1.001	30.31	0.80
Q = 0.180																
1	0.182	1.004	-0.276	0.327	0.596	0.528	-0.686	0.639	0.592	0.862	1.278	1.045	-0.094	1.056	34.49	0.41
2	0.288	0.782	-0.224	0.155	0.456	0.360	-0.491	0.399	0.555	0.677	1.046	0.725	0.064	0.798	30.35	0.37
3	0.180	0.161	-0.203	0.176	0.249	0.119	-0.326	0.173	0.303	0.164	0.629	0.238	-0.022	0.239	26.24	0.19
4	0.326	0.258	-0.080	0.210	0.261	0.167	-0.207	0.220	0.453	0.250	0.661	0.333	0.246	0.333	26.05	0.25
5	0.399	1.394	0.215	0.460	0.232	0.739	0.058	0.897	0.557	1.215	0.499	1.454	0.614	1.458	34.19	1.45
Q = 0.185																
1	0.140	1.220	-0.354	0.384	0.700	0.639	-0.849	0.784	0.635	1.037	1.484	1.266	-0.214	1.279	35.29	0.43
2	0.239	0.846	-0.286	0.130	0.501	0.385	-0.589	0.430	0.542	0.722	1.131	0.772	-0.047	0.856	31.18	0.36
3	0.188	0.212	-0.283	0.173	0.286	0.137	-0.418	0.181	0.323	0.206	0.741	0.275	-0.095	0.274	25.26	0.19
4	0.316	0.266	-0.199	0.240	0.319	0.180	-0.351	0.246	0.469	0.262	0.820	0.359	0.117	0.359	25.54	0.22
5	0.563	0.496	-0.666	0.199	0.177	0.269	-0.691	0.211	0.588	0.496	1.280	0.529	-0.103	0.535	8.05	0.21
Q = 0.190 5																
1	0.177	1.539	-0.399	0.470	0.969	0.804	-1.122	1.010	0.899	1.286	2.021	1.595	-0.222	1.609	36.72	0.39
2	0.350	1.087	-0.307	0.229	0.674	0.502	-0.728	0.582	0.771	0.924	1.499	1.006	0.043	1.111	32.00	0.36
3	0.271	0.151	-0.195	0.178	0.371	0.116	-0.400	0.172	0.476	0.157	0.876	0.233	0.076	0.233	28.94	0.13
4	0.308	0.216	-0.161	0.260	0.380	0.169	-0.373	0.251	0.519	0.228	0.892	0.338	0.147	0.338	29.16	0.19
5	0.439	0.415	-0.427	0.026	0.222	0.210	-0.480	0.103	0.493	0.409	0.973	0.407	0.012	0.416	13.59	0.21

AREA	Ex	Ex(SD)	Ey	Ey(SD)	Exy	Exy(SD)	E3	E3(SD)	E1	E1(SD)	GAMMA	G(SD)	EV	EV(SD)	PS.	PS(SD)
Q = 0.200																
1	0.140	1.684	-0.491	0.520	1.213	0.880	-1.429	1.127	1.078	1.392	2.506	1.748	-0.351	1.762	37.70	0.35
2	0.363	1.166	-0.389	0.246	0.848	0.538	-0.940	0.642	0.915	0.979	1.855	1.077	-0.026	1.191	33.05	0.31
3	0.271	0.224	-0.245	0.182	0.500	0.145	-0.550	0.194	0.576	0.213	1.126	0.289	0.026	0.289	31.34	0.13
4	0.322	0.278	-0.213	0.254	0.529	0.188	-0.538	0.261	0.647	0.272	1.185	0.377	0.110	0.376	31.60	0.16
5	0.559	0.980	-0.475	0.639	0.445	0.587	-0.640	0.702	0.724	0.963	1.364	1.158	0.084	1.170	20.37	0.42

DSC27

AREA	Ex	Ex(SD)	Ey	Ey(SD)	Exy	Exy(SD)	E3	E3(SD)	E1	E1(SD)	GAMMA	G(SD)	EV	EV(SD)	PS.	PS(SD)
		P' =	0,246	ksc				Q =	0,020	ksc						
1	0,010	0,015	-0,029	0,013	0,015	0,010	-0,034	0,013	0,015	0,015	0,049	0,020	-0,019	0,020	19,22	11,57
2	0,006	0,022	-0,030	0,021	0,017	0,015	-0,036	0,021	0,013	0,022	0,049	0,030	-0,024	0,030	21,43	17,77
3	0,020	0,037	-0,034	0,034	-0,005	0,025	-0,034	0,034	0,021	0,037	0,055	0,050	-0,014	0,050	-4,87	26,13
4	0,052	0,084	0,016	0,085	-0,018	0,060	0,009	0,085	0,059	0,084	0,050	0,119	0,069	0,119	-22,18	68,21
5	0,026	0,468	-0,736	0,189	-0,399	0,247	-0,906	0,252	0,196	0,438	1,103	0,495	-0,710	0,504	-23,17	12,88
		P' =	0,240	ksc				Q =	0,040	ksc						
1	96,064	0,001	96,063	0,001	0,001	0,000	96,062	0,001	96,064	0,001	0,002	0,001	0,000	0,001	26,41	13,32
2	96,063	0,001	96,063	0,001	0,001	0,001	96,062	0,001	96,064	0,001	0,001	0,001	0,000	0,001	28,38	25,31
3	96,065	0,002	96,061	0,001	0,001	0,001	96,061	0,001	96,065	0,002	0,004	0,002	0,000	0,002	16,68	14,53
4	96,067	0,004	96,061	0,003	-0,002	0,002	96,061	0,003	96,067	0,004	0,006	0,005	0,000	0,005	-17,50	21,46
5	96,080	0,008	96,051	0,024	-0,018	0,013	96,042	0,022	96,089	0,013	0,047	0,026	0,000	0,025	-25,15	15,83
		P' =	0,235	ksc				Q =	0,060	ksc						
1	0,017	0,015	-0,021	0,013	0,013	0,010	-0,025	0,013	0,021	0,015	0,046	0,020	-0,005	0,020	16,72	12,37
2	0,025	0,024	-0,025	0,020	0,021	0,016	-0,033	0,020	0,032	0,023	0,065	0,031	-0,001	0,031	19,85	13,68
3	0,048	0,040	-0,016	0,039	0,042	0,028	-0,037	0,039	0,069	0,039	0,106	0,056	0,031	0,056	26,35	15,05
4	0,004	0,078	0,003	0,090	0,039	0,060	-0,035	0,084	0,042	0,084	0,077	0,119	0,007	0,119	44,58	44,45
5	0,262	0,110	-0,345	0,365	-0,321	0,196	-0,483	0,342	0,400	0,181	0,884	0,390	-0,083	0,382	-23,33	12,63
		P' =	0,231	ksc				Q =	0,080	ksc						
1	0,085	0,015	-0,074	0,013	0,004	0,010	-0,074	0,013	0,085	0,015	0,159	0,020	0,011	0,020	1,27	3,52
2	0,078	0,022	-0,064	0,017	-0,001	0,014	-0,064	0,017	0,078	0,022	0,142	0,028	0,014	0,028	-0,49	5,59
3	0,115	0,034	-0,063	0,031	-0,022	0,023	-0,065	0,031	0,117	0,034	0,183	0,046	0,052	0,046	-6,99	7,19
4	0,166	0,068	-0,002	0,057	-0,045	0,045	-0,013	0,058	0,177	0,068	0,190	0,089	0,165	0,089	-14,17	13,39
5	0,394	0,307	0,107	0,056	-0,380	0,152	-0,156	0,180	0,657	0,255	0,813	0,303	0,501	0,313	-34,68	10,91
		P' =	0,228	ksc				Q =	0,100	ksc						
1	0,115	0,015	-0,026	0,014	0,004	0,010	-0,026	0,014	0,115	0,015	0,140	0,020	0,089	0,020	1,48	4,17
2	0,097	0,022	-0,009	0,021	0,004	0,015	-0,009	0,021	0,097	0,022	0,106	0,030	0,089	0,030	1,93	8,19
3	0,129	0,039	-0,015	0,034	-0,028	0,026	-0,020	0,035	0,134	0,038	0,154	0,052	0,114	0,052	-10,53	9,63
4	0,115	0,094	-0,004	0,090	0,000	0,065	-0,004	0,090	0,115	0,094	0,120	0,130	0,111	0,130	0,08	31,21
5	0,065	0,434	-0,420	0,076	-0,466	0,214	-0,703	0,232	0,348	0,374	1,051	0,428	-0,356	0,441	-31,27	11,85
		P' =	0,225	ksc				Q =	0,120	ksc						
1	0,145	0,016	-0,071	0,015	-0,003	0,011	-0,071	0,015	0,145	0,016	0,216	0,021	0,073	0,021	-0,91	2,84
2	0,135	0,025	-0,062	0,022	0,006	0,016	-0,062	0,022	0,135	0,025	0,197	0,033	0,073	0,033	1,76	4,78
3	0,146	0,044	-0,096	0,041	-0,011	0,030	-0,096	0,041	0,147	0,044	0,243	0,061	0,051	0,061	-2,62	7,14
4	0,248	0,102	-0,154	0,081	0,029	0,065	-0,156	0,081	0,250	0,102	0,406	0,130	0,094	0,130	4,15	9,19
5	-0,051	0,021	-0,106	1,003	-0,296	0,517	-0,376	0,759	0,219	0,695	0,595	1,035	-0,157	1,004	-42,38	48,42
		P' =	0,228	ksc				Q =	0,140	ksc						
1	0,209	0,016	-0,120	0,016	0,008	0,011	-0,120	0,016	0,209	0,016	0,330	0,022	0,089	0,022	1,36	1,95
2	0,216	0,025	-0,103	0,022	0,019	0,017	-0,104	0,022	0,217	0,025	0,321	0,033	0,113	0,033	3,37	2,96
3	0,223	0,045	-0,081	0,039	0,044	0,030	-0,088	0,039	0,229	0,045	0,316	0,060	0,141	0,060	8,11	5,39
4	0,262	0,103	-0,108	0,107	0,018	0,074	-0,109	0,107	0,263	0,103	0,372	0,148	0,154	0,148	2,77	11,39
5	0,823	0,499	-0,720	0,153	-0,566	0,255	-0,905	0,212	1,009	0,478	1,914	0,513	0,104	0,522	-18,14	7,63

AREA	Ex	Ex(SD)	Ey	Ey(SD)	Exy	Exy(SD)	E3	E3(SD)	E1	E1(SD)	GAMMA	G(SD)	EV	EV(SD)	PS.	PS(SD)
		P' =	0.237	ksc			Q =	0.160	ksc							
1	0.293	0.016	-0.150	0.014	0.001	0.011	-0.150	0.014	0.293	0.016	0.443	0.021	0.144	0.021	0.07	1.38
2	0.288	0.023	-0.147	0.020	0.001	0.016	-0.147	0.020	0.288	0.023	0.435	0.031	0.141	0.031	0.15	2.04
3	0.267	0.042	-0.132	0.032	-0.006	0.026	-0.132	0.032	0.268	0.042	0.400	0.053	0.135	0.053	-0.81	3.78
4	0.272	0.094	-0.050	0.065	0.004	0.057	-0.050	0.065	0.272	0.094	0.322	0.114	0.221	0.114	0.69	10.13
5	0.607	0.319	-0.398	0.220	-0.394	0.192	-0.534	0.233	0.743	0.311	1.277	0.385	0.209	0.387	-19.04	8.61
		P' =	0.242	ksc			Q =	0.170	ksc							
1	0.269	0.019	-0.248	0.014	0.017	0.012	-0.248	0.014	0.270	0.019	0.518	0.023	0.021	0.023	1.87	1.30
2	0.261	0.029	-0.242	0.021	0.035	0.018	-0.245	0.021	0.263	0.029	0.508	0.036	0.019	0.036	3.97	2.02
3	0.220	0.053	-0.212	0.036	-0.008	0.032	-0.213	0.036	0.220	0.053	0.432	0.064	0.007	0.064	-1.07	4.24
4	0.326	0.114	-0.287	0.087	0.032	0.072	-0.288	0.087	0.328	0.114	0.616	0.143	0.040	0.143	3.01	6.66
5	0.895	0.544	-0.558	0.416	-0.382	0.340	-0.653	0.426	0.989	0.540	1.641	0.682	0.336	0.684	-13.87	11.85
		P' =	0.251	ksc			Q =	0.180	ksc							
1	0.312	0.015	-0.292	0.016	0.006	0.011	-0.292	0.016	0.312	0.015	0.604	0.021	0.020	0.021	0.60	1.01
2	0.288	0.021	-0.266	0.019	0.018	0.014	-0.266	0.019	0.288	0.021	0.554	0.028	0.022	0.028	1.83	1.47
3	0.286	0.037	-0.263	0.036	0.017	0.026	-0.264	0.036	0.286	0.037	0.550	0.051	0.023	0.051	1.77	2.67
4	0.284	0.077	-0.195	0.068	0.011	0.051	-0.195	0.068	0.284	0.077	0.479	0.102	0.090	0.102	1.27	6.12
5	0.504	0.116	-0.581	0.490	-0.170	0.258	-0.607	0.486	0.531	0.138	1.137	0.507	-0.077	0.503	-8.70	13.05
		P' =	0.260	ksc			Q =	0.190	ksc							
1	0.384	0.015	-0.323	0.015	0.002	0.011	-0.323	0.015	0.384	0.015	0.706	0.021	0.061	0.021	0.14	0.86
2	0.392	0.024	-0.303	0.021	0.011	0.016	-0.303	0.021	0.392	0.024	0.695	0.032	0.089	0.032	0.92	1.31
3	0.395	0.045	-0.284	0.035	0.018	0.028	-0.285	0.035	0.395	0.045	0.680	0.057	0.111	0.057	1.48	2.38
4	0.471	0.100	-0.190	0.058	0.040	0.058	-0.193	0.058	0.473	0.100	0.666	0.115	0.281	0.115	3.43	4.97
5	0.971	0.098	-0.694	0.164	-0.102	0.097	-0.700	0.164	0.977	0.098	1.678	0.192	0.277	0.191	-3.48	3.32
		P' =	0.269	ksc			Q =	0.199	ksc							
1	0.451	0.017	-0.371	0.017	0.025	0.012	-0.372	0.017	0.452	0.017	0.824	0.024	0.080	0.024	1.70	0.84
2	0.458	0.027	-0.319	0.025	0.014	0.018	-0.319	0.025	0.458	0.027	0.777	0.036	0.138	0.036	1.04	1.34
3	0.502	0.050	-0.326	0.045	-0.020	0.034	-0.326	0.045	0.502	0.050	0.828	0.067	0.176	0.067	-1.39	2.33
4	0.367	0.106	-0.243	0.112	-0.083	0.077	-0.254	0.112	0.378	0.106	0.632	0.155	0.124	0.155	-7.65	7.01
5	0.840	0.491	-0.055	0.771	-0.373	0.463	-0.190	0.750	0.975	0.537	1.165	0.923	0.786	0.914	-19.92	22.74
		P' =	0.280	ksc			Q =	0.210	ksc							
1	0.437	0.016	-0.4[illegible]	0.016	0.010	0.011	-0.485	0.016	0.437	0.016	0.922	0.023	-0.047	0.023	0.60	0.70
2	0.423	0.024	-0.446	0.021	0.001	0.016	-0.446	0.021	0.423	0.024	0.869	0.032	-0.023	0.032	0.03	1.05
3	0.459	0.039	-0.430	0.035	-0.010	0.026	-0.430	0.035	0.459	0.039	0.889	0.053	0.030	0.053	-0.64	1.70
4	0.460	0.096	-0.398	0.078	-0.027	0.062	-0.398	0.078	0.461	0.096	0.859	0.124	0.063	0.124	-1.81	4.12
5	0.365	0.228	-0.765	0.073	-0.416	0.117	-0.902	0.099	0.501	0.218	1.403	0.235	-0.400	0.239	-18.19	4.77
		P' =	0.285	ksc			Q =	0.215	ksc							
1	0.565	0.019	-0.529	0.018	-0.004	0.013	-0.529	0.018	0.565	0.019	1.094	0.026	0.036	0.026	-0.20	0.69
2	0.570	0.028	-0.486	0.023	-0.003	0.018	-0.486	0.023	0.570	0.028	1.056	0.036	0.085	0.036	-0.16	0.97
3	0.586	0.041	-0.456	0.037	0.003	0.028	-0.456	0.037	0.586	0.041	1.042	0.055	0.130	0.055	0.15	1.51
4	0.564	0.071	-0.412	0.073	-0.046	0.051	-0.415	0.073	0.566	0.071	0.981	0.102	0.152	0.102	-2.71	2.97
5	1.041	0.088	-0.769	0.048	-0.243	0.049	-0.801	0.049	1.073	0.088	1.874	0.100	0.273	0.100	-7.51	1.50

AREA	Ex	Ex(SD)	Ey	Ey(SD)	Exy	Exy(SD)	E3	E3(SD)	E1	E1(SD)	GAMMA	G(SD)	EV	EV(SD)	PS,	PS(SD)
		P' =	0.297	ksc				Q =	0.220	ksc						
1	0.645	0.021	-0.628	0.019	0.058	0.014	-0.630	0.019	0.648	0.021	1.278	0.028	0.018	0.028	2.62	0.63
2	0.662	0.033	-0.560	0.023	0.049	0.020	-0.562	0.023	0.664	0.033	1.226	0.040	0.102	0.040	2.31	0.93
3	0.673	0.040	-0.527	0.039	0.030	0.028	-0.528	0.039	0.674	0.040	1.202	0.056	0.146	0.056	1.42	1.32
4	0.615	0.072	-0.440	0.075	0.025	0.052	-0.440	0.075	0.616	0.072	1.056	0.104	0.176	0.104	1.34	2.82
5	0.670	0.075	-0.763	0.035	-0.456	0.041	-0.896	0.040	0.803	0.073	1.699	0.082	-0.093	0.083	-16.24	1.37

DSC28

AREA	Ex	Ex(SD)	Ey	Ey(SD)	Exy	Exy(SD)	E3	E3(SD)	E1	E1(SD)	GAMMA	G(SD)	EV	EV(SD)	PS.	PS(SD)
		P' =	0.247	ksc			Q =	0.022	ksc							
1	0.008	0.012	-0.010	0.010	0.011	0.008	-0.015	0.010	0.013	0.012	0.028	0.016	-0.002	0.016	24.24	16.13
2	-0.024	0.014	0.006	0.013	-0.006	0.009	-0.026	0.014	0.007	0.013	0.033	0.019	-0.019	0.019	11.58	16.52
3	-0.036	0.022	-0.008	0.024	-0.005	0.016	-0.037	0.022	-0.008	0.024	0.030	0.032	-0.045	0.032	9.97	30.91
4	-0.071	0.041	-0.051	0.045	-0.062	0.030	-0.124	0.043	0.001	0.043	0.125	0.061	-0.122	0.061	40.37	13.91
5	-0.244	0.225	0.005	0.237	-0.129	0.163	-0.299	0.226	0.060	0.234	0.359	0.326	-0.239	0.327	22.98	26.04
		P' =	0.243	ksc			Q =	0.040	ksc							
1	0.015	0.009	-0.008	0.009	0.014	0.006	-0.014	0.009	0.022	0.009	0.036	0.013	0.008	0.013	24.74	10.26
2	0.020	0.015	-0.001	0.013	0.009	0.010	-0.004	0.013	0.024	0.015	0.028	0.020	0.019	0.020	21.19	20.50
3	0.049	0.028	0.004	0.029	0.015	0.020	-0.001	0.029	0.053	0.028	0.055	0.040	0.052	0.040	17.11	21.25
4	0.146	0.083	-0.039	0.069	-0.024	0.054	-0.042	0.069	0.149	0.083	0.191	0.108	0.108	0.108	-7.23	16.18
5	-0.238	0.155	0.234	0.030	-0.213	0.082	-0.320	0.146	0.316	0.064	0.636	0.161	-0.004	0.158	21.02	7.26
		P' =	0.235	ksc			Q =	0.060	ksc							
1	0.035	0.012	-0.009	0.011	0.024	0.008	-0.019	0.011	0.046	0.012	0.065	0.016	0.027	0.016	23.72	7.00
2	0.047	0.014	-0.018	0.014	0.014	0.010	-0.021	0.014	0.050	0.014	0.071	0.019	0.028	0.019	11.70	7.84
3	0.017	0.018	-0.001	0.024	-0.004	0.015	-0.002	0.024	0.018	0.019	0.020	0.030	0.016	0.030	-12.90	42.64
4	-0.023	0.038	-0.056	0.050	-0.015	0.031	-0.062	0.049	-0.018	0.039	0.044	0.062	-0.079	0.062	-21.03	40.89
5	0.151	0.001	0.173	0.210	-0.160	0.100	0.002	0.139	0.322	0.150	0.320	0.201	0.324	0.210	42.97	18.78
		P' =	0.224	ksc			Q =	0.080	ksc							
1	-0.004	0.013	-0.039	0.010	0.056	0.008	-0.081	0.011	0.038	0.012	0.118	0.017	-0.043	0.017	36.39	4.02
2	-0.015	0.013	-0.054	0.013	0.030	0.009	-0.071	0.013	0.002	0.013	0.073	0.018	-0.069	0.018	28.45	7.23
3	-0.026	0.026	-0.058	0.024	0.015	0.018	-0.063	0.024	-0.020	0.026	0.044	0.035	-0.083	0.035	21.06	23.28
4	-0.003	0.069	-0.123	0.059	-0.030	0.045	-0.130	0.060	0.004	0.069	0.134	0.091	-0.125	0.091	-13.39	19.38
5	-0.311	0.089	0.078	0.236	0.149	0.122	-0.362	0.112	0.128	0.225	0.490	0.248	-0.234	0.252	-18.75	14.40
		P' =	0.220	ksc			Q =	0.099	ksc							
1	0.083	0.013	0.008	0.011	0.053	0.008	-0.019	0.011	0.110	0.013	0.129	0.017	0.091	0.017	27.28	3.76
2	0.084	0.022	0.021	0.014	0.019	0.013	0.016	0.015	0.090	0.022	0.073	0.026	0.106	0.026	15.60	10.28
3	0.109	0.048	-0.009	0.025	-0.006	0.027	-0.009	0.025	0.109	0.048	0.118	0.054	0.101	0.054	-2.79	13.05
4	0.338	0.114	-0.112	0.072	-0.073	0.067	-0.123	0.073	0.349	0.113	0.472	0.135	0.226	0.135	-8.94	8.17
5	-0.179	0.450	0.131	0.455	0.151	0.321	-0.241	0.452	0.192	0.456	0.433	0.641	-0.048	0.640	-22.20	42.41
		P' =	0.210	ksc			Q =	0.119	ksc							
1	0.020	0.013	-0.120	0.014	0.101	0.010	-0.173	0.014	0.073	0.013	0.246	0.019	-0.100	0.019	27.69	2.23
2	0.007	0.017	-0.096	0.015	0.050	0.011	-0.117	0.015	0.027	0.017	0.144	0.023	-0.089	0.023	22.04	4.54
3	-0.010	0.025	-0.097	0.025	0.040	0.018	-0.113	0.025	0.005	0.025	0.118	0.036	-0.108	0.036	21.18	8.68
4	-0.059	0.054	-0.120	0.059	-0.081	0.040	-0.176	0.058	-0.003	0.056	0.173	0.080	-0.179	0.080	-34.72	13.33
5	-0.267	0.070	-0.078	0.076	-0.090	0.052	-0.303	0.071	-0.042	0.075	0.261	0.103	-0.345	0.103	21.70	11.33
		P' =	0.202	ksc			Q =	0.140	ksc							
1	0.028	0.026	-0.139	0.017	0.200	0.016	-0.272	0.020	0.162	0.023	0.434	0.031	-0.110	0.031	33.68	2.05
2	0.042	0.016	-0.121	0.014	0.123	0.011	-0.187	0.014	0.108	0.016	0.295	0.021	-0.079	0.021	28.23	2.05
3	0.033	0.027	-0.113	0.025	0.111	0.019	-0.173	0.026	0.092	0.027	0.265	0.037	-0.081	0.037	28.27	4.01
4	0.051	0.073	-0.157	0.055	0.096	0.046	-0.194	0.058	0.088	0.070	0.283	0.091	-0.106	0.091	21.30	9.26
5	0.131	0.193	0.273	0.214	0.068	0.144	0.103	0.196	0.300	0.212	0.197	0.288	0.404	0.288	-21.88	41.90

AREA	Ex	Ex(SD)	Ey	Ey(SD)	Exy	Exy(SD)	E3	E3(SD)	E1	E1(SD)	GAMMA	G(SD)	EV	EV(SD)	PS,	PS(SD)
		P' =	0,212	ksc			Q =	0,165	ksc							
1	-0,046	0,066	-0,212	0,033	0,433	0,037	-0,570	0,049	0,312	0,055	0,883	0,075	-0,258	0,074	39,56	2,41
2	0,090	0,019	-0,160	0,020	0,216	0,014	-0,285	0,019	0,215	0,019	0,500	0,027	-0,070	0,027	29,97	1,57
3	0,088	0,024	-0,150	0,027	0,155	0,018	-0,226	0,026	0,164	0,024	0,390	0,036	-0,062	0,036	26,16	2,62
4	0,084	0,044	-0,149	0,060	0,179	0,037	-0,245	0,057	0,181	0,048	0,426	0,075	-0,065	0,075	28,47	5,02
5	0,049	0,162	0,048	0,483	0,172	0,246	-0,123	0,356	0,220	0,355	0,344	0,492	0,097	0,509	44,91	42,49
		P' =	0,220	ksc			Q =	0,169	ksc							
1	-0,146	0,088	-0,245	0,035	0,530	0,048	-0,728	0,064	0,337	0,069	1,066	0,095	-0,391	0,094	42,34	2,53
2	0,027	0,023	-0,181	0,019	0,246	0,015	-0,343	0,020	0,190	0,022	0,533	0,030	-0,154	0,030	33,52	1,59
3	0,044	0,026	-0,176	0,030	0,198	0,020	-0,292	0,028	0,160	0,027	0,453	0,040	-0,132	0,040	30,49	2,51
4	-0,059	0,066	-0,182	0,065	0,204	0,046	-0,333	0,065	0,092	0,065	0,426	0,093	-0,241	0,093	36,65	6,23
5	-0,227	0,239	0,059	0,185	0,213	0,153	-0,340	0,230	0,172	0,200	0,512	0,306	-0,168	0,303	-28,06	17,02
		P' =	0,225	ksc			Q =	0,175	ksc							
1	-0,137	0,097	-0,237	0,038	0,606	0,053	-0,795	0,071	0,421	0,075	1,216	0,105	-0,374	0,104	42,63	2,45
2	0,084	0,023	-0,171	0,019	0,295	0,015	-0,365	0,020	0,278	0,022	0,643	0,030	-0,087	0,030	33,32	1,34
3	0,102	0,032	-0,134	0,030	0,241	0,022	-0,284	0,030	0,253	0,031	0,537	0,044	-0,031	0,044	31,96	2,34
4	0,059	0,085	-0,171	0,075	0,229	0,057	-0,313	0,078	0,200	0,082	0,513	0,114	-0,112	0,113	31,66	6,33
5	0,060	0,090	0,283	0,533	0,202	0,259	-0,059	0,274	0,403	0,458	0,462	0,522	0,343	0,541	-30,55	33,14
		P' =	0,229	ksc			Q =	0,179	ksc							
1	-0,156	0,109	-0,240	0,042	0,665	0,059	-0,864	0,081	0,468	0,085	1,332	0,119	-0,396	0,117	43,20	2,53
2	0,074	0,028	-0,154	0,021	0,296	0,018	-0,357	0,023	0,277	0,026	0,634	0,035	-0,080	0,035	34,49	1,60
3	0,070	0,035	-0,099	0,027	0,208	0,022	-0,239	0,029	0,210	0,032	0,449	0,044	-0,029	0,044	34,01	2,81
4	-0,072	0,078	-0,149	0,048	0,197	0,046	-0,311	0,062	0,090	0,067	0,401	0,092	-0,221	0,091	39,47	6,53
5	-0,035	0,196	-0,251	0,009	0,208	0,103	-0,378	0,106	0,091	0,170	0,469	0,203	-0,286	0,197	31,32	12,09
		P' =	0,236	ksc			Q =	0,184	ksc							
1	-0,136	0,120	-0,321	0,050	0,815	0,066	-1,049	0,088	0,592	0,096	1,641	0,132	-0,457	0,130	41,76	2,28
2	0,108	0,030	-0,248	0,024	0,399	0,019	-0,507	0,026	0,367	0,028	0,874	0,039	-0,139	0,039	32,97	1,27
3	0,116	0,031	-0,213	0,027	0,315	0,021	-0,403	0,028	0,307	0,030	0,710	0,041	-0,097	0,041	31,21	1,66
4	0,159	0,064	-0,237	0,057	0,320	0,043	-0,415	0,058	0,337	0,062	0,753	0,085	-0,078	0,085	29,16	3,25
5	0,062	0,238	0,128	0,168	0,328	0,148	-0,235	0,212	0,425	0,205	0,660	0,296	0,190	0,291	-42,12	12,65
		P' =	0,241	ksc			Q =	0,189	ksc							
1	-0,124	0,124	-0,331	0,052	0,934	0,068	-1,167	0,091	0,712	0,098	1,880	0,136	-0,455	0,134	41,84	2,05
2	0,125	0,032	-0,260	0,028	0,498	0,021	-0,601	0,029	0,466	0,031	1,067	0,043	-0,135	0,043	34,45	1,14
3	0,111	0,037	-0,240	0,030	0,410	0,024	-0,511	0,032	0,382	0,035	0,893	0,047	-0,129	0,047	33,41	1,52
4	0,076	0,101	-0,178	0,067	0,420	0,061	-0,490	0,081	0,387	0,090	0,877	0,122	-0,103	0,122	36,58	3,97
5	-0,229	0,007	0,143	0,196	0,310	0,094	-0,405	0,094	0,319	0,169	0,724	0,189	-0,086	0,196	-29,52	7,65
		P' =	0,245	ksc			Q =	0,196	ksc							
1	-0,108	0,130	-0,357	0,057	0,986	0,071	-1,227	0,096	0,762	0,104	1,988	0,143	-0,465	0,142	41,40	2,05
2	0,142	0,039	-0,271	0,030	0,528	0,025	-0,631	0,033	0,502	0,036	1,133	0,049	-0,129	0,049	34,30	1,24
3	0,132	0,042	-0,221	0,032	0,407	0,026	-0,488	0,035	0,399	0,039	0,887	0,053	-0,089	0,053	33,29	1,71
4	0,019	0,110	-0,274	0,063	0,341	0,064	-0,499	0,080	0,244	0,098	0,743	0,127	-0,255	0,127	33,35	4,91
5	0,402	0,253	-0,306	0,298	0,553	0,194	-0,609	0,288	0,705	0,264	1,313	0,389	0,096	0,391	28,69	8,51

AREA	Ex	Ex(SD)	Ey	Ey(SD)	Exy	Exy(SD)	E3	E3(SD)	E1	E1(SD)	GAMMA	G(SD)	EV	EV(SD)	PS.	PS(SD)
		P' =	0.280	ksc				Q =	0.205	ksc						
1	0.062	0.158	-0.950	0.132	2.228	0.103	-2.729	0.142	1.841	0.147	4.570	0.206	-0.887	0.205	38.60	1.29
2	0.414	0.067	-0.871	0.156	1.609	0.084	-1.961	0.133	1.505	0.102	3.465	0.168	-0.456	0.169	34.12	1.39
3	0.439	0.075	-0.775	0.168	1.384	0.092	-1.679	0.145	1.343	0.111	3.022	0.184	-0.336	0.184	33.16	1.74
4	0.287	0.144	-0.685	0.198	1.250	0.122	-1.540	0.182	1.142	0.162	2.682	0.244	-0.398	0.245	34.38	2.61
5	-0.120	0.111	-0.306	0.434	1.458	0.215	-1.674	0.320	1.248	0.302	2.921	0.431	-0.426	0.448	43.17	4.39

DSC29

AREA	Ex	Ex(SD)	Ey	Ey(SD)	Exy	Exy(SD)	E3	E3(SD)	E1	E1(SD)	GAMMA	G(SD)	EV	EV(SD)	PS.	PS(SD)
		P' =	0.247	ksc			Q =	0.014	ksc							
1	-0.049	0.014	-0.050	0.005	0.006	0.007	-0.056	0.012	-0.043	0.009	0.013	0.015	-0.099	0.015	41.55	33.03
2	-0.037	0.008	-0.054	0.008	0.005	0.006	-0.056	0.008	-0.035	0.008	0.021	0.011	-0.091	0.011	16.20	15.10
3	-0.031	0.014	-0.057	0.014	0.007	0.010	-0.058	0.014	-0.029	0.014	0.029	0.020	-0.088	0.020	15.30	19.28
4	-0.026	0.028	-0.114	0.037	0.008	0.023	-0.115	0.037	-0.025	0.027	0.089	0.046	-0.140	0.046	5.75	14.82
5	0.026	0.056	-0.309	0.079	0.002	0.049	-0.309	0.079	0.027	0.056	0.336	0.097	-0.282	0.097	0.42	8.33
		P' =	0.243	ksc			Q =	0.033	ksc							
1	-0.043	0.014	-0.038	0.006	0.013	0.008	-0.055	0.011	-0.026	0.011	0.028	0.015	-0.081	0.015	50.81	15.39
2	-0.023	0.007	-0.043	0.009	0.000	0.006	-0.043	0.009	-0.023	0.007	0.021	0.011	-0.066	0.011	0.94	15.87
3	-0.026	0.012	-0.060	0.017	-0.003	0.011	-0.060	0.017	-0.026	0.013	0.034	0.021	-0.086	0.021	-6.52	17.63
4	-0.048	0.030	-0.071	0.040	0.017	0.025	-0.080	0.038	-0.039	0.032	0.041	0.050	-0.119	0.050	27.82	34.47
5	-0.146	0.134	-0.275	0.198	0.066	0.121	-0.303	0.190	-0.118	0.140	0.185	0.238	-0.421	0.239	22.88	36.90
		P' =	0.233	ksc			Q =	0.053	ksc							
1	-0.065	0.014	-0.071	0.005	0.016	0.008	-0.085	0.009	-0.051	0.012	0.034	0.015	-0.136	0.015	39.86	12.98
2	-0.051	0.007	-0.066	0.007	0.033	0.005	-0.093	0.007	-0.024	0.007	0.069	0.010	-0.118	0.010	38.77	4.15
3	-0.060	0.011	-0.079	0.014	0.022	0.009	-0.094	0.013	-0.046	0.011	0.048	0.018	-0.139	0.018	33.12	10.41
4	-0.060	0.019	-0.136	0.032	0.014	0.019	-0.139	0.032	-0.057	0.019	0.082	0.037	-0.195	0.037	10.41	12.99
5	0.015	0.067	-0.102	0.037	0.115	0.038	-0.173	0.043	0.086	0.061	0.260	0.076	-0.086	0.076	31.51	8.44
		P' =	0.225	ksc			Q =	0.073	ksc							
1	-0.001	0.015	-0.018	0.008	0.022	0.008	-0.033	0.010	0.014	0.014	0.047	0.017	-0.019	0.017	34.43	10.41
2	0.007	0.007	0.006	0.010	0.038	0.006	-0.032	0.008	0.045	0.008	0.077	0.012	0.014	0.012	44.61	4.45
3	0.013	0.010	0.009	0.015	0.048	0.009	-0.037	0.013	0.060	0.012	0.098	0.018	0.023	0.018	43.85	5.32
4	0.023	0.024	-0.036	0.039	-0.023	0.023	-0.044	0.027	0.032	0.037	0.077	0.046	-0.012	0.046	-19.25	17.36
5	0.030	0.056	-0.098	0.161	0.138	0.087	-0.187	0.092	0.118	0.149	0.305	0.170	-0.068	0.171	32.48	15.86
		P' =	0.214	ksc			Q =	0.093	ksc							
1	-0.053	0.015	-0.084	0.009	0.046	0.009	-0.118	0.011	-0.020	0.014	0.098	0.018	-0.138	0.018	35.71	5.14
2	-0.063	0.009	-0.066	0.010	0.050	0.007	-0.115	0.010	-0.015	0.009	0.100	0.014	-0.129	0.014	44.02	3.91
3	-0.068	0.018	-0.088	0.018	0.054	0.013	-0.133	0.017	-0.023	0.018	0.110	0.025	-0.156	0.025	39.95	6.52
4	-0.101	0.037	-0.083	0.033	0.022	0.025	-0.117	0.035	-0.068	0.034	0.049	0.050	-0.184	0.050	55.50	29.34
5	-0.180	0.255	-0.000	0.250	0.096	0.179	-0.222	0.256	0.041	0.258	0.264	0.357	-0.180	0.357	66.43	38.83
		P' =	0.211	ksc			Q =	0.098	ksc							
1	-0.004	0.017	-0.043	0.009	0.061	0.010	-0.088	0.012	0.041	0.015	0.130	0.019	-0.047	0.019	36.10	4.23
2	0.007	0.008	-0.035	0.011	0.073	0.007	-0.090	0.010	0.062	0.009	0.153	0.013	-0.027	0.013	36.99	2.49
3	-0.006	0.015	-0.043	0.019	0.067	0.012	-0.095	0.018	0.045	0.016	0.140	0.024	-0.049	0.024	37.23	4.88
4	-0.002	0.037	-0.107	0.047	0.036	0.030	-0.118	0.046	0.009	0.038	0.128	0.060	-0.109	0.060	17.33	13.46
5	-0.179	0.081	-0.387	0.262	0.056	0.140	-0.402	0.257	-0.165	0.090	0.237	0.272	-0.566	0.274	14.34	33.37
		P' =	0.207	ksc			Q =	0.103	ksc							
1	0.001	0.016	-0.037	0.011	0.062	0.010	-0.083	0.013	0.048	0.015	0.132	0.020	-0.035	0.020	36.44	4.29
2	0.007	0.011	-0.021	0.012	0.067	0.008	-0.076	0.011	0.062	0.011	0.138	0.016	-0.014	0.016	39.00	3.32
3	-0.027	0.018	-0.059	0.021	0.059	0.014	-0.105	0.020	0.018	0.018	0.124	0.028	-0.086	0.028	37.48	6.36
4	-0.026	0.047	-0.041	0.048	0.030	0.034	-0.065	0.047	-0.002	0.047	0.063	0.068	-0.067	0.068	37.95	30.84
5	-0.128	0.091	0.021	0.151	0.120	0.089	-0.195	0.138	0.088	0.116	0.283	0.179	-0.107	0.176	60.83	17.94

AREA	Ex	Ex(SD)	Ey	Ey(SD)	Exy	Exy(SD)	E3	E3(SD)	E1	E1(SD)	GAMMA	G(SD)	EV	EV(SD)	PS.	PS(SD)
		P' =	0,205	ksc			Q =	0,108	ksc							
1	0,010	0,017	-0,023	0,010	0,077	0,010	-0,085	0,013	0,073	0,015	0,158	0,020	-0,012	0,020	38,79	3,67
2	0,019	0,009	-0,003	0,009	0,087	0,006	-0,080	0,009	0,096	0,009	0,177	0,013	0,016	0,013	41,47	2,04
3	0,023	0,018	0,002	0,015	0,079	0,012	-0,068	0,016	0,092	0,016	0,161	0,023	0,025	0,023	41,25	4,11
4	0,023	0,050	-0,017	0,037	0,063	0,031	-0,064	0,040	0,070	0,046	0,134	0,062	0,007	0,062	36,16	13,32
5	-0,078	0,036	0,308	0,011	0,065	0,018	-0,088	0,034	0,318	0,013	0,407	0,037	0,230	0,037	80,66	2,55
		P' =	0,203	ksc			Q =	0,113	ksc							
1	-0,035	0,017	-0,086	0,013	0,094	0,011	-0,158	0,014	0,037	0,016	0,195	0,021	-0,121	0,021	37,36	3,11
2	-0,039	0,010	-0,074	0,011	0,090	0,008	-0,149	0,011	0,036	0,010	0,185	0,015	-0,113	0,015	39,65	2,32
3	-0,053	0,015	-0,091	0,020	0,078	0,013	-0,153	0,019	0,008	0,017	0,162	0,025	-0,144	0,025	38,28	4,45
4	-0,091	0,031	-0,178	0,049	0,083	0,029	-0,229	0,046	-0,040	0,035	0,188	0,058	-0,269	0,058	31,12	8,78
5	-0,220	0,017	-0,277	0,286	-0,002	0,147	-0,277	0,041	-0,220	0,282	0,057	0,290	-0,497	0,286	-2,48	148,36
		P' =	0,203	ksc			Q =	0,118	ksc							
1	-0,026	0,018	-0,097	0,012	0,108	0,011	-0,175	0,014	0,053	0,016	0,229	0,021	-0,123	0,021	36,00	2,68
2	-0,020	0,008	-0,076	0,008	0,117	0,006	-0,169	0,008	0,072	0,008	0,241	0,011	-0,096	0,011	38,18	1,32
3	-0,026	0,015	-0,083	0,013	0,113	0,010	-0,177	0,014	0,063	0,014	0,235	0,020	-0,109	0,020	37,98	2,43
4	0,011	0,044	-0,090	0,035	0,119	0,028	-0,169	0,036	0,090	0,041	0,260	0,056	-0,079	0,056	33,46	6,17
5	-0,163	0,103	-0,083	0,190	0,208	0,110	-0,335	0,150	0,089	0,151	0,424	0,219	-0,246	0,216	50,47	14,61
		P' =	0,204	ksc			Q =	0,123	ksc							
1	-0,005	0,019	-0,080	0,013	0,103	0,011	-0,153	0,014	0,067	0,017	0,220	0,023	-0,085	0,023	34,96	2,99
2	-0,001	0,009	-0,057	0,012	0,105	0,008	-0,138	0,011	0,080	0,010	0,219	0,015	-0,058	0,015	37,69	1,96
3	-0,012	0,017	-0,060	0,018	0,090	0,013	-0,131	0,018	0,057	0,017	0,188	0,025	-0,073	0,025	37,59	3,83
4	-0,037	0,048	-0,096	0,047	0,058	0,034	-0,132	0,046	-0,001	0,047	0,131	0,067	-0,133	0,067	31,81	14,61
5	-0,310	0,020	-0,094	0,125	0,107	0,065	-0,354	0,060	-0,050	0,110	0,304	0,131	-0,404	0,127	67,62	12,24
		P' =	0,203	ksc			Q =	0,128	ksc							
1	-0,012	0,020	-0,074	0,013	0,120	0,012	-0,167	0,015	0,081	0,018	0,249	0,024	-0,086	0,024	37,70	2,74
2	-0,002	0,010	-0,052	0,010	0,130	0,007	-0,160	0,010	0,105	0,010	0,265	0,014	-0,054	0,014	39,55	1,51
3	0,016	0,017	-0,049	0,017	0,121	0,012	-0,143	0,017	0,109	0,017	0,252	0,024	-0,033	0,024	37,44	2,74
4	0,018	0,050	-0,077	0,045	0,111	0,034	-0,151	0,046	0,092	0,049	0,244	0,068	-0,059	0,068	33,39	7,96
5	0,061	0,056	-0,099	0,399	0,184	0,206	-0,220	0,348	0,182	0,195	0,403	0,401	-0,038	0,403	33,30	28,28
		P' =	0,204	ksc			Q =	0,133	ksc							
1	-0,027	0,019	-0,090	0,013	0,136	0,012	-0,199	0,015	0,081	0,017	0,281	0,023	-0,118	0,023	38,50	2,38
2	-0,030	0,010	-0,068	0,010	0,145	0,007	-0,196	0,010	0,098	0,010	0,294	0,015	-0,097	0,015	41,32	1,41
3	-0,044	0,018	-0,078	0,019	0,149	0,013	-0,211	0,018	0,089	0,018	0,300	0,026	-0,122	0,026	41,79	2,46
4	-0,052	0,049	-0,088	0,050	0,135	0,035	-0,207	0,049	0,067	0,049	0,274	0,070	-0,140	0,070	41,20	7,30
5	0,091	0,162	-0,027	0,106	-0,034	0,096	-0,036	0,115	0,100	0,159	0,137	0,191	0,064	0,194	-14,95	40,01
		P' =	0,205	ksc			Q =	0,138	ksc							
1	-0,018	0,020	-0,116	0,014	0,172	0,012	-0,247	0,016	0,112	0,018	0,359	0,024	-0,134	0,024	37,05	1,94
2	-0,025	0,012	-0,093	0,012	0,177	0,008	-0,240	0,012	0,122	0,012	0,362	0,017	-0,118	0,017	39,60	1,35
3	-0,026	0,023	-0,114	0,016	0,167	0,014	-0,243	0,018	0,103	0,021	0,347	0,028	-0,139	0,028	37,67	2,36
4	-0,025	0,054	-0,125	0,044	0,132	0,035	-0,218	0,046	0,066	0,051	0,284	0,070	-0,151	0,070	34,66	7,02
5	-0,074	0,080	-0,027	0,392	0,101	0,204	-0,155	0,273	0,053	0,286	0,208	0,410	-0,101	0,400	51,56	55,20

AREA	Ex	Ex(SD)	Ey	Ey(SD)	Exy	Exy(SD)	E3	E3(SD)	E1	E1(SD)	GAMMA	G(SD)	EV	EV(SD)	PS.	PS(SD)
		P' =	0.207	ksc			Q =	0.143	ksc							
1	0.037	0.021	-0.075	0.015	0.186	0.013	-0.213	0.017	0.176	0.019	0.389	0.026	-0.037	0.026	36.58	1.89
2	0.032	0.011	-0.062	0.011	0.185	0.008	-0.207	0.011	0.177	0.011	0.384	0.015	-0.030	0.015	37.91	1.15
3	0.016	0.017	-0.045	0.014	0.193	0.011	-0.210	0.014	0.182	0.016	0.393	0.022	-0.028	0.022	40.51	1.57
4	0.056	0.030	-0.047	0.030	0.148	0.021	-0.152	0.030	0.161	0.030	0.314	0.043	0.009	0.043	35.40	3.90
5	0.024	0.126	-0.006	0.046	0.004	0.066	-0.007	0.126	0.024	0.046	0.032	0.134	0.018	0.134	7.75	119.05
		P' =	0.209	ksc			Q =	0.148	ksc							
1	0.032	0.022	-0.110	0.017	0.205	0.014	-0.256	0.018	0.179	0.020	0.435	0.028	-0.077	0.028	35.47	1.82
2	0.018	0.011	-0.100	0.013	0.192	0.008	-0.242	0.012	0.160	0.011	0.402	0.017	-0.081	0.017	36.44	1.20
3	0.022	0.019	-0.107	0.020	0.209	0.014	-0.262	0.019	0.177	0.019	0.439	0.028	-0.084	0.028	36.40	1.80
4	-0.019	0.034	-0.159	0.056	0.203	0.033	-0.304	0.051	0.126	0.041	0.430	0.066	-0.178	0.066	35.56	4.36
5	0.064	0.307	-0.140	0.170	0.345	0.173	-0.398	0.211	0.322	0.269	0.720	0.350	-0.075	0.351	36.74	14.04
		P' =	0.213	ksc			Q =	0.153	ksc							
1	0.024	0.021	-0.091	0.018	0.236	0.014	-0.276	0.019	0.210	0.020	0.486	0.028	-0.066	0.028	38.10	1.65
2	0.046	0.013	-0.082	0.012	0.222	0.009	-0.249	0.012	0.214	0.012	0.464	0.017	-0.035	0.017	36.94	1.06
3	0.054	0.021	-0.096	0.016	0.240	0.013	-0.273	0.017	0.231	0.019	0.504	0.026	-0.041	0.026	36.29	1.47
4	0.063	0.040	-0.086	0.033	0.223	0.026	-0.247	0.034	0.224	0.038	0.471	0.052	-0.023	0.052	35.79	3.13
5	-0.026	0.031	-0.009	0.305	0.385	0.157	-0.403	0.229	0.368	0.198	0.771	0.311	-0.035	0.306	45.60	11.31
		P' =	0.217	ksc			Q =	0.158	ksc							
1	0.039	0.022	-0.113	0.019	0.288	0.014	-0.335	0.019	0.262	0.021	0.597	0.029	-0.073	0.029	37.60	1.38
2	0.025	0.015	-0.093	0.016	0.277	0.011	-0.318	0.015	0.250	0.015	0.568	0.022	-0.067	0.022	39.01	1.11
3	-0.006	0.026	-0.119	0.026	0.265	0.018	-0.333	0.026	0.208	0.026	0.542	0.037	-0.124	0.037	38.97	1.95
4	0.018	0.063	-0.152	0.040	0.150	0.037	-0.240	0.044	0.105	0.059	0.346	0.074	-0.134	0.074	30.27	6.18
5	-0.072	0.059	0.223	0.139	0.383	0.077	-0.336	0.098	0.487	0.112	0.823	0.155	0.151	0.151	55.55	5.30
		P' =	0.222	ksc			Q =	0.163	ksc							
1	0.060	0.024	-0.174	0.022	0.700	0.016	-0.767	0.022	0.653	0.023	1.420	0.032	-0.113	0.032	40.25	0.65
2	0.067	0.017	-0.142	0.016	0.670	0.012	-0.716	0.016	0.641	0.017	1.357	0.023	-0.075	0.023	40.58	0.49
3	0.071	0.026	-0.150	0.029	0.651	0.020	-0.701	0.028	0.621	0.027	1.322	0.039	-0.079	0.039	40.18	0.84
4	0.096	0.058	-0.110	0.055	0.609	0.040	-0.625	0.055	0.612	0.057	1.237	0.080	-0.013	0.080	40.20	1.86
5	0.427	0.586	0.010	0.158	0.480	0.297	-0.305	0.300	0.742	0.510	1.048	0.609	0.437	0.607	33.26	16.79
		P' =	0.228	ksc			Q =	0.165	ksc							
1	0.148	0.028	-0.260	0.026	0.998	0.019	-1.075	0.026	0.963	0.027	2.038	0.038	-0.112	0.038	39.22	0.54
2	0.176	0.021	-0.252	0.018	0.974	0.014	-1.035	0.019	0.960	0.020	1.996	0.028	-0.075	0.028	38.81	0.40
3	0.159	0.028	-0.219	0.024	0.948	0.019	-0.997	0.025	0.937	0.027	1.934	0.037	-0.060	0.037	39.36	0.55
4	0.132	0.042	-0.247	0.046	0.909	0.031	-0.986	0.044	0.872	0.043	1.858	0.062	-0.114	0.062	39.11	0.96
5	-0.268	0.001	-0.457	0.097	1.000	0.050	-1.368	0.074	0.642	0.061	2.010	0.098	-0.725	0.097	42.30	1.37
		P' =	0.238	ksc			Q =	0.169	ksc							
1	0.219	0.055	-0.602	0.052	2.261	0.038	-2.490	0.053	2.107	0.054	4.597	0.076	-0.382	0.076	39.85	0.48
2	0.285	0.046	-0.611	0.051	2.275	0.034	-2.482	0.048	2.156	0.047	4.638	0.068	-0.326	0.068	39.43	0.42
3	0.257	0.055	-0.557	0.047	2.259	0.036	-2.446	0.049	2.145	0.051	4.592	0.072	-0.300	0.072	39.89	0.45
4	0.305	0.093	-0.578	0.097	2.315	0.067	-2.494	0.094	2.221	0.093	4.715	0.134	-0.272	0.134	39.60	0.82
5	0.327	0.237	-0.351	0.207	1.996	0.157	-2.037	0.214	2.013	0.221	4.051	0.315	-0.024	0.315	40.18	2.23

DSC30

AREA	Ex	Ex(SD)	Ey	Ey(SD)	Exy	Exy(SD)	E3	E3(SD)	E1	E1(SD)	GAMMA	G(SD)	EV	EV(SD)	PS.	PS(SD)
		P' =	0.249	ksc			Q =	0.003	ksc							
1	0.161	0.008	0.182	0.009	-0.008	0.006	0.153	0.009	0.170	0.009	0.017	0.012	0.323	0.012	43.19	20.20
2	0.164	0.012	0.168	0.015	-0.001	0.009	0.163	0.012	0.169	0.015	0.006	0.019	0.333	0.019	17.88	95.78
3	0.170	0.019	0.222	0.022	0.007	0.015	0.169	0.019	0.223	0.022	0.054	0.029	0.392	0.029	-8.03	15.51
4	0.125	0.047	0.221	0.053	-0.008	0.035	0.124	0.047	0.222	0.053	0.098	0.071	0.346	0.071	5.21	20.72
5	0.517	0.086	-0.089	0.080	-0.015	0.059	-0.089	0.080	0.518	0.086	0.607	0.117	0.429	0.117	-1.45	5.53
		P' =	0.249	ksc			Q =	0.018	ksc							
1	-0.002	0.010	-0.013	0.010	0.016	0.007	-0.025	0.010	0.009	0.010	0.035	0.014	-0.016	0.014	35.94	11.44
2	-0.008	0.013	-0.003	0.016	0.005	0.010	-0.011	0.014	0.000	0.015	0.012	0.021	-0.011	0.021	-31.35	51.29
3	-0.012	0.021	0.046	0.028	0.014	0.017	-0.016	0.021	0.049	0.027	0.066	0.035	0.034	0.035	-13.46	15.14
4	-0.017	0.040	0.012	0.069	-0.056	0.040	-0.060	0.053	0.055	0.060	0.116	0.080	-0.004	0.080	37.78	19.54
5	0.300	0.279	0.000	0.491	-0.232	0.285	-0.126	0.462	0.427	0.349	0.553	0.576	0.300	0.564	-28.59	29.68
		P' =	0.240	ksc			Q =	0.047	ksc							
1	0.039	0.010	0.011	0.009	0.017	0.007	0.003	0.009	0.048	0.010	0.045	0.013	0.051	0.013	25.51	8.52
2	0.025	0.012	-0.002	0.014	0.010	0.009	-0.005	0.014	0.028	0.013	0.034	0.019	0.023	0.019	18.88	15.83
3	0.025	0.021	0.051	0.021	0.019	0.015	0.014	0.021	0.061	0.021	0.047	0.030	0.076	0.030	-28.51	17.99
4	0.021	0.044	0.054	0.061	-0.004	0.038	0.020	0.045	0.055	0.061	0.035	0.075	0.076	0.075	8.06	62.37
5	0.042	0.008	0.180	0.332	0.111	0.169	-0.020	0.160	0.242	0.285	0.262	0.345	0.222	0.333	-29.10	37.45
		P' =	0.231	ksc			Q =	0.067	ksc							
1	0.190	0.011	0.071	0.012	0.014	0.008	0.069	0.012	0.192	0.011	0.123	0.016	0.262	0.016	6.58	3.67
2	0.187	0.013	0.095	0.014	0.016	0.010	0.092	0.014	0.189	0.013	0.097	0.019	0.282	0.019	10.01	5.66
3	0.202	0.023	0.148	0.022	0.026	0.016	0.137	0.022	0.213	0.023	0.076	0.032	0.350	0.032	21.93	11.92
4	0.179	0.034	0.189	0.051	0.005	0.031	0.176	0.037	0.191	0.049	0.015	0.062	0.368	0.061	-23.64	119.18
5	0.362	0.083	-0.046	0.140	0.196	0.082	-0.126	0.132	0.441	0.092	0.568	0.162	0.316	0.163	21.95	8.17
		P' =	0.226	ksc			Q =	0.087	ksc							
1	0.019	0.011	-0.077	0.009	0.042	0.007	-0.093	0.010	0.035	0.011	0.129	0.015	-0.057	0.015	20.88	3.24
2	0.002	0.015	-0.107	0.015	0.038	0.011	-0.119	0.015	0.014	0.015	0.133	0.021	-0.105	0.021	17.56	4.57
3	-0.011	0.028	-0.097	0.027	0.043	0.019	-0.115	0.027	0.006	0.028	0.122	0.039	-0.108	0.039	22.48	9.12
4	-0.095	0.049	-0.116	0.069	-0.016	0.043	-0.125	0.065	-0.086	0.055	0.039	0.085	-0.211	0.085	-29.40	62.65
5	0.274	0.273	0.219	0.132	0.005	0.150	0.218	0.134	0.275	0.271	0.056	0.305	0.493	0.304	5.60	153.57
		P' =	0.224	ksc			Q =	0.096	ksc							
1	0.105	0.012	-0.015	0.010	0.037	0.008	-0.026	0.010	0.115	0.012	0.142	0.015	0.009	0.015	16.10	3.08
2	0.097	0.017	-0.018	0.015	0.032	0.012	-0.026	0.015	0.105	0.017	0.132	0.023	0.079	0.023	14.69	4.99
3	0.079	0.028	0.023	0.024	0.048	0.019	-0.005	0.025	0.107	0.027	0.112	0.037	0.103	0.037	29.94	9.55
4	0.073	0.058	0.069	0.061	-0.007	0.042	0.063	0.060	0.079	0.059	0.016	0.084	0.142	0.084	-36.33	150.97
5	0.525	0.095	-0.032	0.004	0.111	0.046	-0.054	0.018	0.547	0.092	0.601	0.096	0.493	0.095	10.90	4.52
		P' =	0.217	ksc			Q =	0.106	ksc							
1	0.148	0.012	-0.022	0.011	0.053	0.008	-0.037	0.011	0.163	0.012	0.201	0.017	0.126	0.017	16.03	2.38
2	0.156	0.017	0.003	0.017	0.043	0.012	-0.008	0.017	0.168	0.017	0.176	0.024	0.160	0.024	14.93	3.82
3	0.151	0.029	0.032	0.029	0.035	0.021	0.022	0.029	0.161	0.029	0.138	0.041	0.184	0.041	15.40	8.56
4	0.121	0.080	0.039	0.076	0.036	0.055	0.025	0.076	0.134	0.079	0.109	0.110	0.160	0.110	20.62	28.83
5	0.523	0.102	0.338	0.596	0.371	0.307	0.048	0.464	0.814	0.369	0.766	0.607	0.862	0.604	38.01	22.36

AREA	Ex	Ex(SD)	Ey	Ey(SD)	Exy	Exy(SD)	E3	E3(SD)	E1	E1(SD)	GAMMA G(SD)	EV	EV(SD)	PS,	PS(SD)
		P' =	0,212 ksc				Q =	0,114 ksc							
1	0,098	0,012	-0,076	0,011	0,065	0,008	-0,098	0,011	0,120	0,012	0,218 0,016	0,022	0,016	18,38	2,15
2	0,096	0,016	-0,055	0,016	0,055	0,011	-0,073	0,016	0,114	0,016	0,187 0,022	0,040	0,022	18,00	3,40
3	0,064	0,029	-0,034	0,027	0,061	0,020	-0,063	0,027	0,094	0,028	0,157 0,039	0,031	0,039	25,58	7,18
4	0,073	0,064	0,022	0,055	0,037	0,042	0,002	0,056	0,093	0,062	0,090 0,084	0,095	0,084	27,76	26,83
5	0,687	0,080	0,220	0,415	0,134	0,215	0,184	0,396	0,723	0,132	0,539 0,415	0,908	0,423	15,01	22,26
		P' =	0,210 ksc				Q =	0,127 ksc							
1	0,096	0,013	-0,107	0,013	0,065	0,009	-0,126	0,013	0,115	0,013	0,241 0,018	-0,011	0,018	16,40	2,18
2	0,133	0,017	-0,103	0,020	0,065	0,013	-0,120	0,020	0,150	0,017	0,270 0,026	0,030	0,026	14,62	2,79
3	0,129	0,032	-0,037	0,037	0,107	0,025	-0,090	0,036	0,181	0,033	0,271 0,049	0,092	0,049	26,07	5,18
4	0,103	0,083	0,091	0,075	0,061	0,056	0,035	0,078	0,159	0,078	0,124 0,112	0,195	0,112	42,14	25,85
5	0,706	0,226	0,575	0,009	-0,105	0,111	0,517	0,111	0,765	0,201	0,248 0,218	1,282	0,226	-29,03	25,40
		P' =	0,209 ksc				Q =	0,131 ksc							
1	0,073	0,010	-0,162	0,011	0,085	0,008	-0,189	0,011	0,101	0,010	0,291 0,015	-0,088	0,015	18,00	1,49
2	0,078	0,014	-0,165	0,014	0,068	0,010	-0,183	0,014	0,096	0,014	0,280 0,020	-0,087	0,020	14,59	2,02
3	0,069	0,023	-0,132	0,021	0,081	0,015	-0,160	0,021	0,098	0,022	0,258 0,031	-0,062	0,031	19,39	3,41
4	0,047	0,047	-0,086	0,049	0,027	0,034	-0,091	0,049	0,053	0,047	0,144 0,068	-0,038	0,068	11,33	13,46
5	0,359	0,140	-0,240	0,034	0,017	0,071	-0,241	0,034	0,359	0,140	0,601 0,145	0,119	0,144	1,63	6,80
		P' =	0,206 ksc				Q =	0,141 ksc							
1	0,152	0,015	-0,171	0,016	0,123	0,011	-0,213	0,016	0,194	0,015	0,408 0,022	-0,019	0,022	18,73	1,54
2	0,170	0,018	-0,155	0,020	0,104	0,014	-0,185	0,020	0,200	0,018	0,386 0,027	0,015	0,027	16,36	2,00
3	0,226	0,032	-0,074	0,035	0,128	0,024	-0,122	0,034	0,273	0,032	0,395 0,047	0,151	0,047	20,21	3,41
4	0,235	0,080	-0,009	0,058	0,064	0,050	-0,025	0,060	0,251	0,079	0,276 0,100	0,227	0,099	13,81	10,31
5	0,698	0,408	0,305	0,345	0,227	0,266	0,201	0,349	0,803	0,389	0,602 0,535	1,004	0,534	24,59	25,50
		P' =	0,206 ksc				Q =	0,146 ksc							
1	0,129	0,019	-0,185	0,017	0,161	0,013	-0,253	0,017	0,198	0,019	0,451 0,026	-0,055	0,026	22,94	1,64
2	0,151	0,020	-0,161	0,023	0,126	0,015	-0,206	0,022	0,196	0,020	0,402 0,030	-0,010	0,030	19,50	2,13
3	0,136	0,036	-0,139	0,026	0,147	0,022	-0,203	0,028	0,200	0,034	0,403 0,044	-0,002	0,044	23,52	3,15
4	0,059	0,069	-0,126	0,047	0,148	0,041	-0,208	0,052	0,141	0,064	0,350 0,083	-0,067	0,083	29,04	6,83
5	0,489	0,064	-0,227	0,548	0,127	0,281	-0,249	0,535	0,511	0,113	0,761 0,543	0,262	0,551	9,77	20,75
		P' =	0,206 ksc				Q =	0,157 ksc							
1	0,215	0,023	-0,219	0,021	0,197	0,016	-0,295	0,021	0,292	0,023	0,587 0,031	-0,003	0,031	21,12	1,51
2	0,241	0,019	-0,197	0,021	0,161	0,014	-0,250	0,020	0,294	0,019	0,545 0,028	0,044	0,028	18,15	1,48
3	0,249	0,030	-0,148	0,031	0,209	0,022	-0,238	0,030	0,339	0,030	0,578 0,043	0,101	0,043	23,24	2,13
4	0,245	0,067	-0,102	0,063	0,199	0,046	-0,192	0,063	0,336	0,066	0,529 0,092	0,143	0,092	24,46	5,00
5	0,644	0,320	-0,067	0,495	0,075	0,297	-0,075	0,489	0,652	0,323	0,727 0,587	0,577	0,590	6,01	23,26
		P' =	0,205 ksc				Q =	0,164 ksc							
1	0,311	0,037	-0,513	0,021	0,381	0,021	-0,662	0,026	0,460	0,033	1,123 0,043	-0,202	0,043	21,39	1,09
2	0,335	0,023	-0,501	0,021	0,299	0,016	-0,598	0,022	0,431	0,023	1,029 0,032	-0,166	0,031	17,81	0,88
3	0,397	0,040	-0,478	0,031	0,348	0,025	-0,600	0,033	0,518	0,038	1,119 0,051	-0,081	0,051	19,26	1,30
4	0,642	0,063	-0,500	0,074	0,295	0,048	-0,572	0,071	0,714	0,064	1,286 0,097	0,143	0,097	13,69	2,15
5	1,187	0,157	-0,724	0,122	0,168	0,099	-0,739	0,123	1,201	0,153	1,941 0,200	0,463	0,199	4,99	2,94

AREA	Ex	Ex(SD)	Ey	Ey(SD)	Exy	Exy(SD)	E3	E3(SD)	E1	E1(SD)	GAMMA	G(SD)	EV	EV(SD)	PS.	PS(SD)
		P' =	0.205	ksc			Q =	0.168	ksc							
1	1.904	0.104	-2.999	0.062	2.362	0.061	-3.952	0.078	2.857	0.092	6.810	0.122	-1.095	0.122	21.97	0.51
2	1.871	0.117	-3.056	0.059	2.826	0.066	-4.342	0.082	3.157	0.101	7.500	0.132	-1.184	0.131	24.46	0.50
3	2.100	0.110	-3.238	0.081	3.123	0.068	-4.677	0.090	3.539	0.100	8.217	0.136	-1.138	0.136	24.74	0.48
4	2.326	0.135	-3.113	0.110	3.410	0.087	-4.755	0.118	3.969	0.126	8.725	0.174	-0.786	0.174	25.72	0.57
5	2.574	0.600	-2.935	0.426	3.611	0.366	-4.723	0.480	4.361	0.530	9.085	0.736	-0.361	0.736	26.33	2.33

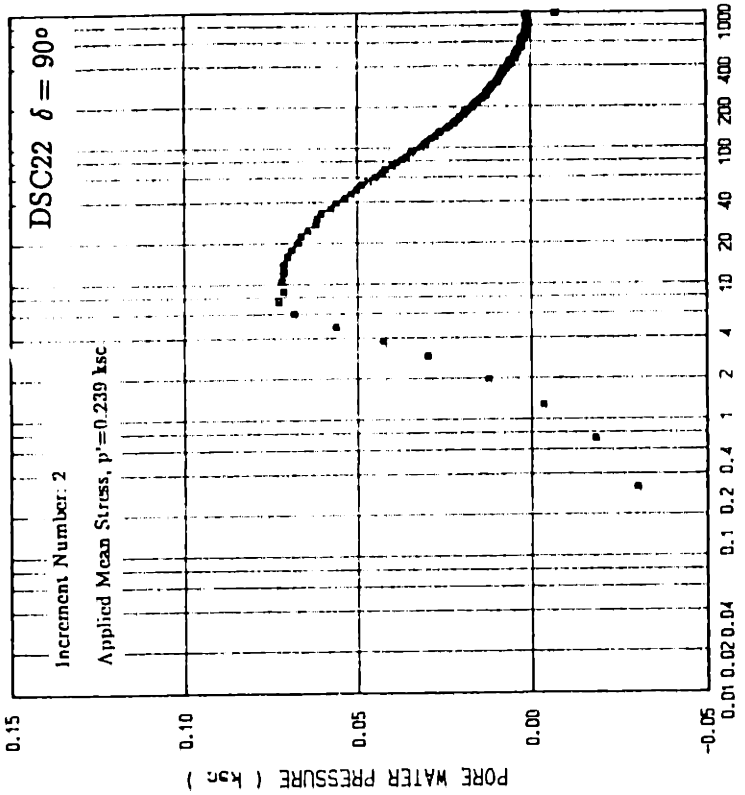

PORE WATER PRESSURE DISSIPATION CURVES

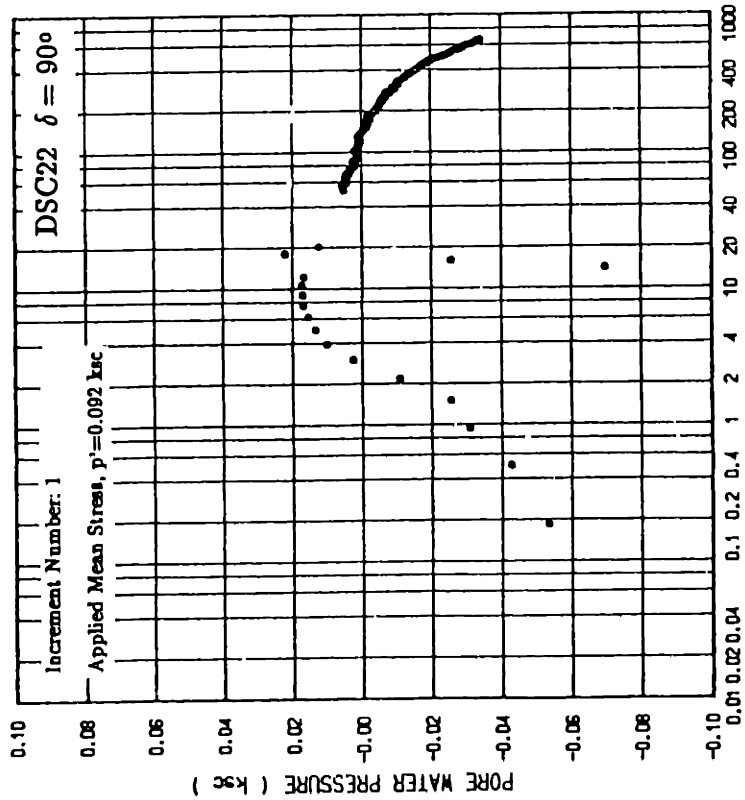

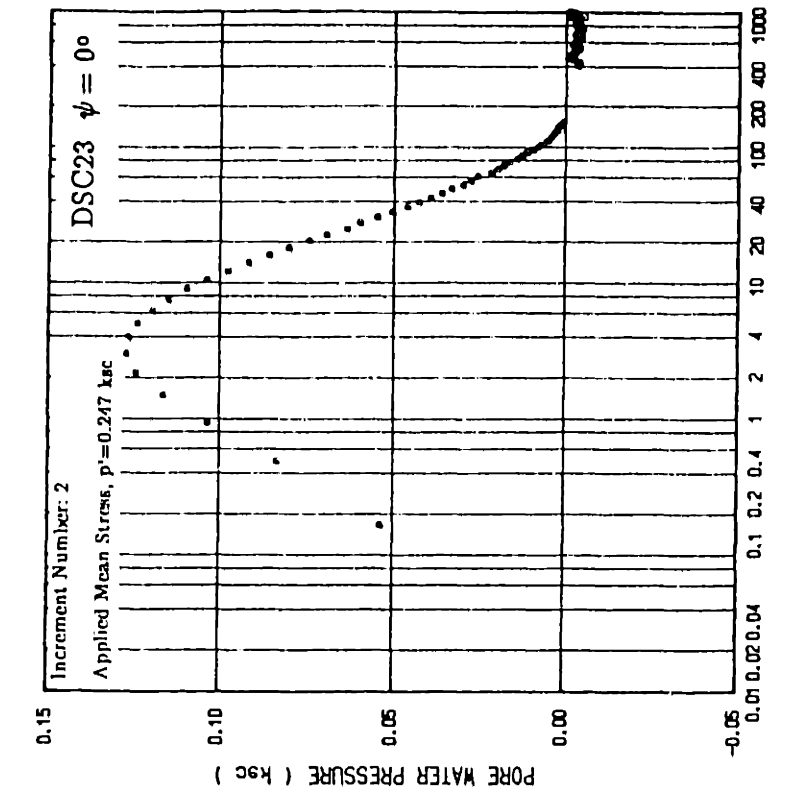
DSC23 ψ = 0°
Increment Number: 2
Applied Mean Stress, p'=0.247 ksc
PORE WATER PRESSURE (ksc)
TIME (in minutes)

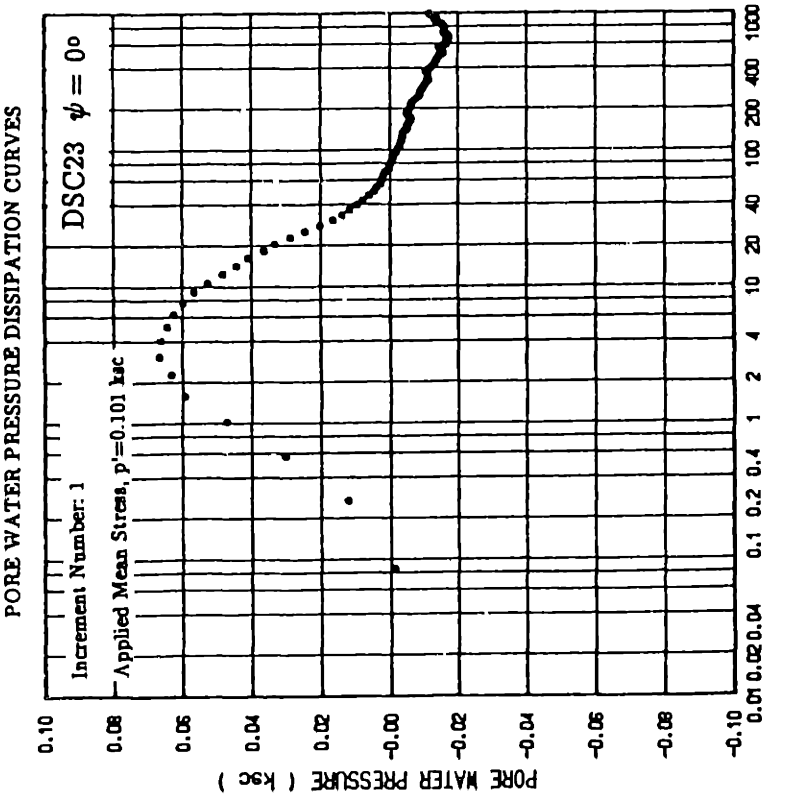
PORE WATER PRESSURE DISSIPATION CURVES
DSC23 ψ = 0°
Increment Number: 1
Applied Mean Stress, p'=0.101 ksc
PORE WATER PRESSURE (ksc)
TIME (in minutes)

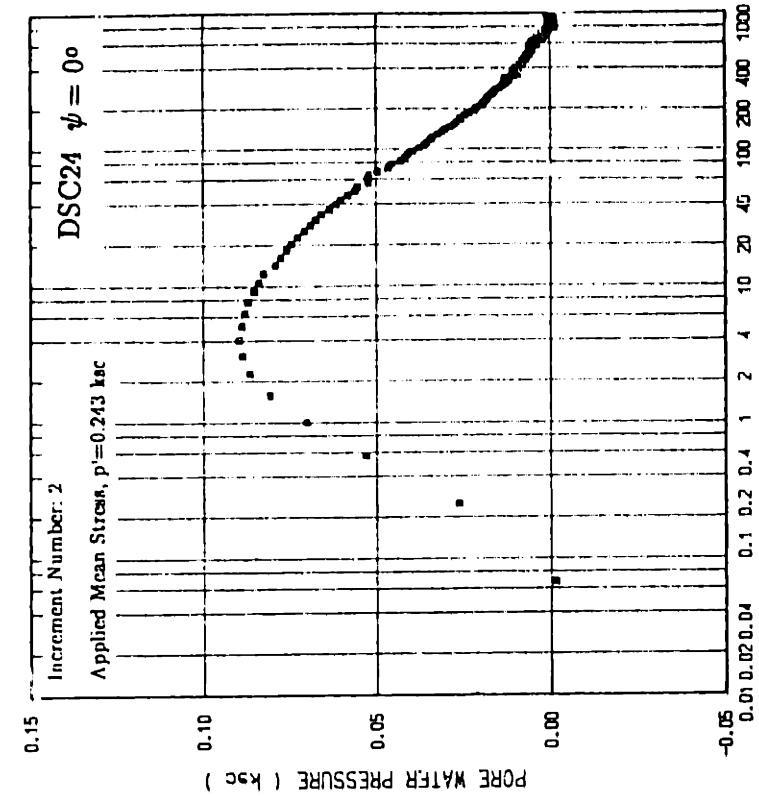

PORE WATER PRESSURE DISSIPATION CURVES

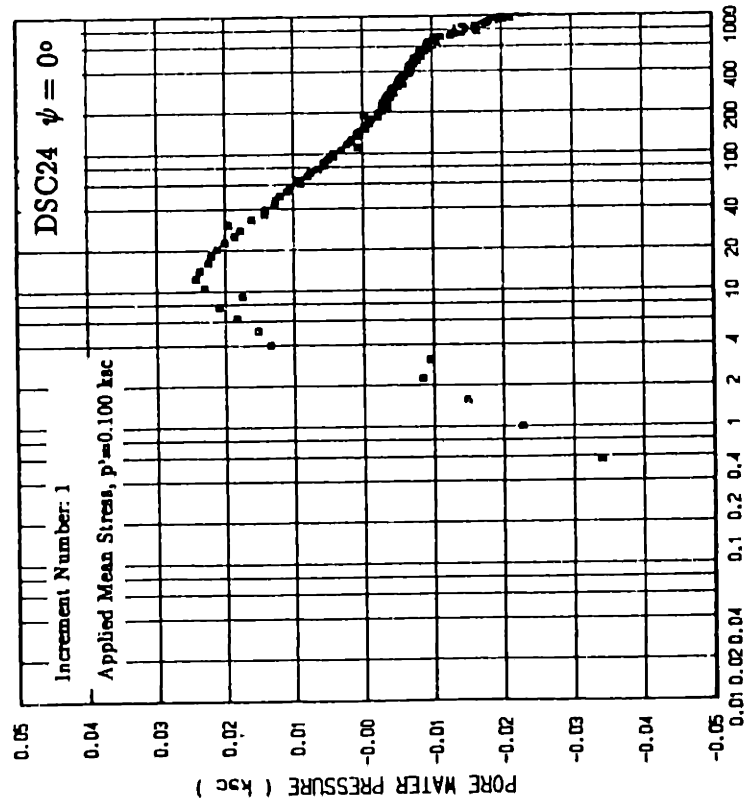

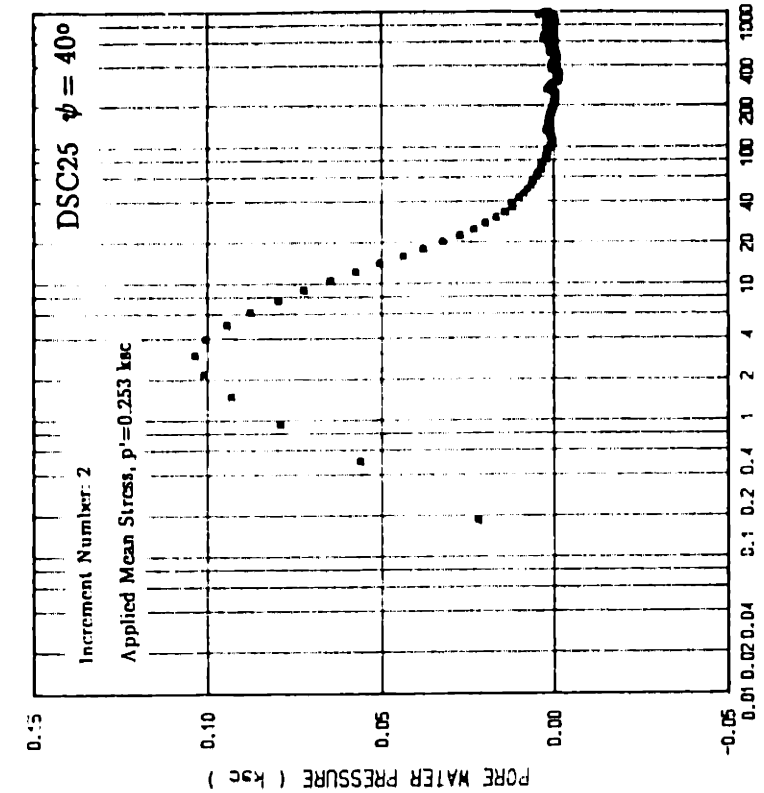
DSC25 ψ = 40°
Increment Number: 2
Applied Mean Stress, p'=0.253 ksc
PORE WATER PRESSURE (ksc)
TIME (in minutes)

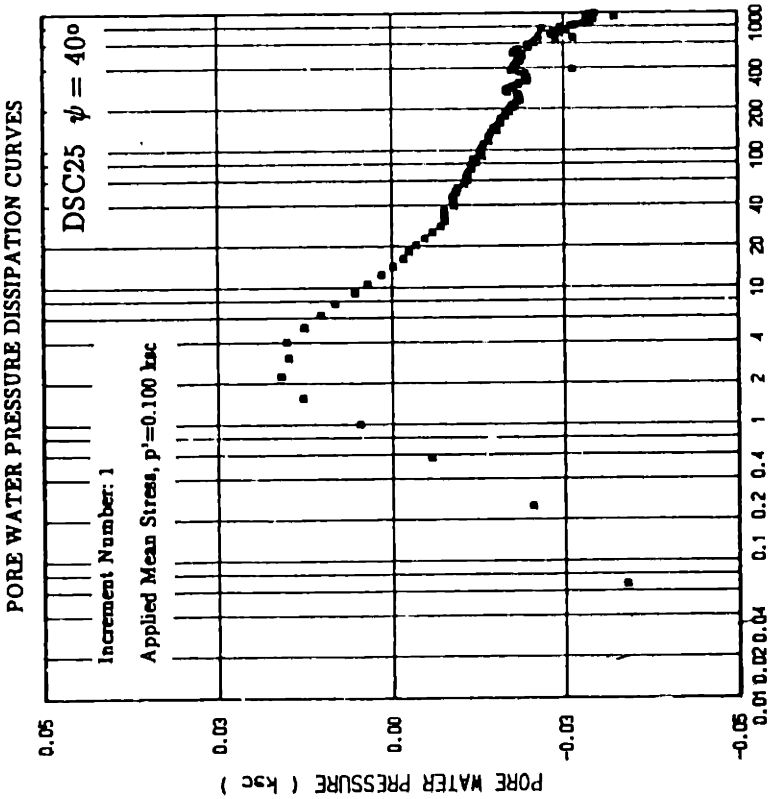
PORE WATER PRESSURE DISSIPATION CURVES
DSC25 ψ = 40°
Increment Number: 1
Applied Mean Stress, p'=0.100 ksc
PORE WATER PRESSURE (ksc)
TIME (in minutes)

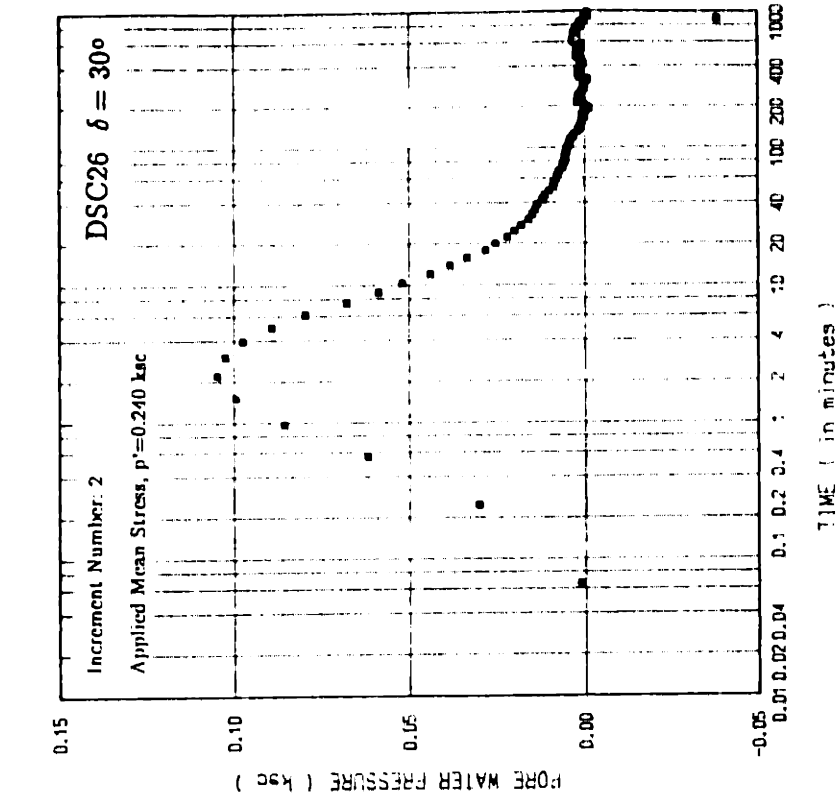

PORE WATER PRESSURE DISSIPATION CURVES

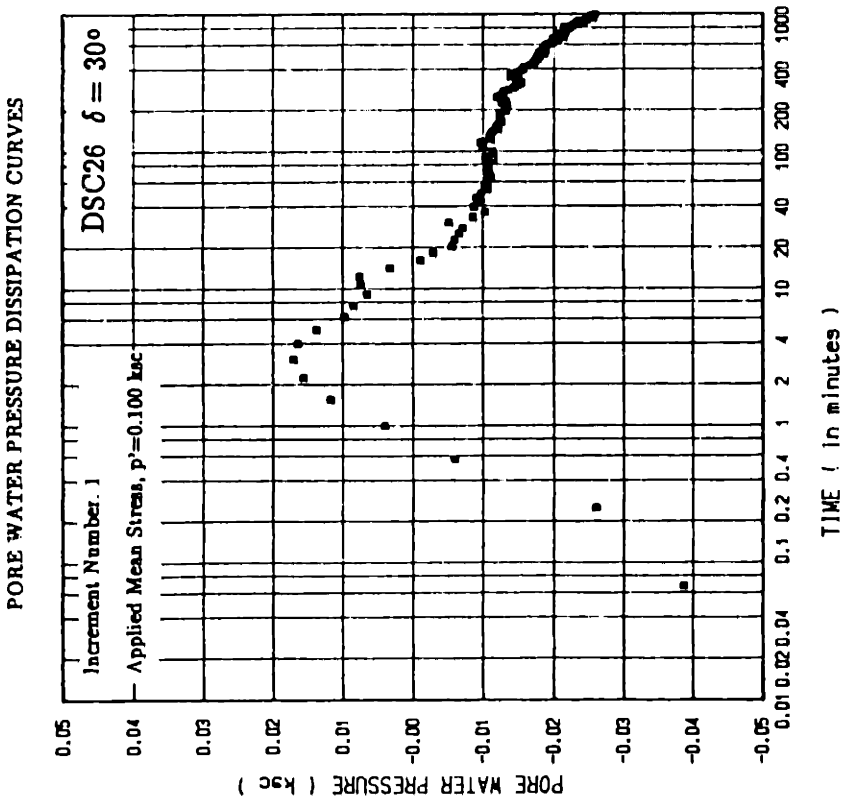

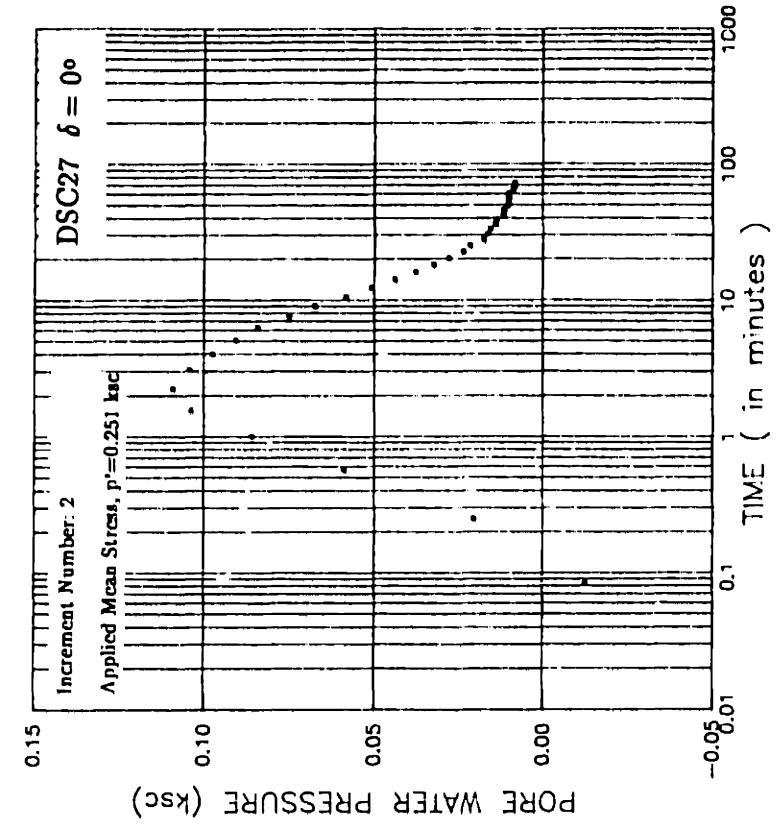
DSC27 δ = 0°
Increment Number: 2
Applied Mean Stress, p'=0.251 ksc
PORE WATER PRESSURE (ksc)
TIME (in minutes)
0.15
0.10
0.05
0.00
−0.05
0.01
0.1
1
10
100
1000

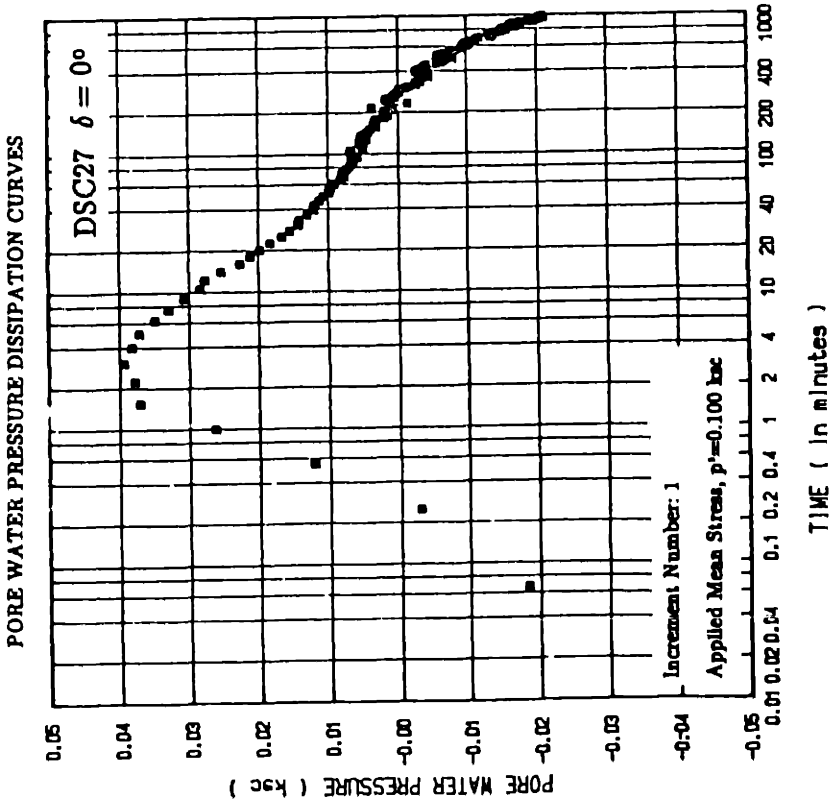
PORE WATER PRESSURE DISSIPATION CURVES
DSC27 δ = 0°
Increment Number: 1
Applied Mean Stress, p'=0.100 ksc
PORE WATER PRESSURE (ksc)
TIME (in minutes)
0.05
0.04
0.03
0.02
0.01
-0.00
-0.01
-0.02
-0.03
-0.04
-0.05
0.01 0.02 0.04 0.1 0.2 0.4 1 2 4 10 20 40 100 200 400 1000

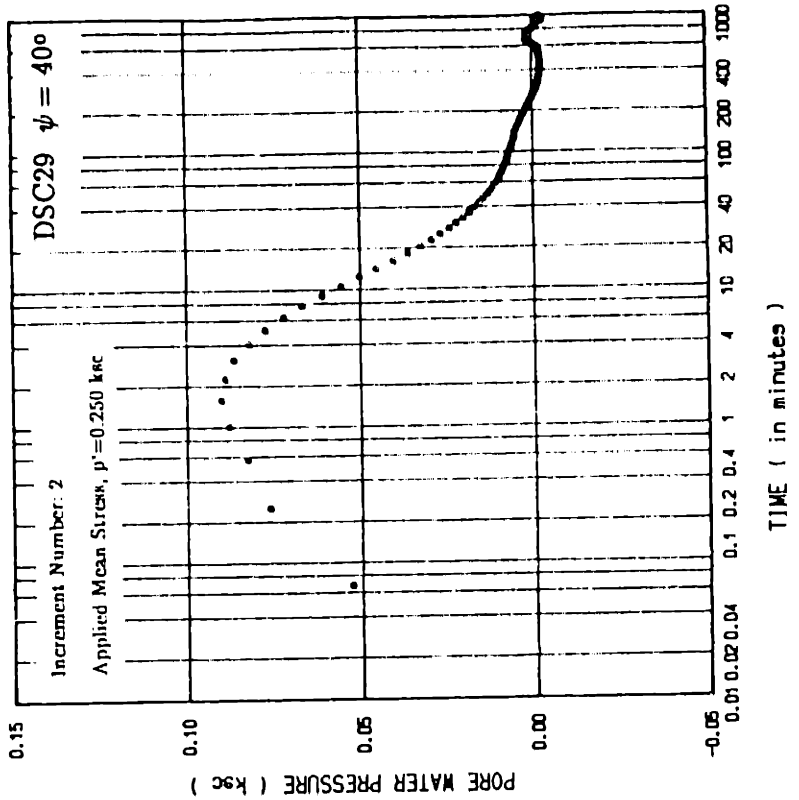

PORE WATER PRESSURE DISSIPATION CURVES

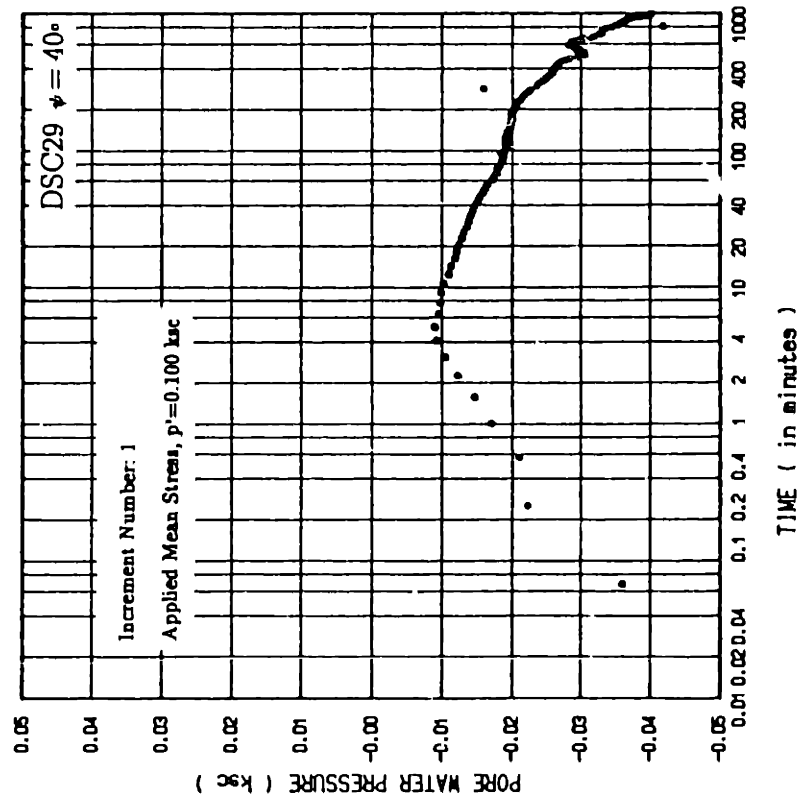

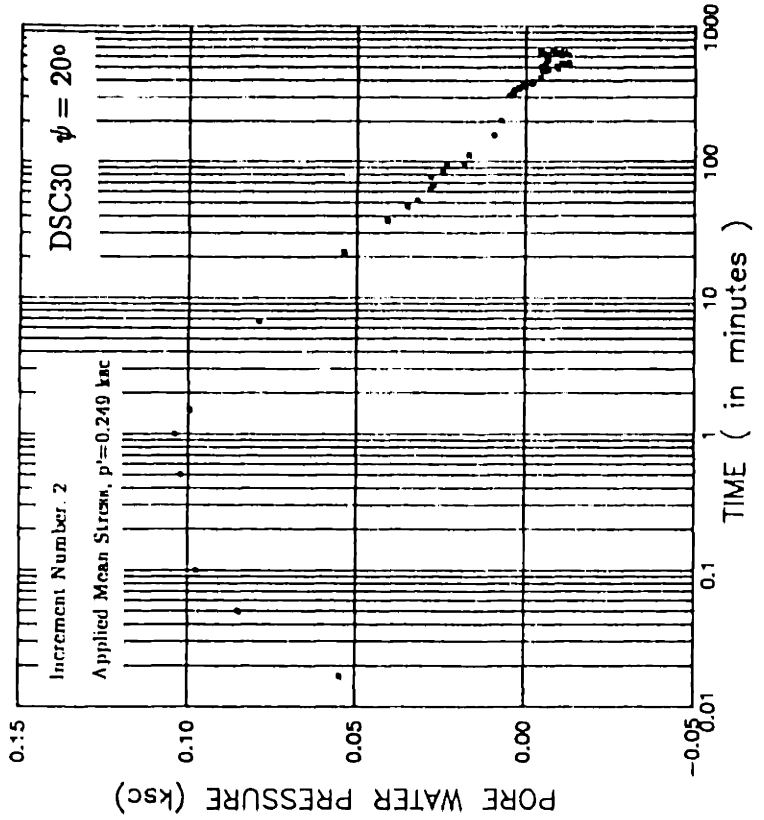
DSC30 ψ = 20°
Increment Number: 2
Applied Mean Stress, p'=0.249 ksc
PORE WATER PRESSURE (ksc)
TIME (in minutes)
0.15
0.10
0.05
0.00
−0.05
0.01
0.1
1
10
100
1000

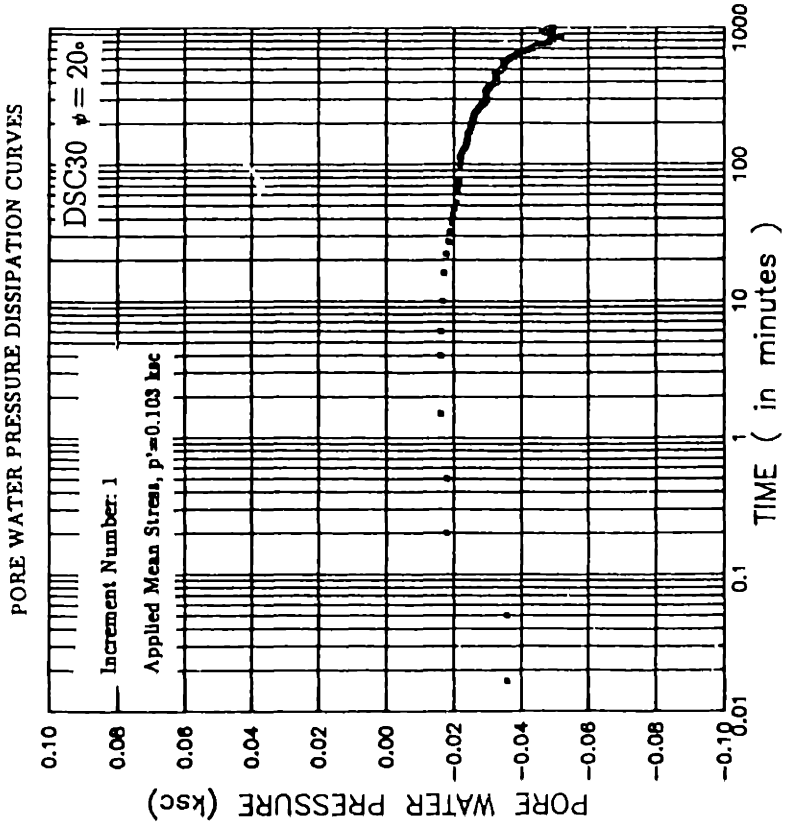
PORE WATER PRESSURE DISSIPATION CURVES
DSC30 ψ = 20°
Increment Number: 1
Applied Mean Stress, p'=0.103 ksc
PORE WATER PRESSURE (ksc)
TIME (in minutes)
0.10
0.08
0.06
0.04
0.02
0.00
−0.02
−0.04
−0.06
−0.08
−0.10
0.01
0.1
1
10
100
1000

DSC21 $\delta = 0^o$

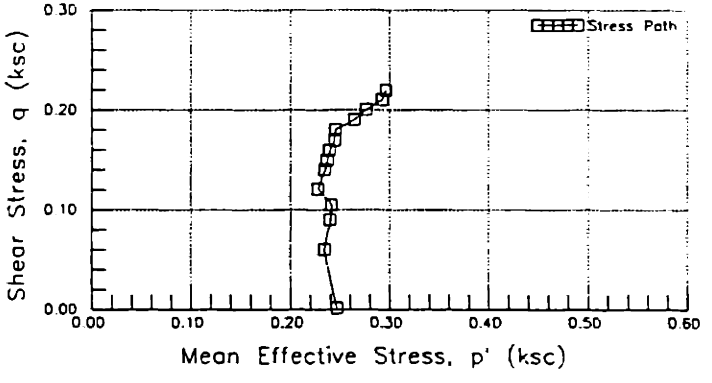

(a) q versus p'

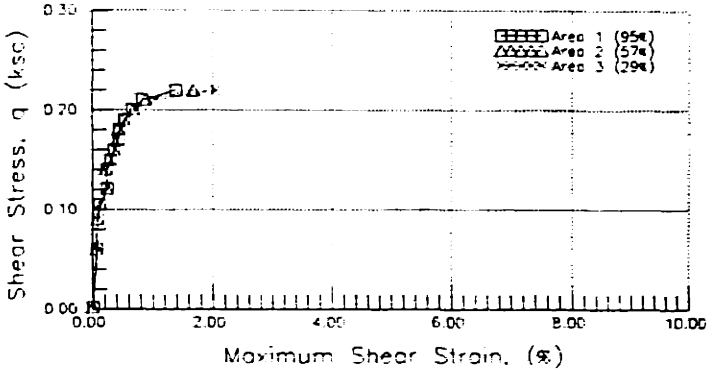

(b) Shear Stress versus Shear Strain

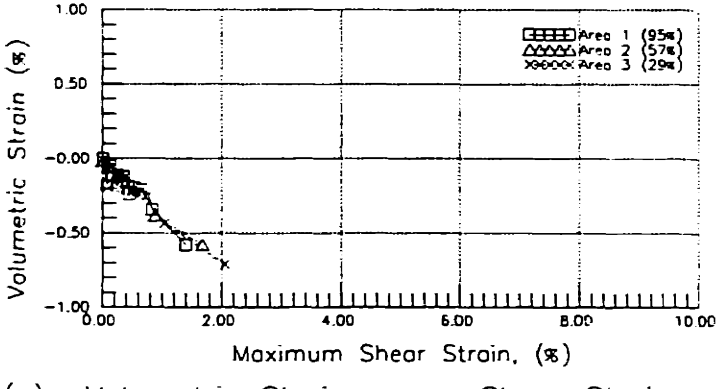

(c) Volumetric Strain versus Shear Strain

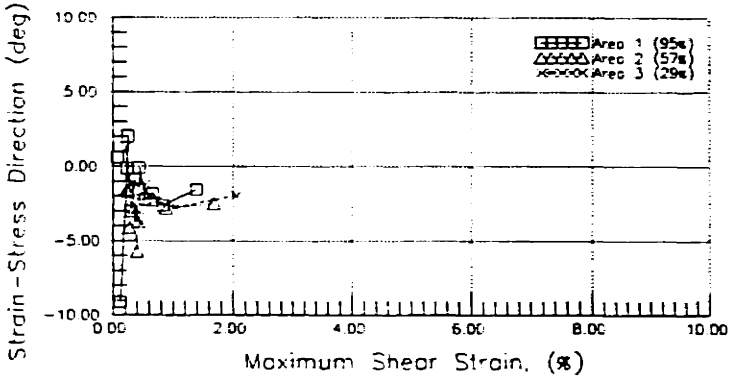

(d) Strain-Stress Direction versus Shear Strain

DSC22 $\delta = 90°$

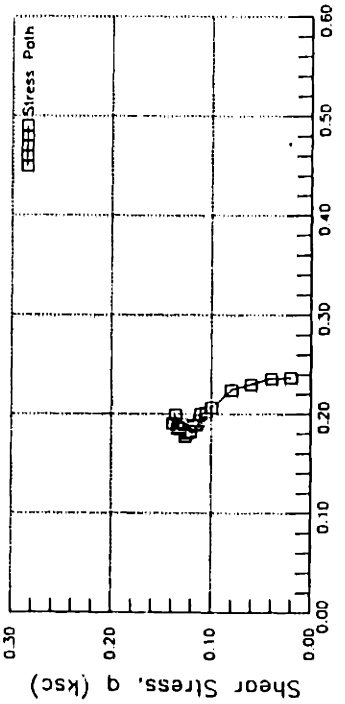

(a) q versus p'

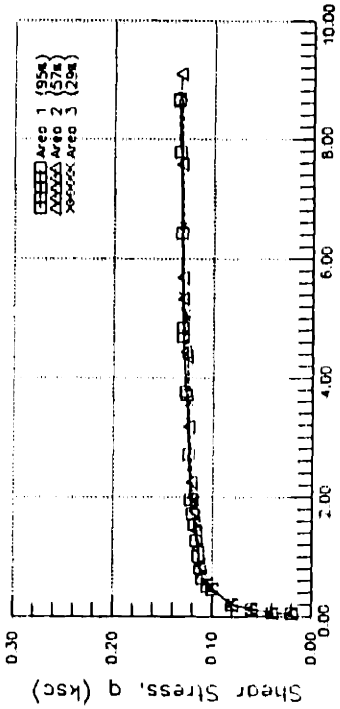

(b) Shear Stress versus Shear Strain

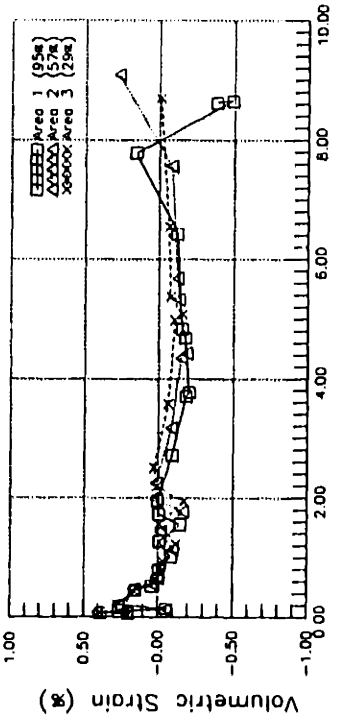

(c) Volumetric Strain versus Shear Strain

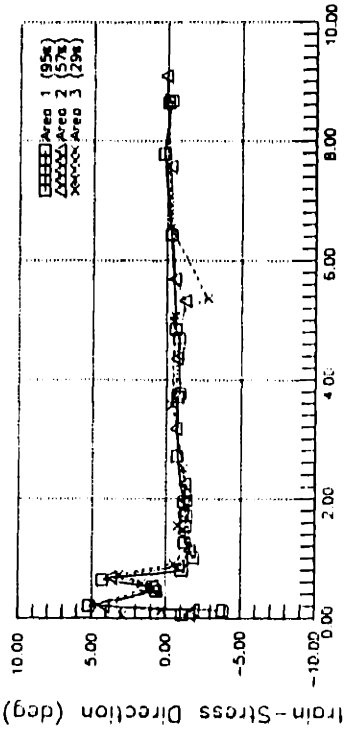

(d) Strain–Stress Direction versus Shear Strain

DSC23 $\psi = 0°$

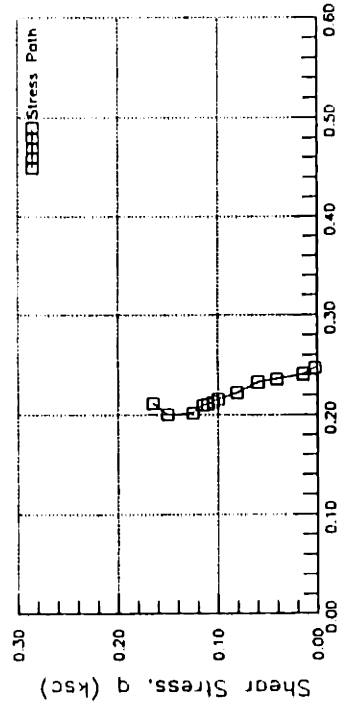

(a) q versus p'

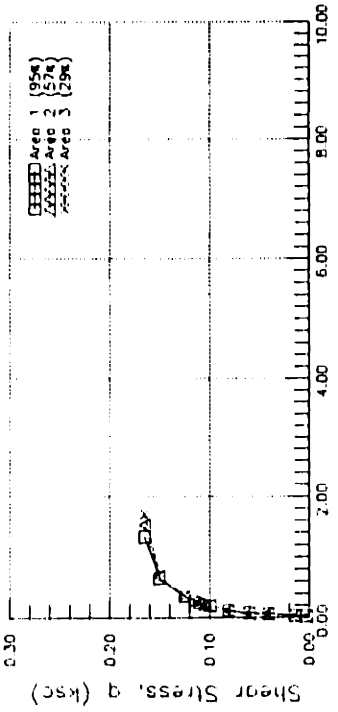

(b) Shear Stress versus Shear Strain

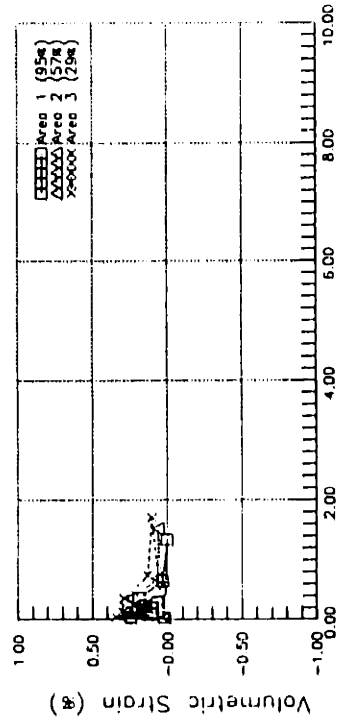

(c) Volumetric Strain versus Shear Strain

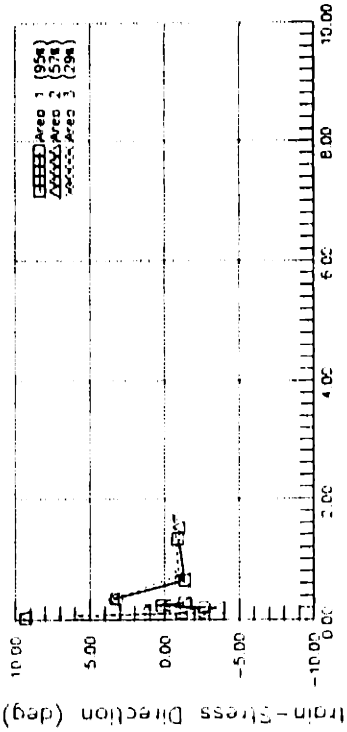

(d) Strain-Stress Direction versus Shear Strain

DSC24 $\psi = 0^o$

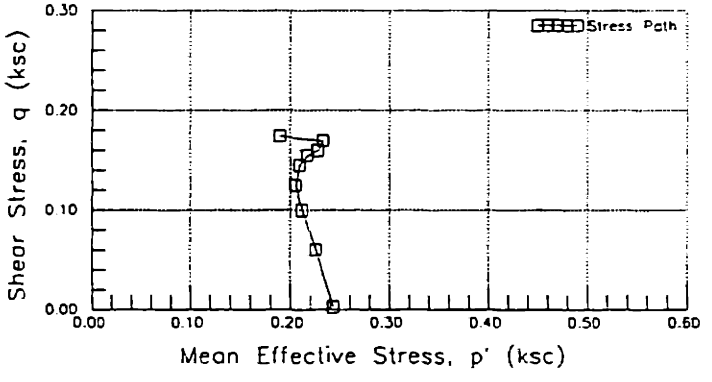

(a) q versus p'

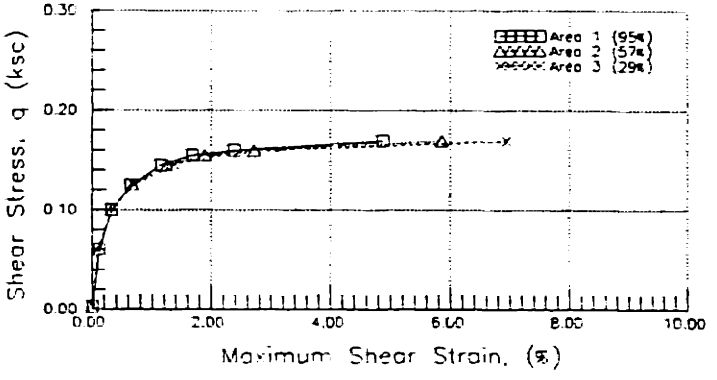

(b) Shear Stress versus Shear Strain

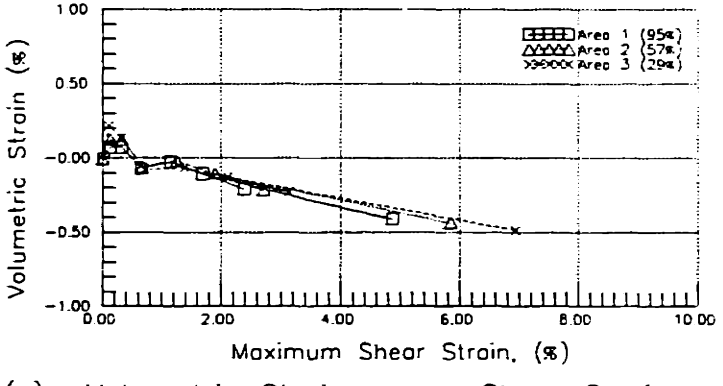

(c) Volumetric Strain versus Shear Strain

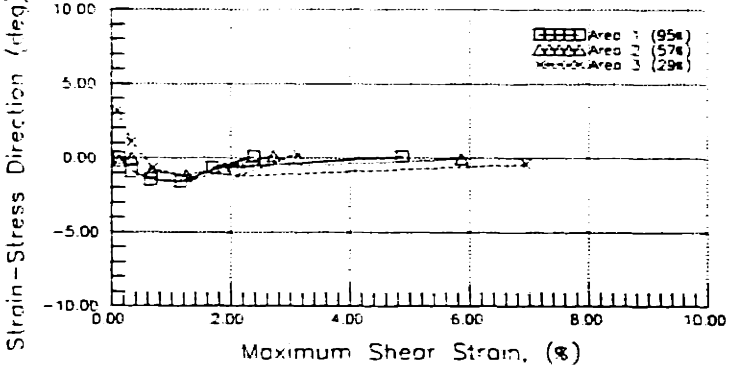

(d) Strain-Stress Direction versus Shear Strain

DSC25 $\psi = 40^{o}$

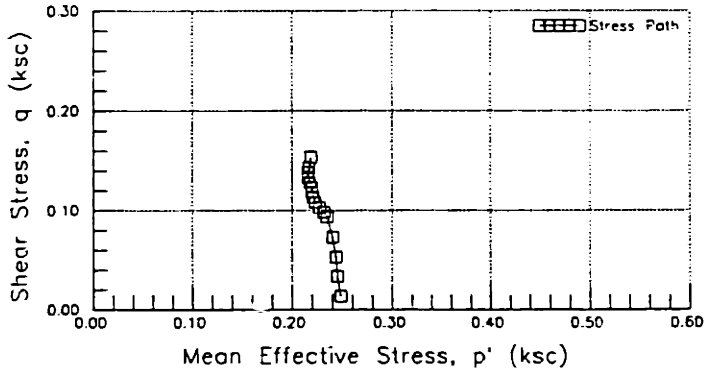

(a) q versus p'

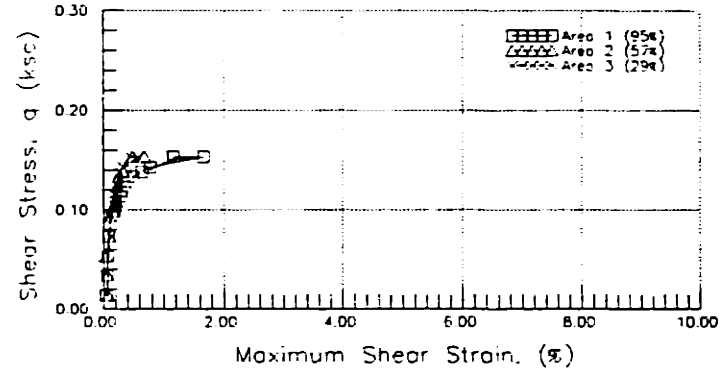

(b) Shear Stress versus Shear Strain

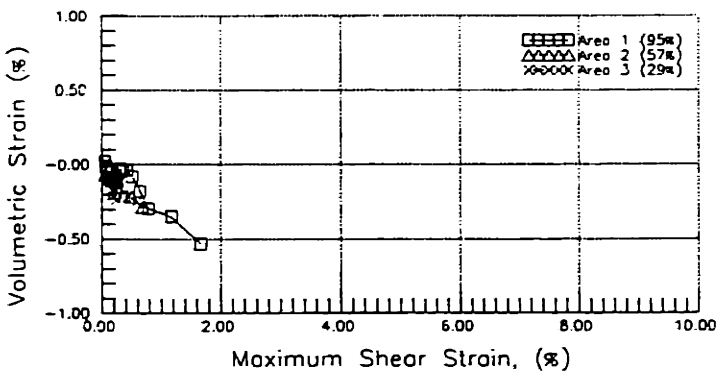

(c) Volumetric Strain versus Shear Strain

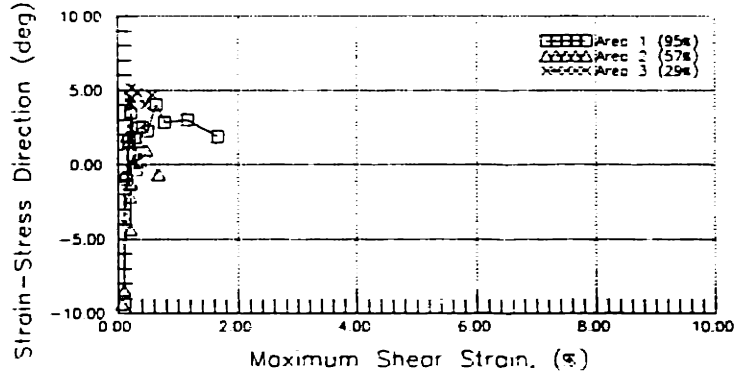

(d) Strain-Stress Direction versus Shear Strain

DSC26 $\delta = 30^o$

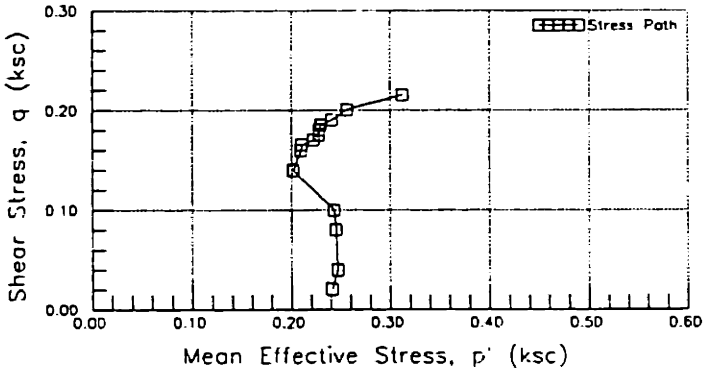

(a) q versus p'

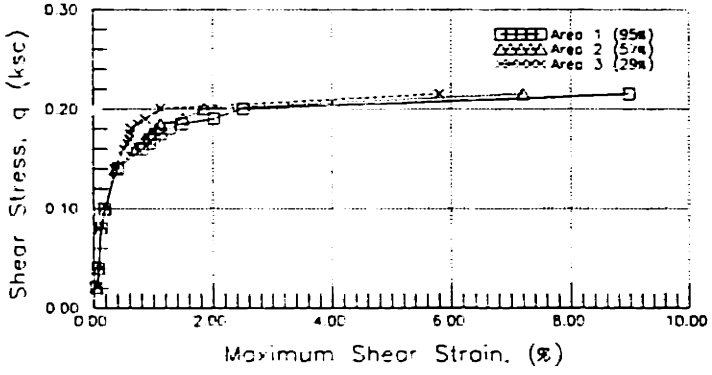

(b) Shear Stress versus Shear Strain

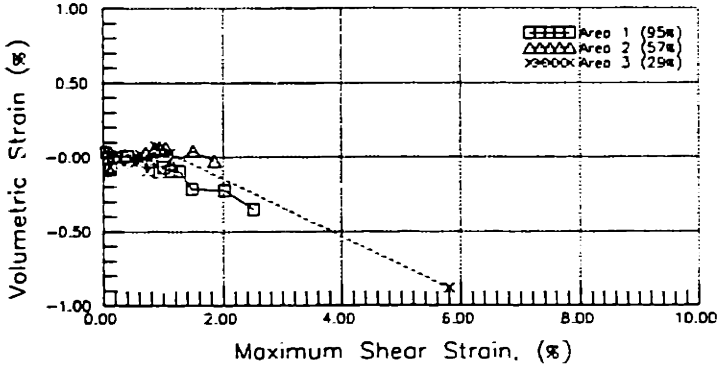

(c) Volumetric Strain versus Shear Strain

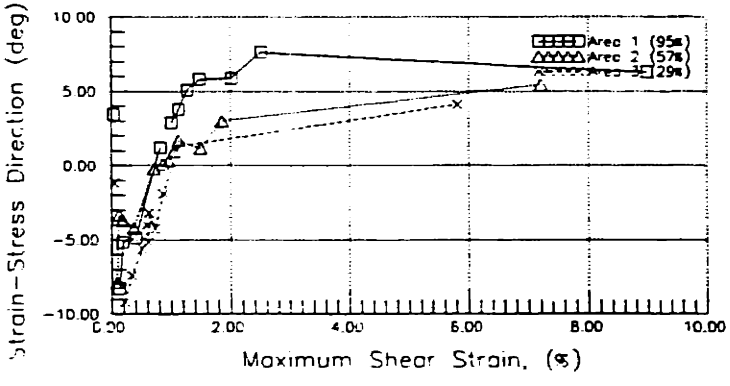

(d) Strain-Stress Direction versus Shear Strain

DSC27 $\delta = 0^o$

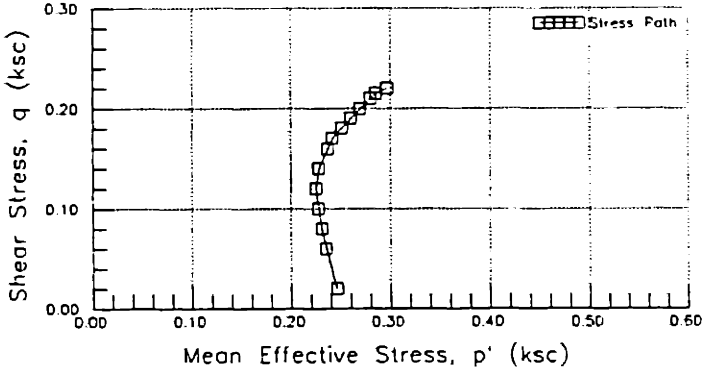

(a) q versus p'

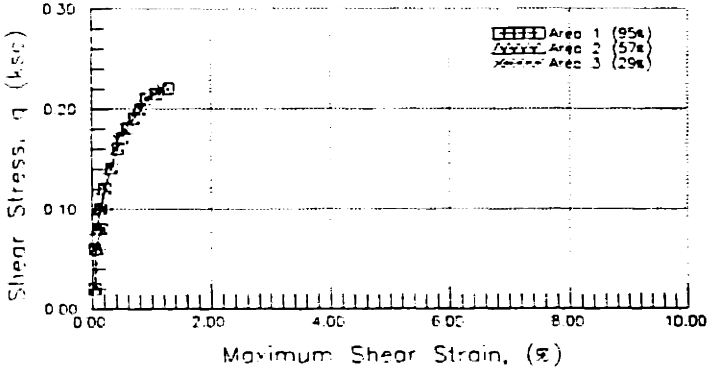

(b) Shear Stress versus Shear Strain

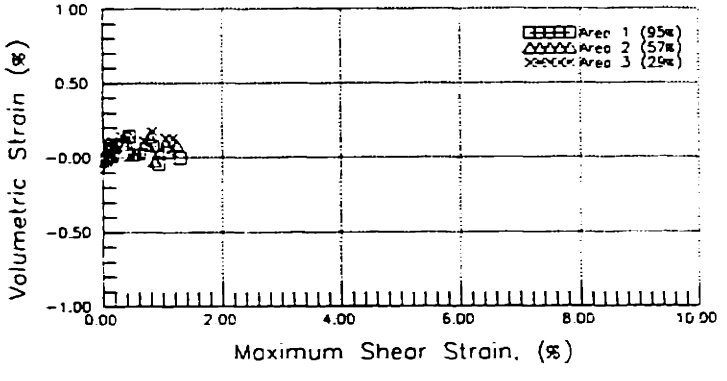

(c) Volumetric Strain versus Shear Strain

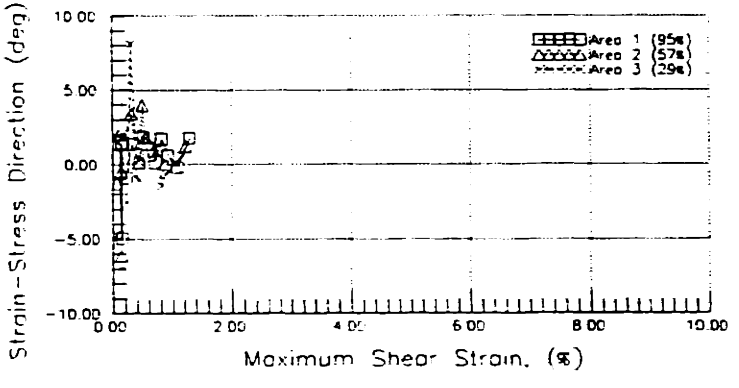

(d) Strain-Stress Direction versus Shear Strain

DSC28 $\delta = 30^{o}$

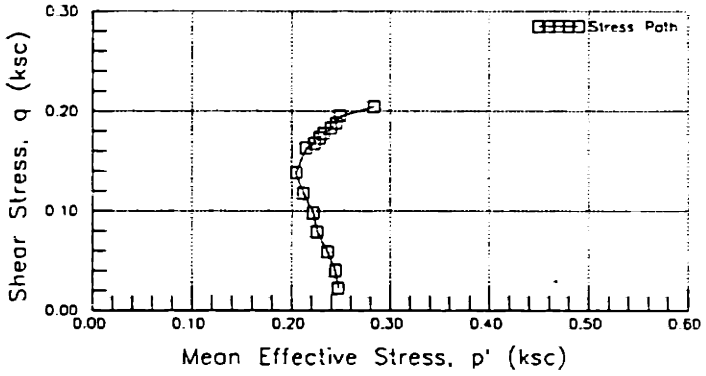

(a) q versus p'

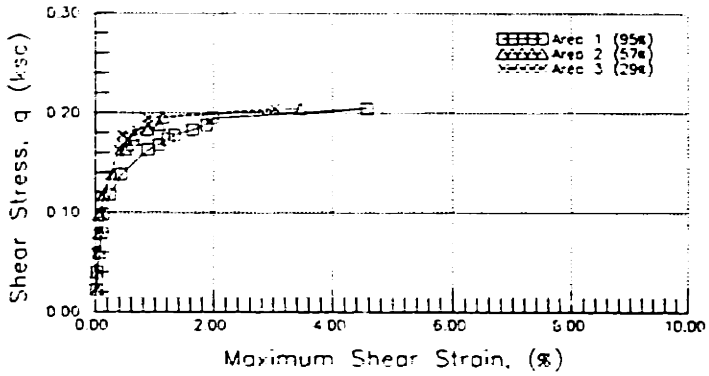

(b) Shear Stress versus Shear Strain

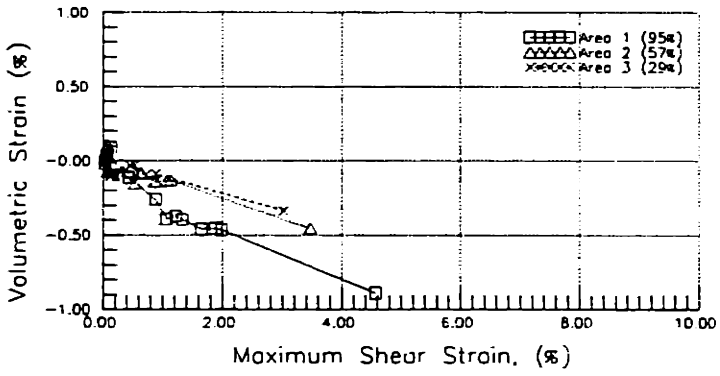

(c) Volumetric Strain versus Shear Strain

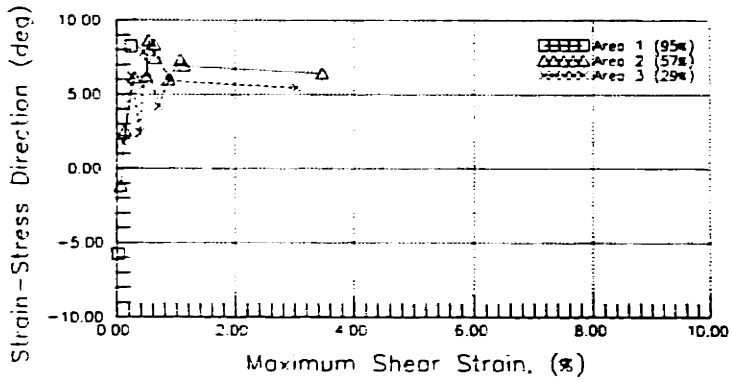

(d) Strain-Stress Direction versus Shear Strain

DSC29 $\psi = 40^o$

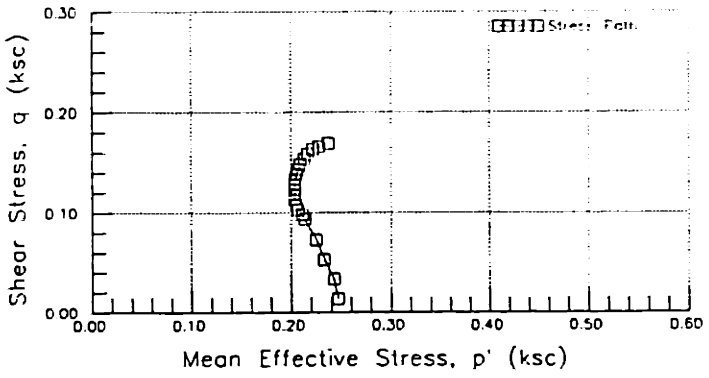

(a) q versus p'

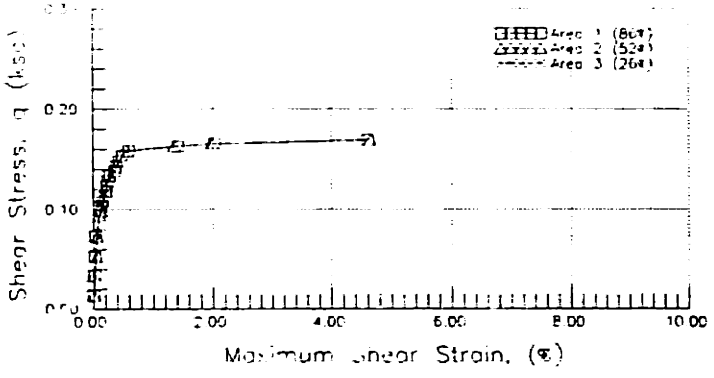

(b) Shear Stress versus Shear Strain

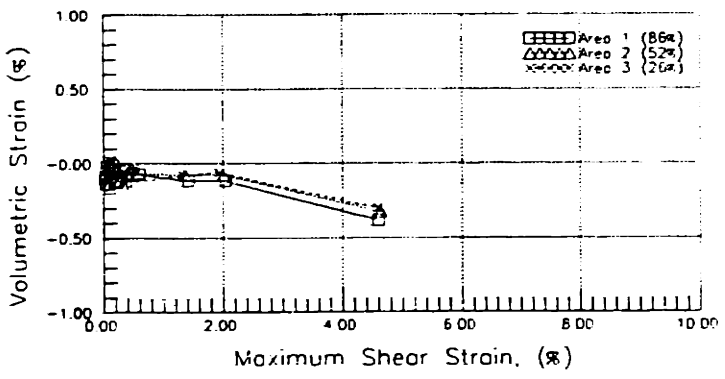

(c) Volumetric Strain versus Shear Strain

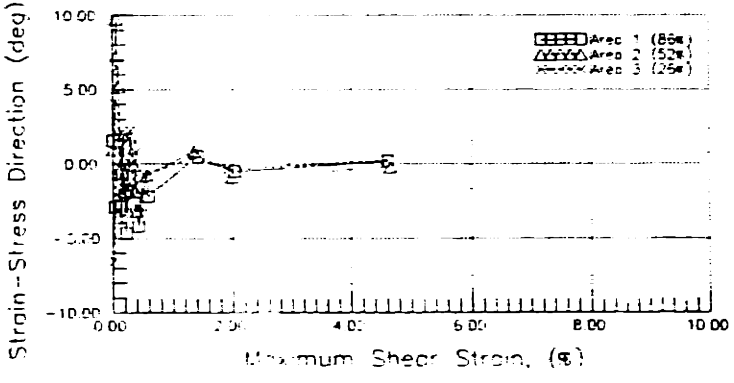

(d) Strain-Stress Direction versus Shear Strain

DSC30 $\psi = 20^o$

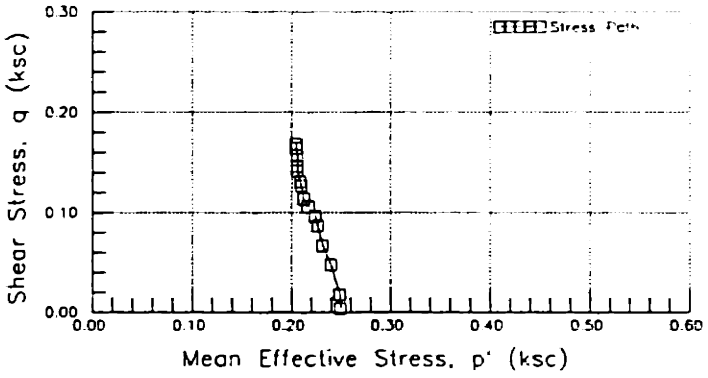

(a) q versus p'

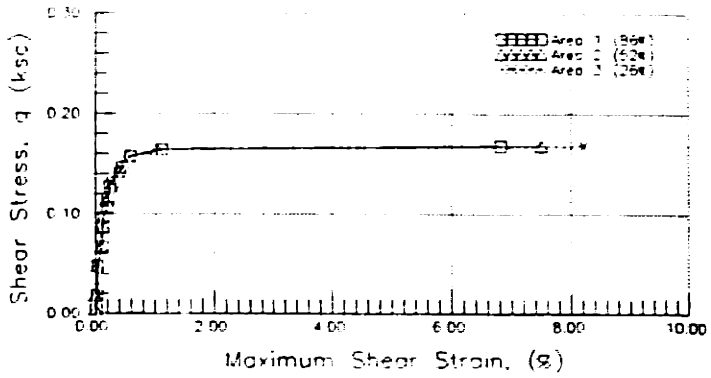

(b) Shear Stress versus Shear Strain

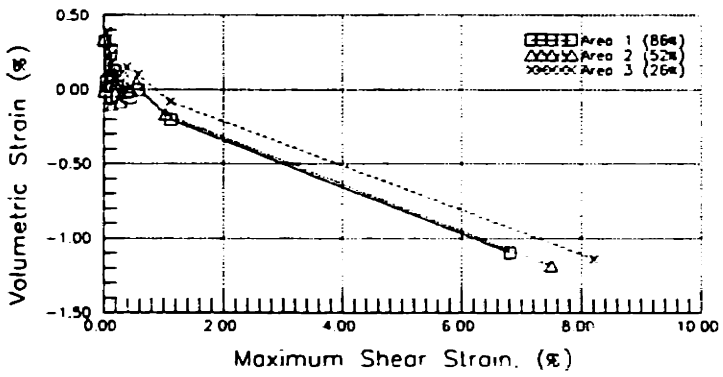

(c) Volumetric Strain versus Shear Strain

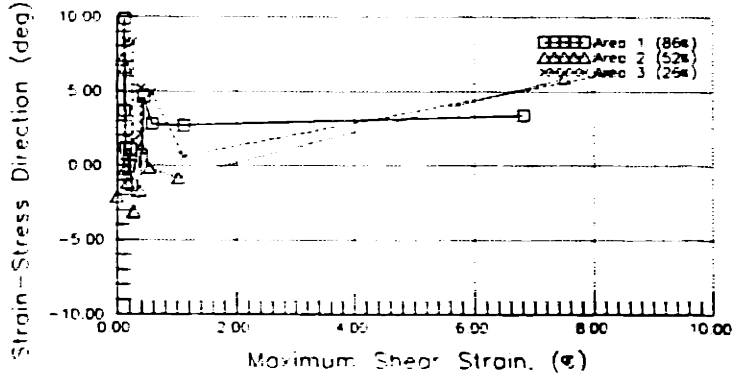

(d) Strain-Stress Direction versus Shear Strain

F.3 CONSOLIDATION RESULTS OF DSC TESTS ON OCR=1 BBC

This section contains:

- Computer printouts of consolidation stress data for DSC tests on OCR=1 BBC.
- Computer printouts of uncorrected consolidation strain data for DSC tests on OCR=1 BBC.
- Computer printouts of corrected consolidation strain data for DSC tests on OCR=1 BBC.
- Plots of consolidation results from DSC tests on OCR=1 BBC.

DSC Consolidation Stresses and Strains for Test DSC31 (δ_{inc}=90°) on Resedimented Boston Blue Clay III.

Film Number	σ'_{vc} (ksc)	σ'_{hc} (ksc)	σ'_{2c}* (ksc)	ϵ_c* (%)	ϵ_{vol}† (%)	ϵ_a† (%)	γ_{max}† (%)	Remarks
1	0.102	0.100	0.079	0.00	0.00	0.00	0.00	σ_2 leaks
2	0.249	0.244	0.114	0.07	0.12	0.12	0.12	
3	0.301	0.261	0.124	0.09	0.24	0.21	0.18	
4	0.360	0.271	0.135	0.11	0.36	0.35	0.33	
5	0.429	0.290	0.150	0.14	0.49	0.49	0.49	
6	0.520	0.321	0.175	0.18	0.78	0.74	0.69	
7	0.619	0.351	0.205	0.24	0.86	0.89	0.93	
8	0.749	0.401	0.256	0.34	1.71	1.45	1.18	
9	0.879	0.469	0.327	0.48	1.98	1.71	1.44	
10	1.000	0.522	0.406	0.63	2.40	2.11	1.82	
11	1.136	0.595	0.525	0.86	3.26	3.26	3.25	Fabric removed
12	1.300	0.678	-	1.15	4.26	3.97	3.67	Assume $\sigma'_2=\sigma'_{hc}$

Notes: * Based on the results of three DSC consolidation tests.
$\sigma_2=10^{[0.537(\sigma_1+\sigma_3)-1.209]}$
* Apparent strain due to Poisson effect of the rubber membrane.
Assuming μ_r=0.25 and E_r=13 ksc, ϵ_c=1.923 x $\Delta\ \sigma_2$
† Corrected strains taken from Area No.1 (86%).

DSC Consolidation Stresses and Strains for Test DSC32 (δ_{inc}=45°) on Resedimented Boston Blue Clay III.

Film Number	σ'_{vc} (ksc)	σ'_{hc} (ksc)	σ'_{2c}* (ksc)	ϵ_c* (%)	ϵ_{vol}‡ (%)	ϵ_R‡ (%)	γ_{max}† (%)	Remarks
1	0.102	0.100	0.069	0.00	0.00	0.00	0.00	Same as DSC34
2	0.249	0.244	0.095	0.05	0.05	0.06	0.07	
3	0.301	0.261	0.091	0.04	-0.02	0.02	0.06	
4	0.360	0.271	0.107	0.07	0.09	0.14	0.15	
5	0.430	0.290	0.132	0.12	0.21	0.24	0.27	
6	0.520	0.321	0.159	0.17	0.40	0.39	0.39	
7	0.620	0.351	0.195	0.24	0.60	0.54	0.48	
8	0.750	0.401	0.234	0.32	0.86	0.81	0.75	
9	0.880	0.469	0.300	0.44	1.22	1.09	0.96	
10	1.000	0.522	0.451	0.73	1.58	1.44	1.30	
11	1.149	0.582	0.561	0.95	2.34	2.02	1.70	
12	1.299	0.676	0.676	1.17	2.39	3.24	4.09	

Notes: * Measured Intermediate Principal Stress.
* Assuming μ_r=0.25 and E_r=13 ksc,
ϵ_c=1.923 x $\Delta\ \sigma_2$
‡ Corrected strains taken from Area No.1 (86%).
† Maximum Shear Strains taken from Area No.1 (86%).

DSC Consolidation Stresses and Strains for Test DSC33 (δ_{inc}=60°) on Resedimented Boston Blue Clay III.

Film Number	σ'_{vc} (ksc)	σ'_{hc} (ksc)	σ'_{2c}* (ksc)	ϵ_c* (%)	ϵ_{vol}‡ (%)	ϵ_a‡ (%)	γ_{max}† (%)	Remarks
1	0.102	0.100	0.069	0.00	0.00	0.00	0.00	
2	0.249	0.244	0.095	0.05	0.05	0.06	0.07	
3	0.301	0.261	0.091	0.04	-0.02	0.02	0.06	
4	0.360	0.271	0.107	0.07	0.09	0.14	0.15	
5	0.430	0.290	0.132	0.12	0.21	0.24	0.27	
6	0.520	0.321	0.159	0.17	0.40	0.39	0.39	
7	0.620	0.351	0.195	0.24	0.60	0.54	0.48	
8	0.750	0.401	0.234	0.32	0.86	0.81	0.75	
9	0.880	0.469	0.300	0.44	1.22	1.09	0.96	
10	1.000	0.522	0.451	0.73	1.58	1.44	1.30	Fabric removed
11	1.149	0.582	0.561	0.95	2.34	2.02	1.70	Error in σ'_{hc}(↓)

Notes: * Measured Intermediate Principal Stress.
* Assuming μ_r=0.25 and E_r=13 ksc,
ϵ_c=1.923 x $\Delta\ \sigma_2$
‡ Corrected strains taken from Area No.1 (86%).
† Maximum Shear Strains taken from Area No.1 (86%).

DSC Consolidation Stresses and Strains for Test DSC34 (δ_{inc}=0°) on Resedimented Boston Blue Clay III.

Film Number	σ'_{vc} (ksc)	σ'_{hc} (ksc)	σ'_{2c}* (ksc)	ϵ_c* (%)	ϵ_{vol}‡ (%)	ϵ_a‡ (%)	γ_{max}† (%)	Remarks
1	0.102	0.101	0.116	0.00	0.00	0.00	0.00	
2	0.249	0.246	0.126	0.02	0.07	0.07	0.07	
3	0.302	0.261	0.109	-0.01	0.05	0.11	0.18	
4	0.360	0.271	0.121	0.01	0.28	0.32	0.36	
5	0.428	0.291	0.131	0.03	-	-	-	
6	0.520	0.322	0.157	0.08	0.35	0.45	0.55	
7	0.619	0.352	0.193	0.15	0.56	0.69	0.81	
8	0.748	0.401	0.244	0.25	0.78	0.94	1.10	
9	0.878	0.468	0.319	0.39	1.09	1.24	1.39	
10	1.000	0.522	0.408	0.56	~1.70	~1.70	~1.70	One σ_v bag leaks
11	1.135	0.595	0.595	0.90	3.05	2.95	2.85	

Notes: * Measured Intermediate Principal Stress.
• Assuming μ_r=0.25 and E_r=13 ksc,
$\epsilon_c = 1.923 \times \Delta \sigma_2$
‡ Corrected strains taken from Area No.1 (86%).
† Maximum Shear Strains taken from Area No.1 (86%).

DSC Consolidation Stresses and Strains for Test DSC35 ($\delta_{inc}=75^{\circ}$) on Resedimented Boston Blue Clay III.

Film Number	σ'_{vc} (ksc)	σ'_{hc} (ksc)	σ'_{2c}* (ksc)	ϵ_c* (%)	ϵ_{vol}‡ (%)	ϵ_a‡ (%)	γ_{max}† (%)	Remarks
1	0.101	0.100	0.092	0.00	0.00	0.00	0.00	
2	0.250	0.247	0.138	0.09	0.11	0.12	0.12	
3	0.301	0.261	0.133	0.08	0.04	0.14	0.23	
4	0.361	0.271	0.159	0.13	0.24	0.28	0.32	
5	0.429	0.290	0.182	0.17	0.45	0.44	0.42	
6	0.521	0.321	0.211	0.23	0.59	0.59	0.59	
7	0.619	0.351	0.248	0.30	0.80	0.77	0.74	
8	0.750	0.401	0.304	0.41	1.16	1.08	1.00	
9	0.879	0.468	0.359	0.51	1.50	1.30	1.18	
10	1.000	0.522	0.409	0.61	1.78	1.69	1.60	
11	1.136	0.594	0.472	0.73	2.84	2.77	2.70	Fabric removed
12	1.300	0.677	0.680	1.13	3.30	3.24	3.18	

Notes: * Measured Intermediate Principal Stress.
* Assuming $\mu_r=0.25$ and $E_r=13$ ksc,
$\epsilon_c=1.923 \times \Delta \sigma_2$
‡ Corrected strains taken from Area No.1 (86%).
† Maximum Shear Strains taken from Area No.1 (86%).

CONSOLIDATION: DSC31 (UNCORRECTED)

AREA	Ex	Ex(SD)	Ey	Ey(SD)	Exy	Exy(SD)	E3	E3(SD)	E1	E1(SD)	GAMMA	G(SD)	EV	EV(SD)	PS.	PS(SD)
	σ_{vc} = 0.249 ksc				σ_{hc} = 0.244 ksc											
1	0.120	0.010	-0.001	0.009	-0.006	0.007	-0.001	0.009	0.120	0.010	0.122	0.014	0.119	0.014	-2.74	3.23
2	0.110	0.013	0.002	0.011	-0.013	0.008	0.001	0.011	0.112	0.013	0.111	0.017	0.112	0.017	-6.80	4.40
3	0.090	0.021	0.006	0.018	-0.003	0.014	0.006	0.018	0.090	0.021	0.084	0.027	0.096	0.027	-2.32	9.28
4	0.023	0.035	-0.033	0.053	-0.025	0.032	-0.042	0.051	0.032	0.038	0.075	0.063	-0.010	0.064	-20.43	24.27
5	0.031	0.250	0.218	0.254	-0.024	0.179	0.028	0.251	0.221	0.255	0.193	0.357	0.249	0.357	7.12	53.12
	σ_{vc} = 0.301 ksc				σ_{hc} = 0.261 ksc											
1	0.187	0.012	0.011	0.011	-0.027	0.008	0.007	0.011	0.191	0.012	0.184	0.016	0.198	0.016	-8.44	2.52
2	0.189	0.016	0.033	0.014	-0.038	0.010	0.025	0.014	0.198	0.015	0.174	0.021	0.223	0.021	-13.13	3.44
3	0.157	0.024	0.045	0.021	-0.024	0.016	0.041	0.022	0.161	0.024	0.121	0.032	0.202	0.032	-11.52	7.66
4	0.088	0.062	0.023	0.067	-0.014	0.046	0.020	0.066	0.091	0.062	0.071	0.091	0.111	0.091	-11.69	36.91
5	-0.158	0.021	0.389	0.569	0.008	0.269	-0.158	0.022	0.389	0.569	0.547	0.570	0.231	0.570	-0.87	28.17
	σ_{vc} = 0.360 ksc				σ_{hc} = 0.271 ksc											
1	0.305	0.017	-0.022	0.012	-0.033	0.011	-0.025	0.012	0.308	0.017	0.333	0.021	0.283	0.021	-5.65	1.82
2	0.332	0.018	-0.010	0.014	-0.037	0.011	-0.013	0.014	0.335	0.017	0.349	0.022	0.322	0.022	-6.06	1.84
3	0.288	0.025	-0.034	0.024	-0.017	0.017	-0.035	0.024	0.289	0.025	0.324	0.034	0.254	0.034	-3.00	3.01
4	0.219	0.061	-0.052	0.059	-0.004	0.042	-0.052	0.059	0.219	0.061	0.271	0.084	0.167	0.084	-0.79	8.93
5	0.208	0.015	0.204	0.068	0.211	0.033	-0.005	0.048	0.417	0.048	0.422	0.066	0.412	0.070	44.72	4.75
	σ_{vc} = 0.429 ksc				σ_{hc} = 0.290 ksc											
1	0.419	0.021	-0.064	0.011	-0.033	0.012	-0.066	0.011	0.422	0.021	0.487	0.023	0.356	0.023	-3.91	1.36
2	0.422	0.017	-0.052	0.014	-0.041	0.011	-0.055	0.014	0.426	0.017	0.481	0.022	0.370	0.022	-4.97	1.31
3	0.383	0.028	-0.066	0.027	-0.027	0.019	-0.068	0.027	0.384	0.028	0.452	0.038	0.316	0.038	-3.44	2.43
4	0.396	0.066	-0.114	0.084	0.000	0.053	-0.114	0.084	0.396	0.066	0.510	0.107	0.282	0.107	0.04	5.98
5	0.097	0.062	0.424	0.354	0.381	0.170	-0.154	0.193	0.676	0.290	0.829	0.346	0.522	0.360	-33.39	12.39
	σ_{vc} = 0.520 ksc				σ_{hc} = 0.321 ksc											
1	0.619	0.017	-0.067	0.012	-0.045	0.010	-0.070	0.012	0.622	0.017	0.692	0.021	0.552	0.021	-3.72	0.85
2	0.620	0.021	-0.057	0.015	-0.074	0.013	-0.065	0.015	0.628	0.021	0.693	0.026	0.564	0.026	-6.20	1.06
3	0.581	0.036	-0.045	0.027	-0.080	0.023	-0.055	0.027	0.592	0.036	0.646	0.045	0.537	0.045	-7.18	2.01
4	0.494	0.092	-0.058	0.047	-0.058	0.052	-0.064	0.047	0.500	0.091	0.564	0.103	0.436	0.103	-5.90	5.25
5	0.362	0.446	0.261	0.118	-0.066	0.243	0.228	0.234	0.395	0.411	0.167	0.473	0.623	0.461	-26.29	80.18
	σ_{vc} = 0.619 ksc				σ_{hc} = 0.351 ksc											
1	0.715	0.024	-0.209	0.015	-0.052	0.014	-0.212	0.015	0.718	0.024	0.930	0.028	0.506	0.028	-3.22	0.86
2	0.753	0.025	-0.173	0.016	-0.070	0.015	-0.179	0.017	0.758	0.025	0.937	0.030	0.579	0.030	-4.29	0.91
3	0.753	0.039	-0.196	0.031	-0.053	0.025	-0.199	0.031	0.756	0.039	0.955	0.050	0.557	0.050	-3.17	1.49
4	0.533	0.078	-0.148	0.074	-0.014	0.054	-0.148	0.074	0.533	0.078	0.681	0.107	0.385	0.107	-1.19	4.51
5	0.628	0.249	-0.033	0.161	0.332	0.152	-0.170	0.177	0.766	0.238	0.936	0.302	0.596	0.297	22.54	9.24
	σ_{vc} = 0.749 ksc				σ_{hc} = 0.401 ksc											
1	1.165	0.026	-0.002	0.016	-0.100	0.015	-0.010	0.016	1.173	0.026	1.183	0.030	1.163	0.030	-4.88	0.73
2	1.236	0.023	0.011	0.017	-0.098	0.014	0.004	0.017	1.244	0.022	1.241	0.028	1.248	0.028	-4.53	0.66
3	1.157	0.034	0.019	0.029	-0.101	0.022	0.010	0.029	1.166	0.034	1.156	0.044	1.175	0.044	-5.04	1.10
4	1.083	0.081	-0.013	0.097	-0.076	0.063	-0.018	0.097	1.088	0.081	1.106	0.127	1.070	0.127	-3.93	3.28
5	0.819	0.008	-0.009	1.055	0.021	0.498	-0.010	1.054	0.819	0.027	0.829	1.054	0.810	1.055	1.47	34.37

AREA	Ex	Ex(SD)	Ey	Ey(SD)	Exy	Exy(SD)	E3	E3(SD)	E1	E1(SD)	GAMMA	G(SD)	EV	EV(SD)	PS.	PS(SD)
	σ_{vc} = 0.879 ksc						σ_{hc} = 0.469 ksc									
1	1.295	0.028	-0.137	0.019	-0.094	0.017	-0.143	0.019	1.302	0.028	1.444	0.033	1.159	0.033	-3.74	0.66
2	1.381	0.025	-0.144	0.019	-0.094	0.016	-0.150	0.019	1.387	0.025	1.537	0.031	1.237	0.031	-3.50	0.58
3	1.309	0.042	-0.125	0.030	-0.104	0.026	-0.132	0.030	1.317	0.042	1.449	0.051	1.184	0.051	-4.12	1.02
4	1.239	0.103	0.018	0.069	-0.029	0.062	0.018	0.069	1.239	0.103	1.221	0.123	1.257	0.123	-1.37	2.90
5	0.751	0.442	0.560	0.188	-0.043	0.251	0.551	0.209	0.760	0.437	0.209	0.482	1.310	0.481	-12.12	67.84
	σ_{vc} = 1.000 ksc						σ_{hc} = 0.522 ksc									
1	1.529	0.033	-0.253	0.021	-0.171	0.019	-0.269	0.021	1.546	0.033	1.815	0.039	1.276	0.039	-5.42	0.61
2	1.644	0.026	-0.222	0.021	-0.169	0.017	-0.237	0.021	1.659	0.026	1.897	0.033	1.422	0.033	-5.14	0.50
3	1.627	0.043	-0.201	0.032	-0.147	0.027	-0.213	0.032	1.639	0.043	1.852	0.054	1.426	0.054	-4.56	0.83
4	1.614	0.110	-0.154	0.095	-0.116	0.073	-0.161	0.095	1.622	0.110	1.783	0.146	1.461	0.146	-3.73	2.35
5	0.597	0.086	0.058	0.788	-0.012	0.374	0.058	0.788	0.597	0.088	0.539	0.793	0.656	0.792	-1.32	39.78
	σ_{vc} = 1.136 ksc						σ_{hc} = 0.595 ksc									
1	2.441	0.044	-0.761	0.046	-0.286	0.032	-0.786	0.046	2.466	0.044	3.252	0.064	1.680	0.064	-5.06	0.56
2	2.573	0.035	-0.615	0.042	-0.268	0.027	-0.637	0.042	2.595	0.035	3.232	0.055	1.958	0.055	-4.77	0.49
3	2.475	0.043	-0.437	0.035	-0.226	0.028	-0.454	0.035	2.492	0.043	2.947	0.055	2.038	0.055	-4.41	0.54
4	2.471	0.103	-0.297	0.079	-0.156	0.065	-0.305	0.079	2.480	0.103	2.785	0.130	2.175	0.130	-3.22	1.34
5	2.222	0.053	0.074	0.203	0.024	0.100	0.074	0.203	2.222	0.053	2.148	0.210	2.296	0.210	0.63	2.66
	σ_{vc} = 1.300 ksc						σ_{hc} = 0.678 ksc									
1	2.859	0.050	-0.767	0.048	-0.292	0.035	-0.791	0.048	2.882	0.050	3.673	0.069	2.092	0.069	-4.58	0.54
2	2.997	0.035	-0.610	0.042	-0.303	0.028	-0.635	0.042	3.022	0.036	3.657	0.055	2.387	0.055	-4.76	0.43
3	2.930	0.044	-0.437	0.035	-0.285	0.028	-0.461	0.035	2.954	0.044	3.415	0.056	2.494	0.056	-4.80	0.47
4	2.920	0.093	-0.302	0.068	-0.290	0.058	-0.328	0.068	2.946	0.093	3.275	0.116	2.618	0.116	-5.10	1.01
5	2.831	0.124	-0.243	0.452	0.062	0.223	-0.244	0.452	2.832	0.124	3.076	0.469	2.588	0.469	1.16	4.15

CONSOLIDATION: DSC32 (UNCORRECTED)

AREA	Ex	Ex(SD)	Ey	Ey(SD)	Exy	Exy(SD)	E3	E3(SD)	E1	E1(SD)	GAMMA	G(SD)	EV	EV(SD)	PS.	PS(SD)
	σ_{vc} = 0.249 ksc				σ_{hc} = 0.246 ksc											
1	0.073	0.014	-0.002	0.012	-0.003	0.009	-0.002	0.012	0.073	0.014	0.075	0.019	0.071	0.019	-2.09	7.21
2	0.096	0.017	0.034	0.016	0.007	0.012	0.033	0.016	0.096	0.017	0.064	0.024	0.129	0.024	6.13	10.68
3	0.106	0.032	0.046	0.027	-0.000	0.021	0.046	0.027	0.106	0.032	0.060	0.042	0.152	0.042	-0.22	20.07
4	0.012	0.078	-0.084	0.061	-0.034	0.050	-0.094	0.063	0.023	0.076	0.118	0.099	-0.071	0.099	-17.63	24.08
5	0.333	0.556	-0.096	0.253	0.133	0.306	-0.133	0.286	0.371	0.538	0.504	0.614	0.237	0.611	15.87	34.92
	σ_{vc} = 0.302 ksc				σ_{hc} = 0.261 ksc											
1	0.143	0.014	-0.033	0.013	-0.005	0.010	-0.033	0.013	0.143	0.014	0.176	0.019	0.110	0.019	-1.62	3.15
2	0.131	0.018	0.027	0.015	0.002	0.012	0.027	0.015	0.131	0.018	0.104	0.023	0.158	0.023	1.21	6.44
3	0.117	0.031	0.031	0.027	0.010	0.021	0.030	0.027	0.118	0.031	0.088	0.041	0.147	0.041	6.54	13.48
4	0.116	0.072	0.040	0.060	0.029	0.047	0.030	0.061	0.126	0.071	0.096	0.094	0.156	0.094	18.73	28.00
5	0.431	0.591	-0.417	0.196	0.086	0.313	-0.426	0.203	0.440	0.588	0.866	0.624	0.015	0.623	5.75	20.71
	σ_{vc} = 0.360 ksc				σ_{hc} = 0.271 ksc											
1	0.327	0.019	-0.032	0.017	0.006	0.013	-0.032	0.017	0.327	0.019	0.359	0.025	0.295	0.025	0.98	2.01
2	0.329	0.027	0.062	0.019	0.015	0.016	0.061	0.019	0.329	0.027	0.268	0.033	0.391	0.033	3.12	3.51
3	0.293	0.043	0.089	0.025	-0.030	0.025	0.084	0.026	0.298	0.043	0.213	0.050	0.382	0.050	-8.25	6.72
4	0.374	0.112	0.044	0.058	-0.010	0.063	0.043	0.058	0.375	0.112	0.332	0.126	0.418	0.126	-1.76	10.89
5	-0.466	0.142	-0.221	0.128	-0.184	0.096	-0.564	0.140	-0.123	0.132	0.442	0.191	-0.687	0.191	28.16	12.41
	σ_{vc} = 0.520 ksc				σ_{hc} = 0.322 ksc											
1	0.390	0.022	-0.156	0.020	0.027	0.015	-0.157	0.020	0.391	0.022	0.549	0.029	0.234	0.029	2.77	1.53
2	0.397	0.028	-0.085	0.018	0.029	0.017	-0.087	0.018	0.398	0.028	0.485	0.033	0.311	0.033	3.42	1.96
3	0.368	0.044	-0.058	0.025	0.020	0.025	-0.059	0.025	0.369	0.044	0.427	0.050	0.310	0.050	2.69	3.37
4	0.273	0.095	-0.087	0.049	0.049	0.054	-0.094	0.050	0.279	0.095	0.373	0.107	0.186	0.107	7.58	8.24
5	0.567	0.446	-0.340	0.068	0.108	0.227	-0.353	0.085	0.580	0.442	0.933	0.452	0.227	0.451	6.70	13.95
	σ_{vc} = 0.619 ksc				σ_{hc} = 0.352 ksc											
1	0.555	0.022	-0.249	0.027	0.029	0.017	-0.250	0.026	0.557	0.022	0.806	0.034	0.307	0.034	2.08	1.21
2	0.617	0.026	-0.138	0.025	0.025	0.018	-0.138	0.025	0.617	0.026	0.756	0.036	0.479	0.036	1.88	1.38
3	0.546	0.034	-0.085	0.034	-0.007	0.024	-0.085	0.034	0.546	0.034	0.632	0.048	0.461	0.048	-0.65	2.17
4	0.545	0.072	-0.122	0.080	0.010	0.054	-0.122	0.080	0.545	0.072	0.667	0.108	0.424	0.108	0.86	4.63
5	0.603	0.258	-0.852	0.103	0.192	0.139	-0.877	0.107	0.628	0.256	1.504	0.278	-0.249	0.278	7.40	5.31
	σ_{vc} = 0.748 ksc				σ_{hc} = 0.401 ksc											
1	0.710	0.026	-0.388	0.036	0.022	0.022	-0.389	0.036	0.710	0.026	1.099	0.044	0.322	0.044	1.15	1.15
2	0.779	0.029	-0.210	0.030	0.002	0.021	-0.210	0.030	0.779	0.029	0.989	0.041	0.570	0.041	0.12	1.20
3	0.795	0.052	-0.170	0.034	-0.027	0.031	-0.171	0.034	0.796	0.052	0.967	0.062	0.625	0.062	-1.62	1.83
4	0.622	0.088	-0.180	0.078	0.025	0.059	-0.181	0.078	0.622	0.088	0.803	0.117	0.441	0.117	1.79	4.18
5	0.613	0.157	-0.411	0.082	0.269	0.089	-0.477	0.088	0.680	0.153	1.157	0.178	0.203	0.177	13.84	4.40
	σ_{vc} = 0.878 ksc				σ_{hc} = 0.468 ksc											
1	0.865	0.029	-0.516	0.037	0.050	0.023	-0.518	0.037	0.867	0.029	1.385	0.047	0.350	0.047	2.08	0.97
2	0.958	0.024	-0.323	0.026	0.055	0.018	-0.325	0.026	0.960	0.024	1.285	0.035	0.635	0.035	2.45	0.79
3	0.943	0.034	-0.234	0.029	0.052	0.022	-0.236	0.029	0.945	0.034	1.182	0.045	0.709	0.045	2.52	1.08
4	0.851	0.058	-0.253	0.061	0.056	0.042	-0.256	0.061	0.854	0.058	1.110	0.084	0.598	0.084	2.90	2.17
5	0.585	0.080	-0.583	0.019	0.048	0.041	-0.585	0.019	0.587	0.080	1.173	0.082	0.002	0.082	2.36	2.01

CONSOLIDATION: DSC33 (UNCORRECTED)

AREA	Ex	Ex(SD)	Ey	Ey(SD)	Exy	Exy(SD)	E3	E3(SD)	E1	E1(SD)	GAMMA	G(SD)	EV	EV(SD)	PS,	PS(SD)
	σ_{vc} = 0.250 ksc				σ_{hc} = 0.247 ksc											
1	0.116	0.011	-0.003	0.008	-0.001	0.007	-0.003	0.008	0.116	0.011	0.119	0.014	0.114	0.014	-0.43	3.34
2	0.155	0.014	0.019	0.009	0.002	0.008	0.019	0.009	0.155	0.014	0.135	0.017	0.174	0.017	0.94	3.52
3	0.170	0.021	0.030	0.017	0.008	0.014	0.029	0.017	0.170	0.021	0.141	0.027	0.199	0.027	3.26	5.58
4	0.230	0.054	0.074	0.035	-0.029	0.032	0.069	0.036	0.235	0.054	0.166	0.064	0.303	0.064	-10.11	11.17
5	0.493	0.609	0.251	0.193	-0.050	0.321	0.242	0.222	0.503	0.596	0.261	0.643	0.745	0.638	-11.14	70.83
	σ_{vc} = 0.301 ksc				σ_{hc} = 0.261 ksc											
1	0.144	0.013	-0.083	0.011	0.022	0.008	-0.085	0.011	0.146	0.013	0.231	0.017	0.060	0.017	5.38	2.07
2	0.181	0.015	-0.081	0.012	0.018	0.010	-0.082	0.012	0.182	0.015	0.264	0.019	0.100	0.019	3.89	2.11
3	0.207	0.026	-0.088	0.022	0.017	0.017	-0.089	0.022	0.208	0.026	0.297	0.034	0.119	0.034	3.26	3.24
4	0.278	0.045	-0.106	0.053	-0.033	0.035	-0.109	0.053	0.280	0.045	0.389	0.070	0.172	0.070	-4.85	5.12
5	0.245	0.216	-0.221	0.128	0.013	0.126	-0.221	0.128	0.245	0.216	0.466	0.251	0.024	0.251	1.64	15.48
	σ_{vc} = 0.361 ksc				σ_{hc} = 0.271 ksc											
1	0.236	0.014	-0.080	0.010	0.005	0.008	-0.080	0.010	0.237	0.014	0.316	0.017	0.157	0.017	0.82	1.52
2	0.306	0.016	-0.068	0.014	-0.008	0.011	-0.068	0.014	0.306	0.016	0.374	0.021	0.239	0.021	-1.25	1.63
3	0.339	0.028	-0.106	0.024	-0.005	0.019	-0.106	0.024	0.339	0.028	0.445	0.037	0.232	0.037	-0.62	2.39
4	0.319	0.070	-0.098	0.082	-0.083	0.054	-0.114	0.082	0.335	0.071	0.449	0.108	0.221	0.108	-10.89	6.88
5	0.703	0.581	-0.158	0.120	-0.167	0.299	-0.189	0.159	0.734	0.570	0.923	0.598	0.546	0.593	-10.57	18.66
	σ_{vc} = 0.429 ksc				σ_{hc} = 0.290 ksc											
1	0.351	0.016	-0.066	0.011	0.013	0.010	-0.066	0.011	0.351	0.016	0.417	0.019	0.285	0.019	1.76	1.31
2	0.436	0.018	-0.043	0.014	-0.003	0.012	-0.043	0.014	0.436	0.018	0.478	0.023	0.393	0.023	-0.35	1.38
3	0.458	0.036	-0.041	0.027	-0.013	0.023	-0.041	0.027	0.458	0.036	0.500	0.045	0.417	0.045	-1.44	2.58
4	0.537	0.092	0.017	0.074	0.071	0.059	0.007	0.075	0.546	0.091	0.539	0.118	0.554	0.118	7.59	6.28
5	0.280	0.507	-0.113	0.193	0.109	0.273	-0.141	0.227	0.308	0.496	0.449	0.549	0.167	0.543	14.46	34.59
	σ_{vc} = 0.521 ksc				σ_{hc} = 0.321 ksc											
1	0.450	0.017	-0.142	0.013	0.025	0.011	-0.143	0.013	0.451	0.017	0.594	0.022	0.308	0.022	2.38	1.04
2	0.561	0.018	-0.149	0.013	0.016	0.011	-0.149	0.013	0.561	0.018	0.710	0.023	0.412	0.023	1.29	0.91
3	0.538	0.029	-0.160	0.018	0.014	0.017	-0.160	0.018	0.538	0.029	0.698	0.034	0.377	0.034	1.11	1.41
4	0.473	0.077	-0.167	0.036	-0.056	0.043	-0.172	0.036	0.478	0.077	0.650	0.085	0.307	0.085	-4.94	3.77
5	0.432	0.546	-0.217	0.129	-0.026	0.283	-0.218	0.130	0.433	0.545	0.652	0.562	0.215	0.561	-2.26	24.88
	σ_{vc} = 0.619 ksc				σ_{hc} = 0.351 ksc											
1	0.558	0.021	-0.179	0.012	0.025	0.012	-0.180	0.012	0.559	0.021	0.738	0.024	0.378	0.024	1.94	0.93
2	0.662	0.022	-0.141	0.015	0.019	0.014	-0.141	0.015	0.663	0.022	0.804	0.027	0.522	0.027	1.34	0.97
3	0.641	0.031	-0.122	0.029	0.020	0.021	-0.122	0.029	0.642	0.031	0.764	0.043	0.519	0.043	1.51	1.60
4	0.668	0.078	-0.057	0.059	0.029	0.049	-0.058	0.059	0.669	0.078	0.728	0.090	0.611	0.098	2.31	3.86
5	0.468	0.558	0.161	0.420	-0.012	0.350	0.160	0.420	0.468	0.557	0.308	0.698	0.628	0.698	-2.20	65.22
	σ_{vc} = 0.750 ksc				σ_{hc} = 0.401 ksc											
1	0.762	0.026	-0.240	0.015	0.011	0.015	-0.240	0.015	0.762	0.026	1.002	0.029	0.522	0.029	0.62	0.84
2	0.913	0.026	-0.206	0.018	0.008	0.016	-0.206	0.018	0.913	0.026	1.119	0.031	0.708	0.031	0.39	0.80
3	0.880	0.042	-0.215	0.030	-0.014	0.026	-0.215	0.030	0.880	0.042	1.095	0.052	0.665	0.052	-0.72	1.35
4	1.074	0.086	-0.234	0.088	-0.062	0.061	-0.237	0.088	1.077	0.086	1.314	0.123	0.840	0.123	-2.73	2.67
5	1.246	0.378	-0.707	0.038	0.201	0.192	-0.728	0.054	1.266	0.377	1.994	0.378	0.538	0.380	5.81	5.48

AREA	Ex	Ex(SD)	Ey	Ey(SD)	Exy	Exy(SD)	E3	E3(SD)	E1	E1(SD)	GAMMA G(SD)		EV	EV(SD)	PS,	PS(SD)
	σ_{vc} = 0.879 ksc						σ_{hc} = 0.468 ksc									
1	0.910	0.027	-0.264	0.014	0.058	0.015	-0.266	0.014	0.912	0.027	1.179	0.031	0.646	0.031	2.83	0.74
2	1.081	0.027	-0.222	0.020	0.065	0.017	-0.225	0.020	1.085	0.027	1.309	0.033	0.860	0.033	2.83	0.73
3	1.134	0.044	-0.179	0.028	0.030	0.026	-0.179	0.028	1.134	0.044	1.314	0.052	0.955	0.052	1.33	1.13
4	1.145	0.104	-0.203	0.068	-0.004	0.063	-0.203	0.068	1.145	0.104	1.348	0.124	0.942	0.124	-0.17	2.65
5	0.614	0.594	-0.435	0.106	0.240	0.304	-0.487	0.165	0.666	0.583	1.154	0.600	0.179	0.603	12.30	14.97
	σ_{vc} = 1.000 ksc						σ_{hc} = 0.522 ksc									
1	1.166	0.034	-0.425	0.016	0.076	0.019	-0.429	0.016	1.169	0.034	1.598	0.037	0.741	0.037	2.74	0.67
2	1.389	0.028	-0.390	0.021	0.061	0.017	-0.392	0.021	1.391	0.028	1.783	0.035	1.000	0.035	1.98	0.56
3	1.383	0.045	-0.310	0.031	0.047	0.027	-0.311	0.031	1.385	0.045	1.695	0.055	1.074	0.055	1.59	0.92
4	1.406	0.128	-0.270	0.077	0.070	0.075	-0.273	0.077	1.409	0.128	1.682	0.149	1.136	0.149	2.39	2.56
5	2.087	1.115	-0.539	0.013	-0.124	0.562	-0.545	0.055	2.093	1.113	2.638	1.117	1.548	1.115	-2.70	12.24
	σ_{vc} = 1.136 ksc						σ_{hc} = 0.594 ksc									
1	1.695	0.043	-0.982	0.027	0.157	0.025	-0.991	0.027	1.704	0.043	2.695	0.050	0.714	0.050	3.34	0.54
2	2.010	0.030	-0.851	0.030	0.155	0.021	-0.860	0.030	2.018	0.030	2.878	0.042	1.158	0.042	3.09	0.42
3	2.060	0.051	-0.732	0.037	0.152	0.031	-0.740	0.037	2.068	0.051	2.808	0.062	1.328	0.062	3.12	0.64
4	2.118	0.133	-0.552	0.036	0.095	0.070	-0.555	0.037	2.121	0.133	2.676	0.138	1.566	0.138	2.03	1.49
5	1.528	0.610	-0.671	0.054	0.237	0.309	-0.696	0.084	1.553	0.608	2.249	0.610	0.857	0.612	6.07	7.83
	σ_{vc} = 1.300 ksc						σ_{hc} = 0.677 ksc									
1	2.183	0.056	-0.967	0.025	0.212	0.030	-0.982	0.025	2.198	0.056	3.179	0.061	1.216	0.061	3.82	0.55
2	2.602	0.040	-0.887	0.028	0.247	0.025	-0.904	0.029	2.619	0.040	3.523	0.049	1.715	0.049	4.04	0.40
3	2.719	0.052	-0.825	0.040	0.208	0.033	-0.837	0.040	2.731	0.052	3.568	0.065	1.894	0.065	3.35	0.52
4	2.669	0.100	-0.767	0.086	0.199	0.066	-0.778	0.086	2.681	0.100	3.459	0.132	1.902	0.132	3.31	1.10
5	2.174	0.614	-0.519	0.101	-0.007	0.314	-0.519	0.101	2.174	0.614	2.694	0.622	1.655	0.622	-0.15	6.67

CONSOLIDATION: DSC34 (UNCORRECTED)

AREA	Ex	Ex(SD)	Ey	Ey(SD)	Exy	Exy(SD)	E3	E3(SD)	E1	E1(SD)	GAMMA	G(SD)	EV	EV(SD)	PS.	PS(SD)
	σ_{vc} = 0.249 ksc				σ_{hc} = 0.246 ksc											
1	0.062	0.013	-0.017	0.009	0.018	0.008	-0.013	0.009	0.057	0.012	0.070	0.015	0.045	0.015	15.29	6.26
2	0.048	0.017	-0.011	0.013	0.014	0.011	-0.007	0.014	0.044	0.016	0.051	0.021	0.037	0.021	16.73	12.04
3	0.064	0.028	0.030	0.023	0.000	0.018	0.030	0.023	0.064	0.028	0.034	0.036	0.094	0.036	-0.82	30.55
4	0.168	0.054	0.055	0.064	0.021	0.042	0.060	0.063	0.163	0.054	0.103	0.084	0.223	0.084	12.24	23.14
5	0.614	0.108	-0.091	0.103	-0.203	0.075	0.019	0.107	0.503	0.104	0.484	0.149	0.523	0.149	-28.61	8.84
	σ_{vc} = 0.301 ksc				σ_{hc} = 0.266 ksc											
1	0.028	0.019	-0.038	0.012	-0.011	0.011	-0.036	0.012	0.026	0.019	0.063	0.022	-0.010	0.022	-10.67	10.11
2	0.072	0.021	-0.050	0.015	0.023	0.013	-0.046	0.015	0.067	0.020	0.114	0.025	0.022	0.025	11.78	6.41
3	0.098	0.032	-0.035	0.028	0.025	0.021	-0.030	0.028	0.093	0.032	0.124	0.043	0.063	0.043	11.78	9.92
4	0.186	0.083	-0.140	0.076	0.079	0.056	-0.115	0.077	0.161	0.083	0.276	0.112	0.045	0.112	17.55	11.62
5	0.838	0.015	0.390	0.045	0.080	0.024	0.406	0.043	0.822	0.019	0.416	0.047	1.228	0.047	11.35	3.28
	σ_{vc} = 0.360 ksc				σ_{hc} = 0.290 ksc											
1	0.115	0.018	-0.072	0.015	0.010	0.011	-0.072	0.015	0.114	0.018	0.187	0.023	0.042	0.023	3.08	3.51
2	0.139	0.022	-0.058	0.014	0.016	0.013	-0.056	0.014	0.138	0.021	0.194	0.025	0.081	0.025	4.80	3.74
3	0.184	0.034	-0.038	0.021	0.027	0.020	-0.034	0.022	0.180	0.034	0.215	0.040	0.146	0.040	7.33	5.38
4	0.237	0.082	-0.073	0.052	0.061	0.049	-0.059	0.055	0.223	0.080	0.283	0.097	0.164	0.097	12.84	9.82
5	0.692	0.307	-0.320	0.069	0.289	0.155	-0.127	0.194	0.500	0.246	0.628	0.311	0.373	0.314	33.62	14.32
	σ_{vc} = 0.430 ksc				σ_{hc} = 0.315 ksc											
1	0.165	0.019	-0.103	0.016	-0.010	0.013	-0.103	0.016	0.164	0.019	0.267	0.025	0.062	0.025	-2.33	2.69
2	0.198	0.022	-0.084	0.020	0.004	0.015	-0.084	0.020	0.198	0.022	0.282	0.030	0.114	0.030	0.74	3.06
3	0.285	0.032	-0.069	0.028	-0.005	0.021	-0.069	0.028	0.285	0.032	0.354	0.043	0.217	0.043	-0.88	3.46
4	0.407	0.061	-0.034	0.067	-0.062	0.045	-0.025	0.066	0.397	0.061	0.423	0.090	0.373	0.090	-8.55	6.13
5	0.930	0.134	-0.036	0.131	-0.207	0.094	0.016	0.131	0.876	0.134	0.860	0.188	0.893	0.188	-14.41	6.26
	σ_{vc} = 0.520 ksc				σ_{hc} = 0.347 ksc											
1	0.271	0.019	-0.116	0.010	0.018	0.011	-0.115	0.011	0.270	0.019	0.385	0.022	0.155	0.022	2.63	1.62
2	0.324	0.024	-0.107	0.016	0.024	0.014	-0.105	0.016	0.323	0.024	0.428	0.029	0.217	0.029	3.28	1.93
3	0.372	0.039	-0.134	0.032	0.008	0.025	-0.134	0.032	0.372	0.039	0.506	0.051	0.238	0.051	0.86	2.87
4	0.440	0.100	-0.194	0.083	-0.061	0.065	-0.188	0.083	0.434	0.100	0.622	0.130	0.247	0.130	-5.67	5.99
5	1.025	0.284	0.519	0.437	0.046	0.262	0.523	0.434	1.021	0.289	0.498	0.521	1.545	0.521	5.35	30.14
	σ_{vc} = 0.620 ksc				σ_{hc} = 0.383 ksc											
1	0.347	0.024	-0.133	0.012	0.015	0.013	-0.133	0.012	0.346	0.024	0.479	0.027	0.213	0.027	1.81	1.59
2	0.433	0.027	-0.106	0.017	0.017	0.016	-0.106	0.018	0.433	0.026	0.539	0.032	0.327	0.032	1.79	1.69
3	0.495	0.043	-0.074	0.031	-0.016	0.026	-0.073	0.031	0.495	0.042	0.568	0.053	0.422	0.053	-1.65	2.66
4	0.495	0.122	-0.099	0.082	0.046	0.074	-0.095	0.084	0.491	0.121	0.586	0.147	0.396	0.147	4.55	7.18
5	0.700	0.409	-0.176	0.339	0.178	0.265	-0.134	0.346	0.658	0.404	0.792	0.531	0.524	0.531	13.39	19.18
	σ_{vc} = 0.750 ksc				σ_{hc} = 0.431 ksc											
1	0.539	0.022	-0.216	0.015	0.020	0.013	-0.215	0.015	0.539	0.022	0.754	0.027	0.324	0.027	1.53	1.02
2	0.648	0.026	-0.203	0.019	0.028	0.016	-0.201	0.020	0.645	0.026	0.846	0.032	0.444	0.032	3.27	1.09
3	0.732	0.043	-0.180	0.037	0.039	0.028	-0.179	0.037	0.730	0.043	0.910	0.057	0.552	0.057	2.48	1.80
4	0.894	0.103	-0.113	0.055	0.152	0.058	-0.088	0.058	0.869	0.101	0.958	0.117	0.781	0.116	9.23	3.48
5	1.136	0.937	-0.143	0.323	0.307	0.491	-0.048	0.451	1.041	0.882	1.090	0.986	0.993	0.991	17.13	25.89

AREA	Ex	Ex(SD)	Ey	Ey(SD)	Exy	Exy(SD)	E3	E3(SD)	E1	E1(SD)	GAMMA	G(SD)	EV	EV(SD)	PS.	PS(SD)
	σ_{vc} = 0.880 ksc				σ_{hc} = 0.476 ksc											
1	0.694	0.026	-0.266	0.015	0.038	0.015	-0.264	0.016	0.692	0.025	0.957	0.030	0.428	0.030	2.28	0.89
2	0.796	0.029	-0.244	0.023	0.057	0.019	-0.241	0.024	0.792	0.029	1.033	0.037	0.552	0.037	3.18	1.04
3	0.915	0.039	-0.237	0.045	0.025	0.030	-0.236	0.045	0.915	0.039	1.151	0.059	0.678	0.059	1.25	1.48
4	1.011	0.105	-0.167	0.068	0.054	0.063	-0.165	0.069	1.008	0.104	1.174	0.125	0.844	0.125	2.64	3.05
5	1.146	0.289	-0.040	0.069	0.206	0.147	0.000	0.099	1.107	0.280	1.107	0.296	1.107	0.298	10.92	7.62
	σ_{vc} = 1.000 ksc				σ_{hc} = 0.519 ksc											
1	0.792	0.026	-0.547	0.022	0.069	0.017	-0.544	0.022	0.788	0.026	1.332	0.034	0.245	0.034	2.98	0.73
2	0.942	0.029	-0.433	0.022	0.117	0.018	-0.423	0.022	0.932	0.028	1.356	0.036	0.509	0.036	4.98	0.76
3	0.999	0.048	-0.347	0.036	0.086	0.030	-0.342	0.037	0.994	0.048	1.336	0.060	0.652	0.060	3.70	1.29
4	1.098	0.121	-0.409	0.065	0.174	0.069	-0.388	0.068	1.077	0.119	1.466	0.138	0.689	0.137	6.86	2.69
5	1.421	0.862	-0.667	0.187	0.389	0.436	-0.585	0.295	1.339	0.830	1.924	0.877	0.755	0.882	11.92	13.00
	σ_{vc} = 1.149 ksc				σ_{hc} = 0.582 ksc											
1	1.128	0.028	-0.584	0.028	0.097	0.020	-0.579	0.028	1.123	0.028	1.702	0.039	0.544	0.039	3.26	0.66
2	1.350	0.028	-0.436	0.024	0.172	0.018	-0.419	0.025	1.333	0.027	1.752	0.037	0.914	0.037	5.66	0.60
3	1.504	0.041	-0.324	0.036	0.166	0.028	-0.309	0.036	1.489	0.041	1.798	0.055	1.100	0.055	5.32	0.88
4	1.740	0.083	-0.264	0.051	0.204	0.049	-0.243	0.052	1.719	0.082	1.962	0.097	1.476	0.097	6.01	1.42
5	1.951	0.766	-0.192	0.298	0.278	0.408	-0.154	0.331	1.913	0.753	2.067	0.820	1.759	0.822	7.81	11.30

CONSOLIDATION: DSC35 (UNCORRECTED)

AREA	Ex	Ex(SD)	Ey	Ey(SD)	Exy	Exy(SD)	E3	E3(SD)	E1	C1(SD)	GAMMA	G(SD)	EV	EV(SD)	PS.	PS(SD)
	σ_{vc} = 0.249 ksc				σ_{hc} = 0.246 ksc											
1	0.062	0.013	-0.017	0.009	0.018	0.008	-0.013	0.009	0.057	0.012	0.070	0.015	0.045	0.015	15.29	6.26
2	0.048	0.017	-0.011	0.013	0.014	0.011	-0.007	0.014	0.044	0.016	0.051	0.021	0.037	0.021	16.73	12.04
3	0.064	0.028	0.030	0.023	0.000	0.018	0.030	0.023	0.064	0.028	0.034	0.036	0.094	0.036	-0.82	30.55
4	0.168	0.054	0.055	0.064	0.021	0.042	0.060	0.063	0.163	0.054	0.103	0.084	0.223	0.084	12.24	23.14
5	0.614	0.108	-0.091	0.103	-0.203	0.075	0.019	0.107	0.503	0.104	0.484	0.149	0.523	0.149	-28.61	8.84
	σ_{vc} = 0.301 ksc				σ_{hc} = 0.266 ksc											
1	0.028	0.019	-0.038	0.012	-0.011	0.011	-0.036	0.012	0.026	0.019	0.063	0.022	-0.010	0.022	-10.67	10.11
2	0.072	0.021	-0.050	0.015	0.023	0.013	-0.046	0.015	0.067	0.020	0.114	0.025	0.022	0.025	11.78	6.41
3	0.098	0.032	-0.035	0.028	0.025	0.021	-0.030	0.028	0.093	0.032	0.124	0.043	0.063	0.043	11.78	9.92
4	0.186	0.083	-0.140	0.076	0.079	0.056	-0.115	0.077	0.161	0.082	0.276	0.112	0.045	0.112	17.55	11.62
5	0.838	0.015	0.390	0.045	0.080	0.024	0.406	0.043	0.822	0.019	0.416	0.047	1.228	0.047	11.35	3.28
	σ_{vc} = 0.360 ksc				σ_{hc} = 0.290 ksc											
1	0.115	0.018	-0.072	0.015	0.010	0.011	-0.072	0.015	0.114	0.018	0.187	0.023	0.042	0.023	3.08	3.51
2	0.139	0.022	-0.058	0.014	0.016	0.013	-0.056	0.014	0.138	0.021	0.194	0.025	0.081	0.025	4.80	3.74
3	0.184	0.034	-0.038	0.021	0.027	0.020	-0.034	0.022	0.180	0.034	0.215	0.040	0.146	0.040	7.33	5.38
4	0.237	0.082	-0.073	0.052	0.061	0.049	-0.059	0.055	0.223	0.080	0.283	0.097	0.164	0.097	12.84	9.82
5	0.692	0.307	-0.320	0.069	0.289	0.155	-0.127	0.194	0.500	0.246	0.628	0.311	0.373	0.314	33.62	14.32
	σ_{vc} = 0.430 ksc				σ_{hc} = 0.315 ksc											
1	0.165	0.019	-0.103	0.016	-0.010	0.013	-0.103	0.016	0.164	0.019	0.267	0.025	0.062	0.025	2.33	2.69
2	0.198	0.022	-0.084	0.020	0.004	0.015	-0.084	0.020	0.198	0.022	0.282	0.030	0.114	0.030	0.74	3.06
3	0.285	0.032	-0.069	0.028	-0.005	0.021	-0.069	0.028	0.285	0.032	0.354	0.043	0.217	0.043	-0.88	3.46
4	0.407	0.061	-0.034	0.067	-0.062	0.045	-0.025	0.066	0.397	0.061	0.423	0.090	0.373	0.090	-8.55	6.13
5	0.930	0.134	-0.036	0.131	-0.207	0.094	0.016	0.131	0.876	0.134	0.860	0.188	0.893	0.188	-14.41	6.26
	σ_{vc} = 0.520 ksc				σ_{hc} = 0.347 ksc											
1	0.271	0.019	-0.116	0.010	0.018	0.011	-0.115	0.011	0.270	0.019	0.385	0.022	0.155	0.022	2.63	1.62
2	0.324	0.024	-0.107	0.016	0.024	0.014	-0.105	0.016	0.323	0.024	0.428	0.029	0.217	0.029	3.28	1.93
3	0.372	0.039	-0.134	0.032	0.008	0.025	-0.134	0.032	0.372	0.039	0.506	0.051	0.238	0.051	0.86	2.87
4	0.440	0.100	-0.194	0.083	-0.061	0.065	-0.188	0.083	0.434	0.100	0.622	0.130	0.247	0.130	-5.67	5.99
5	1.025	0.284	0.519	0.437	0.046	0.262	0.523	0.434	1.021	0.289	0.498	0.521	1.545	0.521	5.35	30.14
	σ_{vc} = 0.620 ksc				σ_{hc} = 0.383 ksc											
1	0.347	0.024	-0.133	0.012	0.015	0.013	-0.133	0.012	0.346	0.024	0.479	0.027	0.213	0.027	1.81	1.59
2	0.433	0.027	-0.106	0.017	0.017	0.016	-0.106	0.018	0.433	0.026	0.539	0.032	0.327	0.032	1.79	1.69
3	0.495	0.043	-0.074	0.031	-0.016	0.026	-0.073	0.031	0.495	0.042	0.568	0.053	0.422	0.053	-1.65	2.66
4	0.495	0.122	-0.099	0.082	0.046	0.074	-0.095	0.084	0.491	0.121	0.586	0.147	0.396	0.147	4.55	7.18
5	0.700	0.409	-0.176	0.339	0.178	0.265	-0.134	0.346	0.658	0.404	0.792	0.531	0.524	0.531	13.39	19.18
	σ_{vc} = 0.750 ksc				σ_{hc} = 0.431 ksc											
1	0.539	0.022	-0.216	0.015	0.020	0.013	-0.215	0.015	0.539	0.022	0.754	0.027	0.324	0.027	1.53	1.02
2	0.648	0.026	-0.203	0.019	0.048	0.016	-0.201	0.020	0.645	0.026	0.846	0.032	0.444	0.032	3.27	1.09
3	0.732	0.043	-0.180	0.037	0.039	0.028	-0.179	0.037	0.730	0.043	0.910	0.057	0.552	0.057	2.48	1.80
4	0.894	0.103	-0.113	0.055	0.152	0.058	-0.088	0.058	0.869	0.101	0.958	0.117	0.781	0.116	9.23	3.48
5	1.136	0.937	-0.143	0.323	0.307	0.491	-0.048	0.451	1.041	0.882	1.090	0.986	0.993	0.991	17.13	25.89

AREA	Ex	Ex(SD)	Ey	Ey(SD)	Exy	Exy(SD)	E3	E3(SD)	E1	E1(SD)	GAMMA	G(SD)	EV	EV(SD)	PS.	PS(SD)
	σ_{vc} = 0.880 ksc						σ_{hc} = 0.476 ksc									
1	0.694	0.026	-0.266	0.015	0.038	0.015	-0.264	0.016	0.692	0.025	0.957	0.030	0.428	0.030	2.28	0.89
2	0.796	0.029	-0.244	0.023	0.057	0.019	-0.241	0.024	0.792	0.029	1.033	0.037	0.552	0.037	3.18	1.04
3	0.915	0.039	-0.237	0.045	0.025	0.030	-0.236	0.045	0.915	0.039	1.151	0.059	0.678	0.059	1.25	1.48
4	1.011	0.105	-0.167	0.068	0.054	0.063	-0.165	0.069	1.008	0.104	1.174	0.125	0.844	0.125	2.64	3.05
5	1.146	0.289	-0.040	0.069	0.206	0.147	0.000	0.099	1.107	0.280	1.107	0.296	1.107	0.298	10.92	7.62
	σ_{vc} = 1.000 ksc						σ_{hc} = 0.519 ksc									
1	0.792	0.026	-0.547	0.022	0.069	0.017	-0.544	0.022	0.788	0.026	1.332	0.034	0.245	0.034	2.98	0.73
2	0.942	0.029	-0.433	0.022	0.117	0.018	-0.423	0.022	0.932	0.028	1.356	0.036	0.509	0.036	4.98	0.76
3	0.999	0.048	-0.347	0.036	0.086	0.030	-0.342	0.037	0.994	0.048	1.336	0.060	0.652	0.060	3.70	1.29
4	1.098	0.121	-0.409	0.065	0.174	0.069	-0.388	0.068	1.077	0.119	1.466	0.138	0.689	0.137	6.86	2.69
5	1.421	0.862	-0.667	0.187	0.389	0.436	-0.585	0.295	1.339	0.830	1.924	0.877	0.755	0.882	11.92	13.00
	σ_{vc} = 1.149 ksc						σ_{hc} = 0.582 ksc									
1	1.128	0.028	-0.584	0.028	0.097	0.020	-0.579	0.028	1.123	0.028	1.702	0.039	0.544	0.039	3.26	0.66
2	1.350	0.028	-0.436	0.024	0.172	0.018	-0.419	0.025	1.333	0.027	1.752	0.037	0.914	0.037	5.66	0.60
3	1.504	0.041	-0.324	0.036	0.166	0.028	-0.309	0.036	1.489	0.041	1.798	0.055	1.180	0.055	5.32	0.88
4	1.740	0.083	-0.264	0.051	0.204	0.049	-0.243	0.052	1.719	0.082	1.962	0.097	1.476	0.097	6.01	1.42
5	1.951	0.766	-0.192	0.298	0.278	0.408	-0.154	0.331	1.913	0.753	2.067	0.820	1.759	0.822	7.81	11.30
	σ_{vc} = 1.299 ksc						σ_{hc} = 0.676 ksc									
1	2.314	0.087	-1.874	0.046	0.132	0.050	-1.870	0.047	2.310	0.087	4.180	0.099	0.440	0.099	1.81	0.68
2	3.018	0.086	-1.979	0.037	0.206	0.047	-1.971	0.038	3.009	0.086	4.980	0.094	1.039	0.094	2.37	0.54
3	3.583	0.098	-2.120	0.050	0.211	0.055	-2.112	0.050	3.575	0.098	5.687	0.110	1.463	0.110	2.13	0.55
4	4.164	0.126	-2.279	0.087	0.174	0.076	-2.274	0.088	4.159	0.125	6.434	0.153	1.885	0.153	1.55	0.68
5	4.293	1.321	-2.641	0.123	0.216	0.656	-2.635	0.180	4.287	1.315	6.922	1.325	1.652	1.327	1.79	5.43

CONSOLIDATION: DSC31 (CORRECTED)

AREA	Ex	Ex(SD)	Ey	Ey(SD)	Exy	Exy(SD)	E3	E3(SD)	E1	E1(SD)	GAMMA	G(SD)	EV	EV(SD)	PS.	PS(SD)
	σ_{vc} = 0.249 ksc						σ_{hc} = 0.244 ksc									
1	0.120	0.010	-0.001	0.009	-0.006	0.007	-0.001	0.009	0.120	0.010	0.122	0.014	0.119	0.014	-2.74	3.23
2	0.110	0.013	0.002	0.011	-0.013	0.008	0.001	0.011	0.112	0.013	0.111	0.017	0.112	0.017	-6.80	4.40
3	0.090	0.021	0.006	0.018	-0.003	0.014	0.006	0.018	0.090	0.021	0.084	0.027	0.096	0.027	-2.32	9.28
4	0.023	0.035	-0.033	0.053	-0.025	0.032	-0.042	0.051	0.032	0.038	0.075	0.063	-0.010	0.064	-20.43	24.27
5	0.031	0.250	0.218	0.254	-0.024	0.179	0.028	0.251	0.221	0.255	0.193	0.357	0.249	0.357	7.12	53.12
	σ_{vc} = 0.301 ksc						σ_{hc} = 0.261 ksc									
1	0.207	0.012	0.030	0.011	-0.027	0.008	0.026	0.011	0.211	0.012	0.184	0.016	0.237	0.016	-8.44	2.52
2	0.208	0.016	0.053	0.014	-0.038	0.010	0.044	0.014	0.217	0.015	0.174	0.021	0.261	0.02	-13.13	3.44
3	0.176	0.024	0.065	0.021	-0.024	0.016	0.060	0.022	0.181	0.024	0.121	0.032	0.241	0.032	-11.52	7.66
4	0.107	0.062	0.042	0.067	-0.014	0.046	0.039	0.066	0.110	0.062	0.071	0.091	0.149	0.091	-11.69	36.91
5	-0.138	0.021	0.408	0.569	0.008	0.269	-0.138	0.022	0.408	0.569	0.547	0.570	0.270	0.570	-0.87	28.17
	σ_{vc} = 0.360 ksc						σ_{hc} = 0.271 ksc									
1	0.345	0.017	0.019	0.012	-0.033	0.011	0.016	0.012	0.348	0.017	0.333	0.021	0.364	0.021	-5.65	1.82
2	0.372	0.018	0.031	0.014	-0.037	0.011	0.027	0.014	0.376	0.017	0.349	0.022	0.403	0.022	-6.06	1.84
3	0.329	0.025	0.006	0.024	-0.017	0.017	0.005	0.024	0.329	0.025	0.324	0.034	0.335	0.034	-3.00	3.01
4	0.259	0.061	-0.012	0.059	-0.004	0.042	-0.012	0.059	0.259	0.061	0.271	0.084	0.248	0.084	-0.79	8.93
5	0.248	0.015	0.244	0.068	0.211	0.033	0.035	0.048	0.457	0.048	0.422	0.066	0.493	0.070	44.72	4.75
	σ_{vc} = 0.429 ksc						σ_{hc} = 0.290 ksc									
1	0.489	0.021	0.006	0.011	-0.033	0.012	0.003	0.011	0.491	0.021	0.487	0.023	0.494	0.023	-3.91	1.36
2	0.491	0.017	0.018	0.014	-0.041	0.011	0.014	0.014	0.495	0.017	0.481	0.022	0.509	0.022	-4.97	1.31
3	0.452	0.028	0.003	0.027	-0.027	0.019	0.001	0.027	0.453	0.028	0.452	0.038	0.455	0.038	-3.44	2.43
4	0.465	0.066	-0.045	0.084	0.000	0.053	-0.045	0.084	0.465	0.066	0.510	0.107	0.420	0.107	0.04	5.98
5	0.167	0.062	0.494	0.354	0.381	0.170	-0.085	0.193	0.745	0.290	0.829	0.346	0.660	0.360	-33.39	12.39
	σ_{vc} = 0.520 ksc						σ_{hc} = 0.321 ksc									
1	0.734	0.017	0.048	0.012	-0.045	0.010	0.045	0.012	0.737	0.017	0.692	0.021	0.783	0.021	-3.72	0.85
2	0.736	0.021	0.059	0.015	-0.074	0.013	0.051	0.015	0.744	0.021	0.693	0.026	0.794	0.026	-6.20	1.06
3	0.697	0.036	0.071	0.027	-0.080	0.023	0.060	0.027	0.707	0.036	0.646	0.045	0.767	0.045	-7.18	2.01
4	0.609	0.092	0.057	0.047	-0.058	0.052	0.051	0.047	0.615	0.091	0.564	0.103	0.667	0.103	-5.90	5.25
5	0.477	0.446	0.376	0.118	-0.066	0.243	0.343	0.234	0.510	0.411	0.167	0.473	0.853	0.461	-26.29	80.18
	σ_{vc} = 0.619 ksc						σ_{hc} = 0.351 ksc									
1	0.890	0.024	-0.034	0.015	-0.052	0.014	-0.037	0.015	0.893	0.024	0.930	0.028	0.856	0.028	-3.22	0.86
2	0.928	0.025	0.002	0.016	-0.070	0.015	-0.004	0.017	0.933	0.025	0.937	0.030	0.929	0.030	-4.29	0.91
3	0.928	0.039	-0.021	0.031	-0.053	0.025	-0.024	0.031	0.931	0.039	0.955	0.050	0.906	0.050	-3.17	1.49
4	0.707	0.078	0.027	0.074	-0.014	0.054	0.027	0.074	0.708	0.078	0.681	0.107	0.735	0.107	-1.19	4.51
5	0.803	0.249	0.142	0.161	0.332	0.152	0.005	0.177	0.941	0.238	0.936	0.302	0.946	0.297	22.54	9.24
	σ_{vc} = 0.749 ksc						σ_{hc} = 0.401 ksc									
1	1.438	0.026	0.272	0.016	-0.100	0.015	0.263	0.016	1.446	0.026	1.183	0.030	1.709	0.030	-4.88	0.73
2	1.509	0.023	0.284	0.017	-0.098	0.014	0.277	0.017	1.517	0.022	1.241	0.028	1.794	0.028	-4.53	0.66
3	1.430	0.034	0.292	0.029	-0.101	0.022	0.283	0.029	1.439	0.034	1.156	0.044	1.721	0.044	-5.04	1.10
4	1.356	0.081	0.260	0.097	-0.076	0.063	0.255	0.097	1.361	0.081	1.106	0.127	1.616	0.127	-3.93	3.28
5	1.092	0.008	0.264	1.055	0.021	0.498	0.264	1.054	1.092	0.027	0.829	1.054	1.356	1.055	1.47	34.37

AREA	Ex	Ex(SD)	Ey	Ey(SD)	Exy	Exy(SD)	E3	E3(SD)	E1	E1(SD)	GAMMA	G(SD)	EV	EV(SD)	PS.	PS(SD)
	σ_{vc} = 0.879 ksc						σ_{hc} = 0.469 ksc									
1	1,705	0.028	0.273	0.019	-0.094	0.017	0.267	0.019	1.711	0.028	1,444	0.033	1.978	0.033	-3.74	0.66
2	1.791	0.025	0.265	0.019	-0.094	0.016	0.260	0.019	1.796	0.025	1.537	0.031	2.056	0.031	-3.50	0.58
3	1.719	0.042	0.285	0.030	-0.104	0.026	0.277	0.030	1.726	0.042	1.449	0.051	2.003	0.051	-4.12	1.02
4	1.648	0.103	0.428	0.069	-0.029	0.062	0.427	0.069	1.649	0.103	1.221	0.123	2.076	0.123	-1.37	2.90
5	1.160	0.442	0.969	0.188	-0.043	0.251	0.960	0.209	1.169	0.437	0.209	0.482	2.129	0.481	-12.12	67.84
	σ_{vc} = 1.000 ksc						σ_{hc} = 0.522 ksc									
1	2.091	0.033	0.309	0.021	-0.171	0.019	0.292	0.021	2.107	0.033	1.815	0.039	2.399	0.039	-5.42	0.61
2	2.206	0.026	0.339	0.021	-0.169	0.017	0.324	0.021	2.221	0.026	1.897	0.033	2.545	0.033	-5.14	0.50
3	2.189	0.043	0.361	0.032	-0.147	0.027	0.349	0.032	2.201	0.043	1.852	0.054	2.549	0.054	-4.56	0.83
4	2.176	0.110	0.408	0.095	-0.116	0.073	0.400	0.095	2.183	0.110	1.783	0.146	2.584	0.146	-3.73	2.35
5	1.159	0.086	0.620	0.788	-0.012	0.374	0.620	0.788	1.159	0.088	0.539	0.793	1.779	0.792	-1.32	39.78
	σ_{vc} = 1.136 ksc						σ_{hc} = 0.595 ksc									
1	3.231	0.044	0.030	0.046	-0.286	0.032	0.004	0.046	3.256	0.044	3.252	0.064	3.260	0.064	-5.06	0.56
2	3.363	0.035	0.176	0.042	-0.268	0.027	0.153	0.042	3.385	0.035	3.232	0.055	3.539	0.055	-4.77	0.49
3	3.265	0.043	0.353	0.035	-0.226	0.028	0.336	0.035	3.283	0.043	2.947	0.055	3.619	0.055	-4.41	0.54
4	3.261	0.103	0.494	0.079	-0.156	0.065	0.485	0.079	3.270	0.103	2.785	0.130	3.755	0.130	-3.22	1.34
5	3.012	0.053	0.864	0.203	0.024	0.100	0.864	0.203	3.012	0.053	2.148	0.210	3.876	0.210	0.63	2.66
	σ_{vc} = 1.300 ksc						σ_{hc} = 0.678 ksc									
1	3.945	0.050	0.319	0.048	-0.292	0.035	0.296	0.048	3.969	0.050	3.673	0.069	4.264	0.069	-4.58	0.54
2	4.083	0.035	0.477	0.042	-0.303	0.028	0.451	0.042	4.108	0.036	3.657	0.055	4.560	0.055	-4.76	0.43
3	4.017	0.044	0.650	0.035	-0.285	0.028	0.626	0.035	4.041	0.044	3.415	0.056	4.667	0.056	-4.80	0.47
4	4.007	0.093	0.784	0.068	-0.290	0.058	0.758	0.068	4.033	0.093	3.275	0.116	4.791	0.116	-5.10	1.01
5	3.917	0.124	0.844	0.452	0.062	0.223	0.843	0.452	3.919	0.124	3.076	0.469	4.761	0.469	1.16	4.15

CONSOLIDATION: DSC32 (CORRECTED)

AREA	Ex	Ex(SD)	Ey	Ey(SD)	Exy	Exy(SD)	E3	E3(SD)	E1	E1(SD)	GAMMA	G(SD)	EV	EV(SD)	PS.	PS(SD)
	σ_{vc} = 0.249 ksc						σ_{hc} = 0.246 ksc									
1	0.073	0.014	-0.002	0.012	-0.003	0.009	-0.002	0.012	0.073	0.014	0.075	0.019	0.071	0.019	-2.09	7.21
2	0.096	0.017	0.034	0.016	0.007	0.012	0.033	0.016	0.096	0.017	0.064	0.024	0.129	0.024	6.13	10.68
3	0.106	0.032	0.046	0.027	-0.000	0.021	0.046	0.027	0.106	0.032	0.060	0.042	0.152	0.042	-0.22	20.07
4	0.012	0.078	-0.084	0.061	-0.034	0.050	-0.094	0.063	0.023	0.076	0.118	0.099	-0.071	0.099	-17.63	24.08
5	0.333	0.556	-0.096	0.253	0.133	0.306	-0.133	0.286	0.371	0.538	0.504	0.614	0.237	0.611	15.87	34.92
	σ_{vc} = 0.302 ksc						σ_{hc} = 0.261 ksc									
1	0.110	0.014	-0.065	0.013	-0.005	0.010	-0.066	0.013	0.110	0.014	0.176	0.019	0.045	0.019	-1.62	3.15
2	0.098	0.018	-0.005	0.015	0.002	0.012	-0.005	0.015	0.098	0.018	0.104	0.023	0.093	0.023	1.21	6.44
3	0.084	0.031	-0.002	0.027	0.010	0.021	-0.003	0.027	0.085	0.031	0.088	0.041	0.082	0.041	6.54	13.48
4	0.084	0.072	0.007	0.060	0.029	0.047	-0.003	0.061	0.093	0.071	0.096	0.094	0.091	0.094	18.73	28.00
5	0.399	0.591	-0.449	0.196	0.086	0.313	-0.458	0.203	0.407	0.588	0.866	0.624	-0.051	0.623	5.75	20.71
	σ_{vc} = 0.360 ksc						σ_{hc} = 0.271 ksc									
1	0.317	0.019	-0.041	0.017	0.006	0.013	-0.041	0.017	0.317	0.019	0.359	0.025	0.276	0.025	0.98	2.01
2	0.319	0.027	0.053	0.019	0.015	0.016	0.052	0.019	0.320	0.027	0.268	0.033	0.371	0.033	3.12	3.51
3	0.284	0.043	0.079	0.025	-0.030	0.025	0.075	0.026	0.288	0.043	0.213	0.050	0.363	0.050	-8.25	6.72
4	0.365	0.112	0.034	0.058	-0.010	0.063	0.034	0.058	0.365	0.112	0.332	0.126	0.399	0.126	-1.76	10.89
5	-0.476	0.142	-0.231	0.128	-0.184	0.096	-0.574	0.140	-0.132	0.132	0.442	0.191	-0.706	0.191	28.16	12.41
	σ_{vc} = 0.520 ksc						σ_{hc} = 0.322 ksc									
1	0.450	0.022	-0.096	0.020	0.027	0.015	-0.098	0.020	0.451	0.022	0.549	0.029	0.353	0.029	2.77	1.53
2	0.456	0.028	-0.026	0.018	0.029	0.017	-0.027	0.018	0.458	0.028	0.485	0.033	0.431	0.033	3.42	1.96
3	0.427	0.044	0.002	0.025	0.020	0.025	0.001	0.025	0.428	0.044	0.427	0.050	0.429	0.050	2.69	3.37
4	0.333	0.095	-0.028	0.049	0.049	0.054	-0.034	0.050	0.339	0.095	0.373	0.107	0.305	0.107	7.58	8.24
5	0.626	0.446	-0.281	0.068	0.108	0.227	-0.293	0.085	0.639	0.442	0.933	0.452	0.346	0.451	6.70	13.95
	σ_{vc} = 0.619 ksc						σ_{hc} = 0.352 ksc									
1	0.684	0.022	-0.120	0.027	0.029	0.017	-0.121	0.026	0.685	0.022	0.806	0.034	0.564	0.034	2.08	1.21
2	0.745	0.026	-0.009	0.025	0.025	0.018	-0.010	0.025	0.746	0.026	0.756	0.036	0.737	0.036	1.88	1.38
3	0.675	0.034	0.044	0.034	-0.007	0.024	0.044	0.034	0.675	0.034	0.632	0.048	0.719	0.048	-0.65	2.17
4	0.674	0.072	0.007	0.080	0.010	0.054	0.007	0.080	0.674	0.072	0.667	0.108	0.681	0.108	0.86	4.63
5	0.732	0.258	-0.723	0.103	0.192	0.139	-0.748	0.107	0.757	0.256	1.504	0.278	0.009	0.278	7.40	5.31
	σ_{vc} = 0.748 ksc						σ_{hc} = 0.401 ksc									
1	0.937	0.026	-0.161	0.036	0.022	0.022	-0.162	0.036	0.937	0.026	1.099	0.044	0.776	0.044	1.15	1.15
2	1.006	0.029	0.017	0.030	0.002	0.021	0.017	0.030	1.006	0.029	0.989	0.041	1.023	0.041	0.12	1.20
3	1.022	0.052	0.057	0.034	-0.027	0.031	0.056	0.034	1.023	0.052	0.967	0.062	1.078	0.062	-1.62	1.83
4	0.848	0.088	0.047	0.078	0.025	0.059	0.046	0.078	0.849	0.088	0.803	0.117	0.895	0.117	1.79	4.18
5	0.840	0.157	-0.184	0.082	0.269	0.089	-0.250	0.088	0.906	0.153	1.157	0.178	0.656	0.177	13.84	4.40
	σ_{vc} = 0.878 ksc						σ_{hc} = 0.468 ksc									
1	1.237	0.029	-0.145	0.037	0.050	0.023	-0.147	0.037	1.238	0.029	1.385	0.047	1.092	0.047	2.08	0.97
2	1.329	0.024	0.048	0.026	0.055	0.018	0.046	0.026	1.331	0.024	1.285	0.035	1.377	0.035	2.45	0.79
3	1.314	0.034	0.137	0.029	0.052	0.022	0.135	0.029	1.316	0.034	1.182	0.045	1.451	0.045	2.52	1.08
4	1.222	0.058	0.118	0.061	0.056	0.042	0.115	0.061	1.225	0.058	1.110	0.084	1.340	0.084	2.90	2.17
5	0.956	0.080	-0.212	0.019	0.048	0.041	-0.214	0.019	0.958	0.080	1.173	0.082	0.744	0.082	2.36	2.01

CONSOLIDATION: DSC33 (CORRECTED)

AREA	Ex	Ex(SD)	Ey	Ey(SD)	Exy	Exy(SD)	E3	E3(SD)	E1	E1(SD)	GAMMA	G(SD)	EV	EV(SD)	PS.	PS(SD)
	σ_{vc} = 0.250 ksc						σ_{hc} = 0.247 ksc									
1	0.116	0.011	-0.003	0.008	-0.001	0.007	-0.003	0.008	0.116	0.011	0.119	0.014	0.114	0.014	-0.43	3.34
2	0.155	0.014	0.019	0.009	0.002	0.008	0.019	0.009	0.155	0.014	0.135	0 017	0.174	0.017	0.94	3.52
3	0.170	0.021	0.030	0.017	0.008	0.014	0.029	0.017	0.170	0.021	0.141	0.027	0.199	0.027	3.26	5.58
4	0.230	0.054	0.074	0.035	-0.029	0.032	0.069	0.036	0.235	0.054	0.166	0.064	0.303	0.064	-10.11	11.17
5	0.493	0.609	0.251	0.193	-0.050	0.321	0.242	0.222	0.503	0.596	0.261	0.643	0.745	0.638	-11.14	70.83
	σ_{vc} = 0.301 ksc						σ_{hc} = 0.261 ksc									
1	0.134	0.013	-0.093	0.011	0.022	0.008	-0.095	0.011	0.136	0.013	0.231	0.017	0.041	0.017	5.38	2.07
2	0.171	0.015	-0.090	0.012	0.018	0.010	-0.092	0.012	0.172	0.015	0.264	0.019	0.081	0.019	3.89	2.11
3	0.198	0.026	-0.098	0.022	0.017	0.017	-0.099	0.022	0.199	0.026	0.297	0.034	0.100	0.034	3.26	3.24
4	0.268	0.045	-0.115	0.053	-0.033	0.035	-0.118	0.053	0.271	0.045	0.389	0.070	0.153	0.070	-4.85	5.12
5	0.235	0.216	-0.231	0.128	0.013	0.126	-0.231	0.128	0.235	0.216	0.466	0 251	0.004	0.251	1.64	15.48
	σ_{vc} = 0.361 ksc						σ_{hc} = 0.271 ksc									
1	0.277	0.014	-0.039	0.010	0.005	0.008	-0.039	0.010	0.277	0.014	0.316	0.017	0.238	0.017	0.82	1.52
2	0.346	0.016	-0.027	0.014	-0.008	0.011	-0.027	0.014	0.347	0.016	0.374	0.021	0.319	0.021	-1.25	1.63
3	0.379	0.028	-0.066	0.024	-0.005	0.019	-0.066	0.024	0.379	0.028	0.445	0.037	0.313	0.037	-0.62	2.39
4	0.359	0.070	-0.057	0.082	-0.083	0.054	-0.073	0.082	0.375	0.071	0.449	0.108	0.302	0.108	-10.89	6.88
5	0.744	0.581	-0.117	0.120	-0.167	0.299	-0.148	0.159	0.775	0.570	0.923	0.598	0.626	0.593	-10.57	18.66
	σ_{vc} = 0.429 ksc						σ_{hc} = 0.290 ksc									
1	0.435	0.016	0.019	0.011	0.013	0.010	0.019	0.011	0.436	0.016	0.417	0.019	0.454	0.019	1.76	1.31
2	0.520	0.018	0.042	0.014	-0.003	0.012	0.042	0.014	0.520	0.018	0.478	0.023	0.563	0.023	-0.35	1.38
3	0.543	0.036	0.044	0.027	-0.013	0.023	0.043	0.027	0.543	0.036	0.500	0.045	0.586	0.045	-1.44	2.58
4	0.622	0.092	0.101	0.074	0.071	0.059	0.092	0.075	0.631	0.091	0.539	0.118	0.723	0.118	7.59	6.28
5	0.364	0.507	-0.029	0.193	0.109	0.273	-0.056	0.227	0.392	0.496	0.449	0.540	0.336	0.543	14.46	34.59
	σ_{vc} = 0.521 ksc						σ_{hc} = 0.321 ksc									
1	0.590	0.017	-0.002	0.013	0.025	0.011	-0.003	0.013	0.592	0.017	0.594	0.022	0.589	0.022	2.38	1.04
2	0.701	0.018	-0.008	0.013	0.016	0.011	-0.009	0.013	0.702	0.018	0.710	0.023	0.693	0.023	1.29	0.91
3	0.678	0.029	-0.020	0.018	0.014	0.017	-0.020	0.018	0.678	0.029	0.698	0.034	0.658	0.034	1.11	1.41
4	0.614	0.077	-0.027	0.036	-0.056	0.043	-0.031	0.036	0.619	0.077	0.650	0.085	0.587	0.085	-4.94	3.77
5	0.573	0.546	-0.077	0.129	-0.026	0.283	-0.078	0.130	0.574	0.545	0.652	0.562	0.496	0.561	-2.26	24.88
	σ_{vc} = 0.619 ksc						σ_{hc} = 0.351 ksc									
1	0.769	0.021	0.032	0.012	0.025	0.012	0.032	0.012	0.770	0.021	0.738	0.024	0.802	0.024	1.94	0.93
2	0.874	0.022	0.071	0.015	0.019	0.014	0.070	0.015	0.874	0.022	0.804	0.027	0.945	0.027	1.34	0.97
3	0.853	0.031	0.090	0.029	0.020	0.021	0.089	0.029	0.853	0.031	0.764	0.043	0.942	0.043	1.51	1.60
4	0.880	0.078	0.154	0.059	0.029	0.049	0.153	0.059	0.881	0.078	0.728	0.098	1.034	0.098	2.31	3.86
5	0.679	0.558	0.372	0.420	-0.012	0.350	0.372	0.420	0.679	0.557	0.308	0.698	1.051	0.698	-2.20	65.22
	σ_{vc} = 0.750 ksc						σ_{hc} = 0 401 ksc									
1	1.081	0.026	0.079	0.015	0.011	0.015	0.079	0.015	1.081	0.026	1.002	0.029	1.160	0.029	0.62	0.84
2	1.232	0.026	0.114	0.018	0.008	0.016	0.114	0.018	1.232	0.026	1.119	0.031	1.346	0.031	0.39	0.80
3	1.199	0.042	0.104	0.030	-0.014	0.026	0.104	0.030	1.199	0.042	1.095	0.052	1.303	0.052	-0.72	1.35
4	1.393	0.086	0.085	0.088	-0.062	0.061	0.082	0.088	1.396	0.086	1.314	0.123	1.478	0.123	-2.73	2.67
5	1.565	0.378	-0.388	0.038	0.201	0.192	-0.408	0.054	1.585	0.377	1.994	0.378	1.177	0.380	5.81	5.48

AREA	Ex	Ex(SD)	Ey	Ey(SD)	Exy	Exy(SD)	E3	E3(SD)	E1	E1(SD)	GAMMA	G(SD)	EV	EV(SD)	PS.	PS(SD)
	σ_{vc} = 0.879 ksc						σ_{hc} = 0.468 ksc									
1	1.335	0.027	0.161	0.014	0.058	0.015	0.159	0.014	1.337	0.027	1.179	0.031	1.496	0.031	2.83	0.74
2	1.506	0.027	0.203	0.020	0.065	0.017	0.200	0.020	1.510	0.027	1.309	0.033	1.710	0.033	2.83	0.73
3	1.559	0.044	0.246	0.028	0.030	0.026	0.246	0.028	1.559	0.044	1.314	0.052	1.805	0.052	1.33	1.13
4	1.570	0.104	0.222	0.068	-0.004	0.063	0.222	0.068	1.570	0.104	1.348	0.124	1.792	0.124	-0.17	2.65
5	1.039	0.594	-0.010	0.106	0.240	0.304	-0.062	0.165	1.091	0.583	1.154	0.600	1.029	0.603	12.33	14.97
	σ_{vc} = 1.000 ksc						σ_{hc} = 0.522 ksc									
1	1.687	0.034	0.096	0.016	0.076	0.019	0.092	0.016	1.690	0.034	1.598	0.037	1.783	0.037	2.74	0.67
2	1.910	0.028	0.132	0.021	0.061	0.017	0.129	0.021	1.913	0.028	1.783	0.035	2.042	0.035	1.98	0.56
3	1.904	0.045	0.212	0.031	0.047	0.027	0.210	0.031	1.906	0.045	1.695	0.055	2.116	0.055	1.59	0.92
4	1.927	0.128	0.251	0.077	0.070	0.075	0.248	0.077	1.930	0.128	1.682	0.149	2.178	0.149	2.39	2.56
5	2.608	1.115	-0.018	0.013	-0.124	0.562	-0.024	0.055	2.614	1.113	2.638	1.117	2.590	1.115	-2.70	12.24
	σ_{vc} = 1.136 ksc						σ_{hc} = 0.594 ksc									
1	2.757	0.043	0.080	0.027	0.157	0.025	0.071	0.027	2.766	0.043	2.695	0.050	2.837	0.050	3.34	0.54
2	3.071	0.030	0.210	0.030	0.155	0.021	0.202	0.030	3.080	0.030	2.878	0.042	3.281	0.042	3.09	0.42
3	3.121	0.051	0.329	0.037	0.152	0.031	0.321	0.037	3.130	0.051	2.808	0.062	3.451	0.062	3.12	0.64
4	3.179	0.133	0.510	0.036	0.095	0.070	0.506	0.037	3.183	0.133	2.676	0.138	3.689	0.138	2.03	1.49
5	2.589	0.610	0.390	0.054	0.237	0.309	0.365	0.084	2.614	0.608	2.249	0.610	2.979	0.612	6.07	7.83
	σ_{vc} = 1.300 ksc						σ_{hc} = 0.677 ksc									
1	3.226	0.056	0.075	0.025	0.212	0.030	0.061	0.025	3.240	0.056	3.179	0.061	3.301	0.061	3.82	0.55
2	3.644	0.040	0.155	0.028	0.247	0.025	0.138	0.029	3.661	0.040	3.523	0.049	3.799	0.049	4.04	0.40
3	3.761	0.052	0.218	0.040	0.208	0.033	0.205	0.040	3.774	0.052	3.568	0.065	3.979	0.065	3.35	0.52
4	3.711	0.100	0.276	0.086	0.199	0.066	0.264	0.086	3.723	0.100	3.459	0.132	3.987	0.132	3.31	1.10
5	3.217	0.614	0.523	0.101	-0.007	0.314	0.523	0.101	3.217	0.614	2.694	0.622	3.740	0.622	-0.15	6.67

CONSOLIDATION: DSC34 (CORRECTED)

AREA	Ex	Ex(SD)	Ey	Ey(SD)	Exy	Exy(SD)	E3	E3(SD)	E1	E1(SD)	GAMMA	G(SD)	EV	EV(SD)	PS.	PS(SD)
	σ_{vc} = 0.249 ksc						σ_{hc} = 0.246 ksc									
1	0.062	0.013	-0.017	0.009	0.018	0.008	-0.013	0.009	0.057	0.012	0.070	0.015	0.045	0.015	15.29	6.26
2	0.048	0.017	-0.011	0.013	0.014	0.011	-0.007	0.014	0.044	0.016	0.051	0.021	0.037	0.021	16.73	12.04
3	0.064	0.028	0.030	0.023	0.000	0.018	0.030	0.023	0.064	0.028	0.034	0.036	0.094	0.036	-0.82	30.55
4	0.168	0.054	0.055	0.064	0.021	0.042	0.060	0.063	0.163	0.054	0.103	0.084	0.223	0.084	12.24	23.14
5	0.614	0.108	-0.091	0.103	-0.203	0.075	0.019	0.107	0.503	0.104	0.484	0.149	0.523	0.149	-28.61	8.84
	σ_{vc} = 0.301 ksc						σ_{hc} = 0.266 ksc									
1	0.020	0.019	-0.046	0.012	-0.011	0.011	-0.044	0.012	0.018	0.019	0.063	0.022	-0.025	0.022	-10.67	10.11
2	0.064	0.021	-0.058	0.015	0.023	0.013	-0.053	0.015	0.059	0.020	0.114	0.025	0.007	0.025	11.78	6.41
3	0.090	0.032	-0.043	0.028	0.025	0.021	-0.038	0.028	0.085	0.032	0.124	0.043	0.048	0.043	11.78	9.92
4	0.178	0.083	-0.148	0.076	0.079	0.056	-0.123	0.077	0.153	0.082	0.276	0.112	0.030	0.112	17.55	11.62
5	0.830	0.015	0.382	0.045	0.080	0.024	0.398	0.043	0.814	0.019	0.416	0.047	1.213	0.047	11.35	3.28
	σ_{vc} = 0.360 ksc						σ_{hc} = 0.290 ksc									
1	0.138	0.018	-0.049	0.015	0.010	0.011	-0.049	0.015	0.137	0.018	0.187	0.023	0.088	0.023	3.08	3.51
2	0.162	0.022	-0.035	0.014	0.016	0.013	-0.033	0.014	0.161	0.021	0.194	0.025	0.127	0.025	4.80	3.74
3	0.207	0.034	-0.014	0.021	0.027	0.020	-0.011	0.022	0.203	0.034	0.215	0.040	0.192	0.040	7.33	5.38
4	0.260	0.082	-0.050	0.052	0.061	0.049	-0.036	0.055	0.246	0.080	0.283	0.097	0.210	0.097	12.84	9.82
5	0.715	0.307	-0.296	0.069	0.289	0.155	-0.104	0.194	0.523	0.246	0.628	0.311	0.419	0.314	33.62	14.32
	σ_{vc} = 0.430 ksc						σ_{hc} = 0.315 ksc									
1	0.236	0.019	-0.032	0.016	-0.010	0.013	-0.031	0.016	0.235	0.019	0.267	0.025	0.204	0.025	-2.33	2.69
2	0.269	0.022	-0.013	0.020	0.004	0.015	-0.013	0.020	0.269	0.022	0.282	0.030	0.256	0.030	0.74	3.06
3	0.356	0.032	0.002	0.028	-0.005	0.021	0.002	0.028	0.356	0.032	0.354	0.043	0.359	0.043	-0.88	3.46
4	0.478	0.061	0.037	0.067	-0.062	0.045	0.046	0.066	0.468	0.061	0.423	0.090	0.515	0.090	-8.55	6.13
5	1.001	0.134	0.035	0.131	-0.207	0.094	0.087	0.131	0.947	0.134	0.860	0.188	1.035	0.188	-14.41	6.26
	σ_{vc} = 0.520 ksc						σ_{hc} = 0.347 ksc									
1	0.394	0.019	0.008	0.010	0.018	0.011	0.008	0.011	0.393	0.019	0.385	0.022	0.401	0.022	2.63	1.62
2	0.447	0.024	0.017	0.016	0.024	0.014	0.018	0.016	0.446	0.024	0.428	0.029	0.463	0.029	3.28	1.93
3	0.495	0.039	-0.011	0.032	0.008	0.025	-0.011	0.032	0.495	0.039	0.506	0.051	0.484	0.051	0.86	2.87
4	0.563	0.100	-0.070	0.083	-0.061	0.065	-0.064	0.083	0.557	0.100	0.622	0.130	0.493	0.130	-5.67	5.99
5	1.148	0.284	0.642	0.437	0.046	0.262	0.646	0.434	1.144	0.289	0.498	0.521	1.791	0.521	5.35	30.14
	σ_{vc} = 0.620 ksc						σ_{hc} = 0.383 ksc									
1	0.539	0.024	0.059	0.012	0.015	0.013	0.060	0.012	0.538	0.024	0.479	0.027	0.598	0.027	1.81	1.59
2	0.625	0.027	0.086	0.017	0.017	0.016	0.087	0.018	0.625	0.026	0.539	0.032	0.712	0.032	1.79	1.69
3	0.687	0.043	0.119	0.031	-0.016	0.026	0.119	0.031	0.687	0.042	0.568	0.053	0.807	0.053	-1.65	2.66
4	0.687	0.122	0.094	0.082	0.046	0.074	0.097	0.084	0.683	0.121	0.586	0.147	0.781	0.147	4.55	7.18
5	0.892	0.409	0.016	0.339	0.178	0.265	0.059	0.346	0.850	0.404	0.792	0.531	0.909	0.531	13.39	19.18
	σ_{vc} = 0.750 ksc						σ_{hc} = 0.431 ksc									
1	0.806	0.022	0.052	0.015	0.020	0.013	0.052	0.015	0.806	0.022	0.754	0.027	0.859	0.027	1.53	1.02
2	0.915	0.026	0.064	0.019	0.048	0.016	0.066	0.020	0.912	0.026	0.846	0.032	0.979	0.032	3.27	1.09
3	0.999	0.043	0.087	0.037	0.039	0.028	0.089	0.037	0.997	0.043	0.910	0.057	1.087	0.057	2.48	1.80
4	1.161	0.103	0.154	0.055	0.152	0.058	0.179	0.058	1.136	0.101	0.958	0.117	1.316	0.116	9.23	3.48
5	1.403	0.937	0.125	0.323	0.307	0.491	0.219	0.451	1.308	0.882	1.090	0.986	1.528	0.991	17.13	25.89

AREA	Ex	Ex(SD)	Ey	Ey(SD)	Exy	Exy(SD)	E3	E3(SD)	E1	E1(SD)	GAMMA G(SD)		EV	EV(SD)	PS.	PS(SD)
	σ_{vc} = 0.880 ksc						σ_{hc} = 0.476 ksc									
1	1.088	0.026	0.128	0.015	0.038	0.015	0.130	0.016	1.086	0.025	0.957	0.030	1.216	0.030	2.28	0.89
2	1.190	0.029	0.150	0.023	0.057	0.019	0.154	0.024	1.186	0.029	1.033	0.037	1.340	0.037	3.18	1.04
3	1.309	0.039	0.157	0.045	0.025	0.030	0.158	0.045	1.309	0.039	1.151	0.059	1.466	0.059	1.25	1.48
4	1.405	0.105	0.227	0.068	0.054	0.063	0.229	0.069	1.402	0.104	1.174	0.125	1.632	0.125	2.64	3.05
5	1.540	0.289	0.355	0.069	0.206	0.147	0.394	0.099	1.501	0.280	1.107	0.296	1.895	0.298	10.92	7.62
	σ_{vc} = 1.000 ksc						σ_{hc} = 0.519 ksc									
1	1.442	0.025	0.138	0.018	0.055	0.015	0.140	0.018	1.439	0.025	1.299	0.030	1.579	0.030	2.42	0.67
2	1.570	0.028	0.171	0.021	0.089	0.018	0.176	0.021	1.565	0.028	1.389	0.035	1.740	0.035	3.69	0.72
3	1.698	0.048	0.240	0.035	0.101	0.030	0.247	0.035	1.691	0.048	1.444	0.060	1.937	0.060	4.02	1.18
4	1.826	0.100	0.284	0.048	0.092	0.055	0.289	0.049	1.821	0.099	1.531	0.111	2.109	0.111	3.45	2.07
5	2.427	0.431	0.542	0.297	0.086	0.261	0.546	0.299	2.423	0.430	1.878	0.523	2.969	0.524	2.63	7.96
	σ_{vc} = 1.149 ksc						σ_{hc} = 0.582 ksc									
1	2.024	0.028	0.312	0.028	0.097	0.020	0.317	0.028	2.019	0.028	1.702	0.039	2.336	0.039	3.26	0.66
2	2.246	0.028	0.460	0.024	0.172	0.018	0.477	0.025	2.229	0.027	1.752	0.037	2.706	0.037	5.66	0.60
3	2.400	0.041	0.572	0.036	0.166	0.028	0.587	0.036	2.385	0.041	1.798	0.055	2.972	0.055	5.32	0.88
4	2.636	0.083	0.632	0.051	0.204	0.049	0.654	0.052	2.615	0.082	1.962	0.097	3.268	0.097	6.01	1.42
5	2.847	0.766	0.704	0.298	0.278	0.408	0.743	0.331	2.809	0.753	2.067	0.820	3.551	0.822	7.81	11.30

CONSOLIDATION: DSC35 (CORRECTED)

AREA	Ex	Ex(SD)	Ey	Ey(SD)	Exy	Exy(SD)	E3	E3(SD)	E1	E1(SD)	GAMMA	G(SD)	EV	EV(SD)	PS.	PS(SD)
	σ_{vc} = 0.249 ksc						σ_{hc} = 0.246 ksc									
1	0.062	0.013	-0.017	0.009	0.018	0.008	-0.013	0.009	0.057	0.012	0.070	0.015	0.045	0.015	15.29	6.26
2	0.048	0.017	-0.011	0.013	0.014	0.011	-0.007	0.014	0.044	0.016	0.051	0.021	0.037	0.021	16.73	12.04
3	0.064	0.028	0.030	0.023	0.000	0.018	0.030	0.023	0.064	0.028	0.034	0.036	0.094	0.036	-0.82	30.55
4	0.168	0.054	0.055	0.064	0.021	0.042	0.060	0.063	0.163	0.054	0.103	0.084	0.223	0.084	12.24	23.14
5	0.614	0.108	-0.091	0.103	-0.203	0.075	0.019	0.107	0.503	0.104	0.484	0.149	0.523	0.149	-28.61	8.84
	σ_{vc} = 0.301 ksc						σ_{hc} = 0.266 ksc									
1	0.020	0.010	-0.046	0.012	-0.011	0.011	-0.044	0.012	0.018	0.019	0.063	0.022	-0.025	0.022	-10.67	10.11
2	0.064	0.021	-0.058	0.015	0.023	0.013	-0.053	0.015	0.059	0.020	0.114	0.025	0.007	0.025	11.78	6.41
3	0.090	0.032	-0.043	0.028	0.025	0.021	-0.038	0.028	0.085	0.032	0.124	0.043	0.048	0.043	11.78	9.92
4	0.178	0.083	-0.148	0.076	0.079	0.056	-0.123	0.077	0.153	0.082	0.276	0.112	0.030	0.112	17.55	11.62
5	0.830	0.015	0.382	0.045	0.080	0.024	0.398	0.043	0.814	0.019	0.416	0.047	1.213	0.047	11.35	3.28
	σ_{vc} = 0.360 ksc						σ_{hc} = 0.290 ksc									
1	0.138	0.018	-0.049	0.015	0.010	0.011	-0.049	0.015	0.137	0.018	0.187	0.023	0.088	0.023	3.08	3.51
2	0.162	0.022	-0.035	0.014	0.016	0.013	-0.033	0.014	0.161	0.021	0.194	0.025	0.127	0.025	4.80	3.74
3	0.207	0.034	-0.014	0.021	0.027	0.020	-0.011	0.022	0.203	0.034	0.215	0.040	0.192	0.040	7.33	5.38
4	0.260	0.082	-0.050	0.052	0.061	0.049	-0.036	0.055	0.246	0.080	0.283	0.097	0.210	0.097	12.84	9.82
5	0.715	0.307	-0.296	0.069	0.289	0.155	-0.104	0.194	0.523	0.246	0.628	0.311	0.419	0.314	33.62	14.32
	σ_{vc} = 0.430 ksc						σ_{hc} = 0.315 ksc									
1	0.236	0.019	-0.032	0.016	-0.010	0.013	-0.031	0.016	0.235	0.019	0.267	0.025	0.204	0.025	-2.33	2.69
2	0.269	0.022	-0.013	0.020	0.004	0.015	-0.013	0.020	0.269	0.022	0.282	0.030	0.256	0.030	0.74	3.06
3	0.356	0.032	0.002	0.028	-0.005	0.021	0.002	0.028	0.356	0.032	0.354	0.043	0.359	0.043	-0.88	3.46
4	0.478	0.061	0.037	0.067	-0.062	0.045	0.046	0.066	0.468	0.061	0.423	0.090	0.515	0.090	-8.55	6.13
5	1.001	0.134	0.035	0.131	-0.207	0.094	0.087	0.131	0.947	0.134	0.860	0.188	1.035	0.188	-14.41	6.26
	σ_{vc} = 0.520 ksc						σ_{hc} = 0.347 ksc									
1	0.394	0.019	0.008	0.010	0.018	0.011	0.008	0.011	0.393	0.019	0.385	0.022	0.401	0.022	2.63	1.62
2	0.447	0.024	0.017	0.016	0.024	0.014	0.018	0.016	0.446	0.024	0.428	0.029	0.463	0.029	3.28	1.93
3	0.495	0.039	-0.011	0.032	0.008	0.025	-0.011	0.032	0.495	0.039	0.506	0.051	0.484	0.051	0.86	2.87
4	0.563	0.100	-0.070	0.083	-0.061	0.065	-0.064	0.083	0.557	0.100	0.622	0.130	0.493	0.130	-5.67	5.99
5	1.148	0.284	0.642	0.437	0.046	0.262	0.646	0.434	1.144	0.289	0.498	0.521	1.791	0.521	5.35	30.14
	σ_{vc} = 0.620 ksc						σ_{hc} = 0.383 ksc									
1	0.539	0.024	0.059	0.012	0.015	0.013	0.060	0.012	0.538	0.024	0.479	0.027	0.598	0.027	1.81	1.59
2	0.625	0.027	0.086	0.017	0.017	0.016	0.087	0.018	0.625	0.026	0.539	0.032	0.712	0.032	1.79	1.69
3	0.687	0.043	0.119	0.031	-0.016	0.026	0.119	0.031	0.687	0.042	0.568	0.053	0.807	0.053	-1.65	2.66
4	0.687	0.122	0.094	0.082	0.046	0.074	0.097	0.084	0.683	0.121	0.586	0.147	0.781	0.147	4.55	7.18
5	0.892	0.409	0.016	0.339	0.178	0.265	0.059	0.346	0.850	0.404	0.792	0.531	0.909	0.531	13.39	19.18
	σ_{vc} = 0.750 ksc						σ_{hc} = 0.431 ksc									
1	0.806	0.022	0.052	0.015	0.020	0.013	0.052	0.015	0.806	0.022	0.754	0.027	0.859	0.027	1.53	1.02
2	0.915	0.026	0.064	0.019	0.048	0.016	0.066	0.020	0.912	0.026	0.846	0.032	0.979	0.032	3.27	1.09
3	0.999	0.043	0.087	0.037	0.039	0.028	0.089	0.037	0.997	0.043	0.910	0.057	1.087	0.057	2.48	1.80
4	1.161	0.103	0.154	0.055	0.152	0.058	0.179	0.058	1.136	0.101	0.958	0.117	1.316	0.116	9.23	3.48
5	1.403	0.937	0.125	0.323	0.307	0.491	0.219	0.451	1.308	0.882	1.090	0.986	1.528	0.991	17.13	25.89

AREA	Ex	Ex(SD)	Ey	Ey(SD)	Exy	Exy(SD)	E3	E3(SD)	E1	E1(SD)	GAMMA	G(SD)	EV	EV(SD)	PS.	PS(SD)
	σ_{vc} = 0.880 ksc						σ_{hc} = 0.476 ksc									
1	1.088	0.026	0.128	0.015	0.038	0.015	0.130	0.016	1.086	0.025	0.957	0.030	1.216	0.030	2.28	0.89
2	1.190	0.029	0.150	0.023	0.057	0.019	0.154	0.024	1.186	0.029	1.033	0.037	1.340	0.037	3.18	1.04
3	1.309	0.039	0.157	0.045	0.025	0.030	0.158	0.045	1.309	0.039	1.151	0.059	1.466	0.059	1.25	1.48
4	1.405	0.105	0.227	0.068	0.054	0.063	0.229	0.069	1.402	0.104	1.174	0.125	1.632	0.125	2.64	3.05
5	1.540	0.289	0.355	0.069	0.206	0.147	0.394	0.099	1.501	0.280	1.107	0.296	1.895	0.298	10.92	7.62
	σ_{vc} = 1.000 ksc						σ_{hc} = 0.519 ksc									
1	1.477	0.026	0.137	0.022	0.069	0.017	0.141	0.022	1.473	0.026	1.332	0.034	1.614	0.034	2.98	0.73
2	1.627	0.029	0.251	0.022	0.117	0.018	0.262	0.022	1.617	0.028	1.356	0.036	1.878	0.036	4.98	0.76
3	1.684	0.048	0.337	0.036	0.086	0.030	0.343	0.037	1.679	0.048	1.336	0.060	2.021	0.060	3.70	1.29
4	1.783	0.121	0.275	0.065	0.174	0.069	0.296	0.068	1.762	0.119	1.466	0.138	2.058	0.137	6.86	2.69
5	2.106	0.862	0.018	0.187	0.389	0.436	0.100	0.295	2.024	0.830	1.924	0.877	2.124	0.882	11.92	13.00
	σ_{vc} = 1.149 ksc						σ_{hc} = 0.582 ksc									
1	2.024	0.028	0.312	0.028	0.097	0.020	0.317	0.028	2.019	0.028	1.702	0.039	2.336	0.039	3.26	0.66
2	2.246	0.028	0.460	0.024	0.172	0.018	0.477	0.025	2.229	0.027	1.752	0.037	2.706	0.037	5.66	0.60
3	2.400	0.041	0.572	0.036	0.166	0.028	0.587	0.036	2.385	0.041	1.798	0.055	2.972	0.055	5.32	0.88
4	2.636	0.083	0.632	0.051	0.204	0.049	0.654	0.052	2.615	0.082	1.962	0.097	3.268	0.097	6.01	1.42
5	2.847	0.766	0.704	0.298	0.278	0.408	0.743	0.331	2.809	0.753	2.067	0.820	3.551	0.822	7.81	11.30
	σ_{vc} = 1.299 ksc						σ_{hc} = 0.676 ksc									
1	3.431	0.087	-0.757	0.046	0.132	0.050	-0.753	0.047	3.427	0.087	4.180	0.099	2.675	0.099	1.81	0.68
2	4.135	0.086	-0.862	0.037	0.206	0.047	-0.853	0.038	4.126	0.086	4.980	0.094	3.274	0.094	2.37	0.54
3	4.700	0.098	-1.003	0.050	0.211	0.055	-0.995	0.050	4.692	0.098	5.687	0.110	3.698	0.110	2.13	0.55
4	5.281	0.126	-1.162	0.087	0.174	0.076	-1.157	0.088	5.276	0.125	6.434	0.153	4.120	0.153	1.55	0.68
5	5.410	1.321	-1.524	0.123	0.216	0.656	-1.517	0.180	5.404	1.315	6.922	1.325	3.887	1.327	1.79	5.43

DSC31 $\delta_{inc} = 90^o$

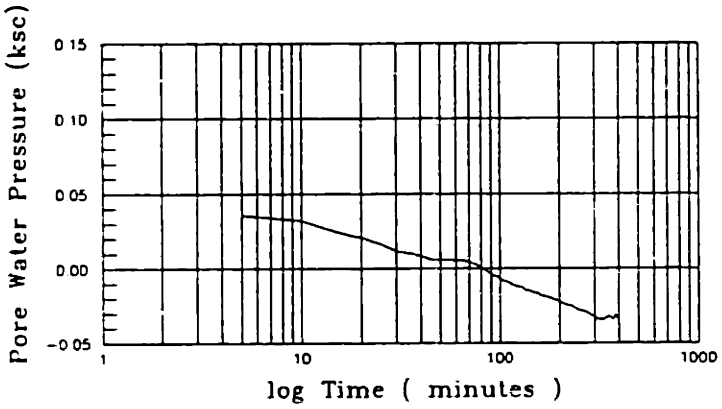

(a) Pore Water Pressure versus Time

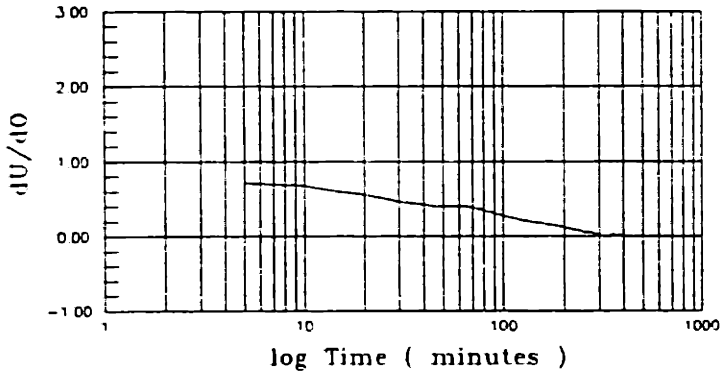

(b) Pore Water Pressure Ratio versus Time

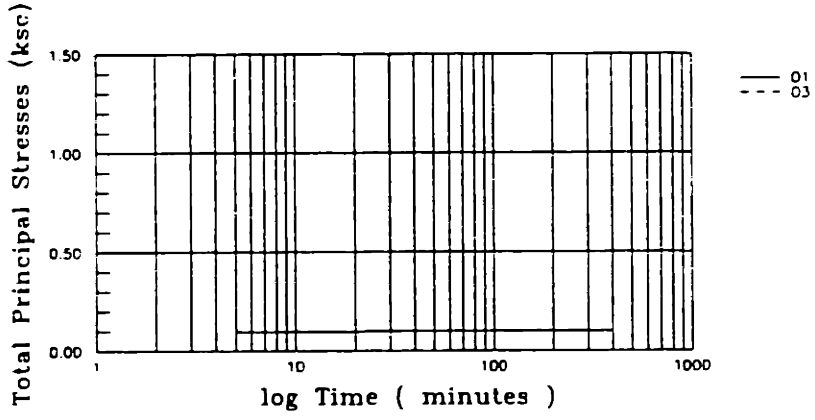

(c) Total Principal Stresses versus Time

Consolidation

Increment Number : 1

At the End of the Increment:

σ_1 = 0.102 ksc (Applied)
σ_3 = 0.100 ksc (Applied)
u = –0.034 ksc (Measured)

ϵ_1 = 0.00±0.00 %
ϵ_3 = 0.00±0.00 %
ϵ_v = 0.00±0.00 %
γ_{max} = 0.00±0.00 %

DSC31 $\delta_{inc} = 90^o$

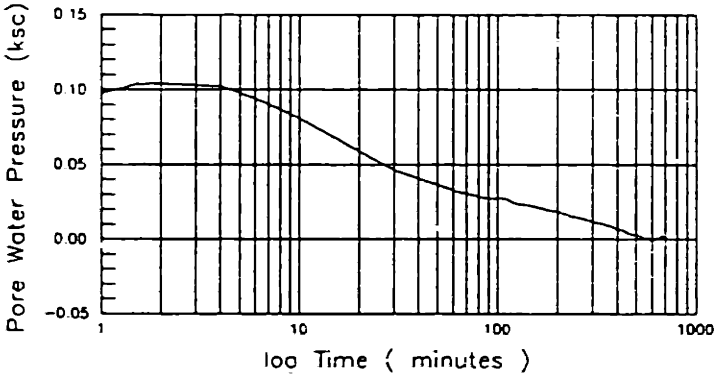

(a) Pore Water Pressure versus Time

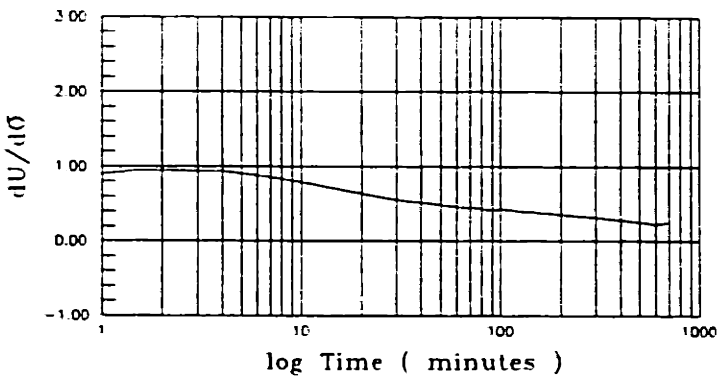

(b) Pore Water Pressure Ratio versus Time

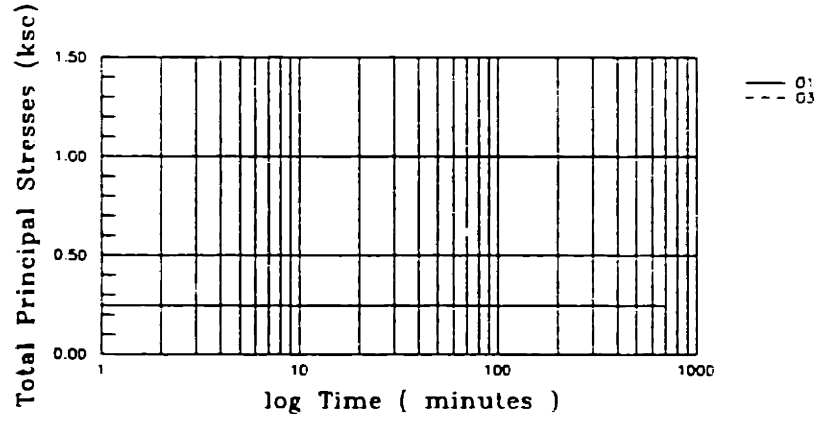

(c) Total Principal Stresses versus Time

Consolidation

Increment Number : 2

At the End of the Increment:

$\sigma_1 = 0.249$ ksc (Applied)
$\sigma_3 = 0.244$ ksc (Applied)
u $= 0.002$ ksc (Measured)

$\epsilon_1 = 0.12 \pm 0.01$ %
$\epsilon_3 = 0.00 \pm 0.01$ %
$\epsilon_v = 0.12 \pm 0.01$ %
$\gamma_{max} = 0.12 \pm 0.01$ %

DSC31 $\delta_{inc} = 90^o$

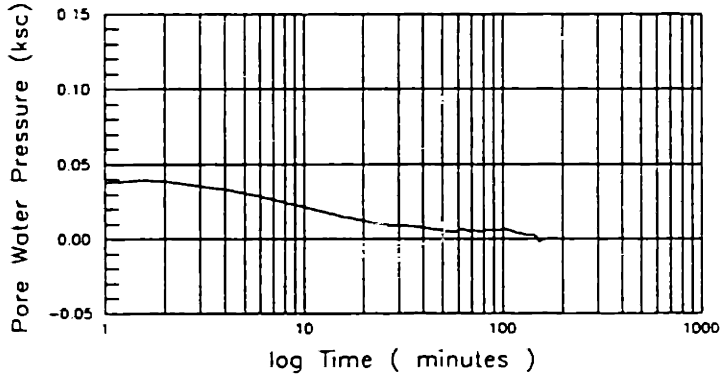

(a) Pore Water Pressure versus Time

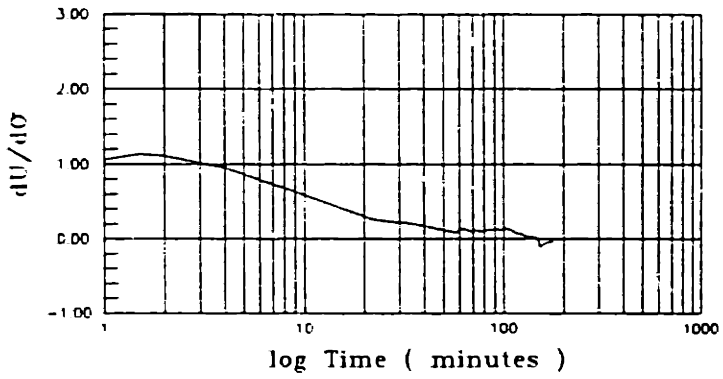

(b) Pore Water Pressure Ratio versus Time

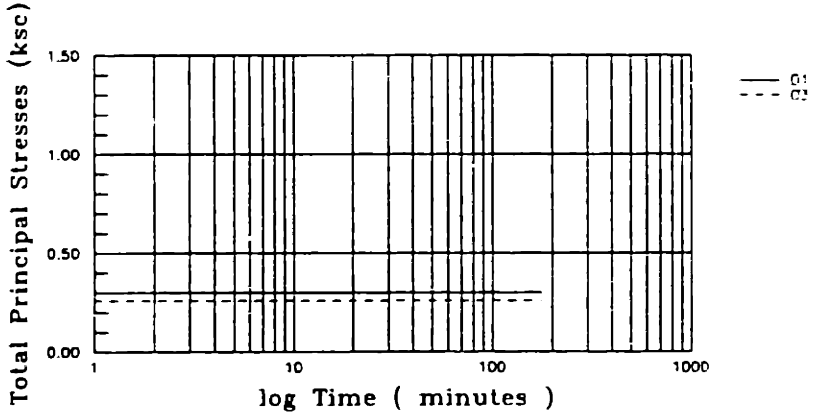

(c) Total Principal Stresses versus Time

Consolidation

Increment Number : 3

At the End of the Increment:

$\sigma_1 = 0.301$ ksc (Applied)
$\sigma_3 = 0.261$ ksc (Applied)
u $= 0.001$ ksc (Measured)

$\epsilon_1 = 0.21 \pm 0.01$ %
$\epsilon_3 = 0.03 \pm 0.01$ %
$\epsilon_v = 0.24 \pm 0.01$ %
$\gamma_{max} = 0.18 \pm 0.01$ %

DSC31 $\delta_{inc} = 90^o$

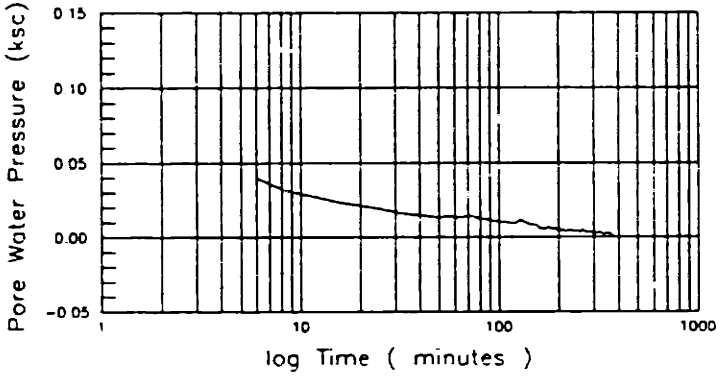

(a) Pore Water Pressure versus Time

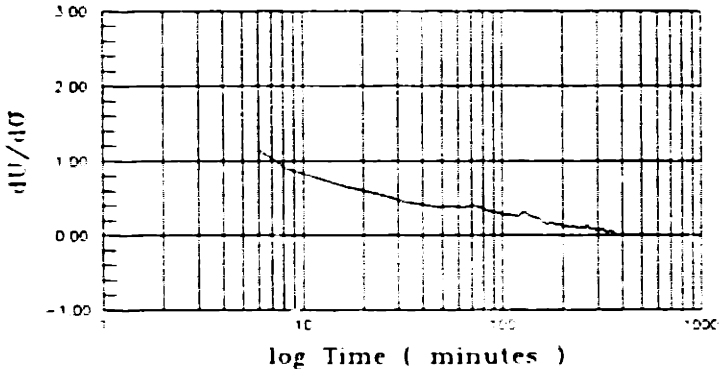

(b) Pore Water Pressure Ratio versus Time

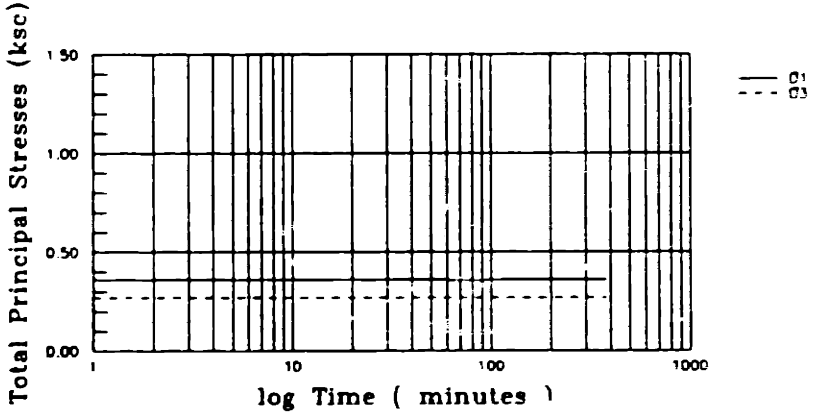

(c) Total Principal Stresses versus Time

Consolidation

Increment Number : 4

At the End of the Increment:

$\sigma_1 = 0.360$ ksc (Applied)
$\sigma_3 = 0.271$ ksc (Applied)
u $= 0.000$ ksc (Measured)

$\epsilon_1 = 0.35 \pm 0.02$ %
$\epsilon_3 = 0.02 \pm 0.01$ %
$\epsilon_v = 0.36 \pm 0.02$ %
$\gamma_{max} = 0.33 \pm 0.02$ %

DSC31 $\delta_{inc} = 90^o$

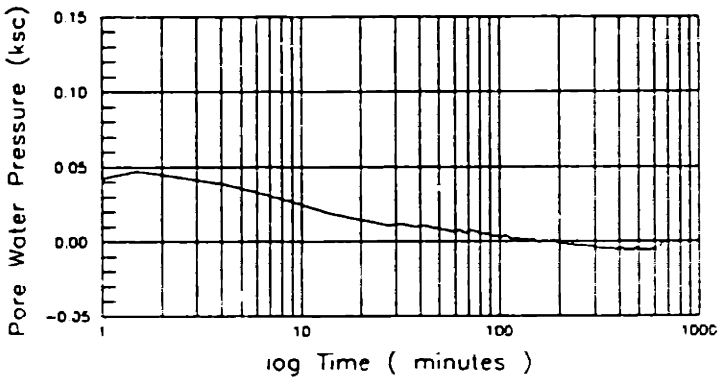

(a) Pore Water Fressure versus Time

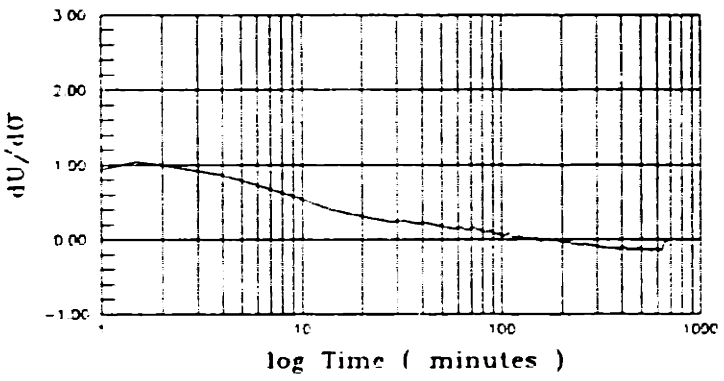

(b) Pore Water Pressure Ratio versus Time

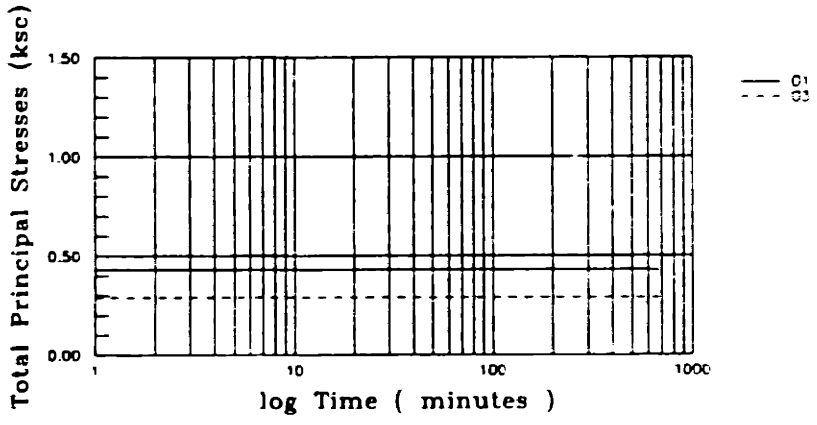

(c) Total Principal Stresses versus Time

Consolidation

Increment Number : 5

At the End of the Increment:

σ_1 = 0.429 ksc (Applied)
σ_3 = 0.290 ksc (Applied)
u =–0.002 ksc (Measured)

ϵ_1 = 0.49±0.02 %
ϵ_3 = 0.00±0.01 %
ϵ_v = 0.49±0.02 %
γ_{max} = 0.49±0.02 %

DSC31 $\delta_{inc} = 90^o$

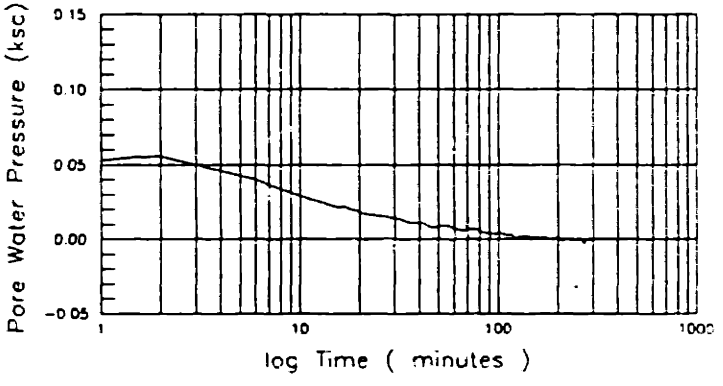

(a) Pore Water Pressure versus Time

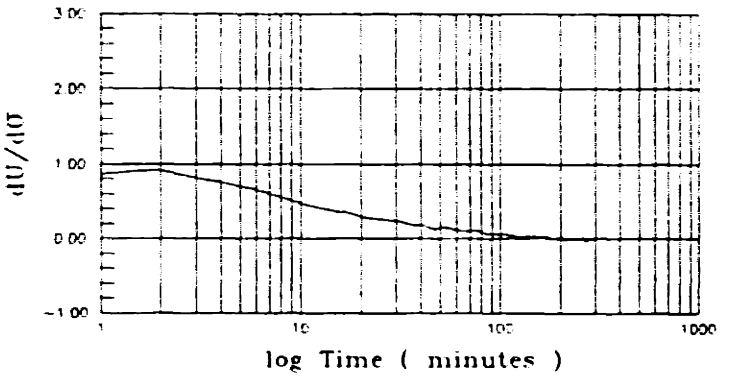

(b) Pore Water Pressure Ratio versus Time

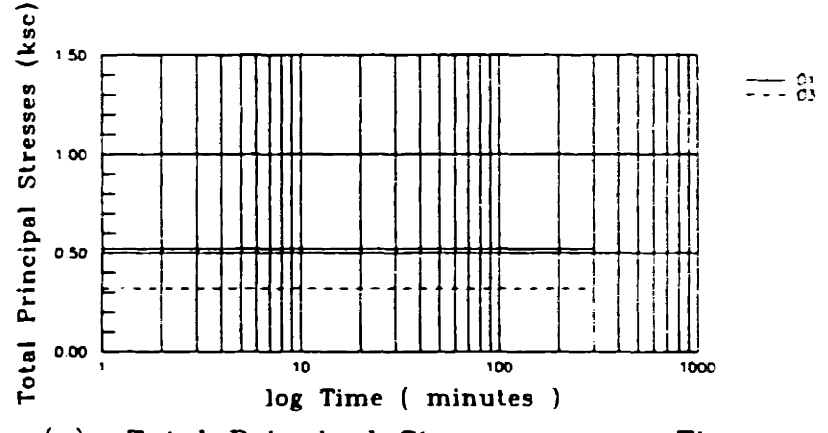

(c) Total Principal Stresses versus Time

Consolidation

Increment Number : 6

At the End of the Increment:

$\sigma_1 = 0.520$ ksc (Applied)
$\sigma_3 = 0.321$ ksc (Applied)
$u = 0.000$ ksc (Measured)

$\epsilon_1 = 0.74 \pm 0.02$ %
$\epsilon_3 = 0.05 \pm 0.01$ %
$\epsilon_v = 0.78 \pm 0.02$ %
$\gamma_{max} = 0.69 \pm 0.02$ %

DSC31 $\delta_{inc} = 90^o$

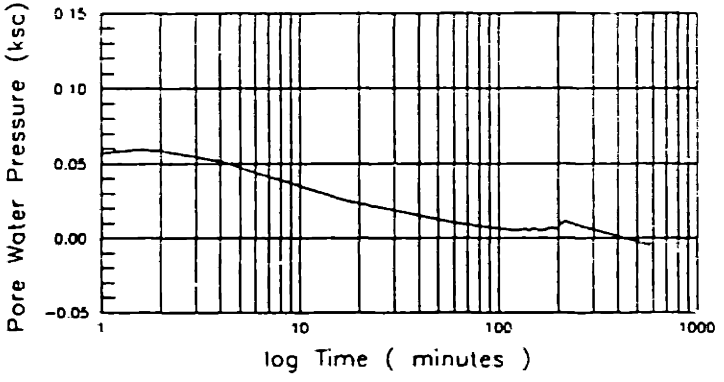

(a) Pore Water Pressure versus Time

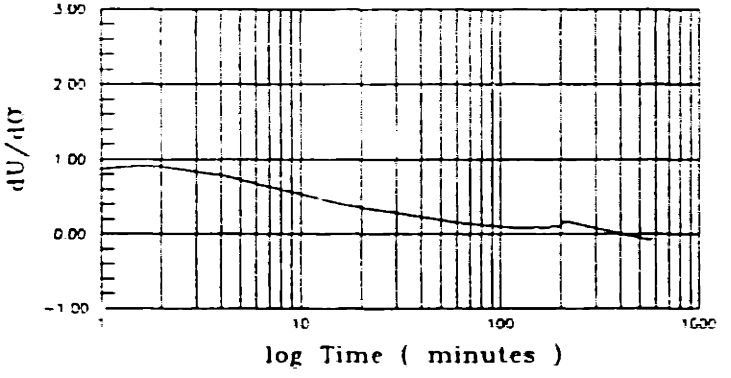

(b) Pore Water Pressure Ratio versus Time

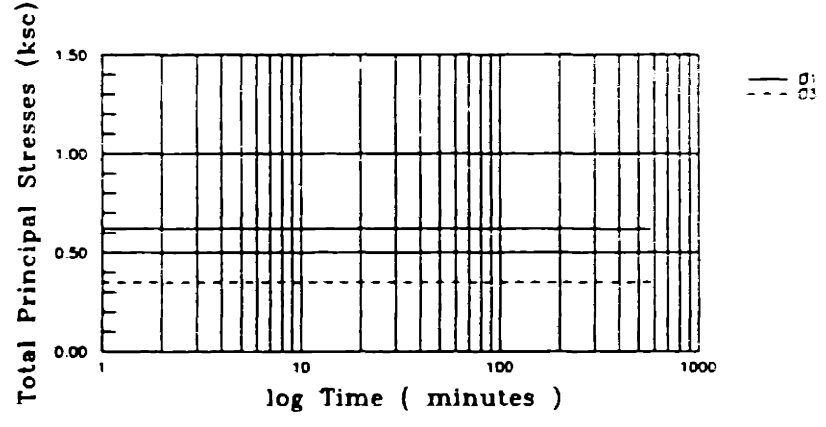

(c) Total Principal Stresses versus Time

Consolidation

Increment Number : 7

At the End of the Increment:

$\sigma_1 = 0.619$ ksc (Applied)
$\sigma_3 = 0.351$ ksc (Applied)
u $= -0.003$ ksc (Measured)

$\epsilon_1 = 0.89 \pm 0.02$ %
$\epsilon_3 = -0.04 \pm 0.02$ %
$\epsilon_v = 0.86 \pm 0.03$ %
$\gamma_{max} = 0.93 \pm 0.03$ %

DSC31 $\delta_{inc} = 90^o$

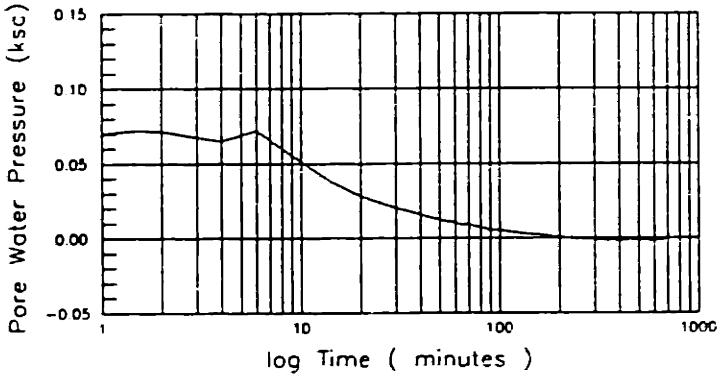

(a) Pore Water Pressure versus Time

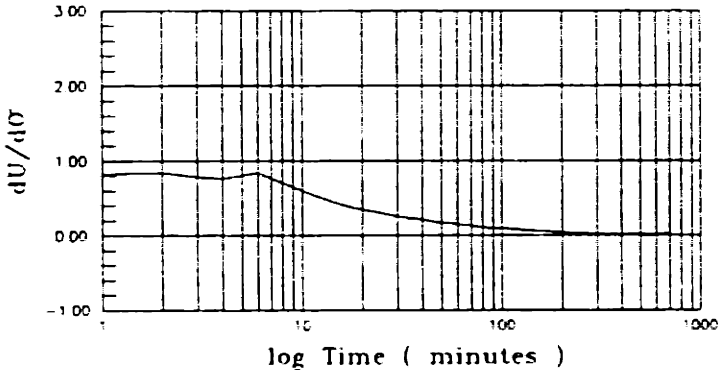

(b) Pore Water Pressure Ratio versus Time

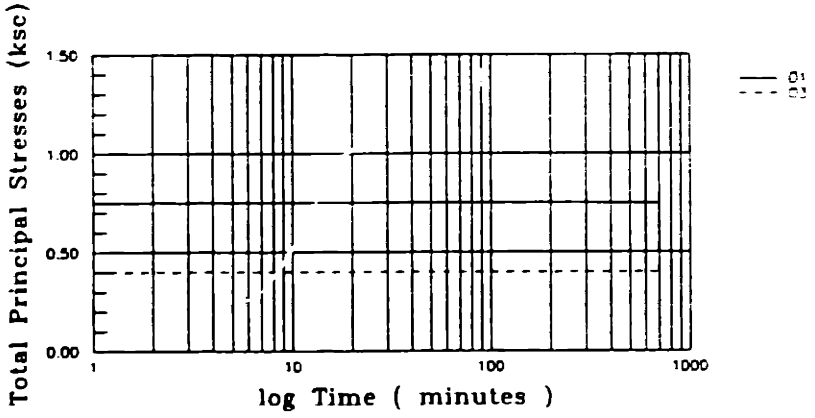

(c) Total Principal Stresses versus Time

Consolidation

Increment Number : 8

At the End of the Increment:

$\sigma_1 = 0.749$ ksc (Applied)
$\sigma_3 = 0.401$ ksc (Applied)
u $= 0.000$ ksc (Measured)

$\epsilon_1 = 1.45 \pm 0.03$ %
$\epsilon_3 = 0.26 \pm 0.02$ %
$\epsilon_v = 1.71 \pm 0.03$ %
$\gamma_{max} = 1.18 \pm 0.03$ %

DSC31 $\delta_{inc} = 90^o$

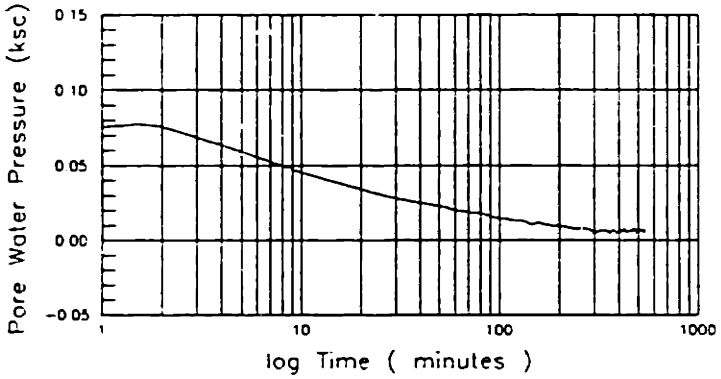

(a) Pore Water Pressure versus Time

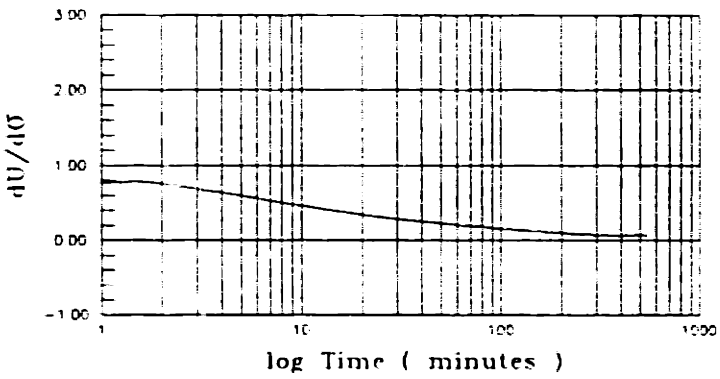

(b) Pore Water Pressure Ratio versus Time

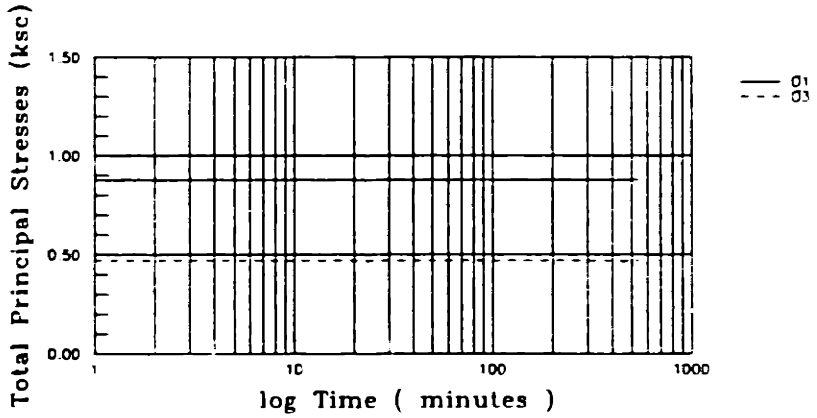

(c) Total Principal Stresses versus Time

Consolidation

Increment Number : 9

At the End of the Increment:

σ_1 = 0.879 ksc (Applied)
σ_3 = 0.469 ksc (Applied)
u = 0.005 ksc (Measured)

ϵ_1 = 1.71±0.03 %
ϵ_3 = 0.27±0.02 %
ϵ_v = 1.98±0.03 %
γ_{max} = 1.44±0.03 %

DSC31 $\delta_{inc} = 90^o$

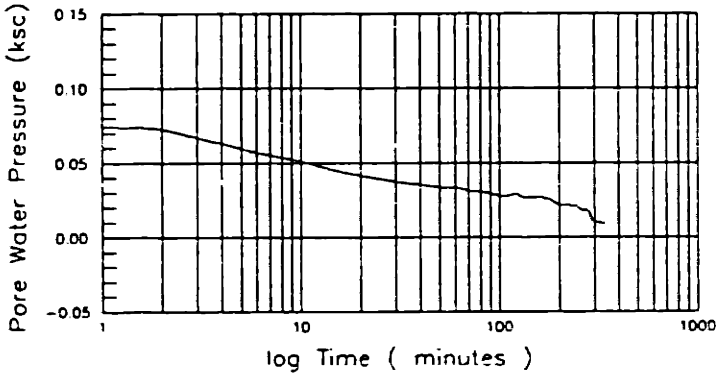

(a) Pore Water Pressure versus Time

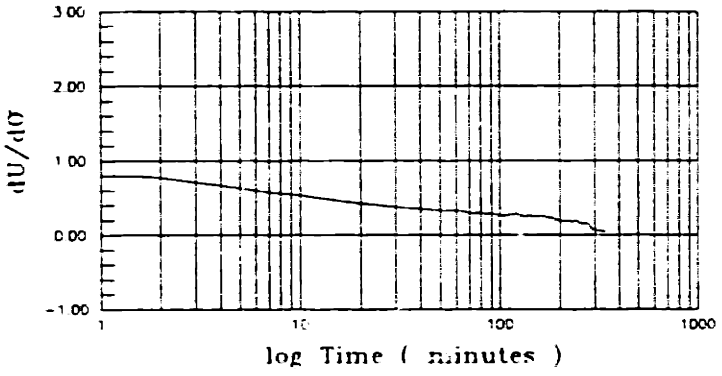

(b) Pore Water Pressure Ratio versus Time

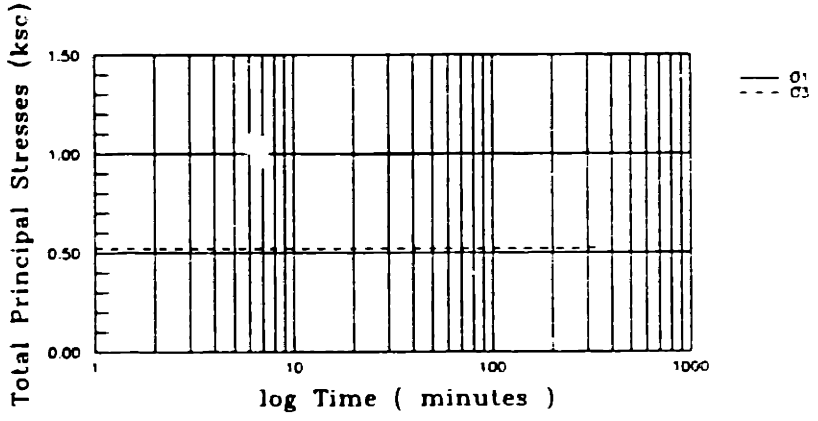

(c) Total Principal Stresses versus Time

Consolidation

Increment Number : 10

At the End of the Increment:

$\sigma_1 = 1.000$ ksc (Applied)
$\sigma_3 = 0.522$ ksc (Applied)
u $= 0.009$ ksc (Measured)

$\epsilon_1 = 2.11 \pm 0.03$ %
$\epsilon_3 = 0.29 \pm 0.02$ %
$\epsilon_v = 2.40 \pm 0.04$ %
$\gamma_{max} = 1.82 \pm 0.04$ %

DSC31 $\delta_{inc} = 90^o$

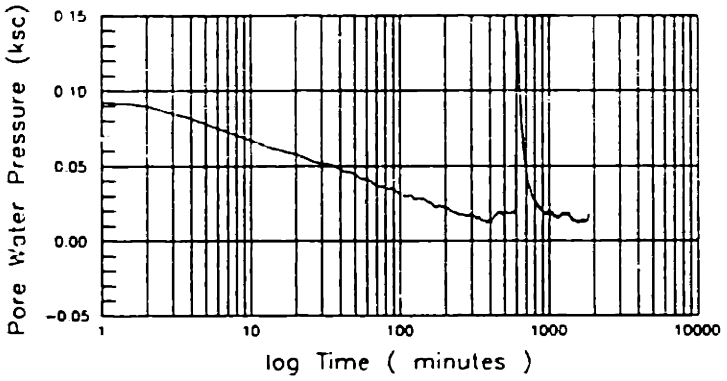

(a) Pore Water Pressure versus Time

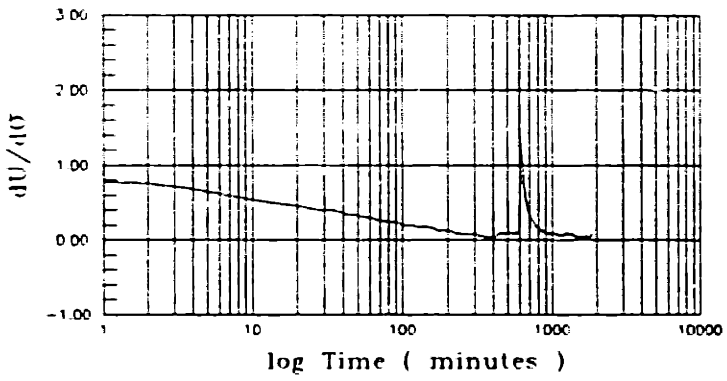

(b) Pore Water Pressure Ratio versus Time

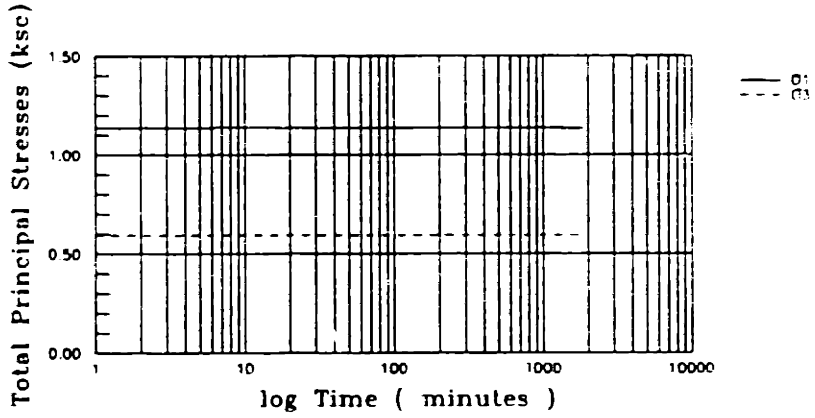

(c) Total Principal Stresses versus Time

Consolidation

Increment Number : 11

At the End of the Increment:

σ_1 = 1.136 ksc (Applied)
σ_3 = 0.595 ksc (Applied)
u = 0.017 ksc (Measured)

ϵ_1 = 3.26±0.04 %
ϵ_3 = 0.00±0.05 %
ϵ_v = 3.26±0.06 %
γ_{max} = 3.25±0.06 %

DSC31 $\delta_{inc} = 90^o$

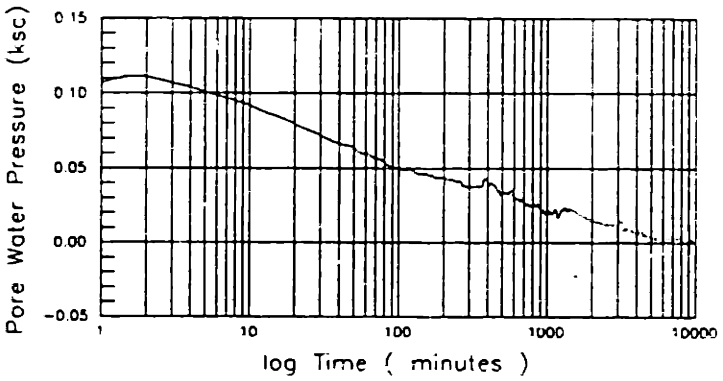

(a) Pore Water Pressure versus Time

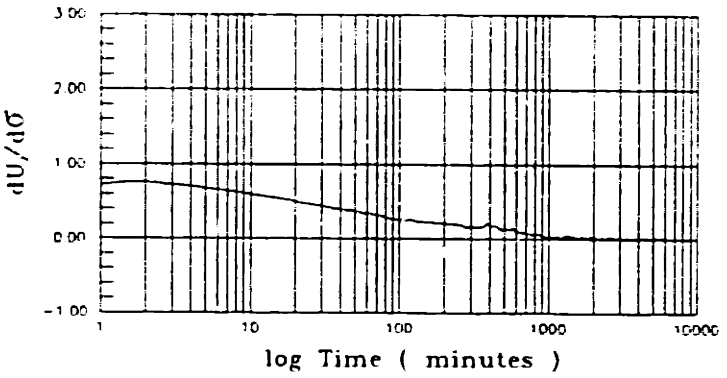

(b) Pore Water Pressure Ratio versus Time

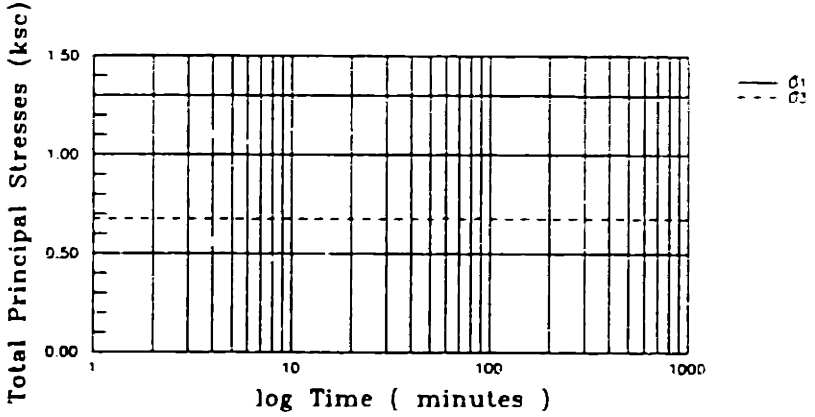

(c) Total Principal Stresses versus Time

Consolidation

Increment Number : 12

At the End of the Increment:

σ_1 = 1.300 ksc (Applied)
σ_3 = 0.678 ksc (Applied)
u = 0.007 ksc (Measured)

ϵ_1 = 3.97±0.05 %
ϵ_3 = 0.30±0.05 %
ϵ_v = 4.26±0.07 %
γ_{max} = 3.67±0.07 %

DSC32 $\delta_{inc} = 45^o$

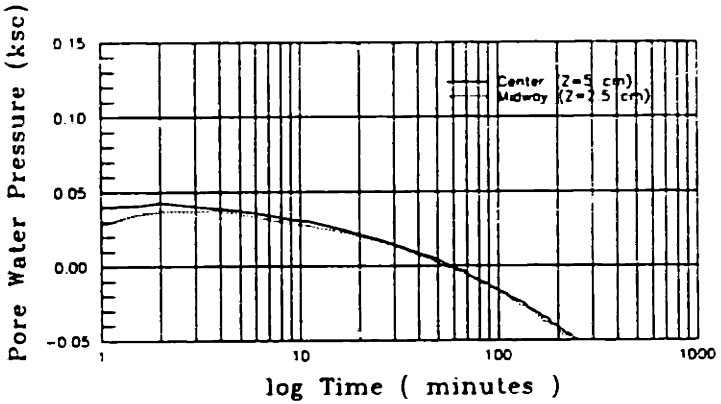

(a) Pore Water P ssure versus Time

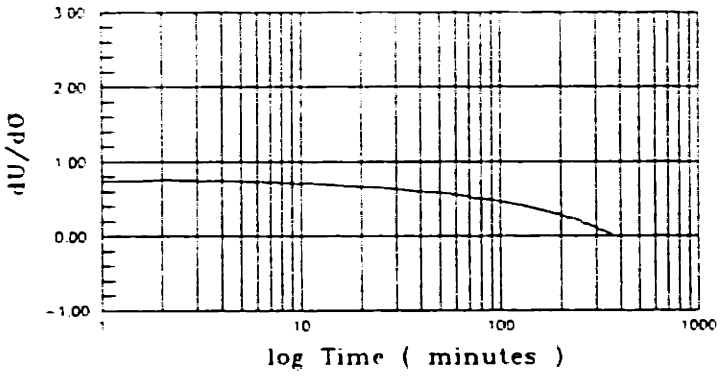

(b) Pore Water Pressure Ratio versus Time

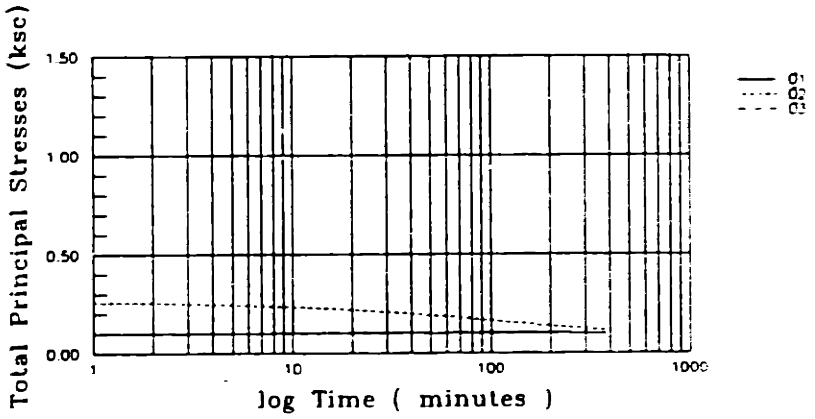

(c) Total Principal Stresses versus Time

Consolidation

Increment Number : 1

At the End of the Increment:

$\sigma_1 = 0.102$ ksc (Applied)
$\sigma_3 = 0.101$ ksc (Applied)
$\sigma_2 = 0.116$ ksc (Measured)
u $= -0.073$ ksc (Measured)

$\epsilon_1 = 0.00 \pm 0.00$ %
$\epsilon_3 = 0.00 \pm 0.00$ %
$\epsilon_v = 0.00 \pm 0.00$ %
$\gamma_{max} = 0.00 \pm 0.00$ %

DSC32 $\delta_{inc} = 45^o$

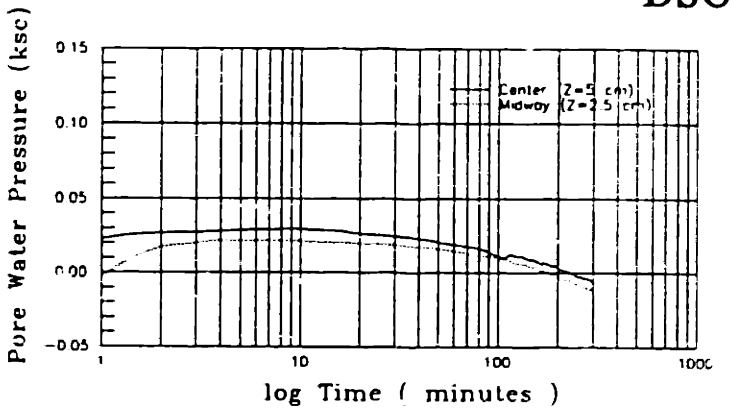

(a) Pore Water Pressure versus Time

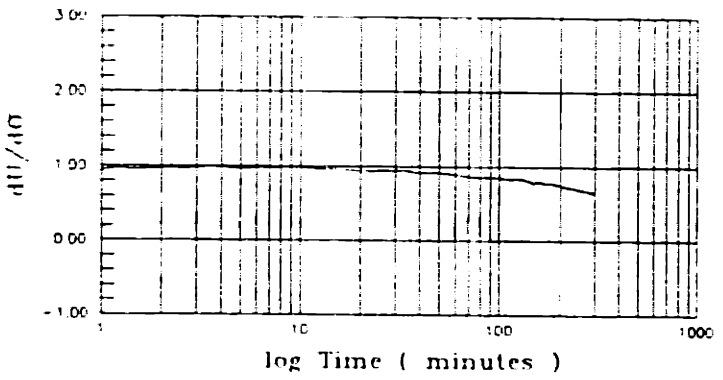

(b) Pore Water Pressure Ratio versus Time

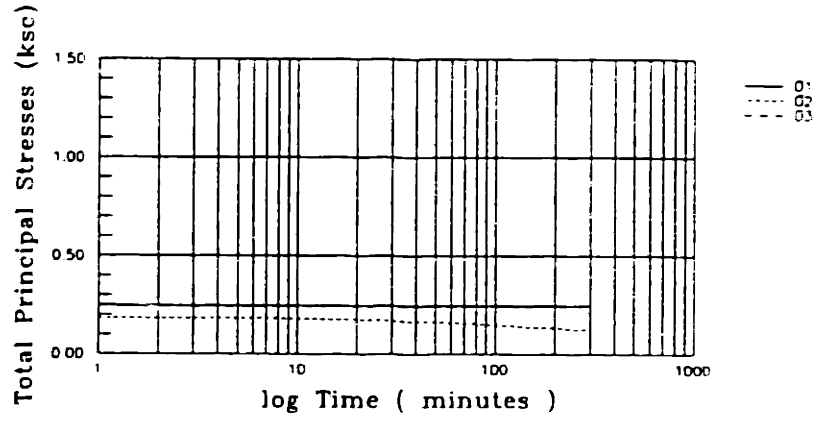

(c) Total Principal Stresses versus Time

Consolidation

Increment Number : 2

At the End of the Increment:

$\sigma_1 = 0.249$ ksc (Applied)
$\sigma_3 = 0.246$ ksc (Applied)
$\sigma_2 = 0.126$ ksc (Measured)
u $= -0.006$ ksc (Measured)

$\epsilon_1 = 0.07 \pm 0.01$ %
$\epsilon_3 = 0.00 \pm 0.01$ %
$\epsilon_v = 0.07 \pm 0.02$ %
$\gamma_{max} = 0.07 \pm 0.02$ %

DSC32 $\delta_{inc} = 45^o$

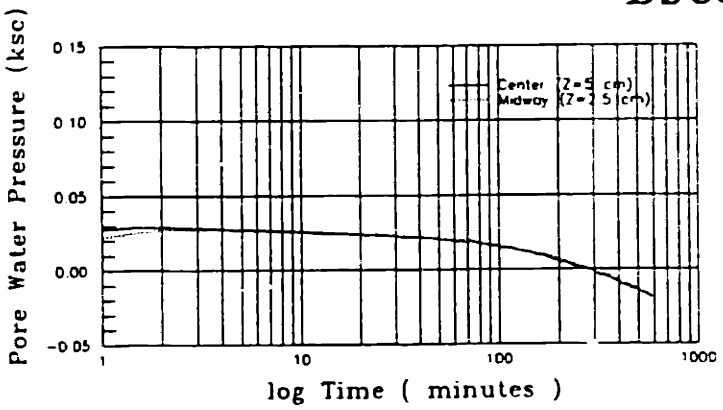

(a) Pore Water Pressure versus Time

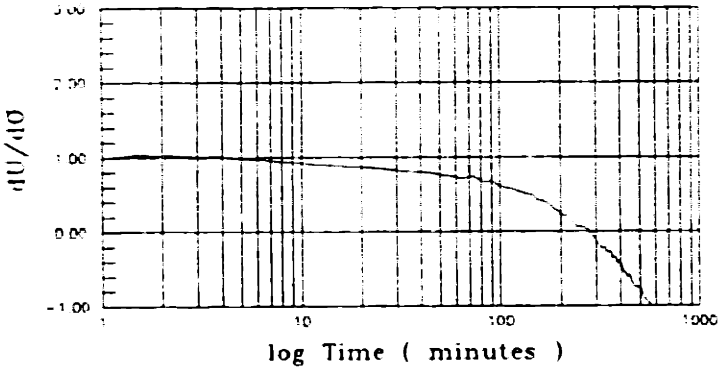

(b) Pore Water Pressure Ratio versus Time

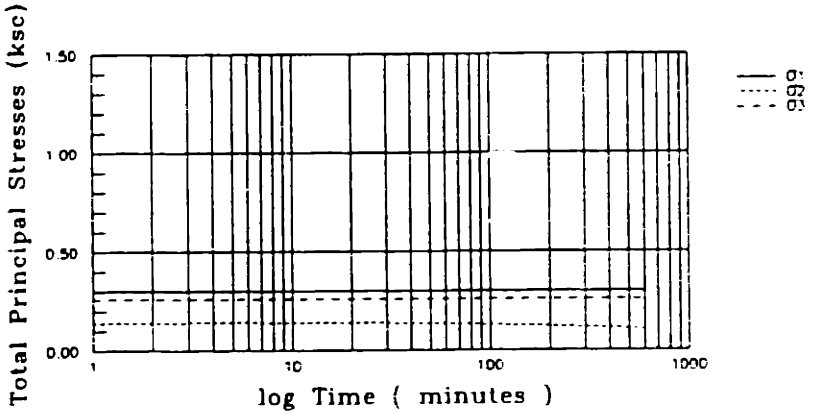

(c) Total Principal Stresses versus Time

Consolidation

Increment Number : 3

At the End of the Increment:

$\sigma_1 = 0.302$ ksc (Applied)
$\sigma_3 = 0.261$ ksc (Applied)
$\sigma_2 = 0.109$ ksc (Measured)
u $= -0.018$ ksc (Measured)

$\epsilon_1 = 0.11 \pm 0.01$ %
$\epsilon_3 = -0.07 \pm 0.01$ %
$\epsilon_v = 0.05 \pm 0.02$ %
$\gamma_{max} = 0.18 \pm 0.02$ %

DSC32 $\delta_{inc} = 45^o$

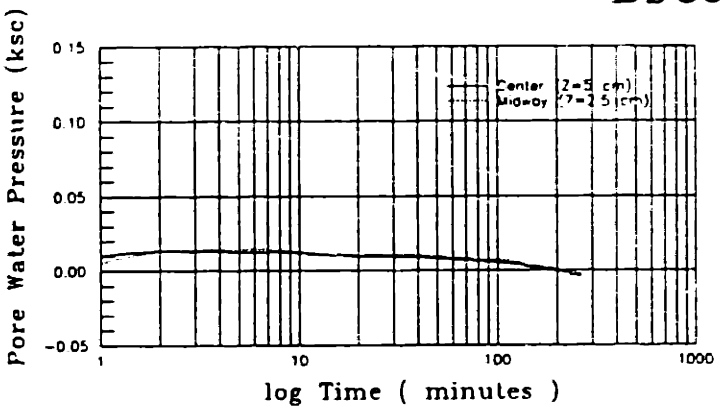

(a) Pore Water Pressure versus Time

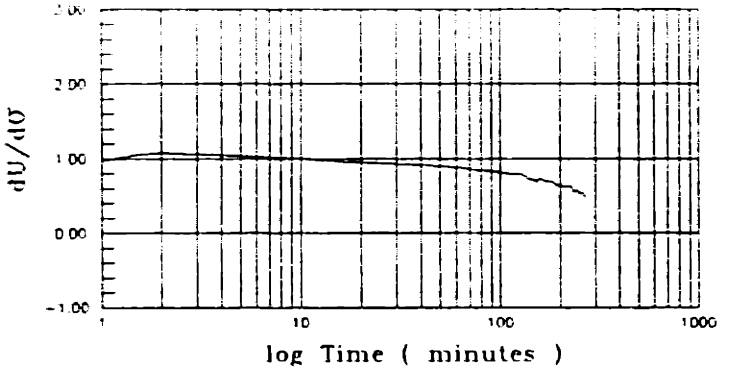

(b) Pore Water Pressure Ratio versus Time

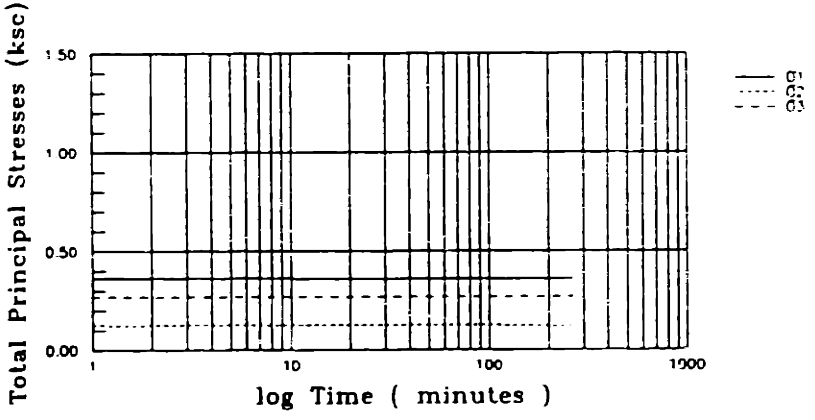

(c) Total Principal Stresses versus Time

Consolidation

Increment Number : 4

At the End of the Increment:

$\sigma_1 = 0.360$ ksc (Applied)
$\sigma_3 = 0.271$ ksc (Applied)
$\sigma_2 = 0.121$ ksc (Measured)
u $= -0.07$ ksc (Measured)

$\epsilon_1 = 0.32 \pm 0.02$ %
$\epsilon_3 = -0.04 \pm 0.02$ %
$\epsilon_v = 0.28 \pm 0.03$ %
$\gamma_{max} = 0.36 \pm 0.03$ %

DSC32 $\delta_{inc} = 45^o$

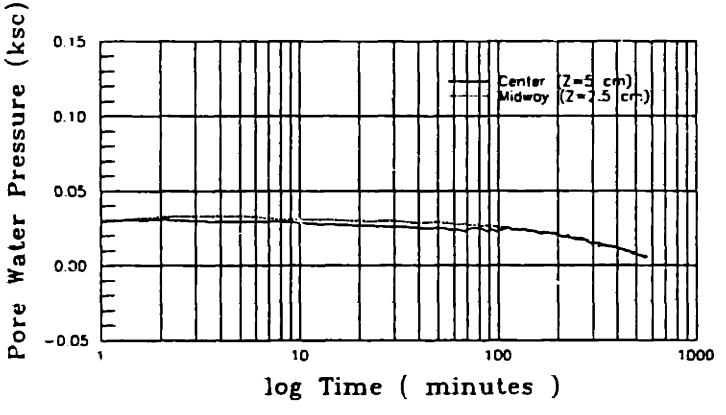

(a) Pore Water Pressure versus Time

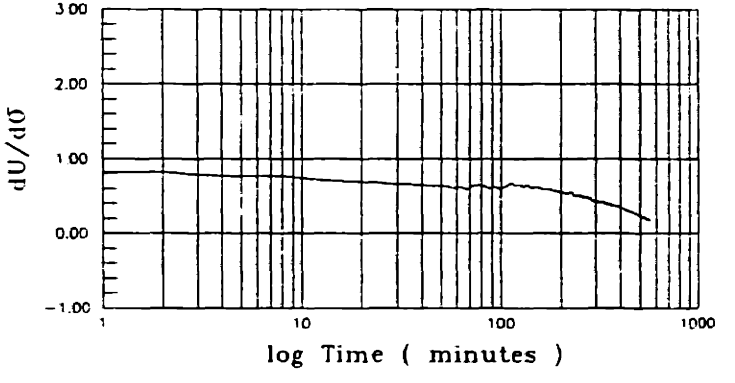

(b) Pore Water Pressure Ratio versus Time

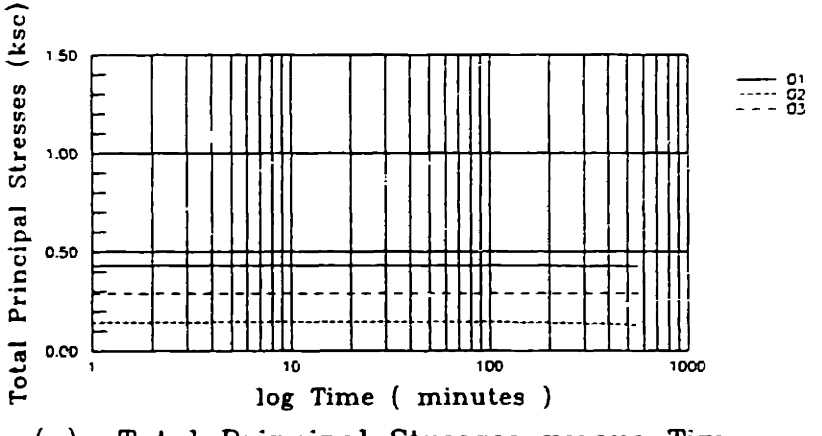

(c) Total Principal Stresses versus Time

Consolidation

Increment Number : 5

At the End of the Increment:

$\sigma_1 = 0.428$ ksc (Applied)
$\sigma_3 = 0.291$ ksc (Applied)
$\sigma_2 = 0.131$ ksc (Measured)
u =–0.004 ksc (Measured)

DSC32 $\delta_{inc} = 45^o$

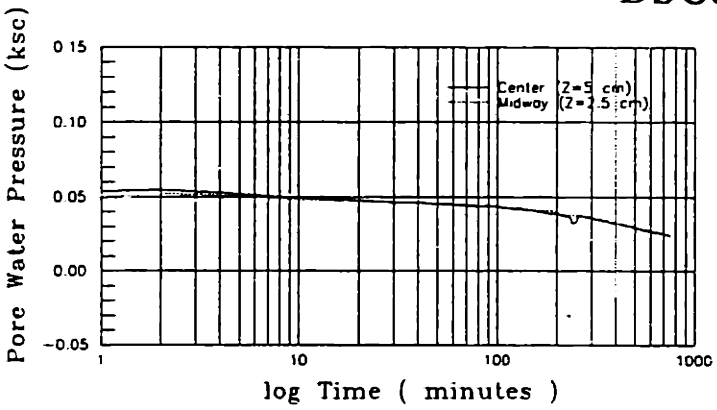

(a) Pore Water Pressure versus Time

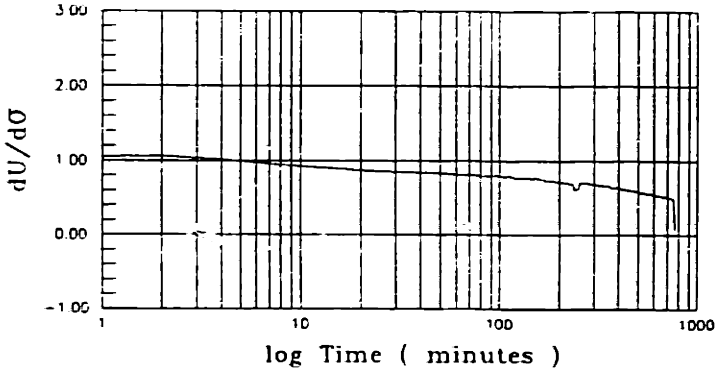

(b) Pore Water Pressure Ratio versus Time

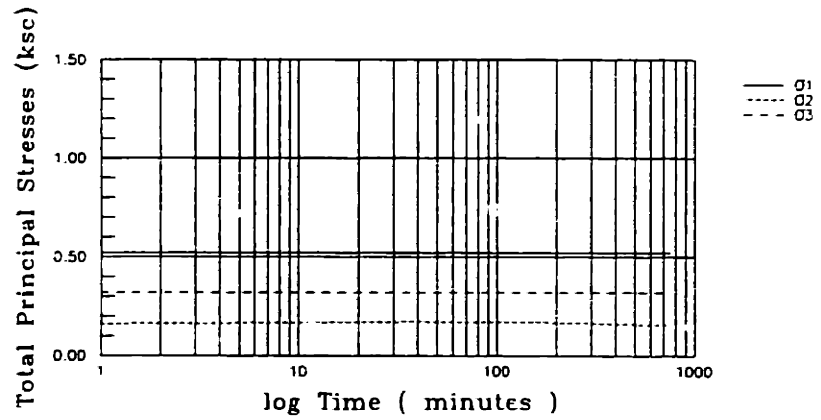

(c) Total Principal Stresses versus Time

Consolidation

Increment Number : 6

At the End of the Increment:

$\sigma_1 = 0.520$ ksc (Applied)
$\sigma_2 = 0.322$ ksc (Applied)
$\sigma_2 = 0.157$ ksc (Measured)
u $= 0.024$ ksc (Measured)

$\epsilon_1 = 0.45 \pm 0.02$ %
$\epsilon_3 = -0.10 \pm 0.02$ %
$\epsilon_v = 0.35 \pm 0.03$ %
$\gamma_{max} = 0.55 \pm 0.03$ %

DSC32 $\delta_{inc} = 45^o$

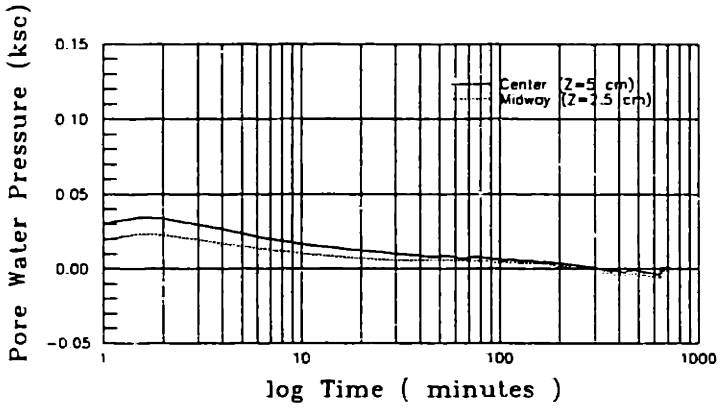

(a) Pore Water Pressure versus Time

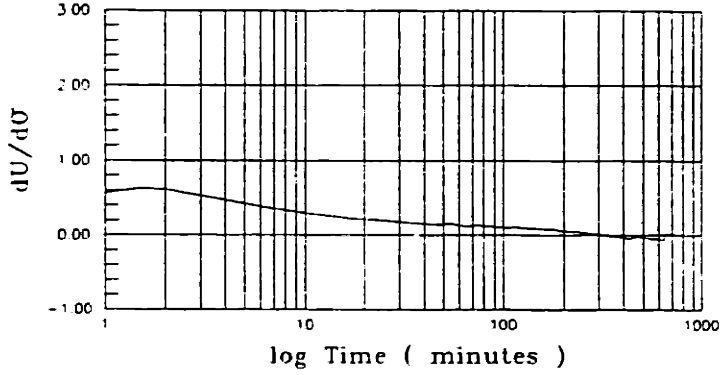

(b) Pore Water Pressure Ratio versus Time

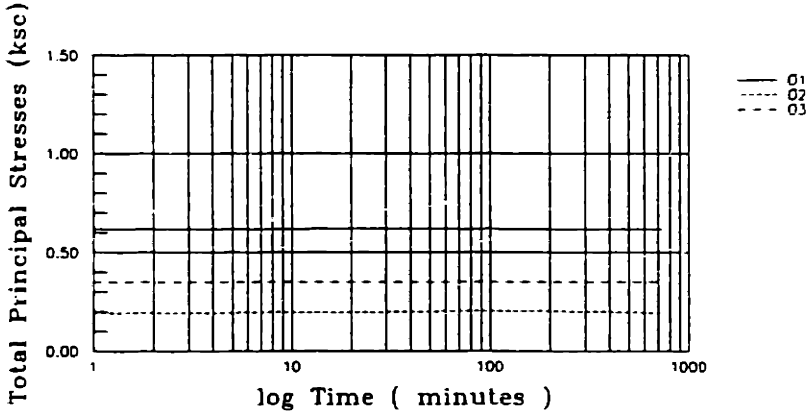

(c) Total Principal Stresses versus Time

Consolidation

Increment Number : 7

At the End of the Increment:

$\sigma_1 = 0.619$ ksc (Applied)
$\sigma_3 = 0.352$ ksc (Applied)
$\sigma_2 = 0.193$ ksc (Measured)
u $= 0.001$ ksc (Measured)

$\epsilon_1 = 0.69 \pm 0.02$ %
$\epsilon_3 = -0.12 \pm 0.03$ %
$\epsilon_v = 0.56 \pm 0.03$ %
$\gamma_{max} = 0.81 \pm 0.03$ %

DSC32 $\delta_{inc} = 45^o$

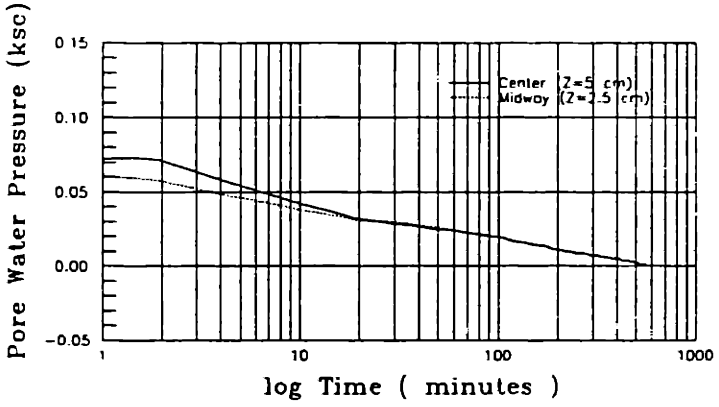

(a) Pore Water Pressure versus Time

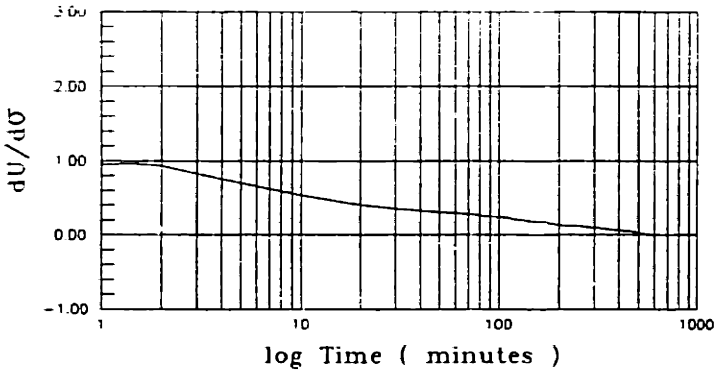

(b) Pore Water Pressure Ratio versus Time

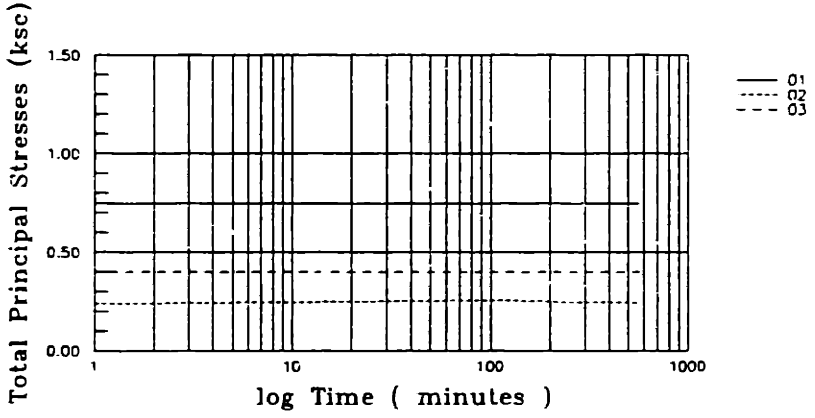

(c) Total Principal Stresses versus Time

Consolidation

Increment Number : 8

At the End of the Increment:

$\sigma_1 = 0.748$ ksc (Applied)
$\sigma_3 = 0.401$ ksc (Applied)
$\sigma_2 = 0.244$ ksc (Measured)
u $= 0.000$ ksc (Measured)

$\epsilon_1 = 0.94 \pm 0.03$ %
$\epsilon_3 = -0.16 \pm 0.04$ %
$\epsilon_v = 0.78 \pm 0.04$ %
$\gamma_{max} = 1.10 \pm 0.04$ %

DSC32 $\delta_{inc} = 45^o$

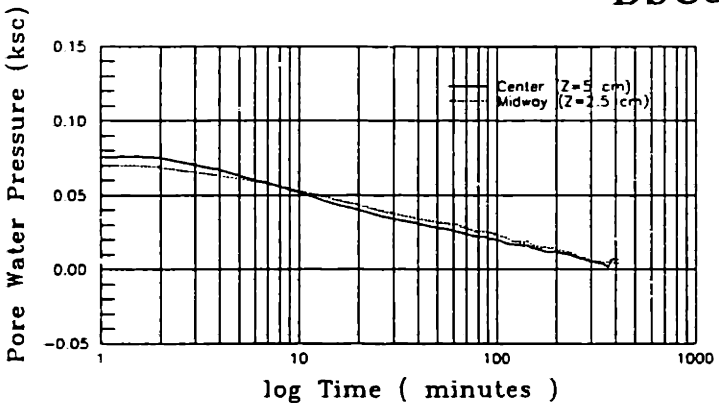

(a) Pore Water Pressure versus Time

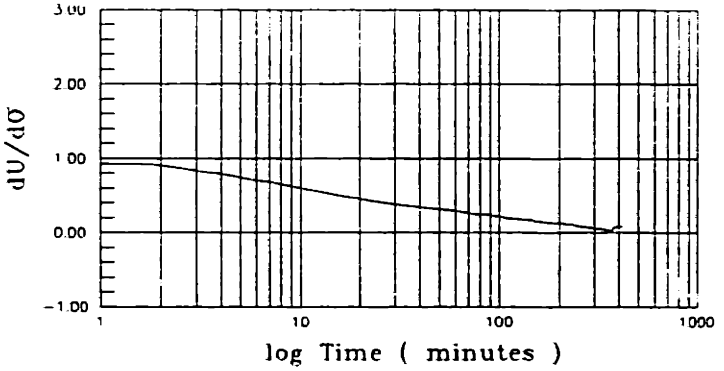

(b) Pore Water Pressure Ratio versus Time

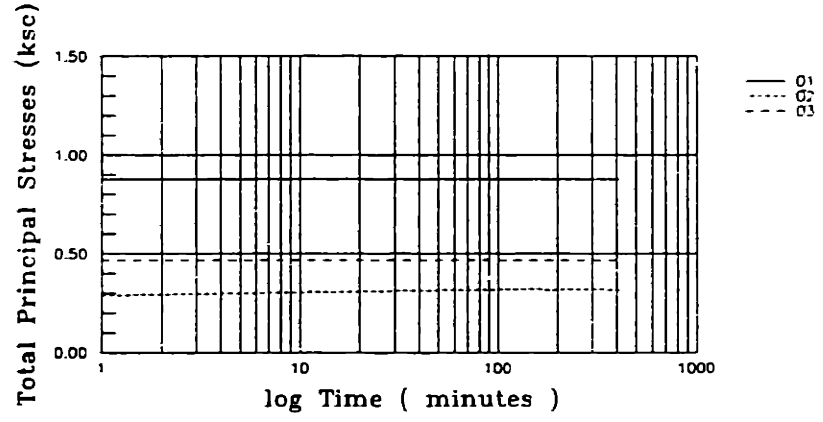

(c) Total Principal Stresses versus Time

Consolidation

Increment Number : 9

At the End of the Increment:

σ_1 = 0.878 ksc (Applied)
σ_3 = 0.468 ksc (Applied)
σ_2 = 0.319 ksc (Measured)
u = 0.007 ksc (Measured)

ϵ_1 = 1.24±0.03 %
ϵ_3 = −0.15±0.04 %
ϵ_v = 1.09±0.05 %
γ_{max} = 1.39±0.05 %

DSC33 $\delta_{inc} = 60^o$

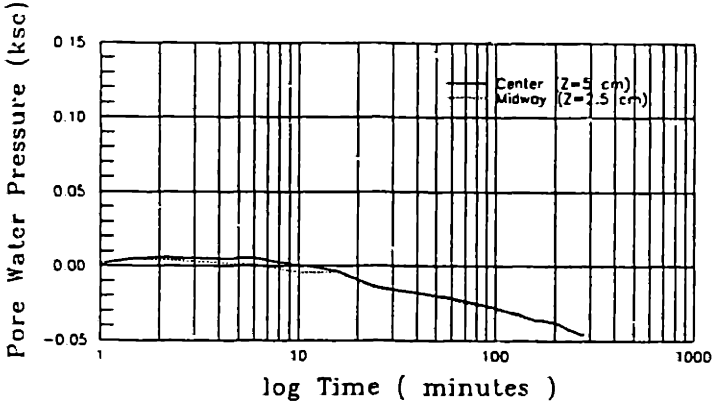

(a) Pore Water Pressure versus Time

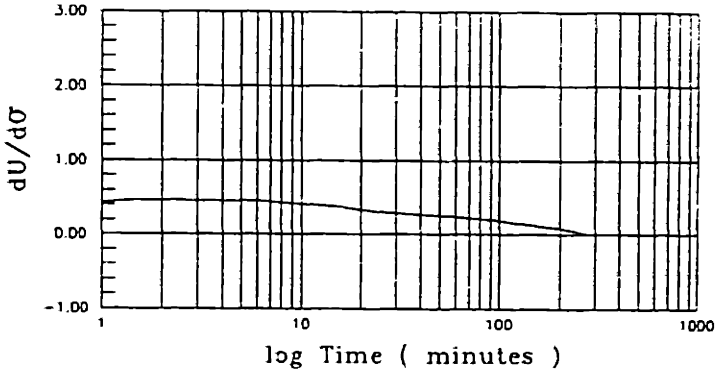

(b) Pore Water Pressure Ratio versus Time

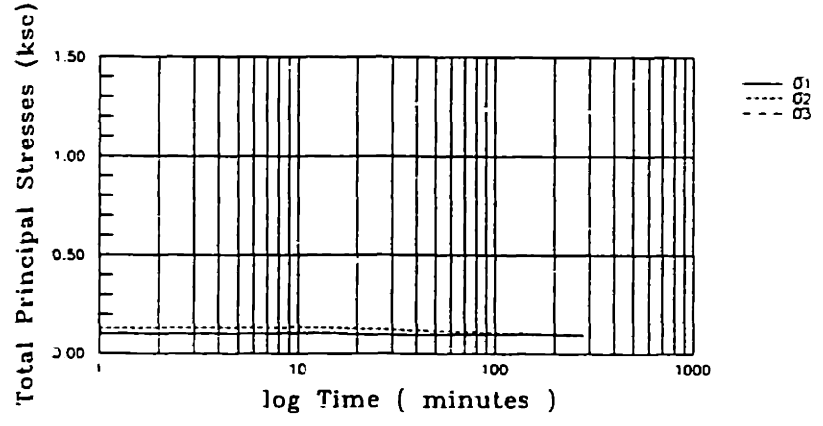

(c) Total Principal Stresses versus Time

Consolidation

Increment Number : 1

At the End of the Increment:

$\sigma_1 = 0.101$ ksc (Applied)
$\sigma_3 = 0.100$ ksc (Applied)
$\sigma_2 = 0.092$ ksc (Measured)
u $= -0.047$ ksc (Measured)

$\epsilon_1 = 0.00 \pm 0.00$ %
$\epsilon_3 = 0.00 \pm 0.00$ %
$\epsilon_v = 0.00 \pm 0.00$ %
$\gamma_{max} = 0.00 \pm 0.00$ %

DSC33 $\delta_{inc} = 60^o$

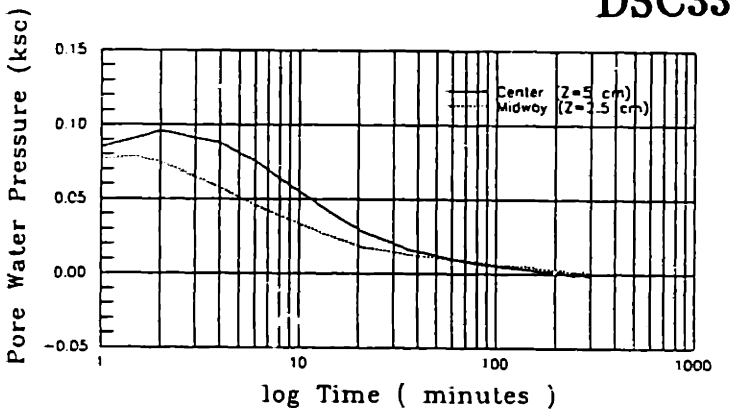

(a) Pore Water Pressure versus Time

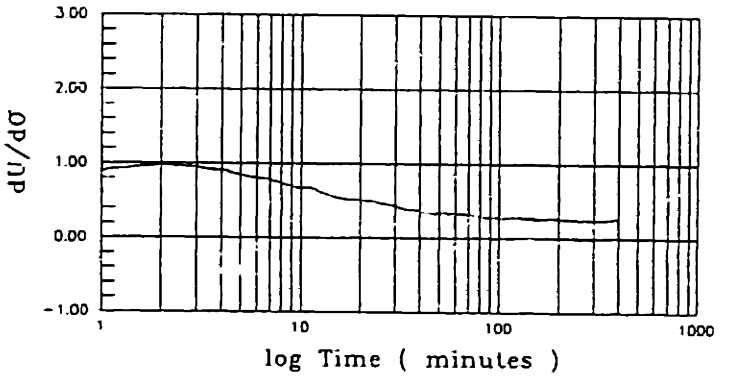

(b) Pore Water Pressure Ratio versus Time

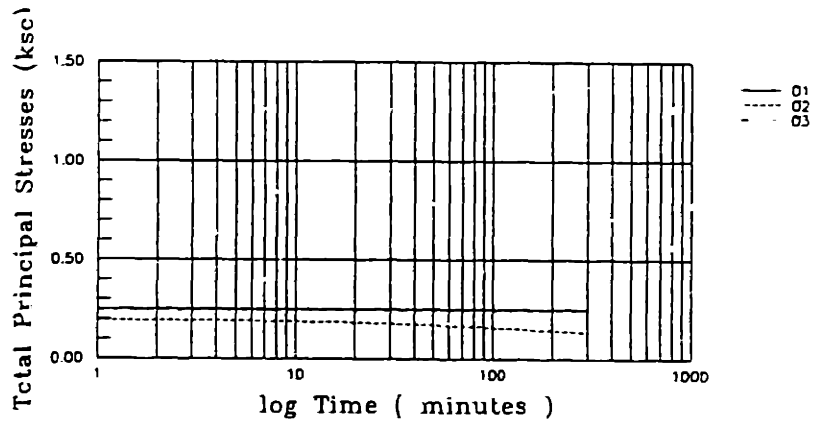

(c) Total Principal Stresses versus Time

Consolidation

Increment Number : 2

At the End of the Increment:

$\sigma_1 = 0.250$ ksc (Applied)
$\sigma_3 = 0.247$ ksc (Applied)
$\sigma_2 = 0.138$ ksc (Measured)
u $= -0.001$ ksc (Measured)

$\epsilon_1 = 0.12 \pm 0.01$ %
$\epsilon_3 = 0.00 \pm 0.01$ %
$\epsilon_v = 0.11 \pm 0.01$ %
$\gamma_{max} = 0.12 \pm 0.01$ %

DSC33 $\delta_{inc} = 60^o$

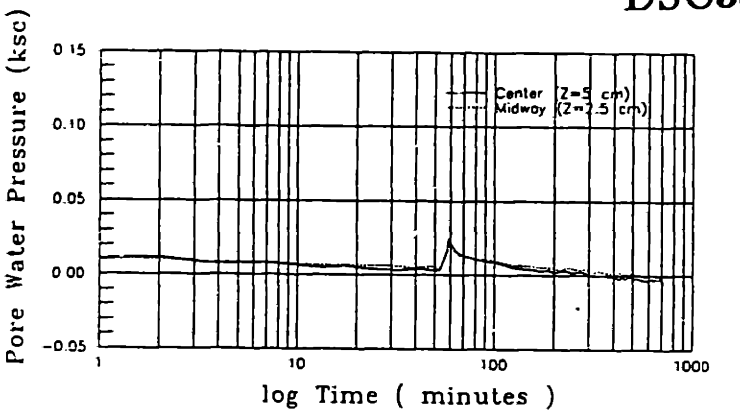

(a) Pore Water Pressure versus Time

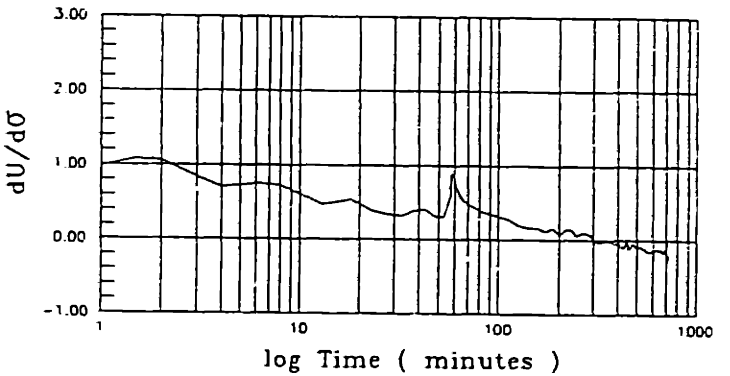

(b) Pore Water Pressure Ratio versus Time

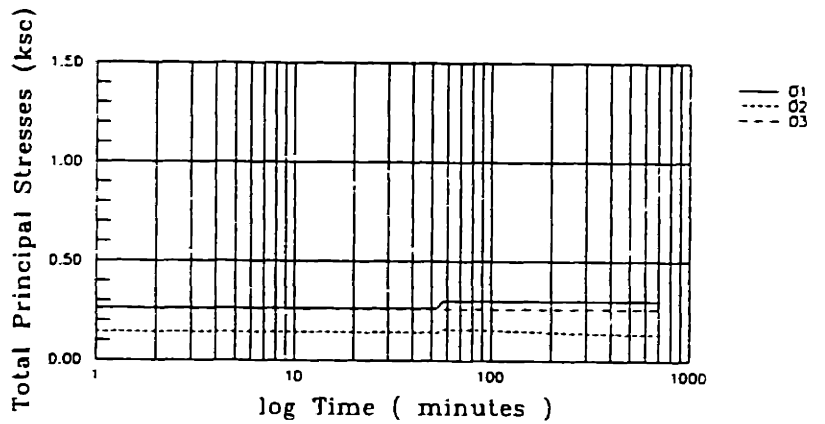

(c) Total Principal Stresses versus Time

Consolidation

Increment Number : 3

At the End of the Increment:

$\sigma_1 = 0.301$ ksc (Applied)
$\sigma_3 = 0.261$ ksc (Applied)
$\sigma_2 = 0.133$ ksc (Measured)
u $= -0.039$ ksc (Measured)

$\epsilon_1 = 0.14 \pm 0.01$ %
$\epsilon_3 = -0.10 \pm 0.01$ %
$\epsilon_v = 0.04 \pm 0.02$ %
$\gamma_{max} = 0.23 \pm 0.02$ %

DSC33 $\delta_{inc} = 60^o$

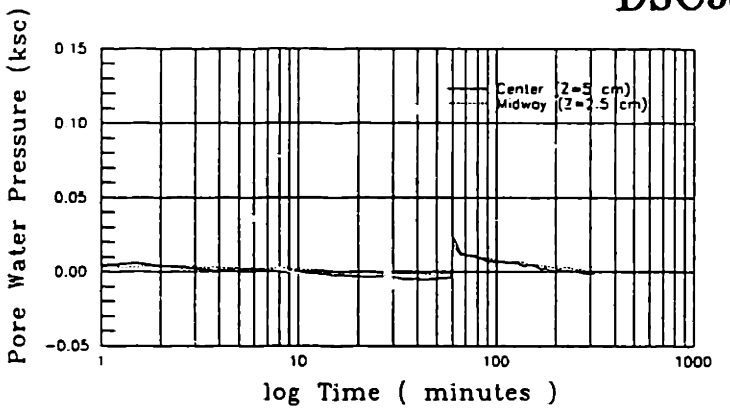

(a) Pore Water Pressure versus Time

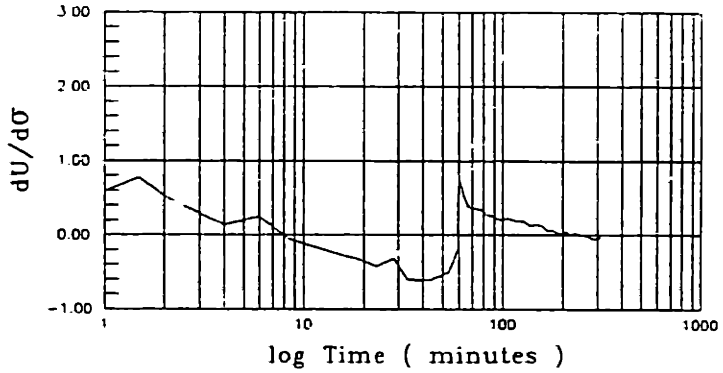

(b) Pore Water Pressure Ratio versus Time

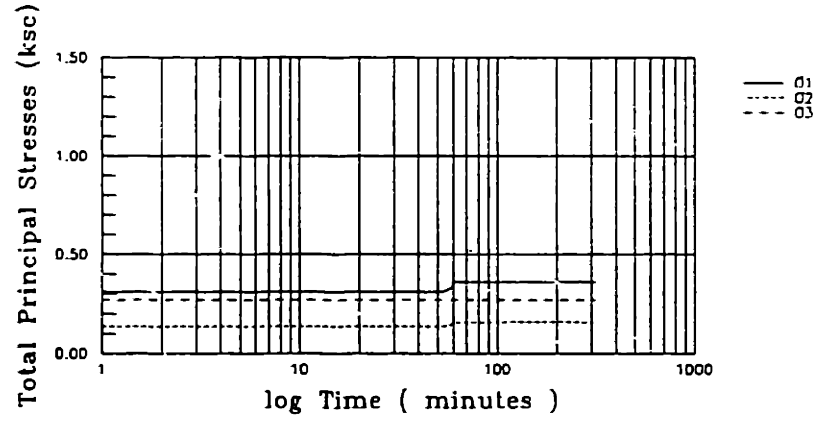

(c) Total Principal Stresses versus Time

Consolidation

Increment Number : 4

At the End of the Increment:

$\sigma_1 = 0.361$ ksc (Applied)
$\sigma_3 = 0.271$ ksc (Applied)
$\sigma_2 = 0.159$ ksc (Measured)
u $= -0.07$ ksc (Measured)

$\epsilon_1 = 0.28 \pm 0.01$ %
$\epsilon_3 = -0.04 \pm 0.01$ %
$\epsilon_v = 0.24 \pm 0.02$ %
$\gamma_{max} = 0.32 \pm 0.02$ %

DSC33 $\delta_{inc} = 60^o$

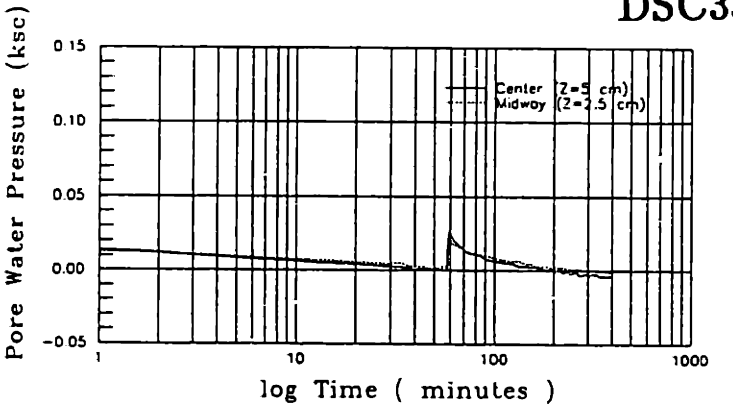

(a) Pore Water Pressure versus Time

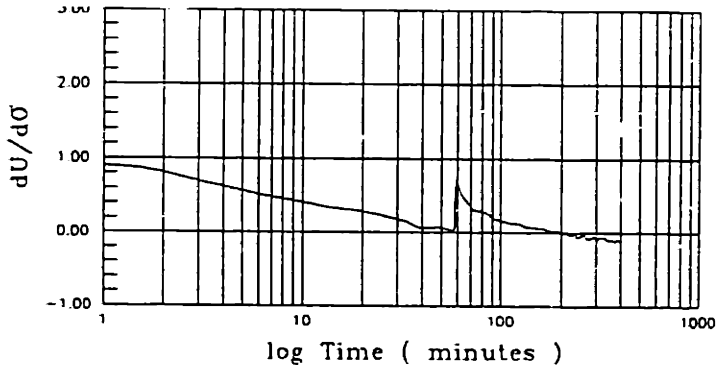

(b) Pore Water Pressure Ratio versus Time

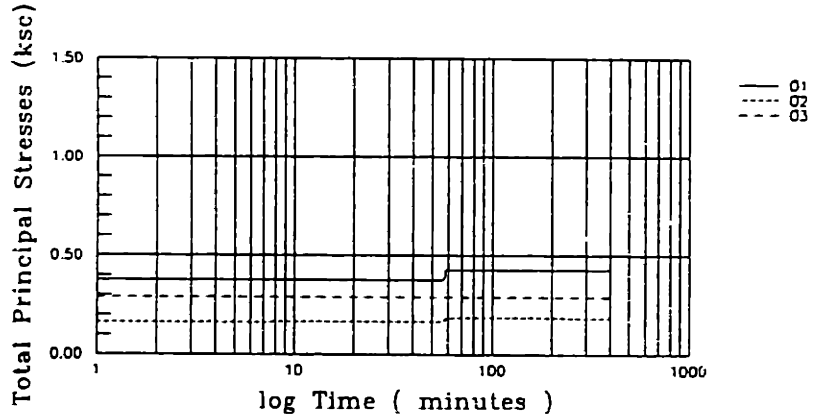

(c) Total Principal Stresses versus Time

Consolidation

Increment Number : 5

At the End of the Increment:

$\sigma_1 = 0.429$ ksc (Applied)
$\sigma_3 = 0.290$ ksc (Applied)
$\sigma_2 = 0.182$ ksc (Measured)
u $= -0.004$ ksc (Measured)

$\epsilon_1 = 0.44 \pm 0.02$ %
$\epsilon_3 = 0.02 \pm 0.01$ %
$\epsilon_v = 0.45 \pm 0.02$ %
$\gamma_{max} = 0.42 \pm 0.02$ %

DSC33 $\delta_{inc} = 60^o$

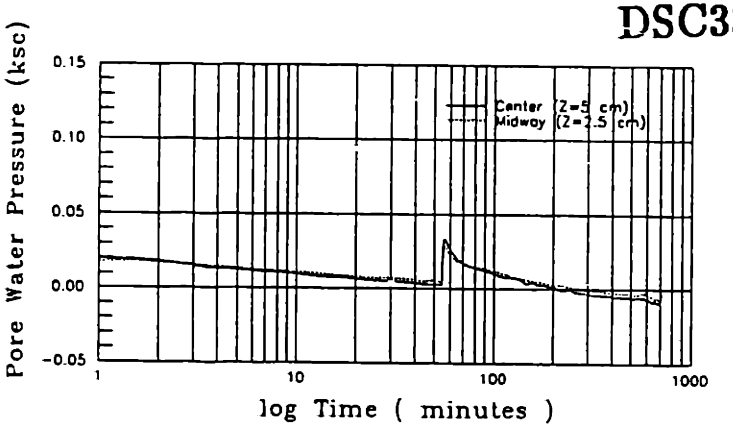

(a) Pore Water Pressure versus Time

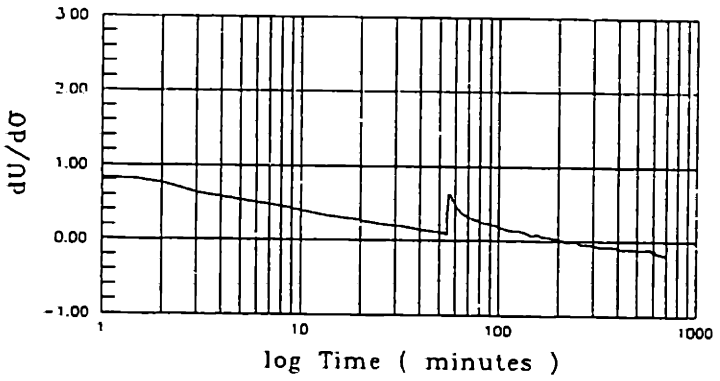

(b) Pore Water Pressure Ratio versus Time

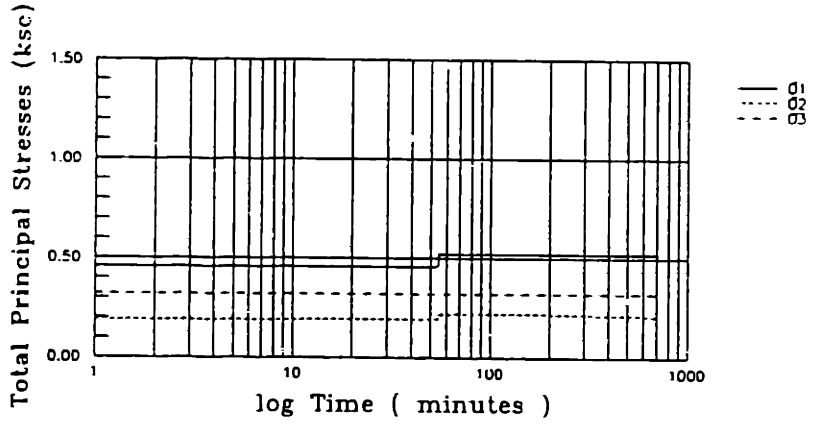

(c) Total Principal Stresses versus Time

Consolidation

Increment Number : 6

At the End of the Increment:

$\sigma_1 = 0.521$ ksc (Applied)
$\sigma_3 = 0.321$ ksc (Applied)
$\sigma_2 = 0.211$ ksc (Measured)
u $= -0.003$ ksc (Measured)

$\epsilon_1 = 0.59 \pm 0.02$ %
$\epsilon_3 = 0.00 \pm 0.02$ %
$\epsilon_v = 0.59 \pm 0.02$ %
$\gamma_{max} = 0.59 \pm 0.02$ %

DSC33 $\delta_{inc} = 60^o$

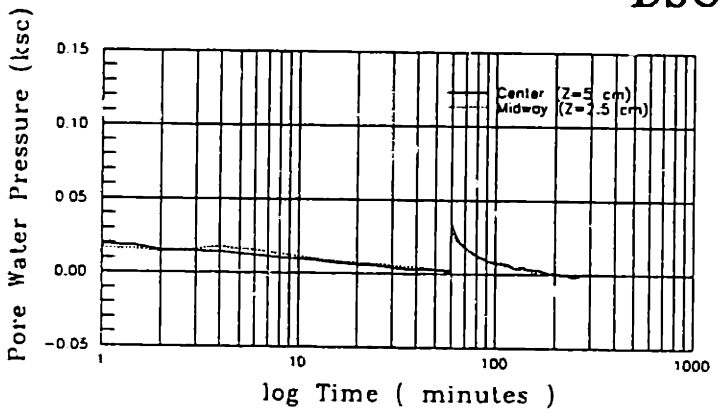

(a) Pore Water Pressure versus Time

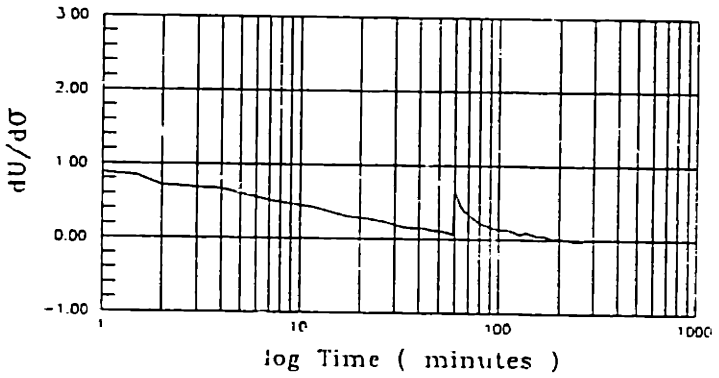

(b) Pore Water Pressure Ratio versus Time

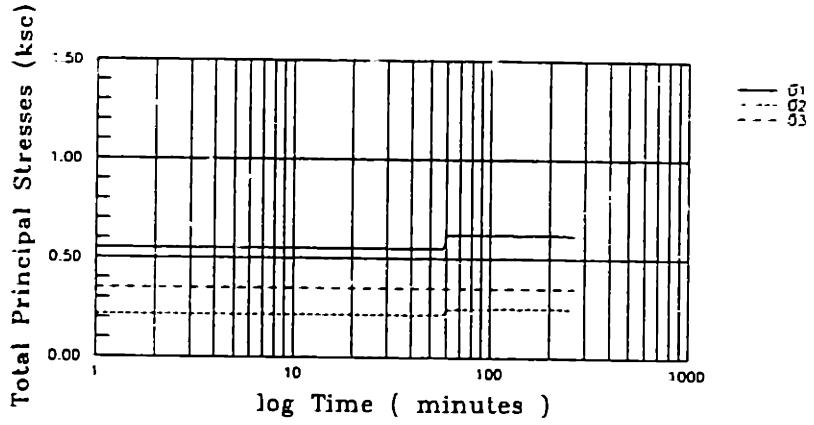

(c) Total Principal Stresses versus Time

Consolidation

Increment Number : 7

At the End of the Increment:

$\sigma_1 = 0.619$ ksc (Applied)
$\sigma_3 = 0.351$ ksc (Applied)
$\sigma_2 = 0.248$ ksc (Measured)
u $= -0.001$ ksc (Measured)

$\epsilon_1 = 0.77 \pm 0.02$ %
$\epsilon_3 = 0.03 \pm 0.01$ %
$\epsilon_v = 0.80 \pm 0.02$ %
$\gamma_{max} = 0.74 \pm 0.02$ %

DSC33 $\delta_{inc} = 60^o$

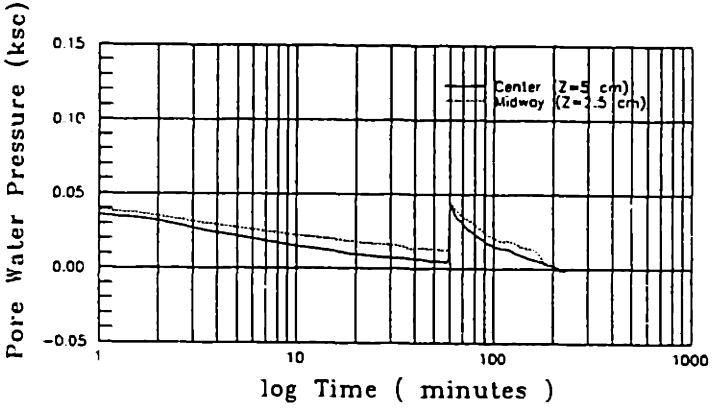

(a) Pore Water Pressure versus Time

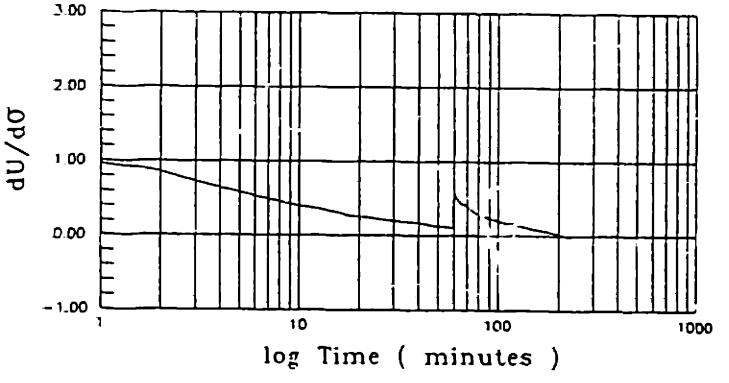

(b) Pore Water Pressure Ratio versus Time

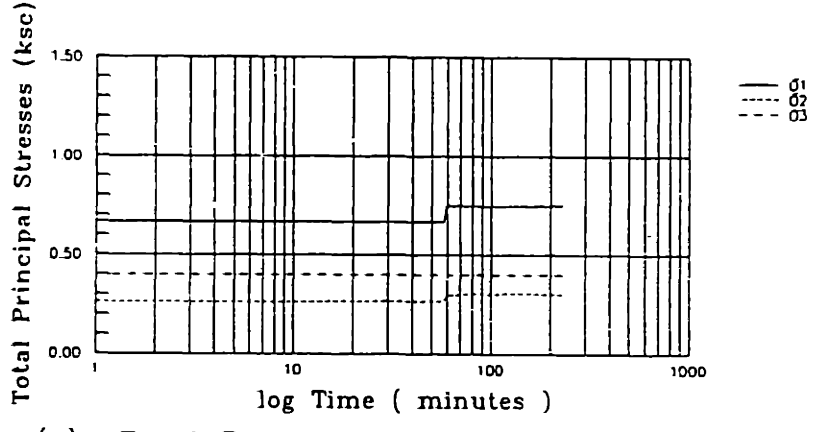

(c) Total Principal Stresses versus Time

Consolidation

Increment Number : 8

At the End of the Increment:

$\sigma_1 = 0.750$ ksc (Applied)
$\sigma_3 = 0.401$ ksc (Applied)
$\sigma_2 = 0.304$ ksc (Measured)
u $= -0.001$ ksc (Measured)

$\epsilon_1 = 1.08 \pm 0.03$ %
$\epsilon_3 = 0.08 \pm 0.02$ %
$\epsilon_v = 1.16 \pm 0.03$ %
$\gamma_{max} = 1.00 \pm 0.03$ %

DSC33 $\delta_{inc} = 60^o$

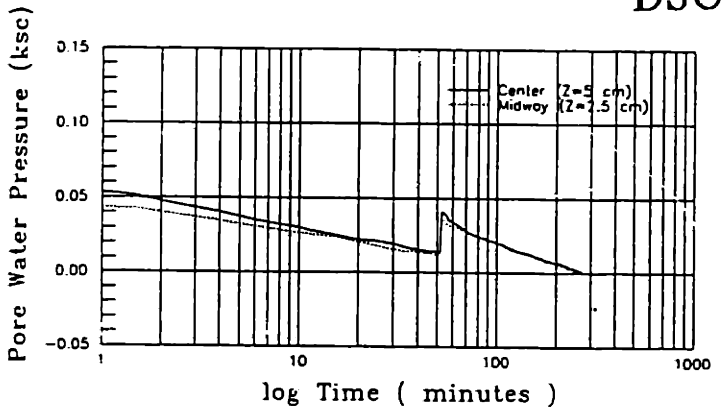

(a) Pore Water Pressure versus Time

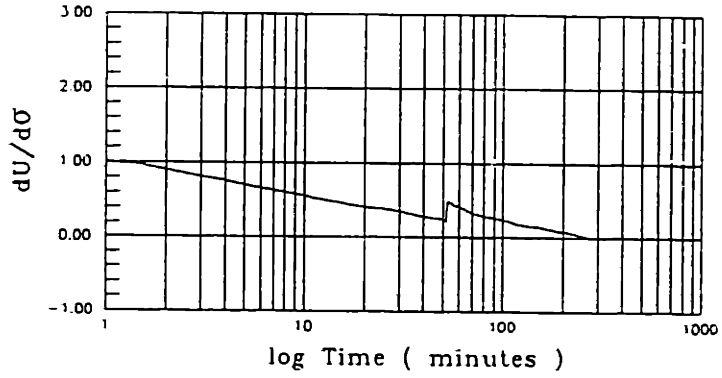

(b) Pore Water Pressure Ratio versus Time

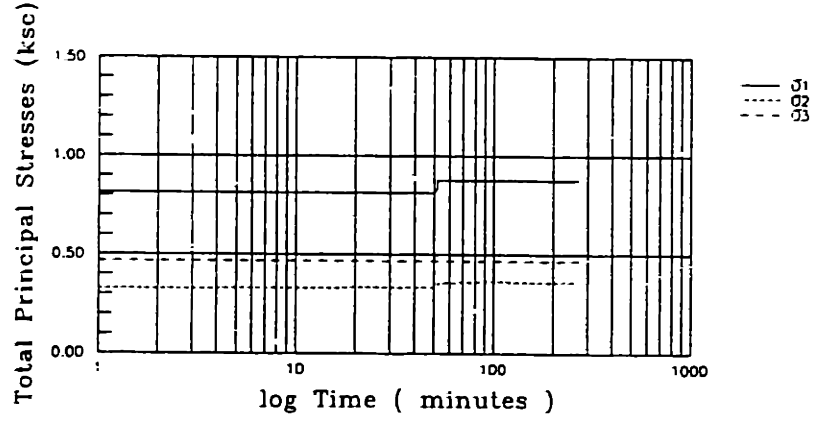

(c) Total Principal Stresses versus Time

Consolidation

Increment Number : 9

At the End of the Increment:

$\sigma_1 = 0.879$ ksc (Applied)
$\sigma_3 = 0.468$ ksc (Applied)
$\sigma_2 = 0.359$ ksc (Measured)
u $= 0.000$ ksc (Measured)

$\epsilon_1 = 1.34 \pm 0.03$ %
$\epsilon_3 = 0.16 \pm 0.01$ %
$\epsilon_v = 1.50 \pm 0.03$ %
$\gamma_{max} = 1.18 \pm 0.03$ %

DSC33 $\delta_{inc} = 60^o$

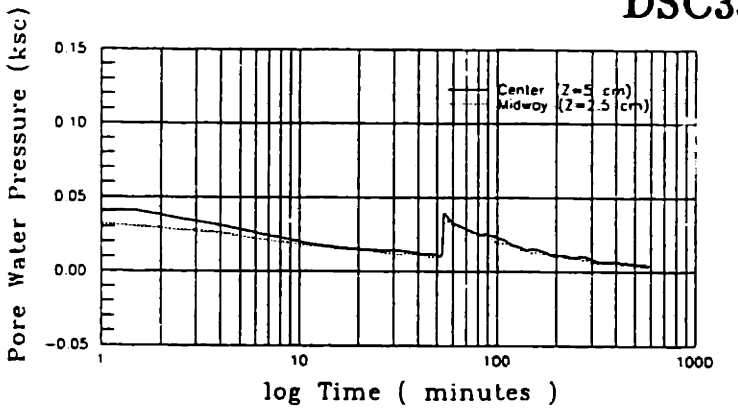

(a) Pore Water Pressure versus Time

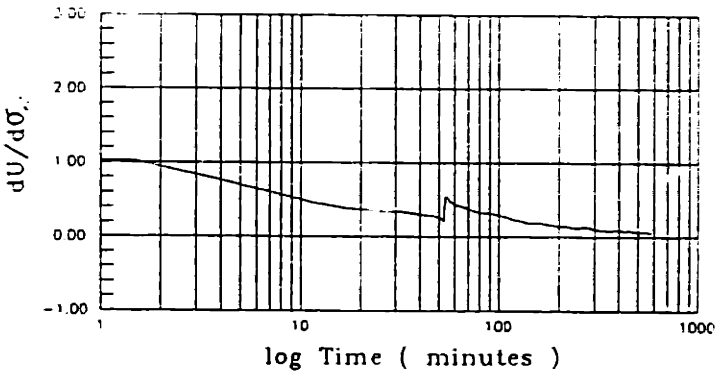

(b) Pore Water Pressure Ratio versus Time

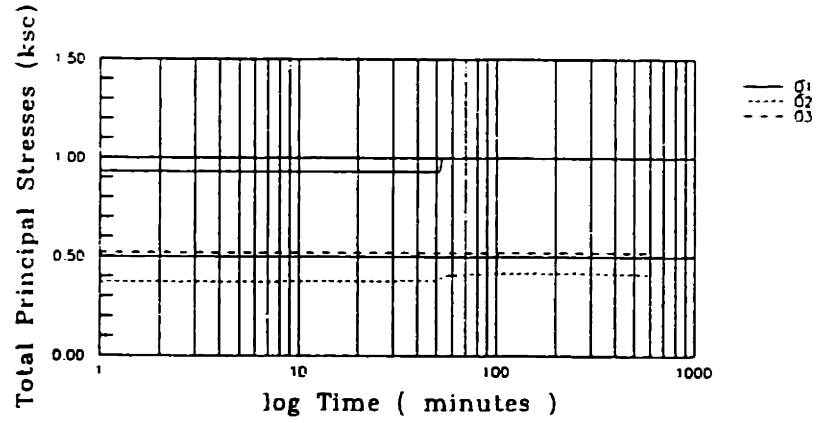

(c) Total Principal Stresses versus Time

Consolidation

Increment Number : 10

At the End of the Increment:

$\sigma_1 = 1.000$ ksc (Applied)
$\sigma_3 = 0.522$ ksc (Applied)
$\sigma_2 = 0.409$ ksc (Measured)
u $= 0.005$ ksc (Measured)

$\epsilon_1 = 1.69 \pm 0.03$ %
$\epsilon_3 = 0.09 \pm 0.02$ %
$\epsilon_v = 1.78 \pm 0.04$ %
$\gamma_{max} = 1.60 \pm 0.04$ %

DSC33 $\delta_{inc} = 60^o$

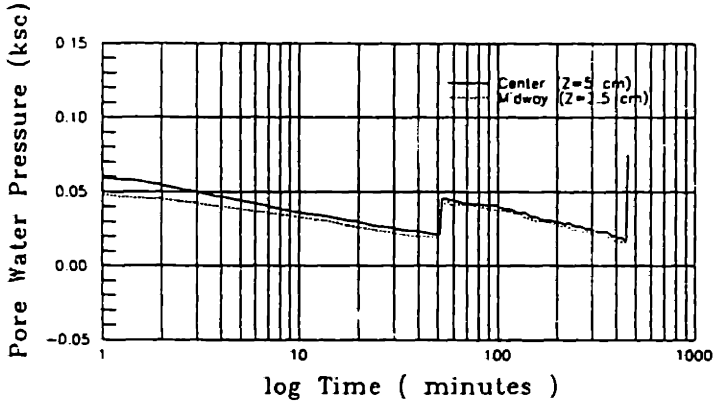

(a) Pore Water Pressure versus Time

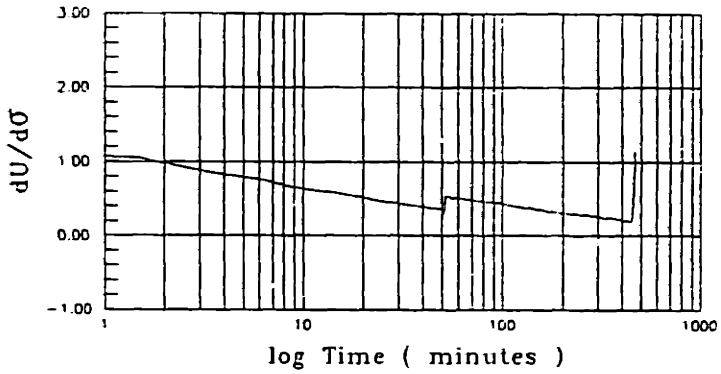

(b) Pore Water Pressure Ratio versus Time

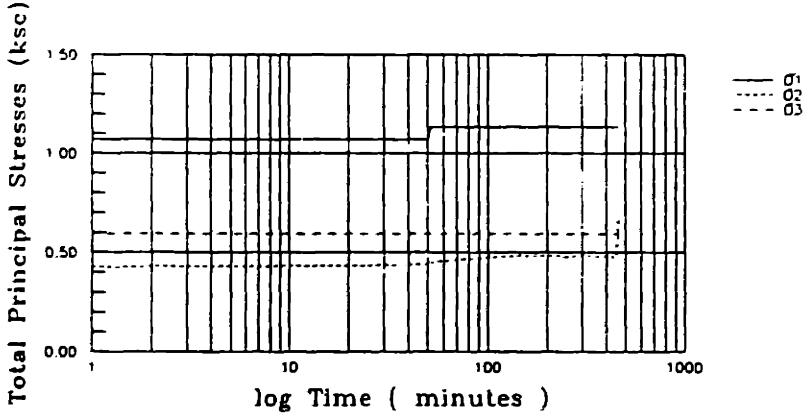

(c) Total Principal Stresses versus Time

Consolidation

Increment Number : 11

At the End of the Increment:

$\sigma_1 = 1.136$ ksc (Applied)
$\sigma_3 = 0.594$ ksc (Applied)
$\sigma_2 = 0.472$ ksc (Measured)
u $= 0.017$ ksc (Measured)

$\epsilon_1 = 2.77 \pm 0.04$ %
$\epsilon_3 = 0.07 \pm 0.03$ %
$\epsilon_v = 2.84 \pm 0.05$ %
$\gamma_{max} = 2.70 \pm 0.05$ %

DSC33 $\delta_{inc} = 60^o$

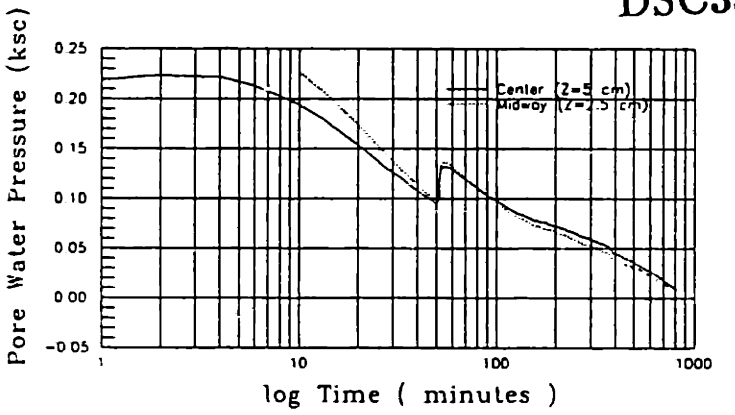

(a) Pore Water Pressure versus Time

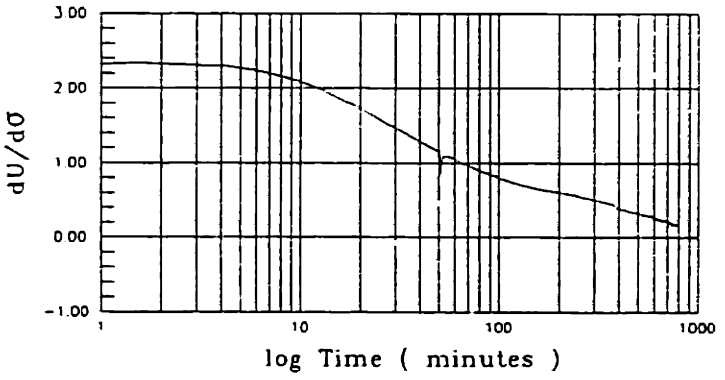

(b) Pore Water Pressure Ratio versus Time

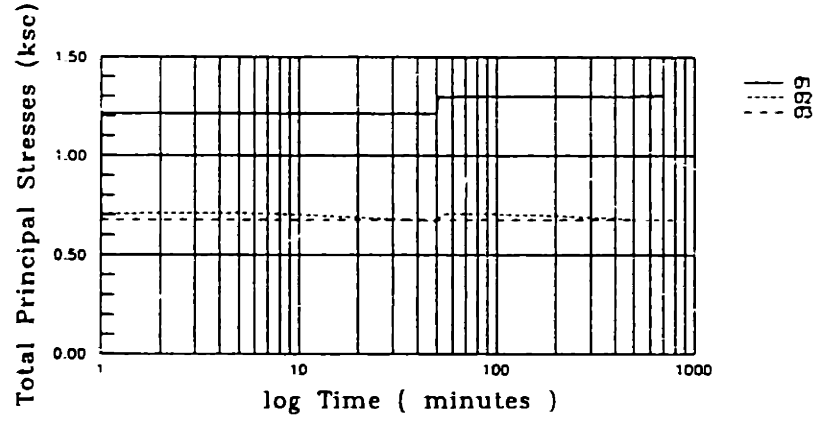

(c) Total Principal Stresses versus Time

Consolidation

Increment Number : 12

At the End of the Increment:

$\sigma_1 = 1.300$ ksc (Applied)
$\sigma_3 = 0.677$ ksc (Applied)
$\sigma_2 = 0.680$ ksc (Measured)
u $= 0.005$ ksc (Measured)

$\epsilon_1 = 3.24 \pm 0.06$ %
$\epsilon_3 = 0.06 \pm 0.03$ %
$\epsilon_v = 3.30 \pm 0.06$ %
$\gamma_{max} = 3.18 \pm 0.06$ %

DSC34 $\delta_{inc} = 0^o$

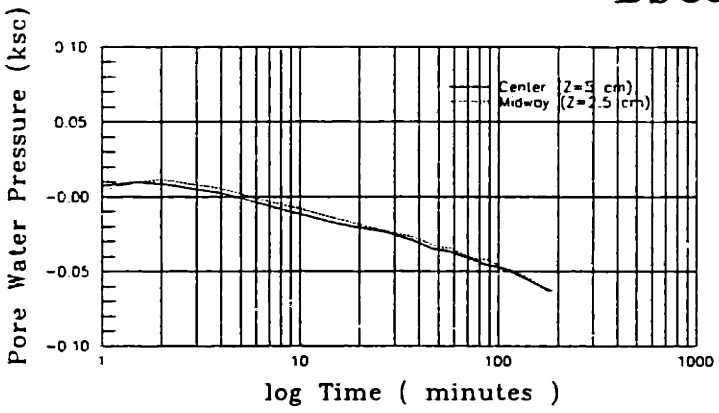

(a) Pore Water Pressure versus Time

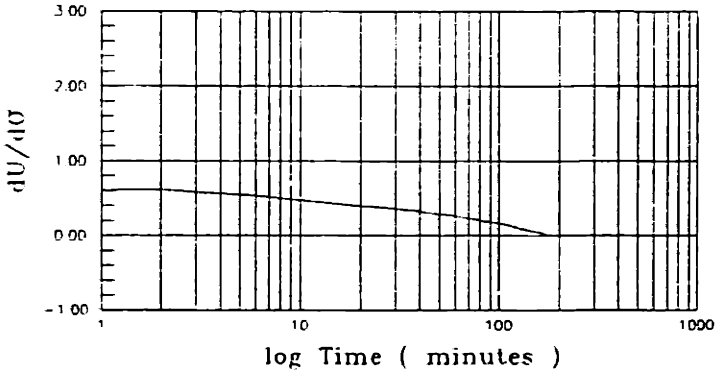

(b) Pore Water Pressure Ratio versus Time

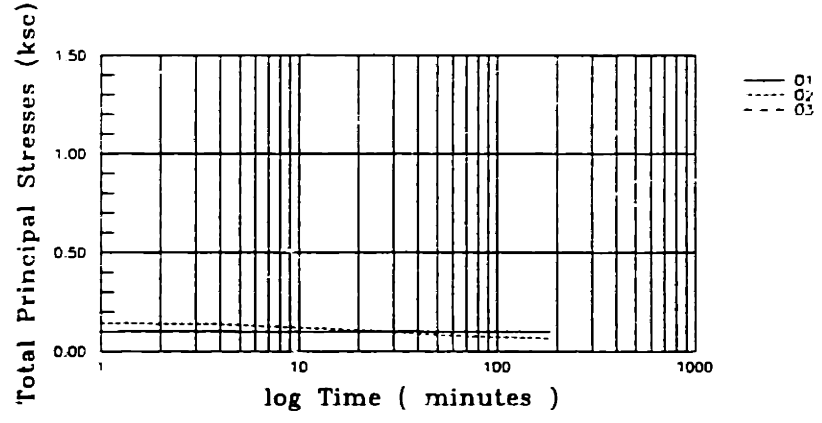

(c) Total Principal Stresses versus Time

Consolidation

Increment Number : 1

At the End of the Increment:

$\sigma_1 = 0.102$ ksc (Applied)
$\sigma_3 = 0.101$ ksc (Applied)
$\sigma_2 = 0.069$ ksc (Measured)
u $= -0.063$ ksc (Measured)

$\epsilon_1 = 0.00 \pm 0.00$ %
$\epsilon_3 = 0.00 \pm 0.00$ %
$\epsilon_v = 0.00 \pm 0.00$ %
$\gamma_{max} = 0.00 \pm 0.00$ %

DSC34 $\delta_{inc} = 0^o$

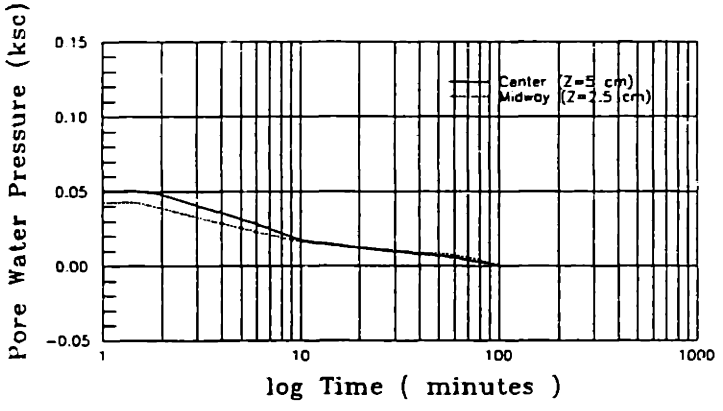

(a) Pore Water Pressure versus Time

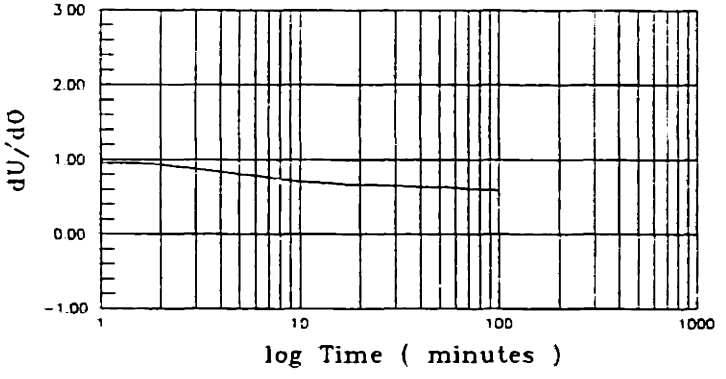

(b) Pore Water Pressure Ratio versus Time

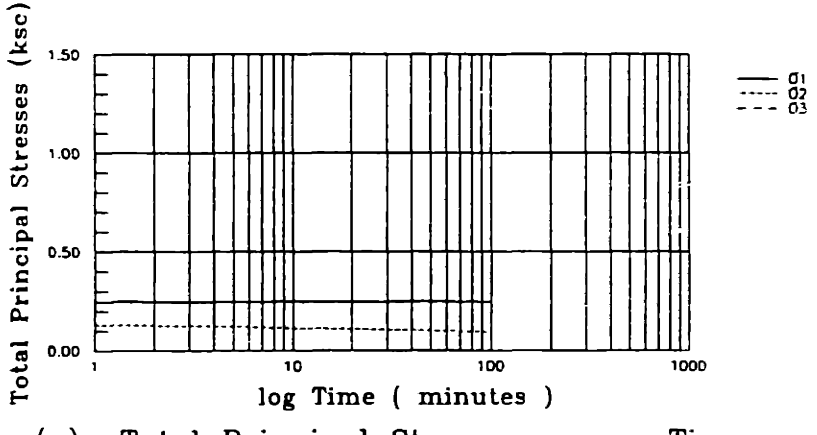

(c) Total Principal Stresses versus Time

Consolidation

Increment Number : 2

At the End of the Increment:

$\sigma_1 = 0.249$ ksc (Applied)
$\sigma_3 = 0.246$ ksc (Applied)
$\sigma_2 = 0.095$ ksc (Measured)
u $= 0.000$ ksc (Measured)

$\epsilon_1 = 0.06 \pm 0.01$ %
$\epsilon_3 = -0.01 \pm 0.01$ %
$\epsilon_v = 0.05 \pm 0.02$ %
$\gamma_{max} = 0.07 \pm 0.02$ %

DSC34 $\delta_{inc} = 0^o$

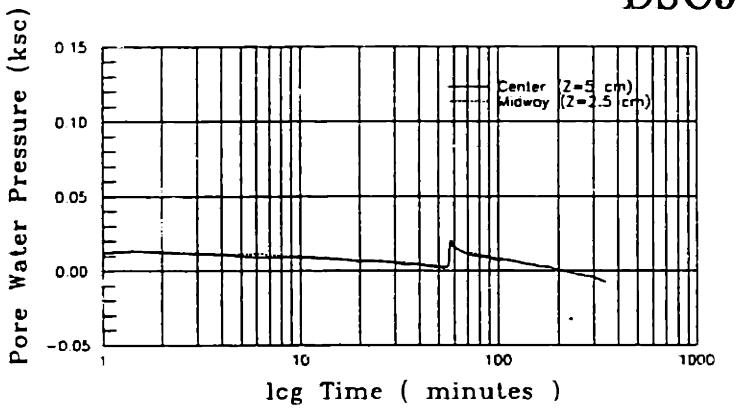

(a) Pore Water Pressure versus Time

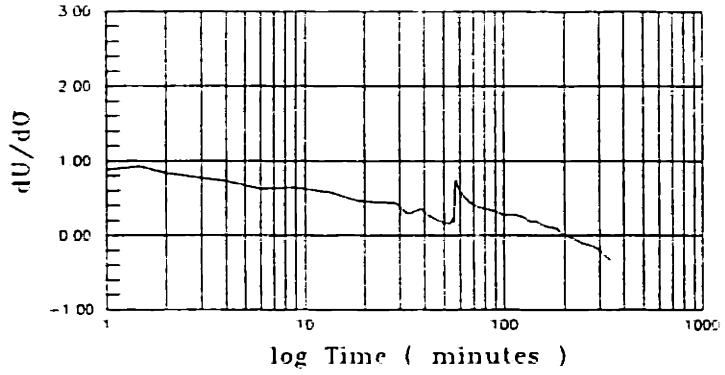

(b) Pore Water Pressure Ratio versus Time

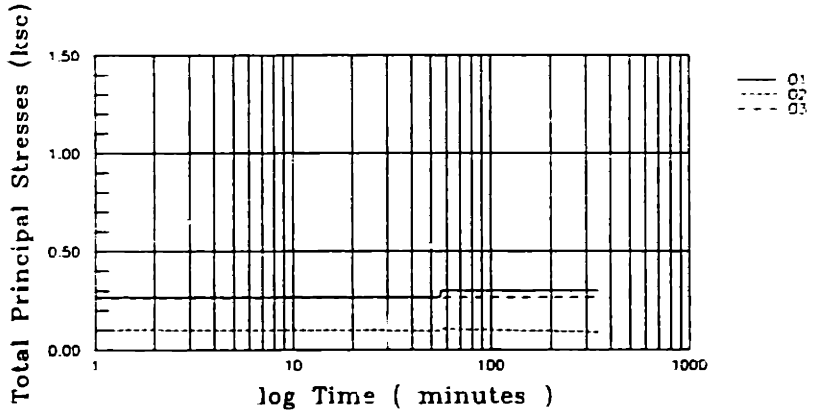

(c) Total Principal Stresses versus Time

Consolidation

Increment Number : 3

At the End of the Increment:

$\sigma_1 = 0.301$ ksc (Applied)
$\sigma_3 = 0.266$ ksc (Applied)
$\sigma_2 = 0.091$ ksc (Measured)
u $= -0.008$ ksc (Measured)

$\epsilon_1 = 0.02 \pm 0.02$ %
$\epsilon_3 = -0.04 \pm 0.01$ %
$\epsilon_v = -0.02 \pm 0.02$ %
$\gamma_{max} = 0.06 \pm 0.02$ %

DSC34 $\delta_{inc} = 0^o$

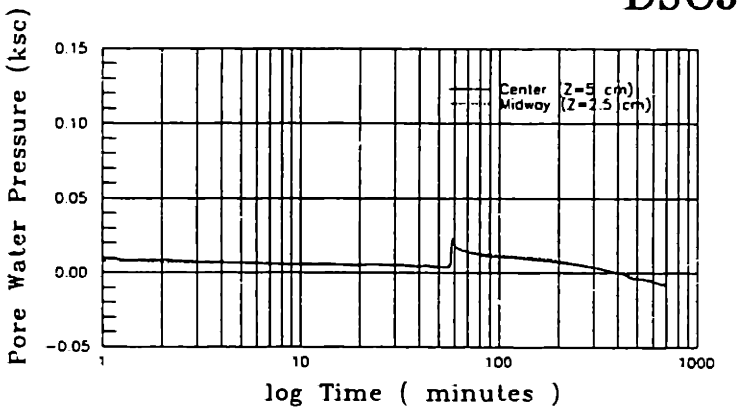

(a) Pore Water Pressure versus Time

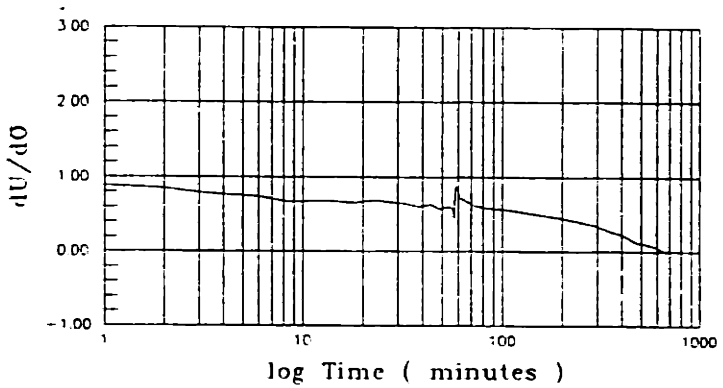

(b) Pore Water Pressure Ratio versus Time

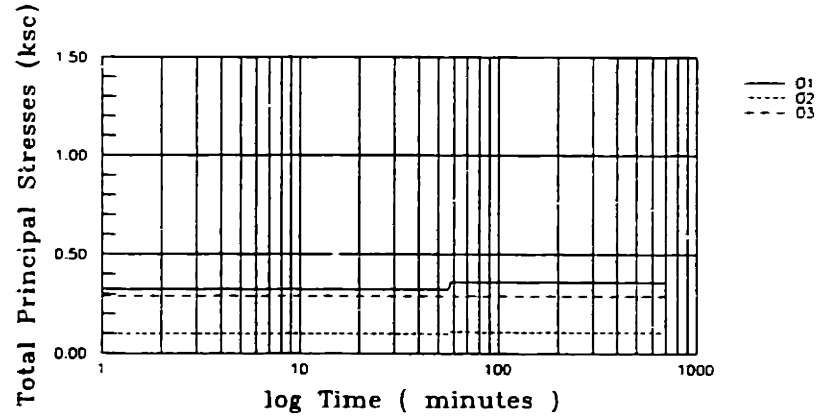

(c) Total Principal Stresses versus Time

Consolidation

Increment Number : 4

At the End of the Increment:

$\sigma_1 = 0.360$ ksc (Applied)
$\sigma_3 = 0.290$ ksc (Applied)
$\sigma_2 = 0.107$ ksc (Measured)
u $= -0.007$ ksc (Measured)

$\epsilon_1 = 0.14 \pm 0.02$ %
$\epsilon_3 = -0.05 \pm 0.02$ %
$\epsilon_v = 0.09 \pm 0.02$ %
$\gamma_{max} = 0.19 \pm 0.02$ %

DSC34 $\delta_{inc} = 0^o$

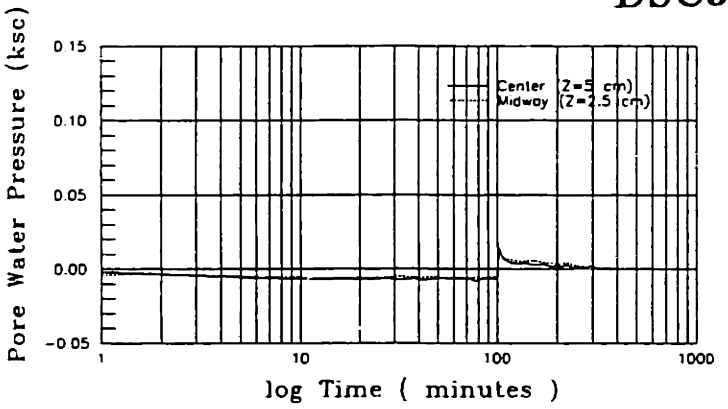

(a) Pore Water Pressure versus Time

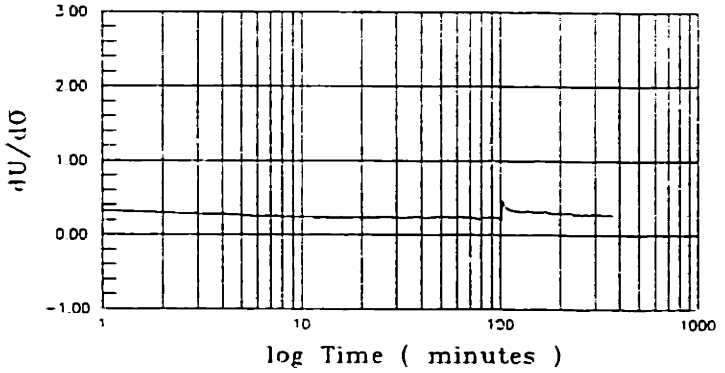

(b) Pore Water Pressure Ratio versus Time

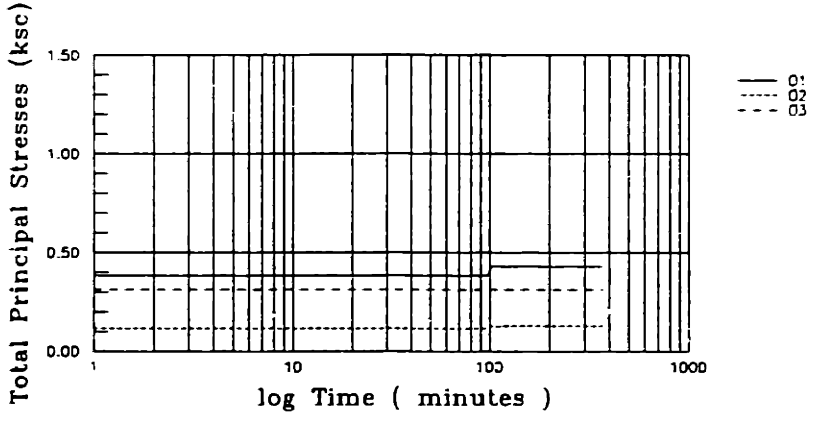

(c) Total Principal Stresses versus Time

Consolidation

Increment Number : 5

At the End of the Increment:

$\sigma_1 = 0.430$ ksc (Applied)
$\sigma_3 = 0.315$ ksc (Applied)
$\sigma_2 = 0.132$ ksc (Measured)
u $= -0.001$ ksc (Measured)

$\epsilon_1 = 0.24 \pm 0.02$ %
$\epsilon_3 = -0.03 \pm 0.02$ %
$\epsilon_v = 0.21 \pm 0.03$ %
$\gamma_{max} = 0.27 \pm 0.03$ %

DSC34 $\delta_{inc} = 0^o$

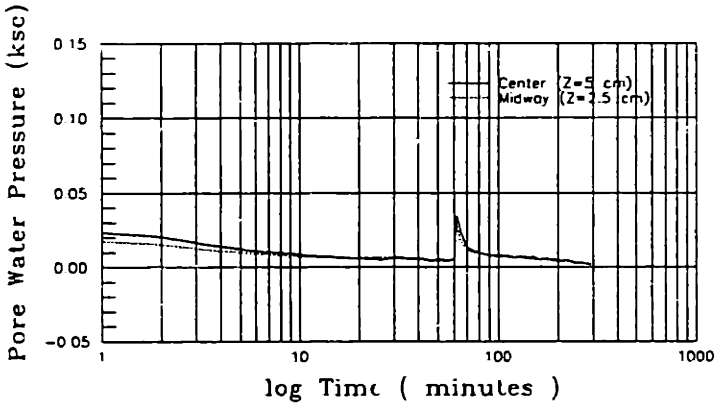

(a) Pore Water Pressure versus Time

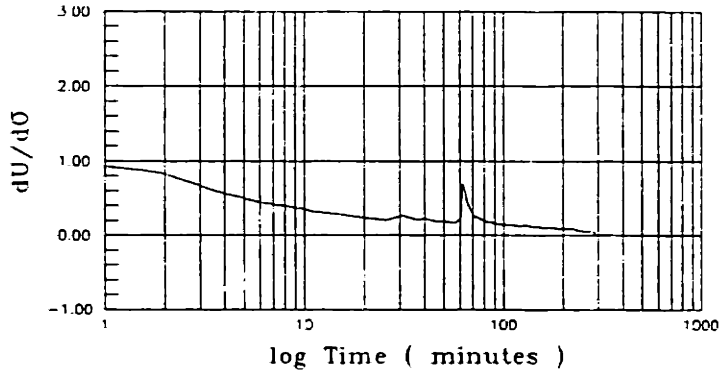

(b) Pore Water Pressure Ratio versus Time

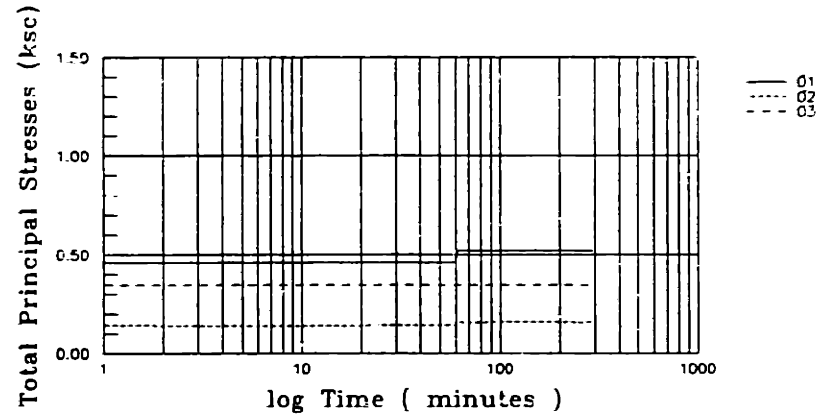

(c) Total Principal Stresses versus Time

Consolidation

Increment Number : 6

At the End of the Increment:

$\sigma_1 = 0.520$ ksc (Applied)
$\sigma_3 = 0.347$ ksc (Applied)
$\sigma_2 = 0.159$ ksc (Measured)
u $= 0.002$ ksc (Measured)

$\epsilon_1 = 0.39 \pm 0.02$ %
$\epsilon_3 = 0.01 \pm 0.01$ %
$\epsilon_v = 0.40 \pm 0.02$ %
$\gamma_{max} = 0.39 \pm 0.02$ %

DSC34 $\delta_{inc} = 0^o$

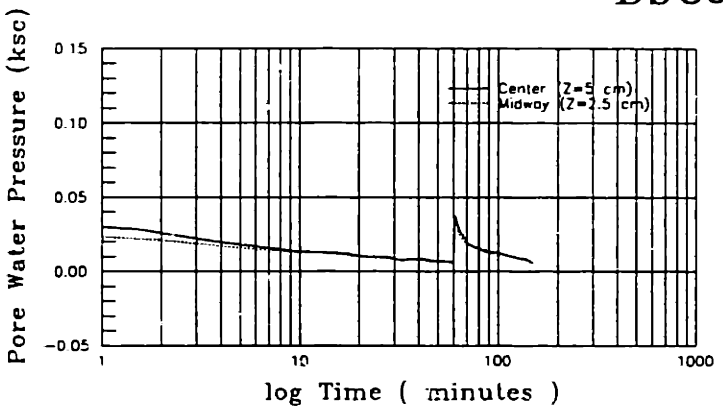

(a) Pore Water Pressure versus Time

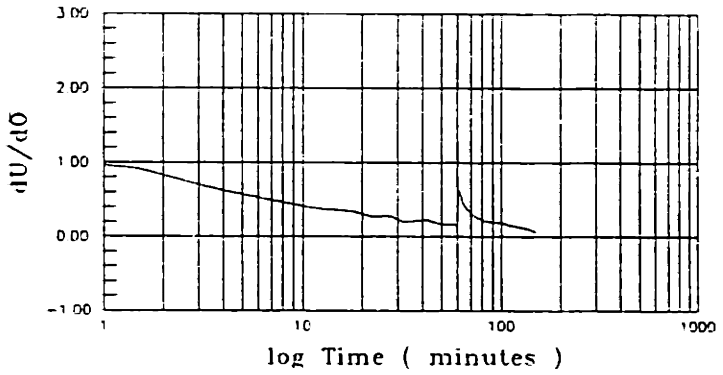

(b) Pore Water Pressure Ratio versus Time

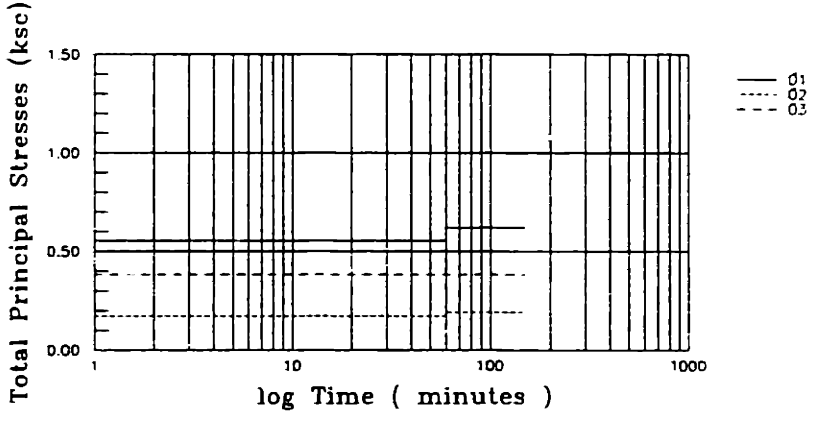

(c) Total Principal Stresses versus Time

Consolidation

Increment Number : 7

At the End of the Increment:

$\sigma_1 = 0.620$ ksc (Applied)
$\sigma_3 = 0.383$ ksc (Applied)
$\sigma_2 = 0.195$ ksc (Measured)
u $= 0.005$ ksc (Measured)

$\epsilon_1 = 0.54 \pm 0.02$ %
$\epsilon_3 = 0.06 \pm 0.01$ %
$\epsilon_v = 0.60 \pm 0.03$ %
$\gamma_{max} = 0.48 \pm 0.03$ %

DSC34 $\delta_{inc} = 0^o$

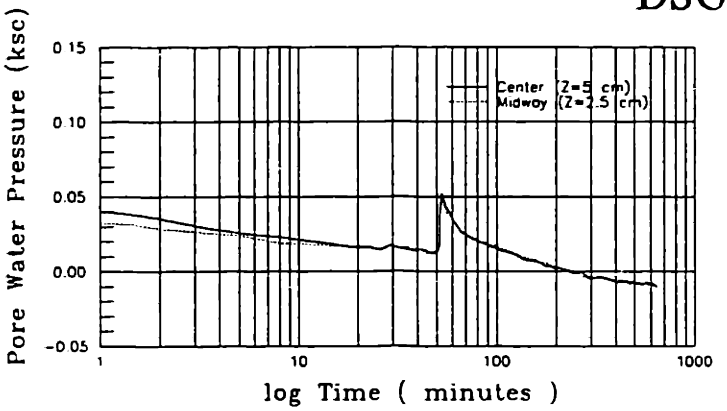

(a) Pore Water Pressure versus Time

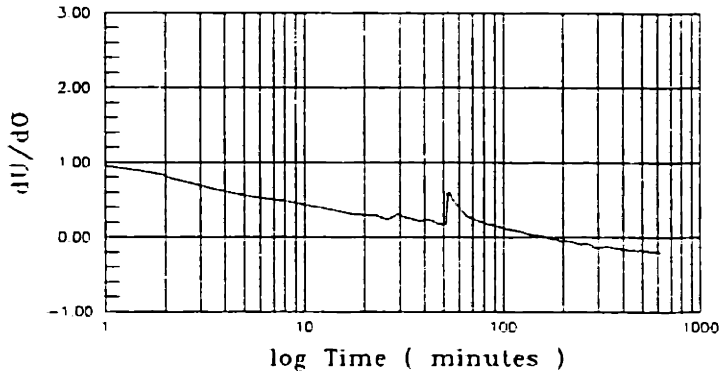

(b) Pore Water Pressure Ratio versus Time

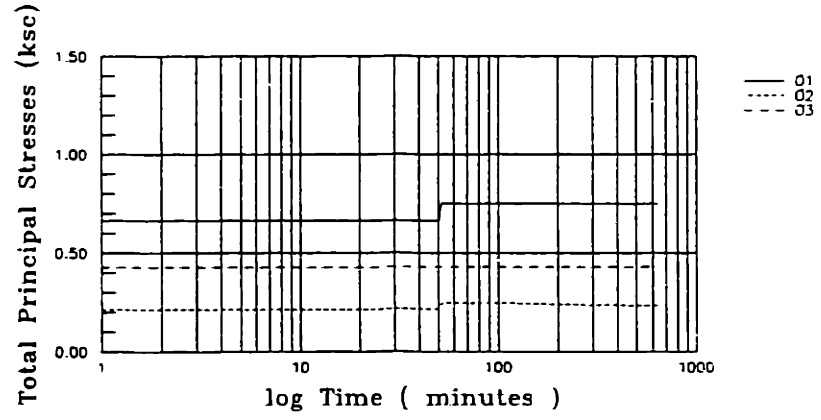

(c) Total Principal Stresses versus Time

Consolidation

Increment Number : 8

At the End of the Increment:

$\sigma_1 = 0.750$ ksc (Applied)
$\sigma_3 = 0.431$ ksc (Applied)
$\sigma_2 = 0.234$ ksc (Measured)
u $= -0.010$ ksc (Measured)

$\epsilon_1 = 0.81 \pm 0.02$ %
$\epsilon_3 = 0.05 \pm 0.02$ %
$\epsilon_v = 0.86 \pm 0.03$ %
$\gamma_{max} = 0.75 \pm 0.03$ %

DSC34 $\delta_{inc} = 0^o$

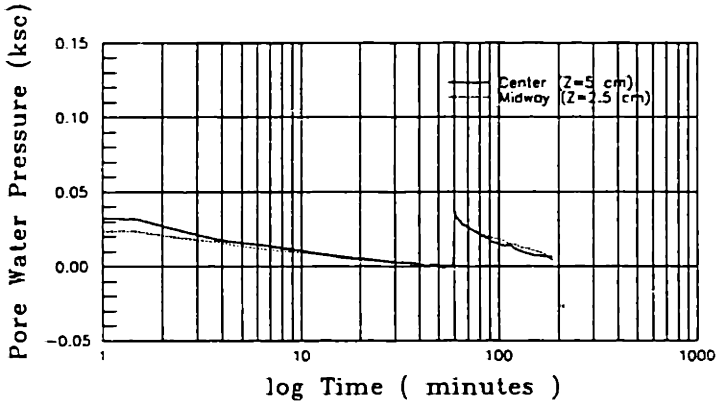

(a) Pore Water Pressure versus Time

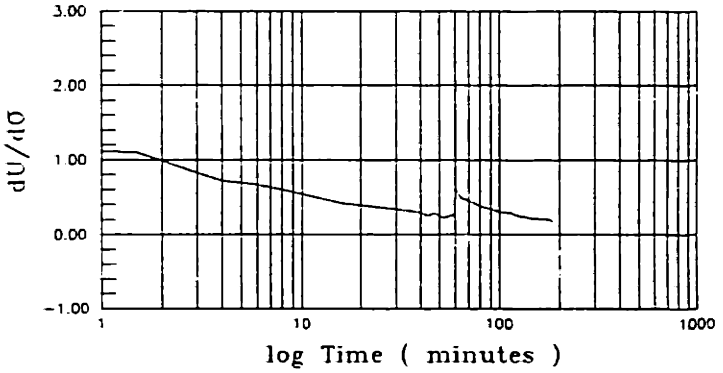

(b) Pore Water Pressure Ratio versus Time

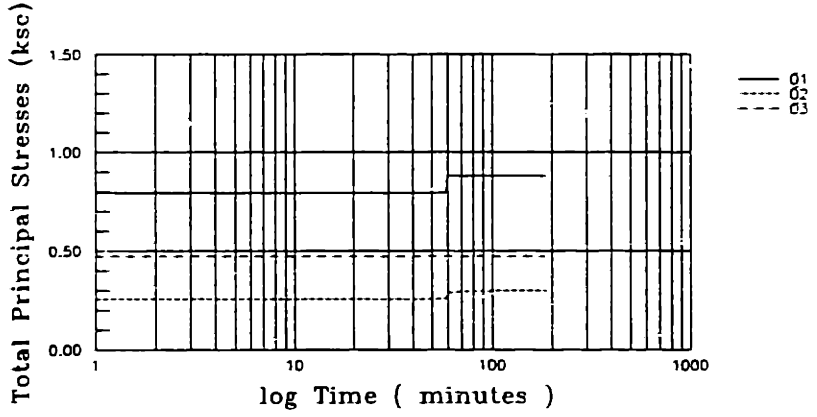

(c) Total Principal Stresses versus Time

Consolidation

Increment Number : 9

At the End of the Increment:

$\sigma_1 = 0.880$ ksc (Applied)
$\sigma_3 = 0.476$ ksc (Applied)
$\sigma_2 = 0.300$ ksc (Measured)
u $= 0.004$ ksc (Measured)

$\epsilon_1 = 1.09 \pm 0.03$ %
$\epsilon_3 = 0.13 \pm 0.02$ %
$\epsilon_v = 1.22 \pm 0.03$ %
$\gamma_{max} = 0.96 \pm 0.03$ %

DSC34 $\delta_{inc} = 0^o$

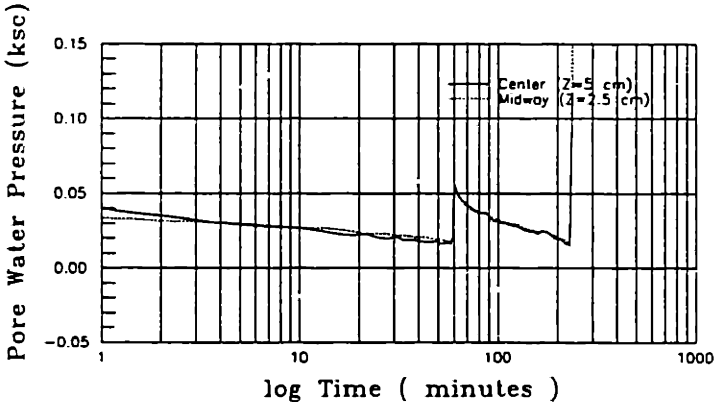

(a) Pore Water Pressure versus Time

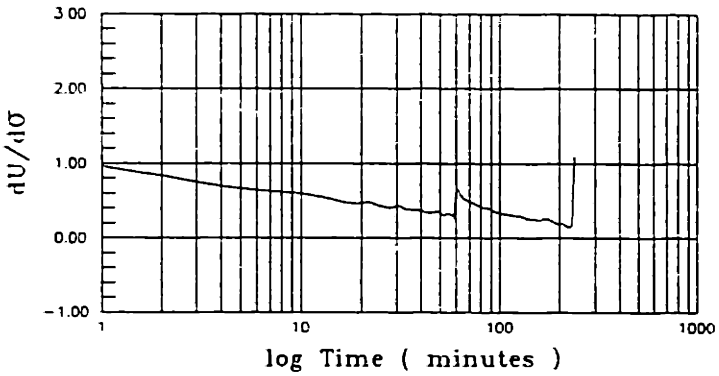

(b) Pore Water Pressure Ratio versus Time

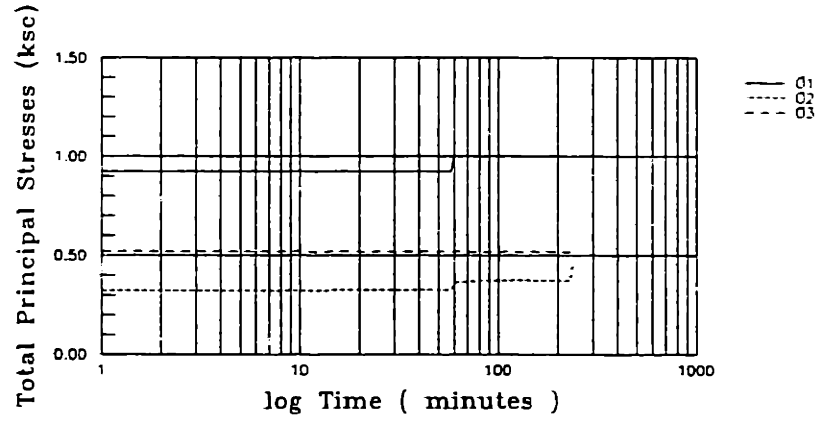

(c) Total Principal Stresses versus Time

Consolidation

Increment Number : 10

At the End of the Increment:

$\sigma_1 = 1.000$ ksc (Applied)
$\sigma_3 = 0.519$ ksc (Applied)
$\sigma_2 = 0.451$ ksc (Measured)
u $= 0.016$ ksc (Measured)

$\epsilon_1 = 1.44 \pm 0.03$ %
$\epsilon_3 = 0.14 \pm 0.02$ %
$\epsilon_v = 1.58 \pm 0.03$ %
$\gamma_{max} = 1.30 \pm 0.03$ %

DSC34 $\delta_{inc} = 0^o$

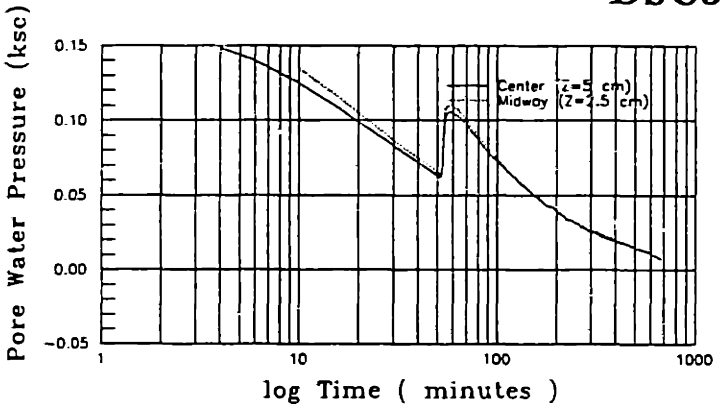

(a) Pore Water Pressure versus Time

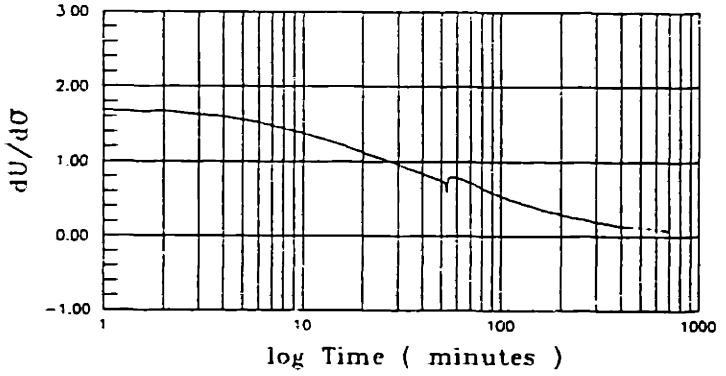

(b) Pore Water Pressure Ratio versus Time

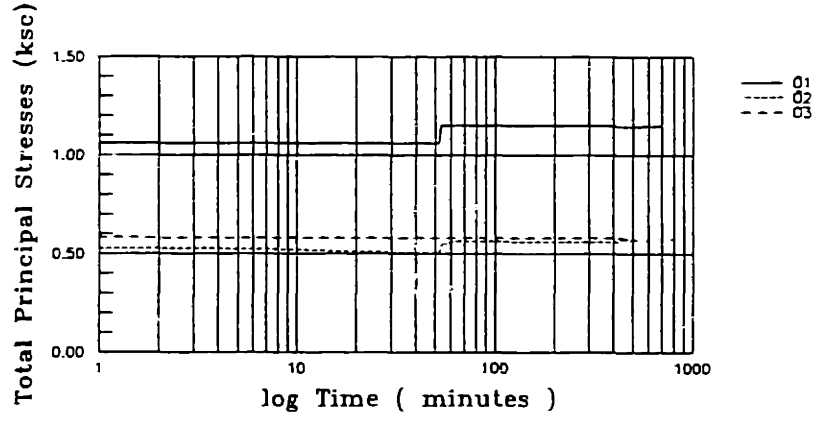

(c) Total Principal Stresses versus Time

Consolidation

Increment Number : 11

At the End of the increment:

$\sigma_1 = 1.149$ ksc (Applied)
$\sigma_3 = 0.582$ ksc (Applied)
$\sigma_2 = 0.561$ ksc (Measured)
u $= 0.009$ ksc (Measured)

$\epsilon_1 = 2.02 \pm 0.03$ %
$\epsilon_3 = 0.32 \pm 0.03$ %
$\epsilon_v = 2.34 \pm 0.04$ %
$\gamma_{max} = 1.70 \pm 0.04$ %

DSC35 $\delta_{inc} = 75^o$

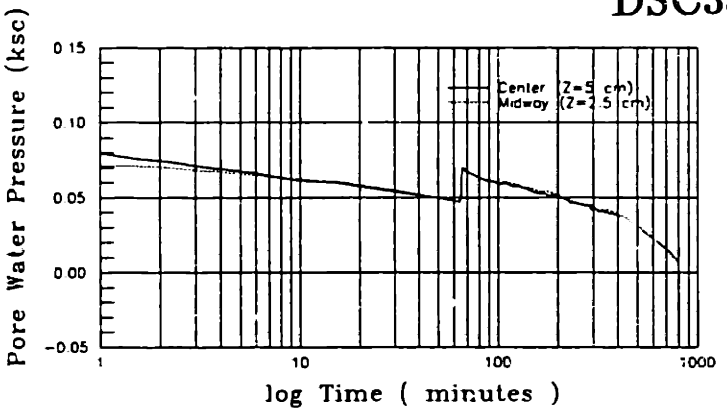

(a) Pore Water Pressure versus Time

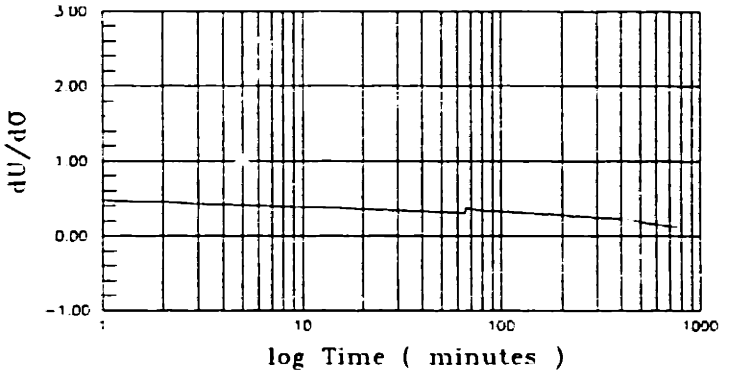

(b) Pore Water Pressure Ratio versus Time

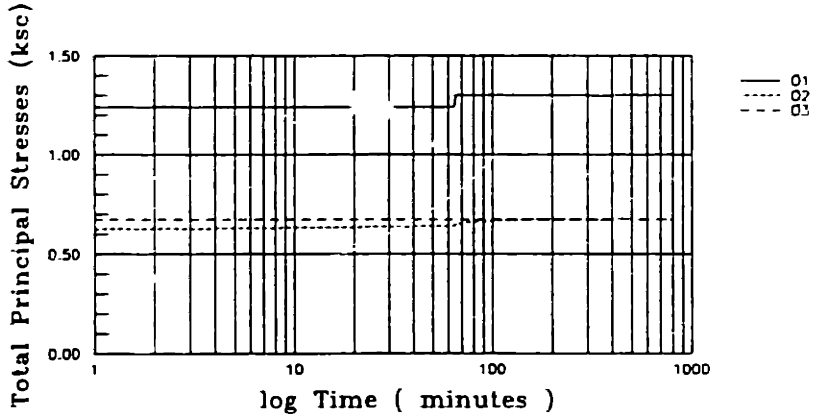

(c) Total Principal Stresses versus Time

Consolidation

Increment Number : 12

At the End of the Increment:

σ_1 = 1.299 ksc (Applied)
σ_3 = 0.676 ksc (Applied)
σ_2 = 0.676 ksc (Measured)
u = 0.037 ksc (Measured)

ϵ_1 = 3.24±0.08 %
ϵ_3 = –0.85±0.05 %
ϵ_v = 2.39±0.10 %
γ_{max} = 4.09±0.10 %

F.4 UNDRAINED SHEAR RESULTS OF DSC TESTS ON OCR=1 BBC

This section contains:

- Computer printouts of incremental stress data for DSC tests on OCR=1 BBC.
- Computer printouts of total stress data for DSC tests on OCR=1 BBC.
- Computer printouts of uncorrected strain data for DSC tests on OCR=1 BBC.
- Computer printouts of corrected strain data for DSC tests on OCR=1 BBC.
- Plots of undrained shear results from DSC tests on OCR=1 BBC.

UNDRAINED SHEAR: DSC31 (INCREMENTAL STRESSES)

FILM No.	DELTA deg	ALFA deg	ΔP ksc	ΔQ ksc	Sig.a mV	Sig.b mV	T a mV	T b mV	U mV	Sig.a ksc	Sig.b ksc	T a ksc	T b ksc	Input V Volts
0	0.000	0.000	0.000	0.000	32.260	17.330	-0.554	-0.492	-0.230	0.000	0.000	0.000	0.000	0.000
1	0.000	0.000	0.000	0.000	32.260	17.330	-0.200	-0.139	-0.230	0.000	0.000	0.000	0.000	10.000
2	0.000	0.000	-0.003	0.011	31.920	17.530	-0.199	-0.139	-0.230	-0.014	0.008	0.000	0.000	10.000
3	0.000	0.000	-0.006	0.031	31.380	17.960	-0.199	-0.139	-0.230	-0.036	0.025	0.000	0.000	10.000
4	0.000	0.000	-0.011	0.050	30.790	18.310	-0.199	-0.139	-0.230	-0.061	0.039	0.000	0.000	10.000
5	0.000	0.000	-0.019	0.071	30.100	18.630	-0.199	-0.139	-0.230	-0.090	0.052	0.000	0.000	10.000
6	0.000	0.000	-0.029	0.091	29.360	18.880	-0.199	-0.139	-0.230	-0.120	0.062	0.000	0.000	10.000
7	0.000	0.000	-0.040	0.111	28.620	19.100	-0.199	-0.139	-0.230	-0.151	0.071	0.000	0.000	10.000
8	0.000	0.000	-0.054	0.130	27.810	19.240	-0.199	-1.390	27.810	-0.185	0.076	0.000	0.000	10.000
9	0.000	0.000	-0.067	0.151	27.000	19.420	-0.199	-0.139	-0.230	-0.218	0.084	0.000	0.000	10.000
10	0.000	0.000	-0.076	0.171	26.310	19.700	-0.199	-0.139	-0.230	-0.247	0.095	0.000	0.000	10.000
11	0.000	0.000	-0.094	0.191	25.400	19.750	-0.199	-0.139	-0.230	-0.285	0.097	0.000	0.000	10.000
12	0.000	0.000	-0.116	0.211	24.380	19.710	-0.199	-0.139	-0.230	-0.327	0.095	0.000	0.000	10.000
13	0.000	0.000	-0.132	0.231	23.500	19.790	-0.199	-0.139	-0.230	-0.363	0.098	0.000	0.000	10.000
14	0.000	0.000	-0.148	0.251	22.640	19.910	-0.199	-0.139	-0.230	-0.399	0.103	0.000	0.000	10.000
15	0.000	0.000	-0.173	0.271	21.560	19.780	-0.199	-0.139	-0.230	-0.444	0.098	0.000	0.000	10.000
16	0.000	0.000	-0.191	0.290	20.660	19.810	-0.199	-0.139	-0.230	-0.481	0.099	0.000	0.000	10.000
17	0.000	0.000	-0.218	0.311	19.520	19.650	-0.199	-0.139	-0.230	-0.528	0.093	0.000	0.000	10.000
18	0.000	0.000	-0.233	0.321	18.900	19.540	-0.199	-0.139	-0.230	-0.554	0.088	0.000	0.000	10.000
19	0.000	0.000	-0.248	0.331	18.300	19.400	-0.199	-0.139	-0.230	-0.579	0.083	0.000	0.000	10.000
20	0.000	0.000	-0.262	0.341	17.720	19.300	-0.199	-0.139	-0.230	-0.603	0.079	0.000	0.000	10.000
21	0.000	0.000	-0.272	0.350	17.260	19.300	-0.199	-0.139	-0.230	-0.622	0.079	0.000	0.000	10.000
22	0.000	0.000	-0.290	0.361	16.570	19.120	-0.199	-0.139	-0.230	-0.651	0.072	0.000	0.000	10.000
23	0.000	0.000	-0.299	0.371	16.100	19.120	-0.199	-0.139	-0.230	-0.670	0.072	0.000	0.000	10.000
24	0.000	0.000	-0.318	0.381	15.400	18.890	-0.199	-0.139	-0.230	-0.699	0.062	0.000	0.000	10.000
25	0.000	0.000	-0.333	0.391	14.800	18.760	-0.199	-0.139	-0.230	-0.724	0.057	0.000	0.000	10.000
26	0.000	0.000	-0.347	0.401	14.240	18.680	-0.199	-0.139	-0.230	-0.747	0.054	0.000	0.000	10.000
27	0.000	0.000	-0.367	0.411	13.490	18.430	-0.199	-0.139	-0.230	-0.778	0.044	0.000	0.000	10.000
28	0.000	0.000	-0.382	0.421	12.900	18.300	-0.199	-0.139	-0.230	-0.803	0.039	0.000	0.000	10.000
29	0.000	0.000	-0.402	0.431	12.170	18.050	-0.199	-0.139	-0.230	-0.833	0.029	0.000	0.000	10.000

FILM No.	DELTA deg	ALFA deg	ΔP ksc	ΔQ ksc	Sig.a mV	Sig.b mV	T a mV	T b mV	U mV	Sig.a ksc	Sig.b ksc	T a ksc	T b ksc	Input V Volts
30	0.000	0.000	-0.414	0.441	11.640	18.000	-0.199	-0.139	-0.230	-0.855	0.027	0.000	0.000	10.000
31	0.000	0.000	-0.430	0.451	11.020	17.850	-0.199	-0.139	-0.230	-0.881	0.021	0.000	0.000	10.000
32	0.000	0.000	-0.451	0.461	10.280	17.590	-0.199	-0.139	-0.230	-0.912	0.010	0.000	0.000	10.000
33	0.000	0.000	-0.466	0.466	9.790	17.340	-0.199	-0.139	-0.230	-0.932	0.000	0.000	0.000	10.000
34	0.000	0.000	-0.481	0.471	9.300	17.080	-0.199	-0.139	-0.230	-0.952	-0.010	0.000	0.000	10.000
35	0.000	0.000	-0.497	0.476	8.810	16.810	-0.199	-0.139	-0.230	-0.973	-0.021	0.000	0.000	10.000
35	0.000	0.000	-0.503	0.476	8.670	16.660	-0.199	-0.139	-0.350	-0.978	-0.027	0.000	0.000	10.000
36	0.000	0.000	-0.518	0.481	8.160	16.400	-0.199	-0.139	-0.230	-1.000	-0.037	0.000	0.000	10.000
37	0.000	0.000	-0.529	0.486	7.780	16.250	-0.199	-0.139	-0.230	-1.015	-0.043	0.000	0.000	10.000
38	0.000	0.000	-0.538	0.491	7.450	16.150	-0.199	-0.139	-0.230	-1.029	-0.047	0.000	0.000	10.000
39	0.000	0.000	-0.549	0.496	7.070	16.010	-0.199	-0.139	-0.230	-1.045	-0.053	0.000	0.000	10.000
40	0.000	0.000	-0.558	0.501	6.720	15.910	-0.199	-0.139	-0.230	-1.059	-0.057	0.000	0.000	10.000
41	0.000	0.000	-0.572	0.508	6.230	15.730	-0.199	-0.139	-0.230	-1.080	-0.064	0.000	0.000	10.000
42	0.000	0.000	-0.586	0.511	5.800	15.450	-0.199	-0.139	-0.230	-1.097	-0.075	0.000	0.000	10.000
43	0.000	0.000	-0.601	0.516	5.330	15.200	-0.199	-0.139	-0.230	-1.117	-0.085	0.000	0.000	10.000
44	0.000	0.000	-0.609	0.520	5.030	15.120	-0.199	-0.139	-0.230	-1.129	-0.088	0.000	0.000	10.000
45	0.000	0.000	-0.612	0.523	4.900	15.090	-0.199	-0.139	-0.230	-1.135	-0.090	0.000	0.000	10.000
46	0.000	0.000	-0.614	0.525	4.810	15.100	-0.199	-0.139	-0.230	-1.138	-0.089	0.000	0.000	10.000
47	0.000	0.000	-0.620	0.527	4.620	15.000	-0.199	-0.139	-0.230	-1.146	-0.093	0.000	0.000	10.000

UNDRAINED SHEAR: DSC32 (INCREMENTAL STRESSES)

FILM No.	DELTA deg	ALFA deg	ΔP ksc	ΔQ ksc	Sig.a mV	Sig.b mV	T a mV	T b mV	U mV	Sig.a ksc	Sig.b ksc	T a ksc	T b ksc	Input V Volts
0	0.000	0.000	0.000	0.000	28.300	15.270	-0.640	0.140	0.020	0.000	0.000	0.000	0.000	0.000
1	45.000	90.000	0.000	0.000	28.300	15.270	-0.285	0.492	0.020	0.000	0.000	0.000	0.000	10.000
2	45.000	90.000	0.000	0.000	28.300	15.270	0.300	0.960	0.020	0.000	0.000	0.000	0.000	10.000
3	0.000	0.000	0.000	0.000	28.310	15.260	0.690	1.510	0.020	0.000	-0.000	0.000	0.000	10.000
4	45.000	-90.000	0.000	0.006	28.300	15.270	1.200	2.020	0.020	0.000	0.000	0.005	0.006	10.000
5	44.279	-39.355	-0.001	0.016	28.280	15.230	1.700	2.500	0.020	-0.001	-0.002	0.015	0.016	10.000
6	44.121	-2.738	-0.002	0.025	28.260	15.190	2.200	2.970	0.020	-0.002	-0.003	0.025	0.025	10.000
7	44.074	-8.093	-0.004	0.035	28.220	15.130	2.700	3.480	0.020	-0.003	-0.006	0.035	0.035	10.000
8	44.043	-14.538	-0.008	0.045	28.150	15.040	3.150	3.950	0.020	-0.006	-0.009	0.044	0.045	10.000
9	43.842	-0.185	-0.013	0.055	28.040	14.890	3.670	4.430	0.020	-0.011	-0.015	0.055	0.055	10.000
10	44.328	-1.201	-0.017	0.065	27.920	14.800	4.180	4.940	0.020	-0.016	-0.019	0.065	0.065	10.000
11	44.830	-6.066	-0.022	0.070	27.770	14.700	4.430	5.190	0.020	-0.022	-0.023	0.070	0.070	10 000
12	45.025	67.522	-0.026	0.075	27.660	14.610	4.670	5.440	0.020	-0.027	-0.026	0.075	0.075	10.000
13	45.119	-5.753	-0.030	0.080	27.570	14.530	4.920	5.670	0.020	-0.030	-0.030	0.080	0.080	10.000
14	45.071	66.450	-0.035	0.085	27.460	14.410	5.120	5.920	0.020	-0.035	-0.034	0.084	0.085	10.000
15	45.220	7.612	-0.039	0.090	27.350	14.320	5.420	6.180	0.020	-0.039	-0.038	0.090	0.090	10.000
16	44.998	-18.419	-0.045	0.095	27.210	14.140	5.660	6.410	0.020	-0.045	-0.045	0.095	0.095	10.000
17	45.023	-47.355	-0.050	0.100	27.090	14.020	5.920	6.660	0.020	-0.050	-0.050	0.100	0.100	10.000
18	44.991	65.418	-0.055	0.105	26.970	13.890	6.170	6.910	0.020	-0.055	-0.055	0.105	0.105	10.000
19	44.985	-67.076	-0.065	0.110	26.730	13.640	6.410	7.170	0.020	-0.065	-0.065	0.110	0.110	10.000
20	45.007	61.555	-0.070	0.115	26.610	13.520	6.660	7.410	0.020	-0.070	-0.070	0.115	0.115	10.000
21	45.084	-6.051	-0.077	0.120	26.440	13.360	6.920	7.660	0.020	-0.077	-0.076	0.120	0.120	10.000
22	44.975	48.889	-0.085	0.125	26.250	13.140	7.160	7.890	0.020	-0.085	-0.085	0.125	0.125	10.000
23	44.794	6.979	-0.096	0.130	26.010	12.850	7.410	8.140	0.020	-0.095	-0.097	0.130	0.130	10.000
24	45.164	7.300	-0.100	0.135	25.860	12.780	7.640	8.390	0.020	-0.101	-0.100	0.135	0.135	10.000
25	45.021	46.916	-0.109	0.140	25.680	12.560	7.880	8.630	0.020	-0.109	-0.108	0.140	0.140	10.000
26	44.919	-3.156	-0.114	0.145	25.560	12.410	8.150	8.890	0.020	-0.114	-0.114	0.145	0.145	10.000
27	44.858	-10.352	-0.118	0.150	25.470	12.300	8.400	9.150	0.020	-0.117	-0.119	0.150	0.150	10.000
28	44.946	-8.991	-0.121	0.155	25.400	12.250	8.640	9.380	0.020	-0.120	-0.121	0.155	0.155	10.000
29	45.068	-6.340	-0.124	0.160	25.300	12.180	8.900	9.630	0.020	-0.124	-0.124	0.160	0.160	10.000

FILM No.	DELTA deg	ALFA deg	ΔP ksc	ΔQ ksc	Sig.a mV	Sig.b mV	T a mV	T b mV	U mV	Sig.a ksc	Sig.b ksc	T a ksc	T b ksc	Input V Volts
30	44.974	-25.555	-0.129	0.165	25.200	12.050	9.140	9.880	0.020	-0.129	-0.129	0.165	0.165	10.000
31	45.100	-1.783	-0.136	0.170	25.010	11.890	9.390	10.120	0.020	-0.136	-0.135	0.170	0.170	10.000
32	45.416	-0.140	-0.143	0.175	24.800	11.770	9.640	10.370	0.020	-0.145	-0.140	0.175	0.175	10.000
33	45.369	0.147	-0.153	0.180	24.560	11.510	9.890	10.620	0.020	-0.155	-0.150	0.180	0.180	10.000
34	45.100	18.859	-0.173	0.185	24.110	10.960	10.130	10.880	0.020	-0.174	-0.172	0.185	0.185	10.000
35	44.955	-5.701	-0.200	0.190	23.480	10.260	10.380	11.110	0.020	-0.200	-0.200	0.190	0.190	10.000
36	45.059	19.701	-0.217	0.195	23.070	9.870	10.630	11.370	0.020	-0.217	-0.216	0.195	0.195	10.000
37	45.029	-13.301	-0.240	0.200	22.520	9.290	10.880	11.600	0.020	-0.240	-0.239	0.200	0.200	10.000
38	45.114	-2.453	-0.320	0.205	20.570	7.300	11.130	11.850	0.020	-0.321	-0.319	0.205	0.205	10.000
39	45.127	-1.872	-0.360	0.207	19.600	6.300	11.230	11.950	0.020	-0.361	-0.359	0.207	0.207	10.000
40	45.979	-0.203	-0.435	0.209	17.640	4.580	11.330	12.050	0.020	-0.442	-0.428	0.209	0.209	10.000

UNDRAINED SHEAR: DSC33 (INCREMENTAL STRESSES)

FILM No.	DELTA deg	ALFA deg	ΔP ksc	ΔQ ksc	Sig.a mV	Sig.b mV	T a mV	T b mV	U mV	Sig.a ksc	Sig.b ksc	T a ksc	T b ksc	Input V Volts
0	60.000	0.000	0.000	0.000	32.280	17.320	-0.640	0.150	-0.560	0.000	0.000	0.000	0.000	0.000
1	0.000	0.000	0.000	0.000	32.280	17.320	0.960	1.740	-0.560	0.000	0.000	0.000	0.000	10.000
2	59.468	1.880	-0.002	0.020	31.990	17.510	1.820	2.630	-0.560	-0.012	0.008	0.017	0.018	10.000
3	59.941	0.461	-0.006	0.040	31.650	17.670	2.680	3.470	-0.560	-0.026	0.014	0.035	0.035	10.000
4	59.891	0.001	-0.009	0.060	31.340	17.830	3.530	4.300	-0.560	-0.039	0.020	0.052	0.052	10.000
5	59.980	0.206	-0.015	0.080	30.950	17.940	4.390	5.170	-0.560	-0.055	0.025	0.069	0.070	10.000
6	59.928	0.097	-0.025	0.100	30.480	17.940	5.250	6.020	-0.560	-0.075	0.025	0.087	0.087	10.000
7	59.936	0.024	-0.035	0.120	30.000	17.940	6.110	6.870	-0.560	-0.095	0.025	0.104	0.104	10.000
8	59.960	0.041	-0.042	0.130	29.690	17.880	6.550	7.310	-0.560	-0.107	0.022	0.113	0.113	10.000
9	59.967	-0.028	-0.048	0.140	29.440	17.870	6.980	7.730	-0.560	-0.118	0.022	0.121	0.121	10.000
10	59.975	-0.088	-0.054	0.150	29.180	17.850	7.410	8.150	-0.560	-0.129	0.021	0.130	0.130	10.000
11	59.948	-0.067	-0.062	0.160	28.870	17.770	7.840	8.580	-0.560	-0.141	0.018	0.139	0.139	10.000
12	59.965	0.087	-0.068	0.170	28.600	17.740	8.250	9.010	-0.560	-0.153	0.017	0.147	0.147	10.000
13	59.959	0.031	-0.075	0.180	28.310	17.690	8.690	9.440	-0.560	-0.165	0.015	0.156	0.156	10.000
14	59.977	-0.019	-0.081	0.190	28.050	17.680	9.130	9.870	-0.560	-0.175	0.014	0.165	0.165	10.000
15	59.978	-0.064	-0.085	0.200	27.830	17.700	9.560	10.290	-0.560	-0.185	0.015	0.173	0.173	10.000
16	59.986	0.116	-0.091	0.210	27.540	17.650	9.970	10.730	-0.560	-0.197	0.013	0.182	0.182	10.000
17	59.941	0.016	-0.099	0.220	27.250	17.580	10.410	11.150	-0.560	-0.209	0.010	0.191	0.191	10.000
18	59.968	-0.025	-0.104	0.230	27.000	17.580	10.840	11.570	-0.560	-0.219	0.010	0.199	0.199	10.000
19	59.965	0.035	-0.112	0.240	26.690	17.510	11.270	12.010	-0.560	-0.232	0.008	0.208	0.208	10.000
20	59.971	0.043	-0.122	0.250	26.330	17.390	11.700	12.440	-0.560	-0.247	0.003	0.217	0.217	10.000
21	60.000	0.050	-0.127	0.260	26.070	17.380	12.120	12.860	-0.560	-0.258	0.002	0.225	0.225	10.000
22	60.015	0.015	-0.136	0.270	25.750	17.310	12.560	13.290	-0.560	-0.271	-0.000	0.234	0.234	10.000
23	59.987	-0.060	-0.142	0.280	25.490	17.270	12.990	13.700	-0.560	-0.282	-0.002	0.243	0.242	10.000
24	59.979	0.030	-0.149	0.290	25.180	17.200	13.420	14.150	-0.560	-0.294	-0.005	0.251	0.251	10.000
25	59.976	0.037	-0.159	0.300	24.840	17.090	13.840	14.570	-0.560	-0.309	-0.009	0.260	0.260	10.000
26	59.982	0.006	-0.168	0.310	24.490	16.990	14.290	15.010	-0.560	-0.323	-0.013	0.269	0.269	10.000
27	59.958	0.013	-0.179	0.320	24.130	16.840	14.700	15.420	-0.560	-0.338	-0.019	0.277	0.277	10.000
28	59.986	0.020	-0.189	0.330	23.740	16.710	15.140	15.860	-0.560	-0.354	-0.024	0.286	0.286	10.000
29	60.010	-0.007	-0.205	0.340	23.230	16.440	15.560	16.270	-0.560	-0.375	-0.035	0.294	0.294	10.000

FILM No.	DELTA deg	ALFA deg	ΔP ksc	ΔQ ksc	Sig.a mV	Sig.b mV	T a mV	T b mV	U mV	Sig.a ksc	Sig.b ksc	T a ksc	T b ksc	Input V Volts
30	59.972	-0.000	-0.223	0.350	22.690	16.110	16.000	16.710	-0.560	-0.398	-0.048	0.303	0.303	10.000
31	60.016	0.038	-0.239	0.360	22.170	15.850	16.420	17.140	-0.560	-0.419	-0.059	0.312	0.312	10.000
32	59.979	0.013	-0.254	0.370	21.710	15.600	16.860	17.570	-0.560	-0.438	-0.069	0.321	0.321	10.000
33	60.014	0.018	-0.265	0.380	21.300	15.440	17.270	17.980	-0.560	-0.455	-0.075	0.329	0.329	10.000
34	59.972	0.084	-0.316	0.390	19.970	14.280	17.690	18.420	-0.560	-0.511	-0.122	0.337	0.338	10.000
35	59.961	-0.002	-0.396	0.395	17.980	12.340	17.930	18.630	-0.560	-0.593	-0.199	0.342	0.342	10.000

UNDRAINED SHEAR: DSC34 (INCREMENTAL STRESSES)

FILM No.	DELTA deg	ALFA deg	ΔP ksc	ΔQ ksc	Sig.a mV	Sig.b mV	T a mV	T b mV	U mV	Sig.a ksc	Sig.b ksc	T a ksc	T b ksc	Input V Volts
0	0.000	0.000	0.000	0.000	28.660	14.940	0.000	0.000	-0.190	0.000	0.000	0.000	0.000	0.000
1	0.000	0.000	0.000	0.000	28.660	14.940	1.594	1.587	-0.190	0.000	0.000	0.000	0.000	10.000
2	0.000	0.000	-0.000	0.010	28.890	14.680	1.594	1.587	-0.190	0.010	-0.010	0.000	0.000	10.000
3	0.000	0.000	-0.005	0.020	29.020	14.320	1.594	1.587	-0.190	0.015	-0.025	0.000	0.000	10.000
4	0.000	0.000	-0.007	0.030	29.200	14.010	1.594	1.587	-0.190	0.022	-0.037	0.000	0.000	10.000
5	0.000	0.000	-0.010	0.040	29.360	13.690	1.594	1.587	-0.190	0.029	-0.050	0.000	0.000	10.000
6	0.000	0.000	-0.016	0.050	29.480	13.280	1.594	1.587	-0.190	0.034	-0.066	0.000	0.000	10.000
7	0.000	0.000	-0.023	0.060	29.550	12.850	1.594	1.587	-0.190	0.037	-0.084	0.000	0.000	10.000
8	0.000	0.000	-0.035	0.070	29.500	12.310	1.594	1.587	-0.190	0.035	-0.105	0.000	0.000	10.000
9	0.000	0.000	-0.050	0.075	29.260	11.810	1.594	1.587	-0.190	0.025	-0.125	0.000	0.000	10.000
10	0.000	0.000	-0.067	0.081	29.010	11.230	1.594	1.587	-0.190	0.015	-0.148	0.000	0.000	10.000
11	0.000	0.000	-0.081	0.084	28.740	10.820	1.594	1.587	-0.190	0.003	-0.165	0.000	0.000	10.000
12	0.000	0.000	-0.093	0.086	28.510	10.470	1.594	1.587	-0.190	-0.006	-0.179	0.000	0.000	10.000
13	0.000	0.000	-0.106	0.088	28.230	10.080	1.594	1.587	-0.190	-0.018	-0.194	0.000	0.000	10.000
14	0.000	0.000	-0.113	0.090	28.090	9.860	1.594	1.587	-0.190	-0.024	-0.203	0.000	0.000	10.000
15	0.000	0.000	-0.125	0.092	27.870	9.500	1.594	1.587	-0.190	-0.033	-0.218	0.000	0.000	10.000
16	0.000	0.000	-0.135	0.094	27.680	9.210	1.594	1.587	-0.190	-0.041	-0.229	0.000	0.000	10.000
17	0.000	0.000	-0.145	0.096	27.490	8.920	1.594	1.587	-0.190	-0.049	-0.241	0.000	0.000	10.000
18	0.000	0.000	-0.154	0.098	27.300	8.630	1.594	1.587	-0.190	-0.056	-0.253	0.000	0.000	10.000
19	0.000	0.000	-0.163	0.100	27.140	8.380	1.594	1.587	-0.190	-0.063	-0.263	0.000	0.000	10.000
20	0.000	0.000	-0.166	0.102	27.110	8.240	1.594	1.587	-0.190	-0.064	-0.268	0.000	0.000	10.000

UNDRAINED SHEAR: DSC35 (INCREMENTAL STRESSES)

FILM No.	DELTA deg	ALFA deg	ΔP ksc	ΔQ ksc	Sig.a mV	Sig.b mV	T a mV	T b mV	U mV	Sig.a ksc	Sig.b ksc	T a ksc	T b ksc	Input V Volts
0	75.000	0.000	0.000	0.000	32.280	17.270	-0.640	0.160	-0.410	0.000	0.000	0.000	0.000	0.000
1	0.000	0.000	0.000	0.000	32.280	17.270	-0.640	0.160	-0.410	0.000	0.000	0.000	0.000	10.000
2	73.079	3.722	-0.001	0.021	31.820	17.650	1.470	2.370	-0.400	-0.019	0.015	0.010	0.013	10.000
3	74.684	0.377	-0.009	0.040	31.220	17.900	1.960	2.770	-0.400	-0.044	0.025	0.020	0.021	10.000
4	74.765	0.614	-0.015	0.060	30.650	18.170	2.440	3.280	-0.400	-0.068	0.036	0.030	0.031	10.000
5	75.012	0.060	-0.028	0.080	29.940	18.300	2.930	3.720	-0.400	-0.097	0.041	0.040	0.040	10.000
6	74.888	-0.070	-0.045	0.100	29.130	18.310	3.450	4.220	-0.400	-0.131	0.042	0.050	0.050	10.000
7	75.018	-0.056	-0.056	0.110	28.640	18.250	3.680	4.450	-0.400	-0.151	0.039	0.055	0.055	10.000
8	74.990	0.067	-0.063	0.120	28.260	18.300	3.930	4.720	-0.400	-0.167	0.041	0.060	0.060	10.000
9	75.003	-0.035	-0.072	0.130	27.840	18.290	4.180	4.950	-0.400	-0.184	0.041	0.065	0.065	10.000
10	74.978	0.021	-0.082	0.140	27.400	18.250	4.420	5.200	-0.400	-0.202	0.039	0.070	0.070	10.000
11	74.997	-0.020	-0.090	0.150	26.980	18.270	4.680	5.450	-0.400	-0.220	0.040	0.075	0.075	10.000
12	74.906	0.070	-0.097	0.160	26.600	18.280	4.930	5.720	-0.400	-0.236	0.040	0.080	0.080	10.000
13	74.986	-0.047	-0.106	0.170	26.190	18.310	5.180	5.940	-0.400	-0.253	0.042	0.085	0.085	10.000
14	75.048	0.034	-0.117	0.180	25.690	18.250	5.410	6.190	-0.400	-0.273	0.039	0.090	0.090	10.000
15	74.997	0.001	-0.125	0.190	25.310	18.270	5.670	6.440	-0.400	-0.289	0.040	0.095	0.095	10.000
16	74.981	0.038	-0.136	0.200	24.830	18.190	5.910	6.690	-0.400	-0.309	0.037	0.100	0.100	10.000
17	74.992	0.009	-0.145	0.210	24.410	18.190	6.160	6.930	-0.400	-0.326	0.037	0.105	0.105	10.000
18	74.993	-0.019	-0.155	0.220	23.950	18.160	6.420	7.180	-0.400	-0.345	0.036	0.110	0.110	10.000
19	74.972	-0.014	-0.169	0.230	23.400	18.010	6.670	7.430	-0.400	-0.368	0.030	0.115	0.115	10.000
20	74.972	-0.038	-0.181	0.240	22.910	17.930	6.920	7.670	-0.400	-0.389	0.026	0.120	0.120	10.000
21	74.985	0.020	-0.195	0.250	22.370	17.800	7.150	7.920	-0.400	-0.411	0.021	0.125	0.125	10.000
22	74.990	-0.003	-0.208	0.260	21.830	17.690	7.410	8.170	-0.400	-0.433	0.017	0.130	0.130	10.000
23	74.998	-0.000	-0.220	0.270	21.350	17.620	7.650	8.410	-0.400	-0.453	0.014	0.135	0.135	10.000
24	74.999	0.002	-0.231	0.280	20.870	17.560	7.900	8.660	-0.400	-0.473	0.012	0.140	0.140	10.000
25	75.011	-0.018	-0.246	0.290	20.300	17.410	8.150	8.900	-0.400	-0.497	0.006	0.145	0.145	10.000
26	75.011	-0.015	-0.258	0.300	19.800	17.330	8.400	9.150	-0.400	-0.518	0.002	0.150	0.150	10.000
27	74.994	-0.012	-0.270	0.310	19.290	17.220	8.650	9.400	-0.400	-0.539	-0.002	0.155	0.155	10.000
28	74.997	0.033	-0.285	0.320	18.730	17.080	8.890	9.660	-0.400	-0.562	-0.008	0.160	0.160	10.000
29	74.991	-0.006	-0.299	0.330	18.180	16.940	9.150	9.900	-0.400	-0.585	-0.013	0.165	0.165	10.000

FILM No.	DELTA deg	ALFA deg	ΔP ksc	ΔQ ksc	Sig.a mV	Sig.b mV	T a mV	T b mV	U mV	Sig.a ksc	Sig.b ksc	T a ksc	T b ksc	Input V Volts
30	75.000	-0.023	-0.312	0.340	17.650	16.830	9.400	10.140	-0.400	-0.607	-0.018	0.170	0.170	10.000
31	75.015	-0.001	-0.325	0.350	17.130	16.720	9.630	10.380	-0.400	-0.628	-0.022	0.175	0.175	10.000
32	74.982	-0.017	-0.342	0.360	16.510	16.500	9.900	10.640	-0.400	-0.654	-0.031	0.180	0.180	10.000
33	75.000	0.003	-0.360	0.370	15.870	16.270	10.130	10.880	-0.400	-0.681	-0.040	0.185	0.185	10.000
34	74.991	0.023	-0.379	0.380	15.200	16.010	10.380	11.140	-0.400	-0.708	-0.050	0.190	0.190	10.000
35	74.991	0.007	-0.404	0.390	14.410	15.620	10.630	11.380	-0.400	-0.741	-0.066	0.195	0.195	10.000
36	74.992	-0.008	-0.428	0.400	13.610	15.220	10.880	11.620	-0.400	-0.774	-0.082	0.200	0.200	10.000
37	74.995	-0.006	-0.455	0.410	12.750	14.770	11.130	11.870	-0.400	-0.810	-0.100	0.205	0.205	10.000
38	74.992	-0.004	-0.472	0.420	12.130	14.560	11.380	12.120	-0.400	-0.836	-0.108	0.210	0.210	10.000
39	74.992	-0.002	-0.497	0.430	11.330	14.150	11.620	12.360	-0.400	-0.869	-0.125	0.215	0.215	10.000
40	74.984	0.015	-0.515	0.440	10.680	13.910	11.870	12.620	-0.400	-0.896	-0.134	0.220	0.220	10.000
41	74.999	0.032	-0.530	0.450	10.090	13.750	12.110	12.870	-0.400	-0.920	-0.141	0.225	0.225	10.000
42	75.010	0.003	-0.535	0.455	9.880	13.760	12.240	12.980	-0.400	-0.929	-0.140	0.227	0.227	10.000
43	74.986	-0.011	-0.539	0.460	9.690	13.760	12.380	13.110	-0.400	-0.937	-0.140	0.230	0.230	10.000
44	75.013	-0.024	-0.543	0.465	9.480	13.770	12.490	13.210	-0.400	-0.946	-0.140	0.232	0.232	10.000
45	74.992	0.005	-0.540	0.470	9.450	13.950	12.620	13.360	-0.280	-0.947	-0.133	0.235	0.235	10.000

UNDRAINED SHEAR: DSC31 (TOTAL STRESSES)

FILM No.	DELTA deg	ALFA deg	P′ ksc	Q ksc	σ_3 ksc	Sig.a mV	Sig.b mV	T a mV	T b mV	U mV	Sig.a ksc	Sig.b ksc	T a ksc	T b ksc	Input V Volts
0	0.000	0.000	0.000	0.000		0.930	0.400	-0.554	-0.492	-0.230	0.000	0.000	0.000	0.000	0.000
1	90.000	-0.001	0.988	0.311	0.677	32.260	17.330	-0.200	-0.139	-0.230	1.299	0.678	-0.000	0.000	10.000
2	0.001	0.001	0.985	0.300	0.677	31.920	17.530	-0.199	-0.139	-0.230	1.285	0.686	0.000	0.000	10.000
3	0.001	0.001	0.983	0.280	0.676	31.380	17.960	-0.199	-0.139	-0.230	1.263	0.703	0.000	0.000	10.000
4	0.001	0.001	0.978	0.261	0.676	30.790	18.310	-0.199	-0.139	-0.230	1.238	0.717	0.000	0.000	10.000
5	0.001	0.001	0.970	0.240	0.674	30.100	18.630	-0.199	-0.139	-0.230	1.210	0.730	0.000	0.000	10.000
6	0.001	0.001	0.959	0.220	0.673	29.360	18.880	-0.199	-0.139	-0.230	1.179	0.740	0.000	0.000	10.000
7	0.001	0.001	0.948	0.200	0.672	28.620	19.100	-0.199	-0.139	-0.230	1.148	0.748	0.000	0.000	10.000
8	87.993	4.017	0.933	0.181	0.669	27.810	19.240	-0.199	-1.390	27.810	1.115	0.754	0.000	-0.025	10.000
9	0.001	0.001	0.921	0.160	0.667	27.000	19.420	-0.199	-0.139	-0.230	1.081	0.761	0.000	0.000	10.000
10	0.002	0.001	0.912	0.140	0.665	26.310	19.700	-0.199	-0.139	-0.230	1.053	0.772	0.000	0.000	10.000
11	0.002	0.001	0.895	0.120	0.662	25.400	19.750	-0.199	-0.139	-0.230	1.015	0.774	0.000	0.000	10.000
12	0.002	0.002	0.873	0.100	0.657	24.380	19.710	-0.199	-0.139	-0.230	0.973	0.773	0.000	0.000	10.000
13	0.003	0.002	0.856	0.080	0.653	23.500	19.790	-0.199	-0.139	-0.230	0.936	0.776	0.000	0.000	10.000
14	0.004	0.003	0.841	0.060	0.647	22.640	19.910	-0.199	-0.139	-0.230	0.900	0.781	0.000	0.000	10.000
15	0.006	0.004	0.816	0.040	0.640	21.560	19.780	-0.199	-0.139	-0.230	0.856	0.776	0.000	0.000	10.000
16	0.012	0.008	0.798	0.021	0.633	20.660	19.810	-0.199	-0.139	-0.230	0.818	0.777	0.000	0.000	10.000
17	0.780	0.558	0.771	0.000	0.622	19.520	19.650	-0.199	-0.139	-0.230	0.771	0.770	0.000	0.000	10.000
18	89.977	-0.017	0.756	0.010	0.617	18.900	19.540	-0.199	-0.139	-0.230	0.745	0.766	0.000	0.000	10.000
19	89.988	-0.009	0.740	0.020	0.612	18.300	19.400	-0.199	-0.139	-0.230	0.720	0.760	0.000	0.000	10.000
20	89.992	-0.006	0.726	0.030	0.608	17.720	19.300	-0.199	-0.139	-0.230	0.696	0.756	0.000	0.000	10.000
21	89.994	-0.004	0.717	0.040	0.602	17.260	19.300	-0.199	-0.139	-0.230	0.677	0.756	0.000	0.000	10.000
22	89.995	-0.003	0.699	0.050	0.596	16.570	19.120	-0.199	-0.139	-0.230	0.649	0.749	0.000	0.000	10.000
23	89.996	-0.003	0.689	0.060	0.592	16.100	19.120	-0.199	-0.139	-0.230	0.629	0.749	0.000	0.000	10.000
24	89.997	-0.002	0.670	0.070	0.584	15.400	18.890	-0.199	-0.139	-0.230	0.600	0.740	0.000	0.000	10.000
25	89.997	-0.002	0.655	0.080	0.579	14.800	18.760	-0.199	-0.139	-0.230	0.575	0.735	0.000	0.000	10.000
26	89.997	-0.002	0.642	0.090	0.575	14.240	18.680	-0.199	-0.139	-0.230	0.552	0.732	0.000	0.000	10.000
27	89.998	-0.002	0.621	0.100	0.568	13.490	18.430	-0.199	-0.139	-0.230	0.521	0.722	0.000	0.000	10.000
28	89.998	-0.002	0.606	0.110	0.564	12.900	18.300	-0.199	-0.139	-0.230	0.496	0.716	0.000	0.000	10.000
29	89.998	-0.001	0.586	0.120	0.557	12.170	18.050	-0.199	-0.139	-0.230	0.466	0.706	0.000	0.000	10.000

FILM No.	DELTA deg	ALFA deg	P′ ksc	Q ksc	σ_2 ksc	Sig.a mV	Sig.b mV	T a mV	T b mV	U mV	Sig.a ksc	Sig.b ksc	T a ksc	T b ksc	Input V Volts
30	89.998	-0.001	0.574	0.130	0.554	11.640	18.000	-0.199	-0.139	-0.230	0.444	0.704	0.000	0.000	10.000
31	89.998	-0.001	0.558	0.140	0.549	11.020	17.850	-0.199	-0.139	-0.230	0.418	0.698	0.000	0.000	10.000
32	89.998	-0.001	0.538	0.150	0.543	10.280	17.590	-0.199	-0.139	-0.230	0.388	0.688	0.000	0.000	10.000
33	89.998	-0.001	0.523	0.155	0.540	9.790	17.340	-0.199	-0.139	-0.230	0.367	0.678	0.000	0.000	10.000
34	89.999	-0.001	0.507	0.160	0.536	9.300	17.080	-0.199	-0.139	-0.230	0.347	0.668	0.000	0.000	10.000
35	89.999	-0.001	0.492	0.165		8.810	16.810	-0.199	-0.139	-0.230	0.327	0.657	0.000	0.000	10.000
35	89.999	-0.001	0.486	0.165	0.532	8.670	16.660	-0.199	-0.139	-0.350	0.321	0.651	0.000	0.000	10.000
36	89.999	-0.001	0.470	0.170	0.525	8.160	16.400	-0.199	-0.139	-0.230	0.300	0.640	0.000	0.000	10.000
37	89.999	-0.001	0.459	0.175	0.518	7.780	16.250	-0.199	-0.139	-0.230	0.284	0.634	0.000	0.000	10.000
38	89.999	-0.001	0.450	0.180	0.515	7.450	16.150	-0.199	-0.139	-0.230	0.270	0.630	0.000	0.000	10.000
39	89.999	-0.001	0.440	0.185	0.510	7.070	16.010	-0.199	-0.139	-0.230	0.255	0.625	0.000	0.000	10.000
40	89.999	-0.001	0.430	0.190	0.507	6.720	15.910	-0.199	-0.139	-0.230	0.240	0.621	0.000	0.000	10.000
41	89.999	-0.001	0.417	0.197	0.504	6.230	15.730	-0.199	-0.139	-0.230	0.220	0.614	0.000	0.000	10.000
42	89.999	-0.001	0.402	0.200	0.499	5.800	15.450	-0.199	-0.139	-0.230	0.202	0.602	0.000	0.000	10.000
43	89.999	-0.001	0.387	0.205	0.496	5.330	15.200	-0.199	-0.139	-0.230	0.182	0.592	0.000	0.000	10.000
44	89.999	-0.001	0.380	0.210	0.502	5.030	15.120	-0.199	-0.139	-0.230	0.170	0.589	0.000	0.000	10.000
45	89.999	-0.001	0.376	0.212	0.505	4.900	15.090	-0.199	-0.139	-0.230	0.165	0.588	0.000	0.000	10.000
46	89.999	-0.001	0.375	0.214	0.506	4.810	15.100	-0.199	-0.139	-0.230	0.161	0.588	0.000	0.000	10.000
47	89.999	-0.001	0.369	0.216	0.518	4.620	15.000	-0.199	-0.139	-0.230	0.153	0.584	0.000	0.000	10.000

UNDRAINED SHEAR: DSC32 (TOTAL STRESSES)

FILM No.	DELTA deg	ALFA deg	P' ksc	Q ksc	σ_2 ksc	Sig.a mV	Sig.b mV	T a mV	T b mV	U mV	Sig.a ksc	Sig.b ksc	T a ksc	T b ksc	Input V Volts
0	0.000	0.000	0.000	0.000		0.930	0.400	-0.640	0.140	0.020	0.000	0.000	0.000	0.000	0.000
1	0.000	0.000	0.865	0.270	0.587	28.300	15.270	-0.285	0.492	0.020	1.135	0.595	0.000	0.000	10.000
2	0.000	0.000	0.865	0.270	0.587	28.300	15.270	0.300	0.960	0.020	1.135	0.595	0.000	0.000	10.000
3	0.000	0.000	0.865	0.270	0.587	28.310	15.260	0.690	1.510	0.020	1.136	0.595	0.000	0.000	10.000
4	0.576	-0.105	0.865	0.270	0.587	28.300	15.270	1.200	2.020	0.020	1.135	0.595	0.005	0.006	10.000
5	1.622	-0.067	0.864	0.271	0.587	28.280	15.230	1.700	2.500	0.020	1.134	0.593	0.015	0.016	10.000
6	2.651	-0.008	0.863	0.272	0.587	28.260	15.190	2.200	2.970	0.020	1.133	0.592	0.025	0.025	10.000
7	3.712	-0.034	0.861	0.273	0.588	28.220	15.130	2.700	3.480	0.020	1.132	0.589	0.035	0.035	10.000
8	4.667	-0.082	0.857	0.275	0.588	28.150	15.040	3.150	3.950	0.020	1.129	0.586	0.044	0.045	10.000
9	5.683	-0.002	0.852	0.278	0.588	28.040	14.890	3.670	4.430	0.020	1.124	0.580	0.055	0.055	10.000
10	6.733	-0.007	0.848	0.279	0.587	27.920	14.800	4.180	4.940	0.020	1.119	0.576	0.065	0.065	10.000
11	7.264	-0.009	0.843	0.279	0.586	27.770	14.700	4.430	5.190	0.020	1.113	0.572	0.070	0.070	10.000
12	7.766	-0.033	0.839	0.280	0.582	27.660	14.610	4.670	5.440	0.020	1.109	0.569	0.075	0.075	10.000
13	8.249	0.007	0.835	0.281	0.583	27.570	14.530	4.920	5.670	0.020	1.105	0.565	0.080	0.080	10.000
14	8.687	-0.103	0.830	0.283	0.583	27.460	14.410	5.120	5.920	0.020	1.100	0.561	0.084	0.085	10.000
15	9.246	-0.020	0.826	0.284	0.583	27.350	14.320	5.420	6.180	0.020	1.096	0.557	0.090	0.090	10.000
16	9.675	-0.001	0.820	0.286	0.585	27.210	14.140	5.660	6.410	0.020	1.090	0.550	0.095	0.095	10.000
17	10.161	0.018	0.815	0.288	0.585	27.090	14.020	5.920	6.660	0.020	1.085	0.545	0.100	0.100	10.000
18	10.625	0.016	0.810	0.290	0.584	26.970	13.890	6.170	6.910	0.020	1.080	0.540	0.105	0.105	10.000
19	11.087	-0.030	0.800	0.292	0.581	26.730	13.640	6.410	7.170	0.020	1.070	0.530	0.110	0.110	10.000
20	11.538	-0.011	0.795	0.293	0.583	26.610	13.520	6.660	7.410	0.020	1.065	0.525	0.115	0.115	10.000
21	12.010	0.008	0.788	0.295	0.582	26.440	13.360	6.920	7.660	0.020	1.058	0.519	0.120	0.120	10.000
22	12.409	0.027	0.780	0.298	0.576	26.250	13.140	7.160	7.890	0.020	1.050	0.510	0.125	0.125	10.000
23	12.813	0.024	0.769	0.301	0.569	26.010	12.850	7.410	8.140	0.020	1.040	0.498	0.130	0.130	10.000
24	13.299	-0.021	0.765	0.301	0.564	25.860	12.780	7.640	8.390	0.020	1.034	0.495	0.135	0.135	10.000
25	13.680	-0.023	0.756	0.304	0.556	25.680	12.560	7.880	8.630	0.020	1.026	0.487	0.140	0.140	10.000
26	14.102	-0.005	0.751	0.307	0.553	25.560	12.410	8.150	8.890	0.020	1.021	0.481	0.145	0.145	10.000
27	14.507	-0.029	0.747	0.310	0.550	25.470	12.300	8.400	9.150	0.020	1.018	0.476	0.150	0.150	10.000
28	14.909	-0.010	0.745	0.312	0.547	25.400	12.250	8.640	9.380	0.020	1.015	0.474	0.155	0.155	10.000
29	15.348	0.009	0.741	0.314	0.545	25.300	12.180	8.900	9.630	0.020	1.011	0.471	0.160	0.160	10.000

FILM No.	DELTA deg	ALFA deg	P' ksc	Q ksc	σ_2 ksc	Sig.a mV	Sig.b mV	T a mV	T b mV	U mV	Sig.a ksc	Sig.b ksc	T a ksc	T b ksc	Input V Volts
30	15.709	-0.015	0.736	0.317	0.541	25.200	12.050	9.140	9.880	0.020	1.007	0.466	0.165	0.165	10.000
31	16.123	0.004	0.729	0.319	0.536	25.010	11.890	9.390	10.120	0.020	0.999	0.460	0.170	0.170	10.000
32	16.599	0.001	0.723	0.320	0.531	24.800	11.770	9.640	10.370	0.020	0.990	0.455	0.175	0.175	10.000
33	16.964	-0.001	0.712	0.323	0.519	24.560	11.510	9.890	10.620	0.020	0.980	0.445	0.180	0.180	10.000
34	17.249	-0.047	0.692	0.327	0.512	24.110	10.960	10.130	10.880	0.020	0.961	0.423	0.185	0.185	10.000
35	17.549	-0.006	0.665	0.330	0.494	23.480	10.260	10.380	11.110	0.020	0.935	0.395	0.190	0.190	10.000
36	17.946	-0.030	0.649	0.333	0.481	23.070	9.870	10.630	11.370	0.020	0.918	0.379	0.195	0.195	10.000
37	18.271	0.010	0.626	0.336	0.466	22.520	9.290	10.880	11.600	0.020	0.895	0.356	0.200	0.200	10.000
38	18.646	0.007	0.545	0.338	0.418	20.570	7.300	11.130	11.850	0.020	0.815	0.276	0.205	0.205	10.000
39	18.787	0.006	0.505	0.340	0.400	19.600	6.300	11.230	11.950	0.020	0.774	0.236	0.207	0.207	10.000
40	19.248	0.006	0.430	0.336	0.370	17.640	4.580	11.330	12.050	0.020	0.693	0.167	0.209	0.209	10.000

UNDRAINED SHEAR: DSC33 (TOTAL STRESSES)

FILM No.	DELTA deg	ALFA deg	P' ksc	Q ksc	σ_2 ksc	Sig.a mV	Sig.b mV	T a mV	T b mV	U mV	Sig.a ksc	Sig.b ksc	T a ksc	T b ksc	Input V Volts
0	60.000	0.000	0.000	0.000		0.930	0.400	-0.640	0.150	-0.560	0.000	0.000	0.000	0.000	0.000
1	0.007	0.004	0.989	0.312	0.678	32.280	17.320	0.960	1.740	-0.560	1.300	0.677	0.000	0.000	10.000
2	1.684	-0.061	0.986	0.302	0.679	31.990	17.510	1.820	2.630	-0.560	1.288	0.685	0.017	0.018	10.000
3	3.417	-0.032	0.983	0.294	0.678	31.650	17.670	2.680	3.470	-0.560	1.274	0.691	0.035	0.035	10.000
4	5.217	-0.000	0.979	0.287	0.678	31.340	17.830	3.530	4.300	-0.560	1.261	0.698	0.052	0.052	10.000
5	7.165	-0.030	0.973	0.280	0.678	30.950	17.940	4.390	5.170	-0.560	1.245	0.702	0.069	0.070	10.000
6	9.156	-0.018	0.964	0.276	0.678	30.480	17.940	5.250	6.020	-0.560	1.226	0.702	0.087	0.087	10.000
7	11.211	-0.006	0.954	0.272	0.673	30.000	17.940	6.110	6.870	-0.560	1.206	0.702	0.104	0.104	10.000
8	12.290	-0.011	0.946	0.271	0.672	29.690	17.880	6.550	7.310	-0.560	1.193	0.700	0.113	0.113	10.000
9	13.337	0.008	0.941	0.270	0.671	29.440	17.870	6.980	7.730	-0.560	1.182	0.699	0.121	0.121	10.000
10	14.389	0.028	0.935	0.270	0.668	29.180	17.850	7.410	8.150	-0.560	1.172	0.698	0.130	0.130	10.000
11	15.443	0.023	0.927	0.270	0.666	28.870	17.770	7.840	8.580	-0.560	1.159	0.695	0.139	0.139	10.000
12	16.486	-0.033	0.921	0.270	0.664	28.600	17.740	8.250	9.010	-0.560	1.148	0.694	0.147	0.147	10.000
13	17.554	-0.013	0.914	0.271	0.663	28.310	17.690	8.690	9.440	-0.560	1.136	0.692	0.156	0.156	10.000
14	18.625	0.008	0.908	0.272	0.657	28.050	17.680	9.130	9.870	-0.560	1.125	0.692	0.165	0.165	10.000
15	19.656	0.030	0.904	0.274	0.656	27.830	17.700	9.560	10.290	-0.560	1.116	0.692	0.173	0.173	10.000
16	20.678	-0.059	0.897	0.275	0.653	27.540	17.650	9.970	10.730	-0.560	1.104	0.690	0.182	0.182	10.000
17	21.665	-0.009	0.890	0.278	0.650	27.250	17.580	10.410	11.150	-0.560	1.092	0.688	0.191	0.191	10.000
18	22.668	0.014	0.884	0.280	0.647	27.000	17.580	10.840	11.570	-0.560	1.081	0.688	0.199	0.199	10.000
19	23.656	-0.022	0.876	0.283	0.644	26.690	17.510	11.270	12.010	-0.560	1.068	0.685	0.208	0.208	10.000
20	24.619	-0.029	0.867	0.286	0.640	26.330	17.390	11.700	12.440	-0.560	1.053	0.680	0.217	0.217	10.000
21	25.557	-0.036	0.861	0.289	0.638	26.070	17.380	12.120	12.860	-0.560	1.043	0.680	0.225	0.225	10.000
22	26.495	-0.011	0.853	0.293	0.631	25.750	17.310	12.560	13.290	-0.560	1.029	0.677	0.234	0.234	10.000
23	27.342	0.049	0.847	0.297	0.628	25.490	17.270	12.990	13.700	-0.560	1.019	0.675	0.243	0.242	10.000
24	28.220	-0.026	0.839	0.302	0.624	25.180	17.200	13.420	14.150	-0.560	1.006	0.672	0.251	0.251	10.000
25	29.037	-0.034	0.830	0.306	0.619	24.840	17.090	13.840	14.570	-0.560	0.992	0.668	0.260	0.260	10.000
26	29.886	-0.006	0.820	0.311	0.614	24.490	16.990	14.290	15.010	-0.560	0.977	0.664	0.269	0.269	10.000
27	30.614	-0.014	0.810	0.316	0.610	24.130	16.840	14.700	15.420	-0.560	0.962	0.658	0.277	0.277	10.000
28	31.424	-0.023	0.799	0.321	0.603	23.740	16.710	15.140	15.860	-0.560	0.946	0.653	0.286	0.286	10.000
29	32.163	0.009	0.783	0.327	0.590	23.230	16.440	15.560	16.270	-0.560	0.925	0.642	0.294	0.294	10.000

FILM No.	DELTA deg	ALFA deg	P' ksc	Q ksc	σ_2 ksc	Sig.a mV	Sig.b mV	T a mV	T b mV	U mV	Sig.a ksc	Sig.b ksc	T a ksc	T b ksc	Input V Volts
30	32.852	0.000	0.766	0.333	0.577	22.690	16.110	16.000	16.710	-0.560	0.902	0.629	0.303	0.303	10.000
31	33.582	-0.053	0.749	0.338	0.567	22.170	15.850	16.420	17.140	-0.560	0.881	0.618	0.312	0.312	10.000
32	34.213	-0.019	0.735	0.345	0.556	21.710	15.600	16.860	17.570	-0.560	0.862	0.608	0.321	0.321	10.000
33	34.864	-0.029	0.723	0.351	0.547	21.300	15.440	17.270	17.980	-0.560	0.845	0.602	0.329	0.329	10.000
34	35.434	-0.139	0.672	0.357	0.510	19.970	14.280	17.690	18.420	-0.560	0.790	0.555	0.337	0.338	10.000
35	35.736	0.004	0.593	0.361	0.444	17.980	12.340	17.930	18.630	-0.560	0.707	0.478	0.342	0.342	10.000

UNDRAINED SHEAR: DSC34 (TOTAL STRESSES)

FILM No.	DELTA deg	ALFA deg	P′ ksc	Q ksc	σ_2 ksc	Sig.a mV	Sig.b mV	T a mV	T b mV	U mV	Sig.a ksc	Sig.b ksc	T a ksc	T b ksc	Input V Volts
0	0.000	0.000	0.000	0.000		0.930	0.400	0.000	0.000	-0.190	0.000	0.000	0.000	0.000	0.000
1	0.000	0.000	0.866	0.284	0.561	28.660	14.940	1.594	1.587	-0.190	1.150	0.582	0.000	0.000	10.000
2	0.000	0.000	0.866	0.294	0.559	28.890	14.680	1.594	1.587	-0.190	1.160	0.571	0.000	0.000	10.000
3	0.000	0.000	0.861	0.304	0.560	29.020	14.320	1.594	1.587	-0.190	1.165	0.557	0.000	0.000	10.000
4	0.000	0.000	0.859	0.314	0.563	29.200	14.010	1.594	1.587	-0.190	1.172	0.545	0.000	0.000	10.000
5	0.000	0.000	0.855	0.324	0.565	29.360	13.690	1.594	1.587	-0.190	1.179	0.532	0.000	0.000	10.000
6	0.000	0.000	0.850	0.334	0.567	29.480	13.280	1.594	1.587	-0.190	1.184	0.515	0.000	0.000	10.000
7	0.000	0.000	0.843	0.344	0.570	29.550	12.850	1.594	1.587	-0.190	1.187	0.498	0.000	0.000	10.000
8	0.000	0.000	0.831	0.354	0.569	29.500	12.310	1.594	1.587	-0.190	1.185	0.477	0.000	0.000	10.000
9	0.000	0.000	0.816	0.359	0.567	29.260	11.810	1.594	1.587	-0.190	1.175	0.457	0.000	0.000	10.000
10	0.000	0.000	0.799	0.366	0.563	29.010	11.230	1.594	1.587	-0.190	1.165	0.433	0.000	0.000	10.000
11	0.000	0.000	0.785	0.368	0.558	28.740	10.820	1.594	1.587	-0.190	1.153	0.417	0.000	0.000	10.000
12	0.000	0.000	0.773	0.370	0.557	28.510	10.470	1.594	1.587	-0.190	1.144	0.403	0.000	0.000	10.000
13	0.000	0.000	0.760	0.372	0.552	28.230	10.080	1.594	1.587	-0.190	1.132	0.387	0.000	0.000	10.000
14	0.000	0.000	0.753	0.374	0.551	28.090	9.860	1.594	1.587	-0.190	1.126	0.379	0.000	0.000	10.000
15	0.000	0.000	0.741	0.377	0.547	27.870	9.500	1.594	1.587	-0.190	1.117	0.364	0.000	0.000	10.000
16	0.000	0.000	0.731	0.378	0.544	27.680	9.210	1.594	1.587	-0.190	1.109	0.353	0.000	0.000	10.000
17	0.000	0.000	0.721	0.380	0.541	27.490	8.920	1.594	1.587	-0.190	1.102	0.341	0.000	0.000	10.000
18	0.000	0.000	0.712	0.382	0.538	27.300	8.630	1.594	1.587	-0.190	1.094	0.329	0.000	0.000	10.000
19	0.000	0.000	0.703	0.384	0.535	27.140	8.380	1.594	1.587	-0.190	1.087	0.319	0.000	0.000	10.000
20	0.000	0.000	0.700	0.386	0.533	27.110	8.240	1.594	1.587	-0.190	1.086	0.314	0.000	0.000	10.000

UNDRAINEL SHEAR: DSC35 (TOTAL STRESSES)

FILM No.	DELTA deg	ALFA deg	P' ksc	Q ksc	σ_z ksc	Sig.a mV	Sig.b mV	T a mV	T b mV	U mV	Sig.a ksc	Sig.b ksc	T a ksc	T b ksc	Input V Volts
0	75.000	0.000	0.000	0.000		0.930	0.400	-0.640	0.160	-0.410	0.000	0.000	0.000	0.000	0.000
1	0.000	0.000	0.988	0.313	0.675	32.280	17.270	-0.640	0.160	-0.410	1.300	0.675	0.000	0.000	10.000
2	1.114	-0.216	0.986	0.296	0.672	31.820	17.650	1.470	2.370	-0.400	1.281	0.690	0.010	0.013	10.000
3	2.107	-0.047	0.978	0.279	0.674	31.220	17.900	1.960	2.770	-0.400	1.256	0.700	0.020	0.021	10.000
4	3.334	-0.122	0.972	0.262	0.673	30.650	18.170	2.440	3.280	-0.400	1.233	0.711	0.030	0.031	10.000
5	4.652	-0.017	0.960	0.247	0.671	29.940	18.300	2.930	3.720	-0.400	1.203	0.716	0.040	0.040	10.000
6	6.248	0.027	0.943	0.232	0.669	29.130	18.310	3.450	4.220	-0.400	1.170	0.717	0.050	0.050	10.000
7	7.076	0.025	0.932	0.224	0.664	28.640	18.250	3.680	4.450	-0.400	1.149	0.714	0.055	0.055	10.000
8	8.035	-0.033	0.925	0.217	0.662	28.260	18.300	3.930	4.720	-0.400	1.133	0.716	0.060	0.060	10.000
9	8.990	0.020	0.916	0.210	0.661	27.840	18.290	4.180	4.950	-0.400	1.116	0.716	0.065	0.065	10.000
10	10.012	-0.013	0.906	0.204	0.656	27.400	18.250	4.420	5.200	-0.400	1.098	0.714	0.070	0.070	10.000
11	11.167	0.014	0.898	0.197	0.653	26.980	18.270	4.680	5.450	-0.400	1.080	0.715	0.075	0.075	10.000
12	12.350	-0.056	0.890	0.192	0.651	26.600	18.280	4.930	5.720	-0.400	1.065	0.716	0.080	0.080	10.000
13	13.600	0.042	0.882	0.186	0.649	26.190	18.310	5.180	5.940	-0.400	1.048	0.717	0.085	0.085	10.000
14	14.952	-0.034	0.871	0.180	0.646	25.690	18.250	5.410	6.190	-0.400	1.027	0.714	0.090	0.090	10.000
15	16.353	-0.001	0.863	0.176	0.643	25.310	18.270	5.670	6.440	-0.400	1.011	0.715	0.095	0.095	10.000
16	17.801	-0.048	0.851	0.172	0.639	24.830	18.190	5.910	6.690	-0.400	0.991	0.712	0.100	0.100	10.000
17	19.354	-0.012	0.843	0.168	0.635	24.410	18.190	6.160	6.930	-0.400	0.974	0.712	0.105	0.105	10.000
18	21.031	0.029	0.833	0.164	0.633	23.950	18.160	6.420	7.180	-0.400	0.955	0.711	0.110	0.110	10.000
19	22.693	0.025	0.818	0.162	0.629	23.400	18.010	6.670	7.430	-0.400	0.932	0.705	0.115	0.115	10.000
20	24.413	0.076	0.807	0.160	0.624	22.910	17.930	6.920	7.670	-0.400	0.912	0.702	0.120	0.120	10.000
21	26.168	-0.045	0.793	0.158	0.621	22.370	17.800	7.150	7.920	-0.400	0.889	0.696	0.125	0.125	10.000
22	28.047	0.009	0.779	0.157	0.617	21.830	17.690	7.410	8.170	-0.400	0.867	0.692	0.130	0.130	10.000
23	29.845	0.001	0.768	0.156	0.613	21.350	17.620	7.650	8.410	-0.400	0.847	0.689	0.135	0.135	10.000
24	31.695	-0.009	0.757	0.157	0.609	20.870	17.560	7.900	8.660	-0.400	0.827	0.687	0.140	0.140	10.000
25	33.536	0.074	0.742	0.157	0.605	20.300	17.410	8.150	8.900	-0.400	0.803	0.681	0.145	0.145	10.000
26	35.347	0.073	0.730	0.159	0.601	19.800	17.330	8.400	9.150	-0.400	0.783	0.678	0.150	0.150	10.000
27	37.050	0.071	0.717	0.161	0.596	19.290	17.220	8.650	9.400	-0.400	0.761	0.673	0.155	0.155	10.000
28	38.773	-0.259	0.702	0.164	0.592	18.730	17.080	8.890	9.660	-0.400	0.738	0.668	0.160	0.160	10.000
29	40.400	0.064	0.689	0.167	0.591	18.180	16.940	9.150	9.900	-0.400	0.715	0.662	0.165	0.165	10.000

FILM No.	DELTA deg	ALFA deg	P ksc	Q' ksc	σ_2 ksc	Sig.a mV	Sig.b mV	T a mV	T b mV	U mV	Sig.a ksc	Sig.b ksc	T a ksc	T b ksc	Input V Volts
30	41.986	0.380	0.677	0.171	0.587	17.650	16.830	9.400	10.140	-0.400	0.693	0.658	0.170	0.170	10.000
31	43.465	0.041	0.663	0.175	0.586	17.130	16.720	9.630	10.380	-0.400	0.672	0.653	0.175	0.175	10.000
32	44.854	5.884	0.664	0.181	0.585	16.510	16.500	9.900	10.640	-0.400	0.646	0.644	0.180	0.180	10.000
33	46.200	0.130	0.628	0.185	0.576	15.870	16.270	10.130	10.880	-0.400	0.620	0.635	0.185	0.185	10.000
34	47.472	0.457	0.610	0.191	0.570	15.200	16.010	10.380	11.140	-0.400	0.592	0.625	0.190	0.190	10.000
35	48.655	0.096	0.584	0.197	0.562	14.410	15.620	10.630	11.380	-0.400	0.559	0.609	0.195	0.195	10.000
36	49.770	-0.080	0.559	0.203	0.555	13.610	15.220	10.880	11.620	-0.400	0.526	0.593	0.200	0.200	10.000
37	50.847	-0.047	0.532	0.209	0.548	12.750	14.770	11.130	11.870	-0.400	0.490	0.575	0.205	0.205	10.000
38	51.834	-0.026	0.515	0.216	0.543	12.130	14.560	11.380	12.120	-0.400	0.465	0.567	0.210	0.210	10.000
39	52.734	-0.011	0.491	0.223	0.538	11.330	14.150	11.620	12.360	-0.400	0.431	0.550	0.215	0.215	10.000
40	53.603	0.086	0.473	0.230	0.535	10.680	13.910	11.870	12.620	-0.400	0.404	0.541	0.220	0.220	10.000
41	54.466	0.160	0.458	0.238	0.531	10.090	13.750	12.110	12.870	-0.400	0.380	0.534	0.225	0.225	10.000
42	54.884	0.013	0.453	0.242	0.530	9.880	13.760	12.240	12.980	-0.400	0.371	0.535	0.227	0.227	10.000
43	55.209	-0.050	0.449	0.246	0.529	9.690	13.760	12.380	13.110	-0.400	0.363	0.535	0.230	0.230	10.000
44	55.614	-0.109	0.444	0.249	0.529	9.480	13.770	12.490	13.210	-0.400	0.355	0.535	0.232	0.232	10.000
45	55.944	0.023	0.448	0.253	0.535	9.450	13.950	12.620	13.360	-0.280	0.353	0.542	0.235	0.235	10.000

UNDRAINED SHEAR: DSC31 (UNCORRECTED)

AREA	Ex	Ex(SD)	Ey	Ey(SD)	Exy	Exy(SD)	E3	E3(SD)	E1	E1(SD)	GAMMA	G(SD)	EV	EV(SD)	PS.	PS(SD)
		P' =	0.978 ksc				Q =	0.261 ksc								
1	0.123	0.013	0.146	0.009	-0.010	0.008	0.120	0.012	0.150	0.009	0.030	0.015	0.270	0.016	20.39	14.49
2	0.141	0.016	0.167	0.010	0.009	0.009	0.138	0.016	0.170	0.011	0.032	0.019	0.307	0.019	-17.65	16.81
3	0.155	0.026	0.155	0.015	0.018	0.015	0.137	0.021	0.173	0.022	0.036	0.030	0.310	0.030	44.53	24.27
4	0.232	0.074	0.165	0.040	0.052	0.041	0.137	0.050	0.260	0.068	0.123	0.083	0.397	0.084	28.48	19.51
5	0.957	0.194	-0.068	0.165	-0.038	0.128	-0.069	0.165	0.958	0.194	1.027	0.255	0.889	0.255	-2.10	7.15
		P' =	0.959 ksc				Q =	0.220 ksc								
1	-0.023	0.009	0.010	0.008	0.000	0.006	-0.023	0.009	0.010	0.008	0.032	0.012	-0.013	0.012	-0.40	10.90
2	-0.041	0.013	0.014	0.012	-0.001	0.009	-0.041	0.013	0.014	0.012	0.055	0.018	-0.027	0.018	0.54	9.19
3	-0.023	0.025	-0.004	0.020	-0.002	0.016	-0.024	0.025	-0.004	0.020	0.019	0.032	-0.028	0.032	6.04	47.17
4	0.026	0.067	0.026	0.040	0.040	0.038	-0.014	0.055	0.065	0.055	0.079	0.077	0.052	0.078	44.81	28.21
5	0.782	0.374	0.052	0.279	0.095	0.235	0.039	0.280	0.794	0.372	0.754	0.467	0.833	0.466	7.28	17.89
		P' =	0.933 ksc				Q =	0.181 ksc								
1	-0.012	0.011	0.041	0.009	-0.007	0.007	-0.013	0.011	0.042	0.009	0.054	0.014	0.029	0.014	7.61	7.48
2	-0.011	0.015	0.071	0.012	-0.011	0.009	-0.013	0.015	0.072	0.012	0.085	0.019	0.059	0.019	7.43	6.39
3	-0.018	0.024	0.055	0.021	-0.027	0.016	-0.027	0.024	0.064	0.021	0.090	0.032	0.037	0.032	18.24	10.06
4	-0.000	0.062	0.019	0.038	-0.041	0.036	-0.033	0.054	0.052	0.048	0.085	0.072	0.019	0.073	38.21	24.64
5	0.334	0.153	-0.243	0.153	0.038	0.108	-0.245	0.153	0.337	0.153	0.582	0.217	0.092	0.217	3.75	10.68
		P' =	0.912 ksc				Q =	0.140 ksc								
1	-0.017	0.012	0.073	0.008	-0.005	0.007	-0.017	0.012	0.074	0.008	0.091	0.014	0.056	0.014	3.33	4.44
2	-0.012	0.014	0.087	0.011	0.018	0.009	-0.016	0.014	0.090	0.012	0.106	0.018	0.075	0.018	-10.16	4.90
3	-0.018	0.025	0.081	0.019	0.000	0.016	-0.018	0.025	0.081	0.019	0.099	0.031	0.063	0.031	-0.21	8.99
4	0.049	0.061	0.054	0.050	0.028	0.040	0.023	0.057	0.079	0.056	0.056	0.079	0.103	0.079	-42.72	40.53
5	-0.026	0.399	-0.161	0.439	0.194	0.296	-0.299	0.422	0.112	0.409	0.411	0.592	-0.188	0.593	35.44	41.31
		P' =	0.873 ksc				Q =	0.100 ksc								
1	-0.054	0.012	0.099	0.010	-0.018	0.008	-0.055	0.012	0.101	0.010	0.157	0.016	0.045	0.016	6.57	2.85
2	-0.049	0.015	0.110	0.013	0.002	0.010	-0.049	0.015	0.110	0.013	0.158	0.020	0.061	0.020	-0.73	3.57
3	-0.051	0.023	0.071	0.020	-0.011	0.015	-0.052	0.023	0.072	0.020	0.124	0.030	0.021	0.030	5.05	6.96
4	0.078	0.028	0.097	0.055	0.023	0.032	0.063	0.039	0.112	0.049	0.049	0.063	0.175	0.062	-33.83	36.37
5	0.227	0.180	-0.253	0.450	-0.128	0.237	-0.286	0.440	0.259	0.206	0.545	0.485	-0.026	0.485	-14.06	25.18
		P' =	0.798 ksc				Q =	0.021 ksc								
1	-0.118	0.013	0.215	0.010	-0.012	0.008	-0.119	0.013	0.215	0.010	0.334	0.017	0.097	0.017	2.07	1.43
2	-0.119	0.014	0.232	0.012	-0.007	0.009	-0.120	0.014	0.233	0.012	0.352	0.019	0.113	0.019	1 16	1.53
3	-0.119	0.024	0.207	0.021	-0.013	0.016	-0.120	0.024	0.208	0.021	0.327	0.032	0.088	0.032	2.23	2.77
4	-0.092	0.058	0.140	0.034	-0.017	0.033	-0.094	0.058	0.141	0.034	0.235	0.067	0.048	0.067	4.15	8.13
5	-0.025	0.116	0.055	0.316	0.321	0.164	-0.308	0.222	0.338	0.244	0.646	0.329	0.030	0.336	-41.46	14.93
		P' =	0.756 ksc				Q =	0.010 ksc								
1	-0.218	0.011	0.255	0.011	-0.015	0.008	-0.218	0.011	0.255	0.011	0.474	0.016	0.037	0.016	1.84	0.95
2	-0.237	0.014	0.255	0.013	-0.024	0.010	-0.238	0.014	0.256	0.013	0.494	0.019	0.018	0.019	2.79	1.10
3	-0.245	0.021	0.210	0.023	-0.021	0.016	-0.246	0.021	0.211	0.023	0.457	0.032	-0.035	0.032	2.64	1.98
4	-0.186	0.055	0.148	0.043	-0.029	0.035	-0.189	0.054	0.151	0.043	0.339	0.070	-0.038	0.070	4.89	5.84
5	-0.003	0.046	-0.125	0.335	0.021	0.164	-0.128	0.329	0.000	0.070	0.128	0.335	-0.126	0.338	9.51	73.07

AREA	Ex	Ex(SD)	Ey	Ey(SD)	Exy	Exy(SD)	E3	E3(SD)	E1	E1(SD)	GAMMA G(SD)	EV	EV(SD)	PS.	PS(SD)
			P' = 0,726 ksc				Q = 0,030 ksc								
1	-0,317	0,013	0,287	0,010	0,005	0,008	-0,317	0,013	0,287	0,010	0,604 0,016	-0,030	0,016	-0,49	0,76
2	-0,324	0,016	0,281	0,013	0,005	0,010	-0,324	0,016	0,281	0,013	0,605 0,020	-0,043	0,020	-0,45	0,96
3	-0,301	0,023	0,261	0,023	-0,015	0,016	-0,301	0,023	0,261	0,023	0,562 0,032	-0,040	0,032	1,52	1,64
4	-0,191	0,043	0,262	0,052	-0,000	0,034	-0,191	0,043	0,262	0,052	0,453 0,068	0,071	0,068	0,04	4,32
5	-0,203	0,027	-0,039	0,517	-0,083	0,251	-0,237	0,197	-0,004	0,478	0,234 0,505	-0,241	0,518	22,71	62,01
			P' = 0,699 ksc				Q = 0,050 ksc								
1	-0,383	0,029	0,439	0,063	0,005	0,035	-0,383	0,029	0,439	0,063	0,822 0,069	0,057	0,069	-0,33	2,46
2	-0,357	0,020	0,333	0,015	-0,012	0,012	-0,357	0,020	0,333	0,015	0,690 0,025	-0,024	0,025	1,00	1,02
3	-0,328	0,027	0,313	0,027	-0,025	0,019	-0,329	0,027	0,314	0,027	0,643 0,038	-0,015	0,038	2,19	1,69
4	-0,327	0,068	0,229	0,057	-0,034	0,044	-0,329	0,068	0,231	0,057	0,560 0,089	-0,098	0,089	3,44	4,55
5	-0,207	0,133	0,256	0,053	-0,135	0,073	-0,243	0,130	0,292	0,062	0,535 0,144	0,049	0,143	15,08	7,82
			P' = 0,670 ksc				Q = 0,070 ksc								
1	-0,374	0,015	0,491	0,016	-0,018	0,011	-0,375	0,015	0,492	0,016	0,866 0,022	0,117	0,022	1,19	0,72
2	-0,368	0,020	0,484	0,015	-0,015	0,012	-0,368	0,020	0,484	0,015	0,852 0,025	0,116	0,025	1,03	0,83
3	-0,356	0,025	0,470	0,024	-0,007	0,017	-0,356	0,025	0,470	0,024	0,826 0,034	0,114	0,034	0,47	1,19
4	-0,271	0,062	0,398	0,049	0,007	0,039	-0,272	0,062	0,398	0,049	0,670 0,079	0,127	0,079	-0,60	3,36
5	-0,023	0,143	0,254	0,362	0,124	0,190	-0,070	0,182	0,302	0,339	0,372 0,388	0,232	0,389	-20,89	29,79
			P' = 0,642 ksc				Q = 0,090 ksc								
1	-0,450	0,016	0,537	0,012	-0,002	0,010	-0,450	0,016	0,537	0,012	0,987 0,020	0,088	0,020	0,13	0,56
2	-0,478	0,018	0,536	0,014	-0,000	0,011	-0,478	0,018	0,536	0,014	1,013 0,023	0,058	0,023	0,02	0,64
3	-0,470	0,029	0,517	0,024	-0,001	0,019	-0,470	0,029	0,517	0,024	0,987 0,038	0,046	0,038	0,06	1,09
4	-0,406	0,072	0,440	0,041	0,013	0,041	-0,406	0,072	0,440	0,041	0,846 0,083	0,034	0,083	-0,90	2,78
5	-0,044	0,099	0,403	0,415	0,014	0,208	-0,044	0,099	0,404	0,415	0,448 0,427	0,360	0,427	-1,80	26,59
			P' = 0,606 ksc				Q = 0,110 ksc								
1	-0,603	0,014	0,639	0,013	-0,003	0,010	-0,603	0,014	0,639	0,013	1,242 0,019	0,035	0,019	0,15	0,44
2	-0,641	0,017	0,649	0,015	0,012	0,012	-0,641	0,017	0,650	0,015	1,291 0,023	0,008	0,023	-0,53	0,51
3	-0,651	0,029	0,648	0,022	0,032	0,018	-0,652	0,029	0,649	0,022	1,301 0,037	-0,003	0,037	-1,43	0,80
4	-0,608	0,075	0,629	0,040	0,015	0,042	-0,608	0,075	0,629	0,040	1,237 0,085	0,022	0,085	-0,67	1,95
5	-0,084	0,073	0,326	0,347	0,063	0,172	-0,094	0,087	0,335	0,342	0,429 0,355	0,242	0,354	-8,55	23,17
			P' = 0,574 ksc				Q = 0,130 ksc								
1	-0,708	0,014	0,811	0,019	-0,008	0,012	-0,708	0,014	0,811	0,019	1,519 0,024	0,103	0,024	0,31	0,45
2	-0,754	0,018	0,871	0,022	-0,002	0,014	-0,754	0,018	0,871	0,022	1,625 0,028	0,117	0,028	0,08	0,50
3	-0,765	0,030	0,835	0,035	-0,007	0,023	-0,765	0,030	0,835	0,035	1,601 0,046	0,070	0,046	0,24	0,83
4	-0,744	0,074	0,792	0,069	-0,026	0,051	-0,745	0,074	0,792	0,069	1,537 0,101	0,048	0,101	0,96	1,88
5	-0,096	0,151	0,973	0,223	0,045	0,133	-0,098	0,151	0,975	0,223	1,073 0,269	0,877	0,269	-2,42	7,11
			P' = 0,538 ksc				Q = 0,150 ksc								
1	-0,816	0,017	1,038	0,019	-0,024	0,013	-0,817	0,017	1,038	0,019	1,855 0,025	0,222	0,025	0,74	0,39
2	-0,904	0,020	1,127	0,021	-0,004	0,014	-0,904	0,020	1,127	0,021	2,031 0,028	0,222	0,028	0,10	0,40
3	-0,916	0,038	1,144	0,031	0,013	0,025	-0,916	0,038	1,144	0,031	2,061 0,049	0,228	0,049	-0,35	0,68
4	-0,878	0,107	1,113	0,039	-0,003	0,056	-0,878	0,107	1,113	0,039	1,991 0,114	0,235	0,114	0,09	1,61
5	-0,247	0,309	1,332	0,010	0,350	0,160	-0,321	0,302	1,406	0,067	1,727 0,309	1,085	0,309	-11,97	5,24

AREA	Ex	Ex(SD)	Ey	Ey(SD)	Exy	Exy(SD)	E3	E3(SD)	E1	E1(SD)	GAMMA G(SD)	EV	EV(SD)	PS.	PS(SD)
		P' =	0.507 ksc				Q =	0.160 ksc							
1	-1.042	0.025	1.125	0.023	-0.015	0.017	-1.043	0.025	1.126	0.023	2.168 0.034	0.083	0.034	0.39	0.45
2	-1.179	0.024	1.201	0.025	-0.014	0.017	-1.179	0.024	1.201	0.025	2.380 0.034	0.022	0.034	0.34	0.41
3	-1.221	0.039	1.224	0.040	-0.022	0.028	-1.222	0.039	1.224	0.040	2.446 0.056	0.002	0.056	0.51	0.65
4	-1.144	0.107	1.232	0.070	-0.062	0.063	-1.146	0.107	1.234	0.070	2.380 0.128	0.088	0.128	1.50	1.52
5	-1.096	0.237	1.238	0.525	-0.065	0.282	-1.098	0.237	1.240	0.525	2.338 0.575	0.141	0.576	1.60	6.91
		P' =	0.470 ksc				Q =	0.170 ksc							
1	-1.293	0.024	1.393	0.029	-0.028	0.019	-1.293	0.024	1.394	0.028	2.687 0.037	0.101	0.037	0.60	0.40
2	-1.438	0.028	1.518	0.031	-0.044	0.021	-1.438	0.028	1.519	0.031	2.957 0.041	0.081	0.041	0.86	0.40
3	-1.515	0.049	1.614	0.040	-0.040	0.032	-1.515	0.049	1.615	0.040	3.130 0.063	0.100	0.063	0.72	0.58
4	-1.521	0.123	1.617	0.081	-0.032	0.073	-1.522	0.123	1.617	0.081	3.139 0.148	0.095	0.148	0.58	1.34
5	-0.557	0.459	1.657	0.035	-0.100	0.237	-0.562	0.459	1.662	0.041	2.224 0.461	1.100	0.460	2.58	6.13
		P' =	0.450 ksc				Q =	0.180 ksc							
1	-1.518	0.026	1.632	0.035	-0.041	0.022	-1.519	0.026	1.632	0.035	3.151 0.043	0.113	0.043	0.75	0.40
2	-1.666	0.027	1.818	0.037	-0.031	0.023	-1.666	0.027	1.818	0.037	3.484 0.045	0.152	0.045	0.51	0.38
3	-1.756	0.048	1.959	0.049	-0.037	0.034	-1.757	0.048	1.959	0.049	3.716 0.068	0.202	0.068	0.56	0.53
4	-1.861	0.097	2.056	0.078	-0.057	0.062	-1.861	0.097	2.057	0.078	3.918 0.124	0.195	0.124	0.83	0.91
5	-1.007	0.478	1.970	0.739	-0.282	0.435	-1.033	0.482	1.997	0.738	3.030 0.879	0.963	0.880	5.36	8.21
		P' =	0.430 ksc				Q =	0.190 ksc							
1	-1.783	0.038	1.948	0.043	-0.061	0.029	-1.784	0.038	1.949	0.043	3.733 0.057	0.165	0.057	0.93	0.44
2	-2.012	0.036	2.179	0.043	-0.082	0.028	-2.014	0.036	2.181	0.043	4.194 0.056	0.167	0.056	1.12	0.39
3	-2.139	0.054	2.332	0.054	-0.091	0.038	-2.140	0.054	2.334	0.054	4.474 0.076	0.193	0.076	1.16	0.49
4	-2.210	0.112	2.460	0.079	-0.078	0.068	-2.211	0.112	2.462	0.079	4.673 0.138	0.250	0.138	0.96	0.84
5	-1.681	0.012	2.247	0.562	-0.130	0.272	-1.685	0.021	2.251	0.562	3.936 0.561	0.567	0.562	1.89	3.96
		P' =	0.402 ksc				Q =	0.200 ksc							
1	-2.397	0.057	2.518	0.059	-0.120	0.041	-2.400	0.057	2.521	0.059	4.921 0.082	0.121	0.082	1.40	0.48
2	-2.762	0.051	2.830	0.063	-0.149	0.041	-2.766	0.051	2.834	0.063	5.600 0.081	0.068	0.081	1.52	0.42
3	-3.018	0.069	3.114	0.071	-0.150	0.050	-3.021	0.069	3.118	0.071	6.139 0.099	0.097	0.099	1.40	0.46
4	-3.189	0.128	3.290	0.085	-0.099	0.076	-3.191	0.128	3.291	0.085	6.482 0.154	0.100	0.154	0.88	0.67
5	-2.330	0.081	3.560	0.315	-0.402	0.158	-2.357	0.083	3.588	0.314	5.945 0.324	1.231	0.325	3.88	1.52
		P' =	0.380 ksc				Q =	0.210 ksc							
1	-3.826	0.087	3.913	0.098	-0.200	0.066	-3.831	0.087	3.918	0.098	7.750 0.131	0.087	0.131	1.48	0.49
2	-4.401	0.088	4.438	0.104	-0.236	0.069	-4.407	0.088	4.444	0.104	8.851 0.137	0.037	0.137	1.53	0.44
3	-4.848	0.096	4.987	0.115	-0.241	0.075	-4.854	0.096	4.993	0.115	9.847 0.149	0.140	0.149	1.40	0.44
4	-5.218	0.154	5.394	0.128	-0.270	0.100	-5.225	0.154	5.401	0.128	10.626 0.200	0.176	0.200	1.46	0.54
5	-5.203	0.759	5.477	0.113	-0.338	0.395	-5.213	0.759	5.488	0.116	10.701 0.768	0.274	0.767	1.81	2.12
		P' =	0.375 ksc				Q =	0.214 ksc							
1	-4.724	0.130	4.891	0.134	-0.245	0.094	-4.730	0.130	4.897	0.134	9.627 0.187	0.167	0.187	1.46	0.56
2	-5.569	0.127	5.660	0.138	-0.302	0.094	-5.577	0.127	5.668	0.138	11.245 0.187	0.091	0.187	1.54	0.48
3	-6.261	0.136	6.420	0.154	-0.300	0.103	-6.268	0.136	6.427	0.154	12.696 0.205	0.159	0.205	1.35	0.46
4	-6.947	0.198	6.895	0.220	-0.298	0.148	-6.954	0.198	6.901	0.220	13.855 0.296	-0.052	0.296	1.23	0.61
5	-6.597	0.469	7.081	0.598	-0.369	0.378	-6.607	0.469	7.091	0.599	13.698 0.760	0.484	0.760	1.55	1.58

AREA	Ex	Ex(SD)	Ey	Ey(SD)	Exy	Exy(SD)	E3	E3(SD)	E1	E1(SD)	GAMMA	G(SD)	EV	EV(SD)	PS.	PS(SD)
		P' =	0.369 ksc					Q = 0.216 ksc								
1	-5.681	0.157	5.777	0.162	-0.289	0.113	-5.688	0.157	5.784	0.162	11.472	0.225	0.096	0.225	1.44	0.56
2	-6.688	0.156	6.705	0.169	-0.343	0.116	-6.697	0.156	6.714	0.169	13.411	0.230	0.017	0.230	1.46	0.49
3	-7.538	0.167	7.657	0.181	-0.370	0.123	-7.547	0.167	7.666	0.181	15.213	0.246	0.118	0.246	1.39	0.46
4	-8.348	0.194	8.420	0.205	-0.325	0.141	-8.355	0.194	8.426	0.205	16.781	0.282	0.072	0.282	1.11	0.48
5	-8.386	0.288	9.037	0.998	-0.635	0.506	-8.409	0.290	9.060	0.998	17.469	1.038	0.651	1.039	2.08	1.66

UNDRAINED SHEAR: DSC32 (UNCORRECTED)

AREA	Ex	Ex(SD)	Ey	Ey(SD)	Exy	Exy(SD)	E3	E3(SD)	E1	E1(SD)	GAMMA	G(SD)	EV	EV(SD)	PS.	PS(SD)
		P' =	0.863	ksc			Q =	0.272	ksc							
1	0.017	0.012	0.027	0.008	0.025	0.007	-0.003	0.011	0.047	0.010	0.051	0.014	0.044	0.015	51.00	8.26
2	0.010	0.017	0.043	0.012	0.016	0.011	0.004	0.016	0.050	0.013	0.046	0.021	0.053	0.021	67.56	13.04
3	0.048	0.030	0.047	0.019	0.043	0.018	0.004	0.025	0.091	0.025	0.087	0.035	0.095	0.036	44.70	11.79
4	0.034	0.085	0.029	0.054	0.053	0.050	-0.021	0.070	0.084	0.071	0.105	0.099	0.063	0.100	43.79	27.20
5	-0.023	0.115	-0.041	0.059	0.127	0.064	-0.159	0.088	0.095	0.092	0.254	0.128	-0.064	0.129	43.05	14.52
		P' =	0.857	ksc			Q =	0.275	ksc							
1	-0.003	0.012	-0.009	0.009	0.024	0.008	-0.031	0.011	0.018	0.011	0.049	0.015	-0.012	0.015	41.41	8.89
2	-0.019	0.019	0.024	0.013	0.032	0.012	-0.036	0.018	0.041	0.014	0.077	0.023	0.005	0.023	61.75	8.60
3	0.006	0.031	-0.004	0.019	0.046	0.018	-0.046	0.025	0.048	0.027	0.093	0.037	0.002	0.037	41.96	11.31
4	-0.004	0.067	-0.030	0.044	0.039	0.040	-0.058	0.053	0.024	0.060	0.082	0.080	-0.034	0.080	35.92	28.24
5	0.096	0.161	-0.078	0.076	-0.075	0.088	-0.107	0.091	0.125	0.154	0.231	0.177	0.018	0.179	69.58	21.92
		P' =	0.848	ksc			Q =	0.279	ksc							
1	0.046	0.014	0.008	0.011	0.034	0.009	-0.012	0.012	0.066	0.014	0.077	0.018	0.054	0.018	30.54	6.75
2	0.036	0.022	0.016	0.015	0.030	0.014	-0.006	0.018	0.058	0.020	0.064	0.027	0.052	0.027	35.91	12.07
3	0.046	0.048	-0.039	0.024	0.053	0.027	-0.064	0.030	0.071	0.045	0.135	0.053	0.006	0.054	25.56	11.34
4	-0.096	0.134	-0.065	0.059	0.035	0.072	-0.119	0.116	-0.042	0.087	0.077	0.145	-0.161	0.147	57.15	54.32
5	-0.053	1.154	0.074	0.568	0.106	0.637	-0.113	1.034	0.134	0.745	0.247	1.272	0.021	1.286	60.53	148.05
		P' =	0.839	ksc			Q =	0.280	ksc							
1	-0.016	0.014	-0.007	0.010	0.058	0.008	-0.070	0.012	0.047	0.012	0.116	0.017	-0.023	0.017	47.17	4.17
2	-0.039	0.023	0.014	0.015	0.054	0.014	-0.072	0.021	0.047	0.018	0.119	0.027	-0.025	0.027	58.05	6.58
3	-0.049	0.038	-0.011	0.024	0.100	0.022	-0.132	0.033	0.072	0.030	0.204	0.045	-0.060	0.045	50.52	6.32
4	-0.065	0.084	-0.101	0.063	0.145	0.052	-0.229	0.073	0.063	0.075	0.291	0.105	-0.166	0.105	41.50	10.34
5	0.105	0.369	0.270	0.134	0.107	0.194	0.052	0.333	0.323	0.200	0.270	0.387	0.375	0.392	63.75	41.16
		P' =	0.830	ksc			Q =	0.283	ksc							
1	0.046	0.015	0.001	0.012	0.051	0.010	-0.032	0.013	0.079	0.014	0.111	0.019	0.046	0.019	33.11	4.91
2	0.031	0.022	0.009	0.015	0.071	0.013	-0.052	0.019	0.093	0.019	0.145	0.027	0.040	0.027	40.72	5.32
3	0.051	0.039	0.002	0.027	0.080	0.024	-0.057	0.032	0.111	0.035	0.168	0.047	0.054	0.047	36.58	8.06
4	0.074	0.111	-0.020	0.070	0.108	0.065	-0.091	0.084	0.145	0.100	0.236	0.131	0.054	0.131	33.33	15.95
5	0.228	0.057	-0.124	0.296	0.237	0.153	-0.244	0.265	0.347	0.144	0.591	0.303	0.103	0.302	26.74	14.62
		P' =	0.815	ksc			Q =	0.288	ksc							
1	0.041	0.014	-0.009	0.012	0.106	0.009	-0.093	0.013	0.125	0.014	0.218	0.019	0.032	0.019	38.24	2.49
2	-0.003	0.021	0.006	0.018	0.077	0.014	-0.075	0.019	0.078	0.019	0.154	0.027	0.003	0.027	46.65	5.04
3	-0.018	0.038	-0.014	0.028	0.077	0.023	-0.094	0.033	0.061	0.033	0.154	0.046	-0.033	0.047	45.76	8.68
4	-0.031	0.069	0.016	0.073	0.094	0.050	-0.105	0.070	0.089	0.071	0.194	0.100	-0.016	0.100	52.03	14.82
5	0.638	0.224	0.176	0.115	0.084	0.125	0.161	0.119	0.653	0.221	0.492	0.252	0.814	0.252	9.98	14.56
		P' =	0.810	ksc			Q =	0.290	ksc							
1	0.001	0.017	-0.024	0.012	0.119	0.010	-0.132	0.014	0.108	0.015	0.240	0.021	-0.023	0.021	42.03	2.46
2	-0.030	0.026	-0.016	0.017	0.111	0.016	-0.134	0.022	0.088	0.022	0.221	0.031	-0.046	0.031	46.73	4.03
3	0.023	0.048	-0.038	0.026	0.120	0.027	-0.132	0.036	0.116	0.041	0.248	0.054	-0.015	0.055	37.83	6.29
4	-0.064	0.119	-0.088	0.072	0.191	0.069	-0.267	0.096	0.115	0.099	0.382	0.138	-0.152	0.139	43.18	10.41
5	0.644	0.303	-0.113	0.196	0.217	0.179	-0.171	0.203	0.702	0.296	0.873	0.361	0.531	0.361	14.93	11.81

AREA	Ex	Ex(SD)	Ey	Ey(SD)	Exy	Exy(SD)	E3	E3(SD)	E1	E1(SD)	GAMMA	G(SD)	EV	EV(SD)	PS.	PS(SD)
		P' =	0.795	ksc			Q =	0 293	ksc							
1	0.226	0.022	0.203	0.024	0.104	0.016	0.110	0.023	0.319	0.023	0.209	0.033	0.428	0.033	41.87	4.47
2	0.276	0.033	0.263	0.027	0.110	0.021	0.160	0.030	0.379	0.030	0.220	0.042	0.539	0.042	43.37	5.52
3	0.319	0.047	0.253	0.035	0.157	0.029	0.125	0.040	0.446	0.042	0.321	0.058	0.572	0.059	39.11	5.22
4	0.236	0.102	0.219	0.071	0.094	0.062	0.133	0.086	0.322	0.088	0.189	0.123	0.455	0.124	42.36	18.78
5	-0.316	0.083	0.024	0.045	0.274	0.047	-0.468	0.075	0.177	0.056	0.645	0.094	-0.292	0.095	60.94	4.17
		P' =	0.780	ksc			Q =	0.298	ksc							
1	0.065	0.017	-0.036	0.015	0.180	0.011	-0.172	0.016	0.201	0.016	0.373	0.023	0.030	0.023	37.15	1.75
2	0.027	0.026	-0.037	0.017	0.155	0.016	-0.163	0.021	0.153	0.023	0.316	0.031	-0.109	0.032	39.15	2.87
3	0.057	0.051	-0.055	0.026	0.164	0.028	-0.172	0.036	0.174	0.044	0.347	0.056	0.002	0.057	35.55	4.69
4	-0.034	0.107	-0.105	0.058	0.193	0.060	-0.266	0.081	0.126	0.090	0.392	0.121	-0.139	0.122	39.79	8.91
5	0.391	0.177	0.191	0.001	0.216	0.087	0.053	0.093	0.529	0.147	0.476	0.175	0.582	0.177	32.51	10.66
		P' =	0.765	ksc			Q =	0.301	ksc							
1	0.033	0.017	-0.084	0.019	0.191	0.013	-0.225	0.018	0.174	0.018	0.399	0.025	-0.051	0.025	36.47	1.82
2	-0.019	0.025	-0.079	0.017	0.166	0.015	-0.218	0.020	0.119	0.022	0.337	0.030	-0.099	0.030	39.87	2.55
3	0.001	0.046	-0.064	0.026	0.165	0.026	-0.199	0.035	0.137	0.039	0.337	0.053	-0.062	0.053	39.47	4.50
4	-0.077	0.096	-0.121	0.056	0.164	0.055	-0.264	0.075	0.066	0.080	0.330	0.110	-0.198	0.111	41.14	9.63
5	-0.007	0.429	-0.069	0.105	0.290	0.217	-0.330	0.293	0.254	0.322	0.584	0.435	-0.076	0.441	41.95	21.66
		P' =	0.751	ksc			Q =	0.307	ksc							
1	0.090	0.018	-0.087	0.024	0.257	0.015	-0.270	0.023	0.273	0.021	0.543	0.031	0.003	0.030	35.48	1.61
2	0.070	0.027	-0.044	0.027	0.223	0.019	-0.217	0.027	0.243	0.027	0.459	0.038	0.026	0.038	37.80	2.39
3	0.067	0.053	-0.030	0.043	0.240	0.034	-0.226	0.047	0.263	0.049	0.489	0.068	0.037	0.068	39.32	3.97
4	0.040	0.131	-0.056	0.101	0.274	0.082	-0.287	0.114	0.271	0.119	0.557	0.165	-0.016	0.166	40.02	8.52
5	-0.279	0.284	0.186	0.163	0.344	0.162	-0.462	0.260	0.369	0.194	0.831	0.325	-0.093	0.327	62.04	11.23
		P' =	0.745	ksc			Q =	0.312	ksc							
1	0.051	0.016	-0.105	0.027	0.306	0.016	-0.343	0.024	0.289	0.021	0.631	0.032	-0.054	0.032	37.83	1.43
2	0.022	0.021	-0.072	0.026	0.282	0.017	-0.311	0.024	0.261	0.023	0.572	0.034	-0.050	0.034	40.30	1.69
3	0.018	0.035	-0.055	0.032	0.262	0.024	-0.283	0.033	0.246	0.034	0.529	0.047	-0.038	0.048	41.03	2.57
4	0.034	0.093	-0.070	0.082	0.301	0.062	-0.324	0.086	0.288	0.088	0.612	0.123	-0.036	0.124	40.10	5.79
5	0.056	0.132	-0.003	0.154	0.185	0.102	-0.161	0.144	0.214	0.141	0.375	0.203	0.054	0.203	40.52	15.48
		P' =	0.736	ksc			Q =	0.317	ksc							
1	0.066	0.019	-0.188	0.031	0.380	0.018	-0.461	0.028	0.339	0.024	0.801	0.037	-0.122	0.036	35.75	1.30
2	0.010	0.025	-0.151	0.033	0.339	0.021	-0.419	0.030	0.278	0.028	0.697	0.041	-0.141	0.041	38.35	1.69
3	0.037	0.045	-0.193	0.042	0.315	0.031	-0.413	0.043	0.258	0.044	0.671	0.061	-0.156	0.061	34.97	2.61
4	-0.063	0.114	-0.217	0.069	0.248	0.066	-0.399	0.087	0.120	0.100	0.518	0.133	-0.280	0.133	36.36	7.37
5	0.748	0.241	0.133	0.089	0.183	0.127	0.083	0.106	0.798	0.232	0.715	0.257	0.881	0.257	15.36	10.24
		P' =	0.723	ksc			Q =	0.320	ksc							
1	0.090	0.022	-0.219	0.036	0.473	0.021	-0.562	0.032	0.433	0.028	0.995	0.042	-0.129	0.042	35.93	1.21
2	0.050	0.028	-0.186	0.035	0.447	0.023	-0.531	0.033	0.395	0.031	0.925	0.046	-0.136	0.045	37.60	1.40
3	0.038	0.041	-0.157	0.033	0.442	0.026	-0.512	0.036	0.393	0.038	0.905	0.053	-0.119	0.053	38.78	1.67
4	-0.012	0.105	-0.279	0.055	0.432	0.059	-0.598	0.076	0.307	0.090	0.905	0.118	-0.291	0.119	36.43	3.76
5	0.284	0.272	-0.050	0.353	0.366	0.224	-0.285	0.330	0.520	0.297	0.805	0.446	0.235	0.445	32.75	15.84

AREA	Ex	Ex(SD)	Ey	Ey(SD)	Exy	Exy(SD)	E3	E3(SD)	E1	E1(SD)	GAMMA	G(SD)	EV	EV(SD)	PS.	PS(SD)
		P' =	0.692 ksc				Q =	0.327 ksc								
1	0.161	0.025	-0.423	0.065	0.746	0.035	-0.932	0.055	0.670	0.042	1.602	0.070	-0.262	0.069	34.31	1.24
2	0.134	0.029	-0.389	0.075	0.686	0.041	-0.862	0.064	0.606	0.049	1.468	0.081	-0.255	0.080	34.56	1.57
3	0.145	0.042	-0.340	0.071	0.631	0.042	-0.774	0.064	0.578	0.054	1.352	0.084	-0.196	0.083	34.50	1.76
4	0.193	0.117	-0.226	0.086	0.598	0.072	-0.651	0.097	0.617	0.107	1.268	0.145	-0.034	0.145	35.35	3.28
5	0.377	0.129	-0.236	0.585	0.529	0.304	-0.541	0.509	0.682	0.314	1.223	0.602	0.141	0.599	29.97	14.00
		P' =	0.649 ksc				Q =	0.333 ksc								
1	0.428	0.037	-0.828	0.121	1.453	0.065	-1.783	0.104	1.383	0.074	3.166	0.129	-0.400	0.127	33.31	1.15
2	0.428	0.050	-0.904	0.151	1.455	0.081	-1.838	0.131	1.362	0.093	3.199	0.161	-0.476	0.159	32.70	1.43
3	0.461	0.078	-0.898	0.170	1.396	0.095	-1.771	0.151	1.333	0.113	3.104	0.189	-0.437	0.188	32.02	1.73
4	0.508	0.115	-0.808	0.173	1.290	0.105	-1.598	0.159	1.299	0.133	2.897	0.209	-0.300	0.208	31.48	2.05
5	0.581	0.372	-0.550	0.123	1.204	0.193	-1.315	0.221	1.346	0.317	2.661	0.389	0.031	0.391	32.42	4.22
		P' =	0.545 ksc				Q =	0.338 ksc								
1	1.259	0.135	-2.719	0.252	3.936	0.144	-5.140	0.226	3.680	0.176	8.820	0.288	-1.460	0.286	31.60	0.93
2	1.649	0.161	-3.377	0.335	4.315	0.188	-5.858	0.302	4.130	0.219	9.987	0.375	-1.728	0.371	29.89	1.07
3	1.963	0.244	-3.826	0.475	4.508	0.270	-6.288	0.434	4.426	0.314	10.714	0.538	-1.862	0.534	28.65	1.43
4	1.731	0.370	-3.854	0.688	4.280	0.394	-6.171	0.629	4.049	0.462	10.220	0.784	-2.123	0.781	28.44	2.19
5	1.019	0.092	-2.942	0.155	3.817	0.091	-5.261	0.141	3.339	0.112	8.600	0.181	-1.922	0.180	31.29	0.60

UNDRAINED SHEAR: DSC33 (UNCORRECTED)

AREA	Ex	Ex(SD)	Ey	Ey(SD)	Exy	Exy(SD)	E3	E3(SD)	E1	E1(SD)	GAMMA	G(SD)	EV	EV(SD)	PS.	PS(SD)
	P' = 0.983 ksc						Q = 0.294 ksc									
1	0.022	0.011	0.007	0.007	0.001	0.006	0.007	0.007	0.023	0.011	0.015	0.013	0.030	0.013	2.59	23.49
2	0.014	0.015	0.003	0.011	-0.002	0.009	0.003	0.011	0.014	0.015	0.011	0.019	0.017	0.019	81.27	47.16
3	-0.000	0.027	-0.002	0.017	-0.002	0.016	-0.004	0.021	0.001	0.024	0.005	0.032	-0.003	0.032	56.53	181.56
4	0.020	0.070	0.018	0.042	-0.012	0.040	0.008	0.056	0.031	0.059	0.023	0.081	0.038	0.081	47.51	101.04
5	-0.204	0.282	0.201	0.013	-0.056	0.137	-0.211	0.278	0.208	0.039	0.420	0.280	-0.003	0.282	7.74	18.61
	P' = 0.964 ksc						Q = 0.276 ksc									
1	0.006	0.012	0.014	0.009	0.029	0.007	-0.020	0.010	0.039	0.010	0.059	0.014	0.020	0.015	48.53	7.07
2	0.005	0.016	0.028	0.014	0.037	0.011	-0.023	0.016	0.056	0.015	0.078	0.022	0.033	0.022	53.70	7.94
3	0.011	0.030	0.019	0.026	0.023	0.020	-0.008	0.029	0.038	0.028	0.047	0.040	0.030	0.040	49.68	24.59
4	0.033	0.074	0.003	0.078	0.043	0.054	-0.028	0.077	0.064	0.075	0.091	0.108	0.036	0.108	35.41	33.76
5	-0.088	0.546	-0.006	0.645	-0.285	0.425	-0.335	0.588	0.242	0.601	0.577	0.851	-0.094	0.845	40.91	42.01
	P' = 0.935 ksc						Q = 0.270 ksc									
1	0.020	0.014	0.050	0.009	0.073	0.008	-0.040	0.012	0.110	0.011	0.150	0.016	0.070	0.017	50.68	3.17
2	0.020	0.020	0.059	0.013	0.080	0.012	-0.043	0.018	0.122	0.016	0.165	0.024	0.079	0.024	51.77	4.16
3	0.038	0.035	0.059	0.026	0.060	0.022	-0.013	0.032	0.109	0.030	0.122	0.044	0.097	0.044	50.02	10.34
4	0.049	0.082	0.084	0.055	0.121	0.049	-0.056	0.071	0.188	0.068	0.244	0.098	0.133	0.099	49.08	11.62
5	-0.325	0.193	0.587	0.424	0.279	0.238	-0.404	0.221	0.666	0.414	1.069	0.466	0.262	0.466	74.29	12.61
	P' = 0.914 ksc						Q = 0.271 ksc									
1	-0.048	0.015	0.015	0.009	0.111	0.008	-0.132	0.013	0.099	0.011	0.231	0.017	-0.033	0.017	52.84	2.14
2	-0.081	0.018	0.024	0.014	0.130	0.011	-0.169	0.016	0.112	0.015	0.281	0.022	0.058	0.022	55.98	2.27
3	-0.022	0.026	0.033	0.024	0.127	0.018	-0.124	0.025	0.135	0.025	0.259	0.035	0.011	0.035	51.15	3.92
4	0.025	0.059	-0.010	0.060	0.115	0.042	-0.109	0.059	0.123	0.059	0.232	0.084	0.015	0.084	40.63	10.37
5	0.087	0.279	0.202	0.045	-0.002	0.137	0.087	0.279	0.202	0.045	0.115	0.282	0.288	0.283	1.10	68.07
	P' = 0.897 ksc						Q = 0.275 ksc									
1	-0.042	0.014	0.041	0.010	0.104	0.009	-0.113	0.013	0.111	0.011	0.224	0.017	-0.001	0.018	55.93	2.23
2	-0.042	0.018	0.047	0.013	0.097	0.011	-0.104	0.016	0.110	0.015	0.214	0.022	0.005	0.022	57.27	2.93
3	-0.041	0.035	0.039	0.025	0.096	0.021	-0.105	0.032	0.103	0.028	0.208	0.042	-0.001	0.043	56.27	5.83
4	-0.017	0.091	0.056	0.055	0.137	0.053	-0.122	0.079	0.161	0.070	0.284	0.106	0.039	0.107	52.43	10.74
5	-0.191	0.433	0.347	0.340	0.083	0.273	-0.204	0.432	0.360	0.343	0.563	0.550	0.156	0.550	81.41	27.83
	P' = 0.876 ksc						Q = 0.283 ksc									
1	-0.054	0.018	0.052	0.013	0.163	0.011	-0.173	0.016	0.171	0.014	0.343	0.022	-0.002	0.022	54.04	1.81
2	-0.058	0.021	0.060	0.017	0.172	0.013	-0.180	0.020	0.183	0.018	0.363	0.027	0.002	0.027	54.46	2.12
3	-0.077	0.033	0.038	0.030	0.168	0.023	-0.197	0.032	0.158	0.031	0.356	0.045	-0.039	0.045	54.47	3.62
4	-0.083	0.047	0.088	0.073	0.222	0.044	-0.236	0.057	0.241	0.066	0.476	0.087	0.005	0.087	55.51	5.22
5	-0.256	0.080	0.297	0.513	-0.103	0.268	-0.274	0.122	0.315	0.504	0.590	0.524	0.041	0.520	10.26	26.06
	P' = 0.853 ksc						= 0.293 ksc									
1	-0.072	0.021	0.097	0.013	0.239	0.012	-0.241	0.019	0.266	0.016	0.506	0.025	0.025	0.025	54.75	1.40
2	-0.057	0.027	0.104	0.018	0.252	0.016	-0.241	0.024	0.288	0.022	0.529	0.032	0.047	0.033	53.88	1.77
3	-0.089	0.045	0.104	0.030	0.205	0.027	-0.220	0.041	0.234	0.035	0.454	0.054	0.015	0.054	57.59	3.42
4	0.087	0.083	0.104	0.064	0.269	0.052	-0.173	0.074	0.365	0.073	0.538	0.104	0.191	0.105	45.94	5.58
5	0.720	0.105	-0.158	0.431	0.262	0.228	-0.230	0.419	0.792	0.156	1.022	0.450	0.563	0.444	15.40	12.78

AREA	Ex	Ex(SD)	Ey	Ey(SD)	Exy	Fxy(SD)	E3	E3(SD)	E1	E1(SD)	GAMMA G(SD)	EV	EV(SD)	PS.	PS(SD)
		P' =	0.830	ksc			Q =	0.306	ksc						
1	-0.104	0.019	0.099	0.014	0.283	0.011	-0.303	0.017	0.298	0.015	0.600 0.023	-0.005	0.023	54.87	1.09
2	-0.130	0.025	0.114	0.019	0.295	0.015	-0.327	0.022	0.311	0.020	0.638 0 030	-0.016	0.030	56.26	1.34
3	-0.145	0.034	0.116	0.034	0.277	0.024	-0.321	0.034	0.292	0.034	0.613 0.048	-0.029	0.048	57.62	2.25
4	-0.165	0.077	0.153	0.082	0.234	0.056	-0.289	0.078	0.277	0.081	0.566 0.112	-0.012	0.112	62.07	5.69
5	0.107	0.104	-0.042	0.343	0.268	0.184	-0.246	0.286	0.311	0.229	0.557 0.369	0.065	0.359	37.22	18.53
		P' =	0.799	ksc			Q =	0.321	ksc						
1	-0.165	0.024	0.132	0.014	0.394	0.014	-0.438	0.021	0.405	0.018	0.843 0.028	-0.033	0.028	55.30	0.95
2	-0.202	0.028	0.140	0.019	0.391	0.017	-0.458	0.025	0.396	0.022	0.854 0.033	-0.062	0.034	56.80	1.13
3	-0.174	0.044	0.169	0.031	0.395	0.027	-0.433	0.041	0.429	0.035	0.862 0.054	-0.004	0.054	56.73	1.79
4	-0.092	0.092	0.319	0.072	0.420	0.058	-0.354	0.086	0.581	0.078	0.935 0.116	0.227	0.116	58.01	3.56
5	0.460	0.360	-0.122	0.401	0.747	0.270	-0.633	0.392	0.971	0.377	1.603 0.541	0.338	0.538	34.35	9.63
		P' =	0.766	ksc			Q =	0.333	ksc						
1	-0.141	0.024	0.253	0.015	0.524	0.014	-0.504	0.021	0.615	0.018	1.119 0.028	0.111	0.028	55.31	0.72
2	-0.154	0.024	0.273	0.020	0.533	0.016	-0.514	0.023	0.633	0.021	1.147 0.031	0.119	0.032	55.91	0.79
3	-0.151	0.040	0.255	0.032	0.517	0.025	-0.503	0.037	0.607	0.034	1.110 0.051	0.104	0.051	55.71	1.31
4	-0.102	0.103	0.417	0.061	0.494	0.059	-0.400	0.093	0.715	0.074	1.115 0.118	0.315	0.120	58.86	3.06
5	-0.402	0.461	0.779	0.050	0.479	0.225	-0.572	0.436	0.949	0.158	1.521 0.462	0.377	0.464	70.47	8.64
		P' =	0.735	ksc			Q =	0.345	ksc						
1	-0.200	0.025	0.252	0.017	0.661	0.015	-0.672	0.022	0.725	0.020	1.397 0.030	0.052	0.030	54.45	0.61
2	-0.193	0.024	0.296	0.022	0.706	0.016	-0.695	0.023	0.798	0.022	1.494 0.032	0.103	0.032	54.55	0.62
3	-0.151	0.038	0.327	0.031	0.676	0.024	-0.630	0.036	0.805	0.034	1.435 0.049	0.176	0.049	54.74	0.98
4	-0.166	0.090	0.326	0.081	0.667	0.060	-0.631	0.087	0.791	0.084	1.422 0.121	0.161	0.121	55.12	2.44
5	-0.034	0.322	0.490	0.032	1.051	0.157	-0.855	0.254	1.311	0.198	2.166 0.316	0.456	0.324	51.99	4.29
		P' =	0.672	ks			Q =	0.357	ksc						
1	-0.315	0.036	0.262	0.021	1.189	0.020	-1.249	0.031	1.197	0.027	2.446 0.041	-0.053	0.041	51.82	0.48
2	-0.291	0.038	0.284	0.026	1.261	0.023	-1.297	0.034	1.290	0.031	2.587 0.046	-0.007	0.046	51.42	0.51
3	-0.275	0.052	0.276	0.041	1.346	0.033	-1.374	0.047	1.374	0.045	2.748 0.065	0.001	0.066	50.78	0.69
4	-0.171	0.119	0 328	0.098	1.416	0.077	-1.359	0.110	1.517	0.106	2.876 0.153	0.158	0.154	50.00	1.53
5	-0.305	0.436	0.782	0.991	1.483	0.553	-1.341	0.684	1.817	0.863	3.158 1.100	0.476	1.083	55.07	9.81
		P' =	0.593	ksc			Q =	0.361	ksc						
1	-0.286	0.084	0.312	0.057	3.014	0.050	-3.015	0.072	3.042	0.070	6.058 0.100	0.027	0.101	47.83	0.48
2	-0.179	0.075	0.222	0.081	3.253	0.055	-3.237	0.077	3.281	0.078	6.518 0.110	0.043	0.110	46.77	0.48
3	-0.114	0.068	0.114	0.077	3.351	0.052	-3.353	0.072	3.353	0.073	6.705 0.103	-0.000	0.103	45.98	0.44
4	0.181	0.099	0.143	0.138	3.386	0.086	-3.225	0.120	3.548	0.120	6.772 0.171	0.323	0.170	44.84	0.72
5	0.129	0.111	0.602	1.087	3.492	0.564	-3.134	0.766	3.866	0.616	7.000 1.126	0.731	1.093	46.94	4.47

UNDRAINED SHEAR: DSC34 (UNCORRECTED)

AREA	Ex	Ex(SD)	Ey	Ey(SD)	Exy	Exy(SD)	E3	E3(SD)	E1	E1(SD)	GAMMA	G(SD)	EV	EV(SD)	PS.	PS(SD)
		P' =	0.859	ksc			Q =	0.314	ksc							
1	0.014	0.014	-0.054	0.012	0.020	0.009	-0.043	0.012	0.003	0.013	0.046	0.018	-0.040	0.018	29.98	11.24
2	0.011	0.023	-0.052	0.015	-0.017	0.014	-0.037	0.020	-0.003	0.018	0.035	0.027	-0.040	0.027	-40.01	22.59
3	0.028	0.040	-0.069	0.028	0.027	0.024	-0.047	0.034	0.007	0.035	0.054	0.048	-0.040	0.049	39.15	25.72
4	0.040	0.077	-0.101	0.070	0.010	0.052	-0.100	0.077	0.040	0.070	0.141	0.104	-0.060	0.104	4.17	21.11
5	0.696	0.418	-0.104	0.107	-0.214	0.210	-0.019	0.159	0.612	0.400	0.632	0.427	0.593	0.432	-21.43	19.19
		P' =	0.850	ksc			Q =	0.334	ksc							
1	0.010	0.016	-0.069	0.011	-0.002	0.010	-0.069	0.011	0.009	0.016	0.079	0.020	-0.059	0.020	-2.12	7.07
2	0.002	0.025	-0.066	0.019	0.001	0.015	-0.066	0.019	0.002	0.025	0.069	0.031	-0.064	0.031	0.96	12.89
3	-0.029	0.044	-0.068	0.037	0.010	0.029	-0.064	0.038	-0.033	0.043	0.031	0.057	-0.097	0.058	20.40	52.63
4	0.172	0.077	-0.275	0.065	0.129	0.050	-0.194	0.073	0.091	0.070	0.285	0.100	-0.102	0.101	32.22	10.11
5	0.219	0.124	-0.022	0.600	0.068	0.315	0.027	0.403	0.170	0.475	0.143	0.630	0.197	0.613	35.81	122.58
		P' =	0.831	ksc			Q =	0.354	ksc							
1	0.122	0.024	-0.058	0.015	0.005	0.014	-0.058	0.015	0.122	0.024	0.181	0.028	0.064	0.028	1.55	4.45
2	0.212	0.026	-0.063	0.021	0.034	0.016	-0.059	0.020	0.207	0.025	0.267	0.032	0.149	0.032	7.35	3.47
3	0.241	0.048	-0.053	0.034	0.054	0.029	-0.042	0.035	0.230	0.046	0.272	0.058	0.188	0.058	11.73	6.12
4	0.035	0.110	-0.128	0.070	-0.004	0.065	-0.128	0.070	0.035	0.110	0.163	0.131	-0.093	0.131	-1.69	22.78
5	0.667	0.907	-1.334	0.129	0.578	0.445	-1.002	0.751	0.335	0.508	1.338	0.895	-0.666	0.917	29.88	19.58
		P' =	0.799	ksc			Q =	0.366	ksc							
1	0.148	0.016	-0.260	0.014	0.011	0.011	-0.260	0.014	0.148	0.016	0.408	0.021	-0.112	0.021	1.56	1.50
2	0.197	0.026	-0.307	0.021	0.022	0.017	-0.306	0.021	0.196	0.026	0.503	0.033	-0.109	0.033	2.50	1.89
3	0.288	0.045	-0.327	0.038	0.049	0.030	-0.323	0.038	0.284	0.045	0.608	0.059	-0.039	0.059	4.68	2.79
4	0.193	0.102	-0.424	0.090	0.034	0.068	-0.422	0.090	0.192	0.102	0.614	0.136	-0.230	0.136	3.20	6.34
5	0.589	0.924	-0.255	0.796	-0.133	0.607	-0.232	0.798	0.566	0.923	0.799	1.219	0.334	1.219	-9.77	43.57
		P' =	0.773	ksc			Q =	0.370	ksc							
1	0.251	0.023	-0.414	0.016	0.006	0.014	-0.414	0.016	0.251	0.023	0.665	0.028	-0.162	0.028	0.49	1.20
2	0.365	0.026	-0.474	0.023	0.020	0.017	-0.474	0.023	0.364	0.026	0.839	0.035	-0.109	0.035	1.36	1.18
3	0.471	0.039	-0.559	0.040	0.041	0.028	-0.558	0.040	0.470	0.039	1.028	0.056	-0.088	0.056	2.26	1.56
4	0.355	0.068	-0.642	0.104	0.027	0.063	-0.642	0.104	0.354	0.068	0.996	0.124	-0.287	0.124	1.56	3.59
5	0.669	0.148	-1.122	0.640	0.482	0.338	-0.932	0.583	0.479	0.312	1.411	0.667	-0.453	0.657	21.52	13.46
		P' =	0.753	ksc			Q =	0.374	ksc							
1	0.345	0.029	-0.596	0.022	0.006	0.018	-0.596	0.022	0.345	0.028	0.941	0.036	-0.250	0.036	0.38	1.10
2	0.504	0.037	-0.693	0.028	0.001	0.023	-0.693	0.028	0.504	0.037	1.197	0.047	-0.189	0.047	0.07	1.11
3	0.610	0.062	-0.825	0.043	0.012	0.038	-0.825	0.043	0.610	0.062	1.436	0.075	-0.214	0.075	0.48	1.50
4	0.651	0.110	-0.760	0.109	-0.022	0.077	-0.759	0.109	0.651	0.110	1.411	0.155	-0.108	0.155	-0.93	3.14
5	1.649	0.440	-1.321	0.931	0.091	0.525	-1.319	0.927	1.646	0.448	2.965	1.030	0.327	1.030	1.75	10.14
		P' =	0.731	ksc			Q =	0.378	ksc							
1	0.484	0.036	-0.805	0.028	-0.001	0.023	-0.805	0.028	0.484	0.036	1.289	0.046	-0.320	0.046	-0.05	1.01
2	0.686	0.045	-0.977	0.029	-0.005	0.026	-0.977	0.029	0.686	0.045	1.664	0.053	-0.291	0.053	-0.19	0.91
3	0.910	0.066	-1.096	0.044	0.005	0.039	-1.096	0.044	0.910	0.066	2.006	0.079	-0.186	0.079	0.16	1.12
4	0.984	0.094	-1.259	0.081	0.084	0.062	-1.256	0.081	0.981	0.094	2.238	0.124	-0.275	0.124	2.14	1.59
5	1.102	0.917	-1.296	0.660	0.101	0.560	-1.292	0.664	1.098	0.914	2.390	1.130	-0.194	1.130	2.43	13.44

AREA	Ex	Ex(SD)	Ey	Ey(SD)	Exy	Exy(SD)	E3	E3(SD)	E1	E1(SD)	GAMMA G(SD)	EV	EV(SD)	PS.	PS(SD)
		P' =	0.712 ksc				Q =	0.382 ksc							
1	0.751	0.044	-1.112	0.043	0.004	0.031	-1.112	0.043	0.751	0.044	1.864 0.062	-0.360	0.062	0.12	0.95
2	1.024	0.050	-1.383	0.040	0.004	0.032	-1.383	0.040	1.024	0.050	2.407 0.064	-0.359	0.064	0.10	0.76
3	1.298	0.060	-1.642	0.048	-0.005	0.038	-1.643	0.048	1.298	0.060	2.941 0.077	-0.344	0.077	-0.10	0.75
4	1.409	0.108	-1.753	0.106	-0.095	0.076	-1.750	0.106	1.406	0.108	3.156 0.152	-0.344	0.152	-1.73	1.38
5	1.644	0.349	-1.671	0.688	-0.391	0.393	-1.623	0.688	1.596	0.351	3.220 0.772	-0.026	0.772	-7.03	7.00
		P' =	0.700 ksc				Q =	0.386 ksc							
1	0.911	0.053	-1.415	0.051	0.004	0.037	-1.415	0.051	0.911	0.053	2.327 0.074	-0.503	0.074	0.10	0.91
2	1.256	0.057	-1.744	0.050	0.026	0.038	-1.744	0.050	1.256	0.057	3.001 0.076	-0.487	0.076	0.50	0.72
3	1.560	0.075	-2.058	0.071	0.054	0.052	-2.057	0.071	1.559	0.075	3.617 0.103	-0.497	0.103	0.86	0.82
4	1.741	0.109	-2.409	0.149	0.124	0.093	-2.406	0.148	1.737	0.109	4.143 0.184	-0.668	0.185	1.72	1.28
5	1.515	0.170	-3.510	1.037	0.135	0.541	-3.506	1.032	1.512	0.198	5.019 1.051	-1.994	1.051	1.55	6.16

UNDRAINED SHEAR: DSC35 (UNCORRECTED)

AREA	Ex	Ex(SD)	Ey	Ey(SD)	Exy	Exy(SD)	E3	E3(SD)	E1	E1(SD)	GAMMA	G(SD)	EV	EV(SD)	PS.	PS(SD)
		P' =	0.972 ksc				Q =	0.262 ksc								
1	0.071	0.015	0.019	0.012	-0.004	0.010	0.01v	0.015	0.071	0.012	0.052	0.020	0.090	0.020	85.28	10.74
2	0.104	0.023	-0.017	0.020	-0.031	0.015	-0.006	0.023	0.093	0.020	0.099	0.030	0.087	0.030	70.57	8.73
3	0.139	0.044	0.042	0.032	-0.026	0.027	0.063	0.040	0.118	0.035	0.055	0.053	0.182	0.054	52.15	27.67
4	0.063	0.084	-0.017	0.063	-0.020	0.052	0.002	0.075	0.044	0.071	0.042	0.103	0.047	0.105	47 14	71.65
5	0.012	0.443	-0.892	0.462	-0.213	0.323	-0.654	0.458	-0.225	0.457	0.429	0.647	-0.879	0.641	41.86	42.80
		P' =	0.932 ksc				Q =	0.224 ksc								
1	0.024	0.016	-0.076	0.013	-0.012	0.010	-0.074	0.016	0.022	0.013	0.097	0.021	-0.052	0.021	82.82	6.02
2	0.088	0.024	-0.073	0.018	-0.038	0.015	-0.062	0.024	0.077	0.018	0.140	0.030	0.015	0.030	73.38	6.10
3	0.127	0.043	-0.079	0.031	-0.057	0.026	-0.054	0.042	0.102	0.033	0.157	0.053	0.048	0.054	66.44	9.68
4	0.231	0.093	-0.194	0.090	-0.119	0.065	-0.139	0.092	0.177	0.090	0.316	0.129	0.037	0.129	65.49	11.71
5	1.158	0.326	-0.024	0.207	-0.327	0.187	0.228	0.247	0.906	0.293	0.678	0.376	1.134	0.386	52.36	16.22
		P' =	0.906 ksc				Q =	0.204 ksc								
1	0.122	0.017	-0.060	0.011	-0.042	0.010	-0.048	0.017	0.110	0.012	0.159	0.021	0.062	0.021	73.94	3.67
2	0.158	0.027	-0.046	0.017	-0.051	0.015	-0.029	0.026	0.141	0.017	0.169	0.031	0.112	0.031	71.22	5.21
3	0.243	0.049	-0.007	0.030	-0.071	0.028	0.028	0.046	0.208	0.033	0.180	0.056	0.236	0.057	63.71	8.95
4	0.207	0.131	-0.009	0.084	-0.043	0.076	0.001	0.129	0.197	0.085	0.197	0.155	0.198	0.155	76.78	22.11
5	0.045	0.973	-0.361	0.321	0.046	0.481	-0.356	0.358	0.039	0.954	0.396	1.020	-0.316	1.025	6.76	70.52
		P' =	0.871 ksc				Q =	0.180 ksc								
1	0.123	0.015	-0.113	0.013	-0.048	0.010	-0.101	0.015	0.112	0.013	0.213	0.020	0.011	0.020	76.38	2.61
2	0.156	0.021	-0.135	0.020	-0.065	0.014	-0.117	0.021	0.138	0.020	0.256	0.029	0.021	0.029	74.61	3.23
3	0.211	0.035	-0.139	0.036	-0.077	0.026	-0.118	0.035	0.190	0.036	0.308	0.051	0.072	0.051	74.84	4.74
4	0.310	0.073	-0.261	0.090	-0.163	0.059	-0.177	0.075	0.227	0.087	0.404	0.117	0.049	0.116	62.98	8.28
5	0.603	0.409	-0.257	0.492	-0.201	0.327	-0.198	0.413	0.544	0.488	0.742	0.643	0.347	0.640	73.59	25.14
		P' =	0.833 ksc				Q =	0.164 ksc								
1	0.230	0.019	-0.192	0.013	-0.105	0.011	-0.157	0.018	0.194	0.013	0.352	0.022	0.037	0.022	71.53	1.80
2	0.283	0.027	-0.214	0.016	-0.111	0.015	-0.184	0.026	0.252	0.016	0.437	0.031	0.069	0.031	74.67	1.99
3	0.316	0.055	-0.229	0.028	-0.107	0.030	-0.204	0.055	0.292	0.028	0.497	0.062	0.087	0.062	77.17	3.46
4	0.277	0.102	-0.345	0.069	-0.128	0.060	-0.314	0.101	0.246	0.070	0.560	0.122	-0.068	0.123	76.39	6.16
5	0.833	0.816	0.005	0.456	-0.145	0.450	0.034	0.810	0.805	0.461	0.771	0.932	0.839	0.935	78.92	33.48
		P' =	0.793 ksc				Q =	0.158 ksc								
1	0.271	0.017	-0.250	0.014	-0.127	0.011	-0.210	0.017	0.230	0.014	0.440	0.022	0.020	0.022	72.34	1.43
2	0.334	0.025	-0.256	0.020	-0.142	0.016	-0.211	0.025	0.289	0.020	0.500	0.032	0.078	0.032	72.59	1.81
3	0.388	0.043	-0.238	0.033	-0.150	0 027	-0.191	0.042	0.341	0.033	0.533	0.054	0.150	0.054	72.75	2.87
4	0.494	0.098	-0.252	0.078	-0.194	0.062	-0.182	0.097	0.424	0.079	0.606	0.125	0.242	0.125	70.06	5.87
5	0.275	0.586	-0.354	0.027	0.010	0.270	-0.354	0.584	0.275	0.054	0.630	0.586	-0.079	0.587	0.95	24.72
		P' =	0.768 ksc				Q =	0.156 ksc								
1	0.322	0.020	-0.317	0.014	-0.161	0.012	-0.262	0.020	0.268	0.014	0.531	0.024	0.005	0.024	71.27	1.28
2	0.356	0.028	-0.351	0.019	-0.162	0.017	-0.304	0.028	0.309	0.019	0.614	0.034	0.005	0.034	74.00	1.55
3	0.412	0.054	-0.348	0.028	-0.178	0.030	-0.295	0.053	0.359	0.030	0.655	0.060	0.063	0.061	73.47	2.59
4	0.435	0.093	-0.447	0.073	-0.206	0.058	-0.386	0.092	0.374	0.074	0.760	0.118	-0.011	0.118	73.58	4.39
5	0.511	0.024	-0.359	0.469	-0.222	0.255	-0.281	0.135	0 433	0.454	0.715	0.482	0.152	0.470	70.79	20.10

UNDRAINED SHEAR: DSC31 (CORRECTED)

AREA	Ex	Ex(SD)	Ey	Ey(SD)	Exy	Exy(SD)	E3	E3(SD)	E1	E1(SD)	GAMMA	G(SD)	EV	EV(SD)	PS.	PS(SD)
		P' =	0.978	ksc			Q =	0.261	ksc							
1	0.123	0.013	0.146	0.009	-0.010	0.008	0.120	0.012	0.150	0.009	0.030	0.015	0.270	0.016	20.39	14.49
2	0.141	0.016	0.167	0.010	0.009	0.009	0.138	0.016	0.170	0.011	0.032	0.019	0.307	0.019	-17.65	16.81
3	0.155	0.026	0.155	0.015	0.018	0.015	0.157	0.021	0.173	0.022	0.036	0.030	0.310	0.030	44.53	24.27
4	0.232	0.074	0.165	0.040	0.052	0.041	0.137	0.050	0.260	0.068	0.123	0.083	0.397	0.084	28.48	19.51
5	0.957	0.194	-0.068	0.165	-0.038	0.128	-0.069	0.165	0.958	0.194	1.027	0.255	0.889	0.255	-2.10	7.15
		P' =	0.959	ksc			Q =	0.220	ksc							
1	-0.028	0.009	0.004	0.008	0.000	0.006	-0.028	0.009	0.004	0.008	0.032	0.012	-0.024	0.012	-0.40	10.90
2	-0.047	0.013	0.008	0.012	-0.001	0.009	-0.047	0.013	0.008	0.012	0.055	0.018	-0.039	0.018	0.54	9.19
3	-0.029	0.025	-0.010	0.020	-0.002	0.016	-0.029	0.025	-0.010	0.020	0.019	0.032	-0.039	0.032	6.04	47.17
4	0.020	0.067	0.020	0.040	0.040	0.038	-0.019	0.055	0.060	0.055	0.079	0.077	0.040	0.078	44.81	28.21
5	0.776	0.374	0.046	0.279	0.095	0.235	0.034	0.280	0.788	0.372	0.754	0.467	0.822	0.466	7.28	17.89
		P' =	0.933	ksc			Q =	0.181	ksc							
1	-0.025	0.011	0.027	0.009	-0.007	0.007	-0.026	0.011	0.028	0.009	0.054	0.014	0.002	0.014	7.61	7.48
2	-0.025	0.015	0.057	0.012	-0.011	0.009	-0.026	0.015	0.059	0.012	0.085	0.019	0.032	0.019	7.43	6.39
3	-0.031	0.024	0.041	0.021	-0.027	0.016	-0.040	0.024	0.050	0.021	0.090	0.032	0.010	0.032	18.24	10.06
4	-0.014	0.062	0.006	0.038	-0.041	0.036	-0.046	0.054	0.038	0.048	0.085	0.072	-0.008	0.073	38.21	24.64
5	0.321	0.153	-0.256	0.153	0.038	0.108	-0.259	0.153	0.323	0.153	0.582	0.217	0.065	0.217	3.75	10.68
		P' =	0.912	ksc			Q =	0.140	ksc							
1	-0.038	0.012	0.052	0.008	-0.005	0.007	-0.038	0.012	0.052	0.008	0.091	0.014	0.014	0.014	3.33	4.44
2	-0.034	0.014	0.066	0.011	0.018	0.009	-0.037	0.014	0.069	0.012	0.106	0.018	0.032	0.018	-10.16	4.90
3	-0.039	0.025	0.060	0.019	0.000	0.016	-0.039	0.025	0.060	0.019	0.099	0.031	0.020	0.031	-0.21	8.99
4	0.028	0.061	0.032	0.050	0.028	0.040	0.002	0.057	0.058	0.056	0.056	0.079	0.060	0.079	-42.72	40.53
5	-0.048	0.399	-0.182	0.439	0.194	0.296	-0.320	0.422	0.091	0.409	0.411	0.592	-0.230	0.593	35.44	41.31
		P' =	0.873	ksc			Q =	0.100	ksc							
1	-0.090	0.012	0.062	0.010	-0.018	0.008	-0.092	0.012	0.064	0.010	0.157	0.016	-0.028	0.016	6.57	2.85
2	-0.085	0.015	0.073	0.013	0.002	0.010	-0.085	0.015	0.073	0.013	0.158	0.020	-0.012	0.020	-0.73	3.57
3	-0.087	0.023	0.035	0.020	-0.011	0.015	-0.088	0.023	0.036	0.020	0.124	0.030	-0.052	0.030	5.05	6.96
4	0.042	0.028	0.060	0.055	0.023	0.032	0.026	0.039	0.075	0.049	0.049	0.063	0.102	0.062	-33.83	36.37
5	0.191	0.180	-0.290	0.450	-0.128	0.237	-0.322	0.440	0.223	0.206	0.545	0.485	-0.099	0.485	-14.06	25.18
		P' =	0.798	ksc			Q =	0.021	ksc							
1	-0.201	0.013	0.132	0.010	-0.012	0.008	-0.201	0.013	0.133	0.010	0.334	0.017	-0.069	0.017	2.07	1.43
2	-0.202	0.014	0.150	0.012	-0.007	0.009	-0.202	0.014	0.150	0.012	0.352	0.019	-0.052	0.019	1.16	1.53
3	-0.202	0.024	0.124	0.021	-0.013	0.016	-0.202	0.024	0.125	0.021	0.327	0.032	-0.077	0.032	2.23	2.77
4	-0.175	0.058	0.057	0.034	-0.017	0.033	-0.176	0.058	0.059	0.034	0.235	0.067	-0.118	0.067	4.15	8.13
5	-0.107	0.116	-0.028	0.316	0.321	0.164	-0.391	0.222	0.256	0.244	0.646	0.329	-0.135	0.336	-41.46	14.93
		P' =	0.756	ksc			Q =	0.010	ksc							
1	-0.331	0.011	0.141	0.011	-0.015	0.008	-0.332	0.011	0.142	0.011	0.474	0.016	-0.190	0.016	1.84	0.95
2	-0.350	0.014	0.142	0.013	-0.024	0.010	-0.351	0.014	0.143	0.013	0.494	0.019	-0.209	0.019	2.79	1.10
3	-0.359	0.021	0.096	0.023	-0.021	0.016	-0.360	0.021	0.097	0.023	0.457	0.032	-0.262	0.032	2.64	1.98
4	-0.300	0.055	0.035	0.043	-0.029	0.035	-0.302	0.054	0.037	0.043	0.339	0.070	-0.265	0.070	4.89	5.84
5	-0.117	0.046	-0.238	0.335	0.021	0.164	-0.242	0.329	-0.113	0.070	0.128	0.335	-0.355	0.338	9.51	73.07

AREA	Ex	Ex(SD)	Ey	Ey(SD)	Exy	Exy(SD)	E3	E3(SD)	E1	E1(SD)	GAMMA	G(SD)	EV	EV(SD)	PS.	PS(SD)
			P' = 0.726 ksc				Q = 0.030 ksc									
1	-0.448	0.013	0.156	0.010	0.005	0.008	-0.448	0.013	0.156	0.010	0.604	0.016	-0.292	0.016	-0.49	0.76
2	-0.455	0.016	0.150	0.013	0.005	0.010	-0.455	0.016	0.150	0.013	0.605	0.020	-0.305	0.020	-0.45	0.96
3	-0.432	0.023	0.130	0.023	-0.015	0.016	-0.432	0.023	0.130	0.023	0.562	0.032	-0.302	0.032	1.52	1.64
4	-0.322	0.043	0.131	0.052	-0.000	0.034	-0.322	0.043	0.131	0.052	0.453	0.068	-0.190	0.068	0.04	4.32
5	-0.333	0.027	-0.169	0.517	-0.083	0.251	-0.368	0.197	-0.135	0.478	0.234	0.505	-0.503	0.518	22.71	62.01
			P' = 0.699 ksc				Q = 0.050 ksc									
1	-0.536	0.029	0.285	0.063	0.005	0.035	-0.536	0.029	0.285	0.063	0.822	0.069	-0.251	0.069	-0.33	2.46
2	-0.511	0.020	0.179	0.015	-0.012	0.012	-0.511	0.020	0.179	0.015	0.690	0.025	-0.332	0.025	1.00	1.02
3	-0.482	0.027	0.159	0.027	-0.025	0.019	-0.483	0.027	0.160	0.027	0.643	0.038	-0.323	0.038	2.19	1.69
4	-0.481	0.068	0.075	0.057	-0.034	0.044	-0.483	0.068	0.077	0.057	0.560	0.089	-0.406	0.089	3.44	4.55
5	-0.361	0.133	0.102	0.053	-0.135	0.073	-0.397	0.130	0.138	0.062	0.535	0.144	-0.259	0.143	15.08	7.82
			P' = 0.670 ksc				Q = 0.070 ksc									
1	-0.551	0.015	0.314	0.016	-0.018	0.011	-0.551	0.015	0.315	0.016	0.866	0.022	-0.237	0.022	1.19	0.72
2	-0.544	0.020	0.307	0.015	-0.015	0.012	-0.545	0.020	0.307	0.015	0.852	0.025	-0.237	0.025	1.03	0.83
3	-0.533	0.025	0.293	0.024	-0.007	0.017	-0.533	0.025	0.293	0.024	0.826	0.034	-0.239	0.034	0.47	1.19
4	-0.448	0.062	0.221	0.049	0.007	0.039	-0.448	0.062	0.221	0.049	0.670	0.079	-0.227	0.079	-0.60	3.36
5	-0.200	0.143	0.077	0.362	0.124	0.190	-0.247	0.182	0.125	0.339	0.372	0.388	-0.122	0.389	-20.89	29.79
			P' = 0.642 ksc				Q = 0.090 ksc									
1	-0.644	0.016	0.343	0.012	-0.002	0.010	-0.644	0.016	0.343	0.012	0.987	0.020	-0.301	0.020	0.13	0.56
2	-0.672	0.018	0.341	0.014	-0.000	0.011	-0.672	0.018	0.341	0.014	1.013	0.023	-0.331	0.023	0.02	0.64
3	-0.665	0.029	0.323	0.024	-0.001	0.019	-0.665	0.029	0.323	0.024	0.987	0.038	-0.342	0.038	0.06	1.09
4	-0.600	0.072	0.245	0.041	0.013	0.041	-0.600	0.072	0.246	0.041	0.846	0.083	-0.355	0.083	-0.90	2.78
5	-0.238	0.099	0.209	0.415	0.014	0.208	-0.238	0.099	0.209	0.415	0.448	0.427	-0.029	0.427	-1.80	26.59
			P' = 0.606 ksc				Q = 0.110 ksc									
1	-1.903	0.014	-0.661	0.013	-0.003	0.010	-1.903	0.014	-0.661	0.013	1.242	0.019	-2.564	0.019	0.15	0.44
2	-1.941	0.017	-0.651	0.015	0.012	0.012	-1.941	0.017	-0.650	0.015	1.291	0.023	-2.592	0.023	-0.53	0.51
3	-1.951	0.029	-0.652	0.022	0.032	0.018	-1.952	0.029	-0.651	0.022	1.301	0.037	-2.603	0.037	-1.43	0.80
4	-1.908	0.075	-0.671	0.040	0.015	0.042	-1.908	0.075	-0.671	0.040	1.237	0.085	-2.578	0.085	-0.67	1.95
5	-1.384	0.073	-0.974	0.347	0.063	0.172	-1.394	0.087	-0.965	0.342	0.429	0.355	-2.358	0.354	-8.55	23.17
			P' = 0.574 ksc				Q = 0.130 ksc									
1	-0.942	0.014	0.576	0.019	-0.008	0.012	-0.942	0.014	0.576	0.019	1.519	0.024	-0.366	0.024	0.31	0.45
2	-0.988	0.018	0.636	0.022	-0.002	0.014	-0.988	0.018	0.636	0.022	1.625	0.028	-0.352	0.028	0.08	0.50
3	-1.000	0.030	0.601	0.035	-0.007	0.023	-1.000	0.030	0.601	0.035	1.601	0.046	-0.399	0.046	0.24	0.83
4	-0.979	0.074	0.557	0.069	-0.026	0.051	-0.979	0.074	0.558	0.069	1.537	0.101	-0.422	0.101	0.96	1.88
5	-0.331	0.151	0.738	0.223	0.045	0.133	-0.333	0.151	0.740	0.223	1.073	0.269	0.408	0.269	-2.42	7.11
			P' = 0.538 ksc				Q = 0.150 ksc									
1	-1.072	0.017	0.782	0.019	-0.024	0.013	-1.073	0.017	0.783	0.019	1.855	0.025	-0.290	0.025	0.74	0.39
2	-1.160	0.020	0.871	0.021	-0.004	0.014	-1.160	0.020	0.871	0.021	2.031	0.028	-0.289	0.028	0.10	0.40
3	-1.172	0.038	0.888	0.031	0.013	0.025	-1.172	0.038	0.889	0.031	2.061	0.049	-0.284	0.049	-0.35	0.68
4	-1.133	0.107	0.857	0.039	-0.003	0.056	-1.133	0.107	0.857	0.039	1.991	0.114	-0.276	0.114	0.09	1.61
5	-0.503	0.309	1.076	0.010	0.350	0.160	-0.577	0.302	1.150	0.067	1.727	0.309	0.573	0.309	-11.97	5.24

AREA	Ex	Ex(SD)	Ey	Ey(SD)	Exy	Exy(SD)	E3	E3(SD)	E1	E1(SD)	GAMMA G(SD)		EV	EV(SD)	PS.	PS(SD)
		P' =	0.507 ksc				Q =	0.160 ksc								
1	-1.312	0.025	0.856	0.023	-0.015	0.017	-1.312	0.025	0.856	0.023	2.168	0.034	-0.455	0.034	0.39	0.45
2	-1.448	0.024	0.932	0.025	-0.014	0.017	-1.448	0.024	0.932	0.025	2.380	0.034	-0.516	0.034	0.34	0.41
3	-1.491	0.039	0.954	0.040	-0.022	0.028	-1.491	0.039	0.955	0.040	2.446	0.056	-0.536	0.056	0.51	0.65
4	-1.413	0.107	0.963	0.070	-0.062	0.063	-1.415	0.107	0.965	0.070	2.380	0.128	-0.450	0.128	1.50	1.52
5	-1.366	0.237	0.968	0.525	-0.065	0.282	-1.368	0.237	0.970	0.525	2.338	0.575	-0.397	0.576	1.60	6.91
		P' =	0.470 ksc				Q =	0.170 ksc								
1	-1.583	0.024	1.103	0.029	-0.028	0.019	-1.583	0.024	1.103	0.028	2.687	0.037	-0.480	0.037	0.60	0.40
2	-1.728	0.028	1.228	0.031	-0.044	0.021	-1.728	0.028	1.229	0.031	2.957	0.041	-0.500	0.041	0.86	0.40
3	-1.805	0.049	1.324	0.040	-0.040	0.032	-1.805	0.049	1.324	0.040	3.130	0.063	-0.481	0.063	0.72	0.58
4	-1.812	0.123	1.326	0.081	-0.032	0.073	-1.812	0.123	1.327	0.081	3.139	0.148	-0.485	0.148	0.58	1.34
5	-0.848	0.459	1.367	0.035	-0.100	0.237	-0.852	0.459	1.372	0.041	2.224	0.461	0.519	0.460	2.58	6.13
		P' =	0.450 ksc				Q =	0.180 ksc								
1	-1.828	0.026	1.322	0.035	-0.041	0.022	-1.828	0.026	1.322	0.035	3.151	0.043	-0.506	0.043	0.75	0.40
2	-1.975	0.027	1.508	0.037	-0.031	0.023	-1.976	0.027	1.509	0.037	3.484	0.045	-0.467	0.045	0.51	0.38
3	-2.066	0.048	1.649	0.049	-0.037	0.034	-2.066	0.048	1.649	0.049	3.716	0.068	-0.417	0.068	0.56	0.53
4	-2.170	0.097	1.746	0.078	-0.057	0.062	-2.171	0.097	1.747	0.078	3.918	0.124	-0.424	0.124	0.83	0.91
5	-1.317	0.478	1.660	0.739	-0.282	0.435	-1.343	0.482	1.687	0.738	3.030	0.879	0.344	0.880	5.36	8.21
		P' =	0.430 ksc				Q =	0.190 ksc								
1	-2.108	0.038	1.623	0.043	-0.061	0.029	-2.109	0.038	1.624	0.043	3.733	0.057	-0.485	0.057	0.93	0.44
2	-2.337	0.036	1.854	0.043	-0.082	0.028	-2.339	0.036	1.856	0.043	4.194	0.056	-0.483	0.056	1.12	0.39
3	-2.463	0.054	2.007	0.054	-0.091	0.038	-2.465	0.054	2.009	0.054	4.474	0.076	-0.457	0.076	1.16	0.49
4	-2.535	0.112	2.135	0.079	-0.078	0.068	-2.536	0.112	2.137	0.079	4.673	0.138	-0.400	0.138	0.96	0.84
5	-2.006	0.012	1.922	0.562	-0.130	0.272	-2.010	0.021	1.926	0.562	3.936	0.561	-0.083	0.562	1.89	3.96
		P' =	0.402 ksc				Q =	0.200 ksc								
1	-2.737	0.057	2.177	0.059	-0.120	0.041	-2.740	0.057	2.180	0.059	4.921	0.082	-0.560	0.082	1.40	0.48
2	-3.102	0.051	2.490	0.063	-0.149	0.041	-3.106	0.051	2.494	0.063	5.600	0.081	-0.613	0.081	1.52	0.42
3	-3.358	0.069	2.774	0.071	-0.150	0.050	-3.362	0.069	2.778	0.071	6.139	0.099	-0.584	0.099	1.40	0.46
4	-3.530	0.128	2.949	0.085	-0.099	0.076	-3.531	0.128	2.951	0.085	6.482	0.154	-0.580	0.154	0.88	0.67
5	-2.670	0.081	3.220	0.315	-0.402	0.158	-2.697	0.083	3.247	0.314	5.945	0.324	0.550	0.325	3.88	1.52
		P' =	0.380 ksc				Q =	0.210 ksc								
1	-4.161	0.087	3.578	0.098	-0.200	0.066	-4.166	0.087	3.584	0.098	7.750	0.131	-0.582	0.131	1.48	0.49
2	-4.736	0.088	4.103	0.104	-0.236	0.069	-4.742	0.088	4.109	0.104	8.851	0.137	-0.633	0.137	1.53	0.44
3	-5.182	0.096	4.652	0.115	-0.241	0.075	-5.188	0.096	4.658	0.115	9.847	0.149	-0.530	0.149	1.40	0.44
4	-5.553	0.154	5.059	0.128	-0.270	0.100	-5.560	0.154	5.066	0.128	10.626	0.200	-0.493	0.200	1.46	0.54
5	-5.537	0.759	5.142	0.113	-0.338	0.395	-5.548	0.759	5.153	0.116	10.701	0.768	-0.395	0.767	1.81	2.12
		P' =	0.375 ksc				Q =	0.214 ksc								
1	-5.051	0.130	4.564	0.134	-0.245	0.094	-5.057	0.130	4.570	0.134	9.627	0.187	-0.487	0.187	1.46	0.56
2	-5.895	0.127	5.333	0.138	-0.302	0.094	-5.904	0.127	5.341	0.138	11.245	0.187	-0.562	0.187	1.54	0.48
3	-6.588	0.136	6.093	0.154	-0.300	0.103	-6.595	0.136	6.100	0.154	12.696	0.205	-0.495	0.205	1.35	0.46
4	-7.274	0.198	6.568	0.220	-0.298	0.148	-7.280	0.198	6.575	0.220	13.855	0.296	-0.706	0.296	1.23	0.61
5	-6.924	0.469	6.754	0.598	-0.369	0.378	-6.934	0.469	6.764	0.599	13.698	0.760	-0.170	0.760	1.55	1.58

AREA	Ex	Ex(SD)	Ey	Ey(SD)	Exy	Exy(SD)	E3	E3(SD)	E1	E1(SD)	GAMMA	G(SD)	EV	EV(SD)	PS.	PS(SD)
			P' =	0.369 ksc				Q =	0.216 ksc							
1	-5.985	0.157	5.473	0.162	-0.229	0.113	-5.992	0.157	5.480	0.162	11.472	0.225	-0.512	0.225	1.44	0.56
2	-6.992	0.156	6.402	0.169	-0.343	0.116	-7.001	0.156	6.410	0.169	13.411	0.230	-0.590	0.230	1.46	0.49
3	-7.842	0.167	7.353	0.181	-0.370	0.123	-7.851	0.167	7.362	0.181	15.213	0.246	-0.490	0.246	1.39	0.46
4	-8.652	0.194	8.116	0.205	-0.325	0.141	-8.658	0.194	8.123	0.205	16.781	0.282	-0.536	0.282	1.11	0.48
5	-8.690	0.288	8.733	0.998	-0.635	0.506	-8.713	0.290	8.756	0.998	17.469	1.038	0.043	1.039	2.08	1.66

UNDRAINED SHEAR: DSC32 (CORRECTED)

AREA	Ex	Ex(SD)	Ey	Ey(SD)	Exy	Exy(SD)	E3	E3(SD)	E1	E1(SD)	GAMMA	G(SD)	EV	EV(SD)	PS.	PS(SD)
		P' =	0.863	ksc			Q =	0.272	ksc							
1	0.017	0.012	0.027	0.008	0.025	0.007	-0.003	0.011	0.047	0.010	0.051	0.014	0.044	0.015	51.00	8.26
2	0.010	0.017	0.043	0.012	0.016	0.011	0.004	0.016	0.050	0.013	0.046	0.021	0.053	0.021	67.56	13.04
3	0.048	0.030	0.047	0.019	0.043	0.018	0.004	0.025	0.091	0.025	0.087	0.035	0.095	0.036	44.70	11.79
4	0.034	0.085	0.029	0.054	0.053	0.050	-0.021	0.070	0.086	0.071	0.105	0.099	0.063	0.100	43.79	27.20
5	-0.023	0.115	-0.041	0.059	0.127	0.064	-0.159	0.088	0.095	0.092	0.254	0.128	-0.064	0.129	43.05	14.52
		P' =	0.857	ksc			Q =	0.275	ksc							
1	-0.001	0.012	-0.007	0.009	0.024	0.008	-0.029	0.011	0.020	0.011	0.049	0.015	-0.008	0.015	41.41	8.89
2	-0.017	0.019	0.025	0.013	0.032	0.012	-0.034	0.018	0.043	0.014	0.077	0.023	0.008	0.023	61.75	8.60
3	0.008	0.031	-0.002	0.019	0.046	0.018	-0.044	0.025	0.050	0.027	0.093	0.037	0.006	0.037	41.96	11.31
4	-0.002	0.067	-0.028	0.044	0.039	0.040	-0.056	0.053	0.026	0.060	0.082	0.080	-0.030	0.080	35.92	28.24
5	0.098	0.161	-0.076	0.076	-0.075	0.088	-0.105	0.091	0.126	0.154	0.231	0.177	0.022	0.179	69.58	21.92
		P' =	0.848	ksc			Q =	0.279	ksc							
1	0.046	0.014	0.008	0.011	0.034	0.009	-0.012	0.012	0.066	0.014	0.077	0.018	0.054	0.018	30.54	6.75
2	0.036	0.022	0.016	0.015	0.030	0.014	-0.006	0.018	0.058	0.020	0.064	0.027	0.052	0.027	35.91	12.07
3	0.046	0.048	-0.039	0.024	0.053	0.027	-0.064	0.030	0.071	0.045	0.135	0.053	0.006	0.054	25.56	11.34
4	-0.096	0.134	-0.065	0.059	0.035	0.072	-0.119	0.116	-0.042	0.087	0.077	0.145	-0.161	0.147	57.15	54.32
5	-0.053	1.154	0.074	0.568	0.106	0.637	-0.113	1.034	0.134	0.745	0.247	1.272	0.021	1.286	60.53	148.05
		P' =	0 839	ksc			Q =	0.280	ksc							
1	-0.025	0.014	-0.017	0.010	0.058	0.008	-0.079	0.012	0.037	0.012	0.116	0.017	-0.042	0.017	47.17	4.17
2	-0.048	0.023	0.004	0.015	0.054	0.014	-0.082	0.021	0.038	0.018	0.119	0.027	-0.044	0.027	58.05	6.58
3	-0.059	0.038	-0.020	0.024	0.100	0.022	-0.141	0.033	0.062	0.030	0.204	0.045	-0.079	0.045	50.52	6.32
4	-0.075	0.084	-0.110	0.063	0.145	0.052	-0.238	0.073	0.053	0.075	0.291	0.105	-0.185	0.105	41.50	10.34
5	0.096	0.369	0.260	0.134	0.107	0.194	0.043	0.333	0.313	0.200	0.270	0.387	0.356	0.392	63.75	41.16
		P' =	0.830	ksc			Q =	0.283	ksc							
1	0.038	0.015	-0.007	0.012	0.051	0.010	-0.040	0.013	0.071	0.014	0.111	0.019	0.031	0.019	33.11	4.91
2	0.023	0.022	0.002	0.015	0.071	0.013	-0.060	0.019	0.085	0.019	0.145	0.027	0.025	0.027	40.72	5.32
3	0.043	0.039	-0.005	0.027	0.080	0.024	-0.065	0.032	0.103	0.035	0.168	0.047	0.038	0.047	36.58	8.06
4	0.066	0.111	-0.027	0.070	0.108	0.065	-0.099	0.084	0.137	0.100	0.236	0.131	0.038	0.131	33.33	15.95
5	0.220	0.057	-0.132	0.296	0.237	0.153	-0.251	0.265	0.339	0.144	0.591	0.303	0.088	0.302	26.74	14.62
		P' =	0.815	ksc			Q =	0.288	ksc							
1	0.038	0.014	-0.013	0.012	0.106	0.009	-0.097	0.013	0.121	0.014	0.218	0.019	0.025	0.019	38.24	2.49
2	-0.007	0.021	0.002	0.018	0.077	0.014	-0.079	0.019	0.075	0.019	0.154	0.027	-0.005	0.027	46.65	5.04
3	-0.022	0.038	-0.018	0.028	0.077	0.023	-0.097	0.033	0.057	0.033	0.154	0.046	-0.040	0.047	45.76	8.68
4	-0.035	0.069	0.012	0.073	0.094	0.050	-0.108	0.070	0.085	0.071	0.194	0.100	-0.023	0.100	52.03	14.82
5	0.634	0.224	0.172	0.115	0.084	0.125	0.157	0.119	0.649	0.221	0.492	0.252	0.806	0.252	9.98	14.56
		P' =	0.810	ksc			Q =	0.290	ksc							
1	-0.005	0.017	-0.030	0.012	0.119	0.010	-0.137	0.014	0.103	0.015	0.240	0.021	-0.035	0.021	42.03	2.46
2	-0.036	0.026	-0.022	0.017	0.111	0.016	-0.139	0.022	0.082	0.022	0.221	0.031	-0.058	0.031	46.73	4.03
3	0.017	0.048	-0.044	0.026	0.120	0.027	-0.137	0.036	0.111	0.041	0.248	0.054	-0.027	0.055	37.83	6.29
4	-0.070	0.119	-0.094	0.072	0.191	0.069	-0.273	0.096	0.109	0.099	0.382	0.138	-0.164	0.139	43.18	10.43
5	0.638	0.303	-0.119	0.196	0.217	0.179	-0.177	0.203	0.696	0.296	0.873	0.361	0.519	0.361	14.93	11.81

AREA	Ex	Ex(SD)	Ey	Ey(SD)	Exy	Exy(SD)	E3	E3(SD)	E1	E1(SD)	GAMMA	G(SD)	EV	EV(SD)	PS.	PS(SD)
		P' =	0.795	ksc			Q =	0.293	ksc							
1	0.218	0.022	0.195	0.024	0.104	0.016	0.102	0.023	0.311	0.023	0.209	0.033	0.413	0.033	41.87	4.47
2	0.268	0.033	0.255	0.027	0.110	0.021	0.152	0.030	0.372	0.030	0.220	0.042	0.523	0.042	43.37	5.52
3	0.311	0.047	0.245	0.035	0.157	0.029	0.117	0.040	0.439	0.042	0.321	0.058	0.556	0.059	39.11	5.22
4	0.229	0.102	0.211	0.071	0.094	0.062	0.125	0.086	0.314	0.088	0.189	0.123	0.440	0.124	42.36	18.78
5	-0.324	0.083	0.017	0.045	0.274	0.047	-0.476	0.075	0.169	0.056	0.645	0.094	-0.307	0.095	60.94	4.17
		P' =	0.780	ksc			Q =	0.298	ksc							
1	0.044	0.017	-0.057	0.015	0.180	0.011	-0.193	0.016	0.180	0.016	0.373	0.023	-0.013	0.023	37.15	1.75
2	0.006	0.026	-0.058	0.017	0.155	0.016	-0.184	0.021	0.132	0.023	0.316	0.031	-0.052	0.032	39.15	2.87
3	0.036	0.051	-0.076	0.026	0.164	0.028	-0.194	0.036	0.153	0.044	0.347	0.056	-0.041	0.057	35.55	4.69
4	-0.055	0.107	-0.126	0.058	0.193	0.060	-0.287	0.081	0.105	0.090	0.392	0.121	-0.182	0.122	39.79	8.91
5	0.370	0.177	0.169	0.001	0.216	0.087	0.032	0.093	0.508	0.147	0.476	0.175	0.540	0.177	32.51	10.66
		P' =	0.765	ksc			Q =	0.301	ksc							
1	-0.011	0.017	-0.128	0.019	0.191	0.013	-0.269	0.018	0.130	0.018	0.399	0.025	-0.139	0.025	36.47	1.82
2	-0.064	0.025	-0.124	0.017	0.166	0.015	-0.262	0.020	0.075	0.022	0.337	0.030	-0.187	0.030	39.87	2.55
3	-0.043	0.046	-0.108	0.026	0.165	0.026	-0.244	0.035	0.093	0.039	0.337	0.053	-0.151	0.053	39.47	4.50
4	-0.121	0.096	-0.166	0.056	0.164	0.055	-0.308	0.075	0.021	0.080	0.330	0.110	-0.287	0.111	41.14	9.63
5	-0.051	0.429	-0.113	0.105	0.290	0.217	-0.374	0.293	0.210	0.322	0.584	0.435	-0.164	0.441	41.95	21.66
		P' =	0.751	ksc			Q =	0.307	ksc							
1	0.025	0.018	-0.152	0.024	0.257	0.015	-0.335	0.023	0.208	0.021	0.543	0.031	-0.128	0.030	35.48	1.61
2	0.005	0.027	-0.109	0.027	0.223	0.019	-0.282	0.027	0.177	0.027	0.459	0.038	-0.105	0.038	37.80	2.39
3	0.001	0.053	-0.095	0.043	0.240	0.034	-0.292	0.047	0.198	0.049	0.489	0.068	-0.094	0.068	39.32	3.97
4	-0.025	0.131	-0.122	0.101	0.274	0.082	-0.352	0.114	0.205	0.119	0.557	0.165	-0.147	0.166	40.02	8.52
5	-0.345	0.284	0.121	0.163	0.344	0.162	-0.527	0.260	0.303	0.194	0.831	0.325	-0.224	0.327	62.04	11.23
		P' =	0.745	ksc			Q =	0.312	ksc							
1	-0.026	0.016	-0.182	0.027	0.306	0.016	-0.420	0.024	0.212	0.021	0.631	0.032	-0.208	0.032	37.83	1.43
2	-0.055	0.021	-0.149	0.026	0.282	0.017	-0.388	0.024	0.184	0.023	0.572	0.034	-0.204	0.034	40.30	1.69
3	-0.059	0.035	-0.132	0.032	0.262	0.024	-0.360	0.033	0.169	0.034	0.529	0.047	-0.192	0.048	41.03	2.57
4	-0.043	0.093	-0.147	0.082	0.301	0.062	-0.401	0.086	0.211	0.088	0.612	0.123	-0.190	0.124	40.10	5.79
5	-0.021	0.132	-0.079	0.154	0.185	0.102	-0.238	0.144	0.137	0.141	0.375	0.203	-0.100	0.203	40.52	15.48
		P' =	0.736	ksc			Q =	0.317	ksc							
1	-0.022	0.019	-0.276	0.031	0.380	0.018	-0.550	0.028	0.251	0.024	0.801	0.037	-0.299	0.036	35.75	1.30
2	-0.079	0.025	-0.239	0.033	0.339	0.021	-0.507	0.030	0.190	0.028	0.697	0.041	-0.318	0.041	38.35	1.69
3	-0.051	0.045	-0.281	0.042	0.315	0.031	-0.502	0.043	0.169	0.044	0.671	0.061	-0.332	0.061	34.97	2.61
4	-0.151	0.114	-0.305	0.069	0.248	0.066	-0.487	0.087	0.031	0.100	0.518	0.133	-0.456	0.133	36.36	7.37
5	0.659	0.241	0.045	0.089	0.183	0.127	-0.006	0.106	0.709	0.232	0.715	0.257	0.704	0.257	15.36	10.24
		P' =	0.723	ksc			Q =	0.320	ksc							
1	-0.017	0.022	-0.327	0.036	0.473	0.021	-0.670	0.032	0.325	0.028	0.995	0.042	-0.344	0.042	35.93	1.21
2	-0.057	0.028	-0.294	0.035	0.447	0.023	-0.638	0.033	0.287	0.031	0.925	0.046	-0.351	0.045	37.60	1.40
3	-0.070	0.041	-0.265	0.033	0.442	0.026	-0.620	0.036	0.285	0.038	0.905	0.053	-0.334	0.053	38.78	1.67
4	-0.120	0.105	-0.387	0.055	0.432	0.059	-0.706	0.076	0.199	0.090	0.905	0.118	-0.507	0.119	36.43	3.76
5	0.177	0.272	-0.157	0.353	0.366	0.224	-0.39[illegible]	0.330	0.412	0.297	0.805	0.446	0.019	0.445	32.75	15.84

AREA	Ex	Ex(SD)	Ey	Ey(SD)	Exy	Exy(SD)	E3	E3(SD)	E1	E1(SD)	GAMMA	G(SD)	EV	EV(SD)	PS.	PS(SD)
		P' =	0.692	ksc			Q =	0.327	ksc							
1	0.017	0.025	-0.567	0.065	0.746	0.035	-1.076	0.055	0.526	0.042	1.602	0.070	-0.551	0.069	34.31	1.24
2	-0.010	0.029	-0.533	0.075	0.686	0.041	-1.006	0.064	0.462	0.049	1.468	0.081	-0.544	0.080	34.56	1.57
3	0.000	0.042	-0.484	0.071	0.631	0.042	-0.918	0.064	0.434	0.054	1.352	0.084	-0.484	0.083	34.50	1.76
4	0.048	0.117	-0.371	0.086	0.598	0.072	-0.795	0.097	0.473	0.107	1.268	0.145	-0.322	0.145	35.35	3.28
5	0.232	0.129	-0.380	0.585	0.529	0.304	-0.685	0.509	0.538	0.314	1.223	0.602	-0.148	0.599	29.97	14.00
		P' =	0.649	ksc			Q =	0.333	ksc							
1	0.224	0.037	-1.032	0.121	1.453	0.065	-1.987	0.104	1.179	0.074	3.166	0.129	-0.808	0.127	33.31	1.15
2	0.224	0.050	-1.108	0.151	1.455	0.081	-2.042	0.131	1.158	0.093	3.199	0.161	-0.884	0.159	32.70	1.43
3	0.257	0.078	-1.102	0.170	1.396	0.095	-1.975	0.151	1.130	0.113	3.104	0.189	-0.845	0.188	32.02	1.73
4	0.305	0.115	-1.012	0.173	1.290	0.105	-1.802	0.159	1.095	0.133	2.897	0.209	-0.707	0.208	31.48	2.05
5	0.377	0.372	-0.754	0.123	1.204	0.193	-1.519	0.221	1.142	0.317	2.661	0.389	-0.377	0.391	32.42	4.22
		P' =	0.545	ksc			Q =	0.338	ksc							
1	0.934	0.135	-3.044	0.252	3.936	0.144	-5.465	0.226	3.355	0.176	8.820	0.288	-2.110	0.286	31.60	0.93
2	1.324	0.161	-3.702	0.335	4.315	0.188	-6.182	0.302	3.805	0.219	9.987	0.375	-2.378	0.371	29.89	1.07
3	1.639	0.244	-4.151	0.475	4.508	0.270	-6.613	0.434	4.101	0.314	10.714	0.538	-2.512	0.534	28.65	1.43
4	1.406	0.370	-4.179	0.688	4.280	0.394	-6.496	0.629	3.724	0.462	10.220	0.784	-2.773	0.781	28.44	2.19
5	0.694	0.092	-3.267	0.155	3.817	0.091	-5.586	0.141	3.014	0.112	8.600	0.181	-2.572	0.180	31.29	0.60

UNDRAINED SHEAR: DSC33 (CORRECTED)

AREA	Ex	Ex(SD)	Ey	Ey(SD)	Exy	Exy(SD)	E3	E3(SD)	E1	E1(SD)	GAMMA	G(SD)	EV	EV(SD)	PS.	PS(SD)
		P' =	0.935	ksc			Q =	0.270	ksc							
1	0.001	0.014	0.030	0.009	0.073	0.008	-0.059	0.012	0.090	0.011	0.150	0.016	0.031	0.017	50.68	3.17
2	0.001	0.020	0.039	0.013	0.080	0.012	-0.062	0.018	0.103	0.016	0.165	0.024	0.040	0.024	51.77	4.16
3	0.018	0.035	0.040	0.026	0.060	0.022	-0.032	0.032	0.090	0.030	0.122	0.044	0.058	0.044	50.02	10.34
4	0.030	0.082	0.064	0.055	0.121	0.049	-0.075	0.071	0.169	0.068	0.244	0.098	0.094	0.099	49.08	11.62
5	-0.344	0.193	0.568	0.424	0.279	0.238	-0.423	0.221	0.647	0.414	1.069	0.466	0.224	0.466	74.29	12.61
		P' =	0.914	ksc			Q =	0.271	ksc							
1	-0.077	0.015	-0.014	0.009	0.111	0.008	-0.161	0.013	0.070	0.011	0.231	0.017	-0.091	0.017	52.84	2.14
2	-0.110	0.018	-0.005	0.014	0.130	0.011	-0.198	0.016	0.083	0.015	0.281	0.022	-0.115	0.022	55.98	2.27
3	-0.051	0.026	0.004	0.024	0.127	0.018	-0.153	0.025	0.106	0.025	0.259	0.035	-0.047	0.035	51.15	3.92
4	-0.004	0.059	-0.039	0.060	0.115	0.042	-0.138	0.059	0.094	0.059	0.232	0.084	-0.043	0.084	40.63	10.37
5	0.058	0.279	0.173	0.045	-0.002	0.137	0.058	0.279	0.173	0.045	0.115	0.282	0.231	0.283	1.10	68.07
		P' =	0.897	ksc			Q =	0.275	ksc							
1	-0.090	0.014	-0.007	0.010	0.104	0.009	-0.161	0.013	0.063	0.011	0.224	0.017	-0.098	0.018	55.93	2.23
2	-0.090	0.018	-0.001	0.013	0.097	0.011	-0.152	0.016	0.062	0.015	0.214	0.022	-0.091	0.022	57.27	2.93
3	-0.089	0.035	-0.009	0.025	0.096	0.021	-0.153	0.032	0.055	0.028	0.208	0.042	-0.098	0.043	56.27	5.83
4	-0.065	0.091	0.008	0.055	0.137	0.053	-0.170	0.079	0.113	0.070	0.284	0.106	-0.057	0.107	52.43	10.74
5	-0.239	0.433	0.299	0.340	0.083	0.273	-0.252	0.432	0.311	0.343	0.563	0.550	0.060	0.550	81.41	27.83
		P' =	0.964	ksc			Q =	0.276	ksc							
1	0.006	0.012	0.014	0.009	0.029	0.007	-0.020	0.010	0.039	0.010	0.059	0.014	0.020	0.015	48.53	7.07
2	0.005	0.016	0.028	0.014	0.037	0.011	-0.023	0.016	0.056	0.015	0.078	0.022	0.033	0.022	53.70	7.94
3	0.011	0.030	0.019	0.026	0.023	0.020	-0.008	0.029	0.038	0.028	0.047	0.040	0.030	0.040	49.68	24.59
4	0.033	0.074	0.003	0.078	0.043	0.054	-0.028	0.077	0.064	0.075	0.091	0.108	0.036	0.108	35.41	33.76
5	-0.088	0.546	-0.006	0.645	-0.285	0.425	-0.335	0.588	0.242	0.601	0.577	0.851	-0.094	0.845	40.91	42.01
		P' =	0.876	ksc			Q =	0.283	ksc							
1	-0.120	0.018	-0.013	0.013	0.163	0.011	-0.238	0.016	0.105	0.014	0.343	0.022	-0.133	0.022	54.04	1.81
2	-0.123	0.021	-0.005	0.017	0.172	0.013	-0.246	0.020	0.117	0.018	0.363	0.027	-0.128	0.027	54.46	2.12
3	-0.143	0.033	-0.027	0.030	0.168	0.023	-0.263	0.032	0.093	0.031	0.356	0.045	-0.170	0.045	54.47	3.62
4	-0.149	0.047	0.022	0.073	0.222	0.044	-0.301	0.057	0.175	0.066	0.476	0.087	-0.126	0.087	55.51	5.22
5	-0.321	0.080	0.231	0.513	-0.103	0.268	-0.340	0.122	0.250	0.504	0.590	0.524	-0.090	0.520	10.26	26.06
		P' =	0.853	ksc			Q =	0.293	ksc							
1	-0.162	0.021	0.007	0.013	0.239	0.012	-0.331	0.019	0.175	0.016	0.506	0.025	-0.156	0.025	54.75	1.40
2	-0.148	0.027	0.014	0.018	0.252	0.016	-0.332	0.024	0.198	0.022	0.529	0.032	-0.134	0.033	53.88	1.77
3	-0.179	0.045	0.014	0.030	0.205	0.027	-0.310	0.041	0.144	0.035	0.454	0.054	-0.166	0.054	57.59	3.42
4	-0.004	0.083	0.014	0.064	0.269	0.052	-0.264	0.074	0.274	0.073	0.538	0.104	0.010	0.105	45.94	5.58
5	0.630	0.105	-0.248	0.431	0.262	0.228	-0.320	0.419	0.702	0.156	1.022	0.450	0.382	0.444	15.40	12.78
		P' =	0.983	ksc			Q =	0.294	ksc							
1	0.022	0.011	0.007	0.007	0.001	0.006	0.007	0.007	0.023	0.011	0.015	0.013	0.030	0.013	2.59	23.49
2	0.014	0.015	0.003	0.011	-0.002	0.009	0.003	0.011	0.014	0.015	0.011	0.019	0.017	0.019	81.27	47.16
3	-0.000	0.027	-0.002	0.017	-0.002	0.016	-0.004	0.021	0.001	0.024	0.005	0.032	-0.003	0.032	56.53	181.56
4	0.020	0.070	0.018	0.042	-0.012	0.040	0.008	0.056	0.031	0.059	0.023	0.081	0.038	0.081	47.51	101.04
5	-0.204	0.282	0.201	0.013	-0.056	0.137	-0.211	0.278	0.208	0.039	0.420	0.280	-0.003	0.282	7.74	18.61

AREA	Ex	Ex(SD)	Ey	Ey(SD)	Exy	Exy(SD)	E3	E3(SD)	E1	E1(SD)	GAMMA	G(SD)	EV	EV(SD)	PS.	PS(SD)
		P' =	0.830	ksc			Q =	0.306	ksc							
1	-0.217	0.019	-0.014	0.014	0.283	0.011	-0.415	0.017	0.185	0.015	0.600	0.023	-0.230	0.023	54.87	1.09
2	-0.243	0.023	0.001	0.019	0.295	0.015	-0.440	0.022	0.198	0.020	0.638	0.030	-0.242	0.030	56.26	1.34
3	-0.258	0.034	0.003	0.034	0.277	0.024	-0.434	0.034	0.179	0.034	0.613	0.048	-0.255	0.048	57.62	2.25
4	-0.277	0.077	0.040	0.082	0.234	0.056	-0.401	0.078	0.164	0.081	0.566	0.112	-0.237	0.112	62.07	5.69
5	-0.005	0.104	-0.155	0.343	0.268	0.184	-0.359	0.286	0.199	0.229	0.557	0.369	-0.160	0.359	37.22	18.53
		P' =	0.799	ksc			Q =	0.321	ksc							
1	-0.309	0.024	-0.012	0.014	0.394	0.014	-0.582	0.021	0.261	0.018	0.843	0.028	-0.321	0.028	55.30	0.95
2	-0.346	0.028	-0.004	0.019	0.391	0.017	-0.602	0.025	0.252	0.022	0.854	0.033	-0.350	0.034	56.80	1.13
3	-0.318	0.044	0.025	0.031	0.395	0.027	-0.577	0.041	0.284	0.035	0.862	0.054	-0.293	0.054	56.73	1.79
4	-0.236	0.092	0.174	0.072	0.420	0.058	-0.498	0.086	0.437	0.078	0.935	0.116	-0.061	0.116	58.01	3.56
5	0.316	0.360	-0.266	0.401	0.747	0.270	-0.777	0.392	0.826	0.377	1.603	0.541	0.049	0.538	34.35	9.63
		P' =	0.766	ksc			Q =	0.333	ksc							
1	-0.336	0.024	0.058	0.015	0.524	0.014	-0.698	0.021	0.421	0.018	1.119	0.028	-0.277	0.028	55.31	0.72
2	-0.348	0.024	0.078	0.020	0.533	0.016	-0.709	0.023	0.439	0.021	1.147	0.031	-0.270	0.032	55.91	0.79
3	-0.345	0.040	0.060	0.032	0.517	0.025	-0.697	0.037	0.413	0.034	1.110	0.051	-0.284	0.051	55.71	1.31
4	-0.296	0.103	0.223	0.061	0.494	0.059	-0.594	0.093	0.521	0.074	1.115	0.118	-0.073	0.120	58.86	3.06
5	-0.596	0.461	0.585	0.050	0.479	0.225	-0.766	0.436	0.755	0.158	1.521	0.462	-0.012	0.464	70.47	8.64
		P' =	0.735	ksc			Q =	0.345	ksc							
1	-0.435	0.025	0.018	0.017	0.661	0.015	-0.907	0.022	0.490	0.020	1.397	0.030	-0.417	0.030	54.45	0.61
2	-0.428	0.024	0.061	0.022	0.706	0.016	-0.930	0.023	0.564	0.022	1.494	0.032	-0.366	0.032	54.55	0.62
3	-0.386	0.038	0.093	0.031	0.676	0.024	-0.864	0.036	0.571	0.034	1.435	0.049	-0.293	0.049	54.74	0.98
4	-0.400	0.090	0.092	0.081	0.667	0.060	-0.865	0.087	0.557	0.084	1.422	0.121	-0.309	0.121	55.12	2.44
5	-0.268	0.322	0.255	0.032	1.051	0.157	-1.089	0.254	1.076	0.198	2.166	0.316	-0.013	0.324	51.99	4.29
		P' =	0.672	ksc			Q =	0.357	ksc							
1	-0.638	0.036	-0.062	0.021	1.189	0.020	-1.573	0.031	0.873	0.027	2.446	0.041	-0.700	0.041	51.82	0.48
2	-0.615	0.038	-0.040	0.026	1.261	0.023	-1.621	0.034	0.966	0.031	2.587	0.046	-0.655	0.046	51.42	0.51
3	-0.599	0.052	-0.048	0.041	1.346	0.033	-1.698	0.047	1.050	0.045	2.748	0.065	-0.647	0.066	50.78	0.69
4	-0.495	0.119	0.004	0.098	1.416	0.077	-1.683	0.110	1.193	0.106	2.876	0.153	-0.490	0.154	50.00	1.53
5	-0.629	0.436	0.458	0.991	1.483	0.553	-1.665	0.684	1.494	0.863	3.158	1.100	-0.171	1.083	55.07	9.81
		P' =	0.593	ksc			Q =	0.361	ksc							
1	-0.736	0.084	-0.138	0.057	3.014	0.050	-3.465	0.072	2.592	0.070	6.058	0.100	-0.873	0.101	47.83	0.48
2	-0.629	0.075	-0.228	0.081	3.253	0.055	-3.687	0.077	2.831	0.078	6.518	0.110	-0.857	0.110	46.77	0.48
3	-0.564	0.068	-0.336	0.077	3.351	0.052	-3.803	0.072	2.903	0.073	6.705	0.103	-0.900	0.103	45.98	0.44
4	-0.269	0.099	-0.307	0.138	3.386	0.086	-3.675	0.120	3.098	0.120	6.772	0.171	-0.577	0.170	44.84	0.72
5	-0.321	0.111	0.152	1.087	3.492	0.564	-3.584	0.766	3.416	0.816	7.000	1.126	-0.169	1.093	46.94	4.47

UNDRAINED SHEAR: DSC34 (CORRECTED)

AREA	Ex	Ex(SD)	Ey	Ey(SD)	Exy	Exy(SD)	E3	E3(SD)	E1	E1(SD)	GAMMA	G(SD)	EV	EV(SD)	PS.	PS(SD)
		P' =	0.859	ksc			Q =	0.314	ksc							
1	0.014	0.014	-0.054	0.012	0.020	0.009	-0.043	0.012	0.003	0.013	0.046	0.018	-0.040	0.018	29.98	11.24
2	0.011	0.023	-0.052	0.015	-0.017	0.014	-0.037	0.020	-0.003	0.018	0.035	0.027	-0.040	0.027	-40.01	22.59
3	0.028	0.040	-0.069	0.028	0.027	0.024	-0.047	0.034	0.007	0.035	0.054	0.048	-0.040	0.049	39.15	25.72
4	0.040	0.077	-0.101	0.070	0.010	0.052	-0.100	0.077	0.040	0.070	0.141	0.104	-0.060	0.104	4.17	21.11
5	0.696	0.418	-0.104	0.107	-0.214	0.210	-0.019	0.159	0.612	0.400	0.632	0.427	0.593	0.432	-21.43	19.19
		P' =	0.850	ksc			Q =	0.334	ksc							
1	0.018	0.016	-0.061	0.011	-0.002	0.010	-0.061	0.011	0.017	0.016	0.079	0.020	-0.044	0.020	-2.12	7.07
2	0.010	0.025	-0.058	0.019	0.001	0.015	-0.058	0.019	0.010	0.025	0.069	0.031	-0.048	0.031	0.96	12.89
3	-0.021	0.044	-0.060	0.037	0.010	0.029	-0.056	0.038	-0.025	0.043	0.031	0.057	-0.081	0.058	20.40	52.63
4	0.180	0.077	-0.267	0.065	0.129	0.050	-0.186	0.073	0.099	0.070	0.285	0.100	-0.087	0.101	32.22	10.11
5	0.227	0.124	-0.014	0.600	0.068	0.315	0.035	0.403	0.178	0.475	0.143	0.630	0.212	0.613	35.81	122.58
		P' =	0.831	ksc			Q =	0.354	ksc							
1	0.134	0.024	-0.046	0.015	0.005	0.014	-0.046	0.015	0.134	0.024	0.181	0.028	0.087	0.028	1.55	4.45
2	0.224	0.026	-0.051	0.020	0.034	0.016	-0.047	0.020	0.219	0.025	0.267	0.032	0.172	0.032	7.35	3.47
3	0.253	0.048	-0.041	0.034	0.054	0.029	-0.030	0.035	0.242	0.046	0.272	0.058	0.211	0.058	11.73	6.12
4	0.047	0.110	-0.117	0.070	-0.004	0.065	-0.117	0.070	0.047	0.110	0.163	0.131	-0.070	0.131	-1.69	22.78
5	0.679	0.907	-1.322	0.129	0.578	0.445	-0.990	0.751	0.347	0.508	1.338	0.895	-0.643	0.917	29.88	19.58
		P' =	0.799	ksc			Q =	0.366	ksc							
1	0.148	0.016	-0.260	0.014	0.011	0.011	-0.260	0.014	0.148	0.016	0.408	0.021	-0.112	0.021	1.56	1.50
2	0.197	0.026	-0.307	0.021	0.022	0.017	-0.306	0.021	0.196	0.026	0.503	0.033	-0.109	0.033	2.50	1.89
3	0.288	0.045	-0.327	0.038	0.049	0.030	-0.323	0.038	0.284	0.045	0.608	0.059	-0.039	0.059	4.68	2.79
4	0.193	0.102	-0.424	0.090	0.034	0.068	-0.422	0.090	0.192	0.102	0.614	0.136	-0.230	0.136	3.20	6.34
5	0.589	0.924	-0.255	0.796	-0.133	0.607	-0.232	0.798	0.566	0.923	0.799	1.219	0.334	1.219	-9.77	43.57
		P' =	0.773	ksc			Q =	0.370	ksc							
1	0.239	0.023	-0.425	0.016	0.006	0.014	-0.425	0.016	0.239	0.023	0.665	0.028	-0.185	0.028	0.49	1.20
2	0.353	0.026	-0.486	0.023	0.020	0.017	-0.485	0.023	0.352	0.026	0.839	0.035	-0.132	0.035	1.36	1.18
3	0.459	0.039	-0.571	0.040	0.041	0.028	-0.569	0.040	0.458	0.039	1.028	0.056	-0.111	0.056	2.26	1.56
4	0.343	0.068	-0.654	0.104	0.027	0.063	-0.653	0.104	0.342	0.068	0.996	0.124	-0.310	0.124	1.56	3.59
5	0.657	0.148	-1.133	0.640	0.482	0.338	-0.944	0.583	0.467	0.312	1.411	0.667	-0.476	0.657	21.52	13.46
		P' =	0.753	ksc			Q =	0.374	ksc							
1	0.322	0.029	-0.619	0.022	0.006	0.018	-0.619	0.022	0.322	0.028	0.941	0.036	-0.297	0.036	0.38	1.10
2	0.481	0.037	-0.716	0.028	0.001	0.023	-0.716	0.028	0.481	0.037	1.197	0.047	-0.235	0.047	0.07	1.11
3	0.587	0.062	-0.848	0.043	0.012	0.038	-0.848	0.043	0.587	0.062	1.436	0.075	-0.260	0.075	0.48	1.50
4	0.628	0.110	-0.783	0.109	-0.022	0.077	-0.782	0.109	0.628	0.110	1.411	0.155	-0.154	0.155	-0.93	3.14
5	1.626	0.440	-1.344	0.931	0.091	0.525	-1.342	0.927	1.623	0.448	2.965	1.030	0.281	1.030	1.75	10.14
		P' =	0.731	ksc			Q =	0.378	ksc							
1	0.447	0.036	-0.841	0.028	-0.001	0.023	-0.841	0.028	0.447	0.036	1.289	0.046	-0.393	0.046	-0.05	1.01
2	0.649	0.045	-1.014	0.029	-0.005	0.026	-1.014	0.029	0.649	0.045	1.664	0.053	-0.364	0.053	-0.19	0.91
3	0.873	0.066	-1.132	0.044	0.005	0.039	-1.132	0.044	0.873	0.066	2.006	0.079	-0.259	0.079	0.16	1.12
4	0.947	0.094	-1.296	0.081	0.084	0.062	-1.293	0.081	0.944	0.094	2.238	0.124	-0.348	0.124	2.14	1.59
5	1.065	0.917	-1.333	0.660	0.101	0.560	-1.329	0.664	1.061	0.914	2.390	1.130	-0.267	1.130	2.43	13.44

AREA	Ex	Ex(SD)	Ey	Ey(SD)	Exy	Exy(SD)	E3	E3(SD)	E1	E1(SD)	GAMMA G(SD)	EV	EV(SD)	PS.	PS(SD)
		P' =	0.712 ksc				Q =	0.382 ksc							
1	0.703	0.044	-1.160	0.043	0.004	0.031	-1.160	0.043	0.703	0.044	1.864 0.062	-0.457	0.062	0.12	0.95
2	0.976	0.050	-1.431	0.040	0.004	0.032	-1.431	0.040	0.976	0.050	2.407 0.064	-0.455	0.064	0.10	0.76
3	1.250	0.060	-1.690	0.048	-0.005	0.038	-1.691	0.048	1.250	0.060	2.941 0.077	-0.440	0.077	-0.10	0.75
4	1.361	0.108	-1.801	0.106	-0.095	0.076	-1.798	0.106	1.358	0.108	3.156 0.152	-0.440	0.152	-1.73	1.38
5	1.596	0.349	-1.719	0.688	-0.391	0.393	-1.671	0.688	1.548	0.351	3.220 0.772	-0.122	0.772	-7.03	7.00
		P' =	0.700 ksc				Q =	0.386 ksc							
1	0.853	0.053	-1.473	0.051	0.004	0.037	-1.473	0.051	0.853	0.053	2.327 0.074	-0.619	0.074	0.10	0.71
2	1.198	0.057	-1.802	0.050	0.026	0.038	-1.802	0.050	1.198	0.057	3.001 0.076	-0.603	0.076	0.50	0.72
3	1.502	0.075	-2.115	0.071	0.054	0.052	-2.115	0.071	1.501	0.075	3.617 0.103	-0.613	0.103	0.86	0.82
4	1.683	0.109	-2.467	0.149	0.124	0.093	-2.463	0.148	1.679	0.109	4.143 0.184	-0.783	0.185	1.72	1.78
5	1.457	0.170	-3.568	1.037	0.135	0.541	-3.564	1.032	1.454	0.198	5.019 1.051	-2.110	1.051	1.55	6.16

UNDRAINED SHEAR: DSC35 (CORRECTED)

AREA	Ex	Ex(SD)	Ey	Ey(SD)	Exy	Exy(SD)	E3	E3(SD)	E1	E1(SD)	GAMMA	G(SD)	EV	EV(SD)	PS.	PS(SD)
		P' =	0.972	ksc			Q =	0.262	ksc							
1	0.071	0.015	0.019	0.012	-0.004	0.010	0.019	0.015	0.071	0.012	0.052	0.020	0.090	0.020	85.28	10.74
2	0.104	0.023	-0.017	0.020	-0.031	0.015	-0.006	0.023	0.093	0.020	0.099	0.030	0.087	0.030	70.57	8.73
3	0.139	0.044	0.042	0.032	-0.026	0.027	0.063	0.040	0.118	0.035	0.055	0.053	0.182	0.054	52.15	27.67
4	0.063	0.084	-0.017	0.063	-0.020	0.052	0.002	0.075	0.044	0.071	0.042	0.103	0.047	0.105	47.14	71.65
5	0.012	0.443	-0.891	0.462	-0.213	0.323	-0.654	0.458	-0.225	0.457	0.429	0.647	-0.879	0.641	41.86	42.80
		P' =	0.932	ksc			Q =	0.224	ksc							
1	0.007	0.016	-0.093	0.013	-0.012	0.010	-0.092	0.016	0.005	0.013	0.097	0.021	-0.086	0.021	82.82	6.02
2	0.071	0.024	-0.091	0.018	-0.038	0.015	-0.079	0.024	0.060	0.018	0.140	0.030	-0.020	0.030	73.38	6.10
3	0.110	0.043	-0.096	0.031	-0.057	0.026	-0.071	0.042	0.085	0.033	0.157	0.053	0.013	0.054	66.44	9.68
4	0.214	0.093	-0.211	0.090	-0.119	0.065	-0.157	0.092	0.160	0.090	0.316	0.129	0.002	0.129	65.49	11.71
5	1.141	0.326	-0.042	0.207	-0.327	0.187	0.211	0.247	0.889	0.293	0.678	0.376	1.099	0.386	52.36	16.22
		P' =	0.906	ksc			Q =	0.204	ksc							
1	0.089	0.017	-0.093	0.011	-0.042	0.010	-0.081	0.017	0.077	0.012	0.159	0.021	-0.003	0.021	73.94	3.67
2	0.125	0.027	-0.079	0.017	-0.051	0.015	-0.061	0.026	0.108	0.017	0.169	0.031	0.047	0.031	71.22	5.21
3	0.210	0.049	-0.040	0.030	-0.071	0.028	-0.005	0.046	0.175	0.033	0.180	0.056	0.171	0.057	63.71	8.95
4	0.174	0.131	-0.042	0.084	-0.043	0.076	-0.032	0.129	0.164	0.085	0.197	0.155	0.133	0.155	76.78	22.11
5	0.012	0.973	-0.394	0.321	0.046	0.481	-0.388	0.358	0.006	0.954	0.396	1.020	-0.381	1.025	6.76	70.52
		P' =	0.871	ksc			Q =	0.180	ksc							
1	0.070	0.015	-0.166	0.013	-0.048	0.010	-0.154	0.015	0.059	0.013	0.213	0.020	-0.095	0.020	76.38	2.61
2	0.103	0.021	-0.188	0.020	-0.065	0.014	-0.170	0.021	0.085	0.020	0.256	0.029	-0.085	0.029	74.61	3.23
3	0.158	0.035	-0.192	0.036	-0.077	0.026	-0.171	0.035	0.137	0.036	0.308	0.051	-0.034	0.051	74.84	4.74
4	0.257	0.073	-0.313	0.090	-0.163	0.059	-0.230	0.075	0.174	0.087	0.404	0.117	-0.057	0.116	62.98	8.28
5	0.550	0.409	-0.310	0.492	-0.201	0.327	-0.250	0.413	0.491	0.488	0.742	0.643	0.241	0.640	73.59	25.14
		P' =	0.833	ksc			Q =	0.164	ksc							
1	0.153	0.019	-0.269	0.013	-0.105	0.011	-0.234	0.018	0.117	0.013	0.352	0.022	-0.117	0.022	71.53	1.80
2	0.206	0.027	-0.291	0.016	-0.111	0.015	-0.261	0.026	0.175	0.016	0.437	0.031	-0.085	0.031	74.67	1.99
3	0.239	0.055	-0.306	0.028	-0.107	0.030	-0.281	0.055	0.215	0.028	0.497	0.062	-0.067	0.062	77.17	3.46
4	0.200	0.102	-0.422	0.069	-0.128	0.060	-0.391	0.101	0.169	0.070	0.560	0.122	-0.222	0.123	76.39	6.16
5	0.756	0.816	-0.072	0.456	-0.145	0.450	-0.043	0.810	0.728	0.461	0.771	0.932	0.685	0.935	78.92	33.48
		P' =	0.793	ksc			Q =	0.158	ksc							
1	0.171	0.017	-0.350	0.014	-0.127	0.011	-0.310	0.017	0.130	0.014	0.440	0.022	-0.180	0.022	72.34	1.43
2	0.234	0.025	-0.356	0.020	-0.142	0.016	-0.311	0.025	0.189	0.020	0.500	0.032	-0.122	0.032	72.59	1.81
3	0.288	0.043	-0.338	0.033	-0.150	0.027	-0.291	0.042	0.241	0.033	0.533	0.054	-0.050	0.054	72.75	2.87
4	0.394	0.098	-0.352	0.078	-0.194	0.062	-0.282	0.097	0.324	0.079	0.606	0.125	0.042	0.125	70.06	5.87
5	0.175	0.586	-0.454	0.027	0.010	0.270	-0.454	0.584	0.175	0.054	0.630	0.586	-0.279	0.587	0.95	24.72
		P' =	0.768	ksc			Q =	0.156	ksc							
1	0.207	0.020	-0.432	0.014	-0.161	0.012	-0.378	0.020	0.153	0.014	0.531	0.024	-0.226	0.024	71.27	1.28
2	0.241	0.028	-0.466	0.019	-0.162	0.017	-0.420	0.028	0.194	0.019	0.614	0.034	-0.226	0.034	74.00	1.55
3	0.297	0.054	-0.464	0.028	-0.178	0.030	-0.411	0.053	0.244	0.030	0.655	0.060	-0.168	0.061	73.47	2.59
4	0.320	0.093	-0.562	0.073	-0.206	0.058	-0.501	0.092	0.259	0.074	0.760	0.118	-0.242	0.118	73.58	4.39
5	0.396	0.024	-0.474	0.469	-0.222	0.255	-0.397	0.135	0.318	0.454	0.715	0.482	-0.079	0.470	70.79	20.10

DSC31 $\delta_{inc} = 90^o$

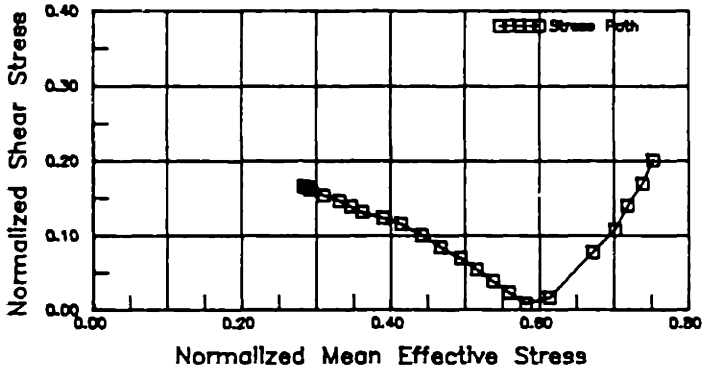

(a) q versus p'

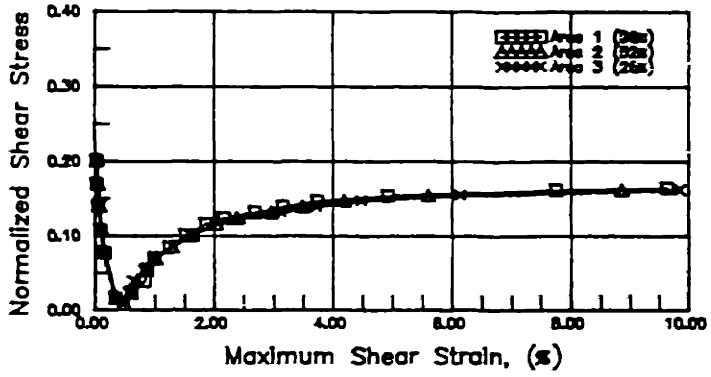

(b) Shear Stress versus Shear Strain

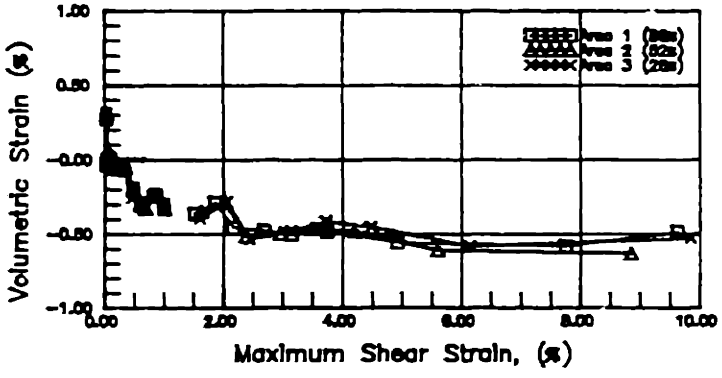

(c) Volumetric Strain versus Shear Strain

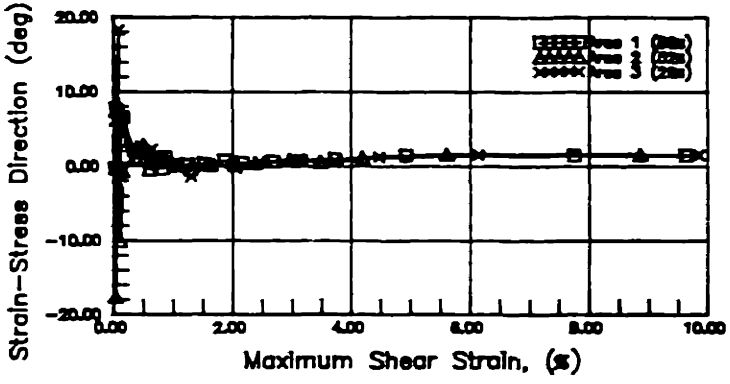

(d) Strain-Stress Direction versus Shear Strain

DSC32 $\delta_{inc} = 45^{o}$

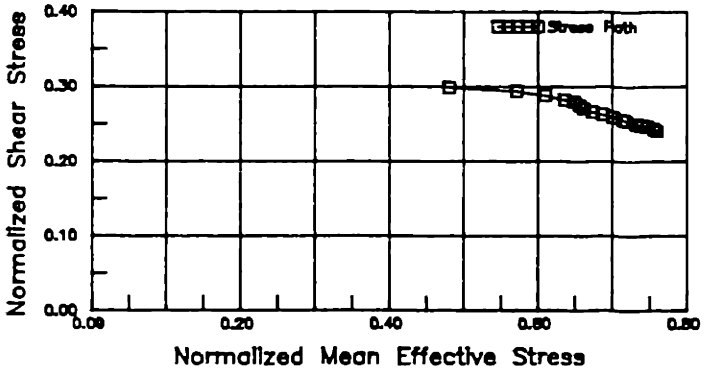

(a) q versus p'

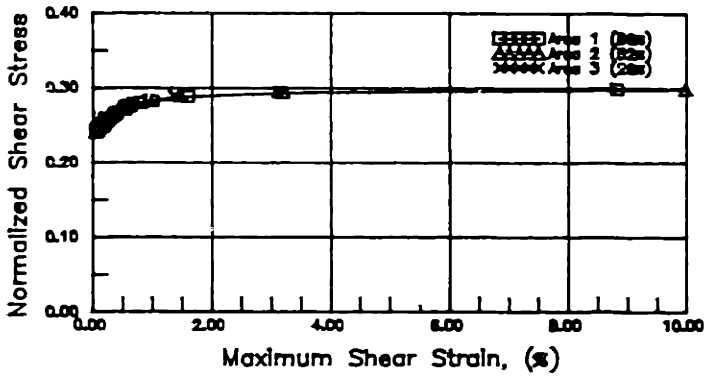

(b) Shear Stress versus Shear Strain

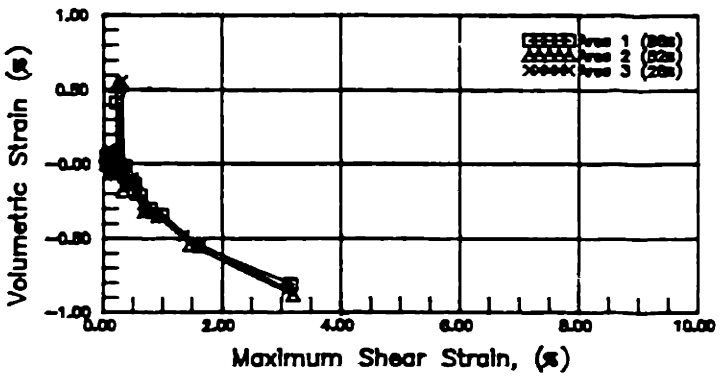

(c) Volumetric Strain versus Shear Strain

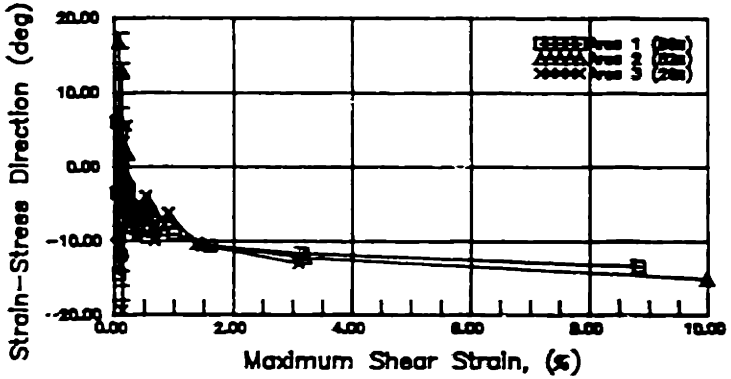

(d) Strain–Stress Direction versus Shear Strain

DSC33 $\delta_{inc} = 60^o$

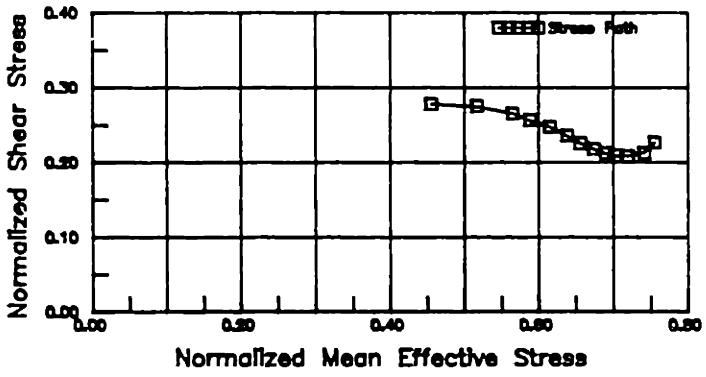

(a) q versus p'

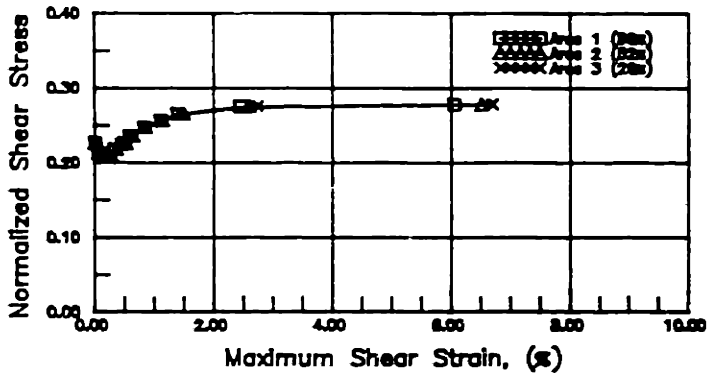

(b) Shear Stress versus Shear Strain

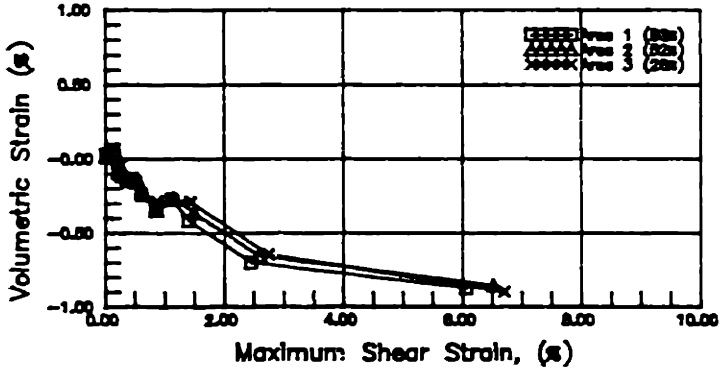

(c) Volumetric Strain versus Shear Strain

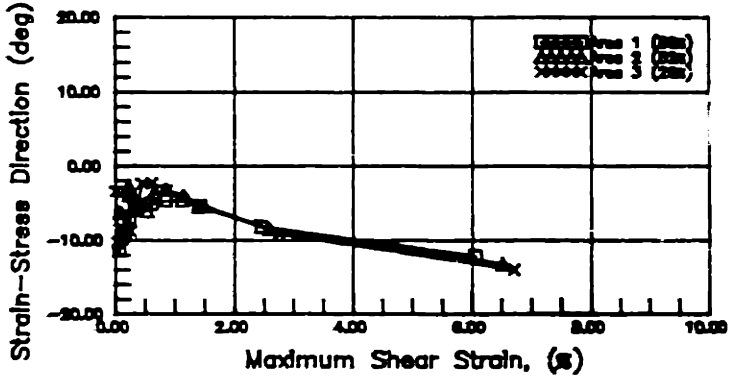

(d) Strain–Stress Direction versus Shear Strain

DSC34 $\delta_{inc} = 0^o$

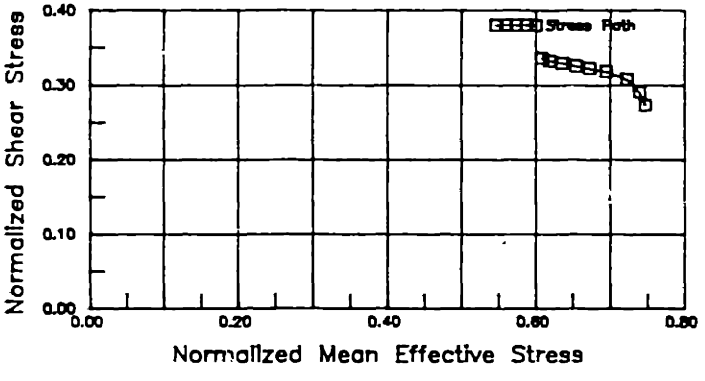

(a) q versus p'

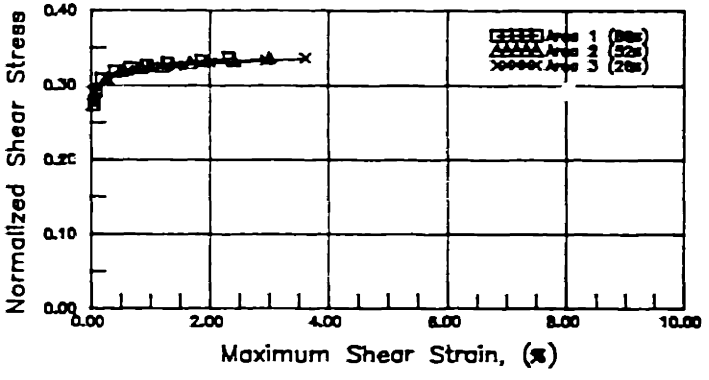

(b) Shear Stress versus Shear Strain

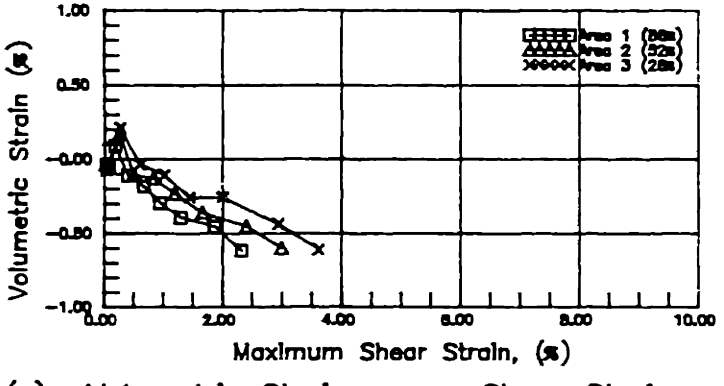

(c) Volumetric Strain versus Shear Strain

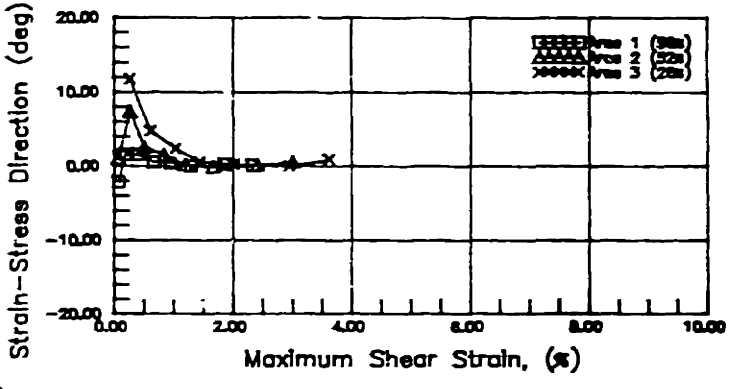

(d) Strain–Stress Direction versus Shear Strain

DSC35 $\delta_{inc} = 75^o$

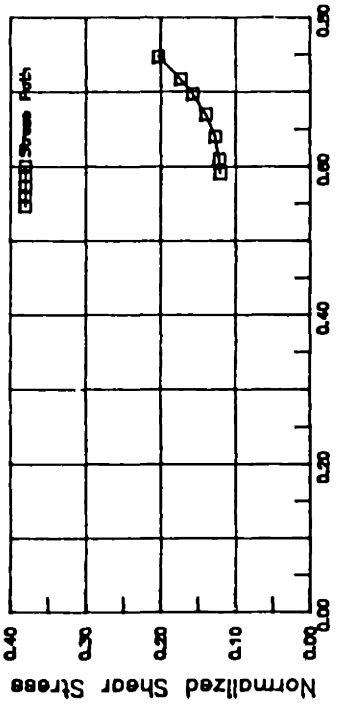

(a) q versus p'

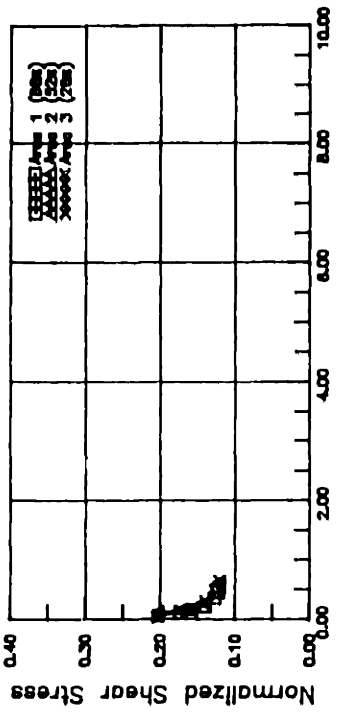

(b) Shear Stress versus Shear Strain

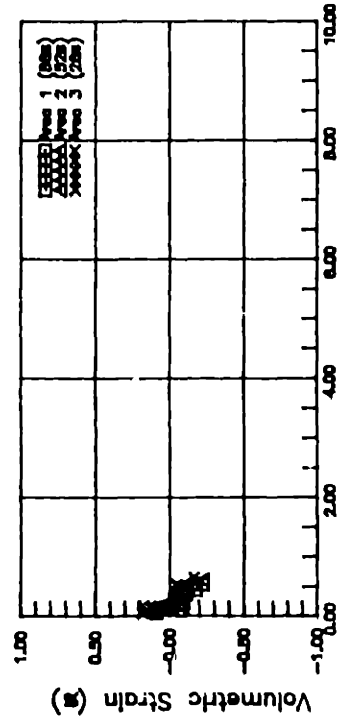

(c) Volumetric Strain versus Shear Strain

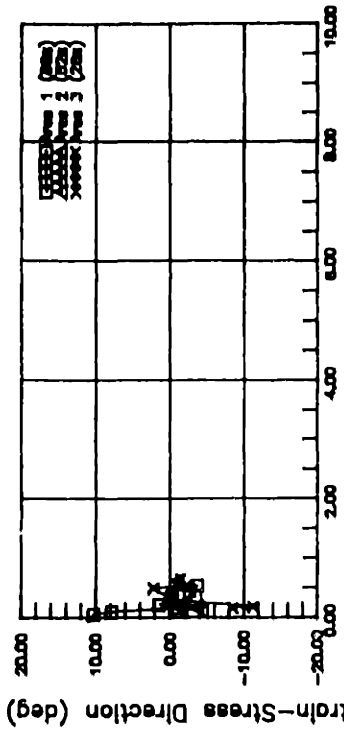

(d) Strain–Stress Direction versus Shear Strain

APPENDIX G

MISCELLANEOUS

G.1 OPTIMIZATION OF STRESS

G.1.1 Introduction

The distortion angle of the DSC sample shown in Figure G.1 can be computed based on the applied stresses only with the assumption that the α angle is equal to β angle, but the actual distortion angle is calculated based on the global strain analysis given by ϵ_{xy} (i.e., $\alpha = \beta = \tan(\epsilon_{xy})$). The calculated distortion angle from the strain analysis does not always match the angle computed from the stress analysis due to the errors in stress and strain measurements. If the calculated distortion angle is not equal to the estimated distortion angle, the Mohr circle of stress will not be centered on the x–axis, which implies that the sample is not in equilibrium. But physically, the sample is stable, therefore the sample has to satisfy the equations of equilibrium. The only possible explanation is that the applied stresses are probably not measured correctly. Rational approach of solving this problem is described in the next section.

G.1.2 Analysis

An optimization technique is used to determine the appropriate stresses which satisfy the equations of equilibrium by assuming that the measurements of the applied stresses and the distortion angle from the global strain analysis have some uncertainty associated with them. The following section describes the optimization approach which is called the Maximum Likelihood Method:

Assuming that there are n independent observations, x_1, x_2, ... x_n. Each of

these variables with normal distribution, has a mean of m_x and a variance of σ_x^2. Then, the likelihood function is given by,

$$L(x_1,x_2, \ldots x_n; \theta) = \prod_{i=1}^{n} f_x(x_i; \theta)$$

where θ is a parameter and f_x is the probability density function. The maximum likelihood estimator, $\hat{\theta}$, is then the value of θ that maximizes the likelihood function $L(x_1,x_2, \ldots x_n; \theta)$. It is sometimes more convenient to maximize the logarithm of the likelihood function instead, which gives,

$$\frac{\partial \ln L(x_1,x_2, \ldots x_n; \theta)}{\partial \theta} = 0$$

If f_x is normal distribution function, then the above equation gives,

$$\sum_{i=1}^{n} \left[\frac{x_i - m_{xi}}{\sigma_{x\,i}}\right]^2 \Bigg|_{\theta} = 0$$

For density functions with two or more parameters (say m parameters), the likelihood function is expressed as,

$$\frac{\partial \ln L(x_1,x_2, \ldots x_n; \theta_1, \ldots, \theta_m)}{\partial \theta_j} = 0; \; j=1, \ldots, m$$

For a normal case, the equation becomes,

$$\sum_{i=1}^{n} \left[\frac{x_i - m_{xi}}{\sigma_{x\,i}}\right]^2 \Bigg|_{\theta_j} = 0; \quad j=1 \text{ to } m \qquad \text{Eq.G.1}$$

In this problem, it is required to estimate $\hat{\sigma}_x$, $\hat{\tau}_{xy}$, $\hat{\sigma}_y$ and $\hat{\xi}$, given σ_a, σ_b, τ_a, τ_b and ξ (see Figure G.2). A quantity, Q, is defined as,

$$Q = \sum_{i=1}^{4} \frac{(\theta_i - \hat{\theta}_i)^2}{\sigma_i^2}$$

$$Q(\xi) = Q\,[\,\xi, \text{Optimal}\,(\sigma_x, \tau_{xy}, \sigma_y |\, \xi)\,]$$

Such that $\frac{\partial Q(\xi)}{\partial \xi} = 0$ for minimum where the corresponding value of ξ will be optimal.

Let the shear and normal stresses acting on two orthogonal planes be, $\underline{X}$, which is,

$$\underline{X} = \begin{bmatrix} \sigma_x \\ \tau_{xy} \\ \sigma_y \end{bmatrix}$$

the normal and shearing components of stress on the plane B (Figure G.2) be:

$$\underline{Y} = \begin{bmatrix} \sigma_\xi \\ \tau_\xi \end{bmatrix}$$

They can be expressed in terms of ξ, σ_x, σ_y and τ_{xy}, which are:

$$\sigma_\xi = \sigma_x \cos^2\xi + \tau_{xy} \sin 2\xi + \sigma_y \sin^2\xi$$
$$\tau_\xi = \tfrac{1}{2}\sigma_x \sin 2\xi + \tau_{xy} \cos 2\xi + \tfrac{1}{2}\sigma_y \sin 2\xi$$

The matrix form of the above equations can then be written:

$$\underline{Y} = \begin{bmatrix} \cos^2\xi & \sin 2\xi & \sin^2\xi \\ 0.5\sin 2\xi & \cos 2\xi & 0.5\sin 2\xi \end{bmatrix} \begin{bmatrix} \sigma_x \\ \tau_{xy} \\ \sigma_y \end{bmatrix} \qquad \text{Eq.G.2}$$

$$\underline{Y} = \underline{H}(\xi)\,\underline{X}$$

where $\underline{H}$ is the transformation matrix.

Let assume the $\underline{X}$ has the following properties:

$$\underline{X} : \underline{X} \sim [\,\underline{m}',\,\underline{\Sigma}'\,]$$

In other words, $\underline{X}$ is assumed to have a mean value of $\underline{m}'$,and a variance of $\underline{\Sigma}'$.

$$\underline{m}' = \begin{bmatrix} \hat{\sigma}_x \\ \hat{\tau}_{xy} \\ 0 \end{bmatrix} \text{ and } \underline{\Sigma}' = \begin{bmatrix} \mathrm{Var}(\hat{\sigma}_x) & 0 & 0 \\ 0 & \mathrm{Var}(\hat{\tau}_{xy}) & 0 \\ 0 & 0 & 10000 \end{bmatrix}$$

Measurements of $\underline{Y}$ can be written as $\underline{Z}$, which is given by,

$$\underline{Z} = \underline{Y} + \underline{\epsilon}$$

where $\underline{\epsilon}$ is normal distribution random variable with mean of zero and a standard deviation equal to σ_ϵ. Its properties are,

$$\underline{\epsilon} \sim [\,\underline{0}\,,\,\underline{\Sigma}_\epsilon\,]$$

Grouping the $\underline{X}$ and $\underline{Z}$ matrices, yields the following,

$$\begin{bmatrix} \underline{X} \\ \underline{Z} \end{bmatrix} = \begin{bmatrix} \underline{I} & \underline{0} \\ \underline{H} & \underline{I} \end{bmatrix} \begin{bmatrix} \underline{X} \\ \underline{\epsilon} \end{bmatrix} = \underline{B}\,\underline{V} \qquad \text{Eq.G.13}$$

and they have properties given by,

$$\begin{bmatrix} \underline{X} \\ \epsilon \end{bmatrix} \sim \left\{ \begin{bmatrix} \underline{m}' \\ \underline{0} \end{bmatrix}, \begin{bmatrix} \underline{\Sigma}' & 0 \\ \underline{0} & \underline{\Sigma}'_\epsilon \end{bmatrix} \right\}$$

The mean matrix is given by,

$$\begin{bmatrix} m' \\ m'_z \end{bmatrix} = \begin{bmatrix} m' \\ \underline{H} m' \end{bmatrix}$$

The variance matrix is,

$$\mathrm{Var}\begin{bmatrix} \underline{X} \\ \underline{Z} \end{bmatrix} = \underline{B}\,\underline{\Sigma}\,\underline{B}^T = \begin{bmatrix} \underline{I} & 0 \\ \underline{H} & \underline{I} \end{bmatrix}\begin{bmatrix} \underline{\Sigma}' & 0 \\ \underline{0} & \underline{\Sigma}'_\epsilon \end{bmatrix}\begin{bmatrix} \underline{I} & \underline{H} \\ \underline{0} & \underline{I} \end{bmatrix}$$

$$= \begin{bmatrix} \underline{\Sigma}' & \underline{\Sigma}'\underline{H}^T \\ \underline{H}\underline{\Sigma}' & (\underline{H}\underline{\Sigma}'\underline{H}^T + \underline{\Sigma}'_\epsilon) \end{bmatrix} \qquad \text{Eq.G.4}$$

The estimate of $\underline{X}$ is represented by $\underline{X}^*(\xi)$ which is,

$$\underline{X}^*(\xi) = \underline{m}' + \underline{\Sigma}_x(\xi)\,\underline{H}^T(\xi)\,\underline{\Sigma}_\epsilon^{-1}\,[\,\underline{Z} - H(\xi)\,\underline{m}'] \qquad \text{Eq.G.5}$$

where $\underline{\Sigma}_x(\xi) = [\,\underline{\Sigma}^{-1} + \underline{H}^T(\xi)\,\underline{\Sigma}_\epsilon^{-1}\,\underline{H}(\xi)\,]^{-1}$

(or equivalently, $\underline{X}^*(\xi) = \underline{m}' + \underline{\Sigma}'\,\underline{H}^T(\xi)\,(\,\underline{H}\,\underline{\Sigma}'\underline{H}^T + \underline{\Sigma}_\epsilon\,)^{-1}\,[\,\underline{Z} - H(\xi)\,\underline{m}'\,]$)

Therefore, the quantity, Q, can be expressed as follows:

$$Q(\xi) = \frac{(\xi - \hat{\xi})^2}{Var(\xi)} + [\underline{X}^*(\xi) - \underline{m}']^T \underline{\Sigma}'^{-1} [\underline{X}^*(\xi) - \underline{m}']$$

$$+ [\underline{H}(\xi)\,\underline{X}^*(\xi) - \underline{Z}]\,\underline{\Sigma}_\epsilon^{-1}\,[\underline{H}(\xi)\,\underline{X}^*(\xi) - \underline{Z}] \qquad \text{Eq.G.6}$$

The derivative of Q is given by,

$\frac{\partial Q(\xi)}{\partial \xi} = 0$ for minimum value of Q.

The above equation cannot easily be solved analytically. Therefore a numerical approach has to be adopted to determine the value of ξ at $\frac{\partial Q(\xi)}{\partial \xi} = 0$ using an iterative process by means of computer program. For a given value of ξ, the value of Q is calculated, and the minimum value of Q is determined from varying the ξ values. The variance of the stresses is determining experimentally which is $(0.007 \text{ ksc})^2$, i.e., 0.000049 ksc^2. The distortion angle is directly related to the shear strain of the sample, therefore the variance of the angle can be assumed to be the same as the variance of the shear strain, ϵ_{xy}.

This analysis is not used in this research because the resulting correction is found to be quite insignificant, which only amounts to about 1% change in the magnitude of the stresses.

G.2 RELATIONSHIP BETWEEN FRICTION ANGLE AND INTERMEDIATE PRINCIPAL STRESS FOR DIFFERENT FAILURE CRITERIA

There are a number of failure criteria commonly used in soil mechanics, e.g., extended Von Mises, Mohr–Coulomb, Lade and Matsuoka failure criteria, etc. The following sections described the relationships between the friction angle (ϕ) and the magnitude of the intermediate principal stress (b). The b parameter is

introduced as a convenient way of expressing the relative value of the intermediate principal stress,

$$b = \frac{(\sigma_2 - \sigma_3)}{(\sigma_1 - \sigma_3)} \qquad \text{Eq.G.7}$$

The stress ratio, R, is given by,

$$R = \frac{\sigma_1}{\sigma_3} \qquad \text{Eq.G.8}$$

The friction angle, ϕ can be expressed as,

$$\phi = \sin^{-1}\left[\frac{R - 1}{R + 1}\right] \qquad \text{Eq.G.9}$$

G.2.1 Extended Von Mises Failure Criterion

The expression for this criterion is,

$$J_2 - I_1^2 K_1^2 = 0 \qquad \text{Eq.G.10}$$

where $J_2 = \frac{1}{6}[(\sigma_1 - \sigma_2)^2 + (\sigma_2 - \sigma_3)^2 + (\sigma_3 - \sigma_1)^2]$

$I_1 = \sigma_1 + \sigma_2 + \sigma_3$

and $K_1 = \frac{1}{\sqrt{3}}\left[\frac{2\sin\phi_{tc}}{3 - \sin\phi_{tc}}\right]$ Eq.G.11

ϕ_{tc} = Friction angle from asymmetric triaxial compression test.

Equation G.11 can be expressed in terms of b and K_1,

$$R = \frac{2\sqrt{6}\ K_1 - \sqrt{6}\ b\ K_1 + \sqrt{2\ b^2 - 2\ b + 2}}{-\sqrt{6}\ K_1 - \sqrt{6}\ b\ K_1 + \sqrt{2\ b^2 - 2\ b + 2}} \qquad \text{Eq.G.12}$$

Since ϕ is a function of R (from Equation G.9) and K_1 is a function of ϕ_{tc} (Equation G.11), therefore the relationship between ϕ and b can be established using Equation G.12.

G.2.2 Mohr–Coulomb Failure Criterion

Mohr–Coulomb failure criterion assumes that the friction angle is independent of the intermediate principal stress, therefore,

Friction angle, $\phi = \phi_{tc}$ = Constant.

where ϕ_{tc} is the friction angle obtained from asymmetric triaxial compression test.

G.2.3 Lade Failure Criterion

Lade and Duncan (1975) proposed the following failure criterion,

$$\frac{(I_1)^3}{I_3} = \text{constant, } K_2 \qquad \text{Eq.G.13}$$

where $I_1 = \sigma_1 + \sigma_2 + \sigma_3$

$I_3 = \sigma_1\ \sigma_2\ \sigma_3$

K_2 can be determined from the equation shown below,

$$K_2 = \frac{\left\{ \left[\frac{1 + \sin \phi_{tc}}{1 - \sin \phi_{tc}} \right] + 2 \right\}^3}{\left[\frac{1 + \sin \phi_{tc}}{1 - \sin \phi_{tc}} \right]} \qquad \text{Eq.G.14}$$

Equation G.14 can be written in terms of R and b,

$$(1+b)^3R^3+(-3b^3+9b+6-bK_2)R^2+(3b^3-9b^2+12-K_2+bK_2)R+(2-b)^3=0 \qquad \text{Eq.G.15}$$

For known values of K_2 and b, Equation G.15 will yield three roots of R, but only one value of R satisfies the condition $R \geq 1$.

G.2.4 Matsuoka Failure Criterion

The Matsuoka failure criterion (Matsuoka, 1974) has the form,

$$\frac{I_1 I_2}{I_3} = \text{constant, } K_3 \qquad \text{Eq.G.16}$$

where $I_1 = \sigma_1 + \sigma_2 + \sigma_3$

$I_2 = \sigma_1\sigma_2 + \sigma_2\sigma_3 + \sigma_3\sigma_1$

$I_3 = \sigma_1 \sigma_2 \sigma_3$

Substituting the above three equations into Equation G.16, the following equation is obtained:

$$(b+b^2)R^3+(2-b^2+4b-bK_3)R^2+(-3b^2+bK_3+5-K_3)R+(2-b-b^2)=0 \qquad \text{Eq.G.16}$$

It can be shown (Wroth, 1984) that $K_3 = 9+8\tan^2\phi_{tc} = 9+8\tan^2\phi_{te}$.

where ϕ_{tc} is the friction angle obtained from asymmetric triaxial compression test, and ϕ_{te} is the friction angle obtained from asymmetric triaxial extension test. The criterion gives $\phi_{tc}=\phi_{te}$.

For known values of K_3 and b, Equation G.16 will yield three roots of R, but only one value of R satisfies the condition $R \geq 1$. The ϕ–b relationship is shown in Figure G.3. Satake (1982) shows that if an associated flow rule is applied to this failure criterion, then the plane strain condition ϕ_{ps} (or R_{ps}) is the maximum value ϕ (or R_f) can have (for all values of b). This means that if b differs from b_{ps}, the ϕ or R_f values corresponding to that value of b will be lower than ϕ_{ps} and R_{ps}.

G.2.5 Illustration of Different Failure Criteria

Figures G.4 to G.7 show the relationship between friction angle versus b value for different failure criteria as function of ϕ_{tc}. Figure G.8 shows the friction angle ratio (ϕ_{te}/ϕ_{tc}) versus the friction angle from the asymmetric triaxial compression test (ϕ_{tc}). Not many experiments have been conducted on homogeneous isotropic granular material, otherwise, one can evaluate the performance of each failure criterion based on these experimental results. One problem encountered by researchers is how to prepare a "homogeneous and isotropic" granular material test sample that eliminates the effects of inherent anisotropy in the testing sample. Until one can solve this problem, then a comparison between experimental data and these failure criteria cannot be made.

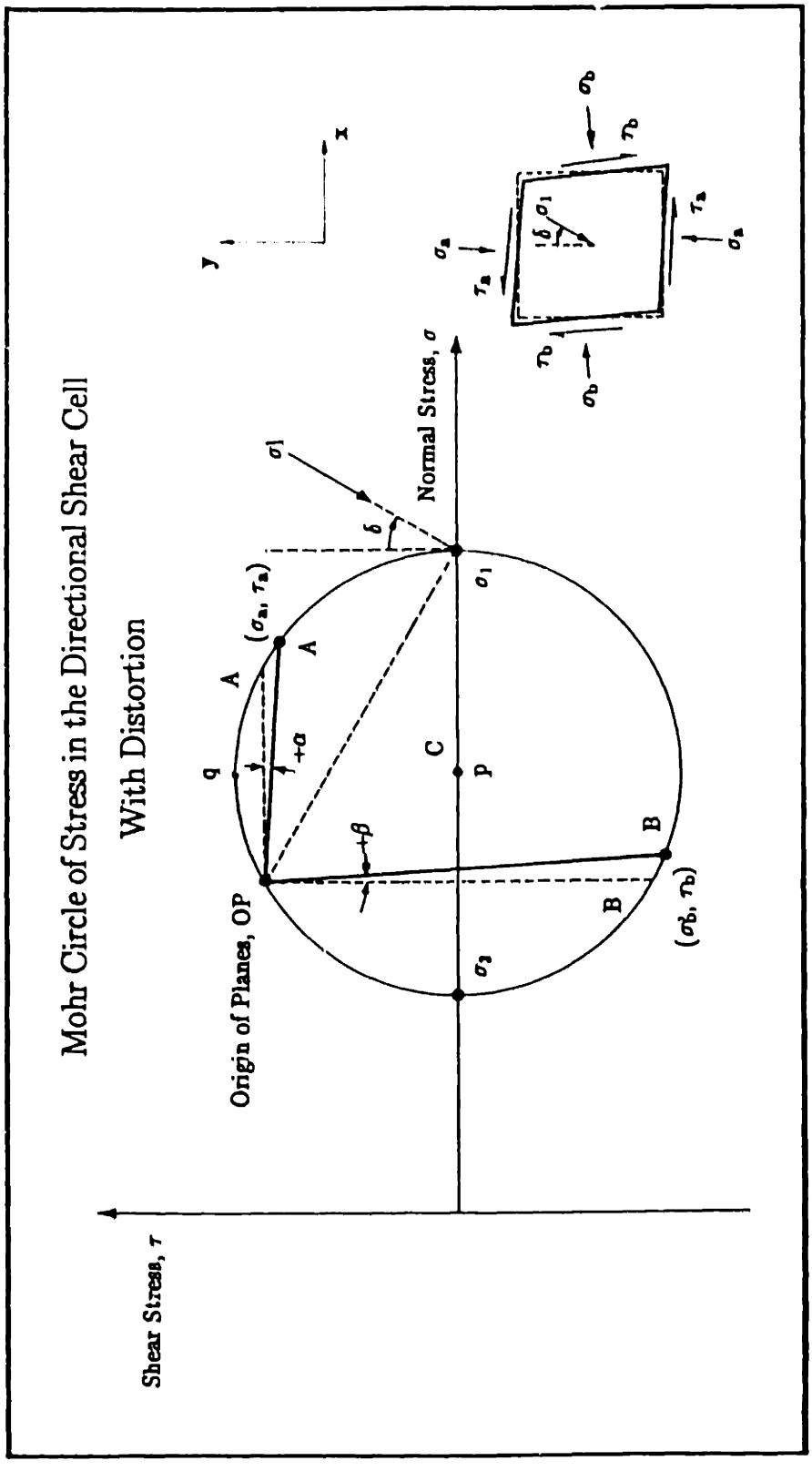

Figure G.1: Mohr Circle of Stress in Directional Shear Cell with Distortion Correction.

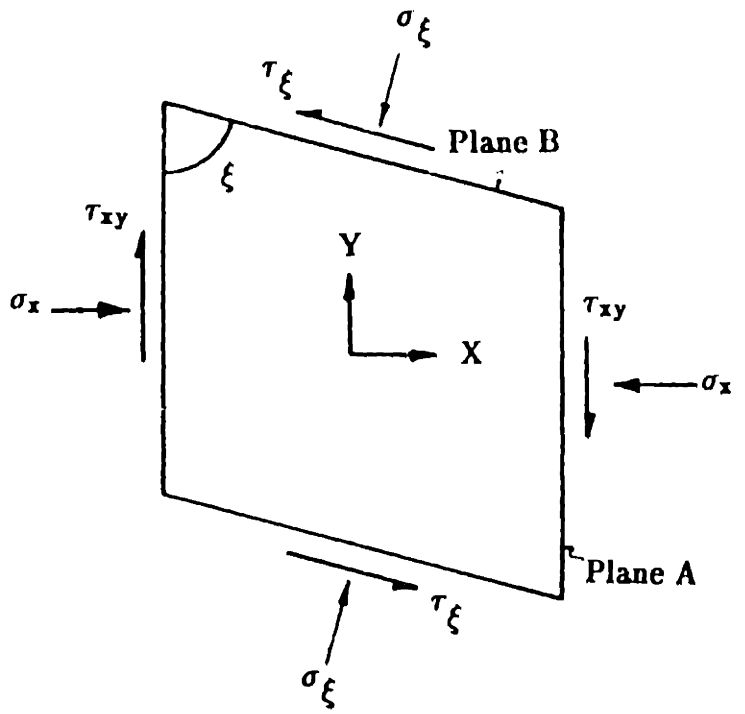

Figure G.2: Normal and Shear Stresses of an Element with Non–Orthogonal Faces.

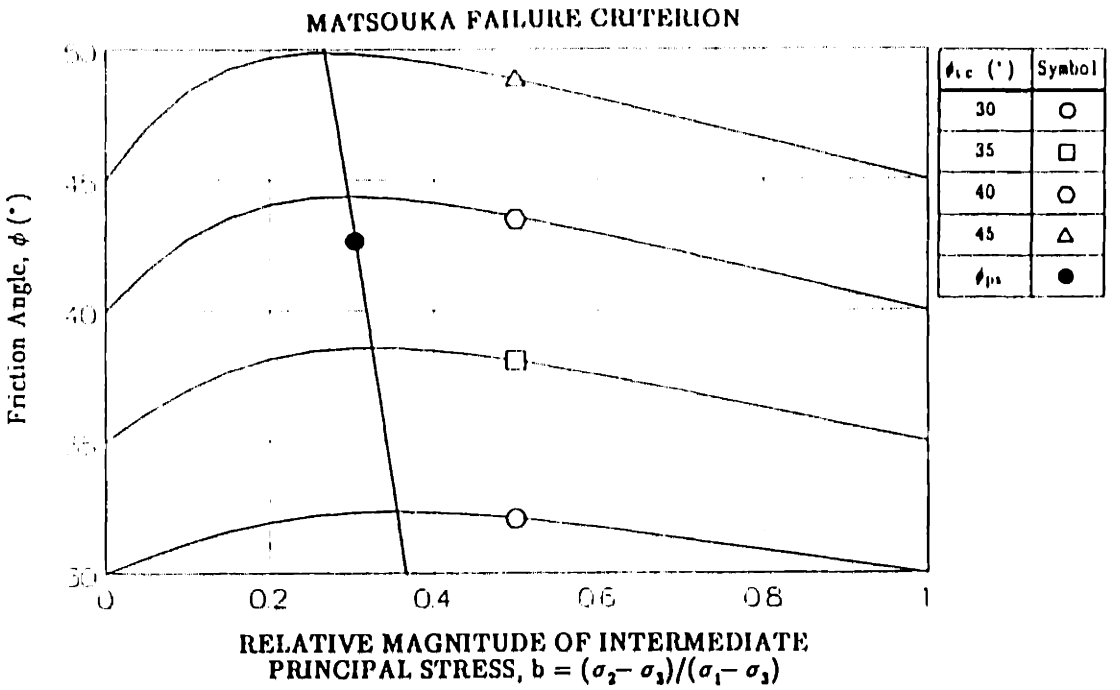

Note: ϕ_{tc}=Friction Angle from Triaxial Compression Test.

Figure G.3: Friction Angle (ϕ) versus Relative Magnitude of Intermediate Principal Stress (b) for Matsuoka Failure Criterion.

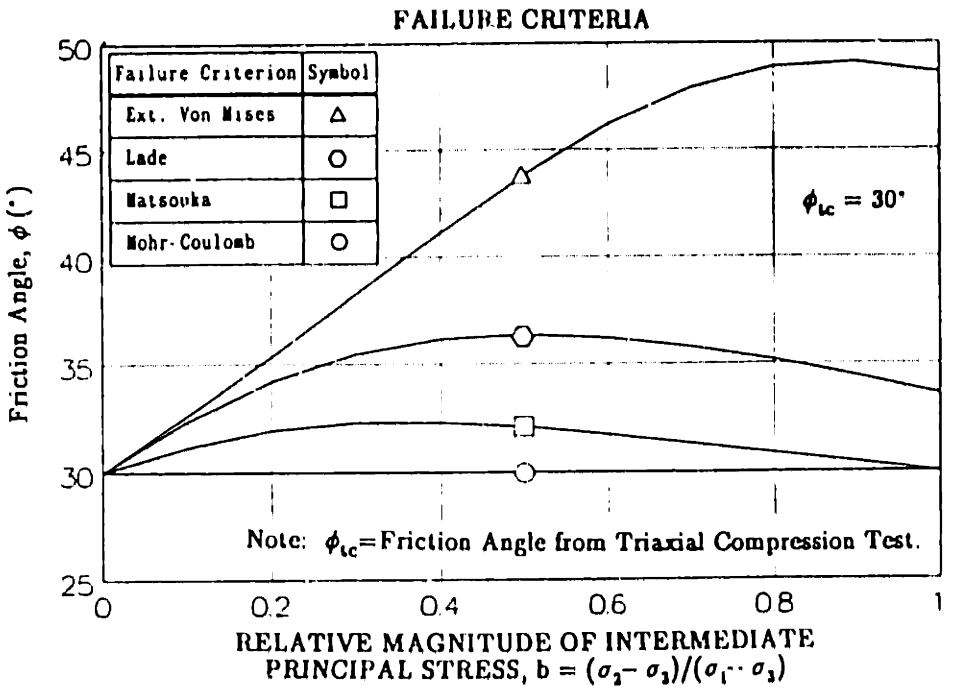

Figure G.4: Friction Angle (ϕ) versus Relative Magnitude of Intermediate Principal Stress (b) for Different Failure Criteria at ϕ_{tc}=30°.

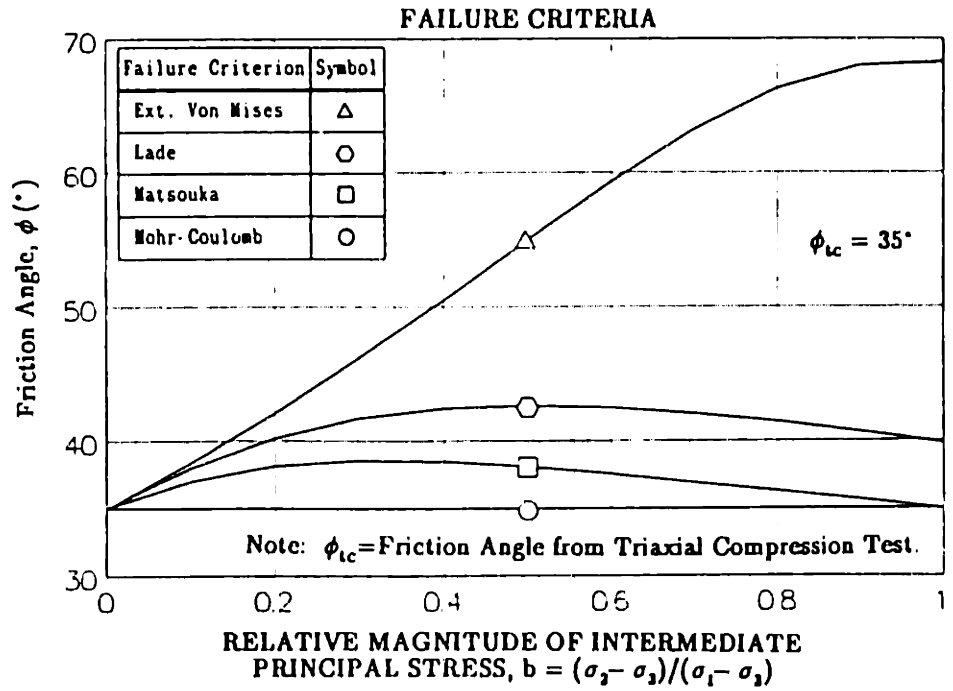

Figure G.5: Friction Angle (ϕ) versus Relative Magnitude of Intermediate Principal Stress (b) for Different Failure Criteria at ϕ_{tc}=35°.

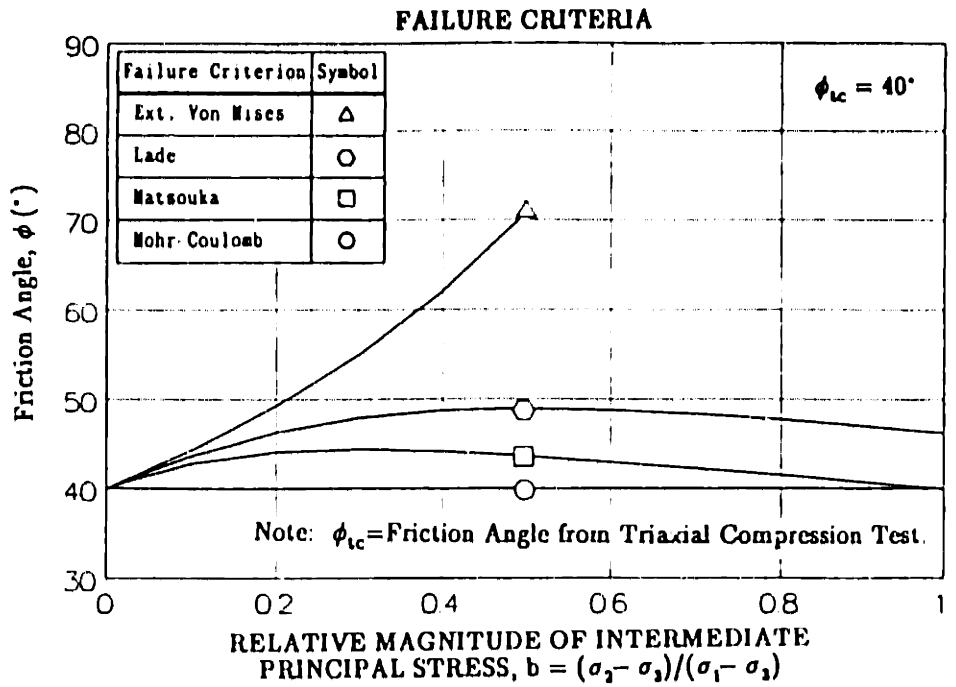

Figure G.6: Friction Angle (ϕ) versus Relative Magnitude of Intermediate Principal Stress (b) for Different Failure Criteria at ϕ_{tc}=40°.

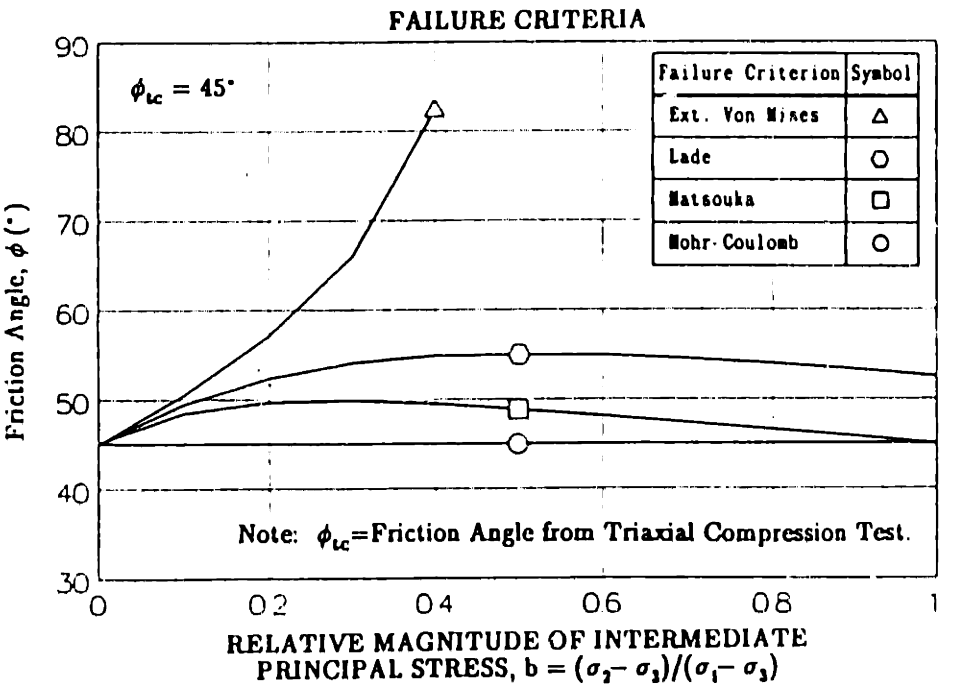

Figure G.7: Friction Angle (ϕ) versus Relative Magnitude of Intermediate Principal Stress (b) for Different Failure Criteria at ϕ_{tc}=45°.

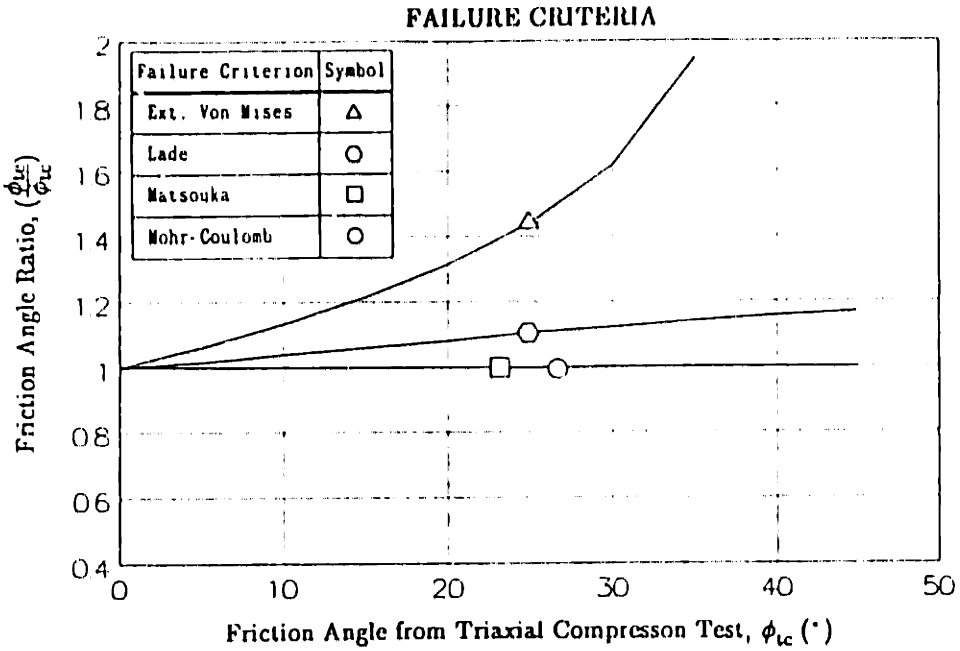

Figure G.8: Friction Angle Ratio (ϕ_{te}/ϕ_{tc}) versus Friction Angle (ϕ_{tc}) for Different Failure Criteria.